ENGINEERING-TRANSPORTATION
LIBRARY

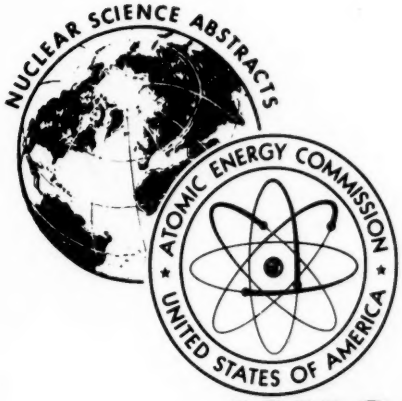

THE UNIVERSITY OF MICHIGAN
JUN 22 1966
ENGINEERING LIBRARY

NUCLEAR SCIENCE ABSTRACTS

Volume 20 Number 10

Abstracts 16158–18183

May 31, 1966

UNITED STATES ATOMIC ENERGY COMMISSION
Division of Technical Information

DEPOSITED BY THE
UNITED STATES OF AMERICA

USAEC DEPOSITORY LIBRARIES

Collections of USAEC reports are maintained in the libraries of the organizations listed below for reference use by the general public. Facilities for making photocopies are available. The USAEC also makes available through these libraries atomic energy reports of countries other than the U. S. that are abstracted in *Nuclear Science Abstracts*.

ALABAMA
Auburn, Auburn University
ALASKA
College, University of Alaska
ARIZONA
Tucson, University of Arizona
ARKANSAS
Fayetteville, University of Arkansas
CALIFORNIA
Berkeley, University of California
Davis, University of California
Los Angeles, University of California
San Diego, Public Library
Stanford, Stanford University
COLORADO
Boulder, University of Colorado
Denver, Public Library
CONNECTICUT
New Haven, Yale University
DELAWARE
Newark, University of Delaware
DISTRICT OF COLUMBIA
Washington, Library of Congress
FLORIDA
Coral Gables, University of Miami
Gainesville, University of Florida
Tallahassee, The Florida State University
GEORGIA
Atlanta, Georgia Institute of Technology
HAWAII
Honolulu, University of Hawaii
ILLINOIS
Chicago, John Crerar Library
Chicago, University of Chicago
Evanston, Northwestern University
Urbana, University of Illinois
INDIANA
Bloomington, Indiana University
Lafayette, Purdue University
IOWA
Ames, Iowa State University
KANSAS
Manhattan, Kansas State University
KENTUCKY
Lexington, University of Kentucky
Louisville, University of Louisville
LOUISIANA
Baton Rouge, Louisiana State University
New Orleans, Tulane University
MARYLAND
Baltimore, Johns Hopkins University
College Park, University of Maryland
MASSACHUSETTS
Cambridge, Harvard University
Cambridge, Massachusetts Institute of Technology
MICHIGAN
Ann Arbor, University of Michigan
Detroit, Public Library
East Lansing, Michigan State University
MINNESOTA
Minneapolis, University of Minnesota
MISSISSIPPI
State College, Mississippi State University
MISSOURI
Kansas City, Linda Hall Library
Rolla, University of Missouri School of Mines and Metallurgy
St. Louis, Washington University
MONTANA
Bozeman, Montana State College
NEVADA
Las Vegas, Nevada Southern University
Reno, University of Nevada
NEW JERSEY
Princeton, Princeton University
Teaneck, Fairleigh Dickinson University
NEW MEXICO
Albuquerque, University of New Mexico
NEW YORK
Albany, The University of the State of New York
Buffalo, State University of New York at Buffalo
Ithaca, Cornell University
New York, Atomic Industrial Forum, Inc.
New York, Columbia University
New York, New York University
Rochester, University of Rochester
Schenectady, Union College
Syracuse, Syracuse University
Troy, Rensselaer Polytechnic Institute
NORTH CAROLINA
Charlotte, Public Library of Charlotte and Mecklenburg County
Durham, Duke University
Raleigh, North Carolina State College
NORTH DAKOTA
Grand Forks, University of North Dakota
OHIO
Cincinnati, University of Cincinnati
Cleveland, Public Library
OHIO (CONT.)
Columbus, Ohio State University
Toledo, University of Toledo
Youngstown, Youngstown University
OKLAHOMA
Norman, University of Oklahoma
Stillwater, Oklahoma State University
OREGON
Corvallis, Oregon State University
Portland, Reed College
PENNSYLVANIA
Philadelphia, University of Pennsylvania
Pittsburgh, Carnegie Library
University Park, Pennsylvania State University
PUERTO RICO
Rio Piedras, University of Puerto Rico
RHODE ISLAND
Providence, Brown University
SOUTH CAROLINA
Columbia, University of South Carolina
TENNESSEE
Knoxville, University of Tennessee
Memphis, Public Library
Nashville, Joint University Libraries
Oak Ridge, Oak Ridge Associated Universities
TEXAS
Austin, University of Texas
College Station, Texas A & M University
Dallas, Southern Methodist University
Houston, Rice University
Lubbock, Texas Technological College
San Antonio, Public Library
UTAH
Salt Lake City, University of Utah
VIRGINIA
Blacksburg, Virginia Polytechnic Institute
Charlottesville, University of Virginia
Norfolk, Old Dominion College
WASHINGTON
Pullman, Washington State University
Seattle, University of Washington
WEST VIRGINIA
Morgantown, West Virginia University
WISCONSIN
Madison, University of Wisconsin
Milwaukee, Public Library
WYOMING
Laramie, University of Wyoming

DEPOSITED BY THE
UNITED STATES OF AMERICA

Volume 20, Number 10, May 31, 1966

NUCLEAR SCIENCE ABSTRACTS

A semimonthly publication of the USAEC Division of Technical Information, Edward J. Brunenkant, Director.
Published by the USAEC Division of Technical Information Extension, Robert L. Shannon, Extension Manager.

Nuclear Science Abstracts covers the international literature on nuclear science and technology and provides the only comprehensive abstracting and indexing of this body of information. Published twice each month since 1947, *NSA* covers technical reports of the U. S. Atomic Energy Commission and its contractors, technical reports of U. S. Government agencies and other governments, universities, industrial and research organizations, as well as patents, books, and journal literature on a world-wide basis. Nearly 350,000 abstracts have appeared in *NSA* through Volume 19. The subject matter covered in *NSA* is described in issue Number 1 and in TID-4552, *Subject Scope of Nuclear Science Abstracts*, available free from the U. S. Atomic Energy Commission, Division of Technical Information Extension, P. O. Box 62, Oak Ridge, Tennessee 37830.

Abstracts are arranged according to a number of subject categories and subcategories. Definitions of categories appear in issues Number 1 and 13. If the language of the original item is not English, the language will be indicated. Translations are not abstracted where an abstract of the original item has appeared in *NSA*.

INDEXES TO NSA

Corporate author, personal author, subject, and report number indexes appear in each issue and are cumulated quarterly, semiannually, and annually. Multi-volume cumulations have been issued as indicated on the following page. Report number indexes for all volumes (1–18) were issued at the end of Vol. 18. At the end of Vol. 19, the indexes for Vols. 1–15 were reissued to include additional public availability information. This cumulation will be a permanent shelf item and will not be reissued. Report number indexes for Vol. 19 are included as a cumulation beginning with Vol. 16.

AVAILABILITY OF PUBLICATIONS ABSTRACTED

The public availability of all U. S. Atomic Energy Commission reports is indicated in the report number indexes. The availability of other reports, when known, is also indicated. The availability of some unnumbered reports is given in the abstract.

Dissertations abstracted in *Dissertation Abstracts* and included in *NSA* are available from University Microfilms, Inc., 315 N. First Street, Ann Arbor, Michigan 48103.

Most of the published literature abstracted in *NSA* is on deposit at the Library, Oak Ridge Associated Universities, Oak Ridge, Tennessee, (a USAEC depository library) and is available through interlibrary loan. When requesting papers from this source, it is important that *NSA* volume and abstract number be cited.

HOW TO OBTAIN NUCLEAR SCIENCE ABSTRACTS

NSA is available on an exchange basis to universities, research institutions, industrial firms, and publishers of scientific information. Inquiries should be directed to the U. S. Atomic Energy Commission, Division of Technical Information Extension, P. O. Box 62, Oak Ridge, Tennessee 37830.

Government agencies may obtain *NSA* free of charge.

NSA is available to the general public on a subscription basis from the Superintendent of Documents, U. S. Government Printing Office, Washington, D. C. 20402, as follows:

For the 24 regular issues, $30.00 domestic, $37.00 foreign. A single issue costs $1.75, plus 25 per cent for foreign mailing. Domestic rates apply to the United States, Canada, Mexico, and Central and South American countries except Argentina, Brazil, British and French Guiana, Surinam, and British Honduras. Foreign rates apply to the countries excepted above and to all other countries throughout the world.

For the quarterly, semiannual, and annual indexes, $22.00 domestic, $25.00 foreign.

Multivolume subject and author indexes are available as follows:

Vols. 1–4 (1948–1950) Johnson Reprint Corporation, 111 Fifth Avenue, New York, N. Y. 10003, $30.00.

Vols. 5–10 (1951–1956) Superintendent of Documents, U. S. Government Printing Office, Washington, D. C. 20402, $5.25.

Vols. 11–15, Subjects, Superintendent of Documents, U. S. Government Printing Office, Washington, D. C. 20402, $19.00.

Vols. 11–15, Personal Authors, Superintendent of Documents, U. S. Government Printing Office, Washington, D. C. 20402, $14.25.

Vols. 11–15, Corporate Authors, Superintendent of Documents, U. S. Government Printing Office, Washington, D. C. 20402, $2.50.

Cumulative Report Number Index, Vols. 1–15, Revised, is available from the Superintendent of Documents, U. S. Government Printing Office, Washington, D. C. 20402, $4.00.

Cumulative Report Number Index, Vols. 16–19, is available from the Superintendent of Documents, U. S. Government Printing Office, Washington, D. C. 20402, $2.50.

Annual Indexes are available separately from the U. S. Government Printing Office as follows:

Vol. 16, Subject and Authors, $9.75.
Vol. 17, Subject and Authors, $12.25.
Vol. 18, Subject and Authors, $12.50.
Vol. 19, Subject and Authors, $12.50.

ACKNOWLEDGMENTS

Agreements between the United States Atomic Energy Commission and the following organizations with regard to providing continuing services and specific literature coverage for *Nuclear Science Abstracts* are gratefully acknowledged:

American Institute of Physics; Atomic Energy of Canada Limited; Atomic Energy Research Establishment, United Kingdom; European Atomic Energy Community (EURATOM); Gmelin Institute; International Atomic Energy Agency; Japan Atomic Energy Bureau—Japan Atomic Energy Research Institute; Netherlands Patent Office; Reactor Centrum Nederland.

TABLE OF CONTENTS

Volume 20, Number 10, May 31, 1966

Category	Page
BIOLOGY AND MEDICINE	1987
General	1987
Ecology	1988
Metabolism, Tissue Distribution, and Toxicology	1988
Radiation Effects on Biochemicals	1992
Radiation Effects on Tissues	1995
Radiation Effects Therapy and Countermeasures	2009
Radiation Hazards and Protection	2009
Radiotherapy and Radiodiagnosis	2010
CHEMISTRY	2014
General	2014
Analytical Procedures	2014
Inorganic and Physical Chemistry	2024
Organic Chemistry	2033
Radiation Chemistry	2035
Radiochemistry	2040
Separation Processes and Procedures	2042
ENGINEERING	2046
General	2046
Applications of Nuclear Explosions	2046
Facilities and Equipment	2046
Heat Transfer and Fluid Flow	2047
Materials Testing	2049
Protective Structures	2050
Space Propulsion	2050
Vacuum Engineering	2051
GEOLOGY, METEOROLOGY, AND MINERALOGY	2052
General	2052
Meteorology	2052
Natural Radioactivity and Fallout	2055
Site Survey and Selection	2060
Techniques and Equipment	2060
Thorium and Uranium Minerals	2061
HEALTH AND SAFETY	2062
INSTRUMENTATION	2069
General	2069
Radiation Detection	2072
Radiation Effects	2082
ISOTOPE TECHNOLOGY	2084
General	2084
Industrial Applications	2084
Power Application	2085
Separation and Production	2085
MATHEMATICS AND COMPUTERS	2087
METALS, CERAMICS, AND OTHER MATERIALS	2088
General	2088
Corrosion	2090
Fabrication	2093
Properties and Structure	2095
Radiation Effects	2106
PHYSICS	2113
General	2113
Accelerators	2114
Astrophysics and Cosmology	2119
Atomic Physics	2121
Cosmic Radiation	2126
Direct Energy Conversion	2128
Elementary Particles and Radiations	2129
Field Theory, Scattering Theory, and Symmetries	2138
Fluid Physics and Thermodynamics	2146
Geophysics	2150
Gravitation, Quantum Mechanics, and Relativity Theory	2153
Low Temperature Physics	2156
Neutron Physics	2162
Nuclear Properties and Reactions	2164
Plasma Physics and Thermonuclear Processes	2190
Shielding	2201
Solid State Physics	2202
REACTOR TECHNOLOGY	2209
General	2209
Auxiliaries and Components	2209
Criticality Studies	2211
Design and Feasibility	2214
Fuels	2215
Power and Power-Breeder Reactors	2215
Process Heat Reactors	2219
Production Reactors	2219
Propulsion and Space	2219
Research and Test Reactors	2220
WASTE DISPOSAL AND PROCESSING	2223
GENERAL AND MISCELLANEOUS	2226
CORPORATE AUTHOR INDEX	INDEX-1
PERSONAL AUTHOR INDEX	INDEX-10
SUBJECT INDEX	INDEX-55
REPORT NUMBER INDEX	INDEX-142

STAFF OF NUCLEAR SCIENCE ABSTRACTS

MANAGING EDITOR

John W. Norris

ASSISTANT MANAGING EDITOR

Donald D. Davis

ASSOCIATE EDITORS

Lawrence T. Whitehead
David E. Bost
Robert C. Kelly
Lee M. Thompson

SUBJECT INDEX EDITOR

Everett J. Hoffman

EVALUATORS

William D. Matheny
John H. Mitchell
Mary H. Newman

ABSTRACTORS

F. S. Armstrong (AECL)
Jane G. Buchanan
D. Lamar Cason
Bennie G. Di Bona
Helen G. Donald
James R. Dulaney
Wells L. Green
Mary Catherine Grissom
Fernando J. Hamilton
Phyllis C. Hansen
Carolyn D. Houston
Rose V. Jermain
Betty L. McDowell
Jean F. Peckham
Mona H. Raridon
Julia Redford
Francis L. Sachs
Lila B. Smith
Charles E. Stuber
Martha J. Thomas
Anne G. Ward
David C. West
Milton O. Whitson
Gabriel O. Ycaza

SUBJECT HEADING SPECIALIST

Robert E. Upchurch

CORPORATE AUTHOR SPECIALIST

Clara L. Fox

DESCRIPTIVE CATALOGING SPECIALIST

J. Paul Meredith

SCHEDULING AND PUBLISHING COORDINATOR

Brainard L. Patton

Communication concerning the editorial policy and content of *NSA* should be addressed to the Managing Editor, *Nuclear Science Abstracts*, AEC Division of Technical Information Extension, P. O. Box 62, Oak Ridge, Tennessee 37830.

Use of funds for printing this publication approved by the Director of the Bureau of the Budget, May 20, 1963

Volume 20, Number 10 May 31, 1966

NUCLEAR SCIENCE ABSTRACTS

BIOLOGY AND MEDICINE

General

16158 (AD-628360) SUPPRESSION OF DNA SYNTHESIS IN WEANLING RAT KIDNEYS BY SHORT-TERM FASTING. Phillips, T. L.; Wachtel, L. W. (Naval Radiological Defense Lab., San Francisco, Calif.). Dec. 14, 1965. 27p. (USNRDL-TR-956).

The effects of restricted food intake on DNA synthesis in the kidney were measured in weanling rats by means of injections of tritiated thymidine followed by an assessment of the number of labeled nuclei in autoradiographs. A marked decrease in renal thymidine uptake occurred after 16 hours of food deprivation. Even when refeeding was initiated after 20 hours food deprivation, DNA synthesis remained depressed for some 24 hours. Furthermore, the mitotic stimulus produced by unilateral nephrectomy was not strong enough to overcome the effects of starvation. The results suggest that in the weanling rat the kidney DNA synthetic system is particularly sensitive to caloric intake, and that this fact must be taken into account in evaluating the effects of whole-body x irradiation on the kidney. (auth)

16159 (ORNL-3900, pp 150-81) BIOLOGY AND MEDICINE. (Oak Ridge National Lab., Tenn.).

Summaries of research and development results are presented on somatic effects of radiation, radiation genetics, methods and chemicals for reducing radiation injuries, molecular level and cellular level mechanisms, terrestrial and freshwater ecology, radiological physics and radiation instruments, and nuclear energy civil effects. (J.R.D.)

16160 (UCRL-14739(Pt.2)) PROGRAM BOOK FOR THE ADVISORY COMMITTEE FOR BIOLOGY AND MEDICINE OF THE UNITED STATES ATOMIC ENERGY COMMISSION. PART II. (Lawrence Radiation Lab., Univ. of California, Livermore). Mar. 10, 1966. Contract W-7405-eng-48. 177p. Dep. mn. CFSTI $5.00 cy, $1.00 mn.

Studies are reported on: radionuclide metabolism in man and other organisms; biochemical and metabolic reactions; the effects of ionizing radiation on biosynthesis and genetics; radionuclide burdens in man and the terrestrial environment; biological ultrastructure; particulate behavior and fallout deposition; and radiation detectors and monitoring systems. (H.G.D.)

16161 THE CAROTENOID PIGMENTS OF A RADIATION-RESISTANT MICROCOCCUS SPECIES. Bamji, Mahtab S; Krinsky, Norman I. (Tufts Univ., Boston). Biochim. Biophys. Acta, 115: 276-84(Feb. 28, 1966).

The carotenoids of a radiation-resistant Micrococcus species from haddock tissue were isolated and characterized by a variety of procedures. These pigments have not been described previously. The four major pigments in stationary-phase cultures all have the same chromophore but differ in the number and type of substituents. The chromophore consists of a β-ionone ring with a conjugated keto group on one end of the carotenoid and a 1,2-alkoxy-3,4-dehydro-γ-ionone portion at the other end. The substituents include tertiary alkoxyls, enolic alkoxyls, and secondary alcohol groups. (auth)

16162 STUDIES ON THE MECHANISM OF EXPERIMENTAL SOFT-TISSUE CALCIFICATION. Gabbiani, G.; Tuchweber, B. (Univ. of Montreal). Can. J. Physiol. Pharm., 43: 177-83(Mar. 1965).

The influence of Pb^{2+}, La^{3+}, and Ce^{3+} salts on calcification was studied in rats. This study is based on the hypothesis that the precipitation of these so-called calcergens with phosphate or carbonate represents the nucleus that elicits the accumulation of calcium salts. Experiments were carried out to test this hypothesis. Animals which received only topical treatment of polymyxin, phosphate, or the combination of both, did not show any calcification. Among the animals prepared by the intravenous injection of various calcergens, precipitation of calcium salts was seen at the polymyxin injection site only in the group treated with lead acetate. On the other hand, all of the calcergens, including La and Ce, were effective in inducing subcutaneous calcification at phosphate, or phosphate plus polymyxin, injection sites. In the animals treated with lead acetate, the deposition of calcium salts at the polymyxin injection site, was seen as a whitish, homogeneous, brittle plaque. In the other groups, no changes were noted at this site. In all animals injected intravenously with a calcergen, a central area of necrosis surrounded by a whitish ring of calcification was observed at the site of phosphate and even more so at the site of phosphate plus polymyxin injections. It is concluded that the addition of phosphate to the extracellular fluid permits the production of calcification by all the calcergens given intravenously, although, with the exception of lead, they usually show no activity in the presence of polymyxin. Localization of calcium salts in the walls and lumens of small vessels, together with the production of central necrosis, suggests that Ce and La do not penetrate readily through capillary walls at sites of mast-cell discharge. This would explain the inactivity when polymyxin is injected at the same time as these calcergens. On the other hand, after the topical injection of phosphate, this compound may be attracted by the circulating calcergen and induces intravascular classification with consequent thrombosis. (BBB)

16163 METOCLOPRAMIDE IN THE TREATMENT OF ROENTGEN DISEASE AND OF THE DIGESTIVE DISORDERS OF ANTICANCEROUS CHEMOTHERAPY. Chassard, J. L.; Pagnon, P.; Treguier, R. J. Radiol., Electrol. Med. Nucl., 46: 857(Dec. 1965). (In French).

Metoclopramide was used to treat nausea in 45 patients who had received radiotherapy or chemotherapy. The drug was very effective in 86% of the cases tried and resulted in improvement in 12%. It is concluded that metoclopramide is particularly useful for digestive disorders accompanying radiation sickness or cancer chemotherapy. (H.G.D.)

16164 THE ANIMAL IN RADIATION EXPERIMENTS. Mueller, G. (Biologiches Institut der Medizinischen Akademie, Magdeburg, Ger.). Radiobiol. Radiotherap., 6: 683-99(1965). (In German).

Sources of errors are inherent in radiobiological experiments depending to a high degree on the animal material used. The ignorance of the respective standards of reactions depending on genotype and of their environmental modifications introduces numerous unknowns into the experiment. The aim of a scientific work must, however, be the elimination of all unknowns, if possible, except the one to be examined. Productivity of experimental work may be considerably increased by the use of uniformly reacting experimental animals. (auth)

16165 DEUTERATED ORGANISMS: CULTIVATION AND USES. Katz, Joseph J.; Crespi, Henry L. (Argonne National Lab., Ill.). Science, 151: 1187-94(Mar. 11, 1966).

Some of the manifestations of deuterium isotope effects in living organisms are discussed. A considerable range of organisms can be grown successfully in fully deuterated form, and the prospects are good that many more organisms will be grown in this form. Particular attention is given to the use of deuterated organisms in conjunction with proton magnetic resonance spectroscopy for following the path of hydrogen in biological systems, for biogenetic studies, and for studies of proteins by nuclear magnetic resonance. (TCO)

16166 BIOLOGICAL CONTAINMENT SYSTEM (Engineering Materials). (Oak Ridge Gaseous Diffusion Plant, Tenn.). (CAPE-1322).

25 drawings.

A containment system is described, which is used in performing normal operations in separating viruses in a virology laboratory. It is 28 ft long, 4 ft wide, 7 ft and 5 in. high, and is constructed of 7 Al sections. Walls and tops are covered with transparent acrylic sheeting. The laboratory safety, sterilization sequences, and controls are automated. The enclosure is sterilized with ethylene oxide and kept under a slight vacuum (1 in. water). Auxiliary systems integrated into the automatically controlled laboratory include the gas fired incinerator, drain sterilizer, double door, gas or steam sterilizer, and uv light exchange compartments. There are three centrifuge systems housed in the laboratory: the A-XII, B, and an unmodified preparative ultracentrifuge. (M.C.G.)

Ecology

16167 THE APPEARANCE OF ACTIVATION PRODUCTS FROM NEUTRON EXPLOSIONS IN FOOD (^{54}Mn). Kistner, G. Atompraxis, 12: 59-60(Jan. 1966). (In German).

Reports about discovering ^{54}Mn in the biological cycle of man increased. Gamma spectroscopic investigations showed that different plants, e.g., wheat, barley, rye, and tea leaves, harvested in recent years were contaminated by ^{54}Mn. Methods for separation of the different radionuclides and the identification of ^{54}Mn are described. (auth).

16168 ENVIRONMENTAL GAMMA RADIATION FROM DEPOSITED FISSION PRODUCTS, 1960-1964. Beck, Harold L. (Atomic Energy Commission, New York). Health Phys., 12: 313-22(Mar. 1966).

Dose rates in air from each important deposited fission product were calculated for the period 1 July 1960 to 1 January 1965 from measured deposition in rainfall at Westwood, N. J. A realistic model was adopted to account for the distribution with depth of the radionuclides in the soil. The calculated dose rates are consistent with in situ γ-spectrometric measurements, indicating that a detailed and reasonably accurate history was obtained of the effect of fallout on external gamma radiation levels. (auth)

16169 ^{137}Cs IN JAPANESE SOIL AND RICE. Yamagata, Noboru (Inst. of Public Health, Tokyo); Kodaira, Kiyoshi; Matsuda, Shunji. J. Radiat. Res., 6: 32-44(Mar. 1965).

Japanese soil and rice collected at 15 localities were analyzed for cesium-137 since 1959 through 1963. The time trend of rice-levels indicates the minimum in 1960 and 1961 and the maximum in 1963, showing more than threefold value of the minimum. A higher dependency was observed of the level of cesium-137 in rice on the fallout rate than either of the cumulative ground deposit or the N-ammonium acetate extractable cesium-137 in soil. Variation with locality is great and the highest rice-level is observed on the northern Japan Sea side, the lowest in the central and southern parts, and intermediate on the northern Pacific side. (auth)

Metabolism, Tissue Distribution, and Toxicology

16170 (AD-628805) WOUNDING RESPONSE IN RELATION TO POLAR TRANSPORT OF RADIOCALCIUM IN ISOLATED ROOT SEGMENTS OF ZEA MAYS. Evans III, E. C.; Vaughan, B. E. (Naval Radiological Defense Lab., San Francisco, Calif.). Jan. 3, 1966. 24p. (USNRDL-TR-963).

Simultaneous, separate determinations of radiocalcium transport in paired corn root segments were demonstrated by a perfusion bridge. Investigations with this new apparatus revealed a heretofore unknown transient in the tracer movement during the first 2 hours after excision. Investigations of the transient suggest that it is a result of wounding and repair, coupled with certain other metabolically mediated processes in organized root tissue. (auth)

16171 (AE-215) AN AUTOMATED ANION-EXCHANGE METHOD FOR THE SELECTIVE SORPTION OF FIVE GROUPS OF TRACE ELEMENTS IN NEUTRON-IRRADIATED BIOLOGICAL MATERIAL. Samsahl, K. (Aktiebolaget Atomenergi, Stockholm (Sweden)). Feb. 1966. 14p. Dep. mn.

An anion-exchange method based on fast selective sorption steps from mixtures of sulfuric, hydrobromic, and hydrochloric acid solutions was developed for the separation of five different groups of radioactive trace elements in neutron-irradiated biological material. The separations are performed automatically with a simple proportioning pump apparatus. The apparatus allows the exact adjustment of influent solutions to the series of ion-exchange columns. The practical application of the method is described in detail. The successful use of the method is practically independent on the level of ^{24}Na activity present in the sample. (auth)

16172 (NYO-2194-1) PATHWAYS OF METABOLISM IN EMBRYONIC DEVELOPMENT. Final Report, June 1, 1958-June 30, 1965. Markert, Clement L. (Johns Hopkins Univ., Baltimore, Md. Dept of Biology). Contract AT(30-1)-2194. 13p. Dep. mn; CFSTI $1.00 cy, $0.50 mn.

Recent results are summarized from a series of studies on metabolic pathways in embryonic development in which radioactive tracers were used to determine the stability and reutilization of the subunits of certain classes of macromolecules. A method was developed for assessing enzyme composition of tissues by the electrophoretic separation of the homogenate in starch, agar, or acrylamide gels and localization of enzymatic activity on the gel by specific staining procedures. The stained gels constitute a zymogram that clearly displays the separated enzymes present in the homogenate. Biological materials used included animals from all the classes of vertebrates and from several invertebrate groups. The molecular and genetic basis for the existence of many enzymes in isozymic forms was studied, with emphasis on the isozymes of lactate dehydrogenase (LDH). These isozymes were found to be under the control of two principal genes each coding for a different polypeptide, with these two polypeptides assembled into tetromers to generate the 5 principal isozymes found in all mammals and birds ex-

amined. In addition, many mammals and birds were found to contain a third gene coding for an LDH subunit found principally in sperm cells. Other studies reported include the progressive synthesis of enzymes during cell differentiation and the influence of genes on protein synthesis, in which the chick embryo was used. Emphasis was placed on the biochemistry and ultrastructure of endodermal cells of the yolk sac membrane at sequential stages of differentiation and the utilization of the yolk in tracing the metabolism of glucose and glycogen by the developing embryo. Data are included from studies on chromosome differentiation in developing embryos of the frog, Rana pipiens, and the genetic control of the isozyme systems for LDH in fish. A list is included of 32 publications that report details of the series of studies. (C.H.)

16173 (PG-Report-686) THE EFFECT OF SODIUM ALGINATE IN INHIBITING UPTAKE OF RADIOSTRONTIUM FROM THE HUMAN GASTROINTESTINAL TRACT. Hesp, R.; Ramsbottom, B. (Production Group, United Kingdom Atomic Energy Authority, Sellafield (England)). 1965. 15p. (CONF-650965-1). Dep. BIS $0.50. HSMO 2s. 6d.

From 1st International Conference on Medical Physics, Harrogate, Eng.

An experiment performed with the co-operation of a normal healthy adult male volunteer has shown that sodium alginate reduced uptake of radiostrontium from the gastrointestinal tract by a factor of about 9. In the first stage of the experiment, 0.36 $\mu C^{85}Sr$ was administered orally 20 minutes after an oral administration of 10g. sodium alginate. Twenty-six days later 0.48 $\mu C^{85}Sr$ was administered orally. In both stages of the experiment samples of excreta and blood were collected, and body retention of ^{85}Sr was measured by means of the Windscale Whole Body Counter. The degrees of inhibition of uptake of radiostrontium affected by sodium alginate, as assessed from urine, blood plasma, and body retention respectively were approximately 9.2, 9.1, and 8.8. (auth)

16174 (RLO-1547-3) A STUDY OF THE MECHANISM OF DIVALENT CATION UPTAKE BY PLANTS. Progress Report, June 1, 1965-May 31, 1966. Moore, David P. (Oregon State Univ., Corvallis). Feb. 28, 1966. Contract AT(45-1)-1547. 15p. Dep. mn. CFSTI $1.00 cy, $0.50 mn.

Progress is reported on studies of: metabolism in the uptake of divalent cations; the effect of concentration, pH, and competitive ions on the rate of uptake; and the basic differences between species in the uptake of divalent cations. Studies on manganese absorption by excised barley roots were continued with emphasis on the interactions between various polyvalent cations as they affect manganese absorption. Both Ca and Sr exhibited a synergism with Mg in their effects on Mn absorption but the effect was weaker than that of Ca-Mg. However, it appeared that Sr could partly substitute for Ca in the Ca-Mg effect. Ferrous iron markedly depressed Mn absorption and also exerted a strong synergistic effect both with Ca and Mg. Ferric iron did not compete with Mn under the conditions of the experiment. The influence of both Zn and La on Mn absorption were also investigated. Experiments on the behavior of UO_2^{++} as a selective inhibitor of ion absorption were continued, and a series of experiments on the differential inhibitory effect of uranyl on ion absorption to pH and UO_2^{++} concentration were conducted. At pH 3.0 UO_2^{++} was found to behave very similarly to other polyvalent cations in its effect on sodium and potassium absorption. Further, potassium absorption was selectively inhibited without materially affecting that of sodium. It was concluded that the divalent form of UO_2 behaved similarly to other divalent cations in the Viets effect, but that the differential inhibition was caused by one or more of the hydrolysis products. The influence of UO_2^{++} on sodium-potassium competition as a function of sodium concentration and potassium concentration was also studied, and it was concluded that sodium and potassium were transported by two sites, one of which was considerably more sensitive to UO_2^{++} than the other. Experiments on the influence of iron on the expression of leaf chlorosis of tomato plants exposed to continuous light indicated that the expression of tomato leaf abnormalities in continuous light was dependent in part on the nutrient status of the plants. (H.G.D.)

16175 (RT/BIO(65)1) MARINE RADIOBIOLOGY. Annual Report for 1963. (Comitato Nazionale per l'Energia Nucleare, La Spezia (Italy). Laboratorio per lo Studio della Contaminazione Radioattiva del Mare). 1965. 20p. (EUR-2239.e). Dep. mn.

Developments are reported for studies on: distribution of inorganic and organic substances in the ecosystem and its components, and analysis of inorganic and organic substances in experimental organisms and their medium; distribution of phytoplankton in the ecosystem and experiments with radioisotopes on predominant phytoplankton species; distribution of zooplankton and its position in the food-chain and experiments with radioisotopes on predominant zooplankton species; and distribution of heterotroph microorganisms and their function in the marine ecosystem, and experiments with radioisotopes on heterotroph microorganisms. Special devices used are described. (P.C.H.)

16176 EFFECT OF PYRIDOXINE ON THE RENAL EXCRETION OF STRONTIUM, CALCIUM, AND PHOSPHATE. Schmid, A.; Zipf, K. Arch. Exp. Pathol. Pharmakol., 250: 282-3(1965). (In German).

Young adult female rats were injected subcutaneously with 0.486×10^{-3} mol/100 g of pyridoxine in 5% aqueous solution, and the renal excretion of Sr was measured. The urine was collected through an indwelling catheter. The rate of excretion of Sr was increased by 77% over normal while Ca excretion was increased only about half of that value. Phosphate excretion was decreased by about 35% below normal. The results indicated some selectivity of pyridoxine to promote Sr excretion that could be of interest in connection with treatment of radiostrontium poisoning. Projection of these results to other animal species would require additional studies, because differences in pyridoxine metabolism are known to exist between various animal species. (BBB)

16177 LIQUID SCINTILLATION COUNTING OF ^{14}C AND ^{3}H SAMPLES USING GLASS-FIBER FILTER-PAPER DISCS. Davies, J. W.; Cocking, E. C. (Univ. of Nottingham, Eng.). Biochim. Biophys. Acta, 115: 511-13(Feb. 28, 1966).

Scintillation counting of biological samples labeled with ^{14}C or tritium on glass-fiber filter discs or cellulose filter-paper discs provides a simple, rapid, and reproducible method for counting aqueous samples under non-aqueous conditions. The method is described. Applications in studies of the uptake of tritiated amino acids and nucleotides by isolated plant protoplasts and in the incorporation of ^{14}C-amino acids and ^{14}C-bicarbonate into proteins and plant tissues are reported. (C.H.)

16178 DISCRIMINATION BETWEEN STRONTIUM AND CALCIUM IN BONE AND THE TRANSFER FROM BLOOD TO BONE IN THE RABBIT. Kshirsagar, S. G.; Lloyd, Elizabeth; Vaughan, Janet (Churchill Hospital, Oxford). Brit. J. Radiol., 39: 131-40(Feb. 1966).

Seven-month-old rabbits were injected intravenously with ^{90}Sr or ^{45}Ca and killed serially at time intervals from ten minutes to 460 days after injection. The uptake of both isotopes was about the same at ten minutes after injection. This uptake represented about one-third of the maximum uptake of ^{45}Ca, which was observed at one day and about half of the maximum uptake of ^{90}Sr, which was observed at four hours. Although the maximum uptake of ^{45}Ca is greater than that of ^{90}Sr the rate of uptake and removal of ^{90}Sr was greater than that of ^{45}Ca. The turnover of both ^{90}Sr and ^{45}Ca was greater in the trabecular bone of the vertebrae and in the ends of the long bones than in the mid-cortex of the femur and tibia at short times after injection. Those portions of bone which showed the highest rates of turnover were found to be associated with relatively lower values for the stable strontium/calcium ratios. This suggested that the net effect of incorporation and release

favored the preferential retention of calcium at metabolically active sites. Measurements of stable strontium and calcium in the whole skeleton and in plasma showed an overall discrimination of about 1.6 in favor of calcium the transfer from blood to bone. (auth)

16179 AN IMPROVED TECHNIQUE FOR THYROIDAL ^{131}I DETERMINATION IN THE SMALL LABORATORY ANIMAL. Premachandra, B. N. (Veterans Administration Hospital, St. Louis. Washington Univ., St. Louis). Endocrinology, 78: 254-60(Feb. 1966).

A technique is described which enables thyroidal ^{131}I measurements to be made with accuracy and reproducibility in the small laboratory animal. For proper positioning of the thyroid and shielding of the detector a lead housing with 2 components placed one above the other is used. The base of the upper unit is made planoconcave with respect to the lower lead shield containing the scintillation detector. Such an arrangement reduces body and background radiation substantially, thereby improving the counting-to-background ratio. In vivo thyroidal ^{131}I has been compared against in vitro thyroidal ^{131}I in 43 rats under various levels of ^{131}I activity with very good agreement in the corresponding determinations (r = +.99). By making in vivo thyroidal ^{131}I measurements in 45 rats with a dual channel analyzer operating in different mode in each channel, the technique described has also been shown to be superior to the use of a radiation spectrometer for reducing body radiation at various intervals after ^{131}I administration. Such a technique may have particular usefulness in minimizing errors due to body and background radiation in long-term thyroidal ^{131}I measurements with repeated radioactivity administration. (auth)

16180 CHANGES IN ^{137}Cs RETENTION AND ROUTES OF ELIMINATION AS EFFECTED BY EXTERNAL FACTORS. McPeak, D. W.; Lodde, G. M.; Parr, W. H. (Army Medical Research Lab., Fort Knox, Ky.). Health Phys., 12: 369-75(Mar. 1966).

Investigations were made to determine the roles that cold and x-irradiation played upon the biological retention of ^{137}Cs in rats. Partial and whole-body x-irradiation increased the retention time, while cold decreased the retention time. Analysis of fecal and urine outputs showed that increased diuresis does not invariably facilitate ^{137}Cs excretion. The possible roles of food ingestion and fecal output were discussed. (auth)

16181 EXPERIMENTAL EPIPHYSEAL CARTILAGE GROWTH ANOMALIES. Storey, E. (Univ. of Melbourne). J. Bone Joint Surg., 47B: 145-56(Feb. 1965).

Stable strontium in the form of $SrCo_3$ was fed to rats at a level of 2.6% in the diet, and the animals were killed at intervals during the next 12 months. Both decalcified and undecalcified sections were prepared and stained in various methods. Strontium in this amount in the diet initially inhibits calcification and induces rickets. Histological changes induced by dietary Sr are described. (TCO)

16182 EFFECTS OF ZINC, CADMIUM, SILVER AND MERCURY ON THE ABSORPTION AND DISTRIBUTION OF ^{64}Cu IN RATS. Van Campen, Darrell R. (Plant, Soil and Nutrition Lab., Ithaca, N. Y.). J. Nutr., 88: 125-30(Jan. 1966).

A technique for placing doses of ^{64}Cu and the accompanying antagonist directly into in vivo ligated segments of rat gastrointestinal tract was used. The following results were obtained: zinc affected ^{64}Cu uptake from the stomach and from the duodenum in the same manner and to about the same extent. In both cases, high levels of zinc depressed ^{64}Cu uptake, but did not produce any change in the tissue distribution pattern. Cadmium depressed ^{64}Cu uptake severely, caused increases in the relative proportions of ^{64}Cu observed in the blood, heart, and spleen, and decreased the proportion retained by the liver. Silver had little effect on ^{64}Cu uptake, but a significantly greater proportion of the absorbed isotope was deposited in the liver, and significantly less was retained by the blood of the silver-treated rats. Mercury produced a moderate, but not statistically significant, lowering of ^{64}Cu uptake, an increase in the relative percentage of ^{64}Cu in the kidney, and a decrease in the proportions of ^{64}Cu retained by the blood and by the liver. Experiments were also conducted to compare the effects of zinc, cadmium, silver, and mercury on the absorption and distribution of ^{64}Cu in rats. The ions used in these studies were chosen because of certain characteristics that they share with one another and with copper. The observations indicated that the effects are widely varied. The only common feature was that each of the four cations did affect copper metabolism. (BBB)

16183 PENETRATION OF ^{239}Pu THROUGH THE SKIN. Khodyreva, M. A. Med. Radiol., 10: 42-6(Oct. 1965). (In Russian).

Plutonium nitrate penetration of intact skin was studied in rabbits. Penetrating ability was assessed by the activity of the blood and internal organs. Blood activity was determined by autoradiography. Plutonium nitrate was absorbed when concentrations of 0.4 to 4 $\mu C/cm^2$ were applied to skin surface. (H.G.D.)

16184 DISTRIBUTION OF URANIUM IN THE ORGANISM OF DOGS AT LONG PERIODS AFTER THE INHALATION OF URANIUM OXIDE. Tikhaya, M. G.; Novikova, A. P.; Parfenov, Yu. D. Med. Radiol., 10: 50-4(Oct. 1965). (In Russian).

Seven mongrel dogs inhaled U_3O_8. The aerosol concentration was 310×10^4 to 634×10^4 mg/l and the exposure time was 60 minutes per day during 5 to 7 days. Larger amounts of aerosols were deposited in the lungs in early stages. After 60 months the uranium concentration in the skeleton exceeded that in the lung. About 10.1% of the retained lung burden is eliminated with biological half-life of 280 days. After 60 months following cessation of exposure the concentration of uranium was greater in the pulmonary lymph nodes than any other tissue and exceeded approximately 550 to 870 times that in the lung. One dog exposed to a single inhalation of poorly soluble uranium aerosols U_3O_8 retained approximately 26% of the inhaled material in the lung after 20 minutes. (auth)

16185 MEASUREMENT OF ^{54}Mn IN POPULATIONS OF UNIO PICTORUM L. (MOLLUSCA, LAMELLIBRANCHIA) OF LAKE MAGGIORE. Ravera, Oscar; Vido, Ludovico (Istituto Italiano di Idrobiologia Dott. Marco De Marchi, Pallanza, Italy). Mem. Ist. Ital. Idrobiol. Dott. Marco De Marchi, 13: 75-84(1961). (In Italian).

The presence of ^{54}Mn was detected in 1960 in specimens of this bivalve, collected at four stations (Fondotoce, Ispra, Angera, and Arona) on this lake, by γ spectrometric and radiochemical methods. The soft tissues contained higher concentrations than the shells, and showed higher variations between samples than those in the shell. For the four respective stations the ^{54}Mn content ($m\mu C/kg$) was 1.10, 2.5, 3.0, and 4.0 for soft parts as compared to 0.15, 0.14, 0.15, and 0.13 for the shell of Unio. The water and sediments of this lake and other molluscs from it have not shown detectable amounts of ^{54}Mn. Samples of U. pictorum from another lake (Lake Varese) also showed appreciable ^{54}Mn content. Radiochemical procedures for separating ^{54}Mn are outlined. It is suggested that ^{54}Mn may originate as an activation product from stable manganese present in the casing of thermonuclear devices. (BBB)

16186 ABSORPTION AND GASTRIC SECRETION OF ^{131}I AND ^{36}Cl IN DAIRY CALVES. Miller, J. K. (Univ. of Tennessee, Oak Ridge). Proc. Soc. Exp. Biol. Med., 121: 291-4(Jan. 1966).

Metabolism of ^{131}I and ^{36}Cl was investigated by simultaneous daily administration of two radioisotopes to milk fed dairy calves. Plasma levels of ^{131}I averaged 1/5 and abomasal ^{131}I contents 3 times corresponding ^{36}Cl values. Thus, net gastric secretion of iodine exceeded that of chlorine by 15 times. Percentages of daily administered ^{131}I and ^{36}Cl, respectively, excreted during the last 3 days

of dosing averaged 15.6 and 12.2% in urine and 31.5 and 0.4% in feces. Chlorine-36 in ingesta from the large intestine was completely water-extractable compared to less than 20% of the ^{131}I in the same samples. (auth)

16187 EFFECT OF IONIZING RADIATION ON IRON METABOLISM OF ORGANISM. Adam, G.; Miltenyi, L.; Hadhazi, Cs.; Mucsi, O. (Medizinische Univ., Debrecen). Radiobiol. Radiotherap., 6: 631-5(1965). (In German).

Radiation effects on iron metabolism were studied in rats exposed to 250 rad doses of ^{60}Co γ rays. Bound iron was assayed in the liver and spleen of animals given tracer doses of $^{59}FeCl$. Electrolytic iron was not bound as well as that of protein complexes. Iron molecules were found in the cytoplasm before and during irradiation and in the vicinity of the cell nucleus after irradiation. The liver was found to be a more important iron depot than the spleen. Radiation injuries to iron metabolism were not verified autoradiographically. (H.G.D.)

16188 EXAMINATIONS OF THE EFFECT OF IONIZING RADIATION ON DISTRIBUTION OF ^{32}P-LABELED YOSHIDA SARCOMA CELLS. Magdon, E.; Baudach, H. (Robert-Roessle-Klinik, Berlin). Radiobiol. Radiotherap., 6: 665-9(1965). (In German).

Phosphorus-32-labeled Yoshida sarcoma cells were transplanted in rats, and the radioactivity was measured at various time intervals in the blood, lungs, liver, spleen, heart, intestine, bones, skin, muscles, and brain. Distribution was found to depend on time, the highest activity at early time increments being detected in pulmonary tissue. Later, activity decreased in the lungs and increased in other tissues, particularly the liver. Irradiation greatly enhanced the rate of decrease of radioactivity in lung tissue, probably because of the rapid destruction of tumor cells in pulmonary tissue. (H.G.D.)

16189 ^{210}Po ANALYSES OF VEGETABLES, CURED AND UNCURED TOBACCO, AND ASSOCIATED SOILS. Berger, K. C.; Erhardt, W. H.; Francis, C. W. (Univ. of Wisconsin, Madison). Science, 150: 1738-9(Dec. 24, 1965).

Analysis of the edible portion of vegetables and samples of green leaf tobacco failed to show ^{210}Po. The cured samples of leaf tobacco and the soils that were analyzed all contained small quantities of the element. Muck soils contained three times as much ^{210}Po as did mineral soils. Solutions used commonly to extract available forms of many mineral elements failed to extract a detectable amount of ^{210}Po. Indications are that ^{210}Po or its radioactive precursors are not taken up from the soil directly by plant roots but rather by sorption in dead, moist plant materials at the atmosphere-plant interface. (auth)

16190 CHANGES IN THYROID ^{131}I ACTIVITY IN OZONE-TOLERANT AND OZONE-SUSCEPTIBLE RATS. Fairchild II, Edward J. (Dept. of Health, Education, and Welfare, Washington, D. C.); Graham, Stuart L.; Hite, Mark; Killens, Richard; Scheel, Lester D. Toxicol. Appl. Pharmacol., 6: 607-13(Sept. 1964).

The effect of O_3 exposures of various concentrations on the thyroid ^{131}I uptake of rats was examined. Single 5-hr exposures of O_3 in concentrations of 4, 2, and 1 ppM produced inhibition of thyroid release of ^{131}I, an effect which was significant for a period of from 48 to 384 hr. Repeated 5-hr exposures to O_3, in either 0.5 or 1.0 ppM concentration on each of 4 days, did not significantly alter thyroid ^{131}I content when measured from 96 to 384 hr. These exposures are known to produce a high degree of tolerance to subsequent challenge. Repeated 5-hr exposures to O_3 in 2 ppM concentrations on each of 2 days, followed 3 days later with a challenge exposure of 4 ppM for 5 hr, not only failed to inhibit thyroid activity, but actually increased the release rate of ^{131}I. Results are discussed relative to a triphasic response characterized primarily by a depression of thyroid function followed by a period of resistance wherein function appears normal, terminating in a phase of thyroid overactivity. These responses to O_3 inhalation indicate that the tolerance phenomenon induced by certain irritant gases is associated with, but not necessarily determined by, a resistant phase of thyroid activity, and furnishes evidence for activation of humorally mediated mechanisms by this gas in concentration as low as 0.5 ppM. (BBB)

16191 SOME EFFECTS OF THE RARE EARTHS AND YTTRIUM ON THE GROWTH AND METABOLISM OF ASPERGILLUS NIGER [Thesis]. Talburt, Dwight Edmond. Fayetteville, Ark., Univ. of Arkansas, 1965. 93p.

Some effects of seven rare-earth elements and yttrium on the growth and metabolism of bacteria, yeast, and molds are described. The gradient-plate technique was adapted to determine the relative sensitivities of various microorganisms to the elements involved. Evidence is presented to support the following conclusion: (1) Yttrium and the rare-earth elements are generally toxic to growth. (2) Bacteria are more sensitive to these elements than the fungi. (3) Some species of fungi are more sensitive to the elements than other species. (4) A ranking of the descending toxicities of the metals for the selected microorganisms follows the order of decreasing atomic number and increasing atomic radius. Colonies of A. niger and some other fungi elaborate oxalic acid during growth, which combines with the metals present to form insoluble oxalates and results in a detoxification mechanism permitting further growth. Hyphae of filamentous fungi on yttrium and rare-earth plates show serious structural change. These damaged hyphae make no futher growth. Yttrium and the rare-earth metals interfere with the metabolism of A. niger as reflected by decrease in total protoplasm, decrease in total acid production, decrease in citric acid production, and decrease in glucose utilization as compared to control cells not treated with these metals. There appears to be no individual rare-earth effect. The degree of the toxic effect of the metals is dependent on the concentration applied. Yttrium and rare-earth binding by A. niger occurs rapidly and reaches a fixed maximum directly related to the protoplasmic mass. Respiration and glucose utilization decrease with increasing quantities of metal. At the maximum metal-binding capacity of the cells, oxygen-uptake responses to added glucose are completely stopped and glucose absorption does not occur. The data indicate that the cell membrane is the primary site of action. (Dissertation Abstr.)

16192 QUANTITATIVE STUDIES OF FACTORS AFFECTING BONE BLOOD FLOW BASED ON BONE CLEARANCE OF RADIOSTRONTIUM (^{85}Sr) [Thesis]. Shim, Sun Shik. Vancouver, Can., Univ. of British Columbia, 1965. 137p.

Factors affecting bone blood flow were studied in rabbits and dogs. A method for estimating bone blood flow was developed using the initial bone clearance of radioactive strontium (^{85}Sr) from blood. The method is based on Fick Principle and is similar to that used in estimating renal plasma flow from clearance of PAH or diodrast. The validity of the method depends on the efficiency of ^{85}Sr removal from blood by bone as indicated by the extraction ratio (ER), the proportion of the ^{85}Sr removed from the blood flowing through bone. The mean effective bone blood flow for 270 bones from 80 rabbits was found to be 9.60 ± 0.19 (SE) ml/min/100 g fresh weight, and for 46 bones from 10 dogs, the average value was 10.15 ± 0.61 (SE) ml/min/100 g fresh weight. Total skeletal blood flow was estimated to be 7.1 ± 0.25 (SE) % of the resting cardiac output in the rabbits and 7.3 ± 0.95 (SE) % of the resting cardiac output in the dogs. The nutrient artery of femur was found to supply 70% of the blood flow to the shaft and ⅓ of the blood flow to the ends. Blood flow to the ends of bone was significantly higher than that to the shaft. Various factors affecting bone blood flow were studied. Section of the sciatic nerve increased blood flow to the bones of the leg and foot. Infusion of epinephrine (2-4 microgram/kg/min) reduced blood flow to tibia and humerus by 74–81% and sharply reduced calcium exchange between blood and the labile calcium storage pool in bone. Immobilization of the leg in a plaster cast for 2 weeks resulted in some decrease in blood flow in tibia and calcaneus but more prolonged immobilization (2 months) caused disuse osteoporosis in these bones and a relative increase in

blood flow. The surgical problem of fractures of the neck of femus was studied, and it was found that such fractures reduced blood flow to the femoral head by 52–83%. (Dissertation Abstr.)

Radiation Effects on Biochemicals

See also CHEMISTRY — Radiation Chemistry

Refer also to abstract 16258.

16193 (EUR-2539,i) SULLA BIOSINTESI DI ACIDO GIBBERELLICO U ^{14}C E DI GLUCOSIO 3-4 ^{14}C. (The Biosynthesis of Gibberellic Acid-^{14}C and 3,4-Glucose-^{14}C). Lucchini, G.; Parisi, B.; Cocucci, S. (Milan Univ. (Italy)). 1966. 28p. Dep. mn.

The organic substrate that gives the optimum gibberellic acid yields and the most favorable ^{14}C labeled precursors for the production of gibberellic acid at moderate cost was sought. The following two routes were studied: inoculation and culture of a small quantity of mycelium in a strongly radioactive medium; and addition to the culture medium, after a certain growth period, of a labeled gibberellic acid precursor. The second route appeared to be the more economical. The specimens obtained were subjected to chemical and biological tests. Carbon-14-labeled glucose was prepared using castor bean endosperms and rat liver. In the first case, $^{14}CO_2$ was supplied to the tissues in a closed atmosphere; in the second $NaH^{14}CO_3$ has injected intraperitoneally to adult male rats. The possibility was also studied of the synthesis of glucose 3,4 ^{14}C from pyruvate 1-^{14}C, using purified glycolytic enzymes. A new technique for the degradation of labeled glucose has been worked out, based on the use of purified enzyme. (auth)

16194 MODIFICATION OF THE ELECTRICAL CONDUCTIVITY OF IRRADIATED BIOPOLYMERS. Furnica, Gheorghe; Radu, Minodora (Institutului de Igiena si Protectia Muncii, Bucharest). Acad. Repub. Pop. Rom., Stud. Cercet. Biochim., 8: 451-4(1965). (In Rumanian).

The effects of large doses of radiation ($1.5-2.0 \times 10^6$ R) on the electrical conductivity of aqueous solutions of γ-globulin and DNA were determined. A ^{60}Co source was used. For the 2% solution of globulin, irradiation produced a 5% decrease in conductivity at 37 to 50°C. Comparison of irradiated and standard solutions after dialysis for 60 hr at 4°C showed a decrease of 31, 29, and 26% for samples irradiated at 10, 37, and 50°C, respectively. But addition of AET (30 mg/ml) produced an increase in conductivity of 18% after dialysis. Irradiation of saturated DNA at 37°C decreased conductivity by 21% (2×10^6 R); or 9.5% decrease was found by irradiation at 50°C. Doses of 1.5×10^6 R at similar temperatures produced changes of less than 5%; but dialyzed (4 days) samples with this dose showed 6–7% decrease. Irradiation with 2.5×10^6 R produced 15% increase at 37°C and 15% decrease at 50°C. (BBB)

16195 EFFECT OF ULTRAVIOLET IRRADIATION ON THE ACID-FASTNESS AND GRAM-POSITIVITY OF MYCOBACTERIA. Murohashi, Toyoho; Yoshida, Konosuke (National Inst. of Health, Tokyo). Amer. Rev. Respirat. Dis., 92: 817-21(Nov. 1965).

Acid-fastness of mycobacteria is lost completely when smears are subjected to uv irradiation for certain periods. The irradiation time required for the complete loss of acid-fastness is different for various mycobacteria, and it is suggested that cell-wall structure of thickness is responsible for the acid-fastness differences of mycobacteria. From a practical standpoint, it would be possible to use this procedure as a very simple in vitro test method for the differentiation of various mycobacteria prior to precise examinations, especially of nonpigmented groups, which are still very difficult to distinguish one from the other. Ultraviolet irradiation that was sufficient to produce a complete loss of acid-fastness did not affect the gram-stainability of all strains of mycobacteria. Thus, the gram-stainability of mycobacteria was kept intact far longer than the acid-fastness, even after the complete loss of the latter by irradiation, suggesting that these two properties are of quite different mechanism. Gram-positivity was not lost by even saprophytic mycobacteria, including M. lacticola, upon irradiation under the conditions described, in less than 20 hours, by which time all types of mycobacteria became completely non-acid-fast. The pore size of cell wall that might result from the destructive effect of uv energy did not seem to be big enough to permit the RNase molecule to pass through it. (BBB)

16196 THE EFFECT OF ULTRAVIOLET EXPOSURE UPON SUCCINIC DEHYDROGENASE ACTIVITY. Ogura, R.; Knox, J. M. (Baylor Univ., Houston, Tex.). Dermatologica, 131: 397-403(1965).

The destruction of enzyme activity in mouse liver homogenate as a result of uv exposure and the ability of certain compounds to prevent, accelerate, or reverse the destruction were studied. In the first experiment, 8-methoxypsoralen was added to the homogenate before irradiation. In the second experiment, glutathione was added after irradiation, and in the third experiment the mice were fed chloroquine for 30 days prior to irradiation. When activity was plotted against exposure time a linear decline of succinic dehydrogenase activity was seen after 5, 10, 15, 20, and 30 min of exposure to uv light. Loss of activity was accelerated by 8 methoxypsoralen. The decrease in succinic dehydrogenase activity following exposure to uv was partially reversed by the addition of glutathione. Chloroquine administration did not prevent or inhibit the decline in activity. The results are discussed in terms of earlier findings. (TCO)

16197 UV-INDUCED PHOTODIMERIZATION OF THYMINE AND 5-HYDROXYMETHYLURACIL IN FROZEN WATER SOLUTIONS. Kalab, D. (Research Department of Bioveta, Ivanovice, Czech.). Experientia, 22: 23-4 (Jan. 15, 1966).

Radioinduced photochemical dimerizations of 5-hydroxymethyluracil and thymine in frozen water solutions were compared and the rates of dimer conversion studied. Water solutions (5×10^{-4} and 10^{-3} M) of both 5-hydroxymethyluracil and thymine were irradiated at 2.537 Å in the frozen state under a bactericidal lamp. Dimer conversion of both compounds were observed in alkaline and neutral solution. A lower rate of dimer conversion was observed in 5-hydroxymethyluracil than in thymine. (F.J.H.)

16198 EFFECT OF ULTRAVIOLET RADIATION ON THE OXIDATION OF CERTAIN KREBS CYCLE SUBSTRATES IN VIBRIO CHOLERAE. Kapoor, N. K.; Sagar, P.; Agarwala, S. C. (Central Drug Research Inst., Lucknow, India). Indian J. Biochem., 2: 237-40(Dec. 1965).

Oxidation of glucose, pyruvate, α-ketoglutarate, succinate, fumarate and malate by V. cholerae cells was found to be affected only by higher doses of ultraviolet radiation. The extent of inhibition varied with the substrate employed. Pyruvate and fumarate oxidation was particularly more sensitive than the oxidation of other Krebs cycle substrates; oxidation of malate and succinate by the cells was relatively resistant to the action of ultraviolet radiation, and the oxidation of glucose is only slightly affected. The effect of ultraviolet radiation on the oxidation of alanine, glutamate and aspartate by the cells was similar to that of the corresponding α-keto acids. The inhibition increased with increases in the incubation period, suggesting that the observed effects do not perhaps represent direct inactivation of preformed enzymes. Elongated cells, formed during post-irradiation growth with lower doses of ultraviolet, oxidized fumarate and pyruvate at rates equal to those by the normal cells. The inhibition of pyruvate oxidation, produced by ultraviolet irradiation of V. cholerae cells was markedly reduced by adding thiourea, ascorbate, xanthine, and sodium thiosulfate to bacterial cell suspensions prior to irradiation. (auth)

16199 IMMUNITY IN EXPERIMENTAL SYPHILIS. IV. SEROLOGICAL REACTIVITY OF ANTIGENS EXTRACTED FROM γ-IRRADIATED TREPONEMA PALLIDUM AND

TREPONEMA REITERI. Miller, James N.; De Bruijn, J. H.; Bekker, J. H. (Univ. of California, Los Angeles. National Inst. of Public Health, Utrecht). J. Bacteriol., 91: 583–7(Feb. 1966).

Ultrasonic lysate preparations extracted from virulent Treponema pallidum, Nichols strain, suspensions exposed to 652,800 R of γ-irradiation exhibited a loss in the serological reactivity of their heat-labile antigens; the heat-stable components of both the lysate and residue antigens were unaffected. The activity of heat-stable, cardiolipin T. pallidum complement-fixing antigen obtained from similarly irradiated organisms was also unaltered. Gamma-irradiation of the cultivable Treponema reiteri with dosages as high as 6,500,000 R failed to alter serologically either the heat-labile or heat-stable component of its lipopolysaccharide-protein (Reiter protein) antigen. The reactivity of the lipopolysaccharide portion of the Reiter protein complex with an antiserum to T. pallidum Nichols indicates previously unsuspected antigenic differences between the rabbit-adapted Nichols strain of the organism and so-called wild human strains of T. pallidum in which this antigen is generally absent. (auth)

16200 REPAIR OF RADIATION-INDUCED DAMAGE TO THE CELL DIVISION MECHANISM OF ESCHERICHIA COLI. Adler, Howard I.; Fisher, William D.; Hardigree, Alice A.; Stapleton, George E. (Oak Ridge National Lab., Tenn.). J. Bacteriol., 91: 737-42(Feb. 1966). (ORNL-P-1741).

Microscopic observations of irradiated populations of filamentous Escherichia coli cells indicated that filaments can be induced to divide by a substance donated by neighboring cells. The observation was made the basis for a quantitative technique in which filaments are incubated in the presence of non-growing donor cells. The presence of donor organisms promotes division and subsequent colony formation in filaments. Donor bacteria do not affect non-filamentous cells. An extract of donor cells retains the division-promoting activity. The extract was partially fractionated, and consists of a heat-stable and a heat-labile component. The heat-stable component is inactive in promoting cell division, but enhances the activity of the heat-labile component. The division-promoting system is discussed as a radiation repair mechanism and as a normal component of the cell division system in E. coli. (auth)

16201 THE EXCRETION OF THYMIDINE WITH THE URINE IN ^{90}Sr-AFFECTED RATS. Uspenskaya, M. S.; Rabinkova, E. V. Med. Radiol., 10: 19-22(Oct. 1965). (In Russian).

The urinary excretion of thymidine was studied under normal conditions and after a single subcutaneous injection of ^{90}Sr in doses of 2 μc or 4 μc/kg body weight. Thymidine excretion was maximum on the 7th day after 2 μc/kg doses and on the 3rd day after 4 μc/kg doses, returning to normal by the 9th day in the former group, but decreasing (30 to 40%) by the 5th to 7th days in the latter group. It is suggested that changes in DNA metabolism and stability may explain the alterations in thymidine excretion. (H.G.D.)

16202 FORMATION OF RIBONUCLEIC ACID DURING THE RECOVERY OF THE DEOXYRIBONUCLEIC ACID SYNTHETIC SYSTEM OF BACTERIA DAMAGED BY ULTRAVIOLET LIGHT. Doudney, C. O. (Univ. of Tex., Houston). Nature, 209: 528-9(Jan. 29, 1966).

The effects of chloramphemicol, 6-azauracil, and acriflavine on DNA synthesis in uv-exposed cultures of E. coli strain WP2 were investigated. The results suggest that RNA is an essential component of the DNA synthesic system in the unirradiated bacterial cell and that post-irradiation RNA formation is necessary for repair or replacement of sites damaged by uv on the DNA template. (G.O.Y.)

16203 THE POSSIBLE FORMATION OF DITHYMINE PEROXIDE IN IRRADIATED DNA. Wang, Shih Yi; Alcantara, Raul (Johns Hopkins Univ., Baltimore). Photochem. Photobiol., 4: 477-81(June 1965).

Observation of the photo-oxidation of the 5-methyl group of thymine derivatives in aqueous solution suggested the formation of dithymine peroxide (TOOT) as the common initial intermediate. The mechanisms for converting TOOT into various oxidation products are discussed. The first reaction involves the homolytic cleavage of the peroxide –O–O-linkage of TOOT to yield 5-hydroxymethyluracil derivatives. The bond energy of O–O is about 35 kcal/mole. Therefore, any wavelength light shorter than 800 mμ, if absorbed, could produce enough energy in breaking this bond. The second reaction depicts a six-membered transition state which collapses to form two 5-formyluracil derivatives from TOOT. In reaction three the aldehyde group is oxidized to its corresponding acid derivative upon irradiation in aqueous solution. An alternative scheme is shown which could result in the formation of one 5-formyluracil and one 5-carboxyuracil from a mixed peroxide of thymine and 5-hydroxymethyluracil. Irradiation of thymine or DNA would result first in the appearance of a thymine radical which, in turn, reacts with molecular oxygen. The resultant peroxide radical then couples with another thymine radical to form dithymine peroxide (TOOT). Stereochemically, TOOT can be considered as an outstanding intermediate for the irradiation of DNA. Also, the identification of 5-formyluracil as a photoproduct may provide a chemical explanation for the crosslinking of DNA to protein. (BBB)

16204 ULTRAVIOLET BLEACHING OF SYNCHRONIZED EUGLENA. Cook, J. R.; Hunt, W. (Univ. of Maine, Orono). Photochem. Photobiol., 4: 877-80(Oct. 1965).

The bleaching response to uv was examined in synchronized populations of Euglena gracilis. Strain Z cells were exposed to a repetitive light-dark cycle of 14 hr light and 10 hr dark, resulting in synchronous division, a doubling of cell number occurring in each dark period. Aliquots for radiation study were taken at cell densities between $5-10 \times 10^4$ cells/ml, well below levels of the stationary phase, and were exposed to the uv source. All irradiation was done in the dark or with a dim red light to prevent photoreactivation. The uv source was a GE germicidal lamp at a distance of 116 cm. The bleaching response of synchronized Euglena was determined at 2 or 3 hr intervals during the 24-hr light-dark cycle. (TCO)

16205 ELECTRON SPIN RESONANCE STUDIES OF ULTRAVIOLET IRRADIATED KERATIN AND RELATED PROTEINS. Dunlop, J. L.; Nicholls, C. H. (Univ. of New South Wales, Sydney). Photochem. Photobiol., 4: 881-90 (Oct. 1965).

The electron spin resonance (ESR) spectra resulting from the uv irradiation of proteins are believed to be produced by several different reactions related to the energy absorptions of the various chromophores present in proteins, particularly those of tryptophan, tryosine, cystine, and phenylalanine. To investigate this phenomenon the formation of free radicals in keratin and related proteins by exposure to uv light was examined by ESR spectroscopy. From a comparison of the spectra obtained and the effects of different wavelengths and the stabilities of the radicals produced, it has been shown that several species of free radicals are produced by the uv irradiation of keratin. However, it was possible to identify only those free radicals associated with the cystine residues. The free radicals produced in keratin by exposure to shorter wavelength irradiation (below 3250 Å) were found to be quite different to those produced at longer wavelengths. The fact that the number of free radicals increased following aeration may appear somewhat anomalous because aeration usually has the opposite effect due to the interaction of oxygen with the free radicals to produce non-radical species. The results of these aeration studies indicate that the formation of free radicals in proteins is more complex than has been suggested by earlier observations; there is no doubt, however, that at least two different free radicals are formed by the uv irradiation of keratin. (BBB)

16206 THE PROPER USE OF SHORT-WAVELENGTH REVERSAL AS A CRITERION OF THE IMPORTANCE OF PYRIMIDINE DIMERS IN BIOLOGICAL INACTIVATION. Setlow, R. B.; Setlow, Jane K. (Oak Ridge National Lab., Tenn.). Photochem. Photobiol., 4: 939-40 (Oct. 1965).

Previous results indicated that dimers contribute to the inactivation of Hemophilus influenzae transforming DNA because some of the thymine-containing dimers are monomerized and the DNA is partially reactivated by short-wavelength following long-wavelength irradiation. Subsequently, other workers using different biological systems have not obtained short-wavelength reversal. The present report re-examines the earlier experimental findings. In the first experiments on H. influenzae DNA, the initial dose of 280-mμ radiation was slightly above the critical level, reversal was observed, and the original implication of dimers in the inactivation of this DNA remains valid. However, Kleczkowski irradiated tobacco mosaic virus with a dose of around 5×10^3 erg/mm^2 at 285 mμ and failed to observe reactivation with subsequent 239-mμ irradiation. His conclusion was that uracil dimers do not influence infectivity and that they are not monomerized by 239-mμ radiation. The analogous experiment with Rhizobium bacteriophage by Kleczkowski similarly provided no information on the importance of dimers, because the dose at 285 mμ was 2.7×10^3 erg/mm^2, much too low for the observation of net monomerization by the subsequent short-wavelength irradiation. This dose would not even significantly affect the subsequent rate of dimerization by the short-wavelength irradiation. If biological reactivation had occurred from short-wavelength irradiation in these systems, the conclusion would have been that dimers were not likely to be involved in killing. It is suggested that caution should also be employed in drawing conclusions about the importance of dimers when the long-wavelength doses are considerably larger than necessary for short-wavelength reversal. (BBB)

16207 REPLY TO A NOTE BY R. B. SETLOW AND JANE K. SETLOW CONCERNING THE PROPER USE OF SHORT-WAVELENGTH REVERSAL OF ULTRAVIOLET LIGHT INACTIVATION OF NUCLEIC ACIDS. Kleczkowski, A. (Rothamsted Experimental Station, Harpenden, Eng.). Photochem. Photobiol., 4: 941-2(Oct. 1965).

After Setlow and Setlow found that the inactivation of transforming DNA from Hemophilus influenzae by long-wave uv irradiation can be partially reversed by short-wave uv irradiation, attempts were made to see whether other nucleic acids behave similarly. In tests made with RNA isolated from tobacco mosaic virus (TMV-RNA) and with a Rhizobium bacteriophage, the phenomenon was not observed by the present author. However, he agrees that the doses of irradiation used may have been less than the critical amount needed for dimerization of uracil or thymine to be reversed by subsequent short-wave irradiation. Whether or not dimerization of either uracil or thymine in TMV-RNA or in the phage contributes significantly to their inactivation by uv, could be found by correlating the rates of inactivation with direct measurements of the rates of dimerization in these materials. However, reasons are given that suggest that dimerization is unlikely to be a significant factor in inactivation of TMV-RNA and of the phage by uv. If inactivation in all systems depends on dimerization similarly, then the amount of dimerization in TMV-RNA, and in the phage inactivated by a small dose of irradiation, should be comparable at least approximately with that in the transforming DNA inactivated to the same extent by a much larger dose. Some of these dimerization should then be reversible by short-wave irradiation, and this should show in a comparable amount of reactivation. However, the experimental results showed no reversal of inactivation. If, at similar proportions of inactivation by long-wave uv, there is very much less dimerization in TMV-RNA or in the phage DNA than in the transforming DNA, it is unlikely that dimerization plays any significant part in the inactivation of TMV-RNA and of the phage. This conclusion is supported by the fact that only about 0.19 J of radiation energy must be absorbed per mg of TMV-RNA, and 0.083 J per mg of phage DNA, to halve their infectivity. These amounts of energy are not likely to produce dimerization to any significant extent. It seems, therefore, that when these materials are irradiated with uv, they lose all their infectivity before appreciable dimerization can occur. (BBB)

16208 INFLUENCE OF SERUM OF IRRADIATED RATS ON JENSEN SARCOMA IN VITRO. III. COMMUNICATION: THE EFFECT OF SERUM OF FRACTIONATEDLY IRRADIATED RATS AFTER THE ADMINISTRATION OF CYSTEIN BEFORE IRRADIATED AND AFTER DIALYSIS. Wagner, H. (Geschwulstklinik, Berlin). Radiobiol. Radiotherap., 6: 645-9(1965). (In German).

The effects of radioprotective agents on growth-inhibiting factors were studied in rats administered cysteine before x irradiation. Growth inhibition by irradiated serum was not observed in the animals given cysteine. Further experiments indicated that the growth inhibiting factor was protein bound. (H.G.D.)

16209 POLAROGRAPHIC DETECTION OF DEHYDROEPIANDROSTERONE IN URINE FOR THE PURPOSE OF DETERMINING RADIATION RESPONSES OF ORGANISM IN TUMOR THERAPY. Riessbeck, K.-H. (Humboldt-Univ., Berlin). Radiobiol. Radiotherap., 6: 651-63(1965). (In German).

After preceding examinations of the excretory behavior of 17-ketosteroids and corticoids (17-ketogenous steroids) in urine, a columnar chromatographic analysis of total 17-ketosteroids showed that dehydroepiandrosterone and 11-hydroxysteroids indicate the effects of tumor radiotherapy on the pituitary-adrenal system. The greater sensitivity of dehydroepiandrosterone as compared to that of 17-ketosteroids was statistically significant. (TCO)

16210 OSTEORADIONECROSES IN THE AREA OF THE HAND. Neumeister, K. (Radiologische Universitatsklinik, Leipzig). Radiobiol. Radiotherap., 6: 701-6(1965). (In German).

Osteoradionecrosis of the first ray of the left hand was reported in a patient 29 years after an overdosage in treating eczema. Radiological criteria of necrotic development and origin of the bone lesion are discussed. (H.G.D.)

16211 MODIFICATION OF THE STABILITY OF COMPLEX METAL-PROTEIN COMPOUNDS IN THE CASE OF PROTEINS SUBJECTED TO THE ACTION OF GAMMA RAYS. Furnica, Gh. (Inst. of Hygiene, Bucharest). Rev. Roum. Biochim., 2: 235-41(1965). (In French).

The Cr-protein complexes formed by albumin and γ globulin were used with γ irradiated and nonirradiated (^{60}Co) samples, using ^{51}Cr as the method for determination of the instability constant. The constant for albumin after 10 hr dialysis is 0.017 for nonirradiated sample, and 0.009 for an irradiated sample; for nondialyzed globulin the nonirradiated sample has a constant of 2×10^{-4}; irradiated, 2×10^{-3}. For dialyzed globulin these values are 5×10^{-5} and 5×10^{-3} respectively. These values increased with increasing dialyzing time; instability to hydrolysis is greatest in the case of the globulin complex for heavy macromolecular fractions. The modification of stability after irradiation indicates the existence of reactions in the macromolecule which occur even after irradiation has ceased for some time; globulins appear to be more sensitive to radiation than albumin, with especial sensitivity found in the heavy fractions. (BBB)

16212 SEROLOGICAL AND PHYSICOCHEMICAL STUDIES ON RADIATION-AGGREGATED HUMAN GAMMA-GLOBULIN [Thesis]. Sweet, George Henry. Lawrence, Kan., Univ. of Kansas, 1965. 55p.

Chemical, physical, and serological investigations were

performed on lyophilized human gamma-globulin (HGG) samples subjected to gamma-irradiation dosages that ranged from 50 electron volts/molecule (ev/m) to 180 ev/m. The solubility of irradiated HGG in neutral 0.85% NaCl decreases as a non-exponential function of the irradiation dose, and several ionizations per molecule are necessary to render the protein completely insoluble. The protein that is insoluble at neutral pH contains molecules that are aggregated by means of disulfide bonds. Irradiated HGG samples that have received doses less than 180 ev/m are completely soluble at pH 2.5 or at pH 10.5 or in reagents that disrupt hydrogen and disulfide bonds. The dissolved samples contain aggregated molecules linked by non-covalent and probably non-polar bonds. The amount of aggregated material in a HGG sample is directly related to the irradiation dose and two or more ionizations within a single molecule causes it to aggregate with other damaged molecules. Purified irradiation-aggregated HGG combines specifically with antibody against native HGG and exhibits precipitin curves similar to those obtained using proteins aggregated by other means. Irradiation-aggregated HGG can be partially degraded by treating the irradiated sample with pepsin or trypsin. The enzyme-treated HGG samples retain the capacity to precipitate anti-native HGG antiserum but they exhibit precipitin curves that are different from precipitin curves exhibited by the untreated samples. The serological reactivity of irradiated HGG is an exponential function of the irradiation dose but antisera of different specificities react differently with the irradiated protein. The results of precipitin reactions between irradiated HGG samples and a hyperimmune antiserum indicate that three or four ionizations within a molecule are necessary to completely destroy its reactivity toward antibody against native HGG. (Dissertation Abstr.)

Radiation Effects on Tissues

Refer also to abstract 16188.

16213 (AD–620403) THE INFLUENCE OF CHRONIC ACCELERATION ON THE EFFECTS OF WHOLE-BODY IRRADIATION IN RATS [Thesis]. Casey, Harold Wilton (California Univ., Davis). 1965. Contract AF33(608)-1045. 77p. CFSTI $3.00 cy, $0.75 mn.

The following conclusions are drawn from the results of the studies combining acute whole-body irradiation and acceleration. Rats survive and physiologically adapt to 3.0 G chronic acceleration. A reduced body mass and depletion of body fat deposits are the only detectable changes from normal rats. Acceleration following exposures to acute whole-body irradiation, with doses in the mid-lethal range, increases radiation mortality. The mortality increases progressively with accelerative forces of 2.0 and 3.0 G. Prior adaptation to acceleration does not influence the increased radiation mortality. The detrimental effects of acceleration are operative only during the first week following irradiation. Pathological lesions in rats dying or sacrificed following acceleration and irradiation are typical of those produced by irradiation and are not modified by acceleration. Deceleration to normal gravity followed by irradiation does not influence the effects produced by radiation. (TAB)

16214 (AD–620438) ABSORPTION OF INTRADERMALLY INJECTED HORSE GAMMA GLOBULIN, A FOREIGN PROTEIN, IN RABBITS FOLLOWING WHOLE BODY GAMMA IRRADIATION [Thesis]. Pryor, William Harold Jr. (Texas Agricultural and Mechanical Univ., College Station). Aug. 1965. Contract AF33(608)-1120. 43p. CFSTI $2.00 cy, $0.50 mn.

Groups of rabbits were exposed to whole-body gamma radiation. Twenty-four hours later a foreign protein, horse gamma globulin, was injected intradermally. Blood samples were taken at 2, 4, 6, 8, 16, and 24 hours postinjection and analyzed for presence of the foreign protein by antigen-antibody double diffusion in agar techniques. An increased quantity of horse gamma globulin would indicate reduced protein localization in situ. One group of animals (200 R) at one sample time (24 hours) showed a statistically significant increase over the control group. It is logically assumed that many radiation effects have a bearing on the amount of horse gamma globulin in the circulating blood, such as peripheral blood flow, hemoconcentration, and the status of various proteolytic enzymes. Therefore, the amount of foreign protein in the blood sample is not a direct measurement of localization capacity, unless these other effects are slight, as at low levels (200 R) and do not overshadow the localization phenomenon. The results of this study indicated that the hypothesis of a direct relationship between whole-body gamma irradiation and localizing capacity of rabbits appears to be correct for a total dose level of 200 R when a 24-hour blood sample is considered. At other dose levels and sampling times, other radiation effects apparently obscure the localizing phenomenon. (TAB)

16215 (AD–628443) THE EFFECTS OF VARIOUS GASES WITHIN THE NASAL CAVITIES OF RATS ON THE RESPONSE OF OLFACTORY BULB NEURONS TO X IRRADIATION. Cooper, G. P.; Kimeldorf, D. J.; McCorley, G. C. (Naval Radiological Defense Lab., San Francisco, Calif.). Dec. 22, 1965. 25p. (USNRDL-TR–958).

Extracellular microelectrode recordings were made from single neurons of the olfactory bulb in anesthetized tracheotomized rats. Air, oxygen, argon, and nitrogen were perfused through the nasal cavities in order to determine whether the response of olfactory bulb neurons to x rays was dependent on the particular gas present within the nasal cavities. Head-only x irradiation (250 KVP, 100 R/minute) produced responses in many neurons during the perfusion of all four gases used. Such responses were ordinarily depressed, however, during argon or nitrogen perfusion as compared with the responses obtained during air or oxygen perfusion. In some cases, argon and nitrogen abolished the response to radiation within 5 minutes. It was concluded that the response of olfactory bulb neurons to x rays was not dependent on the presence within the nasal cavities of any of the gases used. It was also concluded that the response of olfactory bulb neurons to x irradiation depends upon an effect on olfactory receptors, since the response could be modified in most cases by the perfusion of argon and nitrogen. (auth)

16216 (AD–628791) RECOVERY FROM RADIATION INJURY IN DOGS AS EVALUATED BY THE SPLIT-DOSE TECHNIQUE. Ainsworth, E. J.; Leong, G. F. (Naval Radiological Defense Lab., San Francisco, Calif.). Dec. 30, 1965. 27p. (USNRDL-TR–964).

The split-dose technique was used to evaluate recovery from radiation injury in dogs given an initial conditioning exposure to 217 R, which is ~⅔ of the LD_{50}. Based on LD_{50}'s determined at 1, 3, 7, 14, and 20 days after the conditioning exposure, recovery was rapid with 50% recovery occurring by about 3 days. Because of relatively large 95% confidence intervals, the recovery rate per se was difficult to establish. An exponential curve with a recovery half time of 3.1 days may be an acceptable fit to the data. However, between 3 and 20 days the animals' radiosensitivity appeared to change ~ linearly at a rate of ~8.5 R/day.. At 20 days ~40 R of radioresistance was detected, but this was not statistically significant. The numbers of circulating leukocytes were followed for several months after exposure to 150 or 217 R. The leukocyte counts return to only 70–80% of the pre-irradiation values by ~4 months. The data are discussed in terms of the proposed correlation between recovery from radiation injury and basal metabolic rate or changes in the number of circulating leukocytes. (auth)

16217 (AECD-AG–7) EFFECT OF GAMMA-IRRADIATION ON THE SEEDS OF CORCHORUS CAPSULARIS L. AND C. OLITORIUS L. Rahman, Saidur; Mia, M. M. (Atomic Energy Centre, Dacca (Pakistan)). Nov. 1965. 12p. Dep. mn.

The effects of γ rays on jute seeds were studied in order

to determine the critical dose for mutation induction at the highest frequency. Germination, percentage, seedling height, and survival percentage of both Corchorus capsularis and C. olitorius decreased with dose increase. Mitotic studies showed fragments at metaphase, anaphase and telophase in both, but these were more common in C. olitorius. Meiotic studies revealed that most plants were diploid but often had abnormal chromosome associations. Results clearly indicated that C. olitorius was more γ-radiosensitive. (H.G.D.)

16218 (AECD-AG-12) INTERSPECIFIC HYBRIDIZATION IN JUTE. Mia, M. M.; Shaikh, A. Q. (Atomic Energy Centre, Dacca (Pakistan)). Dec. 1965. 5p. Dep. mn.

Hybridization of Corchorus olitorius and C. capsularis was attempted by irradiating seeds with 70 to 100 kR doses of γ-radiation. A total of 120 fruits developed into maturity. The fruits resulting from different cross-combinations showed strong similarity to their female parent but were of smaller size and somewhat different shape. However, the lobed character of male leaves was inherited by the F_1 plants leading to the conclusion that these were hybrids. Pollen fertility was about 20% compared to about 2% in control plants. (H.G.D.)

16219 (AED-C-04-23) BIBLIOGRAPHIEN ZUR KERNFORSCHUNG UND KERNTECHNIK. STRAHLENEINWIRKUNG AUF LEBENDES GEWEBE UND ORGANISMEN. (Bibliographies in Nuclear Science and Technology. Radiation Effects on Living Tissues and Organisms). Stahlhofen, W. (Zentralstelle fuer Atomkernenergie-Dokumentation, Gmelin-Institut fuer Anorganische Chemie und Grenzgebiete, Frankfurt am Main (West Germany)). Jan. 1966. 116p. Dep. mn.

References (352) are given to reports and journals published from 1963 through part of 1965. Separate author, subject, and report number indexes are included. (P.C.H.)

16220 (AED-C-04-24) BIBLIOGRAPHIEN ZUR KERNFORSCHUNG UND KERNTECHNIK. STRAHLENWIRKUNG AUF LEBENDES GEWEBE UND ORGANISMEN. (Bibliographies in Nuclear Science and Technology. Radiation Effects on Living Tissues and Organisms). Stahlhofen, W. (Zentralstelle fuer Atomkernenergie-Dokumentation, Gmelin-Institut fuer Anorganische Chemie und Grenzgebiete, Frankfurt am Main (West Germany)). Jan. 1966. 92p. Dep. mn.

Five hundred fifty references are given to publications on radiation effects on living tissues and organisms. Titles listed are in English, German, and French. Separate author, report number, and subject indexes, as well as table of contents, are included. (H.G.D.)

16221 (AED-C-04-25) BIBLIOGRAPHIEN ZUR KERNFORSCHUNG UND KERNTECHNIK. STRAHLENWIRKUNG AUF LEBENDES GEWEBE UND ORGANISMEN. (Bibliographies in Nuclear Science and Technology. Radiation Effects on Living Tissues and Organisms). Stahlhofen, W. (Zentralstelle fuer Atomkernenergie-Dokumentation, Gmelin-Institut fuer Anorganische Chemie und Grenzgebiete, Frankfurt am Main (West Germany)). Jan. 1966. 110p. Dep. mn.

References (346) are given to reports and journals published from 1963 through part of 1965. Separate author, subject, and report number indexes are included. (P.C.H.)

16222 (AFWL-TR-65-112) EFFECTS OF RADIATION ON SOME SERUM ENZYMES AND TRACE ELEMENTS IN LARGE ANIMALS. Riggsby, William S.; Jones, Norman D.; Godden, William R. (Air Force Weapons Lab., Kirtland AFB, N. Mex. Veterans Administration Hospital, Omaha, Nebr.). Oct. 1965. Contract AF29(601)-62-5217. 34p. CFSTI $2.00 cy, $0.50 mn.

Results are summarized from determinations of serum zinc, copper, malic dehydrogenase (MDH), lactic dehydrogenase (LDH), glutamic-oxalacetic transaminase (SGOT), and glutamic-pyruvic transaminase (SGPT) in large mammals following various types and doses of radiation. The principal subjects were mature sheep although beagle dogs and miniature swine were also used. The radiation sources were a cobalt-60 teletherapy unit, a 250-kvp x-ray therapy unit, and a Godiva II pulsed fission-spectrum neutron reactor. Results indicate that the quantity and type of irradiation received by these animals cannot be determined from these parameters. (auth)

16223 (BNL-8952) THE DEPLETION OF THE INTESTINAL EPITHELIUM OF THE MOUSE FOLLOWING EXPOSURE TO LETHAL WHOLE-BODY RADIATION. Hopper, Arthur F. (Brookhaven National Lab., Upton, N. Y.). [1963]. Contract AT-30-2-GEN-16. 21p. Dep. mn. CFSTI $1.00 cy, $0.50 mn.

Studies were made to analyze the sequence of events occurring in the intestinal epithelium of the mouse following a dose of radiation leading to acute intestinal radiation death. Mice were injected with 100 μC of tritiated thymidine and 45 min. later exposed to 2000 rads of x irradiation at a dose rate of 300 rads/min. Depletion of the crypts of the small intestine occurred in 2½ to 3 days followed by denudation of the villi in 3½ to 4 days. Analysis of grain counts following injection of tritiated thymidine showed that this dose of radiation effectively blocks DNA synthesis in the crypt cells for the first 2½ days after which some synthesis may begin, as indicated by a fall in grain count during the last day. (P.C.H.)

16224 (CEA-R-2848) ACTION DE DOSES FRACTIONNEES DE RAYONS X SUR L'HENOGRAMME ET LA FORMULE PROTEIQUE DE LA SOURIS. (Effect of Fractionated X-Ray Doses on the Hemogram and the Protein Formula of the Mouse). Alix, Denise; Pierotti, Theodore (Commissariat a l'Energie Atomique, Grenoble (France). Centre d'Etudes Nucleaires). Oct. 1965. 32p. Dep. mn.

The effects of small radiation doses on mice were studied. Irradiation in toto was performed at doses of 50, 100, 150 or 200 R according to groups, either as single or as fractionated doses. It was established that changes begin to become evident only after total exposure of 100 R. A decrease of cellular constituents and more often than not an increase of total proteins and γ-globulins occurred. (auth)

16225 (EUR-2715.f) COMPARAISON DES EFFETS DE DIFFERENTS AGENTS MUTAGENES PAR L'ETUDE DE LA MUTAGENESE DE QUELQUES PLANTES-TYPES. Rapport de Synthese, 1962-1964. (Comparison of the Effects of Various Mutagenic Substances by Studying the Mutagenesis of Some Typical Plants. Synthesis Report, 1962-1964). Dommergues, P.; Gillot, J.; Touvin, H.; Bodergat, R.; le Couviour, M. (Institut National de Recherche Agronomique, Dijon (France). Station d'Amelioration des Plantes). Jan. 7, 1966. 34p. Dep. mn.

The findings of three years of research on experimental mutagenesis are reported. It is shown how gamma radiation can profitably be used on plants with vegetative reproduction, for the purpose of either exploring chimera structures or inducing new mutations. A description of the various treatment methods and the culture techniques most likely to produce a high mutagenic yield are given, and a number of partial results obtained with fruit-trees, rose-trees and American carnations are cited. As regards sexually-reproducing plants, treatment, production, and mutation-isolation methods are presented for each of the species studied, in relation to their proper floral biology and to the scheduled research aims. The action of radiation as compared with that of chemical mutagens, including ethyl methane sulphonate and neutral ethyl sulphate is examined. The results reported show that in most cases the chemical treatments had a more intense action in both the surface layers (somatic chimeras on stems, leaves and flowers) and the deep layers (gametes). The advantages to be gained from the mutations thus induced from the standpoint of their agronomic value and from the more fundamental aspect of biochemical, physiological and genetical research are pointed out. (auth)

16226 (NP–15891) MEDICAL SURVEY OF JAPANESE EXPOSED TO FALL-OUT RADIATION IN 1954—A REPORT AFTER 10 YEARS. Kumatori, Toshiyuki; Ishihara, Takaaki; Ueda, Toshio; Miyoshi, Kazuo (National Inst. of Radiological Sciences, Chiba (Japan)). Dec. 1965. 18p. Dep. mn.

Medical examinations were carried out from January to May 1964 on 18 persons exposed to fallout in the middle Pacific Ocean in 1954. Fourteen of them were examined under hospitalization, and the other four were treated as outpatients. In general, these persons had been in good health during the past years. Residual beta burns of the skin were noted in 13 people of the 18 examined. The burns were observed in wrists, external ears, abdominal walls, foot, and leg. Most remarkable ones were those seen in abdominal walls. Ophthalmological studies revealed lens opacities in 7 cases, in which 2 cases showed opacities of posterior capsules. Hematological survey showed that the results of peripheral blood examinations were almost normal, although neutropenia, lymphopenia, co-sinophilia and slight basophilias were observed in one or two cases respectively. Bone marrow examinations revealed slight increase of myeloblasts and M/E ratio in 2 cases. "Mitotically Connected Abnormalities" were found in a few cases. In view of these findings, it was indicated that there is some residual effect of radiation exposure on hematopoiesis on these persons. Chromosome observations of peripheral leucocytes were made in 13 cases. The average rate of chromosome aberrations was much higher than normal. Whole-body counting and determination of urinary excretion of ^{137}Cs and ^{90}Sr were carried out. However, no significant increase of ^{137}Cs or ^{90}Sr was found. In general, the results on Japanese fishermen did not indicate clinically significant late effects of the fallout exposure in 1954. (P.C.H.)

16227 (NYO–3561-2) PROGRESS REPORT [ON USE OF TRITIATED THYMIDINE AS INTERNAL SOURCE OF RADIATION IN STUDY OF LATERAL ROOT INITIATION], ANNUAL, 1965–1966. Stein, Otto L. (Massachusetts Univ., Amherst). Contract AT(30-1)-3561. 10p. Dep. mn. CFSTI $1.00 cy, $0.50 mn.

Corn and pea seedlings were grown in cold thymidine at 0.064, 0.64 and 64mg/l (The latter is 1000 times the concentration available to the plants treated with tritiated thymidine). No effect on primary root length was found in either species. Only in corn was a possible disturbance of lateral root pattern noticed, but only repeat runs with better environmental controls will permit definite conclusions. In pea roots grown in .64 and 64 ppM thymidine no phasing of the mitotic cycle was observed. Roots of corn seedlings were grown from 20 hours in 50 and 150mC/rt of ^3H_2O and then transferred to recovery boxes. Only at the higher concentration was lateral root production inhibited and then along the entire root—similar to effects obtained with x rays at much lower exposures. To date a dosage of ^3H_2O at which only the differentiating pericycle is inhibited similar to the effect of 50μC ^3HT has not been found. (auth)

16228 (NYO–3571-2) THE EFFECTS OF IONIZING RADIATION ON THE GENETIC STRUCTURE OF HETEROZYGOUS OUTBREEDING POPULATIONS OF FOREST TREES. Progress Report, June 1, 1965–May 31, 1966. Stairs, Gerald R. (State Univ. of New York, Syracuse. Coll. of Forestry. State Univ. of New York, Albany). Contract AT(30-1)-3571. 9p. Dep. mn. CFSTI $1.00 cy, $0.50 mn.

Results are reported for studies on pre-meiotic radiosensitivity of male flower buds in Pinus nigra; pollen radiosensitivity in Picea abies, Picea glauca, Pinus nigra, and Pinus resinosa; use of irradiated pollen of Picea glauca in a poly-cross mating scheme; effects of acute irradiation on the pollen of Liriodendron tulipifera used in a diallel mating scheme; and effects of acute irradiation upon clonal material of Populus tremuloides. It was found that male buds irradiated at levels of 500 R and greater result in severe cytological damage. Bud development occurred to exposure levels of 2000 R; although for purposes of mutation breeding it is suggested that exposures be limited to levels below 500 R. Pollen irradiation studies were evaluated by means of in vitro germination. An LD_{50} level was obtained at 200 kR, lethality (less than 1% germination) was observed at 600 kR. At these levels it was assumed that pollen germination was an expression of cytoplasmic tolerance and not of nuclear viability. Breeding studies with irradiated pollen showed that germinable seed was obtained in Picea glauca at 4 kR exposure and in Liriodendron tulipifera at 6 kR exposures; no reduction in seed set was observed at the 4 kR level in Picea glauca. The somatic acute radiosensitivity of Populus tremuloides was investigated; Lethality occurred at 10 kR for irradiated root segments and at 8 kR for shoot pieces. (auth)

16229 (NYO–1472-1) THE ACTION OF RADIATION AND OTHER MUTAGENIC AGENTS. 1. IN INDUCING MUTATION IN DROSOPHILA FEMALES, AND 2. IN CONTROLLING THE ACTION OF SPECIFIC GENES RESPONSIBLE FOR SUPPRESSING UNCONTROLLED GROWTH. Final Report, May 1, 1953–December 31, 1965. Glass, H. Bentley (Johns Hopkins Univ., Baltimore, Md.). Feb. 28, 1966. Contract AT(30-1)-1472. 34p. Dep. mn. CFSTI $2.00 cy, $0.50 mn.

Progress is reported on studies of: the comparative mutagenic effects of ionizing radiations on males and females of Drosophila melanogaster at comparable stages of the germ line; the action of suppressor genes in Drosophila; and the effect of mating pattern on life span in Drosophila. A bibliography of 25 papers published during the contract period is included. (H.G.D.)

16230 (TID–22644) A STUDY OF DNA REPLICATION AND THE IMMEDIATE AND LONG TERM EFFECTS OF RADIATION ON RADIOSENSITIVE AND RADIORESISTANT MAMMALIAN CELLS. Final Report. (Virginia Univ., Charlottesville. Radiobiology and Biophysics Lab.). [1965]. Contract AT(40-1)-2889. 40p. Dep. mn. CFSTI $2.00 cy, $0.50 mn.

DNA replication was evaluated at four organizational levels: molecular, chromosomal, cellular, and intercellular, under the control and in the environment of the intact animal. Mathematical description of the systems shows the similarity of the systems at the different organizational levels. The data imply that constant monitoring through feed-back mechanisms is in operation to insure an orderly replication at the higher organizational levels. The effects of radiation on DNA replication and cell lethality were studied on a radiosensitive asynchronous population of cells in the intestines, and on a semi-synchronous population of radioresistant liver cells under the following conditions: variation of total dose with a constant dose rate; variation in delivery time with a constant total dose; and variation of time between doses with a constant total dose. The depression of DNA synthesis was studied following delivery of total doses ranging from 750 to 24,000R at a constant dose rate of 300R/minute. The parallel depression of both DNA synthesis and labeled cells suggests that a similar radioinduced mechanism is involved in DNA depression and cell lethality. Preliminary studies on radiosensitive (intestines) and radioresistant (liver) organs indicate that the effects of radiation on DNA synthesis are similar. DNA depression following fractionated doses of radiation (375R × 2) and (750R × 2) showed the same characteristic biphasic response curve as the dose rate and dose response studies. A one-month evaluation of the effects of single and multiple doses of radiation on somatic cells was made. The cells were irradiated near the midpoint of the eight hour replicating period of DNA during the first cycle of hepatocytes synthesizing DNA following partial hepatectomy. The results demonstrate that studies can be made on changes in the total population of cells and in a fraction of the cells synchronized within a specific phase of the cell cycle. Preliminary studies indicated that the effects of radiation on DNA synthesis are similar in both radioresistant and radiosensitive cells. In vitro studies were initiated on the relationship between radiation dose and chromosome aberrations in man. (P.C.H.)

16231 (UCRL–16377) DARK RECOVERY AND GLYCEROL PROTECTION FOR DIPLOID SACCHAROMYCES CEREVISIAE. Tobias, C. A.; Amer, N. M.; Ashikawa, J. K.; Lyman, J. T.; McDonald, L. W.; Slater, J. V.; Sondhaus, C. A.; Todd, P. W. (Lawrence Radiation Lab., Univ. of California, Berkeley). Aug. 1965. Contract W-7405-eng-48. 33p. (CONF-650668–1). Dep. mn. CFSTI $2.00 cy, $0.50 mn.

From 2nd International Symposium on Basic Environmental Problems of Man in Space, Paris.

Studies with mice, rabbits, and primates indicated that the matter of radiation exposure to astronauts should be of serious concern for space flights of more than a few days' duration. In space flights of several weeks' or months' duration, accumulation of considerable amounts of proton and α-particle doses, particularly to the outer layers of the body, appears unavoidable. A study of unicellular mammalian cell cultures and of microorganisms showed that high-LET irradiation is more effective than low-LET irradiation in producing lethal effect and that there is interaction between the cellular effects of irradiation and other environmental stresses, including temperature, ultraviolet rays, chemical agents, magnetic fields, and vibration. These injuries are irreversible so that accumulating doses produce accumulating injury. At the cellular level, protection from radiation injury was achieved independently of LET with glycerol, and it was also found in yeast cells that postirradiation dark recovery may occur even from the heaviest ions. (TCO)

16232 (JPRS–34120) THE HYPOPHYSIS AND ADRENALS IN THE PRESENCE OF RADIATION INJURIES TO THE ORGANISM. Kandror, V. I. Translated from pp 13-33; 128-33 of Gipofiz i Nadpochechniki pri Radiatsionnykh Porazheniyakh Organizma, Moscow, 1965. 22p. (TT–66-30562). CFSTI $1.00 cy, $0.50 mn.

The distinct similarity between a number of symptoms of radiation pathology and signs of disturbances in the function of the pituitary and adrenal glands is discussed. It was concluded that many of the symptoms of radiation pathology such as metabolic and morphological changes in the organism, reactivity and resistance of the organism, as well as a certain portion of regenerative phenomena are formed with the direct participation of the hypophysis-adrenal system. (P.C.H.)

16233 COMPLICATIONS AND CAUSES OF DEATH IN POLYCYTHEMIA VERA. Chievitz, Eva; Theide, Torben (Finsen Inst., Copenhagen). Acta Med. Scand., 172: 513-23(1962).

Results and complications of treatment are reported for 250 cases of polycythemia vera, most of which were treated by ionizing radiation. X rays were used alone in 48 patients and combined with cytostatic drugs in 36, while ^{32}P was used alone or with drugs in 52 cases. Among untreated patients 63% died of thrombosis (30 patients), among those treated with venesection 52% (32 patients), while only 21% of the x-irradiated and 35% of the ^{32}P- and chlornaphazine-treated patients died of this complication. (BBB)

16234 STUDIES ON RENAL CLEARANCE. PART II. CHANGES OF KIDNEY AND RENAL CLEARANCE FOLLOWING X-RAY IRRADIATION TO THE KIDNEY IN RABBITS. Hamada, Kunihiko (Hiroshima Univ.). Acta Urol. Jap., 10: 3-26(Jan. 1964). (In Japanese).

Experimental radiation injury of the kidney was produced in rabbits by external local irradiation to the kidney region with various doses of 200 kv x rays. Changes of renal function were studied by renal clearance values, and gross and histologic findings were observed following irradiation. The animals were divided into 5 groups according to the dose of x rays used: 1500 to 6000 R to the left kidney. The mortality rate increased with the dose. It was found that the radiation dose given in this manner should not exceed 3000 R if observations for more than several months are to be made. The values of glomerular filtration rate (GFR), renal plasma and blood flow (RPF, RBF), filtered fraction (FF), and tubular max clearance of p-aminohippurate (Tm_{PAH}) were measured by renal clearance tests before and at various stages after irradiation. The values of GFR, RPF, and RBF immediately after the irradiation slightly and transiently rose above the pre-irradiation values, while a slight but rapid decrease in the value of Tm_{PAH} was observed in early stages postirradiation. However, all of these values slowly decreased subsequently. Values of FF, therefore, showed a slight and transient rise after irradiation, followed by gradual recovery. The gross and histological findings in the irradiated kidney concurred with the changes of renal function measured by renal clearance tests. Grossly, the irradiated kidney showed a transient hypertrophy and congestion with a subsequent tendency of atrophy which was initiated around 2 months after the irradiation. Terminally, atrophic nephrosclerosis was observed and the size of kidney became markedly smaller than control. Histologically, a marked degeneration of the renal tubules, with subsequent displacement of fibrous tissue and round cell infiltration, was observed even in early period post-irradiation. Alterations of glomerulus and vascular system were considerably slower and milder than that of the tubules, but secondary and progressive degeneration attributed to the tubular alterations was observed subsequently in the cortex. Moreover, the larger radiation doses produced in the earlier stages, changes in the glomerulus and vascular system; similar changes were seen in these elements in the nonirradiated kidney in the terminal stage. (BBB)

16235 MICROWAVE HEATING: A STUDY OF THE CRITICAL EXPOSURE VARIABLES FOR MAN AND EXPERIMENTAL ANIMALS. Hoeft, Lothar O. (Wright-Patterson Air Force Base, Ohio). Aerospace Med., 36: 621-2(July 1965).

The maximum safe exposure limit for long-term, whole-body microwave irradiation has been established as an average power density of 0.01 w/cm^2. For intermittent exposure of less than one hr duration a tolerance dosage of 0.01 w-hr/cm^2 is recommended. These limits are based on the thermal effects of microwave radiation. Extrapolation of the results of microwave heating experiments from various species of animals to man has been done frequently without regard for interspecies differences in mass and size; therefore, attempts were made to derive a theoretical basis for extrapolation and to improve experiments designed to investigate nonthermal effects of microwaves. The exposure times required to produce a 5°C temperature rise in man and experimental animals were calculated as a function of the microwave intensity using a simplified model. These calculations show that, while the intensity for which infinitely long exposures are permitted is about the same for all species, higher intensities elevate temperatures quicker in small animals than in larger ones. This difference in heating rates should be taken into account in experiments designed to investigate the nonthermal effects of microwaves. (BBB)

16236 EFFECT OF TEMPERATURE ON SURVIVAL PERIOD OF THE FISH, ORYZIAS LATIPES, FOLLOWING IRRADIATION WITH DIFFERENT X-RAY DOSES. Etoh, Hisami; Egami, Nobuo (National Inst. of Radiological Sciences, Chiba, Japan). Annot. Zool. Jap., 38: 114-21 (Sept. 1965).

In this teleost the dose-survival time curve following x irradiation at 23°C is similar in shape to the curves for laboratory rodents as reported previously. Doses varying from 8 to 64 kR come under the so-called dose-independent range, survival period of fish irradiated with these doses being approximately the same (about 10 days at 23°C). However, if irradiated individual Oryzias or goldfish are kept below 7°C, the survival period may be prolonged to more than 100 days. Further experiments were designed to study the effect of water temperature on the dose-survival time relation in Oryzias latipes. Adult fish were irradiated with 0, 2, 4, 8, 16, or 32 kR of x rays. Temperatures at the time of irradiation were 0, 7, 15, 23, 30, or 37°C, but after irradiation maintained at 23°C. All fish irradiated with 4 kR or more died within 20 days, no sig-

nificant influence of temperature on survival period being observable. When fish irradiated with similar doses of x rays were kept at 6, 12, 16, 23, 30, or 36°C, dose-survival time curves varied considerably at the different temperatures. In those irradiated with 8 kR or more, post-irradiation survival time was shortened with the rise in water temperature after irradiation. In a cool environment (6°C) most irradiated fish survived for more than 120 days. If irradiated fish were transferred to 23°C after having been subjected to cool surroundings (6°C) for a period of 21 days, survival time after the transfer was about the same as that of irradiated fish kept at 23°C after irradiation. If irradiated fish were transferred to water at 6°C after they had been kept at 23°C, the lengths of survival time differed according to the length of the period during which the fish were kept at 23°C. These results indicate that the development of radiation lesions involves both temperature-dependent and temperature-independent phases. (BBB)

16237 RADIATION SURVIVAL OF FOOD PATHOGENS IN COMPLEX MEDIA. **Dyer, John K.; Anderson, A. W.; Dutiyabodhi, Pisawat (Oregon State Univ., Corvallis). Appl. Microbiol., 14: 92-7(Jan. 1966).**

When 15 bacterial species representing genera associated with food-borne diseases were irradiated individually, all except Escherichia coli and Streptococcus faecalis showed typical linear dose-survival curves in Hartsell's broth. The minimal lethal dose (MLD) for the organisms tested ranged from 3.0×10^5 to 6.0×10^5 rad. Salmonella paratyphi B, S. wichita, S. typhi, E. coli, and S. faecalis were found to be the least sensitive to radiation. In commercially canned crabmeat the survival curves of S. typhi, S. paratyphi B, and S. wichita exhibited to varying degrees an initial linear death decline with increasing radiation doses, followed by a distinct tailing effect caused by survival of low numbers at the higher doses. The above species of Salmonella were further individually subjected to γ-radiation in various dilutions of crabmeat. The tailing effect gradually disappeared, with the dose-survival curve tending to become linear as the concentration of the crabmeat decreased. (auth)

16238 THREE METHODS OF ASSESSING THE MUTAGENIC ACTION OF ULTRAVIOLET RADIATION ON THE FUNGUS EMERICELLOPSIS GLABRA. **Schwartz, L. J.; Stauffer, J. F. (Univ. of Wisconsin, Madison). Appl. Microbiol., 14: 105-9(Jan. 1966).**

Colony isolates of the fungus Emericellopsis glabra, developing from uv-irradiated conidia, were examined for variability on the basis of colony morphology, loss of antibiotic-producing capacity on plate assay, and loss of ability to grow in minimal medium. The latter two of these methods are considered to be more objective and reliable in determining the degree of variability induced by uv radiation in this fungus. The highest frequency of variants is obtained at uv dosages that reduce spore survival to levels of 5 to 15%. (auth)

16239 STUDIES ON THE VIRUSES OF ASIATIC INFLUENZA. III. EFFECT OF PHYSICOCHEMICAL FACTORS. **Skurska, Zofia; Lobodzinska, Maria; Biernacka, Irmina (Inst. of Immunology and Experimental Therapy, Wroclaw). Arch. Immunol. Therap. Exp., 13: 178-88(1965)**

Properties of the two lines of the A_2/Wroclaw 11/57 strain of Asiatic influenza virus under the influence of uv rays, RNase, heat, trypsin, ether, and chloroform were examined. The A_2/Wroclaw 11/57 Ea strain is sensitive to equine serum inhibitor, whereas the A_2/Wroclaw 11/57 Eb strain is insensitive to equine serum inhibitor. Ultraviolet irradiation of virus suspensions of known infectious titers was carried out with an Original Hanau LKS 18300 lamp from a distance of 20 cm. The infectious titers of the samples of the suspensions withdrawn at different intervals and the hemagglutination titers were checked. Ultraviolet irradiation of strains A_2/Wroclaw 11/57 Ea and Eb did not produce any change in the characteristics of either line. The hemagglutination and infectious titers of the A_2 strains submitted to uv irradiation are shown. (TCO)

16240 SYNCHRONIZED BUDDING YEAST CELLS. I. VARIOUS EFFECTS OF IRRADIATION AND CYTOSTATIC COMPOUNDS ON METABOLISM AND CELL DIVISION. **Hilz, H.; Eckstein, H. (Univ., Hamburg). Biochem. Z., 340: 351-82(Aug. 11, 1964). (In German).**

Action of various metabolic inhibitors, including ionizing radiation, on synchronized budding of yeast (Saccharomyces cerevisiae) was studied over several generations and their influence on different metabolic parameters is described. Comparative experiments on the action of cytostatic agents point to distinct differences in mechanisms of inhibition. N-Ethyl maleimide and p-chloromercyribenzoate inhibited cell budding and cell proliferation, probably by blocking glycolysis. In contrast, inhibition of respiration was the principal metabolic change seen with organic peroxides such as benzoyl peroxide. X irradiation with 50,000 R destroyed the capacity to form colonies in 95% of the synchronized cells. The irradiated cells nevertheless showed practically no inhibition of respiration and glycolysis in the first few hours postirradiation. They multiplied with only little delay in spite of the fact that they performed but one budding cycle. Syntheses of nucleic acids and of proteins also were delayed but not blocked. Since proliferation stopped after the first budding and the metabolic processes nevertheless continued, giant cells were evidently formed with an increased cell content of protein, RNA, and DNA. A characteristic and probably decisive lesion concerned the distribution of the nuclear material between the original cell and the bud; although partition commenced, it was not, or only partially completed in irradiated cells, and two-cell units resulted, with the nuclear material remaining in or near the bridge between the daughter cells in arrested division. (BBB)

16241 THE HAEMATOLOGICAL COMPLICATIONS OF POLYCYTHAEMIA VERA AND TREATMENT WITH RADIOACTIVE PHOSPHORUS. **Szur, L.; Lewis, S. M.; Path, M. C. (Hammersmith Hospital and Postgraduate Medical School, London). Brit. J. Radiol., 39: 122-30(Feb. 1966).**

Hematological complications developed in 18 of 169 patients with polycythemia vera treated with ^{32}P. The complications are considered under three headings: marrow depression, myelosclerosis, and granulocytic leukemia. Myelosclerosis occurred far more frequently than did leukemia. However, the difficulty in distinguishing between the two during diagnosis is pointed out. It is concluded that if phosphorus-32 therapy for polycythemia does induce either myelosclerosis or leukemia, the causal relationship awaits more proof. (H.G.D.)

16242 MORTALITY FROM CANCER AND OTHER CAUSES AFTER RADIOTHERAPY FOR ANKYLOSING SPONDYLITIS. **Court Brown, W. M. (Western General Hospital, Edinburgh); Doll, Richard. Brit. Med. J., 2: 1327-32(Dec. 4, 1965).**

This survey was designed to investigate the incidence of leukemia in man following exposure to ionizing radiations, and to examine the nature of the relation between the dose of radiation and the extent of the incidence of the disease. Records of patients of 81 radiotherapy centers who had been given radiotherapy for ankylosing spondylitis during the period 1935 to 54 were surveyed. Of 14,554 patients with ankylosing spondylitis who were treated with x rays, more than 98% were traced on or after January 1960, and less complete follow-up information was available for a further three years. The effects of irradiation were assessed by comparing the numbers of deaths observed with the numbers that would have been expected if the patients had suffered the death rates recorded in the population of England and Wales as a whole. The most important finding, apart from the previously reported excess of deaths from leukemia and aplastic anemia, relates to other cancers originating in heavily irradiated tissues. Deaths attributed to these cancers were increased two-fold six or more years after the first treatment, and 15 years after the first treatment the excess showed no

sign of diminishing. The excess was not limited to one or two types of cancer, but many different types contributed to it, in proportion to their normal incidence. In contrasts to these findings, the number of deaths from cancers originating in lightly irradiated tissues was not increased significantly. (BBB)

16243 ACTION OF ^{60}Co γ RAYS ON THE MORTALITY AND FERTILITY OF THE RICE WEEVIL. Laviolette, P.; Nardon, P. (Institut National des Sciences Appliquees, Lyon). Bull. Biol. France Belg., 97: 304-33(1963). (In French).

Survival studies were conducted on the adult insects exposed to 2000 to 111,000 R doses of ^{60}Co γ radiation. The results showed that 5000 and 7000 R are the minimum lethal doses for males and females Sitophilus sasakii, respectively. After a dose of 8000 R the insects died in 12 days. It was shown by studying the distribution of the mortality in time that irradiation induces a heterogeneity in the population by selecting resistant individuals, especially after 6000 R. Examination of the dose-mortality curves showed that death was always delayed. It occurred suddenly after a latent phase, the duration of which was a function of the dose. The variability of response indicated that the sensitivity of the weevils to uncontrolled environmental factors is decreased or increased according to the radiation dose. Radiosensitivity seemed to increase with the age of the insect. Fertility was reduced by half after a dose of 2000 R. A period of sterility appeared after 5000 and 6000 R, and complete sterility occurred after 15,000 R. Fecundity was more resistant to radiation than fertility; some eggs were laid even after 16,000 R. These results indicate the feasibility of employing radiation for the eradication of these insects from cereals and foodstuffs. (BBB)

16244 NOTE ON COMPACT MUTANTS OF LAMBERT CHERRY PRODUCED BY IONIZING RADIATION. Lapins, K. (Canada Dept. of Agriculture, Summerland). Can. J. Plant Sci., 43: 424-5(July 1963).

Compact or dwarf type of growth, a very desirable characteristic, particularly in sweet cherries, (Prunus avium), was produced by ionizing radiation. The compact Lambert variety reported herein appears to be the first mutant produced by ionizing radiation in sweet cherries. Dormant scions of Lambert were treated with 4000 to 5000 R of x rays or with doses of 4.76×10^{12} to 6.95×10^{12} n/cm^2 of thermal neutrons. The scions were grafted, following a 4-week storage period, on trees in the greenhouse. In the next summer, shoots from the grafts were cut back close to their bases, and the lower 10 buds of the cut shoot were used in budding, 2 buds per stock. Many of the resultant nursery shoots, when 1 yr old, showed deviations from the normal Lambert type in shoot growth and leaf characteristics. Two yr after irradiation the trees were planted in the orchard and in the next yr several mutant types were further propagated in the nursery, 10 trees of each mutant. For the three mutants described, 2B-17-4, 2B-17-8, and 2B-17-6, the first two showed striking dwarf characteristics, short shoots and close buds. Leaves of the mutants were slightly reduced in size, normal in shape, and apparently healthy. Leaf area per unit of shoot length was significantly larger in the mutants than in the original variety. The growth cycle of the mutants was not different from that of the regular Lambert. Orchard trees showed characteristically closely spaced spurs in the compact types 2B-17-4 and 2B-17-8, and weak growth in 2B-17-6. Mutants 2B-17-4 and 2B-17-8 shared a common rootstock with a tree of normal growth that showed no evidence of being affected by radiation. In general, the fruit of the compact mutants closely resembled that of ordinary Lambert. Fruit stems of all three compact mutants were relatively short. The stems of the mutant 2B-17-6 were exceptionally thick, a characteristic of great practical importance. (BBB)

16245 NEOPLASMS FOLLOWING IRRADIATION OF THE HEAD. Hazen, Richard W.; Pifer, James W.; Toyooka, Edward T.; Livingood, John; Hempelmann, Louis H. (Univ. of Rochester, New York). Cancer Res., 26: 305-11(Feb. 1966).

In a group of 971 persons given x-ray treatments to the head in childhood, 3 thyroid carcinomas, 1 thyroid adenoma, 1 leukemia, 1 craniopharyngioma, and 2 mixed tumors of the salivary gland have occurred. No thyroid tumors were noted in 417 children treated with radium alone and only 1 thyroid adenoma was reported in 2746 untreated siblings. All thyroid malignancies occurred in a subgroup of 170 children treated in such a way that the pituitary and thyroid glands were probably irradiated. This lends support to the hypothesis that exposure of both glands may be highly carcinogenic. It also suggests that the thyroid glands of children under 15 are as sensitive to the oncogenic action of radiation as those of infants. (auth)

16246 REMARKS ON THE EXTRAPOLATION NUMBERS FROM SURVIVAL CURVES OF VARIOUS POPULATIONS OF CHLORELLA PYRENOIDOSA CHICK AFTER X IRRADIATION. Gilet, Roland (Centre d'Etudes Nucleaires, Grenoble, France). Compt. Rend., 261: 5686-8(Dec. 20, 1965). (In French).

In irradiations of the one-cell organism chlorella, the extrapolation number drawn from survival curves of populations of young cells which should be close to one is in fact larger than that drawn from heterogeneous populations. This poses a problem of the significance of this extrapolation number. (tr-auth)

16247 EFFECT OF MUTATED BACKGROUND GENOTYPE ON MUTANT EXPRESSION IN ARACHIS HYPOGAEA L. Loesch, P. J. Jr. (Univ. of Missouri, Columbia). Crop Sci., 4: 73-8(1964).

This investigation was designed to determine whether putative background genotype effects occur in irradiated peanuts and to determine the extent to which such effects of background genotype, if present, influence the expression of different morphological mutants. Five x ray induced morphological mutants, Cup, Flop, Ilex, Hedera, and Corduroy, descending from a uniform variety of the autogamous polyploid species of A. hypogaea, were hybridized in the X_7 generation. Each mutant was crossed to descendants of the original control, NC4. Mutant F_2 plants of a common phenotypic class, extracted from mutant X mutant families and from mutant X control families were compared in a randomized block design in the F_3 generation. Differences, among and within families, constituted a test of the background genotype hypothesis. Except in a few instances, statistically significant differences among and within F_2 families for plant width, plant height, leaflet length, stem diameter, fruit length, yield of fruit, and mutant expression were obtained in separate tests with mutants Cup and Ilex. Except for leaflet width and mutant grade, statistically significant differences within F_2 families were obtained with the mutant Corduroy. Background effects, for the several mutants, differed in both magnitude and direction. The hypothesis was further substantiated by significant differences in leaflet length among control-type plants extracted from mutant X control families. These results indicated that background effects were separable from the major mutant locus with respect to this character. (BBB)

16248 LOCAL ESTROGEN AND ULTRAVIOLET IRRADIATION IN THE TREATMENT OF TOTAL ALOPECIA (AREATA). Belezos, N. K. (Univ. of Athens). Dermatologica, 131: 304-8(1965).

Satisfactory regrowth of hair is reported in two cases of total alopecia aereata following the local application of an estrogen ointment and uv irradiation. The results of treatment of total or almost total forms of alopecia areata have usually been disappointing. A wide variety of chemical and physical agents have been employed with little or no success. In both cases which are described in detail, estrogen (Progynon) contained in an ointment base was massaged into the affected skin areas for a period of 20 min daily for 20 consecutive days. The total daily dosage of estrogen so applied was from 1.0 to 1.5 mg. This was followed by daily uv irradiation in suberythema

doses for 20 days. This regimen was repeated in both cases after an interval of six weeks. In addition the 12-year old case was given thyroid medication because of clinical evidence of mild hypothyroidism supported by the metabolism studies. A distinct regrowth of abundant but fine and downy (lanugo-like) hair was seen in both patients before the end of the first course of local estrogen treatment. During the 20-day period of uv therapy this fine hair assumed a more natural texture and color. A few small areas of the scalp still showed a somewhat less abundant regrowth of hair at the end of the first course of treatment but were completely covered with normal hair after a second series of local estrogen applications and uv therapy. Undesirable side effects were not observed following the use of female hormones or radiation in these male patients. The topical application of estrogen is preferred to systemic administration since a specific local response is desired rather than usual general effects caused by absorption. It is generally agreed that uv irradiation in the dose used promotes hyperemia. In the cases treated, it is suggested that the uv rays may, in addition to hyperemia, serve as a sensitizing agent to the skin and its glands and so make them more susceptible to the action of the estrogen and/or may act to promote the action of estrogen present in the tissues. (BBB)

16249 INFLUENCE OF γ-RAY RADIATION ON THE GERMINATION OF RAUWOLFIA SERPENTINA BENTH. II. Kawatani, Toyohiko; Hemmi, Seizaburo. Eisei Shikensho Hokoku, No. 81, 181-2(1963). (In Japanese).

Seed of R. serpentina was presoaked in water and irradiated with ^{60}Co γ rays. The effect of irradiation on germination was studied with the seeds immersed in 20 ml of water in a petri dish for 24 hr. The distance from the light source to the center of the seed container was 10 cm. Each sample tested consisted of 200 seeds and the control sample of 700 seeds. Irradiated seeds were sown in a wooden box in a greenhouse the day after irradiation. Germination was observed about $2\frac{1}{2}$ month after sowing. The percentage germination after various doses was as follows: control 79.9%, 1250 R 90.0%, 2500 R 83.5%, 500 R 23.0%, 10,000 R 9.0%, 20,000 R 0%, 40,000 R 0%, and 80,000 R 0%. Thus, a significant depression of germination occurred at doses of 2500 R and higher, the depression being marked at 500 R and total at 20,000 R. (BBB)

16250 HEINZ BODY FORMATION AND CHRONIC RADIATION BURDEN—PRELIMINARY REPORT. Gerhardt, P. (Univ. Tuebingen, Ger.). Fortschr. Geb. Roentgenstr. Nuklearmed., 103: 609-11(1965). (In German).

The Heinz body formation was investigated in 32 normal persons and in 19 persons exposed to long chronic radiation burden. In the 32 normal persons no more than 12% of the erythrocytes carried more than 4 Heinz bodies. In persons with chronic x-ray exposure the number of the Heinz body formations reached pathological proportions. (J.S.R.)

16251 THE RADIOSENSITIVITY OF THE HUMAN SPINAL CORD. Franke, H. (Univ., Hamburg). Fortschr. Med., 81: 345-50(May 21, 1963). (In German).

The tolerance dose and the necrosis dose for the human spinal cord differ, depending on whether diagnosis is made clinically or by autopsy, on whether the degree of injury is transient, unchanging, or progressive, and the accuracy of measurement of the irradiation dose received. The author calculated the radionecrosis dose for the spinal cord from 58 patients treated with 180- to 250-kv x irradiation. The dose reduction by the spine was taken to be 10%. Eight irradiation doses and irradiation times were used. The necrosis dose amounted to about 2500 R one day after the first day of irradiation and to 7000 R within 100 days after the first day of irradiation and varied logarithmically between these intervals. The tolerance dose varied in the same fashion, but it was lower. It was about 1600 R one day after the first day of irradiation and was about 3100 R within 100 days after the first day of irradiation. The tolerance dose was compared graphically with the necrosis dose. Comparison with similar diagrams for human skin showed great differences, and indicated that the dose limits for the spinal cord are much lower. The results confirmed the author's clinical observations and were supported by the differences observed between the pathogenesis of late radiogenic necrosis in human skin and the central nervous system. (BBB)

16252 HORMONAL DEPENDENCY OF MOLTING IN AMPHIBIANS: EFFECT OF RADIOTHYROIDECTOMY IN THE TOAD BUFO BUFO (L). Joergensen, C. Barker; Larsen, Lis Olesen; Rosenkilde, Per (Univ. of Copenhagen,). Gen. Comp. Endocrinol., 5: 248-51(Apr. 1965).

These experiments were performed on two groups of toads, one group of which received subcutaneously 0.9 μC of carrier-free ^{131}I per body weight and the other group 9 μC ^{131}I. The toads had been kept in distilled water for 1 month to improve the efficiency with which injected ^{131}I is retained in the body. In Bufo arenarum 500 μC is known to destroy the thyroid completely in 60 days. Although it was suggested previously that in the toad the thyroids might play a role in normal molting, but one that is subordinate to the adrenals, it was shown that molting is normal even after complete radiothyroidectomy, which could be performed by injecting subcutaneously 9 μC ^{131}I per g. A few small but active thyroidal follicles remained 4 months after injection of 0.9 μC ^{131}I per g body weight. Thus, in the toad, normal molting seems to depend only upon adrenocortical function. It has often been assumed that rhythmic molting in anurans and urodeles is maintained by a corresponding rhythm in endocrine activity. However, the available data support the theory that both in urodeles and anurans the hormones merely exert a permissive action, so that rhythmic processes that are inherent in the skin will result in the formation and shedding of sloughs at intervals when the concentration of the hormones in the blood exceeds critical levels. Thyroxine appears to exert the permissive action in urodeles, and adrenocortical hormone(s) in toads and perhaps in other anurans. (BBB)

16253 INTERCOMPARISON OF PATHOLOGICAL FRACTURES IN BEAGLES INJECTED WITH ^{226}Ra, ^{228}Ra, ^{239}Pu OR ^{90}Sr. Taylor, G. N.; Christensen, W. R.; Jee, W. S. S.; Rehfeld, C. E.; Petermann, P. (Univ. of Utah, Salt Lake City). Health Phys., 12: 361-7(Mar. 1966).

Radium-228 treated beagles exhibited the highest number of radiation induced fractures and the most generalized distribution of fracture sites. The fracture pattern for radium-226 was similar except for a significantly lower incidence in the weight bearing (appendicular) skeleton. Plutonium-239 was characterized by a high percentage of costochondral rib fractures and a very low incidence in the appendicular skeleton. Strontium-90 seldom produced fractures. The healing response was lowest for radium-228, intermediate for plutonium-239 and highest for radium-226. (auth)

16254 STUDIES ON AGE OF ONSET OF DIABETES MELLITUS IN RELATION TO ATOMIC BOMB EXPOSURE. Wada, Sunao; Yamashita, Yoshihiko; Miura, Motoi; Matsuura, Noboru; Yamakido, Michio (Hiroshima Univ.). Hiroshima J. Med. Sci., 13: 265-75(Dec. 1964).

Attempts to compare clinical findings between exposed and nonexposed diabetic atomic bombing survivors residing in Hiroshima failed to show any significant differences between these two groups. (TCO)

16255 ON THE INACTIVATION CRITERIA FOR SINGLE CELLS, SPECIFICALLY IN REGARD TO DIVISIBILITY OF X- AND UV-IRRADIATED SACCHAROMYCES CELLS OF DIFFERENT PLOIDY. Haefner, Klaus (Freie Univ., Berlin). Int. J. Radiat. Biol., 9: 545-8(1965). (In German).

The ability of UV- and X-irradiated haploid, diploid and tetraploid cells of Saccharomyces to divide was investigated by making pedigrees with a micromanipulator. After irradiation four types of cells were observed: cells that never divide; those cells that divide but do not grow to form

visible colonies; cells growing up to visible colonies, which have descendants unable to form a visible colony; and cells that have only descendants forming visible colonies. Quantitative investigations show that the frequency of type 3 cells is high compared with type 4 cells, although type 3 and 4 cells are normally counted as 'survivors.' This result indicates that 'survivors' are not necessarily free of radiation damage causing lethality. The mechanism is discussed, which gives rise to unviable descendants from surviving Saccharomyces cells. A new type of curve is proposed, called curve of lethality, which looks rather for characterizing radiation-induced lethal damage than the usual inactivation curves. (auth)

16256 CYTOLOGIC STUDIES ON LENS EPITHELIUM: A COMPARISON OF EFFECTS ON X-RAYS, MYLERAN, AND TEM. von Sallmann, Ludwig (National Inst. of Neurological Diseases and Blindness, Bethesda, Md.). Invest. Ophthalmol., 4: 471-9(Aug. 1965).

The effects of two alkylating agents, Myleran and triethylene melamine (TEM), and x rays on the lens epithelium were compared. In young male rats of the Osborne-Mendel strain the effects of x rays were observed following local irradiation of the right eye only. Animals were exposed to a dose of 250 or 1000 R. At selected time intervals after treatment, groups of rats were injected intraperitoneally with a water solution of ^{3}H-thymidine, and the animals were killed 1, 4, 8, 12, 16, and 24 hr or later. Autoradiographs of lens were prepared, and the total number of labeled nuclei, mitoses, and degenerate nuclei were counted. Initiation of mitosis was blocked immediately after x irradiation with either dose but cells which had entered mitosis were able to conclude division. Complete mitotic inhibition lasted at least 4 hr when 250 R was used and 24 hr following exposure to 1000 R. The reappearance of dividing figures was followed by an overshoot of mitotic activity. The higher dose prolonged both the period of mitotic suppression and the duration of the overcompensating increase in mitotic counts; however, the sequence of these events was unaffected by the difference in dose. The numbers of cells incorporating ^{3}H-thymidine also decreased after irradiation but less abruptly than mitosis. The time course of suppression of mitotic activity and reduction of ^{3}H-labeled cells during the first postirradiation day indicated that the two effects were not directly related. The immediate response of the mitotic process could not have been the result of interference with DNA formation since the affected cells had attained a full complement of DNA before exposure to the beam. Thus, irradiation attacks the cells at multiple sites of the cycle whereas Myleran inflicts injury to the cells in the G_1 period, with the signs of injury becoming apparent as the cells prepare to divide. TEM seemed to act on some cells in the G_2 period but primarily slows DNA synthesis with resulting prolongation of the S period. (BBB)

16257 LABELING OF PROTEINS WITH RADIOACTIVE IODINE, ESPECIALLY ^{132}I. Herzmann, H. (Inst. for Applied Isotope Research, Berlin). Isotopenpraxis, 1: 30-1(Oct. 1965). (In German).

A device was developed with the aid of which the clinical technician can prepare proteins labeled with ^{132}I shortly before performing the experiment in which they are needed. The device consists of a reaction chamber and an ion-exchange column encased in a plastic container. (J.R.D.)

16258 EFFECTS OF ARGININE DEPRIVATION, ULTRAVIOLET RADIATION, AND X RADIATION ON CULTURED KB CELLS. A CYTOCHEMICAL AND ULTRASTRUCTURAL STUDY. Lane, Nancy J.; Novikoff, Alex B. (Albert Einstein Coll. of Medicine, New York). J. Cell Biol., 27: 603-20(Dec. 1965).

Cultured KB cells (derived from a human oral carcinoma) grown in monolayers were injured by one of three agents: starvation by arginine deprivation or treatment with high doses of either ultraviolet radiation or x-radiation. The different agents produced changes in nucleolar structure and varying accumulations of triglyceride and glycogen. All three agents produced an increase in number and size of lysosomes. These were studied in acid phosphatase preparations, viewed by both light and electron microscopy, and, occasionally, in vital dye, esterase, and aryl sulfatase preparations. Ultrastructurally, alterations in lysosomes suggested that residual bodies developed in a variety of ways, i.e., from the endoplasmic reticulum, multivesicular bodies, or autophagic vacuoles. Following all three agents the endoplasmic reticulum assumed the form of rough or smooth whorls, and, after two of the agents, arginine deprivation or ultraviolet radiation, it acquired cytochemically demonstrable acid phosphatase activity. Near connections between the endoplasmic reticulum and lysosomes raise the possibility that in KB cells, at least when injured, the endoplasmic reticulum is involved in the formation of lysosomes and the transport of acid phosphatase to them. (auth)

16259 ANOMALOUS CONTRACTION OF INVERTEBRATE STRIATED MUSCLE. Stephens, R. E. (Dartmouth Medical School, Hanover, N. H. Marine Biological Lab., Woods Hole, Mass.). J. Cell Biol., 27: 639-49(Dec. 1965).

The phenomenon of A band shortening or contraction was investigated in glycerinated myofibrils of Pecten irradians, Homarus americanus, Cambarus virilis, and Limulus polyphemus through the techniques of ultraviolet microbeam inactivation and polarization microscopy. With the former method, it was shown that these muscles, even though exhibiting the shortening effect, contract in a manner consistent with only the sliding filament model. Intrinsic birefringence studies indicated no significant changes in mass distribution or orientation within the shortened A bands. Except in the case of Limulus muscle, the shortening effect was seen only in contraction under tension. The magnitude of this anomalous phenomenon was dependent upon glycerination time and was duplicated in rabbit psoas muscle through brief trypsin treatment. A band shortening could not be observed in glutaraldehyde-fixed muscle or in myofibrils glycerinated for only short periods. It was concluded that the phenomenon of A band contraction is an artifact induced by the glycerination procedure, possibly through weakening of the sarcomere structure. However, the fact that the A band shortens under tension rather than lengthens poses an interesting paradox. (auth)

16260 THE EFFECT OF ^{60}Co-RADIATION ON DEVELOPMENT AND DNA SYNTHESIS IN THE 11-DAY RAT EMBRYO. Skalko, Richard G. (Univ. of Florida, Gainesville). J. Exp. Zool., 160: 171-81(Nov. 1965).

To investigate radioinduced changes in DNA formation in developing organs, female rats of the Wistar strain were exposed to either 135 or 270 R of ^{60}Co γ radiation on the morning of day 11 (Witschi stage 17). Autopsy on day 20 revealed that the lower dose produced a slight increase in the degree of fetal resorption, no effect on fetal weight, and no malformations in the survivors. The higher dose, on the other hand, produced a large increase in the degree of resorption, a pronounced effect on fetal weight, and many malformations. Radiophosphorus was injected into irradiated and nonirradiated pregnant females to study DNA synthesis in individual litters after irradiation; the ^{32}P-labeled DNA was extracted from embryo homogenates by a modified Schmidt-Thannhauser procedure. DNA synthesis was suppressed in both series of irradiated embryos at 3, 6, and 12 hr after irradiation, the higher dose producing the larger amount of suppression. At 24 hr after irradiation, no significant difference was observed in the degree of DNA synthesis in control and irradiated embryos. No difference was observed between the sp act. of ^{32}P in the acid-soluble fractions of placenta and embryo in control and irradiated litters, indicating that suppression of DNA synthesis reflected a change in the cellular population which is synthesizing DNA. Thus, the primary effect of ionizing radiation is cellular death. The embryo attempts to compensate for this damage by removal of dead cells and reformation of a structurally complete system. This is accomplished by a nonmitotic redirection of undifferentiated cells when the dose is not severe enough to produce structural malformations. With a highly teratogenic dose, however, an increase in mitotic activity apparently accom-

panies the simpler process of removal and redirection of cells. (BBB)

16261 THE EFFECT OF A SINGLE DOSE OF ULTRAVIOLET RADIATION ON EPIDERMAL MELANOCYTES. Pathak, M. A.; Sinesi, S. J.; Szabo, G. (Massachusetts General Hospital, Boston). J. Invest. Dermatol., 45: 520-8(Dec. 1965).

A quantitative histologic and biological study was made of the pigment response to uv radiation of guinea pigs and man. These experimental subjects were exposed to a single dose of radiation and a quantitative histologic study was carried out on the melanocyte population of the epidermis. From a high intensity, 1600-w, xenon light source monochromator, 300-mμ wavelength radiation was delivered in several sites of human skin within the same region to an 8-mm dia region. A dose of 2 MED (minimal erythema dose) equal to 35.6×10^6 erg/0.5 cm^2 was delivered to each site within 6 sec. Likewise, brown or albino guinea pigs were irradiated uniformly on one ear. The response of human skin revealed no changes in the melanocyte density observed for the period of 9 days, at which time the visual pigmentation was augmented distinctly. Cytologic changes observed are described. (TCO)

16262 HYPERBARIC OXYGEN, WHOLE-BODY X IRRADIATION, AND CYCLOPHOSPHAMIDE COMBINATION THERAPY IN MOUSE LEUKEMIA L1210. Lottsfeldt, Fredrik I.; Schwartz, Samuel; Krivit, William (Univ. of Minnesota, Minneapolis). J. Nat. Cancer Inst., 36: 37-43 (Jan. 1966).

Survival of $B6D2F_1/J$ mice with L1210 leukemia after treatment with whole-body x irradiation, hyperbaric oxygen, or cyclophosphamide was studied. Response was determined for irradiation and cyclophosphamide administered individually, in combination, and with and without hyperbaric oxygen. Average survival was increased by only 2 or 3 days after 525 to 1300 R irradiation and by 8.7 days with cyclophosphamide alone. No additive effect could be demonstrated with any two-way combination of the three variables under study. Average increased survival of mice (16.2 days) following treatment with hyperbaric oxygen, 525 R whole-body irradiation, and cyclophosphamide was approximately double that of mice receiving cyclophosphamide alone. The effect was associated with the decreased proportion of mice dying rapidly with relatively normal spleens. It is suggested that hyperbaric oxygen protected the leukemic mice from the toxic effect of radiation and cyclophosphamide. (auth)

16263 INHIBITORY EFFECTS OF X-IRRADIATION ON THE DEVELOPMENT OF MALE CHARACTERISTICS IN FEMALES OF THE TELEOST, ORYZIAS LATIPES, KEPT IN WATER CONTAINING METHYLTESTOSTERONE. Egami, Nobuo; Ohshima, Tamayo; Nakanishi, Yuh H. (National Inst. of Radiological Sciences, Chiba, Japan). Jap. J. Zool., 14: 31-43(Mar. 1965).

In female Oryzia latipes, male sexual characters, e.g., small papillary processes on the rays of the anal fin and leucophores along the distal margin of the caudal fin, may be produced by treatment with androgenic steroids. The inhibitory effects of x irradiation on the occurrence of these anal-fin processes and caudal fin leucophores in androgen-treated Oryzias females are described. When nonirradiated adult females were kept in water containing methyltestosterone (40 μg/l), the anal-fin processes were visible on the fourth or the fifth day of androgen treatment. If females were x irradiated on the second or the third day of androgen administration, the production of anal-fin processes was markedly inhibited, while the appearance of leucophores in the caudal fin was not interfered with. The threshold dose of x rays for inhibiting the anal-fin process formation was about 250 R, and a 4000-R dose nullified the stimulating effect of even the largest dose of androgen tested. The formation of these processes was inhibited if only the posterior part of the body including the anal fin was irradiated, irradiation of the anterior part being ineffective in this respect. Both irradiated and nonirradiated fish were equally capable of taking up androgen from the medium and later liberating it or its metabolites into water. Histologic and cytologic studies, with and without application of colchicine, revealed that, during the course of the androgen-stimulated process formation, mitosis was stimulated in cells of anal-fin rays, and the cell proliferation was suppressed by x rays. This inhibition of hyperplasia of mesenchymal cells by x rays seems to account for the inhibition of the process formation. (BBB)

16264 ON THE PROBLEM OF THE ROLE OF RADIATION IN THE PATHOGENESIS OF BRONCHIAL CARCINOMA. Fuchs, G. (Kaiser-Franz-Joseph-Spitals, Vienna). Krebsarzt, 20: 90-4(1965). (In German).

It has been known for some time now that inhalation of Rn gas or radioactive particles can induce bronchial carcinoma. This was demonstrated in U and Ra mining areas, where autopsies on miners have demonstrated that the incidence of lung carcinomas in miners may be as high as from 40 to 60%. This is also reflected in mortality figures indicating that the average life of Ra miners is only 42 yr as compared to 59 yr in nonminers. Similar results have been demonstrated experimentally. Recently, increased interest and activity in U mining associated with the advent of atomic fission has intensified the possibility of this type of health hazard. In addition, the fact that the range of population exposed to radioactive particles has been increased because of the worldwide distribution of radioactive fallout increases the probability that these will be inhaled into the lung alveoli by large populations. Estimates indicate that the fallout particles contained in 500 m^3 of atmospheric air if inhaled could impose a lung burden of 40 to 50 R/hr. This dose is of the same order of magnitude as received by miners in Ra mines. The discovery of ^{210}Po in tobacco smoke is suggestive of a very similar hazard; ^{210}Po is incorporated into tobacco plants by way of the roots, as ^{210}Pb, and through the leaves from Rn, both of which decay to ^{210}Po. At the temperature of burning cigarettes the ^{210}Pb is vaporized and deposited in the bronchial epithelium. If 2 packs of cigarettes were to be consumed daily over the course of 25 yr, the ^{210}Po deposited in the bronchial epithelium could produce a dose that amounts to about 1000 rem. When considered with the possibility that other cancerogenic substances also may be present in tobacco smoke the α irradiation from ^{210}Po could be important in production of bronchial carcinomas. (BBB)

16265 STUDIES ON THE PRINCIPAL SUBSTANCE INDUCING LEUKOCYTOSIS AFTER X-RAY IRRADIATION (CONTINUED). Ogata, Yoshiya (Univ. of Kumamoto, Japan). Kumamoto Igakkai Zasshi, 38: 673-89(Oct. 25, 1964). (In Japanese).

A substance inducing leukocytosis after x irradiation (designated NPR, Neutropoietin nach Roentogenbestrahlung) was obtained in 0.025% yield from rabbit serum by a method involving salting out with ammonium sulfate, precipitation at the isoelectric point, dialysis, and lyophilization. As a source of postirradiation serum, 2-kg male rabbits were irradiated with x rays; the distance between the tube and the skin was 30 cm, the dose rate was 25 R/min, and the total dose was 200 R. A saturated solution of ammonium sulfate (53.6 g/100 ml) was used for salting out and pH 5.2 to 5.25 was taken as the isoelectric point. NPR was obtained as white, needle-like crystals. It was nondialyzable, sparingly soluble in water, soluble in acid, and alkali, but insoluble in ethanol, acetone, chloroform, and other organic solvents. NPR showed positive reaction with biuret, ninhydrin, Millon's, and xanthoproteic reagents. Acid hydrolysates of NPR were studied by paper chromatography and uv-absorption spectroscopy. It was considered to be high molecular weight polypeptide or protein, without nucleic acid being present. There was no significant difference in the paper electrophoresis pattern and ir-absorption spectrum between NPR and the corresponding fraction extracted from nonirradiated rabbit serum. The mechanism of action of leukocytosis promotion by NPR was explained

in terms of a secondary or tertiary change in structure of the leukocyte-regulating factor which exists in normal body fluid and is increased by stress of various types, e.g., ionizing irradiation. Activation of the factor is probably regulated by the central nervous system and pituitary and adrenal hormones. (BBB)

16266 DISTURBANCE OF THE CONDITIONED REFLEX ACTIVITY IN CHRONIC ACTION OF ^{90}Sr. Klimova, E. N. Med. Radiol., 10: 22-9(Oct. 1965). (In Russian).

Studies were performed in four dogs subjected to daily enteral administration of 0.02 μC/kg ^{90}Sr doses for a period of four years. Tissue dose to the skeleton was 144 rad. No marked clinical manifestations were noted during the four year period. However, more intensive study revealed disturbances of higher nervous activity characterized by wave-like development soon after onset of treatment and evidenced in the deterioration of internal inhibitory responses. (H.G.D.)

16267 THE INFLUENCE OF ^{35}S ON THE GROWTH OF BONES. Levitman, M. Kh. (Inst. of Industrial Hygiene and Occupational Diseases, Academy of Medical Sciences, USSR). Med. Radiol., 10: 29-32(Oct. 1965). (In Russian).

A complete arrest of skeletal growth was observed in four-week-old rats given $Na_2{}^{35}SO_4$ in daily doses of 3 μC/gm os. (H.G.D.)

16268 EXPERIMENTAL RADIATION SICKNESS INDUCED WITH ^{210}Po. Moroz, B. B.; Bezin, G. I.; Vasilievskaya, V. V.; Grozdov, S. P.; Lebedev, B. I.; Ponomar'kov, V. I.; Fedorovskii, L. L.; Fedotov, V. P. Med. Radiol., 10: 57-61(Oct. 1965). (In Russian).

Features peculiar to the clinical course of radiation sickness induced in dogs by ^{210}Po (0.003 μC/kg body weight) are discussed. One of the most important peculiarities of ^{210}Po contamination is development of marked trophic disturbances caused by changes in the nervous and hypophyseal-adrenal systems, the direct action of the alpha-emitter on the tissues, hemodynamic disorders, and chronic hypoxia. (auth)

16269 INVESTIGATION OF THE BIOLOGICAL EFFECTS OF FAST ELECTRONS UNDER CONDITIONS OF CONTINUOUS AND PULSED IRRADIATION OF RAT SKINS. Skuratovich, A. A. Med. Radiol., 10: 62-6(Oct. 1965). (In Russian).

Experiments were performed on rats to determine how the biological effects of continuous and pulsed irradiation with fast electrons (900 kev) differ. Pulse durations of 0.5 and 5 μsec (corresponding to frequencies of 20 and 100 cps) were used. Identical doses of 22,000 rad were delivered in all cases. An area of 2.4 × 2.7 cm on the backs of the animals was irradiated. Effects were judged on the basis of skin reactions and functional indices of the animals (bactericidal properties, galvanic skin resistance, skin temperature and permeability). The experiments showed that exposure to 100 cps pulsed electron irradiation results in a milder skin reaction than if either continuous or 20-cps pulsed irradiation with a frequency of 20 cps is used. The difference in effect is explained by assuming that a refractory period develops in the neuroreceptor apparatus of the skin when tissue becomes nonsensitive to the subsequent impulse. (ATD)

16270 EFFECT OF ULTRAVIOLET-IRRADIATION ON THE TEMPERATE PHAGE-BACTERIA COMPLEX IN VARIOUS STAGES AFTER ITS FORMATION. Ravin, V. K.; Andreeva, I. V. (Inst. of Biophysics, Academy of Sciences, USSR). Microbiology (USSR) (Engl. Transl.), 34: 88-90 (Jan.-Feb. 1965).

Ultraviolet irradiation of Escherichia coli K12S cells infected with λ phage led to phage genome activation irrespective of whether the latter was integrated or not. Infectious centers which are formed after E. coli K12 (λ) uv irradiation are subject to inactivation with acridine dyes. This may be due to transformation of the phage genome in an autonomous stage. (BBB)

16271 A REPORT (BY THE DIRECTOR, BUREAU OF PUBLIC HEALTH). Omuka, Iku (Ministry of Welfare and Health, Tokyo). Nagasaki Igakkai Zasshi, 38: Suppl., 2-4 (Dec. 1963). (In Japanese).

The number of atomic bombing casualties has recently increased with the inclusion of more exposed persons as the distance from the hypocenter has been widened. These casualties have received optimal medical care. The Medicare Act will enhance health protection to eligible casualties and will improve it as the results of clinical studies of the survivors accumulate. The study centers have been established in Hiroshima and Nagasaki Universities in collaboration with the U. S. Atomic Bomb Casualty Commission. Last year, a Japanese-American cultural agreement was developed to further cancer research cooperation between the two countries. The study of casualties in terms of malignancies caused by exposure to the bombings is of great importance. This study is providing vital new data in medical research. The role of the public health today is not only the prevention of disease but also the active promotion of health. In this sense, cross-sectional study is desirable, but long-term study of survivors is still more important. 1950 and 1960, censuses of the Hiroshima and Nagasaki populations have provided valuable information on the fetal casualties. A 40- to 50-yr follow-up study will be necessary to understand the whole spectra of effects of thermonuclear weapon injury, and will be of utmost importance to mankind in general. (BBB)

16272 STATISTICAL OBSERVATIONS OF THE SURVEY ON THE ATOMIC BOMBING CASUALTIES BEFORE THE ENACTMENT OF THE ATOMIC BOMBING MEDICARE LAW (1954-1957). (FIRST REPORT). Shimizu, Kiyoshi (Hiroshima Univ.). Nagasaki Igakkai Zasshi, 38: Suppl., 27-35(Dec. 1963). (In Japanese).

From Feb. 1954 to May 1957 a survey was conducted among 15,510 atomic bomb casualties (6916 males and 8594 females), some by household interview and others by survey in outpatient clinics of four Hiroshima public hospitals. There were 3204 casualties interviewed in 1954, 1219 in 1955, 8102 in 1956, and 2985 in 1957. No sex difference in interviewed persons was noted in 1954 and 1955, but a slight female excess was noted in 1956 and 1957. In both sexes, the 30 to 39 age group was predominant (24.8–29.7%) of the total. Single subjects were most prevalent in the 3rd decade of life, divorced persons highest in the 7th decade; in the 5th and 6th decades, they were most apt to marry. The subjects' distance from the hypocenter was predominantly 1.1 to 2.0 km (41.7–66.4%). The exposed posture was mainly an upright position (40–50%). The percentage of subjects entering Hiroshima within a 3-day-period (August 6–8) after the attack was very low among those interviewed in 1954 and 1955; in 1956, 4% for males and 5% for females in 1957, 10% for males (Aug. 7, 6, 8 in that order) and 7% for female (Aug. 7, 8, 6). Male subjects were exposed mainly outdoors without shelter (36–56.1%), females were usually exposed indoors (48.4–59.1%). The activities engaged in by the subjects following the attack included, in highest frequency, attempts to leave the city, settling, and wandering. Males were most often engaged in escape and wandering; females in giving nursing care and cadaver disposal. These activities were not highly influenced by the exposees distance from the hypocenter. Acute medical conditions in the early postattack phase were chiefly diarrhea, fever, alopecia, and subcutaneous or gingival bleeding. In subjects under 29 years of age and above 50 years of age, diarrhea was the chief problem; in those 30 to 40 years of age, fever was most frequent. For casualties exposed within 1.0 km the main early symptoms were alopecia, diarrhea, and fever; at 1.1 to 4.0 km, diarrhea and fever. Vomiting, diarrhea, and fever were more frequent among those without shelter during the attack. Acute symptoms were frequent in those who escaped from the city after the attack; fever was more severe than the other acute aymptoms and exposure in an upright position resulted in the most severe symptoms. Among medical specialities utilized by these sur-

vivors, internal medicine was the highest in demand, then surgery and ophthalmology. (BBB)

16273 AN ALTERNATIVE MULTI-TARGET EQUATION USEFUL FOR FITTING SURVIVAL CURVES OF X-RAY IRRADIATED PROTOZOA. Calkins, John (Univ. of Kentucky, Lexington). Nature, 209: 172-3(Jan. 8, 1966).

Survival curves of irradiated protozoa do not show the same deviations from the simple multi-target behavior that mammalian cells show. The surviving fraction is 1.0 until quite large doses are delivered, then a small increase in dose produces a large drop in survival. Experimental data from a number of x-ray survival experiments on Parmecuim aurelia are presented. An equation was modified to describe the dose-response equation in such a manner that the dose appears raised to the second power: $S = 1 - (1 - e^{Kx^2})^N$, where S is the surviving fraction, x is the x-ray dose, and K and N are experimentally determined parameters. (M.C.G.)

16274 INHIBITION OF THE ABSORPTION OF D-GLUCOSE IN THE SMALL INTESTINE OF RATS BY X RADIATION. Poppei, H.; Erdmann, K. (Humboldt-Univ., Berlin). Naturwissenschaften, 53: 20(1966). (In German).

Female rats were exposed to whole-body irradiation of 800 R and the absorption of D-glucose in the little intestine was followed for 20 days. The results showed that there is a significant inhibition of the absorption within 33 to 63 min after the end of the irradiation. This inhibition is, for the most part, compensated within two hours after irradiation. After a further decrease the absorption attains a value above normal after about 20 hrs. The absorption again decreases and for the first 8 days after irradiation oscillates. On about the eigth day after irradiation it remains at approximately the same level, somewhat under the normal values. (tr-auth)

16275 EFFECTS OF LOW LEVELS OF IONIZING RADIATION ON THE DEVELOPING CEREBRAL CORTEX OF THE RAT. D'Amato, Constance J.; Hicks, Samuel P. (Univ. of Michigan Medical Center, Ann Arbor). Neurology, 15: 1104-16(Dec. 1965). (TID-21534).

This report describes the development of abnormalities initiated in the cerebral cortex of rats by single exposures to 10- to 40-R doses of 250-kv x rays in fetal or neonatal life, and some mechanisms by which radiation may have brought them about are considered. These doses regularly initiated changes that led to abnormalities of individual neurons and their organization in the cerebral cortex. The threshold dose was about 10 R just after birth and below 10 R in late fetal life. (TCO)

16276 THE EFFECT OF MOISTURE ON RADIOSENSITIVITY IN ROOT-TIPS OF VICIA SATIVA LINN. Sharma, Arun Kumar; Talukdar, Chitra (Univ. of Calcutta). Nucleus (Calcutta), 7: 23-8(June 1964).

In a study of the effect of moisture on the action of x rays, seeds of Vicia sativa were treated in two ways. Some seeds were soaked in water prior to irradiation, while others were irradiated dry and then allowed to germinate. In the first group, two separate sets of seeds were used, those that were germinating at the time of irradiation and those that had not yet germinated but were fully turgid. For presoaked seeds, x radiation doses of 500, 750, 1000, and 4000 R were given and for each dose, two separate sets were used for observation, i.e., germinating and unsprouted seeds. Observations were made after every 24 hr following irradiation for 14 successive days and the results noted. For dry seeds, only the dose of 4000 R was used and observations made as for presoaked seeds. It was shown that in V. sativa moisture has no effect on the manifestation of x-ray action, as far as the chromosome aberration frequency is concerned. In the related species V. faba, radiation damage is increased by water content, which supports the theory of an indirect action of radiation through H^+, OH^-, and HO_2 radicals. But in V. sativa water has no effect in either increasing or decreasing x-ray action. It is suggested that a different mechanism, other than the one suggested for V. faba, is operative. The secondary constriction regions are more susceptible to breakage than any other part of the chromosomes, suggesting that the heterochromatin of these regions is chemically different from the heterochromatin of the other regions. (BBB)

16277 THE BIOCHEMICAL LESIONS INDUCED IN SUBCELLULAR STRUCTURES BY IONIZING RADIATION. II. CATALASE ACTIVITY IN RAT LIVER AND SPLEEN. Dancewicz, Antoni M. (Inst. of Nuclear Research, Warsaw). Nukleonika, 10: 553-7(1965).

The catalase activity of subcellular fractions isolated from rat liver and spleen were determined at 0, 2, or 24 hr after whole-body irradiation of rats with a dose of 750 r. A decrease in enzyme activity was found in whole homogenate and cell sap fraction of the liver at 24 hr after exposure. In spleen the decrease in catalase activity was observed in particulate fractions at 0, 2, and 24 hr after exposure. This decrease was accompanied with an increase in the catalase activity of the cell sap fraction of the spleen. (auth)

16278 MITOTIC DELAY AND THE APPARENT SYNERGISM OF FAR-RED RADIATION AND X-RAYS IN THE PRODUCTION OF CHROMOSOMAL ABERRATIONS. Wolff, Sheldon; Luippold, H. E. (Oak Ridge National Lab., Tenn.). Photochem. Photobiol., 4: 439-45(June 1965). (ORNL-P-340).

Although infrared radiation is not energetic enough to induce breaks in chromosomes, when cells are treated with a combination of x rays and infrared, or even far-red radiation, the yield of chromosome aberrations is increased over that induced by x rays alone. Since chromosome aberrations come from the breakage of the chromosomes followed by the subsequent rejoining (or repair) of the broken ends in new configurations, adjunctive treatment may raise the yield of aberrations by either increasing the yield of breaks or by decreasing the amount of restitution. Experiments to test the hypothesis that the far-red potentiation of x-ray damage to chromosomes is caused by a decrease in restitution indicated that far-red radiation neither increases radiation-induced chromosome breakage nor affects the rejoining of breaks. The results indicate rather that far-red radiation induces a delay of mitosis so that at any given time after x radiation, a different population of cells would be studied if far-red as well as x rays had been given. The experiments were performed with Vicia faba seeds by giving 600 R of x radiation in vacuo followed by a 90-min treatment with far-red radiation, giving 90-min pretreatment with far-red followed by 300 R of x rays in air, and giving 600 R in vacuo, 90-min of far-red radiation, followed by 300 R in air. (TCO)

16279 THE EFFECT OF NATIVE ISOLOGOUS DNA ON THE INCORPORATION OF THYMIDINE-^{3}H INTO U.V. IRRADIATED L-STRAIN CELLS. Djordjevic, O.; Kostic, Lj.; Kanazir, D. (Inst. of Nuclear Sciences Boris Kidric, Belgrade). Photochem. Photobiol., 4: 511-13(June 1965).

The incorporation rate of thymidine-^{3}H in normal unirradiated cells, uv irradiated, and irradiated L-strain cells treated with isologous DNA was studied. A fairly high percentage (60%) of labeled cells was found in normal, control cultures even after 15-min incubation with thymidine-^{3}H. Irradiated cells incorporated thymidine-^{3}H more slowly, thus, for the same time interval, 43% of the cells were labeled. However, in irradiated cultures treated with DNA during the same time interval no incorporation was observed. (TCO)

16280 THE EFFECT OF PROFLAVINE ON U.V.-INDUCED DIMERIZATION OF THYMINE IN DNA. Beukers, R. (Technological Univ., Delft, Netherlands). Photochem. Photobiol., 4: 935-7(Oct. 1965).

In experiments with Bacillus subtilis transforming DNA, when proflavine was present during uv irradiation, protection was found (survival without dye 18%, with dye 45%). However, no restoration could be observed by post-treatment with proflavine + uv. The lack of recovery of biological activity may be due to an irreversible damage to the tertiary structure of the DNA. (BBB)

16281 ETHYLENE FORMATION IN PEA EPICOTYL TISSUES FOLLOWING IRRADIATION WITH γ-RAYS FROM ^{60}Co. Shah, J.; Maxie, E. C. (Univ. of California, Davis). Physiol. Plant., 18: 1115-20(1965).

Pea seeds (Pisum sativum, variety Alaska) were grown for 96 hr in the dark at 27°C. Harvest and transfer of the test material were done in diffuse green light; at other times, all light was excluded. The test material was obtained by harvesting the top 3 mm of each seedling, and irradiation was conducted in the dose range which varied from 1000 to 500 krad at a rate of about 250 krad/hr. Immediately after irradiation, the flasks containing the test materials were attached to a standard manometer for ethylene assay. After a dose of 100 krad a relatively low amount of ethylene was formed initially, reaching a maximum value after 60 min, followed by a gradual decline to the initial value at about 145 min, and to a constant min value at 240 min. The same general pattern was observed at doses up to 250 krad, except for a higher initial production of ethylene with increasing dose. Values for 150 and 200 krad were maximum at 50 min. A break in this pattern was observed at 300 krad, where a low initial concentration and a peak production at 20 min were followed by a progressively declining rate, with minimum values about the same as found in control tissues. With 350 krad, the initial ethylene production was somewhat higher than at 300 krad but showed a progressively declining rate to near that of the control samples at 160 min. Doses of 400, 450, and 500 krad gave the highest values 10 min after treatment, followed by a plateau of lower value, and finally a steep decline. Small ethane peaks were observed with doses of 400 krad and above. In tissues subjected to ionizing radiation, peroxidation of unsaturated fatty acids, which is dependent upon formation of free radicals, must occur. Study of the formation of free radicals in γ-irradiated pea epicotyl tissues was made, but it was not possible to detect any long-lived organic-free radicals. The observed time sequence of ethylene production over the dose range studied, especially at 300 and 350 krad, indicates that formation of the gas is not proportional to dose. It is possible that the in-source production of ethylene may be proportional to dose, but this was not determined. In a nonenzymatic system there should be a proportional increase over the entire dose range. (BBB)

16282 RADIATION EFFECTS ON RENAL ENLARGEMENT IN THE MOUSE. Phillips, T. L.; Vaeth, J. M. (Naval Radiological Defense Lab., San Francisco. Univ. of California, San Francisco). Proc. Soc. Exp. Biol. Med., 121: 161-5(Jan. 1966).

Three hours following unilateral nephrectomy weanling female CF-1 mice were subjected to local abdominal or total-body exposure to either 500 or 600 R. Other groups were given 1350 R to half the abdomen with and without prior nephrectomy. Significant decreases in renal weight gain compared to controls were obtained in the 600 R total-body group and in the locally irradiated animals given 1350 R. When the renal weight changes are compared on the basis of the ratio of renal weight to body weight in percent, an increase from .64 to .95% is seen in animals subjected to nephrectomy alone. The final value in all of the irradiated and nephrectomized groups was similar, ranging from .93 to 1.0%. The results suggest that irradiation in these dose ranges does not exert a direct inhibitory effect on renal weight increase, but it limits body weight gain that influences kidney weight. (auth)

16283 PROTON DOSIMETRY MEASUREMENTS PERFORMED IN SUPPORT OF A SERIES OF PRIMATE IRRADIATIONS. Mitchell, John C. Res. Technol. Briefs, 4: 1-5(Jan. 1966).

Glass rod microdosimeters and alanine were irradiated with protons at 6.8 to 400 Mev. Exposures were made under conditions of minimal scatter as well as in several phantoms which included stationary blocks and rotated Lucite and Masonite cylinders. In addition to these, two specially constructed primate phantoms were irradiated in the same manner as the primates used for the biological experiments. The depth dose measurements are considered in light of calculations made with a digital computer, and the calculated depth dose distributions in representative tissue phantoms are presented for 32, 55, 138, 250, and 400 Mev proton exposures. (auth)

16284 HUMORAL MEDIATION OF RADIATION-INDUCED MOTIVATION IN PARABIONT RATS. Hunt, Edward L.; Carroll, Harold W.; Kimeldorf, Donald J. (Naval Radiological Defense Lab., San Francisco). Science, 150: 1747-8(Dec. 24, 1965).

Parabiont rat pairs with a skin-vascular anastomosis were used to test for a radiation-induced transferable humoral factor that would motivate aversive conditioning in a non-irradiated (shielded) recipient. The shielded partner, by tasting saccharin-flavored fluid shortly after its partner was x-irradiated (360 roentgens), was aversively conditioned to saccharin. This was interpreted as evidence for a humoral motivating factor. (auth)

16285 CHLOROPHYLL MUTATIONS IN EINKORN WHEAT INDUCED BY RADIATION. Fujii, Taro (National Inst. of Genetics, Mishima, Japan). Seiken Ziho, 13: 138-43(Oct. 1962).

When dry dormant seeds of Triticum monococcum, var. flavescens, were exposed to x and γ rays, several types of chlorophyll mutants were obtained. Calculation of mutation rates was usually done on the basis of a single spike. The number of spikes with chlorophyll mutants increased with increasing dose. In one case, 8 spikes among 16 from one individual segregated albina, while in another case, only one was found segregating albina among 60 spikes. Moreover, two or more kinds of chlorophyll mutants appeared in the same X_1 individual, especially in the lot treated with the highest dose, for instance one spike segretating albina and four spikes segregating xantha were observed among 40 spikes from one X_1 individual. Thus the distribution of cluster mutations showed a wide variation. (BBB)

16286 GENETIC AND CYTOLOGICAL STUDIES ON X-RAY INDUCED MUTANTS OF EUROPEAN COMMON WHEAT. Uchikawa, Isamu (Ehime Univ., Matsuyama, Japan). Seiken Ziho, 13: 150-4(Oct. 1962).

Radioinduced mutation studies were conducted with dormant seeds of established normal plants derived from the hexaploid wheat variety Börsum X Scandia III, which was propagated by self-fertilization during six successive generations. The seeds, with a water content of 18.8%, were irradiated with 5, 10, 15, 20, and 25 kR of x rays. In the X_1 generation 3.9% of speltoid chimeras, 0.7% of compactoid chimeras, and 0.3% of plants with additional spikelets were obtained in one experiment, and 4.3% of speltoid chimeras, 0.8% of compactoid chimeras, 2.6% of lax-eared chimeras and 2.8% of plants with additional spikelet were observed in another. Irradiation at a high intensity was more effective than that at low intensity, and the rate of chimeric plants increased in proportion to the x-ray dose. Germination decreased in proportion to the dose. The fertilities of X_1 plants were about 12% lower on the average than those of unirradiated plants. Cytological observations of treated X_1 plants showed about 5 to 6 times more frequent chromosomal irregularities, with multivalents and univalents, misdivision, nondisjunction, fragmentation, and various types of chromosome bridges. In the plants of X_2 generation, various cytogenetic types of speltoids, compactoids, lax-eared, dense-eared, disorderly-eared, short-strawed, bearded, spiral-leaf, narrow-leaf, broad-leaf, trough-leaf types, dwarfs, waxy plants, and macurescens mutants were observed, besides nonheritable deformities of plants with additional spikelets. The rate of mutants increased in proportion to the increase of x ray dose. These mutants are described in detail. (BBB)

16287 EFFECTS OF X-RAYS ON GROWTH, MATURATION, AND FERTILITY OF RATS IRRADIATED AT THE SEVENTH DAY AFTER BIRTH. I. FEMALES. Chu, J.; Hsiung, Y. C. (Academia Sinica, Shanghai). Shih Yen Sheng Wu Hsueh Pao, 8: 54-75(June 1962). (In Chinese).

In 7-day-old female rats exposed to whole-body x irradiation in a single dose ranging from 100 to 400 R, growth, sexual maturation, and fertility were studied. There was a marked retardation of growth after irradiation, as compared with growth of litter-mate controls. During the first two months, the increase in the body weight of the irradiated animals was found to be 10 to 30% (varying according to dose) less than that in the controls. Sexual maturity, as judged by the time of the opening of vagina, was attained earlier in animals exposed to a low dose (100 R) and later in animals exposed to a higher one (400 R) as compared with that of controls. The age at which the animals began regular estrous cycles and subsequently mated was about the same among x-irradiated animals exposed at different dose levels and their litter-mate controls. However, the number of animals which did not mate was markedly higher in experimental group, even though their estrous cycles appeared normal. It is suggested that the latter effect may be due to the insufficient amount of ovarian hormone production caused by irradiation. Results of fertility experiments showed that both the number of fertile matings and litter size were markedly affected by x irradiation. Many experimental animals gave birth to one litter and were sterile thereafter. The relation between the impaired fertility and the depletion of oocytes in irradiated animals was discussed. (BBB)

16288 EFFECTS OF X RAYS ON GROWTH, MATURATION, AND FERTILITY OF RATS IRRADIATED AT THE SEVENTH DAY AFTER BIRTH. II. MALES. **Hsiung, Y. C.; Chu, J. (Academia Sinica, Shanghai). Shih Yen Sheng Wu Hsueh Pao, 8: 76-90(June 1962). (In Chinese).**

Seven-day old male rats were exposed to whole-body x irradiation in a single dose of 300 or 400 R. Growth of the irradiated animals was markedly inhibited, and sexual maturity, as judged by the time at which males first mated with females, seemed to be slightly delayed in all animals and some males were found to show no mating behavior within six months. The fertility of most of the irradiated males was normal on the basis of the litter size and sex ratio of the offspring. However, the number of matings required for successful pregnancy was higher in irradiated males than unexposed animals and in some cases pseudopregnancy occurred in females mated to these irradiated males. The effects of x irradiation on young male and female rats were compared, and the conclusions discussed. (BBB)

16289 INFLUENCE OF WHOLE-BODY X IRRADIATION ON THE ENZYMATIC ACTIVITY OF LACTATE DEHYDROGENASE ISOENZYMES IN VARIOUS ORGANS AND IN THE BLOOD SERUM OF RATS. **Hornung, Guenter; Lehmann, Frank-Guenter; Braun, Heribert (Medizinische Universitaetsklinik, Wuerzburg, Ger.). Strahlentherapie, 128: 595-609(Dec. 1965). (In German).**

The activity of lactate- and α-hydroxybutyrate-dehydrogenase in serum, heart-, liver, and kidney homogenates of rats was determined, following a whole-body x irradiation with 600 R. In addition, the LDH-isoenzymes in serum, heart, liver, kidney, brain, lung, spleen, small bowel, abdominal wall, and thigh muscle were determined using agargel electrophoresis. After the radiation, significantly altered enzyme activities were found in the serum and in the organ homogenates. In all organs examined, there was a decrease of the isoenzyme fractions which were present in high concentration and an increase of the normally lower concentrated fractions. In the serum, there was an increase of those fractions, which decreased in most of the organs following irradiation. (tr-auth)

16290 THE BREEDING OF MEDICINAL PLANTS EXPOSED TO γ-RAY IRRADIATION. I. THE APPEARANCE OF VARIATIONS IN THE X_1 GENERATION OF SEVERAL MEDICINAL PLANTS. **Yamazaki, Tomohisa; Yamanishi, Kiyoshi; Matsuda, Yasuo; Kobayashi, Masao (Meiji Coll. of Pharmacy, Tokyo). Syoyakugaku Zasshi, 18: 20-5(June 1964). (In Japanese).**

For the purpose of developing useful mutants of medicinal plants, the dry seeds of the following species were irradiated: (1) Datura tatula, (2) Pharbitis nil, (3) Linum usitatissimum, (4) Carthamus tinctorius, (5) Capsicum annuum, (6) Perilla frutescens, and (7) Foeniculum vulgare. A 100-C ^{60}Co radiation source was used, giving a dose rate of 50 R/min. Fifty seeds of each plant were placed in a test tube of 0.5 cm dia, covered with cotton stopper, and irradiated with 3, 5, 10, 20, 30, or 50 kR. The percentages of germinated seeds and withered seedlings observed during the 30 days after sowing were variable among the different plants. No change in these percentages was demonstrated in (3) even up to the max dose (50 kR). The germination rate was decreased and the number of withered seedlings increased with the increase of irradiation dosage in (1), (5), (6), and (7). In (2) and (4) there was almost no decrease in germination rate, but the number of abnormal seedlings increased as irradiation dose rose. The height of plants developed from irradiated seeds was also measured. In (1), (3), (4), (5), and (6), the growth of immature plants at 40 days after sowing was inhibited by irradiation and its inhibition was increased as the irradiation dose increased, but in mature plants in the flowering or fruiting period, the irradiation growth-inhibition effect was less. The time of flowering was delayed 2 to 3 days in (1) and 10 to 20 days in (2) and (5), whereas fructification was delayed 3 to 4 weeks in (2) and (5). Seed yield decreased to 12.4% of nonirradiated seeds after 50 kR in (3) and to 47.2% after 20 kR in (5). Some variations on the morphological features and in size of fruit, leaves, stems, and/or flowers were observed in (1), (2) and (6). (BBB)

16291 X-RAY INDUCED SHORTENING OF LIFE SPAN OF ADULT SARCOPHAGA PEREGRINA AND ITS MODIFICATION BY DOSE FRACTIONATION. **Sakka, Masatoshi (Tohoku Univ., Sendai). Tohoku J. Exp. Med., 86: 325-33(Sept. 25, 1965).**

The life span of the adult flies was diminished after x irradiation in the early pupal stage, and imago formation of irradiated pupae was also inhibited. In flies which received a single dose, a linear relation was seen between mean life space and rate of imago formation which suggests that early effects play important roles in delayed effects. Mean life span of control females was longer than the males. With fractionated doses, linearity was lost in the high dose range. Male mortality increased whereas in the female it was nearly constant from the fourth to tenth week, after which it rose rapidly with age. Before the fourth week no significant difference was observed in mortality between sexes. The increase in mortality rate after the fourth week in males was caused by acceleration of aging. On the other hand, in the female, no acceleration of aging in this period was noted. When pupae were irradiated with a single dose of 960 R, high mortality was observed from the beginning of adult life. This arose from residual injury produced during pupal irradiation. The first part of the mortality curve paralleled the controls. Then it reached a shoulder at the fourth week, continued to hold the same value for weeks, and then sharply elevated thereafter. Slope of the last part of the curve simulates again that of the control. Radiation injury produced by a single dose of 960 R accumulated and accelerated aging as evidenced by shortening of the plateau. A linear relation was observed between mean life span and rate of imago formation, but a much higher dose was required to produce an identical effect in fractionated than in single irradiation. Thus, dose fractionation reduced early as well as late effects. As for rate of weekly mortality of irradiated male imagos, two fractions for a total dose of 1920 R was less effective than single one of 1860 R. After single irradiation of 1860 R, adult mortality was high from the beginning of life and reached 100% at the seventh week without a plateau. On the other hand, dose fractionation yielded lower initial mortality. Adults lived as long as eight weeks and a plateau was not demonstrated. Thus radiation injury produced in pupae can be repaired but some of it is still operative in adult life and plays some role in killing adults. (BBB)

16292 RADIOBIOLOGY AT THE CELLULAR LEVEL. Whitmore, G. F. Univ. Toronto Med. J., 38: 283-93 (Apr. 1961).

Results from studies on mammalian cells grown and irradiated in vitro are reviewed. Mention is also made of several in vivo experiments which yielded results comparable with in vitro studies. In discussing the effect of radiation on various parts of the division cycle a simple model is proposed and data offered which support this model. The proposed model considers that the principal effect of radiation is to induce a block in the cell cycle immediately prior to mitosis. Initially this block prevents cells from leaving G2 and entering the mitotic period but does not interfere with the passage of cells through other parts of the cycle; i.e., cells go from G1 into S and from S into G2 at the normal rate but here they are stopped. The evidence presented also seems to indicate that for any one cell, this block may or may not be overcome because of recovery processes acting within the cell. If the block is not overcome, the cell cannot give rise to offspring, but even if the block is overcome, the cell may or may not give rise to viable offspring. The experimental evidence discussed indicates that, whereas radiation damages cells no matter what phase of the cell they are in, the principal effect of radiation is manifested when the cells enter the phase where their further progress through the cycle is blocked. Most of the observed effects of radiation in producing mitotic delay, division delay, and reduced DNA synthesis during the first postirradiation cycle can all be explained by the presence of this block. However, this block may sometimes be overcome with cells again entering mitosis. Even after a dose of 5000 R, 15% of the cells divide at least once. These cells are not radiation survivors in the sense that they escape a hit because at this dose the number of survivors is probably less than one in 10. The cells which escape the block have at least two possible paths open to them; they may carry out one or two abortive divisions before division ceases completely, or they may somehow circumvent the division step and go on to form giant cells. (BBB)

16293 ELECTRON MICROSCOPIC STUDIES ON PHAGOCYTOSIS OF RADIATION-INJURED LYMPHOCYTES IN THE THYMUS OF RATS. Klug, H. (Univ.-Geschwulstklinik der Charite, Berlin). Z. Zellforsch., 68: 43-56(1965). (In German).

Earlier electron microscopic studies of the irradiated thymus have revealed numerous reticulum cells containing cytoplasmic inclusions, presumably representing phagocytized material. Similar changes have been recorded in adrenalectomized animals. To investigate this problem further, the thymus of young rats receiving a single 300 R or three 100 R doses of whole-body dose of x rays was examined by electron microscopy. Other rats were adrenalectomized and x irradiated (two 150 R doses). In electron micrographs the epithelial reticular cells of the thymus show filamentous structures and granules in the cytoplasm; they were, therefore, clearly distinguishable from mesenchymal reticular cells. One to 3 days after irradiation, one or more vacuole-like structures of varying size were observed in the cytoplasm of the epithelial cells. These vacuoles often contained moniliform structures, which appeared to be debris of phagocytized lymphocytes. Following irradiation the cytoplasm of mesenchymal reticular cells likewise showed single or multiple inclusions, which in turn contained electron-dense droplet-like structures. Some of these inclusions were clearly identifiable as remnants of lymphocytes. It is suggested that epithelial as well as mesenchymal reticular cells of the thymus phagocytize lymphocytes damaged by irradiation. However, in each cell type a different mechanism seems to be responsible for the breakdown of the phagocytized lymphocytes. (BBB)

16294 DELAYED AND PERSISTENT EXPRESSION OF INDUCED MUTATIONS IN CHLAMYDOMONAS REINHARDI [Thesis]. Cross, Ronald Allan. Los Angeles, Calif., Univ. of California, 1965. 162p.

A study was undertaken with the ultimate goal of determining the minimum number of functional DNA strands present in each chromosome of the unicellular green alga Chlamydomonas reinhardi. Two basic assumptions were made: 1) an induced recessive mutation will be masked by allelic, non-mutant genetic material; 2) mutant DNA replication and segregation from non-mutant DNA is prerequisite to mutant expression. Experiments were designed to determine patterns of phenotypic expression following the induction of recessive mutations and also to resolve several alternative explanations for the observed patterns. Five mutagens were used: ultraviolet irradiation, ICR-100 (an alkylating agent), ethyl methanesulfonate, nitrosoguanidine and nitrous acid. Mutation from the wild-type to three mutant phenotypes was studied; these were streptomycin resistance, sodium acetate requirement, and high temperature (37°C) sensitivity. A chromosomal mode of inheritance was established for each type of mutant. The majority of induced mutations were latent and were not expressed immediately after treatment. In every case, the frequency of mutations expressed increased very strikingly with time between treatment and assay except when conditions of the experiment prevented cell division. Also, mutants occurred in mixed colonies (mutant and non-mutant cells) more frequently than in pure colonies (mutant cells only). The observed patterns of phenotypic expression fit the expectations of mitotic segregation from polyneme chromosomes (a chromosome having two or more, parallel molecules of DNA). (Dissertation Abstr.)

16295 EFFECTS OF IONIZING RADIATIONS ON PERITRICHS [Thesis]. Sutton, William Wallace. Washington, D. C., Howard Univ., 1965. 95p.

Two peritrichs, Vorticella microstoma and Telotrochidium henneguyi were exposed to various low doses of x-irradiation without any noticeable morphological effects. However, at doses between 2,000 and 5,000 R deviations from the normal were observed in the life cycle. After doses of x rays above 2,000 R conjugation was delayed from the normal 18 to 36-hr span to about 48 hours. Thus conjugation is inhibited until recovery has occurred. After doses of x rays between 2,000 and 5,000 R small pellicular blisters were observed within the first 12 hours after irradiation of recently excysted V. microstoma in the sexual phase of the life cycle. The percentage of blistered organisms was low, and the blisters were transitory and had disappeared after 24 hours. Dosages were increased with no other apparent effects until the organisms were treated with more than 30 kR of x irradiation. Approximately 24 hours are required by V. microstoma and T. henneguyi for recovery from irradiation in the range of 30 to 100 kR; after that growth proceeds rapidly. Gamma irradiation reduced or retarded the growth rate more markedly than usual when the peritrichs were stored at 20°C after irradiation. When stored at 30°C following irradiation, the growth rate was maintained at a level near that of the controls. Observations on the comparative radiosensitivity of the various stages of the life cycle of both peritrichs indicated that the asexual motile (telotroch) stage is more sensitive to irradiation, and the encysted stages are least sensitive or more radio-resistant. The LD_{50} as interpreted from these data is approximately 70 kR for V. microstoma and approximately 75 kR for T. henneguyi when determined 8 hours after ^{60}Co gamma irradiation. (A.G.W.)

16296 RADIATION HYGIENE. Nelson, Neal S.; Rust, John H. (Univ. of Chicago). pp 1-58 of Methods of Animal Experimentation. Vol. 2. Gay, William I. (ed.). New York, Academic Press, 1965.

This review considers the nature of and the assessment of ionizing irradiation effects on biological materials, in terms of the target molecule(s), sensitivity of cells, manifestations of the radiation syndrome, and modification of the radiation response. The following topics of health physics are also reviewed: permissible levels of contamination, monitoring and surveying, reduction of radiation exposure, and control of individual exposure. Biological dose effects are discussed on the basis of the time sequence of radiation

effects and the dose-response curve and its mathematical formulation. From a discussion of differential cell radiosensitivity it is concluded that the order of sensitivity reflects the average life span of the particular cell within the body and the rapidity with which it divides. The time for the injury to be reflected by the organ of which the cells are a part will also be related to the average life of its cell components and to the regenerative capacities of the cells in question. Manifestations of the radiation syndrome are described and discussed. Modification of the radiation response is surveyed and it is concluded that chemical protection is of little practical value. Reasons given for this statement are as follows: (1) Such agents are limited to about a 50% reduction of dose effect; (2) They have a small therapeutic index, i.e., are quite toxic; (3) They are not equally effective against all ionizing radiations; (4) They must be given prior to or during the exposure; and (5) Some have cumulative toxic effects and others become tolerated. Hypotheses advanced to explain chemical protection are also examined. Personnel monitoring for protection against excessive exposure is discussed and various technics and instruments are illustrated. (BBB)

Radiation Effects Therapy and Countermeasures

Refer also to abstracts 16231 and 16490.

16297 (EUR-2548.f) RADIOPROTECTEURS CHIMIQUES. (Rapport Annuel du Avril 1, 1964 au Avril 1, 1965). (Chemical Radioprotectors. Annual Report, April 1, 1964–April 1, 1965). (Liege Univ. (Belgium). Laboratoires de Radiobiologie). 1965. 8p. Dep. mn.

The importance of the biochemical effects of sulfur-containing chemical protectors was confirmed by various ways including: inhibition of carbohydrate metabolism of several systems (isolated cells, tissue homogenates, whole mammal); latent period between injection of radioprotector and appearance of decreased response (test = lethality) of rats and mice to high dose rate x irradiation; appearance of early (a few minutes) lesions (electron microscope) of mitochondria and Golgi apparatus in spleen and lymphoid cells after injection of sulfurous radioprotectors; and alterations of unspecific detoxication hepatic enzyme system. A detailed study was also made on the action of various protectors (administered by local subcutaneous or by intraperitoneal injection) on hair growth and on hair bulb in normal and irradiated animals. Certain curious anomalies in the chemical protection phenomena on that particular test were elucidated. The protective effects of various inorganic salts on barley seeds was also investigated. The importance of the nature of the anion and cation, concentration, time between application and irradiation, and water content of the seeds was established. The mechanism of action of these protectors is different from that of the sulfur containing radioprotectors. The role of water content in the decay of ESR signals in irradiated pea flour was stressed. (auth)

16298 RADIATION SENSITIVITY OF CULTURED MAMMALIAN CELLS: EFFECTS OF SERUM AND TEMPERATURE ON SYNCHRONIZED AND RANDOMLY DIVIDING CULTURES [Thesis]. **Hahn, George Max. Stanford, Calif., Stanford Univ., 1965. 98p.**

In vitro cultures of randomly dividing mammalian cells show variations in response to x rays. An investigation was undertaken to determine if changes in growth conditions of the cultures could be related to variations in their radiosensitivity and if a quantitative relationship could be established between the response of the cultures and the survival parameters of partially synchronized cells. The growth parameters of Chinese hamster cells and to a lesser extent of mouse L cells were modified by varying the amount of fetal bovine serum (FBS) in their medium or by lowering the incubation temperature below 37°C. Survival data, after exposure to 120-kv x rays, showed that the D_{10} of randomly dividing Chinese hamster cells increased with increasing doubling time. Partially synchronized concentrations, were irradiated at various positions in their cell cycle: The survival data showed that the increased doubling time of the cultures were reflected in a lengthening of the early part of the pre-synthetic (G_1) period and that the cells were relatively radiation resistant during this initial portion of the cell cycle. The radiation response over the last 15 hours of the cell cycle was independent of the amount of FBS in the medium. The D_{10}'s of randomly dividing cultures were calculated on the basis of the data obtained from the synchronized cells. These correlated very well with the experimentally obtained values. Experiments performed on cultures growing under suboptimal temperatures showed qualitatively similar results. All the data indicate that the radiation response of arbitrary cultures of cells is governed largely by three factors: (1) the cells' intrinsic radiosensitivity; (2) the structure of the cell cycle in the specific pre-irradiation environment of the culture; and (3) the relative population density of cells occupying various cell states. All three factors can be incorporated into a mathematical model. Computer simulation of radiation experiments and comparison of calculated and measured data reinforce these conclusions. (Dissertation Abstr.)

Radiation Hazards and Protection

See also HEALTH AND SAFETY

16299 EFFECT OF SULPHYDRYL INHIBITORS ON RADIATION SENSITIVITY OF EHRLICH ASCITES TUMOR CELLS. **Damjanovich, S.; Drasil, V. (Univ. Medical School, Debrecen, Hungary). Acta Physiol. Acad. Sci. Hung., 28: 259-63(1965).**

The effect of sulfhydryl inhibitors on radiation sensitivity of Ehrlich ascites tumor cells was investigated. Monoiodoacetic acid (MIAA) was found to sensitize against irradiation, while p-chloromercuribenzoate (PCMB), a more specific SH inhibitor, had no effect. Results are reported from initial experiments of the effect of MIAA and PCMB on proliferation of tumor cells. (TCO)

16300 RADIATION EXPOSURE FROM HEAVY NUCLEI IN SOLAR PARTICLE BEAMS IN SPACE SYSTEMS OF LOW SHIELDING. **Schaefer, Hermann J. (Naval Aerospace Medical Inst., Pensacola, Fla.). Aerospace Med., 37: 1-4(Jan. 1966).**

In extravehicular activity and in the Lunar Excursion Module, the astronaut is protected from environmental ionizing radiation merely by 0.1 to 0.2 g/cm^2 of material. Behind such low shielding, in addition to protons, alpha particles and heavy nuclei in solar particle beams contribute to exposure. Separate analysis of the proton, alpha, and medium heavy fluxes for the November 12, 1960 flare shows that, on the rad dose level, only the alpha component contributes significantly to total dose and does so only in the first 5 millimeters of tissue. On the RBE dose level, the alpha component is the predominant contributor in near-surface regions, becoming equal to the proton dose at 2-millimeter depth in tissue. The contribution of the medium heavy group never exceeds, even in the tissue surface and on the RBE dose level, a few percent of total exposure. No experimental data with laboratory radiations exist that would lend themselves to an interpretation of the peculiar depth dose patterns for flare-produced particles behind low shielding in terms of radiation damage or permissible exposure. (auth)

16301 RADIOCONTAMINATION OF THE ENVIRONMENT AND ITS EFFECTS ON THE MOTHER AND FETUS. I. CLASSIFICATION OF FISSION PRODUCTS AND NEUTRON-ACTIVATED ELEMENTS ACCORDING TO THEIR RATE OF PLACENTAL TRANSFER. **Sternberg, J. (Univ. of Montreal). Int. J. Appl. Radiat. Isotop., 17: 29-40(Jan. 1966).**

Fission products or activated elements can be divided

into different categories, according to their respective rate of placental transfer: there is free transfer for natural metabolites and probably for inert gases and perhaps some discrimination for the periodic relatives of natural metabolites. The colloidal forms of rare earths do not cross the placenta. A large proportion of fission products is constituted by nonmetabolites, whose metabolic fate and placental transfer are unknown. Fetal uptake of fission products is presently limited, especially the variation of tissue concentration as a function of the age of the embryo. There is no evidence that, for a given radiocontaminant, embryo and fetus have the same critical organs as adult tissues. The damaging effect of the radiocontaminant in embryonic tissues may be different from that produced by the same amount of radioactive element in adult tissue, due to the difference in radiosensitivity and also to the different metabolic profile of the cells. The determination of the retention of radiocontaminants by human placentas, obtained from deliveries in different geographic areas of the world is considered. In placentas obtained from normal deliveries of the Montreal area, preliminary measurements indicated a retention of ^{137}Cs in the placentas similar to that calculated from the total-body burden obtained in the literature. No determination was made on placentas of inhabitants of northern Canadian regions. A world-wide determination of placental retention of ^{137}Cs, related to the dietary habits and to the degree of radiocontamination of the geographic area where the placentas are obtained, is proposed. (auth)

16302 THE PROTECTIVE EFFECTS OF TWO DRUGS AGAINST RADIATION INJURY. **Nakashima, Noritsugu; Yamauchi, Yuzuru (Univ. of Kumamoto, Japan). Kumamoto Igakkai Zasshi, 38: 722-6(Oct. 25, 1964). (In Japanese).**

Aspartic acid and Solcoseryl were examined for protective effects against irradiation injury, i.e., prolongation of survival time in mice and decrease hematologic disturbances in rabbits. The 20-g male mice, 10 in each group, were irradiated with x rays under the following conditions: 30-cm distance between the radiation source and skin, dose rate 21.5 R/min, and total whole-body dose 500 R. After irradiation, 0.2 ml 10% aspartic acid solution was injected intraperitoneously daily for 5 days (Group A) or 0.2 ml 1% solution daily for 10 days (Group B). In other mice, 0.2 ml Solcoseryl solution was also injected daily for 5 days (Group C) or 0.2 ml 1% diluted solution daily for 10 days (Group D). The 30-day survival rate was observed. Both aspartic acid and Solcoseryl prolonged longevity and inhibited the postirradiation decrease in body weight of the experimental animals. Two-kg male rabbits, 4 in each group, were irradiated with x rays and injected with 0.5 ml 10% aspartic acid solution daily for 7 days or 0.5 ml Solcoseryl solution for 7 days. Both drugs had some beneficial effects on preventing the usual decrease of red blood cells and hemoglobin level. The decrease of leucocyte count was inhibited and its recovery was promoted by both drugs. Their mode of action is discussed in terms of inhibition of the radioinduced decrease in lymphocytes and promotion of their regeneration. (BBB)

Radiotherapy and Radiodiagnosis

Refer also to abstract 16855.

16303 (AD-626384) IONIZING RADIATION INJURY, PREVENTION AND TREATMENT. Annual Progress Report. **Rothe, William E.; Huycke, Edward J.; Butterfield, James L.; Blumenstock, Jon W. (Army Medical Research Unit, Europe). Oct. 1965. 22p.**

A slight decrease in the average total-body burden cesium-137 of normal persons residing in Germany was observed from January 1964 through May 1965; from approximately 200 to 150 pC Cs-137 per gram body potassium. Clinical studies continued included follow-up testing of persons with carcinoma of the thyroid treated with ^{131}I, iron absorption in anemic patients, and Vitamin B-12 absorption in patients. Continued measurements of body burdens of radium and thorotrast were done in selected persons. The 2-pi liquid scintillation whole body counter was modified to assay whole-body burdens of strontium-90. The minimum sensitivity of such a whole body burden assay is calculated to be 70 nC Sr-90. Measurements of enviromental levels of alpha emitting radioisotopes in water, food, snails, and human teeth and bone were continued. Personnel occupationally exposed to radioisotopes were monitored for possible internal contamination. Adenine was tested as an agent for improving the in vivo viability of red blood cells stored in a standard way for 42 days. Lean body mass changes occurring during airborne training were quantitated in two military groups. (auth)

16304 VALUE OF RADIOACTIVE BRAIN SCANS IN THE DIAGNOSIS OF BRAIN TUMORS AS COMPARED WITH OTHER METHODS. **Bucy, Paul C.; Ciric, Ivan S. (Northwestern Univ. Medical School, Chicago). Acta Neurochir., 13: 113-32(1965).**

The physical and clinical properties of two recently introduced radioactive tracers, ^{203}Hg- and ^{197}Hg-labeled Neohydrin are discussed. Both gave scans of adequate quality for the localization of brain tumors. The advantage of ^{197}Hg is the considerably lesser kidney radiation dose as compared with ^{203}Hg. Mercury-203, a γ (0.28 Mev) emitter which also has low-energy β radiation, has a physical half-life of 48 days. Incorporated in the diuretic Neohydrin its biological half-life is 12 to 24 hr. The total-body radiation dose is greatly reduced in comparison with ^{131}I (290 vs 700 mrad). It has adequate tumor-to-normal brain tissue ratio of about 25. Its biggest disadvantage is the fact that 10% of the injected dose is trapped in the kidneys with a biological half-life of 28 days, thus delivering a considerable radiation to the kidneys. The value of the photoscan was stressed as compared to the dot scan. The simplicity, safety, and lack of discomfort of the radioactive brain scan was emphasized. The difficulties in the detection of brain tumors at the base of the skull and in the posterior fossa were pointed out. In 90 consecutive intracranial tumors the overall evidence of positive and localizing scans was 75.6%. Although the brain scan is the best single localizing procedure in brain tumor diagnosis, it should not be used as a screening test for presence or absence of brain tumors, since a positive scan, generally speaking, means only a lesion (neoplastic or non-neoplastic) with a certain localization and a negative scan has no diagnostic value whatsoever. (BBB)

16305 POSSIBILITIES OF BETA THERAPY OF TUMORS OF THE EYE. **Lommatzsch, P. (Humboldt Univ., Berlin). Ber. Deut. Ophthalmol. Ges., 66: 404 (1964). (In German).**

Patients with epibulbar tumors have been treated with ^{90}Sr applicators at a daily rate of 1,000 rad up to a total dose of 15,000 to 20,000 rad with satisfactory results. Applicators constructed from Ag, filled with ^{90}Sr or ^{106}Ru, and which fit the shape of the eye have been constructed. The applicators contain up to 0.5 mC and produce a dose of about 1000 rad/hr. Studies made in guinea pigs with Brown-Pearce tumors implanted in the anterior chamber indicate that these applicators are suitable for treatment of intraocular tumors. In several instances the tumor regressed completely after irradiation, and the bulbus remained intact. In humans the applicator was used for one case of glioblastoma, causing complete regression, and in another case a mammary metastasis located in the choroid membrane showed satisfactory regression. These applicators are not suitable for tumors less than 5 mm high. The author mentions studies of the isodose pattern obtained with the ^{106}Ru applicator in the anterior pole of the eye, the isodose pattern of the applicator when used for treatment of an intraocular tumor, status of a Brown-Pearce tumor 6 days after implantation in the guinea pig eye, the untreated tumor 3 and 5 weeks after implantation, and the tumor at 4 weeks after β irradiation with a surface dose of 40,000 rad. The scar remaining after regression of the glioblastoma produced by β irradiation with 30,000 rad from a ^{106}Ru applicator is mentioned. (BBB)

16306 THE TREATMENT OF TUMORS IN CHILDREN BY RADIOTHERAPY. Pearson, Dorothy (Christie Hospital and Holt Radium Inst., Manchester, Eng.). Brit. J. Clin. Pract., 19: 363-8 (June 1965).

The effectiveness of radiotherapy of malignant diseases in children, including leukemia and Ewing's tumor, is evaluated with reference to a large number of cases. Some sequelae to irradiation and their prevention are also considered. (TCO)

16307 THE PLACE OF NON-SURGICAL METHODS IN DIAGNOSIS AND MANAGEMENT, AND THE LONG-TERM VALUE OF TREATMENT OF THYROID CANCER. Halnan, Keith E. (Christie Hospital and Holt Radium Inst., Manchester, Eng.). Brit. J. Surg., 52: 736-9 (Oct. 1965).

The use of external radiotherapy, radioiodine, and surgery to treat thyroid tumors is discussed with reference to results in about 300 patients. X-ray therapy has been improved in the last 10 years by the use of megavoltage radiation, which gives better depth doses, avoids undesirably high dose to skin and bone, and especially makes it easier to give homogeneous irradiation to the desired volume while avoiding undesirable areas, such as the spinal cord. Compared with radioiodine, this form of treatment has the advantages of better control of the radiation dose given. An important question is whether the maximum possible or tolerable radiation dose is sufficient either to destroy or to restrain the growth of thyroid carcinoma. Modern radiobiological concepts suggest that the smaller the tumor the lower the radiation dose needed, and that all cells of whatever kind are equally radiosensitive, at least as seen in artificial cell culture. In man, the rate of cell turnover and the possible effects on the tissue stroma, as well as on the tumor itself, are important. It is emphasized that no one treatment will usually be adequate alone; complete surgical excision is not always possible. Combined treatment should therefore be used whenever possible. An ablation dose of 100 mC of radioiodine will give from 20,000 to 50,000 rad to the thyroid; γ radiation alone will represent one-tenth of this, and will irradiate large nonfunctioning nodules. If there are individual tumor cells, or clumps of, say, 10 cells, in the normal thyroid, they will be given an even larger dosage, even if they are completely nonfunctioning, since the β rays will penetrate to a range of about 2 mm. The possibility is also suggested of combining x-ray therapy with radioiodine, giving a full x ray treatment immediately after the second or main treatment dose of radioiodine. (BBB)

16308 ON THE RADIOSENSITIVITY OF CALCIFYING MALHERBE'S EPITHELIOMA. Born, W.; Parra, C. (Albert-Ludwigs-Univ., Freiburg i. B.). Dermatol. Wochschr., 150: 408-14 (Oct. 17, 1964). (In German).

An ulcerated area in the scalp was diagnosed as a spinocellular carcinoma and treated with ^{60}Co contact therapy. The ^{60}Co was incorporated into a plastobalt moulage. A total dose of 5991 R was administered over a three-week period in 5 doses of 1350, 900, 1350, 1266, and 1125 R. Within three weeks of the final irradiation the tumor showed signs of regression. By the end of 8 months the tumor site had healed and the hair had grown back. The tumor recurred about 5 yr later, but was not treated for 5 yr after reappearance. It was then diagnosed as calcifying Matherbe epithelioma. Because of its previous high radiosensitivity it was treated with 15 doses of 300 R each of x irradiation, administered over 18 days. After an interval of three weeks the tumor was irradiated with 16 doses of 300 R each, administered over 18 days. The tumor began to regress within four weeks, and was healed within four months after the last irradiation dose had been given. The favorable results obtained indicate that even though the general opinion is that this type of tumor should be removed surgically, irradiation treatment is effective, especially when surgery cannot be carried out for some reason. However, recurrences of the tumor have also been reported after surgery. (BBB)

16309 IRRADIATION INJURY TO THE COLON. May, James; Loewenthal, John (Univ. of Sydney). Gut, 6: 444-7 (Oct. 1965).

Two patients with irradiation injury to the colon are reported to illustrate the problems of diagnosis and show that there may be a long interval between irradiation and the onset of symptoms. The first patient was a 45-yr-old man in whom a left nephrectomy was performed for a papillary adenocarcinoma of the kidney, and one month later a course of ^{60}Co γ radiation was given in two parallel opposed fields (15 × 15 cm), which included the kidney bed and regional lymphatics. A dose of 300 R was given daily alternating between the anterior and posterior portal, for a total dose of 5500 R delivered over 29 days. The patient remained well until 12 months after irradiation, when he experienced a severe epigastric pain and nausea. An exploratory laparotomy revealed chylous ascites together with a paracolic abscess surrounding that portion of the colon corresponding to a stricture seen in radiographs. The localized area of the descending colon was thickened and indurated and extensively inflamed. A strikingly similar lesion was found on the left side of the transverse colon. The involved portion of the colon was resected and mid-transverse colon anastomosed end-to-end to proximal sigmoid colon. The patient made an uneventful recovery. The second patient was a 47-yr-old woman who had had a squamous cell carcinoma of the cervix treated by radium (one application to give 4000 R to point A) followed one month later by Wertheim's hysterectomy and lymph adenectomy. Histological examination showed residual carcinoma following the radium. One yr later, the patient received a course of ^{60}Co irradiation given by the 360° rotation technique, the tumor volume being a sphere 12 cm in diameter. A tumor dose of 6800 rad (80%) was given. Ten months later she complained of pain in the rectum together with diarrhea and blood passed by rectum. A hard perirectal mass was palpable. Radiography of the abdomen showed a large bowel obstruction. A cecostomy was performed under local anesthesia because of the patient's poor general condition, but she died two days later. These patients illustrate the problem of diagnosis in irradiation injury. In each case the symptoms could have been produced either by recurrent malignancy, a new primary malignancy, or irradiation damage. (BBB)

16310 RARE ISOTOPE MAY HAVE BONE SCAN ADVANTAGES. J. Amer. Med. Ass., 194: 33 (Dec. 27, 1965).

Gallium-86, a rare metal isotope with apparently significant advantages in bone scanning in early clinical use, is discussed. Clinical advantages of ^{68}Ga include a short half life of 1.13 hr and rapid tissue clearance, which enable quick repetition of such tests with less patient exposure to radioactivity; a rapid and apparently preferential localization in bone, kidney, and urinary bladder; decay primarily by positron emission with a relatively small amount of the more penetrating γ rays; and feasibility of obtaining ^{68}Ga from a compact, less expensive generator instead of a cyclotron or other types of accelerator. The ^{68}Ga now can be produced by a parent-daughter generator system, known as a cow, which produces the isotope through controlled decay of a long-lived parent, germanium-68. Gallium-68 citrate has been administered intravenously to 36 patients and, in several instances, bone lesions that had not been visible by x ray were outlined. Highly detailed whole-body scans are obtainable as early as 2 or 2½ hr after administration. The kidney acquires a visible dose within minutes and can be scanned within the hour. Further clinical work is needed before the full use of ^{68}Ga becomes evident. Based on studies in rats, it is estimated the human radiation dose in bones and kidney as about 400 mrad/μC. Whole body dose is estimated at 70 mrad/μC. (BBB)

16311 THE RENOGRAM: RADIOACTIVE ISOTOPES AND RENAL DISEASE. Turner, T. A. (Hertzler Clinic, Halstead, Kan.). J. Kansas Med. Soc., 65: 573-7 (Dec. 1964).

Technics, instrumentation, and clinical examples illustrating the use of radioisotopes in studying renal diseases are reviewed, with particular reference to the use of ^{131}I-Hippuran. Reduction of exposure of the patient by the use of radioisotope rather than urography is emphasized. To perform the renogram with ^{131}I-Hippuran, about 3 μC/kg is injected intravenously; loss into the tissue during injection will result in an erroneous tracing. The addition of a third probe located over the urinary bladder has been advocated by some, the resulting tracing called renocystograms. The curve of the bladder tracing assumes a reciprocal appearance of the renal tracing; that is, it rises as the renal curve falls. Clinical examples are cited wherein repeat injection of contrast media, and delayed urogram films would likely have been informative of renal disease, but this would have necessitated increased radiation exposure, and larger dosage of contrast medium, as well as taking an additional hour or more of time. The renogram usually shows evidence of ureteral obstruction, by an upward slope to the terminal segment of the tracing. This is particularly obvious when compared with the normal falloff of the contralateral kidney tracing. Renograms are often performed on hypertensive patients. This test subjects the patient to less radiation hazard than urograms since a small amount of tagged material needs to be injected and the amount of radiation exposure is minor when compared with a plain film of the abdomen; there should be no hesitancy in performing this test in early pregnancy. (BBB)

16312 RHABDOMYOSARCOMA: CASE REPORT OF LONG TERM PALLIATION BY IRRADIATION. Chadwick, R. O'Neal J. Louisiana State Med. Soc., 117: 265-9 (Aug. 1965).

An unusual case of rhabdomyosarcoma is presented wherein the patient is currently asymptomatic and has no apparent residual tumor as a result of treatment with x rays. Rhabdomyosarcoma, a rare tumor, usually leads to rapid dissemination via the blood and lymphatics with early death of the patient. Both the primary and metastatic foci are reputedly resistant to irradiation, and early radical surgery is ordinarily regarded the best treatment. Unusual instances of radiosensitivity have been reported, but usually it is doubtful that this results in any real addition to the patient's life span. The present case is remarkable in that it represents long-term palliation which was effected solely by orthovoltage x rays in moderate doses. (TCO)

16313 COMBINED SURGICAL AND RADIATION MANAGEMENT OF CARCINOMA OF THE LARYNGOPHARYNX. Hudson, W. R.; Cavanaugh, P. J. (Duke Univ., Durham, N. C.). Laryngoscope, 75: 1123-38(July 1965).

Although carcinoma of the laryngopharynx has long been managed either by surgery or radiation, in view of their limited effectiveness when given alone, the results of combining radiation and surgery into a single therapeutic effort were investigated. Most patients were treated preoperatively with supervoltage therapy, ^{60}Co and ^{137}Cs; however, conventional therapy was used in the more recent patients. Treatment programs and clinical results are described. (TCO)

16314 X-INFLAMMATION IRRADIATION. Portmann, J. (Knappschrafts-Krankenhaus, Ger.). Muenchen. Med. Wochschr., 107: 476-9(Mar. 5, 1965). (In German).

The success and lack of danger from x irradiation for the treatment of inflammatory conditions are generally not recognized at present. The effect of x irradiation with minimal doses on inflammations depends on disturbance of the chemical milieu of the tissue so that recovery, with freedom from recurrences and pain, is brought about. Irradiation of inflammation requires a single minimal radiation dose of only 10 to perhaps as high as 150 R. Doses of this magnitude do not produce discernible morphological or histological changes. The gonadal doses received from these levels of irradiation are extremely small, depending on the localization and amount of dose. In irradiations of the facial area they amount to from 0.008 to 0.015 R. During irradiation of the shoulders, elbows, and extremities gonadal doses may amount to 0.010 to 0.020 R per field. These values are from $1/15$ to $1/30$ of the maximum permissible amounts. The most important conditions that suggest the use of inflammation irradiation include furuncles, panaritivum, abscesses of the sweat glands, mastitis, chronic tonsilitis, spondylosis, herpes zoster, neutritis, arthrosis, hallux valgus, and epichondylitis. (BBB)

16315 STANDARDIZATION OF MEASUREMENTS OF IODINE UPTAKE OF THE THYROID GLAND BY ^{131}I. Gwiazdowski, Bohdan; Chomicki, Oskar; Gwiazdowska, Barbara; Siwicki, Henryk (Inst. of Physical Oncology, Warsaw). Nowotwory, 13: 373-6(1963). (In Polish).

Methods of standardization for measurements of thyroidal ^{131}I uptake as used in the 24-hr uptake test are discussed. A nationwide evaluation program was conducted. This program uses a measurement set that consists of a plastic neck phantom, ^{131}I vials with standardized dimensions, and a long-lived mock I standard, composed of a mixture of ^{133}Ba and ^{137}Cs in a ratio of 13 :1. The activity of the standard is $20 \pm 2\,\mu$C. The methods for measurement that are outlined conform to recommendations of the International Atomic Energy Agency. (TCO)

16316 DUCT LIGATION AND SMALL-DOSE X-RADIATION: A NEW TREATMENT FOR MIKULICZ'S DISEASE. Sage, Harold H. (New York Univ. Coll. of Medicine). Oral Surg., Oral Med., Oral Pathol., 20: 287-93(Sept. 1965).

A new method employing x rays for treating the parotid manifestations of Mikulicz's disease and related problems, such as Sjogren's syndrome, is described with reference to two patients. Ligation of the main parotid duct is performed. Radiation therapy is administered in small doses pre- and postoperatively to diminish parotid secretion and inflammation. It is considered that the salivary symptoms and signs of Mikulicz's disease persist and recur because of incomplete obstruction of the duct system. The treatment method advocated converts this to complete obstruction, and atrophy of the gland ensues. The treatment does not influence the many extrasalivary manifestations of this disease. (TCO)

16317 TOLERANCE OF X-RAY MOVING-BEAM IRRADIATION. Minkov, L.; Thodorov, D. (Univ., Erlangen, Ger.). Radiobiol. Radiotherap., 6: 677-82(1965). (In German).

Fifty-two cases of moving-beam x-ray therapy of carcinomas of the esophagus, lungs, and larger air passages are reported. The general reaction of lung and esophageal carcinomas was severe, whereas carcinomas of larger air passages stood irradiation without complications and with a good local effect, probably because of the smaller volume of irradiated tissue. (H.G.D.)

16318 ESTIMATION OF THE RADIATION DOSE IN DIAGNOSTIC RADIOLOGY: PRACTICAL APPLICATIONS WITH REGARD TO DIFFERENT ORGANS. Stieve, F. E. (Univ., Munich). Radiography, 31: 173-7(Aug. 1965).

In diagnostic radiology radiation damage can be avoided if the regulations on radiation protection are observed. Attention is drawn to cases where a higher radiation danger calls for special precautions for examiner and examinee. Since a risk to staff can be excluded by observation of the regulations on radiation protection, attention should be concentrated on the patient. The demand to produce the best image quality with a minimum dose could be better fulfilled if examination techniques were improved. A table shows how often the various types of radiographic examinations are made in a hospital, and to what extent they contribute to the radiation burden. It was shown that a large portion of the burden is due to radiographs of the pelvis and lower abdomen, whereas radiographs of the skull and extremities are numerically greater but contribute relatively little to the radiation burden. (BBB)

16319 SYMPTOMATIC MEDICATION ASSOCIATED WITH RADIOTHERAPY. Pierquin, B. (Inst. Gustave Roussy, Villejuif, France). Radiol. Clin. Biol., 34: 162-76(1965). (In French).

Treatment of injuries resulting from radiotherapy is discussed. Symptomatic medication is recommended for preventing or retarding the direct and indirect effects of irradiation. It is suggested that the supplementary medications and treatments be prescribed and supervised by the radiotherapist. (H.G.D.)

16320 IRRADIATION PLANNING IN RADIOTHERAPY. Sundbom, L.; Walstam, R. (Karolinska Sjukhuset, Stockholm). Radiologe, 4: 256-62(Aug. 1964). (In German).

In order to obtain the irradiation dose planned in various parts of the body it is necessary to have both exact localization and focussing of the irradiation beam. A focussing apparatus that simulates the movements of the radiation source used is available. Another method is the use of a film which is located at the side where the beam emerges and indicates the movement or location of the beam. However, at high radiation energies the contrast differences between bone and soft tissues is reduced markedly and here the film may not be so useful. Hollow capsules or heavy metal markers placed on the patient are also useful to establish orientation marks. The control films also can be used for a three dimensional exit dose measurement, and thus are worthwhile for correction of dose distribution in patients. Even though corrections or compensation for differences between measurements made under standard conditions and the conditions found in practical therapy are made, variations are often observed. For this reason it is desirable to monitor the dose in the body irradiated as much as possible. However, this type of measurement is only possible in body spaces where ionization chambers or dosimeters can be implanted. These types of measurements can be very important when used, for example, in the oral cavity, bladder, or rectum, to monitor the tumor dose or dose to the radiosensitive tissues surrounding the tumor. (BBB)

16321 A NEW GONAD PROTECTOR. Martin, H. Radiologe, 4: 374-5(Nov. 1964). (In German).

The best protectors commercially available for the male gonads are difficult to fit and so are not used as frequently as they should be during diagnostic radiography. The author describes a protector which shields the gonads against the direct irradiation and most of the scattered irradiation. A Pb plate bent into a tunnel shape ensures shielding from above and the sides. The Pb plate is structurally strengthened by being soldered between two steel plates, and the sharp edges are covered with a plastic rim. The entire tunnel structure is mounted on flexible lamp neck which is based on a heavy metal plate. With this arrangement the entire protector can be kept on the x-ray table, since the foot remains to one side, and the tunnel can be swung aside when not being used. Because the protector is always within reach no special effort is required to use it, and it is more likely to be used. The author presents photographs to indicate the construction and use of the protector. (BBB)

16322 RADIATION OSTEITIS AND RADIATION COLITIS FROM RADIOTHERAPY AND THEIR X-RAY DIAGNOSIS. Kobayashi, Toshio (Kanazawa Univ., Japan). Rinsho Hoshasen, 9: 328-41(May 1964). (In Japanese).

Some cases of late radiation sequelae of therapy are presented. Japanese reports on radiation injury are reviewed. (TCO)

16323 SUBCUTANEOUS NODULES FOLLOWING ^{60}Co TELERADIATION. Muta, Nobuyoshi (Sapolo Medical Coll., Japan). Rinsho Hoshasen, 9: 342-5(May 1964). (In Japanese).

The maximum tissue absorption of ^{60}Co γ rays occurs at a 5-mm depth of the skin, and subcutaneous nodules may appear following irradiation. It is important to differentiate these nodules from recurrences of the cancer. Several cases are described that illustrate the findings. (TCO)

16324 CANCER OF THE BREAST: RESULTS OF TREATMENT IN NORTHERN IRELAND, 1955-1959. Lyons, A. R. (Northern Ireland Radiotherapy Center, Belfast). Ulster Med. J., 34: 33-43(Sept. 1965).

The effectiveness of radiotherapy is reported for 731 cases of breast cancer submitted to irradiation following surgery. Two methods of treatment were employed. In cases which had had simple mastectomy the radiation treatment plan consisted of two large opposed fields to include the axilla, and the supraclavicular region on the affected side, and two tangential field to the chest wall, with a maximum dose of about 4000 rad in three weeks. In other patients, who had radical mastectomy, because the scar was longer the area was not suitable for treatment with the above method, and in those cases a type of treatment using three tangential fields to the chest wall, plus a supraclavicular field in many cases, was employed. Irradiation combined with radical mastectomy leads to an increased incidence of edema of the arm, and because of this, dose to the axilla was reduced by about 12% to 3700 rad. Even with this dose severe edema of the arm occurred. An assessment of the outcome of these treatment methods for breast cancer showed that the extent of surgery had little effect on the 5-yr survival rate, but it was not possible to make any conclusions about the value of radiotherapy. (TCO)

16325 THE USE OF BETA RADIATIONS (^{90}Sr–^{90}Y) IN DERMATOLOGY. Sevin, W.; Lehmann, A. (Staedtische Hautklinik, Stuttgart). Z. Haut., 19: 114-29(Aug. 1, 1965). (In German).

Results from 636 patients who were treated for 381 skin tumors and 420 hemangiomas over a 12-yr period are reported. The treatment consisted of β irradiation from a ^{90}Sr-^{90}Y applicator containing 50 mC of activity with a surface of 0.7 cm^2 or one that contained 400 mC of activity with a surface of 4 to 7 cm^2. In general, total dose administered to the tumors amounted to 8000 rep, administered in three single doses given 10 days apart. For treatment of planotuberous hemangiomas a total of 2000 rep was administered in four single doses of 500 rep each, given at weekly intervals. The healing rate for the skin tumors was 97%, and for the hemangiomas it was 90%. Most of the tumors treated consisted of basiliomas. Less than 8% were spinaliomas. Practically all of the hemangiomas were of the planotuberous type. Almost 38% of the hemangiomas treated were located on the head. The incidence of basaliomas and spinaliomas in the region of the face and ears amounted to from 72 to 74%. (BBB)

16326 LONG-TERM FOLLOW UP IN THE DETECTION AND TREATMENT OF CERVIX CANCER. Stanicek, J.; Dolezel, M. (Univ. J. E. Purkyne, Brno). Zentrahbl. Gynaekol., 86: 1200-5(Aug. 22, 1964). (In German).

Results of treatment and follow up studies made for 40 yr in 2793 patients with cancer of the cervix are reported. The percent treated surgically increased from 12.5 to 52.3% from 1923 to 1962. Starting in 1923 and up to 1962 the detection rate for Stage I rose from 2.5 to 37.0%, and for Stage II it rose from 4.0 to 26.8%. For patients in Stage III and IV, the detection rates decreased from 55.0 to 31.5% and from 38.5 to 4.7%, respectively. The cure rate increased from 2.9 to 49.7%. The authors compare the results in the surgically treated patients with the results of irradiation. Surgical treatment was successful in 52 to almost 82% of the patients where it was used. The cure rate for irradiation treatment ranged from 61.5 to 75.0% for patients with Stage I tumors, from 48.9 to 52.0% for patients with Stage II tumors, and from 15.8 to 17.7% for patients with Stage III tumors. Irradiation treatment methods are briefly described. Radium applicators are used to deliver 6720 mg-hr doses. Under the conditions that the applicators are used the rectum wall receives about 3000 R. Irradiation delivered to various points in the uterus range from 1300 to 6000 R. Other details of the spatial distribution of dose are described. (BBB)

CHEMISTRY

General

Refer to abstract 17158.

Analytical Procedures

See also Separation Processes and Procedures

Refer also to abstracts 16554, 16713, 16823, 16888, 16898, and 17822.

16327 (AAEC/TM-301) POLAROGRAPHIC DETERMINATION OF HYDROGEN PEROXIDE IN IRRADIATED WATER, AND A COMPARISON WITH COLORIMETRIC METHODS. Moore, P. W. (Australian Atomic Energy Commission Research Establishment, Lucas Heights). Oct. 1965. 24p. Dep. mn.

Parameters were established for a polarographic method of measuring hydrogen peroxide in concentrations as low as 10^{-5} M. The method may be extended to measure hydrogen peroxide solutions up to 1.5×10^{-2} M. Comparison with the more commonly used titanium and iodide methods for hydrogen peroxide determination showed the polarographic method to be of similar accuracy above 10^{-4} M and of greater accuracy below 10^{-4} M. The polarographic method has the advantage that dissolved oxygen can be measured on the same sample. (auth)

16328 (AECL-Pak/Lib-10) PLUTONIUM. A Bibliography of Selected Literature. Rafique, M. M. (Atomic Energy Centre, Lahore (Pakistan)). Dec. 1965. 86p. Dep. mn.

References on preparation, production, extraction, and separation of plutonium are given to unclassified reports and journals published during the last 18–20 years. (P.C.H.)

16329 (BNWL-187) PURIFICATION OF RARE EARTHS FROM HANFORD WASTES BY SOLVENT EXTRACTION. Bray, L. A.; Roberts, F. P. (Battelle-Northwest, Richland, Wash. Pacific Northwest Lab.). Feb. 1966. Contract AT(45-1)-1830. 31p. Dep. mn. CFSTI $2.00 cy, $0.50 mn.

Laboratory and hot-cell experiments showed that a good separation of Mn and the rare earths is possible by controlled pH solvent extraction. Because pH control is very difficult in the plant, unreliable results and high product losses occurred in the full-scale tests; the D2EHPA solvent extraction scheme for Mn removal proved impractical. An alternate scheme, based on sulfate precipitation was developed. This process, although complicated by the lack of a centrifuge in the plant, does not require pH control. Preliminary results indicated 85–95% rare earth recovery and an adequate Mn decontamination factor of 50–100. The separation of cerium from trivalent rare earths with D2EHPA was improved by the use of a straight chain hydrocarbon diluent. The effects of radiolysis were markedly reduced and high cerium distribution ratios were maintained. (P.C.H.)

16330 (CEA-R-2851) SORPTION DU ^{90}Sr SUR UN OXYDE D'ALUMINIUM. (Sorption of ^{90}Sr on an Aluminum Oxide). Rzekiecki, Roger (Commissariat a l'Energie Atomique, Saclay (France). Centre d'Etudes Nucleaires). Nov. 1965. 59p. Dep. mn.

The sorption mechanism of an alkaline earth bivalent cation on activated aluminum oxide was compared to the sorption mechanism of a monovalent ion. The selective retention of the alkaline earth cation was used to remove trace amounts of ^{90}Sr from radioactive waste waters. A kinetic study is reported, leading to the calculation of an industrial column. (auth)

16331 (GA-6568) ^{3}He CHARGED PARTICLES IN ACTIVATION ANALYSIS. Final Report. Steele, E. L. (General Atomic, San Diego, Calif. John Jay Hopkins Lab. for Pure and Applied Science). July 15, 1965. Contract AT(04-3)-167. 35p. Dep. mn. CFSTI $2.00 cy, $0.50 mn.

General techniques of ^{3}He activations, as well as some preliminary attempts to circumvent the penetration problem are described. A prime consideration was to determine the potential usefulness of a small cyclotron specially designed for the activation analyst. A variety of experimental results obtained using the Los Alamos cyclotron, illustrating the various special problems and special advantages of ^{3}He activation analysis, are described. These include determinations of c, s, and o in various materials. (P.C.H.)

16332 (GA-6691) VARIABLE-ENERGY NEUTRON ACTIVATION ANALYSIS. Final Report. Steele, E. L. (General Atomic, San Diego, Calif. John Jay Hopkins Lab. for Pure and Applied Science). Sept. 17, 1965. Contract AT(04-3)-167. 44p. Dep. mn. CFSTI $2.00 cy, $0.50 mn.

Results obtained with neutrons produced with deuterons of ≤7 Mev and ^{3}He ions of ≤12 Mev bombarding targets of Li, Be, or B are described. Systems such as the $^{56}Fe(n,p)^{56}Mn - {}^{59}Co(n,\alpha)^{56}Mn$, $^{16}O(n,p)^{16}N - {}^{19}F(n,\alpha)^{16}N$, and $^{52}Cr(n,p)^{52}V - {}^{55}Mn(n,\alpha)^{52}V$ were investigated and found to be amenable to the technique of variable-energy neutron irradiations. Also investigated was the analysis of several copper-base alloys which are generally not feasible by D-T neutron methods, owing to the large amount of ^{62}Cu and ^{64}Cu produced. Short-lived products, such as 5.79-min ^{51}Ti, from the $^{51}V(n,p)^{51}Ti$ reaction, and 2.27-min ^{28}Al, from the $^{31}P(n,\alpha)^{28}Al$ reaction, were selectively produced from predominantly copper samples. Neutron yields from a series of $(^{3}He,n)$ reactions were compared with those from a 14 Mev neutron source (D-T), using the reactions $^{16}O(n,p)^{16}N$ and $^{28}Si(n,p)^{28}Al$ as measures of the fast-neutron yields. It was found that ^{3}He ions of ≤12 Mev produce a fast-neutron flux that is equivalent to a D-T produced flux of approximately 10^{8} n/cm^2-sec per μa of beam current, using either a Li, Be, or B target. In general, the results indicate that the minimum variable-energy neutron source should be able to accelerate protons to 8 to 10 Mev, deuterons to 4 to 5 Mev, and ^{3}He ions to 12 to 15 Mev. Extracted beam currents should be 50 μa, or better. The source should be a cyclotron, in order to conserve on installation space and shielding requirements. Additional beam power would be desirable, in terms of increased sensitivity, but not if the price exceeds the $100,000 range. Ideally, the source would be a variable-energy machine; however, lower particle energies can be obtained from a fixed-energy machine by using stacked-foil techniques. The foil method does increase the low-energy neutron yield with deuterons and produces poor neutron-energy resolutions with protons and ^{3}He ions. (P.C.H.)

16333 (KR-81) ANALYSIS OF THE CHEMICAL STATE OF PLUTONIUM AND FISSION PRODUCTS IN PROCESS FEED SOLUTIONS. Bonnevie-Svendsen, M.; Martini, V. (Institutt for Atomenergi, Kjeller (Norway)). Feb. 1966. 18p. Dep. mn.

The chemical states of plutonium and fission products in reprocessing feed solutions are discussed and the need for simple routine analytical procedures for the characterization of species with different extractability is stressed. The development of an extraction chromatographic procedure for the determination of Pu(III), Pu(VI), and Pu(IV) is described. The main source of error was a light-induced reduction of Pu, which occurred in the presence of excess uranyl nitrate. Performed under exclusion of light, the method is well suited for the sensitive determination of Pu(III) and Pu(VI) in feed solutions. Less than a microgram of Pu is required, and macroconcentrations of U and tech-

nical impurities do not interfere. A fractionation of ruthenium species according to their TBP–extractability can be obtained in the same operation. The possibility for applying a similar procedure to zirconium and niobium is discussed. (auth)

16334 (N–65–18292) THE ESTIMATION OF CERIUM IN COMPLEX CHROMIUM-BASE ALLOYS. Lumley, E. J. (Aeronautical Research Labs., Melbourne (Australia)). Sept. 1964. 20p. (ARL/MET–21).

A gravimetric method for the estimation of cerium was examined, and a method considered applicable to chromium base high-temperature alloys was developed. The results obtained by this method were used in the preparation of x-ray standard specimens; and an x-ray fluorescence method, considered acceptable for giving a quick, approximate assessment of cerium, was evolved. It is considered that the x-ray method would be greatly improved by the use of higher powered sources. (auth)

16335 (NBS-TN–276) RADIOCHEMICAL ANALYSIS: ACTIVATION ANALYSIS, INSTRUMENTATION, RADIATION TECHNIQUES, AND RADIOISOTOPE TECHNIQUES, JULY 1964–JUNE 1965. DeVoe, James R. (ed.) (National Bureau of Standards, Washington, D. C.). Jan. 7, 1966. 155p. GPO $1.00.

Developments in studies on activation analysis, radiation techniques, and radioisotope techniques are reported. Electronics for handling data from pulse height analyzers as well as the use of digital computers for processing these data are described. A Moessbauer spectrometer that uses optical interferometry in the Doppler drive, and the mechanical design for the electromechanical drive are presented. A description of chemical shift of iron compounds is given. Use of a correction factor for certain source detector geometries are described for Moessbauer spectroscopy. A new source of ^{119m}Sn in Pd that produces a very narrow line width is also described. A number of special analyses by activation are described, including Ar in Si, Cl in polystyrene, and Hf in Zr. A beta-gamma sum coincidence gamma spectrometer is also described. (P.C.H.)

16336 (NYO–10175) RESEARCH IN ACTIVATION ANALYSIS. Final Report, August 1, 1963–October 31, 1964. Arino, H.; Kramer, H. H.; Molinski, V. J.; Tilbury, R. S.; Wahl, W. H.; Stier, P. M. (Union Carbide Corp., Tuxedo, N. Y. Nuclear Div.). Dec. 31, 1964. Contract AT(30-1)-2975. 130p. Dep. mn. CFSTI $4.00 cy, $1.00 mn.

Improved radiochemical procedures and neutron activation analysis techniques were developed and are described. A rapid activation analysis method was developed for the simultaneous determination of microgram amounts of tantalum and niobium in various sample materials. Another rapid method was developed for use in determining microgram amounts of magnesium in ores and blood serum. None of these analyses requires more than 30 minutes to complete. Solvent extraction and precipitation were used in the radiochemical separations. Radiochemical procedures were developed to separate sequentially the multiple components of a radioactive mixture. The results show that as many as 12 different neutron-induced radioactive species can be separated from a single neutron-activated sample in just a few hours. The method is capable of determining many more radionuclides in the same sample material, and can be adapted for use as part of an automated separation system for routine laboratory use, either in activation analysis or for fission-product assays. The basic radiochemistry involves ion-exchange resin separations. The method was used to determine many elements in different kinds of sample materials. For example, parts-per-million of W, Cu, Co, Mn, Na, Zn, Ta, Sc, and Sb, and macro amounts of Cr and Fe were determined in ores and minerals. Similar techniques were also used to separate radioelements such as ^{46}Sc, ^{59}Fe, ^{60}Co, and ^{65}Zn from other species and from each other before radioactivity measurement by gamma scintillation spectrometry. Research was also continued in the use of metastable isomers as activation analysis indicators. Nuclear isomers of Zn, Y, Pd, Sn, Ba, Er, Os, Ir, Pt, Ta, and Au were found to be more sensitive indicators under certain conditions than many of the radionuclides normally used. In all instances, the use of cadmium-covered specimens and short irradiations (usually for a few minutes) were used to advantage. Experiments were carried out to detect short-lived isomeric states of Cl, Zr, Ca, and Fe. Nuclear isomers of Cl and Zr, viz., ^{38m}Cl(0.74 sec) and ^{90m}Zr(0.80 sec), are known to exist, but were not detected. No new short-lived radioactivities were found for Ca or Fe. Reactor activation cross sections and cadmium ratios were measured for 29 different nuclear reactions, and new cross-section values were obtained for ^{131m}Ba, ^{89m}Y, ^{197m}Au. ^{191m}Ir, and ^{167m}Er. (92 references). (P.C.H.)

16337 (RMO–3001(Rev.1)(Suppl.)) HANDBOOK OF ANALYTICAL PROCEDURES. Supplement to RMO–3001, Rev. No. 1. Bush, W. E.; Higgins, L. J. (comps. and eds.) (Pitkin (Lucius) Inc., Grand Junction, Colo. Western Uranium Project). June 17, 1965. Contract AT(05-1)-912. 95p. Dep. mn. CFSTI $3.00 cy, $0.75 mn.

Methods are described for: determination of major and minor constituents of silicate rocks and ores; water analysis; radiochemical analysis; and determination of uranium in various media. (P.C.H.)

16338 (RT/CHI–(65)36) DETERMINAZIONE RAPIDA DEL CONTENUTO DI MANGANESE E DI ARSENICO NEGLI ACCIAI COL METODO DI ATTIVAZIONE NEUTRONICA. (Rapid Determination of Manganese and Arsenic Content in Steel by Neutron Activation Analysis). Moauro, A.; Cesarano, C. (Comitato Nazionale per l'Energia Nucleare, Rome (Italy)). Oct. 1965. 17p. Dep. mn.

Neutron activation analysis was used to determine Mn and As in stainless steel specimens. The determination of As after irradiation for two hours was obtained by dissolving the sample in a 37% HCl solution and distilling in HCl gas current. The activity of ^{76}As in the distillate was measured by comparison with the activity of a standard. Mn was determined by 1 minute irradiation in the TRIGA reactor and gamma spectrometry without radiochemical separation by comparing ^{56}Mn activity in the sample and a comparison standard. (auth)

16339 (TID–22662) FEASIBILITY EXPERIMENTS RELATED TO TRACE ANALYSIS OF FLUORINE IN ZINC ELECTROREFINING SOLUTIONS BY FAST NEUTRON ACTIVATION AND COINCIDENCE COUNTING TECHNIQUES. Interim Report No. 3. (Colorado School of Mines Research Foundation, Inc., Golden). Feb. 23, 1966. Contract AT (29-2)-1355. 21p. Dep. mn. CFSTI $1.00 cy, $0.50 mn.

Under the conditions of the experiments described, the detection limit for trace fluorine analysis was found to be 325 ppM in demineralized water based on gamma spectrometry and counting of the 1.37 Mev photopeak. Using coincidence counting between the 0.20 and 1.37 Mev gamma rays the detection limit was lowered to 275 ppM. The detection limit for fluorine in Burt solution from a zinc electrorefining process was determined as 3,250 ppM using gamma spectrometry on the 1.37 Mev gamma alone. Coincidence counting the 0.20 and 1.37 Mev gamma rays lowered the detection limit in this matrix to 293 ppM fluorine, a better than one order of magnitude improvement. The detection limit for fluorine in return electrolyte from a zinc electrorefining process was found to be 240 ppM using coincidence counting. This, and the above detection limits are estimated at the 95% confidence level. However, these detection limits are still two orders of magnitude too high for the technique to be applicable for on-stream analysis and process control in the zinc electrorefining process. A detection limit of 3 ppM fluorine will be required for this process. (P.C.H.)

16340 (USNRDL–TR–970) ION EXCHANGE IN FUSED SALTS. II. THE DISTRIBUTION OF ALKALI METAL AND ALKALINE EARTH IONS BETWEEN CHABAZITE AND FUSED $LiNO_3$, $NaNO_3$, AND KNO_3. Callahan, C. M. (Naval Radiological Defense Lab., San Francisco, Calif.). Dec. 30, 1965. 27p. Dep. mn. CFSTI $2.00 cy, $0.50 mn.

A study was made of the ion-exchange distributions of Na, Ca, K, Ba, Rb, and Cs between the mineral exchanger chabazite and each of the fused salts $LiNO_3$, $NaNO_3$, and KNO_3. The distribution coefficients and the selectivity sequences of the ions varied from salt to salt. The selectivity sequence obtained in fused $LiNO_3$ was taken as the normal one and was in the order of increasing ionic radii of the respective periodic groups. In general the sequence was related to a size-charge effect, and transpositions in this sequence observed in fused $NaNO_3$ and KNO_3 were explained by the influence of the sieving properties of chabazite in depressing the distribution coefficients. In each melt a relationship was found that depended on the size of the preferred cation, the size of the solvent cation, the size of the chabazite channels, and the operation of a two-way traffic mechanism for ion exchange. In these experiments ion charge was less important than ion size in determining selectivity order. (auth)

16341 ANALYSIS OF POLYPHENYLS BY GAS CHROMATOGRAPHY. PART I. RELATIVE RESPONSE OF BIPHENYL AND TERPHENYL WITH RESPECT TO TRIPHENYLMETHANE. Perez Garcia, M. (Junta de Energia Nuclear, Madrid). An. Real Soc. Espan. Fis. Quim. (Madrid), Ser. B, 61: 999-1008(Sept.-Oct. 1965). (In Spanish).

The relative performances of the thermal conductivity and flame ionization detectors towards triphenylmethane were investigated for each of the components of biphenyl and terphenyl mixtures. The influence of the concentration of the compound considered as well as the influence derived from the presence of all other components on the relative performances were studied. A 2-m-long column filled with 50 to 70 mesh sterchamol containing 20% apiezon L was used to carry out the study with the thermal conductivity detector by keeping the column at 300°C and using helium gas as carrier. For the ionization detector use was made of a 2-m-long column filled with 80 to 100 mesh chromosorb P containing 20% silicon rubber Ge-SE-31, which was operated at 255°C using nitrogen as carrier gas. Conclusions were drawn from this investigation with regard to the quantitative analysis of biphenyl, terphenyl, and santowax mixtures. (auth)

16342 RAPID ION EXCHANGE ANALYSIS OF RADIOCESIUM IN MILK, URINE, SEA WATER, AND ENVIRONMENTAL SAMPLES. Boni, A. L. (E. I. du Pont de Nemours and Co., Aiken, S. C.). Anal. Chem., 38: 89-92(Jan. 1966). (DPSPU-65-30-7).

Ion exchange systems were developed to concentrate cesium from biological and environmental samples. An inorganic ion exchanger, potassium cobalt ferrocyanide, was used, either alone or with other ion exchange materials. These systems rapidly, preferentially, and quantitatively concentrate cesium from neutral, acidic, or basic solutions. The difficulty of concentrating trace quantities of cesium in the presence of large amounts of sodium, calcium, and magnesium salts is overcome by use of this exchanger. Methods for the analysis of radiocesium in milk, urine, sea water, fresh water, and miscellaneous environmental samples are discussed. (auth)

16343 DETERMINATION OF RADIOISOTOPES OF CERIUM, BARIUM, LANTHANUM, AND NEPTUNIUM AFTER SEPARATION BY BARIUM SULFATE. Sill, Claude W.; Willis, Conrad P. (Atomic Energy Commission, Idaho Falls, Idaho). Anal. Chem., 38: 97-102(Jan. 1966).

Cerium, barium, lanthanum, and neptunium in quantities from carrier-free tracer levels to about 1 mg were precipitated to better than 99.7% by barium sulfate from strong sulfuric acid solutions containing potassium salts and hydrogen peroxide. Neptunium was removed from the barium sulfate by reprecipitating from concentrated sulfuric acid in the presence of chromic acid. The barium sulfate was then dissolved in alkaline DTPA–TEA solution and radiocerium precipitated in the presence of cerium carrier by addition of hydrogen peroxide. The filtrate was treated with sodium sulfate and acetic acid, which reprecipitated barium as the sulfate and left lanthanum in the aqueous solution. Both lanthanum and neptunium could be reprecipitated from their respective solutions by addition of potassium salts, hydrogen peroxide, and barium chloride. The individual isotopes were then determined preferably by gamma spectrometry although gross beta or gamma counting could be used in some cases. Recovery of each isotope was about 97% for the overall procedure making determination of chemical yields unnecessary. The entire separation scheme requires about 3 hr. The procedure can be applied to air dusts, water, and many kinds of mineralogical and biological materials. (auth)

16344 DATA CONVOLUTION AND PEAK LOCATION, PEAK AREA, AND PEAK ENERGY MEASUREMENTS IN SCINTILLATION SPECTROMETRY. Yule, Herbert P. (General Atomic Div., General Dynamics Corp., San Diego). Anal. Chem., 38: 103-5(Jan. 1966).

Data convolution techniques largely eliminate statistical scatter in scintillation spectra. A computer program applying these techniques to the problems of locating peaks, determining their areas, and estimating their energies with reasonable accuracy is described. The program appears to work very well, and should be of aid in gamma spectrum analysis. (auth)

16345 RAPID X-RAY FLUORESCENCE DETERMINATION OF TRACES OF STRONTIUM IN SAMPLES OF BIOLOGICAL AND GEOLOGICAL ORIGIN. Champion, K. P.; Taylor, J. C.; Whittem, R. N. (Australian Atomic Energy Commission, Sutherland). Anal. Chem., 38: 109-12(Jan. 1966).

A mathematical expression was derived, relating the ratio of line peak to background intensities with sample composition. The treatment was generally similar to that of Kalman and Heller, but led to a matrix effect, which could be called a sample scattering factor. This factor could be calculated from an approximate knowledge of the composition of the sample and published values of coherent and Compton scattering functions. From this a rapid analytical method was developed, which employs no standards other than aqueous solutions of strontium nitrate. Examples are quoted of strontium determinations in a variety of samples analyzed by other methods. (auth)

16346 AN ACCURATE DETERMINATION OF RARE EARTHS AND SCANDIUM IN SOUTH AFRICAN CARBONATITES USING SEPARATION BY ION EXCHANGE CHROMATOGRAPHY. Strelow, F. W. E. (South African Council for Scientific and Industrial Research, Pretoria). Anal. Chem., 38: 127-8(Jan. 1966).

The procedure for determining rare earths in South African carbonatites using ion exchange chromatography and oxalate precipitation is described. A sulfonated polystyrene resin was used as ion exchanger. The equilibrium distribution coefficients of the rare earths in hydrochloric acid were determined. Analytical results for 7 carbonatites are given. The accuracy as well as the precision of the method is shown to be very high. For the procedure described above the amount of rare earths present should not exceed 2 to 2.5 mg. (F.J.H.)

16347 SIMULTANEOUS DETERMINATION OF CALCIUM, COPPER, MANGANESE, AND MAGNESIUM IN SERUM BY NEUTRON ACTIVATION ANALYSIS. Haven, M. C.; Haven, G. T.; Dunn, A. L. (Veterans Administration Hospital, Omaha, Neb.). Anal. Chem., 38: 141-3 (Jan. 1966).

The apparatus, procedure, and reagents used in simultaneous determination of Ca, Cu, Mg, and Mn in serum by neutron activation analysis are described. The serum was irradiated at a flux of 1.1×10^{11} n/cm^2/sec. Results of 21 analyses and of recovery tests are given. The Ca recovery tests were corrected for 90% extraction. Standard spectra for each of the elements were obtained prior to activation of the samples. (F.J.H.)

16348 QUANTITATIVE ANALYSIS OF ^{3}H BY GAS CHROMATOGRAPHY. Liebenberg, Donald H. (Los

Alamos Scientific Lab., N. Mex.). Anal. Chem., 38: 149-50(Jan. 1966). (LA-DC-7044).

The quantitative analysis of ^3He by gas chromatography is described. ^4He carrier gas was supplied at a flow rate of 34.6 ml (1 atm., 0°C) per min. A mass spectrograph analysis was made of the $^3He-^4He$ ratio. The sensitivity of the column to hydrogen, nitrogen, and oxygen was 0.0000624, 0.00168, and 0.00192 mv per ppm. The separation of H_2 and ^3He peaks was obtained at a column temperature of 40°C. Analyses were possible when the H_2-^3He ratio was ~1000. A nearly symmetrical elution peak was obtained, indicating a linear adsorption isotherm. Measurements indicated a value for heat of adsorption of 0.10 ± 0.02 kcal per g mole for ^3He on molecular sieve 5A. (F.J.H.)

16349 THE DETERMINATION OF OXYGEN IN SODIUM. Walker, J. A. J.; France, E. D.; Edwards, W. T. (United Kingdom Atomic Energy Authority, Culcheth, Eng.). Analyst, 90: 727-31(Dec. 1965). (TRG-Report-952).

A method was developed for the determination of oxygen in sodium in the range from 0 to 100 ppm. Sodium is removed by distillation and the oxygen is determined by titration with sulfuric acid. The coefficient of variation for the range from 0 to 100 ppm of oxygen is 10. The effect of titratable impurities associated with sodium oxide in the distillation residue was examined. The possible loss of oxygen as carbon monoxide from the reaction between sodium oxide and carbon was investigated and found to be negligible. (auth)

16350 THE RAPID DISSOLUTION OF PLUTONIUM DIOXIDE BY A SODIUM PEROXIDE SINTER, FOLLOWED BY DETERMINATION OF THE PLUTONIUM CONTENT BY DIFFERENTIAL SPECTROPHOTOMETRY. Milner, G. W. C.; Crossley, D.; Jones, I. G.; Phillips, G. (Atomic Energy Research Establishment, Harwell, Eng.). Analyst, 90: 732-5(Dec. 1965).

A method is described for the dissolution of plutonium dioxide and the determination of the plutonium content by differential spectrophotometry. The plutonium dioxide is brought into solution by mixing with an excess of sodium peroxide and heating at 400°C for 10 min, followed by the addition of a similar amount of sodium hydroxide and reheating for a further 10 min. The cold sinter was then extracted with water and transferred to hydrochloric acid solution containing hydroxylammonium chloride. The solution was heated to decompose the peroxide and reduce the plutonium to the tervalent state. The plutonium concentration was then determined by differential spectrophotometry in 4-cm cells at 565 mμ and compared with standards prepared from plutonium metal. Mean recoveries on 100-mg amounts of plutonium dioxide that were ignited at 850°C were 99.8% with a coefficient of variation of 0.3%. Similar results were obtained on plutonium dioxide that was ignited to 1550°C, by slightly extending the sintering time. (auth)

16351 THE SPECTROPHOTOMETRIC DETERMINATION OF MANGANESE AFTER OXIDATION WITH SODIUM PERXENATE. Bane, R. W. (Argonne National Lab., Ill.). Analyst, 90: 756-8(Dec. 1965).

The use of sodium perxenate in the spectrophotometric determination of manganese is shown to eliminate the necessity of heating, maintaining at near-boiling temperature, and cooling to room temperature before spectrophotometric measurement. Some properties of sodium perxenate of interest in analytical chemistry are reviewed. The determination of manganese in uranium oxides and uranium alloys is described. (M.C.G.)

16352 ANALYSIS OF BERYLLIUM METAL AND ITS COMPOUNDS BY OPTICAL EMISSION SPECTROGRAPHY. Carpenter, L.; Lewis, R. W.; Hazen, K. A. (Bureau of Mines, Boulder City, Nev.). Appl. Spectros., 20: 44-6 (Jan.-Feb. 1966).

Eighteen elements were determined in beryllium in amounts from 5 to 1000 ppM by a d-c-arc method. Samples were dissolved in hydrochloric acid, converted thermally to beryllium oxide, then mixed with graphite and barium carbonate for determining calcium, mixed with cupric oxide for determining boron and molybdenum, and mixed with graphite and germanium oxide for determining the other 15 elements. Spectral transmittances of analytical and internal standard lines were converted to relative-intensity ratios, which were plotted against concentrations of standards to form curves from which concentrations of impurities are read. (auth)

16353 RADIOCHEMICAL SEPARATION OF CARRIER-FREE ZIRCONIUM FROM YTTRIUM OXIDE. Forsberg, S.; Wahlman, L.; Forsling, W. (Research Inst. of Physics, Stockholm). Arkiv Kem., 23: 269-70(1965).

A rapid anion-exchange procedure is described for the separation of carrier-free amounts of zirconium from cyclotron-bombarded yttrium oxide. The nuclide ^{89}Zr was obtained by the reaction $^{89}Y(d,2n)^{89}Zr$. A thin layer of about 1 g of yttrium oxide powder was bombarded with deuterons in the deflected beam of a 225-cm cyclotron. The oxide was dissolved in 150 ml of hot, concentrated HCl. To obtain a sufficiently high adsorption of the zirconium ions on the anion exchange column used, HCl gas was bubbled through the cold yttrium solution until saturated. The 100-200 mesh Dowex-1X8 ion exchange resin used for the separation was previously equilibrated with saturated HCl in a plastic column having an ID of 5 mm and a length of 10 cm. The yttrium solution was eluted and the resin washed with saturated HCl until the effluent was found by evaporation of fractions to dryness, to be free from yttrium, which was only very slightly adsorbed by the resin. Elution was carried out at a low overpressure obtained by HCl gas. Finally, the carrier-free zirconium activity was eluted with 30 ml of very pure 4N HCl. The zirconium source was made by evaporating an eluant fraction to dryness. (BBB)

16354 DETERMINATION OF URANIUM(VI) IN CARBONATE SOLUTIONS FROM THE ABSORPTION IN THE SHORT-WAVE ULTRAVIOLET REGION OF THE SPECTRUM. Dobrolyubskaya, T. S. At. Energ. (USSR), 19: 542-4(Dec. 1965). (In Russian).

The absorption spectrum of a uranyl solution with 0.2 g/l of uranium was compared with the absorption spectrum of uranium(VI) in a carbonate solution containing 0.2 g/l of uranium and 50 g/l of sodium carbonate (with a layer thickness of 0.1 mm). The absorption spectrum of uranium in carbonate solution is characterized by a single wide band with a maximum at 213 mμ. The molar extinction coefficient of uranium(VI) in carbonate solution at 213 mμ was found to be ~72,000, and a method of quantitatively determining uranium(VI) in carbonate solution was developed on the basis of the high extinction coefficient at 213 mμ. The optical density was found to be directly proportional to the uranium concentration. The optical density was increased by 15 to 17% on saturating the carbonate solution with a solution of TBP in kerosine. (TTT)

16355 USE OF DIMETHYL SULFOXIDE AS A SOLVENT IN MEASURING SCINTILLATION MIXTURES. Frimmer, M. (Univ., Giessen, Ger.). Atompraxis, 12: 57-8(Jan. 1966). (In German).

Dimethyl sulfoxide mixes well with water and with organic solvents, and is also a good solvent for numerous organic and inorganic compounds. Thus it is suitable for use in measuring labeled compounds in scintillation mixtures. Experimental results are reported and solubility data given. (auth)

16356 THE POSSIBILITY OF THE RADIOLOGICAL HYDROGEN DETERMINATION IN SOLIDS, ESPECIALLY IN COALS. Bockmann, Rolf; Klusmann, Arno (Technische Hochschule, Aachen). Brennstoff-Chem., 46: 17-20(Jan. 1965). (In German).

Studies on radiological hydrogen determination in liquids on the basis of β absorption are reviewed. The method is accurate, exceeds combustion analysis in speed and leaves

the test substance unaltered. The way in which this analysis method can be transferred to plate-shaped and powdered materials was investigated. The effect of heteroatoms and pore volume was considered and the accuracy limits obtainable were determined. (tr-auth)

16357 THE RAPID AND NONDESTRUCTIVE DETERMINATION OF OXYGEN IN STEELS BY RADIOACTIVATION. Perdijon, J. Bull. Inform. A.T.E.N. (Ass. Tech. Energ. Nucl.), No. 57, Suppl., 3-6(Jan.-Feb. 1966). (In French).

The principle of the radioactivation technique and the nuclear reactions used for the radioactivation of O are reported. A radioactive installation adapted to the determination of O in steel is described. The sensitivity and precision of the installation are reported. (J.S.R.)

16358 PROPERTIES OF THE AMINODIACETATE RESIN DOWEX A-1. II. RELATIVE AFFINITIES OF THE RESIN FOR VARIOUS CATIONS. Rosset, Robert (Ecole Superieure de Physique et de Chimie, Paris). Bull. Soc. Chim. France, No. 1, 59-66(Jan. 1966). (In French).

The order of affinities of the aminodiacetate resin Dowex A-1 for various cations presents a very marked similarity to the order of stability of complexes formed in solution between the same cations and EDTA. The exchange constants were determined for different cation couples. They vary significantly with concentration and composition of the solution in equilibrium with the resin. An interpretation based on the penetration of the solutes into the resin by Donnan equilibrium is given. The cations investigated were Hg^{2+}, UO^{2+}, Cu^{2+}, VO^{2+}, Pb^{2+}, Ni^{2+}, Cd^{2+}, Zn^{2+}, Co^{2+}, Fe^{2+}, Mn^{2+}, Be^{2+}, Ca^{2+}, Mg^{2+}, Ba^{2+}, Sr^{2+}, Cr^{3+}, In^{3+}, Fe^{3+}, Ce^{3+}, Al^{3+}, and La^{3+}. (tr-auth)

16359 SIMULTANEOUS SEPARATIONS OF THE ELEMENTS Ra, Pu, U, Am, AND Cm FROM IRRADIATED THORIUM. Fleury, Alain; Simonoff, Gabriel (Faculte des Sciences, Bordeaux). Bull. Soc. Chim. France, No. 1, 251-2(Jan. 1966). (In French).

A method for the simultaneous separation of the elements Ra, Pu, U, Am, and Cm from irradiated thorium in the presence of a large number of isotopes is presented. Passage of the solution on anion resin separates the elements into two groups. Group A with Ra, Th, Am, and Cm, is not fixed on the resin. Th is eliminated under different conditions on a second anion exchange resin. The extraction of Am–Cm by TBP leaves Ra in the aqueous phase. Group B with Pu and U is fixed on the resin. After elusion Pu is extracted by TTA and U by 8-quinolinol. The extraction yield varies from 62 to 84%, according to the element extracted. The purity of the separations is controlled by the non-interference of the activity of other radioactive isotopes. (tr-auth)

16360 DETERMINATION OF SILICON BY NEUTRON RADIOACTIVATION AND APPLICATION TO NUCLEAR GRAPHITES AND ALUMINA. STUDY OF INTERFERENCES. May, Serge; Piccot, Denis (CEN, Saclay, France). Bull. Soc. Chim. France, No. 1, 332-5(Jan. 1966). (In French).

The determination of silicon in nuclear graphite and alumina by activation was studied. The reaction $^{30}Si(n,\gamma)^{31}Si$ was used. After irradiation the nuclear graphite sample was rapidly burned in oxygen current and the chemical separation of silicon in the form of SiO_2 was made by the entrainment technique. After irradiation alumina was dissolved by alkaline diffusion. Sensitivity of the method is approximately 0.5 ppM. Two interferences can lead to ^{31}Si from the reactions $^{31}P(n,p)^{31}Si$ and $^{34}S(n,\alpha)^{31}Si$. The level of interference of these two reactions is given. The distillation of SiF_4 was used in the calculation of these levels. (tr-auth)

16361 SPECTROPHOTOMETRIC DETERMINATION OF MANGANESE IN BERYLLIUM USING DIETHYLDITHIOCARBAMATE EXTRACTION-SEPARATION AND 2-METHYL-OXINE PHOTOMETRY. Motojima, Kenji; Tamura, Nori (Japan Atomic Energy Research Inst., Tokyo). Bunseki Kagaku, 14: 1150-3(Dec. 1965). (In Japanese).

A method for determining manganese in beryllium was established. The method involves the extraction of manganese into benzene as its diethyldithiocarbamate (DDTC) and the formation of manganese 2-methyl-oxinate in the organic extract. By measuring the absorbance of the organic phase, down to 2 ppM of manganese in beryllium can be determined. Not more than 1 gram of beryllium metal sample is dissolved in hydrochloric acid. To remove interfering metals such as iron and copper, the solution is treated with ammonium citrate and oxine, the pH of the solution is adjusted to 5.0 to 5.5, and the metal oxinates are extracted by shaking with chloroform. The pH of the aqueous solution is then adjusted to 7.5 to 9.5, the solution is treated with 10 ml of 8% DDTC solution, and the manganese DDTC complex is extracted with exactly 10 ml of benzene. The manganese DDTC complex is converted into 2-methyl-oxinate in the benzene solution by adding 0.3 gram of solid 2-methyl-oxine and shaking with 15 ml of 0.1N sodium hydroxide solution. The absorbance of the organic solution is measured at 400 mμ against a reference blank. (auth)

16362 STABLE ISOTOPE DILUTION ANALYSIS. II. DETERMINATION OF ELEMENTS AND COMPOUNDS. Dobkowski, Zbigniew (Katedra Jadrowej Inzynierii Chemicznej Politechniki, Warsaw). Chem. Anal (Warsaw), 10: 519-30(1965). (In Polish).

Tagging by stable isotopic dilution is reviewed for H, C, N, O, S, and other elements. In all cases, a stable isotope is required which has an isotopic abundance much different from the "tagged" element or trace element being analyzed. A mass spectrometer is required to determine the percentage (and absolute quantity) of tagged or trace element present. The application of the method of stable-isotope dilution does not require a quantitative separation of the analyzed substance and is especially suited for the analysis of small samples or trace quantities. 102 references. (TTT)

16363 DETERMINATION OF RARE EARTHS BY NEUTRON ACTIVATION METHOD USING ION-EXCHANGE CHROMATOGRAPHY. ANALYSIS OF SPECTRALLY PURE ERBIUM OXIDE. Minczewski, Jerzy; Dybczynski, Rajmund (Inst. of Nuclear Research, Warsaw). Chem. Anal. (Warsaw), 10: 1113-22(1965).

The procedure for determination of rare earths using neutron activation and ion-exchange chromatography is described. Spectrally pure erbium oxide was investigated. The Er_2O_3 and standard solutions were placed in quartz ampoules and irradiated in the EWA reactor at a neutron flux of 10^{13} n/s cm^2 sec for 20 hr. Following irradiation, the solution was evaporated, the residue dissolved in disodium ethylenediaminetetraacetate, and transferred to the chromatographic column. Elution curves are shown. The activity was calculated from the elution curve. The detection limit for impurities was better than 10^{-9} g or 10^{-3}%. (F.J.H.)

16364 NONDESTRUCTIVE DETERMINATION OF ARSENIC IN ORES AND ROCKS WITH HIGH MANGANESE CONCENTRATION BY NEUTRON ACTIVATION ANALYSIS. Nenov, N.; Popov, Ch.; Tomov, T.; Stefanov, G.; Toelgyessy, J. (Naucno Izsledovatelski Geologiceski Institut, Sofia. Katedra Radiochemie a Radiacnej Chemie Slovenskej Vysokej Skoly Technickej, Bratislava). Chem. Zvesti, 19: 918-24(1965). (In Czech).

A method for determination of arsenic in ores and rocks with more than one percent manganese content was developed using neutron activation analysis without radiochemical pretreatment of the samples. The samples were placed in the reactor for a 20-min irradiation at a neutron flux of 3×10^{12} n/cm^2/sec. The activity of the irradiated samples was measured after a 70-hr decay with 400-channel γ scintillation spectrometer. After 70 hr of decay the residual mass of ^{56}Mn was not measurable and the ^{76}As showed a sharp peak at 0.555 Mev. The sensitivity of the measurement was 5×10^{-6} g with a total relative error of ±15%. (tr-auth)

16365 THE RADIOCHEMICAL LABORATORY OF L'ATOME INDUSTRIEL. Bondy, Charles. Chim. Anal., 48: 23-31(Jan. 1966). (In French).

The techniques used in radioactivation analysis are briefly described. The facilities of the laboratory of l'Atome Industriel for radioactivation analyses are reported. (J.S.R.)

16366 RADIOACTIVATION ANALYSIS OF TITANIUM IN ALUMINUM BY MEANS OF THE REACTION $^{48}Ti(p,n)^{48*}V$. Schweikert, Emile; Albert, Philippe (Centre National de la Recherche Scientifique, Vitry, France). Compt. Rend., Ser. C, 262: 87-90(Jan. 3, 1966). (In French).

A cyclotron delivering a proton beam with variable energy between 3 and 30 Mev and with a current intensity attaining several tens μ amp was used to develop a method for the sensitive determination of titanium in Al by proton irradiation. The experimental study showed that 0.1 ppm of titanium could be determined in zone-purified Al. In industrial aluminum it is necessary to separate the $^{48*}V$ chemically in order to obtain this sensitivity. The interfering isotope is ^{56}Co. (J.S.R.)

16367 RADIOACTIVATION ANALYSIS OF IRON IN ALUMINUM USING THE REACTION $^{56}Fe(p,n)^{56*}Co$. Schweikert, Emile; Albert, Philippe (CNRS, Vitry, France). Compt. Rend., Ser. C, 262: 342-5(Jan. 24, 1966). (In French).

The sensitivity of the determination of iron after neutron irradiation is limited to approximately 10^{-7} or 10^{-8} by weight. The present studies have led to the development of a new analysis method by the radioactivation of iron with protons. This new method makes it possible, for an irradiation time of 2 hrs, to attain a sensitivity higher than that obtained after an irradiation of a week in a neutron flux of equivalent intensity. If the length of proton irradiation is extended to a week, the sensitivity is increased by a factor of 100. (J.S.R.)

16368 DETERMINATION OF CADMIUM IN URANIUM COMPOUNDS BY ATOMIC ABSORPTION SPECTROPHOTOMETRY. Stupar, J.; Podobnik, B.; Korosin, J. (Nuclear Inst. J. Stefan, Ljubljana, Yugoslava). Croat. Chem. Acta, 37: 141-8(1965).

A method is described for a rapid, accurate, and sensitive determination of cadmium in uranium and its compounds. Uranium is separated from cadmium by extraction with tributyl phosphate in kerosene in a continuously operating device. After the appropriate preparation of sample solutions cadmium is determined in the water phase by measuring: (for solutions ranging from 0.05 to 1.5 μg Cd/ml) cadmium absorption in a 15-cm-long acetylene-air-nitrogen flame where 80% methanol solution is atomized; or (for solutions ranging from 0.003 to 0.1 μg Cd/ml) cadmium absorption in a 70-cm absorption cell where the hydrogen-air flame with sample solution is blown in. The sensitivity of the first procedure is 0.015 μg Cd/ml and of the second one 0.001 μg Cd/ml. (auth)

16369 CONTRIBUTIONS TO THE RAPID DETERMINATION OF IMPORTANT RADIONUCLIDES (^{89}Sr, ^{90}Sr, ^{131}I, AND ^{137}Cs) IN FOODSTUFFS AND WATER. II. EXPERIMENTAL PROCEDURES. Bergner, K. G.; Jaegerhuber, P. (Chemischer Landesuntersuchungsanstalt, Stuttgart). Deut. Lebensm. Rundsch, 60: 207-10(July 1964); 253-5(Aug. 1964). (In German).

Methods for determining various radioisotopes in foodstuffs, milk, and water are discussed. The techniques include: separation and determination of ^{131}I, ^{89}Sr, and ^{90}Sr in fresh milk; γ spectrometry of milk (^{131}I, ^{137}Cs, ^{140}Ba–^{140}La, and ^{40}K); separation and determination of ^{131}I in water; separation and determination of ^{89}Sr, ^{90}Sr, and ^{137}Cs in solid foodstuffs and water without decomposition of acid-insoluble ash constituents; and separation and determination of ^{89}Sr and ^{90}Sr in the HCl-insoluble portion of foodstuff and water residues. (TCO)

16370 RADIOACTIVATION DETERMINATION OF PALLADIUM IN BASALTIC AND ULTRABASIC ROCKS. Crocket, James H.; Skippen, George B. (McMaster Univ., Hamilton, Ont.). Geochim. Cosmochim. Acta, 30: 129-41 (Jan. 1966),

Neutron activation analysis was used to determine the Pd content of 23 basaltic rocks, 4 ultrabasic rocks, and a sample of Sudbury quartz diorite. A Pd content of 15.8 ± 1.4 ppb was obtained for 10 analyses of W-1 and compared favorably with 18.5 ppb (average of duplicate analyses) found by Vincent and Smales (1956). It was found experimentally that a U/Pd ratio of 180 caused a 1% interference due to production of Pd isotopes by ^{235}U fission. This potential source of interference was not serious for Pd determination in basalts and ultrabasics by neutron activation but could cause interference in analyses of granitic rocks for Pd. The basaltic rocks analyzed were largely representatives of the nonorogenic intra-oceanic basalts and the continental plateau-building basalts. The oceanic rocks were characterized by less variation in Pd than the continental basalts and averaged 1.9 ± 1.2 ppb (range 0.25 to 3.7 ppb). The latter group was characterized by regional variations in Pd content such that the variation shown by any single province (e.g., Deccan or Columbia River) was considerably less than that shown by the group as a whole. The range of Pd values found for continental basalts was 0.45 to 29.4 ppb. A few basaltic rocks from orogenic regions were also analyzed. Three ultrabasic rocks, an associated chromite, and a quartz diorite from Sudbury, Ontario had a range of 1.3 to 22.2 ppb Pd. Regional trends found in the plateau-building rocks suggested that the Pd content of the source material is an important parameter in producing Pd variations. The Pd data are discussed in terms of recent hypotheses on the petrogenesis of basaltic rocks. (auth)

16371 MEASUREMENT OF RADIOACTIVITY IN EFFLUENTS OF A GAS CHROMATOGRAPH. THE FLAME IONIZATION DETECTOR USED AS A COMBUSTION CHAMBER IN COMBINATION WITH SPECIALLY DESIGNED ABSORBERS. Cramer, W. A.; Houtman, J. P. W.; Koch, R. O.; Piet, G. J. (Reactor Instituut, Delft, Netherlands). Int. J. Appl. Radiat. Isotop., 17: 97-101(Feb. 1966).

A description is given of a specially designed flame ionization detector. From this detector, which is used for quantitative measurement of radioactive components in the effluents of a gas chromatographic column, the combustion products (CO_2 and H_2O) can be recovered quantitatively. The CO_2 is trapped in special absorbers, which are connected with the detector. Subsequent measurement of ^{14}C radioactivity in the absorbing liquid is carried out by heterogeneous scintillation counting with a coincidence counting system. Total ^{14}C activities of 10^{-11} C/fraction can be determined with ±15% accuracy in 1 hr counting time. The method can be very generally used with combustible organic materials containing ^{14}C. By using suitable absorbers, other isotopes such as ^{3}H and ^{35}S can be absorbed in the form of H_2O and SO_2 and might be counted as well. Results of combined gas chromatographic and radioactive analysis of reaction products obtained by γ radiolysis of n-pentane containing about 0.6% 1-pentene-4-^{14}C (specific activity 3.7 mC/mol) are given as an example. (auth)

16372 CHROMATOGRAPHIC SEPARATIONS OF IODIDE, IODATE, TELLURITE AND TELLURATE IONS ON ION-EXCHANGE CELLULOSE PAPERS AND CONTROL OF $Na^{131}I$ GELATIN CAPSULES. Gopal, N. G. S.; Frapart, P. (Centre d'Etudes Nucleaires de Saclay, Gif-sur-Yvette, France). Int. J. Appl. Radiat. Isotop., 17: 129-32(Feb. 1966).

Chromatographic separation of anions of iodine and tellurium in different ionization states on two anion-exchange cellulose papers was studied for use in the control of sodium iodide (^{131}I-labeled) and sodium iodide (^{131}I-labeled) adsorbed on the inside surfaces of gelatin capsules. R_f values are presented in diagrams. In general the more

concentrated the solvent was, the higher the R_f of the ions. (M.C.G.)

16373 TRITIUM MEASUREMENT WITH A LIQUID SCINTILLATION COUNTER. THE APPLICATION OF THE OXYGEN-FLASK COMBUSTION METHOD TO A STRONG COLOURED SAMPLE. Yamazaki, M.; Ishihama, H.; Kasida, Y. (National Institute of Radiological Sciences, Chiba-Shi, Japan). Int. J. Appl. Radiat. Isotop., 17: 134-6(Feb. 1966).

In this method the tritium-labeled colored compounds are completely oxidized and converted into H_2O, CO_2, or SO_2, so a counting efficiency similar to that for tritium activity due to water may be expected in most cases. A good linearity between the radioactivity and the amount of azo compounds was observed when 10 cm^2 of filter paper were burned with the samples. (M.C.G.)

16374 METHOD FOR CALIBRATION OF NEUTRON-γ PROBES USED IN MOISTURE AND DENSITY MEASUREMENT OF SOLIDS. Unger, K. (Inst. for Plant Growing, Berlin). Isotopenpraxis, 1: 21-5(Oct. 1965). (In German).

Three calibrating methods are described and evaluated. One of the methods involves the comparison of probe readings with actual values in situ; another involves calibration of the probe in a calibration chamber of relatively large size; and the third involves calibration of the probe in a chamber of relatively small size. The relations between the flux density of the thermal neutrons and soil moisture and density are discussed. (J.R.D.)

16375 ISOTOPE ANALYSIS OF NITROGEN BY EMISSION SPECTROSCOPY WITH PHOTOELECTRIC RECORDING. Meier, G.; Mueller, G. (Institut fuer Stabile Isotope, Leipzig). Isotopenpraxis, 1: 53-62(Nov. 1965). (In German).

Isotope analysis of nitrogen may be carried out by emission spectroscopy with photoelectric recordings in the range of 0.3 to 99.7 at.% ^{15}N. Some examples show the combinations of apparatus suited for this purpose. The influence of different gases on the results is indicated by some of the spectra given. (auth)

16376 CHEMICAL TREATMENT OF NITROGEN COMPOUNDS FOR ISOTOPE ANALYSIS OF NITROGEN BY EMISSION SPECTROMETRY. Faust, H. (Institut fuer Stabile Isotope, Leipzig). Isotopenpraxis, 1: 62-5(Nov. 1965). (In German).

Methods of chemically treating compounds labeled with ^{15}N are reviewed and an approved micromethod for the chemical treatment of nitrogen compounds for optical isotope analysis of nitrogen is described. It is based on the oxidation of ammonium chloride by sodium hypobromite to N_2. Nitrogen amounts of about (1 to 5) $\times 10^{-6}$ mole are necessary for one sample. The construction of the apparatus and its function are described in detail. (auth)

16377 DETERMINATION OF THE D_2O CONTENT IN WATER BY INFRARED SPECTROMETRY. Knezevic, Z. V. (Boris Kidrich Inst. of Nuclear Sciences, Belgrade). Isotopenpraxis, 1: 69-71(Nov. 1965).

A method for determining the deuterium oxide content in the concentration range from 1 to 100% with a precision of 1 to 0.1 percentage unit is described. Measurements were made with a glass cell 0.6 thick using the infrared spectrum region from 4000 to 4400 cm^{-1}. It was found that glass windows can be also used for absorption cells in the range between 2300 and 3800 cm^{-1} in which very intense OD and OH bands appear. (auth)

16378 SENSITIVITY AND ACCURACY OF MEASUREMENTS IN QUANTITATIVE ANALYSES BY MEANS OF THE BETA-RAY BACKSCATTERING TECHNIQUE. Koch, S.; Schleife, F. (Institut fuer Anwendung Radioaktiver Isotope, Dresden). Isotopenpraxis, 1: 78-81(Nov. 1965). (In German).

Using a measuring probe and the central desk of a mass density gage studies of the efficiency of the beta backscattering technique were made with respect to the qualitative analysis of binary systems. Compact samples produced from mixtures of metallic powders served as the objects measured. Nine different binary systems were studied. The atomic number differences of the two components varied from 1 to 48. The sensitivity and the average error of measuring were determined for different conditions. (auth)

16379 ISOTOPIC ANALYSIS OF SULFUR BY SOLID SOURCE MASS SPECTROMETRY. Zmbov, K. F. (Boris Kidrich Inst. of Nuclear Sciences, Belgrade). Isotopenpraxis, 1: 29-30(Oct. 1965).

The production of SO_2 by catalytic decomposition of the sulfates in the ion source with subsequent ionization of SO_2 molecules by electron impact was found to be the most suitable and convenient method for the isotopic analysis of S. (J.R.D.)

16380 PHOTOMETRIC DETERMINATION OF CERIUM IN SIMPLE AND STAINLESS STEEL. Lev, I. E. (Dnepropetrovsk Metallurgical Inst., USSR). Izv. Vyssh. Ucheb. Zaved., Khim. Khim. Tekhnol., 8: 698-700(1965). (In Russian).

A sensitive photometric method is described for determining small quantities of Ce in simple and stainless steels. The method is based on measuring the intensity of coloring of the yellow product obtained in the oxidation of Ce by o-tolidine. It is shown that the errors in the determinations do not exceed 0.004 to 0.005%, at most. Results are compared with those from previous measurements by other methods. (M.J.T.)

16381 ANALYSIS OF URANIUM IN PHOSPHATE ORES. Tourky, A. Riad; Issa, I. M.; Shalaby, Laila A. (National Research Centre, Cairo). J. Chem. UAR, 5: 53-64(1962).

Egyptian phosphate rocks from different locations were analyzed for their P_2O_5, Ca, Pm, Fe, and Al contents. The optimum conditions for the extraction of phosphoric acid from these rocks by the action of concentration H_2SO_4 were studied, and it was found that a solubilizing agent such as NaCl or H_3PO_4 should be used. Separation of U(VI) from the phosphoric acid leach was accomplished by the anion exchange resin De Acidite FF. The effects of the different ingredients present in the ore, especially ferric iron, on the adsorption of uranium by the resin were also studied. The results indicate that the percentage of uranium in Egyptian phosphate rocks varies from 0.0098 to 0.0191%. Thus, U can be economically extracted from them. The method presented, combining ion exchange and polarographic procedures, is suitable for the determination of uranium in these rocks. The method might also be of value in extraction of uranium as a secondary product provided that the phosphoric acid is used in production of phosphate. (BBB)

16382 REMOVAL OF RADIOSTRONTIUM FROM MILK WITH TRICALCIUM PHOSPHATE AND RESULTING CHANGES IN MILK COMPOSITION. Edmondson, L. F.; Landgrebe, A. R.; Sadler, A. M.; Walter, H. E. (Dairy Products Lab., Washington, D. C.). J. Dairy Sci., 48: 1597-1601(Dec. 1965).

The use of calcium phosphate for coprecipitation of radiostrontium from milk was investigated to evaluate variables which might reduce the phosphate-milk contact heating time so that the processing could be done continuously. A study was also made of changes in milk composition as a result of the phosphate treatment. Tricalcium phosphate was added to milk at the rate of 80 g per liter, and the resulting precipitate, containing ^{85}Sr, was removed by centrifugation. Heating milk to 70°C for 30 min, immediately following addition of phosphate, resulted in removal of 85% of the ^{85}Sr. When the pH of milk was adjusted to 5.4 with H_3PO_4, then to 8.2 with KOH before adding phosphate, 90% removal of ^{85}Sr was obtained by heating to 70°C for only 3 min. When phosphate milk (pH 6.6) was stirred at 5°C for 24 hr, only 60% of the ^{85}Sr was removed. All procedures utilizing calcium phosphate precipitation reduced the milk nitrogen from 23 to 38%.

Usually, more than 45% of the milk calcium, in addition to the added phosphate calcium, was precipitated. Also, a decrease in milk phosphorus occurred in some instances. Several drawbacks to the precipitation procedure for removing radiostrontium from milk are discussed. The usefulness as a fallout countermeasure is limited to the removal of ^{89}Sr and ^{90}Sr. The utilization of milk, if treated with calcium phosphate, would likely be limited to non-beverage products, possibly as dried milk. Since marked deficiencies in the protein (in most cases, also in Ca) occur in treated milk, successful manufacture of sterilized milks and of cheese would be questionable. (BBB)

16383 IMPROVED METHOD FOR THE DETERMINATION OF SCANDIUM BY NEUTRON-ACTIVATION ANALYSIS. **Chung, Koo-Soon; Lee, Chul (Atomic Energy Research Inst., Seoul, Korea). J. Korean Chem. Soc., 8: 88-91(1964).**

A sample of monazite is irradiated for 20 hr in a thermal neutron flux of $\simeq 10^{12}$ neutrons cm^{-2} sec^{-1}. ^{46}Sc is then precipitated with aqueous NH_3 and extracted, as its SCN^- complex, into ethyl ether. The extract is then scintillation counted. The chemical yield of Sc is determined gravimetrically by precipitation with mandelic acid. Contents of $\simeq$10 ppM Sc were measured in this way. (Anal. Abstr.)

16384 RADIOASSAY OF TRITIUM- AND ^{14}C-LABELED POLYMER. **Yang, John Y. (North American Aviation Science Center, Thousand Oaks, Calif.). J. Polym. Sci., Pt. B, 4: 31-4(Jan. 1966).**

Universal application of the liquid scintillation counting technique requires that the polymer sample be converted to water and carbon dioxide by means of combustion. It was found that soot formation can be eliminated by impregnating the polymer sample with a few drops of a cyclohexane solution containing 5% Apiezon W wax and drying in a vacuum oven. By coating the polymer with a black solid, the heat of absorption and, consequently, the combustion of the polymer is made more efficient. This procedure was applied to the radioassay of tritium-labeled polystyrene. The counting efficiency varied from 25 to 33.9%. Counting efficiency in the radioassay of ^{14}C-labeled polystyrene was 48%. (M.C.G.)

16385 SEPARATION CHROMATOGRAPHY OF THE RARE EARTHS BY USE OF DI(2-ETHYLHEXYL)PHOSPHORIC ACID. III. DETERMINATION OF THE YTTRIUM CONTENT IN DYSPROSIUM AND TERBIUM CONCENTRATES. **Grosse-Ruyken, Heinz; Bosholm, Juergen (Technische Univ., Dresden). J. Prakt. Chem., 30: 77-81(1965). (In German).**

A 24 × 0.4 cm (for 1-mg M_2O_3 samples) or 24 × 0.6 cm column was filled with siliconized silica gel (0.03–0.06 mm) charged with 1:1 toluene–di(2-ethylhexyl)phosphorate. The sample was added to the column in 0.5 ml 0.1M HCl. Elution was carried out at 40°C, 0.5 ml/cm^2 min, 20 torr excess pressure. The lower lanthanides were eluted with 10 ml 1.0N HCl; Y was eluted with 5 ml 1.2N HCl. This was reduced to 0.5 ml, and 0.4 ml of 0.05% Arsenazo-I solution was added. Concentrated NH_3 was also added until a red color was obtained. After addition of 2 ml NH_3/NH_4Cl pH 9.1 buffer the solution was brought to 10 ml and the extinction measured at 570 nm. A calibration curve is illustrated. In a mixture of 0.5% Y in Dy a variance of 5% (relative) about the correct value was found. Mixtures of Tb and Y containing 18% Y were also accurately and precisely (±0.1%) analyzed. Four hours are required, of which three represent the separation time on the column. (BBB)

16386 A NEW TYPE OF RADIOMETRIC TITRATOR: REDOX AND CHELATOMETRIC MICROTITRATIONS. **Illaszewicz, A.; Mueller, K.; Spitzy, H. (Technical Univ., Graz). Microchem. J., 10: 1-6(Jan. 1966).**

Radiometric titrations are based on an end-point determination by measurement of the change in counting rates. Radiometric titrations may be divided into three main types; radiometric titrations based on precipitation; radiometric titrations based on complex formation; and radiometric titrations based on redox reactions. Results obtained for the chelatometric titration of copper unknowns are shown. Similar results were obtained in the titration of lead, magnesium, nickel, and zinc. Results of redox titration of arsenious acid by ceric sulfate in 2N sulfuric acid using osmium tetroxide as catalyst are given. A comparison of radiometric titrations with the usual titration procedures is given. (F.J.H.)

16387 DETERMINATION OF ^{14}C, TRITIUM, OR ^{35}S AFTER COMBUSTION OF AN ORGANIC SAMPLE AT A SYSTEM OF NOZZLES. **Kainz, Gerald; Wachberger, Eugen (Univ. of Vienna). Microchem. J., 10: 114-30(Jan. 1966).**

Compounds labeled with ^{14}C, ^{3}H, or ^{35}S are combusted at a system of nozzles. Samples from the milligram range up to 200 mg can be oxidized completely by this technique without individual control for vaporization. Samples exceeding 200 mg can also be combusted, but the gasification of the sample has to be regulated according to the size of the flames at the nozzles. The combustion products are collected in a trap containing methanol, ethanolamine or toluene at −20°C (for ^{35}S at −70°C). Activity is counted with a liquid scintillator spectrometer. Various combustion products reduce the counting efficiency and cause a quenching effect. The dependence of this effect on the amount of heteroatoms was determined for ^{14}C, ^{35}S and ^{3}H. Quenching of halogens, which is especially severe, could be eliminated by silver wool at 600°C. It is shown that the efficiency of the phosphor is decreased remarkably when it is exposed to sunlight and air for a longer time. (auth)

16388 SEPARATION AND DETERMINATION OF CALCIUM, STRONTIUM, AND BARIUM, WHEN PRESENT TOGETHER, BY THE RING OVEN TECHNIQUE. **Chatterjee, R.; Dey, Arun K. (Univ. of Allahabad, India). Microchem. J., 10: 171-4(Jan. 1966).**

The ring oven method was used to separate strontium and barium from calcium as sparingly soluble rhodizonates on filter paper discs. The precipitated rhodizonates, on treatment with bromine vapors, formed soluble barium and strontium bromides, which, when treated with ammonium metavanadate, precipitated barium as metavanadate. The precipitated barium metavanadate was soluble in hydrogen peroxide solutions. The rings obtained by the ring oven technique were developed by an aqueous solution of sodium rhodizonate for strontium and barium and with a freshly prepared aqueous pyrogallol for calcium. For the determinations these rings were compared with standard rings obtained with solutions of known concentrations. The error was within 8%. (auth)

16389 DETERMINATION OF TRACE QUANTITIES OF URANIUM BY CONTROLLED-POTENTIAL DC POLAROGRAPHY IN A TRI-n-OCTYLPHOSPHINE OXIDE EXTRACT. **Belew, W. L.; Fisher, D. J.; Kelley, M. T.; Dean, J. A. (Oak Ridge National Lab., Tenn.). Microchem. J., 10: 301-14(Jan. 1966). (ORNL-P-1540).**

The combination of solvent extraction and controlled-potential d-c polarography directly in the organic extract provided a sensitive and selective method for the determination of uranium. The method should be applicable to a wide range of samples containing trace concentrations of uranium, such as sea water and waste streams. Uranium concentrations as low as 2.4 μg in 250 ml of sample can be determined when a 5-ml polarographic cell is used. If a smaller polarographic cell is used, an evaporation step can be added after the extraction and as little as 0.2 μg of uranium determined in 250 ml of sample. The method compares favorably in precision with colorimetric methods for uranium and is more selective and free from interferences. (auth)

16390 CONTROLLED-POTENTIAL POLAROGRAPHY AND COULOMETRY AS MICROANALYTICAL TECHNIQUES. **Kelley, M. T.; Belew, W. L.; Pierce, G. V.; Shults, W. D.; Jones, H. C.; Fisher, D. J. (Oak Ridge National Lab., Tenn.). Microchem. J., 10: 315-33(Jan. 1966). (ORNL-P-1549).**

The three electrode, controlled-potential technique in

polarography allows the use of very small reference electrodes, such as small calomel or silver-silver chloride electrodes or a quasi-reference electrode, which either have too high a resistance or are too easily polarized to permit their use with a conventional polarograph. The technique also permits the use of solutions of relatively high specific resistance in the polarographic cell, thus permitting the use of organic media or dilute supporting electrolyte, which reduces the problems of blanks from this source. The use of small electrodes facilitates the design of micro polarographic cells. An example of application to polarography on the micro scale is described. Controlled-potential coulometry uses small samples (~0.04 meq) to obtain results of high precision (0.1%). By reducing the size of the cell and the working volume, and by careful attention to details such as purity of reagents and the exclusion of oxygen from the system, it is possible to make the sample size much smaller. By the application of suitable blank correction techniques, it is possible to determine reducible and oxidizable constituents at a level of 0.02 μeq with a precision of 1%. The applicability of controlled-potential coulometry is illustrated by results obtained in the determination of iron, uranium, and plutonium in the range from 0.02 to 7 μeq. (auth)

16391 URANIUM(VI) EXTRACTION FROM HYDROCHLORIC ACID SOLUTIONS BY TRI-N-OCTYLAMINE. Sato, Taichi (Shizuoka Univ., Hamamatsu, Japan). Naturwissenschaften, 53: 37(1966).

The partition of uranium(VI) between hydrochloric acid solutions and solutions of trioctylamine (TOA) in benzene was investigated. The chloride concentration and the water content of the organic phase were determined and an infrared spectral study was made of the organic phases. The results showed that the partition coefficient in the presence of hydrochloric acid passes through a maximum at about 8M initial HCl concentration. When part of the HCl in the aqueous phase is replaced by LiCl, the partition coefficient rises with the total chloride concentration. The results suggest that two amine molecules are associated with each uranium atom in the extraction. Infrared results confirmed this. It was also confirmed that an amine–uranyl chloro complex with the mole ratios of uranium/chlorine/TOA as 1:4:2 is formed by the extraction of uranium. (J.S.R.)

16392 STUDIES ON SEPARATION OF FISSION PRODUCTS BY FLOTATION METHOD. SEPARATION OF ^{137}Cs. Koyanaka, Yoshio (Kyoto Univ.). Radioisotopes, 15: 77-82(1966). (In Japanese).

Flotation proved to be effective in removing ^{137}Cs from its aqueous dilute solution, with the aid of suitable coprecipitant such as cupric or nickel ferrocyanide and pertinent collector such as sodium oleate and octadecylamine acetate. It was found in the experiments on single stage flotation that 90~99% of ^{137}Cs can be removed by optimum choice of the concentrations of coprecipitant and collector, as well as of pH of flotation medium. Multiple flotation for four successive stages gave a decontamination factor of 10^4 to 10^6 with a volume reduction ratio of higher than 50. (auth)

16393 DIRECT DETERMINATION OF SMALL QUANTITIES OF RARE EARTH AND YTTRIUM OXIDES IN THORIA BY EMISSION SPECTROSCOPY. Mykytiuk, A.; Russell, D. S.; Berman, S. S. (National Research Council, Ottawa). Talanta, 13: 175-84(Feb. 1966).

Methods are proposed for the determination of submicrogram quantities of rare earth and yttrium oxides in thorium oxide by emission spectroscopy, without previous separation or concentration of these oxides in the sample. It is possible to volatilize these refractory materials from the thoria using silver chloride as the carrier. The carrier distillation technique in conjunction with relatively high dispersion spectroscopy (0.8–1.1 Å/mm) makes possible analyses at levels that were previously feasible only by preconcentration methods (eg, La_2O_3 and Y_2O_3, 5 ppm; Nd_2O_3 and Sm_2O_3, 10 ppm; CeO_2 and Pr_6O_{11}, 20 ppm in a 10-mg sample of ThO_2). (auth)

16394 REACTIONS OF METALLOCHROMIC INDICATORS ON MICELLES. III. SPECTROPHOTOMETRIC DETERMINATION OF MINUTE AMOUNTS OF LANTHANUM WITH XYLENOL ORANGE. Svoboda, V.; Chromy, V. (Inst. of Pure Chemicals, Brno). Talanta, 13: 237-44(Feb. 1966).

Xylenol orange in the presence of cetylpyridinium bromide is proposed for the spectrophotometric determination of minute amounts of lanthanum (III). A deep blue complex, $La[(XO)(CP)_2]_2$, whose molar absorptivity is 92,000 at 625 mμ, is formed. Beer's Law is obeyed within the limits of 0.08 and 0.8 ppm. The effects of pH, reagent concentration, interfering ions, and time of standing are described. (auth)

16395 ANALYSIS OF RARE EARTH SULFIDES, SELENIDES AND TELLURIDES. Kriege, Owen H.; Theodore, Mary Louise (Westinghouse Electric Corp., Pittsburgh). Talanta, 13: 265-9(Feb. 1966).

The rare earth content of sulfides, selenides, and tellurides was determined by titration with EDTA using Xylenol Orange as indicator. Sulfur was measured by titration of sulfate with lead nitrate solution after removal of rare earths on a cation exchanger. Selenium metal was precipitated from hydrochloric-sulfurous acid solution. Metallic tellurium was deposited from strongly acidic solutions containing sulfurous acid and hydrazine sulfate. An evaluation was made of the accuracy and precision of these methods. (auth)

16396 A NEW PRINCIPLE OF ACTIVATION-ANALYSIS SEPARATIONS. X. SUBSTOICHIOMETRIC DETERMINATION OF TRACES OF GALLIUM. Zeman, Adolf; Ruzicka, Jaromir; Kuvik, Viliam (Faculty of Technical and Nuclear Physics, Prague). Talanta, 13: 271-5(Feb. 1966).

A rapid method for the substoichiometric determination of gallium by neutron-activation analysis was developed. After irradiation and dissolution of the test sample, gallium carrier is added and two preliminary separation steps are performed: the extraction into chloroform of cupferrates from 7N sulfuric acid and of diethyldithiocarbamates from 2 to 3N sulfuric acid. The pH of the remaining aqueous phase is then adjusted to 5.5, the solution extracted with a substoichiometric amount of 8-hydroxyquinoline in chloroform, and the activity of the gallium hydroxyquinolate extract measured. A simultaneously irradiated gallium standard is treated in exactly the same way. From the activities of these two substoichiometric extracts the amount of gallium originally present in the test sample can be calculated. The method was applied to the determination of 10^{-6} to 10^{-3}% of gallium in metallic aluminum and transistor-grade silicon. (auth)

16397 RADIOCHEMICAL DETERMINATION OF CADMIUM ISOTOPES IN RADIOACTIVE DEBRIS. Chu, N.; Salter, L.; Sturniolo, D. (Atomic Energy Commission, New York). Talanta, 13: 283-8(Feb. 1966).

^{109}Cd and ^{113m}Cd were produced in a high altitude nuclear explosion during 1962. Analysis of filters from aircraft and balloon samplers enabled the products of this single detonation to be traced. A radiochemical procedure is presented, which allows determination of the cadmium radionuclides in the course of a sequential analysis for fission products and activation products from nuclear weapons tests. The sensitivity, recovery, and decontamination from other radionuclides are adequate. (auth)

16398 SPECTROPHOTOMETRIC DETERMINATION OF CERIUM WITH SULFANILIC ACID. Sarma, P. L.; Dieter, Lowell H. (Univ. of North Dakota, Grand Forks). Talanta, 13: 347-56(Mar. 1966).

In the presence of other rare earths, cerium(IV) can be determined spectrophotometrically by its reaction with sulfanilic acid with which it produces a red color. Solutions containing 28–210 ppM of cerium absorb at 495 mμ according to Beer's law. Other rare earths, except neodymium, and many common ions do not interfere. Strong oxidizing agents and neodymium in greater than fifty times the concentration of cerium interfere with this method. The

precision depends on the control of pH and time. Cerium alloys were analyzed by this method and the results were compared with those obtained by another spectrophotometric method. (auth)

16399 DETERMINATION OF CERTAIN TRACE IMPURITIES IN URANIUM CONCENTRATES BY ACTIVATION ANALYSIS. Abdel-Rassoul, A. A.; Wahba, S. S.; Abdel-Aziz, A. (Atomic Energy Establishment, Inchass, U. A. R.). Talanta, 13: 381-7(Mar. 1966).

A method is presented for the simultaneous determination of chromium, iron, cobalt, and zinc in samples of uranium concentrates, oxides, and metallic uranium by neutron activation analysis. The method involves adequate decontamination of gross fission product activities by adsorption on silica gel, removal of uranium by solvent extraction, separation of most carrier-free rare-earth activities by coprecipitation with aluminum chloride, and, finally, fractional separation of the elements concerned by ion exchange chromatography. The method can assay ppM of such elements in limited quantities of samples by scintillation γ spectrometric analysis with a reproducibility of 10–15%. (auth)

16400 A COMPARISON OF NEUTRON-ACTIVATION ANALYSIS AND HOT-EXTRACTION ANALYSIS OF THE OXYGEN CONTENT OF STEEL. Pasztor, Laszlo C. (Jones and Laughlin Steel Corp., Pittsburgh); Wood, D. E. Talanta, 13: 389-401(Mar. 1966).

A system developed for the fast neutron activation analysis of the oxygen content of metals was tested comparatively with the conventional vacuum fusion and carrier-gas fusion techniques. The results indicated that neutron-activation analysis is much faster (the total analysis takes only 2 min or less), and more reliable than vacuum fusion and carrier-gas fusion methods because all oxygen present is analyzed. Samples can be much larger than the 0.2–3 g commonly used for the fusion methods. Furthermore, the analysis is non-destructive—the same samples can be reanalyzed as often as desired. The fast neutron analysis system includes a 14-Mev neutron generator producing 10^{11} neutrons/sec, a dual-tube pneumatic transfer system, a 5 × 5 inch NaI(Tl) crystal, a single-channel analyzer, two scalers, and timers and switch-gear. A sample, in a polyethylene bottle, and a Lucite reference are irradiated simultaneously, after which the sample is returned to a detector for counting the ^{16}N gammas from the $^{16}O(n,p)^{16}N$ reaction. The reference is then counted in a second detector; the ratio of the sample counts to the reference counts is proportional to the oxygen content of the sample. Samples with oxygen contents from 0.002 to 0.1% of oxygen were analyzed by neutron activation, then cut in several pieces for hot extraction analysis of the total sample. (auth)

16401 PRECISE TITRIMETRIC DETERMINATION OF URANIUM IN HIGH-PURITY URANIUM COMPOUNDS. Pszonicki, Leon (International Atomic Energy Agency, Vienna). Talanta, 13: 403-8(Mar. 1966).

A procedure was developed for the very precise determination of uranium in high-purity uranium compounds. Uranium(VI) is reduced in a strong hydrochloric acid solution with aluminum in the presence of cadmium ions to uranium(III). It is oxidized to uranium(IV) in the presence of excess orthophosphoric acid and then quantitatively oxidized to uranium(VI) with potassium dichromate using a potentiometric end-point detection. The coefficient of variation based on 20 analyses is ∓0.003%. (auth)

16402 SEPARATION OF TRANSPLUTONIUM ELEMENTS. Stary, Jiri (Faculty of Technical and Nuclear Physics, Prague). Talanta, 13: 421-37(Mar. 1966).

A critical review of the group separation of tervalent lanthanides and actinides and of the separation of individual transplutonium elements are presented. The theoretical principles involved are also discussed. It was concluded that precipitation can be used for the separation of transplutonium elements from a majority of fission products, but not the lanthanides. Ion exchange and solvent extraction are excellent methods not only for group separation of tervalent actinides and lanthanides but also for the selective isolation of adjacent transplutonium elements. An attractive method for the rapid separation of transplutonium elements is electrophoresis. (94 references). (P.C.H.)

16403 SUBSTOICHIOMETRIC DETERMINATION OF MANGANESE BY NEUTRON-ACTIVATION ANALYSIS. Zeman, Adolf; Prasilova, Jarmila; Ruzicka, Jaromir (Faculty of Technical and Nuclear Physics, Prague). Talanta, 13: 457-62(Mar. 1966).

A simple and rapid method for the substoichiometric determination of traces of manganese in various materials by neutron activation analysis was developed. After dissolution of the irradiated test sample, manganese(II) carrier is added and subsequently oxidized by peroxodisulfate to the heptavalent state. The permanganate thus formed is finally extracted into chloroform as tetraphenylarsonium permanganate using a substoichiometric amount of tetraphenylarsonium chloride. This single separation step isolates radiochemically pure manganese-56 in the analysis of a relatively simple material in which interfering elements (gold, rhenium, etc.) are absent. When this is not true, a preliminary separation of manganese from the irradiated sample, based on the extraction of manganese diethyldithiocarbamate into chloroform and followed by stripping of the manganese with dilute sulfuric acid, must be used. A simultaneously irradiated standard containing manganese must be treated in exactly the same way as a test sample. In the materials analyzed by the new method 10^{-5} to 10^{-3}% of manganese was determined. (auth)

16404 INVESTIGATION OF THE SOLVENT EXTRACTION OF CALIFORNIUM, FERMIUM, AND MENDELEVIUM. Gavrilov, K. A.; Gvuzdz, E.; Stary, J.; Seng, Wang Tung (Joint Inst. for Nuclear Research, Dubna, USSR). Talanta, 13: 471-6(Mar. 1966).

Extraction constants for the systems di-(2-ethylhexyl)-orthophosphate/toluene/hydrochloric acid and americium, curium, californium, and fermium were determined. They were then used to select the best conditions for the separation of californium, fermium, and mendelevium by extraction chromatography. The separation factors were much higher than the corresponding ion-exchange methods. (auth)

16405 POTENTIOMETRIC DETERMINATION OF PLUTONIUM BY ARGENTIC OXIDATION, FERROUS REDUCTION, AND DICHROMATE TITRATION. Drummond, J. L.; Grant, R. A. (United Kingdom Atomic Energy Authority, Thurso, Scotland). Talanta, 13: 477-88(Mar. 1966).

A simple and rapid method is described for the routine determination of plutonium with a coefficient of variation of better than 0.2%. It is directly applicable to nitrate solutions containing a large amount of uranium; moderate amounts of iron, molybdenum, fluoride, and phosphate do not interfere. Chromium, cerium, and manganese interfere quantitatively, and the procedure may also prove convenient for the determination of these elements. The plutonium is oxidized to the sexivalent state with argentic oxide in nitric acid solution, and the excess of oxidant is destroyed by reaction with sulfamic acid. A weighed small excess of iron(II) solution is then added, and the excess is titrated potentiometrically with standard potassium dichromate solution using polarized gold indicator electrodes. The whole determination is performed in one vessel at room temperature, and takes about 20 min. (auth)

16406 POLAROGRAPHY OF SOLOCHROME VIOLET RS-METAL COMPLEXES AT HIGH pH. PART I. THE POLAROGRAPHY OF MANGANESE, LANTHANUM, YTTRIUM, ZINC, MAGNESIUM, CALCIUM, AND ALUMINIUM. Palmer, S. M.; Reynolds, G. F. (Loughborough Coll. of Tech., Eng.). Z. Anal. Chem., 216: 202-7(1966).

The polarographic behavior of manganese, lanthanum, yttrium, zinc, magnesium, calcium, and aluminum in the presence of solochrome violet RS at pH 13 is described. Evidence for complex formation with the azo dye is provided for all these species with the exception of calcium

and aluminum. The lack of reaction of calcium was used as the basis of a method for the determination of magnesium in calcium. Results are presented and the limitations of the method are considered. (auth)

16407 CONTRIBUTION TO THE DETERMINATION OF RADIOACTIVITY IN DRINKING AND RAIN WATER. Henke, G. Z. Lebensmittel-Untersuch.-Forsch., 126: 409-17(1965). (In German).

A method for the routine analysis of total α and β activity of drinking water and rainwater is described which depends on coprecipitation and adsorption of fission products from 5-l water samples. The precipitate, which is collected on an 18.5-cm filter, consists of Ni–Cs–Fe(II) cyanides, $Fe(OH)_3$, AgI, $Zr(HPO_4)_2$, alkaline earth carbonates, and active charcoal. A smooth surface is obtained with a dispersion (Neatan) so that total α and β measurements may be counted and a γ spectrum may be measured. The efficiency for 11 radioisotopes and the present fission product mixture in rainwater was tested and on the average lies above 90%. The ^{40}K in water is not detected but may be back calculated. Allowing a doubled error of 20%, the smallest detectable β activity is 1.4×10^{-3} pC/ml, with the correction for ^{40}K, 100-min measurement time, and a background of 22 cpm. (BBB)

16408 PHOTOMETRIC DETERMINATION OF NEPTUNIUM BY MEANS OF XYLENOL ORANGE. Ermolaev, N. P.; Kovalenko, G. S.; Krot, N. N.; Blokhin, V. I. Zh. Anal. Khim., 20: 1336-40(1965). (In Russian).

Neptunium(IV) interacts with xylenol orange in weakly acid media (pH ~ 2). The reagent can be used for photometric determination of neptunium. A method was developed for neptunium determination (in microgram amounts) in pure solutions and in the presence of other elements. One determination takes 3 hr. The experimental error is ±1 μg. (auth)

16409 DETERMINATION OF NITROGEN AND OXYGEN IN UF_6. Turovtseva, Z. M.; Malyshev, V. I.; Noskov, A. S. Zh. Anal. Khim., 20: 1353-8(1965). (In Russian).

A spectrographic method is suggested for determining air admixtures in UF_6. A special vacuum apparatus with a cooled discharge tube of a hollow cathode type was designed for this purpose. Photographic and photoelectric methods were developed for measuring the intensity of the nitrogen bands at λ = 4278 or 4236 Å. A spectrograph with a chamber f = 120 mm was used in the first case and a monochromator was used in the second case. The intensity of the oxygen line at λ = 7772 Å was measured only by the photographic method. The sensitivity of the method was 3×10^{-2}% for nitrogen and 6×10^{-2}% for oxygen. The accuracy was about 5%. The use of an interference light filter with a maximum transmission near or equal to λ = 4278 Å is suggested for detecting large amounts (about 2×10^{-1}%) of air in UF_6. (auth)

16410 OPTIMUM CONDITIONS FOR MEASUREMENTS ON RADIOACTIVE PREPARATIONS. Malykhin, V. M. pp 456-60 of Radioaktivnye Izotopy v Atmosfere i Ikh Ispol'zovanie v Meteorologii. Karol, I. L. (ed.). Moscow, Atomizdat, 1964. (In Russian).

A criterion is derived for optimum conditions for measurements on radioactive preparations, which is based on the quality parameter, $Q = 1/\epsilon^2 T$, where ϵ includes an error factor and T includes the measuring time of a preparation and its background. (G.O.Y.)

16411 METHODS OF MEASUREMENT OF ULTRA-SMALL α ACTIVITIES. Spirin, V. D. pp 461-5 of Radioaktivnye Izotopy v Atmosfere i Ikh Ispol'zovanie v Meteorologii. Karol, I. L. (ed). Moscow, Atomizdat, 1964. (In Russian).

Two methods for the measurement of very small alpha activities are described. (D.C.W.)

16412 QUANTITATIVE RADIOACTIVITY DETERMINATION OF ^{18}O. Amiel, Saadia; Nir, Aharon (to Yeda Research and Development Co., Ltd.). Canadian Patent 723,756. Dec. 14, 1965.

A nondestructive method for determination of the ^{18}O content of a gaseous, liquid, or solid sample is described. Radiation from 4 to 9 Mev from a natural or artificial source converts a very small part of ^{18}O to ^{21}Ne and the procedure may be adapted for a series of samples passed continuously in the path of the source beam. By counting the neutrons emitted by the irradiated sample its ^{18}O content may be estimated. (F.S.A.)

Inorganic and Physical Chemistry

Refer also to abstracts 16781, 16982, 17048, 17218, 17959, 17989, and 18016.

16413 (CEA-R-2703) ETUDE DE L'EAU DE CONSTITUTION DE PLUSIEURS OXYDES A GRANDE SURFACE SPECIFIQUE (GLUCINE, ALUMINE, SILICE–ALUMINE) [THESES]. (Study on the Bound Water of Several High Specific Surface-Area Oxides (Beryllia, Alumina, Silica–Alumina) [Thesis]). Rouquerol, Jean (Commissariat a l'Energie Atomique, Saclay (France). Centre d'Etudes Nucleaires). 1965. 66p. Dep. mn.

Submitted to Paris Univ., France.

The bound water of several oxides (beryllia, alumina, silica-alumina) was studied at different steps of their dehydration (heating temperatures between 150 and 1100°C). The following techniques were used simultaneously: thermal analysis (a new method was developed); nitrogen adsorption (study of the texture); diborane hydrolysis (qualitative and quantitative analysis of surface water); infra-red spectrography (in the absorption range of water); and nuclear magnetic resonance (in the resonance range of protons). Due to these different techniques, five kinds of bound water were observed. Attention is called to the great influence of the thermal treatment conditions on the evolution of the products resulting from the decomposition of alumina α-trihydrate $Al(OH)_3$ and beryllium α-hydroxide, in the course of the dehydration. The peculiar properties of the two kinds of oxides (alumina and beryllia) prepared through a new method of treatment under low pressure and constant speed of decomposition are emphasized. Such particular features concern mainly texture, bound water, and consequently, also catalytic activity. (auth)

16414 (CEA-R-2806) DIFFUSION, MOBILITE ELECTRIQUE ET INTERACTIONS IONIQUES DANS LES SELS FONDUS [THESES]. (Diffusion, Electrical Mobility and Ionic Interactions in Molten Salts [Thesis]). Lantelme, Frederic (Commissariat a l'Energie Atomique, Saclay (France). Centre d'Etudes Nucleaires). 1965. 74p. Dep. mn.

Submitted to Paris Univ., France.

The diffusion and the electrical migration of ions in the molten alkali nitrates $LiNO_3$, $NaNO_3$, and KNO_3 and in their mixtures were examined using stable or radioactive isotope indicators. The results showed that there are large differences in the diffusion coefficients and the electric mobilities when they are compared using the Nernst-Einstein formula. An interpretive model has been put forward which shows the role played by poly-ionic displacements: in a salt AC the particles moving are not only the free ions A^- and C^+ but also the groups $[A_nC_n]^{(n'-n)+}$. The results confirm the importance of electrostatic attraction and of the polarizability of the ions. This mechanism, furthermore, explains the inversions of electrical mobilities often observed in liquid ionic media. (auth)

16415 (CEA-R-2861) MOBILITE DES IONS Rb^+ ET Cs^+ DANS LES GAZ A HAUTE PRESSION. (Mobility of Rb^+ and Cs^+ Ions in Gases at High Pressures). Bacconnet, Eugene (Commissariat a l'Energie Atomique, Saclay (France). Centre d'Etudes Nucleaires). Nov. 1965. 70p. Dep. mn.

Theoretical studies and mobility measurements were made of Rb^+ and Cs^+ ions moving in gases at high pressures (10^{-2} to 25 kg/cm^2). The theoretical study was made by considering the ions and molecules as elastic spheres

and taking into account the electrical polarization forces. The practical work was carried out using the Rb^+ and Cs^+ ions emitted by a thermal source; for velocity measurements a method using an ionic beam cut by four grids was employed. Since the source does not work in atmospheres containing oxygen (even in the combined state) the tests only involved pure gases: nitrogen, argon, and helium at pressures of from 10^{-2} to 12 kg/cm^2. The overall results showed that the Rb^+ and Cs^+ ionic mobilities are very similar and that for fairly short times spent by the ions in the gas, the measurements are in agreement with theory. An increase in these times favors a degradation of the ions which always leads to a decrease in the mobility. This effect was most marked in helium. The gases argon and nitrogen behaved identically towards Rb^+ and Cs^+ ions. (auth)

16416 (NYO-906-68) KINETICS AND STRUCTURAL STUDIES OF CHELATES. β-DIKETONES WITH TRANSITION AND RARE EARTH METALS. Progress Report, June 1, 1966. Cefola, Michael (Brookhaven National Lab., Upton, N. Y.). Contract AT(30-1)-906. 54p. Dep. mn. CFSTI $3.00 cy, $0.50 mn.

Studies were continued on the kinetics of transition metals, such as Cu^{2+}, Ni^{2+}, Zn^{2+}, and Mn^{2+}, with acetylacetone in isopropanol–water mixtures to study the effects of such parameters as dielectric constant and possibly the influence of water on the rate expression. Kinetics of the above metals with other β-diketones were also examined with the purpose of arriving at some conclusions as to the effect of substituents on the rates. All of the experiments were performed at different temperatures so as to obtain some thermodynamic correlations. Supplemental to the investigations, the effects of dielectric on enol-keto percentages of acetylacetone were investigated with the use of NMR and the values thus obtained compared with those attained by the Kurt Meyer method. Preliminary investigations on the $Pr(TTA)_4$ compound indicated the possible use of this chelate for γ dosimetry. (auth)

16417 (ORNL-RMIC-4) LISTS OF AVAILABLE AND DESIRED MATERIALS (ULTRAPURE INORGANIC RESEARCH MATERIALS). (Oak Ridge National Lab., Tenn.). Aug. 1965. Contract W-7405-eng-26. 23p. ORNL Free.

Two lists are included: high-purity inorganic solid-state research materials known to be available (or at least to have been produced); and materials about which information has been requested from the RMIC and for which no source could be found. Although only the highest purity and largest size is given for each material, it should be assumed that for many of the materials shown, lower purities and other forms are probably available. All entries are single crystal unless otherwise specified. (P.C.H.)

16418 (UCRL-16250) VIEWPOINTS OF STABILITY OF METALLIC STRUCTURES. Brewer, Léo (Lawrence Radiation Lab., Univ. of California, Berkeley). Feb. 1966. Contract W-7405-eng-48. 45p. Dep. mn. CFSTI $2.00 cy, $0.50 mn.

The bonding in transition metals is considered and a quantitative procedure developed for the calculation of thermodynamic stability as a function of structure. The values of the enthalpies of sublimation of the bcc and hcp transition metal phases are tabulated for consideration of the possibility of stabilization of unstable structures by high pressure and for other thermodynamic applications. (auth)

16419 (UCRL-Trans-1301(L)) THE PEPTIZATION OF SOLID THORIUM OXIDE. Kohlschuetter, V.; Frey, A. Translated for Univ. of California Lawrence Radiation Lab., Livermore, from Z. Elektrochem., 22: 145-61(1916). 59p. Dep. mn. JCL $5.60 fs, $1.97 mf.

Studies were made to determine the mechanism by which peptization of solid thorium oxide prepared from the oxalate proceeds. Results showed that necessary conditions for obtaining a completely peptizable oxide are that the oxalate is decomposed at a temperature not in excess of 700°C and that it is not maintained at temperatures of the order of 500°C for very long. Peptization is achieved by acids such as HNO_3, HCl, HBr, HI, and H_2SO_4 and by some of their more easily hydrolyzed salts. Complete dispersion of the oxide in the peptizing solution is accompanied by a volume decrease in the system owing perhaps to the extremely fine state of division of the solid. The sols obtained from ThO_2 are milky and turbid, opalescent at high dilution, and sensitive to the addition of electrolytes. The results are explained by the assumption that peptization is brought about by the acid reacting with molecules in the surface of the oxide. This causes the formation of ions, either Th^{4+} or ThO^{2+}, which are or become, directly or indirectly, a constituent of the particle and thereby give it the charge required to turn the particles into a stable sol. Colloidal ThO_2 then is a stage in the transition from the solid oxide to a dissolved chemical compound. (P.C.H.)

16420 THE INFLUENCE OF PHOSPHATE ESTER STRUCTURE AND THE CHARACTER OF METAL IONS OF THE FOURTH SUBGROUP ON DEPHOSPHORYLATION. Trapmann, H.; Devani, M. (Univ., Munich). Arch. Pharm., 298: 253-61(Apr. 1965). (In German).

Samples of solutions containing 1×10^{-5} mole ester per 10 ml, 1 to 5×10^{-5} mole Th, Zr, Hf, or Ti, and various buffers and salts, were examined for hydrolysis of the ester 1 to 144 hr after onset of reaction. Hydrolysis of adenosine-2′-phosphate and its 3′ and 5′ isomers is accelerated by Th and Zr in the order 2′ > 3′ > 5′, and Th is more effective as a catalyst than Zr. In basic solution at the lowest concentration Th is more effective than Hf in promoting hydrolysis of glucose-1-phosphate; at the highest Th > Hf > Zr > Ti. This is generally true in acid medium as well (pH 3.6); but the lower concentration of Th is more effective than the higher, though the opposite is true for Hf. For the hydrolysis of adenosine-3′-phosphate at pH 8.6, increased amount of catalyst increases the rate of dephosphorylation, with Th once again the most effective catalyst. Similar data are also reported for hydrolysis of cocarboxylase; the data indicate a stepwise mechanism for this last reaction. (BBB)

16421 INFLUENCE OF METAL IONS AND OF METAL CHELATES ON THE HYDROLYSIS OF α-D-GLUCOSE 1-PHOSPHATE. Murakami, Yukito; Tanaka, Michio (Kyushu Univ., Fukuoka). Bull. Chem. Soc. Jap., 39: 122-7(Jan. 1966).

The hydrolysis reaction of α-D-glucose 1-phosphate was studied in the presence of several metal ions and metal chelates at 40.0 and 60.0°C, in the pH range of 1.69 to 2.71, and at an ionic strength of 0.10M (KNO_3). The reaction rate was followed by the colorimetric method using a combination of the amidol reagent and 8.3% molybdate solution. Among the metal ions employed, dipositive ions, such as manganese(II), cobalt(II), nickel(II), copper(II), zinc(II), and uranyl ions, were observed to be nearly without effect on the rate of hydrolysis, while iron(III) and thorium(IV) ions demonstrated a negative catalytic effect. On the other hand, all the chelating agents employed tend to restore the reaction rate in reference to the corresponding metal-ion-effected reactions. With the 1:1 thorium(IV)–EDTA and the 1:1 iron(III)–EDTA chelate system, the rate was completely restored. Both iron(III)–kojate and thorium(IV)–Tiron chelate systems restored the reaction rate to a lesser extent. The roles of the chelating agents are discussed. The reaction mechanism in the presence of the catalyst species was considered, and two possible mechanisms were put forward for the present reactions. (auth)

16422 ORGANOPHOSPHORUS–URANYL COMPLEXES STUDIED BY NUCLEAR MAGNETIC RESONANCE SPECTROSCOPY. Burdett, Jane L.; Burger, L. L. (Battelle Memorial Inst., Richland, Wash.). Contract AT(45-1)-1830. Can. J. Chem., 44: 111-18(Jan. 15, 1966).

The effect of extraction of uranyl nitrate on certain neutral organophosphorus compounds was observed by nuclear magnetic resonance (nmr) spectroscopy. Proton and phosphorus chemical shifts were measured for the complexed and uncomplexed material. The effect of complex formation on proton-proton and proton-phosphorus coupling constants was noted. (auth)

16423 HOMOGENEOUS CATALYSIS OF D_2–H_2O EXCHANGE BY RUTHENIUM (III) CHLORIDE: EVIDENCE FOR THE HETEROLYTIC SPLITTING OF HYDROGEN. Halpern, Jack (Univ. of Chicago); James, Brian R. Can. J. Chem., 44: 671-5(Mar. 15, 1966).

The prediction, based on earlier studies of the ruthenium(III) chloride catalyzed oxidation of H_2 by iron(III), that in the absence of iron(III) or other oxidants ruthenium(III) chloride should catalyze homogeneously the isotopic exchange between D_2 and H_2O was confirmed. A kinetic study was made of this exchange reaction in which the dependence of the exchange rate and of the exchange product distribution ($HD:H_2$ ratio) on the concentrations of ruthenium(III), hydrogen ion, and chloride ion were determined. The results, and in particular the observation that the $HD:H_2$ ratio of the exchange product increases with the concentrations of H^+ and Cl^- supported the view that the ruthenium(III)-catalyzed oxidation of D_2 by iron(III) and the D_2-H_2O exchange reaction proceed through related mechanisms involving a common rate-determining step in which D_2 is split heterolytically and a deuteridoruthenium(III) complex is formed. (auth)

16424 ISOTOPE EFFECTS IN MIXTURES OF LIQUID H_2O AND T_2O. Salomon, Mark (State Univ., New Brunswick, N. J.). Can. J. Chem., 44: 689-94(Mar. 15, 1966).

Calculations are presented for the equilibrium tritium isotope effect involving water, hydronium ion, and hydroxide ion. The results are used to predict the kinetic isotope effect in the transfer of protons to a mercury cathode. (auth)

16425 DETERMINATION OF POWDER DENSITY, PARTICULARLY OF URANIUM COMPOUNDS. Dembinski, Wojciech; Deptula, Andrzej (Inst. of Nuclear Research, Warsaw). Chem. Anal. (Warsaw), 10: 1195-8(1965). (In Polish).

A method was developed for determination of powder density with +0.2% precision. The sample was placed under a pressure of 0.2 to 1.0×10^3 kg/cm^2 and weighed in carbon tetrachloride or another liquid of known density. (auth)

16426 CONTRIBUTIONS TO THE CHEMISTRY OF THE RARE EARTHS. XVII. ON THE HYPOPHOSPHITES OF SCANDIUM, YTTRIUM, AND LANTHANUM. Pokorny, J. (Katedra Anorganicke Chemie, Prague). Chem. Zvesti, 19: 628-34(1965). (In Czech).

The hypophosphites of Sc, Y, and La were prepared using solutions of $Sc(OH)_3$, $Y(OH)_3$, and $La_2(CO_3)_3$ in solutions of H_3PO_2. Analysis of the preparations indicated a composition of $M(H_2PO_2)_3$ in each case. Analyses were also carried out using conductometric and oscillometric titrations. The products were crystalline and insoluble in water and the usual organic solvents. The hypophosphite of Sc decomposed in vacuum at 350°C, the Y compound at 450°C, and the La compound at 300–350°C. The ir spectra corresponded in each case to the spectrum of the anion. The important vibration band of hypophosphite at about 2400 cm^{-1} was observed, as well as other absorptions corresponding to P–O bonds. The ir spectra of the new compounds and several other hypophosphites are illustrated and compared with the spectra of the hydroxides. Thermal analysis curves for the Sc and La compounds in vacuum are illustrated. (BBB)

16427 CONTRIBUTIONS TO THE CHEMISTRY OF THE RARE EARTHS. XVIII. ON THE CHLOROACETATES OF SCANDIUM. Pokorny, J. (Katedra Anorganicke Chemie, Prague). Chem. Zvesti, 19: 635-40(1965). (In Czech).

The monochloroacetate, the basic dichloroacetate, and the trichloroacetate of Sc were prepared by solution of the hydroxide in the appropriate acid solution (0.3 mol/25 ml). The product was filtered, then centrifuged, and dried in a vacuum desiccator. Yields were 90%. Analyses of the compounds indicate the formulas $Sc(OOCCH_2Cl)_3$, $ScOH(OOCCHCl_2)_2$, and $Sc(OOCCl_3)_3$. The ir spectra of each compound and of $Sc(OH)_3$ are reproduced. X-ray diffraction patterns were also recorded. The decomposition of these compounds by heat was examined; in 100-200 mg samples, the formation of Cl_2 and $COCl_2$ was observed. Densities of the compounds are: hydroxydichloroacetate, 3.266; monochloroacetate, 2.367; and trichloroacetate, 2.680 g/cm^3. (BBB)

16428 CHROMOGENIC REACTION OF THE URANIUM–ALUMINON CHELATE IN SOLUTION. Sangal, Satendra P. (Univ. of Allahabad, India). Chim. Anal., 47: 662-4 (Dec. 1965). (In French).

The formation of a red (λ_{max} at 540 mμ) 1:1 chelate between the ammonium salt of aurintricarboxylic acid (aluminon) and uranium is described. Its composition was determined by spectrophotometry using the methods of molecular ratio and slope ratio. The value of the stability constant log K obtained by the method of molecular ratio was 4.5 at 25°C. (tr-auth)

16429 STUDY BY INFRARED ABSORPTION OF A DOUBLE NITRATE OF LANTHANUM AND MAGNESIUM BETWEEN 4000 AND 1250 cm^{-1}. Deleplanque, Michel; Kahane, Andre; Serra, Alberto (Faculte des Sciences, Grenoble, France). Compt. Rend., Ser. C, 262: 52-5 (Jan. 3, 1966). (In French).

Infrared absorption spectra were obtained for a hydrated double nitrate between 20 and 290°K. It was deduced that the length of the hydrogen bonds that connect the water molecules in the crystal is more than 2.70 Å. (tr-auth)

16430 URANIUM SEMIPENTOXIDE. Leroy, Jean-Marie; Tridot, Gabriel (Faculte des Sciences, Lille). Compt. Rend., Ser. C, 262: 114-16(Jan. 3, 1966). (In French).

The action of hydrogen sulfide on the amorphous oxides U_3O_8 and UO_3 and on α-UO_3 at room temperature made it possible to isolate, during a solid-gas reaction, uranium semipentoxide. It crystallizes in the hexagonal system with the parameters $\underline{a} = 3.996$, $\underline{c} = 4.117$, and $\underline{c}/\underline{a} = 1.030$. The hypothesis of lacuna structure explains its low stability. At 250°C it decomposes into the two steps, U_3O_8 and U_4O_9, and it oxidizes at room temperature to U_3O_{13}. At temperatures above 160°C hydrogen sulfide leads to uranium dioxide. (tr-auth)

16431 THE SYSTEMS FORMED BETWEEN THE SULFIDES L''S OF THE DIVALENT RARE EARTH ELEMENTS AND THE SULFIDES L''_2S_3 OF THE TRIVALENT RARE EARTH ELEMENTS. Tien, Vovan; Flahaut, Jean; Domange, Louis (Faculte de Pharmacie, Paris). Compt. Rend., Ser. C, 262: 278-81(Jan. 17, 1966). (In French).

The sulfides SmS, EuS, and YbS, designated by L''S, combine with the sulfides L'''_2S_3 of the rare earths and form the combinations $L''L'''_2S_4$ belonging to three crystalline types: cubic Th_3P_4, orthorhombic Yb_3S_4, and orthorhombic $CaFe_2O_4$. The sulfides L''S behave as the sulfides MS of the alkaline earth metals of close ionic radius. The 26 compounds of the Th_3P_4 type obtained are described and the regions of homogeneity formed from these compounds are discussed. (tr-auth)

16432 HETEROGENEOUS EXCHANGE OF PRECIPITATES. X. SYSTEM AgI–I^- (^{131}I)–$UO_2(NO_3)_2$. Despotovic, R. (Inst. Ruder Boskovic, Zagreb). Croat. Chem. Acta, 37: 169-80(1965).

The course of heterogeneous AgI–I^- exchange process at various $UO_2(NO_3)_2$ concentrations (0.00010 to 0.10M) was investigated by means of radionuclide ^{131}I. The course of oxidation $I^- \rightarrow I^0$ was determined in NaI–$UO_2(NO_3)_2$ systems with and without AgI precipitates prepared either in statu nascendi or by drying after isoelectric precipitation. The properties of the systems changed through the change of the initial pI value in the course of the exchange reaction owing to $I^- \rightarrow I^0$, which is reflected in the process of heterogeneous exchange. It was found that in the presence of $UO_2(NO_3)_2$ the course of the heterogeneous exchange reaction on dried AgI precipitates differs from those containing $Co(NO_3)_2$. An increase of the rate of exchange was observed on aging the dried AgI precipitate in the prepared mother liquor. The systems containing AgI precipitate

formed in situ revealed no difference in the course of exchange in the presence of $UO_2(NO_3)_2$ and in the presence of $Co(NO_3)_2$. (auth)

16433 ON THE CAUSE OF FORMATION OF TETRAVALENT Tb COMPOUNDS. Samsonov, G. V. (Inst. of Problems in Metallography, Academy of Sciences, Ukrainium SSR). Dopov. Akad. Nauk Ukr. RSR, No. 11, 1482-4 (1965). (In Ukrainian).

On the basis of the electron configuration of the Tb atom and the conditions determining the possibility of 4f → 5d electron transfers, it was found that in compounds with no metals having high ionization potentials (fluorine, oxygen, nitrogen) electron configurations from $5d^16s^2$ to $5d^26s^2$ may arise, which ensures in the limiting case a tetravalent state of the Tb atom. (auth)

16434 ORGANIC COMPOUNDS OF LANTHANIDE ELEMENTS. PART V. ACETYLACETONE DERIVATIVES OF PRASEODYMIUM AND NEODYMIUM. Mehrotra, R. C.; Misra, T. N.; Misra, S. N. (Rajasthan Univ., Jaipur, India). Indian J. Chem., 3: 525-7(Dec. 1965).

Anhydrous triacetylacetonates of praseodymium and neodymium were prepared by reacting their isopropoxides with anhydrous acetylacetone in dry benzene. By taking the metal alkoxides and acetylacetone in different stoichiometric ratios, a number of alkoxide acetylacetonates were also prepared. A plausible mechanism for these reactions is similar to alcoholysis S_{N^2} reactions. All these products were either sparingly soluble or insoluble in benzene. (auth)

16435 MAGNETIC ANISOTROPY AND NATURE OF CRYSTALLINE ELECTRIC FIELD OF OCTAHYDRATED NEODYMIUM SULFATE. Chachra, S. P. (Univ. of Burdwan, India). Indian J. Pure Appl. Phys., 3: 459-61 (Dec. 1965).

The results of magnetic anisotropy measurements on single crystals of octahydrated neodymium sulfate in the temperature range from 300 to 85°K are explained on the assumption of a suitable single electric field of tetragonal symmetry about the Nd^{3+} ion. The crystal field parameters suggested are: $C_2^0 = 250$, $C_4^0 = 97.0$, $C_6^0 = -70.0$, $C_4^4 = 600$, and $C_6^4 = 0$ cm^{-1}. (auth)

16436 THE MODIFICATION OF STRUCTURES OF TERNARY OXIDES BY CATION SUBSTITUTION. I. SUBSTITUTION OF STRONTIUM FOR BARIUM RUTHENIUM OXIDE AND IN BARIUM IRIDIUM OXIDE. Donohue, Paul C.; Katz, Lewis; Ward, Roland (Univ. of Connecticut, Storrs). Inorg. Chem., 5: 335-8(Mar. 1966).

The effects of variation of the depth of close-packed AO_3 layers on the structures of compounds of the type AMO_3 were studied using the systems $Ba_{1-x}Sr_xRuO_3$ and $Ba_{1-x}Sr_xIrO_3$. It was found that with increasing values of x the nine-layer structure with stacking sequence chh gives way to the four-layer structure (ch,ch) and finally to the three-layer perovskite-type structure (c,c,c). With ruthenium, the successive changes occur when x is about $\frac{1}{6}$ and $\frac{1}{3}$. The iridium case is more complex. Barium iridium oxide has a structure that is based on a superlattice of that of the ruthenium compound. It is probably oxygen deficient. The transformations to the four-layer structure and to the perovskite-type structure occur at somewhat higher strontium content. Some barium is necessary to stabilize the perovskite-type phase. (auth)

16437 THE INFRARED SPECTRA OF RARE EARTH METAL CHLORIDE COMPLEXES OF 2,2'-BIPYRIDYL AND 1,10-PHENANTHROLINE FROM 650 TO 70 Cm^{-11}. Ferraro, J. R.; Basile, L. J.; Kovacic, D. L. (Argonne National Lab., Ill.). Inorg. Chem., 5: 391-5(Mar. 1966).

The infrared spectra of rare earth metal chloride complexes of 2,2'-bipyridyl and 1,10-phenanthroline are reported from 650 to 70 cm^{-1}. From the infrared spectra in this region, frequency assignments are suggested for the ν_{M-N} vibrations. The position of the ν_{M-N} vibration was observed to vary with the properties of the metal and ligand. (auth)

16438 DATA FOR $LaTaO_4$ AND $PrTaO_4$, A NEW STRUCTURE TYPE, AND A SERIES OF NEW RARE EARTH COMPOUNDS, $K_{0.5}Ln_{0.5}Ta_2O_6$, WITH THE $PbNb_2O_6$ STRUCTURE. Wolten, G. M.; Chase, A. B. (Aerospace Corp., El Segundo, Calif.). Inorg. Chem., 5: 484-6(Mar. 1966).

Data on the lattic parameters and the space group of single crystals of $LaTaO_4$ and $PrTaO_4$ are given. Three members of a series of mixed metatantalates were also obtained, $K_{0.5}Ln_{0.5}Ta_2O_6$ where Ln is Ce, Nd, or Pr. The tantalates were obtained from molten KF at 1250°C. The lattice parameters of $LaTaO_4$ and $PrTaO_4$ were measured on single crystals in a goniostat, using CuK_α radiation. A comparison of the lattice parameters with those of the phototype and several other related compounds is given. Metatantalates and orthotantalates are discussed. (F.J.H.)

16439 NATURE OF THE CHEMICAL BOND IN TRANSITION METAL COMPOUNDS WITH BORON. Serebryakova, T. I. (Inst. of Problems in Studies of Materials, Kiev). Izv. Akad. Nauk SSSR, Neorg. Mater., 1: 1811-15 (Oct. 1965). (In Russian).

A review is presented on chemical bonding and electric conductivity of transition metal compounds with boron. Since boron atoms have the electron configuration $2\underline{s}^12\underline{s}^22\underline{p}^1$, they can form stable covalent bonds. The $\underline{s}^2\underline{p}$ configuration can be converted to sp^2 so that numerous structural types and numerous crystal forms are possible. In the borides M_4B and M_2B the boron atoms are isolated from each other. The valence electrons are in the d level of the metal atoms if the metal has a high acceptor capability. In some other units (M_3B_2, MB, MB_2, MB_6) a large fraction of the p electrons form B–B bonds. In the rare earth hexaborides the paired electron bond between boron and metal is directional, and there is a stable three-dimensional covalent bond. For the Ti, V, Cr, and Zr borides the electroresistance is less than that of the metals and for the Nb, Ta, Mo, and W borides it is greater. The capacity to form a large number of boride phases is greater in the latter group than in the former. With increasing boron content of the boride the B–B bond strengthens, and the M–B bond weakens. (TTT)

16440 CERIUM PERRHENATE AND ITS CRYSTAL HYDRATES. Plyushchev, V. E.; Varfolomeev, M. B. (Moscow Inst. of Fine Chemical Tech.). Izv. Vyssh. Ucheb. Zaved., Khim. Khim. Tekhnol., 8: 361-6(1965). (In Russian).

The crystalline hydrates of cerium perrhenate—$Ce(ReO_4)_3 \cdot 4H_2O$ and $Ce(ReO_4)_3 \cdot HeO$—were synthesized. The thermal stability of the synthesized compounds was studied using various methods, and in the process of their dehydration the anhydrous compound $Ce(ReO_4)_3$, stable over a significant temperature interval, was obtained. The identity of cerium perrhenate and its crystalline hydrates was shown by chemical, optical, and x-ray analyses, and some of the properties of these compounds were studied. (M.J.T.)

16441 THERMAL DECOMPOSITION OF ERBIUM AND YTTERBIUM HYDROXIDES. Ambrozhii, M. N.; Dvornikova, L. M. (Saratov State Univ., USSR). Izv. Vyssh. Ucheb. Zaved., Khim. Khim. Tekhnol., 8: 707-11(1965). (In Russian).

The composition of the products of the thermal decomposition of erbium and ytterbium hydroxides was determined more precisely, using data from thermograms and analysis of the hydroxide-water-NaCl system according to the method of the third component, for temperatures from 20 to 270°C. Results of both analytical and graphical analyses are presented. (M.J.T.)

16442 INFRARED SPECTRA OF THE VAPORS ABOVE SULFURIC AND DEUTERIOSULFURIC ACIDS. Chackalackal, Scaria M.; Stanford, Fred E. (Northwestern Univ., Evanston, Ill.). J. Amer. Chem. Soc., 88: 723-8(Feb. 20, 1966).

The infrared absorption spectra in the range 4000 to 400 cm^{-1} of the vapors above liquid H_2SO_4, 1:1 $H_2-SO_4-D_2SO_4$, and D_2SO_4 were measured and assigned to the re-

spective gaseous molecules as well as equilibrium concentrations of SO_3. SO_2 was observed as a decomposition product. Assignment of the frequencies to the normal modes was made using correlations with the related near-tetrahedral molecules $X-SO_2-Y$ and with spectra of the condensed phases. Some frequencies are predicted for H_2CrO_4 and for unassociated gaseous chlorosulfonic acid. (auth)

16443 EFFECT OF THE COMPOSITION OF THE GASEOUS PHASE ON THE ISOTOPIC SEPARATION OF ^{15}N BY CHEMICAL EXCHANGE BETWEEN NITRIC SOLUTIONS AND NITROUS VAPORS. Mahenc, Jean (Institut du Genie Chimique, Toulouse). J. Chim. Phys., 62: 1399-1403(Nov.-Dec. 1965). (In French).

A refluxer was used to study the effect of composition of the gaseous phase on the separation of ^{15}N by chemical exchange between nitric solutions and mixtures of nitric oxide and dioxide. The observations, completed by determination of the profile of the isotopic concentrations along the exchange column showed the importance of the role of absorption of nitrous vapors in the enrichment mechanism. The apparatus also led to a more concentrated sulfuric acid as a by-product of the preparation of ^{15}N. (tr-auth)

16444 CATALYSIS BY ALKALINE AMIDES OF THE ISOTOPIC EXCHANGE BETWEEN HYDROGEN AND LIQUID AMMONIA. Delmas, Robert; Courvoisier, Pierre; Ravoire, Jean (CEN, Saclay, France). J. Chim. Phys., 62: 1423-5(Nov.-Dec. 1965). (In French).

The catalytic action of alkaline amides with respect to the isotopic exchange between hydrogen and liquid ammonia was reexamined. Precise kinetic measurements and the interpretations of the salt effects and the common ion effects indicated a catalysis by the amide ions exclusively. (tr-auth)

16445 POLAROGRAPHIC BEHAVIOR OF HAFNIUM(IV) IN AQUEOUS-ALCOHOLIC MIXTURES. Sancho, J.; Almagro, J.; Pujante, A. (Univ. of Murcia, Spain). J. Electroanal. Chem., 11: 122-7(Feb. 1966).

A polarographic study of hafnium was carried out in lithium chloride (0.1, 0.5 and 1M) in 5, 25, 50, and 75% (v/v) ethanol. One polarographic wave was observed corresponding to a one-electron process agreeing with the microcoulometric study carried out at constant potential and constant current. The observed wave is well-defined and useful analytically. The half-wave potentials were measured against the saturated calomel electrode at different conditions of pH, temperature, and height of mercury column in the concentration range between 10^{-3} and 5×10^{-3}M. The values for the diffusion current constant and the peak potentials obtained in derivative polarography, are also given. (auth)

16446 ON THE KNOWLEDGE OF THE REACTION OF OXALATOHYDRATES OF RARE EARTH METALS WITH HYDROGEN CHLORIDE. I. THERMAL DECOMPOSITION OF THE PRODUCTS REMAINING ON REACTION WITH CONCENTRATED HYDROCHLORIC ACID. Moebius, Rolf; Matthes, Franz (Technische Hochschule, Leuna-Merseburg, Ger.). J. Less-Common Metals, 10: 254-6(Apr. 1966). (In German).

The thermal decomposition of rare earth oxalatochlorides $[RE(C_2O_4)Cl \cdot 3H_2O]$ in air yielded first the unstable monohydrate, then the anhydrous oxalatochloride, and finally the oxychloride. Cerium, however, gave the dioxide. Decomposition of the acid oxalate $[HRE(C_2O_4)_2]$ yielded the oxide, with no intermediate formation of stable lower hydrates or anhydrous compounds. (auth)

16447 ON THE KNOWLEDGE OF THE REACTION OF OXALATOHYDRATES OF RARE EARTH METALS WITH HYDROGEN CHLORIDE. II. REACTION IN THE HYDROGEN CHLORIDE STREAM AT 25 DEG C. Moebius, Rolf; Matthes, Franz (Technische Hochschule, Leuna-Merseburg, Ger.). J. Less-Common Metals, 10: 257-61(Apr. 1966). (In German).

When the hydrated oxalates of rare earth elements are exposed to a stream of hydrogen chloride, the latter is absorbed by their zeolitic water and reacts with the hydrated oxalates of cerium, lanthanum, neodymium, and praseodymium, but is only partial with those of the other rare earth elements. (auth)

16448 ON THE KNOWLEDGE OF THE REACTION OF OXALATOHYDRATES OF RARE EARTH METALS WITH HYDROGEN CHLORIDE. III. REACTION IN THE HYDROGEN CHLORIDE STREAM AT HIGHER TEMPERATURES. Moebius, Rolf; Matthes, Franz (Technische Hochschule, Leuna-Merseburg, Ger.). J. Less-Common Metals, 10: 262-72(Apr. 1966). (In German).

The thermal decomposition of hydrated oxalates in hydrogen chloride was investigated under various conditions. Attempts to heat the rare earth hydrated oxalates in a stream of hydrogen chloride in a tube furnace did not lead to reproducible results. It was, however, established that only from the hydrated oxalates of lanthanum and cerium, and possibly from those of praseodymium and neodymium, could pure anhydrous chlorides be obtained by heating in a stream of hydrogen chloride. (auth)

16449 THERMODYNAMIC PROPERTIES OF URANIUM OXYCARBIDES. Chiotti, P.; Robinson, W. C.; Kanno, M. (Ames Lab., Ames, Iowa). J. Less-Common Metals, 10: 273-89(Apr. 1966). (IS-1249).

The emf of fused-salt cells of the type $U/KCl/LiCl-UCl_3/UO_xC_{1-x}$, C were measured over the temperature range 450–750°C and for oxycarbide compositions of 0.11–0.82 mole fraction UO. Considering the oxycarbide as a pseudobinary solid solution of UO and UC the following relations were derived from the data: $\Delta\bar{G}^{xs}(UC)/(1-X_{UC})^2 = -24{,}000 + (24{,}230 - 44.7T)X_{UC}$ and $\Delta\bar{G}^{xs}(UO)/(1-X_{UO})^2 = -24{,}000 + (24{,}230 - 44.7T)(X_{UC} - 0.5)$ where $\Delta\bar{G}^{xs}$ is the relative excess partial molal free energy in cal/mole for components UC and UO respectively. The standard free-energies of formation of UC and UO at 1023°K are calculated to be −24.7 and −129.6 kcal/mole respectively. (auth)

16450 THE ABSORPTION SPECTRUM OF THE URANYL ION IN PERCHLORATE MEDIA. PART I. MATHEMATICAL RESOLUTION OF THE OVERLAPPING BAND STRUCTURE AND STUDIES OF THE ENVIRONMENTAL EFFECTS. Bell, J. T.; Biggers, R. E. (Oak Ridge National Lab., Tenn.). J. Mol. Spectros., 18: 247-75 (Nov. 1965). (ORNL-P-1376).

The absorption spectrum observed for the UO_2^{2+} ion between 3300 and 5000 Å arose from one or more vibrationally perturbed electronic transitions; some fourteen transitions were observed in this wavelength interval. Each band overlapped the adjacent bands on both the high- and low-frequency side of the band center and resulted in the rather ill-defined (in some areas) summed spectrum observed. Computer techniques, which were developed for the mathematical resolution of complex overlapping spectra, were applied to a study of the fundamental parameters of the absorption spectra of the UO_2^{2+} ion and related systems. The results showed that some prior inferences concerning the character and distribution of the bands in the UO_2^{2+} spectrum are in error. The parameters of the bands obtained from the resolution of the absorption spectrum of uranyl ions and measurements of the intensity distribution and parameters of the resolved fluorescence emission spectrum of uranyl ions in perchlorate media were interpreted with respect to some theoretical models proposed for the vibronic level structure. By the use of very accurate data, with the perchlorate system, an additional band was found in the UV region of the visible range, which was found to be part of the same electronic transition as represented by the bands in the 3325 to 5000 Å region. The parameters of the band distribution used for the previous model will not describe the experimental spectrum. An attempt was made to resolve, by computer techniques, the uranyl absorption spectrum according to the previously proposed model, but the band parameters for this model were converted by the nonlinear least squares computer method to the same resolved absorption bands that were found. A close examination of

the profile and structure of experimental and resolved spectra led to a different assignment of bands in the various levels of a proposed triplet, consisting of bands 1 to 3, 4 to 8, and 9 to 13, as triplet regions 1, 2, and 3, having centers at 21,329, 24,107, and 27,731 cm^{-1}, respectively. (auth)

16451 BANDS OF D_2 AND T_2 ORIGINATING FROM THE LOWEST EXCITED $^1\Sigma_g$ STATES $(1s\sigma)(2s\sigma)^1\Sigma_g$ AND $(2p\sigma)^2{}^1\Sigma_g$. Dieke, G. H. (Johns Hopkins Univ., Baltimore); Cunningham, S. P. J. Mol. Spectros., 18: 288-320(Nov. 1965).

Bands of the two extensive band systems $(1s\sigma)(2s\sigma)^1\Sigma_g \rightarrow (1s\sigma)(2p\sigma)^1\Sigma_u$ and $(2p\sigma)^2\ {}^1\Sigma_g \rightarrow (1s\sigma)(2p\sigma)^1\Sigma_u$ of D_2 and T_2 are presented. The initial states interact strongly and the result of this interaction is a potential curve with two minima, such as computed by Davidson, with which the observations are compatible. The lower vibrational states can be assigned to the individual minima, the higher ones are clearly above the intervening maximum. The presence of perturbations and the comparison between the isotopes resulted in a fairly definite assignment of all vibrational quantum numbers, even though the low states belonging to the far minimum were not located empirically. (auth)

16452 THE SPECTRUM AND STRUCTURE OF THE He_2 MOLECULE. PART III. CHARACTERIZATION OF THE TRIPLET STATES ASSOCIATED WITH THE UAO'S 3s AND 2pπ. Ginter, Marshall L. (Univ. of Chicago). Contracts AF19(628)-2474; Nonr-2121(01). J. Mol. Spectros., 18: 321-43(Nov. 1965).

Existing data on the electronic transitions $3s\ d^3\Sigma_u^+ \rightarrow 3p\sigma\ c^3\Sigma_g^+$, $3s\ d^3\Sigma_u^+ \rightarrow 2p\pi\ b^3\Pi_g$, $3d\sigma\ f^3\Sigma_u^+ \rightarrow b^3\Pi_g$, $3d\pi\ f^3\Pi_\mu \rightarrow b^3\Pi_g$, and $3d\sigma\ f^3\Delta_u \rightarrow b^3\Pi_g$ of He_2 were extended, and the $d^3\Sigma_u^+$ and $b^3\Pi_g$ states described in detail. The partially resolved multiplet splitting for the $b^3\Pi_g$ state is discussed in the light of recent theory as is the applicability of accidental pure precession to the Λ-doubling for the b state. Molecular constants (cm^{-1}) are reported. (auth)

16453 THE RARE EARTH HYDRIDES. Bos, W. G.; Gayer, K. H. (Wayne State Univ., Detroit). J. Nucl. Mater., 18: 1-30(Jan. 1966).

The structures and properties of the rare earth hydrides are reviewed. A critical evaluation of published reports was attempted, particularly in those cases where there is disagreement as to experimental results or their interpretation. The studies of various physical and chemical properties are correlated from two points of view: to establish the existence of similarities, differences, or trends exhibited within the class of compounds; and to establish relations between the properties of a given hydride or group of hydrides so that a clearer understanding of the nature of these compounds will be possible. (auth)

16454 SURFACE CATALYSIS OF THE ORTHOHYDROGEN-PARAHYDROGEN CONVERSION ON CARBON-SUPPORTED GADOLINIUM AND HOLMIUM SULFATES AT 77 DEG K USING ULTRAHIGH-VACUUM TECHNIQUES. Davidson, Eric; Chang, Tiao-hsu; Chapin, Douglas S. (Univ. of Arizona, Tucson). J. Phys. Chem., 70: 347-51 (Feb. 1966).

The rates of orthohydrogen–parahydrogen conversion were investigated at 77°K on several concentrations of $Gd_2(SO_4)_3$ and $Ho_2(SO_4)_3$ catalysts using ultrahigh vacuum techniques. The catalysts were prepared by adsorption of the rare earth ions from dilute aqueous solutions at pH 1 onto carbon. The number of rare earth sites on the catalyst was determined by neutron activation analysis. It was found that exhaustive baking under vacuum at 450°C for 400 to 600 hr led to a plateau in the rate constant vs time-of-heating curves. Rate constants per paramagnetic site were found to be higher at higher site concentrations; a possible explanation postulates adsorption site "cage" structures, which depend on surface site concentrations. The ratio of the rate constants of holmium to gadolinium increased from 2.5 to 3.6 as the rare earth site concentration was increased from 0 to 10^{-5} g-ion/g of carbon. The result was compared to a theoretical ratio of 2.2 calculated on the basis of the Wigner theory. (auth)

16455 REVERSING HYDROGEN ISOTOPE EFFECT ON THE RATE OF THE GAS PHASE DECOMPOSITION OF OXALIC ACID. Lapidus, Gabriel; Barton, Donald; Yankwich, Peter E. (Univ. of Illinois, Urbana). J. Phys. Chem., 70: 407-11(Feb. 1966). (COO–1142-62).

The decomposition of oxalic acid-d_2 vapor at an initial pressure of 0.8 mm was studied between 127 and 156°C. The decomposition appeared to be first order with respect to oxalic acid; observed Arrhenius parameters are: E = 34.5 ± 0.9 kcal $mole^{-1}$ and log A (sec^{-1}) = 14.3 ± 0.5. Comparison of these results with those for oxalic acid revealed a small hydrogen isotope effect, which inverted within the experimental temperature range and which had very great temperature dependence for its magnitude. The size of the temperature dependence seemed explainable by combination of kinetic, equilibrium (between cyclic and noncyclic structures), and tunneling isotope fractionation effects. The magnitude of the observed isotope effect can be explained if there is impressed on this combination a virtually temperature-independent inverse isotope effect such as that described and observed by Rabinovitch and his co-workers. (auth)

16456 HEATS OF IMMERSION IN THE THORIUM OXIDE-WATER SYSTEM. II. NET DIFFERENTIAL HEATS OF ADSORPTION. Holmes, H. F.; Fuller, E. L. Jr.; Secoy, C. H. (Oak Ridge National Lab., Tenn.). J. Phys. Chem., 70: 436-44(Feb. 1966). (ORNL-P-1530).

Net differential heats of adsorption for water on thorium oxide were obtained from the integral heats of immersion of samples containing known amounts of presorbed water. The samples were prepared by the thermal decomposition of thorium oxalate and were carefully characterized as to purity, calcining temperature, particle size, and crystallite size. Surface areas ranged from 1.2 to 14.7 m^2/g. Initial net differential heats of adsorption at low surface coverages ranged from –20 to –30 kcal/mole. In no case did the net differential heat of adsorption decrease to zero with the completion of the first adsorbed monolayer. The results were interpreted in terms of chemisorption involving the formation of surface hydroxyl groups with possibly additional contributions from hydrogen bonding. The samples showed marked dissimilarities with respect to surface heterogeneity. (auth)

16457 CATALYTIC EXCHANGE OF METHANE WITH DEUTERIUM ON PALLADIUM–GOLD ALLOYS. McKee, D. W. (General Electric Research and Development Center, Schenectady, N. Y.). J. Phys. Chem., 70: 525-30 (Feb. 1966).

The rates of the exchange reaction between CH_4 and D_2 were measured on a series of Pd–Au alloy powders in the temperature range from 90 to 200°C. Stepwise exchange was the dominant mechanism in every case and the specific activity of the alloys at 100°C showed a small maximum at a composition of about 10 at. % Au. Increasing concentrations of Au gave rise to a rapid decrease in exchange rate, which became immeasurably small at about 60 at. % Au. The apparent activation energy for the exchange reaction varied between 14 and 23 kcal/mole and showed a shallow minimum at about 20 at. % Au. Possible reasons for this behavior are discussed. (auth)

16458 DISSOCIATION OF ACETIC ACID-d_3 IN AQUEOUS SOLUTION AND RELATED ISOTOPE EFFECTS FROM 0 TO 50 DEG. Paabo, Maya; Bates, Roger G.; Robinson, R. A. (National Bureau of Standards, Washington, D. C.). J. Phys. Chem., 70: 540-3(Feb. 1966).

The dissociation constant of acetic acid-d_3 (CD_3COOH) in water (H_2O) was determined by emf methods at 11 temperatures from 0 to 50°C. From the variation of the dissociation constant with temperature the changes of enthalpy, entropy, and heat capacity for the dissociation process were also derived and compared with similar data for ordinary protoacetic acid in aqueous solution. The pK of the deuterioacetic acid was from 0.012 to 0.016 unit greater than that of the protoacid, and the temperature (22.9°) at which the dissociation constant passed through a maximum was only slightly higher than the corresponding temperature (22.4°)

found earlier for the protoacid. The changes of enthalpy, entropy, and heat capacity accompanying the dissociation of the two acids at room temperature did not appear to differ by an amount significantly greater than the combined errors of the two determinations. (auth)

16459 THE RELATION BETWEEN FORWARD AND BACKWARD UNIDIRECTIONAL RATES OF THE HYDROGEN ELECTRODE REACTION IN THE ISOTOPICALLY MIXED SYSTEM. Enyo, Michio; Yokoyama, Takamitsu (Hokkaido Univ., Sapporo). J. Res. Inst. Catalysis, Hokkaido Univ., 13: 71-6(Jan. 1966).

The validity of the equation, $V_+/V_- = \exp\{-\Delta F/\nu(r)RT\}$, in an isotopically mixed system was investigated with special reference to the hydrogen electrode reaction, where V_+ or V_- is the forward or the backward unidirectional rate of the overall reaction, respectively, $-\Delta F$ its affinity, and $\nu(r)$ the stoichiometric number of the rate-determining step r. It is shown that the equation is formally invariantly valid for the system of any isotopic composition at any magnitude of the isotope effect, ie, the difference in specific rates between the isotopes, by replacing V_+ and V_- with the respective sums of the relevant isotopic contributions and $-\Delta F$ with $-2F\eta$, where η is the electrode potential referred to the rest potential of the same electrode in the same isotopically mixed system and F the Faraday. Applications of the equation thus verified are presented. (auth)

16460 CONTRIBUTIONS TO THE KINETICS AND THE MECHANISM OF HETEROGENEOUS ISOTOPIC EXCHANGE REACTIONS OCCURRING ON THE SURFACE OF SOLID CATALYSTS. I. PREPARATION OF SOLIDS AND DETERMINATION OF THE SURFACES. Latzkovits, Laszlo; Galiba, Ilona; Gal, Dezso (Attila Jozsef Univ., Szeged). Magyar Kem. Foly., 71: 407-10(Sept. 1965). (In Hungarian).

In order to determine the effect of the surface properties of solids on the course of heterogeneous catalytic surface reactions, AgI and other metal iodide crystals were prepared under carefully controlled conditions. The active surface of the crystals was determined by means of F. Paneth's radioactive indicator method. The AgI was prepared in the presence of excess $AgNO_3$, excess KI, and by using equivalent amounts of the precipitants. Solutions labeled with ^{110}Ag and ^{131}I were used for measuring the active surface on the basis of the isotopic exchange reactions. Simultaneous control determinations were made by another method. The results obtained by anionic labeling indicated that the method of preparation affects the surface more strongly if more highly concentrated solutions are used. Comparison of the data obtained by Ag^+ and I^- exchange methods revealed that the former are 6 to 10 times higher than the latter. It appeared probable that Ag^+ exchange in the $AgI-AgNO_3$ system is controlled by self-diffusion and is not affected by the surface charges. Preparation of a precipitate of strictly equivalent composition was found to be exceedingly difficult. (TTT)

16461 DISPERSION RELATION IN LIQUID HELIUM. Borst, Lyle B. (State Univ. of New York, Buffalo). Nature, 209: 187-8(Jan. 8, 1966).

The excitation spectrum in liquid helium obtained from the normal mode representation theory on the assumption of an observed empirical relation is discussed. The complete partition function and thermodynamic functions are given. A comparison of the empirical dispersion relation with the internal energy led to the observation that $C_2P = kT$ at the upper limit of the phonon region and again at P_0 and T_λ (where C_2 is the velocity of second sound near 1°K). The coherence length can be estimated. At P_0, the vibrational quantum number equals 4, the number of states per atomic pair of thermally excited rotors is 27, and the partition function 35000. The number of atoms participating is then 70000. (F.J.H.)

16462 ELECTRON-TRANSFER REACTIONS OF EUROPIUM(II) IN AQUEOUS PERCHLORIC ACID SOLUTIONS. Adin, A.; Sykes, A. G. (Univ. of Leeds, Eng.). Nature, 209: 804(Feb. 19, 1966).

The results of some preliminary experiments on the electron transfer reactions of Eu(II) in aqueous perchloric acid solutions are summarized. The results indicate that the transfers of f-orbital electrons is very difficult. (G.O.Y.)

16463 PLUTONIUM HEXAFLUORIDE SYNTHESIS. Slivnik, Joze. Nukl. Energ., No. 4, 12-13(1965). (In Slovak).

Plutonium hexafluoride was heated in the presence of oxygen to prepare PuO_2. Then HF was passed over the PuO_2 cleaned from possible traces of reduction agents. Fluorine gas was then passed through the vessel. Plutonium hexafluoride was sublimated from the vessel and NMR measurements made. The spectrum indicated that the product was pure. (M.C.G.)

16464 THE EXCITATION AND CHARACTERISTICS OF THE THORIUM SPECTRUM IN ELECTRODELESS DISCHARGE TUBES. Egorov, V. N.; Runkov, O. V. Opt. Spectros. (USSR) (Engl. Transl.), 19: 284-6(Oct. 1965). Translated from Opt. Spektros., 19: 511-14(Oct. 1965).

Reliable electrodeless discharge tubes containing 0.1 to 0.3 mg of thorium were prepared. A comparison was made among the spectra of thorium excited by magnetic fields of very different frequencies. The line-widths of thorium were measured and the causes of broadening of thorium lines in a high-frequency electrodeless discharge are discussed. (auth)

16465 LUMINESCENCE SPECTRA AND THE STRUCTURE OF HYDRATED URANYL NITRATES. Volodko, L. V. Opt. Spectros. (USSR) (Engl. Transl.), 19: 416-20 (Nov. 1965).

Translated from Opt. Spektros., 19: 751-8(Nov. 1965).

An analysis of the luminescence spectra of crystalline hydrates of uranyl nitrate with six, three, and two light and heavy water molecules at 90°K is given. The appearance in these spectra of vibrational frequencies of the nitrate groups and water molecules is established. The probable structure of the considered complexes is discussed. (auth)

16466 THE FLUORESCENCE OF RARE EARTHS. III. EMISSION SPECTRA OF SAMARIUM IN FLUORITE-TYPE PHASES AND IN MULTI-TYPE MIXED PHASES. Muller-Buschbaum, H. K.; Witzmann, H. (Griefswald Univ., Ger.). Opt. Spectros. (USSR) (Engl. Transl.), 19: 420-3(Nov. 1965).

Translated from Opt. Spektros., 19: 759-63(Nov. 1965).

The emission spectrum of samarium in the ThO_2-CeO_2 system was studied. The variations of the spectral position of the emitted lines and their intensities depend upon the composition of the mixed system. The maximum intensity of the characteristic lines of the samarium fluorescence occurs for about 12% CeO_2 in a ThO_2-CeO_2 mixture, permitting a determination of the mean cation radius with which the samarium activator implantation occurs without introducing imperfections. The fluorescence properties of the $CeO_2-Sm_2O_3$ and $(CeO_2-La_2O_3)$-Sm systems are described and discussed. (auth)

16467 INTERPRETATION OF THE FINE STRUCTURE OF THE SPECTRA OF Eu COORDINATION COMPOUNDS OF THE MX_3 TYPE. I. THEORY. SPECTRUM OF Eu BENZOYLACETONATE. Korolkov, V. S.; Kuznetsova, V. V. Opt. Spectros. (USSR) (Engl. Transl.), 19: 423-6 (Nov. 1965).

Translated from Opt. Spektros., 19: 764-70(Nov. 1965).

A method for analyzing the fine structure of the spectra of europium coordination compounds of the type MeX_3 is developed. The spectrum of europium benzoylacetonate is interpreted as an example. (auth)

16468 THERMAL DIFFUSION IN ISOTOPIC HYDROGEN AND HYDROGEN-HELIUM MIXTURES. II. EXPERIMENTAL MEASUREMENTS. Slieker, C. J. G. Physica, 31: 1388-1404(Sept. 1965).

The molecular potential field for the interaction of an asymmetric diatomic molecule with a symmetric one was previously calculated. With these new potential fields ther-

mal diffusion factors for some isotopic hydrogen mixtures and some hydrogen–helium mixtures were calculated. Experiments for the determination of these thermal diffusion factors are described. Moreover, a comparison is made between the experiments of Schirdewahn and the present results. It appears that both results can be brought into agreement if the experimental calculations are done with the initial value of the thermal diffusion factor of the D_2–H_2 system. Schirdewahn's approach to the calculation of thermal diffusion factors of asymmetric molecules is criticized and an effective mass for asymmetric molecules is introduced. (auth)

16469 CATION EXCHANGE AND ADSORPTION OF RADIONUCLIDES ON GLASS SURFACES. Lieser, K. H. (Technische Hochschule, Darmstadt, Ger.). Radio Chim. Acta, 4: 225-7(Dec. 1965). (In German).

The superposition of ion exchange and adsorption processes on glass surfaces was investigated using solutions of K_2CO_3, $Th(NO_3)_4$, $UO_2(NO_3)_2$, $AgNO_3$, $Sr(NO_3)_2$, carrier-free $BaCl_2$, $Ba(NO_3)_2$, $Pb(NO_3)_2$, and $Fe(NO_3)_2$. The amount of the radioactive material adhering to the glass surface was determined as a function of the solution concentration. The results obtained are shown graphically. In the concentration region over 10^{-3} mole/l the effect of the solution concentration caused a significant increase in the amount of radioactive material adhering to the glass surface. At lower concentrations no relation between the amount adhering and the solution concentration was detected. (J.S.R.)

16470 ON THE KNOWLEDGE OF CURIUM(III) PHOSPHATES. Weigel, F.; Haug, H. (Univ., Munich. Univ. of California, Berkeley). Radio Chim. Acta, 4: 227-8 (Dec. 1965). (In German).

The elementary cell of curium(III) phosphate was determined. The lattice constants a = 6.72, b = 6.93, and c = 6.37 Å with $\beta = 104° 6'30''$ were determined. The volume of the elementary cell was calculated as v = 287.7 $Å^3$ with a density of $\rho = 7.83$ g/cm^3. The experimental techniques are described. (J.S.R.)

16471 A HIGH-TEMPERATURE X-RAY STUDY IN A CONTROLLED ATMOSPHERE OF THE SYSTEM URANIUM–OXYGEN. Pialoux, Andre; Dode, Maurice (Faculte des Sciences, Orsay, France). Rev. Hautes Temp. Refract., 2: 319-22(Oct.-Dec. 1965). (In French).

The progressive oxidation of UO_2 to U_3O_8, under known oxygen potentials, was followed using x-rays at high temperature. The attainment of a state of equilibrium is shown by stabilization of the crystal parameters. (auth)

16472 ON URANYL PYROPHOSPHATE COMPLEXES. Dragulescu, C.; Julean, I.; Vilceanu, Nicoleta (Scientific Research Station, Timisoara, Rumania). Rev. Roum. Chim., 10: 809-19(Sept. 1965). (In French).

The reaction of uranyl nitrate with sodium pyrophosphate was studied by potentiometric, conductometric, spectrophotometric, radiometric, and radioelectrophoretic methods. The results obtained showed that the partners constitute one of the relatively few examples of components capable of functioning by turns as a coordination center and as an addendum. The complexes formed can be represented by the following general formulas $[(UO_2)_n P_2O_7]^{(2n-4)+}$ and $[UO_2(P_2O_7)_m]^{(4m-2)-}$, where n = 5 to 2, 1.6 and 1 and m = 1 and 2. The effect of hydrogen ions on the direction of the reaction was also studied using the same methods. (tr-auth)

16473 AN X-RAY AND INFRARED STUDY OF THE PERRHENATE TETRAHYDRATES OF THE RARE EARTHS AND YTTRIUM. Ivanov, V. I.; Varfolomeev, M. B.; Petrov, K. I.; Pervykh, V. G.; Plyushchev, V. E. (Lomonosov Inst. of Fine-Chemical Tech., Moscow). Soviet Phys.-Cryst. (Engl. Transl.), 10: 425-8(Jan.-Feb. 1966).

Translated from Kristallografiya, 10: 509-14(July-Aug. 1965).

The crystal system and space group were determined for these compounds; it was confirmed that there are three types of structure in this series. The cell parameters are reported, together with the infrared absorption spectra for some of the rare earth compounds. Praseodymium perrhenate was found to crystallize from solution as the monoclinic or orthorhombic form under identical conditions. (auth)

16474 AN X-RAY STUDY OF THE OXIDATION OF URANIUM DIOXIDE. Bessonov, A. F.; Strekalovskii, V. N.; Ust'yantsev, V. M. Soviet Phys.-Cryst. (Engl. Transl.), 10: 480-1(Jan.-Feb. 1966).

Translated from Kristallografiya, 10: 570-2(July-Aug. 1965).

High-temperature x-ray patterns of the oxidation of UO_2 were obtained. The phase composition of the UO_2 was monitored continuously during heating in air and during cooling. Isotherms were recorded at 200, 250, 320, and 360°C. The variation in d_{111}, with temperature is shown. It was concluded that the phase transitions during oxidation at 260 to 360°C are: $UO_2 \rightarrow UO_{2+x} \rightarrow \beta UO_2(U_4O_{9+y}) \rightarrow \gamma - UO_2$ (tetragonal) $\rightarrow \alpha - U_3O_8$. The x-ray patterns showed that $\gamma - UO_2$ (tetragonal) is formed only below 400°C and that metastable $\beta - U_3O_8$ is formed only above 320°C. (M.C.G.)

16475 DISTRIBUTION OF DEUTERIUM IN FRACTIONS OBTAINED IN THE PRETREATMENT OF CRUDE OIL. Blaga, Liviu; Blaga, Lucia; Chifu, Alexandra; Ciobotaru, Tamara (Inst. of Atomic Physics, Cluj). Stud. Cercet. Fiz., 17: 893-8(1965). (In Rumanian).

The effect of chemical separation of crude oil on the separation of the hydrogen isotopes was studied on fractions obtained in the pretreatment of asphalt-base and paraffin-base crude oils. The refinery samples were burned in oxygen, normalizing the resulting water with SO_2. The water was then subjected to isotopic determination, using a previously described method. The results indicated that the differences between the deuterium content of the various fractions does not exceed the limits of the experimental error. The deuterium content of the water obtained by burning the oil fractions was found to be lower than that of the city water. It was concluded that isotopic separation and fractionation are independent phenomena. (TTT)

16476 PURIFICATION AND PREPARATION OF SOME CESIUM COMPOUNDS. Simons, E. L.; Cairns, E. J.; Sangermano, L. D. (General Electric Co., Schenectady, N. Y.). Talanta, 13: 199-204(Feb. 1966).

Methods for the purification and preparation of cesium compounds are described. Thermogravimetric data are presented for cesium oxalate and cesium carbonate. (auth)

16477 ULTRASONIC VELOCITY IN AQUEOUS SOLUTION OF THORIUM NITRATE. Prakash, Satya; Srivastava, Som Prakash; Kapur, Shobhay Laxmi (Allahabad Univ., India). Vijnana Parishad Anusandhan Patrika, 7: 117-21 (Oct. 1964). (In Hindi).

Ultrasonic velocities and adiabatic compressibilities in the aqueous solutions of thorium nitrate were measured at 5 mc/sec by the light diffraction method. Ultrasonic velocity increased linearly with concentration and adiabatic compressibility decreased. The variation of apparent molar compressibility with the square root of the concentration did not follow Gucker's formula. According to some studies, the presence of a heavy or complex ion decreases the ultrasonic velocity. But in this case, when the heavy Th^{4+} ion was present, ultrasonic velocity did not decrease, instead it increased linearly. (auth)

16478 A RESIDUAL ACTIVITY METHOD FOR DETERMINATION OF SELF-DIFFUSION COEFFICIENTS IN SOLIDS. Frischat, G. H.; Oel, H. J. (Max Planck-Institut fuer Silikatforschung, Wuerzburg, Ger.). Z. Angew. Phys., 20: 195-201(1966). (In German).

A residual activity method for the determination of self-diffusion in solids is described; as an example ^{22}Na-diffusion in glassy and polycrystalline $Na_2O \cdot 2CaO \cdot 3SiO_2$ was measured. The method is applicable for isotopes of all radiations and for all solids and distinguishes the four important possibilities, viz., surface activity method $1/\mu \gg$

$2\sqrt{Dt}$, $1/\mu \ll 2\sqrt{Dt}$, and $1/\mu \approx 2\sqrt{Dt}$, where μ = absorption coefficient, D = diffusivity, and t = time of diffusion. Theory, experiments, errors, and the advantages of the method for brittle substances are discussed. (auth)

16479 INVESTIGATION ON THE RARE EARTH TERPYRIDYL SYSTEM. IV. TERPYRIDYL COMPLEXES OF HIGHER LANTHANIDES. Sinha, Shyama P. (Cyanamid European Research Inst., Geneva). Z. Naturforsch., 20a: 1661-4(Dec. 1965).

The preparation of terpyridyl chelates of heavier rare earths of the type $M(Terp)(NO_3)_3 \cdot n\,H_2O$ (M = Tb to Yb and n = 0 to 3) is described. Infrared studies of the solid chelates showed the coordinated nature of both terpyridyl and nitrate groups. A spectrochemical series based on the shift of the "breathing" vibration of terpyridyl in the complexes is proposed. (auth)

16480 THE CARBONYL COMPOUNDS OF TECHNETIUM. Hieber, Walter; Lux, Franz; Herget, Camillo (Technische Hochschule, Munich). Z. Naturforsch., 20b: 1159-65(Dec. 1965). (In German).

The carbonyl halogenides of technetium, $Tc(CO)_5X$ (where X = Cl, Br, I), in reactions with N-base ligands (L), organic compounds of phosphorus and its homologs, e.g., isonitriles, yield carbonyl disubstitution compounds $Tc(CO)_3L_2X$. With mercaptans, mercaptides, and dithiocarbamides displacing CO and halogen, polynuclear carbonyl compounds with sulfur linkages are formed. For example, the carbonyl chlorides $Tc(CO)_5Cl$ and $Tc(CO)_3L_2Cl$ in the presence of CO and $AlCl_3$ form the cationic carbonyl compound ions $[Tc(CO)_6]^{\oplus}$ and $[Tc(CO)_4L_2]^{\oplus}$. Such disubstituted carbonyl complexes and alkali alcoholates yield compounds such as $Tc(CO)_3L_2CO_2R$. A special glovebox for carrying out the high-pressure CO reactions is described. With this glovebox, contamination-free operations can be carried out with Tc carbonyls. (tr-auth)

16481 THE DETERMINATION OF STABILITY CONSTANTS OF COMPLEXES FROM A NON-EQUILIBRIUM DISTRIBUTION OF METAL BETWEEN AQUEOUS PHASE AND ION-EXCHANGER. Kyrs, M.; Rais, J. (Inst. of Nuclear Research, Czechoslovak Academy of Sciences, Rez). Z. Phys. Chem. (Leipzig), 230: 303-12(1965).

The possibility and advantages of a method of estimating stability constants of complexes in aqueous phase by studying a non-equilibrial distribution of the metal between the aqueous phase and an ion-exchanger are discussed theoretically. The conclusions were experimentally verified on three systems including Zr(IV), Y(III), Sr, and three different cation exchangers. (auth)

16482 REACTIONS OF LANTHANUM AND NEODYMIUM OXIDES WITH OXIDES OF THE GROUP II ELEMENTS OF THE PERIODIC TABLE. Andreev, A. B.; Keler, E. K. Zh. Prikl. Khim., 38: 2166-74(Oct. 1965). (In Russian).

X-ray, thermographic, selective chemical dissolution, and microscopic methods of analyses were used to detect solid phase reactions between lanthanum and neodymium oxides and the oxides of metals of the second periodic group (BeO, MgO, CaO, SrO, BaO, ZnO, and CdO). Al_2O_3 was added as a third component at ratios of La_2O_3 : RO : Al_2O_3 = 1 : 1 : 1 and 1 : 1 : 2 in a number of experiments. The x-ray and chemical data showed that La_2O_3 and Nd_2O_3 did not react with MgO, CaO, ZnO, SrO, CdO, or BaO on sintering a mixture of the oxides at 1400 to 1500°C. BeO reacted with La_2O_3 and Nd_2O_3 to form beryllates. In the presence of Al_2O_3 as a third component the x-ray data showed that $LaAlO_3$ or $NdAlO_3$ with a perovskite structure was formed as the predominant phase at 1500°C. No ternary compounds could be found in this three-component system. Evidence was found for the intermediate formation of a spinel ($MgAl_2O_4$) at 1200°C, which decomposed to a rare earth aluminate ($LaAlO_3$) at 1400 to 1500°C in the presence of a rare earth oxide (La_2O_3). The addition of 1% B_2O_3 improved the sintering qualities of the oxide mixture. (TTT)

16483 KINETICS OF REDUCTION OF LOW-OXIDE NIOBIUM BY CARBON. Lyubimov, V. D.; Gel'd, P. V.; Shveikin, G. P.; Alyamovskii, S. I. Zh. Prikl. Khim., 38: 2174-81(Oct. 1965). (In Russian).

Samples of NbO_2 were prepared by reducing Nb_2O_5 with hydrogen at 1000°C, and NbO samples were prepared by reacting a mixture of Nb_2O_5 and Nb metal powders at 1200 to 1600°C. The loss in weight of mixtures of NbO_2 + C showed that the reduction began at 1200°C, and the reaction rate increased up to 1600°C. Copious evolution of gas was observed at the initial stages of the reaction. X-ray analysis showed the formation of an intermediate carbide or oxycarbide. NbO was reduced more slowly than NbO_2 by carbon at all temperatures. The reaction rate was not affected on increasing the vacuum from 5×10^{-3} to 1×10^{-1} mm Hg std. The degree of reduction by carbon in one hour at 1400°C was increased from 39 to 56% by increasing the briquetting pressure of the initial mixture of powders from 1250 kg/cm^2 to 20 metric tons/cm^2. Acetylene carbon and charcoal were more effective as reducing agents than were graphite and coke at a briquetting pressure of 2500 kg/cm^2. Additions of soda and potash accelerated the reduction of NbO_2 (almost by a factor of two). The reaction rate for the reduction of NbO_2 was about a factor of two greater with an excess of carbon (NbO_2 + 3C) than it was with an equimolecular mixture (NbO_2 + C). These data indicated that the reduction is a two-stage process. The niobium oxides were reduced by CO gas, which was regenerated by reaction of CO_2 with carbon. (TTT)

16484 CRYSTALLINE STRUCTURE OF CESIUM TETRABROMURANYLATE $Cs_2[UO_2Br_4]$. Mikhailov, Yu. N.; Kuznetsov, V. G.; Kovaleva, E. S. (Kurnakov Inst. of General and Inorganic Chemistry, Academy of Sciences, USSR). Zh. Strukt. Khim., 6: 787-8(Sept.-Oct. 1965). (In Russian).

Crystals of $Cs_2[UO_2Br_4]$ are monoclinic with a = 9.90 ± 0.04, b = 9.808 ± 0.005, c = 6.39 ± 0.02 Å, and β = 103°30′ ± 1°. The space group is $P2_1/c$. The measured density is 4.51 g/cm^3 at 25°C. A total of 760 independent zero reflections were measured with Mo Kα radiation on a spherical single crystal having a diameter of 0.25 mm. The x, y, and z coordinates, respectively, are given in parentheses as follows: U(0,0,0), Cs(0.339, 0.116, 0.068), Br_I(0.026, 0.237, 0.258,), Br_{II}(0.718, 0.061, 0.836), and O(0.039, 0.103, 0.811). The anion complexes $[UO_2Br_4]^{-2}$ are connected by cesium cations Cs^+. The various interatomic distances are given. The coordination number of cesium is equal to 10($4Br_I$ + $4Br_{II}$ + 2O). (TTT)

16485 THE DISSOCIATION ENERGIES OF THE GASEOUS RARE-EARTH MONOXIDES [Thesis]. Ames, Lynford Lenhart. Columbus, Ohio, Ohio State Univ., 1965. 268p.

The dissociation energies of the gaseous rare-earth monoxides were investigated to determine the trends of dissociation energies with atomic number. The dissociation energies of the gaseous monoxides were calculated from the standard heat of the reaction, $M_2O_3(s) \rightarrow 2MO(g) + O(g)$, where M represents any rare-earth element. The thermodynamics of this reaction were investigated, employing the Knudsen effusion method to study the rate of vaporization of the solid rare-earth sesquioxides. A time-of-flight mass spectrometer with a high temperature Knudsen cell molecular beam inlet system was used to identify the vapor species in the vaporization of the sesquioxides. The mass spectrometer was also used to determine the trends in dissociation energies by determining the heat of the isomolecular gas-phase oxygen-exchange reaction, $M_a(g) + M_bO(g) \rightarrow M_b(g) + M_aO(g)$, where M_a and M_b represent different rare-earth elements. The monoxide dissociation energies were found to exhibit a double periodicity with atomic number similar to that observed in the heat of sublimation of the metals. This periodicity is attributed to the energy differences between the $4f^n5d6s^2$ and $4f^{n+1}6s^2$ electronic configurations of the rare-earth atoms and their various ground electronic states. (Dissertation Abstr.)

16486 ISOTOPE EFFECTS AMONG THE OXIDES OF NITROGEN IN THE GASEOUS AND LIQUID PHASES [Thesis]. Jeevanandam, Malayappa. New York, Columbia Univ., 1965. 215p.

The distribution of the stable isotopes of nitrogen between the gaseous nitrogen oxides and their solutions in organic solvents at various temperatures was determined. Nitrogen-15 concentrates in the liquid phase and the effective single-stage separation factor α ranges from 1.009 to 1.040. It increases with decrease of temperature. The influence of non-donor solvents like n-octane, n-heptane, n-hexane, cyclohexane, CCl_4, nitromethane, and "Freon-112" was compared with that of donor-solvents like 1,4-dioxane, 1,3-dioxane, 1,2-dimethoxyethane, dimethyl sulfoxide, and tetrahydrofuran. The results are interpreted in terms of the various equilibria involved. A 100-cm × 1-cm i.d. packed column was used to study the effect of such variables as temperature, concentration of the oxides of nitrogen, flow rate of solvents, and column packing. A marked improvement in the overall separation of ^{15}N over the $NO-N_2O_3$ system is obtained with the use of a carrier solvent. The distribution of the nitrogen and oxygen isotopes, between the gas and liquid phases of $N_2O_4-NO_2$ mixture in a dual-temperature system was determined. Both ^{15}N and ^{18}O concentrate in the liquid phase and the enrichment factor for oxygen is low. When the liquid phase is at 0°C, the observed enrichment factors for nitrogen increase from 1.009 with the gas phase at 27°C to 1.020 with the gas phase at 150°C. At higher gas phase temperatures the enrichment factor decreases. It is more sensitive to temperature changes of the cold bulb than of the hot bulb. A quantitative, spectrophotometric procedure was developed to analyze a gaseous mixture of the oxides of nitrogen. It was applied to the determination of the distribution of the oxides of nitrogen between the liquid and gas phases. (A.G.W.)

16487 THE REACTIONS OF HYDROCARBONS WITH DEUTERIUM ON CHROMIUM OXIDE GEL [Thesis]. Loner, Charles John. Evanston, Ill., Northwestern Univ., 1965. 114p.

The reactions of benzene and cyclohexene with deuterium on chromium oxide gel were studied. This catalyst, when activated at 475°C, will not catalyze the addition of hydrogen to benzene at temperatures below 150°C. This catalyst does, however, possess a high activity for the isotopic exchange of benzene with deuterium. At 80°C, in the gas phase, the exchange reaction is quite rapid, although not as rapid as addition of deuterium to olefins under the same conditions. Exchange of the benzene molecule occurs mainly by a process whereby only one deuterium atom is introduced per adsorption step. The experimental isotopic distribution patterns indicate that the concentration gradients in the catalyst pores are small. With respect to the activity of the catalyst for the benzene–deuterium exchange reaction, activation at 250°C results in low levels of catalyst activity; but catalyst activation at 300°C produces substantial activity. Activation at temperatures slightly higher than 300°C results in almost full development of activity for the exchange reaction. This behavior differs significantly from the development of activity for the hydrogenation of cyclohexene. Full catalytic activity for the addition reaction is obtained by activation above 400°C. It appears that benzene exchange and olefin hydrogenation involve different catalytic sites. Overall exchange of toluene with deuterium on this same catalyst is also quite rapid. On fully activated catalysts, isotopic exchange of the ring hydrogens at 110°C is about 10 times faster than exchange of the methyl hydrogens. The nature of both the mechanisms of these reactions and of the possible catalytic sites upon which they occur is discussed. (Dissertation Abstr.)

16488 THE OSMOTIC AND ACTIVITY COEFFICIENTS OF SOME ALKALI HALIDES IN HEAVY WATER AT 25 deg C [Thesis]. Kerwin, Robert Eugene. Pittsburgh, Univ. of Pittsburgh, 1964. 58p.

The isopiestic ratios of LiCl, NaCl, NaBr, NaI, CsCl, and $ZnSO_4$ to KCl were measured in heavy water. The activity and osmotic coefficients in these solutions were calculated from the isopiestic ratios using the known activity coefficients of $ZnSO_4$ in D_2O, recently determined by J. C. Rasaiah from electromotive force measurements. The results for the alkali halides indicate that the differences between the osmotic and activity coefficients in D_2O and H_2O solutions are linear functions of the composition when the unit of composition is moles of solute per 55.51 moles of solvent, indicated by m′: $\varphi_2(D_2O) - \varphi_2(H_2O) = km'$ and $\ln \gamma_2(D_2O) - \ln \gamma_2(H_2O) = 2km'$. The parameter k thus serves as a measure of the solvent isotope effect on these coefficients and is found to be small in all cases but indicative of electrolyte specificity. It is positive for LiCl, less positive for NaCl, zero for KCl, and slightly negative for CsCl. In the case of the sodium halides k is increasingly positive in the order NaCl < NaI < NaBr. These results may be interpreted either in terms of a small difference in the amount of Bjerrum solvation of the electrolytes in the two media or in terms of the relative influence of the respective electrolytes on the structure of the solvent. The activity coefficients were used along with known solubilities to calculate the standard molal free energies and entropies of transfer from D_2O to H_2O solution for NaCl and KCl. The resulting ΔG^0 values are −116 and −121 cal/mole for NaCl and KCl respectively, i.e., in the direction of spontaneous transfer of these electrolytes from D_2O to H_2O. The corresponding entropy changes are −1.32 and −1.47 eu and may be interpreted in terms of these salts having a greater disruptive effect in the more structured solvent D_2O. (Dissertation Abstr.)

16489 CRYSTALLOGRAPHIC MODIFICATIONS AND KINETICS OF PHASE TRANSFORMATIONS OF La_2O_3, Nd_2O_3, Sm_2O_3, Eu_2O_3, AND Gd_2O_3 [Thesis]. Stecura, Stephan. Washington, D. C., Georgetown Univ., 1965. 150p.

The kinetics of crystal transformations were studied by high-temperature x-ray-diffractometric techniques. The data obtained are interpreted according to the shrinking sphere model theory. Nd_2O_3 cubic-to-hexagonal and Sm_2O_3, Eu_2O_3, and Gd_2O_3 cubic-to-monoclinic transformations obey first order kinetics. The activation energies for these transformations were calculated using the Arrhenius equation. The activation energies for the Nd_2O_3 cubic-to-hexagonal and Sm_2O_3, Eu_2O_3, and Gd_2O_3 cubic-to-monoclinic transformations are 120, 150, 165, and 188 kcal per mole, respectively. The transformations probably occur through the diffusion of oxygen ions. On the basis of kinetic and crystal data, it is concluded that these transitions probably occur by a reconstructive transformation mechanism. Cubic and hexagonal x-ray-diffraction patterns for the sesquioxides were indexed by graphical methods while the monoclinic x-ray patterns were indexed by the analytical Ito's method. Lanthanum sesquioxide crystallizes in a hexagonal (A-type) modification only; neodymium sesquioxide, either in a cubic (C-type) or hexagonal modification or a mixture of both, depending on temperature and times of heating. Samarium oxide, europium oxide, and gadolinium oxide were either cubic or monoclinic (B-form) or a mixture of both, depending upon the decomposition temperatures and times of heating. Hexagonal La_2O_3 and Nd_2O_3, when fired in a high-temperature x-ray diffractometer furnace at temperatures above 1,100°C reacted with the B_2O_3 volatilizing from the alumina ceramic core used in the high temperature x-ray furnace. Boron oxide does not react with either the cubic or the hexagonal modification of Nd_2O_3 below 1,050°C. Sm_2O_3, Eu_2O_3, and Gd_2O_3 cubic and monoclinic modifications are not affected by boron oxide even at temperatures up to 1,450°C. (Dissertation Abstr.)

Organic Chemistry

Refer also to abstract 17959.

16490 (TID–22681) DERIVATIVES OF SOME FIVE-MEMBERED HETEROCYCLES AS POSSIBLE PROTECTIVE

AGENTS AGAINST IONIZING RADIATIONS. Final Report. Potts, Kevin T. (Louisville Univ., Ky. Dept. of Chemistry). Dec. 1965. Contract AT(40-1)-3016. 122p. Dep. mn. CFSTI $4.00 cy, $0.75 mn.

Methods for the synthesis of s-triazole derivatives, ring-fused s-triazole derivatives, meso-ionic compounds of the s-triazole series, and 1,3,4-oxadiazolium salts. The compounds were then evaluated for use in protection of mice against radiation. In general, maximum tolerated doses were given 15–20 min before exposure to 900 R whole-body x radiation. All evaluations were made on a 30-day survival basis. Data on 45 compounds are tabulated. (P.C.H.)

16491 PYROLYSIS OF POLYPHENYLS. PART I. CONTRIBUTION TO THE KINETICS OF THE THERMAL DECOMPOSITION OF TERPHENYLS. Barrera Pinero, R.; Manero Rodriguez, J. (Junta de Energia Nuclear, Madrid). An. Real Soc. Espan. Fis. Quim. (Madrid), Ser. B, 61: 1019-38(Sept.-Oct. 1965). (In Spanish).

Static tests on the thermal stability of commercial terphenyl mixtures and pure p-terphenyl, at temperatures ranging from 400 to 470°C, are described. The pyrolysis was controlled according to the following steps: gas evolution (hydrogen and hydrocarbons); intermediate-boiling compound formation; high-boiling residue formation; and decrease of starting material. Comparative data on decomposition rate and activation energy of the pyrolysis phenomena were tabulated, and a comparison was made with other published values. The kinetics of the reactions are discussed. (auth)

16492 CATALYTIC TRITIUM EXCHANGE REACTIONS WITH TRITIATED ACTIVE METHYLENE COMPOUND. Kudo, Ken-ichi; Adachi, Takayoshi; Hazue, Masaaki; Endo, Michio (Sumitomo Atomic Energy Ind., Ltd., Hyogo, Japan). Bull. Chem. Soc. Jap., 38: 2006-7(Nov. 1965).

The catalytic tritium-hydrogen exchange using ethyl malonate (active methylene-T) (I) as a tritium source is described. It is shown that alkyl hydrogens, by the use of a catalyst, are exchanged with I more easily than with tritium oxide. The catalytic activity of the transition, metals for benzene exchange is, in the following order: with I, Raney Ni > Pd-block > Pt-block; with tritium oxide, Pt-block > Pd-block > Raney Ni. The results of tritium exchange of toluene and m-xylene catalyzed by Pd-block and Raney Ni using I are shown. The effects of water on the isotopic exchange with I are given. (F.J.H.)

16493 THERMODYNAMIC CHARACTERISTICS OF AN ORGANIC COOLING AGENT. Retvari, Laszlo. Energ. Atomtech., 18: 477-80(Oct. 1965). (In Hungarian).

Organic coolants have the advantage that they may be employed at relatively low pressures and high temperatures; thus, the mixture known as Dowtherm A has a vapor pressure of only about 6 atm at 350°C, while if water is used in the same system, a pressure of 168.6 atm must be provided for. The material consists of a eutectic mixture of 26.5 wt. % biphenyl, $(C_6H_5)_2$, and 73.5 wt. % diphenyl oxide, $(C_6H_5)_2O$, with a melting point of 12.5°C and a boiling point of 255°C under 1 atm. The critical parameters are 41 atm and 528°C. Under continuous use, the material is stable up to 385°C and for short periods up to 415°C. Graphs are given for determining the entropy and the enthalpy of the material. Its heat of evaporation under 1 atm is 68.5 kcal/kg. As is the case of organic vapors in general, as the result of adiabatic expansion, the vapor of Dowtherm A becomes superheated while water vapor becomes humid. This fact presents design advantages as there is no need to provide for the removal of the moisture (TTT)

16494 LABELLING OF CORTICOTROPIN WITH ^{125}I. Galskov, A. (Univ. of Copenhagen). Experientia, 22: 63-4(Jan. 15, 1966).

A modification of the methods previously used in labeling corticotropin with ^{125}I and its separation from impurities on a Sephadex G-50 column are described. The yield of labeled corticotropin was about 50 to 60% and the specific activity about 350 to 600 mC/gm corticotropin. (F.J.H.)

16495 PREPARATION OF BROM SULPHALEIN LABELLED WITH ^{82}Br AND ^{197}Hg. Mani, R. S. (Atomic Energy Establishment, Trombay, India). Indian J. Chem., 3: 571-2(Dec. 1965).

Bromosulfaleins (BSP) labeled with ^{82}Br and ^{197}Hg for use in medicine, were prepared by refluxing BSP in acetate buffer solution (pH 4) with 10 to 15 mC of bromine (KBr solution) in the presence of H_2O_2 and by refluxing BSP in acetate buffer solution (pH 5) with ^{197}Hg nitrate solution. Purification of the samples was accomplished by column chromatography using dilute ammonia (3 to 4N) as eluant. Both the labeled bromosulfaleins were quite stable. (auth)

16496 PREPARATION OF ^{131}I-TYROSINES AND ^{131}I-THYROXINE. Abdel-Wahab, M. F.; Megahed, Y. M. (Middle Eastern Regional Radioisotope Centre for the Arab Countries, Cairo). Int. J. Appl. Radiat. Isotop., 17: 132-3(Feb. 1966).

A simple direct method for preparation of ^{131}I-labeled iodotyrosines and L-thyroxine-^{131}I is described. A solution of ^{131}I-labeled KI is mixed with ether and hydrogen peroxide. After 4 hr the ether layer is added to tyrosine or L-thyroxine. Monoiodotyrosine is formed in 8 hr and diiodotyrosine in 24 hr. The ^{127}I in L-thyroxine exchanges with ^{131}I in 48 hr. (M.C.G.)

16497 SOME PROPERTIES OF ORGANIC THORIUM SALTS. Tserkovnitskaya, I. A.; Charykov, A. K. (Leningrad State Univ.). Izv. Vyssh. Ucheb. Zaved., Khim. Khim. Tekhnol., 7: 544-50(1964). (In Russian).

The behavior of thorium salts with various organic acids during their solution in organic solvents was studied. Salts of aliphatic, dibasic, aliphatic-aromatic, displaced benzoic, and doubly displaced benzoic acids were considered. The composition of the salts was studied as a function of the pH values of the precipitate. A series of compounds of organic thorium salts able to be extracted by butyl alcohol was discovered. It was shown that many hydrolyzed thorium salts are capable of floating in organic solvents. Regularities in the composition and extractability of organic thorium salts were examined. (M.J.T.)

16498 STUDY BY INFRARED SPECTROMETRY OF SOME PHENYLMETHANES $(C_6H_5)_2CH_2$, $(C_6H_5)_2CHD$, $(C_6H_5)_2CD_2$, $(C_6H_5)_3CH$, $(C_6H_5)_3CD$. SYNTHESIS OF DEUTERIATED MOLECULES. Gruger, Alain; Lebas, Jeanne Marie (Univ., Paris). J. Chim. Phys., 62: 1318-33 (Nov.-Dec. 1965). (In French).

The infrared spectra of the compounds $(C_6H_5)_2CH_2$, $(C_6H_5)_2CHD$, $(C_6H_5)_2CD_2$, $(C_6H_5)_3CH$, $(C_6H_5)_3CD$, $(C_6H_5)_2CHCl$, and $(C_6H_5)_2CCl_2$ are reported between 400 and 3100 cm^{-1} and the Raman spectra of $(C_6H_5)_2CH_2$, $(C_6H_5)_3CH$, $(C_6H_5)_2CHCl$, and $(C_6H_5)_2CCl_2$ between 200 and 3100 cm^{-1}. The data showed the existence, for certain vibrations, of a significant coupling between the different nuclei. The stability of a large number of frequencies seemed to indicate that the different nuclei are in an identical electronic state. (tr-auth)

16499 VIBRATION SPECTRA OF IMIDAZOLE, IMIDAZOLE (D)-1, IMIDAZOLE (D_3)-2,4,5, AND OF IMIDAZOLE (D_4). PART I. REGIONS BETWEEN 4000 AND 1700 cm^{-1}. Bellocq, Anne-Marie; Perchard, Claudine; Novak, Alexandre; Josien, Marie-Louise (Faculte des Sciences, Bordeaux. Univ., Paris). J. Chim. Phys., 62: 1334-43(Nov.-Dec. 1965). (In French).

The infrared and Raman spectra of imidazole and some deuterated and halogenated derivatives were examined between 4000 and 1700 cm^{-1}. The valence frequencies of the CH vibrators, in the 2 and 4.5 position can be distinguished. It is shown that the maxima of the γNH absorption substructure of the self-associated imidazole are due to combinations of the internal vibrations. The type of the hydrogen bonding NH–N is discussed. (tr-auth)

16500 VIBRATION SPECTRA OF IMIDAZOLE, IMIDAZOLE (D)-1, IMIDAZOLE (D_3)-2,4,5, AND IMIDAZOLE (D_4). PART II. REGIONS BETWEEN 1700 AND 30 cm^{-1}. Perchard, Claudine; Bellocq, Anne-Marie; Novak, Alexandre

(Faculte des Sciences, Bordeaux. Univ., Paris). J. Chim. Phys., 62: 1344-58(Nov.-Dec. 1965). (In French).

An assignment of the ground frequencies of imidazole situated between 1700 and 250 cm^{-1} is proposed. Studies of the absorption spectra of this compound in several states and of the dichroism of an oriented crystal made it possible to identify the A′ and A″ vibrations. Assignment of the bands to vibrations of the CH and NH groupings and to the nucleus was affected by examining the infrared spectra in the solid state and the Raman spectra in aqueous solutions of 4 isotopic species of imidazole. The perturbations of the ground frequency due to association and vibrational coupling are discussed. The frequencies of external vibrations between 200 and 30 cm^{-1} were determined in absorption. (tr-auth)

16501 ISOTOPE EXCHANGE OF ACTIVE METHYL HYDROGENS. III. PREPARATION OF 2,4,6-TRI-d_3-METHYLPYRIDINE, 3,5-DI-d_3-METHYLPHENOL, 3,5-DI-d_3-METHYL-2-ACETYLFURAN, AND 4,6,8-TRI-d_3-METHYLAZULENE, FROM 2,4,6-TRI-d_3-METHYLPYRYLIUM PERCHLORATE. Balaban, A. T.; Gard, E.; Vasilescu, A.; Barabas, A. (Inst. of Atomic Physics, Bucharest). J. Label. Compounds, 1: 266-74(Oct.-Dec. 1965).

From 2,4,6-tri-d_3-methylpyrylium perchlorate, the compounds were obtained by reaction with aqueous or gaseous ammonia, aqueous sodium hydroxide, aqueous hydrogen peroxide, and sodium cyclopentadienide, respectively. The preparation in aqueous solution proved that the nucleophilic additions to the pyrylium ring proceed faster than the dedeuteration. Infrared and nuclear magnetic resonance spectra of these compounds confirm that their methyl groups are deuterated. (auth)

16502 SOLVENT EFFECT IN ISOTOPE EXCHANGE REACTIONS. III. THE INFLUENCE OF THE DIELECTRIC CONSTANT OF THE MEDIA ON THE RATE OF THE EXCHANGE OF THE IODINE ATOMS. Koroes, Endre; Orban, Miklos; Ladanyi, Laszlo; Pataki, Laszlo (Eoetvoes Lorand Tudomanyegyetem Szervetlen- es Analitikai-Kemiai Tanszeke, Budapest). Magyar Kem. Foly., 71: 463-8 (Nov. 1965). (In Hungarian).

The effects of the dielectric constant of benzene–nitrobenzene, chloroform-nitrobenzene, dioxane–water, and ethanol–water mixtures on the iodine isotope exchange reaction between elementary iodine and 1-phenyl-2, 3-dimethyl-4-iodopyrazolone are presented. The deviation from linearity in the increase in polarity during the exchange reaction observed in the case of benzene and nitrobenzene mixtures is attributed to the difference between the microscopic dielectric constant and the measured macroscopic value, while in the ethanol–water and dioxane–water mixtures, the deviation is due to kinetic factors introduced by the increase in the water content. (auth)

16503 KINETIC PROTIUM-DEUTERIUM ISOTOPE EFFECT IN AN INTRAMOLECULAR 1-5 SHIFT OF HYDROGEN. Kloosterziel, H.; Ter Borg, A. P. (Koninklijke/Shell-Laboratorium, Amsterdam). Rec. Trav. Chim., 84: 1305-14(Sept.-Oct. 1965).

The thermal isomerization of 5,8-dideuterocycloocta-1,3, 6-triene to the 1,3,5-isomer was studied. From the rate, as compared with that of the unlabeled compound, and from the distribution of the label in the rearranged material, values were obtained for the primary and secondary kinetic isotope effects. The large value of 5.0 at 120°C for the former corresponded to a nearly symmetrical transition state. (auth)

Radiation Chemistry

See *also* BIOLOGY AND MEDICINE — Radiation Effects on Biochemicals Radiation Effects on Tissues

Refer also to abstracts 16416 and 16583.

16504 (AD-627846) RADIATION-ENHANCED SURFACE ACTIVITY OF GAMMA HMX. Castorina, Thomas C.; Haberman, Jerome; Smetana, Andrew F. (Feltman Research Labs., Picatinny Arsenal, Dover, N. J.). Feb. 1966. 27p. (PA-TR-3282). CFSTI $2.00 cy, $0.50 mn.

The surface activity of one-micron particle size γ-octahydro-1,3,5,7-tetraintro-s-tetrazine (γ-HMX) was enhanced by cobalt-60 gamma irradiation. Surface activity was measured by a radiometric determination of adsorption of carbon-14 labeled stearyl trimethyl ammonium bromide (STAB) from solution. At doses ranging from 5 to 60 Mrads, the enhanced surface activity was found to be related to dose and the evolution of composite gaseous products derived from bulk as well as surface molecules. Although a one-Mrad irradiation of γ-HMX in vacuo produced no change in surface activity, such an irradiation of γ-HMX in contact with water vapor resulted in an enhancement of surface activity that was comparable to the effect of a 15-Mrad dose. Exposure of γ-HMX to NO_2 and NO increased surface activity by 28 and 42%, respectively; irradiation of these samples with one Mrad gave no additional enhancement. The increased rate of thermal decomposition was not specific to radiation-enhanced surface activity promoted by water vapors but was found to be a function of gamma interaction with bulk molecules as well. However, the increased rates of thermal decomposition of unirradiated samples of γ-HMX exposed to NO and NO_2 were attributed solely to thermally unstable reaction products of NO-HMX and NO_2-HMX surface adducts. (auth)

16505 (BNL-949) PROCESS RADIATION DEVELOPMENT PROGRAM SUMMARIES. Fifth Annual Contractors Meeting, October 7–8, 1965. (Brookhaven National Lab., Upton, N. Y.). Contract AT-30-2-GEN-16. 95p. (CONF-651064). Dep. mn. CFSTI $3.00 cy, $0.75 mn.

Twenty-eight articles are included on radiation processed wood-plastic materials; radiation chemistry and radiation synthesis of fluorocarbons, polymers, organometallic compounds, and organic compounds; artificial kidney membranes; radiation engineering; semiconductor device fabrication by neutron transmutation techniques; radiation chemical reactors; HIRDL operations; devices for recording activity of ^{60}Co gamma sources; theory and design of gamma monochromator; radiation effects on optical maser materials; and industrial application of radiation to colloid systems. (P.C.H.)

16506 (BNL-10020) CHEMONUCLEAR AND RADIATION CHEMICAL PROCESS RESEARCH AND DEVELOPMENT. Steinberg, Meyer (Brookhaven National Lab., Upton, N. Y.). Feb. 1966. Contract AT(30-2)-Gen-16. 42p. (CONF-660305-18). Dep. mn. CFSTI $2.00 cy, $0.50 mn.

From American Nuclear Society Topical Meeting, Augusta, Ga.

The guiding principles and some of the latest results in the development of nuclear energy for the synthesis and production of utility and industrial chemicals are presented. It was concluded that fissiochemonuclear processes for the fixation of nitrogen, synthesis of ozone, and production of carbon monoxide and hydrogen are sufficiently interesting from a long-term national goals point of view, to provide ample incentive for a continued orderly development of the science and technology of this field. Radio-induced chemical processes using isotopic and machine sources for chain reaction products will continue attracting further industrial development efforts. (auth)

16507 (INR-671/XVII/C) HYDROFOBIZACJA CELULOZY METODA RADIACYJNEGO SZCZEPIENIA STYRENU NA JEJ POWIERZCHNI. (Hydrophobization of Cellulose by Radiation Induced Grafting of Styrene on its Surface). Bulhak, Zofia; Zielinski, Waclaw (Institute of Nuclear Research, Warsaw (Poland)). 1965. 12p. Dep.

Radiation grafting of cellulose fibers by styrene, bearing in mind the hydrophobization of their surfaces, was carried out. The grafting was performed in pure liquid monomer

and in its solutions in dioxane, chloroform, and several alcohols, at different temperatures, in air, and in nitrogen gas atmosphere. The percentage function of water vapor absorbed and tensile strength of modified fibers was determined. (auth)

16508 (NYO–2771-13) NUCLEAR CHEMISTRY RESEARCH. Annual Report, January 1965–January 1966. Wolke, Robert L. (Wherrett Lab. of Nuclear Chemistry, Univ. of Pittsburgh, Pa.). Contract AT(30-1)-2771. 55p. Dep. mn. CFSTI $3.00 cy, $0.50 mn.

Studies of isomeric yield ratios and excitation functions of (d,p) and (d,n) reactions from approximately 4 to 15 Mev were completed. The (d,p) reactions and one of the (d,n) reactions were found to be in good agreement with distorted wave Born approximation calculations, while another of the (d,n) reactions is better accounted for by compound nucleus theory. The contributions of compound-nucleus-statistical mechanisms to deuteron-induced reactions, specifically (d,2n) and (d,γ) were also studied. It was found that the cross sections and excitation functions of both of these reactions can be almost entirely accounted for by compound-statistical theory, although the (d,2n) cross sections could contain a <25% contribution of a direct mechanism: stripping of a proton followed by evaporation of a neutron. In the determination of the pre-equilibrium, or primordial, charge states of few-Mev light recoiling ions, the target thickness problem now appears to be solved. Studies on the natural radioactivity of ^{113}Cd and spectrometry of the gamma rays from ^{48}Cr were initiated and preliminary results are given. (P.C.H.)

16509 (TID–22666) EFFECTS OF RADIATION QUALITY ON THE RADIOLYSIS OF WATER [Thesis]. Miller, Laurence Frederick (Kansas Engineering Experiment Station, Manhattan). 1966. 259p. Dep. mn. CFSTI $6.00 cy, $1.25 mn.

Kans. State Univ. Eng. Exp. Sta., Spec. Rep. No. 66.

A theoretical investigation was made on problems associated with the prediction of chemical reaction rates and yields of radioinduced chemical reactions. All problems considered were related to the assessment of the effects of radiation quality (energy and type of radiation). Particular emphasis was given to the determination of the energy spectra of electrons resulting from the irradiation of water by 14.6 Mev neutrons and by ^{60}Co gamma rays. Slowing-down spectra for charged particles produced in radiolysis were computed and used as a basis for models for the spur and track structure in irradiated water. Also involved in the establishment of the models were predictions of mean energy loss per spur and mean distance between spurs. These predictions, in turn, were based on empirical estimates of electron-scattering cross sections for low energy electrons and for small energy losses. Estimates of the yields of chemical reactions were based on approximate solutions of the partial differential equations describing simultaneous diffusion and chemical reaction along the tracks of charged particles. Yields were predicted for a simple chemical reaction and compared with experimental results previously determined. (auth)

16510 (NP-tr–1364). REACTION OF ACTIVE NITROGEN WITH ETHYLENE. Ikeda, Masamichi; Shinozaki, Yoshiharu; Meshitsuka, Gisuke. Translated by E. H. M. Colegrave (Atomic Energy Research Establishment, Harwell, Eng.), from Tokyo Metrop. Isotop. Res. Cent. Ann., 3: 57-64(1964). 18p. Dep. mn. JCL $1.60 fs, $0.80 mf.

The products of the reaction between active nitrogen and ethylene were analyzed; acetonitrile, propionitrile, allene, and methylacetylene, previously unconfirmed, were identified. In order to observe the effects of the wall, comparative tests were made under poisoned and unpoisoned conditions. In the former case, due to high nitrogen atom concentration, the yields of reaction products were on the whole greater than in the latter; but little difference was noted in the composition of the reaction products. However, with cyanogen the percentage of reaction product was higher in the poisoned series, while with allene, acrylonitrile, and acetylene the unpoisoned yielded the higher percentage of reaction products. From these results, the reaction mechanisms of the products were studied. (auth)

16511 ELECTRON SPIN RESONANCE ABSORPTION OF HEXANE/SILICA GEL SYSTEMS γ-IRRADIATED AT LOW TEMPERATURES. Kinell, Per-Olof (Swedish Research Councils' Lab., Studsvik); Lund, Anders; Vaenngard, Tore. Acta Chem. Scand., 19: 2113-23(1965).

The system hexane/silica gel and the pure components were irradiated at 77°K with ^{60}Co γ rays at a dose rate of 8 krad/hr to a total dose of about 0.7 ± 0.15 Mrad. Before irradiation the samples were carefully degassed. ESR spectra were recorded at 3-cm wavelength in the temperature range from 77 to 300°K. The absorption intensities at different compositions were measured at 77°K. Of the silica gel resonance lines, one at g = 2.0080 vanished at very low hydrocarbon contents, while another component at g = 2.0008, which showed ^{29}Si hyperfine structure was not influenced by the presence of the hydrocarbon. In the hydrocarbon phase the spectrum changed with the composition of the system and evidence was found for the existence of ethyl radicals. No hydrogen atoms were found in pure silica gel and only very small amounts in the composite systems. The dependence of the free radical yields on the hydrocarbon content is discussed in terms of two simple models. The yields of paramagnetic species in the two phases imply an interaction between the components and the magnitudes of the yields strongly suggest an energy transfer from the silica gel in the formation of free radicals. A saturation effect occurs at a hydrocarbon electron fraction of 0.02. This corresponds to a coverage of 5% of the BET surface. In a model where radicals are produced at active centers, the number of these was found to be about 10^{17} per m^2 BET surface. It was estimated that 5 to 25% of the radiation energy released in the silica gel is transferred to the hydrocarbon. The temperature dependence showed the ethyl radicals to be more stable than the other hydrocarbon radicals. The radicals formed at the lowest hexane contents were less stable than the radicals formed in the pure substance contrary to previously reported results for methane and ethane. (auth)

16512 ELECTRON SPIN RESONANCE STUDIES ON THE TRAPPED FREE RADICALS IN IRRADIATED AQUEOUS HYDROGEN PEROXIDE SOLUTIONS AT LOW TEMPERATURES. Safarik, I.; Mohos, B. (Central Research Inst. for Chemistry, Budapest). Acta Chim. Acad. Sci. Hung., 46: 159-64(1965).

The free radicals formed and trapped in irradiated aqueous H_2O_2 solutions at liquid N_2 temperature were investigated by the ESR technique. The line-shape of the ESR spectrum showed marked variation during the warming of the irradiated sample and similar changes were brought about by the accumulation of radicals when the sample at 77°K was irradiated. It was also found that above a certain temperature no additional variations took place in the spectrum shape at further increases of the temperature or the concentration of radicals. All the observations could be explained by assuming the simultaneous presence of the primary OH and the secondary HO_2 radicals in the sample. (auth)

16513 PROPAGATION OF CLEAVAGE CRACKS IN UNIRRADIATED AND X-RAYED NaCl SINGLE CRYSTALS. Agullo-Lopez, F.; Alvarez Rivas, J. L. (Junta de Energia Nuclear, Madrid). An. Real Soc. Espan. Fis. Quim. (Madrid), Ser. A., 61: 223-32(July-Aug. 1965).

Etch pits observations on cleavage planes of NaCl single crystals are described. The results depended very markedly on the cleavage crack velocity. For slow moving cracks, dense ($\geq 10^7$ cm^{-2}) dislocation bands appeared on the cleavage plane in places where the crack stopped. The depths of these bands were approximately 0.1 mm. They were formed by the screw ends of half-loops lying on the two slip systems nonorthogonal to the cleavage plane. Fast cracks did not cause any of such dislocation arrangements; they left the dislocation density unchanged. For a stopped crack, observations normal to the cleavage plane showed the dislocation pattern at the tip. In this pattern, two narrow arrays, about 1 mm long, consisting of a few edge

dislocation rows arose from the crack tip. In addition, a [100] row of dislocations continuing the crack line was observed. A schematic model that fits all observations is given. The influence of x rays on these results is also presented. No apparent changes were found in the irradiated samples, up to 70,000 R. (auth)

16514 ARTIFICIAL RADIOACTIVE CARBONIZATION. Stach, E.; Depireux, J. Brennstoff-Chem., 46: 7-13(Jan. 1965). (In German).

The carbonization of 4 coal samples from Ruhr coal deposits was increased in the microscopic range by α radiation from a polonium source. The carbon enrichment and the loss of volatile constituents were measured by surface reflection. The process of artificial radioactive carbonization is different from natural radioactive carbonization. (tr-auth)

16515 NITROUS OXIDE AS AN ELECTRON SCAVENGER IN THE RADIOLYSIS OF HYDROCARBONS. Sato, Shin; Yugeta, Rei; Shinsaka, Kyoji; Terao, Terumi (Tokyo Inst. of Tech.). Bull. Chem. Soc. Jap., 39: 156-60(Jan. 1966).

Nitrous oxide was used as an electron scavenger in the radiolysis of hydrocarbons: cyclohexane, cyclohexene, benzene, and their mixtures. Considering that the energy for the formation of an ion pair is about 25 ev in hydrocarbons, 0.4 mole l^{-1} of nitrous oxide is not enough to capture all the electrons ejected from irradiated hydrocarbons. In the case of cyclohexane, 70% of the ejected electrons seem to be captured by 0.4 mole l^{-1} of nitrous oxide. In the case of benzene, $G(N_2)$ is about a half of that for cyclohexane. This was explained tentatively in terms of the ability of benzene to capture electrons. The $G(H_2)$'s in the cases of cyclohexene and benzene have not shown any noticeable dependence on the concentration of nitrous oxide. This shows that hydrogen does not result from the neutralization in these systems. In order to clarify them, the primary processes in the radiolysis of cyclohexane were further considered using the data previously obtained. (auth)

16516 ELECTRON SPIN RESONANCE OF SODIUM POLYPHOSPHATE GLASS IRRADIATED WITH γ RAYS. Miura, Masaji; Hasegawa, Akinori (Hiroshima Univ.). Bull. Chem. Soc. Jap., 39: 196(Jan. 1966).

The relation between the degree of polymerization and the effects of gamma rays on sodium polyphosphate glasses were studied using ESR and optical absorption measurements at room temperature. The ESR spectra of three glasses with different degrees of polymerization show two doublets; the larger doublet is due to a hole trapped by the main chain of polyphosphate while the smaller doublet is due to a hole trapped by the end group. (F.J.H.)

16517 CHEMICAL DOSIMETRY IN IRRADIATION AT HIGH DOSE RATES. I. AQUEOUS SOLUTIONS. Lutgen, P.; Claes, P. (Univ., Louvain, Belg.). Bull. Soc. Chim. Belges, 74: 572-80(Nov.-Dec. 1965). (In French).

Air-free aqueous solutions of ferrous sulfate and oxalic acid were tested as dosimeters for irradiations at high dose rates and nonhomogeneous energy repartition. The extent of the reaction was strongly dose-rate dependent. It appeared that diffusion of the solute to the irradiated zone is the rate determining step. The tested solutions are thus not accurate dosimeters for the irradiations used. (auth)

16518 CHEMICAL DOSIMETRY IN IRRADIATION AT HIGH DOSE RATES. II. ORGANIC LIQUIDS. Lutgen, P.; Claes, P. (Univ., Louvain, Belg.). Bull. Soc. Chim. Belges, 74: 581-90(Nov.-Dec. 1965). (In French).

Hydrogen production by irradiation of organic compounds was investigated for dosimetry purposes. Hydrogen formation during radiolysis of cyclohexane was independent of dose rate and LET, but depended on dose. The usefulness of cyclohexene is lessened by a low $G(H_2)$ which depends on the nature of radiation. Cyclohexane–cyclohexene mixtures with an electronic fraction between 0.05 and 0.1 seemed to possess the features desirable in a dosimeter, especially for irradiations at high dose rates and nonhomogeneous energy repartition. (auth)

16519 ^{60}Co γ-RADIOLYSIS OF HYDROGEN HALIDES AT 77°K. Rumfeldt, R. C.; Armstrong, D. A. (Univ. of Alberta, Calgary). Can. J. Chem., 44: 191-7(Jan. 15, 1966).

Yields of hydrogen formed in ^{60}Co γ radiolyses of pure polycrystalline samples of HBr and HCl at 77°K decrease with increasing dose in the range 0 to 1×10^{18} ev per g. The true initial yields are $G(H_2)_{\text{solid HCl at } 77°K} = 6.3 \pm 0.2$ and $G(H_2)_{\text{solid HBr at } 77°K} = 12.3 \pm 0.3$. Within experimental error these are the same as the respective liquid-phase yields at –79°C. For doses in excess of 2×10^{18} ev per g the dose dependence is no longer significant and the yields tend toward plateau values of 3.2 ± 0.1 and 10.3 ± 0.1 for HCl and HBr respectively. The dose dependence of the hydrogen yields is attributed to the scavenging of a reactive intermediate by the halogen atoms and molecules, which accumulate in the solid matrix as the dose increases. In independent experiments with an apparatus of the Klein–Scheer type it is shown that hydrogen atoms reacted readily with films of HBr at 77°K. There was however, no evidence of a significant reaction with HCl at this temperature. The difference in behavior of the two hydrogen halides may be explained by their different activation energies for reaction with hydrogen atoms. The results of the γ radiolyses are discussed. It is suggested that the dose dependence may be a result of the scavenging of an ionic intermediate rather than a thermal hydrogen atom. (auth)

16520 THE RADIOLYSIS OF ALKALINE AQUEOUS SOLUTIONS CONTAINING HYDROGEN AND OXYGEN. Armstrong, W. A. (Dept. of National Defence, Ottawa, Can.). Can. J. Chem., 44: 737-41(Mar. 15, 1966). (DCBRL–482).

The initial yields of H_2O_2 in aerated water, $G(H_2O_2)^{O_2}$, and in water containing H_2 and O_2, $G(H_2O_2)^{H_2,O_2}$, were measured for alkaline solutions irradiated with ^{60}Co γ rays. $G(H_2O_2)^{O_2}$ decreased with increasing pH from a value of 1.22 in neutral solution to 0.63 in solutions of pH 13.92 and the relation, $G(H_2O_2)^{O_2} = G_{H_2O_2} - \frac{1}{2}G_{OH} + \frac{1}{2}G_{red}$, was valid over the pH range from 7 to 14. $G(H_2O_2)^{H_2,O_2}$ decreased from 3.30 in neutral solution to a minimum of 2.00 at pH 11.35 and then increased to 2.65 pH 13.92. The equation, $G(H_2O_2)^{H_2,O_2} = G_{H_2O_2} + \frac{1}{2}G_{OH} + \frac{1}{2}G_{red}$, which was applicable for neutral solutions, was not valid for basic solutions. A reaction mechanism in accordance with the observed results and the literature values of the rate constants of likely radical reactions was developed. It was assumed that in the alkaline solutions investigated OH radicals react with OH^- ions to form O^- radicals, which react preferentially with O_2 to form O_3^- radicals, which then react either with H_2 or H_2O_2. The increase in $G(H_2O_2)^{H_2,O_2}$ at pH > 12 is attributed to a difference in the rate of reaction of O_3^- with H_2O_2 and HO_2^-, $k(O_3^- + H_2O_2)/k(O_3^- + HO_2^-) = 2.45$. (auth)

16521 MICROSCOPIC VISUALIZATION OF DOSE DISTRIBUTIONS. McLaughlin, W. L. (National Bureau of Standards, Washington, D. C.). Int. J. Appl. Radiat. Isotop., 17: 85-96(Feb. 1966).

Colorless cyanides of triphenylmethane dyes when suitably activated can be made into films that become deeply colored on irradiation with short-wave ultraviolet and ionizing radiations, but are not sensitive to near ultraviolet radiation or visible light. The response range for x rays, γ rays, and electrons is approximately 10^5 to 10^8 rad. Experiments showed that, because of their stability, low energy dependence, and high spatial resolution, these solid systems have excellent potential for visual inspection of high-level dose distributions on a microscopic scale. Since molecular excitations due to low-energy secondaries are most important to over-all radiation effects, the relatively high sensitivity of such dye systems expected in the intermediate and for ultraviolet may represent an advantage in dosimetry. (auth)

16522 THE EFFECT OF PENETRATING RADIATION ON THE PROPERTIES OF POLYAMIDE FIBERS. PART I: FUNDAMENTALS, SAMPLE MATERIALS, CONDITIONS OF IRRADIATION, AND THE METHODS USED FOR EVALUATION. Heger, A. (Institut fuer Technologie der Fasern, Dresden). Isotopenpraxis, 1: 71-8(Nov. 1965). (In German).

A survey of data known on the behavior of polyamides under irradiation with penetrating radiation is given. The materials investigated, the conditions of irradiation, and the methods used for evaluating the results are discussed. (auth)

16523 EFFECTS OF PRELIMINARY γ IRRADIATION AND HEATING ON THE ACTIVITY OF THE $Ag/Ag_2C_2O_4$ CATALYST. Sviridov, V. V.; Branitskii, G. A.; Potanina, L. V. (Belorussian State Univ., USSR). Izv. Vyssh. Ucheb. Zaved., Khim. Khim. Tekhnol., 7: 577-82(1964). (In Russian).

Gamma irradiation (with dose 2.4×10^5 R) of $Ag/Ag_2C_2O_4$ catalysts obtained using partial tribochemical separation of silver oxalate, shows little effect on their activity in hydrogen-peroxide dissociation reactions. Heating the catalysts at 40 and 80°C leads to an increase of the catalytic activity, especially significant in the latter case. Irradiation preceding heating weakens the effectiveness of heating at 40°C. A small radiation dose (2×10^3 R) leads to the same result, if the heating is carried out at 80°C. More significant doses in these conditions lead to a significant intensification of the effectiveness of heating. (M.J.T.)

16524 THE REACTION OF HYDROGEN ATOMS WITH SOME CONJUGATED RING SYSTEMS AT 77 DEG K. Leone, J. A.; Koski, W. S. (Johns Hopkins Univ., Baltimore). J. Amer. Chem. Soc., 88: 656-8(Feb. 20, 1966).

Binary mixtures of naphthalene with methanol and ethanol were irradiated with x rays at 77°K and studied by ESR methods. Previous work determined that, upon irradiation, the hydroxyl hydrogen is liberated and subsequently adds on to the conjugated ring system. With naphthalene, the hydrogen atom adds on in the α position. Molecular orbital calculations of the cyclohexadienyl radical and the corresponding naphthalene radical show good agreement with the data obtained. (auth)

16525 PARAMAGNETIC ABSORPTION OF IRRADIATED GLYCINE. Box, Harold C.; Freund, Harold G.; Budzinski, Edwin E. (Roswell Park Memorial Inst., Buffalo). J. Amer. Chem. Soc., 88: 658-61(Feb. 20, 1966). (NYO-3558-2).

Single crystals of deuterated glycine, $^+ND_3-CH_2-COO^-$, were irradiated at 77°K and subsequently warmed to 165°K. Well-defined electron spin resonance spectra were observed due to either CH_2COO^- or CH_2-COOD. The intensities of sixteen allowed and forbidden transitions calculated on the basis of a simple model agree well with the observed hyperfine patterns. (auth)

16526 REACTIVITY OF HYDROGEN ATOMS TOWARD SOME COBALT(III) COMPLEXES IN AQUEOUS SOLUTIONS. Halpern, Jack; Rabani, Joseph (Univ. of Chicago). J. Amer. Chem. Soc., 88: 699-704(Feb. 20, 1966).

Kinetic studies on the reduction of various cobalt(III) complexes by hydrogen atoms are described. The hydrogen atoms were generated by ^{60}Co γ irradiation of the solutions and the rates of reaction with the cobalt(III) complexes determined by competition with the reaction with ethanol. Rate constants ranging from 3.3×10^{10} to 2.0×10^7 M^{-1} sec^{-1} (at 26°) were determined for the reactions of H atoms with $Co(NH_3)_5I^{2+}$, $Co(NH_3)_5Br^{2+}$, $Co(NH_3)_5NCS^{2+}$, $Co(NH_3)_5$(H-fumarate)$^{2+}$, $Co(NH_3)_5Cl^{2+}$, $Co(NH_3)_5N_3^{2+}$, $Co(NH_3)_3(NO_2)_3$, $Co(NH_3)_5NO_2^{2+}$, $Co(NH_3)_5CN^{2+}$, and $Co(CN)_5^{3-}$, along with upper limits for reactions with a number of other cobalt(III) complexes. In a number of cases the rates of reactions with the corresponding free ligands also were determined. The mechanisms of these reactions and the relation of the observed reactivity patterns for H atoms to those for other reductants are discussed. (auth)

16527 RADIATION-INDUCED GRAFT COPOLYMERIZATION OF BUTADIENE TO POLYETHYLENE AND POLYPROPYLENE. Furuhashi, Akira; Kadonaga, Masao (Nippon Telegraph and Telephone Public Corp., Tokyo). J. Appl. Polymer Sci., 10: 127-41(Jan. 1966).

Polyethylene (PE) and polypropylene (PP) films were irradiated by γ irradiation from a ^{60}Co source in butadiene gas flow and in liquid butadiene. Irradiating in the butadiene gas flow was convenient because the gas state monomer was available directly and little homopolymer was produced. In this case, there was retardative effect on the grafting near the surface of the film and the grafting rate showed the maximum values at 50 to 60°C for high-density PE and PP. Irradiating in the liquid butadiene decreased the retardative effect near the surface. The effect of dose rate I on the grafting rate R_p was represented by $R_p \propto I^{1/4}$ in this case. The grafting rate was always higher in high-density PE than in low-density PE. Results of x-ray diffractometry and electron microscopy indicated that the grafting reaction occurred predominantly near the surface of the crystallite (lamella) of PE and the grafting rate was not affected by the overall crystallinity of the trunk polymer but by the configurational structure, such as the degree of branching or side-chain length. (auth)

16528 STRUCTURE AND PROPERTIES OF CELLULOSE GRAFT COPOLYMERS. I. RADIATION-INDUCED RAYON–STYRENE GRAFT COPOLYMERS. Huang, Robert Y.-M. (International Cellulose Research Ltd., Hawkesbury, Can.). J. Appl. Polymer Sci., 10: 325-41 (Feb. 1966).

Rayon–styrene graft copolymers were prepared by the direct radiation method, with the use of the preswelling technique, by irradiation with γ rays from ^{60}Co. The grafting was carried out in bulk styrene and in styrene–solvent mixtures, such as styrene–methanol and styrene–acetone, to study their effect on the graft copolymerization reaction and the structure of the resulting graft copolymer. The effects of carbon tetrachloride, a chain-transfer agent, were also investigated. Three different types of rayon yarn were used; Fortisan, a modifier-type high wet-modulus rayon, and a high-tenacity tire yarn, in order to study the effect of rayon microstructure on the grafting reaction. The molecular structure of the rayon–styrene graft copolymers was studied by hydrolyzing away the cellulose backbone and measuring the molecular weights of the grafted polystyrene branches. For grafting in bulk styrene, the molecular weights of the grafted polystyrene ranged from 400,000 to 1,000,000, while those of the polystyrene homopolymer formed in the outside solution were of the order of 30,000 to 50,000. The molecular weights of the grafted polystyrene branches tended to increase with per cent grafting in the graft copolymer. For grafting in styrene–methanol and styrene–acetone mixtures, the molecular weights of the polystyrene branches decreased with increasing solvent content. The addition of carbon tetrachloride to bulk styrene resulted in a sharp decrease in the molecular weights of the grafted branches. The grafting frequency or number of polystyrene branches per cellulose chain was calculated from the per cent grafting and the molecular weights of the polystyrene branches. The morphology of the rayon–styrene graft copolymers and some of their physical properties are discussed. (auth)

16529 STUDY OF THE PARAMAGNETIC CENTERS PRODUCED IN IRRADIATED POLYCRYSTALLINE $Mo_7O_{24}(NH_4)_6.4H_2O$. Pascaru, Iancou; Constantinescu, Olimpiu; Constantinescu, Marie; Arizan, Dan (Inst. of Atomic Physics, Bucharest). J. Chim. Phys., 62: 1283-8 (Nov.-Dec. 1965). (In French).

Paramagnetic centers produced by the γ irradiation of $Mo_7O_{24}(NH_4)_6 \cdot 4H_2O$ at the temperature of liquid nitrogen and at room temperature were studied. The EPR spectra were attributed to radicals of the NH^{3+} type and to the pentavalent molybdenum formed by reduction of Mo(VI) in the irradiation process. The behavior of Mo(V) during thermal treatment was explained by an oxidation-reduc-

tion mechanism. The variation of the concentration of Mo(V) produced by the irradiation was studied as a function of the integral dose and as a function of time at temperatures of 125, 150, and 175°C. (tr-auth)

16530 RADIOLYSIS OF BINARY MIXTURES. I. LIQUID PHASE STUDIES WITH BENZENE–METHANOL. Ekstrom, A.; Garnett, J. L, (Univ. of New South Wales, Sydney); J. Phys. Chem., 70: 324-30(Feb. 1966).

Addition of small concentrations of benzene to methanol resulted in a sharp decrease in the radiolysis yields of hydrogen and ethylene glycol. This study suggested that free-radical scavenging is of significant importance. Scavenging products such as cyclohexadiene, cyclohexadiene–methanol, and anisole were formed along with a large number of unidentified products of molecular weight as high as 450. The effect of benzene concentration on the yield of the identified scavenging products was measured. From these data, a reaction scheme is proposed to account for the formation of the scavenging products. (auth)

16531 ELECTRON SPIN RESONANCE OF COLOUR CENTRES IN γ-IRRADIATED PLANAR LEAD HALIDES. Patankar, A. V.; Schneider, E. E. (Univ. of Newcastle-upon-Tyne, Eng.). J. Phys. Chem. Solids, 27: 575-9 (Mar. 1966).

The electron spin resonance spectra of single crystals of two of the planar lead halides, chloride and iodide, irradiated at liquid nitrogen temperatures with γ rays from a cobalt source, have been investigated at 9.5 Gc/sec. In both halides the spectrum as observed at low temperatures consists of two asymmetric lines with g-factors close to 1.999 and 2.006 which are presumably associated with trapped electrons and holes respectively. The halfwidths are 3 and 10 G respectively even at concentrations exceeding 10^{18} cm^{-3} which suggests exchange narrowing, and the relaxation behavior follows the simple Bloch theory. The characteristic line shape and the absence of orientation dependence are explained by assuming that the resonances arise from a random distribution of anisotropic spin systems. The observed line shapes are compared with the theoretical resonance profiles for a powder-like assembly of spins having three unequal g-components. This indicates that the surroundings of the resonance centers have a glass-like structure and suggests that the trapping sites are jogs in dislocation lines. The remarkably high efficiency of generation of radiation centers (only 3 ev absorbed γ energy are required per center) and the high equilibrium concentration of 10^{19} cm^{-3} at a γ-dose rate of 2.2 Mr/hr suggest further that this large scale deformation is produced by a radiation-induced mechanism of multiplication and motion of dislocations. (auth)

16532 EFFECT OF GAMMA RADIATION ON MAGNETIC DIFFUSION IN NICKEL–ZINC FERRITES. Trinkler, E. (Inst. of Physics, Academy of Sciences, Latvian SSR). Latv. PSR Zinat. Akad. Vestis, No. 10, 93-7(1965). (In Russian).

The effects of gamma radiation on the disaccommodation process in nickel zinc ferrites was studied on the radiation circuit of the atomic reactor of the Academy of Sciences, Latvian SSR. Alterations in the activation energy of the disaccommodation process that occurred during gamma-irradiation were compared with alterations in activation energy of the electric conductivity process under the same conditions. The quantitative conformity of the values of the energies compared permitted the existing assumption of the unity of the electronic mechanism responsible for both magnetic and electric properties of nickel zinc ferrites to be confirmed. (auth)

16533 CONTROL OF SELF-IRRADIATION DECOMPOSITION OF TRITIUM-LABELLED COMPOUNDS AT HIGH SPECIFIC ACTIVITY. Evans, E. Anthony (Radiochemical Center, Amersham, Eng.). Nature, 209: 169-71(Jan. 8, 1966).

Results of the investigation of two aspects of the control of the decomposition of tritiated organic compounds from self-decomposition on storage are presented. The two aspects studied are: use of radical scavengers for compounds stored in aqueous solution and storage at very low temperatures (−196°C). Both methods were found to be very effective in reducing the rate of decomposition. The compounds selected for use as radical scavengers were benzyl alcohol, ethyl alcohol, and sodium formate (or formic acid). Solutions of thymidine-2-^{14}C (specific activity 18.3 mC/m mole) at 10 μC/ml containing the scavengers in concentrations ranging from 0.001 to 1% were irradiated with gamma rays to a total dose of 2.5 megarads. The results indicated that benzyl alcohol at 1% concentration was effective in protecting the thymidine-2-^{14}C. Results obtained on keeping selected tritiated nucleosides and amino-acids of specific activity in solutions containing benzyl alcohol, ethanol, and sodium formate as radical scavengers indicated that all three scavengers are effective in reducing the rate of self-irradiation decomposition of the tritium-labeled compounds. The rates of decomposition of a number of tritiated compounds stored at −196°C were examined. The rate of decomposition was reduced, but the use of a protecting solvent was generally necessary. (F.J.H.)

16534 MATRIX ISOLATION OF UNSTABLE HALOGEN RADICAL IONS. Brown, D. M.; Dainton, F. S. (Univ. of Leeds, Eng.). Nature, 209: 195-6(Jan. 8, 1966).

The formation of reduced metal valency states in gamma-irradiated H_2SO_4 glasses at 77°K was observed. The optical absorption produced by gamma-irradiated sodium chloride (0.1 to 1.0M) in H_2SO_4 at 77°K is shown on addition of NaCl the absorption and optical density increased. The peak with λ_{max} = 33mμ was observed only when chloride was present in the glass. A change of extinction coefficient with temperature was observed. The behavior of gamma-irradiated $NaBr-H_2SO_4$ glasses was found to be similar to that described for $NaCl-H_2SO_4$ glasses. The treatment of sodium iodide was just the reverse from that of sodium bromide and chloride. The iodide gave a strong absorption bond at room temperature and a weak bond at 77°K on gamma-irradiation in the region of 380mμ, which is where an absorption due to I_2^- was previously observed in liquid water. (F.J.H.)

16535 STABILITY OF A RADIOACTIVE DRUG—TETRASODIUM 2-METHYL-1,4-NAPHTHAQUINOL DIPHOSPHATE LABELLED WITH TRITIUM. Evans, E. A. (Radiochemical Center, Amersham, Eng.). Nature, 209: 196-7(Jan. 8, 1966).

The decomposition by self-irradiation of the radioactive drug tetrasodium 2-methyl-1,4-naphthaquinol diphosphate labeled in the 5, 6, and/or 7 positions with tritium is described. Its decomposition in isotonic saline solution at different storage temperatures and times are given. The radiochemical purity of the stored drug was determined after various time intervals, by paper chromatography. Less than 10% tritium was actually lost from the molecule by exchange in the aqueous solution during one year of storage, but the decomposition gave rise to three major products, which were not identified. (F.J.H.)

16536 EFFECT OF TEMPERATURE ON THE γ RADIOLYSIS OF WATER VAPOR. Anderson, A. R.; Knight, B.; Winter, J. A. (Atomic Energy Research Establishment, Harwell, Eng.). Nature, 209: 199-200 (Jan. 8, 1966).

Values of $G(H_2)$ from the gamma radiolysis of water vapor ($p \sim 1.5$ atm) were measured at a concentration of 5 mole % cyclohexane, which is sufficient to scavenge all the H atoms produced. The mean yields of H_2 from water vapor are $G(H_2) = 7.0 \pm 0.4$ from 120 to 240°C and $G(H_2) = 10.6 \pm 0.6$ at temperatures >300°C. The observed yields gave $g(e^-) = 3.6$, which agreed with the theoretical value of $g(e^-) = 3.28$ to 3.57 based on $W(H_2O) = 28$ to 30 ev. The enthalpy changes in the process are discussed. (F.J.H.)

16537 STEREOSPECIFIC ADDITION OF HYDROGEN TO FUMARIC ACID IN IRRADIATED SINGLE CRYSTALS OF SUCCINIC ACID. Miyagawa, Ichiro (Duke Univ., Durham, N. C.); Itoh, Koichi. Nature, 209: 504(Jan. 29, 1966).

A high stereospecific efficiency was obtained in the addition of H to fumaric acid by using irradiated, single crystals of succinic acid grown from slowly cooled aqueous solutions of mixtures of succinic and fumaric acids. In the crystals grown from aqueous solutions, only the primary species was detected. In the deuterium-substituted crystals, grown in heavy water, the $DOOCCD_\beta H_\beta{}^1CHCOOD$ species was detected in addition to the primary species. The concentration of $DOOCD_\beta H_\beta{}^1CHCOOD$ increased with the concentration of fumaric acid in the crystal. (G.O.Y.)

16538 CARBOXYLATION OF FORMIC ACID IN AQUEOUS SOLUTIONS UNDER THE INFLUENCE OF U.V.-LIGHT. Getoff, Nikola (Oesterreichischen Akademie der Wissenschaften, Vienna). Photochem. Photobiol., 4: 433-8 (June 1965).

The effects of uv light on the carboxylation of formic acid was investigated in detail to obtain more information about the reaction mechanism. In addition, an attempt was made to compare this mechanism with those proposed for the carboxylation caused by ^{60}Co γ rays. Carboxylation of various organic substances by dissolved carbon dioxide or bicarbonate was achieved by the action of uv light of 184.9 and 253.7 mμ on water. The transformation of formic acid to oxalic acid was examined as a function of uv dose, pH, and formate concentration. For an irradiation period of 12 hr for 0.1M formate, a yield of about 2 mmole/l oxalic acid was obtained. A strong dependence of the carboxylation process on pH was found. The yield of oxalic acid formed rose from 0.08 mmole/l at pH 1.9 to 0.40 at pH 4.5 and reached a saturation value of 0.45 at pH 6 to 10.3. This effect can be explained by the dissociation of the formic acid and formation of (CO_2^-)-radical ion. On the other hand the reduction of CO_2 by e^- aq became very rapid in neutral and alkaline solutions so that an additional formation of CO_2^- was achieved. The (CO_2^-) radical ion in both cases, obtained as a result of the dissociation process of the formic acid or as a reduction product of the hydrated electrons with CO_2, led to the formation of oxalic acid. A sequence of reactions accounting for the process of photochemical carboxylation is outlined. (BBB)

16539 ELECTRON PARAMAGNETIC RESONANCE IN IRRADIATED QUARTZ SINGLE CRYSTALS CONTAINING ALUMINUM IMPURITY. Zil'bershtein, Kh. I.; Ioffe, V. A.; Fedorov, Yu. F. (Inst. of the Chemistry of Silicates, Academy of Sciences, USSR). Soviet Phys.-Cryst. (Engl. Transl.), 10: 607-10 (Mar.-Apr. 1966).
Translated from Kristallografiya, 10: 727-31 (Sept.-Oct. 1965).

Electron paramagnetic resonance was studied in natural and synthetic quartz single crystals containing aluminum impurity, irradiated with x rays at room temperature. A complex spectrum was observed at 77°K. One group of lines consisting of six equidistant components constitutes a signal from a hole center connected with aluminum and is described by a spin Hamiltonian, the form and constants of which coincide with those given in the literature. The variation of this signal with radiation dose, concentration of aluminum impurity, rate of crystal growth, nature of growth pyramids, and annealing temperature of the samples was studied. Some characteristics of a second group of lines found at 77°K and a signal occurring at room temperature are given. (auth)

16540 CHEMICAL SPECIES CONTAINING ^{32}P AND ^{35}S FOLLOWING THE NEUTRON IRRADIATION OF CYSTEINE, CYSTINE AND CYSTEIC ACID [Thesis]. Arrington, Cleon Curtis. Manhattan, Kan., Kansas State Univ., 1965. 93p.

The chemical effects produced by the $^{34}S(n,\gamma)^{35}S$ and $^{32}S(n,p)^{32}P$ nuclear transformations in a series of crystalline sulfur-containing organic molecules were investigated for the purpose of obtaining a more complete understanding of the chemical processes occurring during the recombination of the recoil atom to form stable chemical species. The compounds investigated were the structurally related cysteine, cystine, and cysteic acid. In all of the molecules studied, cysteic acid was found to contain the majority, more than 50%, of the sulfur-35 produced. Sulfate and sulfide were the only ionic sulfur-containing species observed and accounted for 20–30% of the activity. The distribution of the radiolabelled products containing sulfur-35 was found to be affected by the presence of oxygen when cystine was irradiated in air and in vacuo. The phosphorus-32 labelled species produced were found by electrophoretic analyses to be predominantly of an ionic nature. The activity of the "phosphate fraction" was found to be distributed among phosphate, isohypophosphate, hypophosphate and probably polyphosphate ions. For cysteine the "phosphate fraction" accounted for 70% of the total phosphorus-32 activity; for cystine irradiated in air 63%; for cystine irradiated in vacuo only 10% and for cysteic acid 57%. An oxygen effect was observed in the phosphorus-32 distribution for cystine irradiated in air and in vacuo. The interpretation of the results is made in terms of the Seitz-Koehler "displacement spike" model for the interaction of radiation in solids. Mechanistic reactions are proposed in order to explain the results. Useful guidance in these proposals was obtained from the ESR studies of cysteine and cystine and the γ-radiolysis studies of solutions of cysteine and cystine. (Dissertation Abstr.)

16541 ELECTRON SPIN RESONANCE STUDIES OF IRRADIATED NUCLEIC ACIDS AND CONSTITUENTS OF NUCLEIC ACIDS [Thesis]. Pruden, Brenda Lamont. Durham, N. C., Duke Univ., 1965. 124p.

Single crystals of thymidine were grown, irradiated with cobalt-60 γ rays at room temperature and studied by ESR. The principal radical obtained was shown by data on the single crystal to be the product of a hydrogen addition reaction with thymidine, in which an extra hydrogen is added on the $C_{(6)}$ of the thymine base ring. Studies of DNA and powdered thymidine irradiated in vacuum and in hydrogen gas at 300°K were carried out in order to confirm the interpretation of the radical as a hydrogen addition product. An increase in the thymidine resonance was observable in both cases in the samples irradiated in hydrogen. The thymidine radical has a large unpaired electron spin density on $C_{(6)}$ in a $2p_\pi$ orbital, which interacts with the three proton spins of the methyl group and the two protons on $C_{(6)}$. The hyperfine splitting produced by these protons is almost isotropic, indicating hyperconjugative coupling. The methyl protons, which are rotating, produce a splitting of 20.5 gauss per proton, and the $C_{(6)}$ protons give a splitting of 40.5 gauss per proton. The methyl proton coupling yields a value of $\rho = 0.70$ for the electron spin density in the $2p_\pi$ orbital of $C_{(5)}$. The 40.5-gauss coupling of the $C_{(6)}H_2$ group is consistent with couplings found in other radicals formed by addition to a ring, and is larger than the expected value because of conjugation in the ring. The variation of the g-factor with crystal orientation indicates the probable orientation of the plane of the thymine rings. On this model the plane of the ring intersects the crystallographic ab plane along a line approximately parallel to one of the axes a or b, and the normal to the ring forms an angle of approximately 45° with the c axis. ESR spectra of an irradiated single crystal of cytidine were also recorded. The hyperfine pattern is a superposition of at least two radicals, the predominant pattern being a triplet. A probable structure of the radical is considered, and the role of this radical in whole DNA is discussed. (Dissertation Abstr.)

Radiochemistry

See also Separation Processes and Procedures

Refer also to abstract 17968.

16542 (TID-22646) TRACER AND ISOTOPE EFFECT STUDIES IN ORGANIC CHEMISTRY. Annual Progress Report. Fry, Arthur (Arkansas Univ., Fayetteville, Dept. of Chemistry). Jan. 15, 1966. Contract AT(40-1)-3234. 49p. Dep. mn. CFSTI $2.00 cy, $0.50 mn.

Results are reported for studies on: acid-catalyzed ke-

tone rearrangement mechanism studies; tracer studies of reaction mechanisms; oxygen-18 exchange studies; and isotope effect studies. (P.C.H.)

16543 THE COMPOSITION OF TRANSURANIUM ELEMENTS. **Keller, C. (Technische Hochschule, Karlsruhe, Ger. Gesellschaft fuer Kernforschung mbH, Karlsruhe, Ger.). Atompraxis, 12: 13-23(Jan. 1966). (In German).**

Experimental techniques are described for the production of transuranium elements. It was concluded that weighable amounts of the transuranium elements up to fermium can be prepared only by long-time irradiation of uranium or plutonium in high-flux reactors. Nuclear reactions with heavy ions and, to a smaller extent, nuclear explosions, appear to be promising for synthesis of transcurium elements and isotopes. Since these heavy-ion nuclear reactions have extremely small cross sections, only tracer quantities or even few atoms of the elements with $Z > 100$ will probably be produced. Because of the systematics of their formation and disintegration it is expected that the heaviest nuclides have only very short half lives. Therefore they can presumably be identified only indirectly by physical methods. (auth)

16544 CHEMICAL EFFECTS ASSOCIATED WITH THE β-DECAY PROCESS. II. A KINETIC STUDY OF THE CHEMICAL BEHAVIOR OF ^{144}Pr IN THE EDTA COMPLEX SYSTEM. **Shiokawa, Takanobu; Omori, Takashi (Tohoku Univ., Sendai). Bull. Chem. Soc. Jap., 38: 1892-7(Nov. 1965).**

The substitution reaction of ^{144}Ce(III) ions with the ^{144}Pr(III)-EDTA complex in an aqueous solution at 25°C was investigated; the rate-determining step was found to be the acid-catalyzed dissociation of the Pr(III)-EDTA complex. On the basis of this substitution mechanism, the chemical behavior of the ^{144}Pr atoms produced by the β decay of ^{144}Ce was explained in terms of a model that involved the formation of an intermediate complex. The kinetic treatment led to the conclusion that the intermediate, produced as a result of an increase in the nuclear charge by the β decay of the complexed ^{144}Ce, is available for attack by hydroxide ions and protonated EDTA anions and, consequently, produces free ^{144}Pr(III) ions. (auth)

16545 SIMPLE CHEMICAL METHOD FOR THE PREPARATION OF THE TWO α AND β ANOMERS OF DESOXY-2′ ADENOSINE, LABELED WITH ^{14}C. **Pichat, Louis; Dufay, Philippe; Lamorre, Yves (CEN, Saclay, France). Bull. Soc. Chim. France. No. 1, 177-80(Jan. 1966). (In French).**

The action of 2 mmole of the chloro-1 derivative of O-p-toluyl-3,5-desoxy-2-D-ribose on 1 mmole of N_6-acetyladenine-^{14}C-8 in the anhydride mixture of acetic acid at 60°C in the presence of p-toluene sulfonic acid followed by a slow evaporation in the presence of potash as an accepter of the hydrochloric acid led to the fixation at N_9 of the desoxyribose. After deacylation, 18% of the α anomer and 9% of the β anomer of desoxy-2′-adenosine-^{14}C-8 was obtained and 65% of adenosine-^{14}C-8 was recovered. The anomers were separated on a Dowex-1 exchange resin column in the acetate form. (tr-auth)

16546 PREPARATION OF CARRIER-FREE ^{207}Bi FOR BETA-RAY SPECTROMETRY. **Wing, J.; Wahlgren, M. A.; Orlandini, K. A. (Argonne National Lab., Ill.). Int. J. Appl. Radiat. Isotop., 17: 132(Feb. 1966).**

By bombarding a piece of lead containing 0.01% bismuth with 21-Mev deuterons in Argonne's 60-in. cyclotron, 4×10^9 dpm of ^{207}Bi were produced. The irradiated lead was dissolved in 8M chloride-free HNO_3 and the bismuth extracted in 0.5M HNO_3 solution with 0.1M TOPO in cyclohexane. The yield of ^{207}Bi was 90%. (M.C.G.)

16547 THE SYNTHESIS AND ISOTOPIC ANALYSIS OF $CH_3{}^{18}OH$ AND $CH_3{}^{17}OH$. **Borowitz, J. L.; Raviv, A.; Rona, P.; Sadeh, D.; Samuel, D.; Klein, F. S. J. Label. Compounds, 1: 259-65(Oct.-Dec. 1965).**

Methods for synthesis of methanol labeled with ^{18}O or with ^{17}O were evaluated. The best method was considered to be the partial hydrolysis of trimethyl phosphate. Ethanol-^{18}O can be prepared analogously by the partial hydrolysis of triethyl phosphate. The most accurate method for the isotopic analysis of oxygen in methanol is by pyrolysis in a specially designed vessel, the hydrogen being extracted through a palladium tube and the residual carbon monoxide analyzed mass spectrometrically. (auth)

16548 SYNTHESIS OF ^{14}C-LANOSTEROL AND ^{14}C-DESMOSTEROL. **Danieli, B.; Russo, G. (Univ., Milan). J. Label. Compounds, 1: 275-81(Oct.-Dec. 1965).**

The synthesis of lanosterol and desmosterol labeled with ^{14}C in the 25 position by a Wittig reaction between triphenyl-2^{14}C-isopropylidene-phosphorane and the corresponding aldehydes are described. The specific activities obtained are, respectively, 0.539 mC/mM and 0.752 mC/mM and the purities of the compounds, respectively, 96 and 99%. (auth)

16549 PREPARATION OF LABELLED COMPOUNDS BY TRITIOBORATION PROCEDURES. I. CYCLOHEXENE-1-^{3}H. **Buczkowski, Z.; Nystrom, R. F. (Univ. of Illinois, Urbana). J. Label. Compounds, 1: 282-4(Oct.-Dec. 1965).**

Cyclohexene-1-^{3}H was synthesized with a yield of 88% by tritioboration of 1-(N-piperidino)-cyclohexene followed by heating with n-valeric acid. Other unsaturated compounds can be labeled at one olefinic carbon atom with tritium by this method. (auth)

16550 PREPARATION AND PURIFICATION OF ACTINOMYCIN-D-^{3}H BY A SPECIFIC METHOD. **Grosse, N.; Cardinaud, R.; Fromageot, P. (Centre d'Etudes Nucleaires, Saclay, France). J. Label. Compounds, 1: 285-93(Oct.-Dec. 1965). (In French).**

Actinomycin-D was tritiated by exposure to tritium gas. Among the various conditions tested the use of a catalyst made of palladium deposited on alumina, and of an amount of tritium gas corresponding to a gas pressure of 20 torr and to a radioactivity of 2 C for 5 mg of actinomycin results in the highest specific radioactivity of about 200 mC/mM. The activation of the tritium gas by a high frequency electric discharge increases the specific radioactivity only in the absence of the catalyst. The purification of the labeled actinomycin is achieved by formation of a complex with DNA. This complex carries a labeled by-product, which is subsequently separated by thin layer chromatography. (auth)

16551 PREPARATION OF ^{32}P-LABELED COMPOUNDS FROM CARRIER-FREE ^{32}P. **Dubini, M.; Perucca, G. P.; (Donegani Research Inst., Navara, Italy). J. Label. Compounds, 1: 308-9(Oct.-Dec. 1965).**

The preparation of ^{32}P-labeled compounds (e.g., P_2S_5 and $(CH_3O)_2POH$) using a technique based on the reaction of carrier-free ^{32}P present in the residue following distillation of neutron-irradiated sulfur (^{32}S(n,p)^{32}P) is described. The technique is reported to be useful for the preparation of all ^{32}P-labeled compounds whose syntheses require elementary P as raw material. Reaction conditions (temperature, heating time, and exchange yield) are tabulated for three inorganic and three organic compounds. (R.E.U.)

16552 ^{99m}Tc GENERATOR USING Fe_2O_3 AS SORBENT FOR ^{99}Mo. **Bulbulian, S.; Sorantin, H. (Reaktorzentrum, Seibersdorf, Austria). Kerntechnik, 8: 118-19(Mar. 1966).**

For use of ^{99m}Tc as a tracer in biological studies, the isotope must be separated immediately before application from its longer living mother ^{99}Mo. The use of Fe_2O_3 as the sorbent for ^{99}Mo was tested in acid medium at different pH values. The results showed that Fe_2O_3 is a suitable sorbent for ^{99}Mo and that ^{99m}Tc is radiochemically pure with no trace of ^{99}Mo. (J.S.R.)

16553 THE PRODUCTION OF RADIOACTIVE SOURCES BY THE ELECTROSPRAYING METHOD. **Robinson, P. S. (United Kingdom Atomic Energy Authority, Harwell, Eng.). Nucl. Instrum. Methods, 40: 136-40(Feb. 1966).**

The use of the electrospraying technique for the production of radioactive sources, involving a number of modifications to the basic apparatus, is described. The technique

as discussed is suitable both for sources up to 1 mg/cm² thickness and for high-resolution weightless α sources. (auth)

16554 HANDLING ALPHA-ACTIVE SPECIMENS IN THE ELECTRON MICROPROBE X-RAY ANALYZER. Hudgens, C. R.; Roesch, D. L. (Monsanto Research Corp., Miamisburg, Ohio). Contract AT-33-1-GEN-53. Nucl. Instrum. Methods, 40: 157(Feb. 1966).

A description is given of radioactive materials handling in the electron microprobe x-ray analyzer. In the laboratory for which this handling is described the use of uncoated samples is routine. The preparation of the sample and the procedure for its use are described. This procedure is not carried out with strange systems, but usually the contaminating characteristics of the system are learned in the course of preliminary examinations. (J.F.P.)

16555 SECONDARY DEUTERIUM ISOTOPE EFFECT IN ADDITION REACTIONS ON CARBONYL COMPOUNDS. Geneste, P.; Lamaty, G. (Faculte des Sciences, Montpellier, France). Tetrahedron Lett., No. 51, 4633-8(Dec. 1965).

A study was made of secondary isotope effect in nucleophilic addition reactions on carbonyl compounds, since in this type of reaction the steric hindrance caused by the hydrogens to the carbonyl play a dominant role. Use of the nucleophile, borohydride ion, in the reduction of ketones is reported. The values of R_H/R_B (25°C) for the following compounds were: acetone 0.97, diethyl ketone 0.93, acetophenone 0.99, cyclopentanone 0.95, cycloheptanone 0.92, norcamphor 0.93, cyclohexanone 0.88, 4-t-butylcyclohexanone 0.88, and cis-2-decalone 0.94. Four factors responsible for this isotope effect are considered and discussed: inductive effects which are different for D and for H; differences in basicity between deuterated and normal ketones; steric effects; and hyperconjugation (or any other phenomena with conjugative character). The results indicated that hyperconjugation is of greatest importance. The maximum isotope effect, of about 12%, was obtained with compounds having hydrogens (axial) whose position was favorable for maximum hyperconjugation, such as cyclohexanone and 4-t-butylcyclohexanone. Acyclic compounds, which are a mixture of conformation isomers and alicyclic compounds of 5 and 7 carbons in which the hydrogens are less favorably situated, show a considerably diminished isotope effect (4 to 6%). A supplementary indication of the preponderance of the conjugative effect is shown by results with partially deuterated 4-t-butylcyclohexanone which shows that the exchange of the first two hydrogens provides 3/4 of the total isotope effect. It was concluded that in the ketone reduction reaction studied conjugative effects are, in major part if not completely, responsible for the observed isotope effect. However, this may not be the case for all carbonyl addition reactions. (BBB)

Separation Processes and Procedures

See also Analytical Procedures
ISOTOPE TECHNOLOGY — Separation and Production

Refer also to abstracts 16171, 17834, and 18111.

16556 (ORNL-TM-1090) CHEMICAL TECHNOLOGY DIVISION, UNIT OPERATIONS SECTION MONTHLY PROGRESS REPORT, NOVEMBER 1964. Whatley, M. E.; Haas, P. A.; Horton, R. W.; Ryon, A. D.; Suddath, J. C.; Watson, C. D. (Oak Ridge National Lab., Tenn.). Feb. 1966. Contract W-7405-eng-26. 59p. Dep. mn. CFSTI $3.00 cy, $0.75 mn.

One method of removing H_2 and CO from He coolant in gas-cooled reactors is oxidation to H_2O and CO_2 in a fixed-bed of CuO pellets and sorption of the H_2O and CO_2 by molecular sieves. Kinetics of the oxidation reactions were measured and mathematical models were derived to fit the experimental data for two commercially available CuO pellets. These models were generalized to form a basis for design. (auth)

16557 APPLICATION OF CO-CRYSTALLIZATION AND ADSORPTION IN THE SOLUTION OF CURRENT PROBLEMS OF RADIOCHEMISTRY. Mikheev, N. B.; Spitsyn, V. I. (Moscow State Univ.). At. Energy Rev., 3: 3-46(1965).

Improving methods for separation of radioactive elements and isotopes, often present in quantities that cannot be weighed, are discussed. Where physical methods, such as electromagnetic or diffusion, do not apply, the methods used for the solution of this problem are based essentially on the distribution of the components to be separated between phases. The distribution of the elements between the solid and liquid phases offers the basis for the processes of their separation by cocrystallization and adsorption. The distribution of the elements between two liquid phases offers the basis for the extraction method, while the varying distribution of the elements between the fluid and vaporous phases makes possible their separation by the distillation method. Cocrystallization and adsorption are used in the reprocessing of nuclear fuel, for the deactivation of radioactive solutions, and in the separation of radioisotopes as well as in various radiochemical investigations. The effectiveness of the separation of elements by the various methods, including those of cocrystallization and adsorption is shown to depend on the chemical state of the elements to be separated as well as on the physicochemical conditions governing the application of the process. A change in the parameters may influence the effectiveness of the separation of the elements. Adsorption processes on crystal precipitates were studied and this method found an application in chromatography. Since the use of physicochemical methods for separating radioactive substances necessarily involved dealing with highly active materials, the influence of radioactivity on processes that take place in heterogeneous systems was also studied. It was found that in many cases radioactivity affects the state of the system, exerting in this manner an influence on the processes of separation of the elements. (auth)

16558 CONCEPTION OF THE EUROCHEMIC PLANT AND ITS ROLE IN THE STARTUP OF EUROPEAN FUEL CYCLES. Barendregt, T. J.; Rometsch, R. (Eurochemic Co., Mol, Belg.). Atompraxis, 12: 25-9(Jan. 1966).

Eurochemic will be able to reprocess the irradiated fuels discharged from the reactors of its thirteen member countries. Chemical decladding methods were adapted and developed to cope with aluminum, magnesium, stainless steel, and zirconium. Purex-type flowsheets were developed to deal with a variety of uranium fuels of enrichments from natural to 93% ^{235}U. Thus a flexible multi-purpose plant was designed and constructed and is being tested. It employs pulse columns for the main extraction cycles and mixer-settlers for final purification of plutonium and highly enriched uranium. The design throughput is about 5 kg U/day for highest enrichment and 400 kg U/day for power reactor fuels of enrichments of less than 5% ^{235}U. For these fuels the capacity can easily be extended to more than 1000 kg U/day. It is postulated that in the next five years, there will be $25 million worth of uranium recovered and this value can be realized either by re-enrichment in a U. S. diffusion plant or by up-grading by blending in Europe and recycling the blended material through suitable reactors. The recovered plutonium should be worth at least $9 million and can be used in development work for fast breeder reactors or can be recycled to thermal reactors. (auth)

16559 EUROCHEMIC INSTRUMENTATION DEVELOPMENT AND STUDIES. Mongon, A.; Challe, J. Atompraxis, 12: 30-5(Jan. 1966). (In French).

The working conditions that prevail in reprocessing plants and the characteristics of the chemicals dealt with

pose special instrumentation problems and influence their solution from many points of view. These contingencies act in three ways: they limit the choice of suitable methods for conventional measurements; they constitute the prime incentive for development of measuring devices capable of obviating the shortcomings or the inapplicability of better known methods; and they show the need for extensive application of electronic computers, scanning devices, and data loggers. The solutions already adopted at Eurochemic and trends that the Instrument Division Engineers are following are discussed. (auth)

16560 FINAL PURIFICATION OF PLUTONIUM AND CONDITIONING OF THE PRODUCTS. Ludwig, H. B.; Lopez-Menchero, E.; Van Geel, J. (Eurochemic Co., Mol, Belg.). Atompraxis, 12: 36-41(Jan. 1966).

The plutonium tail-end unit of the Eurochemic plant, serving for both tributylphosphate solvent extraction process and a trilaurylamine solvent extraction process is described. The design principles of the equipment and its lay-out are given. (auth)

16561 THE EUROCHEMIC PULSE COLUMNS FOR COUNTERCURRENT LIQUID-LIQUID EXTRACTION. de Witte, R. (Eurochemic Co., Mol, Belg.). Atompraxis, 12: 42-6(Jan. 1966).

The principle of the perforated plate pulse column for liquid-liquid extraction is reviewed and the reasons for using this type of contactor at Eurochemic are mentioned. A description of the Eurochemic pulse columns is given together with a brief discussion on interphase control, pulsation system, capacity, and efficiency in the columns. (auth)

16562 SAFETY PRECAUTIONS TO PREVENT CRITICALITY ACCIDENTS. Schueller, W.; Zuend, H. (Eurochemic, Mol, Belg.). Atompraxis, 12: 47-50(Jan. 1966). (In German).

Fissile material handled outside reactor environments requires careful control in order to avoid an uncontrolled chain reaction. The corresponding safety precautions, which are called criticality control, take advantage of either neutron absorption, or leakage, or restricted moderation to assure a deficient neutron balance. Most frequently applied are the following: safe equipment geometry, limitation of fissile solution concentration, limitation of fissile mass, and neutron poisons. Other important parameters to be considered are the amount of neutron reflection and interaction between groups of individually subcritical units. The applications of criticality control methods are discussed and illustrated by describing how nuclear safety requirements are fulfilled in the different processing stages of the Eurochemic irradiated fuel reprocessing plant. Inherently safe equipment is not always compatible with process or economic requirements and some reliance must often be placed on safe operating procedures. It is emphasized that the necessary controls must be enforced by exhaustive operation manuals and adequate training of plant personnel. (auth)

16563 THE ELECTRODEPOSITION OF RUTHENIUM FROM A RUTHENIUM(III) AND RUTHENIUM(IV) SOLUTION AND A FISSION PRODUCTS SOLUTION. Kobayashi, Yoshii; Yamatera, Hideo; Okuno, Hisateru (St. Paul's Univ., Tokyo). Bull. Chem. Soc. Jap., 38: 1911-15(Nov. 1965).

The electrodeposition of ruthenium from ruthenium chloride and ruthenium nitrosyl chloride solutions was studied and applied to the separation of the radioactive ruthenium contained in fission products. When the amount of ruthenium deposited in a given time was plotted against the cathode potential, the curves for 1×10^{-7} M solutions of chloride and nitrosyl chloride showed a maximum. The decrease in the electrodeposition at lower cathode potentials may be due to the anodic oxidation of ruthenium as well as to the evolution of hydrogen gas at the cathode. The rate of electrodeposition was found to depend on the material used as the cathode, and to be increased by an increase in the temperature and by the addition of platinum or ruthenium carrier. A complete separation of radioruthenium from fission products resulted when electrolysis was carried out with a 0.1 M hydrochloric acid solution of fission products containing carrier ruthenium. The ruthenium electrodeposited on the platinum electrode was completely recovered in the solution by anodic oxidation. (auth)

16564 STUDIES OF THE LIQUID-LIQUID PARTITION SYSTEMS. III. THE SOLVENT EXTRACTION OF AMERICIUM(III) AND EUROPIUM(III) THIOCYANATE COMPLEXES WITH TRIBUTYLPHOSPHATE. Sekine, Tatsuya (Tokyo Coll. of Science). Bull. Chem. Soc. Jap., 38: 1972-8(Nov. 1965).

The two-phase distribution of americium(III) and europium(III) was studied between the hexane solution of tributyl phosphate (TBP) and the aqueous solution of sodium triocyanate at 25°C. From the distribution data when the organic phase was 5% (by volume) TBP in hexane and the aqueous phase was 5M Na(SCN, ClO_4), equilibrium constants were obtained by a least-squares method. A salting-out effect was observed when sodium perchlorate was added to the aqueous phase. This salting-out effect is discussed along with the solvation number of TBP in the adduct complexes in the organic phase. (auth)

16565 SOLVENT EXTRACTION OF EUROPIUM IONS WITH BENZOYLTRIFLUOROACETONE. THE SYNERGISTIC EFFECT OF OXYGEN- AND NITROGEN-CONTAINING SOLVENTS. Shigematsu, Tsunenobu; Tabushi, Masayuki; Matsui, Masakazu; Honjyo, Takaharu (Kyoto Univ.). Bull. Chem. Soc. Jap., 39: 165-9(Jan. 1966).

The synergistic effect of many kinds of oxygen- and nitrogen-containing solvents on the extraction of europium ions with benzoyltrifluoroacetone in n-hexane was studied. The addition of alcohols, esters, ketones, amines, and heterocyclic compounds enhances the extraction, and in general, the solvents with longer carbon chain, especially alcohols and amines, have the larger synergistic effects. At a constant benzoyltrifluoroacetone concentration, the logarithm of the distribution coefficient is linear with pH. The slope of the log D vs pH plot is about 1.5 in the extraction with 0.05M benzoyltrifluoroacetone in n-hexane, but it is 2 in the presence of 0.04M oxygen-containing compound and 3 in the presence of 0.04M nitrogen-containing compound. It may be considered that europium benzoyltrifluoroacetonate forms some adducts with these oxygen- or nitrogen-containing Lewis bases, and that the coordination of nitrogen-containing Lewis bases to the chelates is stronger than that of oxygen-containing ones. Since the solvent extraction of neodymium and lutetium ions with β-diketones was performed as well as that of europium ions, it seems to be a favorable procedure for the extraction of rare earth ions with β-diketones to utilize the adduct formation between β-diketonates and active oxygen- or nitrogen-containing Lewis bases. (auth)

16566 SECOND FORATOM CONGRESS. FUEL ELEMENTS. Boettcher, A. (Etablissement de Recherche Nucleaire, Juelich, Ger.). Bull. Inform. A.T.E.N. (Ass. Tech. Energ. Nucl.), No. 57, 17-28(Jan.-Feb. 1966). (In French).

The effects of the American purposes concerning private ownership and toll enrichment are reviewed. The capacities of existing installations and those under construction for the transformation of fissile material into fuel elements are summarized. A survey is made of the retreatment capacity for irradiated fuels in installations in operation or under design. The effects of fuel cycle factors are discussed. (J.S.R.)

16567 CHROMATOGRAPHIC SEPARATION OF $^{131}I^-$, $^{131}IO_3^-$, AND $^{131}IO_4^-$. Zaduban, M.; Brutovsky, M.; Banas, J. (Radiobiologicke Oddelenie Ustavu Experimentalnej Biologie Slovenskej Akademie Vied, Kosice, Czechoslovakia). Chem. Zvesti, 19: 925-30(1965). (In Czech).

The separation of $^{131}I^-$, $^{131}IO_3^-$, and $^{131}IO_4^-$ in various mobile phases was carried out. The separation was carried out on untreated and treated Whatman paper No. 1.

The paper was treated with $Fe(OH)_3$, $BaSO_4$, and a liquid anion exchange Anex PC-Amin KM sec. The most marked separation was obtained on paper treated with $Fe(OH)_3$ and was obtained in the following mobile phases: ethyl alcohol–water–concentrated ammonia, 0.01 M NaOH, and distilled water. (tr-auth)

16568 KINETICS OF ION EXCHANGE ON THE MINERAL ION EXCHANGER, ZIRCONIUM PHOSPHATE. Ollivier, Jean-Yves; Kikindai, Tivadar (Ecole Centrale des Arts et Manufactures, Paris. CEN, Saclay, France). Compt. Rend., Ser. C, 262: 175-7(Jan. 10, 1966). (In French).

The preponderant role of the diffusion of ions into grains of zirconium phosphate on the kinetics of ion exchange is shown and the coefficient of diffusion can be calculated by applying the Patterson theory. (tr-auth)

16569 REPROCESSING STUDIES AT KJELLER. Kraak, W. (Institutt for Atomenergi, Kjeller, Norway). EuroNuclear, 3: 80-3(Feb. 1966).

The Norwegian/Netherlands fuel reprocessing pilot plant is described. A hot laboratory was constructed containing three large concrete cells and some additional laboratories. The fuel processed in the ND plant is irradiated in JEEP. Each element consists of two parallel aluminum tubes, each containing uranium slugs. A Purex-type process is used to reprocess these elements. The Silex plant was used to study a modified Purex-type process and an amine process. (M.C.G.)

16570 A NEW INORGANIC ION EXCHANGER FOR THE SEPARATION OF CESIUM FROM HIGH LEVEL RADIOACTIVE WASTES. Balon, G.; Beaudet, C. A.; Piret, J. (SERAI, Brussels). EuroNuclear, 3: 85-8(Feb. 1966).

Studies were made to determine the resistance of titanium phosphate (ABEDEMTiA) to gamma radiation and its selective retention of cesium from five different reprocessing solutions. It was found to be possible to perform at least four complete cycles on titanium phosphate with reprocessing solutions that are similar to Marcoule's or Hanford's wastes. The yields at breakthrough were increased for the second and third cycles. This increase was explained as resulting from a saturation of the column with ammonium ions from the eluent after the first elution. (M.C.G.)

16571 SYNERGISTIC EFFECT OF TRI-n-OCTYLAMINE ON THE SOLVENT EXTRACTION OF AMERICIUM BY THENOYLTRIFLUOROACETONE. Newman, Leonard; Klotz, Paul (Brookhaven National Lab., Upton, N. Y.). Inorg. Chem., 5: 461-6(Mar. 1966). (BNL-9313).

The synergistic effect of tri-n-octylamine (R_3N) on the solvent extraction of americium by thenoyltrifluoroacetone (HT) is shown to arise from organic phase reactions $AmT_3 + R_3NHCl = AmT_3R_3NHCl$, $AmT_3 + R_3NHT = AmT_3R_3NHT$, and $AmT_3 + R_3NHClHT = AmT_3R_3NHClHT$, where T^- represents the enolate ion of HT. It was ascertained that the formation constants for each of these reactions are the same. The formation constants were measured in benzene as $\log K_s = 5.03 \pm 0.20$. The formation constant for the addition reaction $AmT_3 + HT = AmT_3HT$ was measured as $\log K_{AmT_3HT} = 0.75 \pm 0.05$. Reasons are presented for the conclusion that in the products of synergism each of the amine species is attached directly to the americium. The synergistic effect was studied for values of pH, which were varied from 1.1 to 5.7. (auth)

16572 URANIUM AND COPPER EXTRACTION BY LIQUID ION EXCHANGE. Joe, E. G.; Ritcey, G. M.; Ashbrook, A. W. (Eldorado Mining and Refining Ltd., Ottawa, Can.). J. Metals, 18: 18-21(Jan. 1966).

The extraction of uranium and copper from sulfuric acid leach slurries by means of liquid ion exchange in a pulse column is discussed. (auth)

16573 RECOVERY OF THORIUM FROM URANIUM SOLUTIONS. Vermeulen, L. W. (Rio Tinto Dow, Ltd., Ontario, Can.). J. Metals, 18: 22-5(Jan. 1966).

The recovery of thorium from uranium ore leach solutions by means of solvent extraction with sulfuric acid is discussed. (auth)

16574 SEPARATION OF SCANDIUM FROM YTTRIUM, LANTHANUM AND THE RARE-EARTH METALS BY ANION-EXCHANGE CHROMATOGRAPHY OF THE SULFATE COMPLEXES. Strelow, F. W. E. (South African Council for Scientific and Industrial Research, Pretoria). J. S. Afr. Chem. Inst., 17: 114-21(1964).

The separation can be effected by passage through AG1-X8 anion-exchange resin (SO_4^{2-} form) and elution with 0.05N H_2SO_4. Scandium is retained by the resin and can be subsequently eluted with 0.5N H_2SO_4. Other metals that are separated from Sc by the same procedure include Al, Be, Mg, Co(II), Mn(II), Cu(II), Ni(II), Zn, Cd, Hg(II), Fe(II), V(IV) and the alkali metals. (Anal. Abstr.)

16575 INVESTIGATIONS ON REPROCESSING OF GRAPHITE–CARBIDE FUEL FOR HIGH-TEMPERATURE REACTORS. Bildstein, H.; Knotik, K. (Reaktorzentrums, Seibersdorf, Austria). Kerntechnik, 8: 110-15 (Mar. 1966). (In German).

For operation of gas-cooled high-temperature reactors, fuel elements are used that consist of a graphite shape in which so-called coated particles are dispersed. Methods for the reprocessing of such graphite-carbide fuels were investigated. Electrolytic and bromination techniques for decomposition of the graphite were investigated. For the decomposition of the coating on the layered particles, burning of the pyrocarbon layer, thermoshock treatment, and thermal chlorination were studied. Various combinations of these decomposition methods in the "head-end" stages were considered. The effect of the fuel composition on the selection of the head-end method was considered. (J.S.R.)

16576 PROCESSING OF URANIUM OXIDE FUEL BY OXIDATION-REDUCTION CYCLE. Mukaibo, Takashi; Kanno, Masayoshi; Miki, Isao (Tokyo Univ.). Nippon Genshiryoku Gakkaishi, 8: 76-80(1966). (In Japanese).

The oxidation-reduction cycle process for reprocessing irradiated and short-cooled uranium oxide fuel was investigated. The experiment was carried out with unirradiated UO_2 pellets, and dummy spent fuel constituting UO_2–Mo and UO_2–Ru pellets. For the first step of the process, an experiment was undertaken on the oxidation and pulverization of UO_2 pellets in flowing air. The weight gain vs. oxidation time curve presented an S-shape, and due to the volumetric change from UO_2 to U_3O_7, pulverization was found to start at an O/U ratio of about 2.34. The particle size of the pulverized UO_2 depended on the oxidation temperature, and, between 325 and 900°C, it decreased with decreasing temperature. U_3O_8 powder with a mean particle size of about 20 μ was obtained by oxidation at temperatures lower than 500°C. Further oxidation at 375°C in air for 1 hr, and reduction at 600°C in hydrogen for another hour reduced the particle size. About 6 cycles of oxidation and reduction were sufficient to obtain a fine UO_2 powder that appeared suitable for cold pressing and sintering. Trials in decontamination indicated that removal of Mo and Ru began at 800 and 900°C, respectively, and was completed at 1,000 and 1,100°C, respectively, in the oxidation state. (auth)

16577 REVIEW OF REACTOR FUEL REPROCESSING PLANT SAFETY IN FOREIGN COUNTRIES. Maruyama, Masatomo (Atomic Fuel Corp., Tokyo). Nippon Genshiryoku Gakkaishi, 8: 81-90(1966). (In Japanese).

Preliminary site surveys and safety control measures associated with reactor fuel reprocessing plants as practiced in foreign countries are reviewed. Representative items selected for description in some detail include the Windscale plant in Britain regarding disposal to sea of liquid radioactive wastes, the Idaho Chemical Processing Plant in the U. S. regarding the release to the atmosphere of gaseous wastes, the Hanford plant in the U. S. regarding the movement of liquid wastes dispersed into the

ground, and the Marcoule plant in France regarding safety control. (auth)

16578 AN ALUMINOSILICATE ION EXCHANGER FOR RECOVERY AND TRANSPORT OF ^{137}Cs FROM FISSION-PRODUCT WASTES. Lewis, R. E.; Butler, T. A.; Lamb, E. Nucl. Sci. Eng., 24: 118-22(1966). (ORNL-P-1411).

A method for recovering fission-product cesium from aged basic fission-product waste with an aluminosilicate ion exchanger (Decalso) was developed and demonstrated. Cesium is selectively absorbed on Decalso from Hanford Purex Supernatant 103A, a basic 9 M $NaNO_3$ solution, and concentrated by a factor of about 8.5. The Decalso column is transported from HAPO to ORNL in shielded containers formerly used for shipping solutions, and the cesium is eluted with ammonium salts for purification and source fabrication. In the period April 1961 to August 1964, 2MCi of ^{137}Cs was recovered from Hanford wastes and transported to ORNL by this procedure. (auth)

16579 EXTRACTION OF URANIUM(VI) BY DI-2-ETHYLHEXYL PHOSPHORIC ACID (D2EHP) AND BY MONOLAURYLPHOSPHORIC ACID (MLPA) FROM PHOSPHORIC ACID SOLUTIONS. Laskorin, B. N.; Smirnov, V. F. Zh. Phikl. Khim., 38: 2226-32(Oct. 1965). (In Russian).

The typical long-chain alkyl phosphates D2EHP and MLPA were synthesized and purified. The extraction of uranyl ions by D2EHP in n-hexane from a 1.04M phosphoric acid solution indicated that the D2EHP was dimerized because of hydrogen bonding. The optical density of D2EHP and of MLPA in n-hexane (D) with respect to pure n-hexane was used to determine the composition of the complex being extracted in the organic phase. The results showed that the ratio of D2EHP to (UO_2^{2+}) was 2:1 in a 0.1 molar series of isomolar solutions. On dilution by a factor of 10 to a 0.01 molar series of isomolar solutions, the ratio of D2EHP to UO_2^{2+} in the extracted complex turned out to be 4:1. At low concentrations of D2EHP in n-hexane (0.01M and lower) each uranyl ion reacted with four molecules of D2EHP. MLPA is more highly associated in n-hexane than D2EHP, and the ratio of MLPA to UO_2^{2+} was found to be equal to 5. In acid solutions it was found that the distribution coefficient for uranium(VI) decreased with increasing concentration of hydrogen ion in H_2SO_4, HNO_3, $HClO_4$, and H_3PO_4 solutions. An increase in the concentration of phosphoric acid to 3.0M led to a sharp decrease in the distribution coefficient for the uranyl ion. (TTT)

16580 URANIUM AND THORIUM EXTRACTION FROM PHOSPHORIC ACID SOLUTIONS BY ACID AND NEUTRAL ALKYLPHOSPHORUS COMPOUNDS. Laskorin, B. N.; Smirnov, V. F. Zh. Prikl. Khim., 38: 2232-6(Oct. 1965). (In Russian).

Di-2-ethylhexylphosphoric acid (D2EHP) extracted uranium from a 1.0M H_3PO_4 solution with a distribution coefficient of about 1 to 3, but on adding 0.05M trioctylphosphine oxide (TOPO) to the 0.1M D2EHP in the organic phase, the distribution coefficient for uranium increased to about 48. With 3.0M H_3PO_4 in the aqueous phase the distribution coefficient fell to about 3.5. For practical use the concentration of H_3PO_4 should be less than 2.0M, where the distribution coefficient is equal to about 7. It is possible to extract uranium(VI) and thorium from a 1.5M H_3PO_4 solution with 0.1M D2EHP + 0.05M DAMP (diamyl methylphosphonate) in n-hexane by four theoretical stages at an organic to aqueous phase ratio of 1. The rare earths, iron, and aluminum are left behind in the aqueous phase, and are thus separated from the uranium(VI) and thorium. Ammonium or sodium carbonate can be used to back-extract the uranium(VI) and thorium from the organic phase. (TTT)

16581 URANIUM SORPTION BY PLATINIZED CARBON. Kuzin, I. A.; Andronov, E. A.; Taushkanov, V. P. Zh. Prikl. Khim., 38: 2332-4(Oct. 1965). (In Russian).

A 0.25 g sample of activated carbon containing 0.08% ash and 0.25% platinum was contacted with 25 ml of a 0.05M solution of NaOH, HCl, HSCN, and CH_3COOH for a period of 4 hr. The results showed that with an oxygen atmosphere the capacity of the activated charcoal was zero for NaOH, 0.188 mg-equiv/g for HCl, 0.412 for HSCN, and 0.823 for the CH_3COOH solution, and with a hydrogen atmosphere to recharge the charcoal the capacity was 0.285 for NaOH, zero for HCl, 0.226 mg-equiv/g for HSCN, and 0.624 for the CH_3COOH solution. These data indicated that HCl is absorbed completely by an ion-exchange mechanism, that thiocyanate is absorbed 44% by ion-exchange and 56% by a specific sorption mechanism, and that CH_3COOH is absorbed 24% by ion exchange and 76% as an undissociated complex. With an initial uranium concentration of 3.57 g/l in solution, the results showed that no uranium is absorbed from a UO_2Cl_2 solution or from a UO_2Cl_2, which is 1.0M in NH_4Cl. On the other hand, the capacity of the activated charcoal for uranium was ~50 mg/g for adsorption from 1.0M NH_4SCN, 30 mg/g from 7.0M NH_4SCN, 26 mg/g from 0.5M CH_3COOH + 0.04M CH_3COONH_4, and 10 mg U/g of charcoal from 10M HCl. These data indicated the formation of uranium complexes. (TTT)

16582 REACTOR FUEL PROCESSING. Volume 8, Number 4. Lawroski, Stephen (ed.). One of the five Quarterly Technical Progress Reviews published for the Division of Technical Information, USAEC. Argonne National Lab., Ill., 1965. 60p. GPO $0.70 Domestic, $0.90 Foreign.

Commercial aspects of fuel reprocessing, mechanical preparation for fuel processing, processing of BeO-based fuels, ion-exchange processes, neptunium recovery processes, recovery and separation of americium and curium, equipment design, process instrumentation, volatility processes, pyrochemical processes, waste processing and disposal, production and properties of uranium oxides and uranium and plutonium carbides, uranium metal production, criticality incidents in fuel processing plants, and compatibility studies with anion exchange resins are discussed. (160 references). (M.C.G.)

16583 DEISTVIE IONIZIRUYUSHCHIKH IZLUCHENII NA IONOOVMENNYE MATERIALY. (Ionizing Radiation Effects on Ion Exchange Materials). Egorov, E. V.; Novikov, P. D. Moscow, Atomizdat, 1965. 399p.

A detailed examination is made of radiation-chemical processes occurring in cation- and anion-exchange resins, in ion-exchange membranes, in sulfurized and oxidized charcoals, and in inorganic ion-exchange sorbents. Possible mechanisms of radiolysis of individual ionites and ionite-solution systems are examined. General information is presented on the composition, properties, and methods of synthesis of ion-exchange materials and on the radiation chemistry of polymers, water, and water solutions. (M.J.T.)

ENGINEERING

General

Refer also to abstracts 17177 and 17184.

16584 (CONF-650922, pp 271-80) SOME MANUFACTURING CONSIDERATIONS IN ECONOMICAL MAGNET DESIGN. McAllister, D. R.; Miller, H. W.

An analysis of the costs of magnets is presented in which the influence of manufacturing techniques and of the selection of coil and core design are considered. (D.C.W.)

16585 (CONF-650922, pp 349-55) SELECTION OF WATER-COOLED CONDUCTORS FOR DC MAGNETS. Pollack, I.

A procedure for selecting a water-cooled hollow conductor for d-c magnets is outlined. A graphical solution for determining the diameter of the coolant hole is presented. (auth)

16586 (CONF-650922, pp 723-32) A 100 KILOGAUSS QUASI-CONTINUOUS CRYOGENIC SOLENOID. PART I. Lontai, Laszlo M.; Marston, Peter G.

A stress analysis is presented for high-field solenoids. Specific results are included for a cryogenic 100-kgauss coil. (D.C.W.)

16587 (CONF-650922, pp 680-3) MEGAGAUSS MAGNETS USING CAPACITOR DISCHARGES. Bitter, Francis.

The production of Mgauss fields in small single-turn coils by the oscillatory discharge of a capacitor is considered. Plans for an installation using a 20 kT capacitor and producing fields of 1 to 5 Mgauss are outlined. (D.C.W.)

16588 (LA-3454) CRYOGENIC EVALUATION LABORATORY TEST OF A (MASONEILAN) CRYOGENIC LOW PRESSURE COUPLING. Liebenberg, D. H. (Los Alamos Scientific Lab., Univ. of California, N. Mex.). Jan. 2, 1966. Contract W-7405-eng-36. 9p. Dep. mn. CFSTI $1.00 cy, $0.50 mn.

The results of the leakage testing of a Masoneilan transfer line coupling are presented. The cooldown tests of the 8-in.-diameter coupling were carried out with the coupling installed in an 8-in.-diameter transfer line and were performed with flow rates of 6 lb/sec of liquid hydrogen. A pressure test of this coupling, rated at 150 psig, was made at 95 psig. Leakage was observed to be at the limit of observational error. (auth)

Applications of Nuclear Explosions

16589 (UCRL-12224-T) THE POTENTIAL APPLICATION OF NUCLEAR EXPLOSIVES FOR THE RECOVERY OF OIL FROM SHALE. Lombard, David B. (Lawrence Radiation Lab., Univ. of California, Livermore). Dec. 1, 1964. Contract W-7405-eng-48. 21p. Dep. mn. CFSTI $1.00 cy, $0.50 mn.

The possibility of using nuclear explosives to break shale for in situ retorting is discussed. Overburden removal by nuclear excavation and mining by caving of a nuclear chimney are also considered. Underground explosions in the 20 to 50 kton range can be used to thoroughly fracture large amounts of oil shale at a cost of $0.57 to $1.20 per barrel of petroleum if a recovery of 25 g/ton is assumed. Explosions of 100 kton would break shale for around $0.32 per barrel. However, shale particle size studies showed that fragment sizes in the nuclear chimney might be suitable for in situ retorting, and that the bulk permeability will be very high. (P.C.H.)

Facilities and Equipment

Refer also to abstracts 17626 and 18165.

16590 (SC-TM-66-49) HIGH PURITY DE-IONIZED WATER CLEANING STATIONS. Marsh, R. C. (Sandia Corp., Albuquerque, N. Mex.). Feb. 1966. Contract AT(29-1)-789. 14p. Dep. mn. CFSTI $1.00 cy, $0.50 mn.

The design, fabrication, and testing of first and second generation integrated high-purity water/laminar flow clean bench cleaning stations are described. The major advantages of these cleaning systems are that they provide high-purity (18 megohm) water in continuously flowing cascade rinse tanks plus a class 100 clean working enclosure. Parts may thus be cleaned and dried in a contamination free environment. The second generation cleaning station described was designed specifically for use in the fabrication of thin film microcircuits. Design specifications and construction details are given. (auth)

16591 (UCRL-14660) HIGH TEMPERATURE TESTING OF GRAPHITE HELICAL-SCREW EXPANDERS AND COMPRESSORS. Wells, W. M.; Hanner, D. W.; McElroy, J. L.; Robinson, E. (Lawrence Radiation Lab., Univ. of California, Livermore). Jan. 21, 1966. Contract W-7405-eng-48. 65p. Dep. mn. CFSTI $3.00 cy, $0.75 mn.

In a simple demonstration, a graphite helical-screw compressor drove an identical expander with temperatures on the low pressure side to 2730°F. Gas temperature on the high pressure side was uncertain in detail, but the temperature in the pyrometric well was as high as 135°F above the outside case temperature. This well temperature was below the actual gas temperature, but the difference was not assessed. Rotational speeds to over 14,000 rpm and tip speeds to 230 fps were achieved in the compressor, which ran for a total of 274 hr at speeds above 500 rpm. Shaft power to the compressor achieved values above 10 hp; shaft power from the expander exceeded 0.9 hp. Efficiency of the expander approached 40%. There were some difficulties with materials. Platinum tubing and thermocouples melted after alloying with silicon. The commercial graphite cement used behaved poorly, although the tests were not critically dependent on the joints. A review of the dependence of the strength of graphite on temperature reveals that the conditions of these tests reveal in small measure the potentialities of graphite. (auth)

16592 OPTIMIZING THE DESIGN OF SUPERCONDUCTING SOLENOIDS. Thomas, E. J.; Bright, C. D. Cryogenics, 6: 10-13(Feb. 1966).

It is apparent from the theory of the superconducting solenoid that the length of wire required to produce a particular maximum field H_m depends upon the shape of the solenoid, and that there is a minimum length corresponding to a particular coil shape. Since the cost of the magnet is determined mainly by the cost of the wire, the optimum shape leads to a minimum in the cost of the magnet. Two design curves that can be used to find simply the optimum solenoid shape and the length of wire required when H_m, the internal bore of the solenoid, and the characteristics and size of the superconducting wire are known are presented. A number of examples of the use of the curves are given. (auth)

16593 PLASMA AND ITS TECHNICAL APPLICATIONS. Pietermaat, F. (Univ. Louvain, Belg.). Electricite, No. 124, 11-22(Sept. 1965). (In French).

The characteristics of plasma are briefly outlined. The use of plasma for fusion, welding, metallization, and cutting is summarized. Plasma induction torches and plasma capacitative torches are described. (J.S.R.)

16594 STUDY OF THE DYNAMIC BEHAVIOR AND THE PROPERTIES CONCERNING AUTOMATIC CONTROL

OF A FOUR-STAGE EVAPORATOR FOR TREATING CONTAMINATED WATERS. Mikoleit, W. (VEB Atomkraftwerk, Berlin). Kernenergie, 8: 597-601(Oct. 1965). (In German).

A multistage evaporator for treating contaminated water was investigated by using an analog computer with regard to its dynamic behavior and its properties in an automatic control system, when electronic control elements are applied. The system of equations and some results of the calculations are given. (auth)

16595 CONSTRUCTION PROBLEMS IN DESIGN OF HOT CELLS. Appelt, H. (Siemens-Schuckertwerke AG, Erlangen, Ger.). Kerntechnik, 8: 26-9(Jan. 1966). (In German).

Some solutions to the work problems in hot cells developed at the Research Laboratory at the Siemens-Schuckertwerke AG were reported. The operating elements on the machines to permit the movements required are described and examples are given. The methods used for changing tools in the cell are reported. (J.S.R.)

16596 EXPERIMENTAL DETERMINATION OF TUNGSTEN HEATER STABILITY IN A VACUUM AT TEMPERATURES UP TO 3273 deg K. Marmer, E. N.; Zhukov, V. V.; Stukanov, A. F. (All-Union Scientific-Research Inst. of Electrothermal Equipment, USSR). Teplofiz. Vysok. Temp., 3: 771-4(Sept.-Oct. 1965). (In Russian).

The test results on a tungsten heater of commercial manufacture in the temperature interval from 2273 to 3233°K are reported. The tungsten evaporation rate and the practical limit of operation of 0.006-m rod heaters were determined. (tr-auth)

16597 60 CHANNEL LOGGER /Q-2226/ (Engineering Materials). (Oak Ridge National Lab., Tenn.). (CAPE-1278).

8 drawings.

A logger used to collect information on paper tape from engineering experiments is described. The tapes are converted into magnetic tapes by means of the CDC 160 A computer, and are then used with the CDC 1604 A computer. (For details, see TID-4100). (J.R.D.)

16598 MACHINE FOR THE EXTRACTION OF THE NUCLEAR CARTRIDGES. Guilloteau, Rene; Petillat, Georges (to Commissariat a l'Energie Atomique). Canadian Patent 724,066. Dec. 21, 1965.

Irradiated nuclear fuel cartridges are stored in light alloy casings about one meter long prior to processing for plutonium recovery. This semi-automatic machine is designed to cut open the casings and dump the fuel while immersed in a large tank of water. One operator sits at a control desk at the top of the tank while another observes the cutting and dumping at a safe distance outside the tank and signals instructions should deformed fuel stick in the casing. Displaced cartridges are removed remotely under water. Hydraulic jacks supply the power for the remote manipulations. (AECL)

Heat Transfer and Fluid Flow

See also PHYSICS — Fluid Physics and Thermodynamics

Refer also to abstracts 16934, 18050, and 18071.

16599 (BAW-1280-34) SODIUM-HEATED STEAM GENERATOR DEVELOPMENT. Quarterly Progress Report, October-December 1965. (Babcock and Wilcox Co., Barberton, Ohio. Boiler Div.). Jan. 15, 1965. Contract AT(11-1)-1280. 35p. Dep. mn. CFSTI $2.00 cy, $0.50 mn.

Design, testing, fabrication, and materials evaluation activities connected with the production of full-scale and 30-Mwt prototype Na-heated superheating steam generators are described. The materials evaluations include studies of the corrosion of Croloy 2¼ steel by sodium hydroxide aqueous solutions, Na-NaOH, and NaH-NaOH mixtures. (T.F.H.)

16600 (COO-1177-15) STEADY FLOW CHARACTERISTICS OF A SINGLE-PHASE NATURAL CIRCULATION LOOP. Technical Report No. 15. Creveling, H. F.; Shoenhals, R. J. (Purdue Research Foundation, Lafayette, Ind.). Jan. 1966. Contract AT(11-1)-1177. 50p. Dep. mn. CFSTI $2.00 cy, $0.50 mn.

One-dimensional steady state single-phase natural circulation flow in a circular loop was analyzed. The resulting correlations are presented for both laminar and turbulent flows for wide ranges of the dimensionless parameters involved. In applying these correlations to a particular case it is necessary to carry out iterative calculations. Example calculations of this kind are given. Experiments were carried out using water, and the measured data were compared with the analytical predictions. (auth)

16601 (GEAP-5067) A PROGRAM OF TWO-PHASE FLOW INVESTIGATION. Eleventh Quarterly Report, October-December 1965. Bijwaard, G.; Staub, F. W.; Zuber, N. (General Electric Co., Schenectady, N. Y.). Jan. 1, 1966. Contract AT(04-3)-189. 76p. (EURAEC-1575). Dep. mn. CFSTI $3.00 cy, $0.75 mn.

Work Performed Under United States-Euratom Joint Research and Development Program.

Experimental data on two-phase flows at constant heat input and a reduced pressure of 0.4 are reported, as measured in glass and metal test sections. The measurements include drift velocity, distribution parameter, void fraction correlations, flow transitions, bubble distributions in annular flows, and void properties with large subcooling. Analytical studies are described in which it is shown that, for two-phase flows in which the bulk liquid is either subcooled or superheated, the effects of nonuniform temperature distributions in the liquid must be taken into account in calculations of vapor void behavior. An analytical expression is derived that can be used to predict the vapor volumetric concentrations in subcooled boiling and boiling at saturated temperatures. A method for taking into account the nucleating characteristics of the heating surface is described. (T.F.H.)

16602 (GEAP-5081) TRANSITION BOILING HEAT TRANSFER PROGRAM. Quarterly Progress Report No. 12, October-December 1965. (General Electric Co., San Jose, Calif. Atomic Power Equipment Dept.). Jan. 3, 1966. Contract AT(04-3)-189. 85p. (EURAEC-1570). Dep. mn. CFSTI $3.00 cy, $0.75 mn.

Work Performed under United States-Euratom Joint Research and Development Program.

A long-term demonstration test with a finned multirod assembly operating in transition and film boiling for 100 hours was performed successfully. Additional fully-developed film boiling data are presented. Three-rod observational tests were completed. Heat transfer results and selected color photographic sequences are presented. An analytical expression is given for the heat transfer from the wall to superheated steam phase in film boiling. Empirical coefficients are shown for the heat transfer between the steam phase and entrained droplets. A relation is given for estimating over-all heat transfer coefficients for fully-developed film boiling. Spatially-dependent film boiling is examined and found to be a result of boundary layer and bulk steam phase superheat development. The effect of fuel pellet heat capacity on the magnitude of cladding temperature fluctuations during transition boiling is analyzed. The result is applied to a typical fuel rod case. The example illustrates how temperature fluctuations of fuel rod cladding can be computed from those measured with heated tubes. Increased heat capacity was found to reduce the magnitude of temperature fluctuations by about 20 percent in the example. (auth)

16603 (NYO-187-7) FORCED CONVECTION BOILING BURNOUT FOR WATER IN UNIFORMLY HEATED TUBULAR TEST SECTIONS [Thesis]. Griffel, Jack (Columbia Univ., New York). May 25, 1965. Contract

AT(30-3)-187. 168p. Dep. mn. CFSTI $5.00 cy, $1.00 mn.

To thoroughly study the effects of the major variables in forced-convective burnout, 402 high-pressure critical heat flux determinations were made with seven uniformly heated, internally-cooled, tubular test sections using water, subcooled at the inlet, as the coolant. An analytical study of annular flow burnout based on observations and dimensional analysis yielded a correlation which relates the critical heat flux to the significant local fluid properties and flow parameters. This equation was used to correlate and study the critical heat flux data obtained together with a selection of additional data points from the major available sources, including data for Freon-12. The equation contains four dimensionless groups and constants determined by regression analysis with a limited portion of the data. Critical heat fluxes calculated by the correlation are in good agreement with the measured values. Observations of the effects of the parameters in subcooled nucleate boiling burnout enabled the formulation of an empirical equation for this regime. The equation relates the critical heat flux only to the mass flow rate and subcooling. In testing the equation with available data it was found that the correlation holds throughout the 60 to 2000 psia pressure range equally well, thus implying that there is no pressure effect on subcooled burnout over this entire range. (auth)

16604 (NYO-3114-13) TWO-PHASE FLOW AND BOILING HEAT TRANSFER. AN ANALYSIS OF THE LIQUID FILM IN ANNULAR FLOW. Interim Report. Turner, J. M.; Wallis, G. B. (Thayer School of Engineering, Dartmouth Coll., Hanover, N. H.). Dec. 1965. Contract AT(30-1)-3114-1. 117p. (EURAEC-1572). Dep. mn. CFSTI $4.00 cy, $0.75 mn.

Work Performed under United States–Euratom Joint Research and Development Program.

An analysis of the liquid film in annular flow was carried out from which the pressure drop can be predicted explicitly in terms of the void fraction, the entrainment and known quantities such as the flow rates, fluid properties and pipe diameter. The analysis is based on the principal hypothesis that the liquid film behaves as though it were part of a single-phase flow of liquid filling the whole pipe. This hypothesis does not correspond exactly to the physical situation since it postulates velocity profiles which are sometimes shaped rather differently from the actual profiles in the film. Nonetheless the hypothesis was adopted to permit the prediction of two-phase pressure drops from single-phase theories. The validity of the analysis, at least for annular upflow, was established by comparing it with 138 data points for annular upflow. As a by-product of this work a theoretical form was discovered for Martinelli's empirical correlation $\varphi_f(\alpha)$. Liquid films in laminar, turbulent and plug flow all give predictions which are numerically the same as the following simple equation: $\varphi_f = [1/(1-\alpha)]$. (auth)

16605 (NYO-3304-8) INVESTIGATION OF BOILING WATER FLOW REGIMES AT HIGH PRESSURE. Report No. 621. Bergles, A. E.; Suo, M. (Dynatech Corp., Cambridge, Mass.). Feb. 1, 1966. Contract AT(30-1)-3304. 61p. Dep. mn. CFSTI $3.00 cy, $0.75 mn.

Flow regime information was obtained for boiling water flowing vertically upward in circular tubes of 0.4 in. diameter and lengths of two to eight feet. Inlet conditions were subcooled, pressures were 500 and 1000 psia, and mass velocities ranged from 0.4×10^6 to 4.0×10^6 lbm/hr-ft^2. Uniform heat fluxes ranging up to the critical heat flux were obtained by direct-current resistance heating. The flow regimes at the exit to the heated section were established primarily by means of an electrical resistance probe. The following major flow regimes were identified: bubbly, slug, froth, and spray annular. The data were presented as flow regime maps in terms of mass velocity and mass quality. The flow regime boundaries were significantly altered by changes in pressure, tube length, and inlet temperature. (auth)

16606 (TID-22621) BASIC STUDIES IN GAS-SOLID SUSPENSION. Quarterly Report No. 65-4, September–December 1965. Peskin, Richard L. (Rutgers–The State Univ. of New Jersey, New Brunswick. Bureau of Engineering Research). Jan. 12, 1966. Contract AT(30-1)-2930. 12p. Dep. mn. CFSTI $1.00 cy, $0.50 mn.

Developments in studies on basic fluid mechanics and heat transfer processes associated with gas-solid suspensions in turbulent flow are reported. This includes research on: Brayton cycle efficiency; thermal deposition force acting on particles; effects of solids on statistical structure of turbulence; heat transfer; mass transfer; and density profile of solids in flow. (P.C.H.)

16607 (TID-22663) A VELOCITY TRANSFER FUNCTION ANALYSIS OF FORCED CONVECTION HEAT TRANSFER [Thesis]. Mahaffey, Michael Kent (Kansas Engineering Experiment Station, Manhattan). 1966. 87p. Dep. mn. CFSTI $3.00 cy, $0.75 mn.

Kans. State Univ. Eng. Exp. Sta., Spec. Rep. No. 56.

A perturbation technique for obtaining the outlet coolant temperature-velocity transfer function for a circular stainless steel tube is described. A computer program is used to evaluate the real and imaginary components of this transfer function for various values of frequency and various initial velocities. After constructing Bode plots using a dimensionless frequency that is inversely proportional to the initial velocity, the transfer function is approximated by a series of lead or lag terms which are linear functions of the initial velocity. This approximate transfer function is used to predict the response of the outlet coolant temperature to a step change in velocity. Predicted responses are compared with experimental data obtained from a pressurized-water heat-transfer loop. (auth)

16608 (ANL-Trans-257) STUDY OF LIQUID METAL BOILING UNDER FORCED CONVECTION. Grass, G.; Kottowski, H.; Milliot, B. (European Atomic Energy Community, Ispra (Italy). Joint Nuclear Research Center). Translated by Elmar K. Wilip (Argonne National Lab., Ill.), from Preprint. Oct, 1965. 32p. Dep. mn. JCL $3.60 fs, $1.16 mf.

Flow patterns in a forced-convection boiling-potassium loop were studied using direct Joule heating and simultaneous electropotential analysis. The boiling was abrupt, leading to the sudden periodic emptying of the test section. A by-pass was introduced to simulate parallel channel flow; marked differences in the boiling behavior were observed. An interpretation of the boiling and condensation phenomena was attempted. (D.C.W.)

16609 CURRENT FEED AND INSTRUMENTATION OF AN ELECTRICALLY HEATED 2,8-Mw SUPERHEATING LOOP. Hitzig, K. (Kernforschungszentrum, Karlsruhe, Ger.). Atomwirtschaft, 11: 86-90(Feb. 1966). (In German).

At the Nuclear Research Center at Karlsruhe, a research circuit was constructed in which the nuclear heat production of a reactor core was electrically simulated with a heating device of high power density. This loop is used for the investigation of various operation and control states of a superheated steam-cooled reactor circuit. It permits extensive research on the individual plant constituents, especially at the input and output. The current supply and the measurement, control, and safety devices of the electrically heated core are described. (tr-auth)

16610 HEAT TRANSFER IN BOILING HYDROGEN, NEON, NITROGEN, AND ARGON. Bewilogua, L.; Knoener, R.; Wolf, G. Cryogenics, 6: 36-9(Feb. 1966).

The heat transfer coefficient in liquid hydrogen, liquid neon, liquid nitrogen, and liquid argon in the range of free convection and bubble-boiling was measured. Two small tubes of diameter 0.6 and 3.0 mm in the form of horizontally suspended windings were used as heaters. Distinct hysteresis was observed with all the measurements. This phenomenon can be satisfactorily explained by a theory due to Stephan. In the cases of nitrogen and argon,

the curve for free convection continues into the region of bubble-boiling, as retardation of boiling occurs. After explosive vaporization of the liquid, however, bubble-boiling begins suddenly and corresponding values are obtained. Pressure dependence of the heat transfer coefficient was also measured for nitrogen and argon. (auth)

16611 RESULTS AND EXPERIENCE OF THE OPERATION OF AN EXPERIMENTAL SODIUM LOOP WITH NATURAL CONVECTION. Sulc, Vlastimil (Inst. for Nuclear Research, Czechoslovak Academy of Sciences, Rez). Jad. Energ., 12: 8-15(Jan. 1966). (In Czech).

The results obtained during the operation of an experimental sodium reactor loop with natural convection at sodium temperatures from 150 to 400°C were reported. The loops were in discontinuous operation for more than a year during which the maximum power output was 5 Kv. The heat exchange of the natural convection in the vertical channels were measured in the range of small Peclet numbers from 6.5 to 20. The results of the measurements in this region seem up to the present time very incomplete. Tests performed during construction, the startup and operation of the loop, and conclusions drawn from some accidents to the loop will help in the improvement of the construction and provision for the safe operation for the first reactor loop. (tr-auth)

16612 HEAT TRANSFER TO LIQUID METALS FLOWING TURBULENTLY IN ECCENTRIC ANNULI. I. Yu, Wen-Shi; Dwyer, Orrington E. Nucl. Sci. Eng., 24: 105-17(1966)

An analytical study was carried out to determine the effects of the degree of eccentricity of the two circles of an annulus on both local and average heat-transfer coefficients for turbulent flow of liquid metals. The study was based on the conditions of heat transfer to or from the inner wall only, uniform heat flux, and fully developed temperature and velocity profiles. The scope of the investigation is indicated by the following ranges of parameters studied: Reynolds number, 5×10^4 to 10^6, Peclet number, 368 to 8000, ratio of outer to inner radius, 1.0 to 4.0, eccentricity, up to 70% of maximum displacement. The results showed that eccentricity can have very great effects on both the local and average heat-transfer coefficients and consequently on the circumferential temperature variations around the annulus walls. At a radius ratio of 1.5 and a Peclet number of 1700, for example, the average coefficient was found to decrease 67 and 93%, when the eccentricity was increased from 0.0 to 0.30 and from 0.0 to 0.70, respectively. Under these conditions, the ratios of total circumferential temperature difference to the difference between the average inner-wall temperature and the stream bulk temperature were found to be 3.20 and 3.55, respectively. (auth)

16613 UNSTATIONARY TEMPERATURE DISTRIBUTION IN CYLINDRICAL AND ANNULAR REACTOR FUEL RODS WITH REGARD TO THE TIME DEPENDENCE OF THE HEAT SOURCE, COOLANT TEMPERATURE, AND HEAT TRANSFER RATIOS. Birkhofer, A. (Technische Hochschule, Munich); Heymann, F. Nukleonik, 8: 51-6 (Jan. 1966). (In German).

The time dependent temperature distribution is calculated in cylindrical and annular fuel rods assuming time dependence of specific power, coolant temperatures, and heat transfer coefficients. The heat transfer equation is solved by means of the eigenvalue method. To homogenize the boundary conditions an appropriate transformation of the heat transfer equation is applied. It was shown that this method is even applicable for relatively complicated geometries and boundary conditions. For most problems it is sufficient to calculate 6 to 8 eigenvalues because of the fast convergence of the solution. (auth)

16614 INVESTIGATION OF CRITICAL THERMAL FLUXES IN FORCED MOTION OF MONOISOPROPYL-BIPHENYL-BENZOL. Naboichenko, K. V.; Kiryutin, A. A.; Gribov, B. S. (Inst. of Engineering Physics, Moscow). Teploenergetika, 11: 81-6(1965). (In Russian).

Results of experimental investigations of heat emission during boiling of monoisopropylbiphenyl-benzol mixtures during forced flow in channels with circular cross sections are reported. (tr-auth)

16615 EFFECTS OF THERMAL DECOMPOSITION OF ORGANIC COOLANTS ON THE HEAT EXCHANGE OF LARGE-VOLUME BOILING. Sterman, L. S.; Vilemas, Yu. (Inst. of Power Engineering, Moscow). Teploenergetika, 11: 86-9(1965). (In Russian).

Results of experimental investigations of the effects of thermal decomposition of organic coolants on critical heat flow and the coefficients of heat exchange in large-volume boiling are reported. (tr-auth)

Materials Testing

16616 RADIOGRAPHIC EXAMINATION THROUGH STEEL USING COLD NEUTRONS. Barton, J. P. (Univ. of Birmingham, Eng.). Brit. J. Appl. Phys., 16: 1833-9 (Dec. 1965).

It is demonstrated that radiography may be successfully performed using cold neutrons. A beam of neutrons of energies below 0.005 ev is conveniently obtained by placing a polycrystalline beryllium neutron filter and a single crystal bismuth gamma-ray filter in a beam tube inside the reactor shield. The emergent beam is relatively free of fast neutrons and gamma rays and therefore requires little extra shielding. The contrast provided by hydrogen and many materials with high absorption cross sections is increased for such sub-thermal neutrons, and smaller quantities can therefore be identified radiographically. Moreover, because the coherent scattering cross section of iron is reduced for neutrons below 0.005 ev, the penetration of the beam is significantly increased. It is also shown that the intensity of scattered neutrons reaching the radiograph is reduced to negligible proportions, and the importance of this result is emphasized. Measurements of radiographic contrast confirm that thicknesses of less than 0.01 in. of plastic or other hydrogenous material will remain equally discernible through at least four inches of mild steel. (auth)

16617 THE ROLE OF NON-DESTRUCTIVE TESTING IN THE MANUFACTURE OF WELDED AND CLAD PRESSURE VESSELS. Litting, B. G. (International Combustion Ltd., Derby, Eng.). Brit. J. Non-Destruct. Testing, 7: 83-9(Dec. 1965).

The role of nondestructive testing and problems encountered in the manufacture of pressure vessels clad with stainless steel are described. Special techniques of nondestructive examination were developed to meet the stringent specification requirements with regard to bonding. A satisfactory welding technique for the M.I.G. cladding of nozzle bores was established. (auth)

16618 VACUUM/GAS LEAK TESTING OF BOILER ELEMENTS FOR NUCLEAR POWER STATIONS. Mitchard, F. S. Brit. J. Non-Destruct. Testing, 7: 97-103 (Dec. 1965).

The reasons for the test are discussed and a comparison made of the methods of testing. Details are also given of the equipment required for the test described, together with an outline of the testing procedure. The results of testing large numbers of flash butt and electric resistance welds are shown. (auth)

16619 EXPERIMENTS WITH FOIL-FILM COMBINATIONS AND COLLIMATORS FOR NEUTRON RADIOGRAPHY. Blanks, B. L.; Morris, R. A. (Los Alamos Scientific Lab., New Mex.). Mater. Eval., 24: 76-80(Feb. 1966).

The Los Alamos Water Boiler Reactor, having a maximum power of 25 kw, was used as a neutron source for neutron radiography. Experiments with various foil-film combinations have verified some of the published results. A neutron beam collimation device was developed to improve the image resolution obtainable with this

system. The application of neutron radiography to the inspection of several reactor components was evaluated. (auth)

Protective Structures

16620 (AD-624370) MAGNITUDE AND DISTRIBUTION OF WEAPON EFFECTS FOR THE DESIGN OF SHELTERS FOR PROTECTION AGAINST FALLOUT. Research Paper P-194. Knapp, H. A. (Institute for Defense Analyses, Arlington, Va. Weapons Systems Evaluation). July 1965. 124p. CFSTI $4.00 cy, $0.75 mn.

Estimates were made of the numbers and yields of weapons which would be detonated in the United States, and to indicate where it is likely that they would be detonated. Data are presented to enable, for any given level of attack directed against populations, a rough allocation of weapons among each of the 213 principal urbanized areas in the United States. The model and data indicate that the Washington (D.C.–Va.–Md.) urbanized area, with 1.8 million persons and covering 340 square miles, would be allocated 3 1-Mt weapons in an attack against the population of the United States consisting of 100 1-Mt weapons airburst at optimum altitude. The model and data indicate this area would receive 12 1-Mt weapons for an attack against the United States consisting of 1000 1-Mt surfacebursts. In each case the entire District of Columbia, consisting of 62 square miles at an average density of 12,400 persons/square mile is subjected to blast levels of at least 5 psi. For an attack against the U. S. population with 300 1-Mt airbursts, or 1000 1-Mt surfacebursts, the model indicates that the entire Washington urbanized area, including Rockville, Maryland, could anticipate blast levels of at least 5 psi. (P.C.H.)

16621 (AD-625867) REUSABILITY OF BUILDINGS AFTER A WARFIRE. Final Report. Troxell, G. E.; Degenkolb, J. K.; Benuska, K. L.; Loya, B. R. (Lin (T. Y.) and Associates, Van Nuys, Calif.). Jan. 1964. Contract OCD-OS-63-172. 70p. CFSTI $3.00 cy, $0.75 mn.

A method for the calculation of a fire resistance rating by utilizing an electronic computer program is reported. The evaluation is divided into two parts; the resistance to interior exposure and the susceptibility to exterior exposure. Resistance to interior exposure is rated by estimating the probable severity of interior fire, assuming ignition of combustible contents, then combining this estimate with the fire resistance and economic value of the building. The reduced economic value, which is calculated as a percentile, is referred to as the Building Reusability Index (BRI). Susceptibility to exterior exposure is evaluated in terms of an Exposure Protection Index (EPI). The rating system was prepared assuming no fire fighting or public utilities were available. (auth)

16622 (ORNL-3918) SHIPPING COST COMPARISONS FOR LEAD-, STEEL-, AND URANIUM-SHIELDED CASKS. Shappert, L. B.; Salmon, Royes (Oak Ridge National Lab., Tenn.). Mar. 1966. Contract W-7405-eng-26. 20p. Dep. mn. CFSTI $2.00 cy, $0.50 mn.

Lead-, steel-, and uranium-shielded casks were compared, based on the total cost of transporting spent fuel from a reactor to a reprocessing site 1,000 miles distant. The unique feature of the comparison was that the costs were compared not on the basis of the same fuel load for each cask, but on the same cask weight. This weight was limited to 25 tons empty weight (or as much as 29 tons loaded), which is about the maximum that can be handled in unrestricted trucktrailer shipments. The total cost, the sum of four separate charges, included handling, freight, insurance, and cask amortization. The results of this comparison indicate that the use of uranium-shielded casks can be economically advantageous, provided that the cost of the cask can be kept in the range of $4.00 to $9.00 per pound of cask weight (empty). The greatest advantage to the reactor operator occurs if he is able to keep the cask in use 100% of the time, or rent a cask when needed. (auth)

16623 (ORNL-TM-1381) ENGINEERING STUDY OF UNDERGROUND HIGHWAY AND PARKING GARAGE AND BLAST SHELTER FOR MANHATTAN ISLAND. Perla, Harold F.; Haller, Harry F. (Holmes and Narver, Inc., Los Angeles, Calif.); Hoffman, George A. (RAND Corp., Santa Monica, Calif.); Jarrett, H. F.; Herbert, W. C. (System Development Corp., Santa Monica, Calif.) Mar. 1966. Contract W-7405-eng-26. 209p. Dep. mn. CFSTI $6.00 cy, $1.25 mn.

For Oak Ridge National Lab., Tenn.

An underground cross-town highway connecting the Lincoln and Queens-Midtown Tunnels in New York City was found to be feasible, either alone or in conjunction with an underground parking garage which could accommodate a large number of vehicles, for use as a blast shelter. The study indicates that at a reasonable cost increase the parking facility and access tunnels can also be made a suitable shelter against blast pressures and ground shock effects from nuclear detonations which result in 100 psi surface overpressure levels above the shelter. Because the depth of burial is suitable for resisting greater overpressures, greater resistance would be possible, at much less than proportional increase in additive cost. The facility in its present concept will safely house 1.8 million people for 30 days, and provides for access during a 15-minute warning period. This capacity is based on the access and bunking concepts presented. The latter provides for bunking 600,000 people during one shift in about 80 percent of the parking area, reserving the other 20 percent of the parking area, the traffic tubes, bunk storage areas, access drifts, and ramps for activities for the other 1,200,000 people. The construction of the cross-town highway and parking area for 30,000 cars is estimated to require approximately $4\frac{1}{2}$ years using conventional techniques and reasonable manpower levels. Through use of equipment and techniques that might be possible after intensive research and development, it is estimated that the same capacity facility can be constructed in approximately 3 years, after 3 years required for equipment research and development, at a substantial decrease in cost. Cost estimates, excluding rights-of-way and personnel supplies for emergency are included. Information on parking facility size and lane justifications and human factors are appended. (P.C.H.)

Space Propulsion

See also ISOTOPE TECHNOLOGY — Power Application
REACTOR TECHNOLOGY — Propulsion and Space

Refer also to abstracts 17904 and 18128.

16624 (N-65-17749) SECONDARY EMISSION EFFECTS IN ION BEAMS [Thesis]. Marazzi, Carlos A. (Colorado State Univ., Fort Collins). Nov. 1964. 57p. (NASA-CR-57119). CFSTI $3.00 cy, $0.50 mn.

It was previously found that when an electron source is introduced into an ion engine, the power of the engine increases notably. An attempt was made to verify the explanation of this effect in terms of space-charge compensation of the ion beam by secondary emission. (D.C.W.)

16625 (N-65-19272) DESCRIPTION AND OPERATION OF SPACECRAFT SERT I ION THRUSTOR FLIGHT TEST. Gold, Harold; Rulis, Raymond J.; Maruna, Frank A. Jr.; Hawersaat, William H. (National Aeronautics and Space Administration, Cleveland, Ohio. Lewis Research Center). Mar. 1965. 19p. (NASA-TM-X-1077). CFSTI $1.00 cy, $0.50 mn.

The SERT I spacecraft was flown into a ballistic trajec-

tory on July 20, 1964, by the Scout launch vehicle. The trajectory provided an experimental period of 47 min. during which the altitude of the spacecraft was above 250 nautical miles. The spacecraft carried two small ion thrustors and telemetered measurements of all major thrustor operating parameters. One of the thrustors operated for approximately 30 min. during which the measured thrust verified the establishment of a neutral ion beam. (STAR)

16626 PERFORMANCE MEASUREMENTS ON A PULSED ABLATING THRUSTER. Goldstein, R.; Mastrup, F. N. (TRW Systems, Redondo Beach, Calif.). AIAA (Amer. Inst. Aeron. Astronaut.) J., 4: 99-102(Jan. 1966).

A new type of pulsed thruster is described, and measurements of the momentum communicated to a pendulum by the gas blast are reported. With the use of a honeycomb collector on the pendulum, the error introduced by reflecting particles was eliminated. At a maximum total electrical discharge energy of 2800 joules, of which approximately 1700 joules were dissipated in the thruster, a momentum of 8150 g-cm/sec was measured. Measurements of mass consumption per shot yielded values ranging from 2-8 mg shot, depending on operation. Momentum and mass consumption measurements point to effective specific impulse values of approximately 1000 sec. Direct measurement of exit velocities using high-speed photography yielded effective specific impulses close to 2000 sec. The two measurements are compatible with each other because the photographic measurements are expected to yield data that are too high. Measured efficiency for conversion of electrical energy dissipated in the thruster into directed thrust-producing flow was determined to be 20%. (auth)

16627 PERFORMANCE CHARACTERISTICS OF A MAGNETIC ANNULAR ARC. Patrick, Richard M.; Schneiderman, Arthur M. (Avco-Everett Research Lab., Everett, Mass.). Contracts NAS 3-5748; AF 49(638)-659. AIAA (Amer. Inst. Aeron. Astronaut.) J., 4: 283-90(Feb. 1966).

The magnetic annular arc is an axisymmetric Hall current plasma accelerator. The data presented are obtained with various propellants for input powers ranging between 10 and 100 kw. Between specific impulses of 3000 and 4000 sec, thrust efficiencies in excess of 50% have been achieved. The current-voltage characteristics of the magnetic annular arc are established, and a qualitative explanation of their nature is presented. The overall arc voltage is shown to be a unique function of the applied bias magnetic-field strength for a given propellant and magnetic-field geometry. A partial theory for this effect is developed. The functional dependence of the thrust on applied bias magnetic-field strength and geometry at constant input power and propellant mass flow rate are described. Data are presented on thermal efficiency obtained from heat balances, and estimates are made of $\omega\tau$ and the effect of ion slip in this device. (auth)

16628 RESEARCH AND DEVELOPMENT OF ELECTRIC PROPULSION. Geis, Jack W. (Wright-Patterson Air Force Base, Ohio). Ann. N. Y. Acad. Sci., 134: 317-41(Nov. 22, 1965).

The relative mission capabilities of chemical and electric rockets are indicated. The cesium contact-ion engine is discussed in detail. (D.C.W.)

16629 EXPERIMENTAL RESEARCH ON ELECTRIC PROPULSION. VII. ANALYSIS OF THE PERFORMANCE OF AN ARC-JET DRIVEN BY MEANS OF HYDROGEN AND NITROGEN. Robotti, Aurelio C.; Oggero, Mario (Politecnico, Turin). Ric. Sci. Rend., Sez. A, 8: 894-901 (July-Aug. 1965). (In Italian).

Experiments are described using a new type of arc-jet, characterized by composite electromagnetic and vortex stabilization and propelled by hydrogen and nitrogen in turn. Attention was particularly directed to the electrical characteristics of the arc and the loss of heat through the electrodes. (auth)

Vacuum Engineering

16630 MEASUREMENT OF PRESSURE IN HIGH AND ULTRAHIGH VACUUM REGIONS USING IONIZATION GAGES: PART I. HOT CATHODE GAGES. Sharma, S. K. (National Physical Lab., New Delhi). J. Sci. Ind. Res. (India), 24: 577-82(Nov. 1965).

The recent developments in the design and operation of hot-cathode ionization gages are reviewed. It is noted that the cold-cathode gage avoids some of the limitations of the hot-cathode gage. (D.C.W.)

16631 EXPERIMENTAL STUDIES OF HYDROGEN CONDENSATION ON TO LIQUID HELIUM COOLED SURFACES. Chubb, J. N.; Pollard, I. E. (Atomic Energy Authority Research Group, Culham Lab., Abindgon, Eng.). Vacuum, 15: 491-6(Oct. 1965).

The process of condensation was explored as used for the very high speed contamination free vacuum pumping of hydrogen which is frequently required in plasma physics experiments. The experimental studies reported confirmed the technical attractions of this pumping technique, and provided some accurate values for sticking coefficients during condensation. Condensation pumping of hydrogen by liquid helium cooled surfaces was performed using an unshielded 63-cm^2 plane condensing surface. Values of sticking coefficients close to unity were obtained with no apparent dependence upon gas flow rate, in the range 1.5×10^{-3} to 17×10^{-3} liter torr cm^{-2} sec^{-1}, upon the condensed gas load, up to 25 liter torr cm^{-2}, or upon the surface temperature, in the range 3.6 to 3.9°K. Monte Carlo computer analysis of the gas flow was used to take account of pressure gradients developed in the test apparatus. The appearance of the layers of condensed hydrogen was sometimes clear and ice-like and sometimes white and frost-like, even with apparently identical experimental conditions. More accurate measurements of sticking coefficients were made by studying the reflection of hydrogen gas molecules from liquid helium cooled surfaces. Monte Carlo analysis of probable molecular histories was used to interpret experimental measurements in terms of sticking coefficients. Results showed that the sticking coefficient for hydrogen on surfaces at 3.5 or 3.7°K varied from 0.98 to 0.99°K for a gas temperature of 100°K, to 0.91 to 0.93°K for a gas temperature of 300°K, and down to between 0.5 and 0.7°K for a gas temperature of 700°K. Condensed hydrogen layers up to several millimeters thick were grown and observed to be quite clear and transparent. Somewhat reduced sticking coefficients were observed as layers of these thicknesses were approached, and this reduction was attributed to thermal conduction limitations in the condensed layer. (BBB)

GEOLOGY, METEOROLOGY, AND MINERALOGY

General

Refer also to abstracts 16742 and 17550.

16632 (AAEC/TM-303) A METHOD FOR DIGITAL COMPUTER PROCESSING OF DATA FROM RADIOISOTOPE SEDIMENT TRACING STUDIES. Hartley, P. E. (Australian Atomic Energy Commission Research Establishment, Lucas Heights). Nov. 1965. 22p. Dep. mn.

A computer method for processing data from radioisotope silt tracing experiments is described. A program to produce iso-activity maps directly was written and used to process data from a silt tracing experiment. Details and listings of the program, principally in Fortran IV for an IBM-7040 with 32,000 words of core storage, are given. The method could be adapted to radioisotope water tracing experiments, and also meteorological, oceanographic, and other geophysical investigations. (auth)

16633 (UCRL-16605) CHEMICAL EVOLUTION AND ORGANIC GEOCHEMISTRY [Thesis]. Belsky, Theodore (Lawrence Radiation Lab., Univ. of California, Berkeley). Jan. 1966. Contract W-7405-eng-48. 134p. Dep. mn. CFSTI $4.00 cy, $1.00 mn.

Structurally-specific biological markers having a wide distribution in marine and non-marine environments and consisting primarily of isoprenoid alkanes were isolated and identified in a variety of sedimental extracts of varying ages. The C_{18}, C_{19} (pristane), C_{20} (phytane), C_{21} isoprenoids, and the C_{27}, C_{28}, and C_{29} steranes were isolated and identified in the oldest known carbon-rich rocks of North America, the 2.7 billion-year-old Soudan shale of Minnesota. The presence of these compounds, which it is felt are indigenous to the rock, indicates that complex, biochemical synthetic mechanisms were in existence over 3 billion years ago, and that life processes probably developed early in the Earth's history some 4 billion-years-ago. The alkane distribution of three known-abiogenic oils was found to differ markedly from the geological oils. There may be differences in the alkanes of marine and non-marine sediments sufficient for telling them apart. Noncontaminative microtechniques were developed for the isolation and identification of alkanes on the microgram level. (82 references). (auth)

16634 THE CARBON, HYDROGEN, AND OXYGEN ISOTOPIC COMPOSITION OF THE HYDROTHERMAL FLUIDS RESPONSIBLE FOR THE LEAD-ZINC DEPOSITS AT PROVIDENCIA, ZACATECAS, MEXICO [Thesis]. Rye, Robert Orph. Princeton, N. J., Princeton Univ., 1965. 117p.

Nearly 50 samples of primary fluid inclusions in calcite, quartz, and sphalerite from several mines at Providencia, Zacatecas, Mexico, were analyzed for deuterium. The range of values recorded for each of the three minerals is −6.8 to −8.3% (relative to SMOW). Detailed studies were made on the carbon and oxygen isotopic composition of four successive calcite generations from three mines. The data indicate only small variations in the isotopic composition of individual generations. Successive generations of calcite, with one exception, have increasingly heavier carbon and oxygen isotopic compositions. This trend coincided with a 150°C decrease in the temperature of mineral deposition. The results can be interpreted to indicate that the oxygen isotopic composition of the hydrothermal fluid was nearly uniform in time and space during ore deposition, and that the trend of $\delta^{18}O$ values with time was a result of increasing isotopic fractionation of oxygen, between the fluid and the calcite, as the temperature of deposition decreased. The results also indicate that the carbon from the source of the fluids was uniform throughout calcite deposition, and that the trend of $\delta^{13}C$ values with time for the bulk of calcite deposition was the result of either increasing isotopic fractionation of carbon with decreasing temperature, or the mixing of limestone carbon with deep seated carbon in the hydrothermal fluid. The oxygen isotopic composition of the hydrothermal fluid, from which calcite precipitated, was calculated. Results show that the bulk of the calcites precipitated from a fluid having an oxygen isotopic composition between 6.4 and 7.9% (relative to SMOW). The isotopic data are interpreted in terms of the origin and history of the hydrothermal fluids responsible for the ore body. The isotopic data strongly point to a magmatic source for the hydrothermal water, and for at least 50% of the carbon in the calcites. The cause of large salinity variations in the Providencia fluid inclusions is shown to be either the result of events at the source of the fluids, or of intermittent incorporation of sedimentary salt by the hydrothermal fluid. (Dissertation Abstr.)

Meteorology

See also Site Survey and Selection

Refer also to abstract 16699.

16635 (RT/PROT(65)40) III ANNUARIO METEOROLOGICO DEL CENTRO DI STUDI NUCLEARI DELLA CASACCIA 1964. (Third Annual Meteorological Report of the Center for Nuclear Studies at Casaccia, 1964). Giudici, G. (Comitato Nazionale per l'Energia Nucleare, Rome (Italy)). Nov. 1965. 120p. Dep. mn.

The results of measurements of atmospheric phenomena observed during 1964 at Casaccia are tabulated. The phenomena measured were atmospheric precipitation, air temperature, relative humidity, atmospheric pressure, amount of sunshine, wind, and vertical thermal gradient. (J.S.R.)

16636 RADIOAKTIVNYE IZOTOPY V ATMOSFERE I IKH ISPOL'ZOVANIE V METEOROLOGII. NAUCHNAYA KONFERENTSIYA PO YADERNOI METEOROLOGII, OBNINSK, 3–6 FEVRALYA 1964. (Radioactive Isotopes in the Atmosphere and Their Use in Meteorology. Scientific Conference on Nuclear Meteorology, Obninsk, Feb. 3–6, 1964. Karol, I. L.; Kirichenko, L. V.; Krasnopevtsev, Yu. V.; Kurganskaya, V. M.; Malakhov, S. G.; Seredag, A.; Yagodovskii, I. V. (eds.). Moscow, Atomizdat, 1964. 492p. (CONF-640208).

Separate abstracts were prepared for the 45 papers included. (G.O.Y.)

For abstracts of individual papers see: 16410, 16411, 16637–16658, and 16688–16708.

16637 EFFECT OF VERTICAL-EXCHANGE INTENSITY ON THE DISTRIBUTION OF NATURAL RADIOACTIVE MATTER IN THE FREE ATMOSPHERE. Shopauskas, K. K. pp 93-101 of Radioaktivnye Izotopy v Atmosfere i Ikh Ispol'zovanie v Meteorologii. Karol, I. L. (ed.). Moscow, Atomizdat, 1964. (In Russian).

Measurements of radioactivity in the atmosphere, made from aircraft over a 4-year period (1960-1963), combined with temperature and wind measurements made for the same period by conventional probes before and after each flight, were used to study and compare the distribution of atmospheric radioactivity under various atmospheric conditions (temperature inversions, extreme convection, neutral temperature stratification) in the atmospheric boundary layer and in free air. It is concluded that in the free atmosphere there is no direct dependence of radioactivity distribution on temperature stratification and that the coefficient of vertical turbulent exchange k, directly measured, is not the same as that derived from the use of temperature and wind data. The distribution of natural radioactivity in the free atmosphere depends not only on k and λ (coefficient of turbulent diffusion and radio-

active decay constant) but also on other factors. The value of k characterizes the effective rate of radon influx into the next higher atmospheric layer, which in turn depends not only on the intensity of vertical turbulent exchange but on such processes as vertical currents, advective transfer, and katafrontally rising air. Averaged over a period of time, the value of k derived from a vertical profile of radioactive decay products depends mostly on the period of half-decay of the parent isotope. (ATD)

16638 EFFECT OF ADVECTION ON RADIOACTIVITY DISTRIBUTION IN THE ATMOSPHERE. Shopauskas, K. K. pp 102-6 of Radioaktivnye Izotopy v Atmosfere i Ikh Ispol'zovanie v Meteorologii. Karol, I. L. (ed.). Moscow, Atomizdat, 1964. (In Russian).

The results are presented of studies of the distribution of radioactivity with height under various climatological conditions (before and after the passage of a warm front, in intramass advection, and with cyclonic circulation over land and water bodies). (ATD)

16639 ESTIMATES OF THE PARAMETERS OF VERTICAL EXCHANGE AND THE AVERAGE RATE OF AEROSOL REMOVAL BY CLOUDS AND PRECIPITATION IN THE LOWER PART OF THE TROPOSPHERE BASED ON NATURAL RADIOACTIVITY DATA OF THE SURFACE BOUNDARY LAYER OF AIR. Karol, I. L.; Vilenskii, V. D. pp 107-19 of Radioaktivnye Izotopy v Atmosfere i Ikh Ispol'zovanie v Meteorologii. Karol, I. L. (ed.). Moscow, Atomizdat, 1964. (In Russian).

A theoretical scheme is discussed for separately calculating the effect of vertical turbulent diffusion of aerosols and their washout by clouds and precipitation on the time that naturally radioactive aerosols remain in the atmosphere. The scheme is checked using measurements of the decay rate of Rn isotopes made in Western Europe and the Moscow region, as well as seasonal measurements of meteorological and soil factors. (ATD)

16640 SEASONAL AND GEOGRAPHICAL CHANGES IN THE ^{210}Pb CONTENT OF THE ATMOSPHERE. Vilenskii, V. D.; Davydov, E. N.; Malakhov, S. G. pp 120-31 of Radioaktivnye Izotopy v Atmosfere i Ikh Ispol'zovanie v Meteorologii. Karol, I. L. (ed.). Moscow, Atomizdat, 1964. (In Russian).

Systematic measurements over a two-year period (1959-1960) of the concentration of Rn and ^{210}Pb in the surface boundary layer of the atmosphere over the Moscow region and on Kheys Island (Franz Josef Land) were used as the basis of a study of the interlatitudinal exchange of air masses in the polar and middle latitudes of the Northern Hemisphere. Measurements of the ^{90}Sr/^{210}Pb ratios made it possible to study the influx of ^{210}Pb and ^{90}Sr into the atmosphere of the polar regions. In addition, an evaluation was made of the seasonal changes in the rate of purification of the ^{210}Pb aerosol-carrier. Instrumentation and techniques are described, and the data are compared with similar data for areas in Greenland, Canada, and Alaska. (ATD)

16641 PLANETARY DISTRIBUTION OF ^{210}Pb IN THE FREE ATMOSPHERE AND ITS USE IN ESTIMATING VERTICAL EXCHANGE PARAMETERS AND WASHOUT OF AEROSOLS BY CLOUDS AND PRECIPITATION, AS WELL AS THE RATE OF EXCHANGE BETWEEN THE TROPOSPHERE AND STRATOSPHERE IN THE NORTHERN AND SOUTHERN HEMISPHERES. Karol, I. L. pp 132-52 of Radioaktivnye Izotopy v Atmosfere i Ikh Ispol'zovanie v Meteorologii. Karol, I. L. (ed.). Moscow, Atomizdat, 1964. (In Russian).

Preliminary results are given for the use of a theoretical three-layer model of the atmosphere (stratosphere, upper troposphere, and aerosol-washout layer) to determine the vertical profile of ^{210}Pb in the extratropical latitudes of the Northern Hemisphere and its use in estimating the exchange rate between these layers and the washout of aerosols by clouds and precipitation. Theoretical formulas are tested with actual measurements, and calculations are made of the annual balance of ^{210}Pb in the stratosphere of both the northern and southern latitudes. (ATD)

16642 DISPERSION OF AEROSOLS IN GLOBAL RADIOACTIVE POLLUTION OF THE ATMOSPHERE. Gaziev, Ya. I. pp 153-63 of Radioaktivnye Izotopy v Atmosfere i Ikh Ispol'zovanie v Meteorologii. Karol, I. L. (ed.). Moscow, Atomizdat, 1964. (In Russian).

Some experimental and theoretical studies of the dispersion of radioactive aerosols are reviewed. The formation of radioactive aerosols during nuclear explosions is considered. (D.C.W.)

16643 DISPERSION OF RADIOACTIVE AEROSOLS IN THE STRATOSPHERE. Gaziev, Ya. I.; Nazarov, L. E. pp 181-5 of Radioaktivnye Izotopy v Atmosfere i Ikh Ispol'zovanie v Meteorologii. Karol, I. L. (ed.). Moscow, Atomizdat, 1964. (In Russian).

The results are presented of studies carried out to determine the dispersion of radioactive aerosols (^{144}Ce, ^{90}Sr, and ^{137}Cs) in the stratosphere (19 to 21 km level and 2 to 3 years after nuclear testing) over the central part of European USSR in 1961. The procedures and instruments used are briefly described. The low rate of influx into the stratosphere of radioactive aerosols from the mesosphere during this period is also discussed. (ATD)

16644 FLUCTUATIONS IN THE DISPERSED COMPOSITION OF RADIOACTIVE AEROSOLS IN THE SURFACE BOUNDARY LAYER OF THE ATMOSPHERE. Gaziev, Ya. I.; Nazarov, L. E. pp 186-92 of Radioaktivnye Izotopy v Atmosfere i Ikh Ispol'zovanie v Meteorologii. Karol, I. L. (ed.). Moscow, Atomizdat, 1964. (In Russian).

A study of coarsely and finely dispersed, artificial, radioactive aerosols in the surface boundary layer of the atmosphere over the Moscow region for the period Jan.–May, 1964 is summarized. (D.C.W.)

16645 RESULTS OF SYSTEMATIC OBSERVATIONS OF HOT PARTICLES IN THE SURFACE BOUNDARY LAYER OF THE ATMOSPHERE IN THE MOSCOW REGION FROM 1961 THROUGH 1963. Makhon'ko, K. P.; Malakhov, S. G. pp 193-206 of Radioaktivnye Izotopy v Atmosfere i Ikh Ispol'zovanie v Meteorologii. Karol, I. L. (ed.). Moscow, Atomizdat, 1964. (In Russian).

The results of systematic observations of hot (10^{-10} to 5×10^{-12} C) aerosol particles in the surface boundary layer of the atmosphere over the Moscow region during the period from Sept. 1961 to Dec. 1963 are presented. (D.C.W.)

16646 RADIOACTIVITY, SIZES, AND COMPOSITION OF α-RADIATING AEROSOLS. Styro, B. I.; Vebra, E. Yu.; Shopauskas, K. K. pp 207-16 of Radioaktivnye Izotopy v Atmosfere i Ikh Ispol'zovanie v Meteorologii. Karol, I. L. (ed.). Moscow, Atomizdat, 1964. (In Russian).

An elaboration is presented of an earlier study of atmospheric samples originally collected at altitudes of 0 to 2 km over the Vilnius area, in which 20 alpha-radiating aerosol particles were discovered. Reexamination of these samples revealed the presence of 42 additional particles of this type. These particles and one particle discovered in studying the radioactive fogs of October 19, 1963, were examined by microphotographic techniques to determine the sizes, composition, and degree of radioactivity. (ATD)

16647 WASHOUT BY PRECIPITATION OF ARTIFICIAL RADIOACTIVE AEROSOLS FROM THE ATMOSPHERE. Burtsev, I. I. pp 217-29 of Radioaktivnye Izotopy v Atmosfere i Ikh Ispol'zovanie v Meteorologii. Karol, I. L. (ed.). Moscow, Atomizdat, 1964. (In Russian).

The mechanisms involved in the fallout of artificial and natural radioactive particles were investigated. The concentrations of ^{90}Sr and ^{90}Y in various types of precipitation were measured at stations in the vicinity of Mt. Elbrus. The intensity and amount of fallout on the ground was also measured. It was found that snow showers with hail were the most effective type of precipitation in the deposition of radioactive particles. (D.C.W.)

16648 WASHOUT OF FISSION PRODUCTS FROM THE ATMOSPHERE. Makhon'ko, K. P.; Malakhov, S. G.; Nekhorosheva, M. P. pp 230-43 of Radioaktivnye Izotopy v Atmosfere i Ikh Ispol'zovanie v Meteorologii. Karol, I. L. (ed.). Moscow, Atomizdat, 1964. (In Russian).

Regular daily observations of the amount, intensity, direction, and types of precipitation were made simultaneously with measurements of the specific radioactivity precipitation (C) in the period 1960–1962 (immediately after nuclear testing and during the moratorium) to determine the relation of C to the precipitation parameters and to the concentration of radioactive materials in atmospheric air, and of the dependence of C on the amount of precipitation. The measurements were averaged for different periods of time (by day, month, and year) and were compared with other results. (ATD)

16649 GLOBAL DISTRIBUTION IN THE ATMOSPHERE AND FALLOUT OF THE RADIOACTIVE PRODUCTS OF NUCLEAR EXPLOSIONS. Karol, I. L.; Malakhov, S. G. pp 244-82 of Radioaktivnye Izotopy v Atmosfere i Ikh Ispol'zovanie v Meteorologii. Karol, I. L. (ed.). Moscow, Atomizdat, 1964. (In Russian).

The results of research on the global distribution in the atmosphere of radioactive products of nuclear explosions and on the fallout on the earth's surface are reviewed. 119 references. (G.O.Y.)

16650 FLUCTUATIONS IN SEASONAL CONCENTRATION OF FISSION PRODUCTS IN THE ATMOSPHERE SURFACE LAYERS OVER THE VICINITY OF MOSCOW AND HEIS ISLAND OF THE FRANZ JOSEF LAND IN 1956 TO 1963. Malakhov, S. G.; Davydov, E. N.; Nekhorosheva, M. P. pp 323-37 of Radioaktivnye Izotopy v Atmosfere i Ikh Ispol'zovanie v Meteorologii. Karol, I. L. (ed.). Moscow, Atomizdat, 1964. (In Russian).

Systematic measurements of the concentration of radioactive aerosol in the atmosphere around Moscow were made during each season of the period between 1956 and 1963 using the FPP-15 filter with a flow of 2000 $m^3\ hr^{-1}$. The concentrations of beta activity, ^{141}Ce, ^{144}Ce, ^{137}Cs, ^{90}Sr, ^{95}Zr + ^{95}Nb, and ^{95}Zr were recorded. Similar measurements were performed at Heis Island. (G.O.Y.)

16651 EFFECT OF VERTICAL DISTRIBUTION OF TEMPERATURE AND WIND VELOCITY ON THE ATMOSPHERIC DIFFUSION OF RADIOACTIVE POLLUTANTS. Berlyand, M. E.; Genikhovich, E. L.; Dem'yanovich, V. K.; Onikul, R. I. pp 380-91 of Radioaktivnye Izotopy v Atmosfere i Ikh Ispol'zovanie v Meteorologii. Karol, I. L. (ed.). Moscow, Atomizdat, 1964. (In Russian).

The inapplicability of the continuously active point source model, which depends on the coefficient of turbulent exchange in the surface boundary layer of the atmosphere, in dealing with atmospheric pollution is discussed. A mathematical model which includes lapse rates, wind velocity, turbulent exchange, and other factors as they actually occur in the thicker boundary layer is presented. (G.O.Y.)

16652 RESULTS OF MODEL EXPERIMENTS ON THE DISTRIBUTION OF POLLUTANTS SETTLING INTO THE LOWER LAYERS OF THE ATMOSPHERE UNDER VARIOUS METEOROLOGICAL CONDITIONS. Byzova, N. L.; Mashkova, G. B.; Osipov, Yu. S. pp 392-402 of Radioaktivnye Izotopy v Atmosfere i Ikh Ispol'zovanie v Meteorologii. Karol, I. L. (ed.). Moscow, Atomizdat, 1964. (In Russian).

The results are presented of a series of theoretical model and field experiments carried out between 1959 and 1963 at the 300-m meteorological tower of the Institute of Applied Geophysics at Obninsk to study the dispersion of effluents from various heights. The aerosols were spherical particles of poly[methyl]-methacrylate powders ranging between 10 and 100 μ in diameter. Measurements were made of four fractions ejected at speeds of 0.27, 0.17, 0.1, and ~0.03 m/sec, at 100 to 200 points, 10 to 20 km away from the source. Meteorological parameters measured included the wind-velocity profiles, wind direction, temperature profile (daytime and nighttime inversions), and such turbulence characteristics as wind-direction pulsations. The results obtained from the field measurements are compared with those derived experimentally. (ATD)

16653 BASIS FOR USING FIBROUS FILTER MATERIALS, FP (PETRYANOV FILTERS). Ogorodnikov, B. I.; Basmanov, P. I. pp 403-18 of Radioaktivnye Izotopy v Atmosfere i Ikh Ispol'zovanie v Meteorologii. Karol, I. L. (ed.). Moscow, Atomizdat, 1964. (In Russian).

The characteristics of various types of fibrous filters [FP(fibrous), V(vinyl), A(aluminum), D(wood, cellulose)] were calculated and compared. A mathematical formalism for using FP filters is given. (G.O.Y.)

16654 ON SOME PROPERTIES OF FIBROUS FILTERS (FP) IN RAREFIED AIR. Petryanov, I. V.; Ogorodnikov, B. I.; Suntzov, A. S. pp 419-34 of Radioaktivnye Izotopy v Atmosfere i Ikh Ispol'zovanie v Meteorologii. Karol, I. L. (ed.). Moscow, Atomizdat, 1964. (In Russian).

The theoretical properties of an ideal aerosol filter are developed and are then modified to account mathematically for various types of real fibrous filters and the diffusion, cascade, inertial, and electrostatic effects to which they are exposed. The results of some experiments in which the formalism was applied to determine certain properties of various types of fibrous filters are presented. (G.O.Y.)

16655 RADIATION-SEDIMENTATION METHOD FOR AEROSOL STUDIES. Verzilov, E. E. pp 446-55 of Radioaktivnye Izotopy v Atmosfere i Ikh Ispol'zovanie v Meteorologii. Karol, I. L. (ed.). Moscow, Atomizdat, 1964. (In Russian).

The bases of radiation-sedimentation methods for aerosol studies are summarized, together with some experiments in which acetylcellulose filters or adhesive layers with acetone were used and were put through a centrifugal beta sedimentometer to analyze the radioactive suspension. (D.C.W.)

16656 EFFECT OF METEOROLOGICAL CONDITIONS ON THE EFFECTIVENESS OF RADIOACTIVE POLLUTANT COLLECTION. Aleksandrov, N. N.; Goroshko, B. B.; Kovalenko, V. G.; Panfilova, G. A. pp 473-80 of Radioaktivnye Izotopy v Atmosfere i Ikh Ispol'zovanie v Meteorologii. Karol, I. L. (ed.). Moscow, Atomizdat, 1964. (In Russian).

The results are presented of comparative tests that were performed to determine the effectiveness of three types of fallout collectors and of experiments that were conducted to determine the coefficient of air passing over a vertical panel. The collectors were plain gauze-covered sheets; framed, sectional, steel sheets painted with nitrocellulose enamel; or glycerine-coated aluminum vessels. The effectiveness of these collectors was tested under various meteorological conditions. (ATD)

16657 MAKING THE COEFFICIENTS OF AEROSOL COLLECTION BY HORIZONTAL SHEETS MORE PRECISE. Pogudin, A. P. pp 481-5 of Radioaktivnye Izotopy v Atmosfere i Ikh Ispol'zovanie v Meteorologii. Karol, I. L. (ed.). Moscow, Atomizdat, 1964. (In Russian).

Daily observations were made over a year's time to measure the coefficient of collection of four types of aerosol collectors: a gauze-covered horizontal panel; a framed, gauze-covered horizontal panel; a water vessel; and an experimental aluminum sheet. The mean arithmetic values of the collection coefficient for a one-day sample using the plain and the framed horizontal panels were almost identical. The water-filled collector yielded a somewhat smaller value than the plain sheet. (G.O.Y.)

16658 METHOD FOR SELECTING CLOUD WATER SAMPLES USING CYCLONE PRECIPITATORS. Pudovkin, I. B. pp 486-9 of Radioaktivnye Izotopy v Atmosfere i Ikh Ispol'zovanie v Meteorologii. Karol, I. L. (ed.). Moscow, Atomizdat, 1964. (In Russian).

A method for selecting cloud water samples using cy-

clone precipitation is briefly described. Some results on aerosol activities in Russia in 1962, measured from cyclone-precipitated water samples, are presented. (G.O.Y.)

Natural Radioactivity and Fallout

See also HEALTH AND SAFETY

Refer also to abstracts 16168, 16647–16649, 16651, 16656, and 16657.

16659 (AD-629527) DISTRIBUTION OF VOLCANIC FALLOUT IN AND ABOUT A ONE-STORY RESIDENCE. Kawahara, F. K.; Crew, R. J. (Naval Radiological Defense Lab., San Francisco, Calif.). Aug. 11, 1965. 64p. (USNRDL-TR-953).

Tests were conducted to study the behavior of fallout in the environment of a one-story residence, using as a fallout simulant naturally deposited volcanic fallout produced by Volcano Irazu in Costa Rica. Particle size distribution of material collected inside the home was similar to that outside. The mass loadings inside were a factor of 50 less than those outside. It was concluded that the ratio of outside fallout dose to inside dose may be reduced significantly in the vicinity of the window through which air is moving. Particle size distribution and mass deposited was uniform from one sample to another in studies conducted outside. Therefore, it was concluded that reclamation tests using uniform distributed synthetic fallout are realistic even when surface configurations are quite complex. (H.G.D.)

16660 (AERE-R-4997) RADIOACTIVE FALLOUT IN AIR AND RAIN: RESULTS TO THE MIDDLE OF 1965. Cambray, R. S.; Fisher, E. M. R.; Brooks, W. L.; Hughes, A.; Spicer, G. S. (Atomic Energy Research Establishment, Harwell (England). Production Group, United Kingdom Atomic Energy Authority, Capenhurst (England)). Nov. 1965. 46p. Dep. BIS $1.40. HMSO 7s.

Samples of atmospheric dust and rainwater were collected from the United Kingdom and overseas. Results are presented of the analyses of these samples for various fission products and certain other radionuclides. The concentrations of the long-lived fission products Cs-137 and Sr-90 in air and rain over the United Kingdom were in 1965, about one third of those for 1964. The average deposition of Cs-137 and Sr-90 in the United Kingdom for the first six months of 1965 was about 40% of that for the corresponding period of 1964. The low yield Chinese explosions of October 1964 and May 1965 temporarily contributed about 3% to the longlived activity. Integration over the world of the deposition of Sr-90 in rain provided an estimate of the total global deposition to the end of 1964. Concentrations of Cs-137 and Sr-90 in the southern hemisphere showed a steady increase to values that by early 1965 were more than double those of 1962 although the annual deposition to the end of 1964 was less than that in the northern hemisphere. Data on concentrations of short-lived fission products from the Chinese explosions and from the Russian underground explosion of January 1965 are appended. (auth)

16661 (ECOM-00392-F) THE INFLUENCE OF LOCAL WINDS ON FALLOUT. Final Report, May–December 1965. Report No. 2. Kangos, James D. (Travelers Research Center, Inc., Hartford, Conn.). Mar. 1966. Contract DA-28-043-AMC-00392(E). 54p. CFSTI.

Information on the structure of the sea breeze obtained by previous observational and theoretical studies is employed to develop a kinematic model of the three-dimensional wind field associated with the sea breeze. Existing information on the structure of the stabilized fallout cloud is used in the numerical computation of the deposition of radioactive particles through a specified sea-breeze circulation. A program is developed for numerical computation of fallout transport through an analytically prescribed three-dimensional sea-breeze circulation and for the computation of its ground deposition pattern. The computer program is utilized to illustrate the fallout deposition patterns obtainable from simple models of the stabilized cloud through alternative models of three-dimensional sea-breeze wind fields. (auth)

16662 (HASL-165) FALLOUT PROGRAM QUARTERLY SUMMARY REPORT, SEPTEMBER 1, 1965–DECEMBER 1, 1965. Hardy, Edward P. Jr.; Rivera, Joseph (Health and Safety Lab., New York Operations Office (AEC), N. Y.). Jan. 1, 1966. 390p. Dep. mn. CFSTI $7.00 cy, $1.75 mn.

This report presents current data from the HASL Fallout Program, the National Radiation Laboratory in New Zealand, Argonne National Laboratory, the Argentine Atomic Energy Commission, U. S. Department of Defense, U. S. Atomic Energy Commission, and the U. S. Weather Bureau. Radionuclide levels in fallout, milk, tap water, diet, surface air, and upper air samples are given in tabular form. Also included are interpretive reports and notes dealing with stable and radioactive strontium in children, global atmospheric radioactivity, anticipated distributions for Cd-109 and Pu-238 from SNAP-9A, and the HASL quality control program. (89 references.) (auth)

16663 (TID-21470) FALLOUT FROM THE NUCLEAR EXPLOSION OF OCTOBER 16, 1964. Kuroda, P. K.; Palmer, B. D.; Attrep, Moses Jr.; Beck, J. N.; Ganapathy, R.; Sabu, D. D.; Rao, M. N. (Arkansas Univ., Fayetteville. Dept. of Chemistry). Contract AT(40-1)-2529. 8p. Dep. mn. CFSTI $1.00 cy, $0.50 mn.

Measurements of the concentrations of twenty fission products in a sample of rain collected at Fayetteville, Arkansas, on October 26, 1964, yielded two mass-yield curves; one for the fresh debris from the Chinese bomb, and another for older debris. The former resembled the mass-yield curve for neutron-induced fission of ^{235}U. Data are tabulated. (auth)

16664 (UCRL-14534, pp 19-22) ESTIMATION OF THE AREA ENCLOSED BY A FALLOUT ISOCONCENTRATION LINE. Kathren, R. L. (Lawrence Radiation Lab., Univ. of California, Livermore).

An equation derived from the classical Sutton equations to predict the area enclosed by a given fallout isoconcentration line is discussed. (auth)

16665 (UCRL-14534, pp 23-7) EFFECT OF VARIATION OF AIRBORNE RADON DAUGHTER CONCENTRATION ON WHOLE-BODY COUNTER BACKGROUND. Lindeken, C. L.; Montan, D. N.; Petrock, K. F. (Lawrence Radiation Lab., Univ. of California, Livermore).

Morning and afternoon airborne radon and thoron daughter concentrations at LRL, Livermore, were determined for the period May through September 1965, and the results are discussed relative to their effect on whole-body counter backgrounds. (auth)

16666 (ORNL-tr-923) ON PLEOCHROIC HALOS IN BIOTITE, HORNBLENDE AND CORDIERITE, AND RELATIONS TO THE α-RAYS OF RADIOACTIVE ELEMENTS. Hoevermann, Georg. Translated for Oak Ridge National Lab., Tenn., from Neues Jahrb. Mineral., Geol. Palaeontal., Beil Bd., 34: 321-400(1912). 91p. Dep. mn. JCL $8.60 fs, $2.93 mf.

Dimensions of the pleochroic halos in biotite, hornblende, and cordierite are reviewed and variations in birefringence were measured. Relations between α-rays of radioactive elements and pleochroic halos were investigated. (132 references). (P.C.H.)

16667 ABNORMALLY LONG α-PARTICLE TRACKS IN BIOTITE (MICA). Gentry, Robert V. (Archaeological Research Foundation, Decatur, Ga.). Appl. Phys. Lett., 8: 65-7(Feb. 1, 1966).

The evidence of giant halos in a small piece of biotite (mica), formed by prolonged alpha-particle emission from radioactive inclusions in the host material, is discussed. The possibility of the giant halos being due to protons from (α,p) reactions on low-Z nuclides rather than long-range alpha particles appears to be extremely doubtful. Also an experiment on induced coloration in

mica was performed in which B-10 enriched boron and ordinary uranium were sandwiched between pieces of mica and subsequently irradiated with a thermal neutron flux. Since no induced coloration in the mica was evident due to the alpha from the $^{10}B(n,\alpha)^{7}Li$ reaction or from ^{235}U fission fragments, it is concluded that the development of giant halos is not due to protons from (α,p) reactions. A microphotograph of one of the giant halos found in this mica is also shown and discussed. (J.F.P.)

16668 STUDY OF THE TRITIUM ACTIVITY OF THE BASIN POURING FROM MONT CENIS. Alvinerie, Jacques (Faculte des Sciences, Bordeaux); Degot, Bernadette; Leveque, Paul; Vigneaux, Michel. Compt. Rend., Ser. D, 262: 32-5(Jan. 3, 1966). (In French).

The distribution of tritium in the waters of the Mont Cenis Lake showed, in 1964, a sharply differentiated stratification. The waters of levels with very little activity up to August 1965 showed, after this date, a sharp increase in the activity. (tr-auth)

16669 SEDIMENTOLOGICAL SIGNIFICANCE OF THE NATURAL RADIOACTIVITY OF THE BEACHES OF THE GULF OF LION. Riviere, Andre; Vernhet, Solange (Faculte des Sciences, Orsay, France). Compt. Rend., Ser. D, 262: 440-3(Jan. 24, 1966). (In French).

Variations of the mean radioactivity showed the regions of sedimentological predominance of the different sources of alluvial deposits and the direction of the littoral transport. A mathematical expression of the variations of radioactivity is given as a function of the distances of advance. (tr-auth)

16670 STABLE ISOTOPIC GEOLOGY OF THE GAS HILLS, WYOMING, URANIUM DISTRICT. Cheney, E. S.; Jensen, M. L. (Univ. of Washington, Seattle. Yale Univ., New Haven). Econ. Geol., 61: 44-71(Jan.-Feb. 1966).

A sulfur, carbon, and oxygen isotopic study of more than 300 samples was made of the sandstone-type uranium deposits of the Gas Hills district, Wyoming. The deposits occur as rolls and blankets in the arkosic, lower Eocene Wind River formation located on the southern edge of the Wind River Basin. Pyrite cement associated with uranium mineralization is isotopically similar to the acid-soluble sulfides produced by anaerobic bacteria in nearby springs and is significantly lighter and more variable in $\delta^{34}S$ composition than undoubted magmatic hydrothermal sulfides. Syngenetic-diagenetic pyrite nodules in barren siltstones have a $\delta^{34}S$ composition of 3.7%, ±10.6%. Isotopic analyses of hydrogen sulfide from neighboring oil fields, pyrite in granitic Precambrian cobbles, and groundwater sulfate from the overlying tuffaceous strata are consistent with, but do not prove, the "volcanic leach" hypothesis of origin for the sulfur of the epigenetic pyrite. The very light $\delta^{34}S$ composition of pyrite associated with jordisite and coalified wood, and the enrichment of ^{34}S in selenium-bearing pyrite and groundwater sulfate of the host Wind River formation suggest limited production of hydrogen sulfide, resulting in isotopically heavy supergene sulfides. The extremely light isotopic composition of pyrite associated with jordisite on the leading edges of roll ore bodies is probably caused by oxidation and re-reduction of previously formed biogenic sulfides. Further evidence of a biogenic origin for these deposits is furnished by the carbon isotopic composition of epigenetic calcite cement (−22%, ±4.0%) that is intimately associated with organic material. The similarity of the $\delta^{13}C$ values of calcite associated with asphalt and the calcite associated with coalified wood implies that the anaerobes derived their energy from both. The heavier isotopic composition of most of the other epigenetic calcites suggests some contamination by sedimentary carbonate during calcite precipitation. The epigenetic calcite cements contain some of the lightest oxygen yet reported for carbonates (mean $\delta_{SMOW}{}^{18}O$ = 5.6%, ±6.0%) and may indicate that the uranium deposits formed during Pleistocene time. This study showed that syngenetic-diagenetic and epigenetic deposits of bacterial origin have distinguishable sulfur and carbon isotopic characteristics. The extremely light $\delta^{34}S$ composition of sandstone-type uranium deposits is believed to be primarily due to the reduction of fairly light sulfate by starved anaerobes in an environment that approximates a closed system. Further enrichment in ^{32}S occurs when these isotopically light sulfides are oxidized to light sulfate which is again reduced to pyrite during the formation of roll ore bodies. (auth)

16671 CONTAMINATION OF ^{90}Sr IN STOCK RAINWATER IN LIGHTHOUSES. Nagasawa, Kakuma; Kido, Yasumasa; Ikebuchi, Hideharu (National Inst. of Hygienic Sciences, Tokyo). Eisei Shikenjo Kenkyu Hokoku, No. 81, 62-71(Oct. 1963). (In Japanese).

Contamination by ^{90}Sr, as a result of nuclear weapon tests by the United States and Russia since 1961, in rainwater collected at lighthouses of the Japanese coastal area was investigated. Ten l of rainwater from each of 14 lighthouses was stored in polyethylene bottles, 100 ml nitric acid was added to each, the solutions were mixed well, and allowed to stand for one week. Strontium (100 mg) and Cs (50 mg) salts were added as carriers, and radioactivity was determined by an LBC-1 type, low-background counter. In general, contamination of water stored by lighthouses on Hokkaido was lower than that of Honshu. Since April, 1962, western Japan started to show obvious radionuclide contamination of rainwater. In June the higher degree of contamination spread throughout Japan. This was considered to result from nuclear weapon tests conducted in the Pacific Ocean. However, the contamination gradually fell later. In January, 1963, a high degree of contamination was seen again, extending to the whole of Japan, including Hokkaido. Highest contamination was demonstrated in Nagaohana in March, 1963. Radioactivity from ^{90}Sr in highly contaminated samples was compared with the max permissible concentrations in drinking water proposed by the International Commission for Radiological Protection for occupationally exposed persons. Radioactivity in most contaminated samples was about 3% of the max permissible concentration. In most cases the contamination in drinking water supplies was much lower than the rainwater values; therefore, the extent of ^{90}Sr contamination was considered to be not likely to cause harmful effects in persons using this drinking water. (BBB)

16672 NOBLE GASES FROM THE PEACE RIVER LALANDE AND ACHILLES METEORITES. Rowe, M. W.; Bogard, D. D.; Manuel, O. K. (Univ. of Arkansas, Fayetteville). Geochim. Cosmochim. Acta, 29: 1199-1202 (Dec. 1965).

The noble gas contents and isotopic abundances were measured for samples of the Peace River, LaLande and Achilles chondrites. The noble gases determined from a single Peace River chondrule were enriched in radiogenic ^{129}Xe and ^{40}Ar. The cosmic ray exposure ages and the potassium−argon gas retention ages were calculated. (auth)

16673 RARE GAS EVIDENCE FOR TWO PAIRED METEORITE FALLS. Heymann, Dieter (Univ. of Chicago). Geochim. Cosmochim. Acta, 29: 1203-8 (Dec. 1965). (COO-382-56; EFINS-65-53).

Rare gas contents were determined by mass spectrometry in meteorites of two so-called paired falls: Accalana−Artracoona−Carraweena and La Lande−Melrose−Taiban. The results showed that Accalana and Carraweena are identical, whereas Artracoona appeared to be an independent fall. The La Lande group included perhaps at least one independent fall, Taiban. A comparison of terrestrial meteorite ages to meteorite fall frequencies showed that the survival of coincidences of octahedrites, and ordinary chondrites, is possible. (auth)

16674 RADIOACTIVITY INDUCED BY COSMIC RAYS IN THE BOGOU METEORITE. Tobailem, J.; Nordemann, D. (Centre d'Etudes Nucleaires de Saclay, France. Centre des Faibles Radioactivites, Gif-Sur-Yvette, France). Geochim. Cosmochim. Acta, 29: 1317-30(Dec. 1965). (In French).

Low background gamma spectrometry was used to determine the activities of gamma emitters contained in a

0.185 kg sample sliced out of the Bogou iron meteorite that fell on 14 August 1962, near Bogou, Republic of the Upper Volta. The following results were obtained: for ^{54}Mn, 483 ± 40 dpm kg^{-1}, at time of fall; for ^{22}Na, 0 ± 4; for ^{60}Co, 14 ± 7; for ^{44}Ti, 3.8 ± 3; for ^{26}Al, 4.3 ± 3; and for ^{40}K, ≤9 ± 6. These results are discussed and compared with those obtained by different authors on Bogou and on other iron meteorites. An upper limit for the exposure age (0.9×10^9y) was computed from the ^{40}K and ^{44}Ti contents and the ratio of ^{40}K to ^{44}Ti production rates. (auth)

16675 STABLE CARBON ISOTOPIC COMPOSITION OF BIOGENIC CARBONATES. Cheney, E. S. (Univ. of Washington, Seattle); Jensen, M. L. Geochim. Cosmochim. Acta, 29: 1331-46(Dec. 1965).

The geology and sulfur isotopic composition of epigenetic pyrite of the Gas Hills district, Wyoming, indicated a bacterial origin for these sandstone-type uranium deposits. The $\delta^{13}C$ value of epigenetic calcite associated with organic materials, however, was heavier than the isotopic composition of calcite of biogenic native sulfur deposits. Stratigraphic and carbon isotopic evidence suggested that contamination by sedimentary carbonate is minimal in the Gas Hills samples. Field and laboratory data showed that anaerobes produce isotopically heavier CO_2 and lighter methane than the associated organic material which they consume as an energy source. The $\delta^{13}C$ values of the salt-dome calcites overlapped the methane field, the Gas Hills values overlapped the CO_2 field, and analyses of Sicilian sulfur limestones were intermediate. Presumably a spectrum of values could be obtained by the oxidation of methane and contamination by the original bacterial CO_2 and sedimentary carbonate. The quantized values of the three deposits were, therefore, evidence of strong geologic control. Methane was stable under the reducing conditions (shown by the presence of uraninite and sulfides) of the Gas Hills, while methane was concentrated and oxidized in the cap rock of salt-domes (mineralogy includes native sulfur), and neither methane nor CO_2 was preferentially lost during the syngenetic precipitation of the Sicilian sulfur limestone. (auth)

16676 MEASUREMENT OF $^{18}O/^{16}O$ RATIOS OF TOTAL OXYGEN OF CARBONATES. Sharma, Taleshwar; Clayton, Robert N. (Univ. of Chicago). Geochim. Cosmochim. Acta, 29: 1347-53(Dec. 1965).

The commonly used phosphoric acid procedure for the determination of oxygen isotope abundances in carbonates involves a large kinetic isotope effect. The value of the fractionation factor, α, defined as;

$$\alpha = \frac{(^{18}O/^{16}O)_{CO_2}}{(^{18}O/^{16}O)_{carbonate}}$$

was measured for several alkaline earth and transition metal carbonates. The value of 1000 ln α ranged from 9.9 to 11.2. The previously used assumption that calcite and dolomite have the same value of α led to an overestimate of the dolomite–calcite oxygen isotope fractionation by 0.8 per mil. (auth)

16677 OBSERVATION OF HOT RADIOACTIVE PARTICLES IN THE ATMOSPHERE DURING 1962–1964. Bykhovskii, A. V.; Zaraev, O. M. (Karpov Inst. of Physics and Chemistry, Moscow). Gig. Sanit., 11: 47-54(1965). (In Russian).

Systematic observations of the content of radioactive aerosols in the atmosphere are reported. The filters through which 150 to 200 thousand cubic meters of the air were drawn, were assayed autoradiographically. Separate hot particles were isolated from the filter and subjected to γ-spectrometry, and by means of a second autoradiograph, a nomograph was drawn for converting the results of autoradiographic assay of filters into values expressing the activity of separate aerosol particles. The presented data point to an abrupt fall in the concentration of hot aerosol particles in the atmosphere during the period 1963 to 1964 when the testing of nuclear weapons in the atmosphere had ceased. (auth)

16678 SOME DATA AND COMMENTS ON ^{22}Na IN FOOD CHAINS. de Bortoli, M.; Gaglione, P.; Malvicini, A. (Joint Nuclear Research Center, Ispra, Italy). Health Phys., 12: 353-9(Mar. 1966).

Measurements of ^{22}Na concentration in fallout, herbage, and milk samples are described together with the method employed, which consists of gamma spectrometry in coincidence with the sum pulses of the gamma rays in cascade. From the data obtained, the ratio of activity of ^{22}Na to ^{137}Cs in fallout appears to be less than the same ratio in milk, which is probably due to greater uptake from soil of the former isotope than of the latter. There are difficulties in calculating the enhancement factors, but they may be estimated to be about 4 in the step herbage-milk and 10 or more in the complete step fallout-milk. (auth)

16679 A GRAPHICAL METHOD FOR THE ESTIMATION OF RADON AND THORON IN ATMOSPHERIC AIR. Abraham, P. (Atomic Energy Establishment, Trombay, India). Indian J. Pure Appl. Phys., 4: 27-9(Jan. 1966).

A graphical method for the estimation of radon and thoron in air by the alpha (or beta) activity measurements of filter paper air samples is described, assuming that radioactive equilibrium exists between the parent gas and the immediate daughter products. Graphs are presented showing the radon and thoron concentrations for ratios of alpha (and beta) activities of the sample at different times after collection, for various sampling periods. The application of the method is illustrated by a calculated example. (auth)

16680 AIRBORNE RADIOACTIVITY AT DELHI. Deb, A. R.; Krishna Murti, G. S. R.; Natarajan, R. (Indian Agricultural Research Inst., New Delhi, India). Indian J. Pure Appl. Phys., 4: 30-2(Jan. 1966).

The radioactivity of the aerosols in open air in the area around the Indian Agricultural Research Institute, New Delhi, was measured by the filter paper method during the period July 1962 to August 1963. The average activity level during the period was found to vary between 2×10^{-13} and 12×10^{-13} curies/liter except on a few occasions. The observed lower average activity level during the monsoon and pre-monsoon months indicates the effect of raindrops and strong winds in removing the activity. A rough estimate of the activity due to nuclear explosion products was made. (auth)

16681 SOME FALLOUT RADIONUCLIDES IN DEEP WATERS AROUND JAPAN. Nagaya, Yutaka; Shiozaki, Masaru; Seto, Yoshio (Maritime Safety Agency, Tokyo). J. Radiat. Res., 6: 23-31(Mar. 1966).

Deep water samples collected in 1963 and 1964 in the adjacent seas of Japan were analyzed radiochemically. Sr–90 and Cs–137 were detected in the deep layers down to 6,000 meters deep and showed approximately uniform vertical distributions below 1,000 meters. Mean concentrations of Sr–90 in deep waters were 0.028 μμc/l in the Pacific and 0.035 μμc/l in the northern Japan Sea, and those of Cs–137 were 0.034 and 0.075 μμc/l respectively. The mean Cs–137/Sr–90 ratios in deep layers of the Pacific showed uniform distribution and the mean value of 1.4, but in the northern Japan Sea, remarkably higher value of 5.5 due to the Sr–90 depletion was found in 1,000 to 2,600 meters layer. Vertical distribution of Ce–144 suggests strong biological retention within the surface layer, and from the apparently uniform distribution in deep layers, 400 meters per month was estimated as the sinking rate of Ce–144. (auth)

16682 CONTAMINATION OF THE BIOSPHERE BY ^{137}Cs FROM WEAPON TEST FALLOUT. Csupka, Stefan; Petrasova, Maria; Carach, Jozef (Regional Station of Hygiene and Sanitation, Bratislava). Jad. Energ., 12: 16-19(Jan. 1966). (In Czech).

The concentration of ^{137}Cs in the precipitation on the territory of western Slovenia was measured in 1962 and 1963. The total β-active precipitation had, in 1963, a tendency to decrease. The specific gravity of the semimonthly activity of ^{137}Cs in the total β activity amounted

in 1962 to 0.9% and in 1963 to 3.2%. In 1963 the activity of ^{137}Cs was 1.3 times higher than the ^{90}Sr. The cumulative value of the radiocesium in 1962 to 1963 amounted to 37.8 nC/m^2. (tr-auth)

16683 THE MEASUREMENT OF GROSS AIR ACTIVITY (LOWER ATMOSPHERE) AT LAHORE. Khan, Umar Hayat; Ahmed, Syed Mansoor. Nucleus (Lahore), 2: 26-9(Apr.-June 1965).

The mechanism of fallout spread and the methods and observations recorded at Lahore, Pakistan are described. Continuous air monitoring is carried out by the fixed filter method. About 3000 to 5000 m^3 of air are sucked through a filter in 24 hr. It is then replaced with another filter. The first filter is then counted for gross activity at different time intervals. Gross activities measured from February 1964 through March 1965 are presented. Results varied from 1.00×10^{-4} to 9.40×10^{-4} μC. (M.C.G.)

16684 DISTRIBUTION OF URANIUM IN SOME NATURAL MINERALS. Hamilton, E. I. (Oxford Univ.). Science, 151: 570-2(Feb. 4, 1966).

The advantages of the fission method over conventional autoradiography for studying the distribution of uranium in natural minerals are described. Relatively high concentrations of uranium associated with micro inclusions in the St. Marks enstatite chondrite were observed and may account for the variation of the uranium concentrations in different samples of this meteorite. (auth)

16685 THE RADIOCHEMICAL MEASUREMENT OF PROMETHIUM ISOTOPES IN NATURE [Thesis]. Attrep, Moses Jr. Fayetteville, Ark., Univ. of Arkansas, 1965. 96p.

The presence of promethium in nature is due to the spontaneous fission of ^{238}U. ^{147}Pm ($T_{\frac{1}{2}}$ = 2.65 years) and ^{149}Pm ($T_{\frac{1}{2}}$ = 53 hours) were isolated and identified in the uranium bearing ore, African pitchblende (42 percent uranium). An analytical scheme devised for its isolation from pitchblende included the development of a fast, reliable ion-exchange separation technique for the separation of the individual rare earths using α-hydroxyisobutyric acid as the eluant. Equilibrium activities of ^{147}Pm and ^{149}Pm are given for depleted uranium and pitchblende samples. Assuming that ^{147}Pm is produced solely by spontaneous fission of ^{238}U in the depleted uranium sample, the spontaneous fission yield was calculated to be 6.1 ± 1.4 percent. A value of 2.5 ± 0.7 percent was obtained for ^{149}Pm. From the pitchblende samples, higher equilibrium ratios were obtained. The ratio of neutron-induced fission of ^{235}U to spontaneous fission of ^{238}U was found to be about 0.10 in African pitchblende for ^{147}Pm. In conjunction with the search for promethium in nature, promethium isotopes were isolated in the first rain in Fayetteville, Arkansas, following the Chinese test of October 16, 1964. Neodymium, samarium, and europium radioactive isotopes were also measured. (Dissertation Isotopes)

16686 L'UTILISATION DES ISOTOPES DANS L'ETUDE GLACIOLOGIQUE DES CALOTTES POLAIRES. (The Use of Isotopes in the Glaciological Study of the Polar Caps). Lorius, C. Mission Paul-Emile Victor No. 253. Paris, Expeditions Polaires Francaises, 1963. 19p.

Reasons for scientific interest in the Antarctic polar cap are briefly indicated. Radioisotopes and their use in age determinations and in the determination of particular levels are discussed. The deuterium cycle in nature is described. It is shown that there is a seasonal variation in the deuterium concentration of precipitations and the isotopic concentration depends on the geographic location and the mean annual temperature. Glaciological uses of the deuterium cycle for study of accumulation and for determination of the ice characteristics are described. (J.S.R.)

16687 CALCULATION OF THE RADIATION DOSE RESULTING FROM NATURAL AND ARTIFICIAL RADIOACTIVE ISOTOPES IN THE GROUND BY GAMMA-RAY SPECTROMETRY. Keil, R. A.; Franke, Th. (Max-Planck-Institut fuer Biophysik, Frankfurt am Main). 12p. (CONF-747-9). ORINS.

From 4th Symposium on Radioactivity in Scandinavia, Risoe, Denmark, Oct. 5-6, 1964.

By means of gamma spectrometry artificial radiation components can be separated from the natural ambient radiation resulting from the natural radioactive isotopes in the ground. A 4.5 × 2 in. NaI(Tl) scintillation crystal and a multichannel analyzer installed in a vehicle were used to study these problems and to estimate the dose rates from natural and artificial gamma radiation fields. Two different methods were developed to obtain total dose rates as well as dose rates from single radioisotopes. The first method uses the calculation of total energy absorbed in the NaI(Tl) scintillator. The relation between absorbed dose in rad and exposure dose in Roentgen is shown. The second method uses the area under the total absorption peak which is proportional to the primary flux of photons of specific energy at the detector. The calibration was carried out by point and plane standard sources of different γ ray energies between 100 kev and 1.8 Mev. If angular response of the detector and soil depth distribution of the nuclides is taken into account, dose rates can be estimated within an error of 10 to 20% as shown in the region of 0.01 to 50 $\mu R/hr$. (auth)

16688 NEW PROBLEMS IN THE INVESTIGATION OF NATURAL RADIOACTIVITY OF THE ATMOSPHERE. Styro, B. I. pp 7-17 of Radioaktivnye Izotopy v Atmosfere i Ikh Ispol'zovanie v Meteorologii. Karol, I. L. (ed.). Moscow, Atomizdat, 1964. (In Russian).

The significant role of aerosols in research on the radioactive pollution of the atmosphere is discussed, and a summarized review of recent research on the nature, distribution, and processes affecting radioactive aerosols is presented. The need for coordinated systematic studies and techniques is stressed. (ATD)

16689 ESTIMATE OF THE RATE OF FORMATION OF CERTAIN RADIOACTIVE ISOTOPES IN THE ATMOSPHERE. Luyanas, V. Yu. pp 18-27 of Radioaktivnye Izotopy v Atmosfere i Ikh Ispol'zovanie v Meteorologii. Karol, I. L. (ed.). Moscow, Atomizdat, 1964. (In Russian).

Some calculations of the production (and concentrations) of radioisotopes by cosmic-ray reactions are discussed. An attempt is made to define more accurately the mechanisms by which tritium is produced. (D.C.W.)

16690 SPECTRA OF THE DIMENSIONS AND MOBILITY OF NATURAL RADIOACTIVE AEROSOLS IN THE ATMOSPHERE. Styro, B. I.; Matulyavichene, V. I. pp 28-39 of Radioaktivnye Izotopy v Atmosfere i Ikh Ispol'zovanie v Meteorologii. Karol, I. L. (ed.). Moscow, Atomizdat, 1964. (In Russian).

Some instrumentation developed for use in separating radioactive ions by size distribution is described. The methods and procedures used in field tests performed during the summer of 1961 along the coast of the Baltic Sea and at Vilnius in 1962 to study the aerosol-size and mobility spectra of RaC′ and Rn are summarized, and the results are compared with other observations. (D.C.W.)

16691 EMISSION OF RADON FROM THE SURFACE OF SOME TYPES OF SOILS IN EUROPEAN USSR AND KAZAKHSTAN. Sisigina, T. I. pp 40-6 of Radioaktivnye Izotopy v Atmosfere i Ikh Ispol'zovanie v Meteorologii. Karol, I. L. (ed.). Moscow, Atomizdat, 1964. (In Russian).

An investigation of the amount of Rn emitted from various types of soils and of fluctuations in the emission from identical soils from several areas in European USSR and in Southwestern Kazakhstan is summarized. The collection and analytical methods and equipment are briefly described. (D.C.W.)

16692 RADON CONCENTRATION AND VERTICAL TURBULENT MIXING IN THE SURFACE BOUNDARY LAYER OF THE ATMOSPHERE. Milin, V. B.; Malakhov, S. G.; Zorina, K. I.; Sisigina, T. I. pp 47-56 of Radioaktivnye Izotopy v Atmosfere i Ikh Ispol'zovanie v Meteorologii. Karol, I. L. (ed.). Moscow, Atomizdat, 1964. (In Russian).

The results of an analysis of simultaneous measurements of Rn concentration in the surface boundary layer of the atmosphere and in the soil, the amount of Rn exhaled from the surface, and the coefficient of vertical turbulent mixing are described. Two series of measurements were made—7 km south of Kirov in the summer of 1950 mainly under convective conditions and in the Moscow region in the summer of 1962 with a surface boundary layer inversion. The effect of vertical turbulent mixing on the concentration of Rn in the surface boundary layer was determined to be of major significance. (ATD)

16693 VARIATION IN THE RADON-CONCENTRATION FIELD IN THE ATMOSPHERE IN THE PRESENCE OF SECTORS WITH NONHOMOGENEOUS EXHALATION VALUES. Kirichenko, L. V. pp 57-72 of Radioaktivnye Izotopy v Atmosfere i Ikh Ispol'zovanie v Meteorologii. Karol, I. L. (ed.). Moscow, Atomizdat, 1964. (In Russian).

Equations are derived for the two-dimensional and three-dimensional determination from localized sources of the field of Rn concentration, taking into account horizontal wind transfer and vertical turbulent diffusion. An analysis is made of experimental data taken from the literature for the vertical wind profile and the profile of the coefficient of vertical turbulent diffusion in the boundary layer and surface boundary layer of the atmosphere. (ATD)

16694 RADON AS AN INDICATOR OF ATMOSPHERIC STABILITY. Sisigina, T. I. pp 73-80 of Radioaktivnye Izotopy v Atmosfere i Ikh Ispol'zovanie v Meteorologii. Karol, I. L. (ed.). Moscow, Atomizdat, 1964. (In Russian).

The results of experimental studies carried out in 1961-1963 from the 300-meter meteorological tower and related facilities on the vertical distribution of Rn in the lower layer of the atmosphere (to 300 m) under various stratification conditions, are presented, and an estimate is made of the coefficients of vertical turbulent mixing using Rn as the tracer. Meteorological data measured from the tower included temperature and wind speed and direction. (ATD)

16695 SEASONAL CHANGES IN RADON AND THORIUM CONCENTRATION IN THE SURFACE BOUNDARY LAYER OF THE ATMOSPHERE. Malakhov, S. G.; Chernysheva, P. G. pp 81-92 of Radioaktivnye Izotopy v Atmosfere i Ikh Ispol'zovanie v Meteorologii. Karol, I. L. (ed.). Moscow, Atomizdat, 1964. (In Russian).

The techniques, procedures, and calculations used to determine the concentrations of Th and Rn decay products in the atmosphere over the Moscow area from 1959 through 1961 are described. The results of these determinations are compared with the amounts of seasonal and daily Rn exhalation from the soil measured in the surface boundary layer of the atmosphere. An attempt is also made to make a comparison with measurements of decay products in the troposphere. (ATD)

16696 FRACTIONATION OF THE RADIOACTIVE PRODUCTS OF A NUCLEAR EXPLOSION. Grechushkina, M. P.; Izrael, Yu. A. pp 164-80 of Radioaktivnye Izotopy v Atmosfere i Ikh Ispol'zovanie v Meteorologii. Karol, I. L. (ed.). Moscow, Atomizdat, 1964. (In Russian).

A review on the fractionation of the radioactive products of nuclear explosions detonated in the air and on the ground is presented. 31 references. (D.C.W.)

16697 SYNOPTIC-CLIMATIC SKETCH MAPS OF GLOBAL STRATOSPHERIC RADIOACTIVE FALLOUT. Dmitrieva, G. V. pp 283-92 of Radioaktivnye Izotopy v Atmosfere i Ikh Ispol'zovanie v Meteorologii. Karol, I. L. (ed.). Moscow, Atomizdat, 1964. (In Russian).

The results of a study that was carried out in 1961, 1962, and (especially) 1963 on the fallout of the radioactive products of thermonuclear explosions and the atmospheric processes producing this fallout over the Northern Hemisphere are presented. (D.C.W.)

16698 AEROSYNOPTIC CONDITIONS FOR THE APPEARANCE ON THE EARTH'S SURFACE OF AREAS OF INCREASED CONCENTRATIONS OF STRATOSPHERIC RADIOACTIVE PRODUCTS. Dmitrieva, G. V.; Kasatkina, V. I. pp 293-306 of Radioaktivnye Izotopy v Atmosfere i Ikh Ispol'zovanie v Meteorologii. Karol, I. L. (ed.). Moscow, Atomizdat, 1964. (In Russian).

Methods that were used to identify the characteristics of various synoptic situations present in the surface boundary layer of the atmosphere over regions which have exhibited especially high radioactivity after thermonuclear explosions and to identify the mechanisms by which radioactive air passes from the stratosphere into the surface boundary layer are described. The data used in these studies were collected from approximately 50 stations in the United States during the IGY. (ATD)

16699 NATURAL AND ARTIFICIAL RADIOACTIVITY OF THE ATMOSPHERE OVER THE OCEANS AND THE RELATIONSHIP TO METEOROLOGICAL FACTORS. Vilenskii, V. D.; Dmitrieva, G. V.; Krasnopevtsev, Yu. V. pp 307-22 of Radioaktivnye Izotopy v Atmosfere i Ikh Ispol'zovanie v Meteorologii. Karol, I. L. (ed.). Moscow, Atomizdat, 1964. (In Russian).

The content and distribution of natural (Rn) and artificial (^{210}Pb and ^{90}Sr) radioactivity in the near-water layer of the atmosphere in the low and equatorial latitudes were studied, together with the relation of this distribution to meteorological conditions. The study was based on data collected on a voyage in the summer of 1960 by a research ship from Odessa across the Black, Mediterranean, and Red Seas and the Indian and Pacific Oceans to Vladivostok. (D.C.W.)

16700 RADIOACTIVE FALLOUT IN VILNIUS IN 1962. Yakovleva, G. V.; Garbalyauskas, Ch. A.; Styrko, B. I.; Shvedov, N. P. pp 338-41 of Radioaktivnye Izotopy v Atmosfere i Ikh Ispol'zovanie v Meteorologii. Karol, I. L. (ed.). Moscow, Atomizdat, 1964. (In Russian).

The radioactive fallout in Vilnius in 1962 was investigated by measuring the ratios ^{141}Ce/^{144}(Ce + Pr) and ^{95}(Zr + Nb)/^{144}(Ce + Pr) using scintillation gamma spectroscopy. A steep increase was found in the total fallout rate between the spring and summer of 1962. This increase reached a maximum in September and fell considerably by December. (G.O.Y.)

16701 FALLOUT OF ^{90}Sr AND ^{137}Cs ISOTOPES IN THE VICINITY OF LENINGRAD IN 1961–1963. Gedeonov, L. I.; Zhilkina, M. I. pp 342-4 of Radioaktivnye Izotopy v Atmosfere i Ikh Ispol'zovanie v Meteorologii. Karol, I. L. (ed.). Moscow, Atomizdat, 1964. (In Russian).

The deposition of ^{137}Cs and ^{90}Sr in the area around Leningrad was studied between 1961 and 1963. The maximum concentrations of both isotopes were observed in June, July, and August of 1962. Most of the deposition of ^{90}Sr was by daily precipitation. (D.C.W.)

16702 ACCUMULATION OF ^{90}Sr AND ^{137}Cs IN THE SOILS OF THE LENINGRAD REGION. Gedeonov, L. I.; Vinogradova, V. K.; Rosyanov, S. P.; Gritchenko, Z. G. pp 345-50 of Radioaktivnye Izotopy v Atmosfere i Ikh Ispol'zovanie v Meteorologii. Karol, I. L. (ed.). Moscow, Atomizdat, 1964. (In Russian).

The results of experiments to measure ^{137}Cs and ^{90}Sr in arenaceous soils between 1958 and 1962 in the environs of Petrokrepost are presented, and the cumulative deposition of these isotopes on the earth's surface is discussed. It is concluded that vertical washout by precipitation is responsible for a large percentage of the surface accumulation of ^{90}Sr and that surface waters washed out the ^{90}Sr into the rivers, seas, and oceans. Contamination through seepage was negligible. It was also found that accumulation on surface soils depends on the physicō-chemical properties of the soil. (G.O.Y.)

16703 DETERMINATION OF ANNUAL ^{90}Sr FALLOUT IN THE POLAR REGIONS BY RECORDING THE ^{90}Sr CONTENT IN THE SEASONAL LAYERS OF SNOW AND ICE IN ICEBERGS OF FRANZ JOSEF AND NORTHERN LANDS.

Davydov, E. N.; Nekhorosheva, M. P. pp 351-6 of Radioaktivnye Izotopy v Atmosfere i Ikh Ispol'zovanie v Meteorologii. Karol, I. L. (ed.). Moscow, Atomizdat, 1964. (In Russian).

Seasonal measurements of ^{90}Sr fallout on the snow layers were performed from towers in the Franz Josef land beginning in the spring of 1960 and from towers in the Northern lands beginning in the spring of 1963. The measurements covered a diameter of 30 to 100 km and were made at heights of less than 500 m in the Franz Josef land and less than 1000 m in the Northern land. The main source of accumulation of ^{90}Sr was precipitation from the atmosphere. When the icebergs and hard snows melted in the summers, the ^{90}Sr was washed out into the ocean. The measurements presented were considered sufficient to characterize the whole polar region. (G.O.Y.)

16704 CHEMICAL COMPOSITION OF ATMOSPHERIC PRECIPITATION AND FALLOUT IN THE VICINITY OF LENINGRAD. Gedeonov, L. I.; Zhilkina, M. I.; Il'inskaya, T. I.; Stepanov, A. V. pp 357-60 of Radioaktivnye Izotopy v Atmosfere i Ikh Ispol'zovanie v Meteorologii. Karol, I. L. (ed.). Moscow, Atomizdat, 1964. (In Russian).

The chemical composition of the fallout in the environs of Leningrad was analyzed by collecting precipitation in Duralumin cells and porcelain vats lined with low-ash filter paper on the bottom and exposed to atmospheric precipitation for periods of one month at a time. The papers were then heated to 450–550°C in a muffle furnace and were weighed. They were then submitted to beta and gamma spectroscopic analyses, which revealed the presence of $^{89-90}Sr$, $^{141-144}Ce$, ^{137}Cs, and ^{91}Y. Some runs showed traces of ^{140}Ba, ^{111}Ag, ^{99}Mo, ^{95}Zn, ^{125}Sb, ^{7}Be, and other related isotopes. The percentage composition of other compounds and elements in the atmospheric precipitation was also determined. (G.O.Y.)

16705 ^{90}Sr IN THE FRESH-WATER RESERVOIRS OF THE SOVIET UNION IN 1961–1962. Sereda, G. A.; Bobovnikova, Ts. I. pp 361-72 of Radioaktivnye Izotopy v Atmosfere i Ikh Ispol'zovanie v Meteorologii. Karol, I. L. (ed.). Moscow, Atomizdat, 1964. (In Russian).

In the period of 1961–1962, a two-part study was made of the ^{90}Sr content of the rivers and reservoirs of the Soviet Union. The first phase consisted of determinations of the ^{90}Sr content in five of the rivers in the Moscow region in relation to global fallout and the content in the soils in these river basins, in the organisms living in the water, and in land-area plant life. The second phase of the study involved the measurement of the ^{90}Sr content in 70 to 100 rivers and reservoirs in the Soviet Unionn (at the rate of 10 samples a year). Statistical analyses of the measurements made over the two-year period established that the minimum number of analyses required to check the ^{90}Sr content in fresh-water reservoirs is one to two samples during low-water periods and a slightly larger number during floods. Since the ^{90}Sr content in materials carried in suspension in the water was found to be negligible, special determinations were not required. The $^{90}Sr/Ca$ ratio was found to be 2 to 11 times larger in the waters of the 60 to 70° North Latitude belt than it was in those located in the middle and low latitudes. This fact was attributed to the higher Ca content in the chernozems, sierozems, and chestnut soils of the forest-steppe and steppe zones in the southern part of the Soviet Union. (ATD)

16706 NATURE OF THE ACCUMULATION OF ATMOSPHERIC AEROSOLS ON OCEAN SURFACES. Popov, N. I. pp 373-9 of Radioaktivnye Izotopy v Atmosfere i Ikh Ispol'zovanie v Meteorologii. Karol, I. L. (ed.). Moscow, Atomizdat, 1964. (In Russian).

Some investigations of the accumulation of radioactive aerosols on land masses and on ocean surfaces are reviewed. (G.O.Y.)

16707 MEASUREMENTS OF β ACTIVITY OF FISSION PRODUCTS. Gritchenko, Z. G.; Gedeonov, L. I.; Flegontov, V. M. pp 435-45 of Radioaktivnye Izotopy v Atmosfere i Ikh Ispol'zovanie v Meteorologii. Karol, I. L. (ed). Moscow, Atomizdat, 1964. (In Russian).

The beta activity of fission products was studied as a function of the weight of the sample and of time after the explosion. The isotopic composition of the samples was determined using gamma spectrometry. It was found that the beta activity of the mixed fission products varied definitely with their age after the explosion. (D.C.W.)

16708 ADSORPTION METHOD OF DETERMINING RADON CONCENTRATION IN THE AIR FROM AN AIRPLANE. Izrael, Yu. A.; Tishchenko, O. P.; Shchetinin, N. N. pp 466-72 of Radioaktivnye Izotopy v Atmosfere i Ikh Ispol'zovanie v Meteorologii. Karol, I. L. (ed.). Moscow, Atomizdat, 1964. (In Russian).

A brief description is given of experimental equipment for the in-flight measurement of the radon content in the atmosphere. The results of some measurements over land areas near the White Sea in 1960 are presented. (G.O.Y.)

Site Survey and Selection

16709 SOME NON-TECHNICAL ASPECTS OF NUCLEAR POWER. PART I. CRITERIA AND SITING OF REACTORS. EuroNuclear, 3: 77-9(Feb. 1966).

Problems concerned with the siting of nuclear power stations, particularly in the densely populated areas of Europe, are discussed. Engineered safeguards variables, gas-cooled reactors, site variables, and siting distances are considered. Initial estimates of distances for reactors of various power levels are listed. (M.C.G.)

16710 AN AUTOMATIC DATA LOGGING SYSTEM FOR METEOROLOGICAL STUDIES IN REACTOR ENVIRONMENT. Joshi, C. W.; Ingle, N. A.; Jathar, N. B. (Atomic Energy Establishment, Trombay, India). Vienna, International Atomic Energy Agency, 1965, Preprint No. CN-22/43, 14p. (CONF-651105-20). ORAU.

From Conference on Nuclear Electronics, Bombay.

An automatic data logging system, which was designed for meteorological studies for the Tarapur power reactor, is described. The system is designed to log data from 256 sensors divided into two groups of 128. (D.C.W.)

Techniques and Equipment

16711 (MIT–1381-13) VARIATIONS IN ISOTOPIC ABUNDANCES OF STRONTIUM, CALCIUM, AND ARGON AND RELATED TOPICS. Thirteenth Annual Progress Report for 1965. (Massachusetts Inst. of Tech., Cambridge. Dept. of Geology and Geophysics). Dec. 1, 1965. Contract AT(30-1)-1381. 112p. Dep. mn. CFSTI $4.00 cy, $0.75 mn.

Information is given on age estimations and isotopic abundances in New England rocks, tektites, Canadian rocks and volcanic material, and sea and surface waters. Rubidium, strontium, argon, potassium, and calcium isotopes were primarily studied. (P.C.H.)

16712 DATING OF THE BEILLARD PEAT BOG BY THE ^{14}C METHOD. Durand, Georges Louis (Faculte des Sciences du Maroc, Rabat, France); Guillet, Bernard Compt. Rend., Ser. D, 262: 28-31(Jan. 3, 1966). (In French).

The Beillard peat bog (Vosges) was previously studied by J. P. Hatt in 1937 from the palynological viewpoint. This peat bog was dated by using the method of pollinicious analysis and the ^{14}C method. The results showed a clear agreement between the two dating methods. (tr-auth)

16713 EVALUATION OF RUBIDIUM AND IRON BIAS IN FLAME PHOTOMETRIC POTASSIUM DETERMINATION FOR K–Ar DATING. Cooper, J. A.; Martin, I. D.; Vernon, M. J. (Australian National Univ., Canberra). Geochim. Cosmochim. Acta, 30: 197-205(Feb. 1966).

The use of a flame photometer for determination of potassium in the presence of rubidium was investigated. An interference effect of 2 parts Rb ≡ 1 part K is observed. This effect is shown to result in considerable error in potassium determination for the K–Ar dating technique when applied to pegmatite and some granitic materials. By use of a selective filter in the optical path of the instrument, the effect can be eliminated. The non-ionic iron interference previously reported was further investigated. It is shown to be significant only for samples of low potassium content such as pyroxenes, some hornblendes, and some tholeiitic basalts. A method for correcting for iron content in such samples is outlined. The practical significance of these two effects in relation to potassium–argon dating is discussed. (auth)

16714 HELIUM IN MAGNETITE [Thesis]. Fanale, Fraser Partington. New York, Columbia Univ., 1964. 157p.

Isotope dilution mass spectrometric uranium, thorium, and helium analyses were performed on several acid-leached magnetites from two Paleozoic ore bodies (Cornwall, Pa. and Santa Rita, New Mexico). The uranium, thorium–helium ages obtained on magnetites from these deposits were found to be in good agreement with estimates based on stratigraphic and absolute geochronological control. Since an excellent correlation of helium content with alpha activity was observed in both suites of samples, it can be concluded that all the observed helium was produced by decay of alpha emitters located in the samples. It is evident that essentially all the helium produced in these samples was quantitatively retained by the magnetite lattice for periods on the order of 10^8 years. Thus it appears that the method, when applied to leached magnetites represents a valuable geochronological tool. However, multiple sample analysis on samples of different activities is necessary to establish that initial helium is not present. Significant "excesses" of helium were found in magnetites from two Pre-Cambrian deposits. The helium contents of these samples were not high relative to most magnetite but their alpha activities were unmeasurably low. Thus it could be established that essentially none of the observed helium was produced by alpha decay in the samples. To establish the origin of the excess, argon measurements were performed on these samples. Significant excesses of argon were also found and the excess He : excess Ar ratios were found to be in reasonable agreement with those observed in beryls and natural gases. Because of this observation and the common characteristics of previously studied samples, it is thought that this gas is typical radiogenic rock gas, the distribution of which in the rock is thought to have been "frozen in" at some point during cooling of the rock. (A.G.W.)

16715 APPLIED GEOCHRONOLOGY. Hamilton, E. I. With a Chapter on Comparative Geochemistry by L. H. Ahrens. New York, Academic Press, Inc., 1965. 278p. $10.00.

The dating of rocks and the related field of isotope abundance studies are discussed. Emphasis is placed on the chemical and physical methods used, the significance of the results, and their interpretation in terms of investigating conventional geological problems. The ^{14}C, K–Ar, Rb–Sr, Re–Os, U–Th–Pb methods of age estimation are among those described. Radiation damage methods and the common lead method are also considered. The dating of modern sediments, meteorite ages, and the geological time scale are discussed. The comparative geochemistry of K, Rb, Ca, Ar, Sr, U, Th, and Pb is considered. (M.C.G.)

Thorium and Uranium Minerals

16716 SECOND FORATOM CONGRESS. URANIUM RESERVES. Closs, H. (Etablissement Federal pour la Recherche Fondamentale, Hanover). Bull. Inform. A.T.E.N. (Ass. Tech. Energ. Nucl.), No. 57, 5-16(Jan.-Feb. 1966). (In French).

The long-term needs in natural U are evaluated for the countries of Europe and compared with the needs of the United States. The natural U reserves of Europe and Western countries are summarized. The long-term stock-piling of natural U is reviewed. An example is given of the presumed evolution of the price of natural U. The possibilities for the production of U concentrates from ores are discussed. The needs for enriched U and Pu and the probable evolution of their prices are considered. (J.S.R.)

16717 STUDIES OF RADIOACTIVE DISEQUILIBRIUM IN MINERALS BY ALPHA-RAY SPECTROSCOPY. Gopalan, K.; Venkatasubramanian, V. S. (Indian Inst. of Science, Bangalore, India). Indian J. Pure Appl. Phys., 3: 478-82(Dec. 1965).

The technique of alpha spectral analysis using a gridded ionization chamber was applied for determination of the relative abundances of the uranium-derived nuclides and hence the degree of radioactive equilibrium in a number of uranium minerals. The types of disequilibria obtained are discussed with special reference to determination of the ages of deposition of uranium in favorable cases. (auth)

16718 THE OUTLOOK FOR URANIUM. A Survey of the U. S. Uranium Market. A Report to the East Central Nuclear Group. Hogerton, John F.; Geller, Leonard; Gerber, Abraham. New York, S. M. Stoller Associates, 1965. 77p.

Information is given on: AEC procurement program for uranium; major U. S. uranium producers; U. S. uranium reserves and resources; projection of U. S. uranium demand; uranium price futures; and business patterns and long-term contracts. The survey was made in order to: collect basic facts about the experience the U. S. has had in finding and producing uranium, and about the current U. S. uranium industry; arrive at a working hypothesis as to uranium price futures and thereby provide inputs needed for analysis of future trends in atomic fuel costs; and develop ideas, from the utility standpoint, about possible future patterns of uranium buying. (P.C.H.)

HEALTH AND SAFETY

See also BIOLOGY AND MEDICINE — Radiation Hazards and Protection
GEOLOGY, METEOROLOGY, AND MINERALOGY — Natural Radioactivity and Fallout

Refer also to abstracts 16226, 16303, 16562, 16665, 16827, 18156, and 18157.

16719 (AEEW-M-568) THE EFFICIENCY OF WHATMAN TYPE ACG/B FILTER PAPERS FOR METHYL IODIDE RETENTION IN AIR. Davis, R. E.; Williams, J. M. E. (Atomic Energy Establishment, Winfrith (England)). Nov. 1965. 10p. Dep. BIS $0.50. HMSO 2s. 6d.

Experiments are described in which charcoal-impregnated glass fiber filter papers Type ACG/B were exposed to methyl iodide vapor and the penetration determined for iodide loadings ranging from 2×10^{-7} to 2×10^{-1} $\mu g/cm^2$ of filter area. Air was subsequently passed through the filters, and at intervals the amount of methyl iodide remaining on them was determined. Penetrations during loading varied from 30% to 80%, but after 10-min elution all filters retained less than 5% of the methyl iodide originally present. (auth)

16720 (AERE-R-4669) FILM DOSIMETRY PRACTICE WITH THE A.E.R.E./R.P.S. FILM HOLDER: A COLLECTION OF EXPERIMENTAL DATA. Adams, N.; Heard, M. J.; Holt, P. D. (eds.) (Atomic Energy Research Establishment, Harwell (England)). Aug. 1965. 88p. Dep.; BIS $2.40; HMSO 12s.

In order to establish film dosimetry procedures for personnel monitoring in two different laboratories, studies were made on: response of film dosimeter to photon and beta radiation; photographic processing; calibration; and dose assessment. The film used was Kodak R.M. contained in a plastic holder. The procedures are supported by experimental measurements made over several years, which are reported. (P.C.H.)

16721 (AWRE-NR-1/66) MEASUREMENT OF THE CRITICAL MASS OF 37 1/2 PERCENT ENRICHED URANIUM IN REFLECTORS OF WOOD, CONCRETE, POLYETHYLENE AND WATER. Lane, R. C.; Perkins, O. J. E. (Atomic Weapons Research Establishment, Aldermaston (England)). Feb. 1966. 20p. Dep. BIS $1.40. HMSO 7s.0d.

The experimental arrangements used in ATLAS, a vertical assembly machine, for measurement of the critical mass of enriched (37½%) uranium in reflectors of wood, concrete, polyethylene, and water are described. The data obtained are presented and discussed. (auth)

16722 (BMwF-FBK-65-03) THEORETISCHE UNTERSUCHUNG DES GROESSTEN ANZUNEHMENDEN UNFALLES BEI DER LAGERUNG HOCHRADIOAKTIVER SPALTPRODUKTE IN SALZFORMATIONEN. (Theoretical Investigation of the Maximum Credible Accident with Regard to the Storage of Highly Radioactive Fission Products in Salt Formations). Brandes, S. (Technische Hochschule, Aachen (West Germany). Institut fuer Elektrische Anlagen und Energiewirtschaft). Oct. 1965. 47p. Dep. mn.

In order to obtain information for dimensioning salt cavities filled with waste, a maximum accident was considered. The spherical heap of fuel elements separated from salt by a layer of air will reach a temperature of more than 100°C so that water, which runs slowly into the cavity, will boil and evaporate. The temperature distributions are calculated for stationary and instationary cases with a given maximum temperature of 100°C in the waste. Fuel elements of the Schulten-type were taken, for those will probably be the first, which might be taken for storage. Because the formation of critical arrangements of waste in salt is possible, the critical radius of the sphere was calculated and found to be 2.9 m. (auth)

16723 (COO-1156-11) FACTORS INFLUENCING THE ACCUMULATION OF FALLOUT ^{137}Cs IN MULE DEER. Whicker, F. W. (Colorado State Univ., Fort Collins. Dept. of Radiology and Radiation Biology). May 1965. Contract AT(11-1)-1156. 238p. Dep. mn. CFSTI $6.00 cy, $1.25 mn.

Factors influencing the accumulation of fallout cesium-137 in a wild population of mule deer, Odocoileus hemionus, in the Cache la Poudre drainage of north-central Colorado were investigated. Air, precipitation, soils, twelve deer forage species, and deer were sampled periodically from various elevations within the study area over a three year period. Experimental sampling designs were primarily factorial with sufficient replication to allow statistical treatment of data. Materials were assayed for Cs-137 using gamma spectrometry. Maximum levels of Cs-137 in deer were observed in 1963. Maximum levels within years occurred during the summer months in animals collected above 8,500 feet elevation. Regression analyses of muscle Cs-137 versus elevation indicated significant correlations. Evidence indicated a high degree of correlation between Cs-137 levels in vegetation and deer. It was concluded that the degree of foliage contamination and food habits were the most important factors contributing to Cs-137 burdens in deer. A Cs-137/K discrimination factor between the diet and muscle of 0.9 was estimated from the rumen samples. Neither sex or age produced statistically significant variations in muscle Cs-137. Inhalation, the drinking of surface waters, and the ingestion of snow were minor sources of Cs-137 intake by deer in comparison to the ingestion of forage. (P.C.H.)

16724 (COO-1156-12) ^{90}Sr IN ANTLERS AND SELECTED BONES OF COLORADO MULE DEER. Farris, Gerald C. (Colorado State Univ., Fort Collins. Dept. of Radiology and Radiation Biology). May 1965. Contract AT(11-1)-1156. 91p. Dep. mn. CFSTI $3.00 cy, $0.75 mn.

Levels of strontium-90 in antlers and various bones of Colorado mule deer (Odocoileus hemionus hemionus) in the Cache la Poudre drainage of north-central Colorado were investigated from July, 1961, through December, 1964. Comparative tests on the strontium-90 activity of femur, scapula, metacarpal, and antler of seven to eighteen month old deer produced highly significant correlation coefficients, indicating a general comparative increase in activity. The correlation coefficient for the antler-femur comparison of adult deer was also found to be highly significant. For the seven to eighteen month old deer, the antler-femur ratio was 0.9 compared to the adult deer ratio of 1.5. Thus, as these elements are taken into the animal, they go into the rapidly growing antler rather than into other bone development. Over the range of values investigated, the adult antler activity was representative of the femur activity for the seven to eighteen month old deer. With the resumption of nuclear testing in September, 1961, the femur bones of seven to eighteen month old deer showed a factor of five increase in strontium-90 during the remainder of the study period. Sex was found not to influence the strontium body burdens in deer up to 17 months old. 97 references are cited. (auth)

16725 (EUR-2543.e) STUDIES ON THE RADIOACTIVE CONTAMINATION OF THE SEA. Annual Report, 1964. Bernhard, M. (Comitato Nazionale per l'Energia Nucleare, La Spezia (Italy). Laboratorio per lo Studio della

Contaminazione Radioattiva del Mare). 1965. 36p. (RT/BIO(65)–18). Dep. mn.

Studies were made on factors that influence the uptake, accumulation, and loss of radioisotopes by marine organisms. A survey was made first of the elements and factors in a sampling area, and next experiments were made on the influencing factors in relation to the data obtained in the survey. The studies and results were divided among five groups: chemistry, botany, microbiology, zoology, and special developments. (P.C.H.)

16726 (GAT–506) ENVIRONMENTAL RADIATION LEVELS AND CONCENTRATIONS. SECOND HALF AND ANNUAL SUMMARIES, 1965. Kalmon, B.; Hulett, S. H. (Goodyear Atomic Corp., Piketon, Ohio). Feb. 18, 1966. Contract AT(33-2)-1. 15p. Dep. mn. CFSTI $1.00 cy, $0.50 mn.

Average environmental radiation and concentration levels in air and water in the vicinity of the Portsmouth Area Gaseous Diffusion Plant for the second half of the calendar year 1965, and for the complete calendar year 1965 are summarized. The results for the first half of 1965 are included in tabular form. For the second half of 1965, both the airborne alpha and beta-gamma activity dropped significantly compared to the first half of 1965. The alpha airborne average for the second half of the calendar year dropped from 16.1 to 9.7% of the maximum permissible concentration. The beta-gamma concentration was less than 0.01% compared to 0.05% for the first half. During the last half of 1965, the average alpha concentration in the water effluents increased while the beta-gamma activity decreased. The highest individual results for alpha and beta-gamma were 12 and 18% of the maximum permissible concentration. Penetrating background exposure rates continued to decline from the 1964 annual average of 48 to 27.7% of the maximum permissible exposure (MPE) in 1965. The second half of 1965 was also lower than the first half of 1965. It was concluded that plant operations have not added appreciably to the general background penetrating radiation. Over-all average concentrations in air and water along with the background exposure rates for both halves of 1965, the over-all 1965 averages, and the over-all 1964 averages are tabulated. (P.C.H.)

16727 (HASL–168) FLIGHT DATA AND RESULTS OF RADIOCHEMICAL ANALYSES OF FILTER SAMPLES COLLECTED DURING 1963. Appendix to Progress Report No. 11 on Project Stardust. Feely, Herbert W.; Friend, James P.; Lagomarsino, Raymond J.; Bogen, Donald C.; Biscaye, Pierre E.; Hardaway, John E. (Isotopes, Inc., Westwood, N. J.). Dec. 1, 1965. Contract DA-49-146-XZ-079. 233p. Dep. mn. CFSTI $6.00 cy, $1.25 mn.

Flight data and results of radiochemical analyses of stratospheric and tropospheric air filter samples collected during 1963 in Project Star Dust are tabulated. The methods used are described. The nuclides measured include fission products, products of neutron activation, and naturally occurring radionuclides. (P.C.H.)

16728 (HASL–169) FLIGHT DATA AND RESULTS OF RADIOCHEMICAL ANALYSES OF FILTER SAMPLES COLLECTED DURING 1964. Progress Report No. 12 on Project Stardust. Feely, Herbert W.; Bogen, Donald C.; Lagomarsino, Raymond J.; Hardaway, John E.; Leo, Micah W. M. (Isotopes, Inc., Westwood, N. J.). Jan. 1, 1966. Contract DA-49-146-XZ-079. 143p. Dep. mn. CFSTI $4.00 cy, $1.00 mn.

Flight data and results of radiochemical analyses of stratospheric and tropospheric air filter samples collected during 1964 in Project Star Dust are tabulated. Methods used are described. The nuclides measured include fission products, products of neutron activation, and naturally occurring radionuclides. (P.C.H.)

16729 (IDO–12049) RADIOLOGICAL APPRAISAL OF THE MONTICELLO PROJECT, SAN JUAN COUNTY, MONTICELLO, UTAH. Paas, Herman J. Jr. (Idaho Operations Office (AEC), Idaho Falls. Health and Safety Div.). Feb. 1966. 25p. Dep. mn. CFSTI $1.00 cy, $0.50 mn.

Measurements and recommendations resulting from a radiological appraisal of the Monticello Project are presented. This appraisal was performed following completion of an erosion control project which included stabilization, covering, and seeding of exposed tailings areas. Evaluation of environmental samples of air, vegetation, and water showed no evidence of radioactive material transport from tailings and ore storage areas. Several hundred dose rate measurements taken over the tailings area showed that the average whole-body exposure to a population maintaining 24-hr/day occupancy would be measurably below the levels believed to be harmful or injurious to health. Similar data were collected at the mill and foundation areas. Except for the generally contaminated foundation area, the site conditions meet criteria that allow release for public usage. Surface occupancy can be permitted on a nonrestricted basis; however, the presence of subsurface contaminants at the tailings area require control, as any disturbance of existing terrain could materially change the radiological conditions found at the time of the survey. (auth)

16730 (NP–15882) RADIOACTIVITY SURVEY DATA IN JAPAN. Number 5. (National Inst. of Radiological Sciences, Chiba (Japan)). Nov. 1964. 26p. Dep. mn.

Radioactivity survey data following the nuclear detonation test conducted on the Chinese mainland, assumed to be at Lake Lop Nor, are reported. Data are given for total beta activity in rain water and atmosphere and ^{131}I content in milk, human urine, atmosphere, rain water, and thyroid glands in cattle and man for 1964. The chemical composition of fallout was also determined. (P.C.H.)

16731 (NP–15883) RADIOACTIVITY SURVEY DATA IN JAPAN. Number 6. (National Inst. of Radiological Sciences, Chiba (Japan)). Feb. 1965. 24p. Dep. mn.

Data obtained from monitoring milk, water supplies, atmosphere and rain water for ^{90}Sr and ^{137}Cs, atmosphere for ^{144}Ce, wheat for ^{90}Sr, and human urine for ^{137}Cs in Tokyo primarily during 1964 are reported. (P.C.H.)

16732 (NP–15898) MEASUREMENT OF AIRBORNE RADIOACTIVITY. (Public Health Service, Rockville, Md.). [196?]. 106p. GPO.

Hazards to man from radioactivity in the atmosphere are discussed, and methods for air sampling, including gross analysis, specific analysis, and surveillance programs, are described. (P.C.H.)

16733 (ORNL–P–1098) ON THE CHOICE OF A FALLOUT SHELTER PROTECTION FACTOR. Blizard, Everitt P.; Upton, A. C.; Wigner, Eugene P. (Oak Ridge National Lab., Tenn.). [nd]. Contract W-7405-eng-26. 9p. Dep. mn. CFSTI $1.00 cy, $0.50 mn.

The appropriate magnitude for a fallout shelter protection factor is discussed. The decrease of radiation intensity, time, and recovery from radiation are considered. It was concluded that the principal uncertainty is whether the maximum damage in terms of increased probability in short-term lethality is the proper criterion for judging the undesirability of a certain radiation history. (P.C.H.)

16734 (TID–22693) POTENTIAL HAZARDS AS A RESULT OF INHALATION OF RADIOIODINES: A LITERATURE SURVEY. Engel, Ronald E. (Public Health Service, Las Vegas, Nev. Southwestern Radiological Health Lab.). Jan. 5, 1966. 95p. ((SWRHL–13r). Dep. mn. CFSTI $3.00 cy, $0.75 mn.

A brief survey was made on the potential hazards to man which might result from releases of radioiodines into the biosphere. The related topic of potential hazards from ingestion of radioiodine is also considered since the determination of total hazard to man must be the ultimate goal of any research program which has been designed to assess the overall public health significance of any radioiodine releases. Research problems are also suggested. (124 references). (P.C.H.)

16735 (TO-B-65-99) DEVELOPMENT OF AN IMPROVED LAND-SURFACE FALLOUT MODEL. Interim Report No. 1, April 1–October 31, 1965. Norment, H. G.; Schwenke, T. W.; Kohlberg, I. (Technical Operations Research, Bulington, Mass.). Jan. 1966. Contract DA-28-043-AMC-01309(E). 181p. (ECOM-01309-1).

A new concept in fallout models, the DOD Fallout Prediction System, is being designed and constructed to serve as a basis for the next generation of fallout prediction models. The model considers in detail the dynamics of cloud rise and growth and provides for fallout particle transport through a three-dimensional time variant atmosphere that includes analytical wind models of local circulation systems such as mountain winds and sea breezes. The model is being programmed for machine computation in a highly modular and flexible fashion to facilitate research usage of the program. Coding is being done exclusively in FORTRAN language. (auth)

16736 (UCRL–14534) HAZARDS CONTROL QUARTERLY REPORT NO. 22, JULY–SEPTEMBER 1965. (Lawrence Radiation Lab., Univ. of California, Livermore). Contract W-7405-eng-48. 60p. Dep. mn. CFSTI $3.00 cy, $0.75 mn.

Progress is reported in eleven papers on hazards control. A separate abstract was prepared for each paper. (J.R.D.)

For abstracts of individual papers see: 16664, 16665, 16737–16741, and 16829–16832.

16737 (UCRL–14534, pp 13-18) DEVELOPMENTS AT THE WHOLE-BODY COUNTER FACILITY. Schmidt, C. T.; Anderson, A. L. (Lawrence Radiation Lab., Univ. of California, Livermore).

Progress is reported on modification of shielding for the facility resulting in background decrease of approximately 30%. Installation of NaI(Tl) detectors for measurement of low-energy radiation is reported, and a computer program for analysis of data from the facility was put into operation. (J.R.D.)

16738 (UCRL–14534, pp 41-3) PORTABLE VACUUM CLEANER FOR RECOVERING SPILLED MERCURY. Gonzales, B. A.; Taylor, R. D. (Lawrence Radiation Lab., Univ. of California, Livermore).

Modification of light-weight vacuum cleaner equipped with centrifugal pump for mercury pickup is described. (J.R.D.)

16739 (UCRL–14534, pp 44-9) USE OF ELECTRONIC FLASH UNITS IN PROXIMITY WITH EXPLOSIVES. Bernardini, E. J. (Lawrence Radiation Lab., Univ. of California, Livermore).

An evaluation of flash units for photographing explosives and high-energy detonators is presented. Safety recommendations and conclusions are included. (J.R.D.)

16740 (UCRL–14534, pp 50-3) REMOVAL OF CARBON DUST FROM A HIGH SPEED PRINTER USING A WET CYCLONE SCRUBBER. Lindeken, C. L.; Taylor, R. D. (Lawrence Radiation Lab., Univ. of California, Livermore).

Design of a wet system which minimizes fire potential is described. Dust deposition in the ductwork is also minimized by collection of the thermoplastic polymer used as a toner near the point of generation. (J.R.D.)

16741 (UCRL–14534, pp 54-6) VACUUM-OPERATED, FOAM-ENTRAINMENT MILK EVAPORATOR. Gaskill, J. R. (Lawrence Radiation Lab., Univ. of California, Livermore).

Development of a vacuum, foam-entrainment evaporator for concentrating milk prior to counting by gamma pulse height analysis is described. (J.R.D.)

16742 (VUF–1014) POST-SHOT HYDROLOGIC SAFETY, PROJECT SHOAL. Final Report. (Hazelton-Nuclear Science Corp., Palo Alto, Calif.). Oct. 30, 1965. Contract AT(29-2)-1229. 54p. Dep. mn. CFSTI $3.00 cy, $0.50 mn.

The Shoal Event, a 12.5 kt on nuclear detonation, one in a series of tests in the Vela Uniform Program, occurred at 1000 hours PST on October 26, 1963, in the granite of the Sand Springs Range, about 45 kilometers southeast of Fallon, Nevada. The Sand Springs Range trends north-south and comprises jointed, faulted, and fault-bounded metamorphosed Paleozoic and Mesozoic marine sediments with a central granitic intrusive body. Re-entry drilling and Hydyme results indicated that the Shoal device detonated as predicted and a rubble chimney 26 meters in radius and 108.5 meters high was formed by the explosion. Significant quantities of radionuclides were produced at Shoal; however, nuclides in ground-water solution were not free to move from the rubble chimney region until aquifer stabilization was achieved and the chimney filled with ground water. It was concluded that slow ground-water flow velocities and radioactive decay preclude the possibility of hazardous aqueous concentrations of radionuclides migrating more than 1000M from the immediate detonation area. (P.C.H.)

16743 (VUF–1021) OFF-SITE SURVEILLANCE FOR THE SALMON EVENT OF PROJECT DRIBBLE. Final Report, October 22, 1964. Carter, Melvin W.; Placak, O. R. (Department of Defense, Washington, D. C.). Feb. 4, 1966. 61p. Dep. mn. CFSTI $3.00 cy, $0.75 mn.

Information and data are compiled to summarize the activities conducted by the Off-Site Radiological Safety Organization relative to the Salmon Event, Project Dribble. Activities prior to the shot, during the active test period, and subsequent to the shot are discussed. Air, plant, and milk samples were monitored and data on radioactive concentrations are tabulated. Of the non-technical aspects, the most significant knowledge gained during the Salmon Event was that large numbers of people can be successfully evacuated, and a comprehensive off-site radiological safety program can be successfully conducted in a populated area if the confidence of the people toward the operation is maintained. (P.C.H.)

16744 (Y-EA–49) Y-12 CLEAN ROOM FACILITIES. Little, J. C. (Union Carbide Corp., Oak Ridge, Tenn. Y-12 Plant). Mar. 14, 1966. Contract W-7405-eng-26. 31p. Dep. mn. CFSTI $2.00 cy, $0.50 mn.

Clean room facilities at the Y-12 plant are described, along with testing methods used to determine contamination. The two methods primarily used to control contamination are the absolute filter and the laminar flow concept of air distribution. Environmental conditions at Y-12 are also discussed. (P.C.H.)

16745 AEROSPACE MEDICINE. Lamb, Lawrence E. (USAF School of Aerospace Medicine, Brooks Air Force Base, Tex.). Advance. Internal Med., 12: 175-232(1964).

Some medical problems encountered in space flight, including those arising from extraterrestrial ionizing radiation, are reviewed. Radiation in space is considered in terms of two general classes: solar and cosmic. Solar radiations provide electrical phenomena, visible light, and energy sources absorbed by the earth and by earth processes. The major portion of the destructive elements of the solar radiations are screened out by the earth's atmosphere. Cosmic radiations include the energies originating throughout the universe, including other planets and the stars of our galaxy, as well as other galaxies within the space continuum. In high concentration, their effects may be damaging since they produce ionizing radiation. Space exploration has defined two areas of excessively high radiation, the Van Allen belts. These areas exist at altitudes of 1400 to 3400 mi and at 8000 to 12,000 mi. They are about in line with the earth's equator, and surround the earth like a huge inner and outer doughnut covering all the earth except the polar regions. The excessively high radiations of this area pose new radiation problems for man in space flight. Traversing high, intensive radiation areas requires rapid penetration, adequate shielding, or both. The absence of significantly increased radiation around the polar areas suggests the possibility of exiting from the earth by the

polar regions to avoid exposure to excessive radiation. It is emphasized that the problems of space radiation are not of the same magnitude as the radiation effects associated with thermonuclear warfare. (BBB)

16746 STANDARDISATION OF RADIOACTIVITY. Lowenthal, G. C.; Oakley, A. E. (Australian Atomic Energy Commission). At. Energy Austral., 9: 19-24(Jan. 1966).

The establishment and maintenance of standards of measurement in the field of radioisotopes are discussed. Establishment of Australian radioactivity standards is described. Standardization procedures include: absolute counting, ionization chamber measurements, and microcalorimetry. Research on electrodeposition techniques, chemical precipitation techniques, and radioisotopic purity is reviewed. (M.C.G.)

16747 ^{226}Ra IN FOOD AND MAN IN BOMBAY AND KERALA STATE (INDIA). Chhabra, A. S. (Atomic Energy Establishment, Trombay, India). Brit. J. Radiol., 39: 141-6(Feb. 1966).

Data are presented on the ^{226}Ra content of various food samples collected from Bombay city and high background areas of Kerala State in India. Comparison of data for the samples of these two areas, shows that the Kerala samples have a ^{226}Ra/g ash content that averages five to ten times higher. An exception is the coconut that is grown profusely in Kerala State; this does not show a higher concentration of ^{226}Ra in spite of the higher availability of ^{226}Ra in the Kerala State soil. From a tentative model formed for the food habits of the people of these two regions, their ^{226}Ra burden has been estimated. The determination of ^{226}Ra in bones and other organs of the human body indicates that a man from high background areas of Kerala State contains about ten times more of this radioisotope than a Bombay citizen. A value of 0.85×10^{-14} g Ra/g ash of bone was found from direct measurements of a single subject from Bombay. (auth)

16748 RADIUM IMPLANT DOSIMETRY WITH A SMALL DIGITAL COMPUTER. Schlessinger, J. E.; Porter, E. H. (New York Univ., N. Y.). Brit. J. Radiol., 39: 147-50(Feb. 1966).

A system for using a small computer for radium implant dosimetry is described, and compared with that in current use at the M.D. Anderson Hospital. The system accepts implants of any geometry, however irregular, and gives results that are accurate enough to be clinically useful. It was made compatible with the Parker-Paterson tables. (auth)

16749 NOMOGRAMS FOR RADIOBIOLOGICALLY-EQUIVALENT FRACTIONATED X-RAY DOSES. Shuttleworth, E.; Fowler, J. F. (Hammersmith Hospital, London). Brit. J. Radiol., 39: 154-5(Feb. 1966).

A nomogram relating total dose, dose per fraction, and number of fractions, to both the equivalent single dose and the equivalent total dose in 30 fractions (for normal tissue reactions) is presented. Based on animal and clinical data, the nomogram is considered alternative to that of Burns, which was based on a cell survival curve. (H.G.D.)

16750 DOSE-RATE AND SURVIVAL CURVES. Barendsen, G. W. (TNO., Rijswijk Z.H., The Netherlands). Brit. J. Radiol., 39: 155-6(Feb. 1966).

Experimental evidence is reviewed that contradicts the suggestion by Porter of a relatively low oxygen enhancement ratio (OER) for low doses of γ or x rays. Even if a difference did exist between the oxygen effects at high and low doses, this would be unlikely to play a significant part in radiotherapy, because of the relatively low daily doses used with high-intensity techniques. (H.G.D.)

16751 COMPUTATION OF X-RAY DIAGNOSTIC EXPOSURE TABLES. Dawson, J. (Royal Hampshire County Hospital, Winchester, Eng.); Phillips, G. M.; Willcox, B. A. M. Brit. J. Radiol., 39: 177-21(Feb. 1966).

A method is described for compiling diagnostic x-ray exposure tables that give exposure factors for a given patient. The necessary calculations are based on the method of least squares and were programmed for an I.C.T. Pegasus digital computer. (auth)

16752 ^{226}Ra CONTENT OF MILK IN FRANCE. I. INTEREST OF THE STUDY. Michon, G. (Centre d'Etudes Nucleaires, Fontenay-aux-Roses, France). Bull. Acad. Vet. France, 38: 141-3(Apr. 1965). (In French).

The maximum permissible quantity of ^{226}Ra is 0.1 μC in the adult, of which 99% is fixed in the skeleton. These values are useful only for those occupationally exposed to the isotope; there are no useful norms established for infants. Likewise, such figures do not reflect the proper values for irradiation of the total population. The maximum permissible genetic dose is defined by reference to the genetic dose due to natural radioactivity. Because the natural radiation level varies from place to place, it is important to define this quantity with accuracy; Ra is one of the chief sources of this activity. Futher, fallout contamination of various foods deserves to be established more firmly for Ra, and a standard may be established to which, for example, ^{90}Sr may be referenced. Certain new limits may in this fashion be established as maximum permissible concentrations for the mean French diet. (BBB)

16753 ^{226}Ra CONTENT OF MILK IN FRANCE. II. EXPERIMENTAL RESULTS. de Dreuille, M.; Michon, G. (Centre d'Etudes Nucleaires, Fontenay-aux-Roses, France). Bull. Acad. Vet. France, 38: 145-9(Apr. 1965). (In French).

Milk samples of 2-l volume were dehydrated, mineralized, dissolved in dilute H_2SO_4, coprecipitated with $BaSO_4$, collected by filtration, washed, and dried. The precipitate was mixed with standard proportions of $CaCO_3$ and $ZnSO_4$, sealed by a disc of Plexiglas, and the emission measured by a $ZnSO_4$ scintillator. One may thus determine 0.15 pC/l. Alternately, by treating the precipitate with H_3PO_4 and then HCl to obtain a solution of $BaCl_2$ and $RaCl_2$ which is degassed. After a certain period of time, the activity of the ^{222}Rn released is measured. In this way, values as low as 0.02 pC/l may be measured. Data are reported for 25 departments of France; values range between 0.05 pC and 1.4 pC (Saone-et-Loire), and may be correlated on a geological map with hercynian regions showing the highest activity. These regions include the armorican plain, the central plain, and the Vosges. More detailed analysis of the regions of areas of milk samples indicates that samples from regions with granulite subsoil average 0.5 pC/l; uraniferous subsoils give values of 3-4 pC/l. The Ra content of water and forage in these regions will be examined. (BBB)

16754 ORGANIZATION OF A CONTROL OF RADIOACTIVE POLLUTION OF MILK: CASE OF RADIOISOTOPES WITH SHORT PERIODS. Michon, G. (Centre d'Etudes Nucleaires, Fontenay-aux-Roses, France). Bull. Acad. Vet. France, 36: 283-5(June 1963). (In French).

The principal fallout isotopes to be found in milk which have a short half-life period are ^{131}I and ^{140}Ba; these isotopes represent a measurable fraction of the total daily ingested I and Ba, since 1 to 3% of daily ingested I comes from milk and 0.01% of ingested Ba is ^{140}Ba in milk. Tolerable limits are 0.7 μC ^{131}I and 4 μC ^{140}Ba. The maximum admissible concentration of ^{131}I in milk may be calculated to be 150 pC/l for a 1-month-old infant and 7500 pC/l for an adult. If the cumulative effective ingestion of I does not exceed ingestible I under equilibrium conditions over a four-month period, the maximum integrated doses are 12,000 pC ^{131}I for a 6-month-old child and 200,000 pC ^{131}I for an adult. Control organization must include enough sampling points to determine inequalities in geographical distribution; frequency of sampling (48 hours) to ensure detection of extreme rapid variations; efficient, rapid expedition, reception and measurement; and permanent control centers at various points to initiate alert and control on short notice. (BBB)

16755 CONTAMINATION BY ^{90}Sr AND ^{137}Cs OF DRY MILK PRODUCTS IN 1962. Nagasawa, Kakuma; Kame-

tani, Katsuaki (National Inst. of Hygienic Sciences, Tokyo). Eisei Shikenjo Kenkyu Hokuku, No. 81, 77-8 (Oct. 1963). (In Japanese).

Contamination of powdered milk by ^{90}Sr and ^{137}Cs as a result of nuclear weapon tests by the United States and Russia in 1962 and 1963 was investigated. Twenty-two whole milk or skim milk powders produced from April 1962 to March 1963 by 7 milk processing plants, as well as milk powders produced in March 1955 and September 1958, were assayed. For the ^{90}Sr assay, 100 g of milk powder was ignited at 450-500° and for ^{137}Cs a 30-g sample was similarly ashed. Radioactivity was measured by an Aloka LBC-1 type gas-flow, low-background counter. Counts were corrected with standard ^{90}Sr and ^{137}Cs samples. Contamination by ^{90}Sr and ^{137}Cs in dry milk products increased after May 1962, and the milk products from Kagoshima in May and from Engaru in August 1962 showed the highest contamination. Thus, dehydrated milk from Kagoshima on August 3, 1962 contained 14.2 $\mu\mu$C/100 g ^{90}Sr, 78 $\mu\mu$C/100 g ^{137}Cs, and in Engaru on September 4, 1962 reached 12.2 $\mu\mu$C/100 g ^{90}Sr, 110 $\mu\mu$C/100 g ^{137}Cs. The milk products from other Japanese cities had contaminations lower than 10 $\mu\mu$C/100 g ^{90}Sr and 70 $\mu\mu$C/100 g ^{137}Cs. These values were much lower than Norway milk products (max contamination in milk powder 48 $\mu\mu$C/l ^{90}Sr, 492 $\mu\mu$C/l ^{137}Co. Conversion of milk powder to one liter of milk can be done by multiplying the $\mu\mu$C value of 100 g milk power by 1.2. (BBB)

16756 IODINE SAMPLING WITH SILVER NITRATE-IMPREGNATED FILTER PAPER. Ettinger, H. J. (Los Alamos Scientific Lab., N. Mex.). Health Phys., 12: 305-11(Mar. 1966).

The use of silver nitrate-impregnated radioiodine filters was evaluated under laboratory and field conditions. Preliminary laboratory tests indicated radioiodine filter efficiencies of 91 to 96 per cent. When sampling a stack effuent containing a variety of reactor waste products radioiodine filter efficiencies of less than 8 per cent were obtained. Sampling effluent gases from hot cells where reactor fuel elements are handled resulted in a median radioiodine filter efficiency of 20 per cent, with efficiencies as high as 96 to 100 per cent under certain operating conditions. Test results show that silver nitrate-impregnated radioiodine filters do not provide a reliable method for monitoring the release of iodine to the atmosphere. (auth)

16757 HEALTH PHYSICS FOR A MAINTENANCE OPERATION ON A HOMOGENEOUS RESEARCH REACTOR. Barrall, R. C.; Brauner, A.; McElroy, W. N.; Smiley, D. C.; Zimbrick, J. D. (Illinois Inst. of Tech., Chicago). Health Phys., 12: 323-31(Mar. 1966).

On 31 August 1962, air samples from the inner subpile room of the IIT Research Institute Reactor indicated an increased level of activity in the air. The activity was identified as ^{138}Cs and ^{88}Rb (both daughters of high-yield fission gases) by half-life and gamma-spectrum analysis. Much smaller quantities of ^{131}I were also found. Subsequently, samples of dehumidifier water showed the presence of ^{131}I. All reactor system pressures, temperatures, excess reactivity and other parameters were unchanged. It was concluded that an extremely small leak was present in the system and further that no hazard was involved in continuing to operate while searching for the leak. Sampling tubes were placed in various locations that were suspected. Dose rates near the recombiner several days after shutdown were as high as 1000 R/hr gamma and a lead-shielded cart was employed to reduce personnel exposures. The leak area was successfully located by the use of the sampling tubes on 17 September and wipe tests on that date indicated that the leak was at a T joint under the aspirator pump. Surveys on 20 September showed a dose rate of 30 R/hr at the location which would be occupied by the welder, and up to 1000 R/hr in the immediate vicinity. Internal decontamination of the system was accomplished on 1 October 1962. A lead-shielded tunnel was constructed in which a welder could lie. Dry runs were made using a wooden tunnel. The dose rate in the shielded tunnel on 2 October 1962 was 0.8 R/hr. The weld was repaired without difficulty. The highest exposure in the operation was slightly over 6 rem with some twenty-two people sharing a combined dose of 58.5 rem. The reactor returned to normal operation on 15 October 1962. (auth)

16758 NEUTRON ACTIVATION OF SULFUR IN HAIR: APPLICATION IN A NUCLEAR ACCIDENT DOSIMETRY STUDY. Petersen, D. F.; Langham, W. H. (Los Alamos Scientific Lab., N. Mex.). Health Phys., 12: 381-4(Mar. 1966).

Incident fast neutron doses sustained by personnel involved in the Wood River Junction, United Nuclear Corporation criticality accident of 24 July 1964, were estimated from induced ^{32}P activity in hair sulfur. Fast neutron doses to the head and pubis of the fatally injured victim were 1200 and 4800 rad respectively, corresponding to total gamma plus neutron dose estimates of ~11,000 and 48,000 rad. Identification of ^{32}P in hair samples from two individuals who entered the area later confirmed the notion that the system either remained critical or that a second excursion occurred. Comparison with the Los Alamos fatality of 1958 indicates that, although doses to the pelvis differed by a factor of 40 and the average total body dose may have differed by about a factor of 3, doses to the head may have been essentially the same (~10,000 rad). Similarities in clinical course and survival of the two cases may reflect the approximately equivalent doses to the upper torso and head. These observations suggest that debilitation from massive radiation exposure may be more dependent on dose to the head and thorax than on average total body dose. (auth)

16759 THERMOLUMINESCENCE DOSIMETRY OF GAMMA RAYS FROM ATOMIC BOMBS IN HIROSHIMA AND NAGASAKI. Ichikawa, Yoneta; Higashimura, Takenobu; Sidei, Tunahiko (Kyoto Univ.). Health Phys., 12: 395-405(Mar. 1966).

Thermoluminescence dosimetry techniques and typical roof tiles were used to obtain the distribution of the gamma ray dose from the atomic bombs dropped on Hiroshima and Nagasaki. Samples of roof tiles were chosen whose exact locations at the time of the bombings were known; none were exposed to the fire that occurred in both cities shortly after the explosions. After being ground, washed and separated by a magnetic method, 300 mg of each sample powder was used to observe the thermoluminescence glow curve contributed from the bomb radiation. The same sample was exposed to ^{60}Co gamma rays and after it had absorbed a known amount of gamma dose, the new glow curve was recorded for calibrating the thermoluminescence sensitivity. The equivalent gamma dose of the bomb radiation was obtained by comparing the bomb glow with the ^{60}Co glow curve. The possible sources of error involved in this dosimetry are discussed in detail and the corrected gamma doses are compared with York's theoretical results. In the case of Nagasaki, the experimental values show excellent agreement with York's values but in the case of Hiroshima, the values were about 30 percent lower than York's. (auth)

16760 FREE-FIELD RADIATION-DOSE DISTRIBUTIONS FROM THE HIROSHIMA AND NAGASAKI BOMBINGS. Auxier, J. A.; Cheka, J. S.; Haywood, F. F.; Jones, T. D.; Thorngate, J. H. (Oak Ridge National Lab., Tenn.). Health Phys., 12: 425-9(Mar. 1966). (ORNL-P-1825).

Recent determinations of air-dose distributions from the Hiroshima and Nagasaki bombings are reported. The ORNL study proposed to determine: the free-field distribution of radiation in air above the air-ground interface; and the shielding factors for structures in which people survived. It is pointed out that the percent probable error in the Hiroshima data is about ±30 because of uncertainties that persist concerning the yield of the weapon dropped there. Data from ORNL are compared with that of York and Wilson. (H.G.D.)

16761 INCORPORATION OF THE CONCEPT OF DISASTER PREPAREDNESS IN THE CURRICULUM OF A

SCHOOL OF VETERINARY MEDICINE. Blenden, D. C. (Univ. of Missouri, Columbia). J. Amer. Vet. Med. Ass., 147: 1515-21(Dec. 15, 1965).

The role of the veterinarian in civil emergencies from natural or man-made causes (thermonuclear war or release of radioactive material from a nuclear reactor) is outlined, with emphasis on instruction in this field. Man-made disasters are an ever-present potential, especially those that might result in widespread trauma, death, and exposure to radiation. Accidental explosions and fires occur from time to time due to human error or neglect. The placement of nuclear power plants and research reactors poses a threat of accidental release of radioactive material. The remote but ever-present threat of enemy attack with nuclear weapons should not be ignored by responsible professional persons and steps be taken to promulgate health concepts of prevention and preparedness. A list is given of the abilities and contributions of the veterinarian during and after a disaster that would be highly valuable to survival of the affected population. (TCO)

16762 SPECIAL PROBLEMS IN THE EMPLOYMENT OF PREGNANT WOMEN IN RADIATION WORK. Cooper, A. G. S. (Queensland Radium Inst., Brisbane). J. Coll. Radiol. Austral., 8: 291(Oct. 1964).

Problems associated with exposure of female radiation workers are considered. Recommendations of international bodies, such as the ICRP, are reviewed. From these recommendations it is suggested that, if a married woman is employed as a radiographer (diagnostic or therapeutic) or as a radioisotope technician she should be warned of the risks in early pregnancy, and if this is suspected any further duty in a radiotherapy establishment should be strictly controlled. Women of reproductive age should not be subjected to planned emergency exposure, nor to any high radiation exposure. Married women radiographers should not be employed in the radium or radon section, nor in any other γ-ray activity. (BBB)

16763 RADIOACTIVE MATERIAL IN THE TEETH OF CHILDREN IN THE NORTHERN NEW JERSEY AREA: CORRELATION WITH ^{90}Sr IN MILK. Kohn, Sidney L.; Gimble, Francis S.; Erk, Vernon (Fairleigh Dickinson Univ., Teaneck, N. J.). J. Dent. Children, 28: 257-62 (Dec. 1961).

A radioautographic study was made of the primary teeth of children born and reared in Northern New Jersey, in attempts to demonstrate the presence of radioactive material such as ^{90}Sr. In an earlier series of samples of adult teeth from Northern New Jersey, a statistically significant increase in density was not obtained; hence the values obtained from these samples were considered comparable to values from controls. The primary tooth of the child from this area showed a deviation of 11 parts per thousand (0.011) of a unit of optical density. It is concluded that radioautography of extracted exfoliated teeth of children demonstrated the presence of radioactive material. Results of comparative densitometry of the radioautographs of the teeth of children from Northern New Jersey and of the teeth of children from St. Louis appear to parallel the differences in concentration of ^{90}Sr in the milk from these areas as published by the U. S. Public Health Service. (BBB)

16764 LOSS OF AN EMITTER IN DEFECTOSCOPIC FIELD WORK. Truelle, Marcel A.; Klener, Vladislav. Prac. Lek., 17: 322-4(Sept. 1965). (In Czech.).

In the course of the defectoscopic examination of steam piping in a town a ^{137}Cs emitter with an activity of cca 1 C was stolen. By using sensitive PGE and N 20 equipment the emitter was found within a relatively short time. The emitter was for more than three hours outside the cover and three boys aged 10–12 years came into contact with it. As exposure to a larger dose could not be ruled out, the boys were sent for examination to the Clinic of Occupational Diseases in Prague. After several weeks the boy who carried the emitter in his pocket, developed mild depigmentation of the skin in the adjacent area of the anterior surface of the thigh. In the spectrum of the left testis temporarily an increase of free fluid was found. Similar accidents can be prevented by careful selection and training of defectoscopic workers and by some technical provisions. (auth)

16765 DETERMINATION OF DOSE IN INTRACAVITARY CONTACT THERAPY WITH ^{60}Co BEADS AND IN INTERSTITIAL THERAPY. Caretti, G.; Chianura, G. (Univ., Bologna). Radiobiol. Radioterap. Fis. Med., 20: 476-88(Nov.-Dec. 1965). (In Italian).

A study is made of the hyperdose found in interstitial and endocavitary contact therapy at the metallic tangency of the radioactive sources with the tissues. Particular attention is given to this problem with reference to cobalt-60 pearl therapy and by controlled photographic dosimetry with ionometric calibration. The contact hyperdose is examined from the point of view of radiotolerance on the part of the patient and radioprotection of the operators. Recommendations for improving distribution of the absorbed radiation are deduced on the basis of attenuation of the contact hyperdoses. (auth)

16766 ON THE RELATION BETWEEN THE TOTAL BETA ACTIVITY AND THE INDIVIDUAL RADIONUCLIDE CONTENT IN FISSION PRODUCT MIXTURES. Hinzpeter, M. (Zentralamt des Deutschen Wetterdienstes, Offenbach am Main, Ger.). Zentrahbl. Biol. Aerosol Forsch. 12: 273-84(Apr. 1965). (In German).

Because a proportionality exists between the ratio of the specific activity in fallout to that of ground air and the ratio of activity of a particular nuclide in fallout to its activity in ground air, it is simpler and less time-consuming to collect radioactive aerosol from a large volume of air on filter paper and send this to a central laboratory for testing than to carry out precipitation analyses. Data are given for the period from 1961 to 1963 for relations between precipitation and total and individual activity of several isotopes during periods of interest, and the equation relating total activity ratios to specific individual isotopic activities is given; four constants are employed, and these differ if the form of precipitation is rain or snow. Correlations of the daily activity for snow and rain for the isotopes ^{95}Zr and ^{140}Ba are plotted on the same graph. The mean error is between 40 and 60% where data range over two orders of magnitude. (BBB)

16767 SEARCH FOR EFFECTIVE DECONTAMINATING SOLUTIONS USED TO REMOVE ^{60}Co FROM DURALUMINUM AND STEEL-3 BY ULTRASONIC CLEANING. Kochergin, S. M.; Moiseenko, S. K. Zh. Prikl. Khim., 38: 2337-9 (Oct. 1965). (In Russian).

The duraluminum and steel samples 2 × 4 cm in size were etched with acid, and after rinsing with water, were contaminated to give an average count rate of 1000 to 1300 counts per minute up to 12,000 to 13,000 counts per minute (a factor of 10 greater than the maximum allowable contamination on equipment surfaces). The samples were placed in an ultrasonic bath at a frequency of ~22,000 cycles/sec and a power of 1 to 1.5 w/cm^2 with a solution temperature of 20°C. Out of a total of 25 different media the following were found to be the most effective for the ultrasonic decontamination of duraluminum: 10% H_2SO_4 + 15 g/l $KMnO_4$, 10% HNO_3, and 10% H_2SO_4 + 15 g/l $K_2Cr_2O_7$. A decontamination of 99.5% was obtained in 2.5, 3, and 5 min with sample weight losses of 0.5, 2.5, and 1% respectively. On aging the ^{60}Co contamination for 4 days it was necessary to increase the agitation time and also the sample weight loss of a factor of 2 in order to obtain 99.5% decontamination. Similar results were obtained with the steel samples. (TTT)

16768 PLUTONIUM ALPHA AIR MONITOR (Engineering Materials). (Lawrence Radiation Lab., Univ. of California, Livermore). (CAPE-1323).

35 drawings.

The continuously indicating plutonium alpha air monitor described is based on the use of a solid-state detector and a single-channel pulse-height analyzer. The resolution of the system excludes 98% of the radon daughter alpha activity and all of the thoron activity. One maximum permissible

concentration (MPC) of ^{239}Pu, 2×10^{-12} $\mu c/cm^3$, can easily be seen within 8 hr of sampling. The monitor consists of an air pump particulate collecting filter; detector (380 mm^2 gold-silicon surface barrier unit); low-noise preamplifier and power supply; linear amplifier, single-channel analyzer, and count-rate meter in one chassis; recorder; and audio alarm. (For details, see TID-4100). (M.C.G.)

16769 ALPHA HAND AND SHOE COUNTER (Engineering Materials). (Lawrence Radiation Lab., Univ. of California, Livermore). (CAPE-1325).

44 drawings.

The instrument described is used in detecting low-level α contamination of personnel. It is automatic and may be used by personnel without radiation monitoring training. The user stands on the machine and inserts his hands in the hand cage, which photoelectrically starts a timed count. Lights indicate when the machine is counting and a high count produces a visual and audible alarm. A recount light indicates when a recount is needed. Air proportional probes are used; one for each hand and shoe. A frisk probe and meter on the side of the machine may be used to monitor clothing. The sensitivity of the machine is such that with a 12-sec count and an alarm level of 4 counts, a 100 count/min source will give an alarm more than 50% of the time and a 300 c/min source has a 99.7% probability of tripping the alarm. (For details see TID-4100). (M.C.G.)

INSTRUMENTATION

General

Refer also to abstracts 16710, 17010, 17195, 17522, 17625, 18030, and 18114.

16770 (CONF-650922, pp 428-30) NMR MAGNETOMETRIC DEVICE WITH FLOWING LIQUIDS. Indreas, Gr.; Scintei, N.

An NMR magnetometer is described with which flowing liquid samples are used to improve the signal-to-noise ratio. The device permits easy measurements of small and inhomogeneous magnetic fields. (D.C.W.)

16771 (CONF-650922, pp 467-71) WIRE ORBIT MEASUREMENTS WITH A PULLEY OF LOW FRICTION. Bichsel, Hans.

A device that was developed for the measurement of the orbit of a charged particle in a magnetic field by simulation of the orbit with a current-carrying wire under tension is described. Some measurements of orbits in the magnet of a charged-particle spectrometer are summarized. (D.C.W.)

16772 (CONF-650922, pp 769-75) CONSIDERATIONS IN APPLYING ACYCLIC GENERATORS FOR PULSE-DUTY IN MAGNET POWER SUPPLIES. Cooney, R. W.; Harvey, L. M.; Horton, M. D.

The application of a flywheel-acyclic generator power supply was programmed and checked on an analog computer for application of a 120,000-kw pulse to a bubble chamber magnet. It was confirmed that the pulse could be generated at 15-sec intervals with apparent economies over other systems. (auth)

16773 (CONF-650922, pp 779-87) STATE OF THE ART FOR PRECISION CURRENT OF FIELD REGULATED POWER SUPPLIES. Kruse, F. W. Jr.

The status of regulated solid-state power supplies for magnets is summarized. Recent developments in the field are emphasized. (D.C.W.)

16774 (CONF-650922, pp 788-96) STATE-OF-THE-ART IN HIGH POWER SILICON CONTROLLED RECTIFIER THYRISTORS. New, T. C.; Nowalk, T. P.

The status of silicon-controlled rectifier thyristors for high-power applications is reviewed. (D.C.W.)

16775 (DESY-65/17) EIN 100 MHz-VORUNTERSETZER IN BIQUINAERER TUNNELDIODEN-TRANSISTOR-SCHALTUNG. (A 100-MHz Prescaler in Biquinary Tunnel Diode Transistor Mode). Nentwich, H. (Deutsche Elektronen-Synchrotron, Hamburg (West Germany)). Dec. 1965. 23p. Dep. mn.

A 100 MHz decimal prescaler is described which operates in the bi-quinary mode with a tunnel-diode flip-flop and a five-stage ring counter. The pulse pair resolution is better than 10 nsec. The unit has gate signal input, reset and optical readout. (auth)

16776 (EGG-1183-1156) AN IMPROVED METHOD OF ROSSI OSCILLATOR-OSCILLOSCOPE COUPLING. Logan, W. L.; Martin, G. P. (Edgerton, Germeshausen and Grier, Inc., Santa Barbara, Calif.). Aug. 20, 1965. Contract AT(29-1)-1183. 47p. Dep. mn. CFSTI $2.00 cy, $0.50 mn.

Methods of exciting the forward deflection plates of EG and G Type 3343 and 3445 oscilloscopes are analyzed, and improved methods are proposed. An analysis of line loss for reactive oscilloscope loads as a function of cable length and oxcillator frequency is given. An alternate technique is then analyzed on the basis of matching the oscilloscope load to a 52-ohm transmission. The results of attempts to define the equivalent circuit between the driving points and the forward capacitance are presented. A method of implementation of matched-line feed is described. (D.C.W.)

16777 (EUR-2702.e) DECIMAL SCANNER FOR THE MODULAR CHAIN. Coppo, N.; Stanchi, L. (European Atomic Energy Community, Ispra (Italy). Joint Nuclear Research Center). Nov. 22, 1965. 12p. Dep. mn.

A decimal scanner that is used to perform the step-by-step variation of a voltage following an external control is described. (D.C.W.)

16778 (NASA-TN-D-3329) HEAT-SHIELD ABLATION MEASUREMENTS USING RADIOISOTOPE TECHNIQUES. Brandon, George W. Jr. (National Aeronautics and Space Administration, Houston, Tex. Manned Spacecraft Center). Mar. 1966. 15p. CFSTI $0.20 cy, $0.50 mn.

A method is presented for applying nucleonic techniques to the measurement of heat-shield surface recession rates during reentry. The method uses a radioactive line source embedded in the heat-shield material. As portions of the radioactive source ablate with the heat-shield during reentry, progressive activity decreases are monitored by a miniaturized detection system. Accuracy of the method is developed and some examples of ablation profiles determined by this method are presented and discussed. (auth)

16779 (PPAD-584D) GUIDE LINE FOR USE OF STANDARD NUCLEAR INSTRUMENT MODULES. Bissell, R. C.; Droege, T. F. (Princeton-Pennsylvania Accelerator, Princeton, N. J.). Feb. 15, 1966. Contract AT(30-1)-2137. 21p. Dep. mn. $1.00 cy, $0.50 mn.

A user's manual which contains most of the drawings, standards and pin assignments that are needed to make effective use of the nuclear instrument module system is presented. (D.C.W.)

16780 (TID-22689) WEIGHING IRRADIATED FUEL SPECIMENS IN WATER. Titus, Albert C. (Knolls Atomic Power Lab., Schenectady, N. Y.). Jan. 3, 1966. Contract W-31-109-eng-52. 13p. Dep. mn. CFSTI $1.00 cy, $0.50 mn.

A method for weighing irradiated fuel elements while suspended from a balance in a water bath is reported. These hot objects create convection currents whose lifting effect causes the reduced weight in water. It was found that stirring-induced counter-currents could be used to essentially eliminate the error, by stirring just hard enough to bring temperature equality above and below the specimen being weighed. For one of the actually observed electrically heated simulated specimens, of 130 grams weight in air, a weight error of -64 mg in water was reduced to ±5 mg. (P.C.H.)

16781 DEUTERIUM ISOTOPE EFFECT ON THE PERFORMANCE OF EUROPIUM CHELATE LASERS. Ross, Daniel L.; Blanc, Joseph; Pressley, Robert J. (RCA Labs., Princeton, N. J.). Appl. Phys. Lett., 8: 101-2 (Feb. 15, 1966).

In studies of the performance of the octacoordinate europium chelate lasers it was found that laser thresholds depend critically on apparently trivial chemical changes of these compounds. Piperidinium tetrakis (4, 4, 4-trifluoro-1-phenyl-1, 3-butanediono) Eu(III), was prepared using a diketone in which the benzene-ring hydrogen atoms were replaced by deuterium, and piperidine fully deuterated except at the 1-(nitrogen) position. The relative quantum yields, lifetimes, and the results obtained in one set of laser experiments at a temperature of 168°K and a concentration of 1.135×10^{-2} M. The fully deuterated chelate has a threshold which is less than 50% of that of the normal compound, while even partial deuteration results in approximately a 40% drop in threshold. The deuteration of the piperidinium ion has nearly the same effect as does deuteration of the ligands; this implies that the cation interacts with the chelated europium ion sufficiently strongly to markedly influence the onset of laser action. (J.F.P.)

16782 A SAFETY DEVICE FOR REDUCING THE RADIATION HAZARD IN X-RAY DIFFRACTOMETRY. Cole, W. F.; Lewis, R. E.; Lancucki, C. J. (CSIRO, Highett, Australia). Austral. J. Instrum. Technol., 21: 105-7(Aug. 1965).

A safety device for use with a modified beam-shutter actuator has been developed. The following features are incorporated: (1) The diffractometer, the ratemeter and/or scaler, the strip chart recorder, and the electronic timer start simultaneously by opening the window of the x-ray tube shield to allow x rays to impinge on the sample. (2) The window of the x-ray shield automatically closes, counting stops, and the motor of the strip chart recorder stops, leaving the x-ray set on when the scan is terminated manually or automatically by means of the scan limit switches. The x-ray set can then be stopped automatically by a time-clock. (3) The window of the x-ray tube shield closes and all the equipment simultaneously shuts down when the scan is automatically terminated by operation of the scan limit switches. As a result the window is open only for the duration of the scan, and is automatically closed whichever way the scan is terminated. (BBB)

16783 STATIC ELECTRICITY IN ANESTHETIC FLOWMETERS ELIMINATED BY RADIOACTIVE PISTOL. Hagelsten, Johs.; Larsen, Ole Steen (Bispebjerg Hospital, Copenhagen). Brit. J. Anaesthesia, 37: 799-800(Oct. 1965).

Sticking of the anesthesia flowmeter bobbin due to accumulation of static electricity may cause a flowmeter inaccuracy of up to 35%. A γ-radioactive static eliminator is described that was constructed especially for decharging of anesthetic flowmeters. The radioactive source consists of 0.1 mC ^{137}Cs. When the bobbin sticks because of static electricity, the flowmeter is ionized by moving the eliminator around the sticking bobbin until it is again rotating freely. If no special measures are taken, 4 to 8 hr will pass until decharging is complete due to natural radioactive radiation. With γ-ray ionization from a static eliminator the electrical charges may be removed in seconds, depending on the strength of the eliminator and the charges present. (TCO)

16784 COMMENT ON A PAPER BY K. KANAYA, H. KAWAKATSU AND H. YAMAZAKI, "AN EVALUATION OF THE ABERRATIONS OF FOCUSED BEAMS OF CHARGED PARTICLES CAUSED BY SPACE CHARGE." Kanaya, K.; Kawaskatsu, H.; Yamazaki, H. (Kamimukodai, Tokyo). Brit. J. Appl. Phys., 17: 143-6(Jan. 1966).

The formulas from which aberration coefficients are obtained with the method of characteristic functions depend critically upon two criteria: whether the system in question is treated as a system with an aperture stop or with a beam of fixed angular aperture at the object plane; the order of the particular aberrations to be calculated. The analysis by Kanaya, Kawakatsu and Yamazaki is examined in the light of this dependence. (auth)

16785 THE EFFECT OF DRIVING PULSE DURATION ON THE THRESHOLD LEVEL OF TRIGGER CIRCUITS. Vojinovic, Mirko. Bull. Boris Kidrich Inst. Nucl. Sci., 16: 163-71(July 1965).

The effect of driving pulse duration on the threshold level was analyzed by using response function of the amplifier obtained by opening the feedback loop of the trigger circuit. The driven transition function was obtained and conditions for transition with rectangular driving pulse shape are given. Calculated and experimental results revealed the importance of the g_m/C_e factor and requirements for sharp cut-off and constant transconductance of the active element. (auth)

16786 A SIMPLE AND FLEXIBLE DIFFERENTIAL AND INTEGRAL PULSE-HEIGHT SELECTOR. Gopalan, K. (Indian Inst. of Science, Bangalore, India). Indian J. Pure Appl. Phys., 4: 20-3(Jan. 1966).

Description and operational details of a differential and integral pulse-height selector circuit are given. The distinguishing feature of the circuit is that it can measure a wide variety of input pulses ranging from 1 μsec. to over 1000 μsec. in length without readjustment. This wide coverage is achieved by replacing the conventional capacitor memory by binary memory in the anticoincidence stage of the instrument. This circuit has, in addition, a simple form, and permits a straightforward extension to multichannel operation independent of incident pulse width. (auth)

16787 ION COLLECTION IN THE BAYARD-ALPERT GAUGE. Comsa, George (Inst. for Atomic Physics, Bucharest). J. Appl. Phys., 37: 554-6(Feb. 1966).

A collecting factor for ions created at a given distance is computed on the basis of a simplified model and under the assumption of a Maxwell distribution of the initial velocities of ions. The factor is independent of the mass of the ion, but is a function of the temperature and takes values differing substantially from unity for usual dimensions of the collector. The effect of the collector dimensions on the x-ray-limited pressure may be analyzed by using an approximate expression for the integral collecting factor. Calculation shows that for very fine collecting wires the collecting factor is affected even by the extremely small momentum transferred to the helium ion from the electron during the ionizing collision. Experiments have confirmed the foregoing considerations, thus opening the way to the measurement of such momenta. (auth)

16788 COLD-CATHODE MAGNETRON GAUGE CHARACTERISTICS. Bryant, Paul J.; Longley, William W. Jr.; Gosselin, Charles M. (Midwest Research Inst., Kansas City, Mo.). Contract NASr-63(06). J. Vac. Sci. Technol., 3: 62-7(Mar.-Apr. 1966).

A description of cold cathode magnetrons operating as gages was developed in terms of the conditions for establishing a discharge and the effects of space-charge buildup. Pressure response curves for NRC type 552 (Redhead) and GCA model 1410 (Kreisman) gages were determined by a conductance-regulated, pressure-ratio method using Bayard-Alpert type gages for upstream pressure reference. Four characteristics of normal magnetrons operated below cutoff are predicted from the discharge mechanism and correlated with test data: an out-of-strike state characterized by a steady pressure-independent gage reading (about 5×10^{-14} torr) due to leakage current; a minimum pressure threshold for operation, 2.7×10^{-12} torr for the NRC 552, 1.7×10^{-10} torr for the GCA 1410; a range (below 10^{-9} torr) of nonlinear pressure-dependent response moderated by space charge buildup; and a range of near linear response corresponding to the region of nearly saturated space charge. (auth)

16789 USE OF MOLYBDENUM IN GETTER ION PUMPS. Jackson, A. G. (Systems Research Labs., Inc., Dayton, Ohio); Haas, T. W. J. Vac. Sci. Technol, 3: 80 (Mar.-Apr. 1966).

A study of gettering materials in ultrahigh vacuum indicates only minor differences for titanium, tantalum, zirconium, and niobium, but the work suggests that molybdenum might offer increased possibilities for the pumping of hydrogen and water in the ultrahigh vacuum range. Molybdenum cathodes were used in a diode ion pump, which was then used to pump a small stainless steel vacuum system, including a partial pressure analyzer capable of measuring partial pressures below 10^{-13} torr. The effects of substituting titanium for the molybdenum were also noted. Finally, one titanium and one molybdenum cathode were used. The initial performance in this case was not so good as the initial results with the molybdenum pump, but it was superior to that using only titanium cathodes. (J.F.P.)

16790 ON THE ANALYSIS OF ELECTRICAL NETWORKS USING THE ZRA 1 TYPE COMPUTER. Griepentrog, E. (VEB Atomkraftwerk, Berlin). Kernenergie, 8: 635-7(Nov. 1965). (In German).

A program was developed for analyzing electrical circuits by using digital computers of the ZRA-1 type. The logic functions occurring in the circuit algebra are brought

into disjunctive normal forms of simple construction. Moreover, if it is desired, the program substitutes variables by given substitutional functions which, of course, must be free from feedback. The program is suitable for setting up conjunctive normal forms, too, due to the duality of the logical operations conjunction and disjunction. (auth)

16791 NUCLEAR RESONANCE MAGNETOMETER WITH FREQUENCY MODULATION. Reimann, R.; Eggensberger, H. (Eidgenoessiche Technische Hochschule, Zurich). Nucl. Instrum. Methods, 40: 9-12(Feb. 1966). (In German).

A new type of NMR magnetometer is described, functioning on the marginal oscillator principle. The usual amplitude modulated receiver is replaced by a frequency modulated receiver. Signal to noise ratio is improved by using frequency discrimination at a higher order harmonic The resulting resonance signal appears as a dispersion signal. (auth)

16792 MULTIPLE-DURATION MONOSTABLE [MULTIVIBRATOR]. Gorodetzky, S.; Zen, J.; Ruscher, J.; Muser, A.; Armbruster, R. (Institut de Recherches Nucleaires, Strasbourg). Nucl. Instrum. Methods, 40: 89-92(Feb. 1966). (In French).

A multiple duration monostable multivibrator is described. Its output pulse width is a multiple of a fixed duration and depends on the time during which the input amplitude exceeds the threshold of the multivibrator. The purpose of this multivibrator is to obtain a gating efficiency of nearly 100% for time fluctuating pulses. The gating efficiency is calculated for pulses of exponential decay. (auth)

16793 VARIABLE-WIDTH PULSE GENERATOR USING AVALANCHE TRANSISTORS AND CHARGE-STORAGE DIODES. Fraser, H. J. (AAEC Research Establishment, Sutherland, N.S.W., Australia). Nucl. Instrum. Methods, 40: 106-8(Feb. 1966).

A variable-width pulse generator is described in which a delay-line-formed avalanche transistor pulser is used to turn off a charge-storage diode. Pulse width is controlled by a variable d-c bias current flowing through the charge-storage diode and is continuously variable from 3–30 ns. The rise time is determined by the avalanche transistor and the fall time by the charge-storage diode. Output is 0–8 v into 50 ohm with a rise time of one ns and a fall time of 2 ns. Two similar circuits are combined to form a double pulser with variable repetition rate 100 kc/s-2 Mc and with variable pulse spacing of 10–200 ns. (auth)

16794 SIMPLE EQUALIZING SYSTEM FOR SMALL DIFFERENTIAL NON-LINEARITY WITH A ONE-NANOSECOND DIGITAL TIME CODER. Meyer, H. (EURATOM, Geel, Belg.). Nucl. Instrum. Methods, 40: 149-52(Feb. 1966).

The main characteristics and principal function of a time coder with direct analog to digital conversion for high-precision time-of-flight experiments are given. A general working-principle diagram of the nanosecond time coder, and a diagram of the step delay with binary coded control are shown. The spectral response with uniform time interval distribution and measurements of a great time interval are also given. (J.F.P.)

16795 METHOD TO CORRECT THE AMPLITUDE DISTORTIONS DUE TO PILE-UP EFFECTS. De Lotto, I. (Consiglio Nazionale delle Ricerche, Milan); Dotti, D.; Mariotti, D. Nucl. Instrum. Methods, 40: 169-72(Feb. 1966).

A method is presented which allows a correction of pile-up distortions based on the experimental evaluation of the pile-up amplitude spectrum. Also pile-up effects in amplitude measurements are examined in order to characterize the cases where the method presented does not apply. The given results show that a good evaluation is allowed for the position of the centroid, for the half-amplitude width of the peaks, and for the peak to valley ratios also in the case of a large pile-up and consequently of an unsymmetrical peak shape. It is noted that the position of the peak of the pile-up spectrum does not affect the position of the reconstructed spectrum except for a rigid shift. (J.F.P.)

16796 ON A PHOTOMULTIPLIER BASE SYSTEM WITH HIGH-VOLTAGE DIVIDER NETWORK REMOTE FROM THE PHOTOMULTIPLIER. Ness, S.; Smith-Saville, R. J. (Univ., Manchester, Eng.). Nucl. Instrum. Methods, 40: 175-6(Feb. 1966).

A photomultiplier base system was recently described by Davis and Spore (IEEE Trans. Nucl. Sci., NS-12, No. 4, 245 (1965)) in which all the usually associated bulk and power dissipation of the dynode-divider network was far removed from the photomultiplier socket in order to increase reliability and accessibility. Such a system was modified for reasons of reliability and accessibility to remote wiring. A single standard 20-core multiway cable was used to couple between all the pins and their bias supplies. This method has the added advantage that the supply end of the cable can be terminated in a standard multiway plug without any complication. (J.F.P.)

16797 THE BRIDGE CELL—A NEW SUPERCONDUCTIVE MEMORY CELL FOR RANDOM-ACCESS WORD-ORGANIZED MEMORIES. Ahrons, R. W. (RCA Electronic Components and Devices, Somerville, N. J.). RCA Rev., 26: 557-73(Dec. 1965).

The bridge cell is a thin-film memory cell based on the phenomenon of superconductivity. It differs from other superconductive memory cells in that each bit is stored in the form of a persistent current whose plane is perpendicular, instead of parallel, to the plane of the thin film. This method of storage leads to inherently high packing densities. An equivalent-circuit model is used to explain the operation of the bridge cell. The model comprises two inductances in parallel with a mutual coupling equal to the lower value of the two inductances. A resistance is in series with the inductance having the lower value. The analysis of this model explains the operation of the cell. The cell can be made by evaporation through masks or by a combination of evaporation and preferential etching. Experiments on evaporated samples have demonstrated that sense voltages higher than one millivolt can be obtained. The cell can be used as an analog memory having an output proportional to the digit-line driving current. The new bridge cell most naturally fits a word-organized memory array. A single cryotron-tree type of decode matrix can be used with the bridge cell, but greater operating speeds can be obtained with a two-level decode matrix. (auth)

16798 TRANSFORMATION OF THE MI-1305 TYPE SPECTROMETER. Alexandru, Gr. (Inst. of Atomic Physics, Bucharest). Stud. Cercet. Fiz., 17: 845-9(1965). (In Rumanian).

The Mi-1305 type mass spectrograph designed for determination of the isotopic concentration may be used for other purposes, if the needed changes are made. In order to reduce the amount of sample required for the measurements, the residual background of the mass spectrum must be reduced and the stability of the ionizing current must be increased. The analyzing magnet also requires a higher current. These conditions were satisfied by carrying out certain design changes. A low-conductivity, 15 to 20 micron diameter orifice was used and the pressure of the reserve chamber was kept below 10^{-2} torr, in order to ensure molecular flow of low molecular weight gases. The new ion source was shielded from the external magnetic field and the ionization chamber was outgassed at 500 to 600°C. Magnetostatic focusing of the electron beam was replaced by an electrostatic system. (TTT)

16799 A DOUBLE-AXIS NEUTRON DIFFRACTOMETER AND GENERAL CRITERIA FOR OPTIMIZATION OF ITS RESOLUTION FOR POWDER INVESTIGATIONS. Stoll, E.; Haelg, W. (Eidgenoessische Technische Hochschule, Zurich). Z. Angew. Math. Phys., 16: 817-20(1965). (In German).

The double-axis neutron diffractometer used in connec-

tion with the Swiss reactor DIORIT is an instrument for either powder or single crystal operation. The precision of the angular movements reaches 10 sec of arc. Positions are measured digitally and a computer forms the 2-to-1 ratios in the case of single crystal operating mode. Suggestions for the optimum adjustments of the instruments for powder investigations are given relative to the selection of the monochromator reflection planes and the contributions of higher-order wave lengths. A ratio for instrument parameters is obtained from analyzing nickel powder defractographs and the results are compared with theoretical predictions. (auth)

16800 AN ELECTRON SPIN RESONANCE SPECTROMETER WITH CONTINUOUSLY VARIABLE FREQUENCY AND HIGH SENSITIVITY. Urban, W. (Technische Hochschule, Karlsruhe, Ger.). Z. Angew. Phys., 20: 215-17 (1966). (In German).

An ESR-apparatus is described, using frequency variation instead of magnetic field variation. A backward wave oscillator is tuned synchronously with the resonator, covering the frequency range from 8 to 13 GHz. Measurements of ESR in diluted single crystals are possible near zero magnetic field. The sensitivity is 5×10^{13} ions per gauss linewidth. A discussion of the signal shapes found in very weak fields is enclosed. (auth)

16801 SPECIFIC GRAVITY APPARATUS, AUTOMATED (Engineering Materials). (Phillips Petroleum Co., Idaho Falls, Idaho. Atomic Energy Div.). (CAPE-1259). 23 drawings.

An automated specific gravity apparatus used in routine analysis of highly radioactive dissolver samples and other samples from enriched-U recovery is described. The falling drop technique used is readily adaptable to remote operation and requires a small volume of sample. The equipment employs a reliable timer system, a controller for automatic and sequential operation of the pipetting and timing events, a print-out reader paralleled with a clock timer, an organic liquid reference tube, and the CPP "Model B" pipetter. With 10-μl aqueous drops and a 6-in. fall, the drop times ranged from 13.7 sec for specific gravity 1.05 to 5.5 sec for specific gravity 1.35. The standard deviation, computed from routine calibration data and a least squares fit, is ±0.0017 in units of specific gravity. (For details, see TID-4100). (auth)

16802 RESOLVING TIMES OF BINARY SCALERS—AN ANALYTICAL STUDY. Choudhury, S. S.; Banerjee, B. M. (Saha Inst. of Nuclear Physics, Calcutta). Vienna, International Atomic Energy Agency, 1965, Preprint No. CN-22/34, 20p. (CONF-651105-13). ORAU.

From Conference on Nuclear Electronics, Bombay.

An analytical study of binary scalers is summarized. The results of calculations of resolving times for a number of practical cases are presented. (D.C.W.)

16803 A LOW-DRIFT SOLID-STATE D-C AMPLIFIER. Wakayama, N.; Furukawa, T. (Japan Atomic Energy Research Inst., Tokyo). Vienna, International Atomic Energy Agency, 1965, Preprint No. CN-22/49, 23p. (CONF-651105-32). ORAU.

From Conference on Nuclear Electronics, Bombay.

A solid-state d-c amplifier, which was developed for the measurement of small currents, is described. (D.C.W.)

16804 RESPONSE CHARACTERISTICS OF A NEW HIGH TEMPERATURE ELECTRON CAPTURE DETECTOR. Yauger, W. L.; Addison, L. A.; Stevens, R. K. (Micro-Tek Instruments Inc., Baton Rouge, La.). 13p. (CONF-651054-1). ORAU. Gmelin, AED-CONF-65-291-1.

From Association of Official Agricultural Chemists, 79th Annual Meeting, Washington, D. C.

An electron capture detector, which uses ^{63}Ni as its electron source and can operate routinely at 300°C, is described. The response of this detector is compared with that of a parallel-plate detector using a tritium source. (D.C.W.)

Radiation Detection

Refer also to abstracts 16505, 16737, 16768, 16769, 17175, 17182, 17253, 17311, 17663, 17864, 17962, and 18025.

16805 (CLOR-43/D) KIESZONKOWY SYGNALIZATOR PRZEKROCZENIA DAWKI PROMIENIOWANIA GAMMA. (Radiation Dose Sensitive Pocket Alarm Monitor). Bukowiecki, B. (Centralne Laboratorium Ochrony Radiologicznej, Warsaw (Poland)). 1965. 8p. Dep.

An instrument that gives an acoustic alarm when a dose of 300 mr is accumulated is described. (D.C.W.)

16806 (CLOR-44/D) OPTYMALIZACJA SPEKTROMETRYCZNYCH STOPNI WEJSCIOWYCH NA TRANZYSTORACH TYPU F.E.T. WSPOLPRACUJACYCH Z POLPRZEWODNIKOWYMI DETEKTORAMI PROMIENIOWANIA JADROWEGO. (Considerations on the Optimalization of F.E.T. Spectrometer Stages Working with Semiconductor Radiation Detector). Bukowiecki, B.; Katkiewicz, W. (Centralne Laboratorium Ochrony Radiologicznej, Warsaw (Poland)). 1965. 21p. Dep.

Some problems in the design of low-noise preamplifiers for use with solid-state detectors are discussed, and the performance and optimization of some amplifier-detector combinations are described. Some experimental results on preamplifiers using specific transistors are included. (D.C.W.)

16807 (CLOR/IBJ-42/D) THE DETERMINATION OF A MIXTURE OF THERMAL-NEUTRON AND GAMMA-RAY EXPOSURES BY FILM BADGES. Musialowicz, T.; Wysopolski, J.; Filipiak, B. (Institute of Nuclear Research, Warsaw (Poland). Centralne Laboratorium Ochrony Radiologicznej, Warsaw (Poland)). 1965. 20p. Dep.

A method of measuring gamma and thermal-neutron doses in mixed fields by the use of film badges is described. (D.C.W.)

16808 (CONF-650922, pp 154-63) MEASUREMENTS OF ION-OPTICAL PROPERTIES OF A HIGH RESOLUTION SPECTROMETER FOR ELECTRON SCATTERING. Penner, S.; Lightbody, J. W.

A double-focusing magnetic spectrometer that was developed primarily for the measurement of electron scattering cross sections is described, and an investigation of the optical properties of the spectrometer by ray-tracing techniques using Ar ions is summarized. (D.C.W.)

16809 (CONF-650922, pp 253-61) A LARGE SPARK CHAMBER MAGNET WITH TAPE WOUND COILS. Yurka, G. E.; Kustom, R. L.; Siljander, W. A.

A 70-ton magnet with a useful volume of 50 × 60 × 30 in. is described. (D.C.W.)

16810 (CONF-650922, pp 366-76) DESIGN AND CONSTRUCTION OF THE MAGNET AND TRANSPORT SYSTEM FOR A LARGE LIQUID HELIUM BUBBLE CHAMBER. Tschopp, Peter A.

The magnet for the liquid-helium bubble chamber of the Rutherford Laboratory is described, together with the system with which the magnet (and bubble chamber) is positioned. (D.C.W.)

16811 (CONF-650922, pp 663-79) 100-300 KG PULSE BUBBLE CHAMBER MAGNET. Bergmann, W. H.

A pulsed magnet is described, the coil of which serves as the chamber body. The fabrication of the coil is outlined. (D.C.W.)

16812 (EGG-1183-1174) O(S)S-10 DIELECTRIC COMPTON DETECTOR DEVELOPMENT REPORT. Report No. L-740. Tolman, E. L. (Edgerton, Germeshausen and Grier, Inc., Santa Barbara, Calif.). Oct. 15, 1965. Contract AT(29-1)-1183. 18p. Dep. mn. CFSTI $1.00 cy, $0.50 mn.

A spherical dielectric Compton detector, which was developed for use in the Weapons Test Program, is described. The calibration and testing of the detector are summarized. (D.C.W.)

16813 (INR-653/IA/D) MEASUREMENT OF THE RATIO OF SLOW TO FAST COMPONENTS OF SCINTILLATION IN STILBENE IN A WIDE RANGE OF dE/dx. Stanislaw, Pszona (Institute of Nuclear Research, Warsaw (Poland)). Sept. 1965. 8p. Dep.

A method of measuring the relative ratio of the slow and fast components of scintillation in organic phosphors as a function of dE/dx of the incident particles is described. Some results are presented for stilbene. (D.C.W.)

16814 (ITEF-386) EFFEKTIVNOST' MAGNITNOGO SPEKTROMETRA DLYA REGISTRATSII K^0-MEZONOV. RASPAD $K^0 \rightarrow \pi^+ + \pi^-$. (Effectiveness of Magnetic Spectrometer for Recording $K^0 \rightarrow \pi^+ + \pi^-$ Decay of K^0 Mesons). D'yuk, F. Zh. (Gosudarstvennyi Komitet po Ispol'zovaniyu Atomnoi Energii SSSR, Moscow. Institut Teoreticheskoi i Eksperimental'noi Fiziki). 1965. 36p. Dep. mn.

The efficiency of a magnetic spectrometer arrangement for the detection of K^0 mesons by the $\pi^+ + \pi^-$ decay mode was investigated. The dependence of the efficiency on the momentum and the decay coordinate of the K^0 meson is presented. (auth)

16815 (JINR-P-2506) ISKROVYE KAMERY V EKSPERIMENTE PO IZUCHENIYU UPRUGOGO RASSEYANIYA π^+-MEZONOV NA PROTONAKH NA UGOL 180 DEG. (Spark Chambers for Studying Elastic Scattering of π^+ Mesons by Protons at 180 deg). Vovenko, A. S.; Gladkii, Ya.; Gus'kov, Y. N.; Lyubimov, A. L.; Matyushin, A. T.; Savin, I. A. (Joint Inst. for Nuclear Research, Dubna (USSR). Lab. of High Energy). 1965. 21p. Dep. mn.

Multiplate spark chambers applied in the experiment on π^+p scattering at 180° are described. The basic characteristics of these chambers and their drift in time are given. The efficiency of recording one particle was measured at the intensive background loading. (auth)

16816 (JINR-P-2528) KONSTRUKTSII GAZOVYKH POROGOVYKH I DIFFERENTSIALNYKH CHERENKOVSKIKH SCHETCHIKOV. (Designs of Gaseous Threshold and Differential Cherenkov Counters). Likhachev, M. F.; Savin, I. A.; Stavinskii, V. S. (Joint Inst. for Nuclear Research, Dubna (USSR). Lab. of High Energy). 1965. 8p. Dep. mn.

Different designs of gaseous Cherenkov counters and their characteristics are considered. (auth)

16817 (JUL-270-RB) EIN AUSGABESYSTEM FUER EINEN VIELKANAL-IMPULSHOEHEN-ANALYSATOR. (A Distribution System for a Multi-Channel Pulse-Height Analyzer). Riepe, G.; Jung, L. (Kernforschungsanlage, Juelich (West Germany). Institut fuer Reaktorbauelemente). May 1965. 21p. Dep. mn

A distribution system is built for an RCL 512-channel analyzer. The system permits the data stored in the multichannel analyzer to be distributed to a tape punch or to an IBM typewriter. The decoding of the channel number and the channel number preselection, and the control of the typewriter and of the tape punch are given. The operation of the counter is outlined. As an example of the use of the distribution system, the stability of the total amplification factor of a γ spectrometer (and, therefore, the position constant of a γ peak) is studied with respect to the change of the multiplier voltage with and without use of an SES stabilizer. (J.S.R.)

16818 (KFK-328) HERSTELLUNG UND UNTERSUCHUNG VON DICKEN BASISFREIEN OBERFLAECHENSPERRSCHICHT-ZAEHLERN. (Preparation and Study of Thick Depleted Surface Barrier Detectors). Meyer, O.; Langmann, H.-J. (Kernforschungszentrum, Karlsruhe (West Germany)). May 1965. 14p. Dep. mn.

The preparation and performance of depleted surface-barrier detectors were studied. Detectors with depletion layers up to 3 mm thick were fabricated, and a method of measuring the resistivity of the bulk material was developed. The best energy resolution, obtained with a 2-mm-thick liquid-air-cooled counter for 1-Mev electrons, was 2.1 kev. (D.C.W.)

16819 (LA-3435) A DOSE MONITORING INSTRUMENT FOR NEUTRONS FROM THERMAL TO 100 Mev. McGuire, Stephen A. (Los Alamos Scientific Lab., Univ. of California, N. Mex.). Aug. 1965. Contract W-7405-eng-36. 25p. Dep. mn. CFSTI $2.00 cy, $0.50 mn.

A proposed neutron monitoring instrument consists of a ^{6}LiI crystal centered in 3-in.-, 10-in.-, and 18-in.-diameter polyethylene spheres. The polyethylene moderates neutrons so that they may be counted as the result of the (n,α) reaction in the crystal. Transport-theory calculations of sphere counting efficiencies use 21-group cross sections from thermal energies to 192 Mev. The monitoring system is found effective for particle accelerators where neutrons up to 100 Mev in energy would be found. (auth)

16820 (LA-DC-7222) QUENCH MONITORING AND EFFICIENCY CALIBRATION THROUGH EXTERNAL STANDARDIZATION. Hayes, F. N. (Los Alamos Scientific Lab., Univ. of California, N. Mex.). [nd]. Contract W-7405-eng-36. 27p. (CONF-641025-1). Dep. mn. CFSTI $2.00 cy, $0.50 mn.

From 9th Symposium on Advances in Tracer Methodology, San Francisco.

It was demonstrated that external standardization not only monitors quenching but also calibrates counting efficiency for ^{14}C, ^{3}H, and ^{32}P over a wide range of quenching. (D.C.W.)

16821 (LAL-1151) AN APPLICATION OF FERMAT PRINCIPLE TO MAGNETIC SPECTROMETERS. Bounin, Paul (Laboratoire de l'Accelerateur Lineaire, Univ. de Paris, Orsay (France)). Jan. 1966. 33p. Dep. mn.

The well-known Fermat principle applied to corpuscular optics is reviewed. It is applied to the particular case of magnetic spectrometers with a symmetry plane. As a consequence a rapid method is given to derive magnets with some specific aberrations cancelled. For example, two already known types of spectrometers are considered, but others may be derived by that method. (auth)

16822 (N-65-19927) THE COSMIC RAY TELESCOPE FOR THE MARINER-MARS MISSION. Final Engineering Report. Lamport, James E. (Enrico Fermi Inst. for Nuclear Studies, Univ. of Chicago, Ill.). [1964]. Contracts NAS7-100; JPL-950615. 19p. (NASA-CR-57515). CFSTI $1.00 cy, $0.50 mn.

For Jet Propulsion Lab., Calif. Inst. of Tech., Pasadena.

The results of some tests of components of the cosmic-ray telescope for the Mariner C space vehicle are presented. Project activities leading up to the launch of the Mariner IV Mars mission are outlined. (D.C.W.)

16823 (NYO-3160-1) INVESTIGATION OF A NEW TYPE NARROW-BAND X-RAY DETECTOR FOR THE IDENTIFICATION OF CHEMICAL ELEMENTS USING RADIOISOTOPE X-RAY SOURCES. Brinkerhoff, Joris M.; Forsyth, Richard (Tracerlab/Research, Waltham, Mass.). Dec. 10, 1965. Contract AT(30-1)-3160. 50p. Dep. mn. CFSTI $3.00 cy, $0.50 mn.

A new type narrow band x-ray detection system for the identification and measurement of chemical elements by means of radioisotope induced x-ray fluorescence was investigated. Good results were obtained for the low, medium, and high atomic number regions. An experimental prototype was constructed for the detection of gold. (P.C.H.)

16824 (NYO-3406-3) SINGLE ELECTRON LIGHT PULSE SIZE DISTRIBUTION FROM A CASCADED IMAGE INTENSIFIER. Technical Report No. 3. Reynolds, Geo. T.; Botos, P. Jr. (Princeton Univ., N. J. Elementary Particles Lab.). Feb. 7, 1966. Contract AT(30-1)-3406. 25p. Dep. mn. CFSTI $1.00 cy, $0.50 mn.

The size distribution of light pulses from the anode of a three-stage cascaded image intensifier was determined at room temperature and at the temperature of dry ice for noise or dark-current pulses and for single photoelectrons from the cathode. (D.C.W.)

16825 (ORNL-TM-1442) STEAM CONDENSATE BETA-GAMMA MONITOR AT THE FISSION PRODUCTS

DEVELOPMENT LABORATORY, BLDG. 3517. Chase, L. H.; Knowles, D. J. (Oak Ridge National Lab., Tenn.). Feb. 17, 1966. Contract W-7405-eng-26. 6p. Dep. mn. CFSTI $1.00 cy, $0.50 mn.

Steam condensate from the Fission Products Development Laboratory is stored in a 2000-gal underground tank, and monitored continuously for beta-gamma radiation, and at intervals is drained into the ORNL Process Waste System. The pumping system for withdrawing samples and the associated radiation monitoring system are described, and a checkout procedure is included. (auth)

16826 (PPAD-574E) A K^+ DETECTOR FOR USE WITH A RAPID CYCLING BUBBLE CHAMBER. Sanders, Harold (Princeton-Pennsylvania Accelerator, Princeton, N. J.). Dec. 6, 1965. Contract AT(30-1)-2137. 25p. (CONF-651001-33). Dep. mn. CFSTI $1.00 cy, $0.50 mn.

From IEEE Nuclear Science Symposium, San Francisco.

A detector system was constructed to detect the decay of K^+ particles generated in nuclear events in the twenty cycles per second hydrogen bubble chamber at the Princeton-Pennsylvania Accelerator. The purpose of this system is to preview each event to minimize the number of nonproductive photographs. Ninety-six large plastic scintillator counters form an array covering 180° of the downstream side of the chamber. Particle discrimination is done by generating a clock timing pulse from counters placed in the incoming beam which enables a set of coincidence gates driven by individual array counters, in such a period as to exclude outputs due to various prompt particles (i.e., the primary beam or the results of various elastic interactions in the chamber). A second level of gating is required to determine if the interaction has occurred during a period in which the chamber was sensitive. The output signal is used to trigger a chamber illuminating flash tube to photograph the event. (auth)

16827 (SZS-9(1965)) 2 ARBEITSTAGUNG UEBER PERSONENDOSIMETRIE, BERLIN, 11. BIS 14. NOVEMBER 1964. ZUSAMMENSTELLUNG. (Second Working Session on Personnel Dosimetry, Berlin, November 11 to 14, 1964. Summary). Herrmann, D.; Kiesewetter, W.; Kraus, W.; Ohlsen, H.; Rothe, W. (Staatliche Zentrale fuer Strahlenschutz, Berlin (East Germany)). Sept. 1965. 33p. (CONF-641129). Dep. mn.

From 2nd Working Session on Personnel Dosimetry, Berlin.

Articles presented at the symposium on personnel dosimetry are reviewed. The discussions are briefly summarized. Topics included are: gamma and neutron personnel dosimetry using photographic films; personnel dosimetry at accidental radiation levels; wrist and hand dosimetry; interpretation of the results of personnel dosimetry; dosimetry in nuclear installations; problems of organization and standardization; and ionization chambers as personnel dosimeters. The results of personnel dosimetry in several countries in 1963 were compared by means of statistical tabulations. (auth)

16828 (TID-22763) THE DETERMINATION OF MIXING AND CIRCULATION IN THE OCEAN WITH RADIOACTIVE TRACERS. Final Report, October 1965. Prospero, J. M. (Miami Univ., Fla. Inst. of Marine Science). Contract AT(40-1)-3146. 26p. (ML-65853). Dep. mn. CFSTI $2.00 cy, $0.50 mn.

In an attempt to reduce the ^{40}K background in sea water and thereby increase the detection sensitivity, an in situ coincidence-counting gamma spectrometer was designed and constructed. However, studies showed that there was no advantage to be gained in using the coincidence counting technique. The detectors were equally if not more effective as single counters. In the energy interval of 0.5 to 1.6 Mev, the instrument has a ^{40}K count rate in sea water that is approximately 8 times that which would be obtained with a 5 × 4 in. NaI(Tl) detector in the energy range 0.25 to 1.6 Mev. For purposes of comparison, the maximum sensitivity to be obtained from a 5 × 4 in. NaI detector and 16 × 12 in. plastic detectors used separately and in pairs was determined for different cases. It was concluded that the sensitivity of the two large detectors used as single detectors is approximately equal to the coincidence counting sensitivity assuming in the latter case that the ^{40}K background is less than one count per hour and that there is no cosmic ray background. (P.C.H.)

16829 (UCRL-14534, pp 1-7) ENERGY ABSORPTION COEFFICIENTS OF DOSIMETRIC LiF. Prevo, C. T.; Cate, J. L. (Lawrence Radiation Lab., Univ. of California, Livermore).

A computer program was developed to calculate the energy absorption coefficient of LiF containing trace amounts of other elements. Experimental results are presented that substantiate the calculations. (auth)

16830 (UCRL-14534, pp 8-12) A SOURCE OF INTERMEDIATE ENERGY NEUTRONS FOR DOSIMETER CALIBRATION. Block, S.; Prevo, C. T. (Lawrence Radiation Lab., Univ. of California, Livermore).

Sb-Be neutron sources moderated with D_2O were developed to provide intermediate energy neutrons for dosimetry calibrations. (auth)

16831 (UCRL-14534, pp 28-31) PERSONNEL ALARM DOSIMETER LE 14507-1. Lakin, R. W. (Lawrence Radiation Lab., Univ. of California, Livermore).

The design of wide-range, personnel-monitoring alarm dosimeter for emergency use including life-saving actions is described. (auth)

16832 (UCRL-14534, pp 32-40) CONVERTING A PORTABLE SURVEY METER'S ION CHAMBER INTO A CONTINUOUS AIR MONITOR BY A SIMPLE EXPEDIENT. Block, S.; Beard, E. (Lawrence Radiation Lab., Univ. of California, Livermore).

Conversion of ion-chamber survey meters and portable electrometers into continuous air monitors is described. (J.R.D.)

16833 STUDY OF THE MULTIPLE SCATTERING CONSTANT IN EMULSION AT GREAT CELL LENGTHS. Bozoki, G.; Gombosi, E.; Jenik, L.; Nagy, E.; Sahini, M. (Central Research Inst. of Physics, Budapest). Acta Phys. Acad. Sci. Hung., 20: 133-48(1966).

The dependence of the multiple scattering constant (K) on cell length is studied in the interval of 0.5 cm ≤ t ≤ 10 cm by means of two different methods. By the "coordinate method" the average value of K is found to be K = 30.2 ± 0.6 in the cell length interval of 0.5 cm ≤ t ≤ 3 cm. When the effect of spurious scattering is taken into account this value decreases to 27.1 ± 1.2. The "angular dispersion" method yields K = 30.2 ± 2.5 for the cell length interval of 3 cm ≤ t ≤ 10 cm. It is found that the spurious scattering depends on the cell length as $d_{sp} = at^n$ where a = (6.84 ± 1.33) · 10^{-3} and n = 1.22 ± 0.17 in the cell length interval of 0.2 cm ≤ t ≤ 3 cm. (auth)

16834 DISPENSER FOR ADDITION OF INTERNAL STANDARD IN LIQUID SCINTILLATION COUNTING. Thomas, Richard C.; Judy, Ray W.; Harpootlian, Harry (Upjohn Co., Kalamazoo, Mich.). Anal. Biochem., 13: 358-60(Nov. 1965).

It was found that a Hamilton repeating dispenser and gastight syringe can be used for rapidly adding a small precisely known volume of internal standard to a large number of samples for liquid scintillation counting. A No. 28 blunt-end needle is attached to the 2.5-ml syringe. The dispenser delivers one-fiftieth the syringe volume each time its button is depressed. Delivery from the dispenser showed a standard deviation of 1.01% for a single addition of internal standard. The corresponding value for a pipet was 1.35%. (M.C.G.)

16835 STATISTICAL CHARACTERISTICS OF FUNCTIONAL RATEMETERS. Skatkin, V. M. At. Energ. (USSR), 19: 544-6(Dec. 1965). (In Russian).

The outlet voltage of a count rate meter will vary due to the statistical nature of the inlet signals. The magnitude of the variation is characterized by the relative statistical error $\delta = \sigma/\bar{u}$, where σ is the average square deviation and $\bar{u}$ is the average voltage. The average value and dispersion

of the outlet voltage are determined for the equivalent network of a current rate meter. Values of $\bar{u}$ and σ are tabulated for a linear meter, summing and difference meters, ratio meters, and log meters. (TTT)

16836 MEASUREMENT OF THE QUANTUM EFFICIENCY OF SCINTILLATION COUNTERS FOR X RAYS. Patla, N.; Kiss, A. E. (Sir John Cass Coll., London). Brit. J. Appl. Phys., 16: 1871-6(Dec. 1965).

The variation of quantum efficiency with wavelength in the range 0.2–2.3 Å is measured by comparison with the efficiency of a proportional counter. Results for NaI(Tl), naphthalene and Naton II (plastic) luminophors used in conjunction with a 9524B EMI photomultiplier show useful efficiencies at the longer wavelengths [NaI(Tl) ~95%; organics ~35%] falling steadily to small values at 0.2 Å. A brief discussion is given of the choice of operating conditions and the relation between quantum efficiency and the modes of interaction of x-ray photons with matter. (auth)

16837 DOSIMETRY OF IONIZING RADIATIONS BY MEANS OF LUMIDOSIMETERS. Delarue, M. R. Bull. Inform. A.T.E.N. (Ass. Tech. Energ. Nucl.), No. 57, 55-61 (Jan.-Feb. 1966). (In French).

The lumidosimeters for the detection of ionizing radiation are mixed metaphosphates of Al, Na, Li, Be, and Ag, where the sensitive element is the Ag. Radiation increases the electron energy level of the valence band up to the level of the conduction band. The electrons thus liberated diffuse and reduce the Ag^+ ions. Ag^0 centers that emit fluorescence under uv excitation are thus formed. The emission of the lumidosimeters under uv excitations are proportional to the radiation dose absorbed. The characteristics of the detection instrument are given. Its use in the precision control of small irradiation doses, control of the accidental irradiation of workers, routine periodic control of the irradiation of workers, equipping armies and civil defense groups, environmental control, biological control, and chemical and high dose control are summarized. (J.S.R.)

16838 INFORMATION PROCESSING FOR HIGH ENERGY CORPUSCULAR PHYSICS EXPERIMENTS. Leveque, A. (Commissariat a l'Energie Atomique, France). Bull. Inform. Sci. Tech., No. 97, 47-54(Oct. 1965). (In French).

The examination unit for photographs taken in the bubble chamber in the high energy corpuscular physics laboratory is described. The main improvements that are under consideration and, in particular, the possibility of measuring the photos automatically are also described. (auth)

16839 PULSE SHAPE DISCRIMINATION IN ORGANIC SCINTILLATORS. Reid, W. B.; Hummel, R. H. Can. Nucl. Technol., 5: 36-41(Jan.-Feb. 1966).

A simple circuit for studying organic scintillators which derives a "fast" signal proportional to the peak amplitude of the anode pulse of a 56 AVP and a "linear" signal proportional to the total charge collected, or pulse height, is described. The quality of a scintillator for pulse shape discrimination can be determined by comparing the amplitude of the fast signal obtained from protons or alpha particles to the amplitude of fast pulses from electrons which give rise to the same pulse height. Plastic phosphors of several compositions and a variety of liquid scintillators were studied using the apparatus. A figure of merit is introduced which is a function of energy and which measures the ability of the system to separate particles of different masses. As a result a liquid was discovered which has both a higher hydrogen atom concentration and a better pulse shape characteristic for neutron detection than scintillators previously used for this application. (auth)

16840 THE ANALYSIS OF TRACK CHAMBER PHOTOGRAPHS USING FLYING SPOT DIGITIZERS. Powell, Brian W. CERN Cour., 6: 7-11(Jan. 1966).

A vast quantity of data pours from the experiments on particle accelerators throughout the world. For example, over 300,000 photographs per week came from the three bubble chambers operating on the CERN PS at the end of 1965. The conventional method of processing these bubble chamber photographs is for each one of them to be examined ("scanned") to see whether it records an interesting particle interaction. The interesting photographs are then passed to hand operated measuring machines to obtain precise measurements of the particle trajectories recorded on the film. Similar measurements are carried out on photographs taken in film spark chamber experiments. The Flying Spot Digitizers at CERN are one of the most fruitful attempts to speed and make more accurate the process of analysis of bubble and spark chamber photographs. There are two types of Flying Spot Digitizer at CERN — the HPD or Hough Powell Device and Luciole, a further development. (auth)

16841 ILLUMINATION OF A BUBBLE CHAMBER BY MEANS OF A RUBY LASER. Gorbunkov, V. M.; Korobkin, V. V.; Leontovich, A. M. (Lededev Physics Inst., Moscow. Moscow Physicotechnical Inst.). Dokl. Akad. Nauk SSSR, 164: 75-7(Sept. 1, 1965). (In Russian).

A concentric-resonator ruby laser (λ = 6943 Å) was used to illuminate particle tracks in a bubble chamber. The resonator consisted of dielectric-coated, concave spherical mirrors with a transmission of ~1% and 50-cm radii placed at a 100-cm distance. The ruby rod, 75 mm long and 9 mm in diameter, was pumped by 0.1-j pulses approximately 0.6 msec in duration from a 4-kj IFK-1500 flash lamp. The laser beam was uniformly distributed with an ~2° angular divergence which was magnified by an f = 50 mm lens to 20°. The experiments were carried out on a bubble chamber model consisting of a plane-parallel plate filled with air bubbles which corresponded to a 25 cm hydrogen bubble chamber. The test object was placed 50 cm from the lens and was illuminated by a concave spherical mirror (radius of curvature, 65 cm; diameter, 23 cm) placed 70 cm from the lens. The laser-illuminated bubble tracks were photographed from a distance of ~50 cm with an f = 53 mm camera on a film with a 70 line/mm resolving power. The excess light was filtered by a combination of an interference filter at λ = 694 mμ with a 30% transmission and a neutral filter with an 11% transmission. The test object was photographed 5 times at different camera angles. The results indicate that the use of a laser illumination system without a filter makes it possible to record bubbles up to 0.06 mm in diameter in hydrogen. Small bubbles in larger chambers (e.g., Wilson's chamber) can be recorded at higher generation energies. Recording at reduced energies can also be effective in cases where low-sensitivity, high-resolution film is used for better contrast and accuracy. (ATD)

16842 A THORON MONITOR. Hiller, D. M. (E. I. du Pont de Nemours and Co., Newport, Del.). Health Phys., 12: 333-40(Mar. 1966).

A commercial ionization chamber device was adapted and calibrated to serve as an accurate, rapid, and convenient thoron monitor for experimental and health physics applications. Calibration was achieved by: deriving a general expression by which the alpha-counting rates of two dust samples (prompt and delayed) can be interpreted in terms of the thoron concentration at the sampling point; and building and using a dual dust collector to obtain the necessary data. The monitor can sense pure thoron concentrations as low as 3.7×10^{-6} μc/l., and can sense pure radon at 0.42 of its thoron sensitivity. (auth)

16843 A MEDICAL X-RAY SURVEY PACKET. Ditchek, T.; Frisoli, A.; Janes, D. (Dept. of Health, Education, and Welfare, Rockville, Md.). Health Phys., 12: 341-4(Mar. 1966).

A mailable packet, the Medical Surpak, that meets some of the requirements for radiation protection surveys of diagnostic medical x-ray installations, is described. The Surpak is mailed to the user of an x-ray machine, who exposes and returns it to the laboratory for processing and analysis. The principal component of the Surpak is X-ray film and the cost including processing and analysis is between 10 and 15 dollars. (auth)

16844 A FILM METHOD FOR ESTIMATING PEAK KILOVOLTAGE, TOTAL FILTRATION AND ROENTGEN OUTPUT OF SELF-RECTIFIED DENTAL X-RAY MACHINES. Winkler, Keith G.; Levin, Sheldon G. (Dept. of Health, Education, and Welfare, Washington, D. C.). Health Phys., 12: 345-52(Mar. 1966).

A film method for determining peak kilovoltage, total filtration, and roentgen output of self-rectified dental x-ray machines is presented. This system is based upon the differential absorption of the x-ray beam by copper and aluminum absorbers as measured by reading optical densities at four points on exposed film. Ratios of relative exposures based upon these densities were used to produce equations for calculating kvp, total filtration, and an exposure factor which corrects for energy dependence of the film. Results are presented of the statistical evaluation of machine-to-machine variation in the estimation of the above mentioned parameters. This method is used by the Public Health Service's Division of Radiological Health for analyzing the Surpak, a package for surveying x-ray machines by mail. (auth)

16845 DEVELOPMENT OF A SENSITIVE LIQUID DOSIMETER FOR INTEGRAL DOSE MEASUREMENT. Gilson, Albert J.; Sprawls, Perry Jr.; Cosper, John H. (Emory Univ., Atlanta). Health Phys., 12: 377-9(Mar. 1966).

A dosimetry system utilizing liquid photographic emulsion was developed. It is most useful in the 0.5 to 6 R range. The average deviation in response was 2.5 per cent or less for paired samples. The concentrations used were within 20 per cent of being tissue equivalent. Variation in response with x-ray energy did not exceed 50 per cent from 16 kev (effective) to ^{60}Co. (auth)

16846 A PORTABLE SCALER. Thorngate, J. H.; Parks, J. E. (Oak Ridge National Lab., Tenn.). Health Phys., 12: 385-93(Mar. 1966). (ORNL-P-1186).

A versatile, battery-operated, transistorized scaler was built for measurements in the field. It has a count capacity of 10^8-1 counts from three transistorized decades and a mechanical register. The scaler has a double pulse resolving time of 7 μsec but is limited to 3×10^3 counts/sec by the register driver circuit. Positive and negative input pulses greater than 100 mv can be counted, and a test signal is available for checking the circuits. Reproducible timed runs from 10 sec to 10 min are possible using a built-in timer. A regulated high voltage supply is included which is variable from 200 to 1500 v with sufficient current to operate a high resistance photo-multiplier tube dynode voltage divider. A special input is provided for use with halogen-quenched geiger tubes. The rechargeable battery will operate the scaler for 20 hr between charges, and a charger is included. The unit is 6 in. high by 9 in. long by 5 in. deep and weighs 10 lb. (auth)

16847 A GLASS DOSIMETER WASHING TECHNIQUE FOR IMPROVED REPRODUCIBILITY. Menkes, Cirel K. (Naval Radiological Defense Lab., San Francisco). Health Phys., 12: 429-33(Mar. 1966).

Accuracy and reproducibility of measurements of fluorescent light output by silver-activated phosphate gloss dosimeters depends largely on the cleanliness of the glass surface. A glass washing and drying technique is reported that appears to reduce errors in readings. Data are presented to show that with the technique, the component error in glass readings due to variations in positioning and glass surface condition is within a standard deviation of about 3% for fluorods exposed to more than 10R, and 0.6% for 6×6 glass squares regardless of exposure. (H.G.D.)

16848 AN IMPROVED PORTABLE FAST NEUTRON DETECTOR. Seaborn, G. B. (Oak Ridge Gaseous Diffusion Plant, Tenn.). Health Phys., 12: 433-4(Mar. 1966). (K-L-6036).

A portable, battery-operated, high sensitivity instrument for detecting fast neutrons is described. The neutron monitor, a redesign of a previous model, utilizes a detector in the form of an ionization chamber filled with ^3He gas at a pressure of 6 atm. The reaction to neutrons is: $^1n_0 + {}^3He_2 \rightarrow {}^3H_1 + {}^1H_1 + 764$ kev. A comparison of the response of the original and redesigned units in the presence of a Pu–Be neutron source indicates that the new unit is more sensitive by a factor of 2/3. (H.G.D.)

16849 LARGE PLASTIC SCINTILLATORS OF PARABOLIC SHAPE. Bhatnagar, K. G.; Bhawalkar, D. V.; Bhiday, M. R. (G. S. Technological Inst., Indore, India). Indian J. Pure Appl. Phys., 3: 500-1(Dec. 1965).

Long (10 cm in the Z-direction) scintillators of rectangular and parabolic cross sections were constructed and their performance was studied with a view to using them in experiments on positron-electron and electron-electron scattering. It was found that these scintillators, when used along with a total reflecting lucite prism, improve the light collecting efficiency considerably giving a better resolution and peak-to-valley ratio. It is suggested that the parabolic shape of the scintillators reduces the possibility of photon trapping in the scintillator between parallel surfaces, thus improving their light-collecting efficiency. (auth)

16850 EFFECT OF THALLIUM CONCENTRATION ON THE PERFORMANCE OF SODIUM IODIDE–THALLIUM ACTIVATED SCINTILLATION CRYSTALS. Ramamurty, G. V. N.; Bhide, G. K. (Atomic Energy Establishment, Trombay, India). Indian J. Pure Appl. Phys., 4: 24-6 (Jan. 1966).

The scintillation performance of sodium iodide crystals doped with thallium iodide was studied for crystals in which the activator (thallium iodide) concentration varies between 0.03 and 0.65 per cent by weight. It is found that in addition to the activator concentration, the thickness of the crystal also influences the pulse height of scintillation. Contrary to earlier reports a decline in the photopeak pulse heights is observed at activator concentrations higher than 0.25 per cent. (auth)

16851 AN EXPERIMENTAL PROPOSAL FOR A NEW METHOD FOR THE MEASUREMENT OF FAST NEUTRON FLUXES. Bucci, Pompeo (CAMEN, Pisa, Italy). Ing. Nucl., 6: 245-9(Sept.-Oct. 1965). (In Italian).

A new method for the measurement of fast neutron fluxes that is based on the phenomenon of the variation of the physical properties of a solid as a result of fast particle bombardment is proposed. After the bombardment of a foil of SiO_2 of fast neutrons, there is a change in the lattice structure and then a variation in the axial ratio c/a of the lattice. After similar treatment, quartz has a decrease of the self-oscillation frequency. This decrease is proportional to the primary oscillation frequency of the irradiation. This variation depends partially on the characteristics of the foil used and partially on the intensity and duration of the irradiation. If the latter is maintained at a constant, it is possible to determine the incident neutron flux. (tr-auth)

16852 DESIGN AND OPERATION OF AN EXTRAPOLATION CHAMBER WITH REMOVABLE ELECTRODES. Loevinger, R. (Stanford Univ., Calif.); Trott, N. G. Int. J. Appl. Radiat. Isotop., 17: 103-11(Feb. 1966).

An extrapolation chamber is described that is suitable for measurements with α, β, or soft x-ray (Grenz ray) sources. Both the thin high-voltage electrode and the thick collecting electrode are readily replaced, allowing use of any suitable material, and any size or shape of plane collecting area, between 1 and 30 mm in diameter. The design allows gaps as small as 0.05 mm over a 5-cm diameter. The peak-to-peak noise level of the assembled unit is about 2×10^{-16} amp, and the leakage current about 5×10^{-17} amp. Associated instrumentation, test procedures and measurement procedures are described. (auth)

16853 A SMALL GAMMA CAMERA—IMPROVEMENTS IN THE RESOLUTION, A SETTING-UP PROCEDURE, AND A DIGITAL PRINTOUT. Wilks, R. J.; Mallard, J. R. (St. Thomas's Hospital Medical School, London). Int. J. Appl. Radiat. Isotop., 17: 113-19(Feb. 1966).

Simple modifications to the image transfer system of a gamma camera with a 5-in. dia crystal are described, together with measurements that show the positioning signals applied to the display become more linearly related to the co-ordinates of the scintillations. Measurements of the inherent resolution of the gamma camera itself (excluding the collimator) showed that logarithmic circuits in the image transfer system provide a resolution much less dependent upon x-ray energy than linear circuits and enable a gain in either the overall sensitivity (×3) or the overall resolution to be achieved. The inherent resolution of the camera is thought to be close to its limit (about 3 mm) for the Anger-type image transfer system. Setting-up procedures are described. A system using a multichannel analyser is presented, which enables a digital print-out of counts from point-to-point in the displayed scan picture to be made. (auth)

16854 METHODS FOR AUTOMATIC PHYSICAL MEASUREMENTS WITH MAGNETIC β SPECTROMETERS. Andreeva, Yu. A.; Beskrovnyi, I. M.; Latyshev, G. D. Izv. Akad. Nauk Kaz. SSR, Ser. Fiz.-Mat. Nauk, No. 2 35-40(May-Aug. 1965). (In Russian).

The automation of measurements on a magnetic beta spectrometer is described by a block diagram which includes the following elements: (1) the spectrometer itself, (2) a control unit which sets the energy at a given value (a current or magnetic field stabilizer), (3) a timer which operates the counter for a given interval of time, (4) a counter such as a multichannel analyzer, (5) a stop and start electronic switch, and (6) a programming unit which coordinates and controls the above units. In making the energy setting a current stabilizer can give excellent results in iron-free spectrometers. A magnetic field stabilizer can be used in spectrometers containing iron and in iron-free spectrometers. The characteristics of various components are described with appropriate literature references for details. (TTT)

16855 ADVANCES IN RADIOISOTOPE INSTRUMENTATION. Perkins, W. H.; Lohmann, Wolfgang (Univ. of Arkansas Medical Center, Little Rock). J. Arkansas Med. Soc., 61: 407-10(Apr. 1965).

Various aspects of new technics and instruments used in medical diagnostic tests employing radioisotopes are surveyed. Scintillation-camera operation is discussed in terms of three main groups of instruments: the γ camera, the positron camera, and the autofluoroscope. Various detector systems are discussed. In a new version of the autofluoroscope a new approach to data transfer is used. With the exception of thyroid visualization the autofluoroscope can be used for all clinical studies that ordinarily require a scanner. The solid state dosimeters and their instrumentation, used to monitor radiation doses in the body, are also considered, and other technological advances in radioisotope work, including data processing and analysis, are discussed. (TCO)

16856 DESCRIPTION OF THE CALORIMETRIC MEASUREMENT OF THE INTENSITY OF LOW ENERGY X RADIATION. Coekelbergs, Roger; Crucq, Andre; Decot, Jean; Degols, Luc; Frennet, Alfred; Timmerman, Lucien (Ecole Royale Militaire, Brussels). J. Chim. Phys., 62: 1277-82(Nov.-Dec. 1965). (In French).

An experimental device making it possible to measure the total energy emitted by a 60-kv x-ray generator is described. The incident radiation is absorbed quasi-totally (>99%) in a thin gold plate well insulated thermally. Heating is measured with an iron-constantan thermocouple. This device also makes it possible to measure the dose absorbed in a sample interposed between the gold plate and the x-ray generator. The absorbed energy is given by the difference between the total incident energy and the energy transmitted. (tr-auth)

16857 SOME PROGRESS IN THE ORTHOGONAL EXPANSION METHOD FOR DEDUCING THERMAL NEUTRON SPECTRA FROM ACTIVATION RATES. Kanda, Keiji (Tokyo Inst. of Tech.). J. Nucl. Sci. Technol. (Tokyo), 2: 533-5(Dec. 1965).

A typical Wigner-Wilkins spectrum which was chosen as the weighting function was numerically analyzed. The calculated spectrum well reproduced the original one in that all the higher mode amplitudes resulted in values smaller than 10^{-7}. From the analysis of spectra other than the weighting function it was found that most spectra, even undermoderated, can be well reproduced provided the spectrum is not too different from the weighting function. Experiments were also performed which demonstrated the practicality of the method used. Four detectors were irradiated, and spectra were measured in two kinds of hexagonal lattices. The continuous neutron spectral curves are given. It is concluded that the practicality of the method is shown, and that this method is valid even in an undermoderated system. (J.F.P.)

16858 ON THE POSSIBILITY OF ABSOLUTE MEASUREMENTS OF RADIOISOTOPE ACTIVITY USING SCINTILLATION GAMMA SPECTROMETRY. Husak, Vaclav; Kleinbauer, Karel; Erban, Jiri (Radioisotope Division of Medical Inst., Olomouci, Czechoslovakia). Jad. Energ., 12: 25-8(Jan. 1966). (In Czech).

Activity measurements that are made with scintillation crystals have significant errors, which may be ascribed to slight differences in the crystals, e.g., different thicknesses in the aluminum covers or in the reflecting layers. More precise measurements were made by a method in which the analyzer channel was placed so as to include the whole photopeak. The low-energy part of the photopeak is thus included, though a small part of the Compton spectrum is neglected. Measurements can then be made within 1 or 2 percent. Measurements made on ^{137}Cs, ^{58}Co, ^{131}I, ^{198}Au, ^{203}Hg, ^{131}I, and ^{51}Cr with plane or well-type scintillation crystals or beta-gamma coincidence method are compared with standard values. The dependence of the performance of plane and well-type scintillation crystals (NaI(Tl)) on the energy of the measured activity is shown mathematically and graphically. (TTT)

16859 ELECTRICAL DETECTION SYSTEM FOR BROAD RANGE MAGNETIC ANALYZER. Koike, Masahiro; Matsuda, Kazuhisa (Tokyo Univ.). Jap. J. Appl. Phys., 5: 153-9(Feb. 1966).

A multicounter system for a broad range magnetic analyzer was developed. Along the paths of analyzed particles, forty proportional counters followed by a scintillation counter were arranged in the focusing plane of the analyzer. The addresses of the proportional counters correspond to the momenta of the analyzed particles. The scintillation counter made a counter telescope with the proportional counters. Backgrounds were much reduced by means of this telescope technique. Forty transistor amplifiers were used for amplification of signals from the proportional counters. After pulse shaping by the forty discriminators, the pulses were led into the corresponding scalers. The forty discriminators were gated by the signals from the scintillation counter. (auth)

16860 ISOTROPIC SPARK CHAMBER. Vorob'ev, G. A.; Rudenko, N. S. (Kirov Polytechnic Inst., Tomsk, USSR). JETP Lett. (USSR)(Engl. Transl.), 3: 37-9(Jan. 15, 1966).

Translated from Zh. Eksp. Teor. Fiz., Pis'ma Redakt., 3: 61-3(Jan. 15, 1966).

A spark chamber with three mutually perpendicular pairs of electrode plates is proposed. (D.C.W.)

16861 A SCINTILLATOR-FILM COMBINATION FOR FAST-NEUTRON DOSIMETRY. Brunnquell, H.; Schneider, H. (Univ., Giessen, Ger.). Kerntechnik, 8: 13-15(Jan. 1966). (In German).

A simple method utilizing a combination of plastic scintillators and films for the dosimetry for fast neutrons is reported. The density curves obtained with irradiation of neutrons alone and of neutrons and γ radiation in combination are given. Density curves as a function of dose for both γ radiation and fast neutrons were obtained. The results show

that the scintillator-film combination described is suitable both for the detection of neutrons and for γ radiation. The plastic scintillator NE102 was used as a luminescent material and the light emission was recorded on highly sensitive polaroid films of the type 410. (J.S.R.)

16862 USE OF LIQUID SCINTILLATORS FOR THE MEASUREMENT OF ISOTOPES EMITTING SOFT β RADIATION. PART III. DETERMINATION OF ^{14}C BY USING AN OPTICAL FILTER. Levay, Bela; Csanyi, Piroska (Eotvos Lorand Univ., Budapest). Magyar Kem. Foly., 71: 356-60(Aug. 1965). (In Hungarian).

The EKCO N 664 A type single-channel liquid scintillation counter was modified for the measurement of ^{14}C, required for the determination of the self-diffusion coefficient of carbon compounds. It was attempted to reduce the phosphorescence in the system by the simultaneous use of an optical filter and a discriminator. The original cells of the apparatus were replaced by plastic-covered glass medicinal bottles provided with an external Al reflector; the optical filter was placed on the lower extremity of the Al reflector. The samples were standardized with ^{14}C-labeled xylene. In the case of a 1000× amplification at 1300 v, the ^{14}C could be determined at room temperature with an efficiency of 78%. Absorption of the phosphorescence of the cell by means of a Chance OX 7 type optical filter with a detection sensitivity of 0.5×10^{-6} μC/ml was achieved by using samples of 16 ml and a duration of 300 seconds, keeping the samples in the dark for one-half hour before the measurement. (TTT)

16863 USE OF LIQUID SCINTILLATORS FOR THE MEASUREMENT OF ISOTOPES EMITTING SOFT β RADIATION. PART IV. INVESTIGATION OF THE INTERACTION BETWEEN THE PHOSPHORESCENCE OF GLASS CONTAINERS AND THE SCINTILLATOR SOLUTIONS. Csanyi, Piroska; Levay, Bela (Eotvos Lorand Univ., Budapest). Magyar Kem. Foly., 71: 360-4(Aug. 1965). (In Hungarian).

The phosphorescence values of the empty and scintillator-filled glass cells of scintillation counters exhibit a difference, interfering with the accuracy of the measurements. This problem was investigated by determining the phosphorescence of the glass, the solvent, and the scintillator individually and after interaction with each other, measuring the changes in the radiation emitted by the glass after excitation with sunlight or mercury-arc light, as a result of the action of various solutions. It was found that a portion of the phosphorescence is absorbed by the liquid scintillator which reemits it at its own characteristic wavelength range. If the absorption band of the solvent or the scintillator lies outside the sensitivity range of the photocathode, while the emission band of the scintillator is within the sensitivity range, the originally not recorded emission of the glass will be shifted into the sensitive region, resulting in an increase of the recorded phosphorescence. This accounts for the high background radiation. Under reversed conditions, the observed phosphorescence of the filled cell will be lower than that of the empty one. Therefore, care must be taken when choosing the optical filter to reduce the phosphorescence to the lowest possible level. Optical filters may be used only to reduce the phosphorescence at the long-wavelength side. (TTT)

16864 USE OF γ SPECTROMETRY FOR THE DETERMINATION OF PLUTONIUM IN THE LIVING ORGANISM. Erokhin, R. A.; Koshurnikova, N. A.; Ternovskii, I. A. Med. Radiol., 10: 37-41(Oct. 1965). (In Russian).

Gamma spectrometry was used for internal detection of ^{239}Pu and ^{241}Am in rats. The technique was found to be useful for qualitative determinations in living tissue and for metabolism studies. The necessity of having phantoms and adhering to similar geometric conditions during measurement is stressed. (H.G.D.)

16865 RADIOMETRIC PROPERTIES OF A LARGE LIQUID SCINTILLATION COUNTER. Belle, Yu. S.; Kostikov, Yu. L; Shamov, V. P.; Shapiro, E. L. Med. Radiol., 10: 67-73(Oct. 1965). (In Russian).

Radiometric properties of a large liquid scintillation counter are described. Applications in radiobiology and radiation protection are presented. (auth)

16866 FHT 800 A: A MEASUREMENT DEVICE FOR MOESSBAUER EFFECT EXPERIMENTS. Faatz, H. Mitteilungsbl. Strahlungsmessgeraete, 6: No. 14, 10-12 (Oct. 1965). (In German).

The FHT 800 A consists of three individual devices: the electromechanical converter, the drive control, and the current supply. Each of these is described. The operation of the device in the modulator range and in multichannel counting operations are discussed. A block diagram is given. (J.S.R.)

16867 BACKSCATTERING OF ELECTRONS FROM PHOSPHORS AND A MATRIX METHOD FOR CORRECTING BACKSCATTERING AND RESOLUTION IN SCINTILLATION BETA SPECTROMETERS. Sen, P.; Patro, A. P. (Saha Inst. of Nuclear Physics, Calcutta). Nucl. Instrum. Methods, 40: 1-8(Feb. 1966).

The response functions for monoenergetic electrons incident on anthracene, plastic, and cesium iodide phosphors were studied. A matrix method for correcting beta spectra for resolution and backscattering was proposed and applied to electron spectra. The difficulties of applying backscattering correction to positron spectra were discussed and a method of eliminating backscattering was studied. The technique has been used to determine the end energy of the weak 1.8-Mev positron group from ^{22}Na. (auth)

16868 HIGH-ORDER DOUBLE FOCUSING IN A MAGNETIC FIELD HAVING THE FORM $1/(r \sin \vartheta)$. Hofmann, A. (Swiss Federal Inst. of Tech., Zurich). Nucl. Instrum. Methods, 40: 13-25(Feb. 1966).

The spectrometer field $H_0a/(r \sin \vartheta)$ discussed can easily be realized by means of conical pole-pieces. Charged particles in this field describe orbits having the form of trochoids. Lafoucrière had already shown that ideal focusing with respect to the azimuthal initial angle ξ_0 is obtained for orbits lying in the plane of symmetry ($\vartheta = \frac{1}{2}\pi$). It is shown that for skew orbits, double focusing is obtained after two or more trochoidal revolutions, provided that a so-called "stable" value is chosen for the parameter $K = p/(\mu_0 e H_0 a)$. Thus for all values of ξ_0 the first and second order aberrations with respect to the angle of elevation ω_0 and one dimension of the source α_0 vanish. For three values of K chosen from a practical standpoint, a numerical calculation has been carried out for the remaining aberrations. Due to its good focusing properties and high dispersive power, this field is very well suited to the construction of β-spectrometer having as high resolution combined with a large value of the transmission and luminosity. In the case of K = 0.309894 and two trochoidal revolutions, the theoretical predictions were verified by experiment. (auth)

16869 MULTIPLE SPECTROMETER CONTROL BY COMPUTER. Beaucage, D. R.; Kelley, M. A.; Ophir, D.; Rankowitz, S.; Spinrad, R. J.; Van Norton, R. (Brookhaven National Lab., Upton, N. Y.). Nucl. Instrum. Methods, 40: 26-44(Feb. 1966). (BNL-9275).

A computer system whose function is to simultaneously operate, control and monitor nine neutron and x-ray spectrometers is described. The spectrometer equipment and the local control station characteristics are presented. The programmed control of the apparatus details asynchronous and synchronous control tasks. A time sharing supervisory system allows semi-automatic and fully automatic operation of the equipment and offers a library of mutually-used computer programs. Communication with the system is through a console typewriter and a complete record of experiment operation is printed. (auth)

16870 A NUCLEAR REACTION POLARIMETER USING POSITION-SENSITIVE PARTICLE DETECTORS. Clegg, T. B.; Barnard, A. C. L.; Swint, J. B. (Rice Univ., Houston, Tex.). Nucl. Instrum. Methods, 40: 45-53(Feb. 1966). (TID-22146).

Position-sensitive solid-state detectors were used in

double-scattering experiments with solid targets. Particles with second scattering angles θ_{lab} from 36 to 144° were observed simultaneously by two of these detectors. Left-right asymmetries were obtained for each detector from consecutive measurements with the detector on opposite sides of the incident beam. A digital computer was used to accumulate data as two-parameter spectra, the two parameters being the positions and energies of the detected particles. Events were labelled to indicate the detector in which they occurred. The polarimeter was used initially to scatter protons twice from ^{12}C. Three sets of measurements were made, so the polarizations were determined (except for a sign) independently of other measurements. A sample angular distribution is shown for the measured polarization of protons elastically scattered from ^{12}C at 6.14 Mev. The data were corrected for the false asymmetry due to the finite geometry. A simple but general calculation is described to make this correction for any polarimeter using two solid targets. (auth)

16871 OPTIMUM ENERGY RESOLUTION OF SEMICONDUCTOR RADIATION DETECTORS WITH PREAMPLIFIERS USING TUBES, FIELD-EFFECT TRANSISTORS, AND BIPOLAR TRANSISTORS. Bilger, H. R. (Oklahoma State Univ., Stillwater). Nucl. Instrum. Methods, 40: 54-60(Feb. 1966).

A uniform treatment of tubes, field-effect transistors (FET's) and bipolar transistors (transistors) in first stages in nuclear-detector preamplifiers is given by introducing equivalent circuits with suitable noise sources. Optimizing the system detector-preamplifier with respect to energy-resolution, it is feasible to obtain a rms-fluctuation of 90 electron-hole pairs with electrometer-type tubes or FET's, whereas with transistors it is feasible to achieve 900 pairs. These values correspond to $\Delta E_{fwhm,Ge} = 0.6$ kev and $\Delta E_{fwhm,Ge} = 6$ kev. (auth)

16872 A MOESSBAUER SPECTROMETER. Bornaz, M.; Filoti, G.; Gelberg, A.; Grabari, V.; Nistor, C. (Inst. for Atomic Physics, Bucharest). Nucl. Instrum. Methods, 40: 61-6(Feb. 1966).

A Mössbauer spectrometer is described with a velocity range of 0.03 to 20 mm/s. The source is driven by an electromagnetic vibrator. The velocity modulated pulses from the detector are displayed on a 400-channel analyzer. Simultaneously with the resonant spectrum, a non-resonant spectrum is measured in order to record the duration of each speed interval. Calibration as well as checks of linearity and stability were performed by measuring the absorption spectra of Fe_2O_3 and Armco-iron. The minimum width of an absorption line was 0.27 mm/s. (auth)

16873 THE DIGITAL RECORDING SYSTEM OF THE AIR SHOWER EXPERIMENT AT KIEL. Boehm, E.; Roose, U. J.; Staubert, R.; Truemper, J. (Univ., Kiel). Nucl. Instrum. Methods, 40: 67-72(Feb. 1966). (In German).

The digital recording system of the extensive air shower experiment at Kiel is described. The scintillator pulse heights occurring simultaneously are digitized using logarithmic analog-to-digital converters and stored in 5 Mc-scalers. After a shower coincidence the amplitude informations are printed and punched by a teleprinter along with indexing number, local time, pressure and fast timing information. Dynode gates triggered by the coincidence are used to avoid disturbance due to photomultiplier noise. (auth)

16874 ON OPTICAL PROPERTIES OF THE NEUTRON CRYSTAL SPECTROMETERS. Popovici, M.; Gelberg, D. (Inst. for Atomic Physics, Bucharest). Nucl. Instrum. Methods, 40: 77-83(Feb. 1966).

The resolution and the luminosity of the crystal spectrometer are investigated taking into account the secondary extinction; the dependence of the luminosity on the mosaic spread of the crystal is calculated. The luminosity of the crystal spectrometer for neutron powder diffraction is established and the optical study of triple-axis crystal spectrometers with elastic and isotropic scatterers is also carried out. (auth)

16875 UNSCRAMBLING OF PROTON RECOIL SPECTRA. Brunfelter, B.; Kockum, J.; Zetterstroem, H.-O. (Research Inst. of National Defence, Stockholm). Nucl. Instrum. Methods, 40: 84-8(Feb. 1966).

A matrix inversion program for unfolding proton recoil spectra was written for the IBM-7090 computer. The program takes into account distortions due to multiple scattering and end effects. It was applied to a stilbene scintillation spectrometer using experimentally determined response functions but should equally well be applicable to other types of proton recoil spectrometers. The results of the application of the program to measurements of the neutron spectrum from a Po–Be-source and of the spontaneous neutron fission spectrum from ^{240}Pu are given. (auth)

16876 A LIQUID HELIUM, TIME-OF-FLIGHT COINCIDENCE NEUTRON POLARIMETER. Miller, T. G. (Army Missile Command, Restone Arsenal, Ala.). Nucl. Instrum. Methods, 40: 93-9(Feb. 1966).

A liquid helium, time-of-flight coincidence neutron polarimeter was developed to measure neutron polarization. The polarizer-analyzer is liquid helium in a specially constructed cryostat. Energy selection is accomplished by time-of-flight techniques and the background is reduced to a negligible amount by requiring fast coincidence between the polarizer-analyzer and the side counters. The counts from both side counters are recorded simultaneously in a 400-channel analyzer by splitting the memory of the analyzer. Measurement of the neutron polarization for the $D(d,n)^3He$ reaction was made using the polarimeter for deuteron bombarding energies between 1.5 and 1.9 Mev at a laboratory angle of 35°. The polarization varies from −16.5% at 1.5 Mev to −21.6% at 1.9 Mev. (auth)

16877 A COMPUTER PROGRAM FOR THE ANALYSIS OF TIME-OF-FLIGHT SPECTRA. Tepel, J. W. (Univ., Hamburg). Nucl. Instrum. Methods, 40: 100-105(Feb. 1966).

A computer program was developed for the automatic analysis of time-of-flight spectra by least square methods. The program will correct multichannel data for background and fit single or overlapping peaks with distributions of an arbitrary predetermined shape. No information on the position or number of lines is necessary. (auth)

16878 ARRANGEMENT FOR POSITION AND ENERGY DETERMINATION WITH SEMICONDUCTOR DETECTORS. Kuhlmann, W. R.; Lauterjung, K. H.; Schimmer, B. (Univ., Cologne). Nucl. Instrum. Methods, 40: 109-12(Feb. 1966). (In German).

Charged particles produce in position-sensitive solid state detectors information proportional to the energy and energy-dependent information proportional to the position. The quotient of the two types of information delivers energy-independent position data. A detector bank of 40 mm length, made of 4 such detectors, was connected to a pulse division circuit, delivering energy information and energy-independent position information. (auth)

16879 A PULSE-DIVISION CIRCUIT. Kuhlmann, W. R.; Schimmer, B. (Univ., Cologne). Nucl. Instrum. Methods, 40: 113-17(Feb. 1966). (In German).

For experiments with detectors for localization of particles a pulse division circuit was evaluated that derived an output pulse from two coincident input signals U_1, U_2, the amplitude of which was proportional to the quotient $Q = U_1/U_2$ of the two input signals. The circuit works in a range $1 \leqq Q < 5$. For $Q = 1$ the input signals may vary in a range $8 < U_{1,2} < 100$ v, for $Q = 3$ in $30 < U_1 < 100$ v and $10 < U_2 < 33$ v. The greatest repetition rate with periodical pulses is about 5 kc for $Q = 3$ and $U_2 = 20$ v, to keep the deviations from the value at low frequencies below 10%. The output signals are so shaped, that they may be analyzed directly by the usual multi-channel-pulse-height-analyzers ($t_r < 0.5$ μsec; $t_f < 3$ μsec). The input signals have to accomplish only one condition: their rise-time t_r must be less than 0.5 μsec. (auth)

16880 POSITION-SENSITIVE COUNTER. Kuhlmann, W. R.; Lauterjung, K. H.; Schimmer, B.; Sistemich, K.

(Univ., Cologne). Nucl. Instrum. Methods, 40: 118-20 (Feb. 1966). (In German).

Charged particles produce in proportional counters with the cathode or the anode of material with suitable resistance an energy-independent information of the position which is a linear function of the location. The resolution of the counter to be described (length 30 cm) amounts to 1.2 mm. (auth)

16881 A PATTERN GENERATOR. Kontos, J. (Democritos Nuclear Research Centre, Athens). Nucl. Instrum. Methods, 40: 121-4(Feb. 1966).

A pattern generating system is described capable of generating trains of pulses that can be associated with patterns consisting of line segments. The output of this system is useful in testing pattern analysis systems in connection with photographs from high energy physics experiments. A transistorized version of the generator was built and tested. (auth)

16882 A SMALL NEUTRON DIFFRACTOMETER. Tunkelo, E.; Kajamaa, J. (Inst. of Tech., Otaniemi, Finland). Nucl. Instrum. Methods, 40: 125-30(Feb. 1966).

The design and performance of a small-neutron diffractometer is presented. The device is located at the 100 kw Triga Mark II reactor. This diffractometer has the monochromator unit inside a radial beam port. As a monochromator, a single crystal of lead is used. The produced neutron beam has a wavelength of 1.10 Å. The properties of this beam and the possibilities of utilization for physical research as well as the required associated instrumentation are described. (auth)

16883 SCATTERING CHAMBER FOR USE WITH SOLID-STATE DETECTORS. Erramuspe, H. J.; Seifert, A. M. (Columbia Univ., New York). Nucl. Instrum. Methods, 40: 155-6(Feb. 1966).

A scattering chamber is described, which was specifically designed to work with solid state detectors mounted internally in a tandem assembly or in multiple arrays. The size of the chamber, which is of simple design, permits working with a large range of solid angles and the rotation assembly covers practically the whole angular range. A vertical cross-sectional view of the chamber, target assembly, exit and entrance pipes and top view, and a ball-bearing-holder diagram are shown. The maximum absolute angular error was estimated to be 0.2, the relative error being 0.1 for a typical polyethylene experiment using the Pupin Columbia University Cyclotron with a proton beam under 15 Mev. (J.F.P.)

16884 COUNTING CHARACTERISTICS OF G-M COUNTERS AT HIGHER INTENSITIES. Lindeman, H. (Technion-Israel Inst. of Tech., Haifa, Israel). Nucl. Instrum. Methods, 40: 159-60(Feb. 1966).

Data are presented showing that the problems involved in the behavior of G-M counters are probably more complicated than might be expected on the basis of Stever's treatment and the measurements of Baldinger and Huber, which are used in Kramer's calculation (Nucl. Instrum. Methods, 32, 37(1965)). An exposure of an oscilloscopic pattern of triggered first pulse and subsequent pulses, showing the form of the peak envelope for a Nuclear Chicago counter, type D 34 is given. The first part of the envelope is nonlinear. The facts presented indicate that the assumptions about the dead time and the recovery time, based on the results of Stever, Baldinger, and Huber, might not describe exactly what is happening in the counter at higher input rates—at least not for all types of counters. (J.F.P.)

16885 CHARGE COLLECTION IN CERTAIN TYPES OF SEMICONDUCTOR RADIATION DETECTORS. Papadakis, A. C. (Post Office Research Station, London). Nucl. Instrum. Methods, 40: 177-8(Feb. 1966).

A discussion of charge collection in semiconductor detectors is given with restriction to the common case where ionization occurs very close to one electrode so that the contribution of one type of carrier is negligible over most of the collection time. Only transit of the remaining carriers needs then be considered, and it is further assumed that recombination and trapping during their transit time is negligible since field perturbations are then most significant. Two stages of charge collection are considered: from a time after ionization until the time when the first of the excess mobile carriers reach the opposite electrode, and from this time until the time when collection of the excess carriers is complete. (J.F.P.)

16886 ISOTROPIC MONOGAP CHAMBER PULSED WITH DAMPED OSCILLATION. Cavalleri, G.; Gatti, E.; Habel, R.; Larocci, E.; Letardi, T.; Visentin, R. (Lab. Nazionali, Frascati, Italy). Nuovo Cimento (10), 41A: 289-91(Jan. 21, 1966).

A damped oscillating pulse with a frequency of 28 MHz, a decay time constant of 0.15 μs, and amplitude of the first oscillation of 12 kv/cm was used to produce the initial streamers for the isotropic monogap chamber. The chamber coupled to the Marx generator by the autotransformer and also particle-track photographs are shown. The preliminary work shows that, using damped oscillation, it is possible to obtain a brightness and a spatial resolution of tracks comparable to or eventually better than those obtained at relatively higher fields employing rectangular pulses. (J.F.P.)

16887 APPLICATION OF HIGH-RESOLUTION SEMICONDUCTOR DETECTORS IN X-RAY EMISSION SPECTROGRAPHY. Bowman, Harry R.; Hyde, Earl K.; Thompson, Stanley G.; Jared, Richard C. (Univ. of California, Berkeley). Science, 151: 562-8(Feb. 4, 1966). (UCRL-16485).

Solid-state devices developed primarily for nuclear gamma spectroscopy have many potential uses in x-ray analysis. Experiments are described which demonstrate their performance. (auth)

16888 LITHIUM-DRIFTED GERMANIUM DETECTORS: APPLICATIONS TO NEUTRON-ACTIVATION ANALYSIS. Schroeder, Gerald L.; Kraner, Hobart W.; Evans, Robley D. (Massachusetts Inst. of Tech., Cambridge). Science, 151: 815-17(Feb. 18, 1966).

Lithium-drifted germanium detectors for high-resolution gamma-ray spectroscopy reduce the need for wet chemistry in neutron-activation analysis. Problems in fields as diverse as geochemistry and the history of 15th-century printing are shown to be susceptible to this analytic technique. (auth)

16889 SEMICONDUCTOR RADIATION DETECTORS. PART III-a. Poenaru, D.; Vilcov, N. (Inst. of Atomic Physics, Bucharest). Stud. Cercet. Fiz., 17: 1017-57 (1965). (In Rumanian).

There are considerable differences in the design of semiconductor detectors, depending on their intended use in nuclear physics experiments. On the basis of the thickness of the space charge region, these detectors are classified as thin detectors with P–N junctions based on surface diffusion or a barrier layer, and thick ones with PIN type junction with a homogeneous semiconductor. The criteria used for selecting specific types are described. Neutron detectors are based on indirect measurements: the neutrons, not having a charge, do not cause ionization but may be detected on the basis of the particles emitted by neutron-generated reactions, such as $^{6}Li(n,\alpha)^{3}H$; $^{3}He(n,p)^{3}H$; $^{10}B(n,\alpha)^{7}Li$. Thus neutron detectors are based on a charged-particle barrier-layer detector with a hydrogen-rich material or a converter containing ^{10}B, ^{6}Li, or ^{3}He. Multiple detector systems are used in experiments with polarized charged particles. The large sensitive volume required for measuring the energy of penetrating particles may be prepared by making use of interstitial impurities of Li in NIP type detectors; the instability of the system may be compensated for by an (n,γ) reaction of ^{30}Si. (140 references). (TTT)

16890 ON THE PREPARATION OF LITHIUM-DRIFTED Ge COUNTER DIODES. Baldinger, E.; Matile, G. (Univ., Basel). Z. Angew. Math. Phys., 16: 822-6(1965). (In German).

The lithium-compensated Ge counters are used for the

detection of γ rays because of their excellent resolution power. The fabrication of these counters and their characteristics are described. (tr-auth)

16891 ON THE POSSIBILITY OF INTRODUCTION OF THE MAXIMUM QUANTITY OF BORON INTO NUCLEAR EMULSIONS. Benisz, J.; Hanus, H. (Pedagogical Academic School, Katowice, Poland). Zesz. Nauk. Wyzszej Szkoly Pedagog. Katowice, Sekc. Fiz., No. 3, 55-6(1962). (In Polish).

Nuclear plates for detection of neutrons (type K-2, 100μ) were impregnated with 0.25, 0.5, 0.75, 1, 1.5, 2, and 2.5% $Na_2B_4O_7 \cdot 10H_2O$. They were then irradiated with thermal neutrons from a Po–Be source (0.4 C) and developed. Tracks of particles were detected by microscopy, and the background was estimated from an untreated plate subjected to the same amount of radiation as the borax-treated plates. The number of tracks detected in a standard number of observations was found to be linearly related to the concentration of borax. Since a saturated $Na_2B_4O_7 \cdot 10H_2O$ solution is 2.7%, this represents the max efficiency obtainable using borax as a neutron detector to activate nuclear plate emulsions. (BBB)

16892 CUTIE PIE, MODEL 4 /Q-2090/ (Engineering Materials). (Oak Ridge National Lab., Tenn.). (CAPE-1276).

2 drawings.

An ionization chamber used with the Cutie Pie Survey Meter is presented. Two designs for the chamber are given. In assembly A, the chamber is fabricated of clear molded, high impact type Polystyrene 3 in. OD, $2^{27}/_{32}$ in. ID, and $5^{3}/_{4}$ in. long. Assembly B has the same dimensions but is fabricated of linen-base Bakelite. (For details, see TID-4100). (J.R.D.)

16893 RADIATION MEASUREMENT UTILIZING COMMUNICATION THEORY. LaPatra, J. W. (Univ. of California, Davis); Wesley, E. J. 19p. (CONF-651001-21). ORAU. Gmelin, AED-CONF-65-293-6.

From IEEE Nuclear Science Symposium, San Francisco.

The application of various aspects of communication theory to the measurement of radiation is considered. (D.C.W.)

16894 NEUTRON DETECTION BY CORRUGATED-PLATE SPARK COUNTERS. Eichholz, G. G.; Templeton, W. M. (Georgia Inst. of Tech., Atlanta). 9p. (CONF-651001-22). ORAU. Gmelin, AED-CONF-65-293-15.

From IEEE Nuclear Science Symposium, San Francisco.

The use of spark counters with grooved-plate electrodes (with neutron-conversion material in the grooves) for neutron detection was investigated. Several types and arrangements of neutron-conversion material were considered. A cylindrical counter consisting of a heavy threaded Al rod mounted in a matching Al tube was developed, in which a set of boron-coated plastic washers serve as neutron converters. (D.C.W.)

16895 BF_3 COUNTERS FOR USE IN FIELD INSTRUMENTATION. Peters, C. W.; Snyder, A. L.; Gallia, A. S. Jr. (Naval Research Lab., San Francisco). 25p. (CONF-651001-23). ORAU. Gmelin, AED-CONF-65-293-11.

From IEEE Nuclear Science Symposium, San Francisco.

A number of different neutron detectors employing arrays of BF_3 counters in hydrogenous moderators were constructed and were tested. Some of the problems of obtaining BF_3 counters with matching mechanical and electrical characteristics from commercial manufacturers are briefly reviewed. Several unexpected problems which arise when BF_3 counters are not used in a controlled environment are discussed. A transient sensitivity to gamma rays in some counter designs immediately after the application of high voltage is noted and explained. A technique for reducing spurious counts due to humidity effects by coating the ceramic high-voltage insulators with Teflon is described. Spurious counts due to inverting and vibrating the BF_3 counters are examined for different sizes of counters. (auth)

16896 NEW POSSIBILITIES OFFERED BY BORON AND URANIUM DETECTORS. Allemand, R.; Delcroix, V. (CEN, Grenoble, France). Vienna, International Atomic Energy Agency, 1965, Preprint No. CN-22/20, 19p. (In French). (CONF-651105-3). ORAU.

From Conference on Nuclear Electronics, Bombay.

Some methods of measuring neutron fluxes in reactors using fission chambers and proportional counters are discussed. Criteria for selecting the type of detector and the type of electronic equipment to be used are considered. (D.C.W.)

16897 IONIZATION CHAMBERS FOR REACTOR CONTROL. Satyanarayana, L.; Rao, E. V. R. (Atomic Energy Establishment, Trombay, India). Vienna, International Atomic Energy Agency, 1965, Preprint No. CN-22/39, 11p. (CONF-651105-29). ORAU.

From Conference on Nuclear Electronics, Bombay.

The design and construction of some ionization chambers for use in reactor control are briefly discussed, and the testing of the chambers is summarized. (D.C.W.)

16898 A MULTI-CHANNEL ANALYSIS SYSTEM FOR LOW LEVELS OF FISSION PRODUCTS IN REACTOR COOLANTS. Ragupathy, S.; Vohra, K. G. (Atomic Energy Establishment, Trombay, India). Vienna, International Atomic Energy Agency, 1965, Preprint No. CN-22/42, 11p. (CONF-651105-28). ORAU.

From Conference on Nuclear Electronics, Bombay.

A multichannel analysis system that consists of an NaI(Tl) crystal and a 256-channel pulse-height analyzer incorporating ferrite-core storage is described. (D.C.W.)

16899 DESIGN AND PERFORMANCE OF NEUTRON THERMOPILES. Cervellati, R.; Gislon, R.; Rispoli, B. (Centro Studi Nucleari della Casaccia, Rome). Vienna, International Atomic Energy Agency, 1965, Preprint No. CN-22/46, 17p. (CONF-651105-11). ORAU.

From Conference on Nuclear Electronics, Bombay.

An analysis of the response of a neutron thermopile is outlined, and the results of some tests of thermocouples are presented and are compared with theoretical predictions. (D.C.W.)

16900 LOW ENERGY α-p PULSE-SHAPE DISCRIMINATION WITH SILICON SURFACE BARRIER DETECTORS. Siffert, P.; Coche, A. (Centre de Recherches Nucleaires, Strasbourg). 22p. (CONF-651001-27). ORAU. Gmelin, AED-CONF-65-293-27.

From IEEE Nuclear Science Symposium, San Francisco.

A system that permits the discrimination between alpha particles and protons with energies greater than 3 Mev is described. (D.C.W.)

16901 HIGH SENSITIVITY DETECTORS FOR FEW-kev X-RAYS. Fisher, P. C.; Meyerott, A. J. (Lockheed Missiles and Space Co., Palo Alto, Calif.). 32p. (CONF-651001-26). ORAU. Gmelin, AED-CONF-65-293-26.

From IEEE Nuclear Science Symposium, San Francisco.

The effect of background counts on the detection sensitivity of gas proportional counters is discussed, and several different geometries that preserve the counter's inherent energy resolution are described. An x-ray experiment designed for use on the first orbiting Astronomical Observatory in the investigation of 2- to 20-kev photons is discussed. The behavior of a complementary system for 0.1- to 6.0-kev photons, using x-ray optics that focus in only one dimension, is also considered. (D.C.W.)

16902 LOW VOLTAGE IONIZATION CHAMBER. Decuyper, J. C.; Gariod, R. (CEN, Grenoble, France). Vienna, International Atomic Energy Agency, 1965, Preprint No. CN-22/9, 22p. (In French). (CONF-651105-5). ORAU.

From Conference on Nuclear Electronics, Bombay.

The properties of low-voltage ionization chambers operating in the recombination mode are studied. (D.C.W.)

16903 RADIATION DETECTORS FOR REACTOR CONTROL. Duchene, J. P.; Roguin, A. (CEN, Saclay,

France). Vienna, International Atomic Energy Agency, 1965, Preprint No. CN-22/12, 10p. (In French). (CONF-651105-8). ORAU.

From Conference on Nuclear Electronics, Bombay.

Some gamma detectors and neutron detectors that are designed for use in the control of reactors are described, together with equipment for connecting the detectors to the measuring units. (D.C.W.)

16904 ELECTRONIC DESIGN OF A SPECTROMETER FOR MONITORING SOLAR X-RAY RADIATION IN SPACE. Mooney, Paul J. (American Machine and Foundry Co., Alexandria, Va.). 13p. (CONF-651057-2). ORAU. Gmelin, AED-CONF-65-313-2.

From IEEE East Coast Conference on Aerospace and Navigational Electronics, Baltimore.

An instrument that was developed to study the spectrum of soft x radiation in the range of 1 to 400 Å is described. The instrument is to be flown with the Orbiting Solar Observatory series of satellites and contains four separate spectrometers and an ion chamber. (D.C.W.)

16905 DETERMINATION OF THE NUMBER OF NEUTRONS EMITTED SIMULTANEOUSLY BY A SOURCE. Gey, Albert; Jacquesson, Jacques (to Commissariat a l'Energie Atomique). Canadian Patent 724,285. Dec. 21, 1965.

^{239}Pu and ^{240}Pu emit neutrons by spontaneous fission. Additional neutrons by the reaction (α,n) will also be present if the fission neutrons strike impurities in the plutonium. A device is designed to determine the ratio of the fission neutrons to those arising from the alpha reaction. Such a determination is desirable when such impurities must be eliminated in a chemical purification process. The device employs two counters. There is a certain time delay or dead time between the detection of the fission neutrons and signal which they produce. The time delay between the alpha neutrons and their signal is distinctly different. A means is provided for observing these time delays from which the numbers of the two kinds of neutrons may be computed. (AECL)

16906 INSTRUMENT FOR THE SIMULTANEOUS AND SEPARATE MEASUREMENT OF ALPHA AND BETA ACTIVITY OF RADIATING NUCLEI. Kiefer, Hans; Maushart, Rupprecht (to Gesellschaft fuer Kernforschung mbH). German Patent 1,205,629. Nov. 25, 1965. Filed Mar. 20, 1963.

An instrument is described that comprises in a common housing two detection systems of which one is a gas-flow counter for the detection of beta particles and the other is a proportional counter sensitive to individual alpha particles which operates in air at atmospheric pressure. A counter window separates the gas-flow counter from the alpha counter, which is provided with openings through which air and alpha particles are admitted into the counter volume of the alpha counter. (Gmelin Inst.)

Radiation Effects

Refer also to abstract 17144.

16907 (N-65-17517) [LOW-ENERGY PROTON EXPERIMENTS]. Monthly Progress Report, Period Ending January 1, 1965. Downing, R. G. (Space Technology Labs., Inc., Canoga Park, Calif.). Jan. 20, 1965. Contract NAS5-3805. 3p. (NASA-CR-60879; STL-4161-6009-SU-000). CFSTI $1.00 cy, $0.50 mn.

A low-energy proton experiment with the STL 2-Mev proton Van de Graaff showed that the slope of the short-circuit density versus the log of the integrated exposure becomes steeper at lower proton energies. Degradation rates as high as 50% per decade were observed in some cases, as compared with the normally observed 20 to 25% per decade slopes under conditions of penetrating radiation and uniform damage. This phenomenon is attributed to the localized region of damage near the junction and also to the open-circuit voltage degradation that is associated with decrease in the form factor of the current-voltage characteristics. It was concluded that the maximum power degradation rate of the cell will decrease far more rapidly relative to the short circuit current degradation under low bombardment than is normally observed with penetrating radiation. (STAR)

16908 (N-65-17526) COMPONENTS IRRADIATION TEST NO. 5: HPA-1002 AND IN1616 DIODES, S2N1724 AND 2N2222 TRANSISTORS, 2N511 FLIP FLOP BISTABLE NETWORK, SN522 OPERATIONAL AMPLIFIER. (Lockheed-Georgia Co., Marietta). July 24, 1964. Contract NAS8-5332). 64p. (NASA-CR-60840; ER-7510). CFSTI $3.00 cy, $0.75 mn.

Two types of diodes, two types of transistors, and two types of microelectronic circuits (an amplifier and a flip flop) were subjected to a radiation environment at a controlled temperature of 37° ± 0.5°C. Irradiation was continued until the specimens had accumulated an average integrated flux of $5.4 \times 10^{14} n/cm^2$ plus an average gamma dose of 7.5×10^6 R. During the irradiation, measurements were made to define V_F and I_R for the diodes; h_{FE}, I_{CBO}, and V_{BE} for the transistors; and output voltages of the amplifiers and flip flops. Test results are indicated and the ranges of radiation exposure over which failures occurred are given. (auth)

16909 (N-65-18250) COMPONENTS IRRADIATION TEST NO. 7: 2N834 TRANSISTORS, IN540 AND IN649 DIODES, SIN752A ZENER DIODES. (Lockheed-Georgia Co., Marietta). Sept. 28, 1964. Contract NAS8-5332. 50p. (NASA-CR-57107; ER-7620). CFSTI $2.00 cy, $0.50 mn.

One type of transistor with specimens from each of three manufacturers, two types of diodes, and one type of Zener diode were subjected to a radiation environment in a controlled temperature chamber to determine the effect of radiation on selected component parameters. Failure criteria for the test were a 50% reduction in h_{FE} of the transistor specimens, a 100% increase in V_F, or an increase in I_R beyond specified maximum values, for the diodes. All specimens failed. Median radiation exposure levels for the transistors were 2.8×10^{13} n/cm² or 8.1×10^5R, $3.4 \times 10^{13} n/cm^2$ or 8.6×10^5R, and 5.0×10^{13} n/cm² or 9.3×10^5R, respectively, for the three suppliers. Specific modes of failure are noted. (STAR)

16910 (N-65-18448) FEASIBILITY STUDY TOWARD DEVELOPMENT OF RADIATION-RESISTANT SOLAR CELL. Final Report, November 1, 1961-January 31, 1963. Cheslow, M.; Kaye, S. (Electro-Optical Systems, Inc., Pasadena, Calif.). Feb. 28, 1963. Contract NAS7-92. 72p. (NASA-CR-57132; EOS-2080-Final). CFSTI $3.00 cy, $0.75 mn.

The results of a feasibility program to develop radiation-resistant solar cells are described. An electric field in the base region which was produced by means of a graded base structure increased the collection efficiency of light-produced carriers from the base region. Comparative results of radiation damage tests with both 1 Mev electrons and 95 Mev protons are presented. The cells were found to be 20 times more radiation resistant than n-on-p cells having 1 ohm cm-base region. A complete theoretical discussion is given. (auth)

16911 EFFECTS OF RADIATION ON ELECTRONIC COMPONENTS. Hamman, Donald J. Battelle Tech. Rev., 15: 2-6(Feb. 1966).

If future space probes are to succeed, more data must be assembled on the effects of radiation on electronic materials and devices. A summary is given of present knowledge concerning the engineering aspects of these effects and the areas in which additional information is needed are delineated. (auth)

16912 ANALYSIS OF THE EFFECT OF FAST-NEUTRON BOMBARDMENT ON THE CURRENT-VOLTAGE CHARACTERISTIC OF A CONDUCTIVITY-MODULATED p-i-n DIODE. Swartz, John M.; Thurston, Marlin O.

(Phylatron Corp., Columbus, Ohio. Ohio State Univ., Columbus). J. Appl. Phys., 37: 745-55(Feb. 1966).

Fast-neutron bombardment of silicon diodes changes the excess carrier diffusion length without significantly changing other diode parameters. Such bombardment is thus a useful tool for investigating diode theory. The technique is applied to an expression for the current-voltage characteristic developed for the wide-based p-i-n diode. For high level injection, there are two current density ranges of interest. First, a range where the base voltage is independent of current density and the total junction voltage v varies as exp (qV/2kT) with current. This region corresponds to unity emitter efficiency at each of the junctions. For higher current densities, the emitter efficiency decreases, and the base voltage increases as the square root of the current density. Also, the total junction voltage varies as exp (qV/kT) with current. The theoretical results are then shown to fit the current-voltage characteristics of experimental wide-based silicon p-i-n diodes. (auth)

16913 THE TRANSIENT RADIATION RESPONSE OF INSULATED GATE FIELD EFFECT TRANSISTORS. Long, David M. (Martin Co., Baltimore). 4p. (CONF-651057-1). ORAU. Gmelin, AED-CONF-65-313-3.

From IEEE East Coast Conference on Aerospace and Navigational Electronics, Baltimore.

The transient response of MOS field effect transistors was investigated by exposing p-channel and n-channel devices to a 600-kev flash x-ray machine. The data show that the response consists primarily of drain-substrate photocurrent and a gate displacement current. The importance of charge scattering in the device response was demonstrated experimentally. One of the devices tested showed an unusually long recovery time of 50 to 100 microseconds. (auth)

ISOTOPE TECHNOLOGY

General

16914 (ORNL–3900, pp 182-93) ISOTOPE DEVELOPMENT. (Oak Ridge National Lab., Tenn.).

Progress in isotope development is summarized in sections on nuclear and radiochemical analyses, radioisotope research, radioisotope technology, and radioisotope safety. (J.R.D.)

16915 INVESTIGATION OF BORON ISOTOPES. Riedel, Jozef Tadeusz (Inst. of Nuclear Research, Warsaw). Przegl. Elektron., 6: 492-7(Oct. 1965). (In Polish).

The results of research in determining the relative isotopic abundances of 10B and 11B in nature are reviewed. A tabulation of the atomic weight is included for a number of major B deposits or mining areas throughout the world. The variation of the ratio 11B/10B is given for a number of chemical forms of boron compounds found in nature, and the ratio is also given for numerous methods of determining the ratio and for the calendar year of each investigation, with the latest ratio (1957) listed as 4.13 ± 0.02. (TTT)

16916 TRITIEVYE IZLUCHATELI. (Tritium Emitters). Gorlovoi, G. D.; Stepanenko, V. A. Moscow, Atomizdat, 1965. 116p.

The fabrication and properties of tritium targets on titanium and zirconium bases are discussed, and methods for saturating targets with tritium or deuterium are described. The uses of tritium sources for ionization gas analysis, as fire alarms, and indicators of consumption, velocity, and direction of gas flow, and as atomic batteries are evaluated. (M.J.T.)

16917 RADIOAKTIVNYE IZOTOPY MOLIBDENA. (Radioactive Molybdenum Isotopes). Rudenko, N. P.; Pastukhova, Z. V. Moscow, Atomizdat, 1965. 48p.

Information on Mo isotopes and the chemistry of Mo is briefly reviewed. The nuclear processes for producing the radioactive isotopes of Mo, the methods for separating them from various irradiated materials, the measurement of their radioactivity, and a method for synthesizing compounds containing radioactive Mo are described. The determination of Mo using activation analysis is discussed. The uses of radioactive Mo isotopes in biology, medicine, agriculture, chemistry, physics, and metallurgy are considered. (M.J.T.)

Industrial Applications

Refer also to abstract 16237.

16918 (AECL-PAK/RB–7) A REVIEW ON THE WHOLESOMENESS OF IRRADIATED FOODS WITH SPECIAL REFERENCE TO WHEAT. Chaudhry, M. A.; Nasiruddin (Atomic Energy Centre, Lahore (Pakistan)). Feb. 1966. 31p. Dep. mn.

The present status of food irradiation is surveyed; potentialities of the technique in developing countries is evaluated; and the need for and possibility of organizing international cooperation in research on food irradiation in Pakistan is considered. The wholesomeness of irradiated foods is reviewed with emphasis on wheat. It is concluded that neither toxicity nor carcinogenicity in irradiated foods can be attributed to the levels of irradiation. (H.G.D.)

16919 (EUR–2619.f) EXAMEN PRELIMINAIRE DES POSSIBILITES ECONOMIQUES LIEES A L'UTILISATION DE L'ENERGIE NUCLEAIRE SOUS SES DIVERSES FORMES DANS QUELQUES PAYS D'OUTRE-MER ASSOCIES A LA COMMUNAUTE ECONOMIQUE EUROPEENNE. (Preliminary Review of the Economic Scope for Various Uses of Nuclear Energy in Certain Overseas Countries Associated With the European Economic Community). Savary, A. (European Atomic Energy Community). Jan. 1966. 79p. Dep. mn.

The use of nuclear techniques in certain African countries associated with the European Economic Community are considered, especially in power generation, production of fresh water from seawater, and the use of radioisotopes in agriculture and hydrology. An analysis of present electricity requirements and of their growth and location over the coming years prompted the conclusion that, in the present state of nuclear technique, nuclear power cannot compete with conventionally generated power. However, agriculture and hydrology appear to be the sectors in which nuclear techniques could usefully be applied and developed. (P.C.H.)

16920 (SGAE-IB/IA–7/1965) RADIOMETRISCHE UND AUTORADIOGRAPHISCHE UNTERSUCHUNGEN BEI DER HERSTELLUNG VON ASBESTZEMENTPRODUKTEN. (Radiometric and Autoradiographic Investigation of the Production of Asbestos Cement Products). Duftschmid, K. E. (Oesterreichische Studiengesellschaft fuer Atomenergie G.m.b.H., Seibersdorf). [1965]. 10p. Dep. mn.

In the production of asbestos cement plates or tubes, the maintenance of optimum mixing conditions is of great importance for the production of a standard quality. By direct neutron irradiation of asbestos component in the reactor, the radioisotope ^{24}Na, which is very useful as an indicator, can be produced. Therefore, an accurate analysis of the asbestos distribution and its fibrous structure in the finished product and a continuous monitoring of the operation of the mixing installation is possible. (tr-auth)

16921 (TID–22627) STUDIES ON THE APPLICATION OF RADIOISOTOPE TECHNIQUES IN STREAM POLLUTION PROBLEMS IN THE PULP AND PAPER INDISTRY. Circular 24. Chatters, Roy M.; Peterson, Richard L. (Washington State Univ., Pullman. Research Div.). 1965. Contract AT(45-1)-353. 11p. Dep. mn. CFSTI $1.00 cy, $0.50 mn.

The development of a radioisotope technique that permits the tagging of fibers and their subsequent identification or tracing without the necessity of introducing any radioactive material into the pulp and paper mill processing system is described. The method involves the treatment of fibers with metallic salts in such a manner as to cause the metal component to become bonded with the cellulose or to be precipitated within the fiber lumen. Successful results were found with $^{140}La(NO_3)_3$. A second and somewhat different radioisotope technique was developed to follow the flow of wood fibers through a mill. The procedure consists of irradiating a specific amount of pulp and introducing it into the mill along with the greater mass of unirradiated pulp. (P.C.H.)

16922 MEASUREMENT OF THE HUMIDITY OF LARGE-LUMP COKE WITH NEUTRONS. Dresia, H. (Staatliche Ingenieur-Schule fuer Maschinenwesen, Essen); Fischoetter, P. Brennstoff-Chem., 46: 13-17(Jan. 1965). (In German).

On the basis of preliminary studies on the measurement of coke moisture with neutrons, an installation for the continuous measurement of the moisture in large-lump broken coke was developed. In a model container, which in its dimensions agrees accurately with that of a coke bunker on a blast furnace, the moisture was systematically measured on broken coke of the fractions from I to IV. In the neutron measurement a coke volume of approximately 0.3 m^3 was used so that a sufficiently representative value was obtained for the moisture of a coke charge. With sufficient gap between measurement site and the coke and the use of neutron reflectors, a measurement value for the coke

moisture was obtained that was linearly dependent on the moisture and independent of the grain fraction. The mean deviation of the measured moisture was approximately 0.5 wt. %. Operational measurements on the coke bunker of a blast oven are discussed. (tr-auth)

16923 SOME OBSERVED DISCREPANCIES IN APPLICATION OF THE TRIANGLE TEST TO EVALUATION OF IRRADIATED WHOLE-EGG MAGMA. Grim, Alfred C.; Goldblith, Samuel A. (Massacushetts Inst. of Tech., Cambridge). Food Technol., 19: 146(Sept. 1965).

Some results are presented on use of the triangle test as a means of evaluating off-flavor produced in irradiated whole-eggs which indicate the importance of presentation of samples to the panel. The ability of trained panel members to identify the odd sample correctly was about 10% higher when they received two untreated and one irradiated sample than with two irradiated and one control sample. It is concluded that in working on the sensory properties of irradiated foods, careful attention should be given to uniform presentation of the samples in all possible combinations. (BBB)

16924 A DENSITY-INDEPENDENT MOISTURE GAUGE USING NEUTRON RADIATION. Schuricht, V.; Hiemann, D. (Institut fuer Anwendung Radioaktiver Isotope, Dresden). Isotopenpraxis, 1: 82-4(Nov. 1965). (In German).

Preliminary investigations showed that the density effect may possibly be compensated in moisture measurements by means of neutrons. An arrangement must yield two counting rates, each of which is linearly dependent only on the water content per unit volume and on the density. By means of a data evaluation device, records of moisture in weight percent may be made in certain time intervals. A combined moisture-density probe and a data evaluating device were mounted and tested by using model substances. It could be shown that the measuring values are nearly independent of density. Repeated calibration control is necessary. (auth)

16925 EFFECT OF HYPOXANTHINE ON THE FLAVOR OF FRESH AND STORED LOW-DOSE-IRRADIATED PETRALE SOLE FILLETS. Spinelli, John (Bureau of Commercial Fisheries Technological Lab., Seattle, Wash.). J. Food Sci., 30: 1063-7(Nov.-Dec. 1965).

The 5′-nucleotides exert a major influence on the flavor of fish, and the most abundant one in fish is 5′-inosine monophosphate (IMP), which after the death of the fish quickly appears in its flesh as the result of the degradation of muscle ATP. IMP is then slowly degradated to hypoxanthine via inosine. Dilute aqueous solutions of hypoxanthine were found to be predominantly bitter. Tests showed, however, that addition of hypoxanthine to fresh and stored low-dose irradiated petrale sole containing less than 10^6 bacteria per g did not alter flavor. Flavor alteration due to added hypoxanthine was detectable in the irradiated fish only when the total bacterial counts exceeded 10^6. To evaluate whether the hypoxanthine that accumulates in stored low-dose-irradiated fish contributes to any flavor change, a study was undertaken to determine certain aspects of flavor imparted by hypoxanthine. To determine whether there was a relation between hypoxanthine content, bacterial counts, and flavor, petrale sole fillets were irradiated at 0.2, 0.3, and 0.4 Mrad. By irradiating the samples at these different dose levels, a wide variation in bacterial counts in fish that were stored for the same length of time was obtained. The results suggest that bacterial growth changes the flavor characteristics of hypoxanthine by either utilizing or altering some of the natural constituents of fish that normally render hypoxanthine tasteless in the fish, or by producing metabolic end products that enhance its flavor-producing properties. (BBB)

16926 INDUSTRIAL MOISTURE MEASUREMENT WITH NEUTRONS. Trost, A. (Messgeraete fuer Kernstrahlung und Zerstoerungsfreie Werkstoffpruefung, Schwarzewald, Ger.). Z. Instrum., 73: 329-36(Dec. 1965). (In German).

The use of neutrons to measure water content of materials in industry is discussed, and a modified method, along with instrumentation and results, is described and illustrated. The nuclear method for moisture gaging is based on the moderation of fast neutrons by hydrogen nuclei and is independent of temperature, pH value, and chemical structure of the material. No contact with the material to be measured is required. The method takes the average value over a large volume and provides an electrical output signal to be used for continuous control. According to the problems encountered in the material examined, depth or surface probes are applied. The method is now being used for glass sand, for concrete production, during road construction, and for sinter mixtures and coke. It also seems promising for other materials containing hydrogen only as moisture or whenever chemically bound hydrogen is present only in small and constant quantities. Radiation protection aspects of the use of the neutron moisture probes are also considered. Safety is best attained by use of a γ-ray-free source, such as ^{241}Am, for generating neutrons. For a stationary probe, 100 mC of ^{241}Am with Be was adequate. (BBB)

Power Application

See also ENGINEERING — Space Propulsion

Refer also to abstracts 17325 and 17326.

16927 (MLM-1297) RADIOISOTOPES FOR HEAT SOURCES. II. CALCULATIONS FOR PREPARATION OF ^{227}Ac BY NEUTRON IRRADIATION OF ^{226}Ra. Foster, K. W. (Mound Lab., Miamisburg, Ohio). July 1, 1965. Contract AT(33-1)-Gen-53. 11p. Dep. mn. CFSTI $1.00 cy, $0.50 mn.

The advantages and disadvantages in the use of actinium-227 as a nuclear heat source material are discussed, and the calculation of optimum neutron irradiation schemes to produce actinium-227 from radium-226 is described. The chief advantages in the use of actinium-227 are the relatively high power density resulting from five alpha-active daughters, and a relatively long half life giving a stable heat output for many years. The chief disadvantages are intense gamma radiation from the various daughters in the decay chain, and low abundance of the starting material, radium-226. Irradiation schemes were optimized to conserve radium rather than for maximum actinium productivity. At present the disadvantages appear to outweigh the advantages for heat source applications. (P.C.H.)

Separation and Production

See also CHEMISTRY — Separation Processes and Procedures

16928 (INSJ-92) PROGRESS REPORT ON INS ISOTOPE SEPARATOR. Kaneko, Kumetaro; Chida, Katsuhisa; Sakai, Mitsuo (Institute for Nuclear Study, Tokyo Univ. (Japan)). Nov. 5, 1965. 15p. Dep. mn.

Characteristics of the INS isotope separator are described, and direct deposition of the separated material on a thin membrane, development of ion source with a high intensity output, and isotope separation are discussed. Separated ^{24}Mg and ^{54}Fe isotopes were deposited on thin foils. The thickness of enriched material was estimated to be of the order of 1 mg/cm^2. The separated isotopes included Cd, Mg, and tin isotopes. (P.C.H.)

16929 CALCULATION OF SQUARED-OFF CASCADES FOR ISOTOPE SEPARATION BY DIFFUSION. Troetsch, E.; Dickel, G. (Univ., Munich). Kerntechnik, 8: 18-22 (Jan. 1966). (In German).

The numerical results obtained previously in the calculation of optimum dimensions for rectangular cascades with random separation factors are applied practically. The individual rectangular cascade are calculated, and the characteristics of the installations composed of several

rectangular cascades are given. The utilization degree was calculated. The transformation theorem is given, and some examples illustrate the use of the formulas derived. (J.S.R.)

16930 SEPARATION OF OXYGEN ISOTOPES BY GAS CHROMATOGRAPHY. Bocola, W.; Bruner, F.; Cartoni, G. P. (Univ. of Naples). Nature, 209: 200-1(Jan. 8, 1966).

Glass capillaries for gas-solid chromatography were used for the separation of ^{16}O from ^{18}O. To prepare adsorbing surfaces, the inner walls of the glass capillaries were etched with an alkaline solution for 6 hr at 100°C and washed to neutrality. The column was dried and activated under a flow of nitrogen at 200°C for 48 hr. The efficiency of this column, measured from the oxygen peak at the working conditions of the chromatogram was approximately 350,000 theoretical plates. At 91.2°K the retention volume ratio for $^{18}O/^{16}O$ was smaller than the vapor pressure ratio for the mixed molecule, and consequently the separation obtained by gas chromatography was less than that expected from the relative volatilities. However, at 80.2°K the differences were larger and the separation factors achieved by gas chromatography increased more rapidly than the vapor pressure ratios. (M.C.G.)

16931 ENRICHMENT OF THE MOLECULAR SPECIES $^{14}N^{15}N$ BY THERMAL DIFFUSION. I. DETERMINATION OF THE PERFORMANCE OF THE COLUMN. Vasaru, Gh. (Inst. of Atomic Physics, Cluj). Stud. Cercet. Fiz., 17: 955-62(1965). (In Rumanian).

In order to provide design data for a laboratory-scale hot-wire type thermal diffusion column for the enrichment of the molecular species $^{14}N\ ^{15}N$ to a desired level, the most important parameters of the experiment, the separation factor q and the specific length l_0 of the column were determined. A gaseous quasibinar mixture containing $^{14}N_2$, $^{14}N\ ^{15}N$ and $^{15}N_2$, at a natural abundance of 99.24, 0.76 and 0.001%, respectively, was used for the experiment. A separation factor of q = 2.32 and a corresponding specific length l_0 = 300 cm were obtained; the theoretical predictions were q = 3.1 and l_0 = 220 cm. This 25% deviation is probably due to the fact that the operation was not carried out at the optimum pressure and to the asymmetric thermal gradients caused by the excentric position of the hot wire. (TTT)

16932 PIERRELATTE—USINE DE SEPARATION DES ISOTOPES DE L'URANIUM. (Pierrelatte—Plant for Separation of Uranium Isotopes). [Paris], Commissariat a l'Energie Atomique, 1964. 38p.

The design and development of the Pierrelatte Isotope Separation Plant is described. The isotopic enrichment processes used are electromagnetic separation, thermal diffusion, centrifugation, expansion in a shock tube, and gaseous diffusion. The principle of each of these methods is described briefly. The characteristics of the plant are given. (J.S.R.)

16933 STABILE ISOTOPE. Katalog fuer Stabile Isotope, Verbindungen und Erzeugnisse mit Angereicherten Stabilen Isotopen. (Stable Isotopes. Catalog for Stable Isotopes, Compounds, and Products with Enriched Stable Isotopes). Leipzig, VEB Deutscher Verlag fuer Grundstoffindustrie, 1964. 208p. (In German and Russian).

This catalog was compiled at the direction of the Permanent Commission on Peaceful Uses of Atomic Energy to publicize the variety of enriched stable isotopes, labeled material, and targets available in the USSR and East Germany. (IIC-M.G.)

MATHEMATICS AND COMPUTERS

Refer also to abstracts 16797, 16873, 17708, and 17709.

16934 AN EXTENSION OF THE FINITE HANKEL TRANSFORM AND APPLICATIONS. Cinelli, G. (Argonne National Lab., Ill.). Int. J. Eng. Sci., 3: 539-59(Oct. 1965).

New finite Hankel transforms with kernels of the form $[J_\mu(\xi_i x)Y_\mu(\xi_i a) - J_\mu(\xi_i a)Y_\mu(\xi_i x)]$ and the corresponding infinite series are introduced, which bring the solution of Bessel's equation with asymmetric endpoint conditions within the realm of integral transform theory. A general solution for the transient temperatures produced in a finite, hollow cylinder by an asymmetrical internal heat source, when radiation takes place on all four surfaces, is accomplished. It is shown how this solution contains Carslaw and Jaeger's results on hollow cylinders as a special case. (auth)

16935 EXISTENCE AND UNIQUENESS THEOREMS IN INVARIANT IMBEDDING. II. CONVERGENCE OF A NEW DIFFERENCE ALGORITHM. Bellman, Richard; Cooke, Kenneth L. (RAND Corp., Santa Monica, Calif.). J. Math. Anal. Appl., 12: 247-53(Oct. 1965).

In order to establish the limiting behavior of equations obtained from an infinitesimal stratification of a medium in the case of the general equations of invariant imbedding, a procedure is used which permits a definition of a generalized solution in a new sense in connection with the application of dynamical programming to the calculus of variations. (J.F.P.)

16936 NUMERICAL SOLUTION OF NON-FREDHOLM (SINGULAR) INTEGRAL EQUATIONS BY MATRIX INVERSION. Jones, C. Edward; Tiktopoulos, George (Princeton Univ., N. J.). J. Math. Phys. (N. Y.), 7: 311-15(Feb. 1966).

It is shown that the simple matrix-inversion techniques often used in numerically solving linear integral equations with a Fredholm-Schmidt (i.e., square-integrable) kernel can also be employed for a wide class of non-Fredholm ("singular") equations. This class includes equations the kernel of which is the sum of a Fredholm-Schmidt kernel and a kernel whose norm (in the operator sense) is less than one. In particular, the integral equations of the so-called "new strip approximation" in particle dynamics belong to this class. (auth)

16937 METHODS OF QUADRATURE FOR EULER TRANSFORM INTEGRALS. Livingston, Peter M. (Univ. of Wisconsin, Madison). J. Math. Phys. (N. Y.), 7: 325-33(Feb. 1966).

Several methods of treating Euler transform integrals exist. One such method follows from the expression of the Euler transform kernel as a bilinear series of independent solutions to the Jacobi equation valid for the integration variable in the real interval -1 to 1 and the transform variable outside. The transform function then is expressed as a series of solutions of the second kind to the Jacobi equation whose coefficients are the expansion coefficients of the function to be transformed in the complete set of Jacobi polynomials, provided the latter exist. Such a series is absolutely convergent for the transform variable not on the real interval cited above. Another method, due to MacRobert, permits quadrature of the Euler transform integral directly for certain integrands. Finally, the expansion of the Euler kernel in a bilinear series of Bessel functions and Neumann polynomials valid for the integration variable on the finite interval, 0 to a, is mentioned, and applied to several integrals. Examples of all three methods are given. (auth)

16938 CORRELATION FUNCTIONS FOR EIGENVALUES OF REAL QUATERNION MATRICES. Mehta, M. L.; Srivastava, P. K. (Univ. of Delhi). J. Math. Phys. (N. Y.), 7: 341-4(Feb. 1966).

The eigenvalue density, the two-, and the three-point correlation functions for the ensemble of real quaternion matrices are calculated. The forms suggest a generalization for the n-point correlation function. The probability that no eigenvalues lie inside a circle of radius r around the origin is also calculated for the ensemble of real quaternion matrices as well as for that of complex matrices. Upper and lower bounding functions for the last probability density are given. (auth)

16939 CANONICAL REALIZATIONS OF LIE SYMMETRY GROUPS. Pauri, M. (Univ., Parma, Italy); Prosperi, G. M. J. Math. Phys. (N. Y.), 7: 366-75(Feb. 1966).

A general theory of the realizations of Lie groups by means of canonical transformations in classical mechanics is given. The problem is the analog to that of the characterization of the projective representations in quantum mechanics considered by Wigner, Bargmann, and others in the case of the Galilei and the Lorentz group. However, no application to particular groups is given. It turns out that the generators y_τ of the infinitesimal transformations in a canonical realization of a Lie group G satisfy relations of the form $\{y_\rho, y_\sigma\} = c^\tau_{\rho\sigma} y_\tau + d_{\rho\sigma}$, where $c^\tau_{\rho\sigma}$ are the structure constants of G and $d_{\rho\sigma}$ are constants depending on the particular realization. It also turns out that any canonical realization of G can be reduced to a fundamental typical form by means of a constant canonical transformation in the phase space of the system. This typical form allows one to obtain a complete characterization of all the possible canonical realizations of G. Once a suitable definition of "irreducible" canonical realization is given, a simple classification can be obtained in terms of the values of certain functions of the generators y_τ (canonical invariants). Recalling the correspondence $\{\ \} \to [\ ]$, formal analogy appears to be achieved with the quantum mechanical case. Even more, a parallel development of the outlined theory in quantum mechanics is of interest in the construction of the invariant operators (even in case of non-semisimple groups) and of complete systems of commuting observables acting within the irreducible representations. (auth)

16940 SUBTRACTOR CIRCUIT WITH INTEGRATED LOGIC ELEMENTS. Stueber, W. (EURATOM, Geel, Belg.). Nucl. Instrum. Methods, 40: 163-5(Feb. 1966).

To avoid channel-width differences introduced by the interpolator system in a nanosecond time coder, an equalizing system was realized, containing a unit to subtract a 3-digit binary number from a 17-digit binary number. The subtractor was built with integrated circuit elements. These were chosen in order to ascertain their properties and possibilities, i.e., how far they can be used without additional conventional elements and how they are able to work together with existing conventional circuits. The principle of subtraction, and the computer program are discussed. The binary subtractor diagram is shown. (J.F.P.)

16941 ON A GENERALIZATION OF THE SPHERICAL COMPLEX FUNCTION. Ikeda, Mineo (Univ. of Hiroshima). Progr. Theoret. Phys. (Kyoto), 34: 695-6 (Oct. 1965). (In French).

The complex spherical function which is a direct generalization of the ordinary spherical function frequently used in mathematical physics is generalized to the case of 4 dimensions. The resulting functions form the space of an irreducible representation of U(4) or SU(4). (M.J.T.)

METALS, CERAMICS, AND OTHER MATERIALS

General

Refer also to abstract 17158.

16942 (ANL–6981) TUNGSTEN–RHENIUM ALLOY THERMOCOUPLES AND THEIR USE IN A UO_2-FUELED REACTOR. Brooks, E. J. (Argonne National Lab., Idaho Falls, Idaho); Kramer, W. C. (Argonne National Lab., Ill.). Nov. 1965. Contract W-31-109-eng-38. 45p. Dep. mn. CFSTI $2.00 cy, $0.50 mn.

Thermocouples of W/W–26 wt % Re and W–5 wt % Re/W–26 wt % Re with ThO_2 insulation and W–26 wt % Re sheathing were calibrated to 2760°C. The W–5 wt % Re/W–26 wt % Re thermocouple had a large change in output between two calibration cycles; explanations are suggested for this behavior. There was no apparent chemical interactions between components. Radial and longitudinal cracking, believed to have been introduced during fabrication, was found in varying degrees in all metallographic sections through the sensing legs of the thermocouples. A unique type of hot junction was incorporated into the design to obviate a welded junction that would have been inherently brittle and fragile. (W.L.G.)

16943 (IITRI–B237-45) PROTECTIVE COATINGS FOR REFRACTORY METALS IN ROCKET ENGINES. Final Report, December 15, 1964–December 15, 1965. (IIT Research Inst., Chicago, Ill.). Jan. 15, 1966. NAS7-113. 117p.

Protective coating systems for use on refractory metal liquid-fueled rocket engine components were developed. Coatings that would be useful in both hydrocarbon and halogen combustion environments were investigated. Primary emphasis was on Hf–Ta alloys, Ir-base coating systems, and composite coatings based on HfO_2. The refractory metal substrate materials employed were ω and Ta-base alloys. Coated nozzles and throat inserts of each of these systems were prepared for engine firing evaluation. Hf–20Ta alloy clad Ta–10W nozzles and throat inserts were prepared by hot spinning of preclad plate. The influence of spinning variables and the use of Ta or Nb diffusion barriers between the Hf alloy and substrate were evaluated. These investigations have demonstrated that Hf–Ta clad Ta–10W is a promising system for temperatures approaching 4000°F. A model was developed for the determination of temperature-dependent stress in plasma sprayed composite nozzles based on HfO_2–W. Tensile properties, elastic modulus and thermal expansion behavior were determined for plasma sprayed ω, monoclinic HfO_2, Y_2O_3 stabilized HfO_2, and a W–50 wt % HfO_2 composite layer. Residual stress measurements of as-fabricated multilayer nozzles were in reasonable agreement with predicted values. The development of Ta–HfO_2 composites based on the controlled oxidation of an Hf–Ta alloy was investigated. The influence of temperature and effective oxygen pressure on the size and distribution of the microconstituents was established. Interdiffusion studies were performed in the systems W–Re, W–Ir, and Ta–W at temperatures to 4000°F to establish layer thickness requirements and material combinations necessary for an effective coating system based on Ir. Fused salt electrolysis and liquid metal slurry coating methods were studied as means for depositing Ir on refractory metal engine components. The slurry coating method was found to be quite effective. (auth)

16944 (NASA-SP–3025) SPACE MATERIALS HANDBOOK. Supplement 1 to the Second Edition Space Materials Experience. Rittenhouse, John B.; Singletary, John B. (Lockheed Missiles and Space Co., Palo Alto, Calif. Research Labs.). 1966. 268p. (ML-TDR–64-40(Suppl.1)). CFSTI $3.00 cy, $1.50 mn.

Materials used in successfully orbited spacecraft are reviewed and tabulated. These materials are discussed, insofar as information is available, as to their contribution to spacecraft performance. Data on the effects of the space environment on materials, as measured in space, are tabulated and discussed; particular attention is given to correlating these data with measurements made with simulated environments. Specific materials for use in various functional categories on a spacecraft are recommended. These recommendations are based on results from both simulated environmental testing and the performance of materials in space as given. Reasons for the materials choices are discussed and some of the further limitations on these choices due to environmental factors are pointed out. (auth)

16945 (ORNL-TM–1161) NINETEENTH METALLOGRAPHIC GROUP MEETING, HELD APRIL 20–22, 1965, OAK RIDGE NATIONAL LABORATORY, OAK RIDGE, TENNESSEE. Gray, R. J. (comp.) (Oak Ridge National Lab., Tenn.). Feb. 1966. Contract W-7405-eng-26. 288p. (CONF-650414). Dep. mn. CFSTI $6.00 cy, $1.50 mn.

Separate abstracts were prepared for the individual papers. For eight papers previously abstracted in NSA, see: 19: 22969, 28739, 34687, 36954, 39092, 20: 751, 7576, and 9499. (W.L.G.)

For abstracts of individual papers see: 16946–16954, 17023, 17024, and 17128.

16946 (ORNL-TM–1161, pp 80–4) A METALLOGRAPHIC TECHNIQUE FOR MEASURING THIN FILMS OF ZIRCONIUM OXIDE AS FORMED ON REACTOR FUEL CLADDING. Owens, C. M. (Westinghouse Electric Corp., Pittsburgh, Pa. Atomic Power Div.).

An improved technique was developed to preserve thin films of zirconium oxide during metallographic preparation. The procedure involves the chemical application of a thin layer of silver which is then heavily plated with copper. Excellent photomicrographs of the oxide can be obtained at 1000 diameters. (auth)

16947 (ORNL-TM–1161, pp 98–102) ACCELERATED EPOXY MOUNTING USING A RADIO-FREQUENCY FURNACE. Crouse, R. S. (Oak Ridge National Lab., Tenn.).

By using a radiofrequency furnace in conjunction with a drying oven, it was possible to mount a metallographic specimen in epoxy in twenty minutes. The usual technique requires three to six hours. The rapid heating promotes both deaeration and impregnation. (auth)

16948 (ORNL-TM–1161, pp 103–11) EVALUATION OF DISSOLVABLE EPOXY SYSTEMS FOR REMOTE METALLOGRAPHIC EVALUATIONS. Ritchie, E. E. (Atomics International, Canoga Park, Calif.); Wade, J. T. (Autonetics, Downey, Calif.).

Evaluation of irradiated materials requires a mounting compound that can be mixed remotely, has low viscosity for remote casting with a room temperature curing cycle, has good abrading characteristics and can be dissolved rapidly without degradation of the sample. Several epoxy systems from different suppliers were evaluated with Bakelite and epoxy mounting rings. The Hysol C-21 system in Bakelite rings with Hysolv 4079 solvent is adequate. Mechanically removing excess epoxy from the specimen greatly reduces the release time. (auth)

16949 (ORNL-TM–1161, pp 112–29) EXPERIENCE WITH COLOR IN METALLOGRAPHY. Gray, R. J.; Crouse. R. S. (Oak Ridge National Lab., Tenn.).

Experience in color metallography using Polaroid's Polacolor and Eastman Kodak's Ektachrome and Ektacolor Professional Processes is described. (auth)

16950 (ORNL-TM–1161, pp 132–45) MICROPHOTOMETER: A VERSATILE INSTRUMENT FOR APPLICATION TO GRAIN ORIENTATION STUDIES AND QUANTITATIVE METALLOGRAPHY. Brock, William W. (National Lead Co. of Ohio, Cincinnati).

A conventional optical microscope was converted to a highly sensitive microphotometer to measure the reflectance property of grains in polished uranium metal samples. Limited measurements performed on alpha-rolled and beta heat-treated uranium samples showed differences in grain orientations. In addition to its use in textural studies, this instrument is expected to aid greatly both in identifying inclusions and in the performance of quantitative metallography. (auth)

16951 (ORNL-TM-1161, pp 159-81) ELECTRICAL DISCHARGE MACHINING IN THE METALLURGICAL LABORATORY. Wilson, J. C. (Oak Ridge National Lab., Tenn.).

Electrical discharge machining (EDM) has proved invaluable for preparing metallurgical specimens. The design, construction, and operation of simple, inexpensive EDM units is described. The capabilities of these machines for such operations as, cutting single crystals to specific orientations with a minimum of deformation, machining spherical, single crystal, oxidation specimens, and cutting cylindrical and flat tensile bars are described. (auth)

16952 (ORNL-TM-1161, pp 182-91) USE OF IMAGE-SPLITTING EYEPIECE. Roman, Harriet R. (Nuclear Metals, West Concord, Mass.).

The image-splitting (or shearing) is achieved by means of a dichroic beam splitter giving color differentiation of the beams. The advantages and disadvantages of this eyepiece and the conventional filar eyepiece was discussed. (auth)

16953 (ORNL-TM-1161, pp 249-66) METALLIC INCLUSIONS IN UO_2. Wolff, U. E.; Rooney, D. M. (General Electric Co., Pleasanton, Calif. Vallecitos Atomic Lab.).

Uranium dioxide as used in reactors and in out-of-reactor tests must be contained in metals. During thermal cycling, the metals tend to interact with the UO_2. Also, the equilibrium between U, O_2, and UO_2 might be shifted during heat treatment. Consequently, in metallographic samples of UO_2 heat-treated outside the reactor, metallic inclusions of different origins are observed. The inclusions are characterized by their various sizes, shapes, arrangements, colors, and reactivities toward etchants. Details on sample preparation are given and possible steps for the identification of inclusions are pointed out. Numerous examples of metallic inclusions are shown. The types of inclusions are correlated with the thermal history of the respective samples. (auth)

16954 (ORNL-TM-1161, pp 267-71) HIGH MAGNIFICATION OPTICAL MICROSCOPY OF CERAMIC MATERIALS. Dvorak, James R. (IIT Research Inst., Chicago, Ill.).

During the course of a study of fracture mechanisms in ceramic materials it was necessary to prepare and photograph, at high magnification, many samples of polycrystalline alumina. It was evident from preliminary examination that the microstructure could not be satisfactorily resolved at higher magnification (×1000 – ×2000) because of the semitransparent nature of the material. Borrowing a technique from the electron microscopist, a shadowing method evolved that proved to be of value in the rapid and satisfactory examination of polycrystalline alumina. This technique may be useful for other materials of a similar nature. (auth)

16955 (LA-tr-66-5) STUDIES ON THE PULVERIZING OF CRYSTALLINE GRAPHITE. Aita, Ryoji; Yoshida, Kunio. Translated for Los Alamos Scientific Lab., Albuquerque, N. Mex., from Tohoku Daigaku Kagakukeisoku Kenkyusho Hokoku, 11: 121-39(1962). 22p. Dep. mn. JCL $2.60 fs, $0.86 mf.

Crystalline graphite was pulverized in a ball mill, a stamp mill using simple impact, a stamp mill fitted with special-shaped shoes, a cutter mill using a shearing action, and an eddy mill using a scraping action. The change in the particle size distribution from the initial –20+28 mesh was measured as a function of pulverizing time. The resultant particles sizes were predominantly –28+35, –100+150, and –270+325. The type of mill used had no effect on the particle size distribution, but did affect the shape of the particles. The particles had the same shape regardless of particle size for the same pulverizing method. Depending on the shape of the pulverizer, the pulverizing process was either a cutting or partial stripping action. (W.L.G.)

16956 (LA-tr-66-6) ON THE SHAPE OF PARTICLE OF NATURAL GRAPHITE PULVERIZED BY THE CUTTER MILL. Aita, Ryoji; Yoshida, Kunio. Translated for Los Alamos Scientific Lab., N. Mex.), from Tohoku Daigaku Kagakukeisoku Kenkyusho Hokoku, 11: 141-60(1962). 20p. Dep. mn. JCL $1.60 fs, $0.80 mf.

The cutter mill was expected to pulverize flakes of natural graphite by a shearing action of the sharp edge of the cutter, the resulting product being flat flakes. It was found that the resulting particles had a spherical shape as a result of the graphite particles colliding with the internal wall of the cutter mill body. (W.L.G.)

16957 (LA-tr-66-11) ABOUT THE MOTION OF BALLS, MILL CHARGE AND THEIR PULVERIZING EFFECT IN THE BALL MILL. Aita, Ryoji; Yoshida, Kunio. Translated for Los Alamos Scientific Lab., N. Mex., from Tohoku Daigaku Kagokukeisoku Kenkyusho Hokoku, 11: 161-88(1962). 30p. Dep. mn. JCL $2.60 fs, $1.10 mf.

The effects of the ball mill design on the pulverizing efficiency of graphite was investigated. Other variables investigated included the rotation speed, the number of balls and amount of graphite in the charge, and the ratio of the charge volume to the mill volume. The best results were obtained with mills having lifters and the charge occupying 70 to 75% of the ball mill volume. (W.L.G.)

16958 (LA-tr-66-12) PULVERIZING OF NATURAL GRAPHITE PARTICLE BY HAMMER MILL. Aita, Ryoji; Yoshida, Kunio. Translated for Los Alamos Scientific Lab., N. Mex., from Tohoku Daigaku Kagakukeisoku Kenkyusho Hokoku, 11: 227-34(1962). 8p. Dep. mn. JCL $1.10 fs, $0.80 mf.

The pulverizing action of the hammer mill was considered to crush the particles of graphite by the striking force between the hammer and the particle of graphite. Contrary to the accepted conception, the particle of graphite became spherical, bending spherically from the periphery of the graphite particle toward the center of the particle, and then this spherical periphery separates from the body splitting into fine powder. The particle size distribution curve shows the first peak at 150 mesh denoting the fine powder separated from the spherical periphery. The next peak is at 325 mesh denoting the finer separated powder from the 150 mesh particle, spherically bending at the periphery and then separating from the body of 150 mesh particle. (auth)

16959 METALLOGRAPHIC TECHNIQUES FOR THE OPTICAL AND ELECTRONIC OBSERVATION OF Zr–2.5 Nb ALLOY. Bassi, A. (CISE, Segrate, Milan); Be, C. A.; Camona, G.; Paganini, L. Energia Nucl. (Milan), 13: 85-6(Feb. 1966).

In the framework of the development of new metallographic techniques based on the use of chemical baths, a polishing bath was studied and set up for the morphological observation of Zr-2.5 Nb alloy as well as a thinning bath for its structural observation in the electron microscope. The baths are briefly discussed. (M.O.W.)

16960 GROWTH AND PREFERENTIAL DOPING OF ZIRCON AND THORITE. Chase, A. B.; Osmer, Judith A. (Aerospace Corp., El Segundo, Calif.). J. Electrochem. Soc., 113: 198-9(Feb. 1966).

$ThSiO_4$ and $ZrSiO_4$ crystals were grown by slow, programmed cooling of $Li_2MoO_4-MoO_3$ melts containing about 6 mole % of the thorite or zircon constituents. The normal habit of the crystals was that of a {110} rod with {111} terminating pyramids. Lanthanide doping caused the {111} faces to become larger and the {110} faces to decrease and finally disappear at high lanthanide concentrations. UO_2 doping had no appreciable effects on the habit, however, the

amount incorporated in the crystal varied according to the crystal face. (W.L.G.)

16961 PURIFICATION OF LITHIUM METAL BY HIGH-VACUUM FRACTIONAL DISTILLATION. Schmidt, Paul H. (Bell Telephone Labs., Inc., Murray Hill, N. J.). J. Electrochem. Soc., 113: 201-4(Feb. 1966).

Mo was used for the crucible, baffle plates, and liner for the stainless steel shell of the distillation apparatus. Distillations performed with an additive of boric oxide in the charge yielded the highest purity distillate. Group II elements, especially Ca, were the most difficult impurities to remove by distillation techniques. (W.L.G.)

16962 NONDESTRUCTIVE DETERMINATION OF THE GRADE OF BERYLLIUM BY RADIOGRAPHY. Abeles, Carl; Waraksa, Irene (Sperry Gyroscope Co., Great Neck, N. Y.). Mater. Eval., 24: 155-7(Mar. 1966).

A nondestructive method is described for determining the grade of beryllium in finished parts. Radiography is used to distinguish between grades S-200 and I-400. These grades are very different in their ultimate tensile strength and precision elastic limit; consequently, they vary greatly in cost. Conventional tests are generally destructive and applied on a sampling basis. By using radiography, 100% evaluation is performed without the time-consuming safety precautions required for handling beryllium in conventional tests. (auth)

16963 COATED COLUMBIUM ALLOYS CAN TAKE HIGH TURBINE HEAT. Talboom, F. P.; Joseph, A. D.; Bradley, E. F. SAE (Soc. Automotive Eng.) J., 90-4 (June 1965).

Nb-27Ta-12W-0.6Zr, Nb-10W-2.5Zr, Nb-10W-1Zr-0.1C, and Nb-Ta-W-Mo alloys were evaluated by tests at 78-2400°F to determine suitability for hollow turbine vanes. The alloys were also tested after coating with Ti-Al, Al-Sn, and Ti-Cr-Si coatings to determine oxidation resistance at 1300 to 2700°F, erosion resistance in a fuel-air combustion atmosphere, thermal shock resistance, impact resistance, and creep rupture properties. Weldability studies showed manual TIG welding to be the most satisfactory for joining the alloys. On the basis of recrystallization temperature, tensile strength, ductility, coated properties, and weldability, the Nb-10W-1Zr-0.1C alloy was selected for the vanes. Actual fabrication procedures involved coining and springback forming to produce the air foil, welding the airfoil trailing edges by TIG methods, precision forging the vane platforms from bar stock at 2000 to 2100°F and joining platform to airfoil by TIG welding. (Rev. Metal Lit.)

16964 ALUMINOTHERMIC PRODUCTION OF ALUMINUM-CERIUM ALLOYS. Pedergin, V. A.; Samsonov, G. V. Soveit J. Nonferrous Metals, 60-3(1964).

Production of Al-Ce master alloy by compacting sintered CeO_2 powder and Al powder into briquettes and sintering in vacuum from 900 to 1600°C is described. The heat of formation of Ce_2O_3, $CeAlO_3$, and metallic Ce and corresponding endothermic and exothermic effects were determined. Selection of optimum grain size of Al powder, density of briquettes, and sintering temperature to prevent oxide impurities in Al-Ce briquettes is described. (Rev. Metal Lit.)

16965 BEEHIVE MELTING FURNACE (Engineering Materials). (Oak Ridge National Lab., Tenn.). (CAPE-1327).

22 drawings.

The inert gas, nonconsumable, button-type furnace is designed for melting and casting laboratory size quantities of reactor metal alloys. It produces homogeneous buttons of desired shape for fabrication. Unique features include a hydroformed copper dome that is effectively cooled to allow high power inputs and which is easily cleaned; interchangeable insert hearths; and a drop casting arrangement. A variety of cylindrical or rectangular shapes can be cast suitable for swaging, forging, or rolling. The tungsten electrode tip may be replaced with a consumable electrode, or a hollow tungsten tip for pseudoplasma melting of nonconducting materials. In operation, the furnace is evacuated and then backfilled to 350 to 500 mm of pressure with high-purity gas. The arc is struck and transferred to a Zr getter button located in a groove around the insert. The getter button removes small quantities of residual air and impurities introduced with the gas. The arc is transferred to the charge to form the button, which is melted several times on each side to insure homogeneity. Buttons are turned over by manipulation with the electrode without opening the furnace. The button mold is removed and the proper insert and mold installed when a drop casting is desired. Then the furnace is evacuated, backfilled and gettered, and the button is melted until the bottom is penetrated and the metal drains into the mold. Button and drop castings of crystal-bar Zr may be produced and also high-purity drop castings of alloys of Ti, Nb, Ta, Mo, etc., have been produced and fabricated into wire and sheet. (For details, see TID-4100.) (TCO)

16966 URANIUM MONOCARBIDE A NEW NUCLEAR FUEL CONCEPT FOR CANADA. Hueston, F. H. (Eldorado Mining and Refining Ltd., Port Hope, Ont.). 23p. (CONF-651019-2). ORAU. Gmelin, AED-CONF-65-294-2.

From 15th Canadian Chemical Engineering Conference, Quebec City.

Techniques for producing UC containing 4.90 ± 0.10 wt % C by prereaction of uranium oxides with graphite followed by skull arc melting and casting were developed. Oxide and graphite powders in 60 kg batches are blended into ½ in. dia spherical agglomerates, dried in air, and reacted at 2000°C in a vacuum to form primary UC. The relation between U/C ratio in the charge and that in the product is complex. Under the conditions used, the reaction will proceed in a satisfactory manner only if the product contains more than 4.55 wt % C. A combination of primary carbide and cast recycle in the ratio of 1:2 was successfully skull arc-melted and cast in a vacuum into ⅝-in. dia rods in 4 kg batches. C is picked up from the electrode so that small additions of U metal may be needed to control the product composition at 4.9% C. (auth)

Corrosion

16967 (AD-628277) FRACTOGRAPHIC ANALYSIS OF Ti-7Al-2Cb-1Ta AND Ti-6Al-4V FRACTURES DEVELOPED IN "WET" FATIGUE. Judy, R. W. Jr.; Crooker, T. W.; Morey, R. E.; Lange, E. A.; Goode, R. J. (Naval Research Lab., Washington, D. C.). July 26, 1965. 17p. (NRL-6330). CFSTI $1.00 cy, $0.50 mn.

Crack-growth-rate studies on Ti-7Al-2Nb-1Ta and Ti-6Al-4V alloys in low-cycle fatigue were performed in air and in a 3.5% salt-water solution. The Ti-7Al-2Nb-1Ta alloy was additionally tested in distilled water. An increase in crack-growth rate at all strain ranges was observed for Ti-7Al-2Nb-1Ta in the wet environments over that in the dry, whereas the Ti-6Al-4V alloys did not appear to be sensitive to a wet environment. At a strain range of 8000 to 9000 microinches/inch, corresponding to about 60% yield strength, the crack-growth rate of Ti-7Al-2Nb-1Ta alloy accelerated and became erratic. Fractographic studies show that the increase in crack-growth rate is due to a change from the ductile mode of fatigue fracture, usually found in dry low-cycle fatigue tests of titanium alloys, to the brittle quasi-cleavage mode of fracture-a fracture mechanism of stress-corrosion cracking. The amount of quasi-cleavage seen on the fatigued fracture surface generally corresponds to the crack-growth-rate increase; thus, it is indicative of the degree of stress-corrosion cracking sensitivity. (auth)

16968 (COO-1319-33) MICROTOPOLOGY OF STRESS-CORROSION CRACKING. A Preliminary Report. Smith, T. J.; Staehle, R. W. (Ohio State Univ. Research Foundation, Columbus). Dec. 1965. Contract AT(11-1)-1319. 71p. Dep. mn. CFSTI $3.00 cy, $0.75 mn.

A preliminary study of the interaction between thin foils and environments, conducted to understand the mechanisms of stress-corrosion cracking, is described. Four alloys

were selected for study: (Fe–15 Ni–20 Cr), (Fe–15 Ni–20 Cr–0.1 P), (Fe–15 Ni–20 Cr–1.5 Si), and (Fe–45 Ni–20 Cr). This selection was based on the known accelerating effects of and the retarding effects of Ni and Si on stress-corrosion cracking in stainless steel compositions. The dislocation structure of each alloy was varied by annealing, straining 5%, and aging. Thin film specimens were first examined in an electron microscope to find the characteristic dislocation structure, then exposed to boiling 42% $MgCl_2$, and finally examined again in the electron microscope. Additional observations were made on these films in ferric chloride, nitric acid, and acetic acid solutions. Observations are interpreted in terms of possible mechanisms of stress-corrosion cracking. (auth)

16969 (EURAEC–1579) THE RELATIONSHIP OF NITROGEN CONTENT OF AUSTENITIC STAINLESS STEELS TO STRESS CORROSION. Quarterly Report No. 438-6, October 1, 1965–December 31, 1965. (Virginia Polytechnic Inst., Blacksburg. Dept. of Metals and Ceramic Engineering). Jan. 1965. Contract AT(40-1)-3208. 17p. Dep. mn. CFSTI $1.00 cy, $0.50 mn.

Work Performed under United States–Euratom Joint Research and Development Program.

A N_2 concentration range of 0.06 to 0.09 % was obtained in wires of type 304 stainless steel by nitriding in different ratios of H_2-NH_3 at 1000°F for 24 hr. Nitrides were not metallographically observed in any of the wires. A dilatometer specimen holder was built and calibrated. (W.L.G.)

16970 (GEAP–4832) SODIUM MASS TRANSFER. XVI. THE SELECTIVE CORROSION COMPONENT OF STEEL EXPOSED TO FLOWING SODIUM. Brush, E. G. (General Electric Co., San Jose, Calif. Atomic Power Equipment Dept.). Mar. 1965. Contract AT(04-3)-189. 153p. Dep. mn. CFSTI $5.00 cy, $1.00 mn.

The partially selective corrosion of type 316 stainless in Na at 1100 and 1200°F contaminated with 12 ppM O_2 is such that Fe behaves nobly, that Mo is neutral, and that Cr, Ni, and Mn behave actively. This results in a compositionally-changed surface layer that is rich in Fe, unchanged in Mo and impoverished in Cr, Ni, and Mn in positions along isothermal flow paths where the Na solvent is unsaturated with respect to the alloying elements. In such regions no oxide film formation is observed and specimen corrosion behavior is characterized by weight losses. The compositional change results in a fcc to bcc transformation at some distance from the interface at an average concentration, of a given active element whose magnitude depends upon the nonlinear transient corrosion rates of Cr and of Ni. Alloy rate control is exerted in a Na boundary layer when the degree of alloying element unsaturation in Na is other than zero. The transformation to linear rate control is accompanied by a transformation from partially selective to full-stoichiometric corrosion behavior. That is, each element corrodes in direct proportion to its bulk alloy composition. This behavior is significant since it means that the compositional change can be ignored in corrosion rate studies, provided that linear rate control exists. At points along the flow path where Na, contaminated with 12 ppM O_2, becomes saturated with the metallic alloying elements, a mechanism change is observed. Cr now behaves nobly, Ni and Mo are neutral, and Fe and Mn behave actively. The mechanism is accompanied by oxide film formation and accompanying weight gains. (W.L.G.)

16971 (N–65–18444) EFFECT OF LOW-DENSITY INERT GAS FLUSH ON OXYGEN–COLUMBIUM REACTION AT 1500 TO 2000 DEG F. Final Quarterly Report. (Aero Vac Corp., Troy, N. Y.). Feb. 14, 1965. 21p. (NASA-CR–57138). CFSTI $1.00 cy, $0.50 mn.

A gas purification system containing a titanium foil getter and a molecular sieve absorption column was able to reduce the impurity content of all gases below 0.3 ppM with the exception of the CO peak. A two-stage magnetic deflection mass spectrometer was designed, constructed, and evaluated for its ability to detect and analyze impurities in a gas stream. A combination of the purification system and the analysis spectrometer was employed to obtain argon spectra at 7×10^{-5} and at 5.5×10^{-5} torr. Only a few peaks were found and full-scale sensitivity was approximately 2 ppM for the first, and 2.5 ppM for the second analysis, respectively. Sensitivities of 0.14 and 0.25 ppM, respectively, of water vapor were found. All spectra showed a peak corresponding to a mass to charge ratio of 16, which was attributed to electrons striking adsorbed oxides on the metallic surface. (STAR)

16972 (NASA-CR–54719) SNAP-8 MATERIALS SEMIANNUAL REPORT FOR JANUARY–JUNE 1965. Derow, H.; Farwell, B. E. (Aerojet-General Corp., Azusa, Calif.). July 1965. Contract NAS5-417. 70p.

Investigations were conducted in support of the design, fabrication, and development testing of various SNAP-8 components. Investigation of a mercury forced-convection corrosion loop was continued with the aim of evaluating the corrosion resistance of 9Cr–1Mo alloy steel (the reference mercury-containment material) for 10,000-hour service. Rubidium is being evaluated as an additive to the mercury to promote boiler conditioning. Data were developed in a continued program to evaluate the effect of the SNAP-8 operating environment on 9Cr–1Mo steel. (auth)

16973 (NASA-TN-D–3275) A STUDY OF SEVERAL OXIDATION-RESISTANT COATINGS ON Cb–10Ti–5Zr ALLOY SHEET AT 2000, 2400, AND 2700 DEG F. Lisagor, W. Barry; Stein, Bland A. (National Aeronautics and Space Administration, Langley Station, Va. Langley Research Center). Mar. 1966. 72p. CFSTI $3.00 cy, $0.75 mn.

Results of a study on the properties of Nb–10Ti–5Zr alloy sheet with 12 oxidation-resistant coatings are presented. Oxidation tests were performed in dry air at 2000, 2400, and 2700°F at atmospheric pressure and also at pressures of 0.5 and 0.05 torr. Mechanical property tests included room-temperature and elevated-temperature tensile tests on both uncoated and coated material before and after exposure and room-temperature bend tests on oxidation coupons before and after exposure. Test results indicate that an upper limit for protection of this alloy from oxidation is approximately 2400°F using modified silicide coatings containing Ti and Cr and that the usefulness of thin-gage coated Nb alloy sheet may be determined by substrate embrittlement rather than by oxidation. Comprehensive metallurgical examinations on as-coated and tested specimens were performed by using x-ray emission and diffraction techniques and electron-probe microanalyzer studies. Substrate thickness decreases due to solid-state diffusion during high-temperature exposures were determined. A possible embrittling mechanism for the coated Nb–10Ti–5Zr alloy sheet is postulated and supported by the metallurgical studies. (auth)

16974 (NP–15889) ULTRASONIC-INDUCED CAVITATION STUDIES IN MERCURY AND WATER. Technical Report No. 3. Garcia, R.; Nystrom, R. E.; Hammitt, F. G. (Michigan Univ., Ann Arbor. Lab. for Fluid Flow and Heat Transport Phenomena). Dec. 1965. 127p.

Ultrasonic-induced cavitation studies were conducted in mercury at 70°F and 500°F and in water at 70°F on a wide variety of materials, which included various refractory alloys, steels, brasses, coppers, etc. The detailed results are given. Comprehensive computer correlations of the cavitation damage data with applicable mechanical and fluid properties were carried out. (M.O.W.)

16975 (NP–15900) A COMPARISON OF THE EFFECTS OF URANIUM AND MOLYBDENUM ALLOYING ADDITIONS ON THE CORROSION RESISTANCE OF AISI TYPE 430 STAINLESS STEEL. Biefer, G. J.; Garrison, J. G. (Department of Mines and Technical Surveys (Canada). Mines Branch). Sept. 1965. 23p. (TB–74). Dept. of Mines and Technical Surveys, Ottawa $0.50.

To compare the effects of U and Mo alloying additions, laboratory corrosion tests were performed on AISI type 430 stainless steels containing 0.24 and 0.55% U, and 1.02 and 2.03% Mo. In comparison with a similar unalloyed steel, both additions brought about qualitatively similar improvements of corrosion resistance both in non-oxidizing sul-

furic acid and hydrochloric acid solutions and oxidizing ferric chloride solution. In these solutions, the corrosion resistance of the Mo-bearing steels was definitely superior to that of the U-bearing steels. In tests in boiling 65% nitric acid, the U-bearing steels and the steel containing 1.02% Mo showed excellent corrosion resistance, resembling that of the unalloyed steel. However, the steel containing 2.03% Mo showed extremely poor corrosion resistance in this medium. Anodic polarization measurements on the steels yielded results which appeared to correlate with the behavior of the steels in the corrosion tests in oxidizing solutions containing the chloride ion. The U content for maximum corrosion resistance appears to lie at 0.5% or less. It is therefore clear that Mo is capable of imparting greater improvements in corrosion resistance to AISI type 430 stainless steel than U, although higher levels of Mo are necessary to achieve this. (auth)

16976 CORROSION RESISTANCE OF STRUCTURAL MATERIALS IN BORON-CONTAINING SOLUTIONS. Belous, V. N.; Gromova, A. I.; Shapovalova, E. T.; Gerasimov, V. V. At. Energ. (USSR), 19: 546-9(Dec. 1965). (In Russian).

The corrosion behavior of stainless steel, titanium, aluminum, lead, and carbon steel was determined in solutions of boric acid, sodium tetraborate, and ammonium tetraborate at 20 and 100°C. The corrosion rate was calculated after removing the corrosion products from the sample. Stainless steel showed a high corrosion resistance of about 0.003 at 20°C and 0.019 g m^{-2} day^{-1} at 100°C after 500 hours of testing. Titanium showed about the same corrosion resistance as stainless steel. In boric acid solution saturated with air, the corrosion of carbon steel was 1.29 g m^{-2} day^{-1} after 500 hours of testing. The corrosion of carbon steel decreased to 0.012 g m^{-2} day^{-1} in alkaline solution. Aluminum possesses satisfactory corrosion resistance in boric acid (0.0156 at 20°C and 0.08 g m^{-2} day^{-1} at 100°C after 500 hours of testing). In the tetraborate solutions the corrosion of aluminum was an order of magnitude higher than it was in boric acid solution. The lead corrosion was 0.43 at 20°C and 0.29 g m^{-2} day^{-1} after 500 hours of testing. (TTT)

16977 THE BEHAVIOR OF COPPER DURING THE OXIDATION OF ZIRCONIUM–COPPER ALLOYS UNDER CARBON DIOXIDE. Guerlet, Jean-Paul; Lehr, Pierre (CNRS, Vitry, France). Compt. Rend., Ser. C, 262: 358-61(Jan. 24, 1966). (In French).

The oxidation of zirconium–copper alloys consists in a selective oxidation of the zirconium. The copper is surrounded in a metallic state in layers of monoclinic zirconia. (tr-auth)

16978 INTERACTION BETWEEN COLUMBIUM AND ALUMINA. Elyutin, V. P.; Lysov, B. S.; Mitin, B. S. Izv. Vyssh. Ucheb. Zaved., Chern. Met., No. 5, 145-7(1965). (In Russian).

An oxide-reinforced composite of Nb powder with 2 to 15% of Al_2O_3 powder was prepared by pressing and sintering in Ar at 1675 to 2275°K for 2 to 10 hr. Electrolytic dissolution of the composite and chemical determination of Al dissolved in Nb as a function of sintering temperature and time is described. The solubility of Al in Nb was found to be less than 1%. (Rev. Metal Lit.)

16979 THE CORROSION OF ZIRCONIUM AND ZIRCALOY-2 AT LOW TEMPERATURES. Cigna, R.; Leach, Llewelyn J. S.; Nehru, A. Y. (Imperial Coll. of Science and Tech., London). J. Electrochem. Soc., 113: 105-9 (Feb. 1966).

The aqueous corrosion of zirconium and Zircaloy-2 was studied as a function of electrode potential, solution pH, and temperature below 100°C. The influence of these variables and of alloying is considered in terms of their effect on the rate and the temperature dependence of corrosion. The relation between the corrosion process and the electronic conduction in the oxide is discussed. (auth)

16980 PHASE STUDIES OF HIGH-NIOBIUM-CONTENT Nb–Zr–O ALLOYS. Marcotte, V. C.; Larsen, W. L. (Ames Lab., Ames, Iowa). J. Less-Common Metals, 10: 229-36(Apr. 1966). (IS-1104).

The mechanism of oxygen addition to the niobium–zirconium alloys from 1 to 15 at. % zirconium was studied in the temperature range 1000–1200°C. The oxygen solubility was found to be less than 180 ppM. As the solubility limit was exceeded, either oxygen-saturated α-Zr or ZrO_2 precipitated, depending on the temperature and zirconium content. (auth)

16981 CHARGING ZIRCALOY-2 WITH HYDROGEN BEYOND THE SOLUBILITY LIMIT. Westerman, R. (Battelle Memorial Inst., Richland, Wash.). Contract AT (45-1)-1350. J. Nucl. Mater., 18: 31-8(Jan. 1966).

Samples of Zircaloy-2 coated with zirconium hydride were both held isothermally and thermally cycled. The maximum temperatures employed were in the vicinity of 400°C. After the treatments the hydrogen concentration of the bulk metal was determined. Long-term isothermal holding did not result in a hydrogen concentration greater than a characteristic terminal solubility. Thermal cycling resulted in hydrogen concentrations much greater than the characteristic terminal solubility, though the levels attained did not appear sufficient to explain the high hydrogen concentrations found in corrosion samples. Possible reasons for the supercharging effect are discussed. (auth)

16982 OXIDATION BEHAVIOR OF Nb AND Nb–V ALLOYS. Mukaibo, Takashi; Kanno, Masayoshi; Yamawaki, Michio (Tokyo Univ.). J. Nucl. Sci. Technol. (Tokyo), 2: 516-24(Dec. 1965).

Nb and Nb–V alloys are promising as high-temperature reactor materials. For this reason their oxidation behavior was studied in the temperature range 485 ~735°C. The specimens were prepared by electron-beam and arc melting. The work included kinetic studies of the oxidation as well as x-ray studies of oxide films. The oxidation reactions of Nb and Nb–V alloys were found to have a very peculiar temperature dependence. The complex oxidation behavior shown by the individual Nb and Nb–V alloys is suggested to be due to the formation of oxide layers with differing compositions in different temperature regions. The formation of a double oxide $NbVO_4$ was identified, and the structure was examined by x-ray diffraction. (auth)

16983 EFFECTS OF SILICON ON THE MECHANICAL PROPERTIES AND INTERCRYSTALLINE CORROSION TENDENCIES OF Cr–Ni–Mo ALLOY. Babakov, A. A.; Svistunova, T. V.; Chermenskaya, N. F. Metalloved. Term. Obrabotka Metal., 12: 6-10(1965). (In Russian).

It was attempted to reduce the intergranular attack of Hastelloy C by decreasing the Si content of the alloy below the usual 1% to a few hundredths of a percent. The alloy thus prepared exhibited a marked change in the secondary phases formed at the grain boundaries, resulting in a marked reduction of the intergranular attack after welding operations. The yield strength of the alloy was found to remain similar to that of the original composition. (TTT)

16984 LIQUID METAL–REFRACTORY REACTION STUDIES. Colligan, G. A.; Phipps, C.; Parille, D. Mod. Casting, 47: 134-43(June 1965).

Preliminary results of studies of the reactions between molten AMS 5350 steel, Inconel 713C alloy, and crucible and mold refractories are given. Optical microscopy, x-ray diffraction and x-ray fluorescent analyses were performed on refractories before and after immersion in molten AMS 5350 and Inconel 713C alloys. The effect of immersion temperature, time, and melting atmosphere are considered on the attack of these molten alloys on crucible and mold refractories. These refractories include alumina, fused silica, zirconium silicate and stabilized zirconia. The results of these investigations on air-melted AMS 5350 alloy indicate that Cr, Mn, and Fe in the oxide formed exhibit extensive attack by solution on all of the refractory materials with the exception of zirconia. (Rev. Metal Lit.)

16985 INVESTIGATION OF THE RATE OF OXIDATION OF METALLIC SCANDIUM. Naumkin, O. P.; Ignatov, D. V. Russ. Met. Mining, No. 5, 101-3(1964).

Oxidation of metallic Sc plates in air in a porcelain crucible from 300 to 900°C and determination of the oxidation rates by weight increments at various temperature points are reported. X-ray and electron diffraction analyses of the oxide film indicate that the film consists of a Sc_2O_3 phase with a substrate of ScN phase. Oxidation kinetics of rare earth metals in terms of their electron orbit structure is discussed. (Rev. Metal Lit.)

16986 A STUDY OF THE OXIDATION MECHANISM OF URANIUM IN MOIST, FLOWING NITROGEN AND IN NITROGEN–OXYGEN MIXTURES [Thesis]. Verink, Ellis Daniel Jr. Columbus, Ohio, Ohio State Univ., 1965. 94p.

The mechanism of oxidation of uranium in moist, flowing gases was studied at 75°C (P_{H_2O} = 33 mm Hg, flow rate 1200 ml/min). Purified nitrogen, oxygen, and nitrogen-oxygen mixtures were employed. In moist nitrogen the kinetic behavior was described by three successive time dependencies: logarithmic, $t^{\frac{1}{3}}$, and linear. The apparent activation energy was low, approximately 10 kcal/mole for each stage. Uranium hydride was formed as a transitory, intermediate product. The final oxidation product was $UO_{(2+x)}$. Hydride is formed at the metal-hydride interface, fed by hydrogen produced by the conversion of hydride to oxide at the hydride-oxide interface. The rate-controlling step is believed to be supply of oxygen ion to the hydride-oxide interface. In moist flowing oxygen, parabolic behavior was observed followed by $t^{\frac{1}{3}}$ time dependency. The oxidation rate was approximately $\frac{1}{20}$ that observed in moist nitrogen. Addition of oxygen to moist, flowing nitrogen inhibits the oxidation reaction. Chemical inhibition results from the combination of oxygen and the by-product hydrogen at the hydride-oxide interface to form water. This restricts the supply of hydrogen to the metal surface reaction. Water reacts with hydride to form a barrier of dense oxide. The effect of various methods of adding oxygen is reported. Electron optical methods correlate the morphology of reaction products with the kinetic data. Shift from coherent to non-coherent reaction products is illustrated. Evidence is presented that uranium is not the diffusing species. Special replication techniques permitted observation of the morphology of the rough outer oxide and of intermediate products at various depths below the surface. (Dissertation Abstr.)

16987 INITIAL OXIDATION OF TUNGSTEN AND TANTALUM [Thesis]. Rausch, Doyle William. Columbus, Ohio, Ohio State Univ., 1965. 125p.

An oxygen-beam technique was used to oxidize atomically clean tungsten and tantalum substrates in the field emission microscope at temperatures between 30 and 1500°C, and oxygen pressures between 10^{-8} and 10^{-4} torr. Many similarities were found in the initial oxidation of both metals. At substrate temperatures below ~500°C, oxidation is not observed. For substrate temperatures between 500 and 1300°C, the reaction on both metals is comprised of three stages: incubation, nucleation, and growth. Each stage is markedly dependent upon substrate crystallography and the preceding stage. Direct observations indicate that the predominant mechanism of oxidation at temperatures below which appreciable oxide evaporation is expected involves the precipitation of oxide microcrystals from supersaturated chemisorbed regions of the substrate. Since the supersaturation required for oxidation decreases as substrate temperature increases, nucleation kinetics have been described in a classical way. For substrate temperatures above ~1300°C, oxide microcrystals were not observed on either metal. (Dissertation Abstr.)

Fabrication

Refer also to abstracts 16328, 17009, 17593, and 17632.

16988 (CONF-650922, pp 305-12) MAGNET COIL FABRICATION. Zimmerman, Ben.

The fabrication and testing of magnet coils is discussed. Methods that will aid in the design of better and more economical coils are noted. (D.C.W.)

16989 (COO–1518-2) FABRICATION OF TUNGSTEN ALLOY TUBING. Progress Report, October 23, 1965–February 1, 1966. Sowman, H. G.; Milner, A.; Rowenhorst, D. D. (Minnesota Mining and Mfg. Co., St. Paul). Feb. 10, 1966. Contract AT(11-1)-1518. 8p. Dep. mn. CFSTI $1.00 cy, $0.50 mn.

Small dia W–26 at. % Re tubing and W–30 at. % Mo–30 at. % Re rod was fabricated by the plastic extrusion of mixtures of the elemental powders and organic binders followed by sintering. Both tubing and rod were ductile in the as-sintered condition. (auth)

16990 (EURAEC–1556) STAINLESS STEEL CLADDING OF HEAVY GAGE STEEL. Quarterly Report No. 5, July 1–September 30, 1965. (Neratoom, N. V., The Hague (Netherlands). Ghent Rijksuniversiteit (Belgium). Soudometal, S. A., Brussels (Belgium)). Contract 008-63-12 TEEB. 5p. (EUR–2697). Dep. mn. CFSTI $1.00 cy, $0.50 mn.

Work Performed under United States–Euratom Joint Research and Development Program.

An alloyed flux was developed that would give the low alloy steel base a composition comparable to AISI 308 stainless steel $\frac{1}{16}$ inch below the surface of the superimposed AISI 304 stainless steel tape. The development tests were performed on flat plates. When the tests were performed on rings, the slag formed by the flux was too fluid and solidified too slowly to be able to support a large molten pool on the curved surface. The effects of the welding parameters on the structure of the deposit was also investigated. (W.L.G.)

16991 (EURAEC–1557) STAINLESS STEEL CLADDING OF HEAVY GAGE STEELS. Quarterly Report No. 6, October 1–December 31, 1965. (Neratoom, N. V., The Hague (Netherlands). Ghent Rijksuniversiteit (Belgium). Soudometal, S. A., Brussels (Belgium)). Contract 008-63-12 TEEB. 5p. (EUR–2698). Dep. mn. CFSTI $1.00 cy, $0.50 mn.

Work Performed under United States–Euratom Joint Research and Development Program.

The mineral composition of the welding flux was changed to give a more viscous slag that would solidify faster and possess a larger surface tension than the flux previously developed. The flux performed satisfactory on flat plates inclined at varying slopes in the direction of welding. The flux will be tested on rings during the next report period. (W.L.G.)

16992 (RPI–2408-4) STUDIES OF SINTERING. Annual Report, [1965]. Lenel, Fritz V. (Rensselaer Polytechnic Inst., Troy, N. Y.). Mar. 1966. Contract AT (30-1)-2408. 38p. Dep. mn. CFSTI $2.00 cy, $0.50 mn.

The procedure for preparing compacts of two or three wires of a silver alloy containing homogeneously dispersed alumina particles is described. The alumina particles act as inert markers. Metallographic inspection of the necks formed between the wires during the initial sintering stage revealed the presence of alumina particles. The rest of the neck filled in with silver as sintering progressed. It is proposed that material transport due to dislocation motion occurred during the early stages of sintering followed by diffusional flow. Spheres of calcium fluoride containing a fine dispersion of stabilized zirconia as markers were sintered on a calcium fluoride plate, which also contained markers, under different externally applied stresses. A sample sintered without an external load showed an area in the neck without markers. In contrast, a sample sintered under pressure showed markers throughout the neck, which also had a considerably larger diameter. Attempts to observe the sintering of ultrafine particles directly under an electron microscope were unsuccessful. (W.L.G.)

16993 (Y-DA–1043) THE ROLE OF POWDER METALLURGY IN THE FABRICATION OF VERY LARGE PARTS. Neeley, A. C.; Googin, J. M.; Asbury, J. J.

(Union Carbide Corp., Oak Ridge, Tenn. Y-12 Plant). Feb. 18, 1966. Contract W-7405-eng-26. 10p. (CONF-660402-2). Dep. mn. CFSTI $1.00 cy, $0.50 mn.

For Presentation at American Society of Tool and Mfg. Engineers, Annual Conference and Tool Show, Detroit.

The fabrication of a lithium hydride reactor shield, a tungsten crucible weighing 1700 lbs, and an aluminum oxide insulator measuring 70 in. in length and 23 in. in dia is described. Each component illustrates the application of basic powder metallurgy techniques that are equally applicable to metal or ceramic powders. (W.L.G.)

16994 KIRKENDALL-EFFECT DENSIFICATION IN A SINTERED TUNGSTEN–MOLYBDENUM POWDER COMPACT. Bradt, R. C.; Lenel, F. V.; Ansell, G. S. (Rensselaer Polytechnic Inst., Troy, N. Y.). Acta Met., 14: 553-4(Apr. 1966).

A layered powder compact was prepared by first pressing a layer of pure Mo powder and then on top of it another layer of a 50/50 wt % mixture of Mo and W powders. This layered compact was then induction sintered in H_2 at 2350°C for 12 hr. Metallographic results showed a densification on the W-rich side and increased porosity on the Mo-rich side of the interface. The faster diffusing Mo caused an increased vacancy concentration on the Mo-rich side of the interface and these vacancies precipitate on the existing pores in the Mo, making them larger and the porosity greater there. On the W-rich side of the interface, the existing pores act as vacancy sources, causing the porosity to disappear.

16995 FUEL CORES FOR PLATE FUEL ELEMENTS. Eschnauer, H.; Wolf, A. Atomwirtschaft, 11: 82-5(Feb. 1966). (In German).

The preparation of fuel cores from uranium–aluminum alloys with highly enriched uranium necessitates very meticulous precautions because of the high material values. The aluminum for fuel and cladding must satisfy rigid specifications. Analyses, mechanical values, and weight are bound to strict tolerances whose maintenance necessitates numerous controls. These are indicated. (tr-auth)

16996 PLUTONIUM-CONTAINING FUEL. Nater, K. A. Atoomenergie Haar Toepass., 8: 1-8(Jan. 1966). (In Dutch).

The fabrication of plutonium-containing fuel elements is described and the advantages of plutonium fuel are discussed. Plutonium can be alloyed with other metals; the most important compounds are discussed. (tr-auth)

16997 SLIP CASTING OF POWDERED CARBIDES. Sakwa, W.; Lesniak, Ch. Giesserei Praxis, No. 8, 157-61(Apr. 25, 1965). (In German).

Production of hard carbide parts of complex configuration from WC by slip casting is described. The mixture used in the tests (WC–6% Co) was selected as the most promising for industrial applications from a series including WC–11% Co, WC–16% TiC–6% Co, WC–14% TiC–8% Co, WC–5% TiC–8% Co. Optimum results were achieved with water as the suspension medium, a pH value of 8.4 to 9.5 for the casting mixture (controlled by the addition of HCl or NH_4OH) and a maximum peptizer (sodium alginate with 9% humidity and 13% ashes) content of 0.2%. The alginate tends to cause porosity, reduce the specific weight of the casting and promotes the formation of inclusions. The mixture was ground in a ball mill for 2 hr and sintered in hydrogen at 1380°C for 1.5 hr. In addition to complex castings the method is suitable for the production of composite and bonded parts with a dimensional tolerance of ±1% of nominal. (Rev. Metal Lit.)

16998 REFRACTORY ALLOY TUBING FOR SPACE POWER SYSTEMS. Buckman, R. William Jr.; Godshall, John L. (Westinghouse Electric Corp., Large, Pa.). Contract AT(30-1)3108. Metal Progr., 89: No. 3, 105-10 (Mar. 1966).

Tubing of B-66 niobium alloy and T-111 tantalum alloy was produced by extruding, rocking, and cold drawing to final size. The properties compare with those for sheet of the same grades. (auth)

16999 A 400-TON COPPER VACUUM TUBE. Blank, Howard A. (American Metal Climax, Inc., New York). Metal Progr., 89: No. 3, 111-16(Mar. 1966).

At the Stanford Linear Accelerator Center, 172,000 oxygen-free copper disks and cylinders were brazed together to form a 10,000 ft waveguide. (auth)

17000 RETORT FURNACE ANNEALS AND BRAZES 266,000 COMPONENTS. Eldredge, Arnold L. (Stanford Linear Accelerator Center, Calif.). Metal Progr., 89: No. 3, 117-22(Mar. 1966).

Production of components of Stanford's linear accelerator continues successfully even after more than 3750 heating cycles in the same furnace. The specially designed pit furnace employs an electrically heated Inconel retort to anneal and braze the components in a protective atmosphere. (auth)

17001 DUCTILITY OF METALLIC URANIUM CONTAINING CARBIDE INCLUSIONS AT ROLLING. Watanabe, Hitoshi (Japan Atomic Energy Research Inst., Tokyo). Nippon Genshiryoku Gakkaishi, 8: 70-5(1966). (In Japanese).

In order to study the effects of nonmetallic inclusions, especially carbides, on the formability of metallic uranium, commercially pure U and U containing 1,000 ppM of carbon were compared as to their rolling characteristics and microstructure. On rolling at 300°C with 12 and 19% reduction per pass, the mean specific rolling pressures were 40 and 52 kg/mm^2 for commercially pure U specimens, but 59 and 61 kg/mm^2 for the U containing 1,000 ppM. On rolling at 600°C with 33% reduction per pass, however, the mean specific rolling pressure of the commercially pure U specimens was the same as that of the U containing 1,000 ppM, about 20 kg/mm^2. This result served to explain the greater ductility of the U matrix observed at higher temperatures. (auth)

17002 EXPERIENCES IN DEVELOPING OF PRODUCTION METHODS FOR REACTOR-GRADE GRAPHITE. Secerov, Mileta; Milicic, Miodrag. Nukl. Energ., No. 4, 2-6(1965). (In Slovak).

Experience in the development of technological procedures for production of reactor-grade graphite and methods for determining the characteristic properties of graphite are discussed. Production of reactor-grade graphite by chemical treatment of natural graphite, by pyrolytic methods from different organic compounds rich in carbon, and from petroleum coke is described. The greatest possibilities were found in the procedure that uses petroleum coke as its starting material. (M.C.G.)

17003 DEFORMED Zr–Ti–O–Fe ALLOY FOR HIGH-PRESSURE CHAMBERS. Shchegoleva, R. P.; Golubeva, L. S.; Litvin, D. F.; Ponyatovskii, E. G.; Zhirkin, Y. N. (Central Scientific-Research Inst. of Ferrous Metals, USSR). Porosh. Met., Akad. Nauk Ukr. SSR, No. 12, 45-7 (Dec. 1965). (In Russian).

A sintered, deformed alloy Zr–Ti–O–Fe designed for use with high-pressure chambers during neutronographic investigations of materials was fabricated. The alloy has a composition corresponding to the zero amplitude of coherent scattering for neutrons (53% Zr, 44.95–43.8% Ti, 0.25–0.40% O and 1.0–2.0% Fe) and to the structure of an unordered solid solution. The ultimate strength of the forgings is 130–150 dan/mm^2. (auth)

17004 PREPARATION OF THIN LAYERS OF ZIRCONIUM CARBIDE BY THE USE OF ELECTROPHORESIS. Savitskaya, Ya. S.; Ekimenko, T. M.; Zhivulina, L. I. Zh. Prikl. Khim., 38: 2222-6(Oct. 1965). (In Russian).

It was found that a thin layer of ZrC (80 to 100 μ) could be deposited on a metal backing using absolute ethyl alcohol (80 ml) as the dispersion medium, 20 g of ZrC powder with a particle size of 2 to 20 μ, and 0.5 to 2 ml of a 5% $HfCl_4$ solution in absolute alcohol to create a charge on the surface of the particle. It was found that the ZrC particle has a positive charge. The best coatings of ZrC were obtained at an electrokinetic potential (ξ-potential) of 19 to 20 mv. An electrode voltage of 30 to 40 volts was optimum. The

coating thickness could be controlled by regulating the time of deposition and the ξ-potential. Conditions could be reproduced to obtain strong, smooth coatings of ZrC. (TTT)

17005 STUDIES IN THE UO_2–ZrO_2 SYSTEM [Thesis]. Wright, Thomas Rea. Columbus, Ohio, Ohio State Univ., 1965. 70p.

In an attempt to develop a solid solution-type nuclear fuel, a selected composition in the UO_2-ZrO_2 system was investigated to determine its fabrication parameters, physical properties, and phase relationship over a defined range of composition and temperature. Densification and homogenization of compacted ball-milled powders were accomplished by sintering from 10 to 15 hr at 1700°C in flowing dry hydrogen. Homogeneous fuel pellets with densities in excess of 97 per cent of theoretical were obtained for property studies. The thermal conductivity of the 50 mole per cent UO_2–50 mole per cent ZrO_2 composition was found considerably lower than that of UO_2 but higher than that of ZrO_2. The linear thermal expansion curve roughly paralleled that of pure UO_2, at a slightly higher value, over the temperature range measured. Electrical resistivity decreased with increasing temperature, as is typical of a ceramic material. In tests of UO_2–20 to 50 mole per cent ZrO_2 compositions, in general, both room-temperature and high-temperature hardness values increased as the ZrO_2 content increased. Homogeneous UO_2–50 mole per cent ZrO_2 pellets were more resistant to cracking under thermal cycling than were inhomogeneous pellets of the same composition. Phase relationships in the UO_2-ZrO_2 system up to 50 mole per cent ZrO_2 were evaluated to determine, as a function of temperature, the equilibrium phases present and the solubility limits of ZrO_2 in UO_2. At 1000°C or above it was found that at low ZrO_2 contents, a single-phase, face-centered-cubic, solid-solution region is present. At ZrO_2 contents greater than 13.5 mole per cent, a two-phase, face-centered-cubic, face-centered-tetragonal region exists at 1000°C. This two-phase region disappears above 1750°C. (Dissertation Abstr.)

Properties and Structure

See also CHEMISTRY — Inorganic and Physical Chemistry
PHYSICS — Solid State Physics

Refer also to abstract 17589.

17006 (AAEC/TM–300) LINEAR THERMAL EXPANSION OF BERYLLIA. Turner, D. N.; Smith, P. D. (Australian Atomic Energy Commission Research Establishment, Lucas Heights). Sept. 1965. 12p. Dep. mn.

Thermal expansion data for beryllia in the temperature range 20–1000°C were obtained by a dilatometric method. Expansion could be expressed to 95% confidence by the expression: % Expansion = 5.86×10^{-4} (T–20) + 4.82×10^{-7} $(T-20)^2 - 1.39 \times 10^{-10}$ $(T-20)^3 \pm 1.44 \times 10^{-2}$ where T is temperature in °C. Sources of error are discussed and comparisons are made with published data. (auth)

17007 (AD–627468) CRYSTAL CHEMISTRY STUDIES. Quarterly Report No. 2, August 13–November 13, 1965. Roy, Rustum; Kachi, S.; McCarthy, G. J.; Muller, O.; White, W. B. (Pennsylvania State Univ., University Park. Materials Research Lab.). Jan. 1966. Contract DA28-043-AMC-01304(E). 32p. CFSTI $2.00 cy, $0.50 mn.

Studies on the crystal chemistry of a series of rare earth–rhenium oxide compounds resulted in the identification of 6 new phases by x-ray and electron probe analysis. Studies on the binary system V–O were completed, and 5 out of 7 intermediate stable phases were found to behave like antiferromagnetic materials, having different Neel points. Methods such as reduction of sesquioxides, oxidation of metals and reaction of metal with sesquioxides were tried in attempts to synthesize SmO and EuO. SmO was successfully prepared by the latter method. (P.C.H.)

17008 (CEA-R–2820) ETUDE DE L'INTERACTION DE PAIRE DANS QUELQUES METAUX NORMAUX [THESES]. (A Calculation of the Pair-Interaction Function in some Normal Metals [Thesis]). Pick, Robert (Commissariat a l'Energie Atomique, Saclay (France). Centre d'Etudes Nucleaires). 1965. 79p. Dep. mn.
Submitted to Paris Univ., France.

The effective pairing interaction between ions in Al, Li, K, and Na was calculated by a second-order perturbation expansion of the wave functions of the conduction electrons. A self-consistent pseudopotential was used. It was shown that the pair interaction function is correctly given to the pseudopotential. (D.C.W.)

17009 (CONF-650922, pp 287-96) SPECIFYING MAGNET STEELS. Marcantonio, Arthur.

The variation of the magnetic properties of low-carbon flat-rolled steel with composition and processing techniques was investigated. (D.C.W.)

17010 (CONF-650922, pp 297-304) TESTING STEELS FOR GRADIENT MAGNETS. Elarde, Paul F.

An electronic hysteresigraph combined with a Babbitt permeameter was used to determine the magnetic properties of steels for use in gradient magnets. The equipment and techniques are described. (D.C.W.)

17011 (CONF-651025–14) CREEP-RUPTURE PROPERTIES OF RHENIUM AND SOME ALLOYS OF RHENIUM AT ELEVATED TEMPERATURE. Flagella, P. N.; Tarr, C. O. (General Electric Co., Cincinnati, Ohio. Nuclear Materials and Propulsion Operation). [1965]. Contract AT(40-1)-2847. 17p. (GE-TM–65-9-12). Dep. mn. CFSTI $1.00 cy, $0.50 mn.

From Symposium on Physical Metallurgy of Refractory Metals, French Lick, Ind.

The stress-rupture and linear creep rate vs stress curves for unalloyed wrought sintered Re show a concave downward curvature when plotted on logarithmic coordinates. This may be related to the high rate of work-hardening required for Re. For the lower stresses at any temperature, the material is less creep-resistant than a linear relation would indicate. At temperatures of 1600, 2200, 2600, and 2800°C, the short-time rupture life for Re is greater than that for arc-cast W. In more prolonged tests, however, the rupture stress of W is greater for identical time periods. Varying the fabrication processing method has a significant effect on the rupture life and the ductility at temperature for W–25Re, although no significant effect was observed on the linear creep rate. Above 1600°C, the larger the grain size, the more ductile the material. Arc-melted material gives the largest grain size and is more ductile as shown in tests at 2200°C. At 1600°C, the ductility is less for larger grain sizes. As with unalloyed Re, the W–25Re alloy developed stress-rupture and linear creep rate vs stress curves with a concave downward curvature on log–log plots. The addition of 50 wt % Re to Mo increases the rupture life and creep resistance over unalloyed arc-cast Mo. The stress-rupture life and creep rate are linear with stress on a log–log plot over the stress range of 2000 to 6000 psi at 1600°C, and 750 to 1000 psi at 2200°C. (auth)

17012 (DRI–1092-226) PHASE EQUILIBRIA OF THE TANTALUM-RICH REGION OF THE TANTALUM–TUNGSTEN–HAFNIUM AND TANTALUM–TUNGSTEN–ZIRCONIUM SYSTEMS. Final Report, September 1, 1964–November 30, 1965. Klodt, Donald T.; Yamamoto, Albert S. (Denver Research Inst., Univ. of Denver, Colo.). Dec. 31, 1965. Contract AT(11-1)-1092. 27p. (DRI–2296). Dep. mn. CFSTI $2.00 cy, $0.50 mn.

The solid-state phase equilibria in the Ta-rich regions of the Ta–W–Hf and Ta–W–Zr alloy systems were investigated at 1600 and 1100°C. Alloys included in the investigation were in the compositional range from 100% Ta up to a maximum of 25 wt % each of W and Hf or W and Zr. The extent of the terminal solid-solution region in each system was investigated for the two isothermal levels and

data are presented as portions of isothermal sections. In the Ta–W–Zr system the maximum solid solubility of Zr and W are both less than 10 wt % in the terminal Ta-rich solid solution at 1600°C and less than 5 wt % at 1100°C. At compositions greater than these amounts a two-phase field of the solid-solution phase and beta-Zr phase exists. The solid solubility of the combined Hf and Ta additions in the Ta-rich solid solution is greater than 10 wt % at 1600°C. A two-phase field of the solid-solution phase plus a phase tentatively identified as W_2Hf exists at greater compositions of W and Hf. X-ray diffraction data for alloys annealed at 1600°C in both systems are presented. (auth)

17013 (INR–632/XIV/PS) APPARATUS FOR INTERNAL FRICTION AND YOUNG'S MODULI MEASUREMENTS IN KILOCYCLE RANGE. Malinowski, W. (Institute of Nuclear Research, Warsaw (Poland)). May 1965. 14p. Dep.

The equipment for internal friction and Young's Moduli measurements is based on the principle of the 3-component quartz resonator method. This method gives the possibility of the evaluation of the amplitude dependent decrements over a wide range of strain amplitudes. The equipment permits to lead continuous measurements in the temperature range from –150°C to room temperature and to about 800°C. The measurements indicate a good behavior and stability of electronic circuits during investigations. (auth)

17014 (INR–645/XIV/PS) NIEKTORE WLASNOSCI OBROBIONEGO CIEPLNIE STOPU U–Mo 1 PERCENT CIEZ. (Some Properties of U–1 wt. percent Mo Alloy after Thermal Treatment). Hofman, A. (Institute of Nuclear Research, Warsaw (Poland)). 1965. 11p. Dep.

Influence of the thermal treatment on the structure and the mechanical properties of U–1 wt % Mo was investigated. The behavior of this alloy under thermal cycling was examined. The experiments showed that by using an appropriate thermal treatment the required structure $\alpha + \gamma$ of the alloy can be obtained. The additions of the Mo improved the mechanical properties and dimensional stability of the alloy under cyclic temperature changes. (auth)

17015 (INR–665/II/PS) A NEUTRON-DIFFRACTION INVESTIGATION OF SOME IRON–TUNGSTEN CARBIDES. Bojarski, Zbigniew; Leciejewicz, Janusz (Institute of Nuclear Research, Warsaw (Poland)). Nov. 1965. 13p. Dep.

The crystal structures of two carbides with the composition Fe_3W_3C and Fe_6W_6C occurring in the ternary system Fe–W–C were redetermined by neutron diffraction. The atomic parameters were refined by the method of least-squares using a computer. A detailed discussion of the crystal structures of both phases is presented. (auth)

17016 (IS–1175) SOLID SOLUBILITY OF SOME GOLD-RICH-RARE-EARTH AND LANTHANIDE-RICH MAGNESIUM ALLOYS. Rider, P. E.; Joseph, R. R.; McMasters, O. D.; Gschneidner, K. A. Jr. (Ames Lab., Iowa State Univ. of Science and Tech.). May. 26, 1965. Contract W-7405-eng-42. 10p. (CONF-650804–2). Dep. mn. CFSTI $1.00 cy, $0.50 mn.

From 8th Rare Earth Research Conference, Ames, Iowa.

The solid solubilities of the rare-earth metals in gold and of magnesium in the lanthanide metals were studied and the observed behaviors were correlated with the Hume-Rothery and Darken-Gurry rules governing solid solution formation. The experimental data can be correlated with these rules provided the modification of the sizes and electronegativities of the solutes as they are placed into the solvent matrix are taken into account, and for the magnesium alloys if we compare the data at some convenient homologous temperature. (auth)

17017 (JPL-TR–32–889) ANALYSIS OF HIGH-TEMPERATURE CREEP IN PYROLYTIC CARBON. Kotlensky, W. V. (Jet Propulsion Lab., Calif. Inst. of Tech., Pasadena). Feb. 15, 1966. 9p.

Data on short-time high-temperature tensile creep parallel to the substrate for two pyrolytic carbons (pyrolytic graphites) characterized by their microstructures as substrate nucleated (SN) and regeneratively nucleated (RN) were analyzed by means of the Dorn method. Over the range of approximately 1.5 to 10% creep strain for the SN material and for creep strains above 1.5% for the RN material, the creep data were found to fit the empirical relationship $\epsilon = A + Bt^n$, where ϵ is the creep strain, t is the time, n is a constant that depends on the material, and A and B are parameters that depend on both the material and the test conditions. The SN material was characterized by n = 0.60, while the RN material had n = 0.42. The same apparent activation energy of about 250 kcal/mole was calculated for both of these carbons. As assumed in the analysis, the structural change that occurs during creep was found to be dependent on the total creep strain, and the same structure was developed at a given load for the same strain, independent of test temperature. These structural changes are discussed briefly with reference to the deformation mechanisms. (auth)

17018 (LRP–20/66) BERYLLIUM PRESSURE BAR HAVING A SUBMICROSECOND RISETIME. Jones, Ieuan R. (Laboratoire de Recherches sur la Physique des Plasmas, Lausanne (Switzerland)). Feb. 1966. 15p. Dep. mn.

The theoretical response of a pressure bar gauge to step-pressure loading was examined experimentally. Theory predicts that a pressure bar constructed from beryllium should have a risetime substantially faster than that of any previous pressure bar gauge described in the literature. Such a gauge was constructed and subjected to step-pressure loading; the time taken for the output signal to increase from 10 to 90% of its final steady value was 0.54 μsec. (auth)

17019 (N–65–17873) RESEARCH ON THE MAGNETIC AND ELECTRICAL PROPERTIES OF SELECTED MATERIALS UNDER EXTREME ENVIRONMENTAL CONDITIONS. Final Report. Moulton, William G. (Alabama Univ., University. Dept. of Physics). Dec. 22, 1964. Contract NAS8-2474. 15p. (NASA-CR–60950). CFSTI $1.00 cy, $0.50 mn.

Single crystals of $PrCl_3$ were prepared and usual parameters of the nuclear quadrupole interactions with the crystal and the orientation of the principles axes of the field gradient tensor determined. The field gradient computed for various Cl positions, is reported. Crystal structure of $PrCl_3$, observed transition frequencies of ^{35}Cl in a field of 1062.7 oersteds, and the frequency shift with temperature are also included. (STAR)

17020 (N–65–18466) DEPOSITION OF TUNGSTEN BY REDUCTION OF THE HEXAFLUORIDE WITH HYDROGEN IN THE VAPOR PHASE. Quarterly Report, November 1, 1964–February 1, 1965. Connor, Jean H.; Brenner, Abner ((National Bureau of Standards, Washington, D. C.). Mar. 12, 1965. Contract AF33(615)-64-1004. 4p.

The evaluation of physical properties of vapor-deposited tungsten was continued. Measurements on hardness and stress are reported. The microhardness of the tungsten samples ranged around 600 knoop with the exception of deposits obtained at 500°C from a mixture of 1.5 H_2 to one WF_6, where the determinations were 850 and 1000 knoop. The deposits obtained above 800°C were not satisfactory for hardness measurements because they consisted primarily of dendrites. With some exceptions, the stress appears to be about 25,000 to 33,000 psi regardless of plating conditions. (STAR)

17021 (N–65–18607) HEMISPHERICAL SPECTRAL EMITTANCE OF ABLATION CHARS, CARBON, AND ZIRCONIA TO 3700 DEG K [Thesis]. Wilson, R. Gale (National Aeronautics and Space Administration, Langley Station, Va. Langley Research Center). Mar. 1965. 30p. (NASA-TN–D–2704). CFSTI $2.00 cy, $0.50 mn.

The initial results of the application of special optical techniques to high-temperature emittance and reflectance studies of an ablation-material char and certain other refractory materials representative of those present in

ablation residues formed during aerospace reentry operations are presented. Spectral hemispherical emittance and reflectance were determined with an image pyrometer integrated with an arc-imaging furnace for carbon, graphite, zirconia, and a phenolic–nylon ablation-material char at wavelengths from 0.37 to 0.72 μm for temperatures from 2100 to 3700°K. Surface-roughness properties of the materials studied were determined from measurements made with a light-section microscope. The dependence of the spectral hemispherical emittance of oxidized carbon at a wavelength of 0.65 μm on its surface-roughness properties was investigated experimentally and the emittance was found to be a linear function of the root-mean-square slope of the surface when the roughness is large compared with wavelength. (auth)

17022 (N–65–18933) HIGH-TEMPERATURE ELECTRICAL PROPERTIES OF INSULATORS AND THEIR COMPATIBILITY WITH REFRACTORY METALS. Summary Report. Havell, Richard F.; Holtz, Frederick C. (IIT Research Inst., Chicago, Ill.). Mar. 3, 1965. Contract NAS3-4104. 169p. (NASA-CR-54125; IITRI-B6016-17). CFSTI $5.00 cy, $1.00 mn.

The d-c resistances of alumina, magnesia, beryllia, and boron nitride were determined in tests between 1100 and 1600°C in nitrogen, hydrogen, and vapors of mercury and cesium. Using the two-probe technique, current measurements were made with tungsten electrodes at voltages between 0 and 180 v d-c over periods of a few hours to 100 hours. The mechanical properties and electrical resistance of tungsten, tantalum, molybdenum, TZM, and Ta–10W were measured after the metals were heated in contact with the above insulator materials in various atmospheres and vacuum, both with and without an applied d-c voltage. These tests were run at elevated temperatures for periods of a few hours to 98 hours. (auth)

17023 (ORNL-TM-1161, pp 208-24) ELECTRON OPTICAL STUDY OF THE EFFECT OF AGING ON CARBIDES IN A NIOBIUM–TUNGSTEN–ZIRCONIUM ALLOY. Willmarth, T. E. (Oak Ridge National Lab., Tenn.).

The kinetics of the aging reaction are explained by illustrating the morphological changes in the carbides, both physical and chemical, taking place during the process. The study indicates that significant transformations are initiated at very early stages of aging, possibly even before 5 minutes. These proceed markedly up to approximately 50 hours, and at this point stabilization of the microstructure is almost complete. (W.L.G.)

17024 (ORNL-TM-1161, pp 236-46) A STUDY OF MICRO-CONSTITUENTS IN INCOLOY 800. Boyko, E. S.; Owens, C. M. (Westinghouse Electric Corp., Pittsburgh, Pa. Atomic Power Div.).

Weld metal cracking encountered in the fabrication of Incoloy 800 components for use in sodium steam generators and fuel rod cladding is related to chemical composition and microconstituents. Precipitates occurring in 2 heats of Incoloy 800 were examined by standard light and electron microscopy techniques and identified by x-ray and electron diffraction. $Cr_{23}C_6$, TiN, and TiC were observed to precipitate in the grain boundaries and matrix of Incoloy 800. The formation of TiC in preference to $Cr_{23}C_6$ due to a higher percentage of Ti appears to refine grain structure and improve weldability. (auth)

17025 (ORNL-TM-1424) ESTIMATED THERMAL CONDUCTIVITY VALUES FOR SOLID AND LIQUID PROMETHIUM. Williams, R. K.; McElroy, D. L. (Oak Ridge National Lab., Tenn.). Mar. 1966. Contract W-7405-eng-26. 34p. Dep. mn. CFSTI $2.00 cy, $0.50 mn.

Using the theory of heat conduction in liquids and the known behavior of other rare-earth elements and metallic melts, the thermal conductivity of liquid promethium is estimated to lie between 0.1 and 0.25 w/cm-°C at the melting point (1080°C) and between 0.1 and 0.36 w/cm-°C at 2000°C. Estimates of the electrical resistivity and thermal conductivity of solid promethium and the self-diffusion coefficient and atomic volume of liquid promethium were also obtained during the course of the survey. (auth)

17026 (RT/ING–(65)17) UNA MISURA DELLA RESISTIVITA ELETTRICA DEL SODIO AD ELEVATA TEMPERATURA: PER LA VERIFICA DELLA LEGGE DI WIEDEMANN-FRANZ-LORENZ. (Electrical Resistivity Measurement of Sodium at Elevated Temperatures, Verification by the Wiedemann-Franz-Lorenz Law). Evangelisti, R.; Isacchini, F. (Comitato Nazionale per l'Energia Nucleare, Rome (Italy)). Nov. 1965. 29p. Dep. mn.

The experimental apparatus adopted for the sodium electrical resistivity measurement in the temperature range 100–1000°C is described. After a short examination of the main characteristics of the measurement method chosen, a detailed analysis is made on the different factors determining the total error which affects the results of the experiment. On the basis of such a valuation the approximation degree of the Wiedemann-Franz-Lorenz equation in the case of liquid sodium is then examined. (auth)

17027 (TID–22712) EFFECTS OF NEUTRON DAMAGE ON THE MECHANICAL PROPERTIES OF PYROLYTIC AND SINGLE CRYSTAL GRAPHITE. Semiannual Progress Report, July 1, 1965–December 21, 1965. Meers, J. T. (Union Carbide Corp., Parma, Ohio. Carbon Products Div.). Feb. 25, 1966. Contract AT(40-1)-3237. 40p. Dep. mn. CFSTI $2.00 cy, $0.50 mn.

The problem of measuring the stress-strain curve for graphite single crystals subjected to basal plane shear was investigated, and the behavior of single crystals under basal plane shear is described and compared with that of the compression-annealed pyrolytic graphite. Work was continued on the production and evaluation of compression-annealed pyrolytic graphite. A careful analysis was made of the optical reflectivity method of measuring the c-axis misorientation of the pyrolytic graphite. Calculations were made to determine the feasibility of measuring c_{13} on compression-annealed pyrolytic graphite; with present measuring techniques, a reliable value of c_{13} probably cannot be obtained directly from experiment. (auth)

17028 (TID–22733) EFFECTS OF NEUTRON DAMAGE ON THE MECHANICAL PROPERTIES OF PYROLYTIC AND SINGLE-CRYSTAL GRAPHITE. Annual Progress Report, April 1, 1964–June 30, 1965. Meers, J. T. (Union Carbide Corp., Parma, Ohio. Carbon Products Div.). Feb. 1, 1966. Contract AT(40-1)-3237. 102p. Dep. mn. CFSTI $4.00 cy, $0.75 mn.

Work on the production, characterization, and measurement of the mechanical properties of unirradiated graphite single crystals, as-deposited pyrolytic graphites, and pyrolytic graphites, which were compression annealed to align the crystallite c-axes, is summarized. Several methods of growing graphite single crystals and several combinations of compression annealing conditions were tried. Material characterization included x-ray methods, optical and electron microscopy, interferometry, and an optical reflectivity technique. A tensile test and shear test for single crystals were devised, and values for shear strengths were obtained from the latter test for natural graphite crystals. Tension and compression stress-strain tests, using resistance strain gages, were made on both as-deposited and compression-annealed pyrolytic graphite. Static torsion tests were also made on both types of pyrolytic graphite. Shear strengths of compression-annealed pyrolytic graphite were obtained by compression-shear tests in addition to results obtained by using the torsion apparatus and the single crystal shear apparatus. Elastic constants were also obtained by the sonic resonance of long thin bars and compound oscillators consisting of graphite specimens with metal end pieces. For the resonant bar method, Timoshenko's equation for the flexural vibrations of a long thin bar was solved, and the solution was used to compute the value of one modulus from the measured resonant frequency and a known value of the other modulus. To make this computation economical for a large number of bars, a program was written for a digital computer. Ultrasonic tests were performed for the determination of two of the elastic constants and their stress dependence. A complete set of elastic compliance and stiffness constants was obtained for as-deposited unirradiated compression-

annealed pyrolytic graphite. An analysis of the data was made to define the limits of accuracy in the data and to deduce a self-consistent set of elastic constants for compression-annealed pyrolytic graphite. (auth)

17029 (ANL-Trans-273) ANNEALING OF URANIUM QUENCHED FROM 100 TO 4.2 DEG K. Jousset, J. C. Translated by J. A. Amy (Argonne National Lab., Ill.), from Acta Met., 14: 193-200(1966). 19p. Dep. mn. JCL $1.60 fs, $0.80 mf.

Zone melted uranium quenched from 100°K in liquid helium shows important increases in resistivity which disappear after annealing at very low temperatures (5 to 30°K) This phenomenon is explained by the existence of a very mobile defect of interstitial nature, as this is confirmed by neutron irradiations at 4.5°K and electron irradiations at 6°K. After quench, isochronal and isothermal annealings were made on samples with different crystalline state and purities. The defect migration energy by the tangents method was also calculated. (auth)

17030 (LA-tr-66-1) MANGANESE CARBIDES. Picon, M.; Flahaut, J. Translated by Gretchen R. Riese and Charles P. Kempter (Los Alamos Scientific Lab., N. Mex.), from Compt. Rend., 245: 62-4(1957). 6p. Dep. mn. JCL $1.10 fs, $0.80 mf.

By combining with graphite at 1,250°C manganese furnishes the orthorhombic or hexagonal carbides CMn_4 and C_2Mn_6 and triclinic or hexagonal C_3Mn_8. In addition, solid solutions of the α metal and of CMn_4 were found with carbon. Hexagonal C_2Mn_6 seemed the least stable; on the other hand, hexagonal C_3Mn_8 which was also obtained in the arc furnace is much more so. (auth)

17031 (ORNL-tr-962) CREEP RUPTURE STRENGTH OF INCOLOY (32Ni-20Cr STEEL). Tomiyasu, Fujio; Takahashi, Kenji. Translated for Oak Ridge National Lab., Tenn., from Zairyo, 13: 35-43(1964). 16p. Dep. mn. JCL $1.00 fs, $0.50 mf.

The high-temperature creep strength of Incoloy was improved by solutions heat treatments that resulted in a grain size of ASTM No. 3-4. The creep strength of welded joints using Inconel welding rods was superior to the coarse-grain Incoloy base plate. Measurements of the creep-stress rate relation yielded an equicohesive temperature of 720°C. The fine-grain specimens (ASTM No. 7-8) were inferior in creep strength at high-temperatures. The high-temperature creep strength of Incoloy was comparable to Inconel and the austenitic stainless steels. (W.L.G.)

17032 THE YTTRIUM OXIDE–TITANIUM DIOXIDE SYSTEM. Ault, J. D.; Welch, A. J. E. (Imperial Coll. of Science and Tech., London). Acta Crystallogr., 20: 410-12(Mar. 10, 1966).

By means of x-ray powder photographs, it is shown that between 29 and 42 mole % of yttrium oxide, a solid solution with a pyrochlore structure exists, while between 46 and 61 mole %, a fluorite-type phase occurs. Between 42 and 46 mole % there is a two-phase region. The phase change mechanism is discussed. (auth)

17033 DISLOCATION WIDTHS IN ANISOTROPIC B.C.C. CRYSTALS. Reid, C. N. (Univ. of Birmingham, Eng.). Acta Met., 14: 13-16(Jan. 1966).

Various dislocation parameters were evaluated for niobium, chromium, molybdenum, vanadium, tungsten, tantalum, and iron, taking into account the elastic anisotropy of these metals. The Peierls-Nabarro treatment indicate that among screw dislocations the conventional ⟨111⟩ dislocation is the easiest to move. However, in the first four metals above, this treatment suggested that the easiest dislocation to move is an edge dislocations with a ⟨100⟩ Burgers vector on a {110} plane. In certain cases considered there were departures in dislocation energy from the results of isotropic elasticity theory; for example, in iron the elastic energy of the ⟨100⟩ screw dislocation exceeded that of the edge. (auth)

17034 THE TANTALUM–ALUMINUM SYSTEM. Raman, A. Aluminium, 41: 318-19(May 1965). (In German).

Alloys containing very pure Al, Ta, and traces of Fe and Nb were melted in an electric-arc furnace and studied from 900 to 1300°C. Phases were examined for Al compositions between 25 and 40% and between 40 and 60%. In the first range, material was heterogeneous and designated $Ta_{17}Al_{12}$; in the second, material was homogeneous only with 58% Al, and was also designated $Ta_{11}Al_{12}$. Lattice parameters and atomic volumes were studied. Alloys with 60 to 75% Al exhibited two phases, $Ta_{12}Al_{17}$ and $TaAl_3$. Effects of impurities upon phase stability are given. (Rev. Metal Lit.)

17035 MONOCLINIC α_b'' PHASE IN THE U–Nb SYSTEM. Mihajlovic, Aleksandar; Malcic, Stjepan. Bull. Boris Kidrich Inst. Nucl. Sci., 16: 143-50(July 1965).

Results of x-ray and metallographic studies of U with 0.5, 1, 2, 3, 4, and 5 Nb on quenching from the gamma region indicated that niobium-rich gamma solid solution transforms into a monoclinic α_b'' martensite. It was also found that α_b' martensite is monoclinic, though its gamma values are smaller than those of α_b''. (auth)

17036 ISOTHERMAL TRANSFORMATION KINETICS OF A URANIUM–1.85 WT. PERCENT NIOBIUM ALLOY. Djuric, Branko. Bull. Boris Kidrich Inst. Nucl. Sci., 16: 151-61(July 1965).

The isothermal transformation of the gamma phase in a uranium–1.85 wt % niobium alloy between 350 and 685°C was studied. It proceeded by three distinct transformation mechanisms: diffusional, bainitic, and martensitic. In the diffusional range typical Widmanstätten precipitation of the beta or alpha phase occurred. (auth)

17037 STUDY OF THE BEGINNING OF THE FRITTING OF URANIUM DIOXIDE. Bacmann, Jean-Jacques; Cizeron, Georges; Delmas, Roger (Centre d'Etudes Nucleaires de Saclay, Gif-sur-Yvette, France). Compt. Rend., Ser. C, 262: 14-17(Jan. 3, 1966). (In French).

The beginning of fritting of uranium dioxide, under hydrogen, was studied by a dilatometric method for temperatures between 700 and 850°C. It was found that the isothermal contraction of the compacts can be expressed in the form of nth power of time whose exponent is close to 0.33. From analysis of the different curves recorded in the temperature interval studied, it was possible to deduce an activation energy of 100 kcal/mol. (tr-auth)

17038 STUDY OF THE DIFFUSION OF CERIUM AND LANTHANUM IN MAGNESIUM. Lal, Krishan; Levy, Viviane (Centre d'Etudes Nucleaires de Saclay, Gif-sur-Yvette, France). Compt. Rend., Ser. C, 262: 107-9(Jan. 3, 1966). (In French).

The diffusion of Ce and La in Mn was studied. The experiments carried out in a heterogeneous system made it possible to determine the activation energies and the frequency factors characterizing these diffusions. (tr-auth)

17039 PLASTIC DEFORMATION OF POLYCRYSTALLINE URANIUM, BY STRAINING AT VARIOUS RATES, BETWEEN 20 AND 850 DEG C. Jean-Louis, Francois; Lacombe, Paul (Ecole des Mines, Paris). Compt. Rend., Ser. C, 262: 315-18(Jan. 24, 1966). (In French).

The effects of the parameters temperature, strain rate, and grain size on the plastic deformation of polycrystalline uranium were studied between 20 and 850°C. It was established that in the α-phase above 20°C uranium has a very good ductility; in the β-phase it is much less ductile; and in the γ-phase it recovers a very high ductility. (tr-auth)

17040 RELATION BETWEEN THE RATIONAL CURVES OF COMPRESSION AND THE DEFORMATION MECHANISMS OF POLYCRYSTALLINE BERYLLIUM. Gasc, Claude; de Fouquet, Jacques (Ecole Nationale Superieure de Mecanique et d'Aerotechnique, Poitiers, France). Compt. Rend., Ser. C, 262: 331-4(Jan. 24, 1966). (In French).

The mechanisms of the plastic deformation between 20 and 400°C of centrifugally cast polycrystalline beryllium were studied from the compression curves taken parallel to the axis of spinning, obtained as a function of the rate and the temperature. The significant increase of the ductility

observed at 150°C results, in particular, from an intervention of slip on a pyramidal plane of the first order following the common direction with the base plane. (tr-auth)

17041 THE USE OF ANOMALOUS SCATTERING OF NEUTRONS IN THE SOLUTION OF CRYSTAL STRUCTURES CONTAINING LARGE MOLECULES. Ramaseshan, S. (Indian Inst. of Tech., Madras). Curr. Sci. (India), 35: 87-91(Feb. 20, 1966).

The differences between x-ray and neutron scattering are discussed and some ways in which the anomalous neutron scattering could be exploited for solution of the phase problem are proposed. The concept of the "heavy atom" in neutron scattering is discussed and its use for determining the phases of reflection is described. (M.C.G.)

17042 CONTINUOUS TRANSITION BETWEEN THE STRUCTURAL TYPES α-$ThSi_2$ AND α-$GdSi_2$ IN THE HOMOGENEITY REGION OF LANTHANUM DISILICIDE. Gladishevskii, E. I.; Kulikova, A. O. (Lvov State Univ.). Dopov. Akad. Nauk Ukr. RSR, No. 11, 1472-4(1965). (In Ukrainian).

On the basis of x-ray analyses and density measurements of ten alloys, the homogeneity region of a solid solution of La in $LaSi_2$ was determined. At 33.3 at. % La it has a crystal structure of the α-$ThSi_2$ type (space group $I4_1/amd-D_{4h}^{19}$; a = 4.322 ± 0.005 Å, c = 13.86 ± 0.02 Å); at 37.8 at. % La, a structure of the α-$GdSi_2$ type (space group $Imma-D_{2h}^{28}$, a = 4.270 ± 0.005 Å, b = 4.170 ± 0.005, c = 14.05 ± 0.02 Å). The solid solution is constructed according to the subtraction type; at the lanthanum-rich boundary of the solid solution the defect of Si atoms is 17.5%. (auth)

17043 SOLID SOLUTIONS OF Ge, Sn, Al, AND Be IN THE COMPOUND V_3Si AND THEIR SUPERCONDUCTIVITY. Savitskii, E. M.; Baron, V. V.; Efimov, Yu. V.; Gladishevskii, E. I. (Lvov State Univ.). Dopov. Akad. Nauk Ukr. RSR, No. 11, 1474-8(1965). (In Ukrainian).

Microscopic and roentgenographic methods were used to investigate the systems V_3Si-V_3X, where X = Ge, Sn, Al, or Be. The existence was established of solid solutions V_3Si-V_3Ge and V_3Si-V_3Sn and the limiting solubility of Al (~8 at. %) and Be (<0.2 at. %) in the compound V_3Si. The critical temperature of transition to the superconducting condition (T_c) of the compound V_3Si decreased gradually on replacing Si with Ge or Sn to values which are characteristic for the compounds V_3Ge or V_3Sn. The introduction of Al or Be also led to a decrease of T_c of V_3Si. (auth)

17044 INTERACTION OF RARE EARTH OXIDES WITH STRONTIUM OXIDE. Lopato, L. M.; Yaremenko, Z. A.; Tresvyatskii, S. G. (Lvov State Univ.). Dopov. Akad. Nauk Ukr. RSR, No. 11, 1493-7(1965). (In Ukrainian).

New compounds were obtained in the systems Re_2O_3-SrO of composition SrY_2O_4, $SrHo_2O_4$, $SrEr_2O_4$, $SrTm_2O_4$, $SrLu_2O_4$, and the existence of the compound $SrYb_2O_4$ was confirmed. Some physicochemical properties of the synthesized compounds were determined. (auth)

17045 PLASMA ANODIZED LANTHANUM TITANATE FILMS. Whitmore, R. E.; Vossen, J. L. (Radio Corp. of America, New York). IEEE (Inst. Elec. Electron. Eng.), Trans. Mater. Packaging, MP-1: 10-15(June 1965).

At the zero-temperature-coefficient point, $La_2Ti_2O_7$ has a dielectric constant of 47 and a Q in excess of 10,000. The dielectric properties are fairly insensitive to changes in composition. The application of plasma anodization to $La_2Ti_2O_7$ is considered, as well as the use of this material as a thin film dielectric. The process involves co-evaporation of La and Ti, followed by plasma anodization. Evaporation and anodization techniques are discussed as are the electrical properties of the resulting films. The advantages of plasma-anodized $La_2Ti_2O_7$ reside in its favorable characteristics, which are outlined. These represent a substantial improvement over the state of the art of evaporable dielectrics in nearly all respects. The only apparent disadvantage of the process is time. Since the glow discharge consists mostly of positive oxygen ions, the rate of anodization is slow. The total anodization time averages between 1 and 3 hr, depending on film thickness. (BBB)

17046 ON THE PHASE TRANSFORMATION OF Cr-Ta AND Cr-Nb ALLOYS. Guseva, L. N. (Baikov Inst. of Metallurgy, USSR). Izv. Akad. Nauk SSSR, Neorg. Mater., 1: 1743-6(Oct. 1965). (In Russian).

In experiments on alloys made from highly purified materials, preliminary work showed that phase conversions in chromium-tantalum alloys take place very slowly, equilibrium being reached only after 120 hr at 1400°C. Microstructure and x-ray analysis studies on cast samples showed, in agreement with published data, that $TaCr_2$ crystallizes in a very stable hexagonal structure of the $MgZn_2$ type with significant amounts of dissolved tantalum. The range of homogeneous composition was from 33 to 42% tantalum. With niobium alloys the compound $NbCr_2$ also crystallized in the $MgZn_2$ type of structure, which changed to the $MgCu_2$ type on cooling. An unknown η-phase was found in all alloys heated 120 hr at 1400°C; it appeared to be of the $TiNi_2$ type. Holding tantalum-chromium alloys at 1500°C for 24 hr formed a γ-phase $TaCr_2$. Phase transformations indicating a polymorphic chromium modification were not found. (TTT)

17047 PHYSICO-CHEMICAL PROPERTIES OF RARE-EARTH SILICIDES. Dvorina, L. A. (Inst. of Problems in Studies of Materials, Kiev). Izv. Akad. Nauk SSSR, Neorg. Mateer., 1: 1772-7(Oct. 1965). (In Russian).

Data obtained on the dependence of silicide microhardness values on loading showed optimum values of 50 to 100 g for scandium and praseodymium, 40 to 50 g for yttrium, 30 to 80 g for lanthanum, and 40 to 100 g for cerium and neodymium. Hardness values in each system were lowest for the phase richest in silicon. This is due to the predominance of the covalent bonds between silicon atoms over the M-Si and M-M bonds, which results in a sharp asymmetry of the electron density. The hardest and most brittle compounds were the monosilicides. Oxidation parameters and equations for the oxidation constants were determined, and scandium silicides were found the most stable to oxidation and cerium silicides the least. Monosilicides were in general the most stable and the metal-rich compounds the least. In most systems the formation of the oxide film in a low-temperature oxidation was a logarithmic function of time. The rate-limiting step in oxidations lasting several hours was the diffusion in the zone at the slag-silicide interface, which the metal or metalloid ions from the crystal lattice must go through to make contact with the oxygen. (TTT)

17048 NATURE OF THE CHEMICAL BOND IN RARE EARTH DICARBIDES. Makarenko, G. N.; Pustovoit, L. T.; Yupko, V. L.; Rud, B. M. (Inst. of Problems in Studies of Materials, Kiev). Izv. Akad. Nauk SSSR, Neorg. Mater., 1: 1787-90(Oct. 1965). (In Russian).

Gas chromatographic analysis of the gas formed by treating Y, La, Ce, Pr, Nd, and Gd carbides with water showed the products to be a mixture of C_2H_2, H_2, CH_4, C_2H_4, and C_2H_6. The percentage of acetylene increased on going from La to Ce, Pr, and Nd, which in fact is related to the electron structure of the rare earths. The acetylene in the GdC_2 product was about the same as that in the LaC_2 product. Physical properties of the dicarbides were measured, and are tabulated and plotted; variation in the specific electroresistance with temperature is shown. After analysis of the data, the molecular model for LaC_2, PrC_2, NdC_2, and CeC_2 was visualized as a tetragonal face-centered unit containing four metal atoms and four C_2 groups, three of them as $(C\equiv)^{2-}$ and one as $(C=)^{4-}$. The chemical bond in the rare earth carbides is thus very complex, with the strongest bond covalent but combined with ionic-metallic bonds. (TTT)

17049 CATION DIFFUSION IN SINGLE-CRYSTAL AND POLYCRYSTALLINE BeO. Austerman, Stanley B.; Wagner, J. W. (Atomics International, Canoga Park, Calif.). J. Amer. Ceram. Soc., 49: 94-9(Feb. 1966).

The diffusion of Be was measured in single crystals of BeO in directions normal and parallel to the hexagonal c axis. The diffusion coefficients, D, in the two directions were nearly equal to each other. The values of D, mea-

sured between 1500 and 2000°C were quite similar to values reported previously for high-density, high-purity, polycrystalline BeO. The single-crystal data, taken in conjunction with polycrystalline data, show that the observed diffusion in polycrystalline BeO proceeds entirely by volume diffusion with no significant diffusion along grain boundaries, although there is some evidence of rapid surface diffusion along microcracks in the surface. The data are interpreted in terms of extrinsic impurity-dependent diffusion via mobile vacancies. (auth)

17050 OBSERVATIONS ON ZETA PHASE IN THE SYSTEM Ta–C. Zaplatynsky, I. (Lewis Research Center, Cleveland). J. Amer. Ceram. Soc., 49: 109-10(Feb. 1966).

The zeta-phase observed in the Ta–C systems is not an equilibrium phase, but rather forms by a diffusionless transformation of the carbon-deficient fcc TaC lattice under compressive stress. It reverts to the TaC structure when the stresses are relieved. (W.L.G.)

17051 PROPOSED METHOD FOR MICROGRAM SURFACE DENSITY MEASUREMENTS BY OBSERVATION OF PROTON-PRODUCED X RAYS. Khan, J. M.; Potter, D. L.; Worley, R. D. (Univ. of California, Livermore). J. Appl. Phys., 37: 564-7(Feb. 1966). (UCRL-12107(Rev. 1).

X-ray production by proton bombardment may be used to determine the surface density of thin films. It is desirable that the energy loss of the protons in the film be small and that the self-absorption of the produced x ray be negligible. To illustrate the method, thin surface films of aluminum are discussed. The aluminum x-ray yield (x rays/proton) as a function of surface density is presented for the range 0 to 115 $\mu g/cm^2$ and at an incident proton energy of 100 kev. Under the conditions of a 10-μA proton current incident on a thick target, a typical detection system would record 10,000 counts/sec with a counter signal-to-noise ratio of 10^4. At a signal-to-noise ratio as low as unity, the calculated surface density is 0.005 $\mu g/cm^2$ or approximately 10^4 atoms/cm^2. Details of the calculation are presented, along with a table of eleven elements to which the method is currently applicable. (auth)

17052 ISOTOPIC MASS DEPENDENCE OF Li DIFFUSION IN RUTILE. Johnson, O. W. (Univ. of Utah, Salt Lake City); Krouse, H. R. J. Appl. Phys., 37: 668-70 (Feb. 1966).

Mass spectrometric measurements of isotope fractionation of interstitial Li in TiO_2 (rutile) were made which indicate, within experimental error, agreement with the expected $M^{-\frac{1}{2}}$ dependence of the diffusion coefficient D. The major source of error apparently was variation of D due to inhomogeneities in the specimen. (auth)

17053 DENSITY OF NIOBIUM. Harding, John T. (California Inst. of Tech., Pasadena). J. Appl. Phys., 37: 928(Feb. 1966).

Data are presented for the density of six niobium spheres. Previous discrepancies in this density value were due to purity variations and porosity in niobium, but high-temperature, high-vacuum outgassing can now produce niobium having consistent mechanical properties. After processing, the Meissner effect, which is very sensitive to impurities, showed that no significant contamination occurred. The weights, densities, and diameters for the six spheres are tabulated. It is noted that this directly determined density value differs by 0.13% from the value calculated from the lattice-spacing constant. (J.F.P.)

17054 ELECTRON TRANSMISSION MICROSCOPY OF POLYCRYSTALLINE BERYLLIUM OXIDE. Kahn, J. S.; Wadleigh, Willa (Univ. of California, Livermore). J. Appl. Phys., 37: 931-2(Feb. 1966). (UCRL-7331).

A description is given of the observations made on micropolycrystals of BeO. These crystals were prepared in a manner analogous to that used in the sintering of bulk material, in order not to restrict the general applicability of the results. The microcrystalline BeO is shown, in which the nature of boundaries and impurity distribution, loops, impurity concentration, interpenetrating grain boundary, twist boundary, and dislocation are indicated. (J.F.P.)

17055 THE HEAT-TREATMENT OF ANODIC OXIDE FILMS ON TANTALUM. IV. ANODIZATION IN PHOSPHORIC ACID SOLUTIONS. Smyth, D. M.; Tripp, T. B.; Shirn, G. A. (Sprague Electric Co., North Adams, Mass.). J. Electrochem. Soc., 113: 100-4(Feb. 1966).

Dielectric measurements were made on tantalum that was anodically oxidized in aqueous phosphoric acid of various concentrations and then heated in air. The resulting dielectric consists of a highly conducting portion adjacent to the tantalum and an outer, nonconducting portion. This structure is interpreted in terms of the distribution of phosphorus incorporated into the oxide and its effect on the diffusion of oxygen during heat-treatment. (auth)

17056 PREPARATION AND LUMINESCENT PROPERTIES OF Ti-ACTIVATED ZIRCONIA. Sarver, J. F. (General Electric Co., Cleveland). J. Electrochem. Soc., 113: 124-8(Feb. 1966).

Very pure monoclinic ZrO_2 prepared from recrystallized zirconium oxychloride and activated with 0.08% Ti^{4+} responds well to 2537 Å and cathode-ray excitation. A room temperature quantum efficiency of 70%, relative to $MgWO_4$, was attained with 2537 Å excitation. The emission band extends from below 4000 to above 6500 Å, peaking at 4800 Å. The phosphor has a broad excitation spectrum and responds almost equally well to wavelengths between 2100 and 2600 Å. At 20°C the response to 2537 Å excitation is about 82% of the maximum response which occurs at about −60°C. The initial decay is exponential with rate constant $\alpha = 1.5 \times 10^5$ sec^{-1}, but the visually detectable persistence lasts several minutes. The long persistence is associated with glow peaks which were found to exist above 20°C. Additional stronger glow peaks occur at lower temperatures. (auth)

17057 HIGH-TEMPERATURE IMMISCIBILITY OF URANIUM MONO- AND DICARBIDES. Sears, Mildred Bradley; Ferris, Leslie M.; Gray, Robert J. (Oak Ridge National Lab., Tenn.). J. Electrochem. Soc., 113: 269-74 (Mar. 1966). (ORNL-P-1754).

The high-temperature, uranium monocarbide–dicarbide immiscibility region was determined by examining the microstructures of specimens with compositions from $UC_{1.1}$ to $UC_{1.8}$, which were prepared by decomposing mixtures containing the sesquicarbide at 1820–2130°C. The low carbon miscibility boundary, which occurs between $UC_{1.1}$ and $UC_{1.2}$ (5.2 and 5.7% carbon), is nearly composition invariant between 1820 and 2070°C. The high carbon miscibility boundary occurs at about $UC_{1.65}$ (7.7% carbon) at 1820°C and the solubility of the monocarbide in the dicarbide phase increases linearly with increasing temperature. The peak of the immiscible region occurs at about $UC_{1.2}$ (5.7% carbon) and a temperature above 2070°C. (auth)

17058 THE ELECTRON METALLOGRAPHY OF DILUTE ALLOYS OF URANIUM WITH IRON AND ALUMINIUM. Marsh, D. J. (United Kingdom Atomic Energy Authority, Preston, Eng.); Slattery, G. F.; Dewey, M. A. P.; Brammar, I. S. J. Inst. Metals, 93: 471-5 (Sept. 1965).

The metallography of two binary alloys and one ternary alloy of uranium with iron and aluminum was studied in detail. In the case of the ternary alloy, a composition appropriate to a uranium fuel element was examined, following heat-treatments designed to simulate the preparation of a fuel rod. The results are discussed with particular emphasis on the relation between the microstructure of an alloy and its resistance to swelling during irradiation. (auth)

17059 DETERMINATION OF THE STRUCTURE OF TANTALUM SUBOXIDES TaO_y ($Ta_{32}O_9$) BY MEANS OF ELECTRON DIFFRACTION. Steeb, S.; Renner, J. (Max-Planck-Institut fuer Metallforschung, Stuttgart). J. Less-Common Metals, 10: 246-9(Apr. 1966). (In German).

Thin monocrystalline films of tantalum, obtained by electropolishing, display superstructure diffraction diagrams when they are heated up to 300°C and then exposed to oxygen at 5×10^{-4} torr pressure. These diagrams correspond to the phase TaO_y. Interpretation of the diagrams shows that the phase TaO_y belongs to the cubic system

(a = 13.4 Å corresponding to $4a_{Ta}$) and possesses the composition $Ta_{32}O_8$. Eighteen oxygen atoms form in each case a dense group consisting of eight primitive cubes with edge length a/8. The midpoints of the groups form a cubic body centered lattice with edge length a. (auth)

17060 MX$_3$ INTERMETALLIC PHASE OF THE RARE EARTHS WITH Hg, In, Tl, Pb. Palenzona, A. (Univ., Genoa). J. Less-Common Metals, 10: 290-2(Apr. 1966).

The REHg$_3$ compounds have the hexagonal Mg_3Cd structure; $EuTl_3$ also belongs to this type. All the other compounds examined had a cubic $AuCu_3$-type of structure. The magnetic properties of the Eu compounds and graphs of the interatomic distances between the rare earth and metal atoms versus the rare-earths trivalent ionic radius are given. (W.L.G.)

17061 THE PHASE DIAGRAM OF PLUTONIUM AT PRESSURES UP TO 75 KBAR. Liptai, R. G.; Friddle, R. J. (Argonne National Lab., Ill.). J. Less-Common Metals, 10: 292-4(Apr. 1966).

The slope of the $\alpha \rightleftharpoons \beta$ phase boundary was observed to decrease with increasing pressure, particularly at pressures over 30 kbar, to zero slope at about 55 kbar. Above 55 kbar, the curve appears to have a negative slope, implying that the density of the β-phase is greater than that of the α-phase. The temperature hysteresis associated with the $\alpha \rightleftharpoons \beta$ transformation was observed to be a function of pressure, decreasing from its maximum value of about 55°C at one atmosphere pressure, to about 5°C at 25 kbars. The $\beta \rightleftharpoons \gamma$ transformation displayed a similar phenomenon. The data for the $\gamma \rightleftharpoons \epsilon$ and $\epsilon \rightleftharpoons$ liquid transformations indicate an increase of temperature hysteresis with pressure, but their magnitudes fall within the limits of experimental accuracy. (W.L.G.)

17062 THE ISOTHERMAL COMPRESSIBILITY OF URANIUM MONOCARBIDE. Kempter, C. P. (Los Alamos Scientific Lab., N. Mex.). J. Less-Common Metals, 10: 294-5(Apr. 1966). (LA-DC-7629).

The linear compression of a UC cylinder was measured at ½-kbar intervals to 7 kbars. From the data, it was calculated that the isothermal coefficient of volume compressibility at 23°C and atmospheric pressure is 6.9×10^{13} cm^2/dyne. (W.L.G.)

17063 TEMPERATURE DEPENDENCE OF THE ELASTIC MODULI IN ALPHA URANIUM SINGLE CRYSTALS. PART IV. (298 DEG TO 923 DEG K). Fisher, E. S. (Argonne National Lab., Ill.). J. Nucl. Mater., 18: 39-54(Jan. 1966).

The single crystal elastic moduli for alpha uranium were measured as a function of temperature between 298 and 923°K. These data, together with those previously reported, permit a description of the elastic properties of uranium at temperatures from 42 to 12°K below the $\alpha \rightarrow \beta$ phase transformation. Abnormal changes in the temperature dependence of certain shear and Young's moduli occurred above 350°K. It is shown that the changes in temperature dependence of the elastic properties are probably responsible for the contraction of b_0 lattice constant with increasing temperature and are reflected in the anomalous increase in the lattice specific heat above 350°K. It is suggested that the anomalies and the marked decrease in temperature dependence of the electrical resistivity above 400°K are associated with a gradual disappearance of magnetic ordering. (auth)

17064 THERMAL EXPANSION OF ALPHA URANIUM. Lloyd, Lowell T. (Argonne National Lab., Ill.); Barrett, C. S. J. Nucl. Mater., 18: 55-9(Jan. 1966).

Thermal expansion of alpha uranium single crystals between 50 and 923°K was compared with the results from previous studies to develop equations as function of temperature for unit cell dimensions and thermal expansion. Coefficients of the polynomial equations for volume per atom and distances between atoms and their respective fraction expansions as a function of temperature are given. The expansion coefficients in the [100] direction increased above 200°K and the expansion coefficients in the [010] direction decreased and became negative at about 300°K. The thermal expansion coefficients along the four nearest neighbor directions in complex crystal structure of alpha-uranium were considered. The coefficients in the d_1 and d_4 directions increased at a nearly constant rate from 50 to 923°K. The coefficient in the d_2 direction was identical to that in the [100] direction. The temperature effect on the coefficient in the d_3 direction was similar to the effect on the [010] direction, but it went through zero near 600°K. The abnormal temperature dependence of the thermal expansion coefficients for the nearest neighbor directions suggested that there were unusual components of the forces in these directions. These unusual forces are given by Fisher in connection with the studies of the elastic moduli in single crystals of alpha-uranium. (F.J.H.)

17065 LOW-FREQUENCY INTERNAL FRICTION OF Al–Al_2O_3 DISPERSED-PHASE ALLOYS (SAP). Mezzetti, F.; Passari, L. (Univ., Ferrara, Italy). J. Nucl. Mater., 18: 70-5(Jan. 1966).

The mechanical properties of Al – Al_2O_3 dispersion-strengthened alloys at high temperature are discussed. Two low-frequency internal friction peaks were found in the alloys. They had similar behavior after heat treatments but seemed to have slightly different activation energies. A grain boundary relaxation mechanism was suggested for both peaks. In order to explain the difference between the two peaks some hypotheses were advanced. It was postulated that the first peak is due to the relaxation mechanism at grain boundaries. With the oxide particles acting as blocking points, the mean distances between them control height and position of the peak. It was assumed that the second peak is related to the Al – Al_2O_3 interfaces present at grain boundaries. The peak characteristics depend on the dimensions of oxide particles. Qualitative and quantitative deductions following Kê's treatment seemed to be in agreement with experimental data, within experimental error. (F.J.H.)

17066 LONG PERIOD MODULATION OF STACKING ORDER IN Au_3Mn. Sato, H. (Ford Motor Co., Dearborn, Mich.); Toth, R. S.; Shirane, G.; Cox, D. E. J. Phys. Chem. Solids, 27: 413-21(Feb. 1966). (BNL-9368).

The crystal structure of Au – Mn alloys near Au_3Mn was determined on both thin film and bulk single crystals utilizing electron, neutron and x-ray diffraction, in order to clarify the long standing controversies concerning the structure of alloys in this composition range. In the single crystal thin films, the Au – Mn alloys form a two dimensional long period superlattice, as determined by Watanabe, over a wide composition range (~22 – ~28% Mn). In a bulk single crystal of composition near 24% Mn, on the other hand, the crystal has basically an ordered face centered cubic lattice, but the stacking order of the close packed planes is modulated in the [111] direction at every fifth layer and the stacking sequence can thus be described as ABCAB. It was also found that the structure of the bulk crystal is extremely sensitive to the composition although all these different structures are closely related. This is therefore an interesting example where the crystal structures are different in bulk and thin film form. A strong resemblance in the physical origin between the modulation of the superlattice by antiphase boundaries in the long period superlattice, and the modulation of the normal lattice by stacking fault boundaries, as in the present case, is emphasized. (auth)

17067 THERMOELECTRIC POWER IN NIOBIUM–ZIRCONIUM ALLOYS. Weinberg, I.; Schultz, C. W. (California Inst. of Tech., Pasadena). Contract NAS7-100. J. Phys. Chem. Solids, 27: 474-6(Feb. 1966).

Measurements were performed on Nb and Nb – Zr alloys containing 1, 1.8, and 3.8 at. % Zr in the temperature range of 9.2 to 330°K. The thermopower of Nb remained positive down to the superconducting transition temperature. Additions of Zr introduced a negative peak at very low temperatures and caused a progressive attenuation of the phonon drag peak at 75°K. The high temperature data was least affected by alloying. It appears that lattice distortion and alterations in the relative importance of umklapp and nor-

mal electron-phonon interactions, as a result of alloying, are the predominant mechanisms leading to phonon drag attenuation at 75°K. (W.L.G.)

17068 ELECTRICAL PROPERTIES OF THORIUM CARBIDES. Auskern, A. B.; Aronson, S.; Sadofsky, J.; Salzano, F. J. (Brookhaven National Lab., Upton, N Y.). J. Phys. Chem. Solids, 27: 613-15(Mar. 1966).

The resistivity, thermoelectric power, and Hall coefficient of hot-pressed $ThC_{0.74}$, $ThC_{0.90}$, $ThC_{0.96}$, and ThC_2 were measured by conventional d-c methods. In addition, samples of $ThC_{0.74}$ and $ThC_{0.90}$ were vacuum annealed at 1800°C for 10 hr. The number of conduction electrons in the different compositions were calculated from the single band model using Hall coefficients corrected for sample porosity. (W.L.G.)

17069 MAGNETIC SUSCEPTIBILITIES OF V, Zr, AND Nb. Suzuki, Haruhiko; Miyahara, Syohei (Hokkaido Univ., Sapporo). J. Phys. Soc. Jap., 20: 2102-3(Nov. 1965).

The temperature variation of the magnetic susceptibilities for vanadium, zirconium, and niobium in the temperature range from 4.2 to 1200°K are reported. The relative values of the magnetic susceptibilities for these metals are shown. The absolute values of these susceptibilities are also listed. (J.F.P.)

17070 THIN FILM DENSITIES. Edgecumbe, J. (Stanford Univ., Calif.). J. Vac. Sci. Technol., 3: 28-30 (Jan.-Feb. 1966). (SLAC-PUB-155).

In order to find film thickness in angstroms, which is important in a variety of thin film work, it is necessary to know the density of the deposit. Contradictory data on thin film deposits exist in the literature. The data reported, using direct methods of measurement, were obtained during the calibration of a quartz crystal monitor and is in agreement with previous data in that films of Al, Au, KCl, and CsI were found to have densities within a few percent of the bulk density. The mass per unit area is plotted against the film thickness for evaporated films of the above materials. (J.F.P.)

17071 JUMP IN VOLUME AND MELTING CURVE OF CESIUM AT PRESSURES UP TO 17,000 kg/cm^2. Bogdanov, V. S. (All-Union Scientific-Research Inst. for Physico-Technical and Radio Measurements, USSR). JETP Lett. (USSR)(Engl. Transl.), 3: 26-8(Jan. 1, 1966).

Translated from Zh. Eksp. Teor. Fiz., Pis'ma Redakt., 3: 44-7(Jan. 1, 1966).

The volume jump in Cs was determined from the break in the continuity of the volume-pressure curve. At the instant of melting, the volume was measured at constant pressure; and the magnitude of its change was determined. The temperature and pressure along the melting curve were measured simultaneously with the volume jump. (D.C.W.)

17072 STUDY ON Al–Zr ALLOYS. PART I. GENERAL EVALUATION OF Zr ADDITION IN IMPROVING RECRYSTALLIZATION CHARACTERISTICS OF ALUMINUM. Nishikawa, Seiichi; Nagashima, Nobuo; Sawaguchi, Tetsuo. Light Metals, No. 69, 21-34(Jan. 1965). (In Japanese).

Aging and recrystallization behavior in Al–Zr alloys are studied by hardness, electrical resistance, and transmission electron microscopic measurements. (Rev. Metal Lit.)

17073 EFFECT OF ELECTRON BOMBARDMENT HEATING ON THE TENSILE PROPERTIES OF TUNGSTEN. Doering, H.; Shahinian, P. (Naval Research Lab., Washington, D. C.). Mater. Res. Stand., 6: 134-8(Mar. 1966).

A comparison was made of the tensile properties of tungsten sheet specimens heated by bombardment with 10-kv electron beams and by thermal radiation. Tests were also conducted at room temperature, 1200 and 2200°C on specimens previously bombarded for prolonged periods at 2400°C. Bombardment heating under conditions, which did not produce surface changes, did not reduce strength. Reduction of strength of specimens with surface damage was greatest at room temperature. Only a slight reduction at 2200°C was noted. (auth)

17074 ON THE PROBLEM OF THE CARBOHYDRIDES. Goretzki, H.; Ganglberger, E.; Nowotny, H.; Bittner, H. (Univ., Vienna). Monatsh. Chem., 96: 1563-6(1965). (In German).

The powder pattern of a $ZrC_{0.6}$ sample that has absorbed H into its crystal lattice was compared with the original carbide and also the pattern of the same sample after the H has been driven off at 1100°C and 10^{-3} torr. The patterns were recorded with thermal neutrons of 1.198 Å wavelength, and data for the carbohydride are tabulated. Nonhydrogenated or dehydrogenated $ZrC_{0.6}$ showed a statistical distribution of the C in the octahedral sites. Additional lines were found in the hydride that are not a second phase; an ordered or partially ordered structure was indicated. Partial occupation of the octahedral interstices by H atoms might explain the alteration in intensity. For $ZrC_{0.5}H_{0.25}$ an antispinel lattice would be approximated. A space group that gives better agreement with experimental intensity measurements is suggested. A slight difference in the lattice from H-free material is suggested. (BBB)

17075 TERNARY PHASES WITH THE $MgZn_2$ TYPE. Ganglberger, E.; Nowotny, H.; Benesovsky, F. (Univ., Vienna). Monatsh. Chem., 96: 1658-9(1965). (In German).

The formation of ternary Laves phases is apparently favored by more favorable adaptation to the characteristic ratio of radii in the presence of a third component. The role of valence electron concentration was also considered. Often the composition of such phases is ABC, but it can also be A_2B_3C or $A_4B_5C_3$. Certain small transition metal atoms and B metals, such as Al, Ga, Si, and Ge, may give Laves phases when substituted into binary compounds. The following new combinations have the C 14 type; the composition, atomic ratio, and the lattice constants a (in Å), c (in Å), and c/a are given for each phase: V–Co–Al, 1:1:1, 4.95, 7.96, 1.607; Nb–Cr–Co, 1:1:1, 4.84, 7.90, 1.631; Nb–Cr–Ni, 1:1:1, 4.85, 7.94, 1.636; Nb–Cr–Ga, 1:1:1, 4.97, 8.22, 1.655; Nb–Cr–Ge, 1:1:1, 4.94, 8.09, 1.636; Ta–V–Si, 2:3:1, 5.00, 8.26, 1.651; Ta–V–Ge, 2:3:1, 5.04, 8.27, 1.640; W–Co–Al, 1:1:1, 4.93, 7.98, 1.617. In the Laves phases $ZrAl_2$ and $HfAl_2$ part of the Al may be replaced by V or Mo, and in $TaFe_2$ Fe may be partially replaced by Al, giving: Zr–V–Al, 1:1:1, 5.30, 8.65, 1.630; Hf–Mo–Al, 1:1:1, 5.30, 8.67, 1.634; Ta–Fe–Al, 1:1:1, 4.93, 8.03, 1.629. (BBB)

17076 ENHANCEMENT OF DUCTILITY IN α-URANIUM. Johnson, R. H.; Sykes, E. C. (Berkeley Nuclear Labs., Eng.). Nature, 209: 192-3(Jan. 8, 1966).

Under stresses about Y/100 and irradiation at 100°C, alpha-uranium exhibited a steady-state creep rate of $\sim 10^{-7}h^{-1}$ and ~ obeyed a pseudo-creep law of the form, $\dot{\epsilon} \simeq (\sigma/Y)\dot{\epsilon}_g$, where Y is the yield strength of the material and $\dot{\epsilon}_g$ the irradiation growth rate of individual crystals. Superplastic flow in alpha-uranium is shown in which the specimen underwent ~170% elongation. To achieve this the uranium specimen was held under constant stress (~1.150 g mm^{-2}) and the temperature changed from 400 to 600°C and back to 400°C every 20 min for 7 days. (F.J.H.)

17077 A C23-TYPE MODIFICATION OF $ThAs_2$. Hulliger, F. (Cyanamid European Research Inst., Geneva). Nature, 209: 499-500(Jan. 29, 1966).

Orthorhombic α-$ThAs_2$ of the C23 type was prepared by reacting As and Th powder at temperatures between 600 and 900°C. Parts of a sample of the C23 type was converted to the C38 modification by heating at 1150°C. Attempts were also made to prepare ThP_2 of the C23 type. (D.C.W.)

17078 RARE EARTH METALS IN STAINLESS STEELMAKING. Nemethy, L. NML (Natl. Met. Lab.) Tech. J. (Jamshedpur, India), 7: No. 1, 41-8(Feb. 1965).

Recent experiments on types 316 and 310 stainless steels confirmed that alloying with rare earth metals cannot be justified, since there is no consistency in the improvement

of any properties. Hot workability, carbide segregation and sensitization, tensile strength, yield strength, elongation, area reduction, hardness, magnetic permeability, austenitic stability, sulfur removal and oxygen removal were examined. Annealing tests conducted at temperatures from 1600 to 2000°F showed only minor differences between properties of steel with and without 0.2% Ce addition. Phase diagrams of Ce–Fe, Ce–Mn, and Ce–Ni binary systems revealed it is unlikely that any of the rare earth metals form intermediate phases with the metallic elements of stainless steels. (Rev. Metal Lit.)

17079 METHODS FOR DETERMINATION OF REACTOR-GRADE GRAPHITE CHARACTERISTICS. Marinkovic, Slobodan. Nukl. Energ., No. 4, 7-11(1965). (In Slovak).

Methods for determining the nuclear, thermal, structural, electronic chemical, and mechanical properties of graphite along with its density, porosity, permeability, and corrosion are described. Methods are also discussed for determining the properties of irradiated graphite. (M.C.G.)

17080 SPECIFIC HEAT OF EUROPIUM AND YTTERBIUM METALS BETWEEN 3 AND 25 DEG K. Lounasmaa, O. V. (Argonne National Lab., Ill. Inst. of Tech., Otaniemi, Finland). Phys. Rev., 143: 399-405(Mar. 11, 1966).

The specific heats of europium and ytterbium metals were measured, using a germanium resistance thermometer, between 3 and 25°K. For europium a sharp peak was found at 16.1°K, indicating that a cooperative transformation takes place in the sample at this temperature. The entropy under the peak is so large that the anomaly must be caused by the bulk specimen and not by impurities. The orgin of this transition, which has not been observed before, is not clear, but various possibilities are discussed on the basis of available experimental information. According to earlier measurements, the electronic specific heat of europium is $C_E = 5.8T$ mJ/mole °K (T in °K); the lattice and magnetic contributions, C_L and C_M, respectively, could not be separated. It is clear, however, that C_M is large, particularly at low temperatures. For ytterbium, which is nonmagnetic, there are only two terms in C_p, namely C_L and C_E. Earlier measurements below 4°K gave $C_E = 2.90T$ mJ/mole °K, and by employing this result C_L was calculated. The Debye temperature Θ decreases from an initial value of 118°K to a minimum of 109°K at 14°K and then rises again slowly. The Θ-versus-T curve is rather similar to that observed for many other metals. (auth)

17081 LATTICE DYNAMICS AND SPECIFIC HEATS OF SOME TRANSITION METALS ON KREBS'S MODEL. Mahesh, P. S.; Dayal, B. (Banaras Hindu Univ., Varanasi, India). Phys. Rev., 143: 443-51(Mar. 11, 1966).

Krebs's model for the lattice dynamics of cubic metals was extended by including the third-nearest-neighbor ionic interactions. The cases of three transition metals, viz, α-iron, molybdenum and tungsten, are discussed. The force constants appearing in the secular equations for the lattice frequencies are estimated from experimental elastic constants and one observed vibration frequency. The phonon dispersion curves for the three major symmetry directions show a good agreement with the results for neutron scattering. The frequency distributions are computed. The theoretical specific heats and Debye parameters also exhibit a good agreement with the experimental data. (auth)

17082 ON THE TEMPERATURE AND STRAIN-RATE DEPENDENCE OF THE FLOW-STRESS OF A SOLUTION-HARDENED NIOBIUM ALLOY. Harris, B.; Peacock, D. E. (Pratt and Whitney Aircraft, North Haven, Conn.). Phys. Status Solidi, 13: K69-K73(1966).

Results of strain-rate change and temperature-change measurements on a Nb–20 Ta–15 W–5 Mo alloy indicate that the deformation of the alloy is not controlled by a thermally-activated mechanism at temperatures of 423°K. (W.L.G.)

17083 SPECIFIC ELECTRICAL CONDUCTIVITIES OF TANTALUM–MOLYBDENUM ALLOY SINGLE CRYSTALS. van Torne, L. I. (Martin Co., Orlando, Fla.). Phys. Status Solidi, 13: 345-50(1966).

The specific electrical conductivities of electron beam zone refined tantalum–molybdenum alloy single crystals were measured at 273, 77, and 4.2°K. It was assumed that the Fermi surface of the alloys is an order of magnitude less than that corresponding to a Fermi sphere and the total scattering cross section behaves like $2\pi(\sqrt{2}\Lambda_F)^2$, where Λ_F is the wavelength of electrons at the Fermi surface. Under these assumptions, the calculated electrical conductivities showed good agreement with the observed conductivities at 4.2°K for tantalum rich alloys. The divergence between calculated and observed conductivities in molybdenum rich alloys is attributed to the contribution of holes to the conductivity. (auth)

17084 EVALUATION OF SPECIFIC HEATS OF TITANIUM, ZIRCONIUM, AND HAFNIUM. Gupta, R. P.; Dayal, B. (Barnaras Hindu Univ., Varanasi, India). Phys. Status Solidi, 13: 257-60(Jan. 1, 1966).

The electron gas model is extended to the three transition metals titanium, zirconium, and hafnium. The theoretic $\theta - T$ curves agree to within 3 to 5% with experimental values. (auth)

17085 PREPARATION OF ZIRCONIUM DIBORIDE. Kuzenkova, M. A.; Kislyi, P. S. (Inst. of Problems in Material Studies, Academy of Sciences, Ukrainian SSR). Porosh. Met., Akad. Nauk Ukr. SSR, No. 12, 8-12(Dec. 1965). (In Russian).

On the basis of x-ray and metallographic analyses it was found that zirconium diboride, obtained by the method of boron carbide reduction at temperatures above 1650°C, contains about 4.94 ± 0.12% ZrB_{12}. One-phase zirconium boride may be obtained at temperatures below 1650°C or at high temperatures with subsequent slow cooling (6 to 8 degrees/min) within a temperature range of 1650 to 1400°C. The microhardness of zirconium dodecaboride was determined as 45 ± 1.5 gn/m². (auth)

17086 PHASE EQUILIBRIUM IN THE TERNARY Zr–Co–C AND Nb–Fe–C SYSTEMS. Fedorov, T. F.; Kuzma, Yu. B.; Skolozdra, R. V.; Popova, N. M. (Lvov State Univ. Baikov Inst. of Metallurgy, USSR). Porosh. Met., Akad. Nauk Ukr. SSR, No. 12, 63-8(Dec. 1965). (In Russian).

The systems Zr–Co–C and Nb–Fe–C were investigated by means of x ray and microscopic analyses. Phase equilibria were established in the cast alloys and at 800°C for Zr–Co–C, and 1050°C for Nb–Fe–C. No ternary carbides were found. The solid solution of the components in the binary compounds was not large. (auth)

17087 THE SYSTEMS FORMED BY LIME WITH THE OXIDES OF TYPE C RARE-EARTH ELEMENTS. Queyroux, F. (Centre d'Etudes de Chimie Metallurgique, Vitry-sur-seine, France). Rev. Hautes Temp. Refract., 2: 307-12(Oct.-Dec.1965). (In French).

The allotropic transformations of the rare-earth oxides and the influence of additions of lime on the stability of the Tl_2O_3 type cubic structure were studied. The essential features are the appearance of a monoclinic B phase in the system $CaO-Yb_2O_3$ and the stabilization of the monoclinic form of the oxide Dy_2O_3. The structure and the stability field of the compounds identified in the systems $CaO-Dy_2O_3$ and $CaO-Yb_2O_3$ were determined. The equilibrium diagram of the system $CaO-Dy_2O_3$ was investigated. (auth)

17088 INCREASE IN THE DIAMETER OF COMPOSITE TUBES USED IN ATOMIC POWER APPLICATIONS. Depoitier, J.; Flipot, A. J. (Centre d'Etude de l'Energie Nucleaire, Mol-Donk, Belg.). Rev. Met. (Paris), 62: 1205-10 (Dec. 1965). (In French).

The thermal expansion of tubes of Al–24% U alloy with aluminum cans on cadmium alloy tubes clad internally and externally with aluminum was measured by means of expansion tools in graphite (between 300 and 550°C) or heat-treated steel (between 300 and 450°C). A formula for the calculation of the expansion force was derived. (TCO)

17089 DIFFUSION OF NICKEL INTO SOLID SOLUTIONS OF INTERMETALLIC COMPOUNDS OF Ni_3Nb AND Ni_3Ta. Kornilov, I. I.; Shinyayev, A. Ya. Russ. Met. Mining, No. 5, 70-1(1964).

Ni_3Nb–Ni_3Ta solid solutions containing 20 to 100% Ni_3Nb, were prepared by vacuum arc melting and homogenizing at 1200°C. The solid solution was doped with Ni-63 isotope and diffusion annealed from 850 to 1250°C. Ni diffusion rates and diffusion activation energies as influenced by chemical composition of solid solution and annealing temperature were measured. (Rev. Metal Lit.)

17090 SELF-DIFFUSION OF NIOBIUM IN SINGLE CRYSTAL AND MOLTEN SPECIMENS. Lyubimov, V. D.; Gel'd, P. V.; Shveykin, G. P. Russ. Met. Mining, No. 5, 100(1964).

The use of Nb-95 isotope to determine self-diffusion coefficients and self-diffusion activation energy of Nb single crystals, molten polycrystalline Nb, and sintered Nb during diffusion annealing from 1700 to 2100°C is described. The relations between self-diffusion coefficients, porosity, and annealing temperatures are reported. (Rev. Metal Lit.)

17091 PHASE DIAGRAMS OF THE SYSTEMS $CbCr_2$–$TiCr_2$ AND $CbCr_2$–Ti. Svechnikov, V. N.; Kocherzhinskii, Yu. A.; Latysheva, V. I. Sb. Nauch. Tr. Inst. Metallofiz., Akad. Nauk Ukr. SSR, No. 19, 192-5(1964). (In Russian).

The section of the ternary Cr–Nb–Ti diagram along the line $NbCr_2$–$TiCr_2$ was studied and plotted by differential, thermal, and x-ray analysis methods. This section is characterized by the regions L, alpha (Cr-base solid solution), beta (low-temperature modification of the compound (Nb, Ti) Cr_2, epsilon (high-temperature modification of the compound (Nb, Ti) Cr_2, alpha, alpha + epsilon, epsilon + L, epsilon + beta, alpha + epsilon + L. The section of the ternary Nb–Cr–Ti diagram along the line $NbCr_2$–Ti was plotted and is identified as a nonquasibinary section. It is characterized by the regions L, alpha, beta, epsilon, gamma (solid solution based on the high-temperature modification of Ti), L + epsilon, L + gamma, beta + epsilon, epsilon + gamma, gamma + beta, gamma + alpha, alpha + beta, L + gamma + epsilon, and alpha + beta + gamma. The following was established: a significant solubility of Cr and Nb in the gamma-solid solution, an insignificant solubility of Ti in $NbCr_2$ and of Nb and Cr in the low-temperature modification of Ti, the eutectoid transformation gamma $\rightleftharpoons$ alpha + beta at 600 and 80% Ti. (Rev. Metal Lit.)

17092 PHASE EQUILIBRIUM DIAGRAM OF THE Hf–Ta SYSTEM IN THE SOLID STATE. Svechnikov, V. N.; Shurin, A. K.; Dmitrieva, G. P. Sb. Nauch. Tr. Inst. Metallofiz., Akad. Nauk Ukr. SSR, No. 19, 206-11(1964). (In Russian).

The phase diagram of the Hf–Ta system was plotted and studied by dilatometric, thermal, microscopic, and x-ray analysis methods. The temperature of the polymorphic transformation of Hf drops to 1020 ± 10°C on adding Ta and, at this temperature, there is a monotectoid equilibrium. The monotectoid point contains about 17% Ta. The maximum solubility of Ta in alpha-phase Hf is 5% at 1020 ± 10°C. The region $beta_1$ + $beta_2$ exists in the range of 17 to 92% Ta. At a content of 35–40% Ta it extends to 1670°C. The solubility of Hf in Ta ($beta_2$-phase) is 6, 8.8, 16, and 33% at 900, 1100, 1300, and 1500°C, respectively. In Hf–Ta alloys containing 10–20% Ta and quenched from the region of the $beta_1$-phase (a Ta solid solution with a high-temperature modification of Hf), a metastable omega-phase is formed (similar to those formed in Ti- and Zr-base alloys). (Rev. Metal Lit.)

17093 INVESTIGATION OF CHROMIUM–IRON–MOLYBDENUM AND CHROMIUM–IRON–TUNGSTEN ALLOYS. Alfintseva, R. A.; Dmitrieva, G. P.; Korobeinikova, V. G.; (and others). Sb. Nauch. Tr. Inst. Metallofiz., Akad. Nauk Ukr. SSR), No. 20, 108-24(1964). (In Russian).

The systems Cr–Fe–Mo and Cr–W–Fe were studied by microscopic, x-ray, and differential thermal analysis methods, by measuring the hot hardness, microhardness, and by determining the high-temperature oxidation resistance. The polythermal sections and the isothermal section at 1100°C (Cr–Fe–Mo), the polythermal sections with a constant content of W and Cr, and the isothermal sections at 1100, 1275, and 1450°C (Cr–Fe–W) were plotted. In the system Cr–Fe–Mo the solubility of Mo in the alpha-phase at 45–65% Cr is 6–7%. It was found that the omega-phase and chi-phase are not formed from the melt, but from the solid alpha-phase. Mo additions stabilize the sigma-phase. The sigma-phase is not oxidation-resistant in air at 1100°C. Regions of sigma, sigma + zeta, alpha + sigma, alpha + sigma + zeta are formed in the system Cr–Fe–W at 1100°C. These regions disappear at 1275°C so that at 1275 and 1450°C, there are regions of alpha, zeta, alpha + zeta, and $alpha_1$ + $alpha_2$ (at 1275°C). The region of the sigma-phase at 1100°C extends to 32% W. The disappearance of the sigma-phase is associated with the nonvariant equilibrium. Additions of W increase the hardness of Fe–Cr alloys both at room and high temperatures, particularly in the region alpha + sigma. The high-temperature oxidation resistance of Cr–Fe alloys does not decrease when W is added. (Rev. Metal Lit.)

17094 EFFECT OF THE DEGREE OF PURITY OF SOME REFRACTORY METALS ON THEIR MELTING POINTS. Pan, V. M. Sb. Nauch. Tr. Inst. Metallofiz., Akad. Nauk Ukr. SSR, No. 20, 130-2(1964). (In Russian).

The change in the melting point of Cr, V, Nb, and Mo on purification of these metals from gas impurities was determined. It was established that, as a result of purification, the melting point rises by 40°C in Cr, by 60°C in V, and by 50°C in Nb. There is a tendency for the melting point of Mo to rise, however, the difference (10°C) is commensurable with the experimental error. (Rev. Metal Lit.)

17095 SUPERCONDUCTIVITY OF BETA-URANIUM. Mathias, B. T. (Bell Telephone Labs., Murray Hill, N. J.); Geballe, T. H.; Corenzwit, E.; Andres, K.; Hull, G. W. Jr.; Ho, J. C.; Phillips, N. E.; Wohlleben, D. K. Science, 151: 985-6(Feb. 25, 1966).

Beta-phase U was stabilized by additions of 1.75 at. % of Cr and Pt. The superconducting transition temperatures were 0.75 and 0.85°K respectfully. The superconducting transition temperature of the Pt-stabilized phase was independent of concentration in the range between 1 and 3%, indicating the solubility limit may have been exceeded. The electronic specific-heat coefficient was significantly higher in the Pt-stabilized phase. Measurements of the ac susceptibility gave transistions about 10 millidegrees in width. It is proposed that the superconducting behavior of alpha-phase U may be due to superconducting filaments of retained stabilized alpha-prime-, beta-, and gamma-phases, or perhaps even filaments of superconducting compounds. It is believed that the beta- and gamma-phase filaments are situated at the grain boundaries and are stabilized by impurities insoluble in the alpha-phase. (W.L.G.)

17096 NEW COMPOUNDS OF RARE EARTHS WITH Mn AND Fe, AND THEIR CRYSTAL STRUCTURES. Kripyakevich, P. I.; Frankevich, D. P. Soviet Phys.-Cryst. (Engl. Transl.), 10: 468-9(Jan.-Feb. 1966).

Translated from Kristallografiya, 10: 560(July-Aug. 1965).

Alloys of Mn with Sm, Gd, Tb, Dy, Ho, Er, Tm, Lu, and Y, and of Fe with Pr, Tb, Dy, Ho, Er, Tm, Lu, and Y were prepared by sintering mixtures of the powered metals. In each of the systems compounds rich in the transition metal were formed with structures of either the Th_6Mn_{23}, Th_2Zn_{17}, or Th_2Ni_{17} type. (M.C.G.)

17097 THE CRYSTAL STRUCTURE OF TERNARY PHASES IN THE Sc–Cu–Al SYSTEM. Teslyuk, M. Yu.; Protasov, V. S. Soviet Phys.-Cryst. (Engl. Transl.), 10: 470-1(Jan.-Feb. 1966).

Translated from Kristallografiya, 10: 561-2(July-Aug. 1965).

The Sc–Cu–Al alloy, prepared in an electric arc furnace, was investigated by x-ray structural methods. With the exception of two lines, the diffraction pattern was in-

dexed with hexagonal symmetry (a = 5.04 and c = 8.24 Å, c/a = 1.68). It was concluded that the alloy consisted principally of the ternary phase ScCuAl with a $MgZn_2$ structure. A ternary phase $ScCu_2Al$ with a structure of the CsCl-type was also postulated. (M.C.G.)

17098 PARAMAGNETISM OF POLYCRYSTALLINE METALLIC GADOLINIUM, HOLMIUM, AND ERBIUM. Pop, Iuliu (Univ. of Cluj). Stud. Cercet. Fiz., 17: 755-9 (1965). (In Rumanian).

The magnetic properties of polycrystalline specimens of Gd, Ho and Er were studied in the paramagnetic region, using a susceptibility balance with a sensitivity of 10^{-8} to 10^{-9} at a mass of 10 mg. A vacuum of 10^{-3} to 10^{-4} mm of Hg was maintained in the system in order to protect the specimens against oxidation; the temperature measurements from liquid nitrogen temperature to room temperature were carried out by means of Cu-constantan thermocouples, using Pt-Pt/Rh thermocouples for measuring elevated temperatures. The results indicated that the three metals exhibit a Langevin-type paramagnetism which is due to electrons with uncompensated spin in the 4f shell. Conductivity electrons and the multiplet structure of the energy levels contribute only negligibly in the case of Gd and Ho and only slightly in the case of Er. The effective magnetic moment data agree with the predictions of Van Vleck's theory. The paramagnetic-ferromagnetic transition range of Ga is quite extended, from 18 to 80°C, and therefore this metal will be further studied in weak fields. (TTT)

17099 METHODS USED FOR THE MEASUREMENT OF THE THERMAL CONDUCTIVITY AND SPECIFIC HEAT ON SMALL SAMPLES. Vasiliu, S. (Inst. of Atomic Physics, Bucharest). Stud. Cercet. Fiz., 17: 971-83(1965). (In Rumanian).

Thermophysical data are of special importance in the development of reactor materials. Published thermal conductivity data vary greatly because the density of sintered products affects strongly the thermal conductivity. Excess oxygen content lowers the value of this property; thus the thermal conductivity of $UO_{2.16}$ with a density of 10.8 g/cm³ was found to be 0.008 cal/cm sec °C at 60°C, while that of the stoichiometric UO_2 with d = 10.0 g/cm³ was 0.02 cal/cm sec °C. Increasing the temperature causes a reduction of the thermal conductivity; irradiation results in a disordering of the lattice and has a similar overall effect on both the thermal conductivity and heat capacity. An apparatus was developed for carrying out thermophysical measurements on small samples. The furnace and the auxiliary equipment were kept under a pressure of 1 mm of Hg in order to reduce the losses during the experiment. Measurements on Al, Cu and ceramic materials indicated an error of 9 to 12% with respect to data published in the literature. (TTT)

17100 THERMODYNAMIC PROPERTIES OF NIOBIUM AT TEMPERATURE RANGE FROM 0 deg K TO MELTING POINT, 2740 deg K. Kirillin, V. A.; Sheindlin, A. E.; Chekhovskoi, V. Ya.; Zhukova, I. A. (Scientific-Research Inst. of High Temperatures, USSR). Teplofiz. Vysok. Temp., 3: 860-5(Nov.-Dec. 1965). (In Russian).

On the basis of known low-temperature measurements of the heat capacity and on the basis of test results on the enthalpy at temperatures from 600 to 2600°K, the thermodynamic properties of niobium (heat capacity, enthalpy, entropy, and isobar-isothermal potential) were calculated for the temperature interval from 0 to 2740°K. The results are presented in the form of tables and empirical equations. (tr-auth)

17101 MOBILITY OF ATOMS IN A MOLYBDENUM–TUNGSTEN ALLOY. Kalinovich, D. F.; Kovenskii, I. I.; Smolin, M. D. (Inst. of Problems in Metallography, Kiev). Ukr. Fiz. Zh., 10: 1365-7(Dec. 1965). (In Ukrainian).

The radioactive isotopes ^{99}Mo and ^{185}W were used to study the diffusion of the two components of an alloy of molybdenum–35 at. % tungsten over the temperature range from 1500 to 2400°C at every 100°C. The temperature parameters of the diffusion process were computed. A comparison was made between the data obtained and the results of studies of other alloys of this system. (auth)

17102 EVAPORATION BEHAVIOR OF NON-GASEOUS FISSION PRODUCTS FROM UO_2. Takagi, J. (NAIG Nuclear Research Lab., Kawasaki, Japan). Z. Naturforsch., 20a: 1566-8(Dec. 1965).

The evaporation behavior of non-gaseous fission products from UO_2 was studied. The release rate of non-gaseous fission products during the post-irradiation annealing of UO_2 was found to be controlled by the proportionality constant. The values of α for Ru, Ce, La, Mo, and Te were determined at temperatures ranging 750 to 1600°C. The general method of treating non-gaseous fission product release from UO_2 is discussed. (auth)

17103 Xe DIFFUSION IN UO_2 SINGLE CRYSTALS. Oi, Noboru (Tokyo Shibaura Electric Co., Ltd., Kawasaki, Japan). Z. Naturforsch., 20a: 1569-71(Dec. 1965).

The release of ^{133}Xe from UO_2 single crystals and UO_2 fine particles was investigated in a He atmosphere in the temperature range from 600 to 2400°C. The D value obtained was D (cm²/sec) = 3.0×10^{-3} (cm²/sec) exp{–63,000 (cal/mol)/RT}. (auth)

17104 INTER-DIFFUSION OF Li ISOTOPES IN LIQUID LITHIUM METAL. Ott, A.; Lodding, A. (Chalmers Univ. of Tech., Goteborg). Z. Naturforsch., 20a: 1578-82(Dec. 1965).

The inter-diffusion coefficient of ^6Li and ^7Li in liquid Li metal was measured by a capillary-reservoir vacuum-lock technique and by mass spectrometric analysis. For the temperature interval from 195 to 450°C and near-normal isotopic composition, the results can be represented by $D = (1.41 \pm 0.12) \times 10^{-3} \exp[-(2825 \pm 90)/(RT)]$. Theoretical relations connecting diffusion and viscosity were well obeyed. Fair agreement was obtained with the Cohen-Turnbull free volume theory, if Li^+ is the diffusing species. (auth)

17105 SEGREGATION PROCESSES AND THE OMEGA TRANSFORMATION IN ZIRCONIUM–NIOBIUM ALLOYS [Thesis]. Houze, Gerald Lucian Jr. Cleveland, Case Inst. of Tech., 1965. 91p.

Single crystal x-ray-diffraction techniques were employed to determine the modes of segregation in Zr-25 and Zr-50 percent Nb alloys, and their role as a pretransition stage in the beta to omega transformation was explored. Segregation in the Zr-50 percent Nb alloy takes place by a cellular reaction at high temperatures, and by the formation of zirconium-rich Guinier-Preston zones at temperatures in the range 350 to 500°C. However, these zones do not lead to the formation of omega in this alloy. The formation of omega during aging of the 25 percent Nb alloy was not preceded by composition fluctuations. It is concluded that segregation within beta is not a necessary pretransition stage in the transformation of beta to omega, and this reaction is discussed in terms of a model that views omega as an ordered arrangement of Zr atoms in two different electronic states. (Dissertation Abstr.)

17106 ACOUSTICAL RELAXATION PROCESSES IN ZIRCONIUM–NIOBIUM ALLOYS [Thesis]. Nelson, Carl Walter. Cleveland, Case Inst. of Tech., 1965. 88p.

The internal friction and Young's modulus of zirconium and some zirconium–niobium alloys were measured from 300 to 4.2°K. An internal friction peak of significant strength was found at 12°K in Zr–5Nb(hcp). It is provisionally concluded that this peak results from a thermally activated relaxation process. No correlation with dislocation processes is found. In addition, two well-defined internal friction peaks were found in annealed and quenched Zr–Nb alloys that undergo the $\beta \rightleftharpoons \omega$ crystallographic transformation. The peak found at approximately 180°K is shown to result from a thermally activated relaxation process. A second peak that appeared at approximately 40°K is also believed to result from a thermally

activated relaxation process. The prestrain and isothermal aging dependence of Q^{-1}_{max} of these two peaks strongly suggests that these peaks are not the result of dislocation relaxation processes. Both peaks are believed to be associated with the $\beta \rightleftharpoons \omega$ crystallographic transformation. A qualitative model for the relaxation that causes the 180°K peak is proposed based on the movement of the coherent interface between the ω transformation product and the β matrix. No relaxation mechanism is proposed for the peak that appears at approximately 40°K. The magnetic susceptibility of these metals has been measured over the temperature range in which $\beta \rightleftharpoons \omega$ transformation is known to occur. The susceptibility of the alloys was found to be temperature independent. (Dissertation Abstr.)

17107 METAL DIFFUSION IN PYROLYTIC GRAPHITE [Thesis]. Hammond, Martin Lewis Stanford, Calif., Stanford Univ., 1965. 206p.

The diffusion coefficients of Nb-95 in pyrolytic graphite (PG) were measured between 1450 and 1950°C in three different types of PG chosen to represent substrate nucleated, combination substrate and regeneratively nucleated, and regeneratively nucleated microstructures. The diffusion coefficients parallel and perpendicular to the deposition surface were determined in as-deposited and partially graphitized PG. A mathematical analysis of diffusion in layered structures was made and correlations between the structure and diffusion parameters noted. The activation energies for Nb diffusion in PG depended only upon direction and were independent of microstructure and state of graphitization. Autoradiography demonstrated that diffusion perpendicular to the layer planes occurs in the primary cone boundaries while the radioactivity is uniformly distributed in the autoradiographs taken for diffusion parallel to deposition plane. Diffusion mechanisms within the crystallites were rejected on the bases of valence and relative atom size. An examination of mechanisms external to the crystallites, combined with an analysis of the relative values of the pre-exponential factors, revealed that the fundamental jump distance for diffusion parallel to the deposition plane is the crystallite diameter, while the jump distance perpendicular to the deposition plane is the layer plane separation distance. This model was confirmed quantitatively by applying the results of an analysis of diffusion in the primary cone boundaries and by utilizing elementary interstitial diffusion theory. In another set of experiments with Re–PG diffusion couples, a metastable carbide of Re was discovered. The carbide has a simple cubic lattice with a unit cell edge of 2.8+ A and reacts with Re to form an eutectic at ~2000°C (±200°C). (Dissertation Abstr.)

17108 MODIFICATION OF EUTECTIC ALLOYS FOR HIGH TEMPERATURE SERVICE [Thesis]. Ashbrook, Richard Louis. Cleveland, Case Inst. of Tech., 1965. 100p.

The high-temperature eutectics Co-10 Al, Co-42 Cr, Co-37 Mo, Co-45 W, Ni-37 Ta, Ni-45 W, and Ni-16 Zr were modified by small additions of Mg, Ca, Y, Ce, La, Ti, Zr, B, Al, and C. Unmodified and modified melts were vacuum melted and solidified at three cooling rates and as investment cast test bars. On the basis of microstructure, nine compositions were chosen for mechanical property determination. The results of stress rupture tests in air at 1800°F as well as room temperature tensile tests of four different high-temperature eutectics showed modification capable of producing substantial improvements in properties. Small additions of B, C, and Ti increased the stress rupture lives of the Co-10 Al, Ni-37 Ta, Co-45 W and Ni-45W up to 23 times and increased room temperature ductility from less than 1 percent to as high as 7.5 percent. The microstructures were altered in several significant ways to provide these improved properties. Stress rupture life was increased by the formation of carbides or borides in the grain boundaries. Room-temperature and high-temperature strength were improved by dispersing a subordinate phase more uniformly throughout the matrix. Replacing large continuous or plate-like constituents with small equiaxed or discontinuous phases improved the ductility. (Dissertation Abstr.)

17109 THE STRUCTURE OF SINTERED MOLYBDENUM–ZIRCONIUM DIOXIDE MATERIALS. Ryval'chenko, M. K.; Padalko, O. V. pp 195-9 of Tr. VII Vses. N-T Konf. Por Met., Erevan, 1964. (In Russian).

The effects of a sintering routine on the structure of Mo–ZrO_2 was determined metallographically and by x-ray. The pieces, obtained hydrostatically and sintered in a vacuum of 10^{-3} mm Hg in H_2 for $2\frac{1}{2}$ hr, experienced grain growth in Mo and formation of coarse inclusions from decomposition in the strengthening phase. (Rev. Metal Lit.)

17110 MAGNIEVYE SPLAVY, SODERZHASHCHIE NEODIM. (Magnesium Alloys Containing Neodymium). Sviderskaya, Z. A.; Rokhlin, L. L. Moscow, Izdatel'stvo Nauka, 1965. 139p.

Results of measurements and data from the literature on the structure of Mg alloys with Nd are correlated. Phase diagrams of Mg–Nd alloys and results of studies on the effects of additional alloying on the properties and structure of Mg–Nd alloys are presented. The thermomechanical processing of these alloys is discussed at length. Pictures of the microstructure of the alloys studied are shown. 173 references. (M.J.T.)

17111 DETERMINATION OF THE CHARACTERISTICS OF INTERDIFFUSION BETWEEN TITANIUM AND MOLYBDENUM FROM THE ATTENUATION OF GAMMA-RAYS. Shinyaev, A. Ya.; Akopyan, V. O.; Sokiryanskii, L. F.; Bogolyubova, I. V. pp 109-14 of Metalloved. Titana. Moscow, Nauka, 1964. (In Russian).

The interdiffusion between Ti and Mo at 905, 1005, 1100, 1110, and 1210°C was studied using a method for determining the concentration of Ti and Mo in the diffusion zone. The method is based on the principle of attenuation of the intensity of a narrow beam of gamma-rays when passing through different micro-areas of the zone. Relations from which the concentration of components from intensity data can be obtained and calculations of interdiffusion coefficients by analytical methods are given. Interdiffusion parameters were found. (Rev. Metal Lit.)

17112 STRENGTH OF THE INTERATOMIC BINDING IN SINGLE-PHASE ALLOYS OF THE Ti–Cb–Cr SYSTEM. Shakhova, K. I.; Budberg, P. B. pp 184-9 of Metalloved. Titana. Moscow, Nauka, 1964. (In Russian).

The modulus of elasticity and shear, measured with an accuracy between 1–1.5%, increase in transition from the single-phase beta region to the two-phase beta plus gamma region. The elastic constant of solid solutions of the metallic compounds are considerably higher than that of the solid solutions of the pure components of the beta-phase. The characteristic temperature and rms lattice atomic displacements for the solid solutions and compounds at 0 and 293°K were calculated from the elastic constant values. With increased Cr, lattice atomic displacements decrease at 0 and 293°K in the beta-solid solution. The binding strength of the solid solutions of the gamma-phase compounds $TiCr_2$ and $NbCr_2$ is evaluated from extrapolating values of the elastic constants. Increased Nb in gamma-solid solution increases the characteristic temperature and decreases rms deviations. The binding strength in the solid solution of the metals is lower than that in the metallic compounds. With increased temperature, the binding forces in the solid solutions of the metals are more weakened than in the solid solution of the metallic compounds. On heating, the hot hardness of single-phase beta-solid solutions soften more than the gamma-phase. (Rev. Metal Lit.)

Radiation Effects

See also CHEMISTRY — Radiation Chemistry

Refer also to abstracts 16505 and 18076.

17113 (AAEC-E-140) THE STRENGTH OF IRRADIATED BERYLLIUM OXIDE FUELLED WITH UO_2–ThO_2.

Hanna, G. L.; Hilditch, R. J. (Australian Atomic Energy Commission Research Establishment, Lucas Heights). July 1965. 14p. Dep. mn.

The mechanical strength of hot-pressed and cold-pressed and sintered dispersions of $(U,Th)O_2$ in BeO was measured before and after irradiation using the diametral compression test. The addition of more than 5 vol % $(U,Th)O_2$ lowered the unirradiated strength to about 60% of the strength of BeO. Irradiation resulted in a marked drop in strength of all coarse dispersions. Hot-pressed fine dispersions behaved similarly to coarse dispersions of the same composition, but the cold-pressed fine dispersions exhibited an apparent increase of strength on irradiation. High temperatures favored the retention of strength during irradiation. (auth)

17114 (AERE-R-5163) DESORPTION STUDIES ON GRAPHITE SURFACES IRRADIATED IN CO_2, CH_4 AND $CO_2/CO/CH_4$ MIXTURES. Bromley, J. (Atomic Energy Research Establishment, Harwell (England)). Feb. 1966. 38p. Dep. BIS $1.00. HMSO 5s.

Desorption between 300 and 600°C under reaction radiation was used to study the surface layers formed by adsorption from CO_2 and $CO_2/CO/CH_4$ gas mixtures on graphite. The adsorbing gas is removed by a 2 hour helium purge at the adsorption temperature and any surface memory removed between experiments by degassing at 600 to 650°C. Out of pile only 1% of the B.E.T. surface can be covered with surface oxide from CO_2 after prolonged exposure at 300°C, but in-pile 2.5% coverage can be obtained in 20 hours with a rise to some 3% after 140 hours. It was found, by desorption and subsequent surface oxidation, that during the surface oxide formation in pile from $^{14}CO_2$ the number of ^{14}C atoms of the gas phase which become attached to the surface by adsorption or exchange processes is only 2% of the number of oxygen atoms that adsorb to form surface oxide. Methane covers 2% of the graphite surface under irradiation but if 4% CO_2 is added to the methane 2% coverage of strongly bound surface oxide is formed and the methane coverage drops to 0.02%. After 114 hours in a 1% $^{14}CH_4/CO/CO_2$ mixture the desorbate contains some 21% of methane, and 20% of the CO and CO_2 desorbed from 300–400°C contains ^{14}C. The adsorbed oxygen must therefore be closely associated with the carbon atoms from the adsorbed methane species. The surface oxide forms more slowly in methane containing mixtures than it does in CO_2. (auth)

17115 (AI-65-264) RADIATION EFFECTS ON SILVER AND ZINC BATTERY ELECTRODES. [PART] II. Interim Report, July–October 1965. Argue, G. R.; Recht, H. L.; McCollum, W. A. (Atomics International, Canoga Park, Calif.). Contract No. 951109. 24p.

For Jet Propulsion Lab., Calif. Inst. of Tech., Pasadena.

The effects of radiation on Ag and Zn electrodes were studied with specific attention given to the Ag electrode. Cd counter electrodes were used with the Ag electrodes in the study pending the availability of suitable Zn electrodes. Material losses from irradiated (7.2×10^7 rads) Ag electrodes of 3.0 gm total weight averaged 60.2, 77.7, and 52.9 mg at 90, 60, and 30% state of charge, respectively; the corresponding losses for the control Ag electrodes were 11.9, 22.7, and 22.4 mg. The predominant Ag species detected in the precipitated material from the irradiated cells was Ag metal. The effects of radiation on electrode capacity appear to be no larger than 5 to 10% in the dose range studied ($\approx 10^8$ rad (H_2O)); both capacity increases (at 90 and 60% state of charge) and decreases (at 30% state of charge) were observed. Considerable scatter was observed in the Ag electrode capacity data. Both the irradiated and the control cell ended up by cycling about an Ag_2O/AgO transition, independent of the state of charge at the beginning of the experiment. H_2 evolution occurred during cell irradiation; none was formed in the control cell. A pressure buildup was observed in irradiated cells; the control cells showed both small increases and decreases in pressure. (auth)

17116 (BNWL-199) CORRELATION OF RADIATION DAMAGE IN BORONATED GRAPHITE. Dahl, R. E. (Battelle-Northwest, Richland, Wash. Pacific Northwest Lab.). Feb. 1966. Contract AT(45-1)-1830. 34p. Dep. mn. CFSTI $2.00 cy, $0.50 mn.

The number of atom displacements caused by fast neutrons and through the nuclear reaction of ^{10}B with thermal neutrons was calculated. An analysis was also made of the effect of whether B was in solid solution or as B_4C. The relative damaging ratio of fast neutron displacements to those caused by the $^{10}B(n,\alpha)^7Li$ reaction was correlated with data on the dimensional changes of boronated graphite exposed in several reactors having neutron spectra with different fast neutron to thermal neutron ratios. (W.L.G.)

17117 (EURAEC-1558) A NEW DETERMINATION OF THE EMBRITTLEMENT IN STEEL USING SMALL SPECIMENS (≈0.2 cc) IN PARTICULAR WITH RESPECT TO IRRADIATION. Progress Report M 66-17-50005, October 1, 1965–December 31, 1965. van Elst, H. C. (Nederlandse Organisatie voor Toegepast Natuurwetenschappelijk Onderzoek, Delft. Centraal Laboratorium). Jan. 3, 1966. Contract 060-64-11-TEEN. 21p. (EUR-2699). Dep. mn. CFSTI $2.00 cy, $0.50 mn.

Work Performed under United States–Euratom Joint Research and Development Program.

The stress wave attenuation test was performed on irradiated Soudotenax and T-1 steel specimens in the temperature interval –50 to 150°C. From the comparison of the evaluated energy absorption as a function of temperature in this test for the irradiated and nonirradiated condition, an estimate of the shift (increase) of the arrest temperature could be given. More clear than the shift in the transition from the ductile to brittle state to higher temperature was the drop in energy absorption. This implies an exhaustion of ductility of which the practical implication is still not yet quite clear, though it presumably implies an enhanced brittleness. (auth)

17118 (EURAEC-1564) IN-PILE CORROSION OF NUCLEAR MATERIALS. Quarterly Report Nos. 9 and 10, March 1, 1965–August 31, 1965. (Centre d'Etude de l'Energie Nucleaire, Brussels (Belgium). Centre d'Etude de l'Energie Nucleaire, Mol (Belgium)). Contract 055-65-3TEEB(RD). 32p. (EUR-2902; R-2361). Dep. mn. CFSTI $2.00 cy, $0.50 mn.

Work Performed under United States–Euratom Joint Research and Development Program.

It is possible that the passivity of stainless steel is enhanced by reactor irradiation in aqueous solutions. In order to check the quality of the surface film a method for coulometric reduction of oxides in 16 N H_2SO_4 was developed. From blank tests on the effect of surface treatment and exposure conditions it was concluded that the optimum surface treatment for irradiation experiments on type 304 stainless steel is as follows: mechanical polishing down to 0.1 μm Al_2O_3, then electrochemical polishing in acetoperchloric acid solution, and exposure to water and different gases (nitrogen, oxygen and air). Capsules for irradiation in the gamma field of spent reactor fuel were designed. Specimens of type 304L stainless steel were irradiated in very pure water. The irradiation dose was 2.7×10^7 rad. No improvement of the oxide film could be detected with the coulometric reduction after this exposure to gamma rays. In former work it was found that the zero-current potential (E_0) of steel when measured in-pile may be considerably lower than when measured in the absence of irradiation. To elucidate this decrease of E_0, the zero-current potential was measured in neutron-irradiated solutions on a platinum electrode. In all solutions except $KHCO_3$ a decrease up to –400 mv was noted. It was also found that the pH values in solutions of pH–5–7 decreased about one unit. It was concluded that these effects must be attributed to irradiation effects on the solution. An explanation was sought by means of redox potential measurements (ferric/ferrous ratio) and comparison with dosimetry results. The potential is strongly dependent on the

purity of the water and the radiation dose. These results furnished a tentative explanation of several radiation effects observed previously, e.g., spontaneous pitting corrosion in some cases while in other cases the steel had a highly passive film after prolonged contact with water in a reactor. Pitting corrosion was studied on boron-containing steels. The results without irradiation are very irreproducible and depend strongly on the preparation of the steel samples. The composition and the heat treatment for resistance are specified. An experiment with low neutron dose rate is in preparation. (auth)

17119 (GAMD-6789) IRRADIATION BEHAVIOR OF GRAPHITE JOINTS AND GRAPHITE-COATED PARTICLES IN A CARBONIZED PITCH MATRIX. Engle, G. B. (General Atomic, San Diego, Calif. John Jay Hopkins Lab. for Pure and Applied Science). Nov. 2, 1965. Contract AT (04-3)-167. 7p. Dep. mn. CFSTI $1.00 cy, $0.50 mn.

The graphite joints showed the same effects of temperature and fast neutron dose and had a contraction comparable to that of solid samples. No change in appearance was noted in the coated particle matrix after irradiation to 1025°C to an exposure of 2.05×10^{21} nvt (E > 0.18 Mev), however, the matrix may have become somewhat stronger during irradiation. (W.L.G.)

17120 (GEAP-4916) IRRADIATION PERFORMANCE OF ALTERNATE CLADDING MATERIALS. Baroch, C. J.; Hoffmann, J. P; Ogawa, S. Y.; Williamson, H. E. (General Electric Co., San Jose, Calif. Atomic Power Equipment Dept.). Sept. 1965. Contract AT(04-3)-189. 115p. Dep. mn. CFSTI $4.00 cy, $0.75 mn.

Three potential alternate cladding materials for boiling water reactor fuel rods were irradiation tested in the Vallecitos Boiling Water Reactor (VBWR). Irradiation data are reported on fuel rods clad with 0.254 and 0.508 mm Incoloy-800 tubing, with Zircaloy-2 tubing lined with a 0.03 mm layer of stainless steel on the inside surface, and 0.127 mm type 304 stainless steel tubing. (auth)

17121 (GEAP-4918) THE PERFORMANCE OF FUEL RODS CONTAINING BORON BURNABLE POISON. Ogawa, S. Y.; Williamson, H. E. (General Electric Co., San Jose, Calif. Atomic Power Equipment Dept.). Sept. 1965. Contract AT(04-2)-189. 57p. Dep. mn. CFSTI $3.00 cy, $0.50 mn.

Two boron burnable fuel element poison designs were irradiation tested in a VBWR test fuel assembly. One design utilized boron as a minor alloying element in the stainless steel cladding material, and the other utilized zirconium diboride intimately mixed with the vibratory compacted UO_2 powder fuel. The irradiation experience of the assembly and the results of post-irradiation examination conducted to ascertain the overall performance of the fuel rods, the changes in the mechanical properties of the borated cladding material, and the behavior of the boron in the UO_2 fuel column are presented. (auth)

17122 (MIT-334-34) EFFECT OF REACTOR IRRADIATION ON SANTOWAX WR: IRRADIATIONS FROM 425 DEG F TO 800 DEG F AT 40 PERCENT FAST NEUTRON FRACTION. Timmins, T. H.; Mason, E. A.; Morgan, D. T. (Massachusetts Inst. of Tech., Cambridge. Dept. of Nuclear Engineering). Feb. 1966. Contract AT(39-1)-334. 241p. Dep. mn. CFSTI $6.00 cy, $1.25 mn.

Santowax WR was irradiated in the M.I.T. In-Pile Loop Facility at temperatures from 425 to 800°F. The irradiations were made in a stainless steel irradiation capsule installed in the central fuel position of the MITR at a fast neutron fraction of the dose rate equal to 0.40 ± 0.04. The maximum dose rate to the coolant in the irradiation capsule was 0.68–0.76 watts/g and the average dose rate to the coolant circulating in the loop was about 0.020 watts/g at the normal MITR power level of 2 Mw. Low temperature (below 350°C) terphenyl irradiation data of M.I.T. and other laboratories were reviewed to determine the apparent kinetics order of radiolysis and the relative degrading effects of fast neutrons and γ rays. At high temperatures (above 350°C), irradiated coolant was found to degrade at rates from 3 to 20 times higher than unirradiated coolant. This phenomenon was interpreted as increased rates of thermal decomposition, or radiopyrolysis, for irradiated coolant. Radiopyrolysis rate constants were calculated in the range 700 to 800°F and compared with pyrolysis rate constants of unirradiated coolant. At these high temperatures, the terphenyl isomer stabilities were in the order para > meta > ortho. Physical property measurements included density, viscosity, melting point, number average molecular weight, and thermal conductivity. Heat transfer measurements showed that standard correlations could be used to determine the heat transfer rates using the physical properties of irradiated coolant. Santowax WR and Santowax OMP heat transfer data were reviewed and the best correlation for all these data was $Nu = 0.023(Re)^{0.8}(Pr)^{0.4} \pm 10\%$. No evidence of scale buildup or fouling of heat transfer surfaces was observed. (91 references). (P.C.A.)

17123 (N-65-17505) X-RAY AND ELECTRON DAMAGE, AND PHOTOCHEMICAL REACTIONS IN CdS SINGLE CRYSTALS AND LAYERS, AND ANNEALING OF THESE DEFECTS. Semiannual Progress Report, July 1–December 31, 1964. Boeer, K. W. (Delaware Univ., Newark. Dept. of Physics). 56p. (NASA-CR-60866). CFSTI $3.00 cy, $0.50 mn.

The investigation included: growth of CdS single crystals by sublimation technique; evaporation of metal contact layers onto CdS in very high vacuum; the level distribution in the band gap of the CdS single crystals using glow curves and spectral distribution of photoconductivity after heat treatment of CdS crystals in ultra-high vacuum; the change in level distribution of CdS after irradiation with x rays between 100 and 300 kev in ultra-high vacuum; and the electrical properties of CdS crystals during heat treatment in sulfur vapor at temperatures between 300 and 750°C. (auth)

17124 (N-65-17608) THE EFFECTS OF RADIATION ON NICKEL–CADMIUM BATTERY ELECTRODES. [PART] III. Interim Report No. 2, June 13–September 13, 1964. Argue, G. R.; Recht, H. L.; McCollum, W. A.; McKenzie, D. E. (Atomics International, Canoga Park, Calif.). Oct. 16, 1964. Contract JPL-950514. 30p. (NASA-CR-60902; AI-64-240). CFSTI $2.00 cy, $0.50 mn.

For Jet Propulsion Lab., Calif. Inst. of Tech., Pasadena.

Experimental results on the loss of capacity of the cadmium electrode in a ^{60}Co radiation field exhibited much scatter although the corresponding blank runs at similar temperature (45°C) outside the radiation field gave more uniform results. The cadmium electrodes of Ni–Cd cells with a single compartment lost about 15% of their ampere hour capacity at 75% of charge during a ^{60}Co γ irradiation of $8.9 \pm 0.2 \times 10^7$ rads (H_2O). Under the same conditions, and with the same dose at 100% and 50% of full capacity, little loss in capacity was observed. Limited data on the amount of material sloughed from the electrodes as a function of state of charge would seem to indicate that less material is lost at 50% of charge than at either 75% or 100%. Also, the Cd/Ni ratio is lower at 50% of charge than at 100%. From data on two runs, in which the electrodes were separated by a porous quartz disc, most of the sloughed material at 50% and 75% of charge came from the cadmium electrode. (auth)

17125 (NASA-CR-404) EFFECTS OF LOW ENERGY PROTONS AND HIGH ENERGY ELECTRONS ON SILICON. Carter, J. R.; Downing, R. G. (TRW Space Technology Labs., Thompson Ramo Wooldridge Inc., Redondo Beach, Calif.). Mar. 1966. Contract NAS5-3805. 57p. CFSTI $0.90 cy, $0.75 mn.

Using Hall effects measurements, the electron energy dependence of the defect introduction rates of the E_c – 0.17 ev, E_c – 0.4 ev, and E_v + 0.3 ev levels was determined. The two levels at E_c – 0.17 ev and E_c – 0.4 ev were found to be relatively insensitive to incident electron energy as predicted by simple displacement theory. The defect introduction rate for the E_v + 0.3 ev level was found to increase rapidly with increasing electron energy. It was

also observed that the energy dependence of the $E_v + 0.3$ ev level appears to be a function of material resistivity in that the dependence becomes steeper at lower resistivities. At resistivities of the order of 15 ohm-cm the energy dependence of the defect introduction rate of the $E_v + 0.3$ ev level was identical to the observed energy dependence of the degradation of minority carrier lifetime in 10 ohm-cm n-p silicon solar cells. Empirically it was observed that this energy dependence appears to be proportional to the second power of the simple displacement theory, suggesting that these defects may be associated with a divacancy or other double displacement type defect. Under low energy proton bombardment in the energy range from 0.2 to 1.9 Mev the degradation rates of open circuit voltage, short circuit current, and maximum power were much greater than normally observed for penetrating radiation. One Mev electron irradiation of 1 and 10-ohm-cm B-doped and Al-doped n-p silicon solar cells indicated that the differences in radiosensitivity as measured by K values cannot be attributed to the dopant material. (P.C.H.)

17126 (NRL-6349) RADIATION DAMAGE SURVEILLANCE OF POWER REACTOR PRESSURE VESSELS. Serpan, C. Z. Jr.; Steele, L. E.; Hawthorne, J. R. (Naval Research Lab., Washington, D. C.). Jan. 31, 1966. 20p. Dep. mn. CFSTI $1.00 cy, $0.50 mn.

The deleterious effect of high energy neutrons upon the mechanical properties of reactor pressure vessel steels has prompted the employment of material surveillance programs in many nuclear power plants. These programs provide for the exposure of test specimens representative of the reactor pressure vessel at in-reactor locations, wherein they will experience the same thermal and radiation damage history as the vessel itself. Evaluation of these specimens, which reveals the progressive changes in the mechanical properties of the vessel, provides a basis upon which operational procedures and maximum lifetime exposure may be formulated for the plant. Pressure vessel surveillance specimens from the Yankee, Army SM-1 and SM-1A, and Big Rock Point reactors were tested. Analysis of the Yankee program was hampered by the fact that only accelerated irradiation rate specimens were available for testing, so the pressure vessel condition was difficult to determine. Unexpectedly, the weld metal specimens from the Big Rock Point program showed a significantly higher mechanical property change, but because of operating temperature variations and overall adherence of material behavior to the nominal, this divergence of performance of the weld should be taken only as a warning for care in evaluating future surveillance specimens. In the Army reactors, the SM-1 and the SM-1A, surveillance programs suffer from not having specimens at the vessel walls. However, when neutron flux measurements and calculations were combined with test teactor material behavior as well as non-vessel wall surveillance material behavior, no significant deviations were observed; thus projections of results to later periods in the reactor lifetime could be made. A review and an analysis of several instances of shortcomings in surveillance programs are presented along with a set of recommendations for consideration in planning new surveillance programs. In utilizing these recommendations, pressure vessel surveillance programs can be made to provide valuable information for use in determining plant operations; at the same time results from these programs may add to the general knowledge of radiation effects in pressure vessel steels or other materials subject to radiation. Recognition of the value of surveillance programs and their conscientious application should further the public acceptance of nuclear reactors as safe alternative power systems. (auth)

17127 (ORNL-3923) EVALUATION AND IRRADIATION EFFECTS STUDIES ON PYROLYTIC-CARBON-COATED FUEL PARTICLES. Morgan, J. G.; Reagan, P. E.; Long, E. L. Jr. (Oak Ridge National Lab., Tenn.). Mar. 1966. Contract W-7405-eng-26. 39p. Dep. mn. CFSTI $2.00 cy, $0.50 mn.

Several different types of pyrolytic carbon coated fuel particles were studied. The particles, about 500μ in dia, contained UC_2, $(U,Th)C_2$, or $(U,Th)O_2$ as the fuel core material. Two types of coatings were used, a two layer (duplex) and a three layer (triplex). Dimensions, densities, coating contamination, and coating structure were determined before irradiation. The particles chosen for the irradiation tests were from three vendors as well as ORNL. The tests were conducted in the ORR in continuously monitored sweep gas experiments. The temperatures of irradiation ranged from 1000 to 1370°C with burnups up to 20% heavy metal. Fractional fission gas release rates of from 10^{-3} to 10^{-6} were measured during irradiation. In two of the tests, about 1% of the coatings failed. The duplex coated particles had spearhead cracks and reactions at the fuel core-coating interfaces. Triplex coated particles did not show this effect. The fission gas released from intact particles appeared to be a result of U contamination in the coatings. (auth)

17128 (ORNL-TM-1161, pp 194-207) PREPARATION OF RADIOACTIVE METALLIC SPECIMENS FOR REPLICATION. Leighton, Stuart A. (General Electric Co., Cincinnati, Ohio. Nuclear Materials and Propulsion Operation).

Electron microscope studies of the structures of irradiated materials require that extreme care be exercised in preparing the specimens for replication. Special procedures must be adopted to assure acceptable results. The details of mounting (using a conductive mount assembly), metallographic preparation, electro-polishing, etching and replication of various specimen surface conditions are given. Typical optical photomicrographs are shown with accompanying electron micrographs illustrating the results achieved with this procedure. (auth)

17129 (ORNL-TM-1407) INTERIM POSTIRRADIATION EXAMINATION OF A EUROPIUM-BEARING CONTROL ROD FROM THE STATIONARY MEDIUM POWER REACTOR. Richt, A. E. (Oak Ridge National Lab., Tenn.). Mar. 1966. Contract W-7405-eng-26. 15p. Dep. mn. CFSTI $1.00 cy, $0.50 mn.

A neutron-absorber element containing Eu was examined nondestructively after 10.1 Mwyr of service in the Stationary Medium Power Reactor (previously referred to as APPR-1). This element, of the type originally designed for Core II service, consists of four composite absorber plates welded to form a square, hollow tube. The stainless steel-clad absorber plates contain a dispersion of 37 wt % Eu_2O_3 in stainless steel as the neutron-absorbing material. Results of this examination indicate that the absorber element is in excellent condition. No evidence of damage was visually apparent, gamma scans showed no indication of abnormalities in the absorber burnup distribution, and the outer dimensions of the element were found to be well within fabrication tolerances. The individual absorber plates were found to be slightly thicker in regions of high burnup; however, the position of this thicker region is characteristic of the as-fabricated plates and not a result of irradiation-induced swelling. The absorber element was placed in temporary storage until arrangements for additional testing in the Stationary Medium Power Reactor are complete. (auth)

17130 DIFFUSE X-RAY SCATTERING FROM NEUTRON-IRRADIATED GRAPHITE. Pant, L. M. (Faculte des Sciences, Orsay, France). Acta Crystallogr., 20: 354-6(Mar. 10, 1966).

The theory of Cochran and Kartha was used to calculate the intensity of diffuse x-ray scattering from neutron-irradiated graphite. The results were compared with the powder patterns reported by Bacon and Warren. It seemed that the displacement, due to the interstitial atom, of atoms directly above or below it decreased at a slower rate with increasing distance (from the interstitial atom) than that given by the inverse-square law. (auth)

17131 THE ROLE OF CORRELATED DEFECTS IN RADIATION-ENHANCED DIFFUSION. Barrett, J. H. (Oak Ridge National Lab., Tenn.). Acta Met., 14: 64-5 (Jan. 1966). (ORNL-P-1341).

It was concluded that under most experimental conditions likely to be encountered, the ratio of the defects destined to recombine with their original partners to the defects destined to migrate to sinks or to recombine with defects other than their original partners is very small and the contribution to radiation-enhanced diffusion of defects undergoing correlated recombination is negligible. Under conditions such that the ratio would be comparable to unity, it seems doubtful that the correlated recombination could be separated from the other annihilation processes. (W.L.G.)

17132 THE EFFECT OF PRESTRAIN AND SUBSEQUENT NEUTRON IRRADIATION ON MOLYBDENUM. Brimhall, J. L.; Mastel, B. (Battelle Memorial Inst., Richland, Wash.). Contract No. AT(45-1)-1830. Acta Met., 14: 539-41(Apr. 1966). (BNWL-SA-300).

The dislocations induced by strain prior to the fast-neutron irradiation neither altered the radiation-induced damage structure nor appeared to play a role in the subsequent deformation of the irradiated Mo. (W.L.G.)

17133 ELECTRON BOMBARDMENT INDUCED CONDUCTIVITY IN FUSED SILICA. Ehrenberg, W.; Gutan, V. B.; Vodopyanov, L. K. (Birkbeck Coll., London). Brit. J. Appl. Phys., 17: 63-9(Jan. 1966).

The electric conductance induced by cathode rays and beta rays in various forms of silica is studied experimentally. The effect is strongest in a crystal and in amorphous specimens containing mainly hydroxyl as impurity, and is very weak in samples made of fused natural quartz. For each beta particle, for example, traversing a platelet 0.18 mm thick of these materials, 300, 100 or 1 elementary charges pass between the electrodes if a potential difference of 500 v exists between them. Metallic impurities greatly reduce the induced conductance; the effect of chlorine is moderate and is estimated quantitatively. The observations can be explained in terms of recombination centers or, alternatively, in terms of exciton generation and decay. (auth)

17134 STUDY BY MAGNETIC HYSTERESIS OF IRON CONTAMINATED BY NICKEL TRACES AND IRRADIATED WITH NEUTRONS. Vigier, Pierre; Moser, Pierre (Centre d'Etudes Nucleaires, Grenoble, France). Compt. Rend., Ser. C, 262: 327-30(Jan. 24, 1966). (In French).

The magnetic hysteresis of very high-purity iron and iron containing very low concentrations of nickel (0.02 to 0.5%) was studied after neutron irradiation at 77°K. The appearance of new hysteresis paths associated with the nickel and their transformations during isochronic anneals suggests the progressive complications of the initial lattice defects. (tr-auth)

17135 INVESTIGATION OF THE INTERACTION OF RADIATION-INDUCED POINT DEFECTS WITH DISLOCATIONS. Gruzin, P. L.; Zharov, Yu. D. Dokl. Akad. Nauk SSSR, 164: 1280-2(Oct. 21, 1965). (In Russian).

The dependence of internal friction on the deformation amplitude and recovery of internal friction in single crystals of spectroscopically pure copper was investigated. Rod-shaped specimens (cross section, $4 \times 4 \times 70$ mm) were subjected to preliminary annealing in vacuum at 800°C for several hours. The method of bending vibrations at a frequency of 2.5–3.5 cps was used to determine the internal friction. Deformation amplitude was within the limits of 10^{-8} to 10^{-6}. Specimens irradiated with 2.2-Mev electrons received an integral dose of 2×10^{18} electrons/cm^2. Amplitude dependence was determined at 20°C, the the range in which internal friction is independent of amplitude, the measurements were made at temperatures of 63, 82, 120, and 150°C. Experimental points representing amplitude-independent friction recovery at 63 and 82°C coincided with the theoretical diagram. At 120°C, the changes of internal friction were insignificant. Annealing at 150°C caused an increase in critical amplitude. The activation energy of the migration of point defects appearing during irradiation was 1 ev. This value coincides with the activation energy of the migration of vacancies in copper. The diagram representing amplitude-dependent internal friction shows the correctness of the Granato-Lücke theory for a dislocation internal friction. The theory is based on a model in which the dislocation is represented by a vibrating string. The energy dissipation in single crystals of copper and other metals is caused by at least two groups of dislocations. Further, some of the dislocations are more strongly secured by defects than others. Variations in the concentration of defects on dislocations are due to different intensity fields. (CFSTI)

17136 LENGTH CHANGES IN ELECTRON-IRRADIATED HIGH-PURITY GERMANIUM. North, J. C.; Buschert, R. C. (Purdue Univ., Lafayette, Ind.). J. Appl. Phys., 37: 639-42(Feb. 1966).

Irradiation of a high-purity intrinsic single-crystal germanium sample at either liquid-helium or liquid nitrogen temperature by 4.5-Mev electrons produced a large initial expansion which approached saturation with flux. The initial expansion at liquid-helium temperature of $\Delta L/L = +78 \times 10^{-24}$ per incident electron/cm^2 is nearly an order of magnitude larger than was observed in either n- or p-type material. The magnitude of this effect is difficult to account for on the basis of the observations of the n- and p-type samples, and the difficulty of interpretation is compounded by the fact that no electric measurements can be made on pure material at low temperatures. Two highly speculative models are briefly discussed. (auth)

17137 IONIZING IRRADIATION EFFECTS ON THE FRACTURE SURFACE ENERGY OF POTASSIUM CHLORIDE. Bhattacharya, Tapan K.; Zwicker, Earl F. (Illinois Inst. of Tech., Chicago). Contract AT(11-1)-1052. J. Appl. Phys., 37: 771-7(Feb. 1966).

The Co-60 gamma-ray-induced changes in the fracture surface energy ϕ of KCl at 300° and 115°K, as measured by the Obreimov-Gilman slow cleavage technique, are given by $\phi = \phi_0 + a_1 D_F^{\frac{1}{2}} + a_2 D_F^{\frac{2}{3}}$, where ϕ_0 is the fracture surface energy of unirradiated crystal, D_F is the F-band optical density per centimeter, and a_1 and a_2 are constants independent of D_F. The square root term represents a plastic-flow contribution which decreases with increasing irradiation and is dominant at room temperature. The two-thirds power term represents an extrinsic point-defect (EPD) contribution which increases with increasing irradiation and dominates at low temperature. The formation of aggregate centers by room-temperature "F-light" bleaching causes an increase in the EPD contribution, which is reversed when the aggregate centers are destroyed by re-irradiation. The external surface energy of Co-60 gamma-ray and 40-kv x-ray irradiated KCl at 300°K, as measured by a pendulum sclerometer, follows a similar relation which is derived under the assumption of a quasistatic friction mechanism. Qualitative observations on spontaneous and forced crack healing in KCl are consistent with the above findings. (auth)

17138 A TEST OF VISCOUS DISLOCATION DAMPING THEORY. Fiore, Nicholas F. (Army Ballistic Research Labs., Aberdeen Proving Ground, Md.). J. Appl. Phys., 37: 878-84(Feb. 1966).

The amplitude-independent dislocation damping of a series of dilute copper-germanium single crystals was studied as a function of composition and frequency. The measurements were performed at room temperature on annealed and γ-irradiated single crystals driven in longitudinal resonance at 80 and 240 kc/sec by means of piezoelectric oscillator. The results indicate that the Granato-Lücke viscous damping analysis cannot account for the observed magnitude and composition dependence of the damping, although the damping is proportional to frequency in agreement with their theory. They further show that a γ-ray dose of 2×10^8 rad is sufficient to suppress the damping to a composition-independent value of 1×10^{-4} which does not decrease with further irradiation. There is evidence that the total damping consists of a composition-dependent edge dislocation loss superposed on a composition-independent screw dislocation loss. (auth)

17139 A PROBLEM ASSOCIATED WITH ELASTIC WAVES PRODUCED BY HEATING OF TARGETS WITH A

PULSED-ION BEAM. Savage, Howard F. (Ames Research Center, Moffett Field, Calif.). J. Appl. Phys., 37: 920-1(Feb. 1966).

In order to verify that the phase lag of elastic waves in a metallic target bombarded by a pulsed ion beam is caused by cyclic heating of the target, a stroboscopic lamp was used to heat the target at the resonant frequency of the transducer. With a darkened aluminum target, the output of the transducer was about twice that obtained with a polished aluminum target. This indicates that the detected elastic waves were generated as a result of a rise in surface temperature and not as a result of radiation pressure. A method of eliminating the cyclic heating of the target is also given. (J.F.P.)

17140 VARIATION OF THE PARAMETERS OF WEAKLY IRRADIATED URANIUM MONOCARBIDE. Bloch, J.; Mustelier, J. P. (CEN, Fontenay-aux-Roses, France). J. Nucl. Mater., 17: 350-5(Dec. 1965). (In French).

The variation of the lattice parameters of uranium monocarbide irradiated at a flux from 7×10^{11} to 2×10^{12} n/cm^2 sec for irradiation periods of 1 to 15 days was studied. The irradiated monocarbide was then annealed for 10 hrs at temperatures to 1000°C in 50° increments. The relative variation of the parameter attained its maximum value after ~1.1×10^{17} fission/cm^2. The effects of annealing on the lattice parameter recovery are graphed and tabulated. The results showed that the effect of the fission products is negligible. An interpretation is given of the three stages of the observed lattice parameter recovery. (J.S.R.)

17141 OBSERVATION OF HELIUM BUBBLES IN IRRADIATED 20 PERCENT Cr–25 PERCENT Ni–Ti STAINLESS STEEL. Rowcliffe, A. F. (United Kingdom Atomic Energy Authority, Warrington, Eng.). J. Nucl. Mater., 18: 60-5(Jan. 1966).

The effects of neutron irradiation on the ductile properties of a 20% Cr–25% Ni–Ti stainless steel at 750°C are discussed. The formation of helium from $^{10}B(n,\alpha)$ reaction is described. From the known concentration of ^{10}B and the neutron dose, the atomic concentration of helium produced by the $^{10}B(n,\alpha)^7Li$ reaction was calculated to be 4×10^{-6}. Tensile specimens were annealed at 1050°C for 30 min and then irradiated at 625°C for 1300 hr in a reactor to a neutron dose of 3.5×10^{20} n/cm^2 (thermal) and 1.5×10^{20} n/cm^2 (fission). Testing was carried out in argon at 750°C at a strain rate of 3×10^{-4}/sec. The high temperature ductility of the steel was severely affected by neutron irradiation. The average total elongation for three irradiated specimens was only 7%, compared with 65% for unirradiated specimens. The diameters of grain-boundary helium bubbles were found to have average values in the range of 45 ± 10 Å (90%). The maximum and minimum for the bubbles were 65 and 25 Å. Annealing for ½ hr at 750°C increased the proportion of bubbles in the range from 60 to 80 Å and 90% of the values fell in the range of 55 ± 15 Å. For those boundaries that contained bubbles, it was estimated that the average density was about 3×10^{10} bubbles per cm^2 of grain boundary surface. The bubble size distribution altered by tensile testing in the grain boundaries is discussed. (F.J.H.)

17142 DEFORMATION POTENTIAL OF IRRADIATION INDUCED TRAPS IN p-TYPE GERMANIUM FROM LENGTH MEASUREMENTS. North, J. C.; Buschert, R. C. (Purdue Univ., Lafayette, Ind.). J. Phys. Chem. Solids, 27: 489-92(Mar. 1966).

When p-type germanium is electron irradiated at liquid nitrogen temperature, a metastable electron trap is formed within the forbidden energy gap. Shifting 5×10^{17} electrons from the valence band to this metastable level produces very little change in length in the sample. This is interpreted to mean that the deformation potential constants are nearly the same for the metastable energy level and the valence band edge. (auth)

17143 OPTICAL OBSERVATION OF INTERSTITIAL LITHIUM IN IRRADIATED LITHIUM FLUORIDE. Farge, Y.; Lambert, M.; Guinier, A. (Faculte des Sciences, Orsay, France). J. Phys. Chem. Solids, 27: 499-502 (Mar. 1966). (In French).

In lithium fluoride crystals irradiated with thermal neutrons at 77°K and studied at the same temperature, a new absorption peak was observed at 5500 Å (2.2 ev). This peak is also observed in crystals irradiated at low temperature with high doses of electrons (1.4 Mev). The crystal excited with 5500 Å polarized light produces a characteristic fluorescence at about 9,100 Å (1.36 ev) whose anisotropy is related to the symmetry of the color center. A model for this center consisting of a lithium atom in the interstitial position ($\frac{1}{4},\frac{1}{4},0$), (antimorph of the H center) is proposed. (auth)

17144 ELECTRON IRRADIATION OF p-TYPE GERMANIUM AT 4.2 DEG K. Whitehouse, J. E. (Purdue Univ., Lafayette, Ind.). Phys. Rev., 143: 520-5(Mar. 11, 1966).

Degenerate p-type germanium samples ($p_0 \simeq 10^{18}$ cm^{-3}) were irradiated at 4.2°K with 4.5-Mev electrons from a microwave linear accelerator. Measurements of electrical conductivity and Hall effect were made during the irradiation and later infrared illumination and heating. Small changes occur during the irradiation and may be described by a carrier removal rate of 0.4 cm^{-1}. Under the same conditions n-type Ge has a removal rate 25 times larger. This result is also in contrast to the case of 1.1-Mev electron irradiation of p-type Ge, where the changes are immeasurably small. Subsequent illumination-induced changes lower the conductivity and may be represented as the sum of two components, each exponential in the time of illumination. Two processes may also be observed during the heating. One, occurring between 30 and 90°K, restores the conductivity; another, between 70 and 110°K, has the reverse effect. Observation of both of the annealing processes is related to the duration of prior illumination. From this information relations between the annealing processes and the stages of illumination-induced change are deduced. A crude analysis of the annealing is attempted and possibilities for the mechanisms are discussed. (auth)

17145 LENGTH CHANGES IN ELECTRON-IRRADIATED n- AND p-TYPE GERMANIUM. North, J. C.; Buschert, R. C. (Purdue Univ., Lafayette, Ind.). Phys. Rev., 143: 609-18(Mar. 11, 1966).

Simultaneous length-change and conductivity measurements of n-type and p-type germanium single crystals were made as a function of irradiation by 4.5-Mev electrons at liquid-helium and liquid-nitrogen temperatures and subsequent isochronal annealing. Changes in length of the samples produced changes in the spacing of a system of parallel-plate capacitors, and these capacitors were compared with a standard capacitor by means of an ac ratio bridge. The sensitivity and long-term stability of the system were such that changes in length on the order of 0.1 Å were detectable. Degenerate n-type material was found to contract during irradiation at both liquid-helium and liquid-nitrogen temperatures. Length and conductivity annealing stages were observed at both 35 and 65°K during isochronal annealing. Length changes in degenerate p-type material were at least an order of magnitude smaller than in n-type. The p-type sample expanded slightly during irradiation at liquid-nitrogen temperature. These length-change results are interpreted in terms of an electronic-volume effect in addition to the usual atomic-volume effect. The measurements helped to confirm the model deduced from the results of electric measurements which predicts that the effect of electron irradiation on germanium is strongly dependent upon the doping of the material. (auth)

17146 REDUCTION IN RADIATION DAMAGE DUE TO CHANNELING OF 51-Mev IODINE IONS IN GOLD. Noggle, T. S.; Oen, O. S. (Oak Ridge National Lab., Tenn.). Phys. Rev. Lett., 16: 395-8(Mar. 7, 1966). (ORNL-P-2000).

Some preliminary observations of the effect of channeling

51-Mev ^{127}I ions in single-crystal gold films on the damage rate, as determined by electron microscope observation of the damage structures, are described. A reduction in the observed damage rate of more than an order of magnitude is reported when channeling occurs. (G.O.Y.)

17147 TRANSMISSION ELECTRON MICROSCOPE STUDY OF NATURAL RADIATION DAMAGE IN ZIRCON ($ZrSiO_4$). Bursill, L. A.; McLaren, A. C. (Monash Univ., Clayton, Victoria). Phys. Status Solidi, 13: 331-43(1966).

Zircons from different localities show considerable variation in physical properties, and it is generally accepted that these variations are the result of α-radiation damage due to the presence of radioactive impurities, in particular, uranium and thorium. Transmission electron microscopy was used to study the radiation damage as a function of α-dose (D) in a number of zircons. No damage was observed in crystals for which $D < 10^{14}$ α/mg. However, black spot contrast was observed in crystals for which $D = 10^{15}$ α/mg. Annealing experiments and electron spin resonance studies suggest that the black spots are due to clusters of oxygen interstitials. Crystals for which $D > 10^{16}$ α/mg were, on x-ray evidence, glassy (metamict). However, the electron diffraction patterns and micrographs showed that these crystals were composed of slightly misoriented zircon crystallites about 100 Å in size. After annealing, these metamict crystals showed dislocation loops and networks and the single crystal character was restored. The dislocation loops appear to lie on {101} planes and have Burgers vectors parallel to ⟨101⟩. Inspection of the crystal structure of zircon suggests that this is a likely slip system for zircon. Both interstitial and vacancy dislocation loops were observed. These results suggest a mechanism for the transformation from normal to metamict zircon and this is discussed. (auth)

17148 CRYSTAL STRUCTURE OF OXIDES AND THEIR NEUTRON IRRADIATION BEHAVIOR AT 80 DEG C. Elston, J. (Centre d'Etudes Nucleaires de Saclay, Gif-sur-Yvette, France). Rev. Hautes Temp. Refract., 2: 323-31 (Oct.-Dec. 1965). (In French).

The behavior of metal oxides of different crystal structures under neutron irradiation was compared. Al_2O_3, MgO, and BeO, whose structures correspond to a close-packing of O^{2-} ions were studied first. Among the other oxides, UO_2 and cubic ZrO_2, which belong to the fluorite-type compounds, are discussed. The irradiation damage is rather small when the structure of the oxide is stable between room temperature and melting point and when the positions available for the displaced ions are of the same nature (octahedral or tetrahedral) as those that are normally occupied. On the contrary, the disturbance is greater when another crystal type of the oxide exists at high temperature. In that case, the neutrons have a similar effect at 80°C as an increase of temperature. Those conclusions apply also to the case of quartz and amorphous silica. (auth)

17149 STRUCTURAL CHANGES IN NEUTRON IRRADIATED α-QUARTZ. Kolontsova, E. V.; Telegina, I. V. (Lomonosov Moscow State Univ.). Soviet Phys.-Solid State (Engl. Transl.), 7: 2207-12(Mar. 1966).

Translated from Fiz. Tverd. Tela, 7: 2730-4(Sept. 1965).

X-ray photographs were taken of neutron-irradiated and unirradiated quartz single crystals at various temperatures: −186, 20, and 750°C. Radiation produces interlocked displacements of the atoms in the crystals. At a definite stage of irradiation ($>5 \times 10^{19}$ n/cm^2 and $<7 \times 10^{19}$ n/cm^2) the structural conformity of the Si−O tetrahedra, which is characteristic of α-quartz, breaks down, and the irradiated crystal structure can be described as a β-quartz type. The original state can be restored by annealing. With a further increase in the integrated current ($>5 \times 10^{19}$ n/cm^2 and $<7 \times 10^{19}$ n/cm^2) the structure differs from that of β-quartz and in its parameters resembles α- and β-quartz. This modification is so stable that it remains even after a prolonged high-temperature anneal (50 hr at 700°C). (auth)

17150 ELECTRICAL PROPERTIES OF INDIUM ANTIMONIDE IRRADIATED BY NEUTRONS AT 77 DEG K AND BY ELECTRONS AT 300 DEG K. Vodopyanov, L. K.; Kurdiani, N. I. (Lebedev Physics Inst., Moscow). Soviet Phys.-Solid State (Engl. Transl.), 7: 2224-7(Mar. 1966).

Translated from Fiz. Tverd. Tela, 7: 2749-53(Sept. 1965).

It is shown that when single crystals of InSb are irradiated by neutrons at 77°K a change in conductivity type occurs in p-type material while n-type samples only change the magnitude of their conductivity. The process of low-temperature annealing was investigated and the activation energy of this process was determined. The effect of defects which are stable at room temperature on the electrical properties was also investigated. (auth)

17151 THE DOPING OF CRYSTALS BY ION BOMBARDMENT [Thesis]. Liberman, Irving. Evanston, Ill., Northwestern Univ., 1965. 84p.

The effect of positive ion bombardment on the electronic properties of selected semiconductors was investigated. Single-crystal wafers of Ge, Si, and the transition metal oxides TiO_2, CoO, and MnO were exposed to inert and reactive gas ions of 10- to 20-kv energy at current densities of approximately 20 mamp/cm^2. Electrical, optical, thermal, and x-ray measurements were performed. The results show that significant changes in crystal properties take place under bombardment, and that doping rather than simple lattice damage is primarily responsible for the resulting electronic behavior. In most cases, conductivity type as well as resistivity could be altered by appropriate choice of the gas ions. Bombardment-induced crystalline damage could not be detected by normal x-ray-diffraction techniques. In the case of hydrogen bombardment of MnO, penetration of ions to depths greater than 25 microns was observed, and significant photoconductivity could be induced. A model was developed, which relates the photoconductive behavior to the bombardment process. It is hypothesized that the hydrogen placed in the lattice increases the free electron lifetime by trapping the thermally or optically generated holes through covalent bonding. N-type behavior and electron photoconduction result. Interpretation of the photoresponse in terms of band to band excitation of carriers provide, as far as is known, the first experimental determination of the optical band gap of MnO. A value of 2.9 ev is obtained. (Dissertation Abstr.)

17152 THE EFFECT OF NEUTRON RADIATION ON THE CREEP PROPERTIES OF TUNGSTEN [Thesis]. Moteff, John. Cincinnati, Univ. of Cincinnati, 1965. 78p.

Creep-rupture testing of recrystallized tungsten in the temperature range of 900° to 1700°C was performed on control specimens and on specimens irradiated at reactor ambient temperature to fast neutron doses ranging up to 8.2×10^{19} nvt. One irradiation at elevated temperature ($1000°C < T < 1350°C$) was performed to a fast neutron dose of about 1.8×10^{20} nvt. Irradiation affects the creep-rupture properties by increasing the time to rupture with a corresponding decrease in the linear creep rate. The lower threshold of the observed radiation-induced strengthening when testing at a temperature of 1100°C appears at a fast neutron dose of about 1×10^{19} nvt. For specimens irradiated at reactor ambient temperatures, the elongation and reduction-in-area parameters are not affected as a result of the irradiation. In the case of the elevated temperature irradiations, however, the specimens tested at both 900 and 1100°C showed severe embrittlement. Specimens irradiated at elevated temperatures showed complete recovery in the time to rupture and in the ductility following an anneal at 1700°C for 30 hours in hydrogen or argon. Post-irradiation heat treatment (annealing) at 1400°C for one hour tends to reduce the radiation-induced strengthening for those specimens tested at 1100°C. Testing irradiated specimens at a lower temperature (900°C), however, indicated that the initial annealing treatment, up to temperatures of 1200°C, would further increase the time to rupture over and above that of the as-irradiated specimen by a significant amount. Further annealing at temperatures from 1300°C up to 1700°C would reduce the time to rupture compared to that of the as-irradiated specimen. Corresponding changes were also observed in the creep rates. (Dissertation Abstr.)

PHYSICS

General

Refer also to abstract 17527.

17153 (AED-C-23-05) HIGH ENERGY PHYSICS. Series C: Bibliographies. Mellentin, K.; Vierk, I. (comps.) (Zentralstelle fuer Atomkernenergie-Dokumentation, Gmelin-Institut fuer Anorganische Chemie und Grezgebiete, Frankfurt am Main (West Germany)). Aug. 1965. 151p. Dep. mn.

A bibliography is presented that consists of approximately 600 articles on experimental and theoretical aspects of general and weak interactions, strong interactions, electromagnetic interactions (photoproduction), strange particles, general physics, methods and instruments, and field theory. (M.O.W.)

17154 (AED-C-23-06) HIGH ENERGY PHYSICS. Series C: Bibliographies. Mellentin, K.; Vierk, I. (comps.) (Zentralstelle fuer Atomkernenergie-Dokumentation, Gmelin-Institut fuer Anorganische Chemie und Grezgebiete, Frankfurt am Main (West Germany)). Aug. 1965. 172p. Dep. mn.

A bibliography is presented that consists of approximately 600 articles on experimental and theoretical aspects of general and weak interactions, strong interactions, electromagnetic interactions (photoproduction), strange particles, general physics, methods and instruments, and field theory. (M.O.W.)

17155 (AED-C-23-07) HIGH ENERGY PHYSICS. Series C: Bibliographies. Mellentin, K.; Vierk, I. (comps.) (Zentralstelle fuer Atomkernenergie-Dokumentation, Gmelin-Institut fuer Anorganische Chemie und Grenzgebiete, Frankfurt am Main (West Germany)). Aug. 1965. 179p. Dep. mn.

A bibliography is presented that consists of approximately 700 articles on both experimental and theoretical physics dealing with general and weak interactions, strong interactions, electromagnetic interaction (photoproduction), strange particles, general physics, methods and instruments, and field theory. (M.O.W.)

17156 (CONF-650922) PROCEEDINGS OF THE INTERNATIONAL SYMPOSIUM ON MAGNET TECHNOLOGY, STANFORD LINEAR ACCELERATOR CENTER, STANFORD UNIVERSITY, STANFORD, CALIFORNIA, SEPTEMBER 8–10, 1965. Brechna, H.; Gordon, H. S. (eds.). (Stanford Linear Accelerator Center, Stanford Univ., Calif.). Oct. 10, 1965. Contract AT(04-3)-400. 856p. Dep. mn. CFSTI $8.50 cy, $3.50 mn.

Separate abstracts were prepared for 62 of the 91 papers presented. Twenty-two papers were previously abstracted in NSA (19: 44811, 44876, 44878, 46965, 47166, 47167, 47170; 20: 627, 932, 939, 940, 990, 1279, 2533, 2544, 2545, 2546, 4775, 5682, 5944, 11387, and 11388). The remaining seven papers deal with converting an ion-optical layout into the design of a practical magnet system; with economics, reliability, and quality control in magnet manufacture and design; with the van der Meer meson (μ) channel; or are résumés of the various sections. (G.O.Y.)

For abstracts of individual papers see: 16584–16587, 16770–16774, 16808–16811, 16988, 17009, 17010, 17175–17206, 17586–17598, and 17874.

17157 (EUR-2620.i) RISOLUZIONE NUMERICA DI UN PROBLEMA DI DIFFUSIONE DEL CAMPO MAGNETICO. (Numerical Resolution of a Magnetic Field Diffusion Problem). Stella, P.; Taroni, A. (European Atomic Energy Community, Ispra (Italy). Joint Nuclear Research Center. European Atomic Energy Community, Ispra (Italy). European Scientific Data Processing Center). Nov. 15, 1965. 42p. Dep. mn.

The numerical solution of a system of nonlinear partial differential equations that represent the diffusion of a magnetic field compressed by a cylindrical liner is outlined. Some results are included. (D.C.W.)

17158 (ORNL-3900, pp 82-149) PHYSICAL RESEARCH. (Oak Ridge National Lab., Tenn.).

Summaries of research and development results are presented on physics and mathematics, chemistry, metallurgy and materials, and controlled thermonuclear reactions. (J.R.D.)

17159 EXPERIMENTAL OBSERVATION OF FOURTH SOUND IN ^{3}He–^{4}He SOLUTIONS. Esel'son, B. N.; Dyumin, N. E.; Rudavskii, E. Ya.; Serbin, I. A. (Physico-Technical Inst. of Low Temperatures, Academy of Sciences, Ukrainian SSR). JETP Lett. (USSR)(Engl. Transl.), 3: 18-20(Jan. 1, 1966).

Translated from Zh. Eksp. Teor. Fiz., Pis'ma Redakt., 3: 32-5(Jan. 1, 1966).

The speed of fourth sound in pure ^{4}He and in a ^{3}He–^{4}He solution was measured as a function of temperature. The results were compared with theoretical predictions. (D.C.W.)

17160 HOW ARE PHYSICAL EQUATIONS TREATED? Kraut, A. Kerntechnik, 8: 129-33(Mar. 1966). (In German).

The formulation of physical equations with their additive errors is illustrated with examples. Magnitudes and their definition are then considered. Equations between magnitudes are given and magnitude equations are compared with the so-called counting value equation. (J.S.R.)

17161 MATEMATICHESKIE MODELI DLYA RASCHETA ELEKTRICHESKIKH I MAGNITNYKH POLEI. (Mathematical Models for Computing Electric and Magnetic Fields). Tozoni, O. V. Kiev, Naukova Dumka, 1964. 304p.

New methods are proposed for computing electromagnetic fields using simulation and computers. The operating principles and construction of models for some specific complex mathematical operations are described. The computation methods of specialized analog machines for calculating electromagnetic fields are discussed. A theory of models of spatially static fields with optimum boundary structure is proposed. Examples of calculation and construction of models with minimum boundary distortion are given, and new methods of simulation are considered. (tr-auth)

17162 MODULATION OF THE FORCES, ACTING ON CONDUCTING BODIES IN THE TRAVELLING MAGNETIC FIELD OF A CYLINDRICAL INDUCTOR. Mikelson, A.; Saulite, U.; Nikolaev, V. Latv. PSR Zinat. Akad. Vestis, Fiz. Tek. Zinat. Ser., No. 3, 23-9(1964). (In Russian).

Recent measurements of the forces acting on conducting bodies in the travelling magnetic field are described. The existence of optimum values of the pole pitch and frequency is found. Experimental results, given as a relation between dimensionless parameters, are presented in diagrams. (auth)

17163 SOME OBSERVATIONS ON THE INTERFERENCE FRINGES FORMED BY X RAYS SCATTERED FROM THIN FILMS. Sauro, J. P.; Bindell, J.; Wainfan, N. (Polytechnic Inst. of Brooklyn). Contract AF-49(638)-1402. Phys. Rev., 143: 439-43(Mar. 11, 1966).

Several aspects of x-ray scattering from thin films were studied. A relation is presented which correctly gives the positions of the interference maxima in the scattered radiation and is shown to reduce to the Kiessig (specular) interference equation under the appropriate conditions. In particular, it is shown experimentally that the phase shift suffered by the x-ray beam upon scattering in the nonspecular directions is the same as the phase shift suffered in the specular scattering. The observed low-angle cutoff of the scattered interference fringe pattern is also

predicted. A previously reported variation in the shape of the specularly reflected beam is discussed, and evidence is presented which indicates that this variation is a result of the angular divergence of the incident x-ray beam. (auth)

17164 STATIONARY CURRENT IN AN AXIALLY SYMMETRIC CONDUCTING BODY WITH A STRONG HALL EFFECT. Bryzgalov, V. I.; Morozov, A. I. (Steklov Mathematical Inst., Academy of Sciences, USSR). Zh. Eksp. Teor. Fiz., 49: 1789-95(Dec. 1965). (In Russian).

The flow of a current in weakly deformed axially symmetric conducting bodies is considered under conditions of a strong Hall effect. By numerical calculations and analytical estimations it is shown that in a fluted conducting body the current is forced out from projecting regions and in the hollow body formed by intersecting flutings the current lines produce thin layers which pass along the walls. The current layers near the walls are calculated. (auth)

17165 STUDY OF BROWNIAN MOVEMENT BY MEANS OF THE MOESSBAUER EFFECT. Bonchev, Ts.; Aidemirski, P.; Mandzhukov, I.; Nedyalkova, N.; Skorchev, B.; Strigachev, A. (Sofia Univ. of Klement Okhridski). Zh. Eksp. Teor. Fiz., 50: 62-8(Jan. 1966). (In Russian).

The question of the resonance absorption of γ-quanta in ^{119}Sn in suspensions of SnO_2 particles in different liquids is discussed. It is shown that with the alteration of the viscosity of the glycerine suspension by diluting the latter with water, at a constant temperature, the width of the line increases in accordance with the law formulated by Singwi and Sjölander. The same is also obtained with the suspension in silicon oil when the viscosity of the latter is altered as a result of temperature change. In the suspensions, unlike the ordinary liquids, the absorption results in crystals, though microscopically small, to which the Debye–Waller factor for the solids applies. The question is discussed of the mechanism of the absorption of the γ-quanta in the suspension according to Frenkel's model for the liquids when the time of settled life of the colloidal particles is taken into consideration. (auth)

17166 ELECTRODYNAMICS OF HOMOGENEOUS ANISOTROPIC AND DISPERSIVE MEDIUM. Viglin, A. S. (Ural Polytechnic Inst.). Zh. Eksp. Teor. Fiz., 50: 85-92(Jan. 1966). (In Russian).

A four-dimensional formalism is employed for determining the electromagnetic field strengths and induction produced by arbitrary sources. The field is found in a medium with given electric and magnetic permeabilities tensors. The formulas are valid also for uniformly moving medium. (auth)

17167 FREE-FALL EXPERIMENTS WITH NEGATIVE IONS AND ELECTRONS [Thesis]. Witteborn, Fred Carl. Stanford, Calif., Stanford Univ., 1965. 133p.

Measurements of the gravitational force on free negative ions and a demonstration of the feasibility of making a similar measurement on free electrons are discussed. Methods and apparatus used to reduce all electric and magnetic forces to values below or near the expected gravitational force on free electrons and free positrons are described. Pulses of electrons in the magnetic ground state (or in some cases negative ions) were guided by a vertical magnetic field along the axis of a 2-cm-diameter vertical OFHC copper drift tube 25 cm high. The number of particles arriving in each of 400 successive time intervals after each emitting pulse was stored in a 400 channel scalar. The forces acting on the particles could be determined from the time-of-flight distribution. Measurements of charge-to-mass ratios made with applied weak electric fields showed that the particles observed in some of the experiments were negative ions with mass between 2 and 5 proton masses. These ions had an unusually long time-of-flight distribution with a pronounced cut-off near 170 milliseconds. Comparison with calculated distribution curves for light negative ions in fields of various strength showed that the gravitational constant for these ions was the same as for neutral bulk matter (980 cm/sec^2) with a standard deviation in the measurement of ±15%. Furthermore, since helium was the only gas likely to be present in the drift tube (at 4.2°K), the mass analysis strongly suggests that the ions composing the distribution were He^-. Theoretical work indicates that such ions exist only in a metastable state whose lifetime before auto-ionization is 1.7×10^{-3} milliseconds. The experimental results suggest a lifetime of more than 170 milliseconds. Analysis of time-of-flight and energy distributions from several experiments demonstrated conclusively that electrons having kinetic energies of 10^{-10} ev for at least 2 cm of their flight had passed through the 2-cm-diameter copper drift tube. (A.G.W.)

17168 YIELD AND ENERGY SPECTRUM OF SECONDARY ELECTRONS GENERATED BY FISSION FRAGMENTS. Whitehead, A. Bruce (California Inst. of Tech., Pasadena). 9p. (CONF-651001-24). ORAU. Gmelin, AED-CONF-65-293-59.

From IEEE Nuclear Science Symposium, San Francisco.

A technique for measuring the yield and energy spectrum of secondary electrons generated by the passage of a fission fragment through a metal foil is described. The electrons are accelerated through an electrostatic potential V and focused on a solid-state detector using a lens. A number N of low-energy secondaries are thus detected as a pulse corresponding to energy NV in coincidence with the fragment. An integral energy spectrum is obtained by using a suppression grid. The technique also yields information about the response of solid-state detectors to electrons in the energy region below 30 kev. (auth)

Accelerators

Refer also to abstracts 16784, 17689, and 17906.

17169 (AD-628928) THE NRL CYCLOTRON PROGRAM. Report of Progress, September 1, 1965. Bondelid, R. O.; Allas, R. G.; Bond, C. D.; Eisele, J. A.; Toth, J. L.; Pieper, A. G.; Shapiro, P.; Theus, R. B. (Naval Research Lab., Washington, D. C.). Oct. 21, 1965. 54p. (NRL-6366).

Construction of the NRL Cyclotron Facility has proceeded to the point at which preliminary assembly of some of the major components has taken place, and preliminary magnetic field measurements are being made. The cyclotron, an improved version of the Oak Ridge Isochronous Cyclotron (ORIC), will furnish large ion currents (up to 1 mA) with variable energy (from 5 to 75 Mev for protons), and a large choice of ion species for research in nuclear physics. The magnet gap of the NRL cyclotron was changed from the vertical plane used in the ORIC to the horizontal plane because an analysis indicates that there will be a large improvement in the intensity of the energy-analyzed beam. This and other changes based on operating experiments at the ORIC were incorporated in the scope of work given to the engineering firm who prepared bid packages, and assisted in the procurement of components, and in the critical path management scheduling of the cyclotron program. An automated system, utilizing a Hall-plate which is positioned by a tape-controlled table, was developed to map the magnetic field of the cyclotron. Computational techniques were developed for analysis of various ion-optic problems. Preliminary analysis of the combination of an energy-analyzing magnet, switching magnets, and quadrupoles was performed so that the beam can be brought into any one of eleven proposed beam paths. Detailed design of three beam paths which will be instrumented initially was completed. A major feature of the cyclotron beam-transport system is an 80-ton, 135-degree, 9-ft-radius energy-analyzing magnet which has an energy resolution better than 5000. The major components of the beam-handling system were designed. These components include vacuum stations, beam stops, slit collimators, beam viewers, and rotating wire scanners. The beam-transport control system provides for remote control and monitoring of all the elements. The requirements for a data-acquisition system were developed for on-line recording, analysis, and treatment of experimental data. A digital computer with time-

sharing capabilities is the principal element in this system. (auth)

17170 (AED-C-18-05) ACCELERATORS. Series C: Bibliographies. Mausberg, W. (Zentralstelle fuer Atomkernenergie-Dokumentation, Gmelin-Institut fuer Anorganische Chemie und Grenzgebiete, Frankfurt am Main (West Germany)). Nov. 1965. 82p. Dep. mn.

A bibliography consisting of approximately 240 articles on various aspects of accelerators is presented. (M.O.W.)

17171 (BNL-10030) SOURCE OF HIGH ENERGY PARTICLES FROM AN INTERNAL TARGET IN THE AGS. Moore, W. H. (Brookhaven National Lab., Upton, N. Y.). Jan. 24, 1966. Contract AT-30-2-GEN-16. 18p. Dep. mn. CFSTI $1.00 cy, $0.50 mn.

The accelerator was pulsed every 2.8 sec and the beam energy upon collision with a beryllium wire was 30.5 Bev. Data are given for the following; total particle flux and average energy, angular distributions in the neighborhood of the target, tunnel background flux, fast particle flux in the tunnel, absorption length in sand, consistency, and energy distribution. (M.O,W.)

17172 (CEA-R-2802) RECHERCHE D'UNE INTENSE SOURCE DE PROTONS PULSEE A LA MICRO-SECONDE [THESES]. (Production of an Intense Source of Microsecond Proton Pulses [Thesis]). Belmont, Jean-Loup (Commissariat a l'Energie Atomique, Grenoble (France). Centre d'Etudes Nucleaires). 1965. 66p. Dep. mn.

Submitted to Grenoble Univ., France.

A duoplasmatron ion source and beam focusing equipment that were developed to provide μsec proton pulses of 100 mamp are described. (D.C.W.)

17173 (CEAL-1029) POSSIBLE USE OF THE CEA DIRECTLY AS A COLLIDING BEAM FACILITY. Robinson, K. W.; Voss, G. A. (Cambridge Electron Accelerator, Mass. Harvard Univ., Cambridge, Mass.). Mar. 2, 1966. Contract AT(30-1)-2076. 13p. Dep. mn. CFSTI $1.00 cy, $0.50 mn.

A discussion of the problems which must be overcome in order to use the CEA directly as a colliding beam facility is presented. (M.O.W.)

17174 (CERN-66-6) WHAT ARE THE EQUATIONS FOR THE PHASE OSCILLATIONS IN A SYNCHROTRON? Hereward, H. G. (European Organization for Nuclear Research, Geneva (Switzerland)). Feb. 10, 1966. 21p. Dep. mn.

The derivation of the equations for the phase oscillations in a synchrotron is discussed with emphasis on the extent to which the Liouvillian damping is given correctly. (D.C.W.)

17175 (CONF-650922, pp 1-26) ELECTROMAGNETS FOR HIGH-ENERGY PHYSICS APPLICATIONS. Brechna, H.

An approach to designing iron-bound magnets using Fabry factors is given. Coil configuration, pole form and shaping, iron boundaries; impurities in ferromagnetic materials, cooling methods and media, and magnet performance are considered. Magnet design features such as reliability, choice of conductor, magnetic materials, and coil insulation are included. Coil damage due to fatigue, electrical breakdown, moisture and other influences on insulation, and environmental conditions are discussed. (auth)

17176 (CONF-650922, pp 27-55) SOME ASPECTS OF MAGNET TECHNOLOGY IN HIGH ENERGY EXPERIMENTAL PHYSICS. Ramm, C. A.

Some aspects of the present state of magnet technology in high-energy experimental physics are illustrated by describing recently constructed magnets. Examples of precise space- and time-dependent magnetic fields and of the requirements for beam optics are given. Techniques for pulsed magnetic fields, for bending and focusing devices, for measuring magnetic moments, and for the production of neutrino beams are discussed. Industrial procedures for the construction of large coils and yokes are outlined. (auth)

17177 (CONF-650922, pp 89-95) THREE-DIMENSIONAL POTENTIAL FUNCTIONS FOR MAGNET DESIGN. Hedin, Bengt.

Several three-dimensional potential functions are studied and their equifield lines or equipotential lines are investigated with a view to pole and magnet design. (G.O.Y.)

17178 (CONF-650922, pp 96-103) CALCULATION OF THE MAGNET PROFILE BY THE METHOD OF EQUIVALENT CURRENTS. Bronca, G; Hamelin, J.; Jaidane, S.

The calculation of magnet profiles by the method of equivalent currents is outlined, and the results of an application of the method to the focusing sector of an accelerator C magnet are presented. (D.C.W.)

17179 (CONF-650922, pp 104-110) THE USE OF CONFORMAL TRANSFORMATION IN MAGNET DESIGN AND THE EXTENSION OF THE SCHWARZ-CHRISTOFFEL TRANSFORMATION. Halacsy, Andrew A.

Using the theory of complex potentials, a transformation equation is derived which conformally maps one half of a t plane at one side of a straight line into the interior of a curve-sided polygon on a z plane. (auth)

17180 (CONF-650922, pp 111-25) THE DESIGN OF VOLUME-MINIMIZED-SPLIT SOLENOID SYSTEMS. Hitchcock, H. C.

A method for the design of volume-minimized, symmetrically separated, right solenoid pairs excited with a uniform winding current density is outlined. (D.C.W.)

17181 (CONF-650922, pp 126-40) THE ORTHOGONAL ANALOGUE MODEL HELPS TO SOLVE MAGNETIC FIELD PROBLEMS DIFFICULT TO BE TREATED BY ANALYTICAL METHODS. Asner, A.; Bossard, P.; Iselin, Ch.

An orthogonal analog model developed for the study of two-dimensional magnetic field problems is described. The application of the model to some problems that cannot be handled reliably by the usual techniques is demonstrated. (D.C.W.)

17182 (CONF-650922, pp 208-17) QUADRUPOLE MAGNET DESIGN. Taylor, Edward A.

A method for calculating the quality of the field in a quadrupole magnet using two-dimensional relaxation was described. The results of several calculations are presented, which show the effect of changing the location of the windings adjacent to the aperture. (G.O.Y.)

17183 (CONF-650922, pp 218-38) THE CERN SLIM BEAM TRANSPORT ELEMENTS. Asner, A.

The beam transport magnets of the CERN proton synchrotron are described. (D.C.W.)

17184 (CONF-650922, pp 239-47) A B-CONSTANT MAGNET POLE DESIGN. Karasawa, Takashi; Motonaga, Shoshichi; Miyazawa, Yoshitoshi; Nakanishi, Noriyoshi; Henmi, Masatake; Kumagai, Hiroo.

The shapes of the pole in which the magnetic induction, B, of iron is constant are presented for a wide range of the ratio of diameter to gap. The shapes are derived from a simple equation with a correction factor k as a function of the ratio of the diameter to the gap. The constancy of B was experimentally confirmed. (auth)

17185 (CONF-650922, pp 248-52) CONTOURED POLES FOR DC ACCELERATOR MAGNETS. Fast, R. W.; Christian, R. S.

The fabrication of contoured poles for the MURA half-scale spiral-sector magnet model, which is a segment of the spiral-sector magnet system required for an FFAG accelerator with a radius of 30 m, is described. A computer-controlled milling machine was programmed to machine the three-dimensional equipotential surface. Some measurements of the magnetic fields in the model are summarized. (D.C.W.)

17186 (CONF-650922, pp 356-65) FABRICATION TECHNIQUES OF SEVERAL COILS IN THE ZERO GRADI-

ENT SYNCHROTRON COMPLEX. Roman, R.; Markley, F.; McKamey, A.

The fabrication, inspection, and testing of the coils used in achromatic bending magnets and the Piccioni extraction magnets of the Argonne Synchrotron are described. (D.C.W.)

17187 (CONF-650922, pp 377-89) ON A CIRCULAR CURRENT SHIM FOR A CYCLOTRON MAGNET. Nakanishi, Noriyoshi; Motonaga, Shoshichi; Miyazawa, Yoshitoshi; Karasawa, Takashi.

The correction of the radial distribution of the magnetic field by circular current shims mounted on the surface of the pole tips was studied experimentally and theoretically using a scale-model magnet and a digital computer. The change of the permeability of iron in strong magnetic fields was taken into account. The shape of the current shims for an ordinary 160-cm variable-energy cyclotron was determined. (D.C.W.)

17188 (CONF-650922, pp 415-20) AUTOMATED LOGGING AND PROCESSING OF THE NRL CYCLOTRON MAGNETIC FIELD DATA. Toth, J. L.; Allas, R. G.; Bond, C. D.; Pieper, A. G.; Theus, R. B.

An automatic data logging and processing system that was developed for the handling of data on the magnetic field of the NRL cyclotron is described. (D.C.W.)

17189 (CONF-650922, pp 421-7) THE DETERMINATION OF MEDIAN PLANES IN CYCLOTRONS WITH HALL PLATES. Smith, Charles G.

The location of the median plane was determined for a large synchrocyclotron using Hall plates rather than the floating-wire technique. The Hall plates are used to measure the horizontal field component. The equipment used to maintain the high angular accuracy that is required for this measurement is described, and the results of measurements on the magnet of the NASA 600-Mev synchrocyclotron are presented. (D.C.W.)

17190 (CONF-650922, pp 431-46) SPECTROSCOPY OF QUADRUPOLE MAGNETS. Cobb, J.; Cole, R.

A method of measuring quadrupole magnetic fields is described. The parameters determined by this method can be used to express the vector magnetic induction of a quadrupole magnet in closed analytical form. (D.C.W.)

17191 (CONF-650922, pp 447-55) PRECISION MAGNETIC FIELD MEASUREMENTS WITH HALL-EFFECT PROBES. Mulady, James R.

A Hall-effect probe that was developed for use in the mapping of cyclotron and beam-transport magnets is described. Some measurements on the magnets of the NASA 600-Mev synchrocyclotron are summarized. (D.C.W.)

17192 (CONF-650922, pp 456-66) BEAM TRANSPORT MAGNET MEASUREMENTS AT DESY. Holm, K.; Steffen, K. G.

A semiautomatic system that was developed for field measurements on beam-transport magnets is described, in which Hall probes are used. (D.C.W.)

17193 (CONF-650922, pp 472-5) A SIMPLE AND CONVENIENT METHOD FOR FIELD MAPPING BY DIFFERENTIAL USAGE OF HALL GENERATORS. Henmi, Masatake; Karasawa, Takashi; Motonaga, Shyoshichi.

A method of measuring magnetic fields is described in which two independently excited Hall generators are used. (D.C.W.)

17194 (CONF-650922, pp 483-6) THE BEHAVIOUR OF HALL-PROBES IN MAGNETIC GRADIENT FIELDS. Berkes, Branko.

The behavior of Hall probes in magnetic fields with strong gradients was studied. (G.O.Y.)

17195 (CONF-650922, pp 487-96) SEARCH COIL MEASUREMENTS OF THE HARMONIC CONTENT OF BEAM TRANSPORT MAGNETS. Lamb, William H. Jr.; Lari, Robert J.

The design equations for a rotating search coil to measure the harmonic content of beam transport magnets are derived. The independent variables are chosen to make the search coils insensitive to the lowest harmonic. A wave analyzer is used to measure the output voltage at the higher harmonics and enables one to calculate the harmonic coefficients. The results of measurements made on a quadrupole magnet are given and agree with theoretical calculations. (auth)

17196 (CONF-650922, pp 497-504) A PRECISION SYSTEM FOR MEASURING WIRE TRAJECTORIES IN MAGNETIC FIELDS. Ratner, L. G.; Lari, R. J.

The design and operational characteristics of a system for measuring particle trajectories by means of a floating-wire analog are described. (auth)

17197 (CONF-650922, pp 536-40) A 90 deg SUPERCONDUCTING BENDING MAGNET FOR 30 Mev PROTONS. Kramer, P.; Hagedoorn, H. L.; Luiten, A. L.

A superconducting magnet that was developed to deflect a 30-Mev proton beam over 90° in a field of 50 kgauss is described. The focusing properties of superconducting solenoids and quadrupole lenses are also compared. (D.C.W.)

17198 (CONF-650922, pp 650-6) THE ARGONNE NATIONAL LABORATORY'S PION FOCUSING HORN. Vogel, H.; Brunk, W.; Roberts, E.; Markley, F.; Pollack, I.; Hinterberger, H.; Telegdi, V. L.; Winston, R.

A pion-focusing device that was developed for use in high-energy neutrino experiments is described. (D.C.W.)

17199 (CONF-650922, pp 686-99) DESIGN AND CONSTRUCTION OF THE EXCITING COILS FOR THE GUIDING MAGNET OF A 4-Gev ELECTRON SYNCHROTRON. Tschopp, Peter A.

The exciting coils for the guiding magnet of the NINA synchrotron are described. The fabrication and testing of the coils are outlined. (D.C.W.)

17200 (CONF-650922, pp 715-22) AN ACHROMATIC 90 deg BENDING MAGNET SYSTEM. Randall, D. D.

It was shown that a single magnet would not be suitable for the bending of a beam of electrons of 100 to 120 Mev, and the use of two 45° bending magnets with a single quadrupole between them was proposed. The residual deviations and divergences that are expected with the latter system were calculated. (D.C.W.)

17201 (CONF-650922, pp 733-44) PRESTRESSING METHOD FOR ASSEMBLING THE ARGONNE ZGS RING MAGNET COILS. Siljander, W. A.

The design, fabrication, and installation techniques by which the prestressing of the ZGS ring magnet coils was accomplished are discussed. (D.C.W.)

17202 (CONF-650922, pp 755-68) MAGNET-SYSTEM POWER SUPPLIES. Gruetter, Fritz.

A survey of power supplies for constant-field and pulsed magnets that are used in high-energy physics is presented. (D.C.W.)

17203 (CONF-650922, pp 776-8) POWER SUPPLY FOR THE MURA MAGNET MODELING PROGRAM. Peterson, F. L.

The power supply that was developed for the MURA FFAG magnet modeling program is described. (G.O.Y.)

17204 (CONF-650922, pp 808-16) RECTIFIER POWER SUPPLIES FOR ZGS EXPERIMENTAL MAGNETS. Rijk, J.

The rectifier power supplies that are used to power the beam-bending and -focusing magnets in the ZGS experimental areas are described. The operation and performance of the power supplies are discussed. (D.C.W.)

17205 (CONF-650922, pp 817-22) PRINCETON-PENNSYLVANIA ACCELERATOR STANDARD MAGNET CURRENT REGULATORS. Riedel, J.

The current regulators that were developed for use with the magnets in the experimental areas at the Princeton Synchrotron are described. The current transducers are discussed in detail. (D.C.W.)

17206 (CONF-650922, pp 823-34) ESTABLISHING THE MAGNETIC FIELD OF A SOLID POLE MAGNET TO WITHIN $\pm$ 0.01 percent. Harris, C. A.; Cobb, J. K.

The problems associated with setting the fields of several magnets in series using only current as an indicator for the calibration of the magnetic field are considered. (G.O.Y.)

17207 (INSJ-93) DEFORMED ION SOURCE AT POSITIVE POTENTIAL IN F. M. CYCLOTRON. Sanada, J. (Institute for Nuclear Study, Tokyo Univ. (Japan)). Jan. 10, 1966. 7p. Dep. mn.

The use of a calutron type ion source and nearly space charge limited current by a deformed shape at positive potential in the F.M. cyclotron is discussed. The calculation of beam orbits was made. The electric field at the deflector was determined by the method of resistance network analogue. (M.O.W.)

17208 (JINR-P-2537) MEDLENNYI VYVOD PUCHKA PROTONOV IZ SINKHROFAZOTRONA. (Slow Ejection of the Proton Beam From the Synchrophasotron). Myznikov, K. P. (Joint Inst. for Nuclear Research, Dubna (USSR). Lab. of High Energy). 1966. 9p. Dep. mn.

A method is described of slow ejection of the proton beam from the synchrophasotron. It is based on using the half-integer parametric resonance of the betatron radial oscillations. A possibility is considered of the technical application of the method to the JINR synchrophasotron. In order to obtain both a slow and fast ejection of the beam from the accelerator along the same direction a method is suggested to combine the considered system of slow ejection with the fast ejection system developed earlier for the JINR synchrophasotron. Such a universal system allows to eject the beam with high efficiency, small emittance and small spread in energy. The ejection time may change within wide ranges from 50 μs up to about 100 ms. (auth)

17209 (LA-3479) QUARTERLY STATUS REPORT ON THE MEDIUM-ENERGY PHYSICS PROGRAM FOR PERIOD ENDING JANUARY 31, 1966. (Los Alamos Scientific Lab., Univ. of California, N. Mex.). Feb. 1966. Contract W-7405-eng-36. 77p. Dep. mn. CFSTI $3.00 cy, $0.75 mn.

Engineering, fabrication, and testing of 805-Mc waveguide structures were continued. Forty cells of a $\beta = 0.708$ (390-Mev protons) cloverleaf cavity system were fabricated and successfully brazed to form a single vacuum-tight tank. Various aspects in the development of r-f power systems are reported. Further development of accelerator control and instrumentation systems is reported. In addition, beam motion, shielding, and activation calculations were made in conjunction with linear accelerators. (M.O.W.)

17210 (LNF-65/37) RIVELATORI DI CORRENTE PER IL LINAC CON TRASFORMATORI DI IMPULSO. (Current Detectors for the Linac with Impulse Transformers. Note No. 293). Renzler, G. (Laboratori Nazionali di Frascati, Comitato Nazionale per l'Energia Nucleare (Italy)). Oct. 26, 1965. 24p. Dep. mn.

Two magnetic detectors constructed at the ADONE Laboratory for the detection of pulsed beams of electrons and positrons from the LINAC are described. The detectors described are two types—one of the pulse transforming type and the other of the reaction type. Circuitry and equations expressing the operation and function of the detectors are given. (J.S.R.)

17211 (LNF-65/45) BEAM OPTICS COMPUTATION FOR PARTICLE TRANSPORT SYSTEMS. Note No. 297. Bassetti, M.; Buonanni, R. M.; Placidi, M. (Laboratori Nazionali di Frascati, Comitato Nazionale per l'Energia Nucleare (Italy)). Dec. 16, 1965. 27p. Dep. mn.

Computation methods for beam transport systems design are presented. The IBM 7040 code, by which the beam injection system for the Adone storage ring was designed, is also described. (auth)

17212 (UCRL-Trans-1305) RADIATION MEASUREMENTS AROUND AN INSUFFICIENTLY SHIELDED TARGET IRRADIATED BY 19.2-Gev/c PROTONS. Charalambous, S.; Dutrannois, J.; Goebel, K.; Rindi, A. (European Organization for Nuclear Research, Geneva (Switzerland)). Translated for Univ. of California Lawrence Radiation Lab., Berkeley), from report CERN/DI/HP/79(Rev.). Oct. 20, 1965. 34p. Dep. mn. JCL $3.60 fs, $1.22 mf.

The CERN proton synchrotron was used to irradiate a beryllium target at 19.2 Bev/c. The radiation escaping from the accelerator was measured. The responses of various detectors were compared. (M.O.W.)

17213 (UCRL-Trans-1312) THE ACCELERATOR MAGNET OF THE GERMAN ELECTRON-SYNCHROTRON (DESY). Hardt, Werner. Translated by Adele B. Herrmann (Univ. of California Lawrence Radiation Lab., Berkeley), from Elektrotech. Z., 84A: 892-7(1963). 25p. Dep. mn. JCL $2.60 fs, $0.95 mf.

Several major problems in the development of the DESY magnet are discussed including the calculation of the pole contour, the shaping of the magnet ends by specially rounded end blocks, and the calculation of the pole surface turns required for corrections during injection. The construction of the magnet is briefly described, and the results of measurements on all sectors of the magnet are presented. (D.C.W.)

17214 THE MILAN UNIVERSITY'S CYCLOTRON. Rosatelli, Carlo Comit. Naz. Energ. Nucl., Notiz., 12: 20-5(1966). (In Italian).

The 45-Mev AVF cyclotron at Milan University is described. Some information is included on the research program that is to be carried out with the accelerator. (D.C.W.)

17215 CONTROL OF RING MAGNET CURRENT OF THE ZERO GRADIENT SYNCHROTRON AT ARGONNE NATIONAL LABORATORY. Praeg, W. F. (Argonne National Lab., Ill.). IEEE (Inst. Elec. Electron. Eng.), Trans. Ind. Electron. Contr. Instrum., IECI-12: 66-77(Nov. 1965).

A functional diagram is shown and a comprehensive account is given of the control of the ring magnet current for the 12.5-Bev Zero Gradient Synchrotron (ZGS) at Argonne National Lab. The motor-generator set of the ring magnet power supply consists of a wound-rotor induction motor rated 15,500 hp at 13,000 v and 893 rpm; two salient pole 3-phase generators, each rated 38,000 kva and 11,000 v at 900 rpm; and a 93-ton flywheel. The total rotating mass is 273 tons. Pulsing power is supplied by a motor-generator-flywheel set via four groups of 12-phase rectifiers. The rectifier groups operate alternately as power rectifiers and power inverters as directed by their phase control circuits. A ZGS pulse demands six distinct modes of operation from its power supply. The amount of demagnetization and rest field is controlled within a few gauss in the period between pulses. During the initial current rise time, $\ddot{B}$ is adjustable within the limits of 18 kG/s$\ddot{B}$and 26 kG/s; $\ddot{B}$ is adjustable, at injection, from zero to 5×10^6 G/s^2. The current is brought close to its flat-top value in the adjustable interval of max voltage. Thereafter, the current flat-tops during a variable transition period (typical flat-top 21,500 G $\pm$ 0.02%). To spill the proton beam on a target, the flat-top is provided with current slope adjustments. Finally, the current decays to its rest field value during an adjustable inversion period. (BBB)

17216 THE RECENT STATE OF BETATRON DEVELOPMENT AND APPLICATION. Eckardt, A.; Geske, G.; Stecher, M. (Friedrich-Schiller-Univ., Jena, Ger.). Kernenergie, 8: 589-97(Oct. 1965). (In German).

Principles of function and construction, fields of application, survey of the betatrons hitherto constructed, and further development are considered. (auth)

17217 NANOSECOND PULSE DEVICE FOR A 2-Mev VAN DE GRAAFF ELECTRON ACCELERATOR. Dehoust, O.; Baierl, H.; Hesse, E. (Technische Hochschule, Munich). Nucl. Instrum. Methods, 40: 131-5(Feb. 1966).

A pulse generator for a 2 Mev Van de Graaff accelerator is described which produces electron pulses with rise and

decay times of 10^{-9} sec. The system is capable of delivering a maximum current of about 5 mamp for a duration in the order of 10^{-8} sec. For longer pulses the current pulse amplitude must be reduced, for example to 1.2 mamp for a 2×10^{-7} sec wide pulse, in order to obtain a good square-topped shape. (auth)

17218 THE PREPARATION OF SELF-SUPPORTING TARGETS OF BRITTLE METALS. Harchol, M. (Hebrew Univ., Jerusalem). Nucl. Instrum. Methods, 40: 158(Feb. 1966).

A method is described which is applicable for the preparation of self-supporting targets of hard metals with large diameters and a broad range of thicknesses. The metal is evaporated onto an aluminum foil of superficial density 170 $\mu g/cm^2$. Targets of Sc, Mn, Co, Y, Ho, and Pr, having about 1.5-cm diameter and thickness ranging from 100 $\mu g/cm^2$ were successfully prepared by this method. A check of residual aluminum was made by looking for gamma rays from proton-induced reactions and also by chemical methods. Both kinds of tests failed to show any sign of residual aluminum. This gives an upper limit of 0.5 mg/cm^2 for the aluminum content of the target. An additional method for the preparation of cobalt foils with thickness greater than 0.5 mg/cm^2 is also given. (J.F.P.)

17219 ON THE PAPER OF LOEBENSTEIN AND SPRINZAK "THE THIRD ORDER ABERRATIONS OF AN ELECTRIC STRONG FOCUSING DOUBLET." Dymnikov, A. D.; Yavor, S. Ya. (Ioffe Inst. of Physics & Tech., Leningrad). Nucl. Instrum. Methods, 40: 161-2(Feb. 1966).

The expression derived by Loebenstein and Sprinzak (Nucl. Instrum. Methods, 25, 162(1963)) for the third order aberrations of the doublet, composed of electrostatic quadrupole lenses, assuming the rectangular model for the field distribution is discussed. It is shown that this expression is not correct. (J.F.P.)

17220 AN IBM 7094 BEAM QUADRUPOLE ABERRATION PROGRAM. Meads, P. F. Jr. (William M. Brobeck and Associates, Berkeley, Calif.). Nucl. Instrum. Methods, 40: 166-8(Feb. 1966).

A very general computing program was written to study the linear properties of a general beam system and to calculate the third-order aberration properties of systems consisting of quadrupole and octopole magnets. The distinctive properties of this IBM 7094 code include a comprehensive method of parameter adjustment, using the linear programming algorithm, to meet up to 12 linear beam conditions and minimize aberrations. Easily used output is provided, including a wide complement of cathode-ray-tube plots. (auth)

17221 METHOD OF INVESTIGATING BETATRON OSCILLATION RESONANCES. Kulikov, O. F.; Moroz, E. M.; Petuchov, V. A.; Shorin, K. N.; Yarov, A. S. (Lebedev Inst. of Physics, Moscow). Nucl. Instrum. Methods, 40: 173-4(Feb. 1966).

The method described for an investigation of betatron oscillation resonances involves synchronous observation of the cross section dynamics of the electron beam and the beam intensity under various artificially created resonance conditions. The method was tested and applied to eliminate particle losses due to resonance antidamping of oscillations in a 680-Mev synchrotron. Photographs are shown of the various effects discussed. (J.F.P.)

17222 DEVELOPMENT OF ELECTROMAGNETS FOR NUCLEAR RESEARCH. Brezinscak, Marijan; Smiljanic, Daniel. Nukl. Energ., No. 4, 17-21(1965). (In Slovak).

Electromagnets developed for use in nuclear research are described. Quadrupole magnets were designed to produce magnetic fields for the focusing of beams of charged elementary particles. The excitation coils of almost all the magnets developed consist of flat coils separately insulated and impregnated. Both solid steel and laminated steel cores are used. (M.C.G.)

17223 ION SOURCES WITH A MAGNETIC FIELD. Teodorescu, I. E.; Marghitu, Silvia (Inst. of Atomic Physics, Bucharest). Stud. Cercet. Fiz., 17: 775-98(1965). (In Rumanian).

Construction and operating characteristics of the Penning and duoplasmatron type ion sources were analyzed, in order to determine the optimum design features of a source intended for use in linear particle accelerators. The study criteria included: formation of a plasma possessing the required ion concentration at the maximum ionization level of the gaseous medium, and the feasibility of utilizing all the ions formed at the highest ratio between the extracted ion flux and the neutral flux. Comparison of the sources revealed that the source originally developed by F. Penning gives satisfactory service in accelerators designed for compactness, simplicity and prolonged operation. Even though the Penning sources do not yield a high extracted ion flux, they remain competitive with the high-frequency sources under the above-mentioned conditions. The extracted ion flux may be increased if the source is used under pulsed operation. The intensities obtained with the duoplasmatron source are an order of magnitude higher than that in high-frequency and Penning sources; however, they require auxiliary equipment, such as high-power input devices and forced-circulation water cooling to remove the heat generated. (TTT)

17224 ACCELERATION OF NEGATIVE HYDROGEN IONS IN THE U-120 CYCLOTRON OF THE INSTITUTE OF ATOMIC PHYSICS. Indreas, Gr.; Tauth, Th. (Inst. of Atomic Physics, Bucharest). Stud. Cercet. Fiz., 17: 887-92(1965). (In Rumanian).

The most probable elementary processes for forming negative H^- ions are: dissociative capture, direct dissociation of the hydrogen molecule after collision with a fast electron and collision of hydrogen molecules or atoms with positive ions or neutral atoms. A high yield of negative ions may be obtained with ion sources that favor elementary processes with a large cross section. The U-120 cyclotron was operated at an induction region of 6.5 to 8 kG, changing the polarity of the electromagnet. The initial proton beam had an average intensity of $I_{\frac{1}{2}20}$ = 180 μamp and E = 6 Mev. Maximum intensity was obtained at relatively high gas flow rates. This high rate could be reduced at creating a larger pressure gradient in the central portion of the cyclotron. Operation of the source with oscillating electrons favors the dissociation process, increasing the intensity of the extracted negative ions. A high vacuum is required for accelerating the negative ions. This is especially important when phasotron operating conditions are employed as the path of the particles increases. (TTT)

17225 IMAGE CHARACTERISTICS OF SHORT MAGNETIC DEFLECTION SYSTEMS FOR ATOMIC BEAMS WITH REGARD TO THE VELOCITY DISTRIBUTION. II. APPROXIMATION THEORY. Becker, G.; Fischer, B. (Physikalisch-Technische Bundesanstalt, Brunswich). Z. Angew. Phys., 20: 71-3(Nov. 1965). (In German).

The numerical calculation of the focusing efficiency of magnetic deflection systems on atoms with a negative effective moment and the defocusing efficiency on atoms with a positive effective magnetic moment requires significant calculation time. An approximation theory for the calculation of these efficiencies is derived in which the central disc of the lens and therefore the N_2 flux are blocked off. (J.S.R.)

17226 LES ACCELERATEURS DE PARTICULES. (Particle Accelerators). Lapostolle, Pierre. Paris, Fayard, 1964. 152p.

The design and purpose of particle accelerators are described for the non-scientific reader. An indication is given of the data that can be obtained with accelerators. (J.S.R.)

17227 POWER SUPPLY SYSTEM FOR RING MAGNET OF ZERO-GRADIENT SYNCHROTRON. Winograd, H.; Millikin, A. D.; Hedin, R. A. (Allis-Chalmers Mfg. Co., Milwaukee). 6p. (CONF-651061-3). ORAU. Gmelin, AED-CONF-65-326-3.

From 21st National Electronics Conference and Exhibition, Chicago.

The power supply system for the ring magnet of the Argonne Synchrotron is described. The system was designed

to deliver d-c pulses with a peak power of 117×10^3 kw with a repetition rate of 15 pulses/min. (D.C.W.)

Astrophysics and Cosmology

Refer also to abstracts 17323 and 17658.

17228 (N-65-18275) DO SOLAR FLARE PROTON EVENTS MEASURE GEOMETRY OF A DIFFUSION PROCESS? Boldt, Elihu (National Aeronautics and Space Administration, Greenbelt, Md. Goddard Space Flight Center). Dec. 1964. 11p (NASA-TM-X-55161; X-311-64-371). CFSTI $1.00 cy, $0.50 mn.

The temporal distribution of protons arriving at earth from solar-flare events is consistent with an isotropic three-dimensional diffusion process. Solar protons that are injected into the interplanetary medium diffuse to earth via scattering from frozen magnetic kinks uniformly distributed over a homogeneous isotropic solar environment. The temporal development of the observed solar-flare proton intensity is a poor indication of the geometry associated with the diffusion process which has been invoked for describing the propagation of the beam. (STAR)

17229 THE ABUNDANCE OF ELEMENTS IN THE SOLAR ATMOSPHERE. Aller, Lawrence H. (Univ. of Michigan, Ann Arbor). Contract AF49(638)-807. Advan. Astron. Astrophys., 3: 1-25(1965).

A brief discussion of the theory and factors influencing the determination of elemental abundances in the solar atmosphere is presented. The role of transition probabilities in abundance determination is discussed. Solar abundance data for several elements are included. (M.O.W.)

17230 SPECTRAL ANALYSIS OF SOLAR FLARES. Svestka, Zdenek (Astronomical Inst. of the Czechoslovak Academy of Sciences, Ondrejov). Advan. Astron. Astrophys., 3: 119-239(1965).

Separate discussions are included on the evidences of Stark broadening of Balmer lines in flares, electron density, optical thickness, electron temperature and deviations from thermodynamic equilibrium, Balmer continuum, filamentary structure of flares, and the consequences of the filamentary structure. (M.O.W.)

17231 SURVEY OF MODERN COSMOLOGY. Zeldovich, Ya. B. (USSR Academy of Sciences, Moscow). Advan. Astron. Astrophys., 3: 241-379(1965).

Separate discussions are presented on the local properties of an expanding universe, properties of the world as a whole, observational predictions from theory, initial stage of evolution (nuclear reactions and thermodynamics), heterogeneities and their evolution in the expanding universe, and general theoretical foundations of cosmology. (M.O.W.)

17232 INTERACTION OF THE SOLAR WIND WITH THE PLANETS. Coleman, Paul J. Jr. (Univ. of California, Los Angeles). AIAA (Amer. Inst. Aeron. Astronaut.) J., 4: 4-9(Jan. 1966).

Properties of the resulting interactions between the solar wind and the magnetosphere are investigated. From observations of the properties of interplanetary medium and development of theoretical models of the solar wind, parameters typical of a quiet solar wind are calculated. The interaction of the solar wind with the dipolar geomagnetic field is described, and the method employed in scaling the observed effects for interaction with dipolar fields of different moments is presented. Speculations concerning interactions of the solar wind with planetary bodies not shielded by magnetic fields are summarized. (B.G.D.)

17233 THE DIFFERENCE IN LANTHANIDE ABUNDANCE PATTERN BETWEEN THE CRUST AND THE CHONDRITE AND ITS POSSIBLE MEANING TO THE GENESIS OF CRUST AND MANTLE. Masuda, Akimasa (Tokyo Univ.); Matsui, Yoshito. Geochim. Cosmochim. Acta, 30: 239-50(Feb. 1966).

First, the following assumptions were made: the earth's lithosphere encountered complete melting at a certain period, successive solidification of the melt resulted in the formation of mantle and crust, the partition coefficient between the solid and liquid phases for lanthanides were constant through all the stages of solidification that led to the formation of mantle, and the initial terrestrial abundance ratios of lanthanides were the same as those observed in chondrites. Mathematical treatment based on these assumptions enabled an interpretation to be made of the pattern variation of lanthanides and their concentration in the average crust and in the Norton County achondrite. In addition a method for estimating the crust-mantle weight ratio independently of geophysics was obtained. A formula was developed for calculation of the partition coefficients of minor elements from the concentration ratios between earth's crust and chondrite. (auth)

17234 NUCLEOSYNTHESIS IN THE EARLY HISTORY OF THE SOLAR SYSTEM. Burnett, D. S. (California Inst. of Tech., Pasadena); Fowler, William A.; Hoyle, F. Geochim. Cosmochim. Acta, 29: 1209-41(Dec. 1965).

The model of Fowler, Greenstein, and Hoyle (FGH) for the nucleosynthesis of D, Li, Be, and B by high energy particles from the Sun during the early history of the solar system was revised. The nuclear calculations were generalized to include a dependence on the duration of the irradiation caused by the long lifetime of ^{10}Be. The first stage of the calculation gave the required spallation yields and time-integrated neutron flux to produce the terrestrial Li, Be, and B abundances and isotopic ratios. The required flux was 4×10^{21} n/cm^2, identical with that obtained by FGH, and did not depend significantly on the choice of irradiation time. The predicted spallation yields depended more strongly on the irradiation time. These were compared with cloud chamber data for ^{16}O + 300 Mev neutrons. The predicted low spallation yield for ^{9}Be, which reflected its low relative abundance, was consistent with the cloud chamber data. Good agreement was not obtained for the B/Li spallation ratio; however, for large values of the irradiation time, this could be due to uncertainties in the parameters. This did not seem possible for short irradiation times, however. The second stage of the calculation gave the required hydrogen concentration, H/Si $\approx$ 1, and dilution factor, $F_d \approx 20$ (approximately the ratio of unirradiated to irradiated material) to give the terrestrial D/H ratio. FGH calculated $F_d = 10$ and H/Si = 8. The amount of water was considerably reduced in the present calculations. Although a loss of O during the formation of the Earth still must be postulated, the amount to be lost is much less than in the FGH case. The nucleosynthesis of ^{13}C in its present terrestrial abundance appeared quite feasible; however, in this case the solar ^{13}C/^{12}C ratio will be much less than that observed terrestrially. The fact that the isotopic composition of Li, Gd, and K in stone meteorites is identical with that found terrestrially implies that the Earth and the meteorites had a common initial history if the basic features of this model are to be retained. A lunar origin for stone meteorites could very well provide the required astrophysical situation to meet this requirement, whereas an asteroidal origin presents many more difficulties. (auth)

17235 DID THE IMP 1 OBSERVE THE MAGNETIC WAKE OF THE MOON OR EARTH? Ivanov, K. G. (Inst. of Terrestrial Magnetism, Ionosphere and Radio Wave Propagation, Academy of Sciences, USSR). Geomagn. Aeronomy (USSR)(Engl. Transl.), 5: 581-3(1965).

Translated from Geomagn. Aeronomiya, 5: 751-3(1965).

It is shown that the magnetic wake of the earth, directed upward along the stream of solar plasma, may have contributed noticeably to the phenomena observed by IMP-1 under sub-Alfven flow of the magnetosphere around the earth. (D.C.W.)

17236 INTERPLANETARY GAS. XI. AN EXOSPHERIC MODEL OF THE SOLAR WIND. Brandt, John C.; Cassinelli, Joseph P. (Kitt Peak National Observatory, Tucson, Ariz.). Icarus, 5: 47-63(Jan. 1966).

Exospheric theory is generalized for the case of an ionized atmosphere, in which the collision cross section is dependent on velocity. A fit to the observed density distribution in the solar corona is used in finding a continuum of energy-dependent "critical levels." The equation of con-

tinuity is used to find a distribution function, valid at large distances from the sun. The effects of fine structure are investigated and a model giving the density, expansion velocity, and kinetic temperature as a function of height is found. An inhomogeneous quiet corona at 2×10^{6}°K gives a proton density of 3 protons/cm^3 and an expansion velocity of 260 km/sec at the orbit of the earth. An active corona, with temperature $4-6 \times 10^{6}$°K, gives an expansion velocity of 460–600 km/sec. Thus, the solar wind appears to be a natural property of the corona, and does not fundamentally depend on the method of treatment (e.g., hydrodynamic versus exospheric, etc.). The problem of the abundances of heavier elements in the solar wind is also discussed; it is concluded that the solar wind abundances (by flux) must be the photospheric values. (auth)

17237 A PRELIMINARY ANALYSIS OF THE ABUNDANCES OF THE RARE EARTHS IN THE SUN. Wallerstein, George (Univ. of California, San Diego). Icarus, 5: 75-8(Jan. 1966).

Using equivalent widths from the Utrecht Atlas and laboratory f values measured at the National Bureau of Standards, the ratios of 11 heavy elements to scandium have been derived from curves of growth of ionized lines. The abundances of Sr, Y, and Zr agree well with spectroscopic determinations from neutral lines by Goldberg, Mueller, and Aller while the agreement for barium is only fair. When the rare earths are compared with abundances from meteorites as summarized by Urey the agreement is good for Ce, Nd, and Sm. La, which is well determined, appears to be surprisingly overabundant, Eu and Gd are represented by few lines and scatter rather badly as does Pr, the presence of whose lines in the sun is doubtful. (auth)

17238 CANYON DIABLO METEORITE: METALLOGRAPHIC AND MASS SPECTROMETRIC STUDY OF 56 FRAGMENTS. Heymann, Dieter (Univ. of Chicago); Lipschutz, Michael E.; Nielsen, Betty; Anders, Edward. Contract AT(11-1)-382. J. Geophys. Res., 71: 619-41 (Jan. 15, 1966). (COO-382-54).

In an attempt to reconstruct the history of the surviving Canyon Diablo fragments, 56 specimens were studied by metallography and mass spectrometry and 5 others by metallography only. Of these, 25 came from the rim of the crater, and 36 from the plains. Fifteen contained diamonds. On the basis of metallographically observable reheating effects, the samples were classified as strongly, moderately, and lightly shocked, corresponding to shock pressures of ≥750 kb, 130–750 kb, and <130 kb. The division among these categories was as follows. Plains: 0, 14, and 86%; rim: 72, 28, and 0%; diamond-bearing: 67, 33, and 0%. To determine the original depth in the meteoroid from which the specimens came, their ^{3}He content was measured. The values vary by a factor of 10^4, ranging from $\leq 0.03 \times 10^{-8}$ to 294×10^{-8} cc STP/g^{3}He. Apparently, the great majority of samples come from the outermost 2 of the meteoroid. There appears to be a distinct grading of shock effects with depth; the mean depth of the lightly shocked specimens is 72 cm, whereas that of the moderately and strongly shocked specimens is 132 cm. Diamond-bearing and rim specimens also come from greater mean depths: 135 and 127 cm, in contrast to the depth of the plains specimens (81 cm). The moderately to strongly shocked specimens, as well as the metallic spherules resulting from the vaporization of the meteorite, show a marked localization northeast and southeast of the crater. The throwout pattern for shocked material seems to have been highly directional, like the lunar ray craters. Measurements of He, Ne, and Ar in 14 of the most gas-rich samples gave a cosmic-ray age of 540 m.y. for 7 and 170 m.y. for 5 samples. The Canyon Diablo object apparently originated in a breakup 540 m.y. ago and suffered a secondary collision in space 170 m.y. ago. (auth)

17239 XENON ANOMALIES IN THE PASAMONTE METEORITE. Rowe, M. W.; Bogard, D. D. (Univ. of Arkansas, Fayetteville). Contract AT-(40-1)-3235. J. Geophys. Res., 71: 686-7(Jan. 15, 1966).

Data on a second sample of the Pasamonte meteorite are reported. The abundance and isotopic ratios of xenon from previous work are compared with those from the data reported. The agreement in the shape of the fission yield curve assumed to result from the spontaneous fission of ^{244}Pu in the two samples of the Pasamonte achondrite is shown and considered to be very good. The largest anomalies ever observed in the mass region 131 to 136 are seen in the xenon from the second sample. The data reported are consistent with spontaneous fission of ^{244}Pu as the main source of excess xenon but not with spontaneous fissions of ^{247}Cm, neutron-induced fission of ^{235}U, or photofission of ^{238}U. (J.F.P.)

17240 X-RAY EMISSION FROM VERY DENSE STARS. Surdin, M. (European Space Technology Center, Delft, Netherlands). Nature, 209: 62-4(Jan. 1, 1966).

A mechanism is proposed that accounts for emission of x-rays from punctual sources. Dynamic oscillations of the main body of a neutron star imply oscillations of the associated magnetic field. Outside the immediate surface of the star, electromagnetic waves are generated. Electrons trapped in the magnetic field of the star emit synchrotron radiation. Both x and γ photons are emitted. (M.C.G.)

17241 A COSMOLOGICAL MODEL. Whittaker, J. M. (Univ. of Birmingham, Eng.). Nature, 209: 491-2(Jan. 29, 1966).

A negative-pressure cosmological model is proposed, which seems to provide a possibility of linking the cosmological parameters with familiar laboratory constants. (G.O.Y.)

17242 ON THE NATURE OF THE QUASI-STELLAR SOURCES. Hoyle, F. (Cambridge Univ., Eng. California Inst. of Tech., Pasadena); Burbidge, G. R.; Sargent, W. L. W. Nature, 209: 751-3(Feb. 19, 1966).

The synchrotron emission from quasi-stellar objects is discussed with emphasis on its importance in relation to the Compton process. It is concluded that either the quasi-stellar objects are at distances of ~10 Mpsec or less, or the physical model associated with these objects must be substantially different from the present theories. (D.C.W.)

17243 LIGHTNING, NOVAE AND QUASARS. Bruce, C. E. R. (Electrical Research Association, Surrey, Eng.). Nature, 209: 798(Feb. 19, 1966).

The release of energy from galaxies is discussed in terms of the electric discharge theory of cosmic atmospheric phenomena and universal evolution. (D.C.W.)

17244 X-RAY ASTRONOMY. Friedman, Herbert (Naval Research Lab., Washington, D. C.). New Sci., 28: 904-6(Dec. 30, 1965).

X-ray astronomy is reviewed. Theories of x-ray sources, including the Crab Nebula are summarized. The techniques and some experiments in x-ray astronomy are considered, and the production of background by galactic cosmic electrons and x radiation are suggested. It is noted that the observed x-ray background flux destroys the steady-state cosmology, which postulates the continuous creation of matter in the form of neutrons to preserve charge neutrality. Future development is also discussed. (J.F.P.)

17245 PRIMEVAL HELIUM ABUNDANCE AND THE PRIMEVAL FIREBALL. Peebles, P. J. E. (Princeton Univ., N. J.). Phys. Rev. Lett., 16: 410-13(Mar. 7, 1966).

The results of a calculation of the primeval abundances of deuterium and helium produced in the big bang are presented. (D.C.W.)

17246 LUNAR X RAYS EXCITED BY ENERGETIC TERRESTRIAL ELECTRONS. Hayakawa, Satio (Nagoya Univ., Japan). Rep. Ionosphere Space Res. Jap., 19: 375-6(1965).

The intensities of lunar x rays excited by energetic electrons associated with the tail of the geomagnetic cavity formed by the solar plasma stream are estimated, and the feasibility of their observation is discussed. (R.E.U.)

17247 TRITIUM DIFFUSION MEASUREMENTS ON FOUR STONE METEORITES. Fechtig, H.; Gentner, W.

(Max-Planck-Institut fuer Kernphysik, Heidelberg). Z. Naturforsch., 20a: 1686-91(Dec. 1965). (In German).

Four stone meteorites were examined for their tritium diffusion constants. Tritium for the diffusion measurements was produced in the meteoritic material by neutron activation and high-energy proton bombardment. The tritium diffusion constants were found to be different for the two tritium production mechanisms. Tritium production by high-energy proton bombardment resembled more the production mechanism caused by cosmic radiation and therefore this diffusion constant was applied for the calculation of tritium losses. In the case of proton-produced tritium, values of D/a^2 were of the order of 10^{-18} sec^{-1}, whereas for tritium produced by neutron activation, the values were between 10^{-10} and 10^{-14} sec^{-1}. Using the D/a^2 values found for one stony meteorite (Alfianello) the tritium loss was of the order of 40% within 10 years. For the other meteorites the tritium loss within 10 years at room temperature was below 1%. (auth)

17248 X-RAY ASTRONOMY: OBSERVATIONAL RESULTS, THEORETICAL ASPECTS AND EXPERIMENTAL PROCEDURES [Thesis]. Bowyer, Charles Stuart. Washington, D. C., Catholic Univ. of America, 1965. 120p.

The results of experiments performed to determine the x-ray emission of the sun were reviewed. The sun's x-ray emission was analyzed in terms of a quiet component and a disturbed component. The average quiet component was found to undergo a variation in intensity that correlates with the sunspot cycle. The theory of solar x-ray emission appears to be adequate to explain the quiet component except at shorter wavelengths where it seriously underestimates the observed flux. The theoretical picture of the disturbed component is only qualitative at this time. The experimental results concerning the recently discovered cosmic x-ray sources were reviewed. Ten sources have been identified to date. A number of the sources, however, that are located near the galactic center are in close proximity and have not been resolved with certainty. The only definitive information on the cosmic x-ray sources other than their approximate locations concerns the source associated with the Crab Nebula. This source has been found to be an extended source approximately one light year in diameter. Theories as to the source mechanisms underlying the cosmic x-ray sources are speculative at present. A large-collecting-area sealed proportional counter was built to obtain information on the cosmic x-ray sources. This detector was sensitive to x rays in the 2 to 8 Å band and had a resolution with ^{55}Fe of 34%. A gas flow large window proportional counter system was built to obtain spectral information from the most intense of the cosmic x-ray sources. This instrument was successfully launched in a rocket on January 21, 1965. No useful data was obtained from the experiment. The causes of its failure are discussed. (Dissertation Abstr.)

17249 THE SPACE RADIATION ENVIRONMENT. Vette, James I. (Aerospace Corp., El Segundo, Calif.). 48p. (CONF-651057-3). ORAU. Gmelin, AED-CONF-65-313-1.

From IEEE East Coast Conference on Aerospace and Navigational Electronics, Baltimore.

A review of the space environment is presented. The solar wind, solar proton events, magnetospheric boundary phenomena, and, especially, the Van Allen radiation belts are discussed. 40 references. (D.C.W.)

Atomic Physics

Refer also to abstract 17225.

17250 (BNL-8850) WAVE FUNCTIONS FOR QUADRUPOLE ANTISHIELDING FACTORS. Sternheimer, R. M. (Brookhaven National Lab., Upton, N. Y.). Jan. 1965. Contract AT-30-2-GEN-16. 28p. Dep. mn. CFSTI $1.00 cy, $0.50 mn.

Some perturbed wave functions that were obtained in a calculation of the quadrupole antishielding factors for Al^{3+}, Cs^+, Cl^-, I^-, Pr^{3+}, and Tm^{3+} are tabulated. Perturbation by the nuclear quadrupole moment is taken into account. (D.C.W.)

17251 (IAE-873) TABLITSY SECHENII FOTOIONIZATSII ATOMA VODORODA. (Tables of Cross Sections of Photoionization of the Hydrogen Atom). Volkov, V. I.; Grechukhin, D. P.; Karpushkina, E. I. (Institut Atomnoi Energii, Gosudarstvennyi Komitet po Ispol'zovaniyu Atomnoi Energii SSSR, Moscow). 1965. 252p. Dep. mn.

Tables are presented of the photoionization cross sections of the hydrogen atom from the (n,l) states for $1 \leq n \leq 15$ and of the radial integrals of the dipole moment which determine the value of the matrix element of the dipole transition of the hydrogen atom from the (n,l) state of the discrete spectrum to the state of the continuous spectrum of the proton-electron system. The calculations were carried out on the basis of perturbation theory. (M.J.T.)

17252 (JINR-P-2522) ZAMECHANIE O MNOGOMERNOI KULONOVSKOI ZADACHE. (A Remark on the Many-Dimensional Coulomb Problem). Kuznetsov, G. I. (Joint Inst. for Nuclear Research, Dubna (USSR). Lab. of Theoretical Physics). 1965. 16p. Dep. mn.

The Fock problem is generalized to the many-dimensional problem. An explicit form of functions realizing representations of class I of groups O(f + 1) and L(f + 1) was obtained. (auth)

17253 (ORNL-3908, pp 90-9) ATOMIC AND MOLECULAR CROSS SECTIONS. Barnett, C. F.; Griffin, D. A.; Krause, M. O.; Ray, J. A. (Oak Ridge National Lab., Tenn.).

Measurements were made to confirm the existence of stable electronic excited states of H_3, similar to those found in H and H_2. Capture into repulsive levels of H_3 dominates the electron capture process, but the capture into all levels is an order of magnitude less than expected. The parameters influencing the charge-transfer conversion of monoenergetic protons into energy-dispersed neutral particle beams were investigated. A 50-kev proton beam was passed through an argon gas cell composed of 11 insulated electrodes arranged to provide a linear decelerating field. Application of a 40-kv retarding field resulted in a nearly flat energy distribution with a 40% conversion efficiency of incident protons to neutrals. Fifty-kiloelectron-volt H_2^+ particles incident on the gas cell exhibited 45% conversion. Engineering modifications have decreased the measured noise width of the silicon surface barrier for measuring low-energy protons. A minimum noise width of 2.75 kev was obtained. The pulse spectrum of 6-kev protons was resolvable with the present geometry. Resolvable pulse spectra were also obtained for 10-kev He^+ and 15-kev N^+ ions. The fast time response of a barium titanate crystal was determined for a pulsed 300-kev H^0 beam. At low power levels (10^{-4} w/cm) the shape of the output signal pulse from the crystal was differentiated; however, as the input power increased, the time response of the crystal was the same as that of the beam. (auth)

17254 ON THE BAND SPECTRUM OF ThO. Edvinsson, Gunnar; Selin, Lars-Erik; Aslund, Nils (Univ. of Stockholm). Arkiv Fys., 30: 283-319(1965).

The extensive band spectrum of the diatomic molecule ThO was studied in the region 5,000 – 11,000 Å. A high frequency, electrodeless discharge was used as a light source. Photographs were taken in a large plane-grating spectrograph. Thorium lines were used for comparison. The analyzed bands belong to seven different band systems. These systems are due to transitions between nine different singlet electronic states, four $^1\Sigma$, three $^1\Pi$, one $^1\Delta$ and one $^1\Phi$ state. The term values of the levels involved were determined by the method of least squares. This involves the solving of a large and strongly overdetermined system of linear equations. The rotational constants were determined from these term vlaues and a high accuracy was obtained. The relative errors of the B and D values are about 10^{-5} and 10^{-3} respectively. Some of the molecular constants in cm^{-1} are given. (auth)

17255 1001 REACTIONS OF THE Ar AND Kr ION DOUBLETS. Hussain, Masud; Kerwin, Larkin (Univ. Laval, Quebec, Can.). Can. J. Phys., 44: 57-65(Jan. 1966).

Ionization probability curves for Ar and Kr were examined up to 1.5 ev above the ionization threshold using an electrostatic electron selector. Structure is observed between the Kr^+ "ground" doublet levels and beyond the Ar^+ $J = \frac{1}{2}$ level. Some of this structure is found to affect the 1001 collision cross section for these ions, which were measured in the primary ion energy range of 500–1300 ev. The cross section for the $J = \frac{1}{2}$ state is found to be larger than that for the $J = \frac{3}{2}$ state in the case of Ar, while the reverse appears to be true for Kr. (auth)

17256 SPUTTERING OF SINGLE-CRYSTAL COPPER. Snouse, T. W.; Haughney, Louis C. (Ames Research Center, Moffett Field, Calif.). J. Appl. Phys., 37: 700-4 (Feb. 1966).

Sputtering yields from the (111), (100), and (110) planes of copper single crystals were measured as a function of normally incident argon-ion energy over the range from 100 to 200,000 ev. A comparison of the ratios of the yield curves as a function of ion energy reveals that lattice "transparency" is apparently not sufficient for a complete theoretical description of the sputtering process. (auth)

17257 ENERGY DISTRIBUTION OF ENERGETIC ATOMS IN AN IRRADIATED MEDIUM. II. SINGLE SPECIES CASE: APPLICATION TO RADIATION DAMAGE CALCULATIONS. Felder, R. M.; Kostin, M. D. (Princeton Univ., N. J.). J. Appl. Phys., 37: 791-6(Feb. 1966).

Collision densities are calculated for a homogeneous time-invariant system of energetic and thermal atoms of a single species. It is assumed that the rapidly moving atoms emanate from a monoenergetic source and undergo only binary elastic collisions with thermal atoms. For a class of interaction potentials whose differential scattering cross sections are independent of the energy of the incident atom, the collision density is found to vary as $1/E$ near the source energy, and as $1/E^2$ at lower energies. For hard-sphere scattering, the $1/E^2$ functionality extends over the entire energy range from zero to the source energy; as the degree of scattering anisotropy increases, the $1/E^2$ range contracts, and the $1/E$ variation covers an increasingly broad interval. Analytical expressions are obtained for the collision densities in both regions. Similar conclusions are reached for a less restricted class of interaction potentials, and the results applied to the calculation of the number of displaced atoms produced by a primary energetic atom. (auth)

17258 TEST OF THE LOW-ENERGY LIMIT OF THE BORN APPROXIMATION. Silverman, S. M. (Air Force Cambridge Research Labs., Bedford, Mass.); Lassettre, E. N. J. Chem. Phys., 44: 2219-20(Mar. 1, 1966).

If the angular distribution of the electron-collision cross sections for a transition is known at any one incident electron energy then, for the energy range for which the Born approximation is valid the total collision cross section may be calculated as a function of incident electron energy. Experimental results were compared with calculations for the $1^1S \rightarrow 3^1P$ transition in helium. Above about 120 ev the optically determined cross sections were larger but the shape of the curve approximately the same. Below 100 ev, however, the shapes of the two curves were different. (M.C.G.)

17259 SOME APPLICATIONS OF THE R-MATRIX THEORY TO REACTIVE AND ELASTIC MOLECULAR SCATTERING. Eu, Byung Chan; Ross, John (Brown Univ., Providence). J. Chem. Phys., 44: 2467-75(Mar. 15, 1966).

Wigner's R-matrix theory of collisions was applied to three topics in molecular scattering. Sufficient conditions are presented for a derivation of an activated-complex theory of chemical reaction rates, and of a statistical theory of reactive collisions. In the statistical theory it was found that the natural choice of the probability of decay of the collision complex into a given channel of the reaction product is a quantity proportional to the rate of production in that channel. Different assumptions were made in the literature on the removal of the dynamics from the probability of decay, and a brief comparison is presented. A connection was noted between the activated-complex and the statistical theory. Last, resonances in the total cross section for elastic scattering at low relative kinetic energy were discussed. Some illustrative calculations were made with the Breit–Wigner one-level formula and the WKB approximation for the eigenstates of the collision complex. (auth)

17260 ANALYSIS OF THE SPECTRUM OF NEUTRAL ERBIUM (Er I). Spector, Nissan (National Bureau of Standards, Washington, D. C.). J. Opt. Soc. Amer., 56: 341-9(Mar. 1966).

First results of a continuing analysis of Er I are given: 30 low levels belonging to $4f^{11}5d6s^2$ and other odd configurations, as well as 138 high levels of even parity are assigned J-values. More than 300 absorption lines are classified. The connection of the odd levels to the $4f^{12}6s^2$ configuration is established, using transitions in the infrared. The energy matrices in intermediate coupling for the subconfiguration $f^{11}(^4I)d$ were calculated and are given. The theoretical formulas were adjusted by a least-squares fit to 19 observed levels designated as $4f^{11}(^4I_{7\frac{1}{2},6\frac{1}{2}})5d6s^2$ resulting in new values for 6 electrostatic and 2 spin-orbit interaction parameters. The rms error was 186 cm^{-1}. Calculated percentage compositions in various coupling schemes show the J_1-j type to be the best for these levels. (auth)

17261 LOW ODD LEVELS OF ERBIUM I. Racah, G.; Goldschmidt, Z. B.; Toaff, S. (Hebrew Univ., Jerusalem). J. Opt. Soc. Amer., 56: 407-8(Mar. 1966).

Using the list of Marquet (Ph.D. thesis, University of California, Berkeley (1964)) all the erbium I levels of Marquet and Behring (J. Opt. Soc. Am., 55: 576 (1965)) and others also were found independently. J values were assigned to these levels on the basis of the J-selection rules. These low odd levels of erbium I are listed for various configurations. Also the Grotrian diagram up to 21,000 cm^{-1} and the parameters for the odd configurations obtained by least squares are given. (J.F.P.)

17262 AUTOIONIZATION OF FAST LITHIUM-LIKE NITROGEN AND OXYGEN IONS AFTER PASSAGE THROUGH A SOLID. Dmitriev, I. S.; Vinogradova, L. I.; Nikolaev, V. S.; Popov, B. M. (Moscow State Univ. Moscow Engineering Physics Inst.). JETP Lett. (USSR)(Engl. Transl.), 3: 20-3(Jan. 1, 1966).

Translated from Zh. Eksp. Teor. Fiz., Pis'ma Redakt., 3: 35-40(Jan. 1, 1966).

The autoionization of fast lithium-like nitrogen and oxygen ions after passing through a solid was investigated. It was found that immediately after leaving the solid target an appreciable fraction of the fast multiply charged ions loses an electron and its charge increases as a result of autoionization. (G.O.Y.)

17263 THE de SITTER GROUP $L_{4,1}$ AND THE BOUND STATES OF HYDROGEN ATOM. Bacry, H. (CERN, Geneva). Nuovo Cimento (10), 41A: 222-34(Jan. 21, 1966).

Assuming that bound states of the nonrelativistic hydrogen atom are basis vectors of a unitary irreducible representation of the 4 + 1 de Sitter group, the generators of this group are built classically in terms of r and p using Poisson brackets. (auth)

17264 PROTON-HYDROGEN ATOM SYSTEM AT LARGE DISTANCES. RESONANT CHARGE TRANSFER AND THE $1s\sigma_g$–$2p\sigma_u$ EIGENENERGIES OF H_2^+. Peek, James M. (Sandia Lab., Albuquerque, N. Mex.). Phys. Rev., 143: 33-5(Mar. 4, 1966).

The resonant charge-transfer reaction of a proton with a hydrogen atom is evaluated in the adiabatic approximation. Previous calculations of this cross section have used various approximations to the energy difference between the $1s\sigma_g$ and $2p\sigma_u$ states of the hydrogen molecule ion H_2^+. This approximation is removed by solving the H_2^+ Schrödinger equation for the eigenparameters required in addition to those previously available in the literature. The resulting

energy differences, found for internuclear separations of $R \leq 40.0\alpha_0$, are used to test the accuracy of large R estimates based on quasiclassical (WKB) and asymptotic arguments. The charge-transfer cross section calculated with the eigenenergies is found to be, at most, a few percent different from earlier results based on energy differences. Firsov's approximation and a recent modification by Smirnov are shown to be highly accurate when used with the eigenenergies. (auth)

17265 IONIZATION PRODUCED BY ENERGETIC GERMANIUM ATOMS WITHIN A GERMANIUM LATTICE. Sattler, A. R. (Sandia Lab., Albuquerque, N. Mex.); Vook, F. L.; Palms, J. M. Phys. Rev., 143: 588-94(Mar. 11, 1966). (LA-DC-7296).

The energy dependence of the ionization produced in germanium by energetic germanium atoms was measured. Germanium solid-state detectors served simultaneously as crystalline Ge sample, neutron target, and ionization detector. The spectrum of ionization produced by prompt Ge recoil atoms energized by monoenergetic neutron bombardment was observed in a pulse-height analyzer, and the edge of the spectrum was identified with the ionization produced by Ge recoil atoms having the calculated maximum recoil energy. The electron-hole pair production of Ge recoils was measured in this manner from 21.4 to 997 kev, using monoenergetic neutrons from 400 kev to 18.6 Mev. In this energy range, the ratio of the ionization produced by a Ge recoil relative to that of an electron of the same energy increased from ~0.15 to ~0.7. At very low Ge recoil energies, most of the energy goes into atomic processes. At high recoil energies, where electronic processes become important, the ionization produced by a Ge recoil appears to approach that for an electron of the same energy. The corresponding partition of energy between electronic processes and atomic processes for an energetic Ge atom in a Ge lattice agrees favorably with predictions of the theory of Lindhard et al. These data together with the earlier results of ionization produced by energetic Si atoms within a Si lattice agree with the A and Z dependence of the partition of energy predicted by Lindhard. (auth)

17266 LONG-RANGE INTERATOMIC FORCES FROM PREDISSOCIATION DATA AND RESONANCES IN ATOMIC SCATTERING. Bernstein, Richard B. (Univ. of Wisconsin, Madison). Phys. Rev. Lett., 16: 385-8(Mar. 7, 1966).

The explicit relations are developed which are needed to make use of the limiting curve of dissociation (LCD) in the determination of long-range interatomic forces from spectra. The close connection between the LCD and the expected pattern of resonances (inverse predissociation) in atom-atom scattering cross sections is also established. (G.O.Y.)

17267 PHOTOELECTRIC ION EMISSION FROM CESIATED SURFACES. Breaux, O. P.; Medicus, G. (Air Force Avionics Lab., Wright-Patterson AFB, Ohio). Phys. Rev. Lett., 16: 392-4(Mar. 7, 1966).

An experiment is summarized in which photoelectric ion emission from cesiated surfaces at room temperature was apparently observed. (D.C.W.)

17268 FINE STRUCTURE AND ISOTOPE SHIFT IN MUONIC LEAD. Anderson, H. L. (Univ. of Chicago); McKee, R. J.; Hargrove, C. K.; Hincks, E. P. Phys. Rev. Lett., 16: 434-9(Mar. 14, 1966).

The fine structure in the K, L, and M x-ray lines of muonic lead was studied. An isotope shift in the 2p-1s transitions was observed. The size and shape of the nuclear charge distribution were calculated from the experimental results. (D.C.W.)

17269 CROSS SECTION AND POLARIZATION OF BALMER ALPHA RADIATION PRODUCED IN CHARGE-EXCHANGE COLLISIONS OF PROTONS WITH N_2. Murray, J. S.; Young, S. J.; Sheridan, J. R. (Univ. of Alaska, College). Phys. Rev. Lett., 16: 439-40(Mar. 14, 1966).

The cross section for the production of Balmer-alpha radiation in charge-exchange collisions of 2- to 35-kev protons with N_2 and the associated polarization of the Balmer-alpha radiation were measured. (G.O.Y.)

17270 CROSS SECTION FORMULAE FOR IONIZATION AND EXCITATION OF ATOMS BY HIGH ENERGY ELECTRONS. Schram, B. L. (FOM-Laboratorium voor Massacheiding, Amsterdam); Vriens, L. Physica, 31: 1431-6 (Sept. 1965).

In the Bethe-Born approximation the cross sections for ionization or excitation of atoms by electrons of high energy E_1, are given by $\sigma = A/E_1 \ln cE_1$ for optically allowed transitions and by $\sigma = B/E_1$ for disallowed transitions. Here A, B and c are constants for a given transition. For ionization or excitation processes to which both types of transitions contribute, the total cross sections are given by $\sigma = A/E_1 \ln c'E_1$. These formulas are frequently simplified using the approximation $cU \approx c'U \approx 4$, where U is the ionization or excitation energy. It is shown that great deviations from these latter approximations occur. (auth)

17271 THE TAMM VARIATIONAL PRINCIPLE AND ITS GENERALIZATION TO THE SCATTERING AMPLITUDE. Moiseiwitsch, B. L. (Stanford Research Inst., Menlo Park, Calif.); Stacey, G. M. Proc. Phys. Soc., 86: 737-43(Oct. 1965).

A variational principle for the phase shift, which is analogous to that originated by Tamm, is derived, and its connection with certain approximations for the phase shift is discussed. Further, the Tamm variational principle is used to establish an integral equation involving the Kato functional. The Tamm variational principle is then generalized to give a variational principle for the scattering amplitude. Finally, application is made to the scattering of electrons by by the static field of a hydrogen atom. (auth)

17272 THE DIPOLE SPECTRUM AND PROPERTIES OF HELIUM. Chan, Y. M.; Dalgarno, A. (Queen's Univ., Belfast). Proc. Phys., Soc., 86: 777-82(Oct. 1965).

Analytical representations of the dipole spectrum of the ground state of helium are derived. From them are calculated the Verdet constant, the mean excitation energies I and I_1 characterizing stopping and straggling of a beam of fast particles absorbed in helium and the leading coefficient $C(a,b)/R^6$ of the long-range interaction between atoms a and b a distance R apart. I is 42.0 ev, I_1 is 73 ev, C(He, He) is 1.471 A.U. and C(He,H) is 2.830 A.U. (auth)

17273 ON THE PRODUCTION OF POLARIZED ELECTRON BEAMS BY SPIN EXCHANGE COLLISIONS. Byrne, J.; Farago, P. S. (Univ. of Edinburgh). Proc. Phys. Soc., 86: 801-15(Oct. 1965).

A method for obtaining beams of polarized electrons, by transfer of polarization from an atomic beam to a cross-fired electron beam, is investigated using the formalism of the Stokes vector and the interaction matrix. The transfer takes place through the mechanism of spin exchange in elastic collisions, and this effect is discussed together with problems arising from the statistical nature of the transfer process. The theoretical requirements for a workable system are translated into practical terms and details are given of a proposed experiment. This incorporates a device capable of trapping electrons of low energy for periods of a few milliseconds. The system is estimated to yield a pulsed beam of electrons of a few ev energy, with an intensity of about 10^{-8} A and a polarization approximately equal to that of the atomic beam. (auth)

17274 ELECTRON CAPTURE BY FAST PROTONS IN HELIUM. Bransden, B. H.; Sin Fai Lam, L. T. (Univ. of Durham, Eng.). Proc. Phys. Soc. (London), 87: 653-5 (Mar. 1966).

Cross sections for the electron capture reaction $p + He(1s^2) \rightarrow H(1s) + He^+(1s)$ are determined within the two-state impact parameter formalism, for a number of approximate helium wave functions. It is concluded that the calculated cross sections are not very sensitive to the helium wave function employed, for a range of proton energies between 30 kev and 10 Mev, and that the simple variational function $\phi(r_1,r_2) = \exp\{-\alpha(r_1 + r_2)\}$ should be adequate for new calculations that are in progress and which go beyond the two-state approximation in an attempt to improve the agreement of the theory with experiment. (auth)

17275 CLASSICAL CALCULATIONS ON ELECTRON CAPTURE. Bates, D. R.; Mapleton, R. A. (Queen's

Univ., Belfast). Proc. Phys. Soc. (London), 87: 657-68 (Mar. 1966).

The classical theory of Thomas on electron capture from heavy atoms by fast nuclei is considered. A modification is introduced. It is found that the predictions of the modified theory are in quite good accord with the measurements of Barnett and his associates. The extent to which the scaled experimental data on a number of gases may be represented by a single curve is striking. Capture from light atoms is also discussed. The approximations made in the classical impulse approximation are here unsatisfactory. A simple classical theory of symmetrical resonance capture in slow encounters is developed. It is remarkably successful. (auth)

17276 ELECTRON CAPTURE BY HELIUM IONS IN NEUTRAL HELIUM. Fulton, Margaret J.; Mittleman, M. H. (Univ. of California, Livermore). Proc. Phys. Soc. (London), 87: 669-76(Mar. 1966).

Two distinct calculations are described. The first describes $He^+ + He$ by a two-atomic-state approximation. It modifies a previous calculation in order to include properly the Pauli principle. It is found that multiple electron exchange which this introduces is not important for the total cross section but is for angular distribution. The second calculation describes $He^{2+} + He$ by a three-atomic-state approximation, allowing for both single and double exchange. It is found that ignorance of He exact wave functions causes conceptual difficulties in the calculation. (auth)

17277 THE STOPPING POWER OF HYDROGEN AND HYDROCARBON VAPOURS FOR ALPHA PARTICLES OVER THE ENERGY RANGE 1 TO 8 Mev. Palmer, Rita B. J. (Royal Free Hospital School of Medicine, London). Proc. Phys. Soc. (London), 87: 681-8(Mar. 1966).

Range-energy relations have been determined experimentally for 8.78 Mev alpha particles in a number of hydrocarbon vapors and in hydrogen. Differential stopping powers at various energies have been determined and mean excitation potentials derived. There is evidence of charge exchange taking place at low energies, but significant deviations from the Bragg rule due to variations in molecular binding were not observed. (auth)

17278 ON THE CAPTURE OF π^- MESONS IN HYDROGEN AND DEUTERIUM. Fursa, A. D. (Inst. of Physics, Academy of Sciences, Ukrainian SSR). Ukr. Fiz. Zh., 10: 1051-5(1965). (In Russian).

The pseudopotential method was used to find the probability of the processes $\pi^-p \rightarrow \pi^0n$ and $\pi^-d \rightarrow \pi^0nn$ originating from the S- and P-mesonic atom states, for π^- and π^0 of the same parity. It is established that the relative contribution of the reaction $\pi^-d \rightarrow \pi^0nn$ with respect to the reactions $\pi^-d \rightarrow nn$ and $\pi^-d \rightarrow nn\gamma$ equals 2.5×10^{-4}. Since the distance between the fine structure levels is considerably greater than the width of the levels, the capture of π^- occurs independently from each level. The probabilities of capture from the various fine structure levels are found. (auth)

17279 ON THE THEORY OF MOLECULAR BEAM PRODUCTION WITH THE HELP OF CYLINDRICAL TUBES. Zugenmaier, P. (Univ., Freiburg i. B.). Z. Angew. Phys., 20: 184-8(1966). (In German).

The intensity distribution and the total flow rate of a molecular beam generated by a tube of arbitrary length in the region of molecular flow ($\lambda \gg a$, $\lambda \gg L$) are calculated. In contrast to earlier works, the density gradient and the density at the end of the tube are determined exactly for the limiting cases of sufficiently long and very short tubes. The intensity distribution for the case of Knudsen flow within the tube ($\lambda \gg a$) is calculated using a method of Giordmaine and Wang. Approximation formulas for the peak intensity and the half-width of the beam are given which are in good agreement with recent experiments. (auth)

17280 MEASUREMENT OF THE g_J-FACTOR OF THE $^5D_4$-GROUND STATE OF ^{56}Fe WITH THE ATOMIC BEAM MAGNETIC RESONANCE METHOD. Kamlah, A.; Penselin, S. (Univ., Heidelberg). Z. Phys., 190: 16-24(1966).

Using a newly built atomic beam magnetic resonance apparatus the Zeeman effect of the ^5D ground state multiplet of ^{56}Fe was studied. The g_J factor of the $^5D_4$ state was determined. (M.O.W.)

17281 MUONIC ATOMS IN THE NEIGHBOURHOOD OF LEAD. Huefner, Joerg (Univ., Heidelberg). Z. Phys., 190: 81-98(1966).

In muonic atoms with deformed nuclei resonances between muonic and nuclear states produce a fine structure in the x-ray spectrum. The nuclear quadrupole moment can be determined from an analysis of this fine structure. The usual calculations of the resonances in muonic atoms are improved; (1) The muonic states are not treated as stationary, (2) The electromagnetic interaction between the muon and the nucleus also contains the magnetic forces and the retardation of the electromagnetic field, and (3) The widths of the muonic transitions (E1, E2 and M1) are calculated without using Siegert's theorem. All corrections are found to be small in most cases. The experimental intensity ratios for muonic Tl, Pb and Bi are discussed in detail. A new type of resonance is proposed for muonic Pb and Bi in order to explain their anomalous intensity ratios. (auth)

17282 RADIATION ANISOTROPY OF THE HYDROGEN ATOM IN AN ELECTRIC FIELD. Lyuboshits, V. L.; Onishchuk, V. A.; Podgoretskii, M. I. (Joint Inst. for Nuclear Research Dubna, USSR). Zh. Eksp. Teor. Fiz., 49: 1938-41(Dec. 1965). (In Russian).

Interference effects in radiative transitions in the hydrogen atom in an external electric field are investigated. It is demonstrated that already in comparatively weak fields the radiation due to the $2P_{\frac{1}{2}} \rightarrow 1S_{\frac{1}{2}}$ and $2P_{\frac{3}{2}}1S_{\frac{1}{2}}$ transitions is noticeably anisotropic and partially linearly polarized. (auth)

17283 THE LORENTZ GROUP AS A DYNAMIC SYMMETRY GROUP OF THE HYDROGEN ATOM. Perelomov, A. M.; Popov, V. S. (Inst. of Theoretical and Experimental Physics, State Atomic Energy Commission, USSR). Zh. Eksp. Teor. Fiz., 50: 179-98(Jan. 1966). (In Russian).

The latent (dynamic) symmetry of the hydrogen atom is considered from the point of view of group theory. It is shown that transition from the compact group 0(4) to its noncompact analog (Lorentz groups) makes feasible the description of the discrete as well as continuous spectrum. In this case the wave function of the continuous spectrum with a given energy $E > 0$ realizes an infinite-dimensional irreducible representation $D(0,\rho)$ of the Lorentz group ($\rho = \sqrt{2/E}$), which belongs to the so-called fundamental series of the unitary representations. Wave functions of discrete spectrum states with a principal quantum number n realize a finite-dimensional representation $D[(n-1)/2,(n-1)/2]$ of the Lorentz group. A wave function symmetry specific for the Coulomb potential is found for continuous spectrum and discrete spectrum states respectively. The special case of states with $E = 0$ (in an attraction field) when the Lorentz group degenerates into the Galilei group is also considered. An expansion of the Coulomb Green function (for $E > 0$) into irreducible representations of the Lorentz group is obtained. An explicit expression for the Green function of the Kepler problem in n-dimensional space is derived and the geometric meaning of the symmetry possessed by the Coulomb wave functions is elucidated. (auth)

17284 IONIZATION OF SYSTEMS BOUND BY SHORT RANGE FORCES UNDER THE ACTION OF AN ELECTROMAGNETIC WAVE. Nikishov, A. I.; Ritus, V. I. (Lebedev Inst. of Physics, Moscow). Zh. Eksp. Teor. Fiz., 50: 255-70(Jan. 1966). (In Russian).

The probabilities for disintegration of neutral and charged systems bound by short range forces under the action of the field of a plane electromagnetic wave are obtained. The angular and energy distributions of the emitted particles, the distributions in number of absorbed photons and also the dependence of the probability on polarization of the electromagnetic wave and polarization of the bound system are considered. The conditions for which the internal structure of the system influences the dependence

of the disintegration probability on the field strength and wave frequency are indicated. The results obtained are valid, in particular, for describing multiquantum disintegration of negative and molecular ions. (auth)

17285 ISOTOPE SHIFT OF THE $K_{\alpha 1}$ X-RAY IN URANIUM [Thesis]. Brockmeier, Richard Taber. Pasadena, Calif., California Inst. of Tech., 1966. 118p.

The first experimental evidence of the isotopic shift of electronic K x rays was found. A two-meter focal length curved-crystal diffraction spectrometer was used to measure the wavelengths of fluorescent $K_{\alpha 1}$ x rays from isotopically pure ^{233}U and ^{236}U samples. The difference in wavelengths was found to be 0.00228 ± 0.00022 x-units. This corresponds to a 1.8 ± 0.2 ev energy difference, the ^{233}U x ray being higher in energy. The result is discussed in terms of the pure volume effect, the even-odd staggering contributions, the change of intrinsic quadrupole moments, and the nuclear compressibility factor. Good agreement between the experimental result and theory is obtained by considering the pure volume effect or by considering the contributions of all four effects choosing the parameter for the nuclear compressibility somewhat higher than inferred from the optical isotope shift measurements. (Dissertation Abstr.)

17286 EFFEKTIVNYE SECHENIYA STOLKNOVENII ELEKTRONOV S ATOMAMI. (Effective Cross Sections of Electron Collisions with Atoms). Veldre, V. Ya. (ed.). Riga, USSR, Izdatel'stvo Zinatne, 1965. 178p.

Six articles are included on calculations of slow-electron collisions with alkali-metal atoms, electron elastic scattering on alkali-metal atoms, excitation of Ne and Ar atoms by electron impact, cross sections of excitation of H atoms in the Born approximation, and lower limits for the phases of electron-hydrogen scattering. (M.J.T.)

17287 IONIZATION CROSS SECTION OF CESIUM AT THRESHOLD. Heil, H.; Scott, B. W. (Hughes Research Labs., Malibu, Calif.). 8p. (CONF-651049-6). ORAU. Gmelin, AED-CONF-65-324-2.

From IEEE Thermionic Conversion Specialist Conference, San Diego, Calif.

Absolute values of the ionization cross section of cesium were obtained near threshold. (D.C.W.)

17288 IVth INTERNATIONAL CONFERENCE ON THE PHYSICS OF ELECTRONIC AND ATOMIC COLLISIONS, UNIVERSITE LAVAL, QUEBEC, CANADA, AUGUST 2-6, 1965. Abstracts of Papers. New York, Science Bookcrafters, Inc. 458p. (CONF-650833).

Separate abstracts were prepared for 19 of the 183 resumes included. The remaining papers deal with experimental and theoretical studies of collisions of atoms, electrons, and molecules. (D.C.W.)

For abstracts of individual papers see: 17289—17306, and 17423.

17289 THE QUASI-STATIONARY-STATE APPROACH TO RESONANCES IN THE SCATTERING OF ELECTRONS FROM ATOMS AND MOLECULES. Herzenberg, A. (Univ. of Manchester, Eng.). pp 1-6 of IVth International Conference on the Physics of Electronic and Atomic Collisions. New York, Science Bookcrafters, Inc.

The quasi-stationary-state approach to resonances in the scattering of electrons from atoms and molecules is discussed. (G.O.Y.)

17290 DOUBLE-INELASTIC COLLISIONS OF EXCITED HYDROGEN ATOMS WITH EXCITED HYDROGEN ATOMS. Pomilla, Frank R.; Milford, S. N. (Grumman Aircraft Engineering Corp., Bethpage, N. Y.). pp 87-93 of IVth International Conference on the Physics of Electronic and Atomic Collisions. New York, Science Bookcrafters, Inc.

The cross sections for double-inelastic collisions of excited hydrogen atoms with excited hydrogen atoms were calculated for center-of-mass energies between 2 kev and 100 Mev. (G.O.Y.)

17291 SPIN-EXCHANGE SCATTERING IN UNIFORM MAGNETIC FIELDS. Glassgold, A. E. (New York Univ., New York). pp 147-50 of IVth International Conference on the Physics of Electronic and Atomic Collisions. New York, Science Bookcrafters, Inc.

Spin-exchange scattering in uniform magnetic fields was studied for collisions in which the atomic systems each have one effective electron (e.g., electrons scattered by hydrogen or by alkali atoms, two alkali atoms, etc.). (G.O.Y.)

17292 FINE STRUCTURE IN THE ENERGY SPECTRA OF ELECTRONS FROM GASES BOMBARDED BY POSITIVE IONS. Rudd, M. Eugene; Lang, David V. (Concordia Coll., Moorhead, Minn.). pp 153-8 of IVth International Conference on the Physics of Electronic and Atomic Collisions. New York, Science Bookcrafters, Inc.

The energy spectra of electrons emitted from various gases after bombardment by protons or hydrogen molecular ions are presented. Rich structures appear in certain energy regions, which may be attributed to auto-ionization electrons from various highly excited atomic states of the gases. (G.O.Y.)

17293 ELASTIC SCATTERING IN HYDROGEN-HELIUM SYSTEMS: MEASUREMENT OF THE "KNOCK-ON" CROSS SECTION. Van Der Valk, Fred; Moore, George E.; Datz, Sheldon (Oak Ridge National Lab.). pp 164-7 of IVth International Conference on the Physics of Electronic and Atomic Collisions. New York, Science Bookcrafters, Inc.

An attempt was made to measure the ratio of the H_2—He and D_2—He total scattering cross sections. A modulated He signal, which was due to knock-on collisions, was observed. The cross sections for knock-on collisions were investigated. (D.C.W.)

17294 THE VELOCITY DEPENDENCE OF THE TOTAL SCATTERING CROSS SECTION OF K ON RARE GASES. Von Busch, F. (Univ., Bonn); Strunck, H. J.; Schlier, C. pp 167-71 of IVth International Conference on the Physics of Electronic and Atomic Collisions. New York, Science Bookcrafters, Inc.

The results of some measurements of the velocity dependence of the total scattering cross section of K on rare gases are summarized, together with some attempts to fit the data. (D.C.W.)

17295 MOLECULAR-BEAM STUDIES OF THE ALKALI-HALOGEN REACTIONS: THE SPECTATOR STRIPPING MODEL. Datz, Sheldon; Minturn, Robert E. (Oak Ridge National Lab., Tenn.). pp 177-80 of IVth International Conference on the Physics of Electronic and Atomic Collisions. New York, Science Bookcrafters, Inc.

A number of alkali atom-halogen reactions of the type $M + X_2 \rightarrow M^+X^- + X$ were studied using crossed-molecular-beam techniques. The reactive scattering distributions were calculated on the basis of a Spectator-Stripping Model. (D.C.W.)

17296 VELOCITY ANALYSIS OF REACTIVE SCATTERING IN CROSSED MOLECULAR BEAMS: INTERNAL ENERGY AND CENTER-OF-MASS ANGULAR DISTRIBUTION OF PRODUCTS. Grosser, Arthur E.; Bernstein, Richard B. (Univ. of Wisconsin, Madison). pp 180-3 of IVth International Conference on the Physics of Electronic and Atomic Collisions. New York, Science Bookcrafters, Inc.

The velocity distributions of excited KBr formed in reactive collisions of velocity-selected K beams with crossed thermal beams of HBr and Br_2 were measured at several laboratory scattering angles and initial relative kinetic energies. The angular distribution of reactive scattering and the distribution function for the internal energy of the KBr were studied on the basis of velocity analyses. (D.C.W.)

17297 ATOMIC INTERACTIONS OF MUONIUM. Mobley, R. M.; Bailey, J. M.; Cleland, W. E.; Hughes, V. W.; Rothberg, J. E. (Yale Univ., New Haven). pp 194-7 of IVth International Conference on the Physics of Electronic and Atomic Collisions. New York, Science Bookcrafters, Inc.

The results of some studies of the reactions of muonium with atoms are briefly discussed, together with two methods of studying reactions of muonium with molecules. (D.C.W.)

17298 STUDIES OF IONIC DRIFT VELOCITIES AND ION-MOLECULE REACTIONS IN A DRIFT-TUBE MASS SPECTROMETER. McDaniel, E. W.; Keller, G. E.; Albritton, D. L.; Miller, T. M.; Martin, D. W. (Georgia Inst. of Tech., Atlanta). pp 239-45 of IVth International Conference on the Physics of Electronic and Atomic Collisions. New York, Science Bookcrafters, Inc.

A drift-tube mass spectrometer which is used for quantitative measurements of ionic drift velocities and qualitative studies of ion-molecule reactions is described. Some data for N^+, N_2^+, N_3^+, and N_4^+ ions in nitrogen are presented, and some preliminary results for H^+ and H_3^+ ions in hydrogen are discussed. (D.C.W.)

17299 THE MEASUREMENT OF LOW-ENERGY CESIUM ION-CESIUM ATOM CROSS SECTIONS BY BEAM TECHNIQUES. Bullis, R. H. (United Aircraft Research Labs., East Hartford, Conn.). pp 263-4 of IVth International Conference on the Physics of Electronic and Atomic Collisions. New York, Science Bookcrafters, Inc.

The total cross sections for cesium ion-atom collisions were measured over an energy range from below 0.1 to 10 ev in a modified Ramsauer cross-section experiment in which significant perturbations, caused by contact potential effects and stray electric fields, were eliminated by using an electroformed collision chamber with reentrant exit and entrance slits. (D.C.W.)

17300 MEASUREMENT OF THE ANGULAR DISTRIBUTION OF ELASTICALLY SCATTERED Cs^+ IONS FROM Ar, Kr, AND N_2. Menendez, Manuel G.; Datz, Sheldon (Oak Ridge National Lab., Tenn.). pp 264-8 of IVth International Conference on the Physics of Electronic and Atomic Collisions. New York, Science Bookcrafters, Inc.

The angular distribution of Cs^+ ions elastically scattered from Ar, Kr, and N_2 was measured in the energy range from 2.3 to 11.6 ev. The results were compared to previous theoretical values. (G.O.Y.)

17301 IONIZATION AND CHARGE-TRANSFER CROSS SECTIONS FOR FAST NEUTRAL HELIUM ATOMS (0.15 to 1.0 Mev). Martin, D. W.; Puckett, L. J.; Taylor, G. O. (Georgia Inst. of Tech., Atlanta). pp 280-4 of IVth International Conference on the Physics of Electronic and Atomic Collisions. New York, Science Bookcrafters, Inc.

Absolute measurements were made of the total cross sections for the production of slow positive ions and free electrons by helium atoms in Ar, He, H_2, and N_2. The energies of the incident particles ranged from 0.15 to 1.0 Mev. (D.C.W.)

17302 AN EXPERIMENTAL STUDY OF CHARGE TRANSFER IN PROTON-ATOMIC HYDROGEN COLLISIONS AT ENERGIES HIGHER THAN 50 kev. Ryding, G.; Gilbody, H. B. (University Coll., London). pp 302-6 of IVth International Conference on the Physics of Electronic and Atomic Collisions. New York, Science Bookcrafters, Inc.

Absolute measurements were made of the total cross section for charge transfer by protons in a target of atomic hydrogen. The results were compared with the predictions of various scattering approximations. (D.C.W.)

17303 THE PROTON-HYDROGEN ATOM SYSTEM AT LARGE DISTANCES. CHARGE TRANSFER AND THE $1s\sigma_g - 2p\sigma_u$ EIGENENERGIES. Peek, James M. (Sandia Lab., Albuquerque, N. Mex.). pp 306-8 of IVth International Conference on the Physics of Electronic and Atomic Collisions. New York, Science Bookcrafters, Inc.

The total charge-transfer cross section for the H, H^+ system was calculated using the eigenenergies for two states of H_2^+. The results were compared with the results of other calculations. (D.C.W.)

17304 ELECTRON CAPTURE INTO EXCITED STATES BY HELIUM IONS INCIDENT ON HELIUM. De Heer, F. J.; Wolterbeek Muller, L.; Geballe R. (FOM-Laboratorium voor Massacheiding, Amsterdam). pp 309-14 of IVth International Conference on the Physics of Electronic and Atomic Collisions. New York, Science Bookcrafters, Inc.

Electron capture into an excited state by helium ions incident on helium gas was investigated at impact energies between 5 and 100 kev. The process considered was $He^+ + He \rightarrow He^* + He^+$. The absolute cross sections were determined for capture into singlet and triplet He(I) levels with principal quantum number n varying between 3 and 6. The degree of polarization was also measured for some of the corresponding spectral lines. (G.O.Y.)

17305 ATOMIC AND IONIC PARTIAL STOPPING POWERS OF HELIUM GAS FOR A HELIUM BEAM. Cuevas, J.; Torres, P.; Allison, S. K. (Univ. of Chicago). pp 347-50 of IVth International Conference on the Physics of Electronic and Atomic Collisions. New York, Science Bookcrafters, Inc.

The measurement of atomic and ionic partial stopping powers of He gas for He beams is discussed, and some results are presented for incident particles in the velocity range from 4.91 to 6.94×10^8 cm/sec. (D.C.W.)

17306 SOME PROPERTIES OF THE GENERALIZED OSCILLATOR STRENGTH AND THEIR RELATION TO INELASTIC SCATTERING OF CHARGED PARTICLES. Inokuti, M.; Platzman, R. L. (Argonne National Lab., Ill.). pp 408-12 of IVth International Conference on the Physics of Electronic and Atomic Collisions. New York, Science Bookcrafters, Inc.

Some of the features of the Bethe surface, especially in the low-K region, are discussed with particular emphasis on the determination of optical properties from scattering data and vice versa. A sum rule is also presented. (G.O.Y.)

Cosmic Radiation

See also Elementary Particles and Radiations
Nuclear Properties and Reactions

Refer also to abstracts 17651 and 17658.

17307 (CONF-651001-34) A SOLAR WIND DEUTERIUM DETECTOR AND CHARGE SPECTRUM ANALYZER. Floyd, Frank W.; Scherb, Frank (Massachusetts Inst. of Tech., Cambridge). [1963]. Contract AT(30-1)-2098. 21p. Dep. mn. CFSTI $1.00 cy, $0.50 mn.

From IEEE Nuclear Science Symposium, San Francisco.

A system is described by which the abundance of deuterium in the solar wind can be determined and the charge distribution in the solar wind can be measured. (D.C.W.)

17308 (N-65-18274) MEASUREMENT OF LOW-ENERGY PRIMARY COSMIC-RAY PROTONS ON IMP-1 SATELLITE. McDonald, F. B.; Ludwig, G. H. (National Aeronautics and Space Administration, Greenbelt, Md. Goddard Space Flight Center). Nov. 1964. 12p. (NASA-TM-X-55160; X-611-64-363). CFSTI $1.00 cy, $0.50 mn.

The intensity and energy spectrum of primary cosmic protons in the energy range of 15 to 75 Mev was investigated using an energy vs energy-loss telescope on the IMP-1 satellite. (D.C.W.)

17309 (N-65-19716) INVERSE COMPTON SCATTERING OF COSMIC RAY ELECTRONS. Jones, Frank C. (National Aeronautics and Space Administration, Greenbelt, Md. Goddard Space Flight Center). Oct. 1964. 33p. (NASA-TM-X-55138; X-641-64-288). CFSTI $2.00 cy, $0.50 mn.

An electron of arbitrary energy in an isotropic thermal radiation field of temperature T is considered. A formally correct expression from $\langle d\epsilon/dt\rangle_{Av}$ is obtained as an asymptotic expansion in the quantity $\epsilon kT/(m_e c^2)^2$. The result $\langle d\epsilon/dt\rangle_{Av} \propto \epsilon^2$ is shown to be the zero-order term in this expansion. It is also shown that the energy-loss rate changes sign at an energy $\epsilon \approx 3/2$ kT as would be expected from thermodynamics. A derivation of the zero-order

term is given from classical radiation theory; from this it is seen that this term also describes the energy-loss rate due to synchrotron radiation as well as from inverse Compton scattering. (STAR)

17310 (AD–623948) MEASURING LOW ENERGY PROTONS ON THE KOSMOS-41 SATELLITE. Vernov, S. N.; Savenko, I. A. (and others). Translated from a Paper Presented at the International Space Science Symposium, 6th, Buenos Aires, May 13–19, 1965. 11p. (FTD-TT–65-1642). CFSTI $1.00 cy, $0.50 mn.

The results of measuring protons with energy 0.4 to 7 Mev and electrons in the outer radiation belt are presented. (M.O.W.)

17311 ON THE VARIATION OF COSMIC RAY MESON INTENSITY AT SEA LEVEL IN CONNECTION WITH ATMOSPHERIC DISTURBANCES. Tanskanen, Pekka J. (Univ. Oulu, Finland). Ann. Acad. Sci. Fenn., Ser. A VI, No. 185, 1-96(1965).

A duplex standard meson telescope for the registration of the meson component of cosmic radiation at ground level is described. Cosmic ray meson intensity variations in connection with atmospheric disturbances are discussed. A linear multiple correlation analysis with permuted aerological parameters was carried out by means of an electronic computer. (auth)

17312 MODULATION OF PROTONS AND α PARTICLES OF SMALL RIGIDITIES AND THE COSMIC-RAY SPECTRUM IN THE GALAXY. Dorman, I. V.; Dorman, L. I. (Inst. of Terrestrial Magnetism, Ionosphere and Radio Wave Propagation, Academy of Sciences, USSR). Geomagn. Aeronomy (USSR) (Engl. Transl.), 5: 516-20 (1965).

Translated from Geomagn. Aeronomiya, 5: 666-72(1965).

The parameters of the dynamic modulation mechanism are found from proton and α particle measurements (it is shown in particular that the dimensions of the modulating volume must be 40–100 AU) and used to determine the intensity of modulation as a function of rigidity for protons and α particles. The cosmic-ray spectrum at small rigidities beyond the modulating volume is also established. It is shown that the "bend" of the spectrum in the region of low energies is completely associated with cosmic-ray modulation in interplanetary space. The expected gradient of cosmic-ray intensity in July 1963 is also found for particles of rigidity R = 1 Bv (3.3%/1 AU for protons and 5.3%/1 AU for α particles) and R = 0.7 Bv (4.1%/1 AU for protons and 7%/1 AU for α particles). (auth)

17313 EFFECTS OF SMALL FLARES IN THE HARD COMPONENT OF COSMIC RAYS OF MAGNETICALLY QUIET AND DISTURBED DAYS. Dorman, L. I.; Ivanov, V. I.; Kolomeets, E. V. (Kazakh State Univ., USSR). Geomagn. Aeronomy (USSR)(Engl. Transl.), 5: 521-4 (1965).

Translated from Geomagn. Aeronomiya, 5: 673-8(1965).

A study of the effects of solar flares on the hard component of cosmic radiation is summarized. (D.C.W.)

17314 SYNCHROTRON RADIATION FROM A PRIMARY COSMIC RAY. Lerche, I. (The Univ., Manchester, Eng.). J. Inst. Math. Appl., 1: 258-68(Sept. 1965).

A description is given of the near field produced by a single charge, whose velocity is close to that of light, moving in a circle in a medium of constant refractive index. The particle's velocity is assumed to be greater than the velocity of light in the medium. It is shown that the resulting radiation pattern differs considerably from that obtained for synchrotron radiation in a vacuum. The physical parameters appropriate to the case of the Earth's atmosphere make it seem unlikely that this mechanism can be used for the detection of cosmic rays. (auth)

17315 ENERGY SPECTRUM OF PRIMARY COSMIC-RAYS. Malhotra, P. K. (Tata Inst. of Fundamental Research, Bombay); Shukla, P. G.; Stephens, S; A.; Vijayalakshmi, B.; Bowler, M. G.; Fowler, P. H.; Hackforth, H. L.; Keereetaveep, J.; Mayes, V. M.; Tovey, S. N. Nature, 209: 567-9(Feb. 5, 1966).

The results of some measurements on the primary flux of protons and heavier nuclei in the energy range from 2.6×10^{12} to 2.6×10^{14} ev are presented and are compared with some other observations. The representation of the energy spectrum by a power law is considered. (D.C.W.)

17316 PRIMARY-ENERGY ESTIMATE FOR JETS BASED ON THE MOMENTUM AND ANGULAR DISTRIBUTIONS OF THE SECONDARIES. Imaeda, K.; Shah, T. P. (Dublin Inst. for Advanced Studies). Nuovo Cimento (10), 41A: 405-16(Feb. 21, 1966).

The overestimation of the primary energy by Castagnoli's method was investigated. Using three distributions: $F(p_t)dp_t = (p_t/p_0^2)\exp[-p_t/p_0]dp_t$, $F(p_t)dp_t = (2p_t/\Delta^2)\exp[-p_t^2/\Delta^2]dp_t$ and $F(p^*)dp^* = p^{*2}dp^*/(\exp[\epsilon^*/kT]-1)$—together with a $\cos^{2\varkappa}\theta^*$ cms angular distribution, formulas for the correction factor $\varkappa$ ($\varkappa\gamma_C = \gamma_{Cast}$) appropriate to Castagnoli's spectrum independent estimate were obtained. $\varkappa$ is found to depend little on the assumed angular distribution, but displays a stronger dependence on the proportion of nonpionic secondaries and their p_t values. For superposed small multiplicity events it is possible for the primary energy to be overestimated by a factor of four. Experimental estimates of $\varkappa$ in the accelerator energy region are reasonably well accounted for by the calculations. (auth)

17317 COSMIC BACKGROUND RADIATION AT 3.2 cm—SUPPORT FOR COSMIC BLACK-BODY RADIATION. Roll, P. G.; Wilkinson, David T. (Princeton Univ., N. J.). Phys. Rev. Lett., 16: 405-7(Mar. 7, 1966).

The microwave background at a wavelength of 3.2 cm was measured. The observed flux is that which would be emitted by a black body at 3.0 ± 0.5°K. (D.C.W.)

17318 OBSERVATION OF ~500-kev PROTONS IN INTERPLANETARY SPACE WITH MARINER IV. Krimigis, S. M.; Van Allen, J. A. (Univ. of Iowa, Iowa City). Phys. Rev. Lett., 16: 419-23(Mar. 7, 1966).

Protons with kinetic energies ~500-kev were observed during a 10-month period of interplanetary flight by the Mariner IV spacecraft. The data were compared with measurements of the intensity of galactic cosmic radiation at the earth and of geomagnetic activity. Two possible explanations of the observations were considered. (D.C.W.)

17319 HIGH-ENERGY γ-RAY ABSORPTION IN SPACE BY A 3.5°K MICROWAVE FIELD. Jelley, J. V. (Atomic Energy Research Establishment, Harwell, Eng.). Phys. Rev. Lett., 16: 479-81(Mar. 14, 1966).

The absorption of high-energy γ rays in space by a universal microwave field with a black-body temperature of 3.5°K was investigated theoretically. (D.C.W.)

17320 SEARCH FOR DISCRETE SOURCES OF COSMIC GAMMA RAYS ABOVE 1 Gev. Oegelman, H. B.; Delvaille, J. P.; Greisen, K. I. (Cornell Univ., Ithaca, N. Y.). Phys. Rev. Lett., 16: 491-4(Mar. 14, 1966).

An attempt was made to observe sources of cosmic γ rays with energies above 1 Bev. Upper limits were assigned to the high-energy γ flux from a number of possible sources. (D.C.W.)

17321 INVESTIGATIONS ON THE MULTIPLY CHARGED NUCLEI OF THE PRIMARY COSMIC RADIATION NEAR THE GEOMAGNETIC EQUATOR USING NUCLEAR EMULSION. PART III. THE LIGHT NUCLEI OF THE COSMIC RADIATION. Durgaprasad, N. (Tata Inst. of Fundamental Research, Bombay). Proc. Indian Acad. Sci., Sect. A, 62: 330-46(Dec. 1965).

A nuclear emulsion stack was exposed over Hyderabad, India (geomagnetic latitude $\lambda = 7.6°N$) under a mean atmospheric depth of 6.8 g/cm^2, on 24 March 1960. The relative and absolute intensities of Be and B nuclei and nuclei of charge $Z \geq 6$ (the S-nuclei) were determined. The intensities were extrapolated to the top of the atmosphere using measured fragmentation parameters involved in collisions of cosmic ray nuclei in graphite. The flux values of Be, B and S nuclei at the top of the atmosphere were determined to be 0.025 ± 0.011, 0.101 ± 0.023, and 1.12 ± 0.10 particles/m^2 sec sr, respectively. The ratios of intensities

B/S, Be/S and Be/B were found to be 0.09 ± 0.02, 0.022 ± 0.008, and 0.25 ± 0.11, respectively. The ratios of intensities were used to compute the amount of matter traversed by the radiation before reaching the vicinity of the earth (2.6 ± 0.6 g/cm^2), to show that the Fermi mechanism of acceleration of particles is not efficient at these energies (1–10 Bev/n) in interstellar space, and to show that preferential acceleration of H_1-nuclei ($Z \geq 20$) is not of overwhelming importance. The derived source composition of nuclei of energy ≥ 7.5 Bev/n suggests that N, O, F and H_3-nuclei ($Z = 10–15$) have similar abundances in the universe and in cosmic rays, and that C and H_1-nuclei are overabundant in cosmic rays. (auth)

17322 COSMIC RAYS IN THE UPPER ATMOSPHERE. Okuda, H.; Yamamoto, Y. (Nagoya Univ., Japan). Rep. Ionosphere Space Res. Jap., 19: 322-38(1965).

Intensities of secondary cosmic rays in the upper atmosphere are calculated to estimate the background radiation for the observation of cosmic ray electrons and γ rays in high altitudes at middle latitudes. The results are represented graphically by altitude dependences and zenith angle dependences for various energies of particles. As for the electronic components, i.e., electrons and γ rays, the altitude dependences of their intensities are in rather good agreement with experimental results, having peak intensities near 120 g/cm^2. (auth)

17323 NEUTRINOS FROM THE ATMOSPHERE AND BEYOND. Reines, Frederick; Sellschop, J. P. F. Sci. Amer., 214: 40-8(Feb. 1966).

The study of high-energy neutrinos produced by cosmic-ray collisions in the earth's atmosphere near Johannesburg, South Africa, is described. An account of the motivation and early results of the study is presented. Also discussed are some conjectures as to the possibility of detecting neutrinos from the sun, the other stars, and intergalactic space. (J.F.P.)

17324 DEPENDENCE OF THE CHEMICAL COMPOSITION OF COSMIC RAYS ON THE NATURE OF THEIR MOTION IN THE GALAXY. Kuzhevskii, B. M.; Syrovatskii, S. I. (Lebedev Inst. of Physics, Moscow). Zh. Eksp. Teor. Fiz., 49: 1950-6(Dec. 1965). (In Russian).

Several models (diffusion and regular) of motion of cosmic rays in the galaxy are considered. A method is indicated which can be employed for choosing between the models on basis of the experimental values of the ratios $^3He/(^3He + ^4He)$ or $D/^4He$. Thus even with the accuracy of the experiments attainable at present a value $^3He/(^3He + ^4He) > 0.15(D/^4He > 0.1)$ would suffice to indicate that the diffusion model is valid whereas a value $^3He/(^3He + ^4He) < 0.15(D/^4He < 0.09)$ would speak in favor of the regular model of motion of cosmic rays in the galaxy. (auth)

Direct Energy Conversion

Refer also to abstract 17521.

17325 (AED-C-15-09) DIRECT CONVERSION OF NUCLEAR ENERGY INTO ELECTRIC ENERGY. Series C: Bibliographies. (Zentralstelle fuer Atomkernenergie-Dokumentation, Gmelin-Institut fuer Anorganische Chemie und Grenzgebiete, Frankfurt am Main (West Germany)). July 1965. 120p. Dep. mn.

A bibliography of approximately 300 articles on various aspects of direct conversion of nuclear energy into electric energy is presented. (M.O.W.)

17326 (AED-C-15-10) DIRECT CONVERSION OF NUCLEAR ENERGY INTO ELECTRIC ENERGY. Series C: Bibliographies. (Zentralstelle fuer Atomkernenergie-Dokumentation, Gmelin-Institut fuer Anorganische Chemie und Grenzgebiete, Frankfurt am Main (West Germany)). Sept. 1965. 96p. Dep. mn.

A bibliography of approximately 240 articles on various aspects of direct conversion of nuclear energy into electric energy is presented. (M.O.W.)

17327 (N-65-19264) CONVERTER PERFORMANCE TEST OF A RHENIUM EMITTER IN CONTACT WITH A CARBIDE FUEL. Final Report. Howard, R. C. (Thermo Electron Engineering Corp., Waltham, Mass.). Mar. 22, 1965. Contract NAS3-4164. 40p. (NASA-CR-54328; TE-64-65). CFSTI $2.00 cy, $0.50 mn.

The test devices DC-1 and DC-2 are described, and the test data obtained from their operation is summarized. The results prove that uranium carbide does not effect the emission from rhenium at temperatures consistent with high power density for at least 200 hr. The consistency of the temperature measurements obtained for DC-1 and DC-2 demonstrated the reliability and reproducibility of the temperature calibration technique employed. The temperature calibration results produced a quantitative measurement of the temperature-drop penalty at the fuel-emitter interface. Although very high contact pressures were obtained between the fuel and the refractory metal surfaces in contact with it, interface temperature differences of 30° to 60°C were observed even after prolonged soaking. Such severe temperature differences can be avoided using cermet fuels metallurgically bonded to emitter materials. (STAR)

17328 SCALING LAWS AND THE ENVELOPE OF ALLOWABLE OPERATING CONDITIONS FOR AN MHD GENERATOR USING INERT GASES. Rosa, R. J. (Avco-Everett Research Lab., Everett, Mass.). Advance. Energy Convers., 5: 265-77(Dec. 1965).

The characteristics of the MHD generator, its temperature and pressure requirements, and the scaling laws that it obeys, are summarized. The aim is to show what conditions are required in a closed cycle number-MHD power plant using equilibrium conductivity only. (auth)

17329 CESIUM-DIODE THERMIONIC CONVERTER FOR LABORATORY EXPERIMENTS. Meyerand, Russell G. Jr.; Bullis, Robert H. (United Aircraft Research Labs., East Hartford, Conn.). Amer. J. Phys., 34: 122-6(Feb. 1966).

A cesium-diode thermionic converter suitable for laboratory instruction is described. The construction of this converter employs only simple glass-blowing techniques so that it can be easily fabricated in a moderately, well-equipped physics laboratory. The use of kovar-to-glass seals and lead-glass sections has been completely eliminated, and the use of oxide glass-to-metal seals has been minimized in the construction of the converter, thereby significantly reducing the probability of cesium attack in seal areas which would seriously limit the useful lifetime of the device. Many interesting and instructive experiments involving thermionic power generation, arc-mode or ignited operation, spectroscopic studies, ion production on high work function surfaces, and the determination of converter current-voltage characteristics can be conducted with this device. (auth)

17330 AN INDUCTIVELY COUPLED AC MHD ELECTRICAL POWER GENERATOR. Koyama, Kenichi; Sekiguchi, Tadashi (Tokyo Univ.). Denki Gakkai Zasshi, 85: 299-308(1965). (In Japanese).

An a-c MHD generator is described and quantitative data calculated for the system are compared with those obtained experimentally. (TCO)

17331 DIRECT CONVERSION INTO ELECTRICAL ENERGY OF GAMMA RADIATIONS EMITTED BY NUCLEAR REACTORS OR RADIOISOTOPES. Roma, Carlo (Univ., Rome). Ric. Sci. Rend., Sez. A, 8: 923-35(July-Aug. 1965). (In Italian).

A new technique of direct conversion of gamma radiation energy into electrical energy is described. It is based on the production of electrons, mainly through the Compton effect, in two electrodes of the same material and insulated in a vacuum, whose thicknesses are in a high ratio between themselves. The electrons produced possess sufficient energy for the range associated with it to permit them to leave the thickness of the electrodes. Assuming the photons to be monoenergetic and their flux density (the flux assumed to be collimated) to be known, current density, theoretical power, and the power dissipated by ionization are determined with the help of statistical considerations. Losses influencing conversion gain are specified. (auth)

17332 CERTAIN SINGULARITIES OF MGD GENERATOR PERFORMANCE AT LARGE HALL NUMBERS. Ivanov, P. P.; Kovbasyuk, V. I.; Stepanov, S. A. (Scientific-Research Inst. of High Temperatures, USSR). Teplofiz. Vysok. Temp., 3: 845-50(Nov.-Dec. 1965). (In Russian).

In MGD generators operating at high Hall numbers, the effects of the sliding of ions and discontinuities of electron temperatures were shown to be substantial on the temperature of the neutral components of the gas. The influence of these effects on the characteristics of the principal types of conducting MGD generators was shown. (tr-auth)

17333 THE ELECTRON EMISSION OF THE Pt-GROUP METALS IN Cs VAPOR. Houston, John M.; Dederick, Preston K. (General Electric Research and Development Center, Schenectady, N. Y.). 21p. (CONF-651049-7). ORAU. Gmelin, AED-CONF-65-324-7.

From IEEE Thermionic Conversion Specialist Conference, San Diego, Calif.

The preliminary results of an investigation of electron emission by Ir, Os, Pd, Pt, Rh, Ru, and W in cesium vapor are presented. (D.C.W.)

17334 ELECTRON EMISSION FROM METALS IN VAPORS OF CESIUM AND FLUORINE. Kaplit, M.; Schrenk, G. L. (Univ. of Pennsylvania, Philadelphia). 11p. (CONF-651049-8). ORAU. Gmelin, AED-CONF-65-324-5.

From IEEE Thermionic Conversion Specialist Conference, San Diego, Calif.

A quantum chemical model for predicting and correlating electron emission from a transition metal in vapors of cesium and fluorine is described. This model is based on the postulates that the fluorine additive and the metallic substrate form a system whose geometry, as a first approximation, is independent of substrate temperature and whose properties are similar to the properties of the metal substrate except for an increase in work function. The adsorption of cesium on this composite structure yields a lower work function than that obtained without the fluorine additive. Theoretical electron emission S curves based on this model are calculated for a cesium–fluorine–molybdenum system. (auth)

17335 LOW WORK FUNCTION COLLECTOR: STRONTIUM TUNGSTATE. Zimmerman, D. R. (General Motors Corp., Indianapolis, Ind.). 7p. (CONF-651049-11). ORAU. Gmelin, AED-CONF-65-324-4.

From IEEE Thermionic Conversion Specialist Conference, San Diego, Calif.

The thermionic emission from a surface of mixed (basic and normal) strontium tungstate was measured in vacuum. The zero-field currents, extrapolated from pulsed Schottky plots, in the range from 1150 to 1400°K are given. The emission is fairly uniform on a large scale as is shown by an electron image photograph. The conversion and activation are repeatable over all surfaces of the same ratio of reactants which were tested. The results from several surfaces of various ratios of $SrCO_3$: W are given. (auth)

Elementary Particles and Radiations

See also Field Theory, Scattering Theory, and Symmetries

Refer also to abstracts 17278, 17805, and 17983.

17336 (AECD/TP-5) PION-NUCLEON COUPLING CONSTANT FROM SPIN-FLIP DISPERSION RELATION. Harun-ar-Rashid, A. M.; Islam, Md. Mazharul; Miah, Md. Hanifuddin (Atomic Energy Centre, Dacca (Pakistan)). July 1965. 13p. Dep. mn.

A set of dispersion relations was used to calculatee coupling constants for pion-nucleon scattering. The analysis is in terms of phase-shifts. (M.O.W.)

17337 (AERE-R-5138) TESTS FOR T-INVARIANCE IN N-N SCATTERING. Phillips, R. J. N. (Atomic Energy Research Establishment, Harwell (England)). Jan. 1966. 12p. Dep. BIS $0.50. HMSO 2s. 6d.

Expressions are given for the polarization tensors of nucleon-nucleon scattering, assuming time-reversal (T) invariance does not hold. Some pairs of tensors, apparently related by T, prove to be equal regardless of T-invariance: others offer genuine tests of T-invariance. (auth)

17338 (DESY-65/10) PAIR PRODUCTION AND HEAVY ELECTRON. Gutbrod, F.; Schildknecht, D. (Deutsches Elektronen-Synchrotron, Hamburg (West Germany)). Oct. 1965. 17p. Dep. mn.

Production of electron-positron pairs is analyzed with the hypothesis of the heavy electron e*. A rough agreement between theory and experiment is found if the coupling constant is suitably chosen as a function of the mass m* of the e*. Comparison with upper limits for this coupling constant taken from inelastic electron-proton scattering indicates that a heavy electron with m* between 120 Mev and 1 Bev cannot explain observed deviations from pure quantum electrodynamics. (auth)

17339 (JINR-E-2557) PLUS PARITY MESONS AND THE 189-PLET OF SU(6). Robaschik, D.; Uhlmann, A. (Joint Inst. for Nuclear Research, Dubna (USSR). Lab. of Theoretical Physics). 1966. 9p. Dep. mn.

The physical chain and the unphysical (u-chain) are used to get two different systems of basis vectors of the 189-plet. The u-chain states are considered to be particle states. The transformation matrices that connect the two bases are calculated, and a mass formula is derived. Some possible assignments of quantum numbers are discussed. (D.C.W.)

17340 (JINR-P-2322) POISKI RASPADA $\pi^0 \to 3\gamma$. (Search for $\pi^0 \to 3\gamma$ Decay). Kut'in, V. M.; Petrukhin, V. I.; Prokoshkin, Yu. D. (Joint Inst. for Nuclear Research, Dubna (USSR). Lab. of Nuclear Problems). 1965. 6p. Dep. mn.

The 70 Mev π^--mesons from a synchrocyclotron were passed through a series of scintillation counters and attenuation filters, and then were stopped in a liquid hydrogen target, where the following charge-transfer reaction took place: $\pi^- + p \to \pi^0 + n$. In order to count the γ quanta from the reaction $\pi^0 \to 3\gamma$, three Cherenkov counters hooked up in a nanosecond coincidence arrangement were placed in a plane perpendicular to the π^--meson beam at mutual angles of 90 and 135°. The counting efficiency was 1%. A total of 66 events showed pulses from all three Cherenkov spectrometers and from the scintillation counters recording the π^--mesons. A time and amplitude analysis of these 66 events showed that the upper limit for the relative probability of the reaction $\pi^0 \to 3\gamma$ was $\lambda < 5 \times 10^{-6}$ (at the 90% confidence level). (TTT)

17341 (JINR-P-2504) UPRUGOE e-d RASSEYANIE I NARUSHENIE CP-INVARIANTNOSTI. (Elastic e-d Scattering and CP-Invariance Breakdown). Dubovik, V. M.; Cheshkov, A. A. (Joint Inst. for Nuclear Research, Dubna (USSR). Lab. of Theoretical Physics). 1965. 8p. Dep. mn.

The cross section for elastic e-d scattering was obtained with account of CP-invariance violation. Using the experimental data the contribution of T-noninvariant form-factor of the deuteron current in the cross section is discussed. A possibility is indicated of checking the C and T invariance hypothesis in electromagnetic interactions of hadrons by using the measurements of asymmetry of angular distributions of recoil deuterons in elastic scattering of electrons by polarized deuterons. (auth)

17342 (JINR-P-2520) ELEKTROMAGNITNYE VZAIMODEISTVIYA X-MEZONA V VYSSHIKH SIMMETRIYAKH. (Electromagnetic Interaction of the X Meson in Higher Symmetries). Bokov, O. G.; Nguen Van Hieu; Sredniava, B. (Joint Inst. for Nuclear Research, Dubna (USSR). Lab. of Theoretical Physics). 1965. 8p. Dep. mn.

Radiative decays of the ninth pseudoscalar meson $\chi(960)$ are treated. Relations were obtained between the coupling constants of one-photon decays of the χ-meson

and the nonet of the vector mesons as well as similar relations for two-photon decays of the nonet of the pseudoscalar mesons in the scheme of intrinsically broken $\tilde{U}(12)$ symmetry. Branching ratios for corresponding processes were calculated. (auth)

17343 (JINR-P-2524) NEKOTORYE EFFEKTY V MODELI KVARKOV. (Some Effects in the Quark Model). Matveev, V. A.; Struminskii, B. V.; Tavkheledze, A. N. (Joint Inst. for Nuclear Research, Dubna (USSR). Lab. of Theoretical Physics). 1965. 10p. Dep. mn.

Using a simple method decay rates for mesons and electromagnetic mass difference for baryons and mesons were calculated in the quark model. (auth)

17344 (JINR-P-2530) NEUPRUGOE π^+-p VZAIMODEISTVIE PRI BOLSHIKH ENERGIYAKH I STATISTICHESKAYA MODEL MNOZHESTVENNOGO ROZHDENYA CHASTITS. (Inelastic π^+-p Interaction at High Energies and Statistical Model of Multiple Particle Production). Zinov'ev, G. M. (Joint Inst. for Nuclear Research, Dubna (USSR). Lab. of Theoretical Physics). 1965. 7p. Dep. mn.

The process of inelastic π^+p interaction in the energy region 1-4 Bev is treated in the statistical model of multiple production of Fermi particles which takes into account the well-known baryon and meson resonances as intermediate states. The results obtained are compared with experiment. (auth)

17345 (JINR-P-2531) PRIMENENIE UNITARNOI SIMMETRII K MNOZHESTVENNOMU ROZHDENIYU MEZONOV. (Application of Unitary Symmetry to Multiple Meson Production). Daibog, E. I. (Joint Inst. for Nuclear Research, Dubna (USSR). Lab. of Theoretical Physics). 1965. 7p. Dep. mn.

It is shown that the Watson theorem concerning the ratio of the average number of charged and neutral mesons in multiple production is generalized to SU(3). The ratio of the number of π pions to that of π^0 and η^0, produced by high-energy nucleon collisions is calculated. A comparison with experiment was made. (auth)

17346 (JINR-P-2534) IZMERENIE VREMENI ZHIZNI π^+-MEZONA. (Measurment of π^+ Meson Lifetime). Dunaitsev, A. F.; Pikhtelev, R. N.; Prokoshkin, Yu. D.; Simonov, Yu. N. (Joint Inst. for Nuclear Research, Dubna (USSR). Lab. of Nuclear Problems). 1965. 12p. Dep. mn.

The mean lifetime of the π^+ meson is measured by the method which is not affected by the background due to the accompanying $\mu^+ \rightarrow e^+$ decay. The stoppings and decay of π^+ mesons were detected by a system of scintillation counters. The pulses from all the counters were displayed on the screen of a high-speed five-ray oscilloscope. A time and height pulse analysis of about 17 thousand oscillograms gave the mean value for the π^+ lifetime to be $\tau_{\pi^+} = (25.85 \pm 0.35)$ns. The main difference of this method from those applied earlier is that it employed a "trap" for positrons appearing in $\mu^+ \rightarrow e^+$ decay, what allowed to decrease this background by more than two orders of magnitude. (auth)

17347 (JINR-P-2547) DVUKHMEZONNAYA ANNIGILYATSIYA BARIONOV V NARUSHENNOI SIMMETRII SL(6,C). (Two-Meson Annihilation of Baryons in Broken SL(6,C) Symmetry). Winternitz, P.; Makarov, A. A. (Joint Inst. for Nuclear Research, Dubna (USSR). Lab. of Theoretical Physics). 1966. 8p. Dep. mn.

The two-meson annihilation of a $p\bar{p}$ pair at rest is considered assuming the SL(6,C) symmetry. Relations between the amplitudes and cross sections of various processes are obtained in good agreement with the experimental data. (auth)

17348 (JINR-P-2556) OB ELEKTROMAGNITNYKH VZAIMODEISTVIYAKH V MODELI KVARKOV. (On Electromagnetic Interactions in the Quark Model). Baldin, A. M. (Joint Inst. for Nuclear Research, Dubna (USSR). Lab. of Theoretical Physics). 1966. 6p. Dep. mn.

It is shown that, starting from the phenomenological interaction of quarks with mesons and from the gauge invariance one can obtain consequences not following from the SU(6) symmetry. It turns out possible, for example, to get the absolute threshold magnitudes for the pion photoproduction cross sections. Sharp differences (experimentally observed) between the cross sections for the reactions $\gamma + p \rightarrow \Sigma^0 + K^+$ and $\gamma + p \rightarrow \Lambda^0 + K^+$, as well as $\gamma + p \rightarrow \Delta^+ + \pi^-$ and $\gamma + p \rightarrow \Delta^0 + \pi^+$ are explained. (auth)

17349 (LAL-1155) DEUTERON ELECTROMAGNETIC FORM FACTORS FOR 3 $f^{-2} < q^2 < 6$ f^{-2}. Benaksas, D.; Drickey, D.; Frerejacque, D. (Laboratoire de l'Accelerateur Lineaire, Univ. de Paris, Orsay (France)). Mar. 1966. 24p. Dep. mn.

Two groups of measurements were made on the elastic scattering of electrons by deuterium; in each case the recoil deuteron was observed instead of the scattered electron. In the first case the spectrometer was set at 45°, so that magnetic scattering was unimportant (about 10%), and the electric form factors of the deuteron were determined. In the second case deuterons were observed at 0°, permitting a direct measurement of the magnetic form factor of the deuteron. Form factors of the neutron were deduced from these measurements for the transfer values $q^2 = 3$, 4, and 5 (f^{-2}). (auth)

17350 (N-65-19395) THE nn SCATTERING LENGTH. Goldberg, Hyman (Paris Univ., Orsay (France). Laboratoire de Physique Theorique et Hautes Energies). Jan. 1965. 20p. (TH-85).

The contribution of the $\pi^\pm\pi^0$ mass difference to the difference in the $^1S_0$ np and nn scattering lengths is calculated by a method due to Dashen and Frautschi. In the calculation only the one-pion-exchange contribution is retained; and the difference $a_{nn} - a_{np} = -4.80F$ is obtained. The deviation of the coupling constants is also estimated, and this is shown to give negligible contribution to the difference. (STAR)

17351 (N-65-19396) 3-PARTICLE NONRELATIVISTIC KINEMATICS AND PHASE-SPACE. Levy-Leblond, Jean-Marc; Levy-Nahas, Monique (Paris Univ., Orsay (France). Laboratoire de Physique Theorique et Hautes Energies). Jan. 1965. 16p. (TH-83).

The kinematics of a nonrelativistic three-particle system is studied. (D.C.W.)

17352 (NEIC-RR-21) THE BIBLIOGRAPHY OF THE NEUTRINO. PART II. (Nuclear Energy Information Center, Warsaw (Poland)). 1966. 441p. Dep.

Subjects included are; properties of the neutrino, neutrinos among decay products, conservation laws, quantum mechanics and field theory for neutrinos, various topics of neutrino theory, elementary particles and weak interactions, neutrino-induced processes, processes of neutrino production, the detection of free neutrinos, neutrino and nuclear astrophysics, geophysics, cosmic radiation, cosmology, and general relativity. (M.O.W.)

17353 THE PROTON-PROTON SINGLET S-STATE INTERACTION. Olsen, J. M.; Skavlem, S. Arbok Univ. Bergen, Mat.-Nat. Ser., No. 3, 1-11(1964).

The low energy proton-proton scattering data are described by means of a three-parameter nonmonotonic potential that is a superposition of two Yukawa potentials. The wave equation is solved by means of a variational method, and the results are tested by numerical integrations for some values of the potential parameters. Corresponding values of admissible potential parameters are plotted graphically. A parabolic relation seems to exist between two of the parameters. The low energy potentials do not fit the 310 Mev proton-proton scattering results. (auth)

17354 DIFFERENTIAL CROSS SECTION FOR PAIR PRODUCTION BY PHOTONS ON ELECTRONS. Mork, K. J. (Institutt for Teoretisk Fysikk N.T.H., Trondheim, Norway). Arkiv Fys. Seminar Trondheim, No. 7, 1-20(1965).

The differential cross section for pair production by unpolarized photons in the field of an electron was computed in lowest order perturbation theory using covariant sums over polarizations. The contributions to the cross section

from the different Feynman diagrams are given separately, and the kinematics of the process are discussed for some cases. (auth)

17355 THE EFFECT OF INELASTIC PROCESSES ON THE P_{11} PHASE SHIFT IN πN SCATTERING. Pisut, J. (Comenius Univ., Bratislava). Czech. J. Phys., 16: 87-94(1966).

Assuming that the neucleon is a bound state in the πN system, the approximate formula for a phase shift in the P_{11} wave was derived. The left-hand cut is approximated by two poles and the effect of inelastic processes on the scattering amplitude of the partial wave P_{11} is discussed in terms of Froissart's method. The values of the inelastic parameter are taken from the experimental data. In this way the agreement with the experimental values of the phase shift in the P_{11} wave for low energies can be obtained. (auth)

17356 A REFORMULATION FOR THE MESON-ATOMIC MODEL OF THE NUCLEON. Sood, P. C.; Trainor, L. E. H. (Panjab Univ., Chandigarh, India. Univ. of Alberta, Edmonton). Indian J. Pure Appl. Phys., 4: 16-19(Jan. 1966).

The motion of a Klein-Gordon particle under the action of two simultaneous, inverse square forces is investigated. One of these forces is taken to be transmitted by a field of mass zero, 4-scalar particles, the other by a field of mass zero, 4-vector particles. It was observed that a variety of energy spectra can be obtained by adjusting the magnitudes and signs of the field strength parameters. The problem is of interest in providing a possible meson-atomic model of the nucleon. (auth)

17357 ON THE ONE CRITERION FOR SELECTING NUCLEON-NUCLEON EVENTS IN NUCLEAR EMULSION. Boos, E. G.; Grigor'eva, G. Ya. Izv. Akad. Nauk Kaz. SSR, Ser. Fiz.-Mat. Nauk, No. 2, 15-17(May-Aug. 1965). (In Russian).

The angular distribution of strongly ionizing tracks was found to be anisotropic in an Ilford G-5 emulsion irradiated with protons having a momentum of 19.8 Bev/c. The asymmetry coefficient was 0.33 ± 0.08. The asymmetry coefficient A was only 0.07 ± 0.07 for a specially selected set of stars (107 events) having two black tracks. The angular distribution of black tracks from nucleon-nucleus reactions (102 events) was isotropic with A = 0.06 ± 0.10. It follows from this analysis that the best agreement in selecting nucleon-nucleon events is attained with a symmetrical distribution of black tracks, and with the additional requirement that the minimum length of the track exceed 500 μ. (TTT)

17358 IDENTIFICATION OF SINGLE- AND DOUBLE-CHARGE PARTICLES BY MEANS OF THE δ-ELECTRON METHOD. Amankulova, D. S.; Kazanskaya, A. P. Izv. Akad. Nauk Kaz. SSR, Ser. Fiz.-Mat. Nauk, No. 2, 41-5 (May-Aug. 1965). (In Russian).

The average density of delta electrons per 1 cm of track length was found to be N = 3.3 ± 0.09 for 19.5 Bev protons, 4.3 ± 0.27 for 17.5 Bev π-mesons, and 3.9 ± 0.25 for 7.5 Bev π-mesons. The density of delta electrons N* is plotted as a function of $p\beta = m\beta^2/\sqrt{1-\beta^2}$ for the proton, deuteron, triton, and helium isotopes. The nature of the energetic particle emerging from an emulsion pile could be determined from these plots. A total of 510 particles having charges Z = 1 and Z = 2 were formed from the interactions of 19.5 Bev protons, and 17.5 and 7.5 Bev π-mesons. Maxima were observed in the number of delta electrons found on the last 3 mm of the particle track. The number of delta electrons were found to be 32 ± 0.69 for the doubly-charged particles and 11 ± 0.27 for the singly charged particles in the last 3 mm of the particle track. This method can be used to discriminate between particles with Z = 1 and Z = 2. (TTT)

17359 INVESTIGATION OF INELASTIC INTERACTIONS OF ANTI-PROTONS WITH NEUTRONS AT 3 Bev/c ENERGY. Botvin, V. A.; Takibaev, Zh. S.; Sharapov, K. V. Izv. Akad. Nauk Kaz. SSR, Ser. Fiz.-Mat. Nauk, No. 2, 70-3(May-Aug. 1965). (In Russian).

An Ilford G-5 emulsion pile was irradiated with a beam of antiprotons having a momentum of 3 Bev/c using the proton synchrotron at CERN. A length of 816.1 m of primary tracks was examined, and a total of 117 cases of inelastic interaction of an antiproton with a neutron were identified. No attempt was made to separate the annihilation events from involving the direct creation of mesons. The distribution of inelastic $\bar{p}$-n interactions according to the number of rays was as follows: 36 ± 5.6% for the single-ray events, 41.0 ± 5.9% for the 3-ray events, 18.8 ± 4.0% for the 5-ray events, and 3.4 ± 1.7 for the 7-ray events. The angular distribution of secondary π-mesons was almost isotropic. The average number of protons and antiprotons per interaction for a $\bar{p}$n event was equal to 0.39 ± 0.07 which is in good agreement with a value of 0.37 for a $\bar{p}p$ event. A proton track was observed in a number of 5 to 7-ray cases. This observation indicates reactions of direct generation rather than annihilation reactions. The direct creation of pions may be due to the interference of two possible processes. The average momentum of the generated pions was $\bar{P}$ = 331 ± 57 Mev/c in the center-of-mass system. (TTT)

17360 ELASTIC SCATTERING OF 5.5-Bev π MESONS ON PROTONS. Azimov, S. A.; Prozorova, E. I.; Yuldashev, A. A. (Inst. of Nuclear Physics, Academy of Sciences, Uzbek SSR). Izv. Akad. Nauk Uz. SSR, Ser. Fiz.-Mat. Nauk, No. 2, 92-3(1965). (In Russian).

An emulsion pile containing 30 layers of emulsion paper was struck by a beam of π^--mesons with 10% μ^--mesons as an impurity. A total of 66 events of π^--p scattering were detected. The elastic scattering cross section for angles greater than 2.4° was found to be equal to $\sigma(\theta > 2.4°) = 5.3 \pm 0.8$ mb. The differential cross section was approximated by the expression: $d\sigma/d\Omega = (d\sigma/d\Omega)_0 \exp(-At)$. Here $t = 2P^2$ (1-cos θ) is the square of the transmitted momentum, and A is the constant. Values of A = 7.7 $(Bev/c)^2$ and of $(d\sigma/d\Omega)_0$ = 34.3 mb/sterad were found from a plot of the experimental data. The total elastic scattering cross section is given as σ = 5.49 ± 0.8 mb with the cross section in the interval of 0 to 2.4° being taken into account. (TTT)

17361 OBSERVATION OF ATOMIC MUONIUM IN CRYSTALLINE QUARTZ. Babaev, A. I.; Balats, M. Ya.; Myasishcheva, G. G.; Obukhov, Yu. V.; Roganov, V. S.; Firsov, V. G. (Inst. of Theoretical and Experimental Physics, Moscow). JETP Lett. (USSR)(Engl. Transl.), 3: 1(Jan. 1, 1966).

Translated from Zh. Eksp. Teor. Fiz., Pis'ma Redakt., 3: 3-4(Jan. 1, 1966).

The asymmetry coefficient in the angular distribution of positrons from the decay of mesons (μ^+) stopped in crystalline quartz at room temperature was measured using an apparatus with which meson (μ^+) spin precession in a magnetic field was observed. (D.C.W.)

17362 USE OF A POLARIZED PROTON TARGET TO DETERMINE ISOBAR PARITY. Dubovikov, M. S. (Inst. of Physics and Tech., Moscow). JETP Lett. (USSR) (Engl. Transl.), 3: 4-6(Jan. 1, 1966).

Translated from Zh. Eksp. Teor. Fiz., Pis'ma Redakt., 3: 8-11(Jan. 1, 1966).

A method is proposed for the determination of the parity of isobars. The method is based on the relations between the polarization effects in parity-conserving processes. (D.C.W.)

17363 REAL PART OF THE pn SCATTERING AMPLITUDE IN THE ENERGY INTERVAL 2 TO 10 Gev. Zolin, L. S.; Kirillova, L. F.; Lu, Ching-chiang; (and others) (Joint Inst. of Nuclear Research, Dubna, USSR). JETP Lett. (USSR)(Engl. Transl.), 3: 8-12(Jan. 1, 1966).

Translated from Zh. Eksp. Teor. Fiz., Pis'ma Redakt., 3: 15-21(Jan. 1, 1966).

Elastic p-d scattering was investigated in the energy range of 1 to 10 Bev. On the basis of the data, as well as information on the p-p scattering amplitude in the same energy range, the real part of the p-n scattering amplitude was evaluated for the energy range of 2 to 10 Bev. (G.O.Y.)

17364 BROKEN UNITARY SYMMETRY AND POSSIBLE Ω^-(1875) RESONANCE. Shekhter, V. M. (Ioffe Inst. of Physics and Tech., Leningrad). JETP Lett. (USSR)(Engl. Transl.), 3: 12-15(Jan. 1, 1966).

Translated from Zh. Eksp. Teor. Fiz., Pis'ma Redakt., 3: 21-6(Jan. 1, 1966).

The width of the Ω^-(1875) resonance was calculated using broken unitary symmetry. (D.C.W.)

17365 ONE METHOD OF SEARCHING FOR QUARKS. Braginskii, V. B. (Moscow State Univ.). JETP Lett. (USSR)(Engl. Transl.), 3: 43-5(Jan. 15, 1966).

Translated from Zh. Eksp. Teor. Fiz., Pis'ma Redakt., 3: 69-73(Jan. 15, 1966).

A modification of Millikan's method is proposed in which the mass of the test body is increased by 4 to 5 orders of magnitude over that of Millikan's mass. Some preliminary results that were obtained using a graphite pellet in a magnetic field as the test body are presented. (D.C.W.)

17366 CONCERNING THE SEARCH FOR SPECIFIC INTERACTIONS BETWEEN μ MESONS AND ν_μ NEUTRINOS AT ULTRAHIGH ENERGIES. Markov, M. (Lebedev Inst. of Physics, Moscow). JETP Lett. (USSR)(Engl. Transl.), 3: 62-3(Jan. 15, 1966).

Translated from Zh. Eksp. Teor. Fiz., Pis'ma Redakt., 3: 98-101(Jan. 15, 1966).

Some interactions of mesons (μ) and neutrinos (ν_μ) at energies on the order of $E \geq 10^{12}$ ev are discussed in terms of a pseudovector-field model. (D.C.W.)

17367 l-DEPENDENCE, SINGULARITIES, AND THE DOUBLE-SPECTRAL FUNCTION. Brehm, J. J. (Northwestern Univ., Evanston, Ill.). Nuovo Cimento (10), 41A: 266-9(Jan. 21, 1966).

It is shown that the l-dependence ansatz for meson (π)-meson (π) interactions leads to the desired exchange pole, the expected Mandelstam spectral curve, and the correct double-spectral function. A Khuri factor is appropriate for two-body exchange and cannot describe a single-particle exchange. Also nothing resembling the double-spectral function emerges. (J.F.P.)

17368 PHOTOPRODUCTION OF PION AND NUCLEON RESONANCES AT ENERGIES UP TO 5.5 Gev. Brall, U. (Technische Hochschule, Aachen); Reimann, G.; (and others). Nuovo Cimento (10), 41A: 270-9(Jan. 21, 1966).

Photoproduction of pions and resonances by protons in the γ energy range between 0.3 Bev and 5.5 Bev is reported. The production of N* (1238) and of the η, ρ and ω mesons was observed. The results of ρ^0 and ω production are compared with the predictions of the one-pion exchange (OPE) model and the diffraction model. (J.F.P.)

17369 A SUM RULE FOR THE TWO-PION DECAY AMPLITUDES OF K MESONS. Sudarshan, E. C. G. (Syracuse Univ., N. Y.). Nuovo Cimento (10), 41A: 283-5 (Jan. 21, 1966). (NYO-3399-41).

A sum rule for the two-meson (π) decay amplitudes of mesons (K) is derived. For this derivation it is assumed that the decay interaction is an arbitrary linear combination of $\Delta I = \frac{1}{2}$, and $\frac{3}{2}$ contributions. Since the two mesons (π) are in an S-wave relation to each other, the only isotopic spins allowed in the final state are I = 2 and I = 0, which are symmetric under the exchange of the two mesons (π). (J.F.P.)

17370 RADIATIVE CORRECTIONS TO INELASTIC ELECTRON SCATTERING WITH DETECTION IN COINCIDENCE. II. de Calan, C.; Fuchs, G. (l'Ecole Polytechnique, Paris). Nuovo Cimento (10), 41A: 286-8 (Jan. 21, 1966).

In previous calculations of the radiative corrections to electron scattering processes of the type $e + A \rightarrow e' + B + C$ where e' and B are detected in coincidence, the radiation emitted by the heavy particles was neglected. The rapidly increasing energy range of experiments leads to an evaluation of this part of the corrections. Corrections are given for the electrodisintegration of deuterium. (J.F.P.)

17371 DISTRIBUTION OF TRANSVERSE MOMENTA IN HIGH-ENERGY MESON PRODUCTION. Friedlaender, E. M. (Inst. of Atomic Physics, Bucharest). Nuovo Cimento (10), 41A: 417-42(Feb. 21, 1966).

A "world survey" of experimental data on the transverse momentum distributions of 5738 secondaries from high-energy inelastic interactions is analyzed. It is shown that the data cannot be fitted satisfactorily by the linear exponential distribution. The baryon data are well described by a Boltzmann distribution while the pion data are a superposition of two Boltzmann distributions with widely differing parameters. Although the combined effect of their mutual variation is to keep the overall transverse momentum practically constant, the values of these parameters and the relative weight of the two partial distributions appear to be quite sensitive to various features of the process of meson production (nature and energy of the primary, nature of the secondary, production of strange particles, etc.). (auth)

17372 ELECTRIC DIPOLE MOMENTS OF FERMI PARTICLES. Salzman, F.; Salzman, G. (Northeastern Univ., Boston). Nuovo Cimento (10), 41A: 443-55(Feb. 21, 1966).

The electric-dipole moments of the nucleons and of the electron and muon are calculated in the intermediate vector boson theory. An intrinsic electric dipole is attributed to the charged vector boson, $W^\pm$. Results are obtained with the regularization procedure proposed by Lee and Yang, both for their so-called ξ-limiting process, and for an alternative limiting procedure which is appropriate only if the W boson does not exist. The theory predicts, for reasonable values of the several parameters, a neutron-electric dipole as large as $1.3(10^{-6})$ nuclear magnetons, which is within a factor two of the present experimental upper bound, and which is readily measurable. The predicted electric dipoles of the other three fermions considered are too small to be measured by techniques currently in use. (auth)

17373 BACKWARD SCATTERING OF HIGH-ENERGY PARTICLES. Blokhintsev, D. I. (Joint Inst. for Nuclear Research, Dubna, USSR). Nuovo Cimento (10), 41A: 481-4(Feb. 21, 1966).

On the basis of the optical model, under very general assumptions, it is shown that in the backward scattering there must be a peak of width $\sim\lambda\!\!\!^{-}/R$ (R is the nucleon "diameter"). The cross section for the backward scattering, unlike the forward scattering, is constant or decreases with increasing energy (depending on the type of the optical model). (auth)

17374 π^+p INTERACTIONS AT 1.6 Gev/c. Daronian, P. (CEN, Saclay, France); Daudin, A.; Jabiol, M. A.; Lewin, C.; Kochowski, C.; Ghidini, B.; Mongelli, S.; Picciarelli, V. Nuovo Cimento (10), 41A: 503-31(Feb. 21, 1966).

A systematic study of π^+p interactions at 1.59 Bev/c in the Saclay HBC 180 l at Saturne is reported. The two-prong reactions allowed study of ρ^+ and N_{33}^{*2+} production. These productions are compared with the predictions of the OPE model for the ρ^+, and the Stodolsky-Sakurai model for N_{33}^{*2+}. In four-prong reactions, N_{33}^{*2+} production is important, and the associated production $\pi^+p \rightarrow N_{33}^{*2+}\eta$ was observed. Finally the cross section values in all different channels are given. (auth)

17375 ALGEBRA OF CURRENTS AND A LOW-ENERGY THEOREM. Okubo, S. (Univ. of Rochester, N. Y.). Nuovo Cimento (10), 41A: 586-98(Feb. 21, 1966). (UR-875-97).

By use of a modified Fubini-Furlan technique, it is shown that a certain commutation relation among spatially integrated currents gives the low-energy Kroll-Ruderman theorem on the photoproduction of a pion by a nucleon. (auth)

17376 $K^- + p \rightarrow \eta + \Lambda$ SCATTERING NEAR THRESHOLD. Pal, B. K. (National Physical Lab., New Delhi). Nuovo Cimento (10), 41A: 599-602(Feb. 21, 1966).

An investigation is made to find the cross section and scattering length for the reaction $K^- + p \rightarrow \eta + \Lambda$. The available experimental information is consistent with a

sharp rise in η-production followed by a sharp drop in a limited energy interval just above the $\eta + \Lambda$ threshold. The channels considered are $\bar{K} + N$ and $\eta + \Lambda$, and the amplitudes are calculated in the Zachariasen-Zemach approximation. (J.F.P.)

17377 ON THE $p\bar{p}$ ANNIHILATION INTO TWO MESONS. Lai, C. S. (Univ. of Chicago). Nuovo Cimento (10), 41A: 606-8(Feb. 21, 1966). (COO-264-295).

The proton-antiproton annihilation at rest into two mesons is studied in the framework of the meson-pole-dominance model in the SU_3 symmetry. It is assumed that vector mesons are dominant in the intermediate states for $p\bar{p}$ annihilation. The coupling constants are determined from the SU_3 symmetry and the known W-ϕ mixing. (J.F.P.)

17378 HIGH-ENERGY BEHAVIOR OF THE REAL PART OF THE SCATTERING AMPLITUDES AND SOME CONSEQUENCES FROM SU_3. Igi, K.; Kawai, T. (Tokyo Univ. of Education). Nuovo Cimento (10), 41A: 609-12 (Feb. 21, 1966).

The dynamical model admitting Regge cuts to Regge poles, which was used to investigate the asymptotic behavior of the real over the imaginary part of the forward scattering amplitude, is applied to calculations of the ratios for high-energy scattering. These ratios are compared with experiment for pp and $\pi^{\pm}p$ scatterings, and predictions are made of these values for $p\bar{p}$, $K^{\pm}p$, $K^{\pm}n$ which are not measured experimentally. Also it is shown that a predicted relation appears to hold where the values are calculated by the same method. (J.F.P.)

17379 TWO-PION DECAY MODES OF $K^{\pm}$ AND K_1^0 MESONS IN SU_3. Das, T.; Mahantappa, K. T. (Univ. of Pennsylvania, Philadelphia). Nuovo Cimento (10), 41A: 618-21(Feb. 21, 1966).

The two-meson (π) decay modes of the mesons ($K^{\pm}$) and (K_1^0) are discussed as an application of a theory of weak interactions in the framework of SU_3. The decay rates and a sum rule are given. (J.F.P.)

17380 ON THE PRODUCTION MECHANISM OF $\bar{K}^{*0}$ (891) IN THE REACTION $K^-p \rightarrow K^-\pi^+n$ AT 3 Gev/c. Verglas, A. (CEN, Saclay, France); Focardi, S.; Minguzzi-Ranzi, A.; Monari, L.; Serra, P. Nuovo Cimento (10), 41A: 629-34(Feb. 21, 1966).

In the study of the three-body final state $K^-p \rightarrow K^-\pi^+n$ for which the cross section is (1.55 ± 0.18) mb, the reaction $K^-p \rightarrow \bar{K}^{*0}n$, $\bar{K}^{*0}\pi^+$ was found to have a cross section of (0.53 ± 0.07) mb. The analysis of the latter reaction favors a one-meson (π) exchange production mechanism. Also a comparison with the reaction $K^-p \rightarrow K^{*-}p$, $K^{*-} \rightarrow \bar{K}^0\pi^-$ confirms the predominance of T = 0 vector meson exchange in this reaction. For this experiment a hydrogen bubble chamber was exposed to a separated meson (K^-) beam with a momentum of (2.985 ± 0.015) Bev/c, and 60,000 pictures were scanned for two-prong events. A Dalitz plot and various distributions for this reaction are shown. (J.F.P.)

17381 ONE-PARTICLE EXCHANGE MODEL FOR INELASTIC PROTON-PROTON SCATTERING. Yock, P. C. M. (Massachusetts Inst. of Tech., Cambridge). Nuovo Cimento (10), 41A: 635-7(Feb. 21, 1966). (MIT-2098-209).

The energy dependences of those proton-proton collisions which can be interpreted as the excitation of an isobar in the final state: $p + p \rightarrow N^{*+} + p$ are examined. In particular the production of the nucleon isobars with masses equal to 1238, 1430, 1512, and 1688 Mev are considered. The observed energy dependences are compared with the theoretical value obtained on the assumption of spin-zero exchange. The production angular distributions are also discussed. (J.F.P.)

17382 POLARIZATION OF THE Σ^0 PARTICLES PRODUCED IN THE REACTION $\pi^- + p \rightarrow K^0 + \Sigma^0$ AT 1.5 AND 1.8 Bev/c. Kim, Young S. (Ohio State Univ., Columbus); Burleson, G. R.; Kalmus, P. I. P.; Roberts, A.; Romanowski, T. A. Phys. Rev., 143: 1028-33(Mar. 25, 1966). (COO-1261-20).

The polarization of the Σ^0 particles produced in the reaction $\pi^- + p \rightarrow K^0 + \Sigma^0$ was measured at 1.5 and 1.8 Bev/c, using a spark-chamber magnet system. The product $\alpha_\Lambda\langle\sigma_{\Sigma^0}\rangle$ was found to be -0.47 ± 0.33, $+0.51 \pm 0.27$, and $+0.82 \pm 0.44$, respectively, in Σ^0 cm angular intervals centered at cos $\theta^* = 0.8, -0.14$, and 0.0 at 1.8 Bev/c; and -0.55 ± 0.23, -0.31 ± 0.38, and -0.82 ± 0.46 at the same production angles at 1.5 Bev/c. The Σ^0 production angular distributions in the backward hemisphere at both momenta are also given. Both polarization and angular distribution are found to vary rapidly with energy. (auth)

17383 K^--p INTERACTION AT 2.24 Bev/c. London, G. W. (Brookhaven National Lab., Upton, N. Y.); Rau, R. R.; Samios, N. P.; Yamamoto, S. S.; Goldberg, M.; Lichtman, S.; Prime, M.; Leitner, J. Phys. Rev., 143: 1034-91(Mar. 25, 1966). (BNL-9542).

K^--p interactions at 2.24 Bev/c were studied in several exposures of the Brookhaven National Laboratory 20-in. hydrogen bubble chamber at the alternating-gradient synchrotron. An account is given of all aspects of the experiment, including: experimental procedures, scanning and measuring techniques, data-reduction methods, and experimental results and their consistency with the current theories of strong and weak interactions. The experimental results are grouped as follows: meson and baryon resonance spectroscopy; other two-body and three-body reactions; the Ξ hyperon; and total cross sections. For completeness, information published elsewhere is included and important details not previously given are added. In addition, a considerable range of new results is reported. (auth)

17384 π^+p INTERACTIONS AT T_π = 450 Mev. Poirier, C. P.; Tilger, C. A.; Alyea, E. D. Jr.; Martin, H. J. Jr.; Scandrett, J. H. (Indiana Univ., Bloomington). Phys. Rev., 143: 1092-5(Mar. 25, 1966).

Elastic and inelastic π^+p interactions at 450 Mev were studied. The inelastic cross section is (4.3 ± 0.4)% of the total cross section. The ratio of the single-pion production cross sections $\sigma(\pi^+p \rightarrow \pi^+\pi^0p)/\sigma(\pi^+p \rightarrow \pi^+\pi^+n)$ is 3.5 ± 1.0. Terms up through $\cos^4\theta_{cm}$ are needed to fit the elastic angular distribution. The effective-mass distributions for π^0 production show (π^+p) isobar formation and are compared with predictions of the Olsson-Yodh isobar model. (auth)

17385 PION PRODUCTION IN ANTIPROTON-PROTON ANNIHILATIONS AT 3.3 AND 3.7 Bev/c. Ferbel, T. (Yale Univ., New Haven); Firestone, A.; Sandweiss, J.; Taft, H. D.; Gailloud, M.; Morris, T. W.; Willis, W. J.; Bachman, A. H.; Baumel, P.; Lea, R. M. Phys. Rev., 143: 1096-1104(Mar. 25, 1966). (BNL-9623).

A study of antiproton-proton collisions at 3.3 and 3.7 Bev/c indicates that (41 ± 4)% of the total interaction cross section can be attributed to annihilation into pions. The average pion multiplicity is 6.5 ± 0.5. The positively charged pions and dipions tend to be emitted backward, while the negatively charged pions and dipions tend to be emitted forward in the center-of-mass system. Although there is a substantial amount of resonance production, especially of ρ and of ω mesons, there is no clear evidence for double or associated resonance production in these final states. A search for new resonances as well as for some of the recently discovered mesons proved unsuccessful. (auth)

17386 MULTIPLE PION PRODUCTION BY 1.89-Bev/c π^-. Christian, R.; Erwin, A. R.; Fechter, H. R.; Schwamb, F. E.; Vegors, S. H.; Walker, W. D. (Univ. of Wisconsin, Madison). Phys. Rev., 143: 1105-9(Mar. 25, 1966).

A report is given of a study of pion-proton interactions in a liquid-hydrogen bubble chamber. A 1.89-Bev/c negative-pion beam incident upon a 14-in.-dia chamber caused interactions from which those with four charged secondaries were selected and measured. Fits were attempted to the following states: $3\pi + p$, $3\pi + p + \pi^0$, and $4\pi + n$. The branching ratios for these three reactions were found to be (64.9 ± 3.3)%, (21.5 ± 1.7)%, and (13.9 ± 1.3)%, respectively. The $3\pi + p$ reaction was found to be dominated by the production of the $\frac{3}{2}$-$\frac{3}{2}$ pion-nucleon isobar, (43 ± 3)% of these events going via this channel. Evidence for the η and ω mesons was found in the $3\pi + p + \pi^0$ final state, (9.0 ± 2.2)% of these events going via the η channel, and (14.0 ± 2.8)% via the ω channel. (auth)

17387 SUM RULES GIVING TESTS OF LOCAL CURRENT COMMUTATION RELATIONS IN HIGH-ENERGY NEUTRINO REACTIONS. Adler, Stephen L. (CERN, Geneva. Harvard Univ., Cambridge, Mass.). Phys. Rev., 143: 1144-55(Mar. 25, 1966).

It is shown that the local commutation relations of the vector and the axial-vector current octets can be studied in nonforward lepton-neutrino reactions. The commutation relations are used to derive sum rules, for fixed q^2 (q^2 = invariant lepton momentum transfer squared), involving the elastic and the inelastic form factors measured in high-energy neutrino reactions. (auth)

17388 EFFECT OF DIPION RESONANCES ON THE PION-NUCLEON SCATTERING AMPLITUDE. Choudhury, S. Rai; Kumar, Aditya; Saxena, R. P. (Univ. of Delhi). Phys. Rev., 143: 1159-63(Mar. 25, 1966).

The effect of the newly discovered dipion resonance at about 730 Mev and of a possible one at about 400 Mev on pion-nucleon scattering is evaluated. Partial-wave dispersion relations are solved via the N/D decomposition by matrix-inversion methods. Two choices of "phase-space" factors are considered. The results, as compared with earlier calculations of a similar type, show marked improvement in P_{33} and P_{11} scattering lengths (with the Martin-Uretsky-type phase-space factor) but continue to disagree violently with experiment on the $S_{1/2}$ $T = 1/2$ scattering length. (auth)

17389 LOW-ENERGY INTERACTION OF Ξ^- WITH PROTON AND DEUTERON. Panchapakesan, N. (Univ. of Chicago). Phys. Rev., 143: 1166-70(Mar. 25, 1966).

The fraction $r_p = \Lambda/(\Lambda + \Xi^0)$ for the reactions $\Xi^- + p \rightarrow \Xi^0 + n$ and $\Xi^- + p \rightarrow \Lambda + \Lambda$ and the fraction $r_d = \Lambda/(\Lambda + \Xi^0)$ for the reactions $\Xi^- + d \rightarrow \Xi^0 + n + n$ and $\Xi^- + d \rightarrow \Lambda + \Lambda + n$ are calculated by solving the Schrödinger equation with one-boson-exchange potentials using coupling coefficients given by the octet model. Calculations are done with and without the conjectured σ meson [$T = 0$, $J = 0$, $m_\sigma \sim 400$ Mev] and for three different values for the coupling coefficient of K* mesons to the baryons. It is found that r_p and $r_d < 10^{-3}$ if the σ is included, and $r_p \sim 0.1$ and $r_d \sim 0.3$ if the σ is not included. The production of Λ particles is thus significant only if the σ is not included. The effect of the Ξ-N channel on the Λ-Λ scattering is also found to be important if the σ meson is not included. (auth)

17390 CALCULATION OF THE NUCLEON MAGNETIC MOMENTS BY DISPERSION-THEORY METHODS. Abarbanel, Henry D. I.; Callan, Curtis G. Jr.; Sharp, David H. (Princeton Univ., N. J.). Phys. Rev., 143: 1225-38 (Mar. 25, 1966).

The magnetic moments of the neutron and proton are calculated within the framework of the S-matrix perturbation theory recently developed by Dashen and Frautschi. In the present context, this method expresses the magnetic moments in terms of a dispersion integral involving photopion production. Evaluation of this integral in terms of contributions from appropriate low-mass intermediate states yields results for the individual magnetic moments which are larger than the experimental values by about a factor of two. The calculation does, however, give an approximately correct value for the ratio of the isovector moment to the isoscalar moment, and a value for the isoscalar moment that agrees with the experimental value to within about a factor of two. (auth)

17391 LINEAR MASS RELATIONS FOR THE ELEMENTARY PARTICLES AND RESONANT STATES. Sternheimer, R. M. (Brookhaven National Lab., Upton, N. Y.). Phys. Rev., 143: 1262-8(Mar. 25, 1966). (BNL-9487).

Previous work on linear mass relations for elementary particles is extended, particularly in connection with several resonant states that have been discovered recently. Two observed resonant states with baryon number B = 2 satisfy very simple mass relations which give support to the compound (quasinucleus) model discussed previously. In terms of the compound model, an interesting regularity was noticed concerning compounds formed from the K and η mesons and members of the baryon octet (N, Λ, Σ, Ξ). A study was also made of mass relations involving the recently discovered mesons and baryon isobars, in particular the particles $\epsilon^0(700)$, D(1280), K*(1400), $f^*(\sim 1500)$, and $N^*_{1/2}(1400)$. (auth)

17392 POSSIBLE TESTS OF $C_{\not\pi}$ AND $T_{\not\pi}$ INVARIANCES IN $l^\pm + N \rightarrow l^\pm + \Gamma$ AND $A \rightarrow B + e^+ + e^-$. Christ, N.; Lee, T. D. (Columbia Univ., New York). Phys. Rev., 143: 1310-21(Mar. 25, 1966). (TID-22364).

A systematic method to test the $C_{\not\pi}$ and $T_{\not\pi}$ invariances of the electromagnetic interaction is to use the inelastic scattering $l^\pm + N \rightarrow l^\pm + \Gamma$ where $l^\pm$ is the charged lepton, N is the target nucleus (or nucleon), and $\Gamma \neq N$ but, otherwise, can be any system of the strongly interacting particles. General expressions for the various possible $C_{\not\pi}$- and $T_{\not\pi}$-noninvariant effects in such reactions are derived and discussed. Similar considerations are also applied to the decay $A \rightarrow B + e^+ + e^-$, where A and B are any complexes of the strongly interacting particles. (auth)

17393 BOSON MASSES. King, R. W. (Purdue Univ., Lafayette, Ind.); Peaslee, D. C. Phys. Rev., 143: 1321-3(Mar. 25, 1966).

A gross mass scale is assigned to the baryon-antibaryon model for bosons: for charge octets $m^2(^3L) - m^2(^1L) \approx 1/2$ Bev^2. For charge singlets the mass formula is less certain but seems to be quite different from that for octets. The quantum number of A parity is pointed out as an inescapable feature of this model; the empirical values of A then rule out quarks for the simplest realization. Interest is remarked in K3π resonances and in possible resolution of the Kπ and K2π modes of the K*(1430). (auth)

17394 NEUTRON EXCHANGE IN THE REACTION $p + p \rightarrow d + \pi^+$. Mathews, J.; Deo, B. (Indian Inst. of Tech., Kanpur, India). Phys. Rev., 143: 1340-5(Mar. 25, 1966).

Several features of observed $p + p \rightarrow d + \pi^+$ cross sections in the Bev region suggest that a one-particle (in this case, one-neutron) exchange mechanism may play a significant role. This possibility was investigated. The treatment of the dnp vertex requires some care; the Fourier transform of the deuteron wave function plays a crucial role in the calculations. The resulting predictions for the angular distribution clearly exhibit the forward peaking which is experimentally observed, although the calculated total cross section, as a function of energy, does not agree very well with experiment. (auth)

17395 DECAYS OF BARYON RESONANCES OF ANY SPIN. Rushbrooke, J. G. (Cambridge Univ., Eng.). Phys. Rev., 143: 1345-53(Mar. 25, 1966).

General formulas are derived relating coupling constants for the strong decay interactions of a baryon resonance B^*_s of any spin s to the observed decay widths, for the decay processes $B^*_s \rightarrow B_{1/2} + P$, $B^*_s \rightarrow B^*_{s'} + P$, and $B^*_s \rightarrow B_{1/2} + V$, where P is a pseudoscalar and V a vector meson. The calculations are carried through within the framework of the Rarita-Schwinger formalism, using interaction Lagrangians incorporating derivative couplings of the pseudoscalar or vector-meson field to free spinor fields. The resulting formulas are compared with the well-known potential-theory expressions. (auth)

17396 MESON PRODUCTION IN ANTIPROTON-NUCLEON ANNIHILATION. Parkinson, Michael (Univ. of Chicago). Phys. Rev., 143: 1359-69(Mar. 25, 1966).

The antiproton-nucleon system at rest and its annihilation are discussed. Final states of two mesons, of many mesons with all but one in a vector resonance, and of two vector resonances are the main concern, although the decay to lepton pairs and other properties of the $\bar{p}$-nucleon system are also considered. The basic assumptions are that annihilations proceed mainly through an intermediate vector meson ($^3S_1$ decay) or pseudoscalar meson ($^1S_0$ decay) and also that SU(3) symmetry is valid for obtaining unknown coupling constants. The unknown parameters in the SU(3) couplings are determined by fitting to experiment, with the following interesting results: $g_{\rho NN} \cong g_{\omega NN}$ and $g_{\eta^* NN} \approx -2g_{\pi NN}$, where η^* refers to the 960-Mev $\eta\pi\pi$ resonance, and the above coupling constants for the ρ and ω are the sum of the γ_μ and $\sigma_{\mu\nu}q_\nu$ coefficients. $g_{\rho NN} \cong g_{\omega NN}$ at $q^2 = -4m_N^2$ is

shown to be consistent with nuclear-force calculations around $q^2 = 0$, and the above value for g_{η^*NN} helps explain the rapid increase with energy of the proton Compton-scattering cross section. The SU(3) $\bar{B}BV$ interaction is determined from the rates for $^3S_1$ annihilations of $\bar{p}p$ to $\pi^+\pi^-\pi^0$, $\pi^+\pi^-$, K^+K^-, and K_1K_2, the VVP coupling from $\omega \to 3\pi$ and $\phi \to 3\pi$, and the $\bar{B}BP$ interaction from the $^1S_0$ decays of $\bar{p}p$ to $K^*\bar{K}^*$, $\rho^0\rho^0$, and $\rho^0\omega^0$. The relation of the SU(3) couplings and the results of broken SU(6) and U(12) are briefly discussed. In particular, it is shown that $d/f = 2$ for $\bar{B}BV$ at $q^2 = -4m_N^2$, in contradiction to the value $^3/_2$ given by SU(6) and U(12); it is also concluded that the d/f ratio is not constant for the $\bar{B}BV$ coupling. A table of relative rates and graphs of expected mass spectra are given for final states consisting of a vector resonance plus pseudoscalar meson, and a comparison with the available experimental evidence is made. The approximate agreement expected is observed. The discussion of the vector-vector final states leads to the prediction that $\Gamma(\bar{p}p \to \rho^0\rho^0) \approx \Gamma(\bar{p}p \to \omega^0\omega^0)$, and it is also determined that $(\bar{p}p \to e^+e^-)/(\bar{p}p \to \pi^+\pi^-) \approx 2 \times 10^{-5}$. Finally it is concluded that the assumptions made are thus far consistent with experiment. (auth)

17397 COUPLED-CHANNEL SCHROEDINGER-EQUATION MODEL FOR HIGH-ENERGY PERIPHERAL COLLISIONS. Wills, John G.; Ellis, David; Lichtenberg, D. B. (Indiana Univ., Bloomington). Phys. Rev., 143: 1375-88 (Mar. 25, 1966).

A model for high-energy pion-nucleon scattering is considered in which there are 3 (or 4) open channels — πN, ρN, πN^* (and ρN^*) — and in which the scattering is determined by coupled Schrödinger equations with Yukawa potentials corresponding to exchange of a single π or ρ meson. All particles are considered spinless for simplicity, and relativistic kinematics are used. The calculations are done numerically on a CDC-3600 computer, in the partial-wave representation, for all values of the orbital angular momentum that contribute significantly to the cross sections. The results are compared with those of 4 other approximations: (1) simple Born approximation, (2) Born approximation modified by absorption parameters taken from elastic scattering, (3) the unitary S matrix obtained by identifying the Born approximation with the K matrix, and (4) Born approximation modified by absorption parameters determined in a self-consistent way from the optical theorem. It is found that none of the approximate methods agree in detail with the coupled-channel Schrödinger-equation results, but that methods (2), (3), and (4) agree qualitatively with the coupled-channel method for the reaction $\pi N \to \rho N$ near the forward direction. (auth)

17398 THEORY OF PARITY-VIOLATING NONLEPTONIC DECAY. Rosen, S. P. (Purdue Univ., Lafayette, Ind.). Phys. Rev., 143: 1388-90(Mar. 25, 1966).

The simplest way of explaining the result $A(\Sigma^+|n\pi^+) = 0$ is to assume an effective parity-violating hamiltonian of the form $(\bar{B} \times B)_{(8)} \times \pi$. With no further assumptions, this hamiltonian predicts two sum rules which are closely related to the Lee-Sugawara triangle, and it imposes an isotopic-spin selection rule $\Delta T < {}^5/_2$. The proposed coupling scheme is a consequence of several dynamical models, and the $\Delta T < {}^5/_2$ rule is consistent with the data on $K \to 2\pi$. (auth)

17399 INEQUALITY FOR ELECTRON AND MUON SCATTERING FROM NUCLEONS. Bjorken, J. D. (Stanford Univ., Calif.). Phys. Rev. Lett., 16: 408(Mar. 7, 1966).

An inequality involving the scattering cross sections and the momentum transfer is presented. (D.C.W.)

17400 PHOTOPRODUCTION CROSS SECTIONS FOR π^+ AND K^+ MESONS AT 3.4 TO 4.0 Gev AND THEIR COMPARISON WITH SU(3). Elings, V. B.; Cohen, K. J.; Garelick, D. A.; Homma, S.; Lewis, R. A.; Luckey, P. D.; Osborne, L. S. (Massachusetts Inst. of Tech., Cambridge). Contract AT(30-1)-2098. Phys. Rev. Lett. 16: 474-7 (Mar. 14, 1966). (MIT-2098-220).

The differential cross sections for the reactions $\gamma + p \to \pi^+ + n$, $\gamma + p \to K^+ + \Lambda^0$, and $\gamma + p \to K^+ + \Sigma^0$ were measured for incident laboratory photon energies between 3.4 and 4.0 Bev. The results agreed with the cross-section inequalities predicted from unbroken SU(3). (G.O.Y.)

17401 GENERAL THEOREM FOR MULTIPLE-PHOTON PROCESSES. Cohan, Norah V.; Hameka, H. F. (Univ. of Pennsylvania, Philadelphia). Phys. Rev. Lett., 16: 478-9(Mar. 14, 1966).

A general theorem for evaluating the time-proportional transition probability between two states of a system of particles in a radiation field is presented. (G.O.Y.)

17402 ANALYSIS OF THE B ENHANCEMENT. Chung, Suh Urk (Univ. of California, Berkeley); Neveu-Rene, Monique; Dahl, Orin I.; Kirz, Janos; Miller, Donald H.; Guiragossian, Zaven G. T. Phys. Rev. Lett., 16: 481-5 (Mar. 14, 1966). (UCRL-16570).

On the basis of some data on π^-p interactions at 3.2 and 4.2 Bev/c, it is shown that the β enhancement can be accounted for in terms of the virtual dissociation of the incident pion, $\pi \to \omega + \rho$, followed by the strongly asymmetric inelastic process $\rho + p \to \pi + p$. Difficulties associated with the interpretation of the B as a resonant state are also discussed. (D.C.W.)

17403 PRODUCTION AND DECAY PROPERTIES OF THE $K_0^*(892)$ PRODUCED IN THE REACTION $K^- + p \to p + \bar{K} + \pi^-$ AT 2.1, 2.45, AND 2.64 Bev/c. Friedman, Jerome H.; Ross, Ronald R. (Univ. of California, Berkeley). Phys. Rev. Lett., 16: 485-91(Mar. 14, 1966). (UCRL-16604).

The total cross section, the differential cross section, and the $K^*(892)$ decay correlations for the interaction $K^- + p \to K^{*-}(892) + p$ were measured. The decay distributions are consistent with the production and decay of a K^* relatively free from interference with other processes. (D.C.W.)

17404 METHOD TO TEST FOR TIME-REVERSAL INVARIANCE VIOLATION IN K DECAYS. Cline, David (Univ. of Wisconsin, Madison). Phys. Rev. Lett., 16: 367-9(Feb. 28, 1966).

A test of time-reversal invariance by the decay $K^+ \to \pi^+ + \pi^0 + \gamma$ is proposed. Some preliminary observations on decays of this type are summarized. (D.C.W.)

17405 ALGEBRA OF CURRENTS AND K_{e3} DECAY. Mathur, V. S.; Okubo, S.; Pandit, L. K. (Univ. of Rochester, New York). Phys. Rev. Lett., 16: 371-4(Feb. 28, 1966). (UR-875-113).

The K_{e3} decay is studied using an algebra of currents that was obtained from the quark model. (D.C.W.)

17406 THE NEUTRINO. Mikaelyan, L. A. (Kyramova Inst. of Nuclear Energy, Moscow). Priroda, No. 9, 24-35(Sept. 1965). (In Russian).

The main facts of neutrino physics are reviewed in a descriptive fashion. Pauli proposed the existence of a small neutral particle to save the laws of conservation which were apparently being violated during beta decay. Fermi called this neutral particle a neutrino. A spin of $^1/_2$ is assigned to the neutrino to conserve momentum. The neutrino was detected from the reaction $\nu + p \to n + e^+$ in the vicinity of a nuclear reactor in 1953. Ordinary water containing cadmium to absorb the neutrons served as the target of the neutrinos which were produced in abundance in the reactor (6×10^{19} neutrinos per second). Davis showed the existence of an antineutrino by irradiating ^{37}Cl (in the form of 4000 liters of CCl_4), and by proving that no ^{37}Ar is formed. The formation of μ-meson neutrinos during decay of a μ-meson is discussed. These neutrinos are different from electron and positron neutrinos. The neutrino spin is discussed briefly. (TTT)

17407 POLARIZATION COEFFICIENTS IN PHOTOPRODUCTION REACTIONS OF PSEUDOSCALAR PARTICLES ON A NUCLEON. Lazarenko, L. O. (Inst. of Physics and Tech., Kharkov). Ukr. Fiz. Zh., 10: 1056-64 (1965). (In Russian).

All polarization coefficients were obtained for photoproduction reactions of pseudoscalar particles on a nucleon.

The coefficients were recorded in covariant form. The coupling relations were found between the polarization coefficients and some consequences of them, useful for the kinematic study of the S-matrix, i.e., for conducting the full experiment in reactions of meson (π) and meson (k) photoproduction. (auth)

17408 DISPERSION THEORY OF MAGNETIC DIPOLE PHOTO-SPLITTING OF THE DEUTERON. Petrov, M. M. (Inst. of Physics, Kiev). Ukr. Fiz. Zh., 10: 1065-70(1965). (In Russian).

The effect of the nonphysical peculiarities on the amplitude of the magnetic dipole photo-splitting of the deuteron at energies close to the photo-splitting threshold is investigated on the basis of dispersion theory. The interaction between the nucleons is described by a non-local Yamaguchi potential. (auth)

17409 COMPTON SCATTERING IN A MAGNETIC FIELD. Tskhakaya, D. D. (Inst. of Physics and Tech., Academy of Sciences, Ukrainian SSR). Ukr. Fiz. Zh., 10: 1277-88(Dec. 1965). (In Ukrainian).

The Compton scattering of photons on a scalar charged particle in a magnetic field is considered. The case of resonance was investigated, as well as the classical relativistic limit for the cross section of scattering. A formula was obtained for the cross section of scattering in the nonrelativistic approximation. (auth)

17410 PHOTOPRODUCTION OF VECTOR MESONS AT HIGH ENERGIES. Tu, Pham Qui (Kiev State Univ.). Ukr. Fiz. Zh., 10: 1295-8(Dec. 1965). (In Ukrainian).

The method of complex angular momenta was used to consider the asymptotic behavior of the cross section of photoproduction of vector mesons. Concrete calculations are presented along with asymptotic expressions obtained for production cross sections of charged and neutral mesons under the assumption that they are determined by isolated poles on the plane of complex momenta. The results are discussed for the case when the amplitude of the processes are determined not only by the poles but by other singularities. (auth)

17411 QUARKS: ASTROPHYSICAL AND PHYSICO-CHEMICAL ASPECTS. Zel'dovich, Ya. B.; Okun, L. B.; Pikel'nev, S. B. Usp. Fiz. Nauk, 87: 113-24(1965). (In Russian).

Various approaches to the search for new stable particles are reviewed: namely, three assumed quarks, having charges 2/3e, $-1/3$e, and $-1/3$e[1-2], as well as others having integral charges. The lightest fractional-charge quark is supposed to be stable in vacuum as well as in contact with ordinary matter (nuclei, electrons). Conditions are given under which integral-charge particles can be stable. Various possible sources of quarks are reviewed, the most powerful being cosmic rays from superstars or quasistars. The annihilation of quarks is then discussed in detail. Since quarks are heavier than nucleons, the process $q_1 + q_1 \rightarrow q_3 + q_{-1}$ is possible, followed by $q_1 + q_{-1} \rightarrow nq_0$ (where the subscript indicates the number of quarks and the minus sign indicates an antiparticle); q_3 is thus an ordinary baryon of three quarks, and q_0 is a meson. Quarks are therefore annihilated via a series of pair collisions. Other likely ways are also traced. Possibilities of detecting quarks are reviewed, including physical-chemical and mass spectroscopic methods. (JPRS)

17412 PREDICTIONS OF UNITARY SYMMETRY FOR HADRON PHOTOPRODUCTION REACTIONS. Dolgov, A. D.; Solov'ev, V. V. (Inst. of Experimental and Theoretical Physics, State Atomic Energy Commission, USSR). Yadern. Fiz., 2: 954-6(Nov. 1965). (In Russian).

In the reaction $\gamma + p \rightarrow$ meson + baryon, the following relations between amplitudes can be readily obtained on the assumption of SU(3) symmetry: (1) $A(p\pi^0) - \sqrt{3}A(p\eta^0) + \sqrt{2}A(\Sigma^+K^0) = 0$ and (2) $A(\Sigma^0K^+ - \sqrt{3}A(K^+\Lambda) + \sqrt{2}A(\pi^+n) = 0$. The available experimental data indicates that $A(\Sigma^+K^0)$ is small, and it follows from (1) that $|A(p\pi^0)|^2 : |A(p\eta^0)|^2 = 3:1$. There is not enough available experimental data to confirm these relationships at present. In the reaction $\gamma + p \rightarrow$ meson + baryon resonance, theory predicts that $|A(\pi^+\Delta^0)|^2 : |A(K^+\Sigma^{*0})|^2 = 2:1$. Experiment gives a value of 2.0 ± 1.7 for this ratio. In the reaction $\gamma + p \rightarrow 2$ mesons + baryon, the following relation between amplitudes is obtained when both mesons are charged: $A(p\pi^+\pi^-) + A(pK^+K^-) + A(\Sigma^+K^+\pi^-) = 0$. In the reaction $\gamma + p \rightarrow 2$ mesons + baryon resonance, the conservation of U-spin leads to a number of relations between reaction amplitudes. More experimental data are needed to confirm these relations. (TTT)

17413 ON THE POSSIBILITY OF INVESTIGATING WEAK NUCLEON-NUCLEON INTERACTIONS. Lobashev, V. M. (Ioffe Inst. of Physics and Tech., Leningrad). Yadern. Fiz., 2: 957-9(Nov. 1965). (In Russian).

The reaction $n^0 + p^1 \rightarrow D^2 + \gamma$ is proposed as a means of studying a weak nucleon-nucleon interaction. A neutron trap in the active zone of a reactor would serve as a strong source of gamma quanta from the above reaction. It is estimated that a collimated beam of 10^{10} to 10^{11} quanta per second could be produced by this reaction. In principle it should be possible to measure a circular polarization on the order of 10^{-7} within a reasonable length of time. In this way it is possible to observe the contribution from a weak nucleon-nucleon interaction. By reversing the magnetic field in polarization counter at a definite frequency it should be possible to detect circularly polarized gamma quanta by electronic means. The fundamental nature of the results justifies the expenditure of a considerable amount of work required to overcome the experimental difficulties. (TTT)

17414 INFLUENCE OF ABSORPTION ON PERIPHERAL PHOTOPRODUCTION OF VECTOR MESONS. Kramer, G.; Schilling, K. (II. Institut fuer Experimentalphysik, Hamburg). Z. Phys., 191: 51-69(1966).

Photoproduction of ρ and ω mesons on nucleons is considered in the peripheral model. The interaction mechanism is assumed to be pseudoscalar and scalar exchange. Absorptive final-state interactions are taken into account. The differential cross section and the angular distribution for the decay are calculated and compared with experimental data. (auth)

17415 DERIVATION OF A WEAK CURRENT IN THE FRAMEWORK OF UNITARY SYMMETRY. Moebius, P. (Univ. of Vienna). Z. Phys., 191: 367-80(1966).

In the framework of unitary symmetry a weak current is derived depending on three parameters. For the calculation of its matrix elements a special method of unitary symmetry-breaking is applied taking into account all corrections due to the baryon mass differences. The matrix elements for the leptonic decays of the pion and kaon are computed and the parameters are determined. A comparison with Cabibbo's treatment of weak interactions is given. The results are also compared with bubble chamber fits and a rather good agreement is found. (auth)

17416 π-MESON-NUCLEON INTERACTION IN THE AXIOMATIC APPROACH. Voronov, B. L. (Lebedev Inst. of Physics, Moscow). Zh. Eksp. Teor. Fiz., 49: 1802-11 (Dec. 1965). (In Russian).

Charge-symmetry interaction between mesons-(π) and nucleons is considered within the framework of the axiomatic approach. A relativistically covariant formulation of the principle of minimal singularity is presented. Together with other familiar principles the latter yields a closed equation set for the S-matrix elements on exit from the mass shell with respect to only one impulse variable. The arbitrariness of the theory reduces to two indefinite real constants corresponding to the $\pi-N$-vertex and meson 4-tail. A perturbation theory solution of the equations yields a renormalized series. (auth)

17417 REAL PART OF THE pp ELASTIC SCATTERING AMPLITUDE AT 2, 4, 6, 8 AND 10 Gev. Kirillova, L. F.; Nikitin, V. A.; Sviridov, V. A. (and others) (Joint Inst. for Nuclear Research, Dubna, USSR). Zh. Eksp. Teor. Fiz., 50: 76-7(Jan. 1966). (In Russian).

Results of measurement of the real part of the pp nuclear elastic scattering amplitude for an energy of 4 Bev and

more refined data for energies of 2, 6, 8 and 10 Bev are presented (the data are treated by taking into account relativistic corrections). The differential cross section was measured in the range $0.003 < |t| < 0.2$ (Bev/c)^2. (auth)

17418 HIGH-ENERGY SUCCESSIVE INTERACTIONS. Feinberg, E. L. (Lebedev Inst. of Physics, Moscow). Zh. Eksp. Teor. Fiz., 50: 202-14(Jan. 1966). (In Russian).

The properties (interaction features) of a particle suffering a sharp momentum change are investigated. The analysis is carried out for two-bremsstrahlung interactions of an electron on fixed centers by standard renormalized quantum electrodynamics. The difference between the present analysis and the usual one is that the time variation of the system functional (assumed initially as a packet) is calculated. It is shown that after the first interaction the particle is in a state in which its subsequent interaction differs from the normal one over a long period of time (which is macroscopically long at very high energies and much greater than the time of passage of the packet). In this state the proper field of the particle differs from the stationary proper field of an ordinary particle with the given momentum. The effect is of a classical nature and is quite large due to relativistic slowing down of the restoration time of the stationary state at high energies. It is not only characteristic for bremsstrahlung and for electrodynamics. The possibility of the existence of the effect for a nucleon interacting strongly with its meson field is discussed and some estimates are presented. (auth)

17419 THE EFFECTS OF INELASTIC CHANNELS ON NN, $\pi\pi$, AND πN ELASTIC SCATTERING CROSS SECTIONS [Thesis]. Coulter, Philip Wylie. Stanford, Calif., Stanford Univ., 1965. 130p.

The results of including inelastic effects in computing elastic scattering cross sections are studied by using the single-channel N/D equations including inelastic unitarity, which were developed by Frye and Warnock. These calculations are compared to the single-channel N/D calculation for elastic unitarity. Three reactions are studied: nucleon-nucleon scattering, pion-pion scattering, and pion-nucleon scattering. The $^1D_2$ partial wave in proton-proton scattering is selected for the first reaction. The calculated values of the real part of the phase shift agree closely with the results of Scotti and Wong (elastic unitarity) for $E_L \leqq 200$ Mev, but the deviation is appreciable at higher energies. The phase shifts peak at about 400 to 500 Mev, depending on the asymptotic behavior of the inelastic factor, and become negative for $E_L \gtrsim 1$ Bev. In pion-pion scattering the $I = 1$, $l = 1$ partial wave is studied in an attempt to compute the width and shape of the ρ resonance. The smallest output width obtained is about 250 Mev as compared to 600 Mev if inelastic effects are neglected. The shape of the resonance is more symmetric if inelastic effects are considered. An argument is presented, which may account for the discrepancy between the input and output widths if the ρ meson can be produced as a quasi-bound state in one of the inelastic channels. The phase shifts for all partial waves with $J \leqq 3/2$ are computed in pion-nucleon scattering. The inelastic factor is taken from Roper's phase shift analysis and the results are compared with the phase shifts obtained by Roper. The results agree reasonably well with Roper's low energy phases with the exception of the S_{11} and P_{11} partial waves. By including the nucleon pole in the direct channel in the generalized potential agreement with Roper for these partial waves at low energy was obtained. It is shown that this is not necessarily evidence for the elementarity of the nucleon. (A.G.W.)

17420 DYNAMICAL EQUATIONS FOR SCATTERING OF PARTICLES WITH SPIN AND ANALYTIC CONTINUATION IN ANGULAR MOMENTUM [Thesis]. de Lany, Vincent Milan. Berkeley, Calif., Univ. of California, 1965. 58p.

Dynamical equations are derived for pion-nucleon scattering and the cross reaction $\pi\pi \rightarrow N\bar{N}$. These equations are a generalization of the equations recently given by Chew and Jones in the new strip approximation to a reaction in which some external particles have spin. A practical difficulty in constructing pole terms in the unequal mass case is discussed. The Froissart-Gribov continuation of the partial-wave helicity amplitudes for $\pi\pi \rightarrow N\bar{N}$ is investigated at $J = 0$ to determine whether the continued amplitudes coincide with the physical amplitudes. It is concluded that it is unlikely that the continued and physical amplitudes will disagree at $J = 0$ in the new strip approximation. (Dissertation Abstr.)

17421 RADIATIVE DECAY OF INTERMEDIATE BOSON [Thesis]. Friedberg, Richard Michael. New York, Columbia Univ., 1962. 47p.

The W particle is a hypothetical charged vector meson playing a role in weak interactions. The radiative decay, $W^- \rightarrow l^- + \bar{\nu} + \gamma$, of this particle is treated in second order perturbation theory. The total decay rate contains an infrared divergence cut off roughly at a photon energy of 10 Mev. Differential and total rates are calculated and the total rate is compared with that of the non-radiative decay, $W^- \rightarrow l^- + \bar{\nu}$. It is found that the ratio of radiative to non-radiative decay is quite insensitive to the magnetic moment parameter of the W meson, but increases substantially with increasing W mass. For a W mass of 1000 Mev, the branching ratio is about 10^{-1} if l^- is e^- or 10^{-2} if l^- is μ^-. It is suggested that the magnetic moment parameter may affect some aspects of the angular distribution. It is noted that if the gyromagnetic ratio of the W is exactly 2, then the $\bar{\nu}$ and γ cannot come off in the same direction. (Dissertation Abstr.)

17422 MESON DECAYS AND THE SIGMA HYPOTHESIS [Thesis]. Faier, Harry. Evanston, Ill., Northwestern Univ., 1965. 110p.

Certain decay modes of the η, K, and X^0 (960) mesons were studied. About three years ago Brown and Singer postulated an $I = 0$ dipion resonance of mass about 400 Mev (the σ meson) to explain the decay branching ratios of the η meson. A quantitative fitting of this theory to the various spectra is presented. The important role of the σ in the decay $X^0 \rightarrow \eta\pi\pi$ is demonstrated. As a further test of the σ idea, the rate and spectra of the K_{e4} decay mode, $K^+ \rightarrow \pi^+\pi^-e^+\nu$ are calculated, assuming that this scalar meson dominates the interaction of the two pions in the final state. Two forms were used for the unstable sigma-propagator: (a) Breit-Wigner, (b) modified Breit-Wigner form with momentum dependent width. A χ^2 fit of the π^0 spectrum in $\eta \rightarrow \pi^+\pi^-\pi^0$ yields best-fit values $m_\sigma = 400$ Mev, $\Gamma_\sigma = 100$ Mev for both forms. However, for these parameters the branching ratio $R = \eta \rightarrow 3\pi^0/\eta \rightarrow \pi^+\pi^-\pi^0$ equals 1.39 ± 0.08 using (a) and 1.19 ± 0.05 using (b), while $R_{expt} = 1.16 \pm 0.15$. For $m_\sigma = 400$ Mev and $\Gamma_\sigma = 100$ Mev, the partial width $\Gamma(\eta \rightarrow \pi^+\pi^-\pi^0)$ is 312 G^2 ev, where G is a dimensionless coupling constant that characterizes the $\eta\sigma\pi$ vertex. The rates $\Gamma(\eta \rightarrow 2\gamma)$ and $\Gamma(\eta \rightarrow \pi\pi\gamma)$ are calculated to be 38 ev and 9 ev, respectively, using a modified version of the Gell-Mann, Sharp, Wagner model. Agreement with experiment results for $G^2 \approx 1/8$. A similar analysis gives $\Gamma(X^0 \rightarrow \eta\pi^+\pi^-) = 2.6\ G^2$ Mev for $m_\sigma = 400$ Mev, $\Gamma_\sigma = 100$ Mev, and $\Gamma(X^0 \rightarrow \pi\pi\gamma) = 57$ kev. Agreement with the experimental ratio is obtained for $G^2 \approx 1/10$. Spectral fits of the σ hypothesis to the τ' data show consistency with the parameters $m_\sigma \approx 400$ Mev and $\Gamma_\sigma \approx 100$ Mev. A similar fit to the odd-pion spectrum in the τ mode gives a χ^2 probability of 30% for these same parameters of the sigma. The $K \rightarrow 3\pi$ branching ratios are calculated and shown to be in accord with the experimental values. The K_{e4} decay mode is studied and agreement with experiment is found for the ratio $r = K^+ \rightarrow \pi^+\pi^-e^+\nu/K^+ \rightarrow \mu^+\nu$, if the dimensionless K_{e4} and $K_{\mu 2}$ axial coupling constants are equated. (Dissertation Abstr.)

17423 POSITRON ANNIHILATION IN THE NOBLE GASES. Jones, G.; Falk, W. R.; Orth, P. H. R. (Univ. of British Columbia, Vancouver, Can.). pp 372-6 of IVth International Conference on the Physics of Electronic and Atomic Collisions. New York, Science Bookcrafters, Inc.

The possibility of studying the momentum-transfer cross sections of positrons in noble gases by a technique that is based on a velocity-dependent annihilation rate for slow positrons in noble gases was investigated. (D.C.W.)

17424 THE TRANSVERSE POLARIZATION OF THE MUON IN THE DECAY $K_L^0 \rightarrow \mu^+ + \pi^- + \nu$. Bartlett, D.;

Friedberg, C.; Goulianos, K.; Hutchinson, D. (Princeton Univ., N. J.). 10p. (CONF-651043-6). ORAU. Gmelin, AED-CONF-65-320-6.

From Weak Interactions Conference, Argonne, Ill.

The transverse polarization of the meson (μ^+) in the decay $K_S^0 \rightarrow \mu^+ + \pi^- + \nu$ was investigated. The spin of the meson (μ^+) was monitored by observing the direction of the electron from its decay. (D.C.W.)

Field Theory, Scattering Theory, and Symmetries

See *also* Elementary Particles and Radiations

17425 (DESY-66/1) APPLICATION OF SPECTRAL REPRESENTATIONS TO THE NONRELATIVISTIC AND RELATIVISTIC BETHE-SALPETER EQUATION. Kramer, G.; Meetz, K. (Deutsches Elektronen-Synchrotron, Hamburg (West Germany)). Jan. 1966. 29p. Dep. mn.

The eigenvalue problem of the scalar Bethe-Salpeter equation is solved by application of the vertical Dyson representation. The method of solution is developed in complete analogy to the solution of Schrödinger's equation by a Stieltjes representation in the case of a Yukawa potential. The eigenvalues are zeros of a characteristic determinant, which can be understood as a generalization of the nonrelativistic Jost function. (auth)

17426 (IC-66/16) DISCRETE DEGENERATE REPRESENTATIONS OF NON-COMPACT UNITARY GROUPS. Raczka, R.; Fischer, J. (International Centre for Theoretical Physics, Trieste (Italy)). Feb. 1966. 43p. Dep. mn.

Two degenerate principal series of irreducible unitary representations of an arbitrary non-compact unitary group U(p,q) are derived. These series are determined by the eigenvalues of the first and second-order invariant operators, which are shown to possess a discrete spectrum. The explicit form of the corresponding harmonic functions is derived and the properties of the discrete representations are discussed in detail. Moreover, the properties of the corresponding degenerate representations of an arbitrary compact U(p) group are derived. (auth)

17427 (IC-66/20) THE STRONG VERTEX ACCORDING TO SL(6,C). Fronsdal, C.; White, R. (International Centre for Theoretical Physics, Trieste (Italy)). Mar. 4, 1966. 11p. Dep. mn.

A non-compact algebra S that contains SL(6,c) as a subalgebra is considered. Its relation to the Poincaré algebra is P $\tilde{+}$ S (semidirect sum). The representations that give theories of the Gürsey-Radicati SU(6) type are determined by the value of a simple degenerate mass, and an irreducible representation of S. These representations are discussed. (M.O.W.)

17428 (JINR-P-2498) O NEKOTORYKH VOZMOZHNYKH OPYTAKH PO PROVERKE IZOTOPICHESKOI STRUKTURY. (On Some Possible Experiments Aimed at Testing the Isotopic Structure of the Electromagnetic Interaction). Grishin, V. G.; Lyuboshits, V. L.; Ogievetskii, V. I.; Podgoretskii, M. I. (Joint Inst. for Nuclear Research, Dubna (USSR)). 1965. 8p. Dep. mn.

Possible experiments are discussed on a test of the $\Delta T = 0,1$ rule in the processes involving γ quanta. (auth)

17429 (JINR-P-2529) O GRUPPAKH SIMMETRII V KLASSICHESKOI I KVANTOVOI MEKHANIKE. (On Symmetry Groups in Clasical and Quantum Mechanics). Winternitz, P.; Smorodinskii, Ya. A.; Uglirzh, M.; Frish, I. (Joint Inst. for Nuclear Research, Dubna (USSR). Lab. of Theoretical Physics). 1965. 18p. Dep. mn.

All potentials having a dynamical symmetry group in a two-dimensional world are found. Classical and quantum motion in these potentials is investigated and it is shown that in all cases the symmetry group is SU(2). The previously known potentials with higher symmetry (Coulomb potential, harmonic oscillator) are obtained as special cases. (auth)

17430 (JINR-P-2565) RASSEYANIE SLOZHNOI CHASTITSY NA SILOVOM TSENTRE. (Scattering of a Complex Particle on the Force Center). Khelashvili, A. A. (Joint Inst. for Nuclear Research, Dubna (USSR). Lab. of Theoretical Physics). 1966. 10p. Dep. mn.

It is proved that it is possible to reduce the problem of a complex particle scattering on the force center to the many-channel problem of particle scattering on a certain "generalized potential" which is dependent on the internal motion of the bound system. A "potential" for the Yukawa interaction is constructed. (auth)

17431 (JINR-P-2569) O MAGNITNOM MOMENTE DIRAKOVSKOI CHASTITSY V POTENTSIAL'NOI YAME. (On the Magnetic Moment of the Dirac Particle in the Potential Well). Bogolyubov, P. N. (Joint Inst. for Nuclear Research, Dubna (USSR). Lab. of Theoretical Physics). 1966. 5p. Dep. mn.

Using the squared Dirac equation an expression is obtained for the magnetic moment of the Dirac particle in a scalar potential well of an arbitrary form. The same is done for the pseudoscalar potential in the limit for the large mass of the particle. (auth)

17432 (NP-15902) ELEMENTARY INTRODUCTION TO ELEMENTARY PARTICLE PHYSICS. Lectures given at The Niels Bohr Institute and NORDITA, Copenhagen. Hamilton, J. (Nordisk Institut for Teoretisk Atomfysik, Copenhagen (Denmark)). 1964/65. 239p. Dep. mn.

Basic ideas involved in elementary particle processes are discussed. In particular, discussions are presented on the phase space factor; the Dalitz-Fermi plot, applications of the Dalitz plot, covariant formulation of transition rates, angular momentum, the operations C, P, T, particle-antiparticle conjugation C, time reversal T, time reversal in field theory, theorems on the CPT and decay processes, meson (K^0) decays, and G-parity. (M.O.W.)

17433 (NYO-3399-13) THE NATURE OF APPROXIMATE SYMMETRIES OF STRONGLY INTERACTING PARTICLES. Sudarshan, E. C. G. (Syracuse Univ., N. Y. Dept. of Physics). [1965]. Contract AT(30-1)-3399. 8p. Dep. mn. CFSTI $1.00 cy, $0.50 mn.

A theory of approximate symmetries of strongly interacting particles is outlined. (D.C.W.)

17434 (NYO-3399-18) DYNAMICAL MIXING OF SPIN AND UNITARY SPIN. Balachandran, A. P. (Syracuse Univ., N. Y. Dept. of Physics). [1965]. Contract AT(30-1)-3399. 5p. Dep. mn. CFSTI $1.00 cy, $0.50 mn.

A completely relativistic model which leads to higher symmetries that mix internal and space-time symmetry variables is described. The symmetry group changes with the internal symmetry multiplets involved in the scattering and is also energy-dependent. (D.C.W.)

17435 (NYO-3399-45) CURRENTS, ALGEBRAS AND DYNAMICAL SYSTEMS. Sudarshan, E. C. G. (Syracuse Univ., N. Y. Dept. of Physics). [1965]. Contract AT (30-1)-3399. 18p. (CONF-651134-1). Dep. mn. CFSTI $1.00 cy, $0.50 mn.

From Eastern Theoretical Conference, Stony Brook, N. Y.

The three facets of symmetry are briefly discussed. Noninvariance groups and their uses, local noninvariance algebras, current and sources, uses of current algebras, and restrictions on local current algebras are discussed. (M.O.W.)

17436 (UCRL-14321-T) THE NON-DYNAMICAL STRUCTURE OF PARTICLE REACTIONS. Moravcsik, Michael J. (Lawrence Radiation Lab., Univ. of California, Livermore). [1965]. Contract W-7405-eng-48. 101p. Dep. mn. CFSTI $4.00 cy, $0.75 mn.

Five lectures dealing with various aspects of elementary particle reactions are presented. Discussions are presented in the following order: (1) the numbers of form factors are derived for a given reaction under various conservation laws; (2) it is shown how both the M-matrix and the observables of a complicated reaction can be reduced to constituents representing simpler reactions; (3) properties of the M-matrix and of the observables were used

to derive some general theorems concerning so-called parity experiments; (4) the mathematical formalism used to calculate observables in terms of form factors for a reaction involving particle of arbitrary spins is discussed; and (5) properties of the experimental observables are derived and these properties are illustrated in terms of a reaction involving four spin-½ particles. (M.O.W.)

17437 INTERMEDIATE FIELDS WITHOUT PARTICLES. Frenkel, A. (Central Research Inst. for Physics, Budapest). Acta Phys. Acad. Sci. Hung., 20: 167-84(1966).

An extension of Bogoliubov's S-matrix theory to include intermediate fields with no corresponding particles in the initial and final states is proposed. The mathematical expression for the complete propagator of an intermediate field indicates that there may be cases when this propagator has the well-known analytic properties of a propagator of an unstable particle (or resonance). It is shown that if application of the formalism to the vector field is possible, a renormalizable theory of weak interactions with intermediate vector boson field can be constructed. In lowest order this theory leads to the same results for the weak decay processes as the usual Fermi theory. (auth)

17438 POTENTIAL SCATTERING. Tang, K. T. (Columbia Univ., New York). Amer. J. Phys., 34: 152-3 (Feb. 1966).

The well-known expression of the scattering amplitude is rederived from the integral representation. The exact equivalence between the integral and differential formulation is explicitly demonstrated. (auth)

17439 EFFECTIVE POTENTIAL IN THE DEGENERATE BOSE LIQUID. Byckling, Eero (Univ. Helsinki. Univ. of Tech., Otaniemi, Finland). Ann. Acad. Sci. Fenn., Ser. A VI, No. 190: 1-7(1965).

The effective interaction in the Bose liquid is obtained in the Nambu representation using Green's function techniques at zero temperature. Inclusion of all the matrix elements of the exact single particle Green's function in the propagators results in a set of 16 scattering matrices. Transformation to the quasiparticle picture decouples the set of scattering matrix integral equations into a set of independent equations. In the center-of-mass approximation with p_4-independent self-energy parts these equations can be solved with previously given methods. (auth)

17440 STUDY OF THE FUNCTIONS L, M, N OF THE NONLINEAR SPINOR THEORY OF ELEMENTARY PARTICLES (CONTINUATION). David, J. H.; Derem, A. Bull. Cl. Sci., Acad. Roy. Belg. (5), 51: 485-96(1965). (In French).

The L, M, N functions were investigated for small λ values. The imaginary parts are calculated by a direct method and the simpler functions to which L, M, N reduce when μ equals unity ($\xi = \eta$) are graphically represented. (M.O.W.)

17441 ON THE RAINICH GEOMETRIZATION OF A VECTOR MESON FIELD IN THE KIBBLE THEORY. Bicak, J. (Charles Univ., Prague). Czech. J. Phys., 16: 95-8(1966).

The variables of a vector meson field are determined within the framework of the Kibble theory as the functions of the metric tensor, affine connection, and their derivatives and a system of differential equations is found for the metric tensor and affine connection which is equivalent to the equations of motion of gravitational and vector meson fields. (auth)

17442 TWO AXIAL OCTETS. Granovskii, Ya. I. (Inst. of Nuclear Physics, Academy of Sciences, Kazakh SSR). JETP Lett. (USSR) (Engl. Transl.), 2: 341-2 (Dec. 15, 1965).

Translated from Zh. Eksp. Teor. Fiz., Pis'ma Redakt., 2: 549-51(Dec. 15, 1965).

The recently discovered nonet of tensor mesons $\underline{9}(2^+)$ = $A_2(1320)$ + K**(1430) + f(1250) + f'(1525) can fit, within the framework of SU(6) symmetry, only in a supermultiplet of dimensionality 405 $\underline{405} = \underline{9}(2^+) + \underline{27}(2^+) + \underline{9}(0^+) + \underline{27}(0^+) + \underline{8}(1^+) + \underline{10}(1^+) + \underline{10}^*(1^+) + \underline{27}(1^+)$. This 405-plet contains two axial octets, which differ in the G-parity of their nonstrange components. The known resonances are identified in the following fashion; $\underline{8}^{(a)} = A_1(1090) + C(1215) + E(1410)$, and $\underline{8}^{(b)} = B(1215) + C'(1330) + D(1280)$. The masses, mixing angles, and widths are briefly discussed. (M.O.W.)

17443 PREDICTION OF MASSES IN MESONIC MULTIPLETS IN THE SIMPLE QUARK MODEL. Anisovich, V. V. JETP Lett. (USSR) (Engl. Transl.), 2: 344-6 (Dec. 15, 1965).

Translated from Zh. Eksp. Teor. Fiz., Pis'ma Redakt., 2: 554-7(Dec. 15, 1965).

Experimental data are presented for comparison with an earlier quark model for determining the masses of higher meson resonances. (M.O.W.)

17444 SEARCH FOR PARITY NONCONSERVATION IN NUCLEAR GAMMA TRANSITIONS. Lobashov, V. M.; Nazarenko, V. A.; Saenko, L. F.; Smotritskii, L. M. (Ioffe Inst. of Physics and Tech., Leningrad). JETP Lett. (USSR)(Engl. Transl.), 3: 47-50(Jan. 15, 1966).

Translated from Zh. Eksp. Teor. Fiz., Pis'ma Redakt., 3: 76-81(Jan. 15, 1966).

The circular polarization of the gamma quanta emitted from ^{181}Ta after the beta decay of ^{181}Hf was measured. An upper limit was established for the polarization of the 482-kev gamma quanta from ^{181}Ta. (D.C.W.)

17445 STRONGLY DECAYING ELEMENTARY PARTICLES. Schmitz, N. (Max-Planck-Institut fuer Physik und Astrophysik, Munich). Naturwissenschaften, 53: 1-8(1966). (In German).

The term "strong decay" is defined. The methods used in the detection and measurement of strongly decaying particles are indicated. The reactions that produce strongly decaying particles are summarized, and the known strongly decaying mesons and baryons are tabulated. (J.S.R.)

17446 OPERATOR AND GENERALIZED GAUGE TRANSFORMATIONS IN QUANTUM ELECTRODYNAMICS. Lam, C. S. (Univ. of Maryland, College Park). Nuovo Cimento (10), 41A: 193-203(Jan. 21, 1966).

Previous studies on the relations between Green's functions are generalized. In the majority of the published literature dealing with this problem, gauge transformations are defined through the change of a generating functional, or equivalently, through certain specified changes of the Feynman rules. The connection between this definition, and the definition of defining a gauge transformation by the addition of the gradient of an operator-valued gauge function to the electromagnetic potential (operator gauge transformation), is studied. It is found that each operator gauge transformation from the radiation gauge may be defined through certain modifications of the Feynman rules in that gauge. However, usually it consists of more modifications than those assumed before. These modifications due to an operator gauge transformation are all of a special type. Modifications of other type may be included, which serves to define generalized gauge transformations. An example of a generalized gauge transformation is given in which the interacting electron propagator coincides with the free one outside any prespecified space-time domain. This example serves to illustrate the many other possibilities of gauge transformations that have not been considered before. A theorem giving a relation between the electron Green's functions in different gauges is also proved. (auth)

17447 RELATIVISTIC TREATMENT OF THE THREE-BODY PROBLEM. Tucciarone, A. (Univ., Rome). Nuovo Cimento (10), 41A: 204-21(Jan. 21, 1966).

The Bethe-Salpeter procedure leading to a relativistic equation for the two-body scattering amplitude cannot be directly applied, in general, to the three-body problem. The difficulties arising in the attempt of applying such a procedure are discussed in the $\lambda\varphi^3$ model. A solution is given leading to a set of equations for the three-body scattering amplitude. The equations found have, in general, nonconnected kernels, and therefore cannot be solved with the Fredholm method. An equivalent set with connected kernels is derived. (auth)

17448 $SU_3 \otimes SU_3$ AND NONLEPTONIC HYPERON DECAYS. Alles, W. (CERN, Geneva). Nuovo Cimento (10), 41A: 280-2(Jan. 21, 1966).

Hyperon nonleptonic decays when an octet meson is emitted and when the weak interaction hamiltonian transforms like the $(8_S^3 + 8_S^1)$ component of the representation 35 of SU_6 are discussed. (J.F.P.)

17449 ANALYTICITY PROPERTIES OF THE SCATTERING AMPLITUDE FOR A VELOCITY-DEPENDENT POTENTIAL. Cirelli, R.; Montaldi, E.; Prosperi, G. M. (Univ., Milan. Istituto Nazionale di Fisica Nucleare, Milan). Nuovo Cimento (10), 41A: 456-80(Feb. 21, 1966).

A method developed in a preceding paper is applied to the study of the analyticity properties of the scattering amplitude relative to a kind of velocity-dependent potential, $V = V_0(r) - \frac{1}{2}[\Delta_2 V_1(r) + V_1(r)\Delta_2]$, which has raised some interest for the description of the low-energy nucleon-nucleon interaction. (auth)

17450 APPROXIMATE CALCULATION OF ASYMPTOTIC OPERATORS. Sirugue-Collin, M. (Univ. d'Aix, Marseille). Nuovo Cimento (10), 41A: 485-502(Feb. 21, 1966).

Asymptotic operators are introduced as creation and annihilation operators of physical particles so that the hamiltonian of the system becomes free when expressed in terms of physical operators. It is shown explicitly on the scalar static model that this is not always possible; hence the necessity of asymptotic conditions is found. An example is also given of calculation using the Machida model. (auth)

17451 COVARIANT MULTIPOLE POLARIZATION OPERATORS AND DENSITY MATRICES FOR ANY SPIN. Sankaranarayanan, A. (Iowa State Univ., Ames). Nuovo Cimento (10), 41A: 532-42(Feb. 21, 1966). (IS–1233).

Covariant multipole polarization operators for a particle with finite nonzero mass and arbitrary spin are constructed by considering the usual multipole expansion of polarization matrices as the rest system operators. Then these multipole operators are used to write down the covariant density matrices and finally their properties are briefly discussed. (auth)

17452 LEVINSON'S THEOREM FOR S-MATRIX THEORY WITH INELASTICITY. Atkinson, D.; Morgan, D. (CERN, Geneva). Nuovo Cimento (10), 41A: 559-75 (Feb. 21, 1966).

A form of Levinson's theorem is stated and proved for a certain class of relativistic, inelastic scattering amplitudes. The notion of the CDD class of an amplitude is introduced. This enables one to use the theorem to say how many elementary particles are associated with the scattering process in question. Lastly, these considerations are generalized, on a less rigorous basis, to include cases in which $\delta(\infty) \neq 0(\pi)$. (auth)

17453 C AND T INVARIANCE AND NUMBER OF SU_3 AMPLITUDES. Ruegg, H. (CERN, Geneva). Nuovo Cimento (10), 41A: 576-85(Feb. 21, 1966).

The implications of C and T invariance, together with P invariance and statistics, for the number of SU_3 amplitudes, are reexamined, especially when the particles involved have spin and some of them baryon number. Meson-meson octet scattering, annihilation of baryon and antibaryon octets into two mesons and into baryon-antibaryon, and baryon scattering are given as examples. It is shown that crossing does not give any new restriction. The crossing of the three "unusual" partial-wave amplitudes occurring in the scattering of four spin-½ particles is discussed. Some experimental implications are given. (auth)

17454 THE ALLOWED LINK-UP BETWEEN RELATIVITY AND INTERNAL SYMMETRY. Cicogna, G. (Scuola Normale Superiore, Pisa, Italy). Nuovo Cimento (10), 41A: 603-5(Feb. 21, 1966).

The allowed linkup between relativity and internal symmetry is shown through a simple approach. It results in a skew position of the Poincaré group with the larger symmetry group G. An important result is that no exact "good" mass formula can be obtained either with a discrete or a continuous mass spectrum, without breaking interactions. (J.F.P.)

17455 SOME REMARKS ON $[SU_4(T) \otimes SU_2(X) \otimes V(Y)]_W$. Buccella, F. (Univ., Florence). Nuovo Cimento (10), 41A: 613-17(Feb. 21, 1966).

The less restrictive predictions of the $[SU_4(T) \otimes SU_2(X)]_W$ subgroup of $SU_6(W)$ are studied. The consequences of the symmetry for this subgroup for the nucleon and hyperon electromagnetic form factors, the baryon-meson coupling, the axial and vector weak currents, the weak nonleptonic hyperon decays, and the forward and backward photoproduction of mesons are discussed. It is also remarked that both Johnson-Treiman relations are lost in this approach. (J.F.P.)

17456 MODELS FOR NONLEPTONIC DECAYS BASED ON THE CHIRAL $U_3 \otimes U_3$ ALGEBRA. Gatto, R. (Univ., Florence. Istituto Nazionale di Fisica Nucleare, Florence); Maiani, L.; Preparata, G. Nuovo Cimento (10), 41A: 622-4(Feb. 21, 1966).

Two models based on alternative assignments of the weak nonleptonic spurions are considered, and S-wave sum rules are derived from the commutation relations. A current × current structure of the weak nonleptonic hamiltonian is not required. The relevant point is the specification of the commutation relations satisfied by the parity-violating and the parity-conserving terms of the nonleptonic hamiltonian. (J.F.P.)

17457 VECTOR-MESON DOMINANCE AND $U_{6,6}$. Papastamatiou, N. J. (Clarendon Lab., Oxford). Nuovo Cimento (10), 41A: 625-8(Feb. 21, 1966).

Using $U_{6,6}$ the couplings of ρ, ω, and ϕ to the baryon current are computed, and the results are compared with experimental fits of the electromagnetic form factors. The agreement in general is found to be very good. (J.F.P.)

17458 RENORMALIZATION OF THE STRANGENESS-CHANGING AXIAL-CURRENT COUPLING CONSTANT. Bar-Nir, I. M. (Tel-Aviv Univ., Israel). Phys. Rev. Lett., 16: 473-4(Mar. 14, 1966).

A method of separating the contributions of the Λ and the Σ^0 to the renormalized axial-vector coupling constant in strangeness-changing beta decay is outlined. (D.C.W.)

17459 REMARKS ON THE FORWARD PEAK AT HIGH ENERGIES. Jin, Y. S. (Brown Univ., Providence). Phys. Rev., 143: 975-7(Mar. 25, 1966). (NYO–2262-105).

In the framework of the axiomatic field theory, it is proved that s-u crossing-symmetric elastic-scattering amplitude of any two stable particles has forward peak at high energies, unless $|\mathrm{Re}f(s,1)/\mathrm{Im}f(s,1)| \to \infty$ or $|f(s,1)| < C(\ln s)^{-1}$. If one exchange amplitude dominates the others, this result also holds for any elastic-scattering amplitude without s-u symmetry. It turns out that the dispersion relation is not essential and the analytic property recently found by Bros, Epstein, and Glaser is sufficient for the proof. In the proof, the properties of the Herglotz function are extensively used. (auth)

17460 BORN APPROXIMATION AND LARGE-MOMENTUM-TRANSFER PROCESSES IN POTENTIAL SCATTERING. Wu, Tai Tsun (Harvard Univ., Cambridge, Mass.). Phys. Rev., 143: 1110-16(Mar. 25, 1966).

Several problems of nonrelativistic scattering by analytic potentials are studied, where both the energy and the momentum transfer are large. The reflection coefficients are found asymptotically from the one-dimensional potentials $Ve^x(1 + e^x)^{-2}$, $Ve^{x/2}(1 + e^x)^{-1}$, and $V \exp(-x^2)$, and the scattering amplitudes for their three-dimensional generalizations $Ve^r(1 + e^r)^{-2}$, $Ve^{r/2}(1 + e^r)^{-1}$, and $V \exp(-r^2)$. The results are compared with these obtained from Born approximation, and it is found that the first Born approximation gives the correct answer asymptotically in the cases $Ve^{x/2}(1 + e^x)^{-1}$ and $Ve^{r/2}(1 + e^r)^{-1}$, but not in the other cases. Conjectures about more general cases are also given. (auth)

17461 HIGH-ENERGY LARGE-MOMENTUM-TRANSFER PROCESSES AND ANALYTICITY IN COORDINATE

SPACE. Wu, Tai Tsun (Harvard Univ., Cambridge, Mass.). Phys. Rev., 143: 1117-34(Mar. 25, 1966).

In nonrelativistic scattering theory, analytic potentials lead to exponentially decreasing differential cross sections for large momentum transfers. An attempt is made to adopt this connection for strong interactions. Since the differential cross section for proton-proton elastic scattering with large momentum transfers decreases exponentially with the momentum transfer, it is postulated that the wave functions of strongly interacting particles are analytic functions of the coordinate variables. This assumption leads in a natural way to an exponential dependence on the transverse momentum transfer. On the basis of this, speculations are made about various scattering processes involving a total of four strongly interacting particles, two incoming and two outgoing. The results are, in some cases, less specific than those of the previous consideration. Since it is natural to consider not only two-particle but also three-particle wave functions, the speculation is also extended to some processes where three particles are produced. (auth)

17462 WAVE FUNCTIONS AND PRODUCTION AMPLITUDES FOR ANY SPIN. Frishman, Y. (Weizmann Inst. of Science, Rehovoth, Israel). Phys. Rev., 143: 1135-8 (Mar. 25, 1966).

Closed formulas are given for the relativistic helicity eigenstates of a wave function for any spin. Helicity amplitudes for the production of higher spin particles are then computed and brought to a simple form for pion and vector-meson exchange. (auth)

17463 CURRENT ALGEBRAS AND APPROXIMATE SYMMETRIES. Oehme, Reinhard (Univ. of Chicago). Phys. Rev., 143: 1138-43(Mar. 25, 1966).

The components of currents involved in weak and electromagnetic interactions are assumed to generate the algebra of chiral U(6) ⊗ U(6). For the hadrons, the spurion scheme of broken U(6,6) symmetry is considered, which implies nonchiral U(6) ⊗ U(6) symmetry for hadrons at rest, and invariance with respect to collinear $U(6)_p$ for particles moving in a given direction. The chiral U(6) ⊗ U(6) commutation relations are evaluated in a single-particle approximation with $U(6)_p$ supermultiplets. It is found that one can obtain U(6) results, even though currents are involved which are not elements of the algebra of $U(6)_p$ or even of nonchiral U(6) ⊗ U(6). There appear, however, factors v/c or 1 − v/c, which either cancel or can be eliminated by taking the appropriate limits. The effect of mass splitting in the single-particle approximation of the commutation relations is evaluated. The relation of these results to the sum rules of Adler and Weisberger is discussed, as well as the relevance of these sum rules for the problem of the damping of semileptonic ΔS = 1 transitions. (auth)

17464 LINE-PROFILE EFFECTS IN STIMULATED SCATTERING. Gatland, I. R. (Georgia Inst. of Tech., Atlanta). Phys. Rev., 143: 1156-8(Mar. 25, 1966).

The enhanced scattering that occurs when an interaction takes place in the presence of a stimulating beam is shown to be an integral of the phase-space density of the stimulating beam over a surface in momentum space. For a narrow line profile this surface may be considered plane and its orientation is determined by the kinematics of the scattering event. An effective band width is defined by normalizing the enhanced scattering with respect to the space density of the stimulating beam, and this is interpreted as being the width of the line profile perpendicular to the plane of integration for the enhanced scattering. This geometric picture gives a simple estimate of the effective band width for use in the general theory of stimulated scattering. The effective band widths are given for some particular line profiles, including those appropriate to laser beams, and the results are applied to some proposed experiments on photon-photon and electron-photon scattering. (auth)

17465 VECTOR-SCALAR FIELDS AND RENORMALIZATION. Kundu, S. K. (Australian National Univ., Canberra). Phys. Rev., 143: 1163-5(Mar. 25, 1966).

A model for vector fields is discussed with a vector coupled to two vectors or two scalar fields. It is shown that the model can be treated adequately with the usual prescription of renormalization theory and does not need any cutoff. An estimate of renormalization for known meson couplings is also presented: $-\delta g/g_0 \sim 0.2$ on this model. (auth)

17466 WEAK AND ELECTROMAGNETIC INTERACTIONS OF THE HADRONS IN BOOTSTRAP THEORY. Dashen, R. F.; Frautschi, S. C. (California Inst. of Tech., Pasadena). Contract AT(11-1)-68. Phys. Rev., 143: 1171-84(Mar. 25, 1966). (CALT-68-52).

The properties of the weak and electromagnetic currents of the hadrons are investigated in the bootstrap theory of strong interactions. In a bootstrap theory, there are many self-consistency conditions relating these weak and electromagnetic parameters to each other. A formalism is developed, which is designed to take the fullest advantage of such bootstrap-like relations. In fact, it is conjectured that the weak and electromagnetic properties of the hadrons are determined to a large extent, and perhaps completely, by self-consistency requirements. Some simple calculations of the weak and electromagnetic parameters pertaining to the octet of baryons and decuplet of resonances are given. The comparison of the results of these calculations with the experimental numbers indicates that the above conjecture holds, at least in this case. (auth)

17467 SELF-CONSISTENT DETERMINATION OF COUPLING SHIFTS IN BROKEN SU(3). Dashen, R. F. (California Inst. of Tech., Pasadena); Dothan, Y.; Frautschi, S. C.; Sharp, D. H. Contract AT(11-1)-68. Phys. Rev., 143: 1185-90(Mar. 25, 1966). (CALT-68-51).

The possibility that certain patterns of SU(3) symmetry breaking are dynamically enhanced in baryon-meson couplings is studied by bootstrap methods. For the strong couplings, a single dominant enhancement is found. It produces very large symmetry-breaking terms, transforming like an octet, as often conjectured. Experimental consequences are listed, such as a reduction of K-baryon couplings relative to π-baryon couplings which is in accord with the experimental weakness of K relative to π production in many circumstances, such as photoproduction and multi-Bev cosmic-ray collisions. For parity-violating nonleptonic couplings, a dominant octet enhancement is again found, which leads to an excellent fit with experiment. For parity-conserving nonleptonic couplings, on the other hand, several different enhancements compete, and the only conclusion that can be drawn is that terms with the "abnormal" transformation properties brought in by strong symmetry-breaking corrections are present. The work provides a dynamical derivation of various phenomenological facts associated with SU(6), such as the dominance of the 35 representation in parity-violating nonleptonic decays. (auth)

17468 S-WAVE BARYON-BARYON SCATTERING IN BROKEN SU(3). Gupta, Sachchidananda; Pande, Lalit Kumar (National Physical Lab., New Delhi, India). Phys. Rev., 143: 1190-3(Mar. 25, 1966).

S-wave baryon-baryon scattering is considered in first-order broken SU(3). Nine sum rules are obtained for the various hyperon-nucleon amplitudes for scattering in the state $^1S_0$, and six for scattering in the state $^3S_1$. One of the sum rules for the state $^1S_0$ involves reactions with nucleon targets only, and can therefore be used for an experimental check. A few other sum rules involve only one reaction with a non-nucleon target and could be useful in estimating the latter. (auth)

17469 FIELD-THEORETIC FORMULATION OF THE OPTICAL MODEL AT HIGH ENERGIES. Torgerson, Ronald (Univ. of Chicago). Phys. Rev., 143: 1194-1215 (Mar. 25, 1966).

Two approximation schemes are studied within the framework of the quantum electrodynamics of massive photons [Q.E.D.(W)], motivated by the semiclassical approximation in potential theory (i.e., the optical model)

rather than Regge pole or cut expectations. In the first scheme a series of Feynman graphs (generalized ladder graphs) that form a natural extension of potential scattering at high energies s and finite momentum transfer t is selected. (They moreover incorporate the effects of crossing symmetry in the s and u channels). In the second scheme a semiclassical approximation is made, without the use of conventional perturbation theory, involving classical currents in the T-product formula for the S matrix. After certain vertex-renormalization and self-energy defects are taken into account, in a general way, an S matrix is found that is identical with that of an optical model whose potential is a superposition of Yukawa potentials. Thus a sufficient (and perhaps necessary) condition for covariance of an optical model is found. Without taking any vertex and self-energy effects into account in either scheme, agreement is found between the two schemes so far up to fourth order. To study the effect of spin in our models a spin-zero object "Π" and a spin-½ object "N" is introduced. Because of the γ_5 invariance of the γ_μ vertex, the helicity-conserving amplitudes for the reactions Π + N → Π + N and N + N → N + N are the same as for Π + Π → Π + Π, namely, A(t)s + B(t)s lns. It is verified that B(t) ≡ 0 up to sixth order. Taken by itself, this form violates unitarity unless B(t) ≡ 0 to all orders. Other ways are also studied to save unitarity in the whole of Q.E.D.(W). Such unitarity considerations are strongly indicative of the importance of an optical term $s\mathcal{f}(t)$ with nonzero real and imaginary parts even when many other series of graphs are taken into account (although other contributions may compete with it near t = 0). The optical contribution, taken alone, provides a natural qualitative explanation for the experimentally suggested constant behavior in the ratio of the real to imaginary part of the forward pp scattering amplitude above 8 Bev/c. Although a similar result is predicted for Kp scattering, it does not apply to πp. (auth)

17470 ALGEBRA OF CURRENTS AND LOW-ENERGY Kπ INTERACTION. Mathur, V. S.; Pandit, L. K. (Univ. of Rochester, N. Y.). Phys. Rev., 143: 1216-19(Mar. 25, 1966). (UR-875-103).

Using the Fubini-Furlan-Adler-Weisberger technique, sum rules were written down for strangeness-changing and strangeness-preserving axial-vector coupling constants. Coupled together, these sum rules provide information on the low-energy interactions of strongly interacting particles. In particular the Kπ system is studied and a case made for the existence of an S-wave resonance near threshold in the I = ½ channel. An evaluation of the KNΛ and KNΣ coupling constants required by the mutual consistency of the sum rules is also presented. (auth)

17471 CURRENT-GENERATED ALGEBRA AND MASS LEVELS OF THE HADRONS. Arafune, J.; Iwasaki, Y.; Kikkawa, K.; Matsuda, S.; Nakamura, K. (Tokyo Univ.). Phys. Rev., 143: 1220-5(Mar. 25, 1966).

The mass splittings of the U(3) [or SU(3)] multiplets of the hadrons are investigated under the following assumptions: (i) The hamiltonian decomposes into an invariant part plus an eighth component of an octet of U(3), and the latter is a space integral of the scalar current transforming like $\frac{1}{2}(q^\dagger\beta\lambda_8 q)$, where q stands for the quark. (ii) An algebra of the positive parity operators generating a nonchiral U(3) × U(3) is a "good symmetry," where the generators consist of the scalar currents and the fourth components of the vector currents. It is shown that if a universal constant with the dimensions of a mass together with the average mass of the multiplet are given, then the splitting is calculated exactly for any multiplet under the above assumptions. A kind of competition of the kinematical group U(3) and the dynamical group U(3) × U(3) can predict the average masses of U(3) multiplets if they belong to the same multiplet of U(3) × U(3). The multiplets that concern us are the $\frac{1}{2}^+$ octet, $\frac{3}{2}^+$ decuplet, $\frac{3}{2}^-$ octet, 0^- nonet, 2^+ nonet, and 1^- nonet. The results show good agreement with experiment. (auth)

17472 DISTINCTION BETWEEN COMPOSITE AND ELEMENTARY PARTICLES IN A MODEL FIELD THEORY. Deshpande, N. G.; Bludman, S. A. (Univ. of Pennsylvania, Philadelphia). Phys. Rev., 143: 1239-46(Mar. 25, 1966).

The Zachariasen model field theory is examined with a view to understanding the behavior of field theory with a nontrivial vertex function in the limit of vanishing renormalization constants Z_1 and Z_3. Two formulations are given for the model, which deals with two scalar relativistic fields A and B with allowed interactions A → B + $\overline{B}$ and B + $\overline{B}$ → B + $\overline{B}$. The model is defined: (1) by specialization of spectral representations for the A-particle propagator and $\overline{B}BA$ vertex functions to allow only elastic unitarity and no crossing in $\overline{B}B$ scattering amplitude; (2) in terms of selected ($\overline{B}B$ chain) diagrams generated by the Fermi interaction $\lambda_0\overline{B}B\overline{B}B$ and the Yukawa interaction $g_0\overline{B}BA$. In both formulations, expressions are derived for the renormalization constants Z_1, Z_3, and $\delta\mu^2$, which generalize earlier works, by allowing poles in the vertex function and inverse propagator, and also allow a complete treatment of the combined (Fermi and Yukawa) interactions. The Zachariasen model is found to be such that when Z_3 → 0: (1) Z_1 → 0 and Z_1^2/Z_3 → 0, g_0^2 → 0, and $\delta\mu^2$ is finite; (2) the poles of the scattering amplitude are no longer propagator poles (elementary particles) but are vertex poles (bound states); (3) the theory is found to develop a redundant zero. The behavior is strikingly different from the earlier models considered, and the significance of this is pointed out. Bounds are obtained on the renormalized coupling constant despite poles of the vertex function, and the distinction between a $Z_3 \neq 0$ elementary particle theory and a $Z_3 = 0$ elementary particle or a bound state is examined with reference to Levinson's theorem on the high-energy behavior of phase shifts. (auth)

17473 GOLDSTONE BEHAVIOR IN SOME MODEL THEORIES. Hellman, W. S.; Roman, P. (Boston Univ.). Phys. Rev., 143: 1247-51(Mar. 25, 1966).

Simple model theories characterized by bilinear interaction structures are studied. The interrelation between nonvanishing vacuum expectation values of the fields, broken vacuum-state invariance, and constant-field translation invariance is pursued, in relation to the appearance of zero-mass particle poles in the propagators. The peculiar role of constant-field translation invariance is discussed. (auth)

17474 DISTORTED-WAVE THEORY OF THE ONE-MESON-EXCHANGE REACTION. Tobocman, W.; Giltinan, D. (Case Inst. of Tech., Cleveland). Phys. Rev., 143: 1252-62(Mar. 25, 1966).

A distorted-wave theory of the one-meson-exchange reaction is derived. The treatment is valid only in the high- and low-energy limits. Only the case of scalar-meson exchange is presented, but the extension of the method to other types of mesons should be straightforward. The distorted-wave one-meson-exchange (DWOME) theory differs from that published by Sopkovich; Dar et al.; Durand and Chiu; Ross and Shaw; Gottfried and Jackson; Omnes; and Ball and Frazer. Calculations are presented comparing the predictions of the two types of DWOME theory for several cases. The two types of DWOME theory are found to give very similar differential cross sections for sufficiently great incident energy. The two formulations are also compared for medium-energy nuclear reactions. In the nuclear realm this becomes a comparison between the distorted-wave Born approximation and a form of the diffraction model. (auth)

17475 SPIN INDEPENDENCE, W SPIN, PARITY, AND SU(6) SYMMETRY. Lipkin, H. J. (Argonne National Lab., Ill.); Meshkov, S. Contract NA-onr-11-65. Phys. Rev., 143: 1269-74(Mar. 25, 1966). (BNL-9630).

The assumption of strict spin independence of strong interactions between elementary particles forbids all three-meson and meson-baryon-baryon couplings, such as ρππ, NNπ, and N*Nπ. It is shown that these catastrophies may be avoided, even in the nonrelativistic limit, by adopting a modified definition of spin independence, i.e., W-spin independence. A nonrelativistic definition of W spin

is obtained, which requires only a trivial change to yield the relativistic description. The consequences of the assumption of W-spin independence are explored. (auth)

17476 REGGEIZATION, MASSLESS PARTICLES, AND VANISHING RENORMALIZATION CONSTANTS. Chester, Arthur N. (California Inst. of Tech., Pasadena). Contract AT(11-1)-68. Phys. Rev., 143: 1275-92(Mar. 25, 1966). (CALT-68-50).

This paper has three purposes: to generalize earlier work on Reggeization in field theories to allow treatment of massless particles; to show that Reggeization occurs in other processes than just vector-spinor scattering; and to recover the one-to-one correspondence between certain poles in the partial-wave amplitudes and dynamical states. In problems involving massless spin-1 and spin-2 mesons, use is made of a modified amplitude defined by Eriksson which contains no infrared divergences and directly yields physical cross sections. It is shown that if the proper experimental procedure is defined, infrared-divergent diagrams do not alter the positions of Regge poles in this amplitude and these diagrams change the residues only to higher orders in the coupling constant. The dilemma about factorization of amplitudes when some of the helicity amplitudes are missing is resolved. These results are then applied to the scattering of photons by spin-½ and spin-0 electrons; in each case, it is found that a dynamical trajectory is formed but that the electron is not Reggeized (does not lie on the trajectory). Then the Compton scattering of gravitons (massless spin-2 particles) by spinor or scalar electrons is calculated. In each case, it is shown that no trajectory is generated near the highest nonsense value available, and that near the electron there is generated only one trajectory. In each case the electron is Reggeized. A theory involving massive spin-2 particles is formulated but not used for calculations. Finally, the dynamical criterion furnished by vanishing renormalization constants is applied to Reggeized particles. This test is found to correctly identify a Reggeized particle as elementary; thus the contribution of a Reggeized particle to the scattering amplitude is essentially different from the contribution of a true dynamical state. This allows certain moving poles to be associated directly with dynamical particles, without regard for amplitudes in other channels. (auth)

17477 BOUND ON THE COUPLING CONSTANT FROM UNITARITY AND ANALYTICITY. Dahmen, H. D.; Reiner, A. S. (Massachusetts Inst. of Tech., Cambridge). Contract AT(30-1)-2098. Phys. Rev., 143: 1295-1302(Mar. 25, 1966). (MIT-2098-200).

Unitarity of the S matrix is used to bound the sum of the pole term and the left-hand contribution appearing in a dispersion relation for a partial-wave scattering amplitude. An upper bound for the coupling constant is then constructed for the case of an arbitrary distribution of any finite number of sign changes in the left-hand cut discontinuity. (auth)

17478 UNSUBTRACTED DISPERSION RELATIONS AND THE RENORMALIZATION OF THE WEAK AXIAL-VECTOR COUPLING CONSTANTS. Weisberger, William I. (Stanford Univ., Calif.). Phys. Rev., 143: 1302-9(Mar. 25, 1966). (SLAC-PUB-143).

Assuming that the equal-time commutation rules for the vector and axial-vector-current octets proposed by Gell-Mann are valid and that the divergence of the $\Delta S = 0$, $\Delta I = 1$ axial current is a strongly convergent operator obeying unsubtracted dispersion relations and dominated by low-frequency contributions, a sum rule is derived for the renormalization of the neutron axial β-decay constant G_A, by the strong interactions. The result agrees with that previously obtained from the assumption that the axial-current divergence is proportional to the pion field. The results are generalized to the strangeness-changing leptonic decays in the context of Cabibbo theory and generalized Goldberger-Treiman relations, and are used to compute the d/f ratio for the weak baryon axial-current coupling and an independent value of G_A. (auth)

17479 GENERAL NONDYNAMICAL FORMALISM FOR REACTIONS WITH PARTICLES OF ARBITRARY SPIN: COMPOSITE REACTIONS AND PARTIAL-WAVE EXPANSIONS. Csonka, Paul L.; Moravcsik, Michael J.; Scadron, Michael D. (Univ. of California, Livermore). Phys. Rev., 143: 1324-39(Mar. 25, 1966). (UCRL-14478-T).

The mathematical techniques developed previously for basic constituent reactions are now extended to composite reactions involving four particles of arbitrary spins and parities. The nondynamical description of the various ways to couple the spins is considered in detail. The coupling together of the initial spins, on the one hand, and of the final spins, on the other, permits the development of the partial-wave expansion of the resulting nondynamical form factors. The Appendices include many specific examples of commonly occurring reactions. (auth)

17480 PARTICLE MASSES AND SU(6) SYMMETRY BREAKING. Harari, H. (Stanford Univ., Calif.); Rashid, M. A. Phys. Rev., 143: 1354-8(Mar. 25, 1966). (SLAC-PUB-153).

The transformation properties of the mass-splitting strong interaction are discussed in the framework of the SU(6) scheme. Using the experimental mass values of the 56 baryons and the 35 mesons, the reduced matrix elements of all the possible mass tensor operators are calculated. It is found that the SU(3) symmetry-breaking terms transform mainly as the 35 representation of SU(6), whereas the SU(3)-conserving, SU(6)-violating terms do not have simple transformation properties. (auth)

17481 COUPLING CONSTANTS IN BROKEN $\tilde{U}(12)$ SYMMETRY. Flamm, D. (Massachusetts Inst. of Tech., Cambridge). Contract AT(30-1)-2098. Phys. Rev., 143: 1369-74(Mar. 25, 1966). (MIT-2098-195).

The effects of SU(3) and $\tilde{U}(4)$ breaking on the coupling constants in $\tilde{U}(12)$ symmetry are investigated using the spurion technique. For an SU(3)-breaking spurion which is a member of 143, only two parameters are introduced in addition to the one for the formal symmetry. All 132 baryon-meson coupling constants can be expressed in terms of these three quantities. For vertices involving pions or ρ mesons, only two parameters are relevant. The effects of $\tilde{U}(4)$ breaking as well as simultaneous $\tilde{U}(4)$ and SU(3) breaking are studied with spurions that belong to the representations 143, 4212, and 5940 of $\tilde{U}(12)$. The sum rules for the coupling constants that follow from the formalism are in reasonable agreement with experiment. (auth)

17482 IS A NON-RELATIVISTIC APPROXIMATION POSSIBLE FOR THE INTERNAL DYNAMICS OF ELEMENTARY PARTICLES? Morpurgo, G. (Univ., Genoa). Physics, 2: 95-105(Oct. 1965).

It is pointed out that, contrary to what is usually implied, the internal dynamics in a compound model of an "elementary" particle is not necessarily relativistic. If the force which binds the constituent objects has a finite range and is not too singular, the relativistic character of the internal motion only depends on the range of such force and on the mass of the constituent particles, not on the depth of the potential well. For instance, for a quark antiquark model of the octet bosons with a quark mass of 5-Bev and a range of the binding force $(5m_\pi)^{-1}$, one has $(p/M)^2 = 1/40$, a non-relativistic situation quite similar to that occurring in nuclei. Starting from this observation it is pointed out that several features of the SU_3 and SU_6 dynamics can be understood by writing a non-relativistic hamiltonian for quarks, in a way similar to that which is used in writing a hamiltonian for a nucleus. More precisely: one can understand why the Gell-Mann–Okubo SU_3 mass formula for baryons works much better than its perturbative derivation would imply; one can obtain the $-3/2$ ratio between the magnetic moments of proton and neutron, due to SU_6, by a very simple calculation, which, at the same time exhibits how peculiar is the situation for the absolute values of the magnetic moments; some interesting aspects of the situation, though implied in the conventional derivation, are masked there under the algebra; the point of view taken leads to the conclusion

that SU_6 should possibly be valid only at non-relativistic energies of the interacting particles. (auth)

17483 MOMENT RELATIONS FOR SCHROEDINGER TWO-BODY CROSS SECTIONS. Roberts, M. J. (London Univ.). Proc. Phys. Soc., 86: 683-91(Oct. 1965).

Recent work on the asymptotic momentum expansion of Schrödinger two-body scattering amplitudes by Buslaev and Hunziker has made it possible to derive identities called 'moment relations' by a method analogous to that used for partial-wave amplitudes (Jost functions). These identities involve the total cross section and the differential cross section in the forward direction. The results are used to derive simple analytic approximations to the total cross section and are compared numerically using a Gauss potential with the cross sections obtained by summing over the first seven partial waves using exact numerical phase shifts and also approximate phase shifts due to Swan. The moment approximations are not so good as those obtained from Swan's phase shifts as far as was tested. (auth)

17484 MINIMAL COUPLING OF MASSLESS CHARGED PARTICLES. Dowker, J. S. (The Univ., Manchester, Eng.). Proc. Phys. Soc., 86: 727-9(Oct. 1965).

The minimal electromagnetic interaction of a charged, massless vector particle is shown to be consistent. (auth)

17485 CHERENKOV INTERACTION IN A UNIFORMLY LOADED WAVEGUIDE. Stekert, J. J. RCA Rev., 26: 510-38(Dec. 1965).

An analysis and computer experiment are carried out on a simple, circularly symmetrical waveguide, homogeneously filled with a uniform dielectric, which is undergoing Čerenkov interaction with a flowing density-modulated electron stream. The dispersion (ω,k) characteristics of the system reveal the presence of two complex root loci for each mode, one denoting evanescence and the other convective instability and gain associated with coupling of the slow space-charge wave to the waveguide mode. The latter loci extend from the region of synchronism for each mode to the immediate vicinity of the dispersion plane origin, thereby presenting an extended frequency region for gain. The gain of the convective instability, however, does peak in the region of mode synchronism. The peak gain is found to be approximately proportional to the cube root of the average beam current, as is the bandwidth at half-peak gain. Peak gain also maximizes as a function of the threshold parameter, βn. The Čerenkov threshold condition, $\beta n = 1$, and the characteristic radiation angle are found to hold for the system. It is concluded that aside from the possible implications of the extended gain region, the differences between this interaction and those of more conventional traveling-wave devices are not fundamental, but are reflections of the specific difference in the properties of the slowing circuits. (auth)

17486 SYMMETRIES IN ELEMENTARY PARTICLE PHYSICS. Mihul, Eleonora (Inst. of Atomic Physics, Bucharest). Stud. Cercet. Fiz., 17: 1079-91(1965). (In Rumanian).

The law of the conservation of spin leads to the unitary SU(2) group. Strangeness is conserved in strong interactions, therefore the SU(2) symmetry group was extended to include also this quantum number, resulting in the derivation of the SU(3) group. In order to include the ordinary spin of the particle, the SU(6) group is used. Studies on the relativistic generalization of the SU(6) group are reviewed. The SL(6) group is also examined within the framework of the SU(6) symmetry, deriving relations between the various formfactors and current matrix elements which are bilinear combinations of a special multiplet wave function. It is pointed out that several authors considered the elementary particles as compound ones. Attention is drawn to the fundamental units, the quarks which determine the overall symmetry of the particles. (TTT)

17487 ON THE TRANSFER THEORY IN NON-EQUILIBRIUM SYSTEMS OF CHARGED PARTICLES IN A STRONG MAGNETIC FIELD. Kalashnikov, V. P. (Inst. of Physics of Metals, Academy of Sciences, Sverdlovsk, USSR). Ukr. Fiz. Zh., 10: 1071-6(1965). (In Russian).

Expressions for charge and energy flows in a non-equilibrium system of charged particles of two types with pair interaction in a quantizing magnetic field are obtained. Kinetic coefficients are constructed for this system, associated with the effect of forces of a statistical nature (temperature gradient, electrochemical potential). (auth)

17488 GROUP THEORETICAL CLASSIFICATION OF TRANSITIONS. Bierter, W.; Simonius, M. (Univ. of Basel). Z. Phys., 191: 91-102(1966).

A formalism is developed and discussed using group theoretical methods, which allows a description of the degree of violation of a given symmetry property for arbitrary compact groups. (auth)

17489 POLARIZATION EFFECTS IN ELECTRON-ELECTRON AND POSITRON-ELECTRON SCATTERING. Holzwarth, Gottfried (Univ., Munich). Z. Phys., 191: 354-9(1966).

The polarization-asymmetries in the cross-sections for electron-electron and positron-electron scattering are investigated numerically in first order perturbation theory in the range from 1 kev to 10 Bev for all angles with regard to polarization-measurements. (auth)

17490 A NEW APPROACH TO POTENTIAL SCATTERING. PART I. FOUNDATION OF THEORY. Klar, H.; Krueger, H. (Univ. Freiburg i. B.). Z. Phys., 191: 409-16(1966).

An approximate integral-representation of the S-matrix in partial-wave expansion is derived for a scalar Schrödinger particle in a central field. The method consists of linearizing Calogero's Riccati equation for the interpolating S-matrix in such a way that the solution of the linearized equation deviates as little as possible from the exact one. The S-matrix thus obtained exhibits exact crossing-symmetry and uniform convergence independent of the coupling constant of the scattering potential. In the weak coupling limit it is especially shown that the method is more accurate than the second Born approximation. The S-matrix is applied to low and high energies. At low energies, a general integral for the scattering length is obtained and at large energies the summation over all angular momenta is carried out yielding an expression for the scattering amplitude. (auth)

17491 A NEW APPROACH TO POTENTIAL SCATTERING. PART II. APPLICATION TO SCATTERING AT LOW AND HIGH ENERGIES. Fluegge, S.; Klar, H.; Krueger, H. (Univ., Freiburg i. B.). Z. Phys., 191: 417-22(1966).

17492 SYMMETRY IN NONLINEAR THEORY OF THE SPINOR FIELD. Chepurnykh, G. K. (Moscow State Univ.). Zh. Eksp. Teor. Fiz., 49: 1779-80(Dec. 1965). (In Russian).

Some restrictions are suggested which remove arbitrariness in choosing the nonlinear term in nonlinear quantum spinor field theory. Quantization of the spinor field is based on invariance of the lagrangian with respect to strong (or Schwinger) space-time reflection (CPT theorem), with respect to strong (or Schwinger) time reversal and with respect to the C-transformation. (auth)

17493 EQUATION OF MOTION FOR A HALF S-MATRIX AND SOME CONSEQUENCES. Sukhanov, A. D. (Moscow Inst. of Radioelectronics and Mining Electromechanics). Zh. Eksp. Teor. Fiz., 49: 1812-23(Dec. 1965). (In Russian).

A formal equation of motion for a "half" S-matrix in quantum field theory is derived which satisfies the integrability condition. Expressions for the Heisenberg field operator and its derivative are obtained in renormalized theory of a scalar self-acting field and the Medvedev equations for Heisenberg "current-like" operators are solved. (auth)

17494 ELECTROMAGNETIC RADIATION EMITTED DURING PASSAGE OF A FAST CHARGED PARTICLE THROUGH A SEMICONDUCTOR. Kheifets, M. I. (Inst. of Physics and Tech., Academy of Sciences, Ukrainian SSR).

Zh. Eksp. Teor. Fiz., 49: 1927-33(Dec. 1965). (In Russian).

The features of emission of associated waves excited by a fast charged particle are investigated by taking into account space dispersion. It is shown that the Cherenkov radiation on transverse waves is distributed over the surface of two or three cones, the number of which depend on the sign of the effective exciton mass and parameters of the semiconductor. The direction of the Cherenkov radiation produced by the additional transverse wave emitted into vacuum depends on the sign of the transverse exciton effective mass. The radiation from the transverse waves can enter vacuum only if the effective mass of the longitudinal exciton is positive and the direction of the radiation coincides with that of the particle motion. Losses due to excitation of the additional waves are calculated. The particle velocity required for excitation of additional waves can be determined from a relation which is presented. It is shown that the width of the emission spectrum on transverse waves can be changed by varying the concentration of free carriers. The emission spectrum produced in vacuum by transverse waves consists of a number of narrow bands. The number and width of the bands depend on the parameters of the semiconductor. (auth)

17495 BOUND STATES OF A NONLOCAL SEPARABLE POTENTIAL. Rokhlenko, A. V. Zh. Eksp. Teor. Fiz., 50: 93-101(Jan. 1966). (In Russian).

A theory of bound states of a nonlocal separable potential is developed by employing the exact expression for the partial harmonics of the S matrix. It is shown that the number of bound states does not exceed the number of attractive terms in the potential function and that the energy levels are a monotonic function of the total coupling constant as well as of the partial coupling constants which characterize each interaction term. The number of bound states and the lowest energy level are estimated. (auth)

17496 DESCRIPTION OF TWO-PARTICLE SCATTERING BY MEANS OF A WHITEMAN-TYPE FUNCTIONAL. Vasilev, A. N. (Leningrad State Univ.). Zh. Eksp. Teor. Fiz., 50: 112-16(Jan. 1966). (In Russian).

Within the framework of the Whiteman axiomatics each physical theory realizes a representation of an algebra A, the elements of which are function chains of finite length $[g_0; g_1(x_1); \ldots; g_n(x_1 \ldots x_n); 0; 0; \ldots]$. A subalgebra $A^{(+)}$ of algebra A is considered which consists of elements of the form $[g_0; 0; g_2(x_1x_2); 0; g_4(x_1x_2x_3x_4); 0; \ldots]$ and one of the representations of the subalgebra is set up in explicit form. An interesting feature of the representation is that the Gilbert space corresponding to it contains only vacuum and two-particle asymptotic states and does not contain asymptotic states with a large number of particles. (auth)

17497 QUANTUM EFFECTS IN MULTIPLE SCATTERING. Kalashnikov, N. P.; Ryazanov, M. I. (Moscow Inst. of Engineering Physics). Zh. Eksp. Teor. Fiz., 50: 117-23(Jan. 1966). (In Russian).

A quantum distribution function is derived which describes multiple scattering of a beam of charged particles as a function of the deviation angle and transverse displacement of the particle. In the classical limit the formula is identical with the classical distribution function for multiple scattering obtained by Fermi. The possibility of recording quantum effects in multiple scattering depending on the properties of the measuring apparatus is investigated. (auth)

17498 INVARIANT PARAMETRIZATION OF THE PRODUCTS OF LOCAL OPERATORS. Cheskov, A. A. Zh. Eksp. Teor. Fiz., 50: 144-55(Jan. 1966). (In Russian).

An invariant parametrization of the matrix elements of the products of local operators with arbitrary spin or tensor dimension prescribed between states with one or several particles of arbitrary mass and spin is obtained. The case of polarizability of a scalar particle in an electromagnetic field is considered. (auth)

17499 ELECTROMAGNETIC PARTICLE PAIR PRODUCTION. Baier, V. N.; Fadin, V. S.; Khoze, V. A. (Novosibirsk State Univ.). Zh. Eksp. Teor. Fiz., 50: 156-68(Jan. 1966). (In Russian).

The electromagnetic pair production cross sections are considered by the method of invariant integration of tensors. The electromagnetic cross section for pair production due to interaction between a photon and charged particle is calculated, recoil and the contribution of dispersion diagrams being taken into account. The exact cross section for annihilation of a particle pair into two charged particle pairs is found. Integration of the fourth rank Compton tensor is carried out over final states of the fermion pairs. (auth)

17500 ON THE LAW OF CONSERVATION FOR FREE FIELDS. Goldman, I. I.; Tevikian, R. V. (Inst. of Physics, Erevan). Zh. Eksp. Teor. Fiz., 50: 199-201(Jan. 1966). (In Russian).

It is shown that free field equations retain their form in nonlocal transformations comprising a group. Correspondingly, all conservation laws for free fields can be generalized and result in conservation of the corresponding nonlocal quantities. (auth)

17501 POSSIBLE RADIATIVE DECAYS OF HEAVY MESONS INVOLVING VIOLATION OF CHARGE PARITY. Zakharov, V. I.; Kaidalov, A. B. Zh. Eksp. Teor. Fiz., 50: 283-5(Jan. 1966). (In Russian).

Radiative decays of f^0, B, A_1, and A_2 heavy mesons are considered in connection with the hypothesis of Bernstein, Feinberg, and Lee regarding the possible nonconservation of C-parity in hadron electromagnetic interactions. Observation of the decays $f^0 \to \pi^0\gamma$ and $A_2^0 \to \pi^0\gamma$, whose probabilities are estimated to be of the order of several percent of the probabilities of the decays due to strong interactions, would be a confirmation of the hypothesis of nonconservation of C-parity in electromagnetic interactions. Of particular interest is the measurement of the ratio of the probabilities of the decays $A_2^0 \to \pi^0\gamma$, $A_2^+ \to \pi^0\gamma$, $A_2^+ \to \pi^+\gamma$, which may serve as a measure of violation of C-invariance in electromagnetic interactions. (auth)

17502 EXCHANGE OF MASSIVE PARTICLES IN THE BETHE–SALPETER EQUATION [Thesis]. Rosner, Jonathan Lincoln. Princeton, N. J., Princeton Univ., 1965. 104p.

Some effects of letting the exchanged particles be massive in a simple Bethe-Salpeter equation were studied. An inhomogeneous linear integral equation is written for the absorptive part of the forward scattering amplitude in a $g\phi^3$ ladder graph model. The solution of this equation is assumed to behave as s^α when $s \to \infty$, where s is the square of the center-of-mass energy. A rigorous proof is given that α can be determined as a characteristic value of a homogeneous equation. Upper and lower bounds on α are obtained as a function of the coupling constant g and the mass μ of the exchanged particles (the rungs of the ladders). As $g \to \infty$, $\alpha/(g/4\pi\mu)^{1/2}$ approaches a constant lying between .858 and 2.01. The dependence of α on the ratio g/μ in the strong-coupling limit is discussed. This result is compared with a corresponding one in the model where the rungs of the ladders are massless. In both models the sides of the ladders have mass m. In the latter model, as $g \to \infty$, $\alpha/(g/4\pi m)$ approaches 1. Whereas the latter behavior corresponds to a general result in nonrelativistic potential scattering, the former does not. The dependence of α on μ in the weak-coupling limit is absent in order g^2. The g^4 term is a definite integral depending on μ. This integral is done in closed form for the special case $\mu = m$. In the small-μ limit, it contains a term proportional to $(\mu^2/m^2)\log(\mu^2/m^2)$, and hence is not analytic at $\mu = 0$. The $g\phi^3$ ladder graph model is compared with a similar model in $\lambda\phi^4$ theory. In the latter model the high energy behavior of the forward scattering amplitude is independent of whether or not the internal particles are massive. (Dissertation Abstr.)

17503 SOME INVESTIGATIONS INTO THE PERATIZATION OF THE SCALAR PARTICLE-GRAVITON INTERACTION [Thesis]. Safko, John Loren. Chapel Hill, N. C., Univ. of North Carolina, 1965. 79p.

The approximation to the interaction of two scalar particles exchanging gravitons by the sum of uncrossed ladder diagrams, known as peratization, has been calculated elsewhere without regulating the divergent diagrams. The same calculation is performed here with regulation, and it is concluded that other researchers using regulators and peratization for the study of weak interactions have taken a wrong contour in the evaluation of the integrals involved. Corrections to peratization due to the non-zero mass of the scalar particles and corrections due to the net four-momentum of the system are discussed. The previously approximated self-energy calculation is discussed and the exact solution is shown to involve an integral that could not be evaluated. Vacuum polarization is investigated by peratization techniques to see if gravity serves as a regulator; however, the complexity of the problem prevented any rigorous conclusions. The single-rung diagram for two spinors exchanging a graviton was calculated and the total interaction was found not to be amenable to peratization. (Dissertation Abstr.)

17504 THE EFFECT OF VECTOR MESONS ON LEPTON PRODUCTION BY THE SCATTERING OF MUON NEUTRINOS AND PROTONS [Thesis]. Dooher, John Patrick. Hoboken, N. J., Stevens Inst. of Tech., 1965. 148p.

The total cross section for the process: $\nu + p \rightarrow \nu + p + \mu^+ + \mu^-$ is calculated using a Weizsäcker-Williams approximation with some added correction terms, while assuming the existence of an intermediate vector meson with a mass of 1.06 Bev. The calculation is done for incoming neutrino laboratory energies greater than 5 Bev. The vector meson is assumed to have an anomalous magnetic moment. The most recent data on high energy proton form factors are used. It is shown that the cross section is at least 10,000 times as large as the cross section for the same process calculated with the four-fermion theory. This calculation serves as a test for the existence of intermediate vector mesons. This calculation also serves as a test for the validity of the Weizsäcker-Williams approximation. It is shown that correction terms to the Weizsäcker-Williams approximation are as large as forty percent of the total cross section. These terms would be small if vector mesons did not exist. The final result is that the cross section varies from a value of 10^{-38} cm^2 approximately, for an incoming neutrino laboratory energy of 5 Bev, to an approximate value of 10^{-37} cm^2 for an incoming neutrino laboratory energy of 20 Bev. The value of the cross section between these two energy values is very close to a linear function of the energy. The results depend on the values of the anomalous magnetic moment of the vector meson K. It is shown that the value of the cross section is nearly fifteen per cent greater for K = 1 than for K = 0. It is thirty per cent greater for K = 1 than for K = –1. Finally, it is pointed out that the cross section for the process $\nu + p \rightarrow \nu + \mu^- + e^+ + p$ is exactly the same as that of the process $\nu + p \rightarrow \nu + \mu^- + \mu^+ + p$ within the range of the validity of the approximation used in this calculation. This is not the case if the four-fermion theory is used to calculate the cross sections. (Dissertation Abstr.)

17505 TRANSVERSE WAVES IN ACCELERATED PARALLEL-FLOW ELECTRON BEAMS WITH CONSTANT MAGNETIC FIELD [Thesis]. Hoeks, Bas. Stanford, Calif., Stanford Univ., 1965. 118p.

The small-perturbed electron motions in an accelerated (space-charge limited) circular cylindrical electron beam in a parallel-flow Pierce-type electron gun were studied. A three-dimensional analysis is restricted to a filamentary beam, in which the electrons interact with the fields due to surface charges only. The resulting second-order differential equation, which describes a purely transverse wave interaction phenomenon, is then solved approximately in terms of first-order WKB solutions and asymptotic series, the WKB form having the advantage of being a fairly good normal mode representation. From the WKB solutions the transformation properties of the accelerated region are established and, by assuming that the electron gun exit terminates into a drifting region, the noise behavior is investigated. Defining the noise fluctuations at the electron gun exit in terms of electric field intensities and those near the cathode in terms of initial displacements and velocities, it is found that (a) for a given beam length the noise fluctuations at the gun exit decrease as the axially applied d-c magnetic field increases, and (b) that for a given value of the axial d-c magnetic field these fluctuations decrease as the beam length increases. (Dissertation Abstr.)

17506 TRANSLATIONS OF THE DISCRETE BOSE–EINSTEIN OPERATORS [Thesis]. Shelupsky, David Irwin. Princeton, N. J., Princeton Univ., 1965. 78p.

The action of the operator translations $a_k \rightarrow a_k + c_k$, $k = 1,2,3, \ldots$, on the members of a certain family of unitarily inequivalent representations of the canonical commutation relations are investigated, the representations being the discrete representations of Garding and Wightman, the c_k, $k = 1,2, \ldots$, a sequence of complex scalar operators. In particular the possibility is considered that these transformations leave invariant the various discrete representations or transform them into each other. The transformation groups leaving invariant the various representations are determined, they are given metricizable topologies in which they are isometrically isomorphic as topological groups to each other, and it is shown that with these topologies the mappings relating them to unitary operators that realize them as unitary similarities on the representations are strongly continuous. A chief result is that the transformations indicated never transform any discrete representation into any other. (Dissertation Abstr.)

17507 ELECTROMAGNETIC MASS DIFFERENCES OF BARYONS, MESONS AND $\frac{3}{2}^+$ RESONANCES [Thesis]. Wojtaszek, Joseph Henry. Rochester, N. Y.; Univ. of Rochester, 1965. 120p.

A theoretical evaluation of the electromagnetic mass differences of the baryons, pseudoscalar mesons, and spin $\frac{3}{2}^+$ resonances is undertaken. The results of previous theoretical ideas are first presented, along with the relations between the mass differences predicted by the groups SU(2), SU(3), and SU(6). Then a dynamical method based on the propagator expansion is proposed, and the contributing processes are derived. When these contributions are evaluated, reasonable agreement with the experimental results can be obtained for the baryons and mesons. In order to obtain this agreement for the K meson, it is found necessary to evaluate the 3-pion contribution to the isoscalar kaon form factor. Also, a resonant model calculation is done for the K + 2π intermediate states in the kaon propagator. The small value observed for the mass difference between the pion-nucleon (3,3) resonances is seen to have a satisfactory explanation, but the other resonance mass differences cannot be explained. Computations were carried out with the IBM 7074 computer. (Dissertation Abstr.)

Fluid Physics and Thermodynamics

See also Plasma Physics and Thermonuclear Processes

Refer also to abstracts 17613 and 17647.

17508 (ARL–65-246) EXPERIMENTAL DETERMINATION OF ION EXCITATION ENERGIES AND DENSITIES IN A LOW PRESSURE DISCHARGE. Corwin, Richard R. (Systems Research Labs., Inc., Dayton, Ohio). Dec. 1965. Contract AF33(615)-1798. 37p. CFSTI $2.00 cy, $0.50 mn.

An experiment is described for measuring the relative population densities of the energy levels of a neon plasma using a "tuneable" helium-neon laser. Absorption measurements of the laser irradiation upon a neon plasma are made. A phase sensitive "lock-in" amplifier is used as a detector, which measures only the absorption of incident laser radiation and thus eliminates erroneous measurement of background light. Two specially constructed plasma diagnostic instruments are described.

The first instrument measures the second derivative of Langmuir probe current with respect to probe voltage, and thus is a measure of the electron velocity distribution in a plasma. This instrument employs a phase sensitive detector which is a theoretically optimum technique for detecting small signals in the presence of noise. The second instrument is a simple logarithmic amplifier which displays, on an oscilloscope, the logarithm of the Langmuir probe current. The slope of the resulting oscilloscope trace is a measure of the electron temperature of the plasma. (auth)

17509 (D-1-82-0469) FIELD-ALIGNED FLOW OF A CONDUCTING FLUID PAST A SOURCE OF MAGNETISM. Winter, D. F. (Boeing Scientific Research Labs., Seattle, Wash. Geo-Astrophysics Lab.); Gerwin, R. A. (Boeing Scientific Research Labs., Seattle, Wash. Plasma Physics Lab.). Oct. 1965. 33p.

A prescribed source of magnetism moves at constant speed through a viscous conducting incompressible fluid with an aligned uniform magnetic field. The velocity and magnetic fields induced at a distance from the source are calculated. The induced fields are also calculated for the case in which the applied field is absent. Although no special symmetry or alignment is assumed, the source is "ideal" in the sense that enclosures (wires or magnets) are infinitesimal in at least two dimensions. Dynamical interactions will occur in a viscous fluid and their effect in the far field is estimated. An estimate is also made of the rate at which energy is dissipated as a consequence of viscous interactions and ohmic heating throughout the fluid, outside the immediate vicinity of the source. (auth)

17510 (IPP-3/25) MICROWAVE INTERFEROMETER MEASUREMENTS OF THE ELECTRON DENSITY DISTRIBUTION BEHIND SHOCK FRONTS AND DISCHARGE PLASMAS. Makios, W. (Institut fuer Plasmaphysik, G.m.b.H., Garching (West Germany)). Dec. 1965. 22p. (CONF-650806-21). Dep. mn.

From 7th International Conference on Phenomena in Ionized Gases, Belgrade.

Previously, various investigators have shown, that in electromagnetically driven shock waves the luminous front is generated from parts of the discharge plasma, in front of which the shock front is propagating. In order to measure the electron density distribution behind the shock front, microwave transmission interferometric measurements were made. The space resolution achieved with horn antennas and focusing lenses was unsatisfactory, because the distance between the shock front and the discharge plasma is of the order of a few wavelengths. With the use of Lecher wires instead of horn antennas, a space resolution of about half a wavelength was obtained. (auth)

17511 (NP-15894) NORMAL IONIZING SHOCK WAVES [Thesis]. Report No. 23. Taussig, Robert T. (Columbia Univ., New York. Plasma Lab.). 1965. Contract AF49(638)-1254. 175p.

Solutions to the steady state jump equations are obtained for a normal ionizing shock wave moving into a nonconducting, stationary gas in an electromagnetic field. The properties of ionizing shock waves common to pure MHD and to ordinary gas shocks are discussed. Some completely novel effects are produced by the upstream electromagnetic field. The shock velocities are bounded for a given upstream electric field strength where the electric field is assumed to lie parallel to the shock plane. For electric fields larger than a critical value, E_c, no steady, compressive shocks exist, and for nonzero electric fields a downstream transverse magnetic field is "switched on" for all shock solutions. Solutions analogous to detonation-deflagration waves were found which meet the Chapman-Jouguet condition. Coupling between electromagnetic and dissociation-ionization effects across the shock is analyzed. Numerical solutions are presented for several electric field strengths in molecular hydrogen using accurate thermodynamic properties and assuming that the gas upstream and downstream from the shock is in chemical equilibrium. The steady state problem of a current-driven shock wave is solved in the context of an electromagnetic annular shock tube. The results agree well with experimental evidence. Evolutionary normal ionizing shock wave solutions are selected and their stability determined in perfect fluid. A theory of shock wave stability in a fully dissipative fluid, based on recent work in magnetohydrodynamics, is outlined. Several illustrative examples are treated along with possible applications of this theory to ionizing shock waves. (auth)

17512 RAYLEIGH'S PROBLEM IN MAGNETOGASDYNAMICS WITH HALL EFFECT. Lu, Pau-Chang (Case Inst. of Tech., Cleveland). AIAA (Amer. Inst. Aeron. Astronaut.) J., 3: 2219-24(Dec. 1965).

The boundary-layer solutions for large times of the velocity and temperature distributions in a gas, induced by the impulsive motion of an infinite flat plate in its own plane, are obtained by using the Kármán-Pohlhausen technique. The gas is assumed to be thermally ionized through a combination of dissipative effects and heat supplied at the plate. The following two examples are given for seeded argon at about 2500°K: (1) with Hall effect (strong magnetic field) and (2) without. (auth)

17513 ACCELERATION OF MAGNETOGASDYNAMIC SOURCE FLOW THROUGH THE SONIC VELOCITY. Hains, F. D. (Boeing Scientific Research Lab., Seattle). AIAA (Amer. Inst. Aeron. Astronaut.) J., 4: 158-60(Jan. 1966).

A two-dimensional magnetogasdynamic source flow, which corresponds to the inviscid flow between plane divergent walls is described. (B.G.D.)

17514 PREDICTION OF MODE TRANSITION IN AN ARC WITH A TRANSPIRATION COOLED ANODE. Cremers, Clifford J.; Birkebak, Richard C. (Georgia Inst. of Tech., Atlanta). AIAA (Amer. Inst. Aeron. Astronaut.) J., 4: 167-9(Jan. 1966).

An attempt to find a parameter to predict mode transition in an arc with a transpiration cooled anode is described. It is found that grouping variables with the dimensions of (1/time) predicted transitions quite well. The parameter is $\mu_0 I^2/4\pi D\dot{m}$, where μ_0 is the permeability of free space, I is the arc current and $\dot{m}$ is the transpirant mass flow; D is the diameter of the cathode jet near the anode which is measured by estimating the size of the anode attachment spot after transition to the mode of lower blowing rate. (B.G.D.)

17515 GENERAL STUDY OF PLANE STEADY FLOWS IN NONEQUILIBRIUM MAGNETOGASDYNAMICS. Bhutani, O. P. (Indian Inst. of Tech., Kharagpur, India). AIAA (Amer. Inst. Aeron. Astronaut.) J., 4: 367-8(Feb. 1966).

A study of small perturbation plane steady flows of infinitely electrically conductive gas that departs from equilibrium and is subjected to an aligned magnetic field is described. Clarification of the role of magnetic and nonequilibrium flow parameters are presented. (B.G.D.)

17516 MAGNETOHYDRODYNAMIC NATURAL CONVECTION IN A CYLINDER. Dunwoody, N. T. (Queen's Univ. of Belfast). AIAA (Amer. Inst. Aeron. Astronaut.) J., 4: 368-9(Feb. 1966).

The effect of a transverse magnetic field on steady, laminar, fully developed natural convection in a vertical cylinder previously considered by Cramer (J. Aerospace Sci. 28: 736(1961)) is evaluated. (B.G.D.)

17517 PHENOMENAS ON ARC-CATHODES IN FLOWING GASES AT LOW PRESSURES. Huegel, Helmut (DVL-Inst. fuer Plasmadynamik, Stuttgart). Astronaut. Acta, 11: 247-51(July-Aug. 1965). (In German).

With arc-heating of flowing gases at low pressures (less than 100 mm Hg) large areas of the cathode are observed to be covered with a fluttering discharge immediately after ignition. Simultaneously, the cathode is losing material. After a short interval the mode of discharge changes suddenly to a stable spotless arc. Moving pictures with up to 5500 frames per second indicate that these phenomena represent different arc types depending on the temperature of the cathode. As long as the cathode is relatively cold the discharge is maintained by several unstable arcs with spots. With the cathode temperature sufficiently high the change takes place to a now stable arc type with a diffuse base.

Preheating the cathode causes an earlier change in discharge mode and thus decreases the loss of electrode material. An attempt is undertaken to give an interpretation of the observed phenomena by means of the "Kontraktionstheorie". According to the character of current transport in the immediate vicinity of the cathode different arc modes are to be expected. In cases of insufficient electron emission by the cathode, where the ion current fraction has a considerable value, a contraction of the arc (spot) is an absolute physical necessity. If however the electron current produced by the emission process is sufficiently high a spotless arc will result. An interpretation of the observed arc motion seems more problematic because of the rather complex aerodynamic, electric and electromagnetic processes involved. (auth)

17518 SPACE-CHARGE CONTROLLED IONIZATION GROWTH IN HYDROGEN. Morgan, C. G.; Evans, C. J.; Williams, W. T.; Davies, A. J. (University Coll., Swansea, Wales). Brit. J. Appl. Phys., 16: 1797-1803(Dec. 1965).

Measurements of the spatio-temporal growth of currents in hydrogen at low pressure p_0 (<15 torr) between plane parallel gold electrodes under the influence of low overvoltage impulses were analyzed by an accurate finite difference method. The growth of the discharge currents was followed from its initial small value ($\leq 10^{-9}$ A) in a uniform electric field to its glow discharge value ($\sim 10^{-4}$ A) in a space-charge distorted field. Estimates of the area of cross section of the discharge channel were made. (auth)

17519 PLASMA OF COMBUSTION PRODUCTS OF $C_2H_2 + O_2$. PART II. CALCULATION OF TRANSPORT COEFFICIENTS. Grycz, Bronislav. Cesk. Cas. Fys., 16: 34-59(1966). (In Czech).

The basic theoretical conceptions necessary for calculating the transport coefficients of the plasma of combustion products are reviewed on the basis of approximate formulas from the kinetic theory of gaseous mixtures. The calculation is performed for the plasma of combustion products of the mixture of $C_2H_2 + \frac{5}{2}\alpha O_2$ with the addition of potassium. The temperature range is $2000 \leqq T \leqq 3000°K$, the pressure p = 1 atm., the coefficient of oxygen deficiency $\alpha = 0.8$, and the partial pressure of the potassium $\epsilon = 10^{-2}$, 10^{-4} atm. (auth)

17520 THE GROWTH OF PRE-BREAKDOWN CURRENT IN HELIUM. Lucas, J. (Univ. of Liverpool). Int. J. Electron., 19: 439-51(Nov. 1965).

The growth of pre-breakdown current across a uniform electric field discharge gap of finite dimensions was calculated for helium. The current was assumed to be amplified by electron ionization and by the production of secondary electrons at the cathode by positive ions, metastable atoms, and non-resonance radiation; allowance was made for the loss of secondary current out of the discharge gap. It was shown that experimental measurements of the pre-breakdown current obtained for the range $3 < E/p < 40$ v cm^{-1} $torr^{-1}$ can not be analyzed to give the electron ionization coefficient (α) without the help of subsidiary experiments to measure the relative abundance and secondary coefficients for the processes producing the secondary electrons. The analysis of these currents by the Townsend equations was shown to give incorrect values of α, especially at the low E/p values where α_T may be several times larger than α. (auth)

17521 AXI-SYMMETRIC LINEAR MAGNETOGASDYNAMIC FLOW WITH A HALL EFFECT IN A TWO-COMPONENT MAGNETIC FIELD. Bertinov, A. I.; But, D. A.; Gorbatkov, S. A. Izv. Akad. Nauk SSSR, Energ. Transp., No. 6, 102-10(1965). (In Russian).

The linear axial symmetrical flow of ideal non-compressible electroconducting gases with the Hall effect in a 2-component magnetic field was shown for continuous and sectioned coaxial electrodes with which the electric force, produced by the Faraday and Hall effects, was reduced. The parameters of the gas and magnetic field were calculated. Final analytical relations were deduced that made it possible to characterize the basic electrodynamic and energetic characteristics of the flow and to obtain the optimization of the output power at different parameters. It was shown that according to the specific electrical output the flow considered yields different types of magnetogasodynamic flows in transverse magnetic fields with separation of energy. However, the absence of insulation in the channel and the possibility of the utilization of compact superconducting magnet systems were discussed. (tr-auth)

17522 TERMINAL PROPERTIES OF ALFVEN WAVE GUIDES. Kliman, G. B.; Rink, R. E. (Massachusetts Inst. of Tech., Cambridge). J. Appl. Phys., 37: 635-8 (Feb. 1966).

Attention is focused on the terminal properties of Alfvén waveguides. The electric input impedance at the terminals of a set of coaxial excitor electrodes is derived. This result is then used to investigate the behavior of a lossy Alfvén wave resonator and the conditions under which the waveguide may be matched by a lumped, active load. Matching with a lossy reactive sheet is also discussed. The discussion is limited to the case of axisymmetric, transverse magnetic field modes since these are of the greatest experimental interest. (auth)

17523 QUANTITATIVE MEASUREMENTS OF THE OPTICAL EMISSION FROM DENSE THETA-PINCH DISCHARGES. Feldman, J. M. (Carnegie Inst. of Tech., Pittsburgh). J. Appl. Phys., 37: 674-81(Feb. 1966).

Measurements of the optical emission of a high luminosity theta-pinch discharge are reported for seven gases over the interval 0.2 to 0.7 μ. The irradiance is typically 0.4 J/100 Å at 450-J input energy. The efficiency is typically 5% to 10%, and the optical pulse duration is approximately 5 μsec. The dependence of the optical output power on bottle material, coupling parameters and input power is discussed. (auth)

17524 PROPAGATION OF A GLOW DISCHARGE INTO THE ANNULAR GAP BETWEEN THE DISCHARGE TUBE WALL AND THE CATHODE. Veron, Harry; Wainfan, Nathan (Polytechnic Inst. of Brooklyn). J. Appl. Phys., 37: 836-41(Feb. 1966).

Time-resolved spectroscopic measurements and electrostatic probe measurements were used to study that part of a high-voltage pulsed glow discharge in hydrogen that propagated into the annular gap between the cathode and the pyrex discharge tube wall. The spectroscopic and probe measurements revealed that a luminous front and a potential wave started to propagate into the annular gap at the same time as the electric field in the cathode fall region at the face of the cathode reached its maximum value. The dependence of the propagation velocity on the discharge parameters is presented and the importance of the secondary emission at the wall of the discharge tube is established as a factor in the propagation of the discharge. (auth)

17525 STEADY MAGNETOGASDYNAMIC FLOW PAST A SOURCE. Crapper, G. D. (Univ. of Leeds, Eng.). J. Inst. Math. Appl., 1: 241-57(Sept. 1965).

An asymptotic solution is presented for the disturbance at large distance from a source placed in a flow of conducting compressible fluid in the presence of an applied magnetic field. The solution is obtained by a Fourier transform method using techniques developed for magnetohydrodynamic waves by Lighthill. The results are discussed in detail for the cases of the undisturbed flow aligned with and perpendicular to the field, although they apply for any angle between the two cases, and show a Mach-cone type of disturbance together with Alfvén waves. (auth)

17526 GROUND-STATE ENERGY OF THE CHARGED BOSE GAS. Wright, Donald (Univ. of Oregon, Eugene). Phys. Rev., 143: 91-5(Mar. 4, 1966).

The ground-state energy of the charged Bose gas at high densities is determined by the method of Green's functions. The pair hamiltonian of Girardeau and Arnowitt is used to calculate the Green's functions. The leading

terms in the high-density expansion are found to agree exactly with those determined by Girardeau using a variational method. (auth)

17527 NEW SERIES EXPANSION IN STATISTICAL MECHANICS. Alexanian, Moorad; Wortman, D. E. (Univ. of California, Livermore). Phys. Rev., 143: 96-103 (Mar. 4, 1966). (UCRL-14325).

A new approximation scheme is applied to thermodynamic variables which have power-series expansions in terms of real parameters. This method is based upon a previously discussed formula designed to overcome the convergence difficulties of the quantum-mechanical Born (perturbation) series. Some properties of the approximation scheme are obtained, and then the method is used to obtain information from power-series expansions such as those met with in thermodynamics and statistical mechanics. In particular, the virial coefficients for several molecular models are used to obtain numerical approximations to the equations of state. The solution for a one-dimensional system of hard rods is obtained exactly in this scheme. For the two-dimensional hard-square lattice gas, the results agree quite well with recent low- and high-density Padé approximants. The qualitative behavior of the solution for a system of hard spheres resembles that of the Mayer theory of condensation. It is noteworthy that the approximation scheme has the property of generating solutions which are monotonically increasing in the density. Thus, no van der Waals loop is obtained. (auth)

17528 FINITE-TEMPERATURE TRANSPORT PROPERTIES OF NORMAL FERMI SYSTEMS. III. DISSIPATIVE EFFECTS IN A SIMPLE PERTURBATIVE MODEL. Watabe, M.; Dagonnier, R. (Univ. Libre, Brussels). Phys. Rev., 143: 110-21(Mar. 4, 1966).

By using the general transport theory of a normal many-fermion system recently developed by Résibois, the collision term is calculated up to fourth order in a coupling parameter. It is shown that the higher order terms can be arranged into the form of the quasiparticle collision term suggested by Landau in the Fermi-liquid theory, except for the transformation operator introduced by Résibois to connect the particle description to the quasiparticle one. We also analyze the three-body collision operator in transport theory from the same quasiparticle point of view to the lowest nontrivial order in the coupling constant. It is shown that the anomalous terms in this operator contain the renormalization effects on the usual two-body collision operator. (auth)

17529 SECOND-ORDER DIFFUSION OF ELECTRONS IN IONIZED GASES. Sodha, M. S.; Srivastava, H. K. (Indian Inst. of Tech., New Delhi, India). Proc. Phys. Soc. (London), 87: 803-8(Mar. 1966).

A solution of Boltzmann's transfer equation was obtained for electrons in an ionized gas in the presence of a non-uniform electron concentration gradient; an explicit expression for f_0 (the isotropic part of the distribution function of electron velocities), correct to terms involving the first power of the second derivative of electron concentration, was obtained. This solution was used to obtain expressions for higher-order electric and thermal current densities in the gas due to the existence of the second derivative of electron concentration. This effect is important when the electron mobility is high (e.g., gases at low pressures) and is negligible in the case of semiconductors. (auth)

17530 CALCULATION OF THE FREE ENERGY ON THE BASIS OF REPRESENTATION OF INTERACTION IN COLLECTIVE VARIABLES. Blazhievskii, L. F. (Lvov State Univ.). Ukr. Fiz. Zh., 10: 1299-1308(Dec. 1965). (In Ukrainian).

To calculate the free energy of an electron gas in the compensating field the representation of interactions by collective variables was used. The spectrum of collective variables is limited by some maximum wave vector k_0. An equation is presented for the free energy in the region of high temperatures. The value k_0 was selected from the conditions of finiteness of potentials. After integration and allowance for group integrals the free energy was represented in the form of an expansion in the parameter $\sqrt{\varkappa\lambda}$ ($\varkappa$ is the Debye radius, λ is the de Broglie wavelength of thermal motion) or in $n^{1/4}$ (n is the density): $F - F_{id} = An^{3/4} + Bn^{5/4} + Cn^2 + Dn^{5/4} + Gn^2 \ln n$. The coefficients of the expansion were calculated. The first term coincided with the known result of Debye-Hückel. (auth)

17531 BREAKDOWN AND HEATING OF GAS BY A LASER BEAM. Raizer, Yu. P. Usp. Fiz. Nauk, 87: 29-64(1965). (In Russian).

A review is made of the heating and breakdown of gases by a focused laser beam. The review considers the breakdown effect, i.e., the formation of ionization in the focal region and formation of the primary plasma, the absorption of the laser beam by the plasma, heating of the gas, and effects observed after the passage of the laser beam. An experimental investigation of the effect of a giant pulse on solid targets and an evaluation of the possibility of heating hydrogen gas to the temperatures required for thermonuclear reaction are discussed. Summaries of the experimental data, followed by a theoretical treatment of the mechanism responsible for the effect are given. The discussion on "the breakdown of gases" includes measurement of the threshold parameters; multiphoton effect; avalanche ionization (qualitative treatment); increase in the electron energy in the field of radiation; and calculation of the avalanche ionization. "Absorption of the beam and heating of the gas," consists of measurement of absorption and scattering of the laser beam and heating of the gas in the breakdown region; light absorption and gas heating waves; breakdown and radiation mechanisms; the spark as a strong explosion; the spark in a magnetic field; generation of plasma by a solid target; and conditions required for a high degree of heating of hydrogen. (ATD)

17532 PLANE GASDYNAMIC FLOWS WITH ORTHOGONAL MAGNETIC AND VELOCITY FIELD DISTRIBUTIONS. Power, Geoffrey (Univ. of Nottingham, Eng.); Walker, Dennis. Z. Angew. Math. Phys., 16: 803-17 (1965).

The two dimensional permanent magnetohydrodynamic flow properties of an elastic, non-viscous, non heat-conducting fluid having an infinite conductivity was considered when the magnetic fields and velocity are orthogonal. It is shown that such a flow can be effectively connected to a four-parameter class of compressible flow of a non-conductor fluid. By emitting an approximate state equation, it is shown moreover that these magnetohydrodynamic flows can be compared to irrotational flows of incompressible and non-conductor fluids on the conditions that the velocity variations are limited. As an example the theory is applied to a flow in a channel. (tr-auth)

17533 ON NONLINEAR THEORY OF BEAM INSTABILITY UNDER CONDITIONS OF THE ANOMALOUS DOPPLER EFFECT. Krasovitskii, V. B.; Kurilko, V. I. (Inst. of Physics and Tech., Academy of Sciences, Ukrainian SSR). Zh. Eksp. Teor. Fiz., 49: 1831-5(Dec. 1965). (In Russian).

The nonlinear problem of excitation of one-dimensional transverse waves by an electron beam moving in a moderating medium with a velocity greater than the phase velocity of the wave is considered in the hydrodynamical approximation. Solutions which are waves with a fixed wave number and time varying amplitude and phase are analyzed. It is shown that in the case of small beam densities the main nonlinear effect restricting increase of the oscillation amplitude is violation of synchronism between the particles and field as a result of slowing down of the beam; this results in an alternation of excitation and absorption of the field by the beam. The maximal oscillation amplitudes are calculated. The possibility of using this effect for removal of beam instabilities by an external field is discussed. (auth)

17534 ANALYTICAL INVESTIGATION OF MAGNETOHYDRODYNAMIC BOUNDARY LAYERS WITH HALL EFFECTS [Thesis]. Pfannebecker, George William. Columbus, Ohio, Ohio State Univ., 1965. 232p.

A laminar, incompressible MHD boundary layer on an electrically insulated semi-infinite flat plate in the presence of applied electromagnetic fields was studied, and the influence of Hall effects on the flow field was considered. Hall effects tend to induce a transverse cross flow, thereby rendering the boundary layer three-dimensional. The governing three-dimensional boundary equations are solved by means of a Blasius power series expansion in the local interaction parameter. Functional coefficients for the series are obtained by the numerical solution of the resulting ordinary differential equations on an IBM 7090 computer. Velocity profiles are presented for selected values of the Hall current parameter, ion slip factor, and electrical loading parameters. Solutions of the energy equation are obtained to establish the temperature distribution in the boundary layer assuming a constant wall temperature. Estimates of wall shearing stress and Nusselt number are presented. It is concluded that the behavior of the MHD boundary layer is quite complex. Reversals in the direction of electric current occurred as a result of applied electric fields. Hall currents are found to induce an appreciable transverse cross flow. In the absence of applied electric fields, the reduction in viscous drag and heat transfer obtained from increasing magnetic field strengths is diminished by Hall effects. Applied electric fields for the generator mode of operation result in an increase in wall shearing stress with increasing magnetic field intensity. Hall currents attenuate this rise in wall friction. Heat transfer is found to be rather insensitive to the magnetic field strength and Hall current for the particular loading parameter considered. Segmenting the electrodes causes a reduction in both wall friction and heat transfer. (Dissertation Abstr.)

17535 THE THERMAL STABILITY OF COMPLETELY CONFINED FLUIDS INCLUDING MAGNETOHYDRODYNAMIC EFFECTS [Thesis]. Sherman, Michael. Cleveland, Case Inst. of Tech., 1965. 288p.

The determination of the conditions needed to induce a state of convective motion in a fluid where a constant temperature gradient is directed parallel to a body force is considered. The fluid is contained in a rather arbitrary region bounded by rigid walls. The principle of exchange of stability is established for arbitrary regions with a generalized thermal boundary condition on the bounding walls. The thermal stability problem is reduced to an eigenvalue problem for the critical Rayleigh number (the stability criterion) and then is reformulated as a variational principle. A method is developed for estimating upper and lower bounds to the critical Rayleigh number for regions in which the critical Rayleigh number cannot be calculated exactly. An extension of the thermal stability problem to include magnetohydrodynamic effects is presented. Here the fluid and the bounding walls are electrical conductors. A constant magnetic field is applied to the configuration. The critical Rayleigh number is a function of an additional parameter, the Hartmann number (ratio of magnetic forces to viscous forces). The procedures previously established for estimating upper and lower bounds to the critical Rayleigh number in the nonmagnetic theory are reformulated for this magnetohydrodynamic problem. (Dissertation Abstr.)

17536 BOUNDARY LAYER THERMODYNAMIC AND HYDRODYNAMIC CHARACTERISTICS OF A FLOWING LIQUID HYDROGEN TANK, WITH AND WITHOUT INTERNAL HEAT GENERATION [Thesis]. Boudreaux, Rodney Ayes. Cincinnati, Univ. of Cincinnati, 1965. 163p.

The turbulent boundary layer within a liquid hydrogen tank of a nuclear rocket stage is considered. Due to wall heat transfer and internal heat generation, an upward convection current emerges. As the tank drains, the acceleration of the fluid in a tapered lower tank predominates the boundary layer characteristics and the downward boundary layer flow attaches to the wall. A method is developed which provides the tradeoff relationships between shield, structure and propellant heating effects based on energy balance. Potential flow and boiling systems were considered for tanks having an arbitrary aft or lower bulkhead shape. The results are incorporated into a nomograph for preliminary design purposes. The position of the attachment of the downward flowing boundary layer to the tank wall is determined by a force balance on a boundary layer volume element. Tank lower contours were systematized through the consideration of source-sink flow. A simple method of determining the equivalent sink strength for actual drain rates and geometry is presented in analytic and graphical form. A set of velocity and temperature profiles was developed for flow at, above, and below the attachment point. Based on these velocity and temperature profiles, universal distribution functions and constants independent of conditions at the edge of the boundary layer and geometry were generated for utilization in the momentum and energy equations. The momentum and energy equations were formulated for computer solution and include draining tank conditions above the point of attachment of the downward boundary layer and static tank (no drainage) comparisons. The analyses were programmed on the IBM 7094 digital computer as separate cases, counterflow and static. (A.G.W.)

Geophysics

Refer also to abstracts 16694, 17232, and 17246.

17537 (JPLAI/LS-541) INTERACTIONS OF SPACECRAFT AND OTHER MOVING BODIES WITH NATURAL PLASMAS. Sterkin, Carol K. (comp.) (Jet Propulsion Lab., Calif. Inst. of Tech., Pasadena). Dec. 1965. Contract NAS-7-100. 182p.

References (829) with abstracts are included for literature on the interactions of moving bodies with ionized media and on ionospheric physics. (D.C.W.)

17538 (N-65-17609) THE MORPHOLOGY OF THE OUTER ZONE ELECTRON DISTRIBUTION AT LOW ALTITUDES FROM JANUARY THROUGH JULY AND SEPTEMBER, 1963 FROM INJUN III. Armstrong, T. (State Univ. of Iowa, Iowa City. Dept. of Physics and Astronomy). [1964]. 86p. (NASA-CR-60905; SUI-64-40). CFSTI $3.00 cy, $0.75 mn.

An intensive study was made of data obtained from the Injun III satellite. Median latitude profiles of the electron population of the low-altitude region of the outer zone for energies $E_e \gtrsim 40$ kev, $E_e \gtrsim 230$ kev, and $E_e \gtrsim 1.6$ Mev were derived. (STAR)

17539 (N-65-18257) TIME VARYING SOLAR CYCLE PROTONS PROGRAM MANUAL. Devaney, R. A.; Blanchard, R. C.; Andary, J. (National Aeronautics and Space Administration, Greenbelt, Md. Goddard Space Flight Center). Oct. 1964. 215p. (NASA-TM-X-55134; X-642-64-278). CFSTI $6.00 cy, $1.25 mn.

A set of programs for the calculation of the variation of the proton population in the earth's radiation belt with the solar cycle is described. (D.C.W.)

17540 (N-65-18914) AN AVERAGE ATMOSPHERE FOR PARTICLES TRAPPED IN THE EARTH'S MAGNETIC FIELD. Hassitt, A. (California Univ., La Jolla, San Diego. Dept. of Physics). Oct. 20, 1964. 23p. (NASA-CR-57165). CFSTI $1.00 cy, $0.50 mn.

Particles trapped in the earth's magnetic field follow orbits which vary over all longitudes and over wide ranges of latitude and altitude. An efficient method of averaging any spatially dependent function over these orbits is described. A Fortran program which computes average atmospheres, using an Anderson and Francis atmosphere and the Jensen and Cain 48-term representation of the earth's magnetic field, is described. This program has been run on the CDC 3600 and IBM 7090 computers. (STAR)

17541 (N-65-19719) EVIDENCE FOR RAPID MOTION OF THE OUTER BOUNDARY OF THE MAGNETOSPHERE. Konradi, Andrei; Kaufmann, Richard L. (National Aeronautics and Space Administration, Greenbelt, Md. Goddard Space Flight Center). Oct. 1964. 24p. (NASA-TM-X-55141; X-611-64-297). CFSTI $1.00 cy, $0.50 mn.

A sudden increase of the particle intensity and of the magnetic field strength on September 25, 1961, was detected by the ion-electron detector and the magnetometer on board Explorer XII outside the earth's magnetosphere. From the physical extent of the region and the energy of the trapped protons, the temporal nature of the event was established. Similarities between particle fluxes as well as between magnetic fields during the increase and within the outer belt make it probable that the increase represents an impulse-like extension of at least a portion of the outer belt. A deduced lower limit on the outward radial velocity of the extension is 156 km/sec. Crude calculations show that either the proton density near the outer edge is less than 100 cm^{-3} or the temperature is greater than 15 ev. (STAR)

17542 ON THE SLANT SPORADIC E REFLECTIONS. Oksman, Juhani (Finnish Academy of Science and Letters, Sodankylae, Finland). Ann. Acad. Sci. Fenn., Ser. A VI, No. 181, 1-18(1965).

The slant E_s traces observed at Sodankylä in the years 1958–60 are examined. Both subtypes of the international classification (the equatorial and the high-latitude subtype) were observed at Sodankylä. A statistical study reveals that the two subtypes have a similar diurnal variation; they are most frequent during the two diurnal maxima of geomagnetic disturbance. The yearly variations are different: the equatorial subtype occurs most frequently in the summer, the high-latitude subtype in the winter. From a comparison with the magnetograms it is concluded that the equatorial subtype is observed when the disturbance belt (ionospheric disturbance current system and the inhomogeneities in the electron density of the E and D regions accompanying it) is located north of Sodankylä, the high-latitude subtype when the belt is more or less overhead. The shape of the E_{ss} traces can be accounted for by two combinations of reflection and scattering, called single scattering and double scattering. The equatorial subtype is seen to be caused almost exclusively by single scattering, the high-latitude subtype mainly by double scattering. The scattering inhomogeneities are deduced to be located partly in the reflecting layer, partly below it. (auth)

17543 HOURLY VALUES OF EQUATORIAL Dst FOR THE IGY. Sugiura, Masahisa (Goddard Space Flight Center, Greenbelt, Md.). Ann. Int. Geophys. Yr., 35: 9-45(1964).

A method of derivation of Dst for the IGY is presented. Using eight magnetic stations in low latitudes, hourly values of Dst are determined for IGY. Three-hourly mean Dst values are compared with corresponding values based on Kertz's Dst indices. Three-hourly mean Dst is also compared with ap indices. It is found that Dst correlates well with ap in gross features and that during magnetic storms activity represented by ap recovers more rapidly than Dst. (auth)

17544 RING CURRENT VARIATIONS DURING THE IGY. Kertz, W. (Technische Hochscule, Brunswick). Ann. Int. Geophys. Yr., 35: 49-61(1964).

The geomagnetic storm-time variations are believed to be due to a ring current, or more likely a current belt, encircling the earth at a distance of a few radii. Three hourly values of the geomagnetic field of this current system for stations at the geomagnetic equator are given. (B.G.D.)

17545 THE QUIET-DAY MAGNETIC VARIATIONS DURING THE IGY. Price, A. T.; Stone, D. J. (Univ., Exeter, Eng.). Ann. Int. Geophys. Yr., 35: 65-269(1964).

A detailed study of the Sq field made possible by hourly value data of the magnetic variations collected at many observatories during the IGY is presented. Topics discussed are methods of analysis and interpretation of the Sq field, precise definition and derivation of the Sq field, choice of a base line from which to measure Sq, nature and sources of observatory data, and reduction of various observatory data to standard forms. A description of the selection of data, and the analysis of data by computer is also presented. Complete listing of observatory stations and hourly values of of the X, Y, Z components of the total Sq field, the daily range and the non-cyclic variation are presented. (B.G.D.)

17546 LABORATORY SIMULATION OF DISTURBANCES PRODUCED BY BODIES MOVING THROUGH A PLASMA AND OF THE SOLAR WIND-MAGNETOSPHERE INTERACTION. Shkarofsky, I. P. (RCA Victor Co., Ltd., Montreal). Astronaut. Acta, 11: 169-82(May-June 1965).

Scaling considerations on two types of geophysical interactions which can be simulated in the laboratory are presented. The laboratory set-ups and the scaling requirements are given. The first geophysical interaction pertains to the motion of a satellite through a tenuous plasma which results in sheaths around the body. Experiments on the wake can be successfully simulated by directing an ionized plasma stream against a (unmagnetized) spherical body. The particular experiments in this field are discussed. Scaling conditions are also presented on the simulation of $V \times B$ sheaths. A satellite, such as Alouette B, with long antennas crossing the earth's magnetic field lines can develop up to 13 volts potential across each half-antenna with associated sheaths as large as one meter. Present experiments are aimed towards simulation of $V \times B$ sheaths and studies of methods to reduce these large sheaths. The second geophysical interaction is concerned with the solar wind interaction with the magnetosphere and with the resulting front interface. Successful simulation of the perturbation in magnetic field at the windward boundary was achieved by directing a plasma stream against a magnetized dipole body. In this regard, the results obtained are briefly illustrated, but a discussion is given on how the scaling is achieved. These experiments were performed without imposing on the plasma stream an additional magnetic field to simulate the interplanetary magnetic field. (auth)

17547 DYNAMICS OF A GEOMAGNETIC TRAP AND ORIGIN OF THE EARTH'S RADIATION BELTS. Pletnev, V. D.; Skuridin, G. A.; Shalimov, V. P.; Shvachunov, I. N. Geomagn. Aeronomy (USSR)(Engl. Transl.), 5: 485-98 (1965).

Translated from Geomagn. Aeronomiya, 5: 626-44(1965).

The interaction of a solar corpuscular stream with the geomagnetic field, leading to the formation of the magnetosphere of the earth and to the penetration of particles into the magnetosphere in the region of neutral points, is examined. As a result of the penetration, drift currents of charged particles appear on the day side of the magnetosphere and form the neutral layer of the magnetic field and a plasma "tail" in the equatorial plane on the night side. The currents of these particles are probably the chief external source producing auroras and the main phase of a magnetic storm. The reverse phase of a storm is associated with a sharp decrease of the pressure of the solar corpuscular stream at the boundary of the magnetosphere and the capture of the drift currents of the penetrating particles at the boundary of the geomagnetic trap (the boundary of the region where the charged particles trapped by the geomagnetic field are localized). The magnetic dissipation of the trapped current during the restoration of the field to the reverse phase leads to the drift of captured particles deeper into the geomagnetic trap and to the simultaneous acceleration of these particles. (auth)

17548 MEASUREMENTS OF PROTONS WITH AN ENERGY OF 0.4- TO 8-Mev ON THE COSMOS 41 SATELLITE. Vernov, S. N.; Savenko, I. A.; Tel'tsov, M. V.; Shavrin, P. I. (Moscow State Univ.). Geomagn. Aeronomy (USSR)(Engl. Transl.), 5: 499-501(1965).

Translated from Geomagn. Aeronomiya, 5: 645-8(1965).

The results are presented of measurements of protons with an energy of 0.4 to 8 Mev in a region where parameter L varies from 3.5 to 10. The maximum intensity of protons with an energy of 0.4 to 3 Mev was 2×10^6 proton/cm^2 sec sterad on L = 3.5 and B = 7.6×10^{-2} gauss. From a comparison of data obtained in the vicinity of the geomagnetic equatorial plane with data at high latitudes for a fixed L = 5, it was found that the vertical pattern has the form $(B/B_{eq})^{-K}$, where $K \approx 1$. The maximum intensity of protons

with an energy of 0.4 to 3 Mev in the region of the geomagnetic equator on L = 3.5 is $\sim 6 \times 10^6$ proton/cm^2 sec sterad. A dependence of the decrease in proton intensity on L of the form L^{-n}, where n = 30, was obtained. But the slope of the proton intensity curve may vary appreciably with increasing L, depending on the geomagnetic situation and the variations of the external electron belt. Intense proton fluxes were detected at large L. (auth)

17549 MICROSTRUCTURE OF THE INITIAL PHASE OF A MAGNETIC STORM ACCORDING TO THE STABILITY OF MICROPULSATIONS. Bol'shakova, O. V. (Inst. of Terrestrial Physics, Academy of Sciences, USSR). Geomagn. Aeronomy (USSR)(Engl. Transl.), 5: 603-5(1965). Translated from Geomagn. Aeronomiya, 5: 775-6(1965).

The microstructure of the initial phase of magnetic storms is discussed in terms of the appearance and development of stable oscillations with small periods. Both recurrent and sporadic storms are considered. (D.C.W.)

17550 SYMPOSIUM ON MAGNETISM OF THE EARTH'S INTERIOR HELD ON 16-20 NOVEMBER 1964, AT THE UNIVERSITY OF PITTSBURGH. J. Geomagnet. Geoelec., 17: 165-541(1965). (CONF-641128).

The symposium covered aspects of the geomagnetic field and its variation originating within the solid earth. Fifty-six papers were presented, in which the existing knowledge of electromagnetic aspects of the solid earth was summarized and important questions which have not yet been solved were clearly pointed out. Sessions were held on the upper mantle project and physics of the earth's interior, world magnetic survey, analysis of the earth's main magnetic field, geomagnetic anomalies, and geomagnetic-secular variation. Also rock magnetism, archaeomagnetism, palaeomagnetism, electromagnetic induction, and electrodynamics were considered. (J.F.P.)

17551 IMPACT OF PLASMA ON A DIPOLE MAGNETIC FIELD. Roberts, J. B. G.; Turner, J. P. (Royal Radar Establishment, Malvern, Eng.). Nature, 209: 755-7 (Feb. 19, 1966).

The impact of a plasma on a dipole magnetic field was investigated. The results show a pinching of the magnetic contour lines and a reversal of the magnetic field similar to geomagnetic form phenomena. (G.O.Y.)

17552 EFFECT OF RESONANCES ON THE ADMITTANCE OF AN R-F PLASMA PROBE SURROUNDED BY AN ION SHEATH. Oya, Hiroshi (Kyoto Univ.). Rep. Ionosphere Space Res. Jap., 19: 243-71(1965).

The effect of resonances (plasma and electron gyro-resonance) on the admittance of an r-f plasma probe surrounded by an ion sheath is theoretically investigated. The parallel plane type probe, with a sharply bounded sheath edge in the hot plasma, is treated with a superimposed steady magnetic field. The theoretical formula for r-f probe admittance is obtained by solving the one-dimensional Boltzmann equation and Poisson's equation for the boundary given by a parallel plane type probe model. It is shown that electron gyro-resonance effect can be observed in the presence of an ion sheath when the equilibrium potential has not a large negative value, and it is also shown that the plasma-resonance is useful to measure the plasma parameters in the ionosphere and exosphere, in the presence of an ion sheath. (auth)

17553 IONOSPHERIC DYNAMO THEORY WITH CONSIDERATION FOR MAGNETOSPHERIC CURRENT ALONG THE GEOMAGNETIC LINES OF FORCE. Maeda, Ken-ichi; Murata, Hiroo (Kyoto Univ.). Rep. Ionosphere Space Res. Jap., 19: 272-85(1965).

The ionospheric dynamo theory is developed considering the vertical current in the conducting layer. The theory can be applied to Sq variation in the solstices, when the wind and electric potential distributions in the dynamo layer are asymmetric with respect to the equatorial plane. "Magnetospheric current" flows along the magneto-flux tube, tending to balance the potentials at conjugate points in both hemispheres. This current is connected to the ionospheric dynamo current. It is assumed that the magneto-flux tube has a certain constant conductivity (longitudinal), and the ionospheric (dynamo layer) conductivity is isotropic. Then the electric potential in the magnetosphere is distributed with a constant gradient along the line of force. In the ionosphere, the potential distribution is obtained through the potential theory as applied to a double layer of electric charge, when the wind distribution is given. The current systems in the ionosphere and the magnetosphere are obtained. Results show that the maximum magnetospheric current is of the order of 10^{-10} amp/m^2. As a first approximation, the horizontal current system in the ionospheric dynamo layer may be determined on the assumption that the vertical current is considered to be zero, even at the solstice. (auth)

17554 DIURNAL VARIATION OF AURORA ZONE GEOPHYSICAL DISTURBANCES. Morozumi, Henry M. (Tokyo Univ.). Rep. Ionosphere Space Res. Jap., 19: 286-98(1965).

A study was made of correlation among the following with special attention to vlf phenomena: (1) vlf noise (1–25 kc broadband); (2) aurora (5577A and white light); (3) ionospheric absorption (30 Mc/s riometer); (4) vlf noise (1 kc/s narrowband); (5) elf (2–30 cps); (6) ulf (0.001–5 cps); (7) variations in the earth's magnetic field (standard magnetograms); and (8) ionospheric phenomena (C-3 ionograms) at Byrd Station during the 1963 austral winter and spring. The phenomena observed showed two peaks in their diurnal appearance on moderately disturbed days, one peak in the evening and the other in the morning, in magnetic time. The evening peak consists of "events," which usually exhibit three phases designated as N-1, N-2, and N-3 (N stands for night). The N-1 phase precedes auroral break-up, and is characterized by vlf hiss and weak aurora. The N-2 phase is the break-up of aurora, and the N-3 phase following the break-up is characterized by vlf chorus and high ionospheric absorption. The phase N-1 tends to dominate early in the evening. In the mid-evening all three phases appear clearly in succession. Late in the evening the N-3 phase predominates over the other two phases. Temporal variation of night events found in this work was briefly compared with the results of the spatial survey by the Injun III satellite. The day event (D) appears to have a sequence similar to that of the night event, in spite of a large difference in their durations. A typical D event lasts more than 5 hours. The most distinct stage of a day event is similar to that of the N-3 phase. However, we occasionally observe vlf hiss burst at the beginning of a D event, just similar to an N-1 phase, and then vlf chorus starts. (auth)

17555 GEOMAGNETIC DIURNAL-VARIATION IN THE NORTH POLAR REGION WITH THE CORRECTED GEOMAGNETIC LATITUDE. Ota, Masaziro (Kyoto Univ.). Rep. Ionosphere Space Res. Jap., 19: 364-6(1965).

A comparison between Hasegawa's geomagnetic variation ovals (contours) for the north polar region and the corrected geomagnetic latitude-circles, suggested by the ovals, is presented. (R.E.U.)

17556 SEASONAL CHANGE OF AURORAL ZONE IN CORRECTED GEOMAGNETIC LATITUDES. Fukushima, Naoshi (Tokyo Univ.). Rep. Ionosphere Space Res. Jap., 19: 367-70(1965).

A systematic latitudinal dependence of the magnitude of the geomagnetic disturbance along the noon and midnight meridians is illustrated for different seasons. A notable result is that the midnight auroral zone is found to be situated at the same latitude both in winter and summer, while the auroral latitude near the noon meridian varies appreciably with season. (R.E.U.)

17557 SPATIAL AND TEMPORAL CHARACTERISTICS OF AURORAL ZONE ELECTRON PRECIPITATION [Thesis]. Rosenberg, Theodore Jay. Berkeley, Calif., Univ. of California, 1965. 137p.

During September and October of 1963, a series of high-altitude balloon flights was conducted from the northern auroral zone. The balloons carried scintillation counters to detect x rays generated in the atmosphere via the bremsstrahlung process and on two occasions on-board

photometers recorded the visible auroral luminosity simultaneously with the x rays. These measurements, combined with observations of the ionospheric absorption of cosmic radio noise by means of riometers, provided data on various spatial and temporal features of precipitating electrons in the energy range from 1 to 200 kev during unexpectedly high solar and geomagnetic activity. It was found that, even though excess radiation was almost always observed to occur simultaneously at two locations within the auroral zone separated by 200 km in the N-S direction, rarely was the precipitation coherent over this spacing when distinct features were examined. It was inferred that regions of coherent electron precipitation are usually localized to less than 200 km in the N-S direction. It was also concluded that the region of similar precipitation is generally far greater in E-W extent than in N-S extent, especially in the late morning and daytime hours. Certain distinct time variations were studied. Long-period pulsations characterized by a nearly sinusoidal modulation of the intensity with periods of 3–5 minutes generally occur between the hours of 0800 and 1200 local time during periods of strong worldwide magnetic activity. It is thought that they arise from hydromagnetic disturbances propagating within the magnetosphere. Short pulsations have half-widths between 2 and 10 seconds with average spacings between bursts varying from 4 to 30 seconds, whereas microbursts have uniform half-widths of about $\frac{1}{4}$ second. Short pulsations definitely occur more often at latitudes south of the auroral zone and favor the hours centered around the dawn meridian, while microbursts do not appear to have a latitude dependence and are centered about 1100 local hours. It was found that quite frequently the behavior of auroral luminosity and x rays do not coincide. It is suggested that two processes are involved in the acceleration and/or precipitation of electrons, each process having a different energy spectrum. (A.G.W.)

17558 PARTIAL ELECTRON VELOCITY SPECTRA FROM CYCLOTRON ABSORPTION OF WHISTLER POWER. Liemohn, H. B. (Southwest Center for Advanced Studies, Dallas). 17p. (CONF-651053–1). ORAU. Gmelin, AED-CONF-65-278-2.

From Joint IEEE-URSI Meeting, Hanover, N. H.

A method is proposed for the determination of partial electron velocity spectra from the power spectra of whistler signals at their upper cutoff. It is assumed that the only frequency-dependent attenuation of the signal is cyclotron resonance absorption by the nonthermal electron component (around 1 kev) in the magnetosphere. According to the theory, the differential density $F = [dN/dv_{||}]_{v_{||}=-u(\omega)}$ is related by an integral equation to the power loss $L(\omega)$ of each whistler, where $v_{||}$ is the velocity component parallel to the local geomagnetic field, u is the resonance speed, and ω is the propagation frequency. The equation is too difficult to solve analytically for F, but over a narrow frequency band $\omega_1 \leq \omega \leq \omega_2$ at the cutoff where L is measurable, an approximate solution is obtained in the form $F = Au^{-n}$ in the range $u_1 \leq u \leq u_2$. The power spectrum of whistlers has not been measured accurately yet, but the sharp cutoffs observed on sonograph traces suggest that $n \geq 9$. The results are compared with previous applications of the theory. (auth)

Gravitation, Quantum Mechanics, and Relativity Theory

Refer also to abstracts 17446 and 17503.

17559 (EUR-2639.f) CALCUL DES COEFFICIENTS DE RACAH, CLEBSCH-GORDAN ET Z. (Calculation of Racah, Clebsch-Gordan, and Z Coefficients). Cao, M. G. (European Atomic Energy Community, Geel (Belgium). Central Nuclear Measurements Bureau). Jan. 1966. 12p. Dep. mn.

The report is concerned with calculating, on an IBM 7090, the Racah, Clebsch-Gordan, and Z coefficients. (auth)

17560 (ITEF-384) ZADACHA TREKH TEL.POLNAYA SISTEMA UGLOVYKH FUNKTSII. (Three-Body Problem. Complete System of Angular Functions). Simonov, Yu. A. (Gosudarstvennyi Komitet po Ispol'zovaniyu Atomnoi Energii SSSR, Moscow. Institut Teoreticheskoi i Eksperimental'noi Fiziki). 1965. 21p. Dep. mn.

The wavefunction of three particles depends on two vectors—the relative coordinates or momenta of the particles—and must be a representation of the permutation group of three particles. A method is proposed for constructing of the complete system of functions for each value of the total angular momentum L, these functions being the irreducible representations of the permutation group. For L = 0 the functions are deduced and written explicitly. They are noted by the values of K—the global six dimensional angular momentum, K being any positive even number, and by ν, going from $-K/2$ to $K/2$ with the interval of two. Symmetric and antisymmetric functions are those with ν multiple of three. (auth)

17561 (JINR-P-2532) p-RAZDELENIE PEREMENNYKH V URAVNENII SHREDINGERA. (p-Separation of Variables in the Schroedinger Equation). Tugov, I. I. (Joint Inst. for Nuclear Research, Dubna (USSR). Lab. of Theoretical Physics). 1965. 18p. Dep. mn.

The $-p$-separation of variables in the generalized Schrödinger equation $\Delta_2 u + (E - V)u = 0$ in the n-dimensional Riemannian space is considered. It is shown that in the Einstein spaces the Schrödinger equation is completely separable, if p is separable. The separation of variables is treated in the invariant form. (auth)

17562 THEORY OF CONGRUENCE IN GRAVITATIONAL FIELDS. I. RED SHIFT AND GEODESICS FROM THE SAME THEOREM. Sueveges, M. (Research Group for Theoretical Physics, Budapest). Acta Phys. Acad. Sci. Hung., 20: 41-50(1966).

A theorem on parallelism is proved. Roughly speaking, the theorem states that physical quantities are congruent under Levi-Civita transport in Riemannian spaces. The three crucial tests of general relativity are deduced from the theorem. (auth)

17563 THEORY OF CONGRUENCE IN GRAVITATIONAL FIELDS. II. THE POSSIBLE COSMOLOGICAL ORIGIN OF THE GROUP L↑. Sueveges, M. (Research Group for Theoretical Physics, Budapest). Acta Phys. Acad. Sci. Hung., 20: 51-8(1966).

A corollary to the theorem proved in part I states that local coordinate systems, defined in the tangent space at any point of the Riemannian manifold, that are obtained from each other by transformations of the holonomy group at that point are physically equivalent. With the aid of this corollary it is proved that if the Universe is a nonvacuum Einstein manifold of signature +2, then the six-dimensional orthochronous proper Lorentz group L↑ is a good local symmetry group in the tangent space at any point of the Universe. Conversely, if L↑, or at least a subgroup of it, is a good local group then the Universe cannot be flat. (auth)

17564 TWO SUBGROUPS OF THE LORENTZ GROUP AND THEIR PHYSICAL SIGNIFICANCE. Janossy, L. (Central Research Inst. for Physics, Budapest). Acta Phys. Acad. Sci. Hung., 20: 115-20(1966).

It is shown that the Lorentz group can be represented as the product of two subgroups. The one subgroup is connected with rotation, the other with translation. The results of the negative relativistic experiments, like the Michelson-Morley experiment, are connected with the invariance of laws with respect to the rotational subgroup, while the positive relativistic effects, like the change of mass with velocity, are connected with the invariance with respect to the translational subgroup. (auth)

17565 ON THE HEISENBERG NONLINEAR SPINOR FIELD EQUATION IN THE PRESENCE OF GRAVITATION FOR A NONLOCAL SPIN CONNECTION. Toro, T. (Univ., Timisoara, Rumania). Acta Phys. Acad. Sci. Hung., 20: 197-9(1966).

Using an expression for the covariant derivative of spinor the Heisenberg-Pauli equation is formulated in terms of integro-differential equations for the case of nonlocal and partially-local spin connection in the presence of gravitation. (L.B.S.)

17566 ON THE ENERGY-MOMENTUM TENSOR AND ON MACROSCOPIC INTERNAL INTERACTIONS IN A GRAVITATIONAL FIELD AND IN MATERIAL MEDIA. Sedov, L. I. Dokl. Akad. Nauk SSSR, 164: 519-22(Sept. 21, 1965). (In Russian).

The equations defining the energy-momentum tensor for a continuous medium in the framework of general relativity are investigated. The general theory is required in order to describe the mechanics of a continuous medium in a gravitational field. The stress tensor is derived starting from a variational (least action) principle, and is found to differ from that of Einstein obtained in the special theory. Although the equations of a continuous medium can be written in terms of purely geometric properties, it is convenient and useful to retain internal stresses. The internal stress tensors in the general and special theories differ by a term depending on local gravitational curvature. (ATD)

17567 INERTIAL ECHO AND COHERENT GRAVITATIONAL WAVES. Kopvillem, U. Kh.; Nagibarov, V. R. (Kazan' Physico-Technical, Inst.). JETP Lett. (USSR) (Engl. Transl.), 2: 329-32(Dec. 15, 1965).

Translated from Zh. Eksp. Teor. Fiz., Pis'ma Redakt., 2: 529-33(Dec. 15, 1965).

New physical phenomena, inertial (or gravitonic) induction and echo, are considered which can possibly be used for generation and reception of coherent gravitational waves (CGW) in a narrow band of optical frequencies under laboratory conditions. Numerical estimates show that the proposed experimental scheme on the detection of CGW can be realized with present-day technical means. (M.O.W.)

17568 NON-EINSTEINIAN GRAVITATION. Polievktov-Nikoladze, N. M. (Tbilisi State Univ., USSR). JETP Lett. (USSR) (Engl. Transl.), 2: 342-4(Dec. 15, 1965).

Translated from Zh. Eksp. Teor. Fiz., Pis'ma Redakt., 2: 551-4(Dec. 15, 1965).

According to Einstein's hypothesis, the invariant Lagrangian density of the free gravitational field is $\Lambda = R/k$, where R is the scalar space-time curvature and $k = 2 \times 10^{-48}$ g/cm-sec^2. An analysis is given which shows that none of the presently known facts proves the incompatibility with experiment of an infinite set of non-Einsteinian expressions for Λ. (M.O.W.)

17569 RADIAL MOTION IN THE SCHWARZSCHILD FIELD AND THE ISSUE OF GRAVITATIONAL COLLAPSE. Israel, Werner (Univ. of Alberta, Edmonton, Can.). Nature, 209: 66-7(Jan. 1, 1966).

It was concluded that the Schwarzschild sphere acts as a unidirectional membrane for particles and light pulses dropped in from outside. The same considerations apply to the homologous gravitational collapse of a pressure-free sphere of mass m. It is shown that the accustomed global assignment of a time-arrow breaks down inside the Schwarzschild sphere. (M.C.G.)

17570 APPROXIMATION METHODS IN MANY-BODY PERTURBATION THEORY. Stoelan, Birger; Cooper, Leon N. (Brown Univ., Providence). Phys. Rev., 143: 209-14(Mar. 4, 1966).

An analysis of some approximations common in the treatment of many-body systems indicates that the inclusion of large numbers of uncancelled exclusion-principle-violating (EPV) processes leads to meaningless results. It is therefore proposed as a criterion for the validity of many-body approximations that there should be no such large-scale inclusion of EPV processes. The graphs generated in the BCS theory are analyzed from this point of view. (auth)

17571 RELATIVISTIC SCHROEDINGER EQUATIONS FOR PARTICLES OF ARBITRARY SPIN. Mathews, P. M. (Brandeis Univ., Waltham, Mass.). Phys. Rev., 143: 978-85(Mar. 25, 1966).

Relativistic wave equations in the Schrödinger form $i\partial\psi/\partial t = H\psi$ for particles of nonzero mass and arbitrary spin are investigated. The wave function ψ is taken to transform according to the representation $D(0,s) \oplus D(s,0)$ of the homogeneous Lorentz group, a unique spin s for the particle being thereby assured without the aid of any supplementary condition. It is shown that the requirement that the Schrödinger equation be invariant under the operations of the Poincaré group, as well as under space and time inversions and charge conjugation, restricts the possible choices of H (as a function of the operators representing the above symmetry operations) to a well-defined class which shrinks to a unique possibility (coinciding with the hamiltonian derived by Weaver, Hammer, and Good) when a further regularity condition of a physical nature is imposed: namely, that the hamiltonian have a unique finite limit in the rest system of the particle. In this process, an ambiguity which exists initially in the definition of operators representing time reversal and charge conjugation gets eliminated. The hamiltonian itself is obtained in explicit form for particles of any spin. (auth)

17572 INVARIANT SCALAR PRODUCT AND OBSERVABLES IN A RELATIVISTIC THEORY OF PARTICLES OF ARBITRARY SPIN. Mathews, P. M. (Brandeis Univ., Waltham, Mass.). Phys. Rev., 143: 985-9(Mar. 25, 1966).

A relativistically covariant Schrödinger equation was previously derived for particles of arbitrary spin s, locally covariant wave functions without redundant components being used to describe states of a particle. Here the invariant scalar product is determined with respect to which the representation of Poincaré transformations on these wave functions is unitary. It is shown that the conventional position and spin operators, not being Hermitian with respect to this scalar product, cannot be observables. New operators that can represent these observables are constructed with the aid of a generalized Foldy-Wouthuysen transformation, which is determined explicitly for arbitrary spin. (auth)

17573 OBSERVABLE CONSEQUENCES OF FUNDAMENTAL-LENGTH HYPOTHESES. Mead, C. Alden (Birkbeck Coll., London). Phys. Rev., 143: 990-1005 (Mar. 25, 1966).

The postulate of the existence of a fundamental length may be expressed in terms of a minimum uncertainty in position measurements, or equivalently as a minimum uncertainty in measurements of the gravitational field. The postulate is expressed mathematically by means of "indeterminate operators," whose properties are discussed. With their aid, it is shown that the postulate of a fundamental length has as a consequence a certain broadening of spectral lines. In the case of a fundamental length of the order of 10^{-13} cm, the predicted broadening is much larger than the widths of nuclear gamma transitions already observed. It is concluded that this fundamental length is already in serious contradiction with experiment. In the case of a fundamental length due to gravitational effects of the order of 10^{-33} cm, as previously suggested by the author, the broadening is too small to have been observed in any experiments done to date. A modified Mössbauer experiment is suggested which should be capable of detecting this small broadening, if it is present. The experiment is difficult, but appears to be possible with presently available techniques. The gravitational-field uncertainties calculated by DeWitt, Peres, and Rosen, and others, lead to a still smaller broadening, which our proposed method would be incapable of detecting. (auth)

17574 INTERACTIONS AND RELATIVITY. Hood, C. Gregory (Boston Univ.). Phys. Rev., 143: 1006-11 (Mar. 25, 1966).

A generalization of special relativity is proposed, which does not rely upon the equivalence principle or the concept of geodesic motions in a Riemannian space. The theory applies to all kinds of interactions provided an expression for the interaction potential energy exists. An invariant interval and Lagrangian are derived, which reduce to the corresponding forms of special relativity when interactions are turned off. For weak gravitational fields it is shown that the theory leads to the three confirmed predictions of general relativity. In addition, a nongravitational red shift is predicted. From the Lagrangian, new expressions for

momentum and energy are derived. Four generalized Lorentz transformations are found which correspond to transformation equations for charged and neutral particles, matter and antimatter. These equations predict an asymmetry in particle-antiparticle lifetimes. Finally, new expressions for the addition of velocities and the transformation of electromagnetic fields are derived. (auth)

17575 ROTATING MASSES AND THEIR EFFECT ON INERTIAL FRAMES. **Brill, Dieter R.; Cohen, Jeffrey M. (Yale Univ., New Haven). Phys. Rev., 143: 1011-15 (Mar. 25, 1966).**

An analysis is given of the stress-energy tensor and geometry produced by slowly rotating bodies. The geometrized mass GM/c^2 of the body is allowed to be comparable to its radius. The geometry is treated as a perturbation of the Schwarzschild geometry, which leads to considerable simplification of Einstein's equations. The rotation of the inertial frame induced by a rotating massive shell is calculated and discussed with particular attention to two limiting cases: (1) for small masses it reduces to Thirring's well-known result; (2) for large masses, whose Schwarzschild radius approaches the shell radius, the induced rotation approaches the rotation of the shell. These and the corresponding results for an expanding and recollapsing dust cloud are examined for their consistency with particular interpretations of Mach's principle. The analytic extension of the rotating exterior metric is a completely source-free rotating solution. It describes a slowly rotating, expanding, and recontracting Einstein-Rosen bridge, which can be taken as a geometrodynamic model for a slowly rotating body. (auth)

17576 NEW INTERPRETATION OF THE EXTENDED SCHWARZSCHILD MANIFOLD. **Israel, Werner (Univ. of Alberta, Edmonton). Phys. Rev., 143: 1016-21(Mar. 25, 1966).**

New analytic extensions of the Schwarzschild and Reissner-Nordström manifolds are presented in which the metric coefficients are simple rational functions of the coordinates, and the complete manifold is covered by a single coordinate patch. A study of radial time-like geodesics leads naturally to an interpretation of the domain inside the Schwarzschild "singularity" involving a breakdown of the global distinction between past and future in this region. According to the new interpretation, and in contrast to presently established views, probes and light signals dropped in toward the center can be recovered by an external observer in a finite time. (auth)

17577 POSITION OPERATORS, GAUGE TRANSFORMATIONS, AND THE CONFORMAL GROUP. **Kastrup, H. A. (Princeton Univ., N. J.). Phys. Rev., 143: 1021-7(Mar. 25, 1966).**

The connection between the Lie algebra of the conformal group and the algebra of quantum mechanics is analyzed, applying a method similar to one considered by Segal. The contraction of the 4-parameter special conformal group yields the position operators, and the contraction of the dilatations yields a phase transformation of the states considered. Quantum mechanics appears in this way as a broken symmetry. Thus one gets a relationship between geometrical gauge transformations and phase transformations, which sheds new light on Weyl's conjecture that geometrical gauge transformations and charge conservation are related to each other. Arguments are given as to why the usual interpretation of the special conformal group as a system of transformations connecting frames of constant relative accelerations hardly can be the right one. The main point is that the physically essential group velocity of the wave packets formed by the eigenfunctions of the special conformal group has the same form as in the case of the plane waves, whereas the physically irrelevant phase velocity has the hyperbolic structure usually discussed. (auth)

17578 PROPOSAL TO CHECK C, P, AND T CONSERVATION AT LARGE MOMENTUM TRANSFER AS A TEST OF CONVENTIONAL QUANTUM ELECTRODYNAMICS. **Weiner, Richard M. Phys. Rev., 143: 1292-4 (Mar. 25, 1966).**

The hypothesis that at large momentum transfer electromagnetic interactions are not C- and/or P-, T-invariant is proposed in connection with the recently observed deviation from conventional quantum electrodynamics. Some experiments are suggested which might verify this assumption and which should serve as an independent test of quantum electrodynamics at large momentum transfer. (auth)

17579 ENERGY TRANSPORT BY THE OZSVATH–SCHUCKING SOLUTION OF THE GRAVITATIONAL FIELD EQUATIONS. **Dehnen, H. (Univ. Freiburg i. B.). Z. Phys., 191: 329-34(1966). (In German).**

The expresssion proposed for the energy-impulse density of the gravitational field is applied to a rigorous solution of the Einstein field equations found by Ozsváth and Schücking. An exact proof is given in a general covariant manner for the physical interpretation of the solution, which was previously given. (tr-auth)

17580 GRAVITATIONAL ELECTRIC EXCHANGE. **Dehnen, H. (Univ., Freiburg i. B.). Z. Phys., 191: 335-42(1966). (In German).**

The influence of the gravitational field on the electromagnetic field is investigated in a general manner. The expected effects are illustrated by two examples and are estimated with respect to their order of magnitude, which were found to be immeasurably small. (tr-auth)

17581 QUANTUM ELECTRODYNAMICS WITH TWO FERMIONS. **Kompaneets, A. S. (Inst. of Chemical Physics, Academy of Sciences, USSR). Zh. Eksp. Teor. Fiz., 49: 1781-8(Dec. 1965). (In Russian).**

It is demonstrated that if two fermions are taken into account and the Lagrangian formalism of quantum electrodynamics is partially rejected, it becomes possible to formulate the equations in such a way that no infinite expressions appear. Both fermions are physical and an equation for the ratio of their masses is derived. (auth)

17582 UNIQUENESS OF THE CENTRAL-SYMMETRIC GRAVITATIONAL FIELD IN VACUUM. **Khrapko, R. I. (Moscow Aviation Inst.). Zh. Eksp. Teor. Fiz., 49: 1884-6 (Dec. 1965). (In Russian).**

It is shown that the coordinate systems usually used for describing part of the Friedman world and the empty region adjacent to it do not satisfy the Liechnerovich continuity conditions. The coordinate system permissible in the Liechnerovich sense possesses the metric found by Petrov and for an empty region it is equivalent to the Schwarzschild coordinate system. (auth)

17583 A PENDULUM GRAVIMETER FOR PRECISION DETECTION OF SCALAR GRAVITATIONAL RADIATION [Thesis]. **Curott, David Richard Francis. Princeton, N. J., Princeton Univ., 1965. 123p.**

A prototype pendulum gravimeter was designed and tested. Constructed of a stable material, quartz, the device enlisted a fused silica fiber as the supporting hinge. This gravitational clock eliminated the usual knife edge limitations upon precision and long term behavior. The period of the simple pendulum mode was determined using electronic counting techniques. Analysis of data indicates a frequency increase of $1.7 \pm .4$ parts in 10^9 per day. The root mean square deviation of less than 8 in 10^8 for daily determinations is predominantly due to building vibrations; hence definite techniques for improvement are suggested. (Dissertation Abstr.)

17584 ASYMPTOTIC MATCHING IN THE RESTRICTED THREE-BODY PROBLEM [Thesis]. **Perko, Lawrence Marion. Stanford, Calif., Stanford Univ., 1965. 144p.**

The motion of a particle of negligible mass in the gravitational field of two point masses m_0 and m_1 as the particle moves from an arbitrary point in three-space to a small neighborhood of the point m_1 is studied in the framework of the restricted three-body problem for $\mu = m_0/m_1$ much less than one. The motion of m_1 with respect to m_0 is assumed to satisfy the two-body equations. Perturbation techniques and the concept of asymptotic matching are used in order to obtain an approximate solution to the problem

for bounded time intervals. An estimation technique based on the construction of a majorizing function is developed and uniform estimates of the errors in position and velocity are computed. Earlier work of P. A. Lagerstrom and J. Kevorkian on restricted three-body problem trajectories for which the initial angular momentum of the particle with respect to m_0 is $0(\mu^{\frac{1}{2}})$ is generalized; an nth order theory including a method of estimation valid for all three-dimensional trajectories that reach a small neighborhood of m_1 with a velocity of 0(1) is developed. The analysis can be easily extended to the restricted four-body problem for particle motion leaving a small neighborhood of m_1 and reaching a small neighborhood of m_2 provided $\mu_1 = m_1/m_0$ and $\mu_2 = m_2/m_0$ are much less than one. This is demonstrated by carrying through the first order perturbation series and asymptotic matching for the restricted four-body problem. Numerical results, which describe the perturbation effect of the earth and Mars on the constants of the Mars-centered perturbed hyperbola as well as the effect of small changes in initial conditions, are given for a large class of earth-to-Mars trajectories in the gravitational field of the earth, Mars, and the sun. (Dissertation Abstr.)

Low Temperature Physics

Refer also to abstracts 16610 and 17197.

17585 (AD–627910) THE TEMPERATURE VARIATION OF THE GINZBURG–LANDAU PARAMETER IN NIOBIUM SINGLE CRYSTALS. Technical Report No. 1. Skinner II, Loren C. (Massachusetts Inst. of Tech., Cambridge. Metals Processing Lab.). Jan. 1966. Contract NR039-087-NRON-3963(16). 47p.

Magnetization measurements were made on high purity Nb single crystals at temperatures from 1.6 to 8.8°K. The crystals were grown by the electron beam floating-zone technique and had resistivity ratios from 100 to 800. The upper and lower critical fields (H_{c2} and H_{c1}) and the slope of the magnetization curve at the upper critical field, H_{c2}, were determined. The value of H_{c2} and the slope at H_{c2} require two separate phenomenological parameters, as was predicted by the Maki-Tsuzuki linear approximation. The temperature dependence of the slope at H_{c2} is best described by the Maki-Tsuzuki theory, but the temperature variation of H_{c2} is best described by the Ginzburg-Bardeen theory. (auth)

17586 (CONF-650922, pp 509-16) A HIGH HOMOGENEOUS FIELD SUPERCONDUCTING MAGNET FOR A POLARIZED PROTON TARGET. Desportes, H.; Tsai, B.

A pair of superconducting Helmholtz coils which are made of a single Cu-coated Nb–Zr wire and generate a 21-kgauss magnetic field with a homogeneity of 10^{-4} is described. Some experimental observations on the performance of the coils are summarized. (D.C.W.)

17587 (CONF-650922, pp 517-24) A HIGH HOMOGENEITY-RICH FIELD SUPERCONDUCTING MAGNET FOR NUCLEAR RESONANCE. Grivet, P.; Sauzade, M.

A superconducting solenoid is described with which a maximum usable field of 58 kgauss with a homogeneity of 10^{-7} over a volume of 150 mm^3 was obtained. (D.C.W.)

17588 (CONF-650922, pp 525-9) MAGNETO-OPTICAL EXPERIMENTS WITH SUPERCONDUCTING MAGNET. Nishina, Yuichiro; Kurita, Susumu; Tanaka, Kunihide.

A superconducting magnet developed for magneto-optical experiments in the region of infrared and visible wavelengths is described. An investigation of the interband absorption and the Faraday rotation in single crystals of GaSe at photon energies near the absorption edge is summarized. (D.C.W.)

17589 (CONF-650922, pp 541-9) THE POTENTIAL OF INTERSTITIAL COMPOUNDS FOR HIGH-FIELD SUPERCONDUCTING MAGNETS. Pessall, N.; Jones, C. K.; Johansen, H. A.

Systematic measurements were made of the critical field, critical current density and critical temperature of some pseudo-binary systems of interstitial compounds (NaCl structure) based on niobium nitride and also of several pseudoternary systems based on niobium carbonitride. A systematization of the superconducting behavior is given, and the potential of this class of materials is discussed. (auth)

17590 (CONF-650922, pp 550-9) TERMINAL CHARACTERISTICS OF SHORT SAMPLES OF SUPERCONDUCTORS AND THEIR EFFECT ON COIL BEHAVIOR. Stekly, Z. J. J.

An investigation of the terminal characteristics of superconducting coils on the basis of measurements of the terminal characteristics of short samples and composite strips is summarized. The analysis of the experimental results is outlined. (D.C.W.)

17591 (CONF-650922, pp 560-7) EXPERIMENTS WITH SUPERCONDUCTING CABLE. Laverick, C.

The performance characteristics of a number of magnets made from various types of superconducting cable were investigated. The effects of variations in the type of impregnating material, the thickness of normal conductor, and the type of insulation used in the cable were studied. (D.C.W.)

17592 (CONF-650922, pp 574-87) DESIGN, CONSTRUCTION, AND PERFORMANCE OF CRYOGENICALLY COOLED AND SUPERCONDUCTING ELECTROMAGNETS. Laurence, James C.; Coles, Willard D.

Some magnets developed at the Lewis Research Center are discussed. Included are a system of coils wound from very pure Al and cooled with liquid Ne and superconducting coils wound from Nb–Sn and Nb–Zr wires and ribbons. (D.C.W.)

17593 (CONF-650922, pp 597-603) STRANDED NIOBIUM–TIN WIRE SOLENOIDS: DESIGN AND FABRICATION TECHNIQUES. Rosner, Carl H.; Benz, Mark G.

Design, construction, and heat-treatment techniques, that are being used in the successful application of Nb–Sn wire (Cryostrand) to high-field superconducting solenoids are discussed in detail. (auth)

17594 (CONF-650922, pp 604-10) A 4500 GAUSS SUPERCONDUCTING MAGNET FOR CORPUSCULAR IONOGRAPHY EXPERIMENTS USED AT CERN. Donadieu, L. J.; Royet, J.

A superconducting magnet that was developed for use in a study of the charge inversion of 70-Mev pions is described. The operational limit of the magnet is 42 kgauss. (D.C.W.)

17595 (CONF-650922, pp 611-14) A CLOSED-LOOP COOLING SYSTEM FOR SUPERCONDUCTING BUBBLE CHAMBER MAGNETS. Kolm, Henry H.

A cooling system for maintaining magnets at the temperature of liquid helium is described. The system is based on the reluctance of liquid helium to solidify at pressures substantially above its critical point. (D.C.W.)

17596 (CONF-650922, pp 615-24) FLUX PUMPS AS POWER SUPPLIES FOR SUPERCONDUCTING COILS. Wipf, S. L.

The output emf of a flux pump and the electrical losses were calculated; and two types of a-c pumps with no moving parts were tested, as well as modifications of two rotating pumps. The experimental results are in agreement with the mathematical treatment. (D.C.W.)

17597 (CONF-650922, pp 625-9) CRYOGENIC COIL FOR MEGAJOULE ENERGY STORAGE. Arp, V.

A hydrogen-cooled aluminum magnet that is being built for a 10^6 J inductive energy storage system is described. (D.C.W.)

17598 (CONF-650922, pp 745-52) NEW MAGNET INSTALLATIONS AT THE KAMERLINGH ONNES LABORATORY. de Klerk, D.

Three magnet installations at the Kamerlingh Onnes Laboratory are described including the power supplies, the coils, and the flux pumps for the superconducting coils. (D.C.W.)

17599 (JINR-P-2480) METOD POLUCHENIYA SVERKHNIZKIKH TEMPERATUR, OSNOVANNYI NA RASTVORENII ^{3}He V ^{4}He. (A Method of Obtaining Superlow Temperature Based on a Dissolution of ^{3}He in ^{4}He). Neganov, B. S.; Borisov, N. S.; Liburg, M. Yu. (Joint Inst. for Nuclear Research, Dubna (USSR). Lab. of Nuclear Problems). 1965. 23p. Dep. mn.

A method is described of obtaining superlow temperatures in a stationary regime. The method is based on a continuous dissolution of liquid ^{3}He in ^{4}He. At a circulation of ^{3}He to be about 1.84×10^{-4} mole/s a temperature of 0.1°K is constantly maintained at the heat supply of 1800 erg/s. When there is no external heat supply the temperature of the solution is kept to be 0.055°K. The temperature variations do not exceed 0.001°K. (auth)

17600 (ORNL-3908, pp 114-48) MAGNETICS AND SUPERCONDUCTIVITY. (Oak Ridge National Lab., Tenn.).

An appropriate way to represent magnetic fields graphically is to trace constant-vector-magnitude curves. It is more effective to use the new concept of "total vector error contours." These two graphical methods are applied to a study of the field configurations of the new large-volume magnet coil systems "C" and "D," which are being built for our magnet laboratory. Other tasks of magnetic field production for thermonuclear research encounter considerable technological difficulties: first, the generation of high fields in small volumes (for instance in the bores of mirror coils) with the additional condition of disturbing by mechanical construction parts the surrounding plasma as little as possible. Two different new designs which try to solve this problem are described. Both showed promising preliminary test results. A second problem is the generation of "magnetic wells" with nonzero field minima. Air-core coil designs are difficult because of the necessary high current densities in the windings. Recently, for this purpose an iron-core design was developed here which needs only low power densities in the coils, allows simple changing of the mirror ratio, and permits ample access to the plasma volume. The work on superconductivity at the Thermonuclear Division is guided by the opinion that for the successful development of superconducting, large-volume, high-field magnets of various shapes (coils, Ioffe bars, etc.), a better understanding of the relevant physical properties of the high-field superconductors is necessary. Recent results on micro Hall probe measurements on Nb-25% Zr cylinders and coils, and investigations on the field distributions in hard-superconducting cylinders with adiabatic field change are described. A note on the macroscopic theory of superconductors of the second and third kind tries to clarify the basic theoretical concepts. (M.O.W.)

17601 A STUDY OF SUPERCONDUCTING COMPOSITE Sn AND Au FILMS. Klokholm, E.; Chiou, C. (IBM Watson Research Center, Yorktown Heights, N. Y.). Acta Met., 14: 565-7(Apr. 1966).

Sn and Sn-Au films were simultaneously deposited on a substrate by vacuum deposition. Next a Au film was deposited followed by a film of Sn. Electron diffraction and microscopy showed that all films were mixed phases rather than composite single layers. The Sn/Au/Sn films were composed of Sn-$AuSn_4$ or $AuSn_4$-$AuSn_2$ depending upon the thickness of the Au film. As the Au thickness increases the Sn content in the mixed phase Sn-$AuSn_4$ decreases. After the stoichiometric composition $AuSn_4$ is reached, further increases in Au film thickness results in the formation of the $AuSn_4$-$AuSn_2$ mixed phase. The ratio of the electrical resistance at 4.2°K to the resistance at 300°K increases rapidly with Au thickness to the amount required for the stoichiometric composition of $AuSn_4$ and then decreases rapidly. The superconducting critical temperature of the films decreased linearly with increasing Au thickness. In the Sn-Au/Au/Sn films, Ag_3Sn crystallites were dispersed in a Sn matrix. The Ag_3Sn was not superconducting. It appears that the formation of the intermetallic compound was the principal cause for the variation of the superconducting properties and not a contact effect between composite layers. (W.L.G.)

17602 EQUIPMENT FOR MEASURING SUPERCONDUCTING PROPERTIES OF SUPERCONDUCTORS FOR STRONG MAGNETIC FIELDS. Litomisky, Miroslav; Ruzicka, Jiri (Ustav Jaderneho Vyzkumu CSAV, Rez, Czechoslovakia). Cesk. Cas. Fys., 16: 27-33(1966). (In Czech).

Equipment used for measuring the critical current density of superconductors in a magnetic field at a temperature of 4.2°K is described. The samples of superconducting materials (wires or strips) can be measured on two different holders: the first is supplied with a current switch working in a helium bath so that during one experiment 10 samples can be measured in constant fields up to 62 kG. In the second holder three samples can be measured simultaneously in magnetic fields up to 83 kG, which are obtained by concentrating the solenoid field by means of ferromagnetic pole pieces placed in a liquid helium bath. The results of some measurements are given. (auth)

17603 MAGNETICS AND SUPERCONDUCTIVITY. Callaghan, Edmund E. Cryog. Eng. News, 17-21(Dec. 1965-Jan. 1966).

The advantages of using low-temperatures to reduce power loss in electronic systems due to resistance are considered. The variation of resistance with temperature, magnetoresistance at low temperatures, and properties of superconductors and superconducting materials are summarized. Also mentioned are the energy storage application of superconductors, the magnetic fields of which can hold large amounts of energy, and the a-c-d-c rectifier, which can be made very small. (J.F.P.)

17604 MAGNETIZATION OF SYNTHETIC FILAMENTARY SUPERCONDUCTORS. A. THE DEPENDENCE OF FLUX JUMPING ON TEMPERATURE AND MAGNETIC FIELD SWEEP RATE. Watson, J. H. P. (Corning Glass Works, Corning, N. Y.). J. Appl. Phys., 37: 516-24(Feb. 1966).

Synthetic high-field superconductors were prepared by impregnating porous glasses of various pore size with indium, using pressures up to 70,000 psi. The magnetic field H_{fj} at which the first flux jump occurred in the initial magnetization of the sample was measured as a function of temperature T and magnetic field sweep rate dH/dt. Values of dH/dt between 24 and 375 Oe/sec were used. For a given value of dH/dt, H_{fj} increased initially as T was lowered, reached a maximum, and finally fell with T. For a given T, H_{fj} was reduced as dH/dt increased. For large values of dH/dt, H_{fj} was almost independent of T and dH/dt. H_{fj} was reproducible to 50 Oe from cycle to cycle except for T < 1.5°K, where the behavior became more erratic. After the sample was warmed to room temperature, H_{fj} was reduced. The samples showed hysteresis in the magnetization. Flux jumping occurred around the hysteresis loop; the values of field at which flux jumps occurred were reproducible from cycle to cycle. The field interval Δ between flux jumps had a temperature dependence similar to H_{fj}; Δ is slightly reduced for large values of the applied magnetic field. The size of the flux jumps were also reduced for large values of magnetic field. For small values of T, the flux jumping behavior became erratic. Measurements of the critical field and transition temperature were made using a low-frequency mutual-inductance technique. The critical field, that is the magnetic field for the normal-superconducting transition, for a sample with a 65-Å pore diameter was 25,770 Oe at 2.67°K. At a reduced temperature of 0.6°K, samples with pore diameters of 65, 117, and 250 Å have critical fields of 156, 102, and 39 times the critical field of bulk indium (176 Oe). The transition temperatures for the samples were 4.24, 4.04, and 3.61°K, respectively, compared with 3.408°K for bulk indium. The over-all behavior of these samples was similar to inhomogeneous type-II superconductors. (auth)

17605 DEVIATIONS FROM BCS BEHAVIOR IN THE TEMPERATURE DEPENDENCE OF THE ULTRASONIC ABSORPTION IN SUPERCONDUCTING TIN. Olsen, Tore; Claiborne, Lewis T.; Einspruch, Norman G. (Texas Instruments Inc., Dallas). J. Appl. Phys., 37: 760-2(Feb. 1966).

The temperature dependence of the attenuation of compressional ultrasonic waves was measured in high-purity single crystals of superconducting Sn. Deviations from BCS behavior were observed. The experimental results are compared on the basis of frequency dependence, state of anneal, deformation, and sample thickness. It is shown that the deviations from BCS behavior are similar to those found for Nb–Zr, Nb–Mo, La, and polycrystalline Sn. It is also demonstrated that the temperature-dependent absorption peaks are not a property of the pure type-I superconductor but are related to both the defect structure and the sample size. (auth)

17606 ULTRASONIC OBSERVATION OF MAGNETIZATION AND FLUX JUMPING IN A SUPERCONDUCTING Nb–Zr ALLOY. Claiborne, Lewis T.; Einspruch, Norman G. (Texas Instruments Inc., Dallas). J. Appl. Phys., 37: 925-6(Feb. 1966).

It is reported that the attenuation of ultrasonic compressional and shear waves by a Nb–3.6% Zr alloy nonideal superconductor in the mixed state is sensitive to the internal magnetic field and to flux jumping. The study was undertaken to determine the effect of field penetration on the temperature-dependent compressional wave absorption structure observed in various type-II and nonideal superconductors in zero external field. Oscilloscope traces of 30-Mc shear wave attenuation, temperature, flux exclusion, and magnetic field are shown as a function of magnetization at 4.2°K. Also given are the compressional wave attenuation, temperature, and magnetic field for nearly adiabatic magnetization at 4.2°K. (J.F.P.)

17607 SUPERCONDUCTIVITY IN THE TRANSITION METAL CARBIDES: $Mo_{4.8}Si_3C_{0.6}$, $Mo_{0.95}Hf_{0.05}C_{0.75}$ AND Mo_2C. Sadagapan, V.; Gatos, H. C. (Massachusetts Inst. of Tech., Cambridge). Contract SD-90. J. Phys. Chem. Solids, 27: 235-8(Feb. 1966).

The superconducting transition temperatures of the following carbides $Mo_{4.8}Si_3C_{0.6}$ (Nowotny phase, hexagonal, $D8_8$-type), $Mo_{0.95}Hf_{0.05}C_{0.75}$ (cubic, Bl type) and Mo_2C (orthorhombic) were found to be 7.6, 14.2, and 12.2°K respectively. The carbon-centered molybdenum-atom octahedron, which is the common crystallographic characteristic of these materials, is believed to be primarily responsible for superconductivity. The role of nonstoichiometry (carbon deficiency) in the superconducting behavior of the carbides and in particular of Mo_2C is discussed. The possibility of obtaining new superconductors among complex ternary and quaternary transition metal phases with the β–Mn, $E9_3$, $E2_1$ and Cr_2AlC structure types is discussed on the basis of their crystallochemical similarities with the carbides studied. (auth)

17608 ULTRASONIC ATTENUATION AND MAGNETIC PROPERTIES OF SUPERCONDUCTING NIOBIUM IN THE MIXED STATE. Ikushima, A. (Osaka Univ.); Fujii, M.; Suzuki, T. J. Phys. Chem. Solids, 27: 327-34(Feb. 1966).

The ultrasonic attenuation coefficient was measured in superconducting niobium as a function of temperature and magnetic field. The observed temperature dependence of attenuation in zero magnetic field agreed rather well with the BCS theory, and the magnitude of the energy gap at 0°K was found to be $(3.5 \pm 0.1)kT_c$. In a magnetic field, the attenuation coefficient began to increase at the initial penetration field, H_{c1}, and reached a value corresponding to the normal state at the upper transition field, H_{c2}. The variation of the attenuation was compared with the behavior of the magnetization of the same specimen, assuming that the effective energy gap in the mixed state is proportional to the square root of the magnetization. Good agreement was found when temperature was close to T_c, whereas a remarkable discrepancy occurred at lower temperatures. The discrepancy was particularly large near H_{c1}. Finally, following the recent theory given by Maki, two parameters, κ_1, κ_2, and their temperature dependence were determined. (auth)

17609 CRITICAL CURRENTS IN SUPERCONDUCTING SINGLE CRYSTAL NIOBIUM DISELENIDE. Spiering, G. A.; Revolinsky, E.; Beerntsen, D. J. (Allis-Chalmers Research Labs., Milwaukee). J. Phys. Chem. Solids, 27: 535-41(Mar. 1966).

Critical current measurements on superconducting $NbSe_2$ single crystals revealed peak effects in addition to the anisotropy reported earlier. In some orientations, the critical current of certain crystals increases with magnetic field for fields higher than about 7 kG. For a particular field in this region, the peak current was usually at an intermediate position rather than when the plane of the crystal was parallel or perpendicular to the magnetic field. Evidence is presented which connects the peak effect anomaly with the degree of nonstoichiometry in the crystal. Mixed state resistivity data are also presented. (auth)

17610 PROPAGATION OF NORMAL REGION IN A SUPERCONDUCTING MAGNET. Shimamoto, Susumu; Ohtsuki, Sozi (Electrotechnical Lab., Tokyo). Jap. J. Appl. Phys., 5: 184-5(Feb. 1966).

The propagation of a normal region at the quenching of a superconducting magnet were investigated in a Nb–25% Zr solenoid. For the purpose of measuring the initiation and propagation of a normal region, taps were attached to the solenoid and the voltages were measured between them at the s-n transition. The result of a quantitative analysis of the oscillogram of the tap voltages and the mechanism of the propagation is discussed. (M.O.W.)

17611 DISPERSION OF SOUND IN SUPERFLUID HELIUM. Khalatnikov, I. M.; Chernikova, D. M. (Inst. of Theoretical Physics, Academy of Scienes, USSR) JETP Lett. (USSR) (Engl. Transl.), 2: 351-5(Dec. 15, 1965).

Translated from Zh. Eksp. Teor. Fiz., Pis'ma Redakt., 2: 566-72(Dec. 15, 1965).

At low frequencies ($\omega\tau \ll 1$) the absorption of sound is investigated with the aid of hydrodynamics equations. The question of sound propagation at not too low frequencies ($\omega\tau > 1$) is considered with the aid of the kinetic equation. These, together with the equations for the continuity of the mass and of the superfluid liquid, constitute a complete system of equations describing the propagation of sound in helium II. (M.O.W.)

17612 JUMP IN SPECIFIC HEAT ON GOING FROM THE SUPERCONDUCTING TO THE NORMAL STATE. Geilikman, B. T.; Kresin, V. Z. (Moscow State Extension Pedagogical Inst.). JETP Lett. (USSR)(Engl. Transl.), 3: 28-30(Jan. 1, 1966).

Translated from Zh. Eksp. Teor. Fiz., Pis'ma Redakt., 3: 48-51(Jan. 1, 1966).

The magnitude of the increase in the specific heat was studied on the basis of the two-band model. It was found that the temperature dependence of the specific heat changes appreciably in the presence of overlapping energy bands. (D.C.W.)

17613 PATH-INTEGRAL CALCULATION OF THE TWO-PARTICLE SLATER SUM FOR ^{4}He. Fosdick, Lloyd D.; Jordan, Harry F. (Univ. of Illinois, Urbana). Contract Nonr-1834(27). Phys. Rev., 143: 58-66(Mar. 4, 1966).

The Wiener integral formulation combined with Monte Carlo sampling was used to compute the two-particle Slater sum for ^{4}He for temperatures ranging from 273 down to 2°K, the lower practical limit for this computational method. This is equivalent to a calculation of the density-independent part of the pair distribution function. A Lennard-Jones 6-12 potential has been used to describe the interaction. Contributions from exchange were found negligible at 5°K and above. Comparisons with the Wigner-Kirkwood expansion are made. The second virial coefficients derived from these results are within two or three percent of the results obtained from the usual phase-shift calculation. (auth)

17614 TEMPERATURE SCALE FOR NEODYMIUM ETHYLSULFATE BELOW 1 DEG K. Blok, J.; Shirley, D. A.; Stone, N. J. (Univ. of California, Berkeley). Phys. Rev., 143: 78-84(Mar. 4, 1966). (UCRL-16345).

A thermodynamic method, γ-ray heating a statistical-mechanical method, and nuclear orientation, were used in

a complementary fashion to determine the final temperature reached on demagnetizing a single crystal of neodymium ethylsulfate (NES) from magnetic fields up to 20 kG, applied along the c axis at 1°K. The temperature scale so established allows nuclear-orientation data to be fitted much more satisfactorily than did the old scale, removing a troublesome S-shaped deviation. Two independent checks were made of the validity of the new scale. The nuclear magnetic moment of ^{137m}Ce is again corrected. The best value, obtained from orientation in both NES and cerium magnesium nitrate lattices is 0.69 ± 0.03 nm, using $\langle r^{-3}\rangle_{4f} = 4.44$ atomic units. (auth)

17615 SECOND-SOUND ATTENUATION ASSOCIATED WITH HOT IONS IN LIQUID He II. Bruschi, L.; Maraviglia, B.; Mazzoldi, P. (Univ., Rome). Phys. Rev., 143: 84-90(Mar. 4, 1966).

An extra attenuation of a second-sound wave associated with the motion of hot ions in liquid helium II was investigated in the range of temperatures 0.87−1.40°K. Such an attenuation manifests itself as a threshold phenomenon at a well-defined electric field E_α, which is found to coincide with the critical field E_C at which a "persistence" of the drift velocity $\langle V_D\rangle$ begins. The existence of a threshold indicates that there is a quite different hydrodynamical regime beyond the threshold. The threshold field has the temperature dependence $E_\alpha = Ae^{-\Delta_s/T}$, with $\Delta_s = 7.69 \pm 0.13$°K. Δ_s varies with pressure analogously to the Δ of rotons measured by neutron diffraction. It is found experimentally that the extra attenuation is an effect strictly associated with the ion. The attenuation is not interpretable in terms of the single-vortex-ring models so far existing. Comparisons are made with analogous experiments where the interaction between second-sound waves and vorticity is investigated. (auth)

17616 EFFECT OF NORMAL-FLUID MOTION ON THIRD SOUND IN LIQUID-HELIUM FILMS. Pollack, Gerald L. (National Bureau of Standards, Washington, D. C. Michigan State Univ., East Lansing). Phys. Rev., 143: 103-9(Mar. 4, 1966).

Some theoretical consequences are derived of a proposed viscous force on the normal-fluid component of the He II film. In contrast with earlier calculations, in which the normal fluid was assumed to be immobile, this new assumption allows large energy attenuations, such as have recently been observed in third sound in He II films and in a wave mode of He II partially clamped in narrow channels. Atkins's three equations describing third sound are modified to take account of energy and entropy transfer associated with normal-fluid motion, and wave modes are obtained which simultaneously satisfy these equations and the normal-fluid equation of motion with a viscous force $-R\nu_n$. The four wave variables are: ζ and T', respectively, the local fluctuations in film thickness and temperature, and ν_s and ν_n, the superfluid and normal-fluid velocities. Attenuation and velocity of the wave mode corresponding to third sound are calculated at temperatures from 1.2°K through T_λ for all values of the dimensionless viscosity coefficient $(R/\omega\rho)$. The maximum calculated attenuation varies from 0.47 cm^{-1} at 1.2°K to 17.3 cm^{-1} at 2.1°K; at the lower temperature the observed attenuation is about 2 cm^{-1}. However, the anomalously rapid decrease in velocity of third sound observed by Everitt, et al., could not be explained in this manner. Evidence for normal-fluid motion in the film is presented, and some feasible experiments for detecting it are described. (auth)

17617 PATTERN OF CURRENT FLOW IN NONIDEAL TYPE-II SUPERCONDUCTORS IN LONGITUDINAL MAGNETIC FIELDS. [PART] I. LeBlanc, M. A. R. (Univ. of Southern California, Los Angeles). Phys. Rev., 143: 220-3(Mar. 4, 1966).

The longitudinal magnetization of a wire of a nonideal type-II superconductor in the presence of a stationary longitudinal magnetic field H_a is seen to oscillate between paramagnetic and diamagnetic as a conduction current is impressed and removed. When a conduction current I near the critical value I_c is present, the longitudinal magnetization is paramagnetic and attains a maximum. With I = 0 after passage of a conduction current $I \lesssim I_c$, the longitudinal magnetization is diamagnetic. This diamagnetic magnetization appreciably exceeds the Meissner-effect diamagnetism exhibited by the sample at corresponding fields. This paramagnetism and diamagnetism have been investigated throughout the range $0 < H_a < H_{c2}$. The variation of the longitudinal magnetization through paramagnetic and diamagnetic states as the conduction current is isothermally varied through a full cycle starting at $I \lesssim I_c$ has also been measured. All of the observations are satisfactorily described by a simple model which requires that macroscopic conduction and induced currents flow in helical paths which seek to preserve the existing magnetic-flux configuration and maintain a constant inward-directed Lorentz-force density throughout the specimen in the presence of a stationary longitudinal magnetic field. (auth)

17618 EFFECT OF ELECTRON-DAMPED DISLOCATIONS ON THE DETERMINATION OF THE SUPERCONDUCTING ENERGY GAPS OF METALS. Mason, Warren P. (Bell Telephone Labs., Murray Hill, N. J. Columbia Univ., New York). Phys. Rev., 143: 229-35(Mar. 4, 1966).

When account is taken of the damping of dislocations by electrons—i.e., by electron viscosity—it is shown that the energy losses due to this source are appreciable and are different in the normal and in the superconducting states. By subtracting off these two losses for the acoustic attenuation measured for these two states, and using the relation between the residual attenuations for the two states determined from the BCS theory, a much better determination of the energy gaps for superconductors is obtained. For lead the value is $2\epsilon_0 = (4.1 \pm 0.1)kT_c$, in good agreement with other methods for measuring the gap. The electron damping of dislocations accounts also for the amplitude effect in the superconducting range first observed by Love and Shaw. Theoretical calculations by Tsuneto have indicated that the ratio of the attenuation in the superconducting to that in the normal state for longitudinal waves should be the same for the region $ql \ll 1$ as that which has been found by BCS in the region $ql \gg 1$. When account is taken of the dislocation damping effect, it is shown that existing data confirm this calculation. (auth)

17619 ENERGY GAP OF SUPERCONDUCTING TIN FILMS IN A MAGNETIC FIELD. Collier, R. S.; Kamper, R. A. (National Bureau of Standards, Boulder, Colo.). Phys. Rev., 143: 323-8(Mar. 4, 1966).

The behavior of clean superconducting thin films of tin in both parallel and perpendicular magnetic fields was observed. The results are quantitatively consistent with an interpretation based on the Ginzburg-Landau theory. For the parallel field one-dimensional numerical solutions of their equations were generated, while for the perpendicular field a refinement of a vortex model proposed by Tinkham which is based on their expression for free energy was used. (auth)

17620 INHERENT LOW-FREQUENCY LOSSES OF THE SUPERCONDUCTING SURFACE SHEATH. Fink, H. J. (Atomics International, Canoga Park, Calif.). Contract AT-(11-1)-GEN-8. Phys. Rev. Lett., 16: 447-50 (Mar. 14, 1966).

It is shown that the low-frequency losses of a superconducting surface sheath are an inherent feature of the critical state of the surface sheath and that flux-pinning is not required to explain the losses. (G.O.Y.)

17621 ELECTRON INTERFERENCE IN A NORMAL METAL INDUCED BY SUPERCONDUCTING CONTACTS. Rowell, J. M.; McMillan, W. L. (Bell Telephone Labs., Inc., Murray Hill, N. J.). Phys. Rev. Lett., 16: 453-6 (Mar. 14, 1966).

An oscillation was observed in the tunneling characteristics of junctions in which electrons tunnel into Ag films backed by superconducting lead. The oscillation was interpreted in terms of electron interference in the normal metal. (D.C.W.)

17622 EFFECT OF ELECTRON-SPIN PARAMAGNETISM ON THE CRITICAL FIELD OF THIN Al FILMS. Strongin, Myron; Kammerer, O. F. (Brookhaven National Lab., Upton, N. Y.). Phys. Rev. Lett., 16: 456-60(Mar. 14, 1966).

The results are presented of measurements of the critical field parallel to the plane of ~100-Å Al films through the field region in which spin paramagnetism limits the critical field. The data are discussed in terms of the simple two-fluid temperature dependence. (D.C.W.)

17623 FLUX PINNING AND FLUX-FLOW RESISTIVITY IN MAGNETICALLY COUPLED SUPERCONDUCTING FILMS. Giaever, I. (General Electric Co., Schenectady, N. Y.). Phys. Rev. Lett., 16: 460-2(Mar. 14, 1966).

The effect of magnetic coupling between two superconducting films on the flux pinning and the flux-flow resistivity was investigated on the basis of some measurements on tin films. (D.C.W.)

17624 SUPERCONDUCTIVITY IN THE CLOSE-PACKED INTERMEDIATE PHASES OF THE V–Ir, Nb–Ir, Nb–Rh, Ta–Rh, Nb–Pt, Ta–Pt, AND OTHER RELATED SYSTEMS. Sadagopan, V.; Gatos, H. C. (Massachusetts Inst. of Tech., Cambridge). Phys. Status Solidi, 13: 423-7(1966).

The superconducting behavior of various close-packed low symmetry intermediate phases in the V–Ir, Nb–Ir, Nb–Rh, Ta–Rh, Nb–Pt, Ta–Pt, Hf–Rh, and Hf–Ir systems was investigated. By considering the σ-phase as a close-packed phase, a smooth relationship was found between its superconducting transition temperature (T_c) and those of the other close-packed phases (of a given system) on the one hand and their composition on the other. In each system the σ-phase exhibited the highest T_c. The normal behavior of the close-packed phases of the pseudobinary systems $NbRu_3-NbPt_3$, $NbIr_3-NbPt_3$, $NbOs_3-NbPt_3$, and $ZrPt_3-NbPt_3$ down to 1.6°K is considered consistent with the model of Gusman and Brout. (auth)

17625 THE ROLE OF INDUCTANCE IN SUPERCONDUCTING ENERGY STORAGE SYSTEMS. Hanrahan, D. J. (Naval Research Lab., Washington, D. C.). Proc. IEEE (Inst. Elec. Electron. Eng.), 54: 67-8(Jan. 1966).

The performance of a superconductor energy storage system is marred by the presence of inductance in either the superconducting switch or the load. The superconducting switch should be made noninductive, and the effects of both load inductance and finite switch resistance may be minimized by a current-step-down out-put transformer. A superconducting energy storage system is shown, and its operation is discussed. (J.F.P.)

17626 A NEW TYPE OF SUPERCONDUCTING MAGNET FOR TRAVELING-WAVE MASERS. Walker, B. J. (Dept. of Defense, Washington, D. C.). Proc. IEEE (Inst. Elec. Electron. Eng.), 54: 96-7(Jan. 1966).

An experimental model of a superconducting magnet designed primarily for use with traveling-wave masers is described. This magnet eliminates the ferromagnetic return path but includes the superconducting shield to obtain the required spatial homogeneity in the air gap. A cross sectional sketch is shown. This design results in a magnet that is considerably lighter in weight and easier to fabricate than the more conventional cyclotron-type superconducting magnet. (J.F.P.)

17627 ELECTRON TUNNELLING EVIDENCE FOR FLUXON ENTRY INTO THIN TYPE II SUPERCONDUCTING FILMS. Sutton, J. (Central Electricity Research Labs., Leatherhead, Eng.). Proc. Phys. Soc. (London), 87: 791-802(Mar. 1966).

Electron tunneling from a normal metal into thin type II superconducting films (Pb–In 20 wt %) was studied as a function of magnetic field H and film thickness (600–7000 Å) at 4.2 and 1.5°K. The behavior at high field confirms the work of Tomasch: surface superconductivity is quenched at H_{c2}, the upper critical field, when H is perpendicular to the film surface, but persists to H_{c3}, the surface sheath-critical field, in a parallel field ($H_{||}$). The degree of surface conductivity is characterized by a current profile ΔI, defined by the tunnel junctions' (I,V) characteristics. For films thicker than 1000 Å, a plot of ΔI against $H_{||}$ exhibits a series of dips which is dependent on film thickness and temperature. At fields where this structure is present, hysteresis is found in decreasing H. The structure and hysteresis are attributed to entry and exit of fluxons from the films. Penetration of $H_{||}$ into a thin film causes fluxon entry to be delayed to a field H_{e0}, greater than H_{c1}, the Abrikosov lower critical field. It is argued that subsequent fluxon entry into a thin film will occur mainly at fields close to H_{en}, at which the spacing of fluxons is such as to permit their hexagonal packing into the film's finite thickness. Reasonable agreement is found between the calculated values for H_{en} and the fields at which the minima of the dips occur in the ($\Delta I, H_{||}$) characteristics. An image calculation of the surface barrier to fluxon entry and escape from thin films shows that their effect becomes less pronounced as film thickness is reduced. It is thought that, in the films used in these experiments, barriers to fluxon entry are rendered ineffective by surface irregularities so that fluxon entry is not delayed above H_{e0}. In a decreasing field fluxons are thought to be trapped by the surface barrier to fluxon escape and cause hysteresis in a plot of ΔI against $H_{||}$. A mechanism is proposed by which the variation in the rate of fluxon entry into the films produces the structure in the ($\Delta I, H_{||}$) characteristics. The argument is based on dubious assumptions as to the microscopic factors governing ΔI. (auth)

17628 PRESENT STATE OF SUPERCONDUCTIVITY PROBLEMS. Abrikosov, A. A. Usp. Fiz. Nauk, 87: 125-42(1965). (In Russian).

Superconductivity studies ranging from the discovery of the phenomenon by Karmerlingh Onnes to recent ideas on the possibility of producing materials which would remain in the superconducting state at room temperature are described. The discovery of the isotope effect by Allen and Maxwell in 1950, followed by the Frohlich-Bardeen concept of an attractive interaction between electrons, are cited as the first step which led to a full explanation of superconductivity in the form of the Bardeen-Cooper-Schrieffer and Bogolyubov theories. The basic formulas of these theories, such as the coupling energy, critical temperature, and temperature dependence of the critical field, are listed and briefly explained. The problem of surface energy, termed as basic to the understanding of the phenomenon, is discussed in greater detail, and it is shown how investigations of surface energy led to Abrikosov's postulate that two kinds of superconductors exist in nature. An outline of the theory of second-kind superconductivity, as proposed by Abrikosov in 1957 and further developed by Gor'kov and other Soviet and Western students of the mixed state is considered. The present-day use of superconductors for the production of strong magnetic fields and in memory devices in computer networks is briefly mentioned, and further practical applications are predicted. Such applications will perhaps be related to recent demonstrations of the possibility of the coexistence of the superconducting and ferromagnetic phases. Though the present simplified model appears to restrict the critical temperatures to beneath 40°K, Abrikosov does not exclude the possibility that other mechanisms of electron attraction will be discovered, which will make the use of very low temperatures unnecessary. (ATD)

17629 EXPERIMENTAL STUDIES ON THE DEGRADATION PHENOMENA IN SMALL SUPERCONDUCTING COILS OF Nb-25 PERCENT Zr. Ruefenacht, J.; Steinemann, A. (Institut Batelle, Geneva). Z. Angew. Math. Phys., 16: 713-20(1965). (In French).

The model of a thermally insulated conducter of the third type permits a simple clarification for the transition into the normal conducting state established in small wire-drawn coils of Nb–25% Zr. The transition occurs for a coil current i that is below the critical value i_c measured on free Nb–25% Zr samples. The model used the concept of a localized temperature increase ΔT_l that was developed through the power loss as a result of the finite spatial displacement of the flux lines in superconducting materials. The experimental results can be transferred to a system of coaxial coils. (tr-auth)

17630 ENERGY LOSSES IN THE FEEDING OF SUPERCONDUCTING COILS WITH MAGNETIC FLUX PUMPS ACCORDING TO H. L. LAQUER. Risch, Rudolf (Brown, Boveri and Cie, Baden, Switzerland). Z. Angew. Math. Phys., 16: 826-30(1965). (In German).

The Joule losses appearing in the flux pump proposed by H. L. Laquer to excite superconducting solenoids were examined. These losses originate in two cryotrons used alternately. Those which appear in the auxiliary circuit are of two types. One type is provoked by the aperture of the cryotron and it can be avoided if the current is increased by stages. The other type is provoked by the increase of the current and it can be reduced if the current is varied very slowly. The losses which appear in the cryotron in parallel with superconducting coil can not be neglected. In the most favorable case they amount to half the energy stored in the solenoid. (tr-auth)

17631 SUPERCONDUCTING HOLLOW CYLINDER AS MAGNETIC LENS. Boersch, H.; Bostanjoglo, O.; Grohmann, K. (Technische Univ., Berlin). Z. Angew. Phys., 20: 193-4(1966). (In German).

The magnetic flux, trapped in a superconducting cylinder, was used for electron-optic imaging. The magnetic field of superconducting lenses can have smaller dimensions and a greater constancy than that of conventional magnetic lenses. (auth)

17632 THE PREPARATION AND SUPERCONDUCTIVITY OF Nb_3Sn DIFFUSION LAYERS WITH ADDITION OF ZIRCONIUM OR TITANIUM. Neubauer, H.; Saur, E.; School, H.-G. Z. Phys., 189: 417-22(1966). (In German).

Vapor pressure and immersion probes were prepared by the diffusion of tin into zirconium- or titanium-containing Nb wires and the transition to superconductivity was investigated. The increase of the transition temperature found by DeSorbo was confirmed at a high concentration range of a supplementary element. (tr-auth)

17633 TEMPERATURE DEPENDENCE OF THE MAGNETIZATION IN THE MIXED STATE OF SUPERCONDUCTING ALLOYS. Neumann, L.; Tewordt, L. (Univ., Hamburg). Z. Phys., 191: 73-80(1966).

The theory of Abrikosov of the immediate subcritical region in the mixed state is extended by means of the generalized Ginzburg-Landau theory to temperatures below T_c and arbitrary mean path l of the electrons. The results for the magnetization and the free energy can still be presented in the form derived by Abrikosov apart from the fact that κ is replaced by a new parameter $\kappa_2(T)$. The slope of the curve κ_2/κ versus $t = T/T_c$ at $t = 1$ is found to decrease monotonically from -0.105 to $-(1.367 - 0.136\,\kappa^{-2})$ as l increases from zero to infinity. The results for short mean free paths are consistent with experiment, in particular, κ_2 is always larger than κ in the vicinity of T_c. But the experimental temperature dependence of κ_2/κ in pure Nb is much higher than the theoretical one. (auth)

17634 INVESTIGATION OF THE EFFECT OF UNIFORM COMPRESSION AND PLASTIC DEFORMATION OF THE SUPERCONDUCTING PROPERTIES OF TITANIUM. Brandt, N. B.; Ginzburg, N. I. (Moscow State Univ.). Zh. Eksp. Teor. Fiz., 49: 1706-14(Dec. 1965). (In Russian).

The superconducting properties of various samples of 99.99% pure titanium iodide are investigated between 0.06 and 0.6°K and the effect of plastic deformation and uniform compression at pressures up to 26000 atm is studied. Plastic deformation and also the state of the sample surfaces are found to have a strong effect on the superconducting transition temperature T_k and critical fields H_k in titanium. Pressures up to ~14000 atm which are close to the hydrostatic pressure do not change or produce only a very small reversible increase of T_k and H_k in single crystal, plastic-deformed or lathe-turned titanium samples irrespective of their superconducting parameters. At pressures between 14000 and 26000 atm a sufficiently reversible increase of T_k and H_k is observed in plastic deformed samples compressed at a mean value of $\approx 0.7 \cdot 10^{-5}$ degree/atm. (auth)

17635 NONLINEAR EFFECTS IN ULTRASONIC ABSORPTION IN SUPERCONDUCTING INDIUM. Bezuglyi, P. A.; Fil, V. D.; Shevchenko, O. A. (Inst. of Physics and Tech. of Low Temperatures, Academy of Sciences, Ukrainian SSR). Zh. Eksp. Teor. Fiz., 49: 1715-17(Dec. 1965). (In Russian).

The absorption of ultrasound in high purity single crystal indium is studied. A strong nonlinear dependence of absorption on amplitude of the sound field is observed in the superconducting state. The results qualitatively agree with the Granato–Lücke model for amplitude-independent absorption of ultrasound on dislocations. (auth)

17636 INVESTIGATION OF THE HIGH-FREQUENCY JOSEPHSON CURRENT. Dmitrenko, I. M.; Yanson, I. K. (Inst. of Physics and Tech. of Low Temperatures, Academy of Sciences, Ukrainian SSR). Zh. Eksp. Teor. Fiz., 49: 1741-53(Dec. 1965). (In Russian).

Results are presented on an experimental investigation of the dependence of the step-like structure of the volt-ampere curves of the Sn–I–Sn superconducting tunnel junctions on temperature, stationary magnetic field strength and size of the junction. It is shown that the steps are due to the interaction between the density wave of the Josephson current and resonance high frequency electromagnetic oscillations in the tunnel junction forming the strip resonator. Cases when the junction width is larger or smaller than twice the depth of penetration of the magnetic field into the transition are investigated. The experimental results qualitatively are in good agreement with the theory. (auth)

17637 EFFECT OF IMPURITIES ON THE SUPERCONDUCTING TRANSITION TEMPERATURE. Baryakhtar, V. G.; Falko, I. I.; Makarov, V. I. (Inst. of Physics and Tech., Academy of Sciences, USSR. Kharkov State Univ.). Zh. Eksp. Teor. Fiz., 49: 1858-67(Dec. 1965). (In Russian).

The effect of diamagnetic impurities on the temperature of the superconducting transition is considered for the case when the topology of the superconductor Fermi surface can be modified by adding impurities. It is shown that under these conditions the dependence of the superconducting transition temperature on the impurity concentration is not linear ($T_k \sim \sqrt{n}\ln n$). Depending on the nature of the change in the Fermi surface topology, the superconducting transition temperature may either increase or decrease with growth of n. (auth)

17638 RESONANCE RADIATION FROM LIQUID HELIUM. Petrov, Yu. V. (Ioffe Inst. of Physics and Tech., Leningrad). Zh. Eksp. Teor. Fiz., 49: 1923-6 (Dec. 1965). (In Russian).

The effect of surrounding fermions and bosons on processes, the final products of which are the same fermions and bosons, is discussed. For liquid ^{3}He this effect leads to a red shift of the upper boundary of the radiation spectrum of the excited atoms by an amount equal to a double Fermi energy and, possibly, to an increase of the lifetime of the atoms in the excited state. For liquid ^{4}He the lifetime in the excited state should decrease and the transparency of the medium at the resonance line should increase. (auth)

17639 EFFECT OF PRESSURE ON THE SUPERCONDUCTING TRANSITION TEMPERATURE. Baryakhtar, V. G.; Makarov, V. I. (Inst. of Physics and Tech., Academy of Sciences, Ukrainian SSR). Zh. Eksp. Teor. Fiz., 49: 1934-7(Dec. 1965). (In Russian).

Expressions for the superconducting transition temperature and critical magnetic field strength derivatives with respect to pressure are obtained in terms of quantities observed experimentally, viz. the electron and lattice compressibility and Grunaisen constants. The formulas derived satisfactorily describe the magnitude and sign of the derivatives $\partial T_k/\partial P$, $\partial H_k/\partial P$ for most of the pure superconductors. (auth)

17640 RELAXATION PHENOMENA IN SUPERFLUID HELIUM. Khalatnikov, I. M.; Chernikova, D. M. (Inst. of Theoretical Physics, Academy of Sciences, USSR). Zh. Eksp. Teor. Fiz., 49: 1957-72(Dec. 1965). (In Russian).

It is shown that the relatively slowest relaxation process in superfluid helium is establishment of equilibrium between the phonon and roton gases. An equation set which describes the propagation of sound waves is derived by taking into account relaxation processes; the equation set is valid for small as well as for large frequency values. (auth)

17641 ATTENUATION OF SECOND SOUND IN ROTATING HELIUM ON TRANSITION THROUGH THE PHASE TRANSFORMATION TEMPERATURE. Andronikashvili, E. L.; Bablidze, R. A.; Tsakadze, Dzh. S. (Inst. of Physics, Academy of Sciences, Georgian SSR). Zh. Eksp. Teor. Fiz., 50: 46-50(Jan. 1966). (In Russian).

The formation of quantized Onsager-Feynman vortexes in rotating helium on transition through the phase transformation point is investigated by the method of second sound attenuation. It is shown that an isotropic mass of vortex nuclei is initially produced which gradually lines up in the system of vortexes aligned along the rotation axis. The relaxation times are measured for various angular velocities and different degrees of overcooling. (auth)

17642 RELAXATION OF ONSAGER-FEYNMAN VORTEXES IN HEATING OF ROTATING HELIUM II ABOVE THE PHASE TRANSFORMATION TEMPERATURE. Andronikashvili, E. L.; Gudzhabidze, G. V.; Tsakadze, Dzh. S. (Inst of Physics, Academy of Sciences, Georgian SSR. Tbilissi State Univ.). Zh. Eksp. Teor. Fiz., 50: 51-4 (Jan. 1966). (In Russian).

The decay of vortex lines in the superfluid component of rotating helium II, which occurs on transition to helium I, is investigated by the oscillating disc method. The decay takes place as a three-step relaxation process. In the first stage decay of the disc oscillations remains unchanged which signifies that in helium I the vortex pattern of the rotating fluid characteristic of helium II and responsible for the additional damping of the disc oscillations is completely conserved. The vortexes subsequently become detached from the disc surface and the damping becomes even lower than would be expected for helium I under the given conditions. Finally, during the third stage of the relaxation the expected stable damping value is gradually attained. The duration of the first of these processes is measured as a function of the velocity of rotation and temperature and also of the degree of roughness of the disc. Possible factors conditioning the prolonged existence of the vortexes in helium I and their subsequent decay are discussed. (auth)

17643 RELAXATION PROCESSES RELATED TO TEMPERATURE CHANGES IN ROTATING HELIUM II. Gudzhabidze, G. V.; Tsakadze, Dzh. S. (Tbilissi State Univ. Inst. of Physics, Academy of Sciences, Georgian SSR). Zh. Eksp. Teor. Fiz., 50: 57-61(Jan. 1966). (In Russian).

Processes related to changes in the elastically plastic properties of rotating helium II and appearing upon change of the liquid temperature are investigated. The study is carried out by cooling helium II as well as by heating it. (auth)

17644 FLOW OF A SUPERFLUID LIQUID IN POROUS MEDIA. Mamaladze, Yu. G.; Cheishvili, O. D. (Inst. of Physics, Academy of Sciences, Georgian SSR). Zh. Eksp. Teor. Fiz., 50: 169-78(Jan. 1966). (In Russian).

A modified equilibrium equation of phenomenological superfluidity theory is proposed for describing helium II in porous media. It is shown that in the vicinity of a large helium II volume the density of the superfluid component in a porous substance increases, the penetration depth of the influence being larger the narrower the pores. The flow of the superfluid component through a porous medium is considered and the critical fluxes at which superfluidity is broken are evaluated. (auth)

17645 COEXISTENCE OF SINGLET AND TRIPLET PAIRS IN AN ANISOTROPIC SUPERCONDUCTOR. Batyev, E. G. (Inst. of Physics of Semiconductors, Siberian Academy of Sciences, USSR). Zh. Eksp. Teor. Fiz., 50: 215-19(Jan. 1966). (In Russian).

It is demonstrated that in a coupling constant range the coexistence of singlet and triplet pairs in an anisotropic superconductor should be possible. (auth)

17646 ON PAIRING WITH AN ORBITAL MOMENT $l \neq 0$. Privorotskii, I. A.; Chesnokov, S. V. (Inst. of Physics and Tech., State Atomic Energy Commission, USSR). Zh. Eksp. Teor. Fiz., 50: 232-42(Jan. 1966). (In Russian).

Two-particle excitations are investigated for the case of pairing with $l = 2$. Stability of the anisotropic state with respect to these excitations is proven. It is shown that the two-particle excitation spectrum satisfies the Landau superfluidity condition. (auth)

17647 ON THE DYNAMICS OF A SUPERFLUID FERMI GAS. Kemoklidze, M. P.; Pitaevskii, L. P. (Inst. of Physics, Academy of Sciences, Georgian SSR. Inst. of Problems in Physics, Academy of Sciences, USSR). Zh. Eksp. Teor. Fiz., 50: 243-50(Jan. 1966). (In Russian).

A nonlinear differential equation is derived, which should be satisfied by the gap Δ in a superfluid Fermi gas. The equation is valid under the condition that the change in Δ over distances of the order of the correlation length v_F/Δ and for times of the order of $1/\Delta$ is small. The deduction is performed for the case of absolute zero temperature. It is shown that the hydrodynamic equations of an ideal liquid are a corollary of the equation derived. (auth)

17648 SPECULAR REFLECTION OF PHONONS IN SUPERFLUID HELIUM BELOW 0.33 DEGREES KELVIN [Thesis]. Rosen, Carol Zwick. Hoboken, N. J., Stevens Inst. of Tech., 1965. 158p.

Specular reflection of phonons was observed in superfluid helium at 0.33°K. At this temperature the phonon mean free path is larger than the dimensions of the focusing apparatus. Phonons emanated in various directions from a small carbon transmitter driven by a 155-cps sinusoidal signal. This caused a 310-cps Joule heating effect, which generated the phonons. Some proceeded directly to a concave fused quartz mirror where they were specularly reflected. When the mirror was sharply focussed, so that the carbon receiver was conjugate to the transmitter, an enhanced signal as much as 14 times greater than the unfocussed phonon background signal was recorded. Thus, phonons were directly manipulated simply by means of a spherical mirror to form the heater image at the carbon detector. (Dissertation Abstr.)

17649 PREPARATION AND PROPERTIES OF SUPERCONDUCTING NIOBIUM–TIN SANDWICHES. Piper, J.; Kebler, R. W.; Binder, I. (Union Carbide Research Inst., Tarrytown, N. Y.). 8p. (CONF-651031–4). ORAU. Gmelin, AED-CONF-65-331-2.

From American Society of Metals Meeting, Detroit.

Flexible ribbons capable of carrying currents of 10^5 amp/cm^2 were prepared by the heat treatment of Nb/Sn/Nb diffusion sandwiches. The effect of the preparation conditions on the structure and superconducting properties of the sandwiches was studied. Cylinders of Nb_3Sn were also fabricated using pairs of concentric hollow cylinders of Nb with Sn interlayers. (D.C.W.)

Neutron Physics

See also REACTOR TECHNOLOGY — Criticality Studies

Refer also to abstract 18006.

17650 (AAEC/E–144) A FUNCTION ARISING FROM SECOND ORDER APPROXIMATIONS TO THE EFFECTIVE RESONANCE INTEGRAL. McKay, M. H.; Pollard, J. P. (Australian Atomic Energy Commission Research Establishment, Lucas Heights). Nov. 1965. 14p. Dep. mn.

A function $K(\theta,a_1,a_\lambda,x_0^*)$, which occurs in the evaluation of second order approximations to the effective resonance integral, is investigated. Various approximations to this function are given for a range of parameters appro-

priate to resonance calculations and a description is given of an economic numerical method of evaluating the function accurately. (auth)

17651 (AD-612192) NUCLEAR PHYSICS AND COSMIC RAYS. Annual Progress Report for Period Ending 1964. (Bartol Research Foundation, Swarthmore, Pa.). Mar. 11, 1965. Contract Nonr377700. 23p. CFSTI $1.00 cy, $0.50 mn.

Information is included on: resonance fluorescence studies on lifetime of the 6.880-Mev level in ^{28}Si, properties of the 4.403 and 4.504-Mev excited states of ^{27}Al, properties of the 7.15-Mev state in ^{31}P, polarization of the resonance radiation from the 2.21-Mev level in ^{27}Al; theoretical studies on excitation of analog states by inelastic electron scattering; cosmic ray studies on isocosms, the cosmic ray equatorial longitude effect, the north and south plateau intensities; atmospheric absorption of nucleonic component, and neutron multiplicity experiments. (TAB)

17652 (CEA-R-2867) RESOLUTION DE L'EQUATION DE DIFFUSION (DEUX DIMENSIONS, PLUSIEURS REGIONS, CONTOURS QUELCONQUES) [THESES]). (Solution of the Diffusion Equation (2 Dimensions, Several Media, Arbitrary Boundary) [Thesis]). Nguyen Luong Than (Commissariat a l'Energie Atomique, Saclay (France). Centre d'Etudes Nucleaires). Nov. 1965. 117p. Dep. mn.

Submitted to Ecole Nationale Superieure de l'Aeronautique, Paris, France.

Quite often practical problems involve relatively complicated geometrical shapes and several very different media. The technique used here (variable mesh spacings) has the following advantages: it enables one to approximate curved contours more easily, distribute the mesh points more economically and smooth out discontinuities due to two very different media (danger of poor convergence). The method of programming by subroutines made available to engineers and scientists who are not well acquainted with numerical analysis a simple and foolproof iterative method: it suffices to pass by all the mesh points and to call the corresponding subroutine each time. (auth)

17653 (LA-3463) NEUTRON CAPTURE CROSS SECTIONS OF SOME RARE EARTH NUCLEI. Bell, George I. (Los Alamos Scientific Lab., Univ. of California, N. Mex.). Jan. 1966. Contract W-7405-eng-36. 16p. Dep. mn. CFSTI $1.00 cy, $0.50 mn.

Statistical theory was used to calculate neutron capture cross sections of some rare earth nuclei for neutron energies of 1 and 10 kev. For nuclei with measured low-energy resonance parameters, these parameters are used in the theory for s-wave capture; for other nuclei, the level density is computed from a semi-empirical expression, and the strength function and Γ_γ are determined by interpolation or extrapolation. Qualitative agreement was found with the experimental values of $\sigma(n,\gamma)$. Particular attention is given to the isotopes of Eu(Z = 63) which probably have larger $\sigma(n,\gamma)$ than any other rare earths. Capture cross sections for the stable Eu nuclei (A = 151, 153) are large because of large strength functions and small competition from compound elastic scattering (i.e. small $\langle\Gamma_n\rangle$). The odd-odd Eu isotopes (especially ^{152}Eu) should have slightly larger $\sigma(n,\gamma)$ (because of even smaller $\langle\Gamma_n\rangle$), but their capture cross sections are unlikely to be more than about 20% larger than that for ^{151}Eu. Results for other nuclei are given. (auth)

17654 (RT/PROT-(65)31) ON THE POSSIBILITY OF OBTAINING A STANDARD SOURCE OF THERMAL NEUTRONS. Mishev, I. T. (Comitato Nazionale per l'Energia Nucleare, Rome (Italy)). Oct. 1965. 9p. Dep. mn.

After corresponding investigations a method was obtained to realize a standard thermal neutron source with 4η geometry using a standard fast neutron source embedded in a paraffin sphere with thickness 7 cm and external radius R. (auth)

17655 NEUTRON FLUX PERTURBATIONS DUE TO INFINITE PLANE ABSORBERS II: EXPONENTIAL FLUX. Williams, M. M. R. (Univ. of Birmingham, Eng.). Brit. J. Appl. Phys., 16: 1841-52(Dec. 1965).

The problem considered is that of the activation of a non-scattering foil placed in an exponential flux. A pair of coupled, non-singular, integral equations for the surface angular distributions were obtained by the Wiener-Hopf method. These were solved numerically. The results indicate that the angular distributions incident on the two faces of the foil are very different from those which exist in the constant source problem. Nevertheless, it was found that provided C, the ratio of scattering to total cross section, lies within the range $0.9 < C < 1.0$, then the flux distortion factors for the two problems are practically identical. An explanation of this is given. (auth)

17656 NUMERICAL SOLUTION OF THE DIFFUSION EQUATIONS WITH THE KANTOROVICH METHOD. Galligani, I. (CCR, Euratom, Ispra, Italy); Giorcelli, M. Energia Nucl. (Milan), 13: 73-81(Feb. 1966).

The time-independent two dimensional neutron diffusion equations are solved with a variational method (Kantorovich's method). This method is particularly convenient when the neutron flux is a smooth function along one of the two directions. A comparison between this method and the finite difference method is made by means of some numerical examples. (auth)

17657 ON THE SPECTRUM OF NEUTRON TRANSPORT EQUATION IN FINITE BODIES. Albertoni, S. (Univ. of Milan. A.R.S. SpA, Milan); Montagnini, B. J. Math. Anal. Appl., 13: 19-48(Jan. 1966).

A general and rigorous theory of the spectrum of the transport equation for thermal neutrons is given. The free-gas model is adopted, and an arbitrary (well-shaped) finite body is considered as a domain for the space variables. The only important assumption is that of isotropic scattering in the laboratory system. The results confirm those of others and prove that the spectrum is made of a continuous part plus a finite number of real eigenvalues, this number being zero if the sample is small enough. (J.F.P.)

17658 A SPECTRAL THEORY FOR THE STATIONARY TRANSPORT OPERATOR IN SLAB GEOMETRY. Bareiss, Erwin H. (Argonne National Lab., Ill.). J. Math. Anal. Appl., 13: 53-92(Jan. 1966).

Patterned after the operational calculus of functional analysis, a spectral theory is constructed over a general function space for stationary transport operators in plane geometry as they occur in neutron theory, radiative transfer, etc. As an application, the general solution of the corresponding transport equations is given in closed form. It is shown that the spectrum of the isotropic transport operator consists of the union of a discrete spectrum of exactly two points, either real or pure imaginary; and a continuous spectrum which extends from ± 1 to $\pm\infty$ of the real axis. If the discrete spectrum of the anisotropic operator consists of two points only, as is the case in practical applications, the spectrum has the same properties as in the isotropic case. Proof and additional properties of the spectrum are derived under the assumption that the scattering functions have the physically important form $f(\Omega,\Omega') = f(\Omega \cdot \Omega') > 0$. (auth)

17659 AGE OF FISSION NEUTRONS TO INDIUM RESONANCE ENERGY IN IRON–WATER MIXTURES. I. EXPERIMENT. Paschall, R. K. (Atomics International, Canoga Park, Calif.). J. Nucl. Energy: Pt. A and B, 20: 25-35(Jan. 1966).

The age of fission neutrons to indium resonance energy (1.46 ev) was measured in mixtures of iron and water. Three different volume ratios of metal-to-water were investigated. The technique of a finite plane fission source with essentially infinite plane detectors was used previously to measure the age in pure water and mixtures of zirconium and water. The general curve of age vs. metal-to-water ratio is not a linear function with iron-water mixtures as it was with zirconium–water mixtures. (auth)

17660 AGE OF FISSION NEUTRONS TO INDIUM RESONANCE ENERGY IN IRON–WATER MIXTURES. II. THEORY. Alter, H. (Atomics International, Canoga Park, Calif.). J. Nucl. Energy: Pt. A and B, 20: 37-54(Jan. 1966).

The Monte Carlo Code, TYCHE-III, was used to calculate

with a high degree of convergence the second, fourth and sixth spatial moments of the slowing-down density distribution at the indium resonance energy, for neutrons originating from a fission source at a point in infinitely extended iron-water moderator. The effects of both inelastic scattering and anisotropy of elastic scattering in oxygen and iron were included. These calculations were compared with the moments of experimentally measured distributions of neutron flux at the indium resonance energy, after applying a suitable correction to the computed slowing down moments. (auth)

17661 DIFFUSION PARAMETERS OF GRAPHITE. Trikha, S. K.; Goyal, I. C. (Univ. of Delhi). J. Nucl. Energy, Pt. A and B, 20: 123-8(Feb. 1966).

The diffusion parameters (diffusion length L and diffusion constant D_0) have been computed for graphite moderator by using two different scattering kernels, one due to Parks and the other based on the Krumhansl and Brooks model of lattice vibrations. The diffusion length for pure graphite moderator comes out to be in good agreement with the experimental results. Calculated values of the decay constant λ for a neutron pulse for large blocks of graphite, agree well with the experimental results, but for smaller assemblies, there is considerable disagreement in the two values. The value of D_0 obtained is fairly close to the experimentally observed value. (auth)

17662 EXISTENCE OF HIGHER TIME DECAY CONSTANTS IN PULSED NEUTRON EXPERIMENTS. Wood, J. (Univ. of Birmingham, Eng.). J. Nucl. Energy, Pt. A and B, 20: 143-6(Feb. 1966).

A discussion is given on how the existence and number of higher eigenvalues (decay constants) in an infinite medium depends upon the nature of the moderator. (B.G.D.)

17663 CALCULATION OF EFFECTIVE CUTOFF ENERGIES TAKING INTO ACCOUNT SCATTERING AND HIGHER RESONANCES OF FILTERS. Tsuchihashi, Keiichiro; Iizumi, Masashi (Japan Atomic Energy Research Inst., Tokyo). J. Nucl. Sci. Technol. (Tokyo), 2: 506-15(Dec. 1965).

A refinement on the calculation of the effective cutoff energies of neutron filters was made by taking into account the scattering and higher resonances of the filters. The effect of scattering is found to be considerable, especially in the case of resonance detectors. With Sm and Gd filters the higher resonances introduce marked deviations of the cutoff energies from those calculated without taking their effect into account. These two factors of scattering and higher resonances cause the epithermal neutron flux from the 1/E-spectrum to strongly affect the cutoff energies. (auth)

17664 SLOW NEUTRON SPECTRA IN MOLECULAR HYDROGEN AT LOW TEMPERATURES. Koppel, J. U.; Young, James A. (General Atomic Div., General Dynamics Corp., San Diego, Calif.). Nukleonik, 8: 40-5(Jan. 1966). (GA-6003).

The integral properties of the scattering cross section for molecular hydrogen at low temperature were computed. In addition, neutron spectra for both space-independent and space-dependent geometries were calculated at 20.4°K, the boiling temperature of liquid hydrogen. (auth)

17665 VALIDITY OF THE CONVOLUTION APPROXIMATION FOR THE VAN HOVE G(r,t) FUNCTION. Nossal, Ralph (Univ. Libre, Brussels. National Bureau of Standards, Washington, D. C.). Phys. Rev., 143: 74-7 (Mar. 4, 1966).

The validity of the convolution approximation is examined by expanding the spatial Fourier transforms of both the true and the approximate Van Hove G(r,t) function in powers of the density. Only the lowest order terms in the expansions are explicitly calculated. However, comparison of the latter indicates that, for intermediate values of k, terms which are retained in the approximation are of magnitude comparable to that of terms which are neglected. It is concluded, therefore, that the convolution approximation fails at low density for intermediate values of k. (auth)

17666 QUASICLASSICAL APPROXIMATION IN THE THEORY OF SLOW NEUTRON SCATTERING. Yul'met'ev, R. M. (Kazan Pedagogical Inst.). Ukr. Fiz. Zh., 10: 1168-75(1965). (In Russian).

Wigner's representations were used to find the asymptotic expansion in $\hbar$ for the law of coherent scattering of slow neutrons by a substance. A correlation is obtained between the scattering laws, calculated by quantum and classical means, making it possible to satisfy the correlation of detailed equilibrium, the rule of sums and the known moments of Placzek. (auth)

17667 NEW DETERMINATION OF THE NEUTRON SCATTERING AMPLITUDE OF ZINC. Fischer, P.; Haelg, W.; Stoll, E. (Eidgenoessische Technische Hochschule, Zurich). Z. Angew. Math. Phys., 16: 820-1(1965). (In German).

The neutron scattering length of zinc was redetermined by means of neutron diffraction on a mixture of zinc and nickel powder. A value of $0.57_3 + 0.001 \times 10^{-12}$ cm was obtained. (auth)

17668 TRANSPORT CALCULATION OF THE DISADVANTAGE FACTOR [Thesis]. Robinson, Alan Hadley. Stanford, Calif., Stanford Univ., 1965. 148p.

The disadvantage factor of a two-region slab lattice was calculated for both the one-velocity and energy-dependent problems. Case's formalism is used for the one-velocity problem, while the method of Ferziger and Leonard is used for the energy-dependent problem. Ferziger and Leonard's method utilizes an energy modal expansion, while retaining completeness in the treatment of the spatial and angular variables. Although a closed form solution was not obtained, the Fredholm equations for the expansion coefficients converge very rapidly under iteration. For numerical work, an IBM 7090 code based on the results was written. The disadvantage factor can be calculated with this code in two seconds for the one-velocity problem and in six seconds for the energy-dependent problem. These results are as accurate as any other method. In the one-velocity case, the use of a computer is not necessary, and hand calculations can be done. Comparisons between the methods developed here and other currently used methods are also given. In addition, an approximate method for cylindrical geometry was found, which yields good results. (Dissertation Abstr.)

17669 APPARATUS FOR THE PRODUCTION OF NUCLEAR REACTIONS ON A PARALLEL ELECTRODE, ESPECIALLY FOR THE PRODUCTION OF NEUTRON PULSES (NEUTRON FULGURITE). Schmidt, Albrecht (to Gesellschaft fuer Kernforschung mbH). German Patent 1,206,095. Dec. 2, 1965. Filed Aug. 27, 1960.

A neutron-generator tube is designed, which comprises a radio-frequency ion source with two opposing electrodes for the extraction and acceleration of ions, which are arranged diametrically in relation to the center of the generated plasma. One of the electrodes is the target, the distance of which from the surface of the plasma is at most twice the diameter of ion beam at the surface of the target. (Gmelin Inst.)

Nuclear Properties and Reactions

Refer also to abstracts 16336, 16508, 17250, 17401, 17444, 17474, 17614, 17994, and 18057.

17670 (AD-629576) LEVELS OF ^{85}Sr POPULATED IN THE DECAY OF ^{85}Y AND ^{85m}Y. Horen, D. J.; Kelly, W. H. (Naval Radiological Defense Lab., San Francisco, Calif.). Nov. 18, 1965. 48p. (USNRDL-TR-962).

Evidence is presented for the existence of two isomers in ^{85}Y with half lives of 2.9 ± 0.2-h and 4.7 ± 0.2-h. Positron, photon, and x-ray measurements, both singles and coincidence, were performed. No evidence was obtained for the existence of an isomeric transition between the two isomers. A tentative decay scheme for 2.9-h ^{85}Y is presented which includes levels in ^{85}Sr at 0.237 (^{85m}Sr, 1/2-), 0.740 (1/2-, 3/2-) and 1.152 (1/2-, 3/2-) Mev. A decay scheme for

4.7-h ^{85}Y is proposed with levels at 0.231 ($^{7}/_{2}$+), 0.769, (0.802), 1.263, 1.353, 1.556, 1.630, 2.118, 2.169, (2.329), 2.351, and 2.779 Mev. Consideration of the data suggests that 2.9-h ^{85}Y has spin and parity $^{1}/_{2}$−, and lies approximately 0.040 Mev above 4.7-h ^{85}Y which has spin and parity $^{9}/_{2}$+. The log ft values suggest that most of the levels populated in the 4.7-h decay have spins and parities $^{7}/_{2}$+, $^{9}/_{2}$ or $^{11}/_{2}$+, the latter being less preferred because of the photon branching ratios. Although additional experimental data are required to make possible a detailed comparison with the even parity level structure of ^{85}Sr as predicted by Talmi and Unna, the apparent preponderance of levels with spins between $^{7}/_{2}$ and $^{11}/_{2}$ indicates one might expect poor agreement. (auth)

17671 (AEEW-M-611) CWF AND TABLE—TWO FORTRAN PROGRAMMES FOR THE CALCULATION OF COULOMB PENETRATION AND SHIFT FACTORS. Norton, D. S.; James, M. F. (Atomic Energy Establishment, Winfrith (England)). Dec. 1965. 14p. Dep. BIS $0.50. HMSO 2s. 6d.

CWF and TABLE are Fortran programs, written for the IBM 7090 and English-Electric Leo Marconi KDF9 computers, that calculate the penetration and shift factors for a charged particle in a Coulomb field. The numerical methods used are those of Lutz and Karvelis. The two programs are very similar. Input to TABLE is in the form of the center-of-mass coordinates. CWF is intended for use in calculating cross sections for neutron-induced reactions which result in charged particle emission, and the input is in the form of the neutron energy in the laboratory frame of reference, together with other necessary reaction data. (auth)

17672 (AERE-R-5053) A COMPUTER PROGRAMME FOR THE CALCULATION OF COMPOUND NUCLEAR CROSS-SECTIONS BY THE HAUSER-FESHBACH THEORY. Wilmore, D. (Atomic Energy Research Establishment, Harwell (England)). Jan. 1966. 14p. Dep. BIS $0.50. HMSO 2s. 6d.

Hauser and Feshbach (Phys. Rev. 87: 366 (1952)) showed that if the processes of formation and decay of the compound nucleus are assumed to be independent then use of the reciprocity theorem allows the differential cross sections in all the reaction channels to be calculated. This calculation requires the transmission coefficient for all the inverse reactions, and these may be calculated from the optical potentials appropriate to these reactions. A computer program is described that carries out this calculation for any mass, charge, and spin of incident particle and target nucleus. The transmission coefficients for the incoming and all the outgoing channels may be fed in directly if they are known, or if not they are calculated from optical potentials. The program then calculates the differential cross section for the elastic scattering of the incident particle and the differential cross sections in all two-body reaction channels, including the compound elastic cross section when the incident particle is re-emitted into the incident channel. The reaction cross sections are all symmetric about 90°. Spin-orbit forces are not taken into account in the calculations. (M.O.W.)

17673 (BNWL-CC-325(Vol.1)) BNW MASTER LIBRARY. VOLUME I. Stewart, K. B. (Battelle-Northwest, Richland, Wash. Pacific Northwest Lab.). Sept. 1, 1965. Contract AT(45-1)-1830. 284p. ORAU.

The BNW Master Library is an evaluated, microscopic neutron cross section library with the data contained on magnetic tape in a form that will allow a computer program to rapidly retrieve and process the neutron cross section data for a particular isotope. The data included is a listing of the library for isotopes ^{1}H to ^{91}Y by the computer program UPDATE. (M.O.W.)

17674 (BNWL-CC-325(Vol.2)) BNW MASTER LIBRARY. VOLUME II. Stewart, K. B. (Battelle-Northwest, Richland, Wash. Pacific Northwest Lab.). Sept. 1, 1965. Contract AT(45-1)-1830. 303p. ORAU.

The BNW Master Library is an evaluated, microscopic neutron cross section library with the data contained on magnetic tape in a form that will allow a computer program to rapidly retrieve and process the neutron cross section data for a particular isotope. The data included is a listing of the library for isotopes ^{90}Zr to ^{161}Gd by the computer program UPDATE. (M.O.W.)

17675 (BNWL-CC-325(Vol.3)) BNW MASTER LIBRARY. VOLUME III. Stewart, K. B. (Battelle-Northwest, Richland, Wash. Pacific Northwest Lab.). Sept. 1, 1965. Contract AT(45-1)-1830. 243p. ORAU.

The BNW Master Library is an evaluated, microscopic neutron cross section library with the data contained on magnetic tape in a form that will allow a computer program to rapidly retrieve and process the neutron cross section data for a particular isotope. The data included is a listing of the library for the isotopes ^{159}Tb to ^{239}Pu by the computer program UPDATE. (M.O.W.)

17676 (CEA-R-2810) ETUDE DES FLUCTUATIONS DES LARGEURS RADIATIVES PARTIELLES ET TOTALES PAR LA CAPTURE DES NEUTRONS DE RESONANCE [THESES]. (Study of the Fluctuations of the Partial and Total Radiative Widths by Neutron Capture Resonance [Thesis]). Huynh Vinh Dinh (Commissariat a l'Energie Atomique, Saclay (France). Centre d'Etudes Nucleaires). 1965. 105p. Dep. mn.

Submitted to Paris Univ., France.

The distributions of partial radiative widths, the effects of correlation between different radiative transitions, fluctuations of total radiative widths Γ_γ from resonance to resonance, the variation of Γ_γ with the mass number, and the existence of potential capture were studied using time-of-flight techniques. (D.C.W.)

17677 (COO-1420-112) BETA-GAMMA CIRCULAR POLARIZATION CORRELATION OF ^{122}Sb. Grabowski, Z. W.; Raghavan, R. S.; Steffen, R. M. (Purdue Univ., Lafayette, Ind. Dept. of Physics). [1964]. Contract AT(11-1)-1420. 14p. Dep. mn. CFSTI $1.00 cy, $0.50 mn.

The angular dependence of the circular polarization of the 566-kev gamma radiation following the first-forbidden 1400-kev β transition of ^{122}Sb is studied. The β-γ circular polarization correlation is consistent with a cos θ dependence. The data confirm that shape and the angular correlations of the 1400-kev β transition of ^{122}Sb are well described by the Coulomb approximation. The ratio of scalar type to vector type matrix element components in this β-transition is studied. The β-γ circular polarization correlation results obtained make possible the reduction of the number of solutions obtained for the six nuclear matrix elements which enter into the $2^- \rightarrow 2^+$ 1400-kev β transition of ^{122}Sb. (auth)

17678 (COO-1420-113) SEARCH FOR HIGHER-ORDER EFFECTS IN ALLOWED β-TRANSITIONS. Grabowski, Z. W.; Raghavan, R. S.; Steffen, R. M. (Purdue Univ., Lafayette, Ind. Dept. of Physics). [1964]. Contract AT(11-1)-1420. 22p. Dep. mn. CFSTI $1.00 cy, $0.50 mn.

The β-γ directional correlations of several allowed β transitions with unusually large ft-values (log ft > 7) were measured. Effects of second-forbidden β components are expected to manifest themselves in small observable anisotropies if these second-forbidden matrix elements are not reduced appreciably by those nuclear structure effects that cause the reduction of the allowed matrix elements. The experimental results for the anisotropy factor $A_2(W)$ in the β-γ directional correlation function $W(\theta) = 1 + A_{22}(W)P_2(\cos\theta)$ are: ^{22}Na(W_0 = 1.69, log ft = 7.4); $A_{22}(\overline{W} = 1.8) = -0.001 \pm 0.005$; ^{56}Co($W_0$ = 3.88, log ft = 8.6), $A_{22}(\overline{W} = 3.3) = -0.001 \pm 0.003$; ^{124}Sb($W_0$ = 2.23, log ft = 7.7), $A_{22}(\overline{W} = 2.0) = +0.002 \pm 0.003$; ^{134}Cs($W_0$ = 2.3, log ft = 8.9), $A_{22}(\overline{W} = 1.9) = +0.003$; ^{160}Tb($W_0$ = 2.1, log ft = 8.1), $A_{22}(\overline{W} = 1.9) = +0.012 \pm 0.006$. Except for the highly deformed ^{160}Tb, no evidence of interference effects with second-forbidden β-components was found indicating that whatever the mechanism that reduces the allowed matrix elements, somehow also reduces the second-forbidden matrix elements. The small anisotropy found in ^{160}Tb may be a result of some K-selection rule effect or may be caused by a competing forbidden β transition. Evidence for the existence of such a β transition which, however, is very difficult to fit into the established ^{160}Tb decay scheme is given. (auth)

17679 (DESY–65/15) HIGHLY POLARIZED COHERENT BREMSSTRAHLUNG FROM A DIAMOND TARGET IN THE Gev REGION. Bologna, G.; Lutz, G.; Schulz, H. D.; Timm, U.; Zimmermann, W. (Deutsches Elektronen-Synchrotron, Hamburg (West Germany)). Nov. 1965. 24p. Dep. mn.

The bremsstrahlung spectra obtained from a diamond radiator at an electron energy of 4.8 Bev is discussed. The work has essentially two results: (1) The exponentially screened potential of the C atom which was used earlier in calculating the bremsstrahlung cross section is not consistent with the experimental spectra. Instead a Hartree type screening potential was used which fits the data very well. (2) The linear polarization obtained from the first peak in a spectrum is much increased, if the orientation of the primary electron momentum is chosen to lie not in the fundamental reference planes of the crystal but at a small angle to one of them. (auth)

17680 (FEI–26) ZAPAZDYVAYUSHCHIE NEITRONY U POROGA DELENIYA TORIYA-232. (Delayed Neutrons of the Fission Threshold of ^{232}Th). Maksyutenko, B. P. (Gosudarstvennyi Komitet po Ispol'zovaniyu Atomnoi Energii SSSR, Obninsk. Fiziko-Energeticheskii Institut). 1965. 4p. Dep. mn.

Emission of delayed neutrons with half lives of 2.2, 5.2, 15.5, and 24 sec was measured in the neutron fission of ^{232}Th at 1.6 to 2.6 Mev, using the T(p,n)^{3}He reaction as a neutron source. Results of relative emission intensities and their accuracy are given. (M.J.T.)

17681 (IAE–966) SPEKTR GAMMA-LUCHEI VOZNIKAYUSHCHIKH PRI ZAKHVATE TEPLOVYKH NEITRONOV V TELLURE. (Spectrum of Gamma-Rays Emitted During the Capture of Thermal Neutrons in Tellurium). Groshev, L. V.; Demidov, A. M.; Shadiev, N. (Institut Atomnoi Energii, Gosudarstevennyi Komitet po Ispol'zovaniyu Atomnoi Energii SSSR, Moscow). 1965. 16p. Dep. mn.

The spectrum of γ rays emitted in the capture of thermal neutrons by Te was measured using a magnetic Compton spectrometer with 0.3% resolution. Identification of the γ lines with the Te isotopes was carried out. Detailed data were obtained for the isotope ^{124}Te. The neutron binding energy of this isotope was determined to be 9410 ± 5 kev. The decay of the initial state of the isotopes ^{124}Te, ^{114}Cd, and ^{118}Sn is examined. (tr-auth)

17682 (INP–428/PL) TRANSVERSE SPIN POLARIZATION IN ODD-MASS DEFORMED NUCLEI. Bochnacki, Zbigniew; Ogaza, Stanislaw (Institute of Nuclear Physics, Krakow (Poland)). Oct. 1965. 11p. Dep. mn.

The spin polarization effect on the value of the magnetic parameter b_0 for the K = ½ rotational bands and on M1 transitions between low-lying states of odd-mass deformed nuclei is considered. The results of numerical calculations for the ground state rotational band of the ^{169}Tm nucleus are presented. (auth)

17683 (INP–430/PL) THE g-FACTOR OF THE 87 kev EXCITED STATE IN ^{155}Gd. Hrynkiewicz, A. Z.; Ogaza, S.; Styczen, J.; Hrastnik, B.; Pudlowska, B.; Kulessa, R. (Institute of Nuclear Physics, Krakow (Poland)). Nov. 1965. 16p. Dep.

The g-factor of the 87-kev state in ^{155}Gd was measured by the observation of the perturbation of angular correlation in the external magnetic field in melted metallic sources, using both integral and differential techniques. The results are in good agreement with the value obtained indirectly from the magnetic hfs-coupling in a liquid source. The structure of the 87-kev level is discussed on the basis of the average value g = –0.376 ± 0.026. (auth)

17684 (JAERI–1085) NELKER: A CODE FOR SCATTERING KERNEL CALCULATION FOR BOUND HYDROGEN. Shimada, Syoichiro (Japan Atomic Energy Research Inst., Tokyo). Dec. 1964. 9p. (In Japanese). Dep. mn.

A description is presented of the NELKER code in FORTRAN-II for IBM-7090. NELKER is a program for calculating the thermal neutron scattering-kernel matrices for bound hydrogen by Nelkin's formulation. In addition to the scattering kernel the program computes the following quantities: differential scattering cross sections, total scattering cross section and transport cross section, and scattering law. Limitations in the code are as follows: the number of energy mesh points ≤60, the number of scattering angles ≤20, and the number of Legendre components of scattering kernel ≤3. The physical formulation of the kernel is also given. (auth)

17685 (JINR–P–2497) O RASPADE ^{159}Ho. (On the Decay of ^{159}Ho). Gromov, K. Ya.; Mukhtasimov, F. N. (Joint Inst. for Nuclear Research, Dubna (USSR). Lab. of Nuclear Problems). 1965. 12p. Dep. mn.

Using a β-spectrograph with a steady uniform magnetic field the conversion electron spectra due to the ^{159}Ho decay were studied. The resolving power of the β-spectrograph is about 0.05%. The accuracy in determining the energy is better than 0.05%. The results of investigations are listed. New γ transitions with the energies: 31.40; 41.14; 85.70; 100.60; 105.30; 132.00; 136.50; 153.05; 185.85; 186.40; 205.90; 217.67; 258.80; 338.70; 356.40; 395.40; 417.00 kev were found. The multipolarities of a number of γ transitions of ^{159}Ho were determined. According to the data obtained a decay scheme of ^{159}Ho is suggested. (auth)

17686 (JINR–P–2512) VLIYANIE SVERKHTONKOGO VZAIMODEISTVIYA V ATOMAKH NA YADERNYE γ-PEREKHODY. (Effect of Atomic Hyperfine Interaction on Nuclear γ-Transitions). Onishchuk, V. A. (Joint Inst. for Nuclear Research, Dubna (USSR). Lab. of High Energy). 1965. 6p. Dep. mn.

A concrete example is taken to illustrate the effect of hyperfine interaction on nuclear γ transitions. It is shown that in atomic states with a fixed projection of the total angular momentum the expressions for the angular distributions of both the polarized and unpolarized γ rays may involve noticeable interference terms. (auth)

17687 (JINR–P–2514) PROTONNYE IZLUCHATELI SREDI IZOTOPOV TELLURA. (Proton Emitters Among Te Isotopes). Vertogradov, L. S.; Karnaukhov, V. A.; Petrov, L. A.; Ter-Akop'yan, G. M. (Joint Inst. for Nuclear Research, Dubna (USSR). Lab. of Nuclear Reactions). 1965. 18p. Dep. mn.

Emitters of delayed protons produced by bombarding ^{92}Mo with ^{20}Ne, ^{22}Ne ions and ^{94}Mo with ^{20}Ne ions were investigated. Proton activities with half lives (4.2 ± 0.2)s, (19 ± 0.7)s, (13 ± 2)s, and 60–80s were found. It is most likely that the first two emitters are isotopes of Te with mass numbers 109 and 111, respectively. On the basis of the data obtained the cross sections for the reactions ^{92}Mo(^{20}Ne,4n)^{108}Te and ^{92}Mo(^{20}Ne,6n)^{106}Te were estimated. (auth)

17688 (JINR–P–2539) RADIOAKTIVNYE SVOISTVA YADER NAIBOLEE TYAZHELYKH ELEMENTOV. (Radioactive Properties of Nuclei of Heaviest Elements (Review)). Flerov, G. N.; Druin, V. A. (Joint Inst. for Nuclear Research, Dubna (USSR). Lab. of Nuclear Reactions). 1966. 23p. Dep. mn.

Experimental and theoretical data on radioactive properties of nuclei of transuranium elements were treated. Special attention is paid to spontaneous fission of nuclei both from the ground and excited (isomeric) state. (auth)

17689 (NP–15783) KVANTOVAYA DEPOLYARIZATSIYA ELEKTRONOV V MAGNITNOM POLE. (Quantum Depolarization of Electrons in Magnetic Field). Baier, V. N.; Orlov, Yu. F. (Akademiya Nauk SSSR, Novosibirsk. Institut Yadernoi Fiziki). 1965. 7p. Dep. mn.

High-energy (E = 6 Bev) electrons or positrons in a storage ring can be strongly polarized in a time of $\tau_{pol.}$ = 190 sec with a magnetic field H = 8000 gauss. Even though the particle energy can be chosen so as to avoid depolarizing resonances caused by radical and azimuthal constituents of the magnetic field, it is possible to obtain electron depolarization at high energies with small perturbations of the magnetic field. The effect is caused by the fact that the energy jump associated with the quantum character of the radiation contains harmonics that give resonances. If the most dangerous harmonics are eliminated, the depolariza-

tion effect will be considerably reduced. Quantum depolarization is investigated under the assumption that the electron trajectory is classical, but that the particle energy undergoes a quantum jump. With a reasonable choice of parameters (particle energy E = 6 Bev, H = 8000 gauss, R = 3000 cm), the analysis indicated that the depolarization time $\tau_{depol.}$ = 25 sec. Thus, the beam is not polarized, and it would be necessary to take special measures to maintain the polarization. However, it should be noted that the polarization is remarkably stable. (TTT)

17690 (NP–15899) AN ENERGY-WEIGHTED M1 SUM RULE. Arbman, G. (Forsvarets Forskningsanstalt, Stockholm (Sweden)). Mar. 1966. 25p. Dep. mn.

An energy-weighted M1 transition sum rule for nuclei is constructed, using shell-model jj-coupled wave functions. The sum is compared to the model-independent energy-weighted E1 sum and is calculated for spherical nuclei in the region $58 \leq A \leq 210$. (auth)

17691 (ORNL-TM–1235) DWBA ANALYSIS OF THE $^{90}Zr(d,p)^{91}Zr$ REACTION AT ENERGIES BETWEEN 3.5 AND 5.5 Mev. Smith, William R. (Oak Ridge National Lab., Tenn.). Nov. 22, 1965. Contract W-7405-eng-26. 13p. Dep. mn. CFSTI $1.00 cy, $0.50 mn.

The distorted-wave Born approximation (DWBA) theory was applied to $^{90}Zr(d,p)^{91}Zr$ angular distributions corresponding to bombarding energies of 3.5, 4.0, 4.5, 5.0, and 5.5 Mev and to levels in the residual nucleus of 0, 1.21, 2.07, and 2.56 Mev of excitation. A single set of parameters, differing slightly from the predictions of proton and deuteron elastic scattering, was found that reproduced most of the angular distributions satisfactorily. However, the spectroscopic factors obtained thereby were, on the average, 30% smaller than those obtained from analysis of 12-Mev data. (auth)

17692 (ORNL-TM–1414) INELASTIC EFFECTS IN STRIPPING AND OTHER DIRECT REACTIONS [Thesis]. Penny, S. K. (Oak Ridge National Lab., Tenn.). Mar. 1966. Contract W-7405-eng-26. 124p. Dep. mn. CFSTI $4.00 cy, $0.75 mn.

Submitted to Univ. of Tennessee, Knoxville.

The distorted-waves theory of direct nuclear reactions, such as deuteron stripping is generalized to include in the distorted waves the effects of the strong inelastic scattering which may be present when the nuclei show collective behavior. The possible changes in parity and angular momentum selection rules are discussed in detail. Formulas are given for the general case, and also for a simple model in which only one level of the target nucleus (assumed even) can be excited. Results of calculations are presented where the simple model is used to predict the angular distributions for three stripping reactions and two cases of inelastic scattering. (auth)

17693 (ORNL-TM–1464) PHASE-SHIFT ANALYSIS OF ELASTIC SCATTERING: THE CODE PEGGY. Owen, L. W. (Oak Ridge National Lab., Tenn.). Mar. 16, 1966. Contract W-7405-eng-26. 12p. Dep. mn. CFSTI $1.00 cy, $0.50 mn.

A least-squares search program was written in FORTRAN for the CDC-1604 computer which analyzes, in terms of phase shifts, the elastic scattering of spin zero and spin one-half particles by spin zero nuclei. Real or complex phase shifts may be used with or without spin-orbit coupling. Differential cross section and polarization angular distributions may be analyzed either separately or simultaneously. (auth)

17694 (STI/PUB/101(Vol.1)) PHYSICS AND CHEMISTRY OF FISSION. VOL. I. Proceedings Series. Proceedings of the Symposium held in Salzburg, 22–26 March 1965. (International Atomic Energy Agency, Vienna (Austria)). 1965. 645p. (CONF-650301(Vol.1)). IAEA: $13.00; S 273,–; £ 3.18.0; F Fr 52,–; DM 45,50.

Separate abstracts are prepared for 27 of the 47 papers presented. Abstracts of 20 papers previously appeared in NSA as 19: 14526, 14527, 15789, 16846, 21225, 21229, 27584, 27585, 29252, 29369, 29373, 29378, 29379, 29381, 29382, 30526, 31230, 31231, 31318, and 20: 6309. (C.E.S.)

For abstracts of individual papers see: 17843–17869.

17695 (STI/PUB/101(Vol. 2)) PHYSICS AND CHEMISTRY OF FISSION. VOL. II. Proceedings Series. Proceedings of the Symposium held in Salzburg, 22–26 March 1965. (International Atomic Energy Agency, Vienna (Austria)). 1965. 481p. (CONF-650301(Vol. 2)). IAEA: $10.00; S 210,–; £ 3.0.0; F Fr 40,–; DM 35,–.

Separate abstracts are presented for 18 of the 33 papers included. Abstracts of 15 papers previously appeared in NSA as 18: 40606, 19: 14508, 16848, 19079, 19093, 29253, 29370–29372, 29374–29376, 29380, 31317, and 20: 8143. (C.E.S.)

For abstracts of individual papers see: 17823–17840.

17696 (UR-875-65) ZERO RANGE DISTORTED WAVE ANALYSIS OF THE $^{16}O(^3He,\alpha_0)^{15}O$ REACTION. Alford, W. Parker; Blau, L. M.; Cline, D. (Rochester Univ., N. Y. Dept. of Physics and Astronomy). Nov. 20, 1964. Contract AT(30-1)-875. 13p. Dep. mn. CFSTI $1.00 cy, $0.50 mn.

Measurements of the $^{16}O(^3He,\alpha)^{15}O$ reaction leading to the ground state of ^{15}O, and the elastic scattering of ^3He from ^{16}O, are analyzed using an optical model in which the radius and diffuseness parameters are different for the real and imaginary parts of the potential well. This form of the optical model potential is found to be necessary in order to obtain agreement between DW calculations and measurements of the $^{40}Ca(^3He,\alpha)^{39}Ca$ reaction. The values of the parameters used for the incident ^3He channel were derived from elastic scattering data using the optical model search code HUNTER, the resulting values of which were essentially the same as those used in the DW analysis of the $^{40}Ca(^3He,\alpha)^{39}Ca$ ground state reaction. With these new optical parameters, the DW calculations reproduced the shape of the measured angular distributions quite well. The measured $^{16}O(^3He,\alpha)^{15}O$ reaction cross sections are about 24 times greater than the zero-range DW calculations. (auth)

17697 (WANL-TME–1028) A NEW CROSS SECTION LIBRARY FOR THE n + ^{235}U REACTIONS. Drawbaugh, D. W.; Gibson, G.; Melnick, M. M. (Westinghouse Electric Corp., Pittsburgh, Pa. Astronuclear Lab.). Nov. 11, 1964. Contract SNP-1. 60p. Dep. mn. CFSTI $3.00 cy, $0.75 mn.

In an enriched undermoderated reactor resonance absorption of epithermal neutrons must be considered. A new set of neutron cross sections of ^{235}U are presented. In particular resonances are included in the experimentally unresolved energy range from ~50 ev to 30,000 ev. Resonance self-shielding and Doppler broadening in this range is handled by a picket fence model for the resonance structure. Account is taken of the fact that within this statistical range there are in general two different distributions for each partial width of a resonance corresponding to different spin states of the compound nucleus. In the unresolved region use is made of the cross section measurements reported by Uttley and those in BNL-325. At low energies, $E < 1.86$ ev, the data of Shore and Sailor is used and at high energies, $E > 3.18 \times 10^4$ ev, data in the BNL-325 report is used. For the experimentally resolved energy region resonance parameters obtained recently by the Saclay group and also parameters given in the BNL-325 1964 supplement are used; smooth background cross sections due to the negative energy resonance are included. Values for the average number of prompt neutrons per fission are obtained from the empirical formulas based on measurements by Moat, Mather and Fieldhouse, and the fission energy spectrum is obtained from the experimental results of Cranberg and Nereson. The variation with energy of the resulting cross sections are shown to compare favorably with various experimental cross sections. Also results of calculations with the GAM, QUERY, and TNS codes are compared with results of integral experiments, viz. the fission integral, the absorption integral, and measured values of $\langle\alpha\rangle$. A comparison is also made of the calculated hydrogen-worth with the measured values for a particular experiment. (auth)

17698 (WANL-TME–1132) XO AND EXT—IBM-7094 PROGRAMS FOR COMPUTING: a. THE RESONANCE CROSS SECTIONS FOR A ZERO TEMPERATURE TARGET

(XO). b. THE MAXWELLIAN DOPPLER BROADENED BREIT-WIGNER RESONANCES (EXT). Gibson, G.; Melnick, M. M. (Westinghouse Electric Corp., Pittsburgh, Pa. Astronuclear Lab.). Mar. 1965. SNP-1. 113p. Dep. mn. CFSTI $4.00 cy, $1.00 mn.

The above mentioned programs are described in detail. (M.O.W.)

17699 (WANL-TME-1317) CURVE PLOT FOR "SCISRS". Melnick, Marian M. (Westinghouse Electric Corp., Pittsburgh, Pa. Astronuclear Lab.). Nov. 1965. Contract SNP-1. 42p. Dep. mn. CFSTI $2.00 cy, $0.50 mn.

The FORTRAN II program, Curve Plot for SCISRS (CPS) is used for plotting cross section data from the SCISRS (Sigma Center Information Storage and Retrieval System) library. The program is given along with results of sample calculations. (M.O.W.)

17700 (ZfK-PhA-17) THE DECAY OF ^{79}Kr. Winter, Georg (Zentralinstitut fuer Kernphysik, Rossendorf bei Dresden (East Germany)). Apr. 1965. 9p. Dep. mn.

The gamma ray spectrum of ^{79}Kr was investigated using a scintillation spectrometer and coincidence techniques. Five new gamma rays with energies of 940, 1030, 1080, 1120, and 1335 kev were observed. They de-excite a new level at 1335 kev. In a further experiment the L/K electron capture ratio of ^{79}Kr was determined by means of a multiwire proportional counter. The experimental value obtained is $P_L/P_K = 0.115 \pm 0.009$. This result is in agreement with recent calculations of Bahcall. (auth)

17701 THE HALF-LIFE OF THE SECOND EXCITED STATE IN ^{133}Cs. Scharbert, T. (Inst. of Nuclear Research, Debrecen). Acta Phys. Acad. Sci. Hung., 20: 185-7(1966).

The lifetime of the 161-kev second-excited level of ^{133}Cs was found to be $T_{\frac{1}{2}} = (9.7 \pm 2.6) \cdot 10^{-11}$ sec from measurements of prompt and delayed coincidences from ^{60}Co and ^{133}Ba, using a time-to-amplitude converter with a slow-fast system and two NaI(Tl) crystals. (L.B.S.)

17702 MEASUREMENT OF THE TOTAL CROSS SECTIONS OF Cs AND Rb FOR NEUTRONS OF 14 Mev ENERGY. Angeli, I.; Hunyadi, I. (Inst. of Nuclear Research, Debrecen). Acta Phys. Acad. Sci. Hung., 20: 193-5(1966). (In German).

The experimental arrangement and the results of measurement of the total cross sections of Cs and Rb for 14-Mev neutrons are discussed. The nuclear radius of ^{133}Cs and the mean value for Rb were also found from the measured cross sections. (L.B.S.)

17703 AN ALPHA-GAMMA AND ALPHA-CONVERSION ELECTRON COINCIDENCE STUDY OF ^{219}Rn, ^{215}Po, AND ^{211}Bi. Valli, K.; Aaltonen, J.; Graeffe, G.; Nurmia, M. (Univ. of Helsinki). Ann. Acad. Sci. Fenn., Ser. A VI, No. 184, 1-17(1965).

An alpha-gamma and alpha-conversion electron coincidence study was made of Rn-219, Po-215, and Bi-211 by means of scintillation and solid state detectors and two-parameter pulse height analysis. New information about the decay of the excited states of the daughter nuclei was obtained. A decay scheme was proposed for Rn-219. (auth)

17704 ON THE A(d, n)(A+1) STRIPPING REACTIONS. Kolltveit, Kristofer. Arbok Univ. Bergen, Mat.-Nat. Ser., No. 7, 1-9(1964).

The stripping amplitude is evaluated in the square well approximation by integrating inside the target nucleus. The main idea is to find a better basis for further investigations where exchange stripping effects are included. The resulting stripping amplitude shows the same angular dependence as former works. (auth)

17705 THE HYPERFINE STRUCTURE OF THE 16 HOUR STATE IN ^{119}Te. Aedelroth, K. E.; Lindgren, L.; Olsmats, M.; Sanner, L. (Univ. of Uppsala). Arkiv Fys., 30: 111-19(1965).

The atomic-beam magnetic-resonance technique was employed to measure the magnetic dipole interaction constant in the 16-hour state of ^{119}Te ($I = \frac{1}{2}$) with the result $|a| = (425 \pm 20)$ MHz. From this value the nuclear magnetic dipole moment is calculated to be $|\mu_I| = 0.27$ nm assuming a pure $5p^4$ electronic configuration. The effect of core polarization is estimated, and when this effect is taken into account the corrected nuclear moment becomes $|\mu_I| = (0.25 \pm 0.05)$ nm. (auth)

17706 THE NATURE OF THE GIANT RESONANCE IN PHOTONUCLEAR REACTIONS. Shevchenko, V.; Yudin, N. (Moscow State Univ.). At. Energy Rev., 3: 3-156(1965).

A review of experimental and theoretical studies of the nature of the giant resonance (dipole and quadrupole collective states) is presented. An account is given of the problems associated with the sum rules for dipole transitions as well as model interpretations of the photoeffect. 338 references. (D.C.W.)

17707 NUCLEON CLUSTERS IN LIGHT NUCLEI. Neudachin, V. G.; Smirnov, Yu. F. (Moscow State Univ.). At. Energy Rev., 3: 157-272(1965).

Various forms of α-clustering of nucleons in light nuclei are considered. The role of the Majorana forces and the characteristic features of the corresponding quantum numbers — the Young orbital diagrams $[\lambda]$ — are discussed. The relation between the shell model and the nucleon clustering model (NCM) is analyzed. Experimental data on the Eλ transition probabilities and the relevant form factors for inelastic scattering are used to describe methods of determining the NCM parameters. A wide range of nuclear reactions is examined. 231 references. (auth)

17708 DATA PROCESSING IN NUCLEAR PHYSICS. Amram, Y. (Commissariat a l'Energie Atomique, France). Bull. Inform. Sci. Tech., No. 97, 35-46(Oct. 1965). (In French).

Some of the problems arising from the use of digital computers for data processing in nuclear physics, are discussed. The ways in which, at the Departement d'Electronique Generale, studies are undertaken are indicated: data collection (preamplifiers...), spark chamber digitization, and design of a special purpose computing unit. (auth)

17709 DATA PROCESSING IN SOME NUCLEAR PHYSICS PROBLEMS. Corge, C. R. (Commissariat a l'Energie Atomique, France). Bull. Inform. Sci. Tech., No. 97, 55-70(Oct. 1965). (In French).

In the nuclear physics field data processing entails data acquisition, data reduction, analysis and simulation. In all of these the computer appears as a powerful tool if not essential. Data reduction is discussed referring to very simple examples. It is shown that computers must be more adapted to experiments and also that more work must be done to improve man-machine communication. (auth)

17710 ON LOW-LYING EVEN-PARITY LEVELS OF ^{18}F NUCLEUS. Narayana, K. L. (Andhra Univ., Waltair, India). Cur. Sci. (India), 35: 38-40(Jan. 20, 1966).

Calculations for nuclei with A = 18 are made using the intermediate-coupling individual particle model with a modified Gaussian potential and Serber and Rosenfeld exchange forces. The nuclei studied are treated as even-even core, A = 16 plus two nucleons in 1d and 2s harmonic oscillator orbitals. The two-nucleon interaction energy matrices for the ten different states of ^{18}F were constructed and diagonalized. The energy level order of ^{18}F and a comparison of the predicted and experimentally observed low-lying levels of ^{18}F are shown. (J.F.P.)

17711 MICROSCOPIC DESCRIPTION OF THE COLLECTIVE VIBRATIONS OF NUCLEI. Lovas, Istvan. Fiz. Szemle, 15: 363-71(Dec. 1965). (In Hungarian).

The model developed for explaining the properties of collective excitations is based on classical analogies, correlating the vibration and rotation of nuclei with oscillations of a liquid and rotations of a solid. The fact that nonclassical physical concepts are involved is expressed only by the quantization of the vibratory and rotational motions. The cases examined more closely include the dipole vibration or giant resonance. The microscopic theory of collective excitations was developed

on the basis of two-body interactions in order to evaluate the collective action of protons and neutrons. Anomalies in the angular distribution of the deuterons from the $^{16}O(p,d)^{15}O$ pick-up reaction may be explained by assuming that the neutron picked up by the proton was in a 1d state characterized by the l = 2 shell at the moment of the reaction. With some modification, the method of study described may be applied to other cases, such as quadrupole vibration excitations. Even though rotational states may be successfully described by the microscopic approach, no uniformly applicable theory has been developed for them. (TTT)

17712 THE HALF LIFE OF ^{32}P. Goodier, I. W.; Pritchard, Daphne H. (National Physical Lab., Teddington, Eng.). Int. J. Appl. Radiat. Isotop., 17: 121-3(Feb. 1966).

Precise measurements were made of the halflife of ^{32}P produced by both the $^{32}S(n,p)^{32}P$ and $^{31}P(n,\gamma)^{32}P$ reactions. Consideration was given to systematic errors including possible radiochemical impurities and a value of 14,290 days was obtained for the halflife of ^{32}P with a statistical error of ±0.014 days evaluated at one standard deviation. (auth)

17713 EFFECTS OF A CASCADE PROCESS ON THE YIELD OF ENERGETIC HELIUM ISOTOPES DURING PRIMARY 9-Bev PROTON REACTIONS WITH PHOTO-EMULSION NUCLEI. Kobzev, V. A.; Takibaev, Zh. S.; Shalagina, E. V. Izv. Akad. Nauk Kaz. SSR, Ser. Fiz.-Mat. Nauk, No. 2, 3-9(May-Aug. 1965). (In Russian).

An attempt is made to explain the mechanism of the formation of alpha particles with a kinetic energy >100 Mev that are emitted during the interaction of 9 Bev protons with emulsion nuclei. The existence of an alpha substructure within the nucleus is assumed. The angle θ_2 of emission of the alpha particle with respect to the direction of the incident cascade nucleon is plotted as a function of the kinetic energy T_2 of the alpha particle from kinematic considerations. The energy of the incident nucleon is varied from 1 to 9 Bev. The angle θ_1 of emission of the recoil nucleus (with respect to the direction of the incident cascade nucleon) is also given as a function of θ_2: $\theta_2 = f(\theta_1)$. The angles θ_1 and θ_2 cannot be determined experimentally, since the angle θ between the beam of primary protons and the direction of motion of the cascade nucleon is unknown. Therefore, a plot of the kinetic energy T_2 of the emitted alpha particle as a function of the angle θ is used for analysis. A total of 69 stars that were formed as a result of the interaction of 9 Bev protons with emulsion nuclei were subjected to an analysis, which showed that the emission of alpha particles could not be explained by the elastic scattering of cascade nucleons on an alpha substructure in the nucleus. No recoil protons (except for two doubtful cases) could be detected. The studies will be continued with the use of 19.5 Bev incident protons. (TTT)

17714 ON THE DIRECT INTERACTIONS IN REACTIONS WITH FINITE NUCLEI IN HIGHLY EXCITED STATES. Ushakov, V. V. Izv. Akad. Nauk Kaz. SSR, Ser. Fiz.-Mat. Nauk, No. 2, 10-14(May-Aug. 1965). (In Russian).

The differential cross section of (n,n') and (n,p) reactions is calculated with the following two assumptions: 1) the nucleus is taken to exist as two independent Fermi gases of protons and of neutrons, and 2) the direct interaction is due to a two-particle collision of the incident nucleon with one of the nucleons of the nucleus. The method of calculation makes no assumptions about whether or not the absorption of the incident nucleons is on the surface or within the volume of the nucleus, about the form of the potential well, or about wave reflection or refraction at the boundary of the nucleus. The reaction is assumed to occur in two stages: 1) the formation of a compound nucleus and 2) its break-up. Expressions are obtained for the differential cross sections of (n,n') and (n,p) reactions that are the same as that given by Brown and Muirhead. (TTT)

17715 PRODUCTION OF HIGH-ENERGY FRAGMENTS BY 7.5-Bev π MESONS. Takibaev, Zh. S.; Tleubergenova, G. A.; Lazareva, T. P. Izv. Akad. Nauk Kaz. SSR, Ser. Fiz.-Mat. Nauk, No. 2, 46-50(May-Aug. 1965). (In Russian).

The yield of fragments with Z > 3 and energy E > 5 Mev per nucleon was investigated by examining the tracks in an emulsion 400 μ thick irradiated with 7.5 Bev π-mesons. A total of 101 events having fragments with Z > 3 were detected. The charge of the fragments was determined from the track width on a section where the track width did not vary. The results showed that Li was present in 58 of the fragments, Be in 22, and B in 11 fragments. The cross section σ for the formation of the fragments with Z > 3 was 6.86 ± 0.68 mb without correcting for geometry, and 24.62 ± 1.29 mb on correcting for geometry. With Z > 4 the corresponding figures are 2.24 ± 0.39 and 8.01 ± 0.74 mb respectively. The charge distribution of the fragments with E > 5 Mev per nucleon did not depend on the nature or energy of the particle forming the fragment. It was shown that the maximum energy of the fragments could not be explained by a fission process. It was noted that the asymmetry for black tracks in stars with fragments increased as compared with the asymmetry in stars without fragments. Apparently a cascade process is primarily responsible for the formation of high-energy fragments. (TTT)

17716 HELIUM PARTICLES EMITTED DURING 17.5-Bev π-MESON COLLISIONS WITH PHOTOEMULSION NUCLEI. Takivaev, Zh. S.; Tleubergenova, G. A.; Lazareva, T. P.; Morozova, P. V.; Kazanskaya, A. P. Izv. Akad. Nauk Kaz. SSR, Ser. Fiz.-Mat. Nauk, No. 2, 51-9(May-Aug. 1965). (In Russian).

Helium particles with a kinetic energy >100 Mev were investigated by irradiating Ilford-G5 emulsion with 17.5 Bev π-mesons at an average π-meson flux of 4.7×10^4 cm^{-2}. Tracks of particles having a different charge were preliminarily separated from the dependence of the range of ionization, and were further identified from the number of delta electrons. A total of 241 helium particles with a kinetic energy greater than 100 Mev were found as a result of a detailed analysis of 21,300 spallations with N > 2. The angular distribution of the emitted helium particles was strongly anisotropic, and the degree of anisotropy did not depend on the energy of the primary π-mesons. The interaction cross-section of 17.5 Bev π-mesons for light and heavy emulsion nuclei were found to be $\sigma_l = 210 \pm 35$ mb, and $\sigma_h = 900 \pm 100$ mb, which values were in satisfactory agreement with calculated values. At least 95% of the interactions involving fast helium particles were emitted from heavy emulsion nuclei (Ag or Br). Nuclear fission or evaporation cannot explain the facts adequately. Rather an intranuclear cascade process must be invoked to explain the emission of fast helium particles. (TTT)

17717 YIELDS OF POTASSIUM ISOTOPES IN HIGH ENERGY BOMBARDMENTS OF VANADIUM, IRON, COBALT, NICKEL, COPPER AND ZINC. Chackett, K. F. (Birmingham, Univ., Eng.). J. Inorg. Nucl. Chem., 27: 2493-2505(Dec. 1965).

Potassium isotopes ^{38}K, ^{42}K, ^{43}K, ^{44}K, and ^{45}K were measured in interactions of protons at 590 Mev and 18.3 Bev with vanadium, iron, cobalt, nickel, copper, and zinc. Absolute cross sections were determined with reference to the $Al(p,3pn)^{24}Na$ reaction and estimates were made of the yield of ^{39}K, ^{40}K, and ^{41}K. The results showed a preferential loss by evaporation and spallation of about twenty nucleons in the bombardments at 18.3 Bev, an effect consistent with published Monte Carlo calculations. Predictions of the ^{39}K, ^{40}K, and ^{41}K cross sections should be of relevance to studies of the potassium content of iron meteorites. (auth)

17718 MEASUREMENT OF THE CAPTURE CROSS SECTION OF SODIUM BETWEEN 10 AND 135 kev. Le Rigoleur, C.; Bluet, J. C.; Bell, H.; Leroy, J. L. (CEN, Cadarache, France). J. Nucl. Energy: Pt. A and B, 20: 67-73(Jan. 1966). (In French).

The neutron capture cross section of sodium was measured relative to the $^6Li(n,\alpha)T$ reaction cross section. This measurement was made by an activation method. The monoenergetic neutron beam was obtained from a Van de

Graaff accelerator, using the $^{7}Li(p,n)^{7}Be$ reaction. The activity of the sodium sample was measured by a sodium iodide scintillator; the efficiency of this counter was determined by comparison with a β-counter in a 4π-geometry. The neutron flux was measured by a ^{6}Li glass scintillator. The cross section shows two resonances at 35 and 55 kev. The 35 kev resonance was not detected by previous total cross-section measurements. (auth)

17719 THE $^{10}B(n\alpha)$ BRANCHING RATIO. Sowerby, M. G. (Atomic Energy Research Establishment, Harwell, Eng.). J. Nucl. Energy, Pt. A and B, 20: 135-9(Feb. 1966).

The $^{10}B(n\alpha)$ branching ratio was measured in the energy range 23 ev – 0.5 Mev. The results show that the ratio is constant for neutron energies up to about 130 kev. (auth)

17720 CALCULATION OF THE CROSS SECTION FOR ^{238}U (n,γ) ^{239}U IN THE ENERGY RANGE 10 Kev-3 Mev. Beynon, T. D. (Woolwich Polytechnic, London). J. Nucl. Energy, Pt. A and B, 20: 146-9(Feb. 1966).

It is shown that the formula of Hauser and Feshbach for the energy averages of fluctuating compound nucleus cross sections in channel-spin representation can be used to evaluate the capture cross sections for ^{238}U for the range 10 kev – 3 Mev by suitable representation of the transmission coefficients and by allowing for the effect of fission competition above 1 Mev. (B.G.D.)

17721 MEASUREMENT OF DISTRIBUTION OF FISSION FRAGMENTS RECOILING INTO ALUMINUM. Mitsui, Hidehiko (Hitachi Ltd., Japan). J. Nucl. Sci. Technol. (Tokyo), 2: 481-4(Dec. 1965).

The distribution of fission fragments recoiled from a thick layer of uranium oxide into aluminum was measured with the application of an anodizing technique to strip layers from aluminum. Details of the procedure are described. The distribution thus determined gave the recoil ranges of the fission fragments: They were 4.06 mg/cm^2 for $^{95}Zr-^{95}Nb$ and 2.67 mg/cm^2 for $^{140}Ba-^{140}La$. The correction factors for these ranges to account for the scattering effect in the uranium oxide layer were estimated. The measured recoil ranges are compared with those previously reported by a number of investigators, and with calculation by semi-empirical formula. (auth)

17722 MEASUREMENT OF THE RESONANCE FISSION INTEGRAL OF ^{233}U. Yasuno, Takehiko (Japan Atomic Energy Research Inst., Tokyo). J. Nucl. Sci. Technol. (Tokyo), 2: 532-3(Dec. 1965).

The resonance fission integral of uranium-233 was measured relative to the resonance capture integral of gold-197. Both the gold and uranium foils were irradiated with and without the cadmium filter. The uranium-233 foil decay curve is shown for bare uranium and then for uranium covered by cadmium. The resonance fission integral for ^{233}U was found to be 838 ± 40 barns. (J.F.P.)

17723 NON EXISTENCE OF THE REPORTED 0.58 Mev GAMMA RAY IN THE DECAY OF ^{42}K. Miyano, Kazumasa (Tokyo Univ.). J. Phys. Soc. Jap., 20: 2094 (Nov. 1965).

An experiment was carried out to check the existence of the 0.58-Mev gamma transition previously reported in the decay of ^{42}K to ^{42}Ca from the third to the second excited state. The obtained coincidence gamma spectrum is shown. Photo peaks due to natural background and one at 0.90 in the peeling-off procedure were observed. But the reported 0.58-Mev gamma ray was not observed. The upper limit of the relative intensity of the 0.58-Mev gamma ray to the 0.90-Mev gamma ray was $5(10)^{-2}$: 1. (J.F.P.)

17724 MEDIUM DEPENDENCE OF CHARGE CHANGING COLLISIONS FOR 9.7 Mev CARBON IONS. Imanishi, Nobutsugu (Kyoto Univ.); Sakisaka, Masakatsu; Fukuzawa, Fumio; Uemura, Yoshiaki. J. Phys. Soc. Jap., 20: 2100-1 (Nov. 1965).

The equilibrium charge distribution for divalent carbon ions at 9.7 Mev was measured in foils of formvar, carbon, aluminum oxide, aluminum, silver, and gold. A systematic dependence of the charge-changing collision on the atomic number of the target material was found. The dependence of the ratio of the cross section for electron loss on that of capture is shown for the various media studied. The degree of ionization is also shown for these media. (J.F.P.)

17725 AN EXPERIMENTAL SURVEY OF NUCLEAR REACTIONS INDUCED BY 57 Mev PROTONS. PART II. (p,d) REACTIONS. Ishizaki, Yoshihide; Kikuchi, Ken; Matsuda, Kazuhisa; Mikumo, Takashi; Nakajima, Yutaka; Nonaka, Itaru; Saji, Yoshio; Suzuki, Arata; Yamaguchi, Hisashi; Eisberg, Robert (Tokyo Univ.). J. Phys. Soc. Jap., 20: 2118-28(Dec. 12, 1965).

With 57-Mev incident protons energy spectra of deuterons from the (p,d) reactions on ^{12}C, ^{27}Al, ^{58}Ni, Ag, Sn, ^{197}Au, and ^{209}Bi were measured by a scintillation counter telescope. Several prominent peaks were observed on ^{12}C, ^{27}Al and ^{58}Ni while very few on Ag, Sn, ^{197}Au and ^{209}Bi. The energy resolution was about 2.5% at half maximum. Angular distributions were obtained for the prominent peaks and were analyzed in terms of $j_l(qr)^2$ and of Butler curves. The peaks are considered to correspond to removal of neutron leaving a hole in a single particle state occupied in the target nucleus. In some cases, however, residual interactions may be taken into account. No clear peak was observed in the region of Q value less than about –25 Mev. (auth)

17726 CIRCULAR POLARIZATION OF THE γ RADIATION FOLLOWING THE STRIPPING REACTION. Zimanyi, Jozsef (Central Research Inst. of Physics, Budapest). Magyar Fiz. Foly., 13: 461-515(1965). (In Hungarian).

The chief difficulty in the theoretical treatment of nuclear reactions arises from the large number of the degrees of freedom of the examined systems. There are, however, certain types of reactions, in which only one or a few degrees of freedom are of importance while the others may be assumed to remain constant. Among the direct reactions, the deuterium stripping reactions have been most extensively examined. The (d,p) stripping reaction describes the noncentric collision of the bombarding deuteron with the target nucleus, resulting in a strong interaction with the loosely held neutron of the deuteron and ultimately in its capture, without affecting the path of the emitted proton. The intermediate system has a short life time and a high energy indeterminancy; the energy dependence of the reaction cross section does not exhibit resonances. The "central force distorted-wave Born approximation" (CFDWBA model) was used to derive the angular distribution and the polarization of the protons and the angular distribution and circular polarization of the subsequent γ emission. It is assumed that the incident deuteron wave and the emitted proton wave interact with the target and final nuclei, but this interaction is assumed not to contain spin-dependent members. The derived theoretical correlation between the various polarizations was experimentally studied using the Dresden cyclotron. The following stripping reactions were examined: $^{10}B(d,p)$ $^{11}*B_{2.14Mev}(\gamma)^{11}B_0$; $^{10}B(d,p)$ $^{11}*B_{4.46}(\gamma)$ $^{11}B_0$ and $^{12}C(d,p)$ $^{13}*C_{3.09}$ (γ) $^{13}C_0$. (TTT)

17727 PHENOMENOLOGY OF NUCLEAR FORCES. [PART] I. Kok, L. P.; van Wageningen, R. (Theoretische Natuurkunde, Groningen, Netherlands). Ned. Tijdschr. Natuur., 31: 205-28(July 1965). (In Dutch).

The present state of knowledge on the phenomenology of nuclear forces is reviewed with respect to the model theories. In part I low-energy phenomena are considered. (J.S.R.)

17728 PHENOMENOLOGY OF NUCLEAR FORCES. [PART] II. Kok, L. P.; van Wageningen, R. (Theoretische Natuurkunde, Groningen, Netherlands). Ned. Tijdschr. Natuur., 31: 297-320(Sept. 1965). (In Dutch).

The equations for the phenomenology of nuclear forces at high energies are derived. The S-matrix formalism, n-p scattering, the amplitude operator, polarization probabilities in nucleon-nucleon scattering, phase analysis, and nucleon-nucleon potentials are discussed. (J.S.R.)

17729 TWO-PROTON AND TWO-NEUTRON BINDING-ENERGY SYSTEMATICS AND ALPHA-DECAY ENERGIES.

Wapstra, A. H. (Instituut voor Kernphysisch Onderzoek, Amsterdam). Nucl. Data, 1: 1-19(Dec. 1965).

The binding energy of two neutrons and of two protons is plotted as a function of N and Z, respectively. The alpha decay energy is plotted as a function of N. The range covered is Z = 10 to 102 and N = 10 to 154. (D.C.W.)

17730 NUCLEAR TRANSITION PROBABILITY, B(E2), FOR $0^+_{g.s.} \rightarrow 2^+_{first}$ TRANSITIONS AND DEFORMATION PARAMETER, β_2. Stelson, P. H. (Oak Ridge National Lab., Tenn.); Grodzins, L. Nucl. Data, 1: 21-102(Dec. 1965). (ORNL-P-1795).

Adopted values for the reduced electromagnetic transition probability, $B(E2)_{ex}$, from the ground state to the first-excited 2^+-state of even-even nuclei are given. Values of β_2, the quadrupole deformation parameter, and of τ, the mean life of the 2^+ state, are also listed. The ratio of the value of β_2 to values expected from the single-particle model is presented graphically as a function of neutron number. As an indication of the extent of collective features in nuclear structure, this ratio seems a better measure than the value of β_2 itself. (auth)

17731 COINCIDENCE METHOD FOR STUDIES OF INTERNAL PAIR FORMATION FROM ANNIHILATION RADIATION. Spring, E. (Univ. of Helsinki). Nucl. Instrum. Methods, 40: 146-8(Feb. 1966).

The internal pair formation coefficient Γ can be determined for a specific transition by a triple-double coincidence method, in which Γ is obtained from the number of internal pairs and gamma rays in coincidence with another transition. This method was used for determination of the internal pair formation of the 2615 kev transition in ^{208}Pb. The result $\Gamma = (4.3 \pm 0.7) \times 10^{-4}$ is in close agreement with the value $\Gamma = (4.5 \pm 0.2) \times 10^{-4}$, which was simultaneously obtained from double coincidence experiments. The method described enables measurement of internal pair formation to a wider extent than before. (auth)

17732 PHASE-SPACE INTEGRALS FOR BETA DECAY AND NUCLEAR MATRIX ELEMENTS. Bahcall, John N. (California Inst. of Tech., Pasadena). Nucl. Phys., 75: 10-16(1966).

The use of phase-space integrals to determine nuclear matrix elements is discussed. The procedure for determining matrix elements is illustrated by analyzing the allowed and superallowed beta decays of isotopes with mass numbers in the range five to ten, utilizing the recent summary of the properties of nuclei in this region compiled by Ajzenberg-Selove and Lauritsen. Some f values for other beta decays of interest are also given. (auth)

17733 NUCLEAR MAGNETIC MOMENTS. Migdal, A. B. (Kurchatov Atomic Energy Inst., Moscow). Nucl. Phys., 75: 441-69(Jan. 1966).

Expressions for the nuclear magnetic moments are given accurately taking into account the nucleon-nucleon interaction. Comparison with experiment makes it possible to determine the constants introduced in the theory and in particular the constant of the spin-spin interaction between the constituent nucleons; the value of this constant is in agreement with other experimental facts. A simple expression, in good agreement with experiment, is obtained for the sum of the magnetic moments of a neutron and a proton in identical states. The equations obtained can be used for the calculation of the matrix form factors of nuclei. (auth)

17734 COULOMB EXCITATION OF LOW-ENERGY STATES IN Ce, Nd, AND Sm ISOTOPES. Eccleshall, D. (Atomic Weapons Research Establishment, Aldermaston, Eng.); Yates, M. J. L.; Simpson, J. J. Nucl. Phys., 78: 481-91(1966).

The even-nuclei ^{140}Ce, ^{142}Ce, ^{142}Nd, ^{146}Nd, ^{148}Nd, ^{150}Nd, ^{144}Sm, ^{148}Sm, and ^{150}Sm and the odd-nuclei ^{143}Nd and ^{145}Nd were Coulomb-excited using oxygens ions. The following B(E2) values for the ground to first excited state transitions in units of e^2b^2 were obtained: ^{140}Ce, 0.27 ± 0.04; ^{142}Ce, 0.42 ± 0.01; ^{142}Nd, 0.42 ± 0.05; ^{143}Nd, 0.047 ± 0.013; ^{144}Nd, 0.44 ± 0.02; ^{146}Nd, 0.65 ± 0.01; ^{148}Nd, 0.96 ± 0.02; ^{144}Sm, 0.25 ± 0.04; ^{148}Sm, 0.70 ± 0.02; ^{150}Sm, 1.37 ± 0.06. The errors quoted are relative errors. In order to obtain absolute errors a 10% error must be added in quadrature to the above. The results are discussed in relation to the energy weighted sum rule and to pairing force theories. (auth)

17735 EFFECTIVE NUCLEON-NUCLEON INTERACTIONS IN THE NUCLEI WITH 29 AND 30 NEUTRONS. Vervier, J. (Centre d'Etude de l'Energie Nucleaire, Mol, Belg.). Nucl. Phys., 78: 497-552(1966).

The energy levels of the nuclei with $20 \leqq Z \leqq 28$, N = 29 and 30 are first calculated under the assumptions that their protons and neutrons outside Z = 20 and N = 28 are in the $1f_{\frac{7}{2}}$ and $2p_{\frac{3}{2}}$ orbits, respectively, and that the effective nucleon-nucleon interactions are given by the experimental spectra of the nuclei with the same Z but N = 28, of ^{56}Co and ^{58}Co. Qualitative agreement with experiment is generally achieved for energy level positions, ground state binding energies, magnetic and quadrupole moments, reduced M1 and E2 transition probabilities and spectroscopic factors for nucleon transfer reactions. The influence of configuration admixtures involving the $2p_{\frac{1}{2}}$ and $1f_{\frac{5}{2}}$ neutron orbits on the nuclei with 29 neutrons is then investigated; the effective proton-neutron interaction is assumed to have a δ-function radial dependence and its strength and spin contribution are determined both from the previous analysis and from the motion of the $2p_{\frac{1}{2}}$ and $1f_{\frac{5}{2}}$ neutron orbits with respect to $2p_{\frac{3}{2}}$ between ^{49}Ca and ^{57}Ni. Satisfactory quantitative agreement with experiment is obtained for energy level positions, spectroscopic factors for the (d,p) reaction on the nuclei with 28 neutrons, magnetic moments and reduced M1 transition probabilities, and, only qualitatively, for β-decay data. (auth)

17736 GAMMA RAYS PRODUCED IN THE ^{56}Fe(n,n'γ)^{56}Fe REACTION. Benjamin, R. W.; Buchanan, P. S.; Morgan, I. L. (Texas Nuclear Corp., Austin). Nucl. Phys., 79: 241-56(1966).

Cross sections for the production of gamma rays by inelastic neutron scattering from iron were measured for incident neutron energies from 0.95 to 4.0 Mev. Angular distributions for nine gamma rays produced by the (n,n'γ) reaction in ^{56}Fe were measured over the same energy range and compared with the theoretical predictions of the Satchler formalism using three different sets of neutron penetrabilities. On the basis of these comparisons, a doublet at 3.45 Mev is proposed and the following spin and parity assignments made to levels in the ^{56}Fe nucleus: 3.45 Mev ($1^+ : 3^+$) and 3.60 Mev (2^+). The possibility of a doublet at 3.12 Mev was also investigated. Branching ratios for the γ rays originating at these levels were determined experimentally. (auth)

17737 THE DIRECT CAPTURE MECHANISM FOR INTERMEDIATE ENERGY NUCLEONS. Gutfreund, H.; Rakavy, G. (Hebrew Univ., Jerusalem). Nucl. Phys., 79: 257-74(1966).

The validity of the direct capture mechanism for protons and neutrons in the range of 10–40 Mev is discussed. The capture cross sections for several nuclei are investigated in detail and the influence of various optical parameters is discussed. It seems that for the heavier nuclei one can obtain the observed cross sections by direct capture theory. Below 20 Mev one is forced to use optical parameters which are inconsistent with elastic scattering analysis. (auth)

17738 MEASUREMENTS OF PROTON-NUCLEUS TRIPLE SCATTERING PARAMETERS NEAR 140 Mev. Jarvis, O. N.; Rose, B.; Taylor, A. E. (Atomic Energy Research Establishment, Harwell, Eng.). Nucl. Phys., 79: 275-96(1966).

Measurements are reported of the triple scattering parameters R, A, and R′ in the scattering of ≈140 Mev protons from Be, ^{10}B, C, Cu and Pb at 8, 10, and 15° lab. From these measurements and data on differential cross sections and polarization, the Wolfenstein parameter β and the amplitudes and relative phases of the central and spin-orbit scattering amplitudes are calculated. On the whole,

consistency was observed between the different types of measurement and the sign of β was determined unequivocally. There appear to be significant differences between the results for ^{10}B and the other light nuclei. These are discussed in the context of possible nuclear-spin-dependent effects. Direct interaction calculations based on known nucleon-nucleon amplitudes do not fit the data. (auth)

17739 MEASUREMENT OF THE ABSOLUTE DIFFERENTIAL CROSS SECTION IN PROTON-CARBON ELASTIC SCATTERING AT 145 Mev. Jarvis, O. N. (Atomic Energy Research Establishment, Harwell, Eng.); Cox, G. F. Nucl. Phys., 79: 297-304(1966). (AERE-R-5006).

The proton-carbon differential cross section for elastic scattering was measured over the angular range 6 to 11° at an energy of 144.8 Mev. The absolute scale of these differential cross section measurements was determined to a precision ±0.5%. (auth)

17740 ANALYSIS OF 140 Mev NUCLEON SCATTERING DATA FOR BERYLLIUM AND CARBON. Jarvis, O. N. (Atomic Energy Research Establishment, Harwell, Eng.). Nucl. Phys., 79: 305-20(1966). (AERE-R-5005).

An analysis was made of the available 140 Mev nucleon elastic scattering data for beryllium and for carbon. These data include the differential cross section and polarization data for protons and neutrons in the region 3 to 20°, some proton triple scattering data and the total and absorption cross sections. With the assumption of charge independence, the data were fitted by means of a simple parametrization from which the phenomenological values of the four forward nuclear scattering amplitudes and of two nuclear radii were obtained. The "spin-orbit" radius is less than the "central" radius in each case. (auth)

17741 QUASI-FREE PROTON-PROTON SCATTERING IN LIGHT NUCLEI AT 460 Mev. Tyren, H. (Univ. of Chicago); Kullander, S.; Sundberg, O.; Ramachandran, R.; Isacsson, P.; Berggren, T. Nucl. Phys., 79: 321-73 (1966).

Quasi-free proton-proton scattering was studied in a number of light nuclei at 460 Mev using two large identical magnetic spectrometers with two-directional focusing and a multichannel electronic detector system. The experiments were carried out in a symmetric geometry. Summed energy spectra and angular correlation distributions of separated components of the spectra are presented. The experimental results for the higher nuclei are analyzed by comparing them with theoretical ones obtained on the basis of the distorted wave impulse approximation. Information on the radii and occupation numbers of the ls and lp orbitals in the nuclei considered is obtained. (auth)

17742 FERMI DECAYS OF DEFORMED ODD NUCLEI. Damgard, Joergen (NORDITA, Copenhagen). Nucl. Phys., 79: 374-8(1966).

The Fermi transitions of ^{156}Eu, ^{170}Lu, and ^{234}Np are forbidden by the isobaric spin selection rule $\Delta T = 0$, and the transition rates are therefore determined by the isobaric spin impurities of the nuclear states. These are calculated by the simple application of a perturbing Coulomb force. The Nilsson wave functions are used for the evaluation of the Coulomb matrix elements. The effect of pairing is also taken into account. (auth)

17743 ENERGY AND ANGULAR DISTRIBUTIONS OF α-PARTICLES IN THE $^{20}Ne(n,\alpha)^{17}O$ REACTION AT 14 Mev. Cevolani, M. (Univ., Bologna); Petralia, S. Nucl. Phys., 79: 379-84(1966).

Energy and angular distributions for α particles in the $^{20}Ne(n,\alpha)^{17}O$ reaction were obtained at E = 14.2 Mev, by using a fast-cycle cloud chamber. Departures from the typical evaporation distribution are observed in the low and high energy parts of the α-particle spectrum; the low energy part, however, is not especially significant owing to the distortion introduced by the $(n,n\alpha)$ reaction. For the high energy α particles the effect can be traced back to a direct interaction. The cms differential cross section peaks at backward angles, an effect which becomes more pronounced for the more energetic α particles. This feature, which is analogous with the reported results for the $^{12}C(n,\alpha)^{9}Be$ and $^{16}O(n,\alpha)^{13}C$ reactions, suggests that heavy particle stripping plays an important role in the $^{20}Ne(n,\alpha)^{17}O$ reaction. (auth)

17744 OSCILLATOR BRACKETS FOR HARTREE-FOCK CALCULATIONS. Baranger, M. (Carnegie Inst. of Tech., Pittsburgh); Davies, K. T. R. Nucl. Phys., 79: 403-16(1966). (ORNL-P-1682).

Some explicit formulas are derived for the oscillator brackets occurring in the calculation of nuclear two-body matrix elements. These formulas are especially adapted to the calculation of brackets with low relative momentum l. There are no restrictions on the radial quantum numbers, which make this method particularly useful for Hartee-Fock calculations. Estimates are given for the computing time. (auth)

17745 THE DENSITY OF ENERGY STATES IN LIGHT NUCLEI. Eder, G.; Kitz, A.; Schwetje, W. (Univ., Giessen, Ger.). Nucl. Phys., 79: 417-26(1966).

The density of nuclear energy states is discussed in its dependence on the single-particle level density and on effective moments of inertia. The oscillator model is used to determine these quantities for oxygen and calcium. (auth)

17746 MATRIX ELEMENTS FOR A THREE-NUCLEON SYSTEM (II). Davies, B. (Univ. of New South Wales, Kensington, Australia). Nucl. Phys., 79: 427-36(1966).

Previous results are extended to include matrix elements of three velocity-dependent operators. The matrix elements are given for arbitrary states of the system. (auth)

17747 MEASUREMENTS OF THE g-FACTORS OF 2^+ STATES IN EVEN NUCLEI UTILIZING HYPERFINE FIELDS IN IRON LATTICE. I. THE 316 kev STATE IN ^{192}Pt AND 328 AND 622 kev STATES IN ^{194}Pt. Agarwal, Y. K.; Baba, C. V. K.; Bhattacherjee, S. K. (Tata Inst. of Fundamental Research, Bombay). Nucl. Phys., 79: 437-48(1966).

The g-factors of the first excited 2^+ state in ^{192}Pt and the first and second excited 2^+ states in ^{194}Pt were measured by the integral γ-γ angular correlation method utilizing the hyperfine magnetic fields at Pt nuclei in dilute Ir-Fe alloys. The following values were obtained: 316-kev state in ^{192}Pt, $g = 0.33 \pm 0.05$, 328-kev state in ^{194}Pt, $g = 0.24 \pm 0.03$, and 622-kev state in ^{194}Pt, $g = 0.15 \pm 0.05$. (auth)

17748 ON THE RESIDUAL NUCLEI OBSERVED IN THE INTERACTIONS OF 25 Gev/c PROTONS WITH HEAVY EMULSION NUCLEI. Makowska, E. (Univ. of Warsaw. Inst. of Nuclear Research, Warsaw); Siemińska, J.; Soltan, M.; Suchorzewska, J.; St. Lorant, S. J. Nucl. Phys., 79: 449-58(1966).

The kinematical analysis of the residual nuclei in the interactions of 25-Bev/c protons with heavy nuclei in low sensitivity nuclear emulsion was made for a sample of 354 stars containing ^{8}Li fragments. The average velocity component in the direction of the beam is $\beta_x = 0.004 \pm 0.002$ for recoils and $\beta_x = 0.015 \pm 0.003$ for ^{8}Li fragments. The average mass number of residual nuclei is found to be about 30. In 30% of all the stars the masses of residual nuclei are comparable to those of other fragments. A correlation of the directions of motion of the residual nucleus and the emitted ^{8}Li fragment is found. (auth)

17749 INVESTIGATION OF THE REACTION $^{3}He(d,p)^{4}He$ INDUCED WITH POLARIZED DEUTERONS FROM 310 TO 2935 kev. Brown, Louis (Carnegie Institution of Washington, D. C.); Christ, Hans A.; Rudin, Hermann. Nucl. Phys., 79: 459-72(1966).

Deuterons from a pressure tank electrostatic generator with a source of polarized ions were used to excite the $^{3}He(d,p)^{4}He$ reaction. The change in the distribution of the protons caused by the polarization was observed at center-of-mass angles 0 and 90° for different orientations of the polarization relative to the beam with deuteron energies from 310 to 2935 kev. The results are expressed as four functions of energy, which are independent of the polarization of the incident beam. The tensor polarization of the deuteron beam is inferred from knowledge of the polarization of a proton beam produced by the same ion source, and this value is compared with the one obtained using an as-

sumed $3/2^+$ s-wave interaction of the ^{3}He reaction. The conclusion is that a fraction of the deuterons react through the $1/2^+$ s-wave channel. The energy dependence of the reaction below 1200 kev confirms this interpretation. The mirror reaction was measured at its resonance and gave identical results. Vector polarization effects in the high-energy region disagree with predictions by stripping theory. Certain technical matters relative to installation of the polarized ion source in the high voltage terminal are discussed. (auth)

17750 TRIPLET-SINGLET TRANSITIONS IN THE D(d, p)T REACTION. Christ, Hans A. (Univ. of Basel); Brown, Louis. Nucl. Phys., 79: 473-5(1966).

The D(d,p)T reaction was induced with polarized deuterons at energies of 400, 850, and 1280 kev. The protons were observed at center-of-mass angles 0 and 90° for various orientations of the polarization relative to the beam and the detectors. The changes in the distribution of the reaction products caused by the polarization were interpreted with the theory of Rook and Goldfarb and indicate that transitions take place between the $^3P_1$ deuteron-deuteron state and the $^1P_1$ triton-proton state. Such transitions are allowed, if a spin-orbit force acts between triton and proton. (auth)

17751 STUDIES OF THE FISSION INTEGRALS OF ^{235}U AND ^{239}Pu WITH CADMIUM AND BORON FILTERS. Hellstrand, Eric (Aktiebolaget Atomenergi, Studsvik, Sweden). Nukleonik, 8: 1-8(Jan. 1966).

The resonance fissions in ^{235}U and ^{239}Pu were studied using cadmium and boron filters. Fission chambers were used as detectors and the experiments were performed in beam geometry. The neutron energy distribution in the beams transmitted through the different filters was determined with a fast chopper. From the cadmium filter measurements the fission resonance integrals were determined. The values obtained were 278 ± 9b for ^{235}U and 301 ± 10b for ^{239}Pu; 0.5 ev < E < 1 Mev. Complementary ^{239}Pu measurements were made in which the fission events were detected from the fission product activity in irradiated foils. Contrary to what was reported elsewhere the value of the ^{239}Pu resonance integral, found in this way, agreed well with that obtained from the fission chamber measurement. The experiments with the boron filters yielded results which, for the thin filter, agreed well with those calculated from the cross section data given in the Karlsruhe compilation. The discrepancy was larger for the thick filter but the values did not disagree outside the common limits of error. (auth)

17752 PRODUCTION OF HYPERFRAGMENTS FROM THE INTERACTIONS OF 3.0-Gev/c AND 5.0-Gev/c K^- MESONS WITH EMULSION NUCLEI. Lemonne, J. (Univ. Libre, Brussels); Sacton, J.; Schorochoff, G.; (and others). Nuovo Cimento (10), 41A: 235-48(Jan. 21, 1966).

A study was made of the production of hyperfragments by the interactions of K^--mesons of 3.0 and 5.0 Bev/c momentum in a nuclear emulsion. The observed frequencies of production, (3.0 ± 0.1)% and (2.2 ± 0.1)% respectively, are significantly smaller than at lower K^--meson momenta, while the range distributions show a relative increase in the number of hyperfragments of range greater than 5 μm. This increase is attributed to a larger contribution from the fragmentation process, which is especially significant at intermediate ranges [(10 ÷ 50) μm], and to greater mean ranges for the heavy hyperfragments, which broaden the peak at short ranges (≤10 μm). The hyperfragments of range less than 10 μm are mainly heavy residual products of silver and bromine nuclei; their mass numbers differ on the average from those of the parent nuclei by about 30 and 35 nucleon masses for 3.0 and 5.0 Bev/c interactions respectively. Eight examples of π^- mesonic decays of heavy hyperfragments, and one probable example of a double hyperfragment, were observed. (auth)

17753 A STUDY OF ^{8}Li FRAGMENTS FROM 28-Gev PROTON INTERACTIONS IN NUCLEAR EMULSION. Chakalakal, D. A.; Barkow, A. G. (Marquette Univ., Milwaukee). Nuovo Cimento (10), 41A: 249-65(Jan. 21, 1966).

A preliminary report on the multiply charged fragments emitted in disintegrations caused by 28-Bev protons in a nuclear emulsion is given. The data were collected from a stack of (4 × 4) inches K-5 nuclear emulsions irradiated by the 28-Bev proton beam at Brookhaven. The analysis of the 179 ^{8}Li fragments observed is carried out on the basis of evaporation theory. Only those ^{8}Li fragments emitted in stars with $n_h \geq 7$ are studied. The results of the investigation suggest the existence of a high nuclear temperature at the time of the emission of the ^{8}Li fragment. This would indicate an earlier emission of ^{8}Li fragments compared to the other nuclear particles. Some supplementary mechanism is necessary to fully explain the experimental data. (auth)

17754 THEORETICAL TOTAL CROSS SECTIONS FOR HIGH-ENERGY NUCLEAR-FIELD PAIR PRODUCTION IN LIGHT ELEMENTS. Soerenssen, A. (CERN, Geneva). Nuovo Cimento (10), 41A: 543-58(Feb. 21, 1966).

The electronic screening constitutes an important correction to the cross section for pair production. For light elements the Thomas-Fermi-Molière model cannot be assumed to yield accurate results. A numerical calculation, based on the Hartree-Fock-Slater approximation is presented for elements ranging from H to Cl and for energies ranging from 10 Mev to 100 Bev. (auth)

17755 OPTICAL ORIENTATION OF ^{201}Hg ATOMS USING THE 1850 A LINE. Novikov, L. N.; Popesku, Ion M. Opt. Spectros. (USSR) (Engl. Transl.), 19: 375-8(Nov. 1965).

Translated from Opt. Spektros., 19: 668-73(Nov. 1965).

The described experiment enables one to pair off the population of the magnetic substates of the ground state of ^{201}Hg atoms by resonance scattering of the unpolarized light of the 1850 Å line of mercury. The nuclear magnetic resonance line is a superposition of two lines of sharply different widths. The narrow line corresponds to resonance with the 6 $^1S_0$ state of ^{201}Hg with a transverse relaxation time $T_2 = 2.8 \times 10^{-2}$ sec. It is suggested that the broad line corresponds to resonance with the metastable 6 $^3P_0$ state of ^{201}Hg with a transverse relaxation time equal to the time between two successive collisions of a mercury atom with the walls of the container. (auth)

17756 MUONIC ATOMS AND CHARGE DISTRIBUTION OF DEFORMED NUCLEI. Acker, H. L.; Marshall, H. (Univ., Freiburg i. B.). Phys. Lett., 19: 127-9(Oct. 1, 1965). (In German).

The primary results obtained in the calculation of the charge distribution of deformed atoms from the x-ray spectra of μ-mesic atoms with strongly deformed nuclei are reported. The muon is treated relativistically. The modified c distribution and the hard core distribution models are considered. (J.S.R.)

17757 DECAY OF NUCLEAR GIANT RESONANCE STATES FOLLOWING ELECTROEXCITATION. Raphael, R.; Ueberall, H. (Catholic Univ. of America, Washington, D. C.). Phys. Rev., 143: 671-5(Mar. 18, 1966).

Nucleon emission following inelastic electron scattering by a nucleus is described as a two-step process, in which a single isolated nuclear level is excited by the incident electron, and then subsequently decays to a state of the daughter nucleus by emitting a proton or neutron. General formulas are derived for the nucleon and electron angular distributions with the help of Racah algebra. Wigner R-matrix theory is then used to interpret the angular distributions in the reactions ^{12}C(e,e'p)^{11}B and ^{16}O(e,e'p)^{15}N with excitation of the ^{12}C and ^{16}O giant dipole states, as measured by Dodge and Barber. (auth)

17758 STUDY OF ^{19}O BY THE ^{17}O(tp)^{19}O AND ^{18}O(d,p)^{19}O REACTIONS. Wiza, Joseph L.; Middleton, Roy. (Univ. of Pennsylvania, Philadelphia). Phys. Rev., 143: 676-82 (Mar. 18, 1966).

A tungsten oxide target enriched to 30% in ^{17}O was bombarded with 12.0-Mev tritons and a similar target enriched to 50% in ^{18}O was bombarded with 12.0-Mev deuterons. In both cases, emitted protons were analyzed using a broad-range multiangle spectrograph. The ^{18}O(d,p)^{19}O reaction

was also studied at a bombarding energy of 11 Mev using a gas target and magnetic analysis. Energy levels up to 6.3-Mev excitation in ^{19}O were determined and no evidence was found for the recently reported levels at 0.348 and 2.617 Mev. Angular distributions were measured and several new spin and parity assignments were made. (auth)

17759 ISOBARIC-SPIN SELECTION RULE IN THE $^{10}B(d,\alpha)^{8}Be$ REACTION AT 7.5 Mev. Browne, C. P. (Univ. of Notre Dame, Ind.); Erskine, J. R. Contract nr-1623(05). Phys. Rev., 143: 683-7(Mar. 18, 1966).

Angular distributions were measured for the $^{10}B(d,\alpha)^{8}Be$ reaction leading to the ^{8}Be levels at 16.62, 16.92, 17.64, and 18.15 Mev. The fact that the total cross section to the 16.62-Mev state is about 115% of that to the 16.92-Mev state shows that, as was revealed earlier for lower bombarding energies, there is a large violation of the isobaric-spin selection rule. The total cross section to the 18.15-Mev state is about 85% of that to the 16.92-Mev state, but the total cross section to the 17.64-Mev state is about 7% of it. Isobaric spin thus does not appear to be a good quantum number for the 16.62- and 16.92-Mev levels, but the 17.64-Mev level does seem to be a nearly pure T = 1 state. (auth)

17760 DEUTERON POLARIZATION FROM THE $^{9}Be(p,d)^{8}Be$ REACTION AT 3 TO 5 Mev. Verbinski, Victor V.; Bokhari, M. Sibtain (Oak Ridge National Lab., Tenn.). Phys. Rev., 143: 688-91(Mar. 18, 1966). (ORNL-P-1759; ORNL-TM-1233).

The polarization of deuterons produced in the $^{9}Be(p,d)^{8}Be$ ground-state reaction was measured at several deuteron emission angles in the region of the stripping peak for proton energies of 3, 4, and 5 Mev. A carbon analyzer via the $^{12}C(d,p)^{13}C$ ground-state reaction was used, along with the relation ϵ (the asymmetry) = $3\ P_p \cdot P_d$, to determine the magnitude and sign of the deuteron polarization. At 3 and 4 Mev the sign near the stripping peak was found to be positive, which is in agreement with earlier experimental findings and with distorted-wave Born-approximation calculations for which deuteron-wave distortion is assumed to predominate. At 5 Mev, however, the sign was measured to be negative, which may be due to a relatively greater proton-wave distortion at this energy. (auth)

17761 PROPERTIES OF THE 4.77- AND 5.16-Mev STATES OF ^{10}B. Alburger, D. E. (Brookhaven National Lab., Upton, N. Y.); Parker, P. D.; Bredin, D. J.; Wilkinson, D. H.; Donovan, P. F.; Gallmann, A.; Pixley, R. E.; Chase, L. F. Jr.; McDonald, R. E. Phys. Rev., 143: 692-711 (Mar. 18, 1966). (BNL-9583).

The energy levels in ^{10}B at 4.77 and 5.16 Mev were studied by means of the reactions $^{11}B(He\text{-}3,\alpha)^{10}Be$ and $^{6}Li(\alpha,\gamma)^{10}B$. In measurements on the $^{11}B(He\text{-}3,\alpha)^{10}B$ reaction (E_{He^3} = 3.5 Mev), alpha particles populating states of ^{10}B were observed at 90° in coincidence with ^{10}B recoil nuclei, ^{10}B recoils and gamma rays, and decay alpha particles, by using two solid-state detectors and a NaI detector. Relative alpha-particle and gamma-ray branching intensities were determined for the decay of the 4.77- and 5.16-Mev states. The ratio of population intensities of the 5.16- and 5.11-Mev states was measured by using a Buechner-type magnetic spectrograph. In the $^{6}Li(\alpha,\gamma)^{10}B$ reaction thick-target gamma-ray yields were measured at resonances for forming the 4.77- and 5.16-Mev states. For the 4.77-Mev state the angular distribution of the predominant 4.05-Mev gamma ray was determined, the 4.77-Mev ground-state transition was detected, and the angular distribution of the 4.77-Mev gamma ray was measured. The intensity of the ground-state gamma-ray branch from the 4.77-Mev level was measured to be (0.5 ± 0.1)%, and the angular distribution of this transition in the $^{6}Li(\alpha,\gamma)^{10}B$ reaction favors an assignment of $J^{\pi} = 3^{+}$ to the 4.77-Mev state. Assignments of either $J^{\pi} = 2^{+}$ or 3^{+} are allowed by the angular distribution of the 4.05-Mev transition from this state. Γ_γ/Γ for the 4.77-Mev level was measured to be $(2.3 \pm 0.3) \times 10^{-3}$. For the $J^{\pi} = 3^{+}$ assignment, partial widths for the 4.77-Mev level were measured to be Γ_γ = 0.033 ± 0.006 ev and Γ_α = 14 ± 3 ev. The partial widths of the 5.16-Mev level were measured as Γ_γ = 2.9 ± 1.1 ev and Γ_α = 0.44 ± 0.09 ev for an alpha-particle branch of (13 ± 4)%. The properties of these and neighboring states are discussed in terms of the independent-particle model. Good agreement is found on some striking features but several points remain to be clarified. (auth)

17762 $^{16}O(\gamma,n)^{15}O$ CROSS SECTION FROM THRESHOLD TO 65 Mev. Cook, B. C.; Baglin, J. E. E.; Bradford, J. N.; Griffin, J. E. (Ames Lab., Ames, Iowa). Phys. Rev., 143: 712-23(Mar. 18, 1966). (IS-1133).

The $^{16}O(\gamma,n)^{15}O$ cross section was measured using least-structure analysis of photonuclear yield functions for energy to 65 Mev. In the giant-resonance energy region considerable structure is reported, in good agreement with structure reported using other methods. The resolution of the least-structure method is comparable to resolution obtained by other methods, and in certain energy regions is superior. The cross section extends to energy above the giant resonance, exhibiting prominent structure to the highest energy measured. Absolute cross sections are reported in good agreement with values obtained elsewhere from yield functions, but approximately 20% higher than measurements made using monochromatic photons. (auth)

17763 $^{12}C(\gamma,n)^{11}C$ CROSS SECTION TO 65 Mev. Cook, B. C.; Baglin, J. E. E.; Bradford, J. N.; Griffin, J. E. (Ames Lab., Ames, Iowa). Phys. Rev., 143: 724-9(Mar. 18, 1966). (IS-1161).

The cross section for the reaction $^{12}C(\gamma,n)^{11}C$ was measured from threshold to 65 Mev using least-structure analysis of yield curves. The giant resonance was resolved into a predominantly triplet structure with peaks at 22.1, 22.75, and 23.6 Mev. No structure was resolved about 40 Mev. The cross section integrated to 65 Mev is 77 ± 6 Mev mb. (auth)

17764 ^{141}Pr PHOTONEUTRON CROSS SECTION TO 65 Mev. Cook, B. C.; Hutchinson, D. R.; Waring, R. C.; Bradford, J. N.; Johnson, R. G.; Griffin, J. E. (Ames Lab., Ames, Iowa). Phys. Rev., 143: 730-5(Mar. 18, 1966). (IS-1160).

The cross section for the reaction $^{141}Pr(\gamma,n)^{140}Pr$ was measured through 65 Mev. Yield curves of ^{140}Pr radioactivity were analyzed by least-structure analysis. Eleven distinct resonances are resolved below 25 Mev with a total integrated cross section to 30 Mev of 1790 ± 100 Mev mb. The cross section falls to zero in the region of 30 Mev and rises slightly with no resolved structure above 35 Mev. The integrated cross section from 30 to 65 Mev is 440 Mev mb. (auth)

17765 NUMBER-CONSERVING APPROXIMATION FOR THE THEORY OF THE PAIRING INTERACTION IN NUCLEI. Dang, Giu Do (Service de Physique Theorique, Orsay, France); Klein, Abraham. Phys. Rev., 143: 735-9(Mar. 18, 1966).

The pairing interaction is studied by means of the equations of motion. An approximation is derived which adheres strictly to particle-number conservation, but is otherwise quite close to the formalism of the Bardeen-Cooper-Schrieffer (BCS) theory. It yields ground-state energies and single-particle properties considerably improved over those of the latter theory, as evidenced by calculations for the model of Pawlikowski and Rybarska, and the model of the Ni isotopes solved exactly by Kerman, Lawson, and MacFarlane. Though it does not yet surpass in accuracy several alternative improvements of the BCS theory, it is capable of systematic further development, including the treatment of more realistic potentials. (auth)

17766 LOW-LYING EXCITED STATES IN ^{115}In AND ^{117}In. Pandharipande, V. R.; Prasad, K. G.; Singru, R. M.; Sharma, R. P. (Tata Inst. of Fundamental Research, Bombay). Phys. Rev., 143: 740-4(Mar. 18, 1966).

The low-lying levels in ^{115}In and ^{117}In were studied by gamma-gamma and beta-gamma directional correlation and life-time measurements. The gamma-gamma directional correlation of the 1306–274-kev cascade in ^{117}In was found to be $W(\theta) = 1 + (0.271 \pm 0.013)P_2(\cos\theta) + (0.026 \pm 0.042)P_4(\cos\theta)$. The measurement of the beta-gamma directional correlation between the beta transition from

^{115}Cd to the 598-kev level in ^{115}In and the following gamma transition of energy 261 kev gave a P_2 coefficient $A_2(W) = -0.16 \pm 0.02$. Based on these measurements it is shown that the levels at 598 and 588 kev in ^{115}In and ^{117}In, respectively, have spin and parity $3/2^-$. The half-life of the 747-kev level in ^{117}In was found to be 4.9 ± 0.2 nsec. (auth)

17767 ELASTIC SCATTERING OF NEUTRONS FROM CARBON AND OXYGEN IN THE ENERGY RANGE 3.0 TO 4.7 Mev. Lister, D.; Sayres, A. (Columbia Univ., New York). Phys. Rev., 143: 745-58(Mar. 18, 1966).

The elastic scattering neutrons from oxygen and carbon was studied in the neutron bombarding energy range 3.0 to 4.7 Mev. Angular distributions were obtained by the method of recoiling gas atoms in a proportional counter. Data were taken over the entire energy range in approximately 25-kev intervals, and in smaller intervals near certain resonances. Differential cross sections for C(n,n)C were obtained relative to the total n-p cross section. Similarly, O(n,n)O differential cross sections as well as the ^{16}O(n,α)^{13}C total cross section were determined relative to the derived C(n,n)C cross sections. A phase-shift search routine was used to find acceptable least-squares fits to a Legendre-polynomial decomposition of the elastic-scattering results. Energy-level parameters were obtained for five states in ^{17}O and are given as follows (in the order: resonance energy relative to the ^{17}O ground state in Mev, spin and parity, and dimensionless reduced width): 7.24($3/2^+$,0.15), 7.69($3/2^-$, 0.07), 7.70($1/2^-$,<0.03), 7.83($1/2^-$,0.04), and 8.07($3/2^-$,0.02). Level parameters were also determined for two states in ^{13}C: 8.27($3/2^+$,0.45) and 8.87($1/2^-$,0.03). (auth)

17768 DEPENDENCE OF PROTON OPTICAL-MODEL PARAMETERS UPON EXPERIMENTAL UNCERTAINTIES. Dickens, J. K. (Oak Ridge National Lab., Tenn.). Phys. Rev., 143: 758-65(Mar. 18, 1966). (ORNL-TM-1267).

The dependence of proton optical-model parameters upon experimental uncertainties was studied for four types of errors. These were errors in over-all normalization, errors affecting the shape of the angular distribution, errors in incident energy, and errors in scattering angle. By varying the data, it is found that the optical-model parameters are affected differently by the four types of errors; this suggests that a single, over-all assigned error is inadequate for error analysis in optical-model studies. The minimum-χ^2 criterion is critically examined as a criterion for obtaining optimum optical-model parameters. The role of the experimental errors in the theoretical analysis is studied. Because the errors associated with the individual cross sections that form an angular distribution are not independent, it is concluded that these data do not make up a collection of several independent random samples, but that, collectively, they resemble a single random sample. This conclusion is statistically important in the study of reaction mechanisms using results of optical-model analysis. (auth)

17769 PHASE-SHIFT ANALYSIS OF T(n,n)T. Tombrello, T. A. (California Inst. of Tech., Pasadena). Contract Nonr-220(47). Phys. Rev., 143: 772-4(Mar. 18, 1966).

A phase shift analysis of the scattering and polarization data for the elastic scattering of neutrons from tritium was made for neutron energies between 1.0 and 6.0 Mev. Although there are insufficient experimental data to allow a unique determination of the phase shifts, a satisfactory solution was obtained by using as a starting point the phase shifts previously obtained for ^{3}He(p,p)^{3}He. The results are similar for these two reactions and a single-level analysis of the phase shifts allows the level parameters of states in ^{4}H and ^{4}Li to be compared. (auth)

17770 NONDYNAMICAL STRUCTURE OF THE ^{3}He(d,p)^{4}He REACTION. Csonka, Paul L.; Moravcsik, Michael J.; Scadron, Michael D. (Univ. of California, Livermore). Phys. Rev., 143: 775-9(Mar. 18, 1966). (UCRL-14506-T).

The parity-conserving reaction $1/2 + 1 \rightarrow 1/2 + 0$ ($1/2$ denoting a particle of spin $1/2$, etc.) is completely described in terms of its six invariant amplitudes. All observables are listed, both for the case when the product of the four intrinsic parities is positive and for the case when this product is negative. The subclass structure of these observables is given. The specific example of the ^{3}He(d,p)^{4}He reaction is examined and consequences of the experimentally found relation between polarization and asymmetry are derived. Specific further experiments are listed which could continue to narrow down the uncertainty in knowledge of the form factors. Experiments determining the product of the four intrinsic parities are also discussed. All proposed experiments are within reach of present-day experimental techniques. (auth)

17771 ^{3}He + p ELASTIC SCATTERING BELOW 1 Mev. Kavanagh, R. W.; Parker, P. D. (California Inst. of Tech., Pasadena). Contract Nonr-220(47). Phys. Rev., 143: 779-82(Mar. 18, 1966).

The cross section at 90° (lab) for elastic scattering of protons by ^{3}He was measured from $E_p = 0.125$ to above 1 Mev. No significant departure of the s-wave phase shifts from the hard-sphere value is seen. Experimental upper limits for the dimensionless reduced width of a $J = 0^+$ state vary from 4×10^{-3} at the lowest energy to 10^{-4} at 1 Mev, and lead to the assignment of $T = 0$ to the 0^+ state at 20 Mev in ^{4}He. (auth)

17772 HARD-CORE POTENTIAL AND THE BOUNDARY-CONDITION MODEL FOR NUCLEAR MATTER. Lee, Y. C. (Bell Telephone Labs., Whippany, N. J.); Wong, K. W. Phys. Rev., 143: 783-9(Mar. 18, 1966).

The usefulness of the boundary-condition model (BCM) for nuclear-matter calculations depends on the uniqueness of its pseudopotential. This uniqueness is examined. A method is proposed for comparing different potentials. Explicit calculations of the average potential energy per particle and the energy gap for nuclear matter are carried out when a hard-core pseudopotential is introduced within the nuclear force range in addition to the pseudopotential of the original BCM. The influence of the hard core with various sizes on the results is discussed. It is found that the results are not sensitive to the hard core as long as the core radius is small, showing that the BCM pseudopotential is effectively quite unique. The fact that the results are affected greatly for larger core radius is linked to the importance of the effect of many-body-correlation. (auth)

17773 PHOTONEUTRON CROSS SECTIONS FOR ^{12}C AND ^{27}Al. Fultz, S. C.; Caldwell, J. T.; Berman, B. L.; Bramblett, R. L.; Harvey, R. R. (Univ. of California, Livermore). Phys. Rev., 143: 790-6(Mar. 18, 1966). (UCRL-7703).

The photoneutron cross sections for carbon and aluminum were measured up to 37 Mev, using nearly monochromatic photons obtained from the annihilation of positrons in flight. For carbon, resonances were observed at 22.0, 23.2, 25.5, 27.1, 28.3, 30.5, and 35.2 Mev, having approximate dipole strengths of 19, 33, 14, 6, 6, 11, and 11%, respectively. The integrated cross section is 46 ± 4 Mev mb. Peaks in the aluminum cross section were observed at 13.8, 14.5, 15.4, 15.7, 16.4, 17.0, 17.7, 18.2, 20.0, 21.5, 22.0, 23.1, and 27.2 Mev. The integral for the cross section $\sigma(\gamma,n) + \sigma(\gamma,2n) + \sigma(\gamma,np)$ is 166 ± 12 Mev mb, while that for $\sigma(\gamma,2n)$ is 6.3 Mev mb. Measurements on the neutron energies indicate that ^{12}C emits neutrons mostly in ground-state transitions, and ^{27}Al mostly by direct interactions. (auth)

17774 INTEGRATED PHOTODISINTEGRATION CROSS SECTION OF HELIUM WITH A VELOCITY-DEPENDENT NUCLEAR POTENTIAL. Srivastava, B. K.; Jain, S. C. (Allahabad Univ., India). Phys. Rev., 143: 797-9(Mar. 18, 1966).

The integrated cross section σ_{int} for the photodisintegration of helium (^{4}He) is calculated by applying the sum rules of Levinger and Bethe and using Irving's wave function. It is assumed that the two-body interaction is central and velocity-dependent both in ^{1}S and ^{3}S states. The value for σ_{int} agrees reasonably well with the experimental results of Gorbunov and Spiridonov and with the theoretical value of Goldhammer and Valk obtained by using hard-core

wave functions and potentials. Moreover, it is found in good agreement with Dohnert and Rojo, that the velocity-dependent potential increases the value of σ_{int} by about 17% over the values obtained with a purely central potential. (auth)

17775 GROUND-STATE (p,n) REACTIONS IN MIRROR NUCLEI AND THE QUASIELASTIC MODEL OF (p,n) REACTIONS. Hansen, Luisa F.; Stelts, Marion L.; Wesolowski, Jerome J. (Univ. of California, Livermore). Phys. Rev., 143: 800-7(Mar. 18, 1966). (UCRL-12176).

The $^{27}Al(p,n)^{27}Si$, $^{29}Si(p,n)^{29}P$, and $^{31}P(p,n)^{31}S$ ground-state reactions were measured using polyethylene "long counters." Absolute cross sections and angular distributions were obtained from 0° to 160° at 10° intervals. The measured angular distributions were compared with the predictions of an optical-model calculation, using an optical potential suggested by Lane, which is a function of the isotopic spins of the incident proton and target nucleus. Since the ground-state (p,n) reactions were measured below the threshold for the excited state, the proton incident energies were between 5.8 and 7.6 Mev. Because of this low proton energy, the optical-model calculations include both Coulomb effects of distortion of the proton wave and the Coulomb energy difference between the incoming proton and the outgoing neutron. Fair agreement between the theoretical and experimental results was obtained for ^{29}Si and ^{31}P using a surface interaction for the imaginary and isobaric parts of the optical potential. Furthermore, the angular distributions from these two nuclei were quite similar in structure, in agreement with the twin-reaction hypothesis of Bloom, Glendenning, and Moszkowski. The neutron angular distributions from ^{27}Al are quite different in structure from those obtained from ^{29}Si and ^{31}P, and attempts to fit them with the optical-model calculation were not successful. A calculation based on distorted-wave single-particle excitation with charge-exchange was also carried out. The results of this calculation agree with those of the optical model for ^{29}Si and ^{31}P. For the ^{27}Al reaction the results of the DWBA calculation are different from those of the optical model, since in the former calculation momentum transfers greater than zero are included; however, neither calculation fitted the ^{27}Al data. (auth)

17776 STRIPPING ANALYSIS OF THE $^{46}Ti(d,p)^{47}Ti$ REACTIONS. Rapaport, J.; Sperduto, A.; Buechner, W. W. (Massachusetts Inst. of Tech., Cambridge). Contract AT(30-1)-2098. Phys. Rev., 143: 808-17(Mar. 18, 1966). (MIT-2098-203).

The (d,p) reactions from a target of isotopically separated ^{46}Ti were studied with the MIT multiple-gap magnetic spectrograph and the MIT-ONR Van de Graaff accelerator using a 7.0-Mev deuteron beam. Forty-seven excited states in ^{47}Ti were observed up to an excitation energy of 4.0 Mev, of which seventeen showed angular-distribution characteristics of a stripping process. Sixty additional energy levels were observed between 4.0 and 6.0 Mev, and angular distributions were obtained for eleven of the most intense of these levels. The ground-state Q value was measured to be 6.665 ± 0.010 Mev, and the proton angular distribution for this state did not show a characteristic stripping curve. Transition strengths and values of the orbital angular momenta of the transferred neutrons were derived from the experimental measurements and from calculations using a zero-range distorted-wave Born-approximation analysis. (auth)

17777 ^{44}Sc ISOMERIC YIELD RATIOS. Tatarczuk, J. R.; Medicus, H. A. (Rensselaer Polytechnic Inst., Troy, N. Y.). Phys. Rev., 143: 818-24(Mar. 18, 1966).

Sc-44 isomeric yield ratios were measured for the three reactions $^{45}Sc(\gamma,n)^{44}Sc$, $^{46}Ti(\gamma,np)^{44}Sc$, and $^{45}Sc(n,2n)^{44}Sc$. Scandium oxide and titanium samples were irradiated with 48-Mev bremsstrahlung to obtain the photo-induced reactions. For the (n,2n) reaction 14-Mev neutrons were used. The yields of ^{44}Sc in the ground and isomeric states were determined by the measurement of the residual gamma activity. A statistical-model calculation of the type used by Huizenga and Vandenbosch was performed in order to obtain the value of the spin cutoff parameter σ consistent with the experimental data. The following isomer yield ratios [(yield of ground state)/(total yield)] were obtained: for $^{45}Sc(\gamma,n)^{44}Sc$, 0.86 ± 0.02; for $^{46}Ti(\gamma,np)^{44}Sc$, >0.98; for $^{45}Sc(n,2n)^{44}Sc$, 0.58 ± 0.02. The experimental results agree with the calculated ratios for values of the spin cutoff parameter σ between 2 and 3. (auth)

17778 DETERMINATION OF NUCLEAR REACTION WIDTHS FROM REACTION YIELD CURVES. Ferry, James A.; Wendt, G.; Palmer, D. W.; Donhowe, J. M. (Univ. of Wisconsin, Madison). Phys. Rev., 143: 825-32 (Mar. 18, 1966).

Problems encountered in measuring narrow resonance widths were studied utilizing several well-known resonances in the $^{27}Al(p,\gamma)^{28}Si$ reaction. Previous measurements had been limited by imperfections of the gap in the electrostatic analyzer. To correct these defects, the surface of each deflection electrode was lapped to a mirror finish and its surface contour was examined by observing the fringe pattern of an optical interferometric device. Another similar device was used to position and measure the gap of the assembled analyzer. The result is a gap constant to ± 0.22 μ over a 4-mm vertical height for $^9/_{10}$ of the analyzer length. The proton beam from the analyzer was calibrated for energy spread by using the measured profile of the gap and the resonance of known width near 774 kev. Thick- and thin-target-yield curves taken over the resonances near 992 and 1317 kev were analyzed, using a Monte Carlo technique, which accurately accounts for the proton energy loss. Despite significant improvement in target-chamber vacuum conditions and resolution of the electrostatic analyzer, target and analyzer uncertainties limited the accuracy of the measured widths to Γ = 90 ± 35 ev and Γ = 85 ± 45 ev for the 992- and 1317-kev resonances, respectively. This study shows that three problems are likely to cause errors in resonance-width and resonance-position measurements. They are: target contamination, treatment of energy loss process, and beam-analyzer imperfections. Examination of methods used previously indicate that these errors tend to compensate. Since compensation under all conditions cannot be expected, this work indicates need for improved measurement methods. (auth)

17779 CROSS SECTIONS FOR THE $^{27}Al(\gamma,\pi^+)^{27}Mg$ REACTION. Walters, William B.; Hummel, John P. (Univ. of Illinois, Urbana). Contract Nonr 1834(05). Phys. Rev., 143: 833-8(Mar. 18, 1966).

Cross sections for the $^{27}Al(\gamma,\pi^+)^{27}Mg$ reaction were determined by measuring the ^{27}Mg radioactivity that was produced in aluminum samples that were irradiated with bremsstrahlung of maximum energy varying from 100 to 300 Mev. The observed yields were corrected for the contributions from secondary neutron reactions. The resulting cross sections have a minimum value of 13 μb at 220 Mev and the integrated cross section to 300 Mev is 1.38 ± 0.24 Mev mb. These values are a factor of about 10 smaller than those reported previously for this reaction. The cross sections for the $^{27}Al(\gamma,\pi^+)$ reaction are compared with those observed previously for similar reactions involving other light target nuclei and are discussed in terms of an extension of the theory outlined by Laing and Moorhouse for reactions of this type. (auth)

17780 ENERGY LEVELS OF ^{31}S. Ajzenberg-Selove, F. (Haverford Coll., Pa.); Wiza, J. L. Phys. Rev., 143: 853-5(Mar. 18, 1966).

An antimony sulfide target was bombarded by 12-Mev ^3He particles from a tandem accelerator. The alpha-particle spectra at 15 and 45° were determined by means of a broad-range spectrograph. Thirty-nine alpha-particle groups were observed corresponding to states of ^{31}S with $E_x < 7.8$ Mev. These results are compared with the known information on the level structure of the mirror nucleus ^{31}P. (auth)

17781 DECAY OF ^{194}Ir AND ^{194}Os. Williams, David C. (Los Alamos Scientific Lab., N. Mex.). Phys. Rev., 143: 855-6(Mar. 18, 1966). (LA-DC-7485).

The abundances of the gamma rays at 293, 301, and 328 kev arising from ^{194}Ir decay were measured and found to be (2.6 ± 0.4)%, (0.39 ± 0.07)%, and (13.0 ± 1.8)%, respectively. These values are substantially lower than those reported in earlier work but are in fair agreement with another recent study of ^{194}Ir decay. Since some recent studies of ^{194}Os decay were made relative to the decay properties of its daughter activity ^{194}Ir, these ^{194}Os data must also be corrected. After correction, the discrepancies between various ^{194}Os studies are considerably reduced. The best values for the energies and abundances, respectively, of the ^{194}Os radiations observed are β_1, 97 ± 2 kev (= Q_β), (67 ± 8)%; γ_1, 43.1 ± 0.3 kev (in coincidence with β_2, 54.5 ± 2 kev), (33 ± 8)%; and γ_2, 82 ± 1 kev, ~0.05%. (auth)

17782 ENERGY LEVELS OF ^{170}Tm. Sheline, R. K. (Florida State Univ., Tallahassee); Watson, C. E.; Maier, B. P.; (and others). Phys. Rev., 143: 857-8(Mar. 18, 1966). (LA-DC-7497).

Twenty-seven levels in ^{170}Tm were observed up to an excitation energy of 1153 kev utilizing 12-Mev deuterons and the reaction ^{169}Tm(d,p)^{170}Tm. The ground-state Q value was determined as 4369 ± 15 kev. Both magnetic Compton and germanium spectrometers were used to measure 16 high-energy gamma rays up to an excitation energy of 868 kev resulting from the capture of thermal neutrons in the reaction ^{169}Tm(n,γ)^{170}Tm. The neutron binding energy observed in this reaction is 6595 ± 2.5 kev. In addition, 177 low-energy gamma rays between 38 and 870 kev were observed in a bent-crystal spectrograph during irradiation of ^{169}Tm with thermal neutrons. The multipolarities of 29 of the transitions were determined from internal conversion measurements with a beta-ray spectrometer. The analysis of these data suggests the existence of 23 levels up to an energy of 720 kev for which assignments were attempted. Three Nilsson configurations 0, in which the proton orbital Ω_p remains $\frac{1}{2}$ + [411↓] and the neutron orbital Ω_n is successively $\frac{1}{2}$ − [521↓], $\frac{7}{2}$ + [633↑], and $\frac{5}{2}$ − [512↑]0, account for 16 states. This analysis leads to the following spectroscopic interpretation (band head energy, kev, in parentheses; spin, parity, and K quantum number in brackets): (ground state), [1−, 1] with superimposed band to 4−; (149.721), [0−, 0] with superimposed band and anomalous spacings of even and odd spin members to 4−; (183.193), [3+, 3] with superimposed rotational members to 5+; (204.452), [2−, 2] with superimposed rotational members to 4−; (447.079), [3−, 3] only member of the band. Seven additional higher energy levels are tentatively assigned, five of which may arise from gamma vibrational bands at 411.45, 661.91, and 719.21 kev built on K = 1−, K = 0− and K = 3+ intrinsic bands, respectively. These are the first gamma vibrational bands postulated in odd-odd nuclei. All states below 425 kev from both (d,p) and direct high (n,γ) excitation are included in these assignments. The Coriolis coupling between the K = 1− and K = 0− bands is clearly observed in the anomalous rotational spacing of the K = 1− band. Calculation of the energies and (d,p) cross sections for the K = 1− and K = 0− bands agrees well with experiment and indicates that only the even members of these bands are appreciably mixed. The M1 transition probabilities within the K = 0 rotational band in ^{170}Tm are shown to be quite large. It is suggested that the high-energy gamma rays in the reaction ^{169}Tm(n,γ)^{170}Tm involve a direct reaction which excludes population of excited proton configurations. (auth)

17783 DOUBLE DECAY PROCESSES IN ^{114m}In. Church, E. L. (Brookhaven National Lab., Upton, N. Y.; Frankford Arsenal, Philadelphia); Gerholm, T. R. Phys. Rev., 143: 879-94(Mar. 18, 1966). (BNL-9547).

A search was made for double internal conversion in competition with the 192-kev E4 transition of ^{114m}In, by measuring the coincidence intensity of equal-energy electrons emitted into separate sections of an orange beta-ray spectrometer. No evidence for double KK, KL, or LL electron ejection was found. The upper limit obtained for the intensity of double K-electron ejection relative to single K conversion may be expressed approximately as: $KK/K < 1.3 \times 10^{-4}$. This limit on KK ejection is appreciably lower than those determined for KL and LL, since the measurements of the latter were restricted to large angular separations between the two electrons, to avoid effects of the scattering in the source of the intense single conversion electrons of the isomeric transition. Interpretation of experimental limits on double electron ejection in terms of double internal conversion requires the knowledge of the contributions of a variety of additional scattering processes. Quantitative estimates of these processes are not yet available for ^{114m}In, but qualitative estimates indicate that their intensities may be comparable with the present experimental upper limits. If the contribution of these scattering processes is taken to be zero, and the present KK limit is interpreted directly in terms of the double-conversion formalism of Eichler, an approximate equivalent limit on double gamma-ray emission is obtained: $\gamma\gamma/\gamma < 3 \times 10^{-4}$. This is to be compared with the direct limit on double gamma-ray emission set by Grabowski, Gustafsson, and Bäckström: $\gamma\gamma/\gamma < 3 \times 10^{-5}$. Both of these upper limits are significantly less than the dimensional estimate for an allowed double E2 cascade proceeding through nearby 3+ states in ^{114}In. Such states, composed principally of d-neutron configurations, are expected on the basis of systematics, but have not yet been identified. It is pointed out that the present situation is analogous to the well-known presence of inhibited particle E2 transitions in nearby Sn, Cd, and Sb isotopes, which have received an explanation in terms of pairing-correlation effects. It is emphasized that a similar explanation is available here, both for the inhibition of the double gamma-ray process, and the inhibition of the competing E4 transition. These suggestions are illustrated by calculations based on the extended shell model of Kisslinger and Sorensen, as simply applied to odd-odd ^{114}In. The present results are then interpretable as further evidence of the effects of pairing correlations in the tin region. (auth)

17784 EFFECTS OF ANGULAR MOMENTUM IN THE DECAY OF SAMARIUM COMPOUND NUCLEI. Kaplan, Morton (Yale Univ., New Haven). Phys. Rev., 143: 894-9 (Mar. 18, 1966).

Excitation functions for a series of neutron-emitting compound nucleus reactions leading to the product ^{142}Sm were measured. By using heavy-ion (HI) beams as bombarding projectiles, it was possible to produce compound nuclei with the same excitation energies but with differing angular momenta. Nine reactions of the type (HI,xn), where x = 4 to 8, were studied, spanning a region of excitation energies from 40 to 105 Mev. The cross-section maxima are all in the vicinity of 500 mb and occur at energies above threshold corresponding to 4.8−6.3 Mev per emitted neutron. For the same compound nuclei, the effects of increasing angular momentum are to shift the excitation-function peaks toward higher energies and to considerably broaden their width. With increasing number of neutrons emitted, the apparent (extrapolated) threshold energies become increasingly displaced from the true thresholds. Both these displacements and the positions of the excitation function peaks correlate with angular momentum, but it is not possible to distinguish linear relations from quadratic ones. (auth)

17785 SCATTERING OF 150- AND 300-Mev POSITRONS AND ELECTRONS FROM BISMUTH. Browman, A.; Grossetete, B.; Yount, D. (Ecole Normale Superieure, Orsay, France). Phys. Rev., 143: 899-910(Mar. 18, 1966).

Positrons and electrons from the Orsay linear accelerator were scattered from bismuth at 6, 10, 15, and 20° at 300 Mev, and at angles having similar momentum transfers at 150 Mev. In addition to electron-positron ratios, relative and absolute cross sections were measured and are given here for the present experiment as well as for the high- and the low-resolution experiments reported earlier. The latter data extend to 45° at 300 Mev ($q^2 \approx 1.4$ F^{-2}). The combined data from the three experiments are internally consistent and are in general agreement with the partial-wave predictions based on earlier electron scattering results. However, the electron-positron ratio in the neighbor-

hood of the 6°, 300-Mev point disagrees by 2.2 standard deviations with the partial-wave predictions and also with the value for the ratio obtained at the corresponding 150-Mev point when the latter is scaled to 300 Mev by means of a "model-independent" scaling law. The present data thus confirm the discrepancy noted earlier in which the results of Goldemberg, Pine, and Yount at 5° and 300 Mev disagreed with the partial-wave predictions and with the scaled results of Miller and Robinson taken at energies below 170 Mev. (auth)

17786 DECAY OF ^{108m}Ag. Kistner, O. C.; Sunyar, A. W. (Brookhaven National Lab., Upton, N. Y.). Phys. Rev., 143: 918-22(Mar. 18, 1966). (BNL-9584).

The decay of the long-lived isomer (>5 yr) of ^{108}Ag was investigated with scintillation and proportional-counter spectrometers employing coincidence techniques. Conversion-electron measurements with a high-transmission "orange"-type spectrometer and a high-resolution $\pi\sqrt{2}$ double-focusing spectrometer together with gamma-gamma angular-correlation measurements served to establish the multipolarities of most of the observed transitions. ^{108m}Ag was found to decay 8.5% of the time via a two-step isomeric cascade consisting of a 30.4-kev M4 transition followed by a 79.4-kev E1 transition. The remaining 91.5% of the decays proceed by an electron-capture transition to a 1770-kev level in ^{108}Pd. This level then decays to the ground state of ^{108}Pd via a 722.7 ± 1.0 kev, 613.9 ± 0.6 kev, 433.6 ± 0.5 kev triple gamma cascade. Two excited states at 79.4 ± 0.5 and 109.8 ± 0.5 kev are established in ^{108}Ag, with proposed spins and parities of 2- and 6+, respectively. The half-life of the 79-kev level was shown to be $\leq 10^{-9}$ sec. The spins and parities of the 1770- and 1048-kev levels in ^{108}Pd are assigned as 6+ (possibly 5+) and 4+, respectively. (auth)

17787 DECAY OF ^{149}Nd. Helmer, R. G.; McIsaac, L. D. (Phillips Petroleum Co., Idaho Falls, Idaho). Phys. Rev., 143: 923-42(Mar. 18, 1966).

The level structure of ^{149}Pm was studied from the decay of 1.7-h ^{149}Nd. Studies were made of the internal-conversion electron spectrum with magnetic spectrographs, and of the gamma-ray spectrum with NaI(Tl) and Ge(Li) detectors. Gamma-gamma coincidence experiments were carried out with NaI(Tl) and Ge(Li) detectors. Beta-gamma coincidence measurements were made with combinations of proportional counters and anthracene, NaI(Tl), and Ge(Li) detectors. The half life of ^{149}Nd was found to be (1.73 ± 0.01) h. About seventy gamma-ray transitions from 30 to 1456 kev were observed. The transitions with intensities greater than 1% of the decays have the following energies, transition intensities, and multipolarities: 30.0 (~6%, E2), 59.0 (~2), 74.4 (~2), 97.0 (~3, M1), 114.3 (38, M1), 155.9 (6.2, E1), 188.8 (2.0), 198.9 (1.4), 208.2 (2.6), 211.3 (24, M1), 240.3 (6.5, M2), 267.7 (7), 270.3 (10, E1), 326.6 (4.5), 349.1 (1.5), 423.6 (7), 443.5 (1.1), 540.5 (6.5), 556.4 (1.1), and 654.7 (8.4). The 240-kev transition has a half life of 41 μsec which agrees with the M2 assignment based on the internal-conversion coefficients. From previous lifetime measurements for states at 114 and 270 kev, hindrance factors were computed for the following gamma-ray transitions: 114 kev (M1, 350), 270 kev (E1, $\sim 5 \times 10^5$), 155 kev (E1, $\sim 5 \times 10^5$), and 59 kev (E1, $\sim 5 \times 10^4$). The 30-kev transition between the 270- and 240-kev levels appears to be enhanced by a factor of about 80. A level scheme is proposed which includes about sixty transitions. There are well-established excited states 114.3, 188.8, 211.4, 240.3, 270.2, 387.6, 538.0, 654.8, and 768 kev. (auth)

17788 TERNARY FISSION OF HEAVY COMPOUND NUCLEI IN THORITE TRACK DETECTORS. Fleischer, R. L. (General Electric Co., Schenectady, N. Y.); Price, P. B.; Walker, R. M.; Hubbard, E. L. Phys. Rev., 143: 943-6(Mar. 18, 1966).

A thorite ($ThSiO_4$) track detector was used to study fission induced by reactions between 400-Mev Ar ions and Th nuclei in the detector. Both binary and ternary fissions were observed. The cross section for binary fission is 3.0 ± 0.4 b. The angular distribution of fragments from the ternary fissions indicates compound-nucleus formation. The cross section for ternary fission is approximately $\frac{1}{30}$ of that for binary fission. (auth)

17789 NUCLEAR-RESONANCE FLUORESCENCE IN ^{159}Tb. Raghavan, R. S. (Franklin Inst., Swarthmore, Pa.). Phys. Rev., 143: 947-52(Mar. 18, 1966).

Levels at 363 and 580 kev in ^{159}Tb populated in the decay of ^{159}Gd were investigated by the resonance-fluorescence method using the centrifuge technique. Powdered terbium oxide (Tb_4O_7) was used as the resonance scatterer. From the resonance scattering cross sections and known branching ratios, the mean lives of the levels were computed to be: τ(363-kev level): $(2.2 \pm 0.15) \times 10^{-10}$ sec; τ(580-kev level): $(1.1 \pm 0.15) \times 10^{-12}$ sec. Angular-distribution studies revealed that the 363-kev γ ray previously identified as E1 was predominantly dipole in character, with an ⟨M2⟩/⟨E1⟩ amplitude ratio $\delta = -(6^{+}_{-}\frac{1}{2})\%$. These studies also showed that attenuations due to extranuclear fields in the oxide scatterer were very small. In the case of the 580-kev γ ray, the measured angular distribution confirmed the earlier assignment of spin ½ for this level. Estimates of the B(E2) of this γ ray derived from Coulomb excitation, combined with the above value of the mean life, gave the ⟨E2⟩/⟨M1⟩ amplitude ratio of the 580-kev γ ray as $\delta = \pm(3 \pm 1.5)\%$. (auth)

17790 HIGH-ENERGY FISSION OF ^{238}U. Sugarman, Nathan; Muenzel, Helmut; Panontin, J. A.; Wielgoz, Karoline; Ramaniah, M. V.; Lange, Gerald; Lopez-Menchero, Emilio (Univ. of Chicago). Phys. Rev., 143: 952-? (Mar. 18, 1966). (EFINS-65-64).

The results of a study of the thick-target recoil properties of fission products from the 450-Mev proton fission of ^{238}U are reported. The average kinetic energy, the average cascade deposition energy, and the average anisotropy of an isolated product are calculated from the recoil results. The characteristics of the most probable fission products, and of the primary fragments leading to them, are then calculated. The average total kinetic energy of the primary fragments is found to be 163 ± 8 Mev and the average separation of their charge centers at the scission point is 18.4 ± 0.5°F. The angular distribution of the fission fragments is somewhat anisotropic, favoring perpendicular emission of fragments for low cascade deposition energies and forward-backward emission for high deposition energies. The momentum-deposition energy relation obtained from the Monte Carlo intranuclear cascade calculations leads to an average cascade deposition energy of 123 Mev for the fission process, somewhat lower than the value 147 Mev calculated for all cascade nuclei. The cascade deposition energy, calculated from recoil results, for formation of a specific nuclide agrees with that determined from an analysis of its excitation function to about 20%. (auth)

17791 FOUNDATIONS FOR HARTREE-FOCK CALCULATIONS WITH SINGULAR POTENTIALS. Shakin, Carl; Waghmare, Yeshwant R. (Massachusetts Inst. of Tech., Cambridge). Contract AT(30-1)-2098. Phys. Rev. Lett., 16: 403-5(Mar. 7, 1966).

A theoretical foundation for the application of effective interaction in nuclear Hartree-Fock calculations is developed using the unitary model-operator approach. (G.O.Y.)

17792 EXPERIMENTAL OBSERVATION OF M1 AND E2 HYPERFINE STRUCTURE IN THE MUONIC K AND L X RAYS OF BISMUTH. Ehrlich, R. D.; Fryberger, D.; Jensen, D. A.; Nissim-Sabat, C.; Powers, R. J.; Sherwood, B. A.; Telegdi, V. L. (Univ. of Chicago). Contract Nonr 2121(25). Phys. Rev. Lett., 16: 425-9(Mar. 14, 1966).

An experimental investigation of the hyperfine structure of muonic Bi is summarized. (G.O.Y.)

17793 MAGNETIC DIPOLE AND ELECTRIC QUADRUPOLE HYPERFINE EFFECTS IN ^{209}Bi MUONIC X RAYS. Bardin, T. T.; Barrett, R. C.; Cohen, R. C.; Devons, S.; Hitlin, D.; Macagno, E.; Nissim-Sabat, C.; Rainwater, J.; Runge, K.; Wu, C. S. (Columbia Univ., New York). Phys. Rev. Lett., 16: 429-34(Mar. 14, 1966).

The effects of the electric quadrupole moment and the magnetic dipole moment on the hyperfine structure of ^{209}Bi were investigated on the basis of measurements on the muonic K and L x rays from ^{209}Bi. (D.C.W.)

17794 MASS OF ^{8}He FROM THE FOUR-NEUTRON TRANSFER REACTION ^{26}Mg(α,^{8}He)^{22}Mg. Cerny, J.; Cosper, S. W.; Butler, G. W.; Pehl, R. H.; Goulding, F. S.; Landis, D. A.; Detraz, C. (Univ. of California, Berkeley). Phys. Rev. Lett., 16: 469-73(Mar. 14, 1966). (UCRL-16705).

The existence of ^{8}He was verified, and the mass of ^{8}He was determined using the reaction ^{26}Mg(α,^{8}He)^{22}Mg. (D.C.W.)

17795 INTERNAL CONVERSION. Hollander, J. M. (Univ. of California, Berkeley); Rasmussen, J. O.; Hamilton, J. H. Phys. Today, 19: 58-60(Feb. 1966).

A conference on conversion electrons from nuclei is reviewed. New and experimental techniques that lead to increasing knowledge of L-subshell ratios, K, L, and M particle parameters and conversion coefficients in complex and short-lived decays and new results were discussed. It is emphasized that with few exceptions theory has achieved outstanding overall success in explaining and correlating experimental data. Most deviations reported are small, but it is suggested that much information may be in them. (J.F.P.)

17796 THE DISCOVERY OF HEAVY HYPERNUCLEI. Zakrzewski, Janusz (Univ. of Warsaw). Postepy Fiz., 16: 525-43(1965). (In Polish).

The most important investigations relating to the discovery of heavy hyperfragments are reviewed, discussing the conditions and methods of producing these particles, including the decay of mesonic and nonmesonic hyperfragments, their classification, means of production, and experimental techniques for identifying and studying hyperfragments. A serious problem area is the identification of hyperfragments in nuclear emulsions in studies of production and decay processes, and in track measurements. A major difficulty relates to the difficulty of determining which nucleus in the emulsion was involved in the production or decay of hyperfragments. Since it is not possible to load nuclear emulsions with adequate percentages of heavy elements such as uranium, it is important to supplement nuclear emulsion work with investigations utilizing such detectors as hydrogen and xenon bubble chambers. (TTT)

17797 SEARCH FOR LEVEL STRUCTURE NEAR 2.86 Mev IN ^{10}B. Maydan, D.; Vass, D. G. (Univ. of Edinburgh). Proc. Phys. Soc., 86: 817-20(Oct. 1965).

^{9}Be(d,n)^{10}B neutron time-of-flight spectra are presented. These spectra provide no evidence for the formation of any level near 2.86 Mev in ^{10}B for 600 kev deuterons. (auth)

17798 A MEASUREMENT OF WIDE-ANGLE BREMSSTRAHLUNG AT 28 Mev. Hague, J. F.; Jennings, R. E.; Rand, R. E. (London Univ.). Proc. Phys. Soc. (London), 87: 633-9(Mar. 1966).

The absolute differential cross section for the production of bremsstrahlung was measured for photons emitted at 93° by 27.6 Mev electrons scattered by ^{27}Al. The shape of the energy spectrum is in good agreement with theory but the ratio of the experimental to theoretical cross section predicted by the formula of Biel and Burhop is 1.23 ± 0.07. Full details of the experiment and analysis are given. (auth)

17799 THE SCATTERING OF HIGH-ENERGY ELECTRONS BY ^{7}Li. Murray, G.; Strachan, C. (Univ. of Aberdeen, Eng.). Proc. Phys. Soc. (London), 87: 641-52 (Mar. 1966).

The interaction between the constituent nucleons in a nucleus and the Møller field of a scattered electron is used in the two-component form derived from the covariant interaction by the Foldy–Wouthuysen transformation. The kinematics of electron-nucleus scattering with disintegration of the nucleus are given. The shell model is used for the nucleus and the electrodisintegration of ^{7}Li is discussed where a proton is emitted and the resulting ^{6}He nucleus is left in either its spinless ground state or its first excited state (J = 2). Expansion of the fields in terms of multipoles is avoided because of the high momentum transfer and wave functions with the correct translational properties are used. (auth)

17800 INTERPRETATION OF THE STRUCTURE OF ^{7}Li FROM PROTON SCATTERING. Mahalanabis, J.; Jackson, D. F. (Battersea Coll. of Tech., London). Proc. Phys. Soc. (London), 87: 677-9(Mar. 1966). (UCRL-14444).

The interpretation of the data on 150 to 185 Mev proton scattering from ^{7}Li is discussed in terms of the shell model and the unified model. The shell model calculations fail to fit the small-angle inelastic scattering from the first excited state, while an interpretation of the proton scattering data in terms of the unified model appears to be in conflict with other experimental data. (auth)

17801 AN EXACT DIAGONALIZATION OF THE QUADRUPOLE AND PAIRING FORCES IN THE NUCLEAR d-s SHELL. Broglia, R.; Maqueda, E.; Bes, D. R. (Facultad de Ciencias Exactas y Naturales, Buenos Aires). Rev. Union Mat. Argent. Asoc. Fis. Argent., 22: 107-22(1965).

The pairing plus quadrupole interaction were diagonalized for four identical particles in the N = 2 shell of the harmonic oscillator. The states of the basic representation are classified according to the SU3 coupling scheme. The energy levels and wave functions are calculated for different values of the relative intensity of the two forces. The results are compared with the predictions of the vibrational and asymmetric rotor models. (auth)

17802 ALPHA PARTICLE EXCITATIONS IN ATOMIC NUCLEI. Simons, Lennart (Univ. of Helsinki). Soc. Sci. Fenn., Comment. Phys.-Math., 31: 1-16(1965).

Certain light nuclei, in particular ^{40}Ca and ^{32}S, are regarded as temporarily consisting of an alpha-cluster and a residual nucleus. In an earlier work the case was considered for these particles being in the ground state. A treatment is presented of their excited states. After taking the spin-orbit coupling into consideration single levels and spectra are obtained. Good agreement with experimentally determined levels is obtained in some cases, especially if it is assumed that an alpha-cluster can be temporarily excited to about 2.38 Mev, corresponding to a state with spin and parity 2^{+}. (auth)

17803 ANGULAR DISTRIBUTION OF NEUTRONS FROM THE ^{12}C(α,n)^{15}O REACTION AT AN E_{α} = 14 Mev. Alevra, A.; Dumitrescu, R.; Lukas, I. R.; Magda, M. T.; Martalogu, N.; Plostinaru, D.; Poenaru, D.; Trutia, E.; Vilcov, I.; Vilcov, N. (Inst. of Atomic Physics, Bucharest). Stud. Cercet. Fiz., 17: 761-4(1965). (In Rumanian).

Reactions due to particles heavier than deuterons are of special interest in deuteron stripping reactions because they yield a great variety of information in nuclear spectroscopy; the formation of compound nuclei must thereby be taken into consideration. Thus, the angular distribution of the ^{12}C(α,n)^{15}O reaction could reveal whether a compound nucleus or direct interaction is involved in the reaction. For this reason, the angular distribution of neutrons corresponding to the ground state of the residual ^{15}O was determined at E_{α} = 14 Mev, at which only relatively low energy, <3.4 Mev, neutrons are obtained. The measurements were carried out on the cyclotron of the Institute by using the time-of-flight method. Colloidal graphite deposited on tantalum served as the target. A marked peak in the angular distribution implied that direct interaction may be involved in the reaction; however, the bombardment energies could lead to an excitation in the compound nucleus between the 17.65- and 17.50-Mev levels. In order to establish the relative importance of these processes, measurements must be carried out at other bombardment energies and backscattering angles. (TTT)

17804 DIFFUSION AND CAPTURE OF ARGON IN NEUTRON-IRRADIATED CALCIUM FLUORIDE. ON THE PROBLEM OF THE TRANSFER REACTION AND RADIATION DAMAGE IN SOLID BODIES. Lagerwall,

Torbjoern. Trans. Chalmers Univ. Technol., Gothenburg, No. 307, 1-141(1965). (In German).

An account is given of an investigation concerning the creation of argon from calcium by neutron irradiation and the diffusion of the argon atoms in calcium fluoride single crystals. The cross section for the reaction $^{44}Ca(n,\alpha)^{41}Ar$ was determined by β-γ coincidence measurements to be 0.061 mb. The mobility of Ar in the CaF_2 lattice is inferred from kinetic studies of rare gas diffusion out of the crystal at different temperatures, and an expression for the diffusion coefficient is given. The corresponding entropy of activation is also calculated. The solubility of Ar in CaF_2 and the effects of radiation damage on Ar diffusion are given. The investigation of age determinations by the K–Ar method is also discussed. (J.F.P.)

17805 DETERMINATION OF DEUTERON POLARIZATION PARAMETERS FROM EXPERIMENTS ON DOUBLE SCATTERING BY NUCLEI. Malko, A. I. (Inst. of Physics, Kiev). Ukr. Fiz. Zh., 10: 1077-82(1965). (In Russian).

A method is described for determining the polarization parameters of deuteron beams obtained by means of elastic scattering by nuclei according to the data of experiments on double scattering by nuclei of three different elements. A system of nonlinear algebraic equations is presented, the numerical solution of which enables one to find these parameters. (auth)

17806 POLARIZATION OF PRODUCTS OF ^{6}Li BREAK-UP IN THE ELECTROMAGNETIC FIELD OF THE NUCLEUS. Tartakovskii, V. K.; Ismatov, E. (Inst. of Physics, Kiev. Khar'kov State Univ.). Ukr. Fiz. Zh., 10: 1289-94(Dec. 1965). (In Ukrainian).

^{6}Li break-up in the electromagnetic field of the nucleus was considered on the basis of a cluster model. Polarization, quadrupolarization, and azimuthal asymmetry in the angular distribution of the reaction products were investigated. It is shown that with an escape angle of the deuteron $\vartheta = 11°$ and $\theta = 15°$, polarization is as high as 13%. When the incident beam is polarized, with fixed escape angles of the particles, the differential cross section may vary within wide limits (up to 40%), depending on the azimuthal angle. Quadrupolarization is in general small and may be perceptible only in cases when the reaction cross section is very small. (auth)

17807 CHARACTERIZATION OF THE ^{9}B EXCITED STATES POPULATED BY ^{9}Be-DECAY. Baghdikian, M. (Univ. Libre, Brussels). Univ. Brux., Inst. Phys. Bull., No. 21, 1-29(July 1965).

As the ^{9}B lifetime is very short, its spin and parity can be determined by angular correlation of its decay products. The ^{9}B populated by the $^{9}_{\Lambda}Be \rightarrow$ decay ($^{9}_{\Lambda}Be \rightarrow {}^{9}B + \pi^{-}$) can be observed in emulsions through the decay reactions $^{9}B \rightarrow {}^{8}Be + p$, $^{8}Be \rightarrow \alpha + \alpha$. The angular correlations of the ^{9}B decay products are computed here and curves are represented for different possible ^{9}B spins: $1/2^{-}$, $1/2^{+}$, $3/2^{-}$, $3/2^{+}$, $5/2^{-}$, $5/2^{+}$ and for the first ^{8}Be states 0^{+} and 2^{+}. (auth)

17808 NEW ISOTOPES ^{157}Eu, ^{157}Ho, AND ^{156}Er. Zhelev, Zh. T.; Kalinnikov, V. G.; Kudryavtseva, A. V.; Lebedev, N. A.; Makarov, S. P.; Muziol, G.; Kherrman, E. (Joint Inst. for Nuclear Research, Dubna, USSR). Yadern. Fiz., 2: 956-7(Nov. 1965). (In Russian).

Rare earth fractions were separated from a tantalum target irradiated with 660-Mev protons. Erbium and holmium fractions were isolated 2 hours after the irradiation. Daughter activities of dysprosium and holmium were isolated by extraction chromatography from an erbium fraction free of holmium. The 330 kev photopeak of ^{157}Dy ($T_{1/2}$ = 8.2 hr) was identified. The halflife of ^{157}Er was found to be 24 minutes from the amount of ^{157}Dy which accumulated in three successive separations. In a similar manner, the halflife of ^{157}Ho was found to be 18 minutes. An attempt was made to determine the halflife of ^{156}Er by following the increase and decrease of positron-emitting holmium isotopes in the erbium fraction. It was concluded that the upper limit for the halflife of ^{156}Er was 10 to 12 minutes. (TTT)

17809 NEUTRON CROSS SECTIONS FOR SOME THRESHOLD REACTIONS. Lagerwall, Torbjoern (Hahn-Meitner-Institut fuer Kernforschung, Berlin. Chalmers Univ. of Tech., Goteborg). Z. Naturforsch., 20a: 1583-7(Dec. 1965).

Three neutron reactions leading to production of the rare gases ^{41}Ar and ^{135}Xe were investigated. Single-crystal samples of KF, CaF_2, and BaF_2 were irradiated in the Berlin reactor, and the target-free absolute activities of the rare gas isotopes were measured by a β-γ coincidence method. The calculated cross sections are: $^{41}K(n,p)^{41}Ar$, $\sigma = (2.73 \pm 0.41)$ mb and $\sigma_0 = (98.6 \pm 14.8)$ mb; $^{44}Ca(n,\alpha)^{41}Ar$, $\sigma = (61.1 \pm 9.2)$ μb and $\sigma_0 = (64.7 \pm 9.7)$ mb; and $^{138}Ba(n,\alpha)^{135}Xe$, $\sigma = (1.9 \pm 0.3)$ μb and $\sigma_0 = (4.9 \pm 0.7)$ mb. The first sets of values were valid for a fission-neutron spectrum. The second sets were calculated for the high-energy plateau. They can be considered as valid for 15-Mev neutrons. (auth)

17810 THE CONVERSION ELECTRON SPECTRUM OF ^{104}Rh AFTER NEUTRON CAPTURE. Bieber, Erhard (Technische Hochschule, Munich). Z. Phys., 189: 217-41(1966). (In German).

The β spectrometer at the Munich Research Reactor was newly calibrated with a photographic method. The smallest obtainable line half-value width was 0.07% in the pulse measurement rod. The introduction of a bismuth shield between the reactor core and the steel tube and the use of a new magnetic field control led to a greater detection sensitivity and increased measurement accuracy. The origin of the background was investigated. In the measurement of the conversion electron spectrum of ^{104}Rh 70 lines were found. These belong to 55 transitions. In many cases the multipole classification of these transitions could be determined. Therefore it was possible to give spin and parity values for some levels in the low energy term scheme of ^{104}Rh. An expansion of the level scheme given by Gruber was proposed. (tr-auth)

17811 THE LIFETIME OF THE $^{23}/_{2}$ THREE-PARTICLE STATE OF ^{177}Hf AND ITS DECAY THROUGH A K-FORBIDDEN GAMMA TRANSITION. Bodenstedt, E.; Radeloff, J.; Buttler, N.; Meyer, P.; Schaenzler, L.; Forker, M.; Wagner, H.-F.; Krien, K.; Plingen, K.-G. (Univ., Bonn). Z. Phys., 190: 60-80(1966). (In German).

An isomeric state of ^{177}Hf with $T_{1/2} = (1.12 \pm 0.10)$ s was found by a fast chemical separation of the hafnium daughter from the 155d ^{177m}Lu activity. The same halflife was measured by observing the delayed β-γ-coincidences. A systematic investigation of the whole region $5s \geqq T_{1/2} \geqq 10^{-7}$ s by the technique of delayed coincidences gave no further isomerism. The observed halflife to the $^{23}/_{2}$ three particle state of ^{177}Hf was assigned at 1315 kev and it was assumed that the second hypothetical three particle state at 1337 kev does not exist. The $^{21}/_{2}$ rotational state of the $K = {}^{9}/_{2}$ band is populated by a strongly converted 14.16 kev γ-transition from the isomeric state at 1315 kev. The 14.16 kev M_1 and N_1 conversion lines were observed by use of a double focusing magnetic β-spectrometer. The isomerism is caused by the K-selection rule. The retardation of the following three-γ-transitions by different degrees of K-forbiddenness is discussed. The pulse height spectrum, measured by means of a Li-drifted Ge-detector, does not show the 36.52 kev-γ-transition which was previously assumed to populate the 1301 kev-state. In addition to the known γ-transitions a 40.9 kev-line was found. This is probably the transition between the 1301.1 kev and the 1260.3 kev-states. (auth)

17812 ON AN ISOMER OF ^{197}Au. Smend, F.; Weirauch, W.; Schmidt-Ott, W.-D.; Flammersfeld, A. (Univ., Goettingen, Ger.). Z. Phys., 191: 1-9(1966). (In German).

^{197m}Au was produced from Au by fast neutron irradiation and investigated using scintillation and semiconductor gamma spectrometers. The following results were obtained: Half-life $T_{1/2} = (7.5 \pm 0.2)$ sec; conversion coefficients of the 130.5 kev isomeric transition: $\alpha_{K130.5} = 0.9 \pm 0.3$ and $\alpha_{tot\,130.5} = 28 \pm 4$, indicating an E3 multipolarity. Conversion coefficients of the subsequent 278.5 kev transition: $\alpha_{K278.5} = 0.32 \pm 0.04$ and $\alpha_{tot\,278.5} = 0.44 \pm 0.10$.

This transition was identified as M1 with an E2 admixture of (13 ± 13)%. The 278.5 kev level decays either by this transition (98.5%) or by a 202 kev−77 kev cascade (1.5%). The experimental gamma transition probabilities are in reasonable agreement with the theoretical values calculated from the model of Kisslinger and Sorensen. (auth)

17813 STUDY OF THE NUCLEAR LEVELS OF ^{10}B AND ^{11}B BY INELASTIC ELECTRON SCATTERING. Spamer, E. (Technische Hochschule, Darmstadt, Ger.). Z. Phys., 191: 24-43(1966). (In German).

Cross sections as a function of momentum transfer and angle were measured for inelastic electron scattering from ^{10}B and ^{11}B. Primary energies between 32 and 57 Mev, and scattering angles from 92 to 165° were used. For the levels at 8.93 and 8.56 Mev in ^{11}B, and 7.477 and 6.01 Mev in ^{10}B the following multipolarities and radiation widths to the ground state (in ev) were deduced: 4.0 ± 0.6 (M1); 0.72 ± 0.30 (M1) + 0.40 ± 0.10 (E2); 12.0 ± 2.2 (M1) and 0.122 ± 0.020 (E2), respectively. Transition radii were evaluated for the levels mentioned, and for the 2.12 Mev state in ^{11}B. (auth)

17814 ON THE INCLUSION OF CORE EXCITATIONS IN THE QUASI-PARTICLE THEORY OF NUCLEAR STRUCTURE. Werner, E. (Univ., Heidelberg). Z. Phys., 191: 381-94(1966).

It is shown how the existence of several dominant poles in the spectral representation of the two-point function modifies Migdal's quasi-particle description of nuclear structure. The discussion is restricted to the case where the additional poles are due to the coupling of single-particle states with core-excitations. A prescription is given for the calculation of the ratios of single-particle or single-hole strengths measured in stripping or pick-up reactions. (auth)

17815 DEUTERON AND α-PARTICLE PICKUP IN THE INTERACTION BETWEEN ^{10}B AND ^{16}O. Shumilov, S. N.; Klyucharev, A. P.; Rutkevich, N. Ya. (Inst. of Physics and Tech., Academy of Sciences, Ukrainian SSR). Zh. Eksp. Teor. Fiz., 49: 1754-63(Dec. 1965). (In Russian).

The reaction $^{16}O + {}^{10}B \rightarrow {}^{14}N + 3\alpha - 2.8$ Mev due to the interaction between 100-Mev ^{10}B ions and ^{16}O nuclei of the photographic emulsion is studied. The excitation function of the reaction has a maximum at a ^{10}B energy of 60 Mev. The ^{14}N angular distribution in the cms has two maximums, one in the small angle and the other in the large angle range. They are due to α-particle and deuteron pickup from ^{16}O respectively. The reaction proceeds via formation of the ^{12}C nucleus. Excitation and decay of this nucleus into three α-particles are considered. (auth)

17816 CONTRIBUTION TO THE THEORY OF DIFFRACTION SCATTERING OF PARTICLES BY COMPLEX NUCLEI. Inopin, E. V.; Kresnin, A. A. (Inst. of Physics and Tech., Academy of Sciences, Ukrainian SSR). Zh. Eksp. Teor. Fiz., 49: 1796-1801(Dec. 1965). (In Russian).

Problems connected with the method of analysis of experimental data on diffraction scattering of particles by complex nuclei proposed recently are considered. The theory is compared with the experiments on scattering of α-particles on a number of nuclei from various regions of the periodic system. The analysis shows that the method considered yields a correct description of diffraction scattering. (auth)

17817 INELASTIC DIFFRACTION SCATTERING TREATED BY THE COMPLEX ANGULAR MOMENTUM METHOD. Inopin, E. V.; Tishchenko, B. I.; Shebeko, A. V. (Inst. of Physics and Tech., Academy of Sciences, Ukrainian SSR). Zh. Eksp. Teor. Fiz., 49: 1824-30(Dec. 1965). (In Russian).

A simple analytic expression for the inelastic scattering cross section of a zero spin particle is deduced on the basis of the complex angular momentum method. The expression obtained contains the well known Blair phase rule. The results are compared with experimental data on α-particle scattering on a number of nuclei. The comparison indicates a very satisfactory qualitative agreement between the theory proposed and the experiments. (auth)

17818 QUADRUPOLE AND NUCLEAR SPIN INTERACTION VIA THE OPTICAL PHONON VIRTUAL FIELD. Nagibarov, V. R. (Kazan Inst. of Physics and Tech., Academy of Sciences, USSR). Zh. Eksp. Teor. Fiz., 49: 1836-42(Dec. 1965). (In Russian).

Interaction of nuclear spins and energy migration over orbital levels via the optical phonon virtual field is considered. The mechanism is due to interaction between quadrupole moments (nuclei and electron shells) and the electric field gradient of the optical oscillations. For distances between the quadrupoles r_{ij} of the order of the lattice parameters the cross relaxation transition probability depends on r_{ij} as $1/r_{ij}^{10}$; for distances considerably exceeding the lattice constant it varies as $1/r_{ij}^{4}$ and $1/r_{ij}^{8}$. Numerical estimations show that processes of this type are quite effective. (auth)

17819 QUANTUM-STATISTICAL THEORY OF DYNAMIC POLARIZATION OF NUCLEI. Buishvili, L. L. (Inst. of Cybernetics, Academy of Sciences, Georgian SSR). Zh. Eksp. Teor. Fiz., 49: 1868-74(Dec. 1965). (In Russian).

A quantum-statistical analysis of the dynamic polarization of nuclei is carried out, by taking into account diffusion of nuclear spins as well as dipole interaction of electron spins. A set of integro-differential equations is obtained for the nuclear Zeeman, electron Zeeman and dipole pool temperatures. Various particular cases are discussed. (auth)

17820 SEMICONDUCTOR DETECTOR STUDIES OF RECOILS FROM 15-Mev DEUTERONS ON ^{12}C [Thesis]. Sodd, Vincent Joseph. Pittsburgh, Univ. of Pittsburgh, 1964. 145p.

A method is described by which recoiling residual nuclei from nuclear reactions are counted and analyzed with good resolution as they escape from thin targets during accelerator bombardments. The properties of the silicon surface barrier detectors used are described. Spectra of 1- to 8-Mev ^{10}B, ^{12}C, ^{13}C, and ^{13}N recoils from 15-Mev deuteron-induced reactions of carbon were obtained as a function of detector bias, target thickness, and thickness of interposed absorber. Applications of the method to studies of the range, energy loss, and charge-state distributions of low-energy heavy ions are described. The equilibrium charge-state distributions of ^{12}C ions with velocities between 8.77 and 9.77 × 10^8 cm/sec and of ^{13}C ions with velocities between 7.08 and 8.46 × 10^8 cm/sec were determined. The ions were produced as recoils from ^{12}C (d,d′) and ^{12}C(d,p) reactions induced by 15-Mev deuterons, equilibrated during the process of escaping from the carbon targets, subjected to magnetic analysis, and detected with a low-resistivity Si surface-barrier detector. The data join smoothly to previous results, which are predominately at higher velocities. (Dissertation Abstr.)

17821 ENERGY DEGRADATION OF FISSION FRAGMENTS IN LIGHT MATERIALS [Thesis]. Mulas, Pablo M. Princeton, N. J., Princeton Univ., 1965. 175p.

A surface barrier silicon detector was used to determine average energy versus distance curves for ^{252}Cf fission fragments in H_2, D_2, N_2, and "Mylar." In all cases the energy loss was substantially greater than that predicted by the integrated form of the Bohr equation. The magnitude of the discrepancy increased with the atomic number of the stopping material. Attempts were made to fit the present data and that of previous workers on heavier materials with the expression $E = E^0(1 - f)^n$. E is the average energy of a group of fragments of original average energy E^0, which have travelled a fraction f of their total range. No correlation was found between the value of the exponent n and the various stopping media. The average energy-distance curve in H_2 obtained in these experiments and a semiquantitative treatment of the ionization produced by fission fragments enabled the calculation of w, the differential energy expended per ion-pair, for the average mass fission fragment of ^{252}Cf as a function of the fragment energy. (Dissertation Abstr.)

17822 YADERNAYA SPEKTROSKOPIYA I NEITRONOAKTIVATSIONNYI ANALIZ. (Nuclear Spectroscopy and Neutron Activation Analysis). Riga, USSR, Izdatel'stvo Zinatne, 1965. 84p.

Four articles on conversion electrons in the radiative capture of thermal neutrons by nuclei are presented, including the spectrum of internal-conversion electrons emitted in thermal-neutron capture by ^{164}Dy and by ^{165}Ho, excited levels of ^{177}Lu, and isomer-formation cross-section ratios in ^{116}In. Seven articles on methods and techniques of neutron activation analysis are given, including identification of elements, determination of Al in semiconducting Si, determination of Se in Cu, determination of Fe in blood, induced radioactivity in polyethylene from neutron irradiation, electromagnetic pendulum for activation of samples in neutron beam, and pneumotransporter of samples. (M.J.T.)

17823 BORON PILE $\bar{\nu}$ MEASUREMENTS. Colvin, D. W.; Sowerby, M. G. (Atomic Energy Research Establishment, Harwell, Eng.). pp 25-37 of STI/PUB/101 (Vol. 2).

Accurate absolute measurements of $\bar{\nu}$, the average number of neutrons per fission, were made with the boron pile. The experimental method is described and results are presented of the $\bar{\nu}$ values obtained for the thermal-neutron-induced fission of ^{233}U, ^{235}U, ^{239}Pu, and ^{241}Pu, the spontaneous fission of ^{240}Pu and ^{252}Cf, and the fast neutron-induced fission of ^{235}U in the energy range 100 kev to 2.6 Mev. (auth)

17824 PROMPT-NEUTRON EMISSION FROM ^{235}U FISSION FRAGMENTS. Cornell, T.; Maslin, E. E.; Rodgers, A. L. (Atomic Weapons Research Establishment, Aldermaston, Eng.). pp 67-72 of STI/PUB/101 (Vol. 2).

A gadolinium-loaded large liquid scintillation counter is being used in conjunction with a neutron beam from the HERALD reactor to study neutron emission in the fission process. In particular, the neutron emission from individual fission fragments is observed. A fission-fragment detector comprising two gold-silicon surface barrier counters operating in coincidence is situated at the edge of a 1-m-diam. spherical scintillation tank. The solid-state counters are placed on opposite sides of an evaporated fissile deposit on a thin nickel backing. A system of collimators selects for measurement only those fission events that have fragments travelling in the direction along the incident neutron beam and along the axis of the scintillator. Numbers of neutrons detected within 10 μs of a fission event are recorded. The angular correlation of neutron emission with fragment direction is used to associate the neutrons with the particular fission fragment that emitted them. Energies of both fragments are available from the solid-state counters, and identification of fragment mass and of the total kinetic energy of the fragment pair is made. The number of neutrons emitted by each fragment of the pair has been measured as a function of both the fragment mass and the total kinetic energy of the pair for thermal neutrons incident on ^{235}U. The usual asymmetry in the distribution of excitation energy between the heavy and light fragments is observed. The variation of the number of neutrons from the pair as a function of mass ratio is also determined. (auth)

17825 FISSION-NEUTRON SPECTRA OF ^{235}U, ^{239}Pu AND ^{252}Cf. Conde, H.; During, G. (Research Inst. of National Defence, Stockholm). pp 93-102 of STI/PUB/101 (Vol. 2).

Measurements of the fission neutron spectra from the neutron-induced fission of ^{235}U and ^{239}Pu, and the spontaneous fission of ^{252}Cf, were made. The spectra were measured with a time-of-flight technique using a plastic scintillator as the fission-neutron detector. The low energy part of the ^{252}Cf fission-neutron spectrum (below 0.3 Mev) was also measured with a ^{6}Li-glass detector replacing the plastic scintillator. The fissile materials were mounted in xenon-gas scintillation chambers. The primary neutrons were produced by a 2.5-Mev Van de Graaff accelerator with top terminal pulsing. The resolving time-of-flight equipment was better than 3 ns. Results fitted to Maxwellian distributions, $\sqrt{E}e^{-E/T}$, are presented for neutron-induced fissions of ^{235}U at 40 kev and 1.5 Mev of incident neutron energy and for ^{239}Pu at 40 kev. Results are also given for the fission-neutron energy spectrum of ^{252}Cf. (auth)

17826 LIQUID SCINTILLATOR EXPERIMENT FOR MEASURING $\bar{\nu}$ FOR ^{241}Pu. Boldeman, J. W. (Australian Atomic Energy Commission Research Establishment, Lucas Heights, New South Wales). pp 103-9 of STI/PUB/101 (Vol. 2)

A 1-m-diam. tank of gadolinium-loaded liquid scintillator is being used for measurement of the number of prompt neutrons per neutron fission event for various target materials including ^{241}Pu. Incident neutrons range in energy from thermal to 6 Mev. The thermal-neutron measurements use a collimated beam from the 10-kw reactor, MOATA. Neutrons of higher energy are produced with a 3-Mev Van de Graaff accelerator. The target material is incorporated in a methane proportional counter mounted at the center of the liquid scintillator and within an evacuated flight path. Coincident pulses between this fission counter and the liquid scintillator indicate a fission event. Following each such event, pulses resulting from the detection of prompt neutrons in the liquid scintillator are counted for 40 μs. The number of pulses per fission event is converted to a pulse amplitude for recording in a pulse-height analyzer. The Van de Graaff accelerator is operated with externally triggered pulsing of such a kind that, during the 40-μs counting time, the d-c proton or deuteron beam is interrupted, easing background problems especially in the case of ^{241}Pu where only small amounts of material are available. At the same time there is essentially no loss in duty cycle. The efficiency of the liquid scintillator tank will be determined, using the accepted $\bar{\nu}$ value for the spontaneous fission of ^{252}Cf. After making the usual corrections, a relative accuracy of 1% is expected for the $\bar{\nu}$ measurement. (auth)

17827 PROMPT AND DELAYED GAMMA-RAYS FROM FISSION. Maier-Leibnitz, H.; Armbruster, P.; Specht, H. J. (Technische Hochschule, Munich. Kernforschungsanlage, Juelich, Ger.). pp 113-23 of STI/PUB/101 (Vol. 2).

The following data about gamma-rays from fission are reported and discussed. Total prompt gamma-ray spectrum, and average number and energy of gamma-rays; x rays in prompt fission, and excitation of x rays in matter; gamma spectra as a function of the mass ratio in fission, gamma lines in those spectra, and Doppler effect; anisotropy in gamma emission relative to the direction of fragments; average gamma energy and gamma spectra as a function of mass of the fission products; delayed gamma rays; delayed gamma rays as a function of fission product mass. (auth)

17828 AVERAGE NUMBER AND ENERGY OF GAMMA-RAYS EMITTED AS A FUNCTION OF FRAGMENT MASS IN ^{235}U THERMAL-NEUTRON-INDUCED FISSION. Maier-Leibnitz, H.; Schmitt, H. W.; Armbruster, P. (Oak Ridge National Lab., Tenn.). pp 143-61 of STI/PUB/101 (Vol. 2).

The average number and energy of gamma rays emitted as a function of fragment mass in ^{235}U thermal-neutron-induced fission were measured. A three-parameter correlation experiment was performed in which two silicon surface barrier detectors were used to measure the fission product energies, and a 5-in-diam., 4-in-thick NaI(Tl) scintillation crystal was used to measure the gamma-ray energies. Extreme care was taken in the experimental arrangement to avoid counting direct fission neutrons, scattered gamma rays and neutrons, and other false events. Data were recorded event-by-event in a system similar to that used in previous energy correlation experiments, and were analyzed according to a "weighting method" proposed by Maier-Leibnitz. The total number and energy of the gamma rays for both fragments as a function of mass ratio were obtained directly. The number and energy of gamma rays for individual fragment masses were determined by making use of the variation in laboratory angular distribution and energy of the gamma-rays emitted from moving fragments. In particular, the 0 to 180° ratio of the number

of gamma rays from a moving source emitting isotropically in its center-of-mass system is proportional to $1 + 2 \times 2v/c$; similarly the 0 to 180° ratio in total gamma energy is proportional to $1 + 2 \times 3v/c$. Thus by comparing appropriate ratios in the analysis for light and heavy fragments moving towards or away from the gamma detector, one obtains these quantities as a function of individual fragment mass. Results of preliminary analyses show interesting similarities in behavior to those for neutrons. Both the total energy and average quantum energy of gamma rays are essentially constant over most of the range of mass ratios; however a broad minimum is observed for the total energy in the region where $M_H \sim 130$, i.e., where $Z_H \sim 50$ or $N_H \sim 82$. An increase is observed in the total energy as the mass ratio approaches unity. The number and energy of gamma-rays emitted from individual fragments are observed to increase in both fragment groups and show similar mass dependence, as has been observed for prompt neutrons. The average quantum energy in the mass range of closed shells seems to be higher. (auth)

17829 THE ANGULAR DISTRIBUTION OF GAMMA-RAYS FROM THE FISSION OF ^{235}U. **Graff, G.; Lajtai, A.; Nagy, L. (Central Research Inst. of Physics, Budapest).** pp 163-7 of STI/PUB/101(Vol. 2).

The angular distribution of gamma rays from thermal-neutron-induced fission was measured with respect to the axis of fission. The gamma radiation intensities were found to be higher in the direction of fission-fragment motion than in that normal to it. The anisotropy proved to be nearly the same for photon threshold energies of 120 and 600 kev. (auth)

17830 DELAYED NEUTRONS AND PHOTONEUTRONS FROM FISSION PRODUCTS. **Amiel, S. (Atomic Energy Research Center, Yavne, Israel).** pp 171-96 of STI/PUB/101(Vol. 2).

Most studies of the delayed neutrons from fission have involved analysis of the kinetic behavior of fission chain-reacting systems, analysis of the gross neutron decay (resolved into six groups with approximate half lives of 0.2, 0.5, 2, 6, 22 and 55 s) and some measurements of the neutron spectra (the energies extend from 0.1 to 1.2 Mev, peaking in the range 0.2 to 0.5 Mev). Rapid separations of fission-produced halogens have indicated seven isotopes (^{87}Br, ^{88}Br, ^{89}Br, ^{90}Br and ^{137}I, ^{138}I, ^{139}I), and rare gas analysis has indicated 1.5-s Kr and 6-s Rb as definite delayed neutron precursors. These identified precursors account for some 80% of the total delayed neutron yields. Theoretical predictions of possible precursors point to a few tens of such nuclides to be found mainly in regions just above closed neutron shells. Total neutron yields are observed to increase with mass number and decrease with atomic number of the fissioning nuclide. Yields are nearly independent of the energy of the incident fissioning neutron at energies up to several Mev. In this range observed group yields, especially of the long-lived precursors, are in fairly good agreement with fission mass and charge distributions, and calculated neutron emission probabilities. Further detailed studies of delayed neutron precursors (particularly in the difficult short half life region) require development of ultra-fast radiochemical separation procedures (or on-line isotope separation) and fast neutron spectroscopy of high resolution and efficiency. A knowledge of the intensities and gamma spectra of fission products is of practical importance in reactor technology, particularly with respect to gamma heating, shielding and radiation effects. Gamma rays of energies greater than 2.23 and 1.67 Mev cause emission of photoneutrons from deuterium and beryllium respectively, and are important in the kinetics of heavy water and beryllium-moderated reactors. The rate of photoneutron emission after fission represents the composite decay of the corresponding gamma-ray-emitting nuclides in the mixture of fission product chains. The gross photoneutron decay curves from both D_2O and beryllium were resolved into nine groups with half lives ranging from a few seconds to ~13d. Each of these groups represents a complex composite of nuclides. Detailed information on the constituents of these groups is important for reactors in which fission products fractionation may take place and affect relative group abundances. Such information exists only for the longer-lived fission products whose properties and yields are well known, and where experimental results are in agreement with calculated values based on fission mass and charge distributions and decay schemes. The characterization of individual nuclides in the more complex short-lived groups is indeed a formidable task, but this information is of considerable practical and theoretical importance, and warrants further extensive study. (auth)

17831 COMPARISON OF OBSERVED DELAYED-NEUTRON ABUNDANCES WITH CALCULATED FISSION YIELDS OF NEUTRON PRECURSORS. **Hermann, G.; Fiedler, J.; Benedict, G.; Eckhardt, W.; Luthardt, G.; Patzelt, P.; Schuessler, H. D. (Univ., Mainz).** pp 197-213 of STI/PUB/101(Vol. 2).

Cumulative fission yields of known and predicted delayed-neutron precursors were calculated using recent mass- and charge-distribution data. These yields were then compared with abundances of the 55-, 22-, 6-and 2-s neutron periods in various low-energy fission reactions, i.e., neutron emission probabilities were calculated by minimizing the deviations between observed and calculated abundances. The number and kind of precursors involved in each period have been varied as well as the assumptions made on most probable primary charge and its dispersion. The abundances reported in low-energy fission can be explained satisfactorily by the known precursors. Some of the predicted precursors may be present but their calculated contributions are comparatively small. Some other predicted precursors lead to bad agreement with abundance data and to unlikely emission probabilities. Several questionable mass-assignments of precursor nuclides are corroborated. Emission probabilities were used for estimating delayed-neutron abundances in 14-Mev neutron fission. The values obtained are much smaller than reported abundances. This discrepancy cannot be accounted for by unknown precursors, at least for fission of ^{232}Th and ^{238}U by 14-Mev neutrons, since only a relatively small fraction of the delayed-neutron activity remains after a rapid halogen separation. Therefore, the absolute abundances for both reactions are remeasured by a new method that involves no absolute counting. Preliminary abundances obtained are much lower than the reported values, and are in good agreement with the expected value. (auth)

17832 VARIATION OF RELATIVE YIELDS OF DELAYED NEUTRONS. **Maksyutenko, B. P.** pp 215-19 of STI/PUB/101(Vol. 2). (In Russian).

The relative yields of delayed neutrons from uranium-238 on fission by neutrons with average energies of 1.5, 2.3, 3.8, 5.75, 6.5, and 15 Mev were measured. The decay curves were processed on a computer by the least-squares method for set half life values. This method makes it possible to assess, independently of accuracy of identification, the deformation of the decay curve of the delayed neutrons, and consequently to judge the changes in yield of the different groups. The rounded-off values of the half-lives used in the calculations were 55, 24, 15.5, 5.2, and 2.2 s. In a number of experiments the shorter-lived groups could not be separated because of the length of time (5.5 s) needed to switch off the ion current on the Van de Graaff accelerator. The results are given in the form of the ratio between the yield of each group and the first (with a half life of 55 s). The ratio between the yields of the group changes unevenly. Where fission is induced by neutrons in the 2.3 to 6-Mev energy region (the region between the "steps" in the fission cross section), this ratio either does not change (for the groups with half lives of 5.2 and 0.5 s) or decreases smoothly with increase in energy by from 10 to 40% (for the groups with half lives of 24, 15.5 and 2.2 s). At an energy of 6.5 Mev (where the n, nf reaction already occurs) the ratio of the yields is sharply increased as compared to that at $E_n = 5.75$ Mev, except for the group with a half life of 15.5 s, in which the opposite tendency is observed. There is also a sharp change in the ratio of the yields in the region of the first "step" in the fission cross section,

i.e. close to the fission threshold of uranium-238 at E_n = 1.5 Mev. At a neutron energy of 15 Mev a decrease in the ratio of the yields is again apparent. The ratio of the yields for uranium-235 and plutonium-239 in the range 0.025 ev-6 Mev follows the pattern observed for uranium-238 over the corresponding range. (auth)

17833 RESEARCH FOR DELAYED-NEUTRON PRECURSORS IN ANTIMONY AND ARSENIC FISSION PRODUCTS. del Marmol, P.; de Mevergnies, M. Neve; Speecke, A. (CEN-SCK, Mol, Belg.). pp 225-31 of STI/PUB/101 (Vol. 2).

Antimony and arsenic fission products are isolated by a fast radiochemical procedure and their activity measured by neutron counting. Irradiations are performed at the BR2 reactor in an external beam of 1.5×10^9 n/cm^2·s and fission products of arsenic and antimony can be isolated from 2 g ^{235}U with a chemical yield of about 40% in two seconds. The whole process is performed automatically. A 2-s half-life is observed that cannot be attributed to halogen or rare gas delayed-neutron precursors and thus must be produced by arsenic or antimony. (auth)

17834 SHORT-LIVED ANTIMONY AND ARSENIC ISOTOPES FORMED IN FISSION. Tomlinson, L. (Atomic Energy Research Establishment, Harwell, Eng.). pp 233-40 of STI/PUB/101(Vol. 2).

The application of a new technique for the rapid separation of short-lived antimony and arsenic isotopes from fission products is described. The gamma spectra of ^{128}Sb, ^{129}Sb, and ^{130}Sb were measured and previous observations confirmed. A new delayed-neutron activity of 2-s half life was detected. The experimental data indicate that this activity is due to two isotopes, one of antimony and the other of arsenic. These are tentatively assigned to ^{135}Sb and one of the isotopes ^{85}As or ^{87}As. (auth)

17835 RECENT EXPERIMENTS ON THE BETA ACTIVITY OF FISSION PRODUCTS FROM THE THERMAL-NEUTRON FISSION OF ^{233}U, ^{235}U, AND ^{239}Pu. Specht, H. J.; Seyfarth, H. (Technische Hochschule, Munich). pp 253-62 of STI/PUB/101(Vol. 2).

The build-up of beta-activity of fission products from the low-energy fission of ^{233}U and ^{235}U was measured as a function of the time t after starting the irradiation of the fissionable material with thermal neutrons. By differentiating the beta-activity divided by the constant fission product rate one obtains the mean beta-decay rate $\beta(t)$ per fission as a function of the time t after fission. The uranium targets were mounted within a 4π proportional counter, coincident conversion electrons and γ rays being thereby eliminated. The background of fast neutrons and γ rays was strongly reduced by using a neutron beam tube with a liquid nitrogen-cooled bismuth single crystal filter. The fission product rate was measured with the same counter. The measurements cover the time interval from 0.01 s to 10 h. The results are compared with other experimental data and existing theories. The total number of beta-decays per fission was found to be 5.25 ± 0.2 and 5.93 ± 0.2 for ^{233}U and ^{235}U respectively compared with theoretical values of 5.27 and 6.10 respectively. (auth)

17836 NUCLEAR FISSION AT HIGH AND MEDIUM ENERGY OF EXCITATION. Perfilov, N. A. (Radioinstitut, Leningrad). pp 283-306 of STI/PUB/101(Vol. 2). (In Russian).

A review of experimental research on nuclear fission at high and medium energy of excitation is given. Certain aspects of nuclear fission theory in this range of energy are also considered. (auth)

17837 RANGES OF IODINE AND BROMINE ISOTOPES PRODUCED IN THE INTERACTION OF HIGH-ENERGY PROTONS WITH URANIUM. Brandt, R. (CERN, Geneva. Max-Planck-Institut fuer Kernphysik, Heidelberg). pp 329-42 of STI/PUB/101(Vol. 2).

Conventional range experiments using a thick uranium foil together with aluminum catches and monitors are carried out at the two CERN accelerators with 0.55- and 18.2-Bev protons. Iodine (or bromine) is chemically isolated and separated in the CERN radioisotope separator. This gives carrier-free samples containing essentially only one pure radioactive isotope. The chemical yield is determined also. The analysis of the data gives directly the range for each isotope in uranium. All iodine isotopes have the same range at 0.55-Bev proton energy, i.e., they are all produced in a fission process. It was known previously that neutron-rich iodine isotopes have about the same range whether the proton energy is above or below 1 Bev, and that neutron-deficient iodine isotopes show a drastic decrease of about one half when the proton energy increases above 1 Bev. It is shown that this decrease in range occurs rather suddenly, giving a step-function in the range–versus–iodine isotopic mass curve. The neutron-deficient isotopes having a decreased range above 1-Bev proton energy are the same as those for which a strong increase in their excitation function above 1 Bev has been observed. Bromine isotopes show essentially the same range behavior. The strong increase in the production of neutron-deficient isotopes is again observed at high bombarding energies. The discussion is concentrated on these neutron-deficient isotopes. They are produced essentially only above 1 Bev and have at the higher bombarding energy only about one half the range of normal fission products, indicating that they are produced by a process other than fission. These findings will be discussed in the light of "spallation" and "fragmentation" models, both terms being redefined. (auth)

17838 FISSION CROSS-SECTIONS OF ^{181}Ta, Re, Pt, ^{197}Au, Pb, Bi, Th, ^{235}U AND ^{238}U FOR PROTONS WITH ENERGY OF 150-660 Mev. Kon'shin, V. A.; Matusevich, E. S.; Pegushevskii, V. I. pp 349-52 of STI/PUB/101 (Vol. 2). (In Russian).

The measurements were carried out on the synchrocyclotron of the Joint Institute for Nuclear Research, with a maximum proton energy of 660 Mev. The fission events were recorded by visual observation of the fission-fragment tracks left on glass after treating. The absolute recording efficiency was determined by the number of ^{235}U and ^{239}Pu fissions in a known thermal-neutron flux, and the number of ^{235}U fissions in a neutron flux from a Ra-α-Be standard source. The proton flux was determined by measuring the absolute number of β disintegrations of ^{24}Na occurring in the ^{27}Al(p,3pn)^{24}Na reaction (whose cross section is known with an accuracy of ±5%), using a scintillation gamma spectrometer. Samples were irradiated both in an external proton beam and within the chamber of the synchrocyclotron. The fission cross sections were measured in the proton energy range 150–660 Mev. The corrections applied are discussed. The results of the measurements are compared with earlier figures, and the dependence of fissility of the nuclei investigated on the parameter Z^2/A is determined. (auth)

17839 VARIATION OF FISSION-FRAGMENT KINETIC ENERGY DISTRIBUTION, MASS DISTRIBUTION, AND YIELD OF LONG-RANGE ALPHA PARTICLES IN THE RESONANCE-NEUTRON-INDUCED FISSION OF ^{235}U AND ^{239}Pu. Melkonian, E.; Mehta, G. K. (Columbia Univ., New York). pp 355-68 of STI/PUB/101(Vol. 2).

These measurements were undertaken to obtain additional information on the fission process, and to investigate the application of this information to the assignment of J-values to resonance levels, as the usual methods of determining J-values are of limited applicability in the case of fissile isotopes. An earlier study of ^{235}U showed that the fission-fragment kinetic energy and the alpha yield varied significantly from level to level, and fell into two groups suggestive of the two possible J-values. Measurements on ^{239}Pu are reported. A study of 19 levels shows 15 levels with high average kinetic energy and 4 levels with low average kinetic energy, the former being assigned J = 1 and the latter J = 0 on the basis of the expected ratio of population of the two spin states and also for maximum compatibility with other determinations. Some variation of relative alpha-particle yield was found. It is concluded that there are definite variations of kinetic energy of the fragments from level to level; the variation in the case of ^{235}U is correlated with the relative yield of symmetric

fission; there is some indication in the case of ^{239}Pu that the variation of fragment energy is correlated with the J-values; and the relative yield of alpha particles varies in an expected fashion. (auth)

17840 VARIATION OF THE BINARY-TO-TERNARY FISSION RATIO FOR ^{235}U IN THE THERMAL-NEUTRON-ENERGY REGION. Deruytter, A. J.; Neve de Mevergnies, M. (CEN-SCK, Mol, Belg.). pp 429-37 of STI/PUB-101 (Vol.2)).

The slow chopper installed at BR1 was used to make an accurate determination of the binary-to-ternary fission ratio for ^{235}U in the neutron-energy range from 0.005 to 0.2 ev. Large gold-silicon surface-barrier detectors are used for the consecutive measurement of long-range α particles (absorber in) and fission fragments (absorber out). The time analysis is done with a 100-channel time-of-flight analyzer. A one-meter flight-path and a rotor speed of 50 rev/s is used. The B/T ratio was also measured with a high statistical accuracy (about 1%) in intense beams with well-defined neutron spectra, i.e., a "cold neutron" beam, a beam extracted from a thermal column and a beam of 0.3-ev neutrons produced by crystal diffraction. The B/T ratio exhibits a small and smooth variation in the energy range considered. This effect seems to be correlated with measurements of some other fission parameters in the same neutron-energy range. (auth)

17841 WEAK ALPHA AND ELECTRON-CAPTURE DECAY IN ^{208}Po AND ^{209}Po [Thesis]. Hagee, G. Richard. Cincinnati, Univ. of Cincinnati, 1965. 132p.

The weak alpha and electron-capture decay of ^{208}Po and ^{209}Po were investigated in order to derive a self-consistent decay scheme. Techniques of single alpha, gamma, and conversion electron spectroscopy were used and were supplemented by alpha-gamma, gamma-gamma, and conversion-electron gamma coincidence methods. New alpha groups were found having energies of 4.22 Mev with 2.44×10^{-4}% abundance in ^{208}Po decay and of 4.11 Mev, 4.31 Mev, and 4.617 Mev with 5.66×10^{-4}%, 1.46×10^{-4}%, and 0.48% abundance respectively in ^{209}Po decay. Conversion-electron studies of the 263 kev gamma characterize it as an M1 + E2 transition. Changes in the spin assignments for the 761-kev level in ^{205}Pb from $(^9/_2^-)$ to $(^3/_2^-)$ and for the 576-kev level from $(^3/_2^-)$ to $(^5/_2^-)$ are suggested. Electron-capture decay in ^{209}Po was measured as 0.263%. The K-shell conversion coefficient for the associated 900-kev gamma ray was determined as 1.7×10^{-2}, which characterizes it as an M1 + E2 transition. Total electron-capture branching in ^{208}Po decay was measured as 1.81×10^{-3}%. The predominant electron-capture feeding was determined as 77.4% to the 921-kev (2^+) level with branching to the 630-kev (3^+) and 1074-kev (3^+) levels of 19.0% and 3.6% respectively. Log ft values of 13.7 and 14.3 for decay to the (2^+) and (3^+) levels are in agreement with assignments as second forbidden and second forbidden unique transitions respectively. Conversion-electron measurements show that gamma rays of 291, 534, 565 and 599 kev are M1 radiation with small admixtures of E2 in certain cases. A gamma-ray triad of 534, 565, and 599 kev in the electron-capture decay of ^{208}Po was resolved by means of a gamma-ray conversion-electron coincidence technique using semiconductor detectors for electron measurements. Details of the decay schemes obtained are internally consistent and agree well with experimental and theoretically calculated energy levels obtained elsewhere by other methods. (Dissertation Abstr.)

17842 NUCLEAR RESONANCE FLUORESCENCE USING RECOIL BROADENED GAMMA RAYS FROM THE RADIATIVE CAPTURE OF THERMAL NEUTRONS [Thesis]. Dowdy, Edward Joseph. College Station, Tex., Texas A and M Univ., 1965. 73p.

A beam of 7.3-Mev gamma rays, with an energy spread of ±1.85 kev was produced utilizing the recoil broadening of the 7.3-Mev to ground state transition in the de-excitation of the ^{15}N compound nucleus formed in the $^{14}N(n,\gamma)^{15}N$ reaction. This recoil broadened beam was used to resonantly excite an energy level near 7.3 Mev in lead. The angular distribution of the resonance scattered gamma rays was measured and found to fit the $(1 + \cos^2\theta)$ distribution of a dipole transition. From a comparison of the resonance scattering yield with a natural lead scatterer and with a radiogenic lead scatterer, it was concluded that ^{206}Pb could not be responsible for the resonant effect. The ground state transition width of the resonantly excited level was measured by means of a resonance self-absorption experiment and found to be 1.04 ± .25 ev, assuming that the level that was excited is a level in ^{208}Pb. (Dissertation Abstr.)

17843 REVIEW OF FISSION THEORY. Swiatecki, W. J. (Univ. of California, Berkeley). pp 3-9 of STI/PUB/101(Vol. 1).

A survey of the present state of fission theory is attempted. The basic requirements of a theory of a physical process are outlined and against this background the state of fission theory is summarized, with special emphasis on developments in the past few years. An attempt is made to bring out the most important outstanding problems to be settled by future experiments and theory. (auth)

17844 STUDY OF FISSION FOLLOWING (d,p) AND (t,p) REACTIONS IN URANIUM ISOTOPES. Eccleshall, D.; Yates, M. J. L. (Atomic Weapons Research Establishment, Aldermaston, Eng.). pp 77-84 of STI/PUB/101(Vol. 1).

The fission of ^{233}U, ^{234}U, ^{235}U, ^{236}U, and ^{238}U induced by (d,p) and (t,p) reactions was studied, at a bombarding energy of 13 Mev. The protons were detected in an annular counter system situated at about 170° to the beam, and the proton spectrum in coincidence with fission fragments was recorded. The annular counter system consisted of an E-ΔE telescope with a thin (0.002-in.) surface barrier semiconductor counter in front of a thick surface barrier counter in which the protons were stopped. The particles were identified using a conventional pulse multiplier. The fission fragments were detected in other surface barrier counters at 90, 135, and 170°. For this latter angle the annular ΔE counter was used to detect the fission fragments, since it was found that of the various particles emerging from the target only the protons were in coincidence with fission fragments. Differences in the fission thresholds deduced from the ^{234}U (t,pf) and ^{235}U (d,pf) reactions were observed, indicating that the (t,p) reaction feeds fissioning states of lower excitation in the compound nucleus. A difference in the behavior of the fission-fragment angular distributions for these two reactions was also observed at energies close to the fission threshold. Both effects provide evidence for a detailed structure consistent with the existence of the low-lying collective excitations at the saddle point of fission, analogous to those observed at the stable shape. (auth)

17845 DEPENDENCE OF FISSION-FRAGMENT PRIMARY CHARGE ON NUCLEAR STRUCTURE. Armbruster, P. (Kernforschungsanlage Juelich, Ger.). pp 103-19 of STI/PUB/101(Vol. 1).

Assuming a quasi-static scission configuration the potential energy of this configuration was calculated. The energy release between saddle point and scission point was maximized using the liquid drop model and taking into account the mass dependence of the deformability of the fission fragments. The leading terms that determine the charge distribution depend on the Coulomb and the asymmetry energy of the scission configuration. The deformability of the fragments shows dependence from nuclear structure. A term proportional to the difference of the deformation energies of the two fragments gives rise to a strong influence from this nuclear structure effect. In the region of closed shells the difference in the deformation energies is much the same as the total deformation energy. A term comparable to the Coulomb energy term has to be taken into account in these mass regions. The calculated Z_p-values were compared to experimental results for ^{235}U. Calculated Z_p-values for ^{252}Cf are given. (auth)

17846 SHELL EFFECTS IN NUCLEAR FISSION. Geilikman, B. T. (Kurchatov Inst. of Atomic Energy, Moscow). pp 121-26 of STI/PUB/101(Vol. 1). (In Russian).

The important part played by shell effects in nuclear fission has been reliably established experimentally and forms the basis of the theory of asymmetry of fission and other properties of fission fragments. However, from the theoretical point of view there are certain difficulties in understanding these effects, since at the moment of scission the fragments are considerably deformed. When the shell effects are calculated in succession, the energy of the fissioning nucleus before scission may be presented in the form of the sum of the energies of the spherical fragments taking shell effects into account, the Coulomb interaction energy of the fragments and their deformation energy. The deformation energy of the fragments should be calculated not using the elasticity values of the fragements according to the drop model, but, for very low deformations, the single particle elasticity values taking into account the magic effects, with a gradual transition to the drop values for deformations at which the levels of neighboring shells intersect. The single-particle elasticity values can be obtained from the experimental data on the Coulomb excitation of the nuclei. In Vandenbosch's calculations of fragment deformation, the elasticity of the fragments was based on the condition of coincidence between the deformation energy of the fragments and the experimental values for their excitation energy. However, in this case the elasticity was assumed to be constant at all deformations, and for this reason, although the elasticity values found in Vandenbosch do show magic effects, they differ considerably in magnitude from the experimental elasticity values (see above). The calculations of Vandenbosch also failed to take into account the magic effects for nondeformed fragments that lead to a reduction in the energy of the magic nucleus. Therefore, according to these calculations fission should be symmetrical, since the elasticity and consequently also the deformation energy (at the same deformation) are greater for magic than for nonmagic nuclei. In fact, since the energy gain for magic spherical fragments is greater than the loss resulting from the increase in elasticity, the formation of magic and near-magic fragments, i.e., asymmetrical fission, is energetically advantageous. This energy gain is essentially connected with the fact that because of the high elasticity value at low deformations the magic fragments are so little deformed that the deformation energy does not compensate for the difference in mass of magic and nonmagic fragments. Apart from the deformation energy, the kinetic energy of the separating degrees of freedom at the moment of scission should be taken into account when calculating the excitation energy of fragments. For the shell effects of the fragments to play an important part in fission, the process of deformation of the nucleus on descending from the saddle point (in the case of threshold fission) must be, as in fact it is, fairly slow with respect to the nucleonic degrees of freedom, i.e., $\tau_{def} \gg \tau_{nucleon}$ (τ_{def} is the descent time, $\tau_{nucleon} \sim \hbar/\Delta E_{nucleon}$, and $\Delta E_{nucleon}$ is the distance between the nucleon levels). In this case nucleonic shells are formed before scission. At the same time $\tau_{def} \ll \tau_{rot}$, i.e., the process of descent is fast with respect to the rotational degrees of freedom ($\tau_{rot} \hbar/\Delta E_{rot}$). In the case of fission of an excited nucleus with fairly high excitation energy at the saddle point, $\Delta E_{nucleon}$, may be so low that not only $\tau_{def} \ll \tau_{rot}$ but also $\tau_{def} \ll \tau_{nucleon}$, i.e., the process of descent is accelerated with respect to all the degrees of freedom. In this case the density matrix of the nucleus does not change on moving from the saddle point. This would seem to explain the fact that the theoretical angular distribution of fragments at fission of an excited nucleus agrees with the experimental value only when the parameters determining the rotational state of the nucleus (moment of inertia) at the saddle point and not at the scission point are used. (auth)

17847 PAIRING EFFECTS IN FISSION OF EVEN-EVEN COMPOUND NUCLEI NEAR THE THRESHOLD. Strutinskii, V. M.; Pavlinchuk, V. A. (Kurchatov Inst. of Atomic Energy, Moscow). pp 127-33 of STI/PUB/101(Vol. 1). (In Russian).

The effects connected with discreteness of the number of excited quasi-particles at the saddle point, which are caused by nucleon pairing, are analyzed. The weak dependence of density of the internal states in the range $(2-4)\Delta$ in comparison with the exponential dependence characteristic of high energies is shown to lead to a marked reduction in $d\bar{\nu}/dE$ in this energy range. At lower energies it would be reasonable to expect a sharp reduction in the $\bar{\nu}$ by ~0.2, corresponding to a reduction in internal excitation energy by $2\Delta = \sim 1.5$ Mev. However, as a result of the presence in the gap of the so-called β- and γ-vibration levels, which contribute to the internal excitation of the fissionable nucleus, there is a jump $\Delta\bar{\nu} = \sim 0.1$ at an energy of 0.6-0.7 Mev above the threshold, which corresponds to the position of these states. The dependence of $\bar{\nu}(E)$ calculated on the basis of these considerations is compared with the experimental figure for ^{235}U. It follows from an analysis of these and other effects that an applicable value for Δ_0 is ~0.7 Mev, i.e., approximately the same as for nuclei in the ground state. (auth)

17848 FISSION DISTRIBUTION IN NEUTRON-INDUCED FISSION OF ^{230}Th, ^{238}Pu, AND ^{241}Am. Vorotnikov, P. E.; Dybrovina, S. M.; Shigin, V. A.; Otrotsenko, G. A. (Kurchatov Inst. of Atomic Energy, Moscow). pp 157-69 of STI/PUB/101(Vol. 1). (In Russian).

The angular distribution of fragments in the neutron-induced fission of ^{230}Th, ^{238}Pu, and ^{241}Am was measured in the neutron energy range 100-1200 kev. Measurements were also made for ^{241}Am at neutron energies of 4 and 5 Mev, and the dependence of the fission cross section of ^{238}Pu on neutron energy in the 50-1400 kev range was likewise determined. The partial fission cross sections for the different K-bands were derived for ^{230}Th on the basis of the angular distributions obtained, using fission cross sections taken from another paper, and also the neutron capture cross sections of the neutron permeabilities calculated by the optical coefficients of adhesion. The following band sequence was established: $1/2^-$, $3/2^-$, $3/2^+$; the energy interval between the bands is ~100 kev. The pattern of the cross section for band $1/2^-$ shows in the sub-barrier region (at a neutron energy of 860 kev) the same dip as the total fission cross-section. This pattern in the sub-barrier region cannot be explained by the normal change in neutron width, as it can be in the case of fission above the barrier, and gives grounds for assuming the presence of some other mechanism powerfully affecting the fission cross section. The angular distributions of the fragments can be explained satisfactorily only on the assumption that there is an energy shift between the individual states within the bands. This indicates that the widths of the levels at the saddle are probably less than the distances between the levels themselves. Assuming that the levels are rotatory, a value of about 4 kev is obtained for $\hbar^2/2J$. From analyzing the anisotropy of Pu^{238} fission, we may assume the band sequence $1/2^+$, $3/2^-$, $1/2^-$. In the case of ^{241}Am fission, the angular distributions show a weak energy dependence and little anisotropy; this is explained by the large number of participating states. The measurements at 4 and 5 Mev made it possible to determine the value of K_0^2, and to compare it with the data for ^{237}Np. This comparison shows that the energy dependence of K_0^2 for odd-odd compound nuclei is apparently identical with that for even-odd nuclei. (auth)

17849 ANGULAR ANISOTROPY OF FISSION AND THE LIQUID DROP MODEL. Strutinskii, V. M. (Kurchatov Inst. of Atomic Energy, Moscow). pp 171-84 of STI/PUB/101(Vol. 1). (In Russian).

The results of calculations of the moments of inertia of the nucleus at the saddle point are given for the liquid model of potential energy, which takes into account the effect of blurring of the edge of the nucleus in the form of a correction to surface tension depending on the curvature of the effective surface (the GN-correction). If the GN-correction is applied when $\Gamma < 0$, the form of the nucleus at the saddle point is closely dependent on the basic fissionability parameter Z^2/A. Unlike the normal liquid drop model, the value J_{eff} obtained in this way is in good agreement with the experimental figure found by Huizenga et al. from the angular anisotropy of fission, and at the same values $\Gamma \approx -0.1$

and $(Z^2/A)_{crit} \approx 45$, which agree best of all with other data. The data on the magnitude of J_{eff} make it possible to determine direct from the experiment and independently of the model the parameter $(Z^2/A)_{crit}$ for the excited nuclear model. (auth)

17850 CROSS-SECTIONS FOR LOW-ENERGY NEUTRON-INDUCED FISSION. Rae, E. R. (Atomic Energy Research Establishment, Harwell, Eng.). pp 187-203 of STI/PUB/101(Vol. 1).

The main features of neutron-induced-fission cross sections and their interpretation are outlined. Some emphasis is placed on recent improvements in the quality of the measurements and in attempts at quantitative interpretation of certain aspects of the data. (auth)

17851 MEASUREMENT AND ANALYSIS OF THE FISSION CROSS-SECTION OF ^{239}Pu FROM 0 TO 5 kev. de Saussure, G.; Blons, J.; Jousseaume, C.; Michaudon, A.; Pranal, Y. (Centre d'Etudes Nucleaires, Saclay, France). pp 205-18 of STI/PUB/101(Vol. 1). (In French).

The cross section of ^{239}Pu for low-energy neutrons was measured between 0.16 ev and 5 kev by the time-of-flight method, with a gas scintillator containing 310 mg of ^{239}Pu. Under the best conditions and at high energy, the resolving power of the measurement was 3 ns/m. The Saclay linear accelerator was used as a pulsed neutron source. The measurement consisted in the successive determination of the fission rate (by means of a gas scintillator) and the incident neutron energy spectrum (by means of a BF_3 counter whose efficiency was proportional to $E^{-\frac{1}{2}}$). The background was determined by interposing black resonance screens in the neutron beam. The quantity $\sigma_F\sqrt{E}$ is proportional to the ratio of the fission rate to the counting-rate of the BF_3 detector. It was calibrated by reference to the resonance at 7.8 ev, the parameters of which are known. At the discrimination threshold, adjusted to an alpha-ray build-up rate of 1 counts/s, an efficiency of 65% for the detection of fissions was obtained. The fission cross section was measured in several sequences to observe the various energy ranges with sufficient resolving power. A detailed description is given of the experimental apparatus, the tests with the scintillator and the experimental conditions in which the various measurement sequences were carried out. A curve showing the fission cross section as a function of energy is included. The results of an analysis of the resonance parameters are also reported. (auth)

17852 MEASUREMENT OF FISSION CROSS-SECTIONS FOR NEUTRONS OF ENERGIES IN THE RANGE 40-500 kev. White, P. H.; Hodgkinson, J. G.; Wall, G. J. (Atomic Weapons Research Establishment, Aldermaston, Eng.). pp 219-33 of STI/PUB/101(Vol. 1).

Measurements were made of the fission cross section of ^{233}U, ^{234}U, ^{236}U, ^{237}Np, ^{239}Pu, and ^{241}Pu at several neutron energies between 40 and 500 kev. Measurements in this energy range are of importance in reactor calculations especially in fast dilute systems where the neutron flux is high in the 10-100-kev energy range. Recent measurements of the ^{235}U fission cross section gave absolute values slightly lower than previous data. The present series of measurements are made relative to the new values of the ^{235}U fission cross section using back-to-back ionization chambers. The fissile foils were assayed by α-assay, direct weighing and coulometry. Good agreement was obtained between these assays. The fission measurements have an estimated accuracy of between 1 and 2% and, combined with the error on the ^{235}U fission cross section, give a final error of about 3% in the fission cross sections. The results together with those of previous measurements are given, and the corrections for fission fragment absorption, backgrounds, and scattering are discussed. (auth)

17853 ANALYSIS OF THE FISSION CROSS-SECTION OF ^{233}U FOR NEUTRONS OF ENERGIES BETWEEN 1.7 AND 30 ev. Nifenecker, H.; Perrin, G. (Centre d'Etudes Nucleaires, Saclay, France). pp 245-53 of STI/PUB/101(Vol. 1). (In French).

The cross section of ^{233}U for resonance neutrons was analyzed by the least-squares method. The need for using a multilevel formalism, the statistical distributions of level spacing and partial widths are considered. By the use of a study of level spacing as a starting point, particular attention is paid to the possibility of obtaining information on the relation of population of resonances of different spin. (auth)

17854 FISSION CROSS-SECTION MEASUREMENT OF ^{235}U AND ^{239}Pu FOR LOW-ENERGY NEUTRONS. Fraysse, G. (EURATOM, C.C.R., Ispra, Italy); Prosdocimi, A. pp 255-80 of STI/PUB/101(Vol. 1).

Fast detection with a double gaseous scintillator and low geometry counting with a solid-state ion chamber were applied to determine the fission cross section of ^{235}U and ^{239}Pu. Monochromatic neutron beams of 0.0322, 0.0626 and 0.275 ev were supplied by two crystal spectrometers at the EL3 reactor in CEN-Saclay. The monitoring of the neutron flux was done by reference to the counting of a grid ion chamber mounted with a boron layer. Both alpha and fission rates were measured, and the results at the reference energy of 0.0253 ev were calculated: $(\sigma_F)_0^{235}U = 582 \pm 10$ b and $(\sigma_F)_0^{239}Pu = 738 \pm 7$ b. (auth)

17855 THE FISSION CROSS-SECTION OF ^{240}Pu FOR 0.03-2.0 Mev NEUTRONS. De Vroey, M.; Ferguson, A. T. G.; Starfelt, N. (Atomic Energy Research Establishment, Harwell, Eng.). pp 281-5 of STI/PUB/101 (Vol. 1).

The fission cross section of ^{240}Pu was measured for neutrons having energies between 0.030 and 2.0 Mev. The substantial values of the cross section below the "threshold" at 200 kev are confirmed. The cross section can be fitted on the assumption that at low energies only p-wave neutrons can induce fission using values of average resonance parameters derived from adjacent nuclei. (auth)

17856 INTERACTION OF NEUTRONS WITH ^{235}U NUCLEI IN THE ENERGY RANGE 2 ev-30 kev. Wang, Shih-ti; Wang, Yung-ch'ang, Dermendzhiev, E.; Ryabov, Yu. V. (Joint Inst. for Nuclear Physics, Dubna, USSR). pp 287-305 of STI/PUB/101(Vol. 1). (In Russian).

The fast pulsed reactor was used to measure the total cross section, the fission cross section and the radiative capture cross section of ^{235}U by the time-of-flight method with a resolution of ~0.04 μs/m. The flight length was 1000 m. The time spectra were recorded by 2048-channel time analyzers. To measure the total cross sections by the transmission method, a resonance-neutron scintillation counter with lithium glass was used. The fission, radiative-capture, the total cross sections were measured by the auto-indication method using a large liquid scintillation detector with cadmium added to the solution. The sample to be investigated was placed in the axis of a cylindrical opening in the vessel, in a geometry close to 4π. The volume of the detector was scanned by 32 FEU-24 photomultipliers. The fissions were identified by the delayed coincidences between the scintillations corresponding to the recording of the prompt gamma rays and the moderated prompt fission neutrons. Radiative capture is not accompanied by a delayed pulse. The efficiency of recording fissions and radiative capture was ~50 and ~25% respectively, while the background (expressed as a percentage of the strong resonances) was ~1 and ~15% respectively. The area method was used to obtain the parameters $g\Gamma_n$, Γ, Γ_f, and Γ_γ for a number of low-lying levels. The average widths of $\bar{\Gamma}_\gamma$ and $\bar{\Gamma}_f$ over all the levels were (42 ± 3) mv and (51 ± 6) mv respectively. The levels were divided into two systems with $\alpha_1 < 1 (\bar{\alpha}_1 \sim 0.5)$ and $\alpha_2 > 1 (\bar{\alpha}_2 \sim 1.5)$ and $\Gamma_f^1 \approx 72$ mv and $\bar{\Gamma}_f^2 \approx 25$ mv respectively, which may be connected with the two spin values 3^- and 4^- of the compound nucleus. The energy dependence of the ratio of radiative-capture to fission cross sections was obtained in the neutron-energy range from 2 ev to 30 kev. Measurements using a sample of ^{238}U instead of ^{235}U made it possible to take into account experimentally the contribution of the radiative capture of ^{238}U to α. (auth)

17857 THE EXCITATION FUNCTION AND THE ISOMERIC YIELD RATIO FOR THE 14-ms FISSIONING ISO-

MER FROM DEUTERON IRRADIATION PLUTONIUM. Flerov, G. N. (Joint Inst. for Nuclear Research, Dubna, USSR); Pleve, A. A.; Polikanov, S. M.; Ivanov, E.; Martalogu, N.; Poenaru, D.; Vilcov, N. pp 307-14 of STI/PUB/101(Vol. 1).

In the past two years several workers have reported the existence of a spontaneous fission phenomena, with an anomalous short lifetime, explained as a fission from an excited state. Further studies are made on the excitation of the isomeric state by the deuteron bombardment of a plutonium target enriched in the 242-isotope. The cross section of the excitation, as well as the isomeric yield ratio, was measured at different bombarding energies. The deuteron beam energy was varied between 7 and 12 Mev by both the cyclotron regime and the aluminum absorbers. The experimental technique used was based on the recoil method. The nuclei, knocked out from the target by the deuterons, are caught on a rotating disk and carried in front of several glass detectors for counting the fission fragments. The cross section of the 14-ms isomer, at a deuteron energy of 12 Mev, was determined to be about 4×10^{-30} cm^2. This value is a hundred times greater than that obtained with heavy ions. The excitation function shape verifies the assumption that the isomer is produced via the (d,2n) process proving that ^{242}Am is the spontaneously fissioning nucleus. For measuring the ground state (d,2n) cross section the activation method was used, catching the knocked-out nuclei on an aluminum foil (the reaction ^{242}Pu (d,2n) leads to an alpha transition of 6.1 Mev energy). The (d,2n) cross section rises rapidly with the bombarding energy, attaining a value of $\sigma_n \sim 7.5$ mb for 12 Mev. The small value of the isomeric yield ratio ($\sim 5 \times 10^{-4}$) thus obtained leads one to conclude that the total angular momentum of the excited state responsible for fission is high. (auth)

17858 SYMMETRY OF NEUTRON-INDUCED ^{239}Pu FISSION IN RESONANCE REGION. Cowan, G.; Bayhurst, B. P.; Prestwood, R. S.; Gilmore, J. S.; Knobeloch, G. W. (Los Alamos Scientific Lab., N. Mex.). pp 347-54 of STI/PUB/101(Vol. 1). (LA-DC-7558).

Symmetry of fission produced in ^{239}Pu by time-of-flight energy-resolved neutrons was radiochemically measured in the resonance region by a neutron time-of-flight method, called the "wheel" method. Data were obtained from 200 to 600 ev in energy intervals ranging from 10 to 25 ev in width, containing 3 to 12 resonances per sample. Both increases and decreases in symmetry of fission were observed as compared with thermal neutron fission of ^{239}Pu. Measured by the ratio of ^{115}Cd, a "valley" fission product, to ^{99}Mo, a "peak" fission product, the symmetric yield decreased by 18% at 250 ± 4 ev, 29% at 307 ± 5 ev, and 33% at 395 ± 6 ev. The symmetric yield increased by 16% at 206 ev. The average symmetry of fission over the energy region 196 to 585 ev showed a decrease of 8% from the thermal value. Changes in the ratio ^{111}Ag/^{99}Mo appeared to be about one-third as great as changes in the ^{115}Cd/^{99}Mo ratio from level to level. The ratio ^{140}Ba/^{99}Mo showed no systematic changes from the thermal value within analytical error and the average is within 1% of the thermal ratio, which permits the assumption that ^{99}Mo and ^{140}Ba yields are not variable for resonance fission and are the same as in thermal fission. (auth)

17859 DETERMINATION OF THE PRIMARY NUCLEAR CHARGE OF FISSION FRAGMENTS FROM THEIR CHARACTERISTIC K-X-RAY EMISSION IN SPONTANEOUS FISSION OF ^{252}Cf. Glendenin, L. E.; Unik, J. P.; Griffin, H. C. (Argonne National Lab., Ill.). pp 369-84 of STI/PUB/101(Vol. 1).

The distribution of nuclear charge in the spontaneous fission of ^{252}Cf was determined directly by simultaneous measurement of the masses and characteristic K-x-ray energies associated with the primary fission products. The x rays were detected by a thin NaI (Tl) crystal (or by an argon-filled proportional counter) in coincidence with a pair of solid-state detectors for the complementary fission fragments. Preliminary to the three-parameter study of the charge-mass distribution the gross characteristics of the K x rays were examined in some detail. The average yield of K x rays is 0.55 ± 0.1 per fission (the heavy group accounting for 70% of the total). From delayed-coincidence and fragment time-of-flight experiments it was found that about 30% of the x rays are emitted within 0.1 ns after fission, another 30% between 0.1 and 1 ns, 25% between 1 and 10 ns, the remainder appearing as two delayed components of equal intensity with half lives of ~30 and ~100 ns. These characteristics indicate that the x rays arise from internal conversion during de-excitation of the primary fission fragments, an interpretation supported by the observed yield (~1 per fission) of 50–300-kev electrons emitted within 2 μs of fission. In the three-parameter experiments the yield and energy of K x rays emitted in the first centimeter (ns) of fragment flight were determined as a function of fragment mass. The yield of K x rays per fragment is a pronounced saw-tooth function of mass, rising from <0.01 in the region below mass 92 (N ~ 50) to 0.1 in the light group, falling abruptly to near-zero in the mass region 128–132 (Z ~ 50), rising to 0.2 in the region of the heavy group mass-yield peak, and then increasing rapidly beyond mass 148 (region of deformed nuclei) to a maximum of 1 around mass 158. The observed correlation of K x ray energies with fragment mass leads to a smooth primary charge (Zp) function in better agreement with the empirical rule of equal charge displacement (ECD) than with other postulates for charge division in nuclear fission. (auth)

17860 FISSION YIELDS OF SOME ISOTOPES IN THE FISSION OF ^{232}Th BY REACTOR NEUTRONS. Wyttenbach, A.; Von Gunten, H. R. (Eidgnoessisches Institut fuer Reaktorforschung, Wuerenlingen, Switzerland). pp 415-21 of STI/PUB/101(Vol. 1).

The fission yields of the longer-lived isotopes produced in the fission of ^{232}Th are not very well known; existing data show rather large discrepancies and/or uncertainties. Since it was felt that at least some of these discrepancies arise from difficulties in measuring the absolute activities of the fission products, the fission yield of 10 selected isotopes whose decay schemes are well understood were measured. The thorium foils were irradiated in a position at the edge of the core of the SAPHIR swimming pool reactor. Following irradiation, the thorium was dissolved after addition of appropriate carriers. The fission products of interest were determined by conventional radiochemical methods that had to be modified slightly to ensure good decontamination from the abundantly formed ^{233}Pa. The chemical yields were determined by gravimetric methods. Counting was done preferentially on a γ-spectrometer that was calibrated at 11 different energies by standards either obtained from the IAEA or prepared by $4\pi\beta$-counting. In the case of ^{90}Sr, ^{106}Ru, and ^{144}Ce a β-proportional counter was used that had been calibrated for these isotopes. In addition to the sought elements, ^{99}Mo was isolated from each foil to serve as an internal monitor for the number of fissions taking place. The experiment thus gave the ratio of the yield of the sought element to the yield of ^{99}Mo. This ratio "R" was obtained for ^{90}Sr, ^{103}Ru, ^{106}Ru, ^{111}Ag, ^{112}Pd, ^{131}I, ^{137}Cs, ^{140}Ba, ^{141}Ba, ^{141}Ce, and ^{144}Ce. Results indicate the existence of a third peak in the yield mass curve in the region of symmetric fission. Yields of fission products relative to the ^{99}Mo yields are given, and the absolute yields calculated by assuming ^{99}Mo = 2.78%. This number was derived from the work of Iyer et al., and was obtained by normalizing the area under the yield mass curve to 200%. (auth)

17861 NEUTRON-INDUCED FISSION OF ^{227}Ac, ^{231}Pr, AND ^{237}Np: MASS DISTRIBUTION. Iyer, R. S.; Jain, H. C.; Namboodiri, M. N.; Rajkishore, M. Rajagopalan; Ramaniah, M. V.; Rao, C. L.; Ravindran, N.; Sharma, H. D. (Atomic Energy Establishment Trombay, India). pp 439-48 of STI/PUB/101(Vol. 1).

Results of radiochemical studies on the mass distribution in the neutron-induced fission of actinium-227, protactinium 231, and neptunium-237 were presented. This work was carried out as part of a program to determine the mass distribution in the fission of heavy elements as a function

of Z and A. All irradiations were carried out in the core of the swimming-pool type reactor APSARA with cadmium shielding wherever necessary. Relative yields of several fission product nuclides were obtained by a method involving a comparison of the fission product activities from the respective targets with those formed from uranium-235 simultaneously irradiated. Thermal-neutron fission yields of uranium-235 were assumed. These results indicate a predominantly asymmetric mass distribution in all the three cases, and also a distinct though small symmetric peak in the case of actinium-227. (auth)

17862 THE ENERGY RELEASE IN LOW-ENERGY FISSION. **Fraser, J. S. (Atomic Energy of Canada Ltd., Chalk River, Ont.). pp 451-66 of STI/PUB/101(Vol. 1).**

Recent advances in semiconductor detector and time-of-flight techniques have led to precise measurements of the fragment kinetic energies in thermal neutron and spontaneous fission. The resolution obtainable is limited by the effects of the prompt neutron recoil. Detailed measurements of the variation of the kinetic energy release with neutron bombarding energy have been correlated with the number of prompt neutrons emitted. An interpretation of this correlation in terms of channel effects has been proposed. The fine structure observed in the kinetic energy measurements has been shown to be connected with the extra energy available from the pairing energy in even-even fragments. (auth)

17863 THERMAL-NEUTRON-INDUCED FISSION OF ^{235}U, ^{233}U, AND ^{239}Pu. **Thomas, T. D. (Princeton Univ., N. J. Brookhaven National Lab., Upton, N. Y.); Gibson, W. M.; Safford, G. J. pp 467-80 of STI/PUB/101(Vol. 1).**

Solid-state detectors were used to measure the kinetic energies of the coincident fission fragments in the thermal-neutron-induced fission of ^{235}U, ^{233}U, and ^{239}Pu. Special care was taken to eliminate spurious events near symmetry to give an accurate measure of such quantities as the average total kinetic energy at symmetry. For each fissioning system over 10^6 events were recorded. As a result the statistics are good enough to see definite evidence for fine structure over a wide range of masses and energies. The data were analyzed to give mass yield curves, average kinetic energies as a function of mass, and other quantities of interest. For each fissioning system the average total kinetic energy goes through a maximum for a heavy fragment mass of about 132 and for the corresponding light fragment mass. There is a pronounced minimum at symmetry, although not as deep as that found in time-of-flight experiments. The difference between the maximum average kinetic energy and that at symmetry is about 32 Mev for ^{235}U, 18 Mev for ^{233}U, and 20 Mev for ^{239}Pu. The dispersion of kinetic energies at symmetry is also smaller than that found in time-of-flight experiments. Fine structure is apparent in two different representations of the data. The energy spectrum of heavy fragments in coincidence with light fragment energies is greater than the most probable value. This structure becomes more pronounced as the light fragment energy increases. The mass yield curves for a given total kinetic energy show a structure suggesting a preference for fission fragments with masses ~134, ~140, and ~145 (and their light fragment partners). Much of the structure observed can be understood by considering a semi-empirical mass surface and a simple model for the nuclear configuration at the saddle point. (auth)

17864 SIMULTANEOUS MEASUREMENTS OF FLIGHT TIMES AND ENERGIES OF FISSION FRAGMENTS. **Andritsopoulos, G.; Cornell, T.; Rodgers, A. L. (Atomic Weapons Research Establishment, Aldermaston, Eng.). pp 481-9 of STI/PUB/101(Vol. 1).**

An alternative way of measuring the prompt neutron emission is described. Fragment time-of-flight apparatus is mounted in an evacuated tube that passes laterally through the thermal column of the 5-Mw research reactor HERALD. A centrally positioned thin source produces 3×10^5 fissions s^{-1}. Fragments travel distances of 180 and 300 cm respectively to the terminal detectors, and in passing through a VYNS film, positioned 180 cm from the source along the longer flight path, eject electrons that are used to form a reference time-signal. Essentially the times of flight of both fission fragments are measured simultaneously with the kinetic energy of one of the pair. This is achieved by using a surface barrier counter for the 300-cm detector. The difficulty of maintaining good timing and energy resolutions simultaneously is overcome by routing the pulse to the charge sensitive preamplifier through a delay line amplifier from which a fast timing pulse is derived. The collected data enables the fragment mass to be determined both before and after prompt neutrons have been emitted. Hence the experiment provides a means for studying the behavior of neutron emission from individual fragments. The experimental uncertainties are those associated with the measurement of small differences, and an appraisal is made of the errors and calibrations that enter into the measurements. Of particular importance, the response of the surface barrier counter to fission fragments is obtained directly from the collected data from events in which the neutron emission is low. These calibrations are used in the measurements of post-neutron mass. (auth)

17865 FISSION-FRAGMENT ANGULAR, ENERGY, AND MASS DIVISION CORRELATIONS FOR THE ^{234}U(d,pf) REACTION. **Vandenbosch, R. (Univ. of Washington, Seattle); Unik, J. P.; Huizenga, J. R. pp 547-60 of STI/PUB/101(Vol. 1).**

The fission of the compound nucleus ^{235}U in the neighborhood of its fission threshold was studied by means of the ^{234}U (d,pf) reaction. A three-parameter analyzer was used to record simultaneously the two fission-fragment kinetic energies and the proton energy for each coincident event. The excitation energy at which fission occurs is defined by the kinetic energy of the stripped proton. The variation of angular anisotropy with excitation energy shows considerably more structure than that obtained by Lamphere for the same nucleus resulting from fast-neutron bombardment of ^{234}U. At least eight fission channels at the saddle point were observed for the energy region between threshold and 2 Mev above threshold. Nilsson-type calculations of single particle energies for deformed nuclei have been made for the larger deformations more nearly describing the saddle-point configuration. The single particle states identified by Lamphere are consistent with those calculated to be close to the Fermi surface for reasonable saddle-point deformations. The primary motivation for this experiment was to search for a possible correlation between mass asymmetry and angular anisotropy. Mass yields obtained from the correlated fragment energies show no variation of the anisotropy with mass ratio, in contrast with experiments where the excitation energy at which fission is occurring is not fixed and where a dependence of anisotropy on mass ratio was observed. There is therefore, no evidence from anisotropy measurements that the properties of the saddle point influence the final mass division. The average total kinetic energy release in fission varies by less than 0.5% for the different saddle-point channels observed. The variation of total kinetic energy with mass ratio was also investigated. (auth)

17866 A STUDY OF THE MASS SPECTRA OF FISSION FRAGMENTS AFTER PROMPT NEUTRON EMISSION. **Signarbieux, C.; Ribrag, M. (Centre d'Etudes Nucleaires, Saclay, France). pp 561-71 of STI/PUB/101(Vol. 1). (In French).**

The distribution of the masses of fission fragments, following neutron emission, was obtained by simultaneously measuring the velocity and energy of each particle. The special feature of this method is that it is essentially independent of the initial energy of the fragments, so that one can use relatively thick targets of fissionable material ($0.1\ mg/cm^2$). The energy measurement is made by gold-silicon surface barrier detector; the velocity measurement was made on a flight path of 130 cm, with a total resolving power of 1.5 ns. The "starting" detector consisted of a windowless photomultiplier that detected directly the secondary electrons emitted by a thin metallic sheet during the passage of the fission fragments. The "stop" signal is

picked up directly, by means of a transformer, on the semiconductor detector. The results given relate to the thermal fission of ^{235}U, and are compared with the results obtained by the radiochemical method. (auth)

17867 NEUTRONS AND KINETIC ENERGY OF FRAGMENTS IN FISSION OF HEAVY NUCLEI. Apalin, V. F.; Gritsyuk, Yu. N.; Krutikov, I. E.; Lebedev, V. I.; Mikaelyan, L. A. (Kurchatov Inst. of Atomic Energy, Moscow). pp 587-99 of STI/PUB/101(Vol. 1). (In Russian).

The distribution of excitation energy and kinetic energy depending on the mass of the fragment formed in heavy-isotope fission by thermal neutrons is experimentally investigated. The excitation energy is shown to have a low minimum in the region of the double-magic fragment (M ~ 132), to increase in the symmetrical fission area and to be at its maximum for fragments complementary to magic. The kinetic energy of the fragments measured for ^{235}U correlates with the excitation energy. The total energy release according to the experimental data is in good agreement with calculations according to Milton's mass tables in every case except that of strongly asymmetric fission. In the measurements conducted, the ratio of the maximum of the fragment yield curve to the minimum (after neutron escape) was 500 : 1. (auth)

17868 MULTI-PARAMETER INVESTIGATIONS OF FAST FISSION FRAGMENTS. D'yachenko, P. P.; Kuz'minov, B. D. pp 601-10 of STI/PUB/101(Vol. 1). (In Russian).

A number of investigators have noted the peculiar dependence of kinetic energy on the mass of the fragments. This dependence differs considerably for the fission of nuclei by thermal neutrons, neutrons with an energy of 14 Mev and α particles. It may be that this is a result of the difference not only in excitation energy, but also in the moment introduced by the particle causing fission. It is obviously difficult to deny the part played by nuclear shells in the formation of fragments according to mass, and in this connection the study of the kinetic energy of fragments as a function of their mass is of great interest, as are the corresponding investigations of the widths of distribution of the kinetic energy. Particular attention is given to the characteristics of symmetrical fission of ^{235}U, and it is found that when tails appear in the apparatus spectra of the fission fragments, there occur in the symmetrical mass-region pulses with a most probable total energy of ~120 Mev. Actual symmetrical fission events correspond to a total mean energy of ~155 Mev. The kinetic energy of paired fragments was measured using two surface-barrier silicon counters. The impulses are analysed for amplitude by a two-dimensional 128 × 128 channel analyser with a memory on ferrite. The neutron source used was the BR-5 fast neutron reactor, the mean energy of the fast neutron spectrum being ~250 kev. Layers of fissile isotopes with a thickness of 20-30 $\mu g/cm^2$ were used. The fission of ^{235}U by thermal neutrons gave an experimental curve for the mass yield with a 250 : 1 ratio between peak and valley. Comparison of the characteristics of the fragments (kinetic energy and mass distribution) showed no noticeable difference in the fission of ^{235}U by thermal and fast neutrons. The total kinetic energy of the fragments in the symmetrical fission of ^{235}U by thermal and fast neutrons proved to be identical, equalling ~155 Mev, which agrees, within the limits of experimental error, with the corresponding figures for fission of ^{235}U by neutrons with an energy of 14 Mev and of ^{232}Th by α particles. (auth)

17869 ANGULAR ANISOTROPY AND MASS ASYMMETRY OF ^{232}Th FISSION FRAGMENTS. Kuz'minov, B. D.; Sergachev, A. I. pp 611-17 of STI/PUB/101(Vol. 1). (In Russian).

Angular anisotropy of fragments with different masses in the fission of thorium-232 by fast neutrons is investigated. The masses of the fragments were determined by simultaneous recording of the kinetic energy of paired fragments in a double ionization chamber with grids. The direction of flight of the fragments was determined using a mechanical collimator. The neutrons causing fission had an extended spectrum, but the contribution of fissions via the (n,n'f) reaction did not exceed a few per cent. The fragments were sorted out according to energy by a two-dimensional 128 × 128 channel analyser with a memory on ferrite. The dependence of angular anisotropy on the mass of the fragments and on their kinetic energy with fixed mass is discussed. The first dependence makes it possible to judge the degree to which the saddle point affects the distribution of the fragments according to mass, while the second gives information about the degree to which the configuration of the nucleus at the moment of breakdown affects the angular anisotropy of the fragments. (auth)

17870 A NEW DESIGN OF RATIO CIRCUIT FOR FISSION-FRAGMENT STUDY. Patwardhan, P. K.; Indurkar, V. S. (Atomic Energy Establishment, Trombay, India). Vienna, International Atomic Energy Agency, 1965, Preprint No. CN-22/32, 20p. (CONF-651105-27). ORAU. From Conference on Nuclear Electronics, Bombay.

A pulse-voltage dividing circuit, which was developed for use in studies of the mass distributions of fission fragments in multi-parameter experiments, is described. (D.C.W.)

17871 COMPTES RENDUS DU CONGRES INTERNATIONAL DE PHYSIQUE NUCLEAIRE, PARIS, 2–8 JUILLET 1964. VOLUME II. COMMUNICATIONS. (Proceedings of the International Congress of Nuclear Physics, Paris, July 2–8, 1964. Volume II. Summaries). Gugenberger, P. [(ed.)]. Paris, Centre National de la Recherche Scientifique, 1964. 1230p. (CONF-502(Vol.2)).

Experimental and theoretical papers are presented in five sections on: nuclear forces; nuclear matter; nuclear structure and models; reaction mechanisms; and radioactivity: weak interactions. Abstracts are included of each of the contributed papers. (L.B.S.)

Plasma Physics and Thermonuclear Processes

See also Fluid Physics and Thermodynamics

Refer also to abstracts 17510, 17552, and 17600.

17872 (AD–627988) IONIZATION AND RECOMBINATION IN ALKALI-SEEDED COLLISION-DOMINATED PLASMAS. Curry, B. P. (Aro, Inc., Arnold Air Force Station, Tenn.). Oct. 12, 1965. 48p. (AEDC-TR-65-260).

At electron densities greater than 10^{12}/cc, ionization and recombination proceed predominantly by sequential transitions between adjacent energy levels induced by collisions with free electrons. Similar models for this process were developed by various investigators. Closed-form expressions were developed for ionization and recombination of effective one-electron atoms by modifying the Byron model and determining analytically the critical energy level in equilibrium with the free electrons, using a simplified quantum mechanical model of the alkali atoms. The reaction rate coefficients calculated from these expressions agree satisfactorily with available experimental data and with numerical calculations of other investigators. (auth)

17873 (CLM-R-49) AN APPARATUS FOR THE DETECTION AND ENERGY ANALYSIS OF FAST NEUTRAL ATOMS. Mason, D. W.; Schofield, J. M. S. (Culham Lab., United Kingdom Atomic Energy Authority, Abingdon (England)). Oct. 1965. 18p. Dep. BIS $0.60. HMSO 3s.

The apparatus was constructed to measure the energy and time dependence of the flux of neutral atoms emitted, due to the process of charge exchange, from plasma contained in a magnetic mirror machine. As the momentum change of the ions in this process is negligible the energy measurements, which are made outside the trap are simply related to the distribution function of the plasma ions within it. The atoms pass through a water vapor cell where approximately 6% are re-ionized. This fraction is electrostatically analyzed and counted using a scintillation technique. Measurements of the ionization efficiency and the

scattering losses in the water vapor cell are described. (auth)

17874 (CONF-650922, pp 630-42) DESIGN AND FABRICATION OF INTEGRAL COOLANT PASSAGE CRYOGENIC COILS FOR HIGH POWER DENSITY. Boozenny, A.; Payne, J. R.

A solenoidal magnet with integral coolant passages is described, and the performance of the coils in the plasma containment device (adiabatic mirror-cusp) for which it was designed is compared with that of conventional coils. The techniques used in the fabrication of the coils are also described. (D.C.W.)

17875 (IPP–1/35) ENTWICKLUNG EINER LASER-BELEUCHTUNG FUER DAS MACH-ZEHNDER INTERFEROMETER. (Development of a Laser Light Source for the Mach-Zehnder Interferometer). Beck, R. (Institut fuer Plasmaphysik, G.m.b.H., Garching (West Germany)). Mar. 1965. 48p. Dep. mn.

A laser light source for the Mach-Zehnder interferometer is reported which is used for measurements of electron density in a plasma. In order to take framing camera or smear pictures of the interference pattern during a pinch discharge, the luminous density of the laser surface should be constant during a period of about 15 μs. To achieve these properties, a laser having a special resonator with great mirror distance and a strong optical pump was developed. Laser theory was extended to this type of laser with external mirrors and estimations were made of the resonator quality and of the duration and strength of optical pumping, for which constant laser emission is to be expected. For sufficiently strong optical pumping continuous laser operation was indeed observed. Intensity measurements made simultaneously at different points of the laser surface indicate a strong correlation of the emission from different portions of the laser surface. In order to test the uniformity of the luminous density framing-camera pictures of the laser surface during the emission were taken. They show that the laser is in oscillation in transversal modes. To get an understanding of these modes some details of the theory of optical resonators are presented and applied to the set up. The theoretical predictions are in good agreement with the experimental results. Framing-camera pictures show moreover, that a portion of the laser surface emits light of constant intensity. This region is used as a light source for the interferometer. Photographs of the interference pattern demonstrate that it is possible to produce many more interference fringes by using a laser than by one of the usual light sources. It is therefore possible to measure great changes in electron density which produce great displacements of the interference fringes. (auth)

17876 (IPP–1/37) MESSUNG HOHER ELEKTRONENDICHTEN MIT EINER NEUARTIGEN MIKROWELLEN-REFLEXIONSSONDE AN EINEM LINEAREN Z-PINCH. (Measurement of High Electron Densities on a Linear Z Pinch Using a New Microwave Reflection Probe). Hermansdorfer, H. (Institut fuer Plasmaphysik, G.m.b.H., Garching (West Germany)). June 1965. 54p. Dep. mn.

A new microwave reflection probe allowing the local measurement of electron densities well above the critical density is described. To show its applicability measurements on a z-pinch are reported. The probe was tested on a fast z-pinch discharge without preionization and stabilization. At different radii the time development of the electron density during the first implosion phase was measured. The experiments gave some interesting features of the discharge. The applicability of the reflection probe within the limits common to all probes in plasma physics is thus shown. (auth)

17877 (IPP–6/44) STREUUNG ELEKTROMAGNETISCHER WELLEN AN PLASMAZYLINDERN. (Diffraction of Electromagnetic Waves on Plasma Cylinders). Luenow, W; Tutter, M. (Institut fuer Plasmaphysik, G.m.b.H., Garching (West Germany)). Nov. 1965. 54p. Dep. mn.

The diffraction of electromagnetic waves on a cylindrical plasma is numerically computed. The calculations are made using the geometrical optic approximation and using the wave equation (exact solution). The electric field vector of the incident wave is taken to be parallel to the axis of the cylinder. The calculation is carried out for constant electron density and for a Gaussian density distribution. (auth)

17878 (LA–3437) SPHERICAL HARMONIC REDUCTION OF THE FOKKER-PLANCK EQUATION. Oliphant, Thomas A. Jr. (Los Alamos Scientific Lab., Univ. of California, N. Mex.). Aug. 1965. Contract W-7405-eng-36. 40p. Dep. mn. CFSTI $2.00 cy, $0.50 mn.

The Fokker-Planck equation is reduced to a form that is useful from the viewpoint of doing practical calculations of problems involving configuration space as well as velocity space. The basic technique is a spherical harmonic decomposition in velocity space that reduces the number of independent variables by two. As an example, the application of the method to a problem with theta-pinch geometry is outlined. (auth)

17879 (LRP–19/65) ETUDE D'UNE DECHARGE HAUTE FREQUENCE AXIALE. (Study of an Axial High-Frequency Discharge). Heym, A.; Weibel, E. S. (Laboratoire de Recherches sur la Physique des Plasmas, Lausanne (Switzerland)). Dec. 1965. 20p. Dep. mn.

The measurements made on a high-frequency linear discharge fed by a generator giving a 30 Mw for 10 periods at a frequency of 2 MHz were reported. The analysis of the results of the magnetic probe measurements and of photographic measurements taken with a turning mirror channel showed the shock waves and the mass movements in this discharge. The study of the time evolution of the magnetic field profile made it possible to estimate the electron temperature of the plasma. The existence of a negative resistance of the field in the limited shell at certain moments of the period made it possible to interpret the light emitted in the vicinity of the walls as the results of the bombardment of the walls by electrons. The results show that a linear discharge confined by walls in which the initial pressure is 60 or 100 μ Hg of hydrogen is present in the form of a ring whose temperature is of the order of 6 ev. The rings surround a hot nucleus carrying a small current and is formed by the energy and material contribution of successive shock waves appearing at each semiperiod. The mean velocities measured move in the direction of a compression up to the fourth period, then in the direction of an expansion up to eighth period, and are annulled toward the end of the discharge. The results at 25 μ of Hg do not appear fundamentally different from those at 60 and 100 μ, although the photography does not show the existence of a nucleus. Theoretical limitations made it impossible to make conclusions on the values of the temperature and velocity in this case. (tr-auth)

17880 (MATT–437) ON THE INITIAL TRANSIENT OF A THERMONUCLEAR REACTOR. Mills, Robert G. (Princeton Univ., N. J. Plasma Physics Lab.). Mar. 1966. Contract AT(30-1)-1238. 34p. Dep. mn. CFSTI $2.00 cy, $0.50 mn.

During the period when a thermonuclear reactor is brought into operation, the temperatures and densities of the components of the plasma undergo significant changes. This period of time is of interest since it bears on the possibility of establishing the steady state conditions necessary for a successful reactor. The history of a thermonuclear plasma is traced during its first milliseconds of development. (auth)

17881 (N–65-19804) FOCUSSED MICROWAVE SYSTEMS FOR PLASMA DIAGNOSTICS. Carswell, A. I.; Richard, C. (RCA Victor Co., Ltd., Montreal (Quebec). Research Labs.). Dec. 1964. Contract DRB-PD-69-400007. 184p.

The use of focused microwave beams for plasma diagnostics was investigated both theoretically and experimentally. Scalar diffraction theory was used to describe the amplitude and phase behavior of a microwave beam in the focal region of a lens system, and simplified expressions for the beam properties are presented in terms of an effective beam width and field depth. Dielectric lenses were

used to produce focused microwave beams at 10 and 35 Bc/sec; the properties of the laboratory systems are compared with the theoretical predictions. The dependence of the focal properties on such parameters as lens illumination, microwave frequency, lens F-number, and image position were studied in some detail. The properties of a double lens system for multiple focused beam plasma diagnostics are also described. The limitations of focused beams for quantitative measurements of plasma properties are discussed. (STAR)

17882 (N-65-19862) EXPERIMENTAL INVESTIGATION OF THE FUNDAMENTAL MODES OF A COLLISIONLESS PLASMA. Quarterly Report No. 1, March 10–June 10, 1964. Malmberg, J. H. (General Atomic, San Diego, Calif. John Jay Hopkins Lab. for Pure and Applied Science). June 22, 1964. Contract NAS7-275. 6p. (NASA-CR-57469; GACD-5403). CFSTI $1.00 cy, $0.50 mn.

Modifications of the experimental machine and the development of instruments for the experiment are reported. Measurements on the plasma properties are also discussed. The probe manipulators necessary for the experiment were built, and the electromagnetic coupling between the probes was greatly reduced by using a shielding technique. The signal-to-noise ratio of the receiver was also materially improved. A number of measurements on the geometry of the plasma and on the noise in the plasma were made. (STAR)

17883 (NP-15784) ISSLEDOVANIE DREIFOVOI NEUSTOICHIVOSTI V KALIEVOI PLAZME. (Investigation of Drift Instability in Potassium Plasma). Buchel'nikova, N. S. (Akademiya Nauk SSSR, Novosibirsk. Institut Yadernoi Fiziki). 1965. 17p. Dep. mn.

A plasma was formed by heating potassium vapor to 2000°K on tungsten. The plasma was cylindrical and limited on the ends by the heated tungsten plates. A magnetic field of 400 to 3000 gauss was directed along the cylinder axis. The plasma density was a maximum on the axis, and decreased with radius. The radius was R = 2 cm, and the distance between the end plates was L = 36 cm. The plasma was strongly ionized, and was collision-free at densities of 1.0×10^9 to 1×10^{10} cm^{-3}. The direction of electron drift was found from the change in phase shift of signals from two probes. It was found that drift oscillations were excited in a region of frequencies from 1.5–2 up to 70–80 kilocycles per second. In this case the state of the plasma was weakly turbulent. The amplitudes of the oscillations in density $\tilde{n}$ and in potential $\tilde{\nabla}$ were measured. It was found that within 20%, $\tilde{n}/n = e\tilde{\nabla}/T$. The oscillations were potential. At densities of 1×10^9 to 1×10^{10} cm^{-3}, the value of $\tilde{n}/n$ did not depend on the magnetic field or density. On increasing the density above 7 to 10×10^{10} cm^{-3}, the amplitude ($\tilde{n}/n$) decreased due to damping of the instability as a result of an increase in the number of ion-ion collisions which have a stabilizing effect. The diffusion coefficient was measured from the plasma flow transverse to the magnetic field. Its value was found to be 10^2 cm^2/sec at densities of 1×10^9 to 1×10^{10} cm^{-3}. This value significantly exceeded the classical value of 0.5 for $n = 1 \times 10^9$ and H = 1000 gauss. The anomalous diffusion was due to drift instability. (TTT)

17884 (NP-15886) INTRODUCTION TO GENERAL DYNAMICAL SYSTEMS, STABILITY AND WAVES. Rijnhuizen Report 65-27. Broer, L. J. F. (Stichting voor Fundamenteel Onderzoek der Materie, Jutphaas (Netherlands). Instituut voor Plasma-Fysica). Dec. 1965. 43p. Dep. mn.

An introduction to wave propagation and stability theory in general is presented. The classical theory of stability, to which Liapounow has made the most important contributions, is discussed. The extension of the theory of the stability of dynamical systems to continuous system is discussed. (M.O.W.)

17885 (ORNL-3908) THERMONUCLEAR DIVISION SEMIANNUAL PROGRESS REPORT FOR PERIOD ENDING OCTOBER 31, 1965. (Oak Ridge National Lab., Tenn.). Mar. 1966. Contract W-7405-eng-26. 172p. Dep. mn. CFSTI $5.00 cy, $1.00 mn.

Separate abstracts were prepared for the 9 included sections. (M.O.W.)

For abstracts of individual sections see: 17253, 17600, and 17886–17892.

17886 (ORNL-3908, pp 1-17) INJECTION AND ACCUMULATION: SINGLE-PASS EXPERIMENTS (DCX-1). Dunlap, J. L.; Edwards, R. S.; Haste, G. R.; Massengill, L. A.; Nielsen, C. E.; Postma, H.; Reinhardt, R. G.; Schill, W. J.; Wells, E. R.; Young, R. A. (Oak Ridge National Lab., Tenn.).

The axial oscillation amplitudes and the energy spread of trapped protons were deliberately increased in attempts to stabilize the instability driving proton losses to permit the accumulation of higher densities. The threshold density for this instability could be increased by nearly two orders of magnitude by these techniques. However, the maximum thresholds remained below the density at which proton losses occur, and the limiting plasma density, 1 to 2×10^8 cm^{-3}, was not increased significantly. A number of experiments relating directly to the problem of mode assignment for the instability were performed. These experiments included studies of threshold variations with energy spread, with changes in the distribution of trapped protons in radial oscillation amplitude, and with changes in the shape of the magnetic field. Some instability growth-time measurements were also made. The results of the experiments are in agreement with the theory of the negative mass instability. Progress in analytic calculation of orbits and orbit frequencies and results of injecting into mode I and mode II discharges are also reported. (auth)

17887 (ORNL-3908, pp 18-31) INJECTION AND ACCUMULATION: MULTIPLE-PASS EXPERIMENTS (DCX-2). Bell, P. R.; Culver, J. S.; Davis, R. C.; (and others) (Oak Ridge National Lab., Tenn.).

Experiments were carried out in which the plasma properties were studied with hydrogen arc dissociation and hydrogen and nitrogen gas dissociation. The densities obtained vary, depending on the conditions, from 1×10^8 ions/cm^3 to several times 10^9 ions/cm^3, somewhat lower than those obtained with the lithium arc dissociation. The highest densities are obtained with the hydrogen arc used as a dissociator despite the fact that the pressure could not be reduced in these experiments below $\sim 5 \times 10^{-6}$ torr. In the case of gas dissociation, a quantitative use of the energy analyzer data was made to determine directly the trapped proton density, and the results agree with the usual measurements using the integral of the charge-exchange flux following beam turnoff. It appears that in the case of gas dissociation, the evidence suggests fairly good accountability of the injected beam from the charge-exchange flux at equilibrium. Surprisingly, the trapped density is observed to rise to a peak as the pressure is increased and then falls at pressures above 2×10^{-5} torr. This behavior is shown to be due to variations in the energy spread as a result of the presence of the microinstability. Studies of the pitch-angle distribution in gas breakup were made. In certain instances no central peak was observed. The interpretation of these results in terms of what limitations for the density may be expected is still ambiguous. Radio-frequency measurements were made with improved calibrated probes which show electric fields at the probes in excess of 100 v/cm for some of the harmonics. The variation of the behavior of the harmonic spectra as a function of gas pressure and energetic particle density is also described. (auth)

17888 (ORNL-3908, pp 32-51) ELECTRON-CYCLOTRON HEATING. (Oak Ridge National Lab., Tenn.).

The EPA Facility was modified extensively and will henceforth be called INTEREM for Injection of Neutrals and Trapping on an Electron Resonance Environmental Medium. The injected 20-kev neutral beam current has increased in magnitude. As a result of these improvements, the density of 20-kev ions trapped in the electron-cyclotron plasma has increased to $\sim 3 \times 10^7$ ions/cm^3. Hot-ion instabilities were not observed in the presence of the

environmental plasma medium. The neutral beam was also used to measure the cold-ion density in the environmental plasma. A description of the 2-kw, 8-mm continuous-wave microwave source used to form the electron-cyclotron plasma in the ELMO Facility is given. Experimental results show that the multicomponent plasma might have as many as four rather distinct energy groups. The results of some density and temperature measurements using bremsstrahlung diagnostics, neutron intensities, diamagnetic measurements, and axial currents are presented. It is shown that two types of instabilities can be induced in a hot-electron plasma produced by electron-cyclotron heating in a magnetic mirror. One type results in radial loss of particles across magnetic field lines and appears to be due to the growth of flutes. The other results primarily in loss along magnetic field lines and appears to be due to the mirror instability. Both types are accompanied by radio-frequency oscillations and result in the loss, per event, of ~10% of the energy stored in the plasma. (auth)

17889 (ORNL–3908, pp 52–89) PLASMA PHYSICS. Alexeff, Igor; Jones, W. D.; Neidigh, R. V.; Peed, W. F.; Stirling, W. L. (Oak Ridge National Lab., Tenn.).

Ion and electron temperatures and densities are being measured in the burnout experiments. The power density of Burnout V was increased. Deuterons up to 170 kev were analyzed, and corresponding neutron fluxes from wall reactions were observed. A wide-angle optical system was used to study the light emitted from the plasma of Burnout V. As expected, in mode II operation, the central arc is observed to fade and is replaced by a dim glow throughout the entire plasma container. Development of hot-electron plasmas continues. In an annular shell trapped between magnetic mirrors, two feed arcs operating simultaneously contribute to an electron density of 10^{12} cm^{-3} and temperature of 100 ev. Electrons of 100 kev at 5×10^{8} cm^{-3} density are found on both the inside and outside of the shell. Ionic sound wave studies were continued, and verified that γ, the adiabatic compression coefficient for the plasma electrons, is unity, as is expected on theoretical grounds. An electron-emitting hot probe was found to be a supersensitive ion-wave detector, apparently because the ion wave perturbs a space-charge sheath surrounding the probe. A simple model was used to predict which gases in cylindrical discharge tubes tend to produce moving striations and which do not. A study of Langmuir probes shows that in small, quiescent plasma systems of low density, Langmuir probes are not always satisfactory. In these systems, Langmuir probes can be supplemented by a simple "decay" technique for density measurements. Calculations for the momentum probe (magnetic analyzer) for plasma studies were extended to include the effects of electric potentials placed on the probe. Studies of the macroscopic cross-field mass motion (fluting) from the hydrogen arc continued in a modified magnetic field geometry. The addition of a pair of coils inside the main mirror coil pair enables one to produce a field with a radial minimum on the axis. For the largest depth of this magnetic well, correlated signals which may be identified as flutes still appear, although their radial velocity is reduced, perhaps by an order of magnitude. The radial density profile is also narrowed. Flutes were also observed in the plasma, produced apparently by a streaming interaction (turbulent heating), in the uniform field of beta tank D, using the PIG-configuration plasma source. The observed flute velocities, of the order of $\sim 2 \times 10^{6}$ cm/sec, are somewhat higher than are observed in the gas arc facility. At large radii these flutes cannot be observed, but fluctuations in the ion current appear which may be interpreted as a rigid rotation of the plasma body at a frequency with a period of 2 μsec. In calutron beam work during this period, the Ca^{+} beam passing through a homogeneous magnetic field was studied. Further spectroscopic studies of the energetic carbon arc suggest for the first time a possible leveling off of the heating mechanism in very long, magnetically confined carbon arcs. (M.O.W.)

17890 (ORNL–3908, pp 100–7) HIGH-CURRENT ION-BEAM PRODUCTION AND INJECTION. Davis, R. C.; Hall, R. R.; Kelley, G. G.; Morgan, O. B.; Stratton, R. F.; Babler, G. M. (Oak Ridge National Lab., Tenn.).

Research on ion sources and facilities for extracting, focusing, and handling ion beams for direct application into present thermonuclear devices and potential application into future devices has continued. Intense direct-current hydrogen ion beams, either atomic or molecular, are now available over an energy range of 4 to 600 kev with total beams of from 200 ma to 1 amp. The fraction of the total beam usable for various experiments is indicated by imposing various degrees of collimation. (auth)

17891 (ORNL–3908, pp 108–13) PLASMA THEORY AND COMPUTATION. (Oak Ridge National Lab., Tenn.).

A concentrated effort was made to obtain a comparison between theory and experiment in two important instances: the low-density instability in DCX-1 and the flutelike instabilities which can be excited in the PTF machine. The importance of these particular cases stems from the general questions they bear upon: the domain of relevance of negative-mass instability theory, and the broad question of finite length and cold-plasma effects respectively. In a quite separate area, the long-range program to obtain a complete theoretical description of plasma transport phenomena has progressed to a most important point. The formulas derived earlier to describe "anomalous" diffusion rates due to specified fluctuation spectra were studied from several viewpoints. Work now in progress is aimed at predicting the fluctuation spectrum to be expected on the basis of the nonlinear development of plasma instabilities. This information would then permit a general diffusion calculation, which might give answers to the question of what levels of instability are tolerable in a fusion plasma. (auth)

17892 (ORNL–3908, pp 149–53) VACUUM STUDIES, SPUTTERING, ADSORPTION, AND DIFFUSION OF GASES IN METALS. (Oak Ridge National Lab., Tenn.).

Further consideration of tritium inventory problems in a thermonuclear reactor was made. The data found in the literature were analyzed and show that tritium inventory control is associated with the primary factors, temperature, metal cleanliness and purity, and bombarding flux of energetic atoms or ions. An experimental study was conducted using low-energy bombardment in a glow discharge; the study yielded results in agreement with the detailed literature study. Part of the continuing studies of vacuum systems and components included a study of the periodic pressure bursts frequently observed in vacuum systems. In the particular system used for this study, the gases were identified with water and carbon dioxide effusing from the pump flange elastomer gasket and not air or background gases in the vacuum system. Oil transport in vacuum systems was previously found to be by a surface transport process for a mixed hydrocarbon oil. The results of a study using a high-mass-resolution mass analyzer on the mobility of a trisiloxane oil could be interpreted most simply by assuming a vapor-phase transport mechanism. The subject of transport mechanisms of high-molecular-weight materials is still moot. Measurements with a refrigerated McLeod gage indicate that the "Hg vapor pumping effect" can be eliminated by immersing the gage in a region where the ambient temperature is –15°C. Calibration of a commercial capacitive differential manometer was made to determine the usefulness of such a gage for a pressure standard in measuring condensable vapors. Sputtering ratios were measured for 30-kev D^{+} ions on tungsten, molybdenum, copper, and 316 stainless steel. Sputtering ratios range from 0.03 for copper to 0.007 for the stainless steel. (auth)

17893 (SU-IPR–44) STUDIES OF PLASMA OSCILLATIONS. Quarterly Status Report No. 23, June 1–August 31, 1965. Crawford, F. W. (Stanford Univ., Calif. Inst. for Plasma Research). Nov. 1965. Contract AT(04-3)-326. 33p. Dep. mn. CFSTI $2.00 cy, $0.50 mn.

Experimental and theoretical research during this period is reported on ion wave propagation and positive column instabilities, electron beam probing of plasmas, beam-plasma interactions, and positive column resonances and propagation. (M.O.W.)

17894 (SU-IPR-47) STUDIES OF PLASMA OSCILLATIONS. Quarterly Status Report No. 24, September 1, 1965–November 30, 1965. Crawford, F. W. (Stanford Univ., Calif. Inst. for Plasma Research). Jan. 1966. Contract AT(04-3)-326. 45p. Dep. mn. CFSTI $2.00 cy, $0.50 mn.

Further experimental and theoretical research is reported on ion wave propagation and positive column instabilities, electron beam probing of plasmas, beam-plasma interactions, and positive column resonances and propagation. (M.O.W.)

17895 (AEC-tr-6669) NUCLEAR FUSION (TRANSLATED SELECTED ARTICLES). Translated from Nucl. Fusion, 5: 7-16; 20-40; 85-6(1965). 83p. Dep. mn. CFSTI $3.00 cy, $0.75 mn. JCL $8.10 fs, $2.69 mf.

Abstracts for the three included papers appeared previously in NSA as; 19: 33460, 33462, and 33467. (M.O.W.)

17896 MICROFIELD APPROXIMATIONS IN PLASMAS. Root, Richard M. (Florida State Univ., Tallahassee). AIAA (Amer. Inst. Aeron. Astronaut.) Student J., 3: 49-51 (Apr. 1965).

Previous approximations made in attempts to solve the fundamental problem of determining the electric field distribution within a plasma, or ionized gas, are considered, and Monte Carlo methods were used to develop the probability distribution of the microscopic electric field in an ionized gas expressed as a function of a normalized magnitude of the field. These methods were used to run a theoretical experiment on a large computer. Statistical sampling techniques were used to determine the microfield of the plasma. For assurance that this method will give the probability distribution, Bernoulli's theorem was invoked. (TCO)

17897 LORENTZ FORCE MAXIMIZATION IN CONTINUOUS FLOW HALL CURRENT PLASMA ACCELERATORS. Henry, Roger P. (Univ. of Toronto). AIAA (Amer. Inst. Aeron. Astronaut.) J., 4: 165-6(Jan. 1966).

Lorentz forces used to produce accelerations are the result of a current crossed with an applied magnetic field. Practical limitations on maximum steady magnetic fields and maximization of current density between electrodes limit the production of large Lorentz forces in Hall current plasma accelerators. Seeding of the plasma flow to produce greater conductivity is discussed as one means for increasing the Lorentz force. (B.G.D.)

17898 MEASUREMENT OF THE THERMAL RADIATION FROM AN ARGON PLASMAJET. Cremers, C. J. (Georgia Inst. of Tech., Atlanta); Pfender, E. AIAA (Amer. Inst. Aeron. Astronaut.) J., 4: 376-7(Feb. 1966).

The total radiated energy emitted by a Thermal Dynamic Corporation F-40 plasma torch as a function of angle from the nozzle axis and as a function of the flow rate was measured by means of a thermopile. The thermopile response is discussed. (B.G.D.)

17899 USE OF LANGMUIR PROBES FOR LOW-DENSITY PLASMA DIAGNOSTICS. Mawardi, O. K. (Case Inst. of Tech., Cleveland). Amer. J. Phys., 34: 112-20 (Feb. 1966).

A review is given of the theory of operation of the single and double Langmuir probe. The method of using the double Langmuir probe for the purpose of measuring the temperature and density of electrons in a plasma is described. A laboratory experiment using Langmuir probes is suggested and sample calculations pertaining to such an experiment are given. (auth)

17900 ON THE POSSIBILITY OF EXCITATION HEATING OF IONS TO HIGH TEMPERATURE. McNally, J. Rand Jr.; Skidmore, M. R.; Jenkins, P. M.; Francis, J. E. Jr. (Oak Ridge National Lab., Tenn.). Appl. Opt., 5: 187-94(Feb. 1966). (ORNL-P-1716).

Cyclic or chainlike inelastic collision processes are invoked as an hypothesis to explain the grossly nonthermodynamic properties of energetic carbon and gas-fed carbon arcs confined by magnetic fields. Elastic collisions between the fast electrons ($\nu_- > \nu_+$ but $E_- \ll E_+$) and the hot ions appear to be only about one-tenth as efficient a process for heating the ions as the proposed multiple inelastic collision process, which is called excitation-heating. In addition, a revised treatment of the rate of energy transfer from hot carbon ions to the very cold electrons ($\nu_- < \nu_+$) reduces the conventional ion cooling rate by a factor of about 6. (auth)

17901 SPECTROSCOPY OF PLASMAJETS AND ELECTRIC ARCS. Tourin, Richard H. (Warner and Swasey Co., Flushing, N. Y.). Appl. Spectros., 20: 1-5(Jan.-Feb. 1966).

Spectroscopy is considered as a means to study the ways in which energy is transferred within and from plasmajets and electric arcs. For this purpose, measurements of spectral intensities and line widths were applied to measure thermodynamic properties of the hot ionized gases. Methods, apparatus, and applications are illustrated by examples. (auth)

17902 SOME SPECTROSCOPIC MEASUREMENTS OF A SUPERSONIC PLASMAJET. Shipley, K. L. (Sandia Corp., Albuquerque, N. Mex.). Appl. Spectros., 20: 6-11 (Jan.-Feb. 1966).

Typical results of spectroscopic data from argon and nitrogen supersonic plasma jets are presented. The purpose of this study was to determine which of these spectroscopic data give suitable information for temperature determination. Spectral-line-intensity and hydrogen-line broadening techniques were used. For the argon jet, the results from line-intensity measurements of ionized and un-ionized atoms generally gave reliable information; results from hydrogen-line broadening measurements indicated temperatures from 6% to 20% less than intensity measurements. Spectrographic data were compared with enthalpy measurements. For the nitrogen plasma jet, the N_2^+ (0,0) band was used to determine a rotational temperature. (auth)

17903 SMALL-TIME SOLUTION OF SNOWPLOUGH EQUATIONS FOR A PLASMA ACCELERATOR. Bakken, Jon Arne. Arbok Univ. Bergen, Mat.-Nat. Ser., No. 4, 1-15(1964).

The snowplough equations for an idealized plasma accelerator energized from a condenser bank are solved with respect to current and current sheet position to the second order of a characteristic parameter S. Approximate small-time formulas are given. Dimensionless variables are employed. Ohmic losses are neglected. (auth)

17904 ELECTRIC ARC IN A SUPERSONIC PLASMA JET. Huegel, Helmut; Krause, Siegfried; Peters, Theo. Astronaut. Acta, 11: 238-46(July-Aug. 1965). (In German).

Recently the interest in the development of plasma thrustors with magnetic acceleration has grown considerably at the expense of purely thermal arc jet engines. Most promising is selfmagnetic acceleration of the plasma although this requires radial components of the current within the electric arc. These are ideally realized by means of an expanding supersonic free jet. The fundamental problem thus was to investigate the general behavior of electric arcs in supersonic gas streams. Among other items the question arose whether it would be possible to heat a supersonic gas stream in a channel (ramjet); this has not yet been achieved satisfactorily by chemical combustion. An electric arc which burns transversely to a supersonic plasma jet is considered. It appears that a stable arc cannot be achieved without a stabilizing transverse magnetic field. The arc forms a sheath in the jet boundary. A stable arc, however, is maintained in a coaxial cold argon flow at pressures above 4 mm Hg and currents higher than 360 A. Proceeding from this fact the mentioned experiments with models of arc-ramjet engines have been performed. It appears that heating within the engine is possible in subsonic flow, whereas the possibility of supersonic flow heating has not yet been established. Finally, the indicated experiments with an arc discharge are discussed, in which the arc plasma is accelerated by electromagnetic forces

produced by its own magnetic field. These experiments encourage further work on the subject. They are intended to be continued especially in connection with the development of plasma thrustors and plasma wind tunnels. (auth)

17905 HETERODYNE GENERATION BY ELECTROMAGNETIC FIELDS IN GASEOUS PLASMA. **Bloch, S. C.** (Univ. of South Florida, Tampa). Brit. J. Appl. Phys., 16: 1853-60(Dec. 1965).

It is shown that the original work of Bailey and Martyn concerning ionospheric cross modulation also contains the elements of the theory of heterodyne generation occurring when electromagnetic fields interact in a plasma. Mixing of fundamental frequencies in the 5–9 Mc region was observed in air plasma in the laboratory, at pressures ranging from 0.025 to 2 torr. Heterodynes, accompanied by harmonic generation, included those of the forms $f_i \pm f_j$ and $2f_i \pm f_j$. Power densities at the fundamental frequencies were less than one mw cm^{-3}. (auth)

17906 ANALOGUE COMPUTER TECHNIQUES USED TO STUDY CHARGED PARTICLE TRAJECTORIES IN A MAGNETIC FIELD. **Read, A. H.** (United Kingdom Atomic Energy Authority, Abingdon, Eng.). Brit. J. Appl. Phys., 16: 1861-70(Dec. 1965).

An analog computer solution of the equations of motion of a charged particle in a magnetic field system is described. Flow diagrams are given for two possible computer arrangements. A photoformer technique for generating the magnetic field functions is used. This allows rapid changes of the field profile to be made on a Polaroid slide bearing an image of the profile. Some of the practical problems encountered when using this technique are discussed and suitable ways of overcoming them are presented. (auth)

17907 ON THE DIFFUSION THEORY OF THE LOW-VOLTAGE ARC PLASMA. **Popescu, I.; Brandus, L.; Moldovan, C.; Musa, G.** (Physics Inst. of the S.R.R. Academy, Bucharest). Brit. J. Appl. Phys., 17: 129-31(Jan. 1966).

The thermo-diffusion term in the particle flux equations is considered according to the experimental data, which show a large variation of the electron temperature across the low-voltage arc plasma. For the case of an infinite plane parallel plasma and a constant electric field the electron diffusion coefficient at the cathode edge is estimated and it is compared with the classical theoretical expression. (auth)

17908 EXPERIMENTAL STUDY OF THE PLASMA CREATED BY FOCUSING OF A LASER BEAM IN AIR. **Floux, Francis; Veyrie, Pierre** (Centre d'Etudes de Limeil, Villeneuve-Saint-Georges, France). Compt. Rend., 261: 3771-3(Nov. 8, 1965). (In French).

The plasma created by the focusing of a laser beam is modified very rapidly during the first 60 nsec. The cinematographic recording is compared to the evolution to the absorption of the luminous energy. (tr-auth)

17909 HIGH-FREQUENCY HEATING OF LOW-PRESSURE PLASMA. **Klima, R.** (Inst. for Plasma Physics, Prague). Czech. J. Phys., 15: 697-9(1965). (In Russian).

The theoretical implications of cyclotron heating of electrons, resulting in the formation of a plasma at a high-frequency field frequency of $\omega \approx 2|\Omega_0|$, whereby Ω_0 is the cyclotron frequency of electrons, were reviewed. By generalizing the hamiltonian previously derived for a specific case, simplified equations were obtained for describing the motion of charged particles. Amplitudes of the individual resonance harmonics were obtained for specific concrete cases. The results indicated an instability in the motion of the particles or an absorption of the high-frequency energy in the case of $N_\omega \approx 2|\Omega_0|$, N = 1, 2, 3, ... Accordingly, either a paramagnetic resonance, or, - in the case of even values of N, - forced oscillation resonance is initiated. The exponential amplitude growth increment $\bar{q}^1$ may be determined from the literature data. It can be also shown that high-frequency resonance discharge occurs only in specific density ranges of the particles. (TTT)

17910 A SIMILARITY PARAMETER IN THEORY OF PLASMA FLOWS. **Morozov, A. I.; Solov'ev, L. S.** Dokl. Akad. Nauk SSSR, 164: 80-3(Sept. 1, 1965). (In Russian).

A similarity analysis is made of a two-fluid, fully ionized plasma flow under steady state conditions. A vector potential is defined for electrons and ions as $n_e v_e = \mathrm{rot}\,\bar{\Psi}_e$, $n_i v_i = \mathrm{rot}\,\bar{\Psi}_i$, which, when combined with Maxwell's equation, yields $H = (4\pi e/c)(\bar{\Psi}_i - \bar{\Psi}_e) + H_0$. The similarity parameter for the flow is defined by $\xi = (c|H - H_0|_{charact}/4\pi|\bar{\Psi}_i|_{charact})$. For the case of a flow in a coaxial channel of arbitrary cross section ξ becomes $\xi = (|\dot{N}_e - \dot{N}_i|/|\dot{N}_i|) = (I_p/I_\Pi)$. Because of the fact that Ψ is a three-dimensional vector, one can construct three ξ parameters. In the absence of dissipation terms and for $m_e/M \to 0$, the magnetic field degenerates into an electron component where one can show that ξ takes on the physical meaning of a "charge exchange" parameter. (ATD)

17911 WAVE PROPAGATION IN PLASMA. **Share, Irwin** (Hofstra Univ., Hampstead, N. Y.). Electro-Technology (N. Y.), 76: 59-72(Nov. 1965).

Various aspects of the interaction of electromagnetic waves and plasma are reviewed, and applications of this interaction to situations of practical interest in communication and in electron devices are examined. Basic expressions are developed which describe the behavior of electromagnetic waves in plasma; then phenomena of practical importance are related to these expressions. The plasmas considered in this article are made up of electrons, positive ions, and neutral particles. In the propagation of an electromagnetic wave in an infinite uniform plasma medium, considered first, is wave propagation in the absence of a magnetic field. Then, the more general and complicated case is considered wherein the wave passes through a uniform, nonvarying magnetic field. Orbit theory is used primarily to treat the motions of individual charged particles in electric and magnetic fields. Before a discussion of the communication aspects of wave propagation in naturally occurring plasmas, the formation of the major natural plasmas is examined, and some key properties of these plasmas are pointed out. The use of a plasma column as a variable microwave phase shifter or attenuator is discussed. Some plasma devices are considered as well as current research directed toward plasma amplifiers and solid-state plasma devices. It may be possible to use the nonlinear propagation characteristics of plasma for parametric amplification and harmonic generation. (BBB)

17912 MACROSCOPIC CHARACTERISATION OF A TWO-FLUID ANISOTROPIC WARM PLASMA. **Cheng, D. K.; Chen, H. C.** (Syracuse Univ., New York). Electron. Lett., 1: 277-8(Dec. 1965).

Two "compressivity tensors" are proposed, which, together with the permittivity tensor and the permeability, will characterize the macroscopic electromagnetic properties of an anisotropic warm plasma under the two-fluid model. A set of four governing equations is formulated, which is both mathematically concise and amenable to meaningful physical interpretation. (auth)

17913 SLOW-WAVE PROPAGATION IN A NONUNIFORM PLASMA. **Pinder, D. N.** (Battersea Coll. of Tech., London). Electron. Lett., 1: 291(Dec. 1965).

The propagation of electromagnetic waves along a coaxial line filled with three concentric dielectric annuli, one of which is a plasma possessing a nonuniform charge density, is considered. A variational technique is used to find the dispersion curve for the lowest-order circularly symmetric slow wave which may propagate in the system. (auth)

17914 INTERNATIONAL DEVELOPMENTS IN CONTROLLED THERMONUCLEAR FUSION. **Dougal, Arwin A.** (Univ. of Texas, Austin). IEEE (Inst. Elec. Electron. Eng.), Spectrum, 3: 87-93(Feb. 1966).

Progress in the study of controlled thermonuclear fusion is reviewed. The discussion includes the basic principles, the superdense plasma pinch, thermal losses which limit the peak plasma temperature, ion cyclotron resonance

heating, plasma instabilities and turbulence, electron or ion beam-plasma injection, and irradiation by a giant pulse laser. Marked progress has been made toward controlled thermonuclear fusion especially in the ability to produce interesting plasmas with diverse physical characteristics in the laboratory. But a workable reactor concept has not yet been developed. Universal and micro-instabilities continue to be unsolved problems. (J.F.P.)

17915 SCATTERING OF ELECTROMAGNETIC WAVES BY PLASMA. Khan, R. M.; Khan, T. P. (Jadavpur Univ., Calcutta). Indian J. Phys., 39: 347-51(July 1965).

The case of reflection and refraction of plane electromagnetic wave by plasma in an applied magnetic field is treated. The component of the magnetic field perpendicular to the plane of incidence in the reflected wave provides an easy means of analyzing the physical features of the plasma. (auth)

17916 DIOCOTRON INSTABILITY IN PLASMAS AND GAS DISCHARGES. Knauer, W. (Hughes Research Labs., Malibu, Calif.). J. Appl. Phys., 37: 602-11(Feb. 1966).

The wave interaction underlying the diocotron effect is re-examined and a physical model of the instability presented. A wave analysis is then given for circular, wall-enclosed charge layers with finite length in the axial direction. Circular layers are of particular interest, since they apply to various plasma, discharge, and electron device geometries. Their instability behavior is found to be similar in many respects to the behavior of linear charge sheets, described in earlier work by R. W. Gould. In contrast to linear sheets, however, circular layers are unstable only when their thickness is sufficiently small. This effect is associated with the inability of charge perturbations to have a wavelength which exceeds the layer circumference. Data are presented for the magnitude of growth in various configurations and for the critical layer width at which growth terminates. (auth)

17917 NONLINEAR LIMITING OF THE DOUBLE-STREAM INSTABILITY. Mihran, Theodore G. (General Electric Co., Schenectady, N. Y.). J. Appl. Phys., 37: 624-30(Feb. 1966).

The double-stream instability in finite-diameter beams was investigated by numerical experiments on a digital computer using the disk electron model. The nonlinear level is found to be a quadratic function of the linear-theory double-stream parameters $\omega\delta/\omega_q$. Computed electron trajectories show electron trapping to be the cause of r-f current saturation. A simple analytic trapping theory is given which predicts observed peak nonlinear current levels to within a factor of three. This investigation suggests that current conversion efficiencies approaching 50% can be achieved by operating near the upper edge of the gain band. On the other hand, nonlinear behavior occurs at perturbation levels of the order of 1% for weak instabilities near the lower edge of the gain band. The time to reach the nonlinear level is surprisingly short in most cases, ranging from 2 to 30 plasma wavelengths, depending on gain and excitation level. (auth)

17918 RAPID ELECTRON-DENSITY OSCILLATIONS ON THE AXIS OF A THETA PINCH. Gerardo, J. B.; Bialecke, E. P.; Hirsch, R. L. (Univ. of Illinois, Urbana). J. Appl. Phys., 37: 756-60(Feb. 1966).

A detailed temporal history of the electron density on the axis of a theta pinch is presented. During the magnetic compression, oscillations are superimposed on the electron density. The amplitude of these oscillations is, under some conditions, as large as 50% of the maximum value attained in the pinched state. These density variations are ascribed to radial hydromagnetic oscillations. The electron density measurements were made by means of a spherical laser interferometer and these were correlated with electron density measurements using Stark broadening techniques. (auth)

17919 A NOTE ON THE UNIFIED THEORY OF NON-LINEAR OSCILLATIONS OF A COLD PLASMA. Freidberg, J. P.; Sasiela, R. (Polytechnic Inst. of Brooklyn, N. Y.). J. Math. Anal. Appl., 12: 488-90(Dec. 1965).

A limitation of the time dependent solution to the cold plasma equation obtained by Dolph (Math. Anal. Appl. 5(1962)) is presented. (B.G.D.)

17920 EXCITATION OF PLASMA OSCILLATION BY PARAMETRIC RESONANCE. Kato, Kiyoe; Yoseli, Morihiro; Kiyama, Satoru; Watanabe, Shinsuke (Electrotechnical Lab., Tokyo). J. Phys. Soc. Jap., 20: 2097-8(Nov. 1965).

An experiment was performed on parametric resonance in plasma. Typical patterns displayed on the cathode ray tube and the plasma-electron frequency versus discharge current, with strong oscillation indicated, are shown. The results confirm that the oscillation may be excited by the parametric resonance in the oscillation system with the characteristic frequency, but details of the mechanism for such excitations are obscure. (J.F.P.)

17921 ANOMALOUS BREMSSTRAHLUNG AND ANOMALOUS CYCLOTRON EMISSION FROM PARTIALLY IONIZED GASES. Tanaka, Shigetoshi; Honzawa, Tadao; Takayama, Kazuo (Nagoya Univ., Japan). J. Phys. Soc. Jap., 20: 2099-2100(Nov. 1965).

Radio wave emissions from partially ionized gases of xenon, krypton, argon, neon, and helium were studied in the frequency range from 20 to 1000 Mc. The characteristics of both the anomalous bremsstrahlung and cyclotron emission which were observed are similar and are described. The occurrence of these emissions was observed in xenon, krypton, and argon, but was not observed in neon and helium plasmas. The radio-frequency emission from a plasma is shown as a function of the magnetic field with the detecting frequency as a parameter. It is concluded that anomalous bremsstrahlung as well as the anomalous cyclotron emission is ascribed to the negative absorption effect in plasma. (J.F.P.)

17922 REEMISSION OF IONICALLY PUMPED H_2 AND He FROM A STAINLESS STEEL SURFACE. Martin, G.; Lewin, G. (Princeton Univ., N. J.). Contract AT(30-1)-1238. J. Vac. Sci. Technol., 3: 6-10(Jan.-Feb. 1966). (MATT-336).

H_2 and He discharges in a stellarator produce copious wall bombardment by the plasma ions. The re-emission rate of the gas was measured for times of 0.06 to 10^5 sec after bombardment. The rate was approximately proportional to $t^{-0.6}$ for He and $t^{-0.75}$ for H_2. The re-emission is also calculated assuming diffusion of the gas in the solid and taking into account the finite nonuniform initial distribution. It follows from the analysis that the rate is proportional to t^{-n} where n approaches 0.5 or 1.5 as the ratio of re-emission to bombarding time approaches zero or infinity. (auth)

17923 SEARCH FOR RAMAN SCATTERING OF ELECTROMAGNETIC WAVES IN THE MICROWAVE BAND WITH THE AID OF A TURBULENT PLASMA. Demidov, B. A.; Fanchenko, S. D. JETP Lett. (USSR) (Engl. Transl.), 2: 332-4(Dec. 15, 1965).

Translated from Zh. Eksp. Teor. Fiz., Pis'ma Redakt. 2: 533-7(Dec. 15, 1965).

It is shown that in the theory of Raman scattering of electromagnetic waves by the electronic oscillations of a bound plasma that the Raman-scattering signal can yield very valuable information on the level of the turbulent oscillations. Using a toroidal plasma installation, a search for the scattering of electromagnetic waves from an external source was made. Various details of the search are presented. (M.O.W.)

17924 STATES WITH POPULATION INVERSION IN A SELF-COMPRESSED DISCHARGE. Kulagin, S. G.; Likhachev, V. M.; Markuzon, E. V.; Rabinovich, M. S.; Sutovskii, V. M. (Lebedev Inst. of Physics, Moscow). JETP Lett. (USSR)(Engl. Transl.), 3: 6-8(Jan. 1, 1966).

Translated from Zh. Eksp. Teor. Fiz., Pis'ma Redakt., 3: 12-14(Jan. 1, 1966).

Negative-temperature states were observed in a pinched 15-kamp discharge in spectrally pure argon at 10^{-2} mm Hg. The self-compressed discharge generated a 0.2-μsec pulse. (G.O.Y.)

17925 UNSTABLE STATES OF A PLASMA IN A TRAP WITH COMBINED FIELD. Baiborodov, Yu. T.; Gott, Yu. V.; Ioffe, M. S.; Yushmanov, E. E. JETP Lett. (USSR) (Engl. Transl.), 3: 58-60(Jan. 15, 1966).

Translated from Zh. Eksp. Teor. Fiz., Pis'ma Redakt., 3: 92-6(Jan. 15, 1966).

The results are presented of a detailed investigation of some distinct unstable states of plasma that are observed in a trap with a combined field (minimum-induction type) under certain injection conditions. A possible interpretation of the physical nature of the instability is outlined. (D.C.W.)

17926 THERMONUCLEAR INVESTIGATION. I. INTRODUCTION. Rietjens, L. H. Th. (FOM-Instituut voor Plasma-Fysica, Rijnhuizen, Netherlands). Ned. Tijdschr. Natuur., 31: 149-52(May-June 1965). (In Dutch).

The status of thermonuclear power is summarized. (D.C.W.)

17927 THERMONUCLEAR INVESTIGATIONS. II. EQUILIBRIUM, CONFINEMENT, INSTABILITIES, AND STABILIZATION. Weenink, M. P. H. (FOM-Instituut voor Plasma-Fysica, Rijnhuizen, Netherlands). Ned. Tijdschr. Natuur., 31: 153-63(May-June 1965). (In Dutch).

Energy equilibrium in the plasma, confinement of the plasma in a finite space, and stability of the equilibrium configuration are considered theoretically. (J.S.R.)

17928 THERMONUCLEAR INVESTIGATION. III. EXPERIMENTS. Rietjens, L. H. Th.; Braams, C. M.; de Kluiver, H.; Minardi, E.; Ornstein, L. Th. M. (FOM-Instituut voor Plasma-Fysica, Rijnhuizen, Netherlands). Ned. Tijdschr. Natuur., 31: 164-89(May-June 1965). (In Dutch).

Experimental studies on the production and heating of plasma, injection of plasma and particles, plasma confinement in open systems, and plasma confinement in closed systems are summarized. (J.S.R.)

17929 THERMONUCLEAR INVESTIGATIONS. IV. THE ENERGY BALANCE FOR THERMONUCLEAR REACTORS. Minardi, E. (FOM-Instituut voor Plasma-Fysica, Rijnhuizen, Netherlands). Ned. Tijdschr. Natuur., 31: 190-6(May-June 1965). (In Dutch).

The extent to which the energy balance of a thermonuclear reactor is favorable is considered. The operating conditions for a fusion reactor, energy losses in a thermonuclear reactor, end losses in a magnetic mirror, and cyclotron radiation are briefly discussed. (D.C.W.)

17930 ENERGY EMITTED BY ARGON PLASMA IN SPECTRAL LINES. Yakubov, I. T. Opt. Spectros. (USSR) (Engl. Tansl.), 19: 277-9(Oct. 1965).

Translated from Opt. Spektros., 19: 497-500(Oct. 1965).

The energy of an argon plasma in equilibrium at various pressures, temperatures, and layer thicknesses was calculated. The calculation included the emission in numerous spectral lines as well as the continuous spectrum. (auth)

17931 BREMSSTRAHLUNG IN THE INFRARED REGION FROM THE PLASMA OF THE ELECTRODELESS INDUCTION DISCHARGE. Dushin, L. A.; Kononenko, V. I.; Pavlichenko, O. S.; Nikolskii, I. K. Opt. Spectros. (USSR) (Engl. Transl.), 19: 378-81(Nov. 1965).

Translated from Opt. Spektros., 19: 674-9(Nov. 1965).

The bremsstrahlung in the near infrared region from an electrodeless induction discharge in hydrogen was investigated. The bremsstrahlung in the wavelength range from 1.8 to 9.5 μ was recorded with a germanium-gold alloy photoresistor, which was operated at liquid nitrogen temperature. By using the results of the measurements of the temperature of plasma electrons, the plasma density was determined from the intensity of the bremsstrahlung. Conclusions are drawn concerning the possibility of using this method for the analysis of a dense plasma. (auth)

17932 METHOD FOR THE DETERMINATION OF ATOMIC-RESONANCE LINE-OSCILLATOR STRENGTHS FROM WIDTHS OF OPTICALLY THICK EMISSION LINES IN T-TUBE PLASMAS. Lincke, R.; Griem, H. R. (Univ. of Maryland, College Park). Phys. Rev., 143: 66-73 (Mar. 4, 1966).

Using the neutral-helium resonance line as an example, a method is described for the measurement of the product of oscillator strength, Stark width, and ground-state density. Directly measured is the width of the line (as emitted by an essentially homogeneous but optically thick layer), which is proportional to the square root of the above product. A T tube is filled with a known helium-hydrogen mixture, and the temperature is calculated from the measured intensity ratios of helium and hydrogen lines. Measured widths of (optically thin) visible lines yield electron densities, which then give the theoretical Stark width of the ultraviolet line. These densities are also used in Saha equations to calculate the ground-state density from the measured temperature and the mixing ratio. This leaves the oscillator strength as the only unknown, whose accuracy is limited in the helium case mostly by the error in the ground-state density to about 25%, when the plasma is sufficiently dense and long-lived for local thermal equilibrium to hold. (auth)

17933 ECHO PROCESSES IN A PLASMA. Herrmann, G. F.; Whitmer, R. F. (Lockheed Palo Alto Research Lab., Calif.). Phys. Rev., 143: 122-9(Mar. 4, 1966).

The generation of echoes in classical systems is discussed with particular reference to cyclotron echoes in a plasma. A system of oscillators subjected to a sequence of pulses will produce an echo if the interaction contains appropriate nonlinear terms. A formal description of the echo mechanism is given for the case where nonlinear effects are confined to the times at which pulses are present, with emphasis on wave-propagation aspects. Diagrams are introduced for the classification of various nonlinear processes. The generation of echoes in a plasma interacting with microwave pulses propagating normal to an applied magnetic field is analyzed in a small-signal approximation. Echoes are found to arise from nonlinear terms associated with the convective motion of the electrons, and from the interaction with the magnetic component of the microwave pulses. Equations for the echo amplitude, in terms of the pulse widths and intensities, are given for transverse and longitudinal propagation. (auth)

17934 LONGITUDINAL PLASMA OSCILLATIONS NEAR ELECTRON CYCLOTRON HARMONICS. Buchsbaum, S. J.; Hasegawa, Akira (Bell Telephone Labs., Murray Hill, N. J.). Phys. Rev., 143: 303-9(Mar. 4, 1966).

A theory is developed for longitudinal plasma oscillations (normal modes) which are excited in a warm plasma column at microwave frequencies in the presence of a strong magnetic field. The oscillations manifest themselves as a set of absorption peaks near the harmonics of the electron cyclotron frequency. Good agreement is found between the observed positions of the peaks and a model calculation. The important property of the oscillations is that they are confined to a region near the axis of the plasma column, and are "quantized" by the shape of the electron density distribution. (auth)

17935 A CONVERGENT EXPRESSION FOR THE PARTITION FUNCTION OF A PARTIALLY IONIZED HYDROGEN PLASMA. Dekeyser, R. (Rijksuniversiteit, Utrecht). Physica, 31: 1405-17(Sept. 1965).

The partition function of a hydrogen plasma is derived, partly classically and partly quantum-mechanically, avoiding in this way at the same time the close distance and the high orbit divergences. The result is exact in the small density and infinite temperature limit, but can be considered as a good approximation also for conditions, where the ionization is incomplete. From this a Saha equation is derived, which contains an effective lowering of the ionization potential. An expression is obtained for the pressure, which is not simply the sum of the known pressures of the neutral and ionized parts, but has a correction from the transitions between these parts. (auth)

17936 THEORETICAL AND EXPERIMENTAL STUDIES OF WATER VAPOR PLASMA RADIATION. Golubev, V. A.;

Moskvin, Yu. V.; Khovrin, S. K. Teplofiz. Vysok. Temp., 3: 669-76(Sept.-Oct. 1965). (In Russian).

The contribution of different optical processes to the integral radiation of water plasma was analyzed and the effects of the radiating current under the experimental conditions were calculated. The measurement of the integral radiation energy was made in the temperature range from 10,000 to 18,000°K in the plasma jet emitted at atmospheric pressure from electric-arc heaters with water stabilizers. The theoretical and experimental data agreed satisfactorily. (tr-auth)

17937 EXPERIMENTAL DETERMINATION OF ARGON PLASMA HEAT-CONDUCTANCE FACTOR. Asinovskii, E. I.; Kirillin, A. V. (Scientific-Research Inst. of High Temperatures, USSR). Teplofiz. Vysok. Temp., 3: 677-85(Sept.-Oct. 1965). (In Russian).

The measurement of the thermal conductivity of argon plasma was made on a device having an electric arc stabilized with chilled copper walls. The dependence of the intensity of the electric field and the radial distribution of the temperature of the arc current was measured for different diameters of the stabilizing channel (4, 6, and 8 mm). It was shown that in similar types of arcs the heat transfer did not appear to be purely conductive. A method for the processing of the experimental data was proposed that made it possible to determine both the coefficient of the heat conductivity and the complete coefficient of radiation of the argon plasma. The experimental results obtained were compared with theory. (tr-auth)

17938 INVESTIGATION OF THE PERFORMANCE OF A DIRECT-CURRENT PLASMATRON. German, V. O.; Morozov, M. G. (Scientific-Research Inst. of Mechanics, USSR). Teplofiz. Vysok. Temp., 3: 765-70(Sept.-Oct. 1965). (In Russian).

A plasmatron with continuous current of 300 kvt and air-stabilized arcs is described. The model developed made it possible to produce plasma jets with a diameter of 30 mm, temperatures of 2500 to 4500°K, and velocities of 350 to 750 m/sec. The length of continuous operation was 2 hrs. Investigations of the electrical parameters and of the rotation of the plasma showed the existence of oscillations, categorized according to frequency into three groups: of the order of 1, 10^3, and 10^4 Hz. The influence of various parameters can reduce the amplitude of the low-frequency oscillations. (tr-auth)

17939 PLASMA FLOW BETWEEN ELECTRODES WITH WEAK LONGITUDINAL CONDUCTIVITY. Morozov, A. I.; Shubin, A. P. Teplofiz. Vysok. Temp., 3: 827-37(Nov.-Dec. 1965). (In Russian).

The stationary non-viscous surface flow of highly conducting plasma in narrow channels under the effects of transverse magnetic fields was shown in the presence of the Hall effect. The electrodes were connected in series to the sections. It was shown that in the presence of weak dissipation between sections and strongly impressed Hall effect, thin pre-anode boundary layers were formed. The corrections to the isothermal flow, producing dissipation, were calculated in the linear approximation. (tr-auth)

17940 EFFECTS OF IONIZATION REACTIONS ON PLASMA THERMAL CONDUCTIVITY. Krinberg, I. A. (Inst. of Geochemistry, Academy of Sciences, Siberian SSR). Teplofiz. Vysok. Temp., 3: 838-44(Nov.-Dec. 1965). (In Russian).

The effect of ionization reactions on the thermal conductivity of plasma was investigated. It was shown that in spite of some original equation systems, the expressions for the thermal conductivity, dependent on the transfer of the energy of ionization reactions, have the same form as in the case of dissociation reactions investigated by Butler and Brokaw. The formulas for the calculation of the thermal conductivity were obtained in some individual cases. (tr-auth)

17941 THE FLUCTUATIONS AND SCATTERING OF PARTICLES IN A TURBULENT PLASMA. Akhiezer, I. O. (Physicotechnical Inst., AN Ukrainian SSR). Ukr. Fiz. Zh., 10: 1161-7(1965). (In Russian).

An investigation was made of a stationary distribution of the turbulent fluctuations in a plasma consisting of cold ions and hot electrons moving with respect to the ions at a velocity of sound s. The case of a low supercriticality $1 - s/u \ll 1$ was considered. It was found that at some definite values of the wave vector almost all the turbulent waves propagate inside a narrow cone around the direction u, the angle of aperture of this cone being much smaller than the Cherenkov angle. At some other values almost all turbulent waves propagate along the surface of the Cherenkov cone. From an investigation of the interaction of charged particles with a turbulent plasma it was found that the intensity of interaction is determined by the level of fluctuations in the plasma. The dependence of the change in the energy of the particle per unit time on the magnitude and direction of its velocity is determined by the character of the spectral and angular distribution of fluctuations in the plasma. Thus, the scattering of particles in plasma can be used for experimental checking of the theory of plasma turbulence. (ATD)

17942 MAGNETODYNAMIC INSTABILITY OF PLASMA BEAM. Shih, Chang-ho. Wu Li Hsueh Pao, 21: 1700-4 (Sept. 1965). (In Chinese).

Whenever the velocity of a plasma beam is greater than the Alfven velocity estimated from the fully ionized background, the relative small fluctuations of the flow are unstable. This instability is similar to that involved in the relation of the sun and the earth. Under certain conditions, if sufficient number of neutral particles are present, as it might be the case in the ionosphere, the effect of such instabilities must be taken into account. Examination of the instability resulting in a partially ionized background revealed that the conditions for instability in strong or weak interactions, when $\omega \ll \gamma_i$ differ markedly from those in a fully ionized medium. The presence of neutral particle has a strong effect. However, if disparity in the beam density results in a condition of $F \gg 1$, the weak interaction instability becomes dependent only on the beam density and high-density beams become very unstable. In the case of $F \ll 1$, strong interactions take place, rendering weaker the conditions of instability. This type of instability might be one of the mechanisms responsible for the magnetic pulsations of the earth or for the magnetic fluxes produced by nuclear explosions in space. (TTT)

17943 PLASMAS UNDER THE INFLUENCE OF STATIONARY CROSSED ELECTRIC AND MAGNETIC FIELDS. Joshi, V. (Technische Hochschule, Munich). Z. Angew. Phys., 20: 237-44(1966). (In German).

In a low pressure glow discharge system, a static electric field between two condenser plates used as anodes, and a stationary magnetic field were applied, the latter being generated by means of external electromagnetic coils oriented perpendicularly to the E-field. Both fields, in turn, were oriented perpendicularly to the axis of the electric discharge. Under the simultaneous application of these fields, the ions emitted—mainly in the anode drop range between the condenser plates—were accelerated towards the cathode. The dependence of the directed velocity, and the ion- and electron temperatures on the electric and magnetic fields, respectively, and their proportions in respect of the gas pressure as parameters, were investigated. There were measured directed ion velocities up to 10^7 cm/sec (by H_2 about 200 ev). The values determined by experiment were in good agreement with the theoretically expected ones. (auth)

17944 ELECTROMAGNETIC RADIATION FROM PLASMAS OF HIGH TEMPERATURE AND DENSITY. Eberhagen, A. (Institut fuer Plasmaphysik, Garching, Ger. Univ. of Maryland, College Park). Z. Angew. Phys., 20: 244-57(1966). (In German).

A survey is presented of the electromagnetic radiation emitted from high-temperature and high-density plasmas. Continuum radiation and line emission from these plasmas are treated for wavelengths from the x-ray region of the spectrum up to the region of microwaves. The distribution of the electromagnetic radiation in the different wavelength ranges is described, and the different possibilities to obtain

information on the physical properties of the radiation source are discussed. A short review is given of the energy losses of the plasma by the different types of radiation. (auth)

17945 ON THE DISCHARGE OF THE Θ-PINCH AT HIGH INITIAL DENSITIES. Meiners, Dieter (Technische Hochschule, Hanover). Z. Naturforsch., 20a: 1711-21 (Dec. 1965). (In German).

A linear Θ-pinch discharge without preionization was investigated in helium within that range of density in which the mean free path of electrons between two elastic collisions diminishes to such a low value that the electrons cannot gain the ionization energy in the induced electric field over this distance. Compared to observations at low densities in this high-density range the instant of the first breakdown in the discharge tube was found to be shifted to later half-cycles with increasing initial pressure. In addition, the further development of the discharge at high initial densities showed a very different structure compared to the low-density behavior. Comparison of optical observations with measurements of the current density distribution obtained by means of magnetic probes (using a special difference method because of the very small plasma currents) showed that in the half cycle immediately following the breakdown, a typical shock wave pinch is produced at high densities. The regions near the axis were heated only by an ionizing shock, while the contraction of the current sheath, which initially started the shock, was stopped very early in far outer regions. During the following half-cycle quite a different behavior of the discharge was observed because of the enhanced electrical conductivity: the contraction ran much faster and therefore the separation between the shock front and the driving current sheath decreased. (auth)

17946 RESONANT OHMIC DAMPING OF LINEARIZED MAGNETOACOUSTIC WAVES. Tasso, H. (Institut fuer Plasmaphysik, Garching, Ger.). Z. Naturforsch., 20a: 1722-3(Dec. 1965).

The linearized perturbation equations of the classical magnetohydrodynamic modes can be reduced for a cylindrical symmetry and static equilibrium to one second-order equation. When the resistive plasma in static equilibrium is infinite and homogeneous or when it is incompressible, there is no overstability. The perturbations are damped and in the neighborhood of singularities they are shown to be strongly damped in a resonant way. It appeared that without resistivity there are waves that propagate nearly perpendicular to the longitudinal magnetic field in the neighborhood of the singularities and with a small resistivity resonant damping occurs. Two cases are considered: a homogeneous, infinite, compressible plasma and an inhomogeneous, incompressible plasma with constant longitudinal current density and a vacuum outside. (M.C.G.)

17947 ELECTRON-ION BREMSSTRAHLUNG OF NON-RELATIVISTIC PLASMAS. Schiller, Diethard H. (Univ., Timisoara, Rumania). Z. Phys., 191: 360-6 (1966). (In German).

An investigation was made of the bremsstrahlung from nonrelativistic plasmas, in which the electrons were averaged according to the Fermi-Dirac distribution instead of the usual Maxwell-Boltzmann distribution. This allowed not only the case of a nondegenerate, but also that of a degenerate electron component of the plasma to be treated simultaneously. In the first case, it is possible to estimate correction terms to known results, which were again found as the first approximation of the present results. These correction terms, which are shown for the case in which the energy distribution function is derived from the Maxwell-Boltzmann distribution, are found to be about one order of magnitude smaller than the correction terms usually considered, that originate from a correction of the interaction cross section (in the zero-Born approximation). For the second (degenerate) case the physical conditions are investigated, which correspond e.g., to those in the inside of white dwarfs. (tr-auth)

17948 PLASMA INSTABILITY IN A STRONG HIGH-FREQUENCY FIELD. Gorbunov, L. M.; Silin, V. P. (Lebedev Inst. of Physics, Moscow). Zh. Eksp. Teor. Fiz., 49: 1973-82(Dec. 1965). (In Russian).

It is shown that a collisionless plasma in a strong external high frequency field is unstable with respect to build-up of nonpotential oscillations. Such instability is possible for frequencies of the external field which are lower than the electron Langmuir frequency as well as for those that are higher and this makes it qualitatively different from instability of potential oscillations. The instability considered arises under conditions when the electron oscillation amplitude in an external field exceeds the Debye radius of the plasma particles. (auth)

17949 INVESTIGATION OF DRIFT WAVES OF A NON-POTENTIAL NATURE IN A STATIONARY MAGNETO-ACOUSTIC PLASMA. Vdovin, V. L.; Rusanov, V. D.; Frank-Kamenetskii, D. A. Zh. Eksp. Teor. Fiz., 50: 39-45(Jan. 1966). (In Russian).

Magnetic noise is studied in an arrangement in which the plasma is produced by the magneto-acoustic method in a glass tube located in a stationary magnetic field. The plasma continuously flows along the axis into the measuring volume, in the center of which the magnetic field strength changes from 700 to 2500 Oe. The hydrogen plasma was studied at pressures ranging from 5×10^{-3} to 10^{-3} torr. The active high-frequency power introduced into the discharge is 4 kw. Within the indicated pressure range the electron temperature varied from 4 to 10 ev. The electron concentration in the center of the chamber is 5×10^{11} to 5×10^{12} cm^{-3}. Intense (~0.05 Oe) nonpotential electric noise with first harmonic frequencies of the order of 100 kc/s was detected and investigated in the 50 to 500 kc/s range by means of magnetic probes. The dependence of the noise on the plasma parameters is investigated. The results are discussed from the point of view of excitation of drift inhomogeneous Alfven waves in the plasma. (auth)

17950 QUASILINEAR THEORY OF CURRENT INSTABILITY IN A PLASMA. Rudakov, L. I.; Korablev, L. V. Zh. Eksp. Teor. Fiz., 50: 220-31(Jan. 1966). (In Russian).

The problem of the passage of a current in a two-temperature plasma ($T_e \gg T_i$) is solved. The electric field strength E is assumed to be given and sufficiently large so that Coulomb collisions do not interfere with the free acceleration of most of the electrons. Ion-acoustic oscillations are excited in the plasma as a result of current instability. Interaction between the electrons and ion-acoustic oscillations is considered in the quasilinear approximation. In this approximation electrons are scattered on the oscillations almost elastically with a frequency $\sim \nu^{-3}$. Thus during a period of time $t < t_0 \approx \sqrt{T_e M}/eE$ the current remains stationary and is $j \approx -e\sqrt{T_e/M}$. Subsequently, due to heating of the electrons, runaway electrons appear and the current begins to grow. (auth)

17951 INTERACTION BETWEEN ELECTRON BEAMS AND A NON-ISOTHERMAL PLASMA AND THE NONLINEAR STABILIZATION OF BEAM INSTABILITY. Kovrizhnykh, L. M. (Lebedev Inst. of Physics, Moscow). Zh. Eksp. Teor. Fiz., 50: 251-4(Jan. 1966). (In Russian).

A method for stabilization of beam instability by setting up sufficiently strong ion-acoustical oscillations in the plasma is described. It is indicated that pulsating spectra may exist in the beam-plasma system. (auth)

17952 RECOMBINATION LINE INTENSITIES IN AN ATTENUATED HYDROGEN PLASMA [Thesis]. Clarke, William Henry. Los Angeles, Calif., Univ. of California, 1965. 108p.

The populations of the discrete atomic states of hydrogen, at low densities and high temperatures, were calculated by a statistical equilibrium approach. The earlier work of Menzel and Baker and others was extended to cover the quantum numbers l as well as n. The range of the computation was also greatly extended so that all levels of astrophysical interest could be considered. Because of this con-

siderable extension of the earlier work, completely new techniques had to be derived for the computation of the radiative transition probabilities required. Recursive procedures were found, which are suitable for such calculations. In addition, the effects of collisional redistribution upon the state populations were included, at least to a first approximation. On the basis of the state populations obtained, theoretical line decrements for the Balmer and Paschen series of hydrogen and the Pickering and Pfund series of ionized helium were obtained, which agree more closely with observations than either the Menzel-Baker b(n) decrements or the pure radiative decrements calculated by the b(n,l) method. (Dissertation Abstr.)

17953 TWO-STAGE MAGNETIC MIRROR COMPRESSION EXPERIMENT USING A ROTATING PLASMA SOURCE [Thesis]. Forsen, Harold Kay. Berkeley, Calif., Univ. of California, 1965. 150p.

A two-stage magnetic mirror compression experiment was constructed to investigate a rotating plasma as a clean, high-temperature plasma source. Kilovolt deuterons are created in the crossed electric and magnetic fields of the first stage and are transferred or injected into the second stage. The purity and trapping of the plasma is limited by electrode effects. Ionization takes place in the coaxial system, which has a radial electric field of 7.10^5 v/m and an axial magnetic field of 11 to 20 kG. The 10^{17} particles are injected into the field region by a fast-acting valve in the central anode. Particles ionized in these $\vec{E} \times \vec{B}$ fields have equal energy in gyromotion and in drift motion. If the electric field is turned off, the drift energy is removed but the energy of gyromotion remains. The plasma is in contact with the electrodes, therefore high mass impurities are liberated from the electrodes and contaminate the plasma. Measurements are made on the plasma to determine energy density, ion energy distribution, electron temperature, impurity content, and neutron flux. To transfer the plasma out of the first stage to the second stage, two methods are used: one involves sequentially energizing the first stage magnetic field coils to move the plasma into the second stage mirror field; the other involves ionization in a gradient field, which directly injects the plasma into the second stage. In the process of transfer, the plasma leaks out of the first stage. The escaping deuterons are given additional axial acceleration by the fringing electric field at the tip of the anode, which extends through the first stage and ends between the two stages. This tip acceleration made trapping by the available fields and rise times impractical. (Dissertation Abstr.)

17954 ANOMALOUS DIFFUSION ACROSS A MAGNETIC FIELD IN AN RF DISCHARGE [Thesis]. Powers, Edward Joseph Jr. Stanford, Calif., Stanford Univ., 1965. 125p.

An experimental investigation of plasma diffusion across a static magnetic field in an r-f (29.3 Mc) discharge is reported. It was carried out using helium and argon discharges primarily, with hydrogen and nitrogen discharges used to a lesser extent. The operating pressure range varied from 0.02 to 1.0 mm Hg. A model of a diffusion-dominated r-f discharge in a static magnetic field is developed. The model, which assumes that electrons and ions are lost only by classical collisional diffusion processes, indicates that the amplitude variation of the r-f electric field may be used as a measure of the plasma loss. It predicts that as the magnetic field is increased from zero the r-f electric field required to sustain a constant-density discharge should decrease monotonically. Experimentally it was observed that as the magnetic field is increased from zero the r-f electric field initially decreases, but starts to rise when the magnetic field exceeds a critical value B_c. The discharge voltage and power varied in a similar manner. It is shown that the unexpected rise in the afore-mentioned parameters may be interpreted in terms of a rise in the plasma diffusion rate across the static magnetic field. The transition to this anomalous diffusion is accompanied by the onset of low-frequency fluctuations in the tens of kilocycles range. Increasing the magnetic field beyond the critical field results in a growth in the amplitude of the fluctuations and in the introduction of higher frequency components into the noise spectrum. The critical magnetic field was observed to be insensitive to the type of gas used and to increase with increasing pressure and decreasing tube radius. The r-f discharge critical field data are compared with those obtained by other researchers. (A.G.W.)

17955 THERMAL CESIUM PLASMA [Thesis]. Cutler, William Herbert. Stanford, Calif., Stanford Univ., 1965. 229p.

Thermal cesium plasma is generated by thermal ionization of cesium on a hot tungsten surface, at a temperature sufficient for emission of electrons as well as ions. The devices considered consist of one or two ionizers in the form of flat spiral filaments or disks of tungsten, mounted within a glass envelope that has been evacuated and charged with cesium. The devices are usually operated in an axial magnetic field, which contains the plasma in a column having the same diameter as the ionizer(s). The principal diagnostic tool is the Langmuir probe. Measurements of radial plasma density profiles give information about diffusion of plasma across the magnetic field. These measurements are compared with theories based on ambipolar diffusion on the one hand, and free motion of ions in the magnetic field on the other. The measured diffusion lies between extremes represented by the two theories. Oscillations of the unsymmetric diode were observed and explained rather completely by a computed simulation model. Measurements of plasma resistivity parallel to the magnetic field were obtained, which agree closely with the theoretical resistivity of a fully ionized plasma. Quiescent operation of the two-ionizer device was achieved, and the predicted bistable states of positive and negative space potential were observed during quiescent operation. Ion acoustic waves were observed in the unsymmetric diode under special conditions. The wave velocity is higher than predicted, and the waves are highly damped for diode voltages outside a very small range. This high damping suggests that the diode voltage has a profound effect on the shape of the electron velocity distribution in the diode. (A.G.W.)

17956 PLASMA INTERACTION WITH A CYLINDRICAL MAGNETIC FIELD [Thesis]. Henson, Robert Maurice. College Station, Tex., Texas A and M Univ., 1965. 74p.

A combination of the sonic diffuser and plasma jet theories was formed into a theory that explains the behavior of a plasma injected axially into a cylindrical magnetic field. The theory utilizes the plasma properties—density, temperature, and velocity—to predict streaming or stagnation in critical magnetic fields in accordance with Tuck's criterion. However, the theory embodies the fact that a highly directed plasma velocity is not the only requirement necessary for streaming to occur in a converging magnetic field. (Dissertation Abstr.)

17957 THE QUASI-LINEAR THEORY OF ELECTROSTATIC INSTABILITIES [Thesis]. Bodner, Stephen Elliott. Princeton, N. J., Princeton Univ., 1965. 91p.

In the last decade there has been a great deal of interest in the collision-free plasma. The collective effects are described by the Vlasov equation and Maxwell's equations. Vlasov's equation is nonlinear and so to make analysis tractable one usually linearizes the equation by expanding in some small perturbation. Clearly if the perturbation is unstable the linear approximation will break down. The problem, then, is to determine the time behavior of instabilities using the nonlinear Vlasov equation. In order to determine to what level the unstable perturbations grow and also the new equilibrium state that the plasma will seek, a rigorous asymptotic expansion procedure on the nonlinear Vlasov equation is used, that takes into consideration the different physical time scales of the system. The method is applied to two instabilities: the electron plasma instability and the ion wave instability. The first is simpler mathematically and the second is experimentally important to the Sherwood program. It is shown that for high-temperature ratios of electrons to ions the instability stabilizes quickly

at a very low amplitude that is experimentally negligible. The methods of analysis used will form the basis of solving for the limiting amplitude for other types of instabilities. (Dissertation Abstr.)

17958 TEORIYA TURBULENTNOI PLAZMY. (The Theory of Turbulent Plasma). Vedenov, A. A. Moscow, Akademiya Nauk SSSR Institut Nauchnoi Informatsii Itoginauki, 1965. 115p.

Methods of describing a plasma are surveyed. Discussions are given of high- and low-frequency oscillations in a plasma, plasma stability, beam-plasma interactions, wave-particle interactions in a plasma, anomalous diffusion and electric conductivity, convection and convective instability, helical instability, the excitation of turbulence, plasmon-plasmon and plasmon-particle interactions, transfer coefficients in a turbulent plasma, and the scattering of electromagnetic waves in a turbulent plasma. (M.J.T.)

17959 KINETIKA I TERMODINAMIKA KHIMICHESKIKH REAKTSII V NIZKOTEMPERATURNOII PLAZME. (Kinetics and Thermodynamics of Chemical Reactions in Low-Temperature Plasma). Polak, L. S. (ed.). Moscow, Izdatel'stvo Nauka, 1965. 255p.

Fourteen articles are included on a method of calculating kinetic variations of chemical reactions in plasma jets, calculations of forced quenching of acetylene during its synthesis from methane in plasma jets, control of methane-to-acetylene conversion process by forced change of plasma-jet temperature regime, study of Maxwellization of nonequilibrium Ar-methane mixture by Monte-Carlo method, production of acetylene from methane in plasma jets, production of acetylene and olefin from hydrocarbons by direct run-through in a plasma jet, oxidation of methane in in plasma jets, kinetics and thermodynamics of nitrogen-oxide formation in plasma jets and optimization of this process, mechanisms of quenching chemical-reaction products in plasma jets, optical pyrometer for plasma jets, a h-f electrodeless plasmatron for obtaining pure Si and its oxides, the uhf plasmatron and its chemical applications, and a literature survey of chemical processes in plasma and plasma jets. (M.J.T.)

17960 METHOD AND DEVICE FOR THE ACCELERATION OF ELECTRICALLY CHARGED PARTICLES OF AN IONIZED GAS. Consoli, Terenzio; Hall, Richard B. (to Commissariat a l'Energie Atomique. Boeing Co.). German Patent 1,206,532. Dec. 9, 1965. Priority date Apr. 29, 1963, France.

A device is designed for accelerating a plasma submitted to a static magnetic field created by a coil parallel to the plasma, which consists of a resonant cavity subjected, by means of a loop, to an a-c electromagnetic field, the length of the cavity being equal to half of the wavelength of the electromagnetic field. The mean force acting on an electron entering the cavity through a central opening at one end is made continually accelerative by varying the pitch of turns of the coil and by choosing the frequency of the alternating field and the intensity of the static field in such a manner that, in the transversal symmetry plane of the cavity, the cyclotron frequency of the plasma ions is equal to the frequency of the alternating field and that the mean force acting on the electrons is varying along the axis of the cavity according to a predetermined linear function. (Gmelin Inst.)

Shielding

Refer also to abstract 16300.

17961 (ORNL-TM-1212) OGRE-G—AN OGRE SYSTEM MONTE CARLO CODE FOR THE CALCULATION OF GAMMA-RAY DOSE RATE AT ARBITRARY POINTS IN AN ARBITRARY GEOMETRY. Trubey, D. K.; Emmett, M. B. (Oak Ridge National Lab., Tenn.). Jan. 17, 1966. Contract W-7405-eng-26. 31p. Dep. mn. CFSTI $2.00 cy, $0.50 mn.

An OGRE system gamma-ray Monte Carlo code was written for the calculation of dose rate at arbitrary points by statistical estimation. The 05R general geometry routine GEOM was utilized to provide almost completely arbitrary material and statistical weight geometries. Input source parameters may be read to specify point source configurations or binary tapes may be read to provide the initial particle parameters for arbitrary source configurations. (auth)

17962 (ORNL-TM-1237) GAMMA-RAY ATTENUATION COEFFICIENTS FOR GERMANIUM. Chapman, G. T. (Oak Ridge National Lab., Tenn.). Mar. 2, 1966. Contract W-7405-eng-26. 5p. Dep. mn. CFSTI $1.00 cy, $0.50 mn.

An interpolation method was used to determine the γ-ray attenuation coefficients of germanium. If the region of the atomic numbers, Z, is relatively small and the γ-ray energy is not too close to the k-shell energies for the elements in this range of Z, the attenuation coefficients will vary smoothly and not too drastically as a function of Z. (auth)

17963 (ORNL-tr-1059) COMPUTATION OF THE THICKNESS OF LEAD SHIELDING AGAINST GAMMA RADIATION. Hoenig, Arnost. Translated for Oak Ridge National Lab., Tenn., from Inzenyrske Stavby, 7: 303-9(1965). 18p. Dep. mn. JCL $1.60 fs, $0.80 mf.

Calculated gamma buildup factors for the dose rate are given in detailed tables and diagrams, relative to lead with a density of 1.00 g/cm^3. (M.O.W.)

17964 (ORNL-tr-1061) COMPUTATION OF THE THICKNESS OF WATER SHIELDS AGAINST GAMMA RADIATION. Hoenig, Arnost. Translated for Oak Ridge National Lab., Tenn., from Inzenyrske Stavby, 9: 399-404 (1965). 13p. Dep. mn. JCL $1.60 fs, $0.80 mf.

Calculated gamma buildup factors for the dose rate are given in detailed tables and diagrams, relative to water with a density of 1.00 g/cm^3. (M.O.W.)

17965 SOME TECHNIQUES APPLICABLE TO THE SHIELDING OF NUCLEAR PARTICLES FROM SPACE. Barrett, M. J. (Nuclear Utility Services, Inc., Washington, D. C.). AIAA (Amer. Inst. Aeron. Astronaut.) J., 4: 9-13(Jan. 1966).

A phenomenological model of the effects of charged particles incident on a homogeneous medium yields equations of the dose deposition as a function of depth. In the high-energy interval 50–500 Mev, this dose is dominated, close to the medium surface, by the slowing down of the particles. Away from the surface layer, secondary particles due to nuclear interactions become the dominant dose-depositing mechanism. The simple mathematical formulas presented are in reasonable agreement with Monte Carlo calculations and measurements. (auth)

17966 GRAPHING SELF-ABSORPTION CURVES WITH ORDINARY GAMMA-RAY ABSORPTION DATA. Rabinoff, Carter V.; Boekelheide, Irving (Chico State Coll., Calif.). Amer. J. Phys., 34: 130-2(Feb. 1966).

Ordinary experimental gamma-ray absorption data can be graphed to closely approximate the theoretical self-absorption curves of W. R. Dixon. To do so emphasizes the point of Dixon's work for the student and gives additional insight into the nature of absorption. A method for accomplishing this is described. (auth)

17967 PRACTICAL CALCULATION METHODS OF NEUTRON SHIELDING OF REACTORS. AN HISTORICAL CONSIDERATION. Verschuur, K. A. Atoomenergie Haar Toepass., 7: 251-8(Dec. 1965). (In Dutch).

A bibliographic review is given of the historical development of calculation methods of reactor neutron shielding. The developments made in the period from 1950 to 1957 are briefly indicated. The developments in America, England, and other European countries from 1957 to 1964 are summarized. (J.S.R.)

17968 SHIELDING CALCULATIONS FOR BETA RADIATION SOURCES OF HIGH ACTIVITY. Hennen, N. M. (Boelkow GmbH, Ottobrunn, Ger.). Kerntechnik, 8: 23-6 (Jan. 1966).

Shielding calculations were made for β radiation sources of high activity using a ^{90}Sr and ^{90}Y source. The calculation was carried out in the following manner. The radioactive preparation was considered as a source of photons with 11 energy groups. For each group the flux density after penetration of an absorber shield and a vacuum gap was determined. Calculations were also made of the ion dose output. Numerical calculations were made for specific examples. (J.S.R.)

17969 DEVICE FOR CALCULATION OF GAMMA SHIELDING PROBLEMS. Tschirf, E.; Pfeiffer, K. (Oesterreichische Hochschule, Vienna). Kerntechnik, 8: 115-17(Mar. 1966). (In German).

A device for the calculation of γ shielding and its operation are described. Two examples illustrate the use of the device. (J.S.R.)

17970 ENERGY LOSS OF 53-Mev ELECTRONS IN GRAPHITE. Theissen, H.; Gudden, F. (Technische Hochschule, Darmstadt, Ger.). Z. Phys., 191: 395-7 (1966). (In German).

The energy loss and the half width of the resulting energy distribution were measured for 53 Mev electrons passing through graphite absorbers. The absorbers had thicknesses between 0.3 and 5 g/cm^2. While the measured energy loss agrees with the prediction of theory, the measured half width is larger than the theoretical one for absorber thicknesses exceeding about 1 g/cm^2. (auth)

Solid State Physics

See also CHEMISTRY — Inorganic and Physical Chemistry
METALS, CERAMICS, AND OTHER MATERIALS — Properties and Structure

Refer also to abstracts 17081, 17084, 17588, and 17804.

17971 (AD-299256) ELECTRETS. PART II. A BIBLIOGRAPHY. Johnson, Virginia Ann (Harry Diamond Labs., Washington, D. C.). Sept. 30, 1962. 124p. (TR-1074). CFSTI $2.75 cy, $0.75 mn.

A bibliography containing over 300 abstracted references and an author index is presented. The references cover the technical literature on electrets: thermoelectrets, photoelectrets, and radioelectrets; and are arranged under these categories. (auth)

17972 (IAE-942) TABLITSA ANTIFERROMAGNETIKOV. (Table of Antiferromagnetics). (Institut Atomnoi Energii, Gosudarstvennyi Komitet po Ispol'zovaniyu Atomnoi Energii SSSR, Moscow). 1965. 26p. Dep. mn.

Near the Néel temperature T_n the magnetic susceptibility ordinarily attains a maximum, and the specific heat c has a characteristic λ-shape. Although the results of neutron diffraction measurements can serve as a definite criterion for the existence of antiferromagnetic order, the presence of the above anomalies can indicate the occurrence of antiferromagnetism with a very high degree of probability. The table contains almost all the antiferromagnetics known up to 1965. Only directly measured values are given. The crystal structure or magnetic structure, the Néel temperature T_n (°K), the molar susceptibility, type of transition and other data are presented for about 200 metals and compounds. The rare earth metals and their alloys are not included in the table, but rare earth compounds are included. (143 references.) (TTT)

17973 (IS-1106) COMPUTER PROGRAM FOR FERMI SURFACE STUDIES. Anderson, J. R.; Rhyne, M. K. (Ames Lab., Iowa State Univ. of Science and Tech.). June 1965. Contract W-7405-eng-82. 74p. Dep. mn. CFSTI $3.00 cy, $0.75 mn.

A FORTRAN computer program used to calculate cross-sectional areas of the Fermi surface and cyclotron masses is described. The application of this program to the face-centered-cubic metal lead, based on an orthogonalized-plane-wave interpolation model, is given. (auth)

17974 (IS-T-63) KERR MAGNETO-OPTIC EFFECT AS APPLIED TO RARE-EARTH METALS [Thesis]. Gongwer, Nancy Ruth (Ames Lab., Iowa State Univ. of Science and Tech.). Nov. 1965. Contract W-7405-eng-82. 52p. Dep. mn. CFSTI $3.00 cy, $0.50 mn.

Polarized monochromatic light from a filtered mercury arc source was reflected from the surface of permalloy films. The light was then passed through a Glan Thompson analyzer to a viewing lens which permitted visual or photographic observations of domains. A small electromagnet was used to change the magnetization and the domain walls were observed to move as the domains changed shape and size. Maximum contrast between adjacent domains was obtained at angles of incidence between 25° and 30°. Calculations of the magneto-optic rotation for gadolinium, terbium, and dysprosium showed that the effect should be about 2.5 times as large as for iron. When a polished terbium single crystal was used in place of the permalloy, it was found that the incident light was diffusely scattered because of impurity inclusions in the sample. Domains in terbium were therefore not observable. Higher purity single crystals will be needed for this type of domain observation. (auth)

17975 (NYO-2047-36) INVESTIGATIONS OF RADIATION EFFECTS IN METAL OXIDES AND AZIDES BY ELECTRON SPIN RESONANCE. Progress Report, February 1, 1965–January 31, 1966. Bartram, Ralph H.; Gilliam, Otis R. (Connecticut Univ., Storrs. Dept. of Physics). Jan. 31, 1966. Contract AT(30-1)-2047. 86p. Dep. mn. CFSTI $3.00 cy, $0.75 mn.

Radioinduced defects in single crystals of metal oxides, alkali azides and crystals of related structure are investigated experimentally and theoretically. The crystals are irradiated by use of a Van de Graaff electron accelerator, the Brookhaven Research Reactor, ^{60}Co gamma sources, or ultraviolet light and changes in the defect structure are observed by electron spin resonance (ESR). Investigations were continued on the trapped F_2^- ion in electron-irradiated KHF_2. Several electronic temperature controllers and programmers were constructed which permitted the growth of improved large crystals of KHF_2 for associated optical and ESR measurements. Some ESR measurements on reactor-irradiated Al_2O_3 were made at 35-Gc/sec to enhance the resolution of poorly resolved components. A study of radiation effects in electron-irradiated Al_2O_3 is continuing with different sample specimens and with different irradiation conditions than previously employed. An investigation of defects in $CaMoO_4$ caused by gamma-ray irradiation is in progress. Theoretical investigations of radiation effects in ionic crystals are conducted with the objective of accounting quantitatively for the optical and ESR absorption spectra of radiation-induced defects, and of understanding the radiation-damage mechanism. A calculation of wave functions for F′-centers in alkali halides was completed. A theory was developed to explain the anomalous g shift of F-centers in alkaline-earth oxides, sulfides and selenides, in terms of configuration mixing, and a manuscript is being prepared for publication. A molecular orbital calculation of $(AlO)^{3-}$ in Al_2O_3 verified the triplet ground state and yielded a reasonable optical absorption band. It became apparent that electron correlation plays a dominant role in the zero-field splitting. (M.O.W.)

17976 (NYO-2047-36, App.1) PARAMAGNETIC RESONANCE OF F_2^- IONS TRAPPED IN ELECTRON-IRRADIATED POTASSIUM BIFLUORIDE. Otto, Fred B.; Gilliam, O. R. (Connecticut Univ., Storrs). 20p.

ESR spectra attributed to F_2^- molecular ions located at two inequivalent anion sites were observed after electron bombardment of single crystals of potassium bifluoride (KHF_2) at 77°K. The molecular axis of the F_2^- ion lies along [110] or along [1$\bar{1}$0], and the spectrum for each site consists of four hyperfine resonances. They derive from a hole interacting equally with two nuclei of spin ½ giving an effective nuclear spin of 0 or 1 and a highly anisotropic

A tensor. For z||[110], x||[001] and y||[1$\bar{1}$0], components of the g and A tensors for 77°K are: $g_z = 2.0020 \pm 0.001$, $g_x \cong g_y = 2.0168 \pm 0.001$, $A_z = 955.4 \pm 1$ G and $A_x \cong A_y = 21 \pm 4$ G. At room temperature $g_z = 2.0024 \pm 0.001$, $g_x \cong g_y = 2.0180 \pm 0.0015$, $A_z = 928.8 \pm 1$ G, $A_x = 35.5 \pm 1$ G and $A_y = 25.5 \pm 3$G. The crystal changed from colorless to intense green upon electron irradiation with optical absorption bands at 2.0 and 4.1 ev. As the sample was brought to room temperature, the 2.0-ev band rapidly annealed, whereas the 4.1-ev band showed annealing behavior similar to the spin resonances, remaining about two days. The ESR spectra resulted from electron energies >0.15 Mev but not from 10^6 R ^{60}Co gamma-ray irradiations. All ESR measurements were made at 9.2 Gc/sec. (auth)

17977 (NYO-2047-36, App.2) WAVE FUNCTIONS FOR F' CENTERS IN ALKALI HALIDES. La, S. Y.; Bartram, R. H. (Connecticut Univ., Storrs). 30p.

The point-ion-lattice model of Gourary and Adrian is used to investigate F'-centers in alkali halides. Ground-state energies and wave functions are determined by series solution of the Hartree-Fock equation for two electrons in a square-well potential of depth-$\alpha_M e^2/b$ and range b, where α_M is the Madelung constant and b the interionic distance. The difference between the point-ion and square-well potentials is subsequently treated as a perturbation, and an additional correction for polarization is derived from the semi-continuum model. An analogous calculation of ground state energies for F-centers is performed in order to determine F'-band energies. The theoretical F'-band energies which can be compared with experiment are: NaCl, 2.40 ev; KCl, 2.42 ev; KBr, 1.91 ev. These are in fair agreement with Pick's experimental values: NaCl, 2.43 ev; KCl, 1.65 ev; KBr, 1.38 ev. The wave functions are more diffuse than Pekar's but are still concentrated primarily in the vacancy. In order to verify the method, F-band energies were also calculated, in good agreement with experiment. (auth)

17978 (NYO-3402-2) MAGNETO-THERMODYNAMICS OF PARA- AND ANTIFERROMAGNETS. Annual Report, March 1, 1965-March 1, 1966. Butera, R. A. (Pittsburgh Univ., Pa. Dept. of Chemistry). Contract AT(30-1)-3402. 26p. Dep. mn. CFSTI $2.00 cy, $0.50 mn.

Construction and performance testing of the magneto-thermodynamic apparatus are described in detail. Brief discussions on the preparation of single crystals of $MnBr_2 \cdot 4H_2O$ and $MnBr_2$, and a spherical polycrystalline praseodymium sample are presented. (M.O.W.)

17979 (UCRL-12386) COMPRESSION OF LITHIUM HYDRIDE. Stephens, D. R. (Lawrence Radiation Lab., Univ. of California, Livermore). Feb. 4, 1965. Contract W-7405-eng-48. 13p. Dep. mn. CFSTI $1.00 cy, $0.50 mn.

The compressions of ^{7}LiH, ^{7}LiD, ^{6}LiH, and ^{6}LiD were measured to 40 kb at 25°C. The compressibilities at P = 0 were in good agreement with reported best values. However, simple ionic models did not predict the observed variations in compressibility. This was interpreted as due to the partially covalent nature of LiH. (auth)

17980 (ANL-Trans-274) THERMALLY ACTIVATED PROCESSES IN THE DEFORMATION OF NEUTRON-IRRADIATED COPPER SINGLE CRYSTALS. II. DISLOCATION MOTION IN THE PRESENCE OF AN OBSTACLE SPECTRUM AND EVALUATION OF MEASUREMENTS. Diehl, J.; Seidel, G. P.; Niemann, L. Translated by Elmar K. Wilip (Argonne National Lab., Ill.), from Phys. Status Solidi, 12: 405-19(1965). 21p. Dep. mn. JCL $2.60 fs, $0.83 mf.

A theoretical treatment of the thermally activated motion of dislocations in the presence of obstacles of different size leads to an Arrhenius equation. In this equation the activation energy at different stresses (or temperatures) is determined by different parts of the size spectrum, and the pre-exponential factor depends explicitly on stress and temperature. This result was applied to experimental data. Information was obtained regarding the number, size, and size distribution of the dislocation obstacles. The obstacles most likely consist of stacking fault discs containing an average of 20 to 30 vacancies. (auth)

17981 ELECTRON SPIN RESONANCE STUDIES OF IRRADIATED SILVER HALIDES. Greenslade, D. J. (The Univ., Nottingham, Eng.). Brit. J. Appl. Phys., 16: 1921-2(Dec. 1965).

No electron spin resonance signals were observed in pure silver halides previously irradiated with gamma rays, ultraviolet or visible light. Impure samples showed a resonance similar to that reported by Smith and Ingram, but further experiments indicate that their interpretation requires modification. (auth)

17982 THERMOLUMINESCENCE OF CALCIUM OXIDE ACTIVATED BY THE ELEMENTS OF THE IVa GROUP OF THE PERIODIC TABLE. Schwartz, Laurent-Marcel; Janin, Joseph (Univ., Lyon). Compt. Rend., 261: 3782-5(Nov. 1, 1965). (In French).

The thermoluminescence of calcium oxide activated by one of the four elements Ti, Zr, Hf, and Th after excitation by ultraviolet or γ rays at a dose of approximately 2 Mrad was studied. The results showed that the γ irradiation of the calcium oxide activated by Zr, Hf, or Th causes a very intense thermoluminescence whereas the fluorescence of the products is very low. With Ti the thermoluminescence is much less developed and no long-duration phosphorescence was observed at −190°C. A progressive modification of the thermoluminescence curves was established from Ti to Th. The maximum at high temperature, which is practically alone with Ti does not exist with Th, on the contrary the maxima which appear around 0°C have a considerable importance with Zr, Hf, and Th. The temperatures of the maxima of thermoluminescence differ little for γ or ultraviolet excitations, but the emission becomes less intense if before irradiation with the ultraviolet the sample is exposed to a γ irradiation and heating to 350°C. (tr-auth)

17983 POSITRON ANNIHILATION IN CADMIUM SULFIDE MONOCRYSTALS. Borisov, M.; Ivanchev, N.; Marinov, M.; Bonchev, L. (Inst. of Physics, Bulgarian Academy of Sciences). Compt. Rend. Acad. Bulg. Sci., 18: 801-4(1965). (In Russian).

The electron structure of a material may be clarified on the basis of γ-spectrum measurements of the annihilating radiation, from the correlation between the 2γ quanta involved in the two-photon annihilation process, and the lifetime of the positrons. The angular correlation was chosen as being the most convenient from the experimental point of view. After being slowed down to thermal velocities within about 10^{-12} sec, the probability that the positrons will be annihilated by the internal shell electrons is very small; valence electrons with energies from 1 to 10 ev participate in this process. Deviation of the energy from the annihilating γ quanta from $h\gamma_0 = m_0c^2$ (whereby m_0 is the mass of the electron or positron at rest) and deviation of the direction of the emitted quanta from 180° depend on the energy. Such experiments were carried out on CdS single crystals, attempting to determine angular distribution changes attributable to the specific resistivity of the crystals which ranged from 10^{10} ohm/cm (in the dark) to a few ohm/cm in the case of crystals doped with Cd. The results revealed a definite difference in the angular distribution of the two materials, although the curves were quite similar in shape. They indicate that in the high-resistivity crystals, positron annihilation events by high-pulse electrons predominate. When valence electrons were involved, the angular distribution of the quanta depended on the electron-filled valence zone. In the low-resistivity crystals, donor-level electrons from the stoichiometrically excessive amount of Cd participate in the positron annihilation process. (TTT)

17984 ON THE SENSITIVITY OF PHOTOCATHODES TO X-RAYS. Jedlicka, M. (Vacuum Electronic Research Inst., Prague). Czech. J. Phys., 16: 132-7(1966). (In German).

The electron emission from photocathodes exposed to X-rays was investigated. Measurements were performed on emitters made of platinum, Ag-Mg alloy, known photoelectric layers of Sb-Cs, Sb-Na-K-Cs and Te-Cs-Sb-Na-K and of a KCl layer. The greatest sensitivity—par-

ticularly in the region of soft radiation—was found in substances with small electrical conductivity. Finally some results of measurements are discussed. (auth)

17985 MAGNETIZATION OF IRON–BERYLLIUM ALLOYS. Aldred, A. T. (Argonne National Lab., Ill.). J. Appl. Phys., 37: 671-4(Feb. 1966).

Saturation magnetizations of bcc iron–beryllium alloys were measured, and the results were used to calculate mean atomic magnetic moments. The linear rate of change of moment with solute concentration was found to be -2.262 ± 0.108 Bohr magnetons per atom. This was considered to be consistent with a model where beryllium, a nontransition metal solute, dilutes a constant iron moment. (auth)

17986 CRITICAL SCATTERING OF POLARIZED NEUTRONS IN NICKEL. Drabkin, G. M.; Zabidarov, E. L.; Kasman, Ya. A.; Okorokov, A. I. (Ioffe Physico-Technical Inst., Leningrad). JETP Lett. (USSR) (Engl. Transl.), 2: 336-8(Dec. 15, 1965).

Translated from Zh. Eksp. Teor. Fiz., Pis'ma Redakt., 2: 541-4(Dec. 15, 1965).

A study was made of critical small-angle neutron scattering for the purpose of investigating phase transitions. Polarization measurements were made on a single-crystal nickel sample placed in a 10 Oe magnetic field. Detailed results are presented for the polarization of neutrons scattered through 10.2 minutes of angle. (M.O.W.)

17987 SCATTERING OF POLARIZED NEUTRONS IN MAGNETS NEAR THE PHASE-TRANSITION POINT. Maleev, S. V. (Ioffe Physico-Technical Inst., Leningrad). JETP Lett. (USSR) (Engl. Transl.), 2: 338-40(Dec. 15, 1965).

Translated from Zh. Eksp. Teor. Fiz., Pis'ma Redakt., 2: 545-8(Dec. 15, 1965).

Drabkin et al. investigated the scattering of polarized neutrons in nickel at temperatures close to the Curie temperature. The usefulness of the data obtained from experiments of this type was investigated. The results are presented. (M.O.W.)

17988 THE MOESSBAUER EFFECT ON ^{161}Dy IMPURITY NUCLEI IN METALLIC GADOLINIUM. Lukashevich, I. I.; Sklyarevskii, V. V.; Aleshin, K. P.; Samoilov, B. N.; Stepanov, E. P.; Filippov, N. I. JETP Lett. (USSR) (Engl. Transl.), 3: 50-2(Jan. 15, 1966).

Translated from Zh. Eksp. Teor. Fiz., Pis'ma Redakt., 3: 81-5(Jan. 15, 1966).

The magnetic properties of Gd were investigated by studying the hyperfine splitting of the gamma rays from ^{161}Dy nuclei in a Gd lattice. Two systems of hyperfine splittings were observed and were attributed to two different states of the electron shell of the Dy ions. (D.C.W.)

17989 APPLICATIONS OF THE MOESSBAUER EFFECT. Wegener, H. (Univ., Erlangen, Ger.). Mitteilungsbl. Strahlungsmessgeraete, 6: No. 14, 3-8(Oct. 1965). (In German).

The physical basis of the Mössbauer effect is briefly indicated and the effects that can modify the frequency of the Mössbauer quanta are described. On the basis of some examples it is shown how information on the physical and chemical properties can be obtained from the Mössbauer spectra. (J.S.R.)

17990 INFLUENCE OF SELF-ABSORPTION ON ABSOLUTE MEASUREMENT OF THE MOESSBAUER FRACTION. Lejeune, S. (Univ. Libre, Brussels). Nucl. Instrum. Methods, 40: 141-5(Feb. 1966). (In French).

The influence of self-absorption for Mössbauer f measurements is considered theoretically and experimentally. Neglecting the ordinary mass attenuation is shown to lead to errors which can be very important for small fractions. Measurements with a stainless steel source are in good agreement with theoretical expressions which take account of ordinary mass attenuation. (auth)

17991 THE SCINTILLATION EXCITATION MECHANISM IN THALLIUM-ACTIVATED SODIUM IODIDE. Zakharko, Ya. M.; Chepelev, V. V. Opt. Spectros. (USSR) (Engl. Transl.), 19: 462-3(Nov. 1965).

Translated from Opt. Spektros., 19: 831-3(Nov. 1965).

The temperature dependence of the x-ray luminescence yield of NaI(Tl) crystals was studied to determine the roles of exciton and recombination mechanisms of excitation. The possibility of an electron-hole interaction in the final excitation of the activation luminescence centers was investigated. (L.B.S.)

17992 HYPERFINE MAGNETIC FIELDS AT NUCLEI OF INDIUM IN IRON AND NICKEL. Holliday, R. J.; Shirley, D. A.; Stone, N. J. (Univ. of California, Berkeley). Phys. Rev., 143: 130-2(Mar. 4, 1966). (UCRL-16437).

Hyperfine magnetic fields for In in Fe and Ni were determined by nuclear orientation of ^{114m}In in Fe and Ni alloys. A ^{57}Co thermometer was used in each case. The results are: H_{hf} (In in Fe) $= -295 \pm 10$ kG; H_{hf} (In in Ni) $= -42 \pm 5$ kG. (auth)

17993 NORMAL-FERMI-LIQUID THEORY FOR ELECTRONS IN SOLIDS. Jones, B. L.; McClure, J. W. (Univ. of Oregon, Eugene). Phys. Rev., 143: 133-47(Mar. 4, 1966).

A Landau-type Fermi-liquid theory for interacting electrons moving in a fixed periodic potential is derived. Two methods are used: the Green's-function method, which gives a more physical description of the system but does not give all the desired results, and the many-body perturbation-theory approach, which is complete but is more complicated. The Green's-function formalism of Kadanoff and Baym is adapted to inhomogeneous systems by rewriting it in operator form. A kinetic equation for an energy-dependent, single-particle density matrix is then derived. The quasiparticle concept is introduced and a formal solution of the kinetic equation is given and discussed. These developments are specialized to the periodic potential and a transport equation of the Landau-Boltzmann type is derived for quasiparticles moving within a single energy band. Expressions for the density and current density are then identified from a continuity equation. Although this work does not treat real transitions between energy bands, the Green's-function method suggests a plausible form for a Landau-like theory which includes such transitions. The perturbation-theory treatment follows the work of Luttinger and Nozières, who derived Landau's theory for systems without a lattice potential. When the perturbation theory is expressed in terms of Bloch functions, the quantities involved become matrices between different energy bands. However, it is shown that many of the key results of Luttinger and Nozières can be suitably generalized. The perturbation-theory calculation shows that when the periodic potential is present the change in quasiparticle energy can still be expressed in terms of the variation of the quasiparticle distribution function, and that the results obtained from the Green's-function approach are exact in the case of slowly varying external fields. (auth)

17994 GAMMA-GAMMA ANGULAR-CORRELATION STUDY OF ^{169}Tm IN LUTETIUM IRON GARNET. Koicki, S.; Koicki, A.; Wood, G. T.; Caspari, M. E. (Univ. of Pennsylvania, Philadelphia). Phys. Rev., 143: 148-56 (Mar. 4, 1966).

The attenuation and rotation of the integral angular correlation of the $\frac{7}{2}$(177-kev)$\frac{7}{2}$(131-kev)$\frac{3}{2}$ γ-γ cascade in ^{169}Tm following electron capture of ^{169}Yb was measured in dilute solutions of ^{169}Yb in polycrystalline samples of lutetium iron garnet at room temperature and at liquid-nitrogen temperature with and without applied magnetic field. The same measurements were also performed on the $\frac{7}{2}$(198-kev)$\frac{5}{2}$(110-kev)$\frac{3}{2}$ γ-γ cascade at liquid-nitrogen temperature. From these experiments the magnetic hyperfine field acting at the nuclei of the Tm^{3+} ions, the electronic relaxation time at the Tm^{3+} ions, and the ratio of the g factors of the $\frac{7}{2}$+ and $\frac{5}{2}$+ spin states in ^{169}Tm could be deduced. At room temperature the time-averaged magnetic hyperfine field in the direction of the magnetizing field $\langle H_{int}^{z} \rangle$ was 206 kOe and agreed within 10% with that cal-

culated from molecular-field theory using the free-ion model with an exchange field of 196 kOe and neglecting inner-core exchange-polarization effects. The value of $\langle H_{int}^2 \rangle$ at liquid-nitrogen temperature averaged over all sites was 523 kOe. Neglecting quadrupole effects, the electronic relaxation time of the Tm^{3+} electrons was estimated to be 3.8×10^{-13} sec at room temperature and 1.8×10^{-12} sec at liquid-nitrogen temperature, consistent with an inverse dependence of the relaxation time on the absolute temperature. The ratio of the g factors was determined to be $g_{\frac{1}{2}}/g_{\frac{3}{2}} = 1.28 \pm 0.12$. (auth)

17995 NUCLEAR SPIN RELAXATION IN GALLIUM METAL. Hammond, R. H.; Wikner, E. G.; Kelly, G. M. (General Atomic Div., General Dynamics Corp., San Diego, Calif.). Phys. Rev., 143: 275-8(Mar. 4, 1966).

The nuclear spin-lattice relaxation time T_1 was measured in a fine powder of gallium metal from near the superconductivity transition temperature 1.1°K to near the melting point 307°K. The experiments were performed with pure nuclear quadrupole resonance using pulsed-nuclear-resonance techniques. Between approximately 4.2 and 300°K the product of T_1 and the absolute temperature is found to be temperature-dependent, varying from 1.01 sec°K between 1.1 and 4.2°K to 0.73 sec°K at 300°K. The relaxation mechanism is magnetic in origin, as determined from the ratio of the relaxation times for the ^{69}Ga and ^{71}Ga nuclei. Various explanations for the temperature dependence of T_1T are discussed. (auth)

17996 SYSTEMATIC VARIATION OF QUADRUPOLE CRYSTAL-FIELD SHIELDING IN RARE-EARTH ETHYL SULFATES. Blok, Johan; Shirley, D. A. (Univ. of California, Berkeley). Phys. Rev., 143: 278-83(Mar. 4, 1966). (UCRL-16318).

Quadrupole-coupling constants were obtained from measurements on ^{140}La, ^{154}Eu, ^{159}Gd, and ^{177}Lu nuclei oriented in neodymium ethyl sulfate at temperatures down to 0.01°K. These results are combined with the other available quadrupole-coupling data on La, Dy, Tm, and Lu in ethyl sulfate lattices to determine the quadrupole-antishielded term transforming as Y_2^0 in the crystal-field potential, i.e., $(1 - \gamma_\infty)\, A_2^0$. This term increases fairly slowly throughout the rare earths, with an average value of approximately $(3 \times 10^4\ cm^{-1})a_0^{-2}$. These values were compared with theoretical estimates of -80 for γ_∞ to yield the quantities A_2^0. Comparison of the A_2^0's with the corresponding V_2^0's taken from optical spectroscopy, using Hartree-Fock radial moments $\langle r^2 \rangle$ for the $4f$ electrons, together with some extrapolation, gives a complete set of shielding factors $(1 - \sigma_2)$ for the crystal-field component V_2^0. These factors vary from 0.6 in Lu^{3+} to 0.4 in Eu^{3+} and drop to -0.2 in La^{3+}. Thus not only is there substantial shielding of V_2^0, but this shielding seems to vary considerably in the $4f$ series. The σ_2's are typically larger by about 50% than theoretical estimates. (auth)

17997 ELECTRON-PARAMAGNETIC-RESONANCE ABSORPTION BY TRIVALENT NEODYMIUM IONS IN SINGLE CRYSTALS OF LANTHANUM TRICHLORIDE AND LANTHANUM ETHYL SULPHATE IN ZERO MAGNETIC FIELD. Erickson, Lynden E. (Univ. of Chicago). Phys. Rev., 143: 295-303(Mar. 4, 1966).

Measurements of magnetic-dipole transition frequencies of $^{143}Nd^{3+}$ and $^{145}Nd^{3+}$ occurring substitutionally for La^{3+} in $LaCl_3$ were made for the first time in the absence of an external magnetic field. The sensitive [10^{13} spins/(Mc linewidth)], versatile, cavity-type, variable-frequency (1000–4600 Mc) spectrometer developed for these experiments is described. Measurements of magnetic-dipole transition frequencies of $^{143}Nd^{3+}$ and $^{145}Nd^{3+}$ in $La(C_2H_5SO_4)_3 \cdot 9H_2O$ made at low field by Bleaney were repeated at zero magnetic field. The results are summarized in terms of a least-squares best fit of the spin hamiltonian $H = AS_zI_z + B(S_xI_x + S_yI_y) + P[I_z^2 - \frac{1}{3}I(I+1)]$ to the data. The spin-hamiltonian parameters are independent of temperature between 4 and 15°K. Theoretical interpretation of the spin-hamiltonian parameters yielded $^{143}\mu_N/^{145}\mu_N = 1.60892 \pm 0.00010$, $^{143}g_n\langle r^{-3} \rangle = (11.59 \pm 0.10) \times 10^{24}\ cm^{-3}$, and $^{143}\mu_N = (1.10 \pm 0.10)$ nm for the $LaCl_3$ crystal; and $^{143}\mu_N/^{145}\mu_N = 1.60886 \pm 0.00029$, $^{143}g_n\langle r^{-3} \rangle = (11.56 \pm 0.10) \times 10^{24}\ cm^{-3}$ and $^{143}\mu_N = (1.10 \pm 0.10)$ nm for the $La(C_2H_5SO_4)_3 \cdot 9H_2O$ crystal assuming $\langle r^{-3} \rangle = (36.9 \pm 4.5) \times 10^{24}\ cm^{-3}$. The close agreement of $g_n\langle r^{-3} \rangle$ for the two crystals implies that $\langle r^{-3} \rangle$ is independent of the host for these two crystals. (auth)

17998 NUCLEAR SPIN RELAXATION IN MOLYBDENUM METAL. Narath, Albert; Alderman, Donald W. (Sandia Lab., Albuquerque, N. Mex.). Phys. Rev., 143: 328-34 (Mar. 4, 1966).

The ^{95}Mo and ^{97}Mo nuclear spin-spin and spin-lattice relaxation rates in molybdenum metal were studied in the temperature range $1 \leq T \leq 4$°K. The transverse relaxation process is found to have an exponential time dependence (corresponding to a Lorentzian line shape) with characteristic times $T_2(^{95}Mo) = 10 \pm 1$ msec and $T_2(^{97}Mo) = 14 \pm 1$ msec which are independent of temperature. At 4.0°K the longitudinal relaxation times are $T_1(^{95}Mo) = 8.9 \pm 0.2$ sec and $T_1(^{97}Mo) = 7.6 \pm 0.2$ sec. The ratio $T_1(^{95}Mo)/T_1(^{97}Mo) = 1.17 \pm 0.03$ is larger than the square of the nuclear moment ratio, $(\mu^{97}/\mu^{95})^2 = 1.0424$. This anomaly is attributed to an electric quadrupole process due to d-band conduction electrons. This process contributes significantly to the relaxation rate of ^{97}Mo but not to that of ^{95}Mo because of the large difference in nuclear quadrupole moments ($Q^{97}/Q^{95} = 9.2$). The known moment ratios are used to partition the observed rates into nuclear magnetic dipole (R_μ) and nuclear electric quadrupole (R_Q) contributions. The resulting values of R_Q yield quadrupole moment estimates $Q^{95} = (0.12 \pm 0.03) \times 10^{-24}\ cm^2$ and $Q^{97} = (1.1 \pm 0.2) \times 10^{-24}\ cm^2$. An approximate separation of R_μ into contact, core-polarization, and orbital rates has been achieved. The principal contribution to the Knight shift and to the conduction-electron susceptibility is shown to arise from the orbital magnetization of the d band. The results of this study provide an upper-limit estimate of about 3 for the electron-phonon enhancement of the s-electron specific heat. (auth)

17999 MAGNETIC AND STRUCTURAL PROPERTIES OF EUROPIUM METAL AND EUROPIUM MONOXIDE AT HIGH PRESSURE. McWhan, D. B. (Bell Telephone Labs., Murray Hill, N. J.); Souers, P. C.; Jura, G. Phys. Rev., 143: 385-9(Mar. 11, 1966).

The change of the Néel temperature of europium metal and of the Curie temperature of EuO with pressure was measured up to 90 kbar by resistivity and initial-permeability methods, respectively. The compressibility of Eu and EuO was determined relative to NaCl in the same range of pressure by powder x-ray diffraction methods. The compressibility is represented by the Birch equation; for Eu, $B_0 = 124$ kbar and $\xi = 0.9 (dB/dp = 2.8)$ and the standard deviation is 1.8; for EuO, $B_0 = 1070$ kbar and ξ was assumed to be zero and the standard deviation is 2.8. For Eu, $d \ln T_N / d \ln V \approx 0$ down to $V/V_0 = 0.8$. The initial slope for EuO is $d \ln T_c / d \ln V = -6 \pm 2$. The results are discussed in terms of the theories of exchange interaction in the heavy rare-earth metals and the europium chalcogenides. (auth)

18000 ELECTRON-NUCLEAR INTERACTION IN ANTIMONY METAL. Hygh, E. H.; Das, T. P. (Univ. of California, Riverside). Phys. Rev., 143: 452-69(Mar. 11, 1966).

The field gradient at the nuclei due to the conduction electrons in antimony metal is calculated using an approximation for their wave functions in keeping with available information concerning the Fermi surface of antimony metal. It is shown that the Wannier functions for antimony can be closely approximated by a set of orthogonalized atomic orbitals (OAO) which are mixed by the noncentral terms in the one-electron hamiltonian. The mixing of the s-like and p-like OAO is seen to be analogous to the concept of s-p hybridization in the simple chemical picture of the solid. Combined with earlier calculations of the field gradient due to the ion cores, the total field gradient comes out as eq = 1998×10^{12} esu/cm^3 as compared to 1889×10^{12}

esu/cm^3, the experimental value of the gradient based on Hewitt and William's quadrupole-resonance data and Murakawa's values of the quadrupole moments of the ^{121}Sb and ^{123}Sb nuclei. In addition, the direct contributions to the isotropic and anisotropic Knight shifts were calculated from the spins of the conduction electrons near the Fermi surface. These are found to be $\delta_{iso} = +0.07\%$ and $\delta_{ax} = -0.05\%$. It is hoped that when experimental values of these quantities become available in the future a comparison with the theoretical values of the direct contributions will permit an assessment of the importance of other contributors to the Knight shift such as core polarization and orbital effects. (auth)

18001 NORMAL VIBRATIONS IN ALUMINUM AND DERIVED THERMODYNAMIC PROPERTIES. Gilat, G.; Nicklow, R. M. (Oak Ridge National Lab., Tenn.). Phys. Rev., 143: 487-94(Mar. 11, 1966). (ORNL-P-1638).

The experimental phonon-dispersion curves of aluminum at 80 and at 300°K were analyzed in terms of axially symmetric Born–von Kármán force-constant models, including 8 nearest neighbors. The resulting models were used to compute a frequency distribution function $g(\omega)$ at each temperature from which various thermodynamic properties were derived. The specific-heat curve predicted by the $g(\omega)$ appropriate to 80°K fits excellently the experimental results in the temperature range 20 to 80°K. At higher temperatures the experimental results deviate from this calculated curve and approach the curve appropriate to $g(\omega)$ at 300°K. Similar behavior is found for the experimental Debye-Waller coefficient in the range above 100°K. It is concluded that inelastic-neutron-scattering data and thermodynamic data are compatible in the range of sufficiently low temperatures where deviations from the quasiharmonic approximation are small, provided a good force-constant model as well as a statistically adequate $g(\omega)$ are available. There is evidence that the quasiharmonic approximation in aluminum is invalid at room temperature at least for the extreme low-frequency part of $g(\omega)$. (auth)

18002 RELATIVISTIC ELECTRONIC STRUCTURE IN CRYSTALS. II. FERMI SURFACE OF TUNGSTEN. Loucks, T. L. (Ames Lab., Ames, Iowa). Phys. Rev., 143: 506-12(Mar. 11, 1966). (IS-1232).

The relativistic augmented-plane-wave method developed previously is applied to tungsten. Relativistic effects on the energy bands and the Fermi surface are presented. The angular dependence of de Haas–van Alphen frequencies, as well as other experimental results, is determined from the theoretical Fermi surface. A comparison with experimental results supports the general conclusion that relativistic effects reduce the size of the Fermi surface of tungsten. (auth)

18003 ORDERING OF INTERSTITIAL IMPURITIES IN NIOBIUM. Van Landuyt, J.; Gevers, R.; Amelinckx, S. (SCK-CEN, Mol, Belg.). Phys. Status Solidi, 13: 467-86 (1966).

An ordering phenomenon in niobium was studied by electron microscopy and by electron diffraction. The phenomenon is found in parts of niobium foils subjected to an annealing treatment in vacuum. Domains are formed which, on the basis of the present model, are due to the ordering of interstitial oxygen atoms. The insertion of the interstitials on a superlattice in the niobium matrix causes a deformation of the latter in a ⟨110⟩ direction. The domain structure results from the fact that several orientations are possible for the superlattice. Further evidence for this ordering is deduced from the presence of superlattice dislocations and of supplementary spots in the diffraction patterns. The superlattice is deduced from the diffraction data and a composition Nb_2O is attributed to this metallic oxide phase. The domains are revealed by fringe contrast at the boundaries and by the change in background intensity. Both contrast effects are associated with the slight deformation due to the ordering. A discussion is included of a second type of fringe pattern which is often observed in annealing niobium. Patterns of this type have previously been attributed to the presence of stacking faults; it is shown here that they are due to plate-shaped precipitates of some oxide phase in the niobium matrix. (auth)

18004 ISOMERIC SHIFT OF THE 23.8-kev γ LINE OF ^{119}Sn IN VARIOUS ALLOY PHASES. Pobell, F. (Nebenstelle Reaktorstation, Garching, Ger.). Phys. Status Solidi, 13: 509-17(1966). (In German).

Measurements are made of the isomeric shift of the 23.8-kev γ line of ^{119}Sn in alloys of tin with six of its neighbors in the periodic system. The measurements are made over the complete range of concentration of the alloys. The isomeric shift is constant within a single phase. The transition to a new phase results in a strong change in the s-electron density within the ^{119}Sn nucleus. The results are discussed and compared with knight-shift measurements. (auth)

18005 ELECTRON SPIN RESONANCE OF SULFUR AND SELENIUM RADICALS IN ALKALI HALIDES. Schneider, J. (Univ., Freiburg i. B.); Dischler, B.; Raeuber, A. Phys. Status Solidi, 13: 141-57(Jan. 1, 1966).

Three classes of paramagnetic radical molecules were detected in alkali halides by electron spin resonance: S_3^- and Se_3^-, SO_2^-, and SeO_2^-, and radicals formed by four equivalent sulfur or selenium atoms. The S_3^- and Se_3^- radicals occupy a trivacancy site formed by one metal and two halide vacancies. The C_2-axis of the radical is orientated along a face diagonal axis of the crystal. A hyperfine interaction of the unpaired electron with three ^{33}S or ^{77}Se nuclei is observed. The unpaired electron is localized in a Π-type molecular orbital formed by atomic p-orbitals normal to the plane of the molecule. The S_3^- and Se_3^- centers are stable at room temperature. The electronic structure of the SO_2^- and SeO_2^- radicals is found to be analogous to that of S_3^- and Se_3^-. However, these radicals probably occupy only one halide vacancy site. Internal rotation is observed for SO_2^- and SeO_2^-, resulting in isotropic ESR-spectra at elevated temperatures. Radicals formed by four equivalent sulfur or selenium atoms are detected in x-irradiated chalcogen-doped alkali halide crystals. (auth)

18006 EFFECT OF EXCITONS ON THE SCATTERING OF NEUTRONS BY CRYSTALS. Glauberman, A. E.; Ruvinskii, M. A. (Lvov State Univ.). Phys. Status Solidi, 13: 233-8(Jan. 1, 1966).

An investigation was made of the magnetic scattering of slow neutrons by non-localized Mott excitons, and nuclear scattering by polarizing excitons of the Dykman-Pekar type. It is shown that the effective cross sections for magnetic scattering by one exciton are equal, to within at least an order of magnitude, to the corresponding quantities for magnetic scattering by free electrons. The cross sections are also comparable with the cross sections for scattering by the electrons of impurity centers. The cross section for nuclear scattering by a polarizing exciton is of the same order as in the case of a polaron. (auth)

18007 OBSERVATIONS OF PRIMARY DEFECTS IN CRYSTALS OF LITHIUM FLUORIDE IRRADIATED WITH THERMAL NEUTRONS AT 77 DEG K. Comes, R.; Lambert, M.; Perret, R.; Guinier, A. (Univ. Paris, Orsay, France). Phys. Status Solidi, 13: 265-8(Jan. 1, 1966). (In French).

It is shown that lithium fluoride crystals, irradiated with thermal neutrons, contain primary-defect zones rich in point defects. For a dose of 1.7×10^{18} thermal neutrons/cm^2, half the crystal volume is occupied by these zones. The zones disappear for temperatures above 110°K. (auth)

18008 ZEEMAN-FIELD-DEPENDENT QUADRUPOLAR INTERACTION IN RARE-EARTH TRICHLORIDES. Ghatikar, M. N. (Saha Inst. of Nuclear Physics, Calcutta). Proc. Phys. Soc. (London), 87: 727-9(Mar. 1966).

The contribution to the nuclear quadrupolar interaction from Zeeman-field-dependent terms of the form S_iH_j $(I_z^2 - \frac{1}{3} I(I+1))$ was estimated for a number of rare-earth trichlorides and compared with other contributions. Dy^{3+} is the interesting case where this contribution is of comparable magnitude with the contributions from other terms. The expected change in the Mössbauer pattern for Dy^{3+} at different Zeeman fields has been discussed. (auth)

18009 MOESSBAUER ABSORPTION IN THE PRESENCE OF ELECTRON SPIN RELAXATION. Bradford, E.; Marshall, W. (Atomic Energy Research Establishment, Harwell, Eng.). Proc. Phys. Soc. (London), 87: 731-47 (Mar. 1966).

The theory necessary to discuss Mössbauer absorption in the presence of electron spin relaxation effects is formulated and formulas given for both polarized and unpolarized gamma rays incident on single crystals or polycrystals. A perturbation theory is used to calculate spectra in the range where the electron spin relaxation is fast but nevertheless produces observable effects. Some typical cases are discussed and compared with other theoretical results. The absorption spectra for ^{57}Fe in a cubic metal is calculated assuming the electron spin relaxes by the Korringa mechanism. Special attention is given to the spectra of hemoglobin cyanide where the relaxation of electron spin is by processes typical of insulators and good agreement is found with experiment. (auth)

18010 EXCITATION TRANSFER FROM THE CRYSTAL LATTICE TO RARE EARTH IONS. Zhabotinskii, M. E.; Rudnitskii, Yu. P.; Tsapkin, V. V.; Ellert, G. V. (Inst. of Radio Engineering and Electronics, Academy of Sciences, USSR). Zh. Eksp. Teor. Fiz., 49: 1689-94(Dec. 1965). (In Russian).

The possibility of effective excitation energy transfer from the crystal lattice to activator ions is confirmed experimentally. Results of investigation of energy transfer from the cesium tetrachloride uranyl lattice to the rare earth ions are presented. It is shown that an essential role in this transfer is played by migration of uranyl ion excitation along the crystal lattice. (auth)

18011 LANDAU DAMPING AND RESONANCE DAMPING OF MAGNETOPLASMA WAVES IN BISMUTH. Khaikin, M. S.; Edelman, V. S. (Inst. of Problems in Physics, Academy of Sciences, USSR). Zh. Eksp. Teor. Fiz., 49: 1695-1705(Dec. 1965). (In Russian).

The magnetic field strengths restricting the strong damping region of magnetoplasma waves are measured, the damping being due to cyclotron resonance of the current carriers which is shifted by the Doppler effect. Landau damping of magnetoplasma waves is detected; the magnetic field strengths and wave velocities at which it arises are measured. The experiments are carried out with a plane bismuth single crystal in which the binary axis is parallel to the normal to the surface and at a frequency of 9.5 Bc and temperature of 1.5°K. The following quantities were determined. The Fermi velocity of holes in the basis plane, $v_{\Phi_2} = (2.35 \pm 0.1) \cdot 10^7$ cm/sec; Fermi velocity of electrons in the basis plane, the value of which along the binary axis is $v_{\Phi_3} = (11.3 \pm 0.5) \cdot 10^7$ cm/sec; the effective hole mass at the Fermi surface limiting point in the basis plane $m_x^* = (0.220 \pm 0.002)\, m_0$. The results are compared with some parameters of the Fermi surface. (auth)

18012 MAGNETOSTRICTION OF RARE EARTH METALS IN THE PARAMAGNETIC, ANTIFERROMAGNETIC AND FERROMAGNETIC REGIONS. Belov, K. P.; Levitin, R. Z.; Ponomarev, B. K. (Moscow State Univ.). Zh. Eksp. Teor. Fiz., 49: 1733-40(Dec. 1965). (In Russian).

The magnetostriction of the rare earth metals Tb, Dy, Ho and Er (polycrystalline samples) is measured in pulsed magnetic fields up to 150 kOe at temperatures between 90 and 300°K. The magnitude of the magnetostriction is found to be large (of the order of 100×10^{-6}) in all metals in the paramagnetic region. Magnetostriction due to transition from the antiferromagnetic to ferromagnetic state is observed in Ho, In, Tb, and Dy. In the ferromagnetic state the magnetostriction is respectively 3300×10^{-6} and 2200×10^{-6}. (auth)

18013 LOW-FREQUENCY PROPERTIES OF A SEMICONDUCTOR PLASMA IN A STATIONARY ELECTRIC FIELD. Bass, F. G.; Khankina, S. I.; Yakovenko, V. M. (Inst. of Radiophysics and Electronics, Academy of Sciences, Ukrainian SSR). Zh. Eksp. Teor. Fiz., 50: 102-11 (Jan. 1966). (In Russian).

Some features of the propagation of electromagnetic waves connected with the appearance of a negative differential conductivity are discussed. Dispersion relations are obtained for the transverse and longitudinal electromagnetic and electroacoustic waves in a semiconductor located in a stationary electric or magnetic field. It is shown that in a certain frequency range amplification or generation of waves should arise as a result of change of the sign of the conductivity. The amplification increments of the wave amplitudes are found. (auth)

18014 POSSIBILITY OF SUPER-THERMAL CONDUCTIVITY IN SEMICONDUCTORS. Kozlov, A. N.; Maksimov, L. A. Zh. Eksp. Teor. Fiz., 50: 131-4(Jan. 1966). (In Russian).

The possible existence of an undamped energy flow in a two-band system with pairing is demonstrated. The Landau criterion for superfluidity is proven for the case of crystal periodicity. The superfluid motion is stable with respect to umklapp-processes and scattering on impurities. (auth)

18015 CHANGE OF RESONANCE NUCLEAR PARAMETERS DURING SCATTERING ON REGULAR SYSTEMS. Kagan, Yu.; Afanas'ev, A. M. Zh. Eksp. Teor. Fiz., 50: 271-80(Jan. 1966). (In Russian).

Scattering on nuclear systems with a low-lying resonance level is considered. It is found that if the nuclei form a regular one-dimensional chain or a two-dimensional lattice, the elastic width Γ_1' and position of the resonance level significantly change. It is demonstrated that the change in the width is related to the lifetime of the collective excited state of the nuclear system. The lifetime of such a state and the width may respectively be larger or smaller than the lifetime (width) of an isolated excited nucleus. It is shown that in the case of a three-dimensional crystal the elastic width vanishes in general and the energy dependence of the resonance interaction is defined exclusively by the inelastic width Γ_2. (auth)

18016 I. THE EMISSION AND ABSORPTION SPECTRA OF SOME SIMPLE MOLECULES TRAPPED IN SOLID RARE GASES. II. THEORY OF ELECTRONIC RELAXATION IN THE SOLID PHASE [Thesis]. Frosch, Robert Peter. Pasadena, Calif., California Inst. of Tech., 1965. 228p.

In Part I a study of the spectral properties of simple molecules trapped in liquid helium-cooled rare gas matrices and the equipment used are described. Measurements were made of the phosphorescence lifetimes of C_6H_6, C_6D_6, $C_{10}H_8$, and $C_{10}D_8$ in at least one of the following solids: Ar, Kr, and Xe. The $a^4\Pi \rightarrow X^2\Pi$ and the $B^2\Pi \rightarrow X^2\Pi$ transitions of NO were excited in Ar and Kr using x rays, and the resulting spectra were measured and interpreted. The radiative lifetime of the NO quartet state was measured in Ne, Ar, and Kr and found to be 156, 93, and 35 msec, respectively, in these solvents. C_2H_2 and C_2D_2 were deposited in Ar, Kr, and Xe and submitted to x-ray damage. The well-known Swan bands of C_2 were observed in both emission and absorption. Both the upper and lower states of the Swan system have ΔG values in the solid more than 10% greater than the gas phase values. In addition two new C_2 band systems with 0-0 bands in Ar at 22,973 and 19,619 cm^{-1}, respectively, and with a common lower state were tentatively identified. These systems apparently have not been reported in the gas phase. A transient system was seen in the emission of a deposit of C_2H_2 in Kr that may be due to HC_2. Another series observed when C_2H_2 is deposited in either Kr or Xe is apparently diacetylene phosphorescence. Part II presents a theory of electronic relaxation in solid media. The theory indicates that rates of electronic relaxation in solids depend in an important way on the electronic coupling between initial and final states and on the vibrational overlap between initial and final states. The theory has been successful in explaining the effect of deuterium substitution and the heavy atom effect on relaxation rates. Only a small temperature effect is predicted. (Dissertation Abstr.)

18017 PROCEEDINGS OF THE SYMPOSIUM ON ACCURACY IN X-RAY INTENSITY MEASUREMENT, SUFFERN, NEW YORK, FEBRUARY 24, 1965. Abrahams, S. C. (ed.). Transactions of the American Crystallographic Association, Volume 1, 1965. Pittsburgh, Polycrystal Book Service, 1965. 122p. $3.50. (CONF-650202(Vol.1)).

Papers (6) are presented dealing with the sources and treatment of errors in intensity measurements and with measurement techniques. (D.C.W.)

REACTOR TECHNOLOGY

General

Refer also to abstracts 16757 and 18070.

18018 (CONF-651101–73) A NON-DESTRUCTIVE ELECTRICAL METHOD OF STUDYING THE DENSITY DISTRIBUTION OF A RANDOMLY PACKED BED. Zablocki, H. S.; Rudo, F. S.; Cutler, J. A.; Coler, M. A. (Markite Co., New York). 1965. Contract AT(11-1)-Gen-14. 20p. Dep. mn. CFSTI $1.00 cy, $0.50 mn.

From 13th Conference on Remote Systems Technology, Washington, D. C.

A nondestructive electrical probing technique, which revolves around the judicious use of electrodes without invading a bed of any desired geometry is described. The technique was used to survey the density distribution within a packed bed. The results showed that this method shows promise for making detailed studies of the interior of packed beds and since they are based on electric signals might well be adapted even for dynamic systems for analysis and feedback instrumentation. (P.C.H.)

18019 (IDO–17146) SPERT PROJECT. Quarterly Technical Report, July–September 1965. Crocker, J. G. (ed.) (Phillips Petroleum Co., Idaho Falls, Idaho. Atomic Energy Div.). Feb. 1966. Contract AT(10-1)-205. 39p. Dep. mn. CFSTI $2.00 cy, $0.50 mn.

Operation of the Capsule Driver Core (CDC) was begun in the Spert IV facility; measurements were made of control and transient rod worths, fuel rod worths, and neutron flux distributions. Explosive tests were performed to determine the relative performances of 304 and 304L stainless steels under dynamic loads. As part of the explosive testing program, a water velocity transducer was developed. Specifications were prepared for UO_2 fuel rods to be used in the CDC fuel testing program. A two-dimensional diffusion technique was developed for use in the calculation of Doppler reactivity feedback in low-enrichment cores similar to the PBF core. The technique was applied to the Spert I oxide core. A method was also developed for calculating the energy density in the fuel at the end of a power excursion. (D.C.W.)

18020 (ORNL–3900, pp 2–81) REACTOR DEVELOPMENT. (Oak Ridge National Lab., Tenn.).

Summaries of progress are presented on EGCR development, fuel shipment studies, applied and basic reactor physics, development of reactor fuels and materials, reactor controls development, heat transfer and fluid mechanics research, reactor fuel processing, Th microsphere preparation, MSRE development, evaluation of reactors, space reactor studies, nuclear desalting studies, HFIR development, nuclear safety studies, and studies on radioactive waste disposal. (J.R.D.)

18021 PROCEDURE FOR RAPID START-UP; ANALYSIS ON AN ANALOGUE COMPUTER AND COMPARISON WITH RESULTS OF REACTOR TRIALS. Caillet, C.; Deat, M.; Furet, J.; Weill, J. (CEN, Saclay, France). Vienna, International Atomic Energy Agency, 1965, Preprint No. CN-22/21, 22p. (In French). (CONF-651105–10). ORAU.

From Conference on Nuclear Electronics, Bombay.

An automatic starting procedure is described by which a reactor can pass from any unknown subcritical state to a subcritical state very close to criticality with satisfactory speed and safety. The results of an analog study of the procedure are compared with experimental observations on a reactor. (D.C.W.)

Auxiliaries and Components

Refer also to abstracts 16896, 16899, and 16903.

18022 MEASUREMENT DEVICES FOR NUCLEAR REACTORS. Leiter, Edgar. A E G Mitt., 55: 582–9 (1965). (In German).

Measurement devices for nuclear reactors developed by the AEG are described. The devices are assembled by the unit system from smaller units. The basic units are plug elements on which the units are mounted by printed circuit techniques. Transistors and semiconductor diodes were used. The operation, measurement properties, technical data, and the construction of the following groups of instruments were described: logarithmic pulse channel, linear and logarithmic direct current channel, difference amplifier for the measurement of reactor periods, mean value and comparison unit for the safety system, testing instrument, and net instrument. (tr-auth)

18023 DETECTORS FOR REACTOR INSTRUMENTATION. Beck, Juergen. A E G Mitt., 55: 590-3(1965). (In German).

The neutron flux for a reactor is monitored with three measurement channels, the start-up, power, and safety channels. Each of these channels requires a special detector. After a brief indication of the physical bases of neutron detection, the construction of neutron detectors was explained. Descriptions are given of individual detector types of the reactor instrumentation of the AEG with a summary table of the technical data. (tr-auth)

18024 EXPERIENCES WITH THE EXPERIMENTAL MEASURING SYSTEMS OZH-1 AND OZH-2. Bollok, L.; Mathe, I. G.; Selley, G. Energia Atomtech., 18: 570-7 (Dec. 1965). (In Hungarian).

The measuring devices OZH-1 and OZH-2 were used in loop experiments, carried out in the Hungarian VVRS experimental reactor during 1963 and 1964, respectively. Both series of experiments were aimed at the determination of radiation polymerization of organic compounds under the operational parameters of pressure, temperature, and flow rate of atomic power plants. Specially designed pumps were incorporated into the systems which differed only in details of the flow diagram. In OZH-1, the liquid was outgassed in the secondary circuit, within the biological shield, determining the amount of gas formed by level measurements in the pump vessel outside of the shield; samples were taken under atmospheric pressure. In OZH-2, the external circuit was eliminated, sending the gases through a condenser into the gasometer. In both cases, the temperature was controlled by electric heaters and nitrogen gas was used to pressurize the system. OZH-1 was operated under a pressure of 1 atmosphere at a maximum temperature of 250°C at a reactor power of 2 Mw for 1011 hours while OZH-2 was kept under 7 atmospheres at 350°C at 2.5 Mw for 550 hours. The results served to determine radiation-induced decomposition under dynamic conditions under a pressure required to avoid boiling; data were also collected on the corrosion resistance of structural materials and on heat transfer characteristics of organic agents. No accidents were experienced with either system; work stoppage was caused only by the breakage of a gasket and power failure. (TTT)

18025 FUEL ROD SCANNER FOR REACTOR POWER DENSITY DISTRIBUTION MEASUREMENT. Kobayashi, Setsuo; Matsuoka, Kenichi (Hitachi Ltd., Japan). J. Nucl. Sci. Technol. (Tokyo), 2: 485-7(Dec. 1965).

A fuel rod scanner with an automatic decay correction system was manufactured to measure the reactor power density distribution by the γ-activity from an irradiated fuel rod. The detection head is a scintillation counter surrounded with Pb shield. A fuel rod travels on this head by the feed mechanism operated by compressed air force. Main advantages are that this mechanism does not give any oscillation to the fuel rod in moving and settles the measuring point accurately within ±0.01 mm. It is hardly possible to calculate the correction for decay of the fission product because it includes many kinds of decays and it has decay constant varying with time. Therefore, an automatic correction for decay time is highly desirable.

A system of automatic decay correction, combining an automatic fuel rod scanner and electronic circuits, is used which effects the remote and automatic counting with minimal personnel. The effect of background counts in measuring and monitor channels and the pulse pile-up at high counting rate in electronic circuits are discussed in detail. In case of predominant background counts it is preferable to make a measurement so as to satisfy the following equation, $B_M/B = P/N_i^{Pri}$, where B_M, B are background counts in monitor and measuring channels respectively and P, N_i^{Pri} a preset count in monitor channel and an observed count in measuring channel. (auth)

18026 EVOLUTION OF SAFETY SYSTEMS FOR THE CONTROL OF C.E.A. REACTORS. Furet, J. (CEN, Saclay, France). Vienna, International Atomic Energy Agency, 1965, Preprint No. CN-22/17, 24p. (In French). (CONF-651105-16). ORAU.

From Conference on Nuclear Electronics, Bombay.

Safety criteria in the control of reactors are outlined, and the requirements on the control systems of reactors are discussed. Safety in the control of reactors at shutdown is briefly considered, together with the measurement of reactivity. (D.C.W.)

18027 TRANSISTORIZED INSTRUMENTS FOR REACTOR CONTROL AND FLUX MEASUREMENT. Venkateswarlu, U.; Chakravarti, S. N.; Majumdar, B. (Atomic Energy Establishment, Trombay, India). Vienna, International Atomic Energy Agency, 1965, Preprint No. CN-22/38, 14p. (CONF-651105-31). ORAU.

From Conference on Nuclear Electronics, Bombay.

A log amplifier, a period amplifier, and a linear amplifier are discussed in which a current-sensitive operational d-c amplifier with 100% negative feedback is used. The d-c amplifier is described in detail. (D.C.W.)

18028 THE USE OF MODULATED GAIN DETECTORS AND A DIGITAL DATA STORAGE UNIT TO RECORD PULSED REACTOR EXCURSIONS. Launois, M. (CEA, Paris). Vienna, International Atomic Energy Agency, 1965, Preprint No. CN-22/14, 21p. (In French). (CONF-651105-24). ORAU.

From Conference on Nuclear Electronics, Bombay.

A system for recording pulsed reactor excursions is described, in which a current detector, a sampling circuit, a coder, and a digital storage unit are used. (D.C.W.)

18029 FAST PERIOD METER WITH INTEGRATED CIRCUITS. Lacour, J. (CEN, Grenoble, France); Delcroix, V.; Pinon, Y.; Tattegrain, A. Vienna, International Atomic Energy Agency, 1965, Preprint No. CN-22/24, 25p. (In French). (CONF-651105-23). ORAU.

From Conference on Nuclear Electronics, Bombay.

A system that was designed for the measurement of the power doubling time of the CABRI reactor at Cadarache during the exponential phase of the transient state produced by a step change in reactivity is described. (D.C.W.)

18030 REDUCING THE EFFECTS OF ELECTRICAL INTERFERENCE ON NUCLEONIC INSTRUMENTS. Cox, R. J.; Harrison, D. (Atomic Energy Establishment, Dorchester, Eng.). Vienna, International Atomic Energy Agency, 1965, Preprint No. CN-22/27, 19p. (CONF-651105-4). ORAU.

From Conference on Nuclear Electronics, Bombay.

The causes of interference between electric systems are outlined, and some methods of measuring the sensitivity of instruments to interference are described. The results of some measurements on actual systems are presented. (D.C.W.)

18031 A LOGICAL-ELEMENT SYSTEM FOR REACTOR CONTROL. Emelyanov, I. Ya.; Filippov, A. G.; Umanskaya, S. L.; Rabichev, V. A.; Shevchenko, V. V. (Inst. of Atomic Energy, Moscow). Vienna, International Atomic Energy Agency, 1965, Preprint No. CN-22/57, 22p. (In Russian). (CONF-651105-9). ORAU.

From Conference on Nuclear Electronics, Bombay.

The structure of systems for the control and protection of reactors is described. Systems which use summation of the power variation signals coming from individual channels are shown to have advantages over systems which sum the currents from several ionization chambers. The structure of control systems is discussed for cases in which asynchronous and step-type motors are used to drive the reactivity control units and in which the rods are moved simultaneously with electric synchronization or are moved in turn (in a spiral). The problems of the logical processing of emergency variation signals for the power and the rate of change in power of the reactor are discussed. The possibility is shown of obtaining on computers, both continuously and as the operator requires, information on the equipment parameters to be monitored and on the state of the measuring and auxiliary channels. (auth)

18032 REACTIMETERS. Chauvet, G.; Gariod, R.; Tournier, E. (CEN, Grenoble, France). Vienna, International Atomic Energy Agency, 1965, Preprint No. CN-22/22, 23p. (In French). (CONF-651105-12). ORAU.

From Conference on Nuclear Electronics, Bombay.

A system is described with which the reactivity of a reactor can be measured directly and instantaneously, particularly during reactivity transients. (D.C.W.)

18033 POWER MEASUREMENTS AND AUTOMATIC REACTOR CONTROL BY CHERENKOV OR GAMMA RADIATION. Weiss, H. (Oesterreichische Hochschule, Vienna). Vienna, International Atomic Energy Agency, 1965, Preprint No. CN-22/2, 21p. (CONF-651105-33). ORAU.

From Conference on Nuclear Electronics, Bombay.

A system that was developed for the measurement of reactor power on the basis of the Cherenkov and gamma radiation from the reactor core is described. (D.C.W.)

18034 SOLID-STATE NEUTRON FLUX MONITORING INSTRUMENTS FOR THE NUCLEAR REACTOR. Furukawa, T.; Wakayama, N. (Japan Atomic Energy Research Inst., Tokyo). Vienna, International Atomic Energy Agency, 1965, Preprint No. CN-22/48, 15p. (CONF-651105-18). ORAU.

From Conference on Nuclear Electronics, Bombay.

A transistorized picoammeter, a log-N amplifier, and a period meter that were developed for the neutron flux monitoring system of the materials testing reactor (JMTR) are described and discussed. (D.C.W.)

18035 PRESENT STATE OF DEVELOPMENT IN REACTOR CONTROL INSTRUMENTATION DESIGN IN FRANCE. Furet, J.; Weill, J. (CEN, Saclay, France). Vienna, International Atomic Energy Agency, 1965, Preprint No. CN-22/16, 24p. (In French). (CONF-651105-17). ORAU.

From Conference on Nuclear Electronics, Bombay.

The status of neutron-flux monitoring instrumentation in France is summarized. (D.C.W.)

18036 DEVELOPMENT OF FISSION PRODUCT DETECTORS FOR THE DETECTION OF BURST FUEL ELEMENT CANS. Graftieaux, J.; Roguin, A. (CEN, Saclay, France). Vienna, International Atomic Energy Agency, 1965, Preprint No. CN-22/13, 18p. (In French). (CONF-651105-19). ORAU.

From Conference on Nuclear Electronics, Bombay.

Three types of detection systems that have been developed for use in gas-cooled reactors are discussed. Some methods for the detection of failures in water-cooled reactors are also briefly considered. (D.C.W.)

18037 DESCRIPTION OF TWO REACTIVITY MEASURING APPARATUSES. Deiss, M.; Furet, J. (CEN, Saclay, France). Vienna, International Atomic Energy Agency, 1965, Preprint No. CN-22/11, 18p. (In French). (CONF-651105-6). ORAU.

From Conference on Nuclear Electronics, Bombay.

Two systems that were developed for the measurement of the reactivity of reactors are described. The theoretical bases of the systems are outlined. (D.C.W.)

18038 DESIGN FOR EXPERIMENTAL REACTOR SAFETY CIRCUITS INVOLVING NUMERICAL DATA PROCESSING. Di Giacomo, C. (Groupement Atomique Alsacienne Atlantique, Le Plessis-Robinson, France). Vienna, International Atomic Energy Agency, 1965, Preprint No. CN-22/10, 15p. (In French). (CONF-651105-7). ORAU.

From Conference on Nuclear Electronics, Bombay.

The principles underlying the design of the safety circuits for a heavy-water-cooled and heavy-water-moderated reactor are outlined. The problems of redundancy of measurements and of inter-signal coincidences are stressed. The safety circuits are then described, and some tests are summarized by which the operation of the circuits is checked. (D.C.W.)

18039 GUIDE TUBES FOR NUCLEAR REACTORS. Alfille, Lucien; Gewiss, Claude; Ropers, Jean (to Commissariat a l'Energie Atomique). Canadian Patent 724,288. Dec. 21, 1965.

To avoid heating the liquid moderator the fuel elements are contained in thermally insulated guide tubes. The insulation consists of three layers of roughened metal strips helically wound onto the guide tubes and secured with collars at the ends. The helical strips are wound in different directions so as to enclose poorly conducting gas between the roughened spots or ridges. Materials are chosen with respect to minimum neutron absorption and suitable mechanical properties. (AECL)

18040 SUPPORTING-POST FOR THE SOLID MODERATOR PILE OF A NUCLEAR REACTOR. Rouge, Pierre; Manee, Roger (to Commissariat a l'Energie Atomique). Canadian Patent 724,289. Dec. 21, 1965.

The supporting posts for a vertical reactor, which uses a solid moderator, consists of a rigid central steel part and a hexagonal annular portion also of steel. The annular elements do not rest on each other but on rings projecting from the central core which bears all the weight. A ball and socket joint at the bottom, and interlocking keys allow small movement caused by changing temperature but stability of the assembly is maintained against the risk of earthquakes. Coolant flows in space between the central and annular parts. Disposition of the fuel is not stated. (AECL)

18041 ELECTROMAGNETIC JACK FOR CONTROL RODS IN MARINE NUCLEAR REACTORS WITH A CENTER LATCH SYSTEM. Schreiber, Franz (to Siemens-Schuckertwerke Aktiengesellschaft). German Patent 1,206,102. Dec. 2, 1965. Filed Apr. 28, 1964.

A magnetic jack with a lift coil, a grip coil, and a hold coil surrounding internal magnetizable elements to which the control rod is attached is equipped with a latch system for fixing the control rod in the shutdown position even in case of capsizing. This capsizing latch system is actuated magnetically by the lift coil. (Gmelin Inst.)

18042 DEVICE FOR THE MOVEMENT OF A CONTROL ROD IN A NUCLEAR REACTOR. Filloleau, Etienne; Haffemayer, Marcel; Maulard, Jean (to Commissariat a l'Energie Atomique). German Patent 1,206,534. Dec. 9, 1965. Priority date June 27, 1961, France.

A device is described that comprises a control differential gear having an output element that produces the displacement of the control rod, a first input element adapted to be rotated in both directions by a power unit, and a second input element adapted to be rotated in the direction that moves the control rod toward its safety position by an actuating device. The first input element can be rotated at substantially different speeds in each direction and the actuating device comprises at least one spring to rotate the second input element. The output element is a ring gear which meshes with a rack carried by an operating bar supporting the control rod. (Gmelin Inst.)

18043 METHOD AND APPARATUS FOR THE MEASUREMENT OF THE PERIODIC VARIATION OF THE NEUTRON FLUX DENSITY IN A NUCLEAR REACTOR. Passe, Jean (to Commissariat a l'Energie Atomique). German Patent 1,206,535. Dec. 9, 1965. Priority date May 17, 1963, France.

The current supplied by an ionization chamber located in the reactor core is amplified and transmitted under control of a timing circuit for a duration equal to Δt to a first integrator, and for a second duration equal to Δt to a second integrator. A voltmeter allows reading the two integrated potentials, and the variation of the neutron flux density in time is determined from the ratio of these potentials, by which the measure does not depend on the small variations of the current of the ionization chamber. (Gmelin Inst.)

18044 DEVICE FOR SHUTDOWN OF NUCLEAR REACTORS WITH AN ELECTROMAGNETIC COLLISION MOMENTUM GENERATOR. Eiweck, Ladislaus (to Gesellschaft fuer Kernforschung mbH). German Patent 1,206,536. Dec. 9, 1965. Filed Oct. 21, 1964.

An electromagnetic collision momentum generating device which comprises a coil, a ferromagnetic yoke, and a magnetizable element adjacent to the yoke to which the control rod is attached is improved in that the magnetizable element is a permanent magnet. (Gmelin Inst.)

Criticality Studies

Refer also to abstract 17656.

18045 (AI-66-16) TUNGSTEN RESONANCE INTEGRALS AND DOPPLER COEFFICIENTS. Second Quarterly Report, October–December 1965. Carpenter, S. G.; Otter, J. M.; Paschall, R. K.; Royden, H. N. (Atomics International, Canoga Park, Calif.). Feb. 11, 1966. Contract NAS3-7982. 29p. (NASA-CR-54888).

The spectra of real and adjoint fluxes at the sample position at the center of the Sodium Graphite Reactor Critical Assembly (SGR-CA) were calculated with a one-dimensional diffusion code using 15 energy groups. Fifteen-group sample cross sections were calculated for a number of sample materials and sizes. These cross sections, together with the calculated spectra, were used in a perturbation theory calculation of sample reactivities and Doppler coefficients. Some sample cross sections were recalculated by using the cross section definition appropriate to unperturbed fluxes. Perturbation theory calculations made by using these cross sections were in good agreement with most experimental results. Work on Monte Carlo calculation of resonance integrals and Doppler coefficients has started. Self-shielding of the 1/v contribution to the resonance integral and reactivity effects due to sample thermal expansion were estimated with the aid of Wigner's rational approximation to the escape probability for a lump. The indicated thermal expansion effect is quite large for samples not under cadmium. The first set of radial flux maps using tungsten and gold foils was completed. The reactivity of a natural-tungsten slug was measured as a function of temperature up to 1250°K, both bare and under cadmium. The measured points lie on a smooth curve with little scatter. Each reactivity is determined with a precision of about 0.002 to 0.004 cents; the maximum reactivity change from room temperature is about 0.12 cents. Auxiliary measurements were carried out that demonstrate the insignificance of the effects of scattering by heavy elements in the sample. Preliminary calibration of the epithermal sensitivity of the oscillator was carried out with gold and uranium samples. (auth)

18046 (BNL-9644) MONTE CARLO METHODS IN RESONANCE ABSORPTION. Levine, Melvin M. (Brookhaven National Lab., Upton, N. Y.). Oct. 1965. Contract AT(30-2)-Gen-16. 30p. (CONF-660203-1). Dep. mn. CFSTI $2.00 cy, $0.50 mn.

From National Topical Meeting on Reactor Physics in the Resonance and Thermal Regions, San Diego, Calif.

A review of the use of the Monte Carlo methods in the calculation of neutron resonance absorption is presented. The principles of the method are outlined, and the results of some Monte Carlo calculations are presented. A number of Monte Carlo codes are briefly discussed. (D.C.W.)

18047 (KR-78) DATAPREP-II—A REACTOR LATTICE HOMOGENIZATION AND BIGG-II DATA PREPARATION COMPUTER CODE. Stamm'ler, R. J. J.; Tverbakk, O. P.; Weiss, Z.; Doederlein, J. M. (Institutt for Atomenergi, Kjeller (Norway)). Dec. 1964. 66p. Dep. mn.

The physics of the DATAPREP-II computer code is de-

scribed. This code provides a reactor lattice homogenization in the fast, resonance, and thermal energy ranges, allowing heterogeneous thermal reactors to be treated by standard homogeneous multigroup codes. A User's Manual is also provided, including a test case. The code is written in FORTRAN-63 for the CDC-3600 computer at the Kjeller Computer Installation. (auth)

18048 (ORNL-P-1967) NEUTRON FLUCTUATION MEASUREMENTS AT OAK RIDGE NATIONAL LABORATORY. Fry, D. N.; Roux, D. P.; Ricker, C. W.; Stephenson, S. E.; Hanauer, S. H.; Trinko, J. R. (Oak Ridge National Lab., Tenn.). [nd]. Contract W-7405-eng-26. 18p. (CONF-660206-2). Dep. mn. CFSTI $1.00 cy, $0.50 mn.

From Symposium on Neutron Noise, Waves, and Pulse Propagation, Gainesville, Fla.

The difference in the effective delayed-neutron fraction in a circulating-fuel reactor with and without circulation of the fuel in the primary loop was studied by neutron power-spectral-density (NPSD) measurements with the MSRE at zero power. Subcritical reactivity measurements were made on the first HFIR core at the ORNL Critical Facility using the NPSD technique. The possibility that the onset of nucleate boiling in the ORR could be detected by NPSD measurements was also investigated, as well as the use of pulse-type neutron detectors in NPSD measurements. (D.C.W.)

18049 (RT/FI(65)42) ESAME COMPARATIVO DEI METODI DI CALCOLO DEI FATTORI DI SVANTAGGIO. (Comparative Examination of Methods for Disadvantage Factor Calculations). Tondinelli, L. (Comitato Nazionale per l'Energia Nucleare, Rome (Italy)). Nov. 1965. 39p. Dep. mn.

The theoretical principles are examined on which the disadvantage factor calculations in the monoenergetic approximation are based, namely diffusion theory, transport theory, collision probabilities method, and Monte Carlo method. The comparison of the results obtained when these methods are applied to hydrogenous moderated lattices emphasizes the convenience of the Amouyal-Benoist method. (auth)

18050 (STL-372-22) KINETIC STUDIES OF HETEROGENEOUS WATER REACTORS. Quarterly Progress Report for Period Ending June 30, 1965. Neal, L. G.; Wentz, L. B.; Wright, R. W. (TRW Systems, Redondo Beach, Calif. Applied Thermodynamics Dept.). July 30, 1965. Contract AT(04-3)-372. 47p. Dep. mn. CFSTI $2.00 cy, $0.50 mn.

Studies are carried out of pressure-wave generation by impacts of water on molten Al in vacuum; on pressure generation by temperature transients in metal surfaces in closed water systems; and on the performance of hydrodynamic-instability models in reproducing measured data. (T.F.H.)

18051 (TRG-Report-1014) REACTOR PHYSICS CALCULATIONS WITH THE ARGOSY CODE. Tyror, J. G. (Reactor Group, United Kingdom Atomic Energy Authority, Sellafield (England)). June 30, 1965. 31p. Dep. BIS $0.90. HMSO 4s. 6d.

Recommendations are presented for using the ARGOSY code, processing output from ARGOSY and applying the processed output to reactor problems. (D.C.W.)

18052 (WAPD-T-1836) FEW, LONG TIME INCREMENT DEPLETION CALCULATIONS FOR APPROXIMATING BY SYNTHESIS A MANY, SHORT-TIME INCREMENT DEPLETION CALCULATION. Flanagan, Charles A. (Bettis Atomic Power Lab., West Mifflin, Pa.). Nov. 1965 Contract AT-11-1-GEN-14. 14p. (CONF-651101-68). Dep. mn. CFSTI $1.00 cy, $0.50 mn.

From 13th Conference on Remote Systems Technology, Washington, D. C.

Calculational studies are performed to evaluate the capability of flux synthesis methods to give the desired results when the trial function flux distributions are obtained from a few-time-step depletion calculation. Furthermore, region (or block) depletion is used in the synthesis calculations and the resultant flux distributions are compared to "truth" values. (auth)

18053 ON THE COMPARISON OF THE THEORETICAL AND EXPERIMENTAL PARAMETERS FOR HOMOGENEOUS URANIUM-WATER CRITICAL ASSEMBLY. Kochenov, A. S.; Lyashchenko, N. Ya. At. Energ. (USSR), 19: 463-4(Nov. 1965). (In Russian).

The P_1 approximation of the neutron transport equation and the single-velocity thermal-neutron diffusion equation were used for the calculations; the energy range was divided into 12 groups, including the thermal range for the slowing-down equation. The critical assembly used for the experimental determinations consisted of 70 × 35 × 250 mm holders, with 250 × 70 × 2.7 mm fuel sheets pressed from polyethylene and U_3O_8 with a ^{235}U content of 90%. Foils of Al, Cu, and stainless steel were used as covering. It was found that the assembly was quasi-homogeneous when the hydrogen and ^{235}U concentration ratio was $\rho H/\rho^{235}U \gtrsim 50$. For a value of this ratio of about 50, the water gap between the foils amounted to about 5 mm, or equal to the mean free path of the thermal neutrons in water; therefore at >50, the effect of the heterogeneity must be taken into account, and the method may be used only in the first case. For the calculation it was assumed that the assembly was spherical, with a 50-mm thick water reflector. Comparison of the results revealed agreement between theory and experiment. Thus, this method of calculation may be used for determining the critical dimensions of homogeneous, epithermal reactors using a hydrogenous moderator. (TTT)

18054 ON THE OPTIMUM CONTROL OF A NUCLEAR REACTOR BY THERMAL PROCESSES. Kurbatov, I. M.; Leonchuk, M. P.; Trofimov, A. S. At. Energ. (USSR), 19: 537-40(Dec. 1965). (In Russian).

With a given change in reactor power $q(\tau)$ during an excursion, control of the reactor is achieved by changing the coolant flow G (τ) to maintain a linear change in exit temperature $\theta(\tau,1)$. The minimum of a functional must be found. The optimum rate of changing from one power level to another can be selected from the conditions of the minimum. On assuming that the change in reactor power of (τ) is arbitrary, the control parameters are found from the condition of a minimum time for the transient process. The thermal processes in the reactor channel are described by a set of equations in partial derivatives, whose solution is approximated by a set of ordinary differential equations with the use of successive approximations. The minimum of the functional is obtained. The rise and fall of the reactor power as a function of time τ are given at various values of G and q. (TTT)

18055 A MEASUREMENT OF THE HYPERFINE STRUCTURE OF THE THERMAL NEUTRON FLUX DISTRIBUTION IN ORGANIC-COOLED UC CLUSTERED FUEL ELEMENTS IN A D_2O MODERATED LATTICE. Boeuf, A.; Tassan, S. (CCR, Euratom, Ispra, Italy). Energia Nucl. (Milan), 13: 57-66(Feb. 1966).

The detailed hyperfine structure distribution of the thermal flux in 7-, 6-, and 4-rod UC clustered fuel elements, cooled by an organic compound, in a D_2O moderated lattice, was measured by activation of Dy microdetectors. The measured distributions were satisfactorily described by simple empirical expressions. (auth)

18056 FEEDBACK DUE TO ELASTIC WAVES AND DOPPLER COEFFICIENT DURING THE EXCURSIONS OF A PULSED FAST REACTOR. Randles, J. (EURATOM, Ispra, Italy). J. Nucl. Energy: Pt. A and B, 20: 1-16(Jan. 1966).

In order to assess the inherent self-regulation of a pulsed fast reactor during the course of a single pulse, a formalism is developed for describing the feedback of reactivity. Because of the rapidity of the process considered, the only phenomena which are thought to be of importance are the Doppler effect and the axial thermal expansion of the fuel pellets. Since the latter effect gives a delayed negative reactivity component, systems with a (prompt) negative or zero Doppler coefficient present no problem. If the Doppler coefficient is positive, however, the axial expansion and Doppler reactivity feedbacks compete against each other and the system is then only self-regulating if the former acts quickly enough to dominate over the latter within the

timescale of the pulse. This competition between the axial expansion effect and a positive Doppler effect is the focal point of interest. It is shown that the elongation of the pellets can be expressed as a superposition of longitudinal elastic waves excited by the thermal shock accompanying the pulse. From this it is deduced that the delay in the reactivity feedback due to axial expansion arises basically from the time required by longitudinal elastic waves to propagate from the ends to the center of the fuel pellets. In order to derive a condition which ensures that the axial expansion effect is able to override the Doppler effect and provide an inherent shut-down tendency in accident conditions, the general formalism is applied to a simple model. From this model it is shown that the system is inherently self-regulating only if the Doppler coefficient is less than a certain limit, the value of which is derived explicitly as a function of certain reactor parameters. It is thought that this formula for the upper limit of the Doppler coefficient will be very useful in design and safety studies of pulsed (or burst) fast reactors. (auth)

18057 MONTE CARLO ANALYSIS OF SOME ENRICHED ^{235}U FAST CRITICAL ASSEMBLIES. Benzi, V.; Cupini, E.; De Matteis, A. (CNEN, Bologna). J. Nucl. Energy: Pt. A and B, 20: 17-24(Jan. 1966).

A Monte Carlo strategy adopted for an analysis of some highly enriched ^{235}U fast critical assemblies is briefly described. Moreover a twenty-group cross section set for ^{235}U and ^{238}U giving a satisfactory agreement between the results of calculation and experiment is reported. (auth)

18058 FLAT FLUX IN A SLAB REACTOR WITH NATURAL URANIUM. Bartosek, V.; Zezula, R. (Nuclear Research Inst., Czechoslovak Academy of Sciences, Rez). J. Nucl. Energy, Pt. A and B, 20: 129-34(Feb. 1966).

On the basis of two-group theory a nonlinear differential equation for fuel distribution is formulated which generates a flat thermal flux in a slab reactor with resonance escape probability depending on the density of fuel. An iterative procedure for solving this equation is described which was employed for numerical calculation of fuel density distribution in a homogeneous slab reactor with D_2O and natural uranium. (auth)

18059 A VARIATIONAL PRINCIPLE FOR RATIOS IN CRITICAL SYSTEMS. Lewins, J. (Univ. of Washington, Seattle). J. Nucl. Energy, Pt. A and B, 20: 141-3(Feb. 1966).

A variational principle from which arbitrary ratios in critical systems can be calculated in a stationary manner is presented. This principle enables the perturbation expression to be derived concisely using a compact operator notation in a generalized X variable (position and velocity) that incorporates the usual exact and approximate models of reactor theory. (B.G.D.)

18060 ON THE BURN-UP CHARACTERISTICS OF LARGE Pu–U FAST REACTORS. Nishihara, Hiroshi; Ohta, Masao (Kyoto Univ.). J. Nucl. Sci. Technol. (Tokyo), 2: 525-31(Dec. 1965).

Breeding ratio, effective multiplication factor k_{eff} and sodium-void reactivity effect of Pu–U fast reactors having a 3,000 l core volume are investigated as functions of burnup. Following results are obtained: Initial breeding ratio does not fail to be a measure for roughly estimating breeding character. By charging Pu fuel in the internal blanket situated inside core region, k_{eff} of the system remains almost constant along with burnup. The variation of sodium-void reactivity due to fuel burnup of the above system does not seem to be serious. (auth)

18061 NUMERICAL TREATMENT OF THE KINETIC REACTOR EQUATIONS. Griepentrog, E. (VEB Atomkraftwerk, Berlin). Kernenergie, 8: 610-13(1965). (In German).

The numerical methods described result in an essential shortening of the time necessary for the calculations as compared to the well known methods of solving the kinetic reactor equations. With the same efficiency, they may be applied to all systems of decay type equations, e.g., occurring in shielding problems, calculations of reactor burnup values, etc. Special methods of a type as simple as possible are yet more efficient although the intervals here must be chosen smaller since, on the other hand, only some few operations are necessary in each step. (auth)

18062 EFFECT OF DISTRIBUTION OF FISSILE MATERIAL ON CRITICAL MASS. Clark, H. K. Nucl. Sci. Eng., 24: 133-41(1966). (CONF-650602-27).

The influence of the distribution of ^{235}U, ^{239}Pu, and ^{233}U in water on the minimum critical mass, the minimum critical concentration per unit length of cylinder, and the minimum critical mass per unit area of slab surface is calculated. Two energy groups are employed in the calculations with parameters normalized to force agreement between calculations and experiments performed with water-reflected spheres containing uniform aqueous solutions having a wide range of concentrations. Calculations made with these parameters for a water-reflected cylinder, in which the optimum distribution for minimum mass was approximated within five coaxial regions, agree well with experimental results. Minimum critical masses, concentrations per unit length of cylinder, and masses per unit area calculated for ^{235}U, ^{239}Pu, and ^{233}U are, respectively, 768 g, 16.9 g/cm, 0.417 g/cm^2; 492 g, 10.6 g/cm, 0.266 g/cm^2; and 571 g, 13.5 g/cm, 0.362 g/cm^2. (auth)

18063 HETEROGENEITY CALCULATION FOR FAST REACTORS BY A PERTURBATION METHOD. Storrer, F.; Khairallah, A.; Cadilhac, M.; Benoist, P. Nucl. Sci. Eng., 24: 153-64(1966).

A perturbation method is described for the calculation of the heterogeneity effects on the multiplication factor and on the flux in fast reactors. It differs from the conventional perturbation method in that it uses an adjoint flux that is different from, but simply related to, the conventional adjoint. This new adjoint flux follows from the use of the collision-probability concept in the integral transport equation. The first-order changes in both the multiplication factor and the flux are simply expressed in terms of the conventional flux and adjoint flux obtained from homogeneous calculations. A procedure is described for the computation of higher-order changes. Qualitative results, as well as numerical results, are given. The application of the method to Doppler calculations in heterogeneous reactors is outlined. (auth)

18064 REACTOR NOISE ANALYSIS BY PHOTON OBSERVATION. Gelinas, R. J.; Osborn, R. K. Nucl. Sci. Eng., 24: 184-92(1966).

A set of moment equations is given for a reactor system in which neutron fluctuations are observed by detecting high-energy prompt photons that arise from neutron interactions. Attention is restricted to a one-speed "point-reactor" model in which delayed neutrons and photons are ignored. Expressions for the ratio of the variance to mean of the particles arising from the detection of photons are computed, as well as for the power spectral density of the detection rates. Comparison of these results with the corresponding expressions from conventional neutron-detecting noise analysis shows a striking similarity, and it is suggested that noise analysis by photon detection possesses certain other characteristics that endorse its feasibility in principle. (auth)

18065 CONSISTENCY IN THE ANALYSIS OF HIGH-BUCKLING CRITICAL EXPERIMENTS. Eich, W. J.; Williams, H. T. Jr. (Westinghouse Atomic Power Div., Pittsburgh). Nucl. Sci. Eng., 24: 209-11(1966).

In the determination of the effective multiplication factor corresponding to critical assemblies, the experimentally determined material buckling has generally been used in accounting for leakage. In compilations of this effective multiplication factor much scatter is encountered due to uncertainties in the measured bucklings of the smaller critical assemblies. This systematic difficulty is illustrated in a table which lists the characteristics of three lattices that are very similar. Tables are also presented showing comparisons of effective multiplication factors for various types of calculations, a comparison of interface reaction rates, and three fast-group reflector constants. (J.F.P.)

18066 MEASUREMENT OF THE TRANSFER-FUNCTION WITH STATISTICAL METHODS. Matthes, W. (EURATOM, Ispra, Italy). Nukleonik, 8: 21-32(Jan. 1966).

The source transfer-function of a (subcritical) reactor can be experimentally determined by correlation measurements. The formulas for the interpretation of the measurements are derived by starting from the linear relation between input X and output Y of the system: $Y(t) = \int dX(t')H(t',t)$ where the transfer-function $H(t',t)$ is the output of the system at time t for an input of $dX(t') = 1$. The inherent stochastic transfer properties of the system can be described by letting H be a stochastic quantity and applying the above formula to the discrete time series of events at the input and at the output. Correlating the output Y with an arbitrary (stochastic) process leads to a correlation function which can be measured in the time- or frequency domain under the assumption of ergodicity of the system. The different correlation methods in use are briefly discussed from this general point of view. (auth)

18067 THE REACTOR KINETICS EQUATION AS A DIRECT CONSEQUENCE OF THE BOLTZMANN EQUATION. Belleni-Morante, A. (Univ., Florence). Nukleonik, 8: 33-7(Jan. 1966).

The reactor kinetics equation was deduced directly from the Boltzmann equation and proved to be a differential-difference equation of retarded type. The common kinetic equation was compared with the retarded one and it was found that the latter leads to solutions which are less stable than those of the common equation. (auth)

18068 PARTICULAR SOLUTIONS OF THE ENERGY-DEPENDENT BOLTZMANN EQUATION. Mueller, Karl-Heinz (CCR EURATOM, Ispra, Italy). Nukleonik, 8: 38-40(Jan. 1966).

The Carleman-Kupradse method for solving a coupled set of integral equations with sectional holomorphic kernels combined with a method based on a variation procedure, of removing the energy from the field of free variables, allows the construction of particular solutions of the neutron transport equation. The nuclear data enter the calculation only after they are weighted and integrated over the energy variables (E,E'). Thus, the procedure allows the use of cross sections in a numerical form (e.g., the usual energy group representation). An approximate solution can be found from a linear system of algebraic equations. (auth)

18069 THE INTEGRAL NUCLEUS METHOD IN NUCLEAR REACTOR PHYSICS. Rosescu, Th. Stud. Cercet. Fiz., 17: 799-844(1965). (In Rumanian).

The kernel method is one of the rigorous ones used for solving the neutron transport equation. It was derived from the observation that the nucleus of the integral transport equation represents in some specific cases a solution for the neutron diffusion or slowing-down equations. The use of kernels allows a differential or integral-differential equation with given boundary conditions to be transformed into an integral equation that contains the conditions implicitly. The equations also make it possible to transform a nonhomogeneous equation which is difficult to solve into a homogeneous equation with nonhomogeneous boundary conditions or vice-versa; a choice may be made at will, depending on the difficulties encountered. If the kernel satisfies a linear equation, it may be used by superimposition to obtain the neutron flux or the slowing-down density, which is due not to an isolated source but to a distribution of sources. It is thus possible to establish correlation between point, linear and plane nuclei and to treat reactors in which fission occurs as a series of distributed sources. The physical interpretation of the theory is emphasized, pointing out the potential application of the method in reactor physics calculations. (26 references) (TTT)

18070 NEKOTORYE VOPROSY FIZIKI I TEKHNIKI YADERNYKH READTOROV. (Certain Problems in Physics and Technology of Nuclear Reactors). Yurova, L. N. Moscow, Atomizdat, 1965. 156p.

Eleven articles are included on the theory and methods of calculating nuclear reactors and the thermophysical parameters of hydrogenous liquids. Discussions are given on the existence and uniqueness of a positive solution of the neutron-transport equation taking slowdown into account, effective methods of calculating two- and three-dimensional reactors, computer calculations of fast reactors, critical parameters of a reactor without reflector and the neutron spatial-angular distribution in the material-parameter approximation, the effect of the capability of unloading the side screen of a fast breeder reactor on its doubling time, subcritical uranium-water assemblies for physical studies, heat transfer during boiling of subcooled water and ethyl alcohol in pipes, heat transfer during forced convection in a pipe and during high thermal loading, critical boiling during forced movement of acetone, benzene, and monoisopropylbiphenyl, and the density of organic compounds. (M.J.T.)

Design and Feasibility

18071 (TID-22665) NOISE ANALYSIS APPLIED TO A LIQUID-SOLID FLUIDIZED BED [Thesis]. Timmons, Darrol Holt (Kansas Engineering Experiment Station, Manhattan). 1966. 139p. Dep. mn. CFSTI $4.00 cy, $1.00 mn.

Kans. State Univ. Eng. Exp. Sta., Spec. Rep. No. 65.

An experimental and theoretical study of the application of noise analysis to the determination of the dynamic behavior of a copper–water fluidized bed system is summarized. (D.C.W.)

18072 THE HOMOGENEOUS SUSPENSION REACTOR PROJECT. Went, J. J. (KEMA, Arnhem, Netherlands). EuroNuclear, 3: 89-92(Feb. 1966).

A single-zone circulating suspension reactor system, utilizing a mixed U–Th oxide, is being studied. For a large heavy water moderated reactor fueled with a $^{232}ThO_2$–$^{233}UO_2$ suspension, the reaction rate $^{233}Pa \rightarrow {}^{234}Pa$ (relative to the reaction rate $^{233}Pa \rightarrow {}^{233}U$) was calculated as a function of neutron flux at 180°C. Fuel costs are considered and research questions being studied are listed. The KSTR suspension test reactor is described along with the zero-energy reactor for investigating the nuclear stability of a circulating suspension system. (M.C.G.)

18073 THERMAL BREEDING BY UTILIZING THE THORIUM–URANIUM FUEL CYCLE. Wenzel, P. (VEB Atomkraftwerk, Berlin). Kernenergie, 8: 625-35(Nov. 1965). (In German).

Breeding is possible in both fast and thermal reactors with the thorium-uranium cycle. The state of reactor development and fuel utilization is reviewed. Uranium and thorium resources are considered. The neutron physics of thorium-uranium fueled thermal reactors is discussed. Thorium-fueled thermal reactors are also described. The technology of the thorium-uranium fuel cycle is reviewed. (68 references). (M.C.G.)

18074 REACTOR OPTIMIZATION. Lewins, J. Nucl. Energy, 20-6(Jan. 1966).

A general theory for the optimization of an inhomogeneous steady-state system is outlined. The optimum fuel distribution in a lattice cell, in terms of the maximum thermal utilization, is treated as an example. (D.C.W.)

18075 NUCLEAR REACTOR WITH AQUEOUS FUEL SOLUTION AND A CATALYTIC RECOMBINER. Flora, John W. (to North American Aviation Inc.). German Patent 1,205,633. Nov. 25, 1965. Priority date Sept. 4, 1956, United States.

A nuclear reactor is designed, which comprises a core, an aqueous uranyl solution disposed in the core as the active fuel, a canopy positioned above the core for containment of overflow solution and a catalytic hydrogen-oxygen recombiner positioned in the canopy. A relatively large throat connects the solution vessel and the canopy, the throat forming annular overflow container with the canopy. Baffle means are positioned at the exit of the throat in the canopy, the baffle means directing core solution overflow into the annulus, and drain holes are provided in the annulus connecting with the solution vessel for the flow return of the overflow solution to the solution vessel. (Gmelin Inst.)

Fuels

Refer also to abstract 16566.

18076 (ORNL-TM-1385) A COMPUTER PROGRAM FOR PREDICTING COATED-PARTICLE BEHAVIOR. Prados, J. W. (Oak Ridge National Lab., Tenn.). Mar. 1966. Contract W-7405-eng-26. 32p. Dep. mn. CFSTI $2.00 cy, $0.50 mn.

A computer program is developed for use in calculating conditions under which the pyrolytic-carbon coatings of fuel microspheres would be expected to fail. Working equations and a listing of the Fortran-63 source program are presented, together with instructions for furnishing input data. (auth)

18077 THE BOILER SUPER-HEATING ELEMENTS FOR THE SUPER-HEAT REACTOR OF THE AEG. Schwarzwaelder, Rainer. A E G Mitt., 55: 594-603 (1965). (In German).

The present study is limited to the tube shaped boiler super-heating elements of the AEG. The reactor uses uranium dioxide in sintered form or compressed by vibration as a fuel element. Stainless steel and nickel alloys were used as the cladding material. These elements are described. The principal difficulties in the development of such elements (corrosion and erosion, mechanical stability of the fuel claddings at high temperatures and under irradiation, heat distribution, and construction) were indicated and the development work already carried out is reported. (tr-auth)

18078 IMPROVEMENT OF HEAT TRANSFER OF A FUEL ELEMENT WITH POLYZONAL SPIRAL FINNING BY MODIFYING ENTRY CONDITIONS. Becirspahic, Sulejman; Vehauc, Aleksandar; Kulundzic, Predrag. Bull. Boris Kidrich Inst. Nucl. Sci., 16: 127-41(July 1965).

Channel entry conditions of a fuel element model with polyzonal spiral finning were modified to investigate their effect on heat transfer at the beginning of finning in the Re number range from 20,000 to 80,000. Distribution of the St number along the fuel element and its dependence on the position, and the minimum and average St number as a function of the Re number were determined. The modifications give a more uniform distribution of the St number over the fuel element. (auth)

18079 DISPERSIONNYE TEPLOVYDELYAYUSHCHIE ELEMENTY YADERNYKH REAKTOROV. (Dispersion Fuel Elements for Nuclear Reactors). Samoilov, A. G.; Kashtanov, A. I.; Volkov, V. S. Moscow, Atomizdat, 1965. 344p.

The construction, properties, and application of dispersion-type fuel elements are discussed. The characteristics of various materials used in fabricating dispersion fuels are considered, including U–O, U–C, U–N, U–Si, U–S, and Pu–O compounds. Processes involved in the fabrication of dispersion fuel elements are described, including melting, casting, powder metallurgy, and canning. The mechanical and physical properties of dispersion compositions prepared by various processes are compared. The radiation resistance of dispersion-type fuel elements is considered, with discussions of radiation effects on the properties of the construction materials, the changes in the properties of the fissioning phase, and results of irradiation testing. (M.J.T.)

18080 NUCLEAR REACTOR FUEL ELEMENT CLUSTER. Schmidt, Gerhard (to Gesellschaft fuer Kernforschung mbH). German Patent 1,203,888. Oct. 28, 1965. Filed Aug. 17, 1963.

Spacing of elongated fuel rods in clusters is maintained by axially directed cooling fins extending radially from the surface of the rods, which are provided with cooperating hooks. (Gmelin Inst.)

18081 FUEL ELEMENT FOR NUCLEAR REACTORS. Wallace, Walter Paul; Simnad, Massoud T. (to General Dynamics Corp.). German Patent 1,205,632. Nov. 25, 1965. Priority date June 8, 1960, United States.

A nuclear fuel element is designed, which comprises a solid fuel body made of a homogeneous mixture of uranium and zirconium hydride with a closely fitting aluminum container disposed around the fuel body, the fuel body having a reduced cross section adjacent to the ends thereof, whereby the fuel element has a reduced tendency to irreversibly elongate. A coating of lubricant capable of withstanding operating temperatures of 2000°C or more is disposed at the interface between the fuel body and the container. (Gmelin Inst.)

Power and Power-Breeder Reactors

Refer also to abstracts 16618 and 17328.

18082 (AECL–2390) WORLD AND CANADIAN ENERGY TODAY AND TOMORROW. PART I. THE ROLE OF NUCLEAR ENERGY. Merlin, H. B. (Atomic Energy of Canada Ltd., Chalk River (Ontario)). [nd]. 22p. (CONF-660110–1). Dep. mn. AECL $0.50.

From Canadian Electrical Assn. Eastern Zone Meetings, Halifax, Nova Scotia.

Uses and sources of energy in the world today, future growth in demand for electricity, and the role of nuclear energy in meeting this demand are reviewed. Canada's electrical systems are also briefly reviewed. (auth)

18083 (CVNA–63) RADIOLOGICAL ENVIRONMENTAL SURVEY MANUAL. King, H. T.; Jones, M. B. (Carolinas Virginia Nuclear Power Associates, Inc., Parr, S. C.). Sept. 15, 1960. Contract AT(30-1)-2289. 28p. Dep. mn. CFSTI $2.00 cy, $0.50 mn.

An environmental radiological survey program consisting of regularly scheduled collections, and radioactivity analyses of water, milk, soil, plants, animals, and airborne particles is provided for present and future evaluation of background radioactivity levels in the plant site and surrounding area. (M.O.W.)

18084 (CVNA–96) A NARRATIVE SUMMARY OF ON-SITE METEOROLOGICAL TESTS AT PARR, SOUTH CAROLINA. Courtney, F. E. (Lockheed Nuclear Products, Marietta, Ga.). Nov. 1961. 61p.

For Carolinas Virginia Nuclear Power Associates, Inc., Parr, S. C.

Six test series were conducted on the reactor site. These tests were all planned to document the behavior of the environment in relation to potential reactor operations. Within each test series several individual tests were conducted making a total of some nineteen individual tests. Included is a description of each test, the conclusions drawn as a result of each test, and the significance of the test results in terms of future reactor operations. (M.O.W.)

18085 (CVNA–173) CVTR INITIAL CORE LOADING. Glass, C. D. (Carolinas Virginia Nuclear Power Associates, Inc., Parr, S. C.). Mar. 22, 1963. 31p.

The operations involved in the initial core loading of the CVTR are summarized. The present locations of the core components are discussed. (M.O.W.)

18086 (CVNA–174) CVTR INITIAL CRITICALITY. (Carolinas Virginia Nuclear Power Associates, Inc., Parr, S. C.). Apr. 4, 1963. Contract AT(30-1)-2289. 23p. Dep. mn. CFSTI $1.00 cy, $0.50 mn.

The following data obtained at the CVTR are summarized; nuclear instrumentation response during the addition of D_2O to the Primary Coolant System, nuclear instrumentation response during the addition of D_2O to the moderator tank, the initial approach to criticality, and the nuclear instrumentation overlap. (M.O.W.)

18087 (CVNA–250) CAROLINAS VIRGINIA NUCLEAR POWER ASSOCIATES, INC. RESEARCH AND DEVELOPMENT PROGRAM. Quarterly Progress Report, July–September 1965. (Westinghouse Electric Corp., Pittsburgh, Pa. Atomic Power Div.). Contract AT(30-1)-2289. 80p. Dep. mn. CFSTI $3.00 cy, $0.75 mn.

Measurements and analytic studies in CVTR are reported, including: neutron fluxes and spectra at 44 Mwt; pD effects in coolant; core thermal-hydraulic characteristics in approach to 65-Mw operation; core physics, reactivity coefficients, control-rod worths, flux-wire measurements and their analysis, Xe transient effects on control-rod worths, and axial hot-channel factors; metallurgical inspection of components; high-power and high-burnup operation analyses; and safety-hazards analysis. (T.F.H.)

18088 (INR-669/C) SALT-BOILING FAST REACTOR "SAWA". Taube, M.; Kowalew, A.; Mielcarski, M.; Poturaj-Gutniak, S. (Institute of Nuclear Research, Warsaw (Poland)). Dec. 1965. 17p. Dep. mn.

A fast-breeder reactor is proposed in which $AlCl_3$ circulating in a closed cycle serves as the coolant. The fissionable and fertile materials used in the reactor are $^{239}PuCl_3$ and $^{238}UCl_3$, respectively. An analysis of the mass and energy balance in the core is outlined. (D.C.W.)

18089 (NAA-SR-Memo-10178) THE WATER CHEMISTRY OF HERMETICALLY-SEALED BOILING WATER REACTORS. Haroldsen, G. O. (Atomics International, Canoga Park, Calif.). Aug. 10, 1964. Contract AT-11-1-GEN-8. 52p. Dep. mn. CFSTI $3.00 cy, $0.50 mn.

To provide a basis for establishing the requirements of the water purification system for a hermetically-sealed boiling water reactor (such as COMPACT or its predecessor, SNAP 4), an extensive literature survey is made of corrosion rates and of corrosion-product deposition rates in 300-series stainless-steel systems containing high-purity, high-temperature water. After a stable oxide film is formed, the rate of corrosion remains low, generally reported as 5 to 10 mg/dm^2mo. Within reasonable limits, dissolved oxygen, dissolved hydrogen, pH, and temperature do not significantly affect the rate, which is already low. Although much has been written about crud deposition and scale formation, the information is largely qualitative, and the data do not allow firm, quantitative estimates to be made. It is clear, however, that maximum water purity minimizes deposition. Based on presently available information, it appears that fouling in the COMPACT reactor, over its intended core life of 10,000 hours, can be precluded by maintaining the level of impurities at about 10 ppb. It is probable that a ten-fold increase in this amount could be tolerated, but experimental verification is required. It is feasible that a mixed bed deionizing system, to purify the total condensate flow and a 0.5% side stream from the reactor core, could reduce the impurity concentration to 10 ppb. Here again experimental verification is needed. Less well established is the basis for designing a deionizing system with a 10,000 hour life that can remove both filterable and dissolved impurities. (auth)

18090 (NUS-246) REACTOR OPERATION'S SAFETY ANALYSIS MONTHLY REPORT NO. 4, MARCH 1 TO MAY 31, 1965. (Nuclear Utility Services, Inc., Washington, D. C.). July 16, 1965. Contract AT(11-1)-651, Subcontract Nos. 4 and 5. 162p. Dep. mn. CFSTI $5.00 cy, $1.00 mn.

For Rural Cooperative Power Association, Elk River, Minn.

The sensitivity of the fission-product monitor was calculated, and the use of a deoxygenating resin in the primary purification system of the ERR was evaluated. The radioiodine peaking which has occurred regularly with almost every plant startup at Elk River during the last year was investigated. Tests were performed on the rod clutch coil circuit to verify design calculations on the replacement of a potentiometer, capacitor, and resistor with a zener diode circuit. The reasons for the bowing of some of the fuel tubes in the two fuel elements that were removed from the core in Nov. 1964 were investigated. A study was also made of the control rods in order to provide support for a technical specification change to permit operation of the regulating rod beyond the limit of 3.4% elongation at fracture. (D.C.W.)

18091 (RT/FI(65)45) PROGETTO NEUTRONICO PRELIMINARE DEL P.R.O.-II CORE (UO_2-SS). (Preliminary Neutronic Project of PRO-II Core (UO_2-Stainless Steel)). Cardosi, G.; Panzeri, D. (Comitato Nazionale per l'Energia Nucleare, Rome (Italy)). Nov. 1965. 32p. Dep. mn.

The results of analysis and calculations executed in the preliminary neutronic project of PRO II Core (UO_2 fuel – SS cladding) are presented. (auth)

18092 (TRG-Report-1039) THE USE OF DOUNREAY FAST REACTOR AS A MATERIALS TESTING REACTOR. Birss, I. R.; Bishop, T. P. (Reactor Group, United Kingdom Atomic Energy Authority, Dounreay (Scotland)). Dec. 14, 1965. 22p. Dep. BIS $0.60. HMSO 3s.

An introduction to the Dounreay Fast Reactor as a Materials Testing Reactor is presented. The facilities which are available for irradiation experiments, the environment which an experiment will experience, and the methods used to calculate doses, heat ratings and burnups are described. The methods are to some extent dictated by the method of presentation of neutron data. (auth)

18093 (UNC-5142) PERFORMANCE EVALUATION OF HEAT EXCHANGERS FOR SODIUM-COOLED REACTORS. Quarterly Technical Progress Report, October 1, 1965–December 31, 1965. Dischinger, R. H. (United Nuclear Corp., Elmsford, N. Y.). Jan. 20, 1966. Contract AT(11-1)-1452. 32p. Dep. mn. CFSTI $2.00 cy, $0.50 mn.

Procedures are completed for evaluation of the performance of and design methods used for an intermediate heat exchanger and a steam generator. These procedures utilize a CDC-1604-A computer to derive observed performance from actual test data, and to calculate predicted performance consistent with test conditions and in accordance with the design methods and assumptions. The structural portion is checked out using sample data. (auth)

18094 (WAPD-MRP-115) PRESSURIZED WATER REACTOR (PWR) PROJECT. Technical Progress Report, October 22, 1965–January 21, 1966. (Bettis Atomic Power Lab., Pittsburgh, Pa.). Contract AT(11-1)-Gen-14. 105p. Dep. mn. CFSTI $4.00 cy, $0.75 mn.

Separate discussions are presented on PWR development and engineering. Among these include the reactor mechanical and thermal design, reactivity aspects, metallurgy of core materials, and core engineering. Assemblies 1, 2, 3, and 4 of core 2 of the Shippingport PWR were considered. (M.O.W.)

18095 (WCAP-3385-52) SAXTON PLUTONIUM PROGRAM. MECHANICAL, THERMAL AND HYDRAULIC DESIGN OF SAXTON PARTIAL PLUTONIUM CORE. Bassler, E. A.; Fischer, D. C.; Georges, N. J.; McCabe, E. A. (Westinghouse Electric Corp., Pittsburgh, Pa. Atomic Power Div.). Dec. 1965. Contract AT(30-1)-3385. 47p. (EURAEC-1491). Dep. mn. CFSTI $2.00 cy, $0.50 mn.

Work Performed under United States–Euratom Joint Research and Development Program.

The mechanical design and the thermal and hydraulics design for Saxton Core II, which contains nine centrally located PuO_2-UO_2 fuel assemblies and twelve peripheral UO_2 assemblies are described. Design guidelines for the PuO_2-UO_2 portion of Saxton Core II included: 20,000 Mwd/tonne peak rod average burnup, 16 kw/ft maximum heat rate in the rods, at end of design life, internal gas pressure to be less than external reactor operating pressure, and fuel rod outside diameter, length, and lattice spacing to be the same as for the UO_2 rods in Cores I and II. (auth)

18096 (ORNL-tr-987) RAPSODIE REACTOR—PRELIMINARY STUDIES IN THE FABRICATION OF CONTROL ROD MECHANISMS: TESTS OF THE NEW GRIPPER. Jacquelin, R. (Commissariat a l'Energie Atomique, Cadarache (France). Centre d'Etudes Nucleaires). Translated for Oak Ridge National Lab., Tenn., from report PNR/SEPR-65.018. May 25, 1965. 23p. Dep. mn. JCL $2.60 fs, $0.89 mf.

The testing of a prototype gripper for the control rods of the Rapsodie reactor is summarized. (D.C.W.)

18097 FAST POWER REACTORS. Kazachkovsky, O. D. (Inst. of Atomic Reactors, Melekess, USSR); Lytkin, V. B. At. Energy Rev., 3: 47-87(1965).

The development of nuclear power on a large scale, such as can be obtained only through the use of fast reactors is discussed. The basic physical characteristics of fast power reactors are considered: high breeding ratios, high power density in the core, high concentration of fissile material, and use of a liquid-metal coolant. The various types of fuel that can be used and possible methods of its chemical reprocessing are reviewed. The economic characteristics of fast power reactors are considered together with possible means of further improving them. (auth)

18098 THE DEVELOPMENT OF COATED-PARTICLE FUEL FOR HIGH-TEMPERATURE REACTORS. Huddle, R. A. U. (Atomic Energy Establishment, Winfrith, Dorset, Eng.). Atompraxis, 12: 54-7(Jan. 1966).

The thinking that led to the concept of coated-particle fuel for high-temperature reactors and the basic philosophy employed in the development program are discussed in relation to the Dragon Reactor Experiment. Fundamental aspects concerning the fabrication and behavior of such fuel are considered with particular attention paid to the choice of process and product. The actual methods chosen for development are described and their advantages discussed in relation to the requirements of the fuel element development program. The results obtained in the irradiation program demonstrated the suitability of coated particle fuel for use in the Dragon Reactor Experiment and proved the feasibility of such fuel for high-temperature power reactors. (auth)

18099 FUTURE FUEL NEEDS OF NUCLEAR POWER PLANTS. Wagemann, K. (Institut fuer Reaktorentwicklung, Juelich, Ger.). Atomwirtschaft, 11: 66-71(Feb. 1966). (In German).

Previous publications and pertinent data on the world reserves of uranium ores indicate significant variations. In the present study, on the basis of various estimated values, relations were derived between the present reserves of fissionable material and the nuclear energy needs to be expected. The fuel necessary to cover these energy needs was determined without going into specific reactor types. The parameters used in the calculations are the specific power, the conversion ratio or the doubling time, and the availability of breeder reactors. (tr-auth)

18100 FUEL UTILIZATION IN A JOINT ECONOMY OF CONVERTERS AND BREEDERS. Steinert, C. (Siemens-Schuckertwerke AG, Erlangen, Ger.). Atomwirtschaft, 11: 72-6(Feb. 1966). (In German).

Energy production and fuel utilization of a nuclear economy can exist in very different ratios to each other when different types of reactors are considered and compared with each other. For a joint economy of converters and breeders operating on a uranium-plutonium cycle it was shown how the conversion potential, breeding potential, doubling time, and rise of the nuclear energy production affects the fuel utilization. (tr-auth)

18101 SIMPLIFIED METHOD FOR THE CALCULATION OF THE FUEL COST FRACTION. Gruemm, H. Atomwirtschaft, 11: 76-81(Feb. 1966). (In German).

The fuel cost components of energy production costs of nuclear power plants is composed of a series of components. For prognosis and type comparison the fuel cost problem was generalized under simplified assumptions giving the lowest possible sources of error. The calculation leads to a compact approximation formula which considers all essential parameters and cost components. This formula, based on the present-worth method, can detect the fixed and variable cost components. (tr-auth)

18102 ON THE COST REGRESSION IN NUCLEAR POWER PLANTS. Gudehus, H. Atomwirtschaft, 11: 93-5(Feb. 1966). (In German).

The cost reduction dependent on the installation size is much higher in nuclear power plants than in conventional power plants. The extent of this reduction contains however still many uncertainties. The results of the probable cost decrease are discussed. (J.S.R.)

18103 THE 50-Mw BOILING WATER REACTOR OF DODEWAARD. Mostert, P. Atoomenergie Haar Toepass., 8: 11-19(Jan. 1966). (In Dutch).

The boiling water reactor at Dodewaard is the first Dutch nuclear power station. The power plant is operated by General Electric but, in so far as possible, the components were constructed by Dutch industry. After a complete description of the reactor, the physical aspects of the reactor core are reported. (tr-auth)

18104 SECOND FORATOM CONGRESS. PRESENT TYPES OF NUCLEAR POWER PLANTS. Jaroschek, K. (Ecole Superieure Technique, Darmstadt, Ger.). Bull. Inform. A.T.E.N. (Ass. Tech. Energ. Nucl.), No. 57, 29-48 (Jan.-Feb. 1966). (In French).

The present nuclear reactors in operation in Great Britain, France, Italy, the Federal Republic of Germany, Austria, Belgium, Spain, and Switzerland are reviewed. A comparative examination is made of the development plans. (J.S.R.)

18105 CLADDING TEMPERATURES USED IN AN AUTOMATIC CONTROL PROCEDURE FOR A POWER REACTOR. Roussel, F.; Yung, J. M. Bull. Inform. A.T.E.N. (Ass. Tech. Energ. Nucl.), No. 57, 49-54(Jan.-Feb. 1966). (In French).

The most significant parameters in the control of a gas–graphite reactor are the effect of the control rods on the reactor, the role of the cladding temperatures, and the measurement of the CO_2 output. The automatic control systems possible for the operation of a graphite–gas nuclear power reactor are indicated. The control system of the EDF-1 reactor is outlined. Possible future developments are indicated. (J.S.R.)

18106 SIMULATION OF NUCLEAR PLANTS AND C.N.E.N.'S ACTIVITIES IN THIS FIELD. Mathis, Agostino Comit. Naz. Energ. Nucl., Notiz., 11: 21-8(Dec. 1965). (In Italian).

The concepts of simulation and the most appropriate methods and tools of calculus are considered. The contributions made by simulation methods to the design of nuclear plants, and the work done by C.N.E.N. in this field are reviewed. (auth)

18107 LOW-CAPACITY ATOMIC POWER STATIONS. Mathe, I. Gyoergy; Selley, Gabor. Energ. Atomtech., 18: 266-70(May-June 1965). (In Hungarian).

The low-capacity, 0.2 to 20 Mw(e) power stations present special advantages in areas, where the use and storage of conventional fuels, such as coal, oil, natural gas, hydroelectric power or imported electricity is too costly and the requirements are low. Three factors are of special importance in making the small, nuclear power station competitive: the transportation and storage costs of nuclear fuels are very low; construction, installation and testing of the small plants require much less time than that of large power stations; the small units may be mass-produced, thus further reducing the cost. In addition, they may serve as training schools for the personnel of projected larger plants. The small plants are especially useful in remote areas, polar research posts, tropical forests, desert regions and mountainous areas. The units may be transported disassembled or they may be mounted ready for operation on barges or trailers. Pressurized water reactors, fueled with high enriched uranium and operating with relatively low exit temperatures of 270 to 300°C have been used; examples include the Soviet TES-3 and the United States PM-2A and PM-3A stations, used in Greenland and in the Antarctic, respectively. Boiling water type reactors, rated at less than 1 Mw, are used primarily for military support operations. In the nitrogen-cooled, water-moderated ML-1 reactor the gas turbine is operated directly by the coolant. Organic reactors are limited to temperatures below 400°C; they present the advantage of low original investment cost. Examples of these reactors include the Soviet Arbus and the U. S. Direct-Cycle Diphenyl Reactor. (TTT)

18108 EVALUATION OF THE FIRST BR3 CORE. Fedrighini, A. C. (FIAT, Turin); Forti, G.; Moncassoli, A. M. Energia Nucl. (Milan), 13: 67-72(Feb. 1966).

Results are presented from an analysis of experimental data obtained during the operation of the first Belgian Reactor BR-3. The theoretical evaluation of the stationary behavior of the BR-3 core was carried out by a detailed analysis of the following items: fast constants, thermal constants, reactivity coefficients, control rod worth, and core lifetime. For each item a brief discussion of the obtained results is reported. (auth)

18109 IMPROVEMENTS AND LIMITATIONS IN THE VAPOR CYCLE OF THE MAGNOX REACTORS. Ruggiero, Umberto (Univ., Bari, Italy). Ing. Nucl., 6: 231-44 (Sept.-Oct. 1965). (In Italian).

Because of the industrial importance of CO_2-cooled reactors of the Magnox type, the research made to improve the yield is examined and analyzed on the basis of the latest studies. Solutions with vapor cycles with double and single pressures and repeated superheating are considered. The results are examined critically and the possible improvements are evaluated with respect to the most recent developments. The problem of the humidity of the vapor in the turbines is discussed. The increase of the input temperature of the gas in the reactor and the stability of the maximum output value, the limits of use of cycles with double pressure, and the advantages offered by the simple cycle with repeated superheating are discussed. (tr-auth)

18110 EXPERIMENTS RELATING TO THE CONTROL OF FISSION-PRODUCT RELEASE FROM ADVANCED GAS-COOLED REACTORS. Collins, D. A.; McIntosh, A. E.; Taylor, R.; Yuille, W. D. (United Kingdom Atomic Energy Authority, Seascale, Eng.). J. Nucl. Energy, Pt. A and B, 20: 97-122(Feb. 1966).

It has been shown that iodine released from irradiated AGR fuel elements may be present in three forms: elemental iodine vapor, iodine carried on solid particles, and vapor compounds of iodine, principally methyl iodide. Other fission products, specifically tellurium, cesium, barium/lanthanum, strontium and ruthenium are present entirely as solid particles. The relative amounts of the three forms of iodine depend on such factors as the fuel-element temperature and irradiation level, the gas composition and temperature and the sorption/desorption history of the iodine on surfaces. Methyl iodide can comprise an appreciable percentage of the total iodine released. A trapping system consisting of a combination of high-efficiency filters and activated carbon beds can provide adequate protection against the escape of the released fission products (apart from the rare gases) provided that the capacity of the carbon for methyl iodide is not exceeded. A coconut-shell-based carbon (Type SC II), chosen for its performance against elemental iodine, will retain methyl iodide with high efficiency only up to a loading of about 5 g/te carbon at 100°C and much less at room temperature. An alternative coal-based carbon (Type 207 B) has excellent performance in relatively dry gas up to a loading of about 500 g/te carbon both at room temperature and at 100°C. The performance of scaled-down trapping plants containing each of these types of carbon has been demonstrated against the fission products released from overheated AGR fuel specimens in laboratory-scale experiments. (auth)

18111 GERMAN POLICY OF REACTOR DEVELOPMENT. Pretsch, J. (Bundesministerium fuer Wissenschaftliche Forschung, Bad Godesberg, Ger.). Kerntechnik, 8: 9-12(Jan. 1966). (In German).

The basic German policy with respect to reactor development is briefly outlined. The individual development programs, comprehensive survey of all development programs, test reactors, and fast breeders and high temperature reactors are considered. The German plans for the processing of irradiated fuels are also indicated. (J.S.R.)

18112 CONTROL OF THE OBRIGHEIM NUCLEAR POWER PLANT. Aleite, W. (Siemens-Schuckertwerke AG, Erlangen, Ger.). Kerntechnik, 8: 15-18(Jan. 1966). (In German).

The Obrigheim Nuclear Power Plant is scheduled for operation in 1968. The power control of the power plant, especially the control of the reactor, is described. The reactor and its circuits are briefly considered, and the systems used for the control of the reactor power are discussed. A simplified block diagram of the reactor power control is given. The manual and automatic controls for the control rods are described. (J.S.R.)

18113 DUNGENESS "A" POWER STATION COMES ONTO LOAD. Nucl. Energy, 4–9(Jan. 1966).

The Dungeness A power plant is briefly described, and its operating parameters are summarized. The departures from established practices for reactors of this type are noted. (D.C.W.)

18114 THE SPECIALIZED USE OF OPTICAL INSTRUMENTS IN THE CONSTRUCTION OF NUCLEAR POWER STATIONS. Stevens, G. Nucl. Energy, 32-42(Feb. 1966).

The application of some specific optical instruments in the construction of nuclear power stations is discussed. (D.C.W.)

18115 CONTROL OF REACTIVITY IN HIGH CONVERSION RATIO, PLUTONIUM-FUELED THERMAL POWER REACTORS. Srikantiah, G. Nucl. Sci. Eng., 24: 175-83 (1966).

Methods of long-term reactivity control for plutonium-fueled D_2O-moderated reactors that favor high conversion ratios are considered. One method uses annular gaps around the fuel elements that can be selectively filled with the D_2O moderator. Reactivity compensations ranging from 8 to 15% can be achieved with gaps of 6- to 8-cm thickness and a corresponding reduction in conversion ratio of 3 to 5%. In the second method, depleted uranium sleeves that can be removed as required during long-term operation are utilized around fuel elements in annular regions of the reactor. Sleeves of only 0.2-cm thickness, around fuel elements in the central region of the reactor, provide reactivity compensations of up to 10% and actually increase the conversion ratio in the design studied. Average conversion ratios of about 0.90 are obtained in a large D_2O-cooled and -moderated reactor using Zircaloy pressure tubes at fuel burnup of 10^4 MWd/t. The average conversion ratios would increase to about 0.97 if beryllium-based pressure tubes could be developed. (auth)

18116 DYNAMICS OF NUCLEAR FUEL CYCLES. Gruemm, H. Nukleonik, 7: 443-51(Oct. 1965). (In German).

The internal conditions (limited by the common fission and breeder substance change) of an expanding nuclear energy economy consisting of populations of various reactor types are investigated. A flexible formalism "the mass flux image" that makes it possible to survey the various strategies for the introduction of nuclear energy and which yields the substance change is derived. The formulation is made on the basis of the following assumptions. The total nuclear energy and the mean load factors for the individual populations are given. The power fractions of the individual types entering into the system are valid as given. The nuclear energy needs, the power fraction, the substance change, and the current production are taken as continuously varying magnitudes. For the mass flux image data blocks are used in which,the parameters characterizing the individual reactor types are summarized as time functions. (J.S.R.)

18117 INTERNATIONAL MARKETING OF NUCLEAR POWER PLANTS. Nehrt, Lee C. Indiana University Social Science Series No. 22. Bloomington, Ind., Indiana University Press, 1966. 416p. $6.00.

Atomic energy laws, treaties, agreements, policies, and regulations in the domestic, international, and foreign spheres and the ways in which they affect the foreign marketing of nuclear power plants by domestic reactor manufacturers are discussed. The period studied ends in mid-1962. A series of case studies are presented to illustrate the effects of the framework of nuclear power. (M.C.G.)

18118 TEKHOLOGICHESKII I TEPLOTEKHNICHESKII KONTROL NA ATOMNYKH ELEKTRICHESKIKH STANTSIYAKH. (Technological and Thermotechnical Control of Nuclear Power Stations). Shal'man, M. P. Moscow, Moskovskii Energeticheskii Institut, 1965. 135p.

Sources of radioactive contamination of coolant and equipment and conditions for safe reactor operation are reviewed. Special technological control and the organization of control systems in nuclear power stations are discussed. Control of fuel-can integrity and detection of leaks are considered. Apparatus used in control systems, including ionization chambers, proportional counters, scintillation counters, multichannel devices, and automatic devices, is considered. Organization and automation of thermotechnical and power control are discussed, and apparatus used for control of pressure, temperature, power level and output, water regime, and gas regime is described. (M.J.T.)

18119 SAFETY SYSTEMS AND THE MEASUREMENT OF NEUTRON FLUX. Meiffren, J.; Decool, F. (CEA, Marcoule, France). Vienna, International Atomic Energy Agency, 1965, Preprint No. CN-22/19, 36p. (In French). (CONF-651105-26). ORAU.

From Conference on Nuclear Electronics, Bombay.

The original flux measurement system and safety devices are briefly discussed, and the improved systems are described. (D.C.W.)

18120 CARBON DIOXIDE-COOLANT GAS OF THE G.2 AND G.3 REACTORS: LEAKS, ANALYSIS, ACTIVITY. Meiffren, J.; Dupay, F. (CEA, Marcoule, France). Vienna, International Atomic Energy Agency, 1965, Preprint No. CN-22/18, 73p. (In French). (CONF-651105-25). ORAU.

From Conference on Nuclear Electronics, Bombay.

The systems used for chemical analysis of the coolant gas of the G2 and G3 reactors, for the measurement of the activity of the coolant gas, and for leak measurements on the coolant loops are described, and results obtained in operation of the reactors are presented. (D.C.W.)

18121 STATIC PROGRAMMING OF DATA HANDLING. Kovanic, P. (Inst. of Nuclear Research, Czechoslovak Academy of Sciences, Rez). Vienna, International Atomic Energy Agency, 1965, Preprint No. CN-22/56, 22p. (CONF-651105-22). ORAU.

From Conference on Nuclear Electronics, Bombay.

A method of digital data handling is proposed. The theoretical bases of the method are outlined, together with some applications of the method to the control of nuclear power plants and reactors. (D.C.W.)

18122 DESIGN FACTORS INFLUENCING THE CONTAINMENT OF INTERNAL EXPLOSION IN FAST REACTORS. Samuels, D. E. J. (Atomic Weapons Research Establishment, Southend-on-Sea, Eng.). 15p. (CONF-651009-17). ORAU. Gmelin, AED-CONF-65-307-18.

From Conference on Safety, Fuels, and Core Design in Large Fast Power Reactors, Argonne, Ill.

A study of the sequence of events following a core explosion and of the loading and response mechanisms occurring in the structure is summarized. (D.C.W.)

18123 A PARAMETER STUDY OF LARGE FAST REACTOR MELTDOWN ACCIDENTS. Meyer, R. A.; Wolfe, B.; Friedman, N. F. (General Electric Co., San Jose, Calif.). 28p. (CONF-651009-21). ORAU. Gmelin, AED-CONF-65-307-43.

From Conference on Safety, Fuels, and Core Design in Large Fast Power Reactors, Argonne, Ill.

The energy release from a fast reactor meltdown accident was studied to assess the importance of the various parameters involved. Modified Bethe-Tait calculations for a spherical 1000-Mwe oxide-fueled reactor were performed as a function of Doppler coefficient, neutron lifetime, pressure-energy relation, core composition, power flattening, and initial starting conditions. Calculations were also made for a cylindrical version of the Bethe-Tait equations. It was shown that with a large Doppler coefficient, one becomes relatively insensitive to the reactor parameters except for the heat capacity of the fuel and that for reactivity inputs of the order of tens of dollars per second, a large but attainable Doppler effect can limit the explosive energy release to a magnitude for which containment has been engineered in presently operating fast reactors. (auth)

Process Heat Reactors

18124 EFFECT OF THE UTILIZATION FACTOR ON THE ECONOMY OF HEAT-GENERATING ATOMIC POWER STATIONS. Halzl, Jozsef; Torma, Miklos. Energ. Atomtech., 18: 257-65(May-June 1965). (In Hungarian).

Recent economic studies indicated that heat-generating reactors become competitive only if the requirements are very high. Low-capacity, uneconomical plants are built primarily for the purpose of reducing the original investment costs while training the personnel. In such cases it was found preferable to build heat- rather than electricity-generating plants, basing the calculations on the performance of a small, 62.5-Mw, OMR-type power reactor which is able to satisfy a demand of 47×10^6 kcal/hour. Further calculations were carried out to improve the utilization factor, using the nuclear power cost data compiled for the 1961 general conference of IAEA. This parameter may be improved by taking certain administrative steps, such as operation during the night and during holiday periods, and by changes in the design. Use of a condensing system, inclusion of a fossile-fuel fired peak-load boiler and of a Ruths or Marguerre-type heat-storage unit were considered. The efficiency is also increased if the power plant is used as the central heat-supply station for several industrial complexes, especially if their peak-load periods do not coincide. Night-time operation of heat pumps is also recommended. (TTT)

Production Reactors

18125 (RL-SA-25) PENETRATION SEALS FOR N-REACTOR PLANT. Hoffman, Roy C.; Strong, Grant H. (General Electric Co., Richland, Wash. Hanford Atomic Products Operation). Mar. 8, 1965. Contract AT(45-1)-1350. 35p. Dep. mn. CFSTI $2.00 cy, $0.50 mn.

Gas tight seals between nuclear reactor ventilation system zones are a requirement for electrical system wall penetrations. These seals must prevent uncontrolled release of radioactivity. Seals were designed for the N-Reactor which represent an economical solution to the problem. (auth)

Propulsion and Space

See also ENGINEERING — Space Propulsion

18126 (EUR-2629.i(Vol.1)) NAVE CISTERNA A PROPULSIONE NUCLEAR (CON REATTORE DI TIPO COMPATTO AD ACQUA IN PRESSIONE A CIRCOLAZIONE FORZATA). Progetto Intermedio. (Nuclear-Powered Tanker (with Compact-Type Forced-Circulation Pressurized-Water Reactor). Intermediate Project). (FIAT, Turin (Italy). Sezione Energia Nucleare. Ansaldo S.p.A., Genoa (Italy)). Sept. 27, 1965. 456p. Dep. mn.

The results of a design study for a nuclear-powered tanker using a forced-circulation pressurized-water reactor are presented. (D.C.W.)

18127 (GA-6753(Pt.1)) GRAPHITE INTERFACE STUDIES. Technical Summary Report, May 16, 1963-September 30, 1965. Neill, J. M.; Bardes, R.; Beyster, J. R.; Young, J. A. (General Atomic, San Diego, Calif. John Jay Hopkins Lab. for Pure and Applied Science). Oct. 11, 1965. Contract AT(04-3)-167. 100p. Dep. mn. CFSTI $3.00 cy, $0.75 mn.

Neutron spectra in Be and graphite were studied experimentally and theoretically. Neutron spectra across temperature discontinuities in graphite, across interfaces

between poisoned and unpoisoned graphite, and across interfaces between Be and graphite were investigated. A more accurate lattice frequency spectrum was obtained for graphite, and the neutron total cross section of Be was calculated and was compared with experimental data. The effect of coherent scattering in Be on the differential reaction rate was also studied. It was concluded that the bound kernels for Be and graphite are superior for reactor calculations to the free-atom scattering kernel. (D.C.W.)

18128 DEVELOPMENT PROBLEMS OF NUCLEAR ROCKET ENGINES. Beveridge, J. H. (Aerojet-General Corp., Sacramento, Calif.). Ann. N. Y. Acad. Sci., 134: 304-16(Nov. 22, 1965).

The development and testing of the NERVA engine are briefly discussed. The major technical problems of the nuclear rocket engine are stressed, together with solutions to these problems. (D.C.W.)

18129 SHIP REACTOR DEVELOPMENT IN JAPAN. von zur Muehlen, M. (Gesellschaft fuer Kernenergieverwertung in Schiffbau und Schiffahrt mbH, Hamburg). Atomwirtschaft, 11: 91-2(Feb. 1966). (In German).

The construction of the oceanographic research ship of 6900 BRT plant as the first Japanese Atomic Ship has still not begun since the cost is higher than the budgeted means. However preliminary planning is still proceeding on the basis of a pressurized water reactor. The principal nuclear data and the data for ship and conventional machinery are tabulated. (J.S.R.)

18130 AUTOMATIZATION OF A NUCLEAR-SHIP REACTOR PLANT. Haebler, D. v. (Siemens-Schuckertwerke AG, Erlangen, Ger.). Kerntechnik, 8: 133-6(Mar. 1966). (In German).

The automated startup sequence of a nuclear-ship reactor plant was investigated and an example is given of the results obtained. In the study only the recooling system, the volume control system, the safety feed system, the components of the cooling circuit, and the coolant purification were considered. The sequence of steps in the startup from the cold state are shown in block diagram. (J.S.R.)

18131 AN EFFECT OF NUCLEAR-REACTOR OPERATION IN SPACE. Carpenter, Donald G.; Denfeld, Richard E.; Kronlund, Kenneth H. (Air Force Academy, Colo.). Nature, 209: 64(Jan. 1, 1966).

The effects of space environment on a reactor system are considered. It is suggested that the reactor system might achieve a noticeable positive potential while in operation. The magnitude of this effect was determined from some rough approximations. For a 1 Mw(t) reactor in a polar orbit at 1000 km the electrostatic energy stored was calculated to be 100 joules. (M.C.G.)

18132 SUDOVYE ATOMNYE ENERGETICHESKIE USTANOVKI. (Naval Nuclear Power Installations). Kudinov, N. N. Leningrad, Izdatel'stvo Sudostroenie, 1964. 332p.

The classification, construction, and properties of the basic equipment for naval nuclear power installations are described. The physical principles of the production of nuclear energy are reviewed. The basic theory of nuclear reactors and of the heat exchange in their active zone is presented. The main types and construction plans of existing and proposed nuclear power stations and nuclear ships are discussed. Methods for determining the steam–water cycle parameters and the efficiency of naval reactors are considered. Descriptions are given of the basic forms of nuclear fuel, materials for constructing basic equipment for reactors, materials used for biological shielding, methods for reloading reactors with fuel, auxiliary systems for naval nuclear power stations, and means of radiation safety control on nuclear ships. (M.J.T.)

Research and Test Reactors

Refer also to abstracts 16882 and 18092.

18133 (EUR-2625.e) THE BR2 TESTING REACTOR AND ITS CONNECTED LABORATORIES. Annual Progress Report, 1964. (Centre d'Etude de l'Energie Nucleaire, Mol (Belgium)). Nov. 3, 1965. 38p. Dep. mn.

The reactor and the associated laboratories are briefly described, and the fabrication and development of the irradiation devices used in the reactor are discussed. The research program carried out at the reactor is also outlined. (D.C.W.)

18134 (GEAP-4966) VIBRATION OF SEFOR FUEL RODS IN PARALLEL FLOW. Quinn, E. P. (General Electric Co., San Jose, Calif. Atomic Power Equipment Dept.). Sept. 1965. Contract AT(04-3)-540. 35p. Dep. mn. CFSTI $2.00 cy, $0.50 mn.

Tests were performed with a full-scale SEFOR fuel rod assembly to determine the rod vibration resulting from fluid flow. The maximum vibration for a normal rod assembly corresponding to reactor conditions was found to be 0.001 inch at 67 cps. Larger vibration at lower frequencies was measured for two other assemblies with a reduced number of axial supports. (auth)

18135 (IDO-17135) IN-TANK IRRADIATION FACILITIES AT THE TEST REACTOR AREA (STANDARD PRACTICES GUIDE). Ackaret, R. L.; Richardson, A. S. (Phillips Petroleum Co., Idaho Falls, Idaho. Atomic Energy Div.). Jan. 1966. Contract AT(10-1)-205. 81p. Dep. mn. CFSTI $3.00 cy, $0.75 mn.

An aid is presented for planning and designing capsule experiments for irradiations in the Test Reactor Area (TRA) facilities. Facilities available for capsule irradiations are described. Standard capsules and capsule holders or baskets are also described. A generalized discussion of typical designs of various types of capsules is included. In addition, the requirements for irradiation of capsule experiments are presented. (auth)

18136 (IS-1320) SURVEY OF ENVIRONMENTAL RADIOACTIVITY. Voss, Milo D. (Ames Lab., Iowa State Univ. of Science and Tech.). Dec. 1965. Contract W-7405-eng-82. 38p. Dep. mn. CFSTI $2.00 cy, $0.50 mn.

The environmental monitoring program is the pre-operational program for the Ames Laboratory Research Reactor (ALRR). The pre-operational environmental program consists of gross alpha and beta determinations of air, soil, vegetation, river water, bottom sediment, precipitation, and well-water samples. This report includes data for the period January 1, 1965 to December 31, 1965. The data indicate that the ALRR has not been a contributor to environmental radioactivity in the Ames area. The conclusion is reached that radioactivity levels recorded represent background conditions from atmospheric fallout and naturally occurring radioactivity. (auth)

18137 (KR-82) ORGANIC COOLED IRRADIATION LOOP IN THE HFR AT PETTEN. Boehler, Torstein; Skreppen, Helge (Institutt for Atomenergi, Kjeller (Norway)). Nov. 1965. 22p. Dep. mn.

The organic-cooled irradiation loop in the High Flux Reactor is described, and operating experience with the loop is summarized, together with the irradiation program. The loop is being used for studies of the effects of fast neutrons on pressure-vessel steels. (D.C.W.)

18138 (TID-22697) PROGRESS REPORT ON NORA PROJECT, OCTOBER 1–DECEMBER 31, 1965. (Institutt for Atomenergi, Kjeller (Norway)). Feb. 1966. Contract AT(30-1)-3498. 49p. (NC-73). Dep. mn. CFSTI $2.00 cy, $0.50 mn.

Two new H_2O moderated cores were investigated in NORA. A few macroscopic flux measurements and some intracell neutron density measurement were carried out in the two cores. A partial analysis of these measurements is presented. Reactivity worth measurements were made for several types of control rods. Both experimental and theoretical work for determining the zero power noise in NORA is discussed. (M.O.W.)

18139 TANGENTIAL CHANNELS AND CONSTRUCTION OF THE THERMAL COLUMN IN THE VVR-M REACTOR. Vasil'ev, G. Ya.; Konovalov, E. A.; Pankov, V. G.; Yashin, D. A. At. Energ. (USSR), 19: 465-7(Nov. 1965). (In Russian).

The design of the VVR-M reactor of the A. F. Ioffe Institute included 9 horizontal beamholes and a thermal column. The disturbing background γ radiation may be reduced by designing the beamholes in a tangential direction with respect to the core surface, allowing them to reach into the Be reflector or the water behind it. In that case only the secondary and induced γ radiation will be present. During Nov. 1961 and Sept. 1963 channels were drilled through the shielding, passing also through the thermal column. Water-filled plugs were fitted into the steel pipes lining the beamholes through the concrete. The various physical parameters, such as thermal neutron flux, Cd ratio, fast neutron flux, and γ radiation dose were determined in all the channels while the reactor was operated at 10 Mw with precisions of 20, 15, 40, and 20%, respectively. (TTT)

18140 THE INFLUENCE OF THE VVR-M ACTIVE ZONE CONFIGURATION ON THE NEUTRON SPECTRA FROM THE HORIZONTAL CHANNEL. **Vertebnyi, V. P.; Vlasov, M. F.; Kirilyuk, A. L. At. Energ. (USSR), 19: 467-8(Nov. 1965). (In Russian).**

The shape of the slow-neutron spectrum emitted by the core is effected by the core configuration in the vicinity of the beam. In order to obtain the highest neutron yield in a given spectral range with the lowest fast-neutron flux admixture, the optimum core configuration was determined on the basis of data obtained by the time-of-flight method. Replacement of a light moderator by a heavy one may increase the resonance neutron yield; therefore such tests were carried out in the beamholes of the VVR-M reactor of the Academy of Sciences, determining the changes in the spectrum caused by changes in the core near the beamhole. The following neutron sources were used in these experiments: a. fuel elements only; b. fuel elements with a 5.5-cm thick water layer; and c. fuel elements with a 5-cm thick Be layer. The results indicated an intensity gain of nearly 2 for water and Be; the signal/background ratio was also increased by a factor of nearly 2. In the resonance region the count rate was about 1.4 times higher in the case of Be, as compared with the other two cases. Thus, the configuration including the Be moderator was considered to be the best one. (TTT)

18141 REACTOR FOR UNIVERSITY INSTRUCTION. **Raszl, Karoly. Energ. Atomtech., 18: 527-35(Nov. 1965). (In Hungarian).**

During the decade of the fifties more than 60 reactors were placed in operation at educational institutions in the United States. This development was slower in Europe but even so, by 1964, 34 university reactors were installed there. Design of these reactors must take into account that they are to be used for demonstrating reactor operation problems—startup, shutdown; reactor physics experiments—determination of critical mass, reactor period, rod characteristics; nuclear physics measurement—absorption and scattering cross section measurements; engineering studies—activation of coolant and corrosion products; mechanical and electrical engineering studies; radiation chemistry experiments—preparation of short-half-life isotopes, etc. A reactor satisfying these requirements was designed for use at the Technical University, with a maximum power level of 10 kw. The fuel elements consisted of U containing 10% of ^{235}U clad with Al. The core was surrounded by a graphite ring to reduce the critical mass and to increase the volume available for experiments. Light water served as moderator, coolant and reflector. Details of the experimental beamholes, safety and control equipment and the radiation protection system are given together with the architectural features of the reactor building. The latter was affected by the location of the existing buildings on the campus and by the level of the ground water table connected with the Danube River. (TTT)

18142 DISTRIBUTION OF SOME FISSION PRODUCTS BETWEEN CORE AND RECOMBINER OF L54M REACTOR. PART 5. EFFECT OF Cu^{2+} CONCENTRATION IN THE FUEL ON THE ESCAPE PROBABILITY OF IODINE. **Lazzarini, E.; Sangiust, V.; Terrani, M. (CESNEF, Milan). Energia Nucl. (Milan), 13: 82-4(Feb. 1966).**

It is shown that copper ions in the fuel of the L54M reactor displace the iodine from elementary form to others, perhaps iodide and iodate, which have negligible vapor pressure. As a consequence the transfer of iodine from core to recombiner is lowered by the presence in the fuel of copper ions. (auth)

18143 CALCULATION OF LATTICE PARAMETERS OF THE WWER CORE FOR COMPARISON WITH EXPERIMENTAL RESULTS ON CRITICAL ASSEMBLIES. **Mueller, A.; Zenker, W. (VEB Atomkraftwerk, Berlin). Kernenergie, 8: 602-5(1965). (In German).**

Lattice parameters for assemblies of fuel element bundles of the WWER type with uniform and different ^{235}U enrichment were calculated by the programs GRUPA and EMMI and compared with the values determined experimentally on critical assemblies. Although the calculational methods are relatively simple, a good agreement resulted between the experimentally determined and the calculated values of the material buckling B_m^2, an effective migration area M_m^2 and the infinite multiplication factor k_∞ of the lattice. (auth)

18144 DYNAMIC BEHAVIOR OF A RESEARCH REACTOR. **Wolter, W. (VEB Atomkraftwerk, Berlin). Kernenergie, 8: 606-10(1965). (In German).**

With a digital computer program the dynamic behavior of of 10 Mw(th) research reactor WWRM was determined at reactivity change rates of 0.01 and 0.1%/s. Because the reactivity change between zero and full power is small, the neutron density exceeds the values at nominal power; partially there are considerable neutron density peaks. (auth)

18145 INDIVIDUAL REACTOR CELL TEMPERATURE COEFFICIENT MEASUREMENTS. **Chrysochoiedes, N. G. (Nuclear Research Center Democritus, Athens). Kerntechnik, 8: 30-2(Jan. 1966).**

A new experimental approach is given for studying reactor temperature coefficients. The method consists in measuring the temperature coefficient of each individual cell of the core and reflector by separately heating the individual cell coolant while the temperature of the rest of the reactor remains constant. The measurements are performed at very low power levels so that no temperature perturbations are produced by fission heat. The experiments were made at the Democritus Swimming Pool Reactor but they could be applied to other types of reactors where provisions were made for circulating the coolant. (auth)

18146 IRRADIATION POSSIBILITIES AND SAFETY CONSIDERATIONS CONCERNING SIMPLE IRRADIATIONS AT THE REACTOR FR 2. **Dienst, W.; Marth, W. (Kernforschungszentrum, Karlsruhe, Ger.). Kerntechnik, 8: 121-7(Mar. 1966). (In German).**

In simple irradiation experiments it is necessary to know the geometric dimensions of the channels, their neutron and γ flux densities, reactivity limitations, and the cooling of the sample in the individual positions. These data are presented for the FR 2 reactor by means of diagrams and tables. (J.S.R.)

18147 MEASUREMENT OF THE SLOW NEUTRON SPECTRUM OF A NEUTRON BEAM FROM THE UA-RR-1 REACTOR BY TIME-OF-FLIGHT SPECTROMETER. **Hamouda, I.; Maayouf, R.; Stupak, A.; Nesterenko, V.; Salama, M.; El-Ela, M. Abu (Atomic Energy Establishment, Cairo). Nucl. Instrum. Methods, 40: 153-4(Feb. 1966).**

The measurement of the thermal neutron spectrum of one of the horizontal channels of the UA-RR-1 reactor, using the time-of-flight method, is described. Neutrons from a horizontal channel of 60-mm diameter are chopped by a mechanical chopper. A schematic diagram of the arrangement of this mechanical chopper and a schematic diagram of the position of fuel elements at the beam exit are shown. The slow neutron spectrum of the beam, the experimental points, and the Maxwellian spectrum for T = 325°K are given. The obtained results are in good agreement with those which were obtained under similar conditions. (J.F.P.)

18148 THE NEW SWIMMING POOL REACTOR. OSIRIS WILL GO CRITICAL AT SACLAY IN 1966. Goujon, Jean Sci. Progr.-Nature, No. 3366, 395-8(Oct. 1965). (In French).

The neutron economy, heat exchangers, and safety and operability of the Osiris swimming pool reactor are briefly described. (J.S.R.)

18149 SOME DESIGN ASPECTS OF INSTRUMENTATION FOR CONTROL AND SAFETY OF ZERO ENERGY REACTOR ZERLINA. Venkateswarlu, U.; Viswanathan, L.; Pansare, M. G.; Nagle, A. K. (Atomic Energy Establishment, Trombay, India). Vienna, International Atomic Energy Agency, 1965, Preprint No. CN-22/36, 23p. (CONF-651105-30). ORAU.

From Conference on Nuclear Electronics, Bombay.

Some of the special conditions that exist in the Zerlina reactor are described, and their influence on the design of the neutron-flux instrumentation of the reactor is discussed. (D.C.W.)

18150 APPARATUS FOR MEASURING FAST DOUBLING TIMES OF THE CABRI REACTOR. Friedling, G. (CEN, St. Paul-lez-Durance, France). Vienna, International Atomic Energy Agency, 1965, Preprint No. CN-22/8, 28p. (In French). (CONF-651105-14). ORAU.

From Conference on Nuclear Electronics, Bombay.

An apparatus that was developed for the measurement of doubling times as short as 1 msec in the Cabri reactor is described. The theoretical accuracy and bases of the apparatus are briefly discussed. (D.C.W.)

18151 AUTOMATIC CONTROL SYSTEM OF THE PEGGY REACTOR. Friedling, G. (CEN, St. Paul-Lez-Durance, France). Vienna, International Atomic Energy Agency, 1965, Preprint No. CN-22/23, 21p. (In French). (CONF-651105-15). ORAU.

From Conference on Nuclear Electronics, Bombay.

The automatic control system that was designed to replace the original control system of the PEGGY reactor is described. (D.C.W.)

18152 CONTROL AND SAFETY ASSEMBLY FOR REACTORS OF VERY HIGH FLUX. Jover, P.; Uberschlag, J.; Furet, J. (CEN, Saclay, France). Vienna, International Atomic Energy Agency, 1965, Preprint No. CN-22/15, 12p. (In French). (CONF-651105-21). ORAU.

From Conference on Nuclear Electronics, Bombay.

An automatic system that was developed for the correction of the gain of the amplifiers for the effects of disturbances in the detectors is described. (D.C.W.)

WASTE DISPOSAL AND PROCESSING

See also BIOLOGY AND MEDICINE — Ecology
CHEMISTRY — Radiochemistry
CHEMISTRY — Separation Processes and Procedures
HEALTH AND SAFETY

18153 (AED-C-01-12) AUSGEWAEHLTES SCHRIFTTUM NACH SACHGEBIETEN. BAUWESEN. BESEITIGUNG RADIOAKTIVER ABFALLSTOFFE. TEIL I. (Selected Literature According to Subject Field. Construction Engineering. Disposal of Radioactive Waste Material. Part I). (Zentralstelle fuer Atomkernenergie-Dokumentation, Gmelin-Institut fuer Anorganische Chemie und Grenzgebiete, Frankfurt am Main (West Germany)). 1965. 142p. Dep. mn.

Abstracts of 127 papers dealing with various aspects of the disposal of radioactive waste material are presented. (M.O.W.)

18154 (AED-C-01-13) AUSGEWAEHLTES SCHRIFTTUM NACH SACHGEBIETEN. BAUWESEN. BESEITIGUNG RADIOAKTIVER ABFALLSTOFFE. TEIL II. (Selected Literature According to Subject Field. Construction Engineering. Disposal of Radioactive Waste Material. Part II). (Zentralstelle fuer Atomkernenergie-Dokumentation, Gmelin-Institut fuer Anorganische Chemie und Grenzgebiete, Frankfurt am Main (West Germany)). 1965. 99p. Dep. mn.

Abstracts of 84 papers on various aspects of radioactive waste disposal are presented. (M.O.W.)

18155 (BNWL-157) TRANSIENT THERMAL BEHAVIOR IN FIXATION OF RADIOACTIVE MATERIALS. Jansen, G. Jr.; DeMier, W. V. (Battelle-Northwest, Richland, Wash. Pacific Northwest Lab.). Jan. 1966. Contract AT(45-1)-1830. 123p. Dep. mn. CFSTI $4.00 cy, $0.75 mn.

Dimensionless correlations are given for the thermal history of cylindrical, infinite-slab, and annular heat-generating radioactive material containers after fixation at elevated temperatures. The maximum temperatures attained are presented as functions of heat generation rate, initial temperature, container geometry, thermal conductivity, and environmental heat transfer coefficients. The effect of heat losses through the ends of a solid cylindrical container is also presented for steady state conditions. Several examples are given as an aid to calculations. Computer programs for more detailed estimation of thermal histories in slabs, cylinders, and annuli are appended. (auth)

18156 (BNWL-SA-453) VOLATILIZATION OF FISSION PRODUCTS FROM HIGH LEVEL CERAMIC WASTES. Albrethsen, A. E. (Battelle-Northwest, Richland, Wash. Pacific Northwest Lab.). Feb. 8, 1966. Contract AT (45-1)-1830. 17p. (CONF-660208-5). Dep. mn. CFSTI $1.00 cy, $0.50 mn.

From Symposium on Solidification and Long-Term Storage of Highly Radioactive Wastes, Richland, Wash.

Volatilization was established as the predominant mechanism of fission product release from simulated high level solidified waste of differing phosphate content when exposed to high temperatures. Waste representative of fuel ranging from 20,000 to 100,000 Mwd/t exposure was used. Cesium-137 was found to be the isotope of greatest radiological concern from the standpoint of airborne release during a shipping accident fire. Fractional release rates at 1100°C for cerium, ruthenium, and strontium were at the lower detection limits of the experiment (approximately 10^{-3} percent/hour) while average cesium release rates of about ½ percent/hour were observed under the same exposure conditions. (auth)

18157 (BNWL-SA-466) DISPOSAL OF RADIOACTIVE WASTES INTO FRESH WATER. Honstead, J. F. (Battelle-Northwest, Richland, Wash. Pacific Northwest Lab.). Sept. 24, 1965. Contract AT(45-1)-1830. 36p. Dep. mn. CFSTI $2.00 cy, $0.50 mn.

Studies were made on the dilution, dispersion, deposition, removal, and transformation, and reconcentration of radioactive materials in fresh waters in order to estimate the movement and fate of the radionuclides in a water system, and also to estimate the degree of hazard involved. The processes of metabolic concentration by fish and wildlife are also considered. Aquatic foodstuffs were monitored for ^{32}P and ^{65}Zn. It was concluded that discharge of waste water into a fresh water system should be accompanied by an intensive monitoring program which includes special studies that detect the behavior and fate of radionuclides in the biological communities affected. (P.C.H.)

18158 (BNWL-SA-467) THE WASTE SOLIDIFICATION ENGINEERING PROTOTYPES TECHNICAL PROGRAM. Cooley, C. R.; Platt, A. M. (Battelle-Northwest, Richland, Wash. Pacific Northwest Lab.). Feb. 1, 1966. Contract AT(45-1)-1830. 25p. (CONF-660208-6). Dep. mn. CFSTI $1.00 cy, $0.50 mn.

From Symposium on Solidification and Long-Term Storage of Highly Radioactive Wastes, Richland, Wash.

The objectives and future plans for the Waste Solidification Engineering Prototypes are discussed. The emphasis on specific safeguard, technical, and economic evaluations and the program steps to achieve demonstration of solidification methods are outlined for an Oak Ridge National Laboratory pot calcination and rising level glass process, a Pacific Northwest Laboratory spray solidification process, and a Brookhaven National Laboratory phosphate glass process. Plans for the first portion of the program are reviewed. (auth)

18159 (BNWL-SA-514) SURVEY OF METHODS FOR THE TREATMENT AND DISPOSAL OF GLASS MELTER CONDENSATES CONTAINING SULFURIC ACID. Mercer, B. W.; Touhill, C. J.; Coleman, L. F.; Svoboda, C. J. (Battelle-Northwest, Richland, Wash. Pacific Northwest Lab.). Feb. 2, 1966. Contract AT(45-1)-1830. 14p. (CONF-660208-7). Dep. mn. CFSTI $1.00 cy, $0.50 mn.

From Symposium on Solidification and Long-Term Storage of Highly Radioactive Wastes, Richland, Wash.

Methods for the treatment of sulfuric acid condensate from the phosphate glass melter were investigated. Projected fission product concentrations in the condensate were estimated to be more than 100 C/gal (predominantly ruthenium) when processing wastes from 20,000 Mwd/t fuel. Two general approaches were taken for the treatment and disposal of the condensate: conversion of the condensate or the sulfate contained therein to solids which retain all or a portion of the fission products; and separation of the sulfate from the fission products which would be recycled to the glass process. (auth)

18160 (CEA-R-2894) DISPOSITIF DE RECUPERATION D'EFFLUENTS RADIOACTIFS. (Device for Recovering Radioactive Waste). Mas, Roland (Commissariat a l'Energie Atomique, Saclay (France). Centre d'Etudes Nucleaires). Nov. 1965. 9p. Dep. mn.

A new system is presented, which consists essentially of a standard reservoir of stainless steel fixed in a concrete well lined with stainless steel. Each reservoir has a standard lid on which are placed all the accessory devices, which are standardized. The new reservoirs offer a great degree of security, and are interchangeable; the wells are easy to decontaminate and it is possible to work

in a well without any danger of the personnel being irradiated by neighboring reservoirs. (P.C.H.)

18161 (ISO-SA-1) OPERATING EXPERIENCE ON IN-TANK SOLIDIFICATION OF RADIOCHEMICAL WASTES. Shefcik, J. J. (Isochem Inc., Richland, Wash.). [nd]. Contract AT(45-1)-1851. 19p. (CONF-660208-8). Dep. mn. CFSTI $1.00 cy, $0.50 mn.

From Symposium on Solidification and Long-Term Storage of Highly Radioactive Wastes. Richland, Wash.

Operation of the First In-Tank Solidification Unit is described. Radiochemical waste solutions are evaporated within a 750,000-gallon underground tank by sparging with air electrically heated to 1200°F. The air sparger is also an air-lift circulator used for agitation. To minimize entrainment, most of the heat is transferred to the solution by passing the air down the hollow wall of the circulator-sparger. Stud fins improve heat transfer. The off-gas is filtered and dehumidified, producing effluent streams low in residual radioactivity. Decontamination factors of $>10^4$ are obtained. Radiochemical wastes are added as evaporation occurs. After concentration by a factor of 4 to 6, the concentrate will solidify on cooling. (auth)

18162 (NP-15754) THE MINIMUM ATMOSPHERIC DILUTION OF LONG-TERM AND SHORT-TERM EMISSIONS FROM THE EUROCHEMIC CHIMNEY. Alderhout, J. J. H. (European Company for the Chemical Processing of Irradiated Fuels, Mol (Belgium)). June 1965. 27p. (ETR-173). Dep. mn. CFSTI $2.00 cy, $0.50 mn.

An estimate was made of the minimum long-term average atmospheric dilution (for routine emissions) and the minimum short-term atmospheric dilution (for accidental release) for the Eurochemic main plant chimney. The estimates were made with the aid of the Gaussian plume model. The results showed that a non-depositing, long-term, continuous emission of one curie per second from the Eurochemic plant chimney can be estimated to give rise to an average air concentration at ground level of a maximum of approximately 2×10^{-7} C/m^3 at the most unfavorable spot. This spot lies in the direction 240° (ENE) at some 3 kilometers from the Eurochemic stack. A non-depositing, short-term emission of one curie from the Eurochemic plant chimney can be estimated to give rise to a total integrated concentration of a maximum of approximately 3×10^{-5} C s/m^3 during the most unfavorable weather conditions (fumigation). The place of maximum total integrated concentration lies at about 0.5 km from the Eurochemic stack. It is thought that the values found are realistic though conservative ones. (auth)

18163 (NP-15859) HYDRODYNAMICS OF THE DISPOSAL OF LOW-LEVEL LIQUID RADIOACTIVE WASTES IN SOIL. Final Report. Mackrle, Vladimir; Dracka, Oldrich; Svec, Jan (Czechoslovak Academy of Sciences, Prague. Inst. of Hydrodynamics). 1965. IAEA Contract No. 98. 142p. Dep. mn.

The general aspects of liquid flow carrying suspension through a porous medium was studied in order to obtain data that might serve in evaluating the applicability of injection for the disposal of the radioactive sludge. Theoretical and laboratory studies were made on: injection of diluted suspension; injection of concentrated sludge; and two-dimensional filling of geological formations. The results offer a theoretical basis for the formulation of the requirements for a suitable geological structure as well as for the technology of injection. (P.C.H.)

18164 (NP-15874) THE EVAPORATION OF RADIOACTIVE WASTES BY SOLAR ENERGY. Report No. 2 (Final). Amarantos, S.; Hatzikakidis, A. ("Democritus" Nuclear Research Center, Athens (Greece)). Dec. 1965. Contract 224/RB. 33p. Dep. mn.

The feasibility of using solar energy in the evaporation of radioactive wastes was studied. A semi-pilot plant device (solar evaporator) was designed and constructed based on the existing information on the various applications of solar energy. The solar evaporator was installed in the open air and operated for almost three months (September to November 1965). The results showed that solar evaporation of radioactive liquids in open air is possible without the danger of contaminating the environment. Also, the following evaporating capacities were received: approximately 20 liters per eight hours (8.00–16.00) when the maximum temperature of the evaporated liquid was approximately 50°C. (auth)

18165 (ORNL-P-1987) PROJECT SALT VAULT: DESIGN AND DEMONSTRATION OF EQUIPMENT. Schaffer, W. F. Jr.; Boegly, W. J. Jr.; Parker, F. L.; Bradshaw, R. L.; Empson, F. M.; McClain, W. C. (Oak Ridge National Lab., Tenn.). [1964]. Contract W-7405-eng-26. 36p. (CONF-660208-4). Dep. mn. CFSTI $3.00 cy, $0.50 mn.

From Symposium on Solidification and Long-Term Storage of Highly Radioactive Wastes, Richland, Wash.

Handling, transfer, and storage techniques applicable to high-level solid waste disposal operations were successfully demonstrated with short-cooled ETR fuel assemblies. The design of Project Salt Vault equipment for the encapsulation of the fuel assemblies, cross country shipment, transfer from the surface to the mine level, movement within the mine, and transfer into storage is described. The operations are unique in that high-level radioactive materials are transferred from a shipping cask on the surface to the mine level 1000 feet below without the use of hot cells. (auth)

18166 (TID-22531) INVESTIGATION OF MATERIALS AND METHODS FOR FIXATION OF LOW AND MEDIUM LEVEL RADIOACTIVE WASTE IN STABLE SOLID MEDIA. Progress Report, February 1–October 31, 1965. Rastogi, R. C.; Sehgal, J. D.; Thomas, K. T. (Atomic Energy Establishment, Trombay (India)). Dec. 4, 1965. Contract No. 261/US. 48p. Dep. mn. CFSTI $2.00 cy, $0.50 mn.

The results of fusion studies on incinerator ash from the pilot incinerator and synthetic chemical treatment plant sludge obtained as secondary wastes in the treatment of radioactive liquid effluents are described. The leaching characteristic of the fused mass and the volume reduction obtainable were studied. A method for evaluating loss on volatilization during firing, using stable cesium salt and flame photometry for the estimation of volatilized cesium, is described. Results are presented. Details of a pilot furnace under fabrication, proposed to be used for preparing 20–50 kg batches of glass using inactive wastes, and suggestions for future work are also included. (auth)

18167 ROLE OF WASTE MANAGEMENT AT EUROCHEMIC. Marcus, F. R. (Eurochemic Co., Mol, Belg.). Atompraxis, 12: 50-3(Jan. 1966).

More waste streams of different compostions are created in the multipurpose plant than in any other known processing plant in operation. A major task of Eurochemic is considered to be to demonstrate that waste management can be done in a simple, safe, and economic manner despite the unfavorable plant location and the extremely low discharge limits. The different waste groups and their handling, the principles for design of equipment, and the development work to solve the problem of decladding waste that is specific to Eurochemic are discussed. (auth)

18168 SOFTENING AND DECONTAMINATING WASTE WATER BY CAUSTIC-CARBONATE PRECIPITANTS IN A SLOWLY-STIRRED SLUDGE-BLANKET COLUMN. Schonfeld, E.; Davis, W. Jr. (Oak Ridge National Lab., Tenn.). Health Phys., 12: 407-15(Mar. 1966).

In order to reduce the concentration of calcium in low-radioactivity-level process waste water and thereby make the water more suitable as a feed to a countercurrent foam column in which strontium and other radioactive nuclides can be removed, a modified lime-soda precipitation process was developed. The process consists in adding sodium carbonate and sodium hydroxide to the water to a concentration of 0.005 M each (calculated before chemical reaction) and using a slowly stirred, suspended-bed sludge column to remove (by a filtering action) the resulting calcium carbonate and magnesium hydroxide. With this procedure, and with Fe^{3+} (a few parts per million) as a coagulant, the residual hardness of the water was reduced at 5 ppm (as $CaCO_3$) or less. This low value was achieved with

sludge columns of diameter up to 9 in., at water flow rates up to 60 gal/ft^2/hr, at sludge-height to column-diameter values of 4 to 0.5, and at stirring-paddle peripheral rates of 5 to 10 in./sec. With ORNL low-radioactivity-level process waste water as feed, the radionuclide decontamination factors across the sludge column were as follows: 10 to 15 for ^{90}Sr, 30 to 40 for ^{144}Ce, 10 to 50 for ^{60}Co, 1.7 to 2.2 for ^{106}Ru and 1.1 for ^{137}Cs. The calcium concentration can be reduced to a point such that it will not significantly interfere with subsequent removal of strontium in a foam separation column. The degrees of softening and decontamination are significantly better than can be achieved in the ORNL lime-soda plant. The process is being evaluated on a 15,000 gal/day basis. (auth)

18169 PROJECT SALT VAULT: A DEMONSTRATION DISPOSAL OF HIGH-LEVEL RADIOACTIVE SOLIDS IN LYONS, KANSAS, SALT MINE. Boegly, W. J. Jr.; Bradshaw, R. L.; Empson, F. M.; Schaffer, W. F. Jr.; Parker, F. L.; Blomeke, J. O. (Oak Ridge National Lab., Tenn.). Health Phys., 12: 417-24(Mar. 1966).

The demonstration of the disposal of high-level radioactive waste solids in salt mines is reported. Fourteen irradiated fuel assemblies from the Engineering Test Reactor will serve as a source of radiation, since high-level solidified wastes do not exist at the present time. The assemblies will be placed in a circular array of holes in the floor of a newly mined area (14 ft above the existing mine floor) with one can in the center and the other six cans located peripherally, spaced 5 ft on centers. During the course of the 2-year test, four sets of assemblies will be used to achieve a peak dose in the salt of about 8×10^8 rad and the temperature of the salt adjacent to the center hole will be maintained at 200°C with supplementary electrical heaters. A second radioactive array, located in the existing mine floor, will receive the fuel canisters which are removed from the main array at the end of each 6-month period. The purpose of this array is to study the problems that may be encountered if the waste containers are located in salt interbedded with water-bearing shale. A third array, consisting only of heaters, will be operated as a control to determine those effects due solely to heat. In addition to the radioactive and control arrays, a rib-pillar located between the main radioactive array and the control array will be heated electrically around its base to produce significant information on salt flow characteristics and mine stability at elevated temperatures. Preparation of the four experimental rooms will involve the mining of approximately 19,000 tons of salt. Placing of the first fuel assembly cans in the mine is expected to take place in November 1965. (auth)

18170 UTILIZATION OF MULTICLONE DUST FOR DECONTAMINATING SEWAGE WATERS CONTAINING ^{137}Cs AND ^{90}Sr/^{90}Y. Otto, R.; Hecht, P. (Institut fuer Angewante Radioaktivitaet, Leipzig). Kernenergie, 8: 643-5(Nov. 1965). (In German).

The results of some experiments concerning the use of multiclone dust for decontaminating sewage waters containing ^{137}Cs and ^{90}Sr/^{90}Y are given. Multiclone dust is a product of gasifying coke in the Winkler generator. Studies carried out on a laboratory scale using model waters showed that the surface-active material is suitable for the separation of the radionuclides mentioned. (auth)

18171 DECONTAMINATION OF RADIOACTIVE WASTES OF THE KARLSRUHE NUCLEAR RESEARCH CENTER FROM 1963 TO 1965. Krause, H.; Nentwich, O. (Kernforschungszentrum, Karlsruhe, Ger.). Kerntechnik, 8: 105-10(Mar. 1966). (In German).

A vapor compression evaporator and an installation for the fixation of radioactive wastes in bitumens were constructed. The amount and activity of the waste processed is given. The procedures followed in the decontamination are outlined and the decontamination factors obtained in each step are discussed. (J.S.R.)

GENERAL AND MISCELLANEOUS

18172 (BNWL–208) AN EVALUATION OF THE USE OF SELECTIVE DISCHARGES FROM LAKE ROOSEVELT TO COOL THE COLUMBIA RIVER. Jaske, R. T. (Battelle-Northwest, Richland, Wash. Pacific Northwest Lab.). Feb. 1966. Contract AT(45-1)-1830. 88p. Dep. mn. CFSTI $3.00 cy, $0.75 mn.

The general operation of the annual Columbia River cooling program for 1963, 64, and 65 is reviewed. The evaluation includes the complete development of the river including Wells Dam and is drawn from the parametric variation of Grand Coulee mixed discharge temperatures. It was concluded that reported effects have been somewhat overstated due to two primary causes: the incorrect assumption that the spill flow is drawn primarily from the upper 5 to 10 ft of the lake; and an unfortunate accumulation of temperature data inaccuracies emanating from the temporary or expedient installation of data input sources. Additional research on the formation and scope of subsurface jet flow in Lake Roosevelt and other large reservoirs in the system is essential to develop an optimal plan which will minimize river temperatures. (P.C.H.)

18173 (LA–3455) REZONE—A PROPOSAL FOR ACCOMPLISHING REZONING IN TWO-DIMENSIONAL LAGRANGIAN HYDRODYNAMICS PROBLEMS. Browne, Philip L. (Los Alamos Scientific Lab., Univ. of California, N. Mex.). Sept. 21, 1965. Contract W-7405-eng-36. 20p. Dep. mn. CFSTI $2.00 cy, $0.50 mn.

A proposed numerical experiment is described, in which an attempt is made to provide a code that will rezone a two-dimensional Lagrangian hydrodynamics problem by allowing mass and the related momenta and internal energy to be transferred from one zone to another as the grid lines are moved through the material. (auth)

18174 (NP–15771) REPORT ON THE ACTIVITIES OF THE DANISH ATOMIC ENERGY COMMISSION, APRIL 1, 1964–MARCH 31, 1965. (Atomenergikommissionen, Roskilde (Denmark)). Oct. 1965. 96p. Dep. mn.

Continued activities along the lines of those in previous years are reported. Work by the atomic power committee toward development of atomic power stations is discussed. Work done in the various departments and sections at Risø is summarized. Activities directed toward international cooperation in peaceful uses of atomic energy are reported along with other activities such as Greenland geological investigations, education and training, presentation of general information, programming the visit of NS Savannah, operation of the Atomic Energy Commission library, and patent administration. Information is also included on administration, mutual assistance with other nations in radiation accidents, and publications. (J.R.D.)

18175 (ORNL–3900) ANNUAL REPORT, 1964. (Oak Ridge National Lab., Tenn.). Contract W-7405-eng-26. 208p. Dep. mn. CFSTI $6.00 cy, $1.25 mn.

Information on research and development progress is reported in four sections. A separate abstract was prepared for each section. A fifth section on training, education, and information centers is also included. (J.R.D.)

For abstracts of individual sections see: 16159, 16914, 17158, and 18020.

18176 (SCL–DR–66–6) MATERIALS MARKING SYSTEM. Wishart, R. C. (Sandia Corp., Livermore, Calif.). Feb. 1966. Contract AT(29-1)-789. 17p. Dep. mn. CFSTI $1.00 cy, $0.50 mn.

A marking system for positive identification of material samples exposed to a nuclear blast environment is described. The system involves assigning a unique notch to each material sample prior to exposure. (TCO)

18177 (TID–3733) BIBLIOGRAPHIES OF ATOMIC ENERGY LITERATURE. Issued or in Progress During the Period, December 1965–January 1966. (Division of Technical Information Extension (AEC), Oak Ridge, Tenn.). 16p. DTI Extension Free.

Seventy-six references are given to bibliographies on atomic energy issued or in preparation during the period Dec. 1965 through Jan. 1966. Subject, author, and report number indexes are included. (P.C.H.)

18178 (TID–22703) AN EVALUATION OF EXISTING CRITERIA FOR JUDGING THE QUALITY OF SCIENCE EXHIBITS. Final Report. Shettel, Harris H.; Reilly, Pamela C. (American Institutes for Research, Pittsburgh, Pa.). Nov. 1965. 86p. Dep. mn. CFSTI $1.00 cy, $0.75 mn.

A rating scale for evaluating scientific and technical exhibits is presented. The scale was also tested to determine its reliability and adequacy of coverage. On the basis of the data obtained from the tryouts, the scale was revised so as to combine or eliminate redundant items, to clarify ambiguously-worded items, and to incorporate new items dealing with features considered important aspects of exhibit effectiveness by the tryout subjects and the project staff, but which had not been documented through the literature survey. The revised scale was thus more rational and less empirical than the original scale. An annotated bibliography of the exhibit literature that was used to develop the rating scale is appended. The initial and final versions of the scale are also included as appendices. (96 references). (P.C.H.)

18179 (Y–1508) POLYVINYL PLASTISOL QUALITY STUDY. Schmitt, C. R. (Union Carbide Corp., Oak Ridge, Tenn. Y-12 Plant). Mar. 9, 1966. Contract W-7405-eng-26. 20p. Dep. mn. CFSTI $2.00 cy, $0.50 mn.

Laboratory studies were made on samples of various production quantities of polyvinyl chloride plastisols to determine the cause of cracks, blisters, and other imperfections in flexible molds made from the material by heat curing. Moisture was found to be the major troublesome contaminant of those batches that produced cured molds of inferior quality. Although the quality of the plastisol could be upgraded by vacuum treatment to remove moisture, degradation re-occurred after subsequent exposure to a moist atmosphere. (auth)

18180 EURATOM'S ROLE IN THE CREATION OF A NUCLEAR INDUSTRY. Ydo, H. J. (EURATOM, Brussels). EuroNuclear, 3: 83-4(Feb. 1966).

Creation of a nuclear industry in the European Atomic Energy Community is discussed. The market, the industry, and problems in the development of nuclear industry are considered. (M.C.G.)

18181 RESEARCH CENTRES IN EUROPE. NO. 14. SACLAY. EuroNuclear, 3: 93-100(Feb. 1966).

Research programs at Saclay are reviewed. The EL-2, EL-3, and OSIRIS research reactors are described. The Van de Graaffs, cyclotrons, linear accelerators, and Saturne proton synchrotron are described, and research programs being carried out with them are discussed. Critical facilities and active handling facilities are described. Physics research and reactor developments are considered. Studies on nuclear materials and scientific support work are discussed. (M.C.G.)

18182 ATOM ENERZHISININ KHALG TESERRUFATYNDA TETBIGI (ENERKETIKADA, NEFT SENAJESINDE VE TEKHNIKADA). (Utilization of Atomic Energy in the National Economy (Power Production, Petroleum Industry, and Technology)). Shirinov, Kh. Baku, Azerbajchan Dovlet Neshrijjaty, 1965. 240p. (In Azerbaidzhan).

Following a brief discussion of nuclear fission phenomena and concepts, detectors and counters and basic principles of nuclear reactors, the following reactor materials and their properties are considered: uranium, thorium, plutonium,

uranium compounds, ceramics, graphite, beryllium, and zirconium. Various types of reactors are described, with some details on the HFIR, Indian Point, Voronezh, Consolidated Edison, General Electric, gas-cooled, graphite-sodium, and homogeneous reactors and other specific installations. Heat-exchange systems are discussed, and the SNAP concepts are illustrated. Radioisotope gages mentioned include those for neutron-gamma and gamma-gamma logging in petroleum fields and gages for thickness, level, and density measurements. Ionization gages, gages for measuring snow depths, and the portable GUP-Co-50 gamma source unit are described. Among tracer uses discussed are pipeline leak detection, labeled fertilizers for plant growth studies and brain tumor and thyroid studies. Dosimetry and instrumentation are also covered. (TTT)

18183 NUCLEAR ENERGY IN THE NETHERLANDS—ORGANIZATION, LEGISLATION, TRAINING. The Hague, Interdepartmental Committee on Nuclear Energy, [1965]. 53p.

The organization of studies on nuclear energy in the Netherlands is described. Legislation on transport and storage of radioactive materials, operation of nuclear installations, exploration and processing radioactive ores, imports and exports, public health and protection of labor, and third-party liability is reviewed. Training is also considered. (M.C.G.)

CORPORATE AUTHOR INDEX

This index contains entries for this period for all report literature and, in addition, for certain published literature items for which it is felt that a corporate approach is especially desirable, e.g., symposia, conference proceedings, and meetings.

Each entry under a corporate author is a shortened version of the title of the publication, followed by the *NSA* volume and abstract number. Report numbers are given in parentheses.

The phrase "Progress report" is abbreviated as "Prog. rpt.," permitting a more rapid and complete alphabetical arrangement of the titles without changing the location of the progress report titles in relation to the other titles.

A

AERO VAC CORP., TROY, N. Y.
Prog. rpt. on O–Nb reaction at 1500 to 2000°F, final, 2/14/65, 20: 16971 (N-65-18444)

AEROJET-GENERAL CORP., AZUSA, CALIF.
Prog. rpt. on SNAP-8 materials, semiannual, 1–6/65, 20: 16972 (NASA-CR-54719)

AERONAUTICAL RESEARCH LABS., MELBOURNE (AUSTRALIA).
Estimation of cerium in chromium-base alloys, 20: 16334 (N-65-18292)

AIR FORCE WEAPONS LAB., KIRTLAND AFB, N. MEX.
Effects of radiation on serum enzymes and trace elements in large animals, 20: 16222 (AFWL-TR-65-112)

AKADEMIYA NAUK SSSR, NOVOSIBIRSK. INSTITUT YADERNOI FIZIKI.
Investigation of drift instability in potassium plasma, 20: 17883 (NP-15784)
Quantum depolarization of electrons in magnetic field, 20: 17689 (NP-15783)

AKTIEBOLAGET ATOMENERGI, STOCKHOLM (SWEDEN).
Selective sorption of trace elements in neutron-irradiated biological material, 20: 16171 (AE-215)

ALABAMA UNIV., UNIVERSITY. DEPT. OF PHYSICS.
Magnetic and electrical properties of selected materials, 20: 17019 (N-65-17873)

AMERICAN INSTITUTES FOR RESEARCH, PITTSBURGH, PA.
Evaluation of existing criteria for judging quality of science exhibits, 20: 18178 (TID-22703)

AMES LAB., IOWA STATE UNIV. OF SCIENCE AND TECH.
Computer program for Fermi surface studies, 20: 17973 (IS-1106)
Kerr magneto-optic effect as applied to rare-earth metals, 20: 17974 (IS-T-63)
Solid solubility of gold-rich rare-earth and lanthanide-rich magnesium alloys, 20: 17016 (IS-1175)
Survey of environmental radioactivity, 20: 18136 (IS-1320)

ANSALDO S.p.A., GENOA (ITALY).
Nuclear-powered tanker, 20: 18126 (EUR-2629.i(Vol.1))

ARGONNE NATIONAL LAB., IDAHO FALLS, IDAHO.
Tungsten–rhenium alloy thermocouples and use in UO_2-fueled reactor, 20: 16942 (ANL-6981)

ARGONNE NATIONAL LAB., ILL.
Tungsten–rhenium alloy thermocouples and use in UO_2-fueled reactor, 20: 16942 (ANL-6981)

ARKANSAS UNIV., FAYETTEVILLE. DEPT. OF CHEMISTRY.
Fallout from nuclear explosion of October 16, 1964, 20: 16663 (TID-21470)
Prog. rpt. on tracer and isotope effect studies in organic chemistry, annual, 1965, 20: 16542 (TID-22646)

ARMY MEDICAL RESEARCH UNIT, EUROPE.
Prog. rpt. on ionizing radiation, injury, prevention, and treatment, annual 10/65, 20: 16303 (AD-626384)

ARO, INC., ARNOLD AIR FORCE STATION, TENN.
Ionization and recombination in alkali-seeded collision-dominated plasmas, 20: 17872 (AD-627988)

ATOMENERGIKOMMISSIONEN, ROSKILDE (DENMARK).
Prog. rpt. on activities, annual, 4/64–3/65, 20: 18174 (NP-15771)

ATOMIC ENERGY CENTRE, DACCA (PAKISTAN).
Effect of γ irradiation on seeds of Corchorus capsularis and C. olitorius, 20: 16217 (AECD-AG-7)
Interspecific hybridization in jute, 20: 16218 (AECD-AG-12)
Pion-nucleon coupling constant from spin-flip dispersion relation, 20: 17336 (AECD/TP-5)

ATOMIC ENERGY CENTRE, LAHORE (PAKISTAN).
Bibliography on Pu, 20: 16328 (AECL-Pak/Lib-10)
Review on wholesomeness of irradiated foods with special reference to wheat, 20: 16918 (AECL-PAK/RB-7)

ATOMIC ENERGY ESTABLISHMENT, TROMBAY (INDIA).
Prog. rpt. on fixation of low- and medium-level radioactive waste in stable solid media, 2–10/65, 20: 18166 (TID-22531)

ATOMIC ENERGY ESTABLISHMENT, WINFRITH (ENGLAND).
CWF and TABLE—two FORTRAN programs for calculation of Coulomb penetration and shift factors, 20: 17671 (AEEW-M-611)
Efficiency of Whatman-type ACG/B filter papers for methyl iodide retention in air, 20: 16719 (AEEW-M-568)

ATOMIC ENERGY OF CANADA LTD., CHALK RIVER (ONTARIO).
World and Canadian energy today and tomorrow. I., 20: 18082 (AECL-2390)

ATOMIC ENERGY RESEARCH ESTABLISHMENT, HARWELL (ENGLAND).
Computer program for calculation of compound nuclear cross sections by Hauser-Feshbach theory, 20: 17672 (AERE-R-5053)
Desorption studies on graphite surfaces irradiated in CO_2, CH_4, and $CO_2/CO/CH_4$ mixtures, 20: 17114 (AERE-R-5163)
Film dosimetry practice with AERE/RPS film holder, 20: 16720 (AERE-R-4669)
Radioactive fallout in air and rain: results to middle of 1965, 20: 16660 (AERE-R-4997)
Tests for T invariance in N-N scattering, 20: 17337 (AERE-R-5138)

ATOMIC WEAPONS RESEARCH ESTABLISHMENT, ALDERMASTON (ENGLAND).
Measurement of critical mass of 37.5% enriched U in reflectors of wood, concrete, polyethylene, and water, 20: 16721 (AWRE-NR-1/66)

ATOMICS INTERNATIONAL, CANOGA PARK, CALIF.
Evaluation of dissolvable epoxy systems for remote metallographic evaluations, 20: 16948 (ORNL-TM-1161, pp 103-11)
Prog. rpt. on radiation effects on Ag and Zn battery electrodes, 7–10/65. II., 20: 17115 (AI-65-264)
Prog. rpt. on radiation effects on Ni–Cd electrodes. III., 6–9/13/64, 20: 17124 (N-65-17608)
Prog. rpt. on tungsten resonance integrals and Doppler coefficients, 6–12/65, 20: 18045 (AI-66-16)
Water chemistry of hermetically sealed boiling water reactors, 20: 18089 (NAA-SR-Memo-10178)

AUSTRALIAN ATOMIC ENERGY COMMISSION RESEARCH ESTABLISHMENT, LUCAS HEIGHTS.
Function arising from second-order approximations to the effective resonance integral, 20: 17650 (AAEC/E-144)
Linear thermal expansion of beryllia, 20: 17006 (AAEC/TM-300)
Method for digital computer processing of data from radioisotope sediment tracing studies, 20: 16632 (AEEC/TM-303)
Polarographic determination of H_2O_2 in irradiated H_2O, 20: 16327 (AAEC/TM-301)
Strength of irradiated BeO fueled with UO_2–ThO_2, 20: 17113 (AAEC-E-140)

AUTONETICS DIV., NORTH AMERICAN AVIATION, INC., DOWNEY,

CALIF.
Evaluation of dissolvable epoxy systems for remote metallographic evaluations, 20: 16948 (ORNL-TM-1161, pp 103-11)

B

BABCOCK AND WILCOX CO., BARBERTON, OHIO. BOILER DIV.
Prog. rpt. on Na-heated steam generator, 10–12/65, 20: 16599 (BAW-1280-34)
BARTOL RESEARCH FOUNDATION, SWARTHMORE, PA.
Prog. rpt. on nuclear physics and cosmic rays, annual, 1964, 20: 17651 (AD-612192)
BATTELLE-NORTHWEST, RICHLAND, WASH. PACIFIC NORTHWEST LAB.
BNW master library. I., 20: 17673 (BNWL-CC-325(Vol.1))
BNW master library. II., 20: 17674 (BNWL-CC-325(Vol.2))
BNW master library. III., 20: 17675 (BNWL-CC-325(Vol.3))
Correlation of radiation damage in boronated graphite, 20: 17116 (BNWL-199)
Disposal of radioactive wastes into fresh water, 20: 18157 (BNWL-SA-466)
Evaluation of use of selective discharges from Lake Roosevelt to cool Columbia River, 20: 18172 (BNWL-208)
Purification of rare earths from Hanford wastes by solvent extraction, 20: 16329 (BNWL-187)
Transient thermal behavior in fixation of radioactive materials, 20: 18155 (BNWL-157)
Treatment and disposal of glass melter condensates containing sulfuric acid, 20: 18159 (BNWL-SA-514)
Volatilization of fission products from high-level ceramic wastes, 20: 18156 (BNWL-SA-453)
Waste solidification engineering prototypes technical program, 20: 18158 (BNWL-SA-467)
BETTIS ATOMIC POWER LAB., PITTSBURGH, PA.
Prog. rpt. on PWR Project, 10/22/65–1/21/66, 20: 18094 (WAPD-MRP-115)
BETTIS ATOMIC POWER LAB., WEST MIFFLIN, PA.
Approximating by synthesis a many, short-time increment depletion calculation, 20: 18052 (WAPD-T-1836)
BOEING SCIENTIFIC RESEARCH LABS., SEATTLE, WASH. GEOASTROPHYSICS LAB.
Field-aligned flow of a conducting fluid past a source of magnetism, 20: 17509 (D-1-82-0469)
BOEING SCIENTIFIC RESEARCH LABS., SEATTLE, WASH. PLASMA PHYSICS LAB.
Field-aligned flow of a conducting fluid past a source of magnetism, 20: 17509 (D-1-82-0469)
BROOKHAVEN NATIONAL LAB., UPTON, N. Y.
Chemonuclear and radiation chemical process research and development, 20: 16506 (BNL-10020)
Conference on process radiation development, summaries, Brookhaven National Lab., 10/65, 20: 16505 (BNL-949)
Depletion of intestinal epithelium of the mouse following exposure to lethal whole-body radiation, 20: 16223 (BNL-8952)
Monte Carlo methods in resonance absorption, 20: 18046 (BNL-9644)
Prog. rpt. on kinetics and structural studies of chelates, annual, 6/65–6/66, 20: 16416 (NYO-906-68)
Source of high-energy particles from an internal target in the AGS, 20: 17171 (BNL-10030)
Wave functions for quadrupole antishielding factors, 20: 17250 (BNL-8850)

C

CALIFORNIA UNIV., DAVIS.
Influence of chronic acceleration on effects of whole-body irradiation in rats, 20: 16213 (AD-620403)
CALIFORNIA UNIV., LA JOLLA, SAN DIEGO. DEPT. OF PHYSICS.
Average atmosphere for particles trapped in the earth's magnetic field, 20: 17540 (N-65-18914)
CAMBRIDGE ELECTRON ACCELERATOR, MASS.
Possible use of the CEA directly as a colliding beam facility, 20: 17173 (CEAL-1029)
CAROLINAS VIRGINIA NUCLEAR POWER ASSOCIATES, INC., PARR, S. C.
CVTR initial core loading, 20: 18085 (CVNA-173)
CVTR initial criticality, 20: 18086 (CVNA-174)
On-site meteorological tests at Parr, South Carolina, 20: 18084 (CVNA-96)
Radiological environmental survey manual, 20: 18083 (CVNA-63)
CENTRALNE LABORATORIUM OCHRONY RADIOLOGICZNEJ, WARSAW (POLAND).
Determination of mixture of thermal-neutron and γ exposures by film badges, 20: 16807 (CLOR/IBJ-42/D)
Optimalization of FET spectrometer stages working with semiconductor radiation detector, 20: 16806 (CLOR-44/D)
Radiation-dose-sensitive pocket alarm monitor, 20: 16805 (CLOR-43/D)
CENTRE D'ETUDE DE L'ENERGIE NUCLEAIRE, BRUSSELS (BELGIUM).
Prog. rpt. on in-pile corrosion of nuclear materials, 3–8/65, 20: 17118 (EURAEC-1564)
CENTRE D'ETUDE DE L'ENERGIE NUCLEAIRE, MOL (BELGIUM).
Prog. rpt. on BR2 testing reactor and connected laboratories, annual, 1964, 20: 18133 (EUR-2625.e)
Prog. rpt. on in-pile corrosion of nuclear materials, 3–8/65, 20: 17118 (EURAEC-1564)
COLORADO SCHOOL OF MINES RESEARCH FOUNDATION, INC., GOLDEN.
Prog. rpt. on fast neutron activation analysis for determination of trace F in Zn electrorefining solutions, 2/66, 20: 16339 (TID-22662)
COLORADO STATE UNIV., FORT COLLINS.
Secondary emission effects in ion beams, 20: 16624 (N-65-17749)
COLORADO STATE UNIV., FORT COLLINS. DEPT. OF RADIOLOGY AND RADIATION BIOLOGY.
Factors influencing accumulation of fallout ^{137}Cs in mule deer, 20: 16723 (COO-1156-11)
Strontium-90 in antlers and selected bones of Colorado mule deer, 20: 16724 (COO-1156-12)
COLUMBIA UNIV., NEW YORK.
Forced convection boiling burnout for water in uniformly heated tubular test sections, 20: 16603 (NYO-187-7)
COLUMBIA UNIV., NEW YORK. PLASMA LAB.
Normal ionizing shock waves, 20: 17511 (NP-15894)
COMITATO NAZIONALE PER L'ENERGIA NUCLEARE, LA SPEZIA (ITALY). LABORATORIO PER LO STUDIO DELLA CONTAMINAZIONE RADIOATTIVA DEL MARE.
Prog. rpt. on marine radiobiology, annual, 1963, 20: 16175 (RT/BIO(65)-1)
Prog. rpt. on radioactive contamination of the sea, annual, 1964, 20: 16725 (EUR-2543.e)
COMITATO NAZIONALE PER L'ENERGIA NUCLEARE, ROME (ITALY).
Comparative examination of methods for disadvantage factor calculations, 20: 18049 (RT/FI(65)-42)
Determination of manganese and arsenic content in steel by neutron activation analysis, 20: 16338 (RT/CHI-(65)36)
Electrical resistivity measurement of Na, 20: 17026 (RT/ING-(65)17)
Possibility of obtaining a standard source of thermal neutrons, 20: 17654 (RT/PROT-(65)31)
Preliminary neutronic project of PRO-II core (UO_2–stainless steel), 20: 18091 (RT/FI(65)45)
Third annual meteorological report of Center for Nuclear Studies at Casaccia, 1964, 20: 16635 (RT/PROT(65)-40)
COMMISSARIAT A L'ENERGIE ATOMIQUE, CADARACHE (FRANCE). CENTRE D'ETUDES NUCLEAIRES.
Rapsodie reactor—fabrication of control rod mechanisms, 20: 18096 (ORNL-tr-987)
COMMISSARIAT A L'ENERGIE ATOMIQUE, GRENOBLE (FRANCE). CENTRE D'ETUDES NUCLEAIRES.
Effect of fractionated x-ray doses on hemogram and protein formula of the mouse, 20: 16224 (CEA-R-2848)
Production of intense source of microsecond proton pulses, 20: 17172 (CEA-R-2802)
COMMISSARIAT A L'ENERGIE ATOMIQUE, SACLAY (FRANCE). CENTRE D'ETUDES NUCLEAIRES.
Bound water of several high specific surface-area oxides, 20: 16413 (CEA-R-2703)
Calculation of pair-interaction function in some normal metals, 20: 17008 (CEA-R-2820)
Device for recovering radioactive waste, 20: 18160 (CEA-R-2894)
Diffusion, electrical mobility, and ionic interactions in molten salts, 20: 16414 (CEA-R-2806)
Fluctuations of partial and total radiative widths by neutron capture resonance, 20: 17676 (CEA-R-2810)
Mobility of Rb^+ and Cs^+ ions in gases at high pressures, 20: 16415 (CEA-R-2861)
Solution of the diffusion equation, 20: 17652 (CEA-R-2867)
Sorption of ^{90}Sr on an aluminum oxide, 20: 16330 (CEA-R-2851)
CONNECTICUT UNIV., STORRS.
Paramagnetic resonance of F_2^- ions trapped in electron-irradiated KF_2, 20: 17976 (NYO-2047-36, App.1)
Wave functions for F′ centers in alkali halides, 20: 17977 (NYO-2047-36, App.2)
CONNECTICUT UNIV., STORRS. DEPT. OF PHYSICS.
Paramagnetic resonance of F_2^- ions trapped in electron-irradiated KF_2, 20: 17976 (NYO-2047-36, App.1)
Prog. rpt. on investigation of radiation effects in metal oxides and azides, annual, 2/65–1/66, 20: 17975 (NYO-2047-36)

Wave functions for F' centers in alkali halides, 20: 17977 (NYO-2047-36, App.2)

CULHAM LAB., UNITED KINGDOM ATOMIC ENERGY AUTHORITY, ABINGDON (ENGLAND).
Apparatus for detection and energy analysis of fast neutral atoms, 20: 17873 (CLM-R-49)

CZECHOSLOVAK ACADEMY OF SCIENCES, PRAGUE. INST. OF HYDRODYNAMICS.
Prog. rpt. on hydrodynamics of disposal of low-level liquid radioactive wastes in soil, final, 1965, 20: 18163 (NP-15859)

D

DELAWARE UNIV., NEWARK. DEPT. OF PHYSICS.
Prog. rpt. on radiation damage in CdS, 7–12/64, 20: 17123 (N-65-17505)

"DEMOCRITUS" NUCLEAR RESEARCH CENTER, ATHENS (GREECE).
Prog. rpt. on evaporation of radioactive wastes by solar energy, final, 12/65, 20: 18164 (NP-15874)

DENVER RESEARCH INST., UNIV. OF DENVER, COLO.
Prog. rpt. on phase equilibria of Ta-rich region of Ta–W–Hf and Ta–W–Zr systems, final, 9/64–11/65, 20: 17012 (DRI-1092-226)

DEPARTMENT OF DEFENSE, WASHINGTON, D. C.
Off-site surveillance for Salmon Event of Project Dribble, 20: 16743 (VUF-1021)

DEPARTMENT OF MINES AND TECHNICAL SURVEYS (CANADA). MINES BRANCH.
Effects of U and Mo alloying additions on corrosion resistance of AISI type 430 stainless steel, 20: 16975 (NP-15900)

DEUTSCHES ELEKTRONEN-SYNCHROTRON, HAMBURG (WEST GERMANY).
Application of spectral representations to nonrelativistic and relativistic Bethe-Salpeter equation, 20: 17425 (DESY-66/1)
Highly polarized coherent bremsstrahlung from a diamond target in Bev region, 20: 17679 (DESY-65/15)
Pair production and heavy electron, 20: 17338 (DESY-65/10)
100-MHz prescaler in biquinary tunnel diode transistor mode, 20: 16775 (DESY-65/17)

DIVISION OF TECHNICAL INFORMATION EXTENSION, (AEC), OAK RIDGE, TENN.
Bibliographies of atomic energy literature, 20: 18177 (TID-3733)

DYNATECH CORP., CAMBRIDGE, MASS.
Investigation of boiling water flow regimes at high pressure, 20: 16605 (NYO-3304-8)

E

ECOLE NATIONALE SUPERIEURE DE L'AERONAUTIQUE, PARIS (FRANCE).
Solution of the diffusion equation, 20: 17652 (CEA-R-2867)

EDGERTON, GERMESHAUSEN AND GRIER, INC., SANTA BARBARA, CALIF.
An improved method of Rossi oscillator-oscilloscope coupling, 20: 16776 (EGG-1183-1156)
Compton detector development report, 20: 16812 (EGG-1183-1174)

ELECTRO-OPTICAL SYSTEMS, INC., PASADENA, CALIF.
Development of radiation resistant solar cell, 20: 16910 (N-65-18448)

ENRICO FERMI INST. FOR NUCLEAR STUDIES, UNIV. OF CHICAGO, ILL.
Cosmic-ray telescope for Mariner-Mars mission, 20: 16822 (N-65-19927)

EUROPEAN ATOMIC ENERGY COMMUNITY.
Biosynthesis of Gibberellic Acid-^{14}C and 3,4-Glucose-^{14}C, 20: 16193 (EUR-2539.i)
Calculation of Racah, Clebsch-Gordan, and Z coefficients, 20: 17559 (EUR-2639.f)
Comparison of effects of mutagenic substances by studying mutagenesis of plants, 20: 16225 (EUR-2715.f)
Decimal scanner for the modular chain, 20: 16777 (EUR-2702.e)
Nuclear-powered tanker, 20: 18126 (EUR-2629.i(Vol.1))
Numerical resolution of magnetic field diffusion problem, 20: 17157 (EUR-2620.i)
Prog. rpt. on BR2 testing reactor and connected laboratories, annual, 1964, 20: 18133 (EUR-2625.e)
Prog. rpt. on chemical radioprotectors, annual, 4/64–4/65, 20: 16297 (EUR-2548.f)
Prog. rpt. on marine radiobiology, annual, 1963, 20: 16175 (RT/BIO(65)-1)
Prog. rpt. on radioactive contamination of the sea, annual, 1964, 20: 16725 (EUR-2543.e)
Review of economic scope for various uses of nuclear energy in certain overseas countries, 20: 16919 (EUR-2619.f)

EUROPEAN ATOMIC ENERGY COMMUNITY, GEEL (BELGIUM). CENTRAL NUCLEAR MEASUREMENTS BUREAU.
Calculation of Racah, Clebsch-Gordan, and Z coefficients, 20: 17559 (EUR-2639.f)

EUROPEAN ATOMIC ENERGY COMMUNITY, ISPRA (ITALY). EUROPEAN SCIENTIFIC DATA PROCESSING CENTER.
Numerical resolution of magnetic field diffusion problem, 20: 17157 (EUR-2620.i)

EUROPEAN ATOMIC ENERGY COMMUNITY, ISPRA (ITALY). JOINT NUCLEAR RESEARCH CENTER.
Decimal scanner for the modular chain, 20: 16777 (EUR-2702.e)
Numerical resolution of magnetic field diffusion problem, 20: 17157 (EUR-2620.i)
Study of liquid metal boiling under forced convection, 20: 16608 (ANL-Trans-257)

EUROPEAN COMPANY FOR THE CHEMICAL PROCESSING OF IRRADIATED FUELS, MOL (BELGIUM).
Minimum atmospheric dilution of long-term and short-term emissions from the Eurochemic chimney, 20: 18162 (NP-15754)

EUROPEAN ORGANIZATION FOR NUCLEAR RESEARCH, GENEVA (SWITZERLAND).
Radiation measurements around an insufficiently shielded target, 20: 17212 (UCRL-Trans-1305)
What are the equations for the phase oscillations in a synchrotron, 20: 17174 (CERN-66-6)

F

FELTMAN RESEARCH LABS., PICATINNY ARSENAL, DOVER, N. J.
Radiation-enhanced surface activity of gamma HMX, 20: 16504 (AD-627846)

FIAT, TURIN (ITALY). SEZIONE ENERGIA NUCLEARE.
Nuclear-powered tanker, 20: 18126 (EUR-2629.i(Vol.1))

FORSVARETS FORSKNINGSANSTALT, STOCKHOLM (SWEDEN).
An energy-weighted M1 sum rule, 20: 17690 (NP-15899)

G

GENERAL ATOMIC, SAN DIEGO, CALIF. JOHN JAY HOPKINS LAB. FOR PURE AND APPLIED SCIENCE.
Helium-3 charged particles in activation analysis, 20: 16331 (GA-6568)
Irradiation behavior of graphite joints and graphite-coated particles in carbonized pitch matrix, 20: 17119 (GAMD-6789)
Prog. rpt. on fundamental modes of collisionless plasma, 3/10–6/10/64, 20: 17882 (N-65-19862)
Prog. rpt. on graphite interface studies, 5/63–9/65, 20: 18127 (GA-6753(Pt.1))
Variable-energy neutron activation analysis, 20: 16332 (GA-6691)

GENERAL ELECTRIC CO., CINCINNATI, OHIO. NUCLEAR MATERIALS AND PROPULSION OPERATION.
Creep rupture properties of Re and Re alloys, 20: 17011 (CONF-651025-14)
Preparation of radioactive metallic specimens for replication, 20: 17128 (ORNL-TM-1161, pp 194-207)

GENERAL ELECTRIC CO., PLEASANTON, CALIF. VALLECITOS ATOMIC LAB.
Metallic inclusions in UO_2, 20: 16953 (ORNL-TM-1161, pp 249-66)

GENERAL ELECTRIC CO., RICHLAND, WASH. HANFORD ATOMIC PRODUCTS OPERATION.
Penetration seals for N-reactor plant, 20: 18125 (RL-SA-25)

GENERAL ELECTRIC CO., SAN JOSE, CALIF. ATOMIC POWER EQUIPMENT DEPT.
Irradiation performance of alternate cladding materials, 20: 17120 (GEAP-4916)
Performance of fuel rods containing boron burnable poison, 20: 17121 (GEAP-4918)
Prog. rpt. on transition boiling heat transfer program, 10–12/65, 20: 16602 (GEAP-5081)
Sodium mass transfer. XVI., 20: 16970 (GEAP-4832)
Vibration of SEFOR fuel rods in parallel flow, 20: 18134 (GEAP-4966)

GENERAL ELECTRIC CO., SCHENECTADY, N. Y.
Prog. rpt. on two-phase flow investigation, 10–12/65, 20: 16601 (GEAP-5067)

GHENT RIJKSUNIVERSITEIT (BELGIUM).
Prog. rpt. on stainless steel cladding of heavy gage steel, 7–9/65, 20: 16990 (EURAEC-1556)
Prog. rpt. on stainless steel cladding of heavy gage steels, 10–12/65, 20: 16991 (EURAEC-1557)

GOODYEAR ATOMIC CORP., PIKETON, OHIO.
Environmental radiation levels and concentrations, second half and annual summaries, 1965, 20: 16726 (GAT-506)

GOSUDARSTVENNYI KOMITET PO ISPOL'ZOVANIYU ATOMNOI ENERGII SSSR, MOSCOW. INSTITUT TEORETICHESKOI I EKSPERIMENTAL'NOI FIZIKI.
Effectiveness of magnetic spectrometer for recording $K^0 \rightarrow \pi^+ + \pi^-$ decay, 20: 16814 (ITEF-386)

Three-body problem complete system of angular functions, 20: 17560 (ITEF-384)
GOSUDARSTVENNYI KOMITET PO ISPOL'ZOVANIYU ATOMNOI ENERGII SSSR, OBNINSK. FIZIKO-ENERGETICHESKII INSTITUT.
Delayed neutrons of the fission threshold of ^{232}Th, 20: 17680 (FEI-26)
GRENOBLE UNIV. (FRANCE).
Production of intense source of microsecond proton pulses, 20: 17172 (CEA-R-2802)

H

HARRY DIAMOND LABS., WASHINGTON, D. C.
Bibliography on electrets. II., 20: 17971 (AD-299256)
HARVARD UNIV., CAMBRIDGE, MASS.
Possible use of the CEA directly as a colliding beam facility, 20: 17173 (CEAL-1029)
HAZLETON-NUCLEAR SCIENCE CORP., PALO ALTO, CALIF.
Post-shot hydrologic safety. Project Shoal, 20: 16742 (VUF-1014)
HEALTH AND SAFETY LAB., NEW YORK OPERATIONS OFFICE (AEC), N. Y.
Prog. rpt. on fallout program, 9–12/65, 20: 16662 (HASL-165)
HOLMES AND NARVER, INC., LOS ANGELES, CALIF.
Underground highway and parking garage and blast shelter for Manhattan Island, 20: 16623 (ORNL-TM-1381)

I

IDAHO OPERATIONS OFFICE (AEC), IDAHO FALLS. HEALTH AND SAFETY DIV.
Radiological appraisal of Monticello Project, San Juan County, Monticello, Utah, 20: 16729 (IDO-12049)
IIT RESEARCH INST., CHICAGO, ILL.
High magnification optical microscopy of ceramic materials, 20: 16954 (ORNL-TM-1161, pp 267-71)
High-temperature electrical properties of insulators, 20: 17022 (N-65-18933)
Prog. rpt. on protective coatings for refractory metals, final, 12/64–12/65, 20: 16943 (IITRI-B237-45)
INSTITUT ATOMNOI ENERGII, GOSUDARSTVENNYI KOMITET PO ISPOL'ZOVANIYU ATOMNOI ENERGII SSSR, MOSCOW.
Spectrum of γ-rays emitted during capture of thermal neutrons in tellurium, 20: 17681 (IAE-966)
Table of antiferromagnetics, 20: 17972 (IAE-942)
Tables of cross sections of photoionization of the hydrogen atom, 20: 17251 (IAE-873)
INSTITUT FUER PLASMAPHYSIK, G.M.B.H. GARCHING (WEST GERMANY).
Development of a laser light source for the Mach-Zehnder interferometer, 20: 17875 (IPP-1/35)
Diffraction of electromagnetic waves on plasma cylinders, 20: 17877 (IPP-6/44)
Measurement of high electron densities on linear Z pinch using new microwave reflection probe, 20: 17876 (IPP-1/37)
Microwave interferometer measurements of electron density distribution behind shock fronts and discharge plasmas, 20: 17510 (IPP-3/25)
INSTITUT NATIONAL DE LA RECHERCHE AGRONOMIQUE, DIJON (FRANCE). STATION D'AMELIORATION DES PLANTES.
Comparison of effects of mutagenic substances by studying mutagenesis of plants, 20: 16225 (EUR-2715.f)
INSTITUTE FOR DEFENSE ANALYSES, ARLINGTON, VA. WEAPONS SYSTEMS EVALUATION DIV.
Magnitude and distribution of weapon effects for design of shelters for protection against fallout, 20: 16620 (AD-624370)
INSTITUTE FOR NUCLEAR STUDY, TOKYO UNIV. (JAPAN).
Deformed ion source at positive potential in f-m cyclotron, 20: 17207 (INSJ-93)
Prog. rpt. on INS isotope separator, 11/5/65, 20: 16928 (INSJ-92)
INSTITUTE OF NUCLEAR PHYSICS, KRAKOW (POLAND).
g-Factor of 87-kev excited state in ^{155}Gd, 20: 17683 (INP-430/PL)
Transverse spin polarization in odd-mass deformed nuclei, 20: 17682 (INP-428/PL)
INSTITUTE OF NUCLEAR RESEARCH, WARSAW (POLAND).
Apparatus for internal friction and Young's moduli measurements in kilocycle range, 20: 17013 (INR-632/XIV/PS)
Determination of mixture of thermal-neutron and γ exposures by film badges, 20: 16807 (CLOR/IBJ-42/D)
Hydrophobization of cellulose by radiation-induced grafting of styrene on its surface, 20: 16507 (INR-671/XVII/C)
Measurement of ratio of slow to fast components of scintillation in stilbene in a wide range of dE/dx, 20: 16813 (INR-653/IA/D)
Neutron-diffraction investigation of iron–tungsten carbides, 20: 17015 (INR-665/II/PS)
Salt-boiling fast reactor "SAWA", 20: 18088 (INR-669/C)
Some properties of U–1 wt. percent Mo alloy after thermal treatment, 20: 17014 (INR-645/XIV/PS)
INSTITUTT FOR ATOMENERGI, KJELLER (NORWAY).
Analysis of chemical state of Pu and fission products in process feed solutions, 20: 16333 (KR-81)
DATAPREP-II—reactor lattice homogenization and BIGG-II data preparation computer code, 20: 18047 (KR-78)
Organic-cooled irradiation loop in the HFR at Petten, 20: 18137 (KR-82)
Prog. rpt. on NORA Project, 10–12/65, 20: 18138 (TID-22697)
INTERNATIONAL ATOMIC ENERGY AGENCY, VIENNA (AUSTRIA).
Conference on physics and chemistry of fission, Salzburg, 3/65. II., 20: 17695 (STI/PUB/101(Vol.2))
Conference on physics and chemistry of fission, Salzburg, 3/65. I., 20: 17694 (STI/PUB/101(Vol.1))
INTERNATIONAL CENTRE FOR THEORETICAL PHYSICS, TRIESTE (ITALY).
Discrete degenerate representations of non-compact unitary groups, 20: 17426 (IC-66/16)
Strong vertex according to SL(6,C), 20: 17427 (IC-66/20)
ISOCHEM INC., RICHLAND, WASH.
In-tank solidification of radiochemical wastes, 20: 18161 (ISO-SA-1)
ISOTOPES, INC., WESTWOOD, N. J.
Prog. rpt. on radiochemical analyses of filter samples collected under Project Stardust, 1963. Appendix, 20: 16727 (HASL-168)
Prog. rpt. on radiochemical analyses of filter samples collected under Project Stardust, 1964, 20: 16728 (HASL-169)

J

JAPAN ATOMIC ENERGY RESEARCH INST., TOKYO.
NELKER: code for scattering kernel calculation for bound hydrogen, 20: 17684 (JAERI-1085)
JET PROPULSION LAB., CALIF. INST. OF TECH., PASADENA.
Analysis of high-temperature creep in pyrolytic carbon, 20: 17017 (JPL-TR-32-889)
Cosmic-ray telescope for Mariner-Mars mission, 20: 16822 (N-65-19927)
Interactions of spacecraft and other moving bodies with natural plasmas, 20: 17537 (JPLAI/LS-541)
Prog. rpt. on radiation effects on Ag and Zn battery electrodes, 7–10/65. II., 20: 17115 (AI-65-246)
Prog. rpt. on radiation effects on Ni–Cd electrodes. III., 6–9/13/64, 20: 17124 (N-65-17608)
JOHNS HOPKINS UNIV., BALTIMORE, MD.
Prog. rpt. on effects of radiation and other mutagenic agents on inducing mutation in Drosophila, final, 5/53–12/65, 20: 16229 (NYO-1472-1)
JOHNS HOPKINS UNIV., BALTIMORE, MD. DEPT. OF BIOLOGY.
Prog. rpt. on pathways of metabolism in embryonic development, 6/58–6/65, 20: 16172 (NYO-2194-1)
JOINT INST. FOR NUCLEAR RESEARCH, DUBNA (USSR).
Possible experiments aimed at testing isotopic structure of electromagnetic interaction, 20: 17428 (JINR-P-2498)
JOINT INST. FOR NUCLEAR RESEARCH, DUBNA (USSR). LAB OF HIGH ENERGY.
Designs of gaseous threshold and differential Cherenkov counters, 20: 16816 (JINR-P-2528)
Effect of atomic hyperfine interaction on nuclear γ transitions, 20: 17686 (JINR-P-2512)
Slow ejection of proton beam from the synchrophasotron, 20: 17208 (JINR-P-2537)
Spark chambers for studying elastic scattering of π^+ mesons by protons at 180°, 20: 16815 (JINR-P-2506)
JOINT INST. FOR NUCLEAR RESEARCH, DUBNA (USSR). LAB OF NUCLEAR PROBLEMS.
Decay of ^{150}Ho, 20: 17685 (JINR-P-2497)
Measurement of π^+ meson lifetime, 20: 17346 (JINR-P-2534)
Method of obtaining super-low temperature based on a dissolution of ^3He in ^4He, 20: 17599 (JINR-P-2480)
Search for $\pi^0 \to 3\gamma$ decay, 20: 17340 (JINR-P-2322)
JOINT INST. FOR NUCLEAR RESEARCH, DUBNA (USSR). LAB OF NUCLEAR REACTIONS.
Proton emitters among Te isotopes, 20: 17687 (JINR-P-2514)
Radioactive properties of nuclei of heaviest elements, 20: 17688 (JINR-P-2539)
JOINT INST. FOR NUCLEAR RESEARCH, DUBNA (USSR). LAB OF THEORETICAL PHYSICS.
Application of unitary symmetry to multiple meson production, 20: 17345 (JINR-P-2531)
Elastic e-d scattering and CP-invariance breakdown, 20: 17341 (JINR-P-2504)
Electromagnetic interaction of the X meson in higher symmetries, 20: 17342 (JINR-P-2520)
Electromagnetic interactions in the quark model, 20: 17348 (JINR-P-2556)
Inelastic π^+-p interaction at high energies and statistical model,

20: 17344 (JINR-P-2530)
Magnetic moment of Dirac particle in the potential well, 20: 17431 (JINR-P-2569)
On the many-dimensional Coulomb problem, 20: 17252 (JINR-P-2522)
p-Separation of variables in the Schroedinger equation, 20: 17561 (JINR-P-2532)
Plus-parity mesons and the 189-plet of SU(6), 20: 17339 (JINR-E-2557)
Scattering of complex particle on the force center, 20: 17430 (JINR-P-2565)
Some effects in the quark model, 20: 17343 (JINR-P-2524)
Symmetry groups in classical and quantum mechanics, 20: 17429 (JINR-P-2529)
Two-meson annihilation of baryons in broken SL(6,C) symmetry, 20: 17347 (JINR-P-2547)

K

KANSAS ENGINEERING EXPERIMENT STATION, MANHATTAN.
Effects of radiation quality on radiolysis of water, 20: 16509 (TID-22666)
Noise analysis applied to a liquid-solid fluidized bed, 20: 18071 (TID-22665)
Velocity transfer function analysis of forced convection heat transfer, 20: 16607 (TID-22663)
KERNFORSCHUNGSANLAGE, JUELICH (WEST GERMANY). INSTITUT FUER REAKTORBAUELEMENTE.
Distribution system for multichannel pulse-height analyzer, 20: 16817 (JUL-270-RB)
KERNFORSCHUNGSZENTRUM, KARLSRUHE (WEST GERMANY).
Preparation and study of thick depleted surface-barrier detectors, 20: 16818 (KFK-328)
KNOLLS ATOMIC POWER LAB., SCHENECTADY, N. Y.
Weighing irradiated fuel specimens in water, 20: 16780 (TID-22689)

L

LABORATOIRE DE L'ACCELERATEUR LINEAIRE, UNIV. DE PARIS, ORSAY (FRANCE).
Application of Fermat principle to magnetic spectrometers, 20: 16821 (LAL-1151)
Deuteron electromagnetic form factors, 20: 17349 (LAL-1155)
nn Scattering length, 20: 17350 (N-65-19395)
LABORATOIRE DE RECHERCHES SUR LA PHYSIQUE DES PLASMAS, LAUSANNE (SWITZERLAND).
Axial high-frequency discharge, 20: 17879 (LRP-19/65)
Beryllium pressure bar having a submicrosecond risetime, 20: 17018 (LRP-20/66)
LABORATORI NAZIONALI DI FRASCATI, COMITATO NAZIONALE PER L'ENERGIA NUCLEARE (ITALY).
Beam optics computation for particle transport systems, 20: 17211 (LNF-65/45)
Current detectors for the linac with impulse transformers, 20: 17210 (LNF-65/37)
LAWRENCE RADIATION LAB., UNIV. OF CALIFORNIA, BERKELEY.
Accelerator magnet of German electron synchrotron (DESY), 20: 17213 (UCRL-Trans-1312)
Chemical evolution and organic geochemistry, 20: 16633 (UCRL-16605)
Dark recovery and glycerol protection for diploid Saccharomyces cerevisiae, 20: 16231 (UCRL-16377)
Stability of metallic structures, 20: 16418 (UCRL-16250)
LAWRENCE RADIATION LAB., UNIV. OF CALIFORNIA, LIVERMORE.
Compression of lithium hydride, 20: 17979 (UCRL-12386)
Converting portable survey meter's ion chamber into continuous air monitor, 20: 16832 (UCRL-14534, pp 32-40)
Effect of variation of airborne radon daughter concentration on whole-body counter background, 20: 16665 (UCRL-14534, pp 23-7)
Energy absorption coefficients of dosimetric LiF, 20: 16829 (UCRL-14534, pp 1-7)
Estimation of area enclosed by a fallout isoconcentration line, 20: 16664 (UCRL-14534, pp 19-22)
High-temperature testing of graphite helical-screw expanders and compressors, 20: 16591 (UCRL-14660)
Non-dynamical structure of particle reactions, 20: 17436 (UCRL-14321-T)
Personnel alarm dosimeter LE 14507-1, 20: 16831 (UCRL-14534, pp 28-31)
Portable vacuum cleaner for recovering spilled mercury, 20: 16738 (UCRL-14534, pp 41-3)
Potential application of nuclear explosives for recovery of oil from shale, 20: 16589 (UCRL-12224-T)
Prog. rpt. on hazards control, 7–9/65, 20: 16736 (UCRL-14534)
Program book for Advisory Committee for Biology and Medicine, 20: 16160 (UCRL-14739(Pt.2))
Removal of C dust from high-speed printer, 20: 16740 (UCRL-14534, pp 50-3)
Source of intermediate-energy neutrons for dosimeter calibration, 20: 16830 (UCRL-14534, pp 8-12)
Use of electronic flash units in proximity with explosives, 20: 16739 (UCRL-14534, pp 44-9)
Vacuum-operated, foam-entrainment milk evaporator, 20: 16741 (UCRL-14534, pp 54-6)
Whole-body counter facility, 20: 16737 (UCRL-14534, pp 13-18)
LIEGE UNIV. (BELGIUM). LABORATOIRES DE RADIOBIOLOGIE.
Prog. rpt. on chemical radioprotectors, annual, 4/64–4/65, 20: 16297 (EUR-2548.f)
LIN (T. Y.) AND ASSOCIATES, VAN NUYS, CALIF.
Reusability of buildings after a warfire, 20: 16621 (AD-625867)
LOCKHEED–GEORGIA CO., MARIETTA.
Components irradiation test No. 5, 20: 16908 (N-65-17526)
Components irradiation test No. 7, 20: 16909 (N-65-18250)
LOCKHEED MISSILES AND SPACE CO., PALO ALTO, CALIF. RESEARCH LABS.
Space materials handbook, 20: 16944 (NASA-SP-3025)
LOCKHEED NUCLEAR PRODUCTS, MARIETTA, GA.
On-site meteorological tests at Parr, South Carolina, 20: 18084 (CVNA-96)
LOS ALAMOS SCIENTIFIC LAB., UNIV. OF CALIFORNIA, N. MEX.
Cryogenic evaluation laboratory test of cryogenic low-pressure coupling, 20: 16588 (LA-3454)
Dose-monitoring instrument for neutrons from thermal to 100 Mev, 20: 16819 (LA-3435)
Neutron capture cross sections of some rare earth nuclei, 20: 17653 (LA-3463)
Prog. rpt. on medium-energy physics, 1/66, 20: 17209 (LA-3479)
Quench monitoring and efficiency calibration through external standardization, 20: 16820 (LA-DC-7222)
REZONE—proposal for accomplishing rezoning in two-dimensional lagrangian hydrodynamics problems, 20: 18173 (LA-3455)
Spherical harmonic reduction of Fokker-Planck equation, 20: 17878 (LA-3437)
LOUISVILLE UNIV., KY. DEPT. OF CHEMISTRY.
Prog. rpt. on derivatives of five-membered heterocycles as radiation-protective agents, final, 12/65, 20: 16490 (TID-22681)

M

MARKITE CO., NEW YORK.
Non-destructive electrical method of studying the density distribution of a randomly packed bed, 20: 18018 (CONF-651101-73)
MASSACHUSETTS INST. OF TECH., CAMBRIDGE.
Solar wind deuterium detector and charge spectrum analyzer, 20: 17307 (CONF-651001-34)
MASSACHUSETTS INST. OF TECH., CAMBRIDGE. DEPT. OF GEOLOGY AND GEOPHYSICS.
Prog. rpt. on variations in isotopic abundances of Sr, Ca, and A and related topics, annual, 1965, 20: 16711 (MIT-1381-13)
MASSACHUSETTS INST. OF TECH., CAMBRIDGE. DEPT. OF NUCLEAR ENGINEERING.
Effect of reactor irradiation on Santowax WR, 20: 17122 (MIT-334-34)
MASSACHUSETTS INST. OF TECH., CAMBRIDGE. METALS PROCESSING LAB.
Temperature variation of Ginzburg-Landau parameters in Nb single crystals, 20: 17585 (AD-627910)
MASSACHUSETTS UNIV., AMHERST.
Prog. rpt. on use of tritiated thymidine as internal source of radiation in study of lateral root initiation, annual, 1965–66, 20: 16227 (NYO-3561-2)
MIAMI UNIV., FLA. INST. OF MARINE SCIENCE.
Determination of mixing and circulation in the ocean with radioactive tracers, 20: 16828 (TID-22763)
MICHIGAN UNIV., ANN ARBOR. LAB. FOR FLUID FLOW AND HEAT TRANSPORT PHENOMENA.
Ultrasonic-induced cavitation studies in mercury and water, 20: 16974 (NP-15889)
MILAN UNIV. (ITALY).
Biosynthesis of Gibberellic Acid-^{14}C and 3,4-Glucose-^{14}C, 20: 16193 (EUR-2539.i)
MINNESOTA MINING AND MFG. CO., ST. PAUL.
Prog. rpt. on fabrication of W alloy tubing, 10/23/65–1/1/66, 20: 16989 (COO-1518-2)
MOUND LAB., MIAMISBURG, OHIO.
Radioisotopes for heat sources. II., 20: 16927 (MLM-1297)

N

NATIONAL AERONAUTICS AND SPACE ADMINISTRATION,

CLEVELAND, OHIO. LEWIS RESEARCH CENTER.
Description and operation of spacecraft SERT I ion thrustor flight test, 20: 16625 (N-65-19272)
NATIONAL AERONAUTICS AND SPACE ADMINISTRATION, GREENBELT, MD. GODDARD SPACE FLIGHT CENTER.
Do solar flare proton events measure geometry of a diffusion process? 20: 17228 (N-65-18275)
Evidence for rapid motion of outer boundary of the magnetosphere, 20: 17541 (N-65-19719)
Inverse Compton scattering of cosmic-ray electrons, 20: 17309 (N-65-19716)
Measurement of low-energy primary cosmic-ray protons on IMP-1, 20: 17308 (N-65-18274)
Time varying solar cycle protons program manual, 20: 17539 (N-65-18257)
NATIONAL AERONAUTICS AND SPACE ADMINISTRATION, HOUSTON, TEX. MANNED SPACECRAFT CENTER.
Heat-shield ablation measurements using radioisotope techniques, 20: 16778 (NASA-TN-D-3329)
NATIONAL AERONAUTICS AND SPACE ADMINISTRATION, LANGLEY STATION, VA. LANGLEY RESEARCH CENTER.
Hemispherical spectral emittance of ablation chars, carbon, and zirconia to 3700°K, 20: 17021 (N-65-18607)
Oxidation-resistant coatings on Nb-10Ti-5Zr alloy sheet at 2000, 2400, and 2700°F, 20: 16973 (NASA-TN-D-3275)
NATIONAL BUREAU OF STANDARDS, WASHINGTON, D. C.
Prog. rpt. on radiochemical analysis, 7/64–6/65, 20: 16335 (NBS-TN-276)
Prog. rpt. on W deposition, 11/64–1/65, 20: 17020 (N-65-18466)
NATIONAL INST. OF RADIOLOGICAL SCIENCES, CHIBA (JAPAN).
Medical survey of Japanese exposed to fallout radiation in 1954, 20: 16226 (NP-15891)
Radioactivity Survey Data in Japan, No. 5, 11/64, 20: 16730 (NP-15882)
Radioactivity Survey Data in Japan, No. 6, 2/65, 20: 16731 (NP-15883)
NATIONAL LEAD CO. OF OHIO, CINCINNATI.
Microphotometer: application to grain orientation studies and quantitative metallography, 20: 16950 (ORNL-TM-1161, pp 132-45)
NAVAL RADIOLOGICAL DEFENSE LAB., SAN FRANCISCO, CALIF.
Distribution of volcanic fallout in and about a one-story residence, 20: 16659 (AD-629527)
Effects of various gases within nasal cavities of rats on response of olfactory bulb neutrons to x irradiation, 20: 16215 (AD-628443)
Ion exchange in fused salts. II., 20: 16340 (USNRDL-TR-970)
Levels of ^{85}Sr populated in decay of ^{85}Y and ^{85m}Y, 20: 17670 (AD-629576)
Recovery from radiation injury in dogs as evaluated by the split-dose technique, 20: 16216 (AD-628791)
Suppression of DNA synthesis in weanling rat kidneys by short-term fasting, 20: 16158 (AD-628360)
Wounding response and polar transport of ^{45}Ca in isolated root segments of Zea mays, 20: 16170 (AD-628805)
NAVAL RESEARCH LAB., WASHINGTON, D. C.
Analysis of Ti–7Al–2Nb–1Ta and Ti–6Al–4V fractures, 20: 16967 (AD-628277)
Prog. rpt. on NRL cyclotron, 9/65, 20: 17169 (AD-628928)
Radiation damage surveillance of power reactor pressure vessels, 20: 17126 (NRL-6349)
NEDERLANDSE ORGANISATIE VOOR TOEGEPAST NATUURWETENSCHAPPELIJK ONDERZOEK, DELFT. CENTRAAL LABORATORIUM.
Prog. rpt. on determination of embrittlement in steel, 10–12/65, 20: 17117 (EURAEC-1558)
NERATOOM, N. V., THE HAGUE (NETHERLANDS).
Prog. rpt. on stainless steel cladding of heavy gage steel, 7–9/65, 20: 16990 (EURAEC-1556)
Prog. rpt. on stainless steel cladding of heavy gage steels, 10–12/65, 20: 16991 (EURAEC-1557)
NORDISK INSTITUT FOR TEORETISK ATOMFYSIK, COPENHAGEN (DENMARK).
Elementary introduction to elementary particle physics, 20: 17432 (NP-15902)
NUCLEAR ENERGY INFORMATION CENTER, WARSAW (POLAND).
Bibliography of the neutrino. II., 20: 17352 (NEIC-RR-21)
NUCLEAR METALS, WEST CONCORD, MASS.
Use of image-splitting eyepiece, 20: 16952 (ORNL-TM-1161, pp 182-91)
NUCLEAR UTILITY SERVICES, INC., WASHINGTON, D. C.
Prog. rpt. on Elk River reactor operations safety analysis, 3–5/65, 20: 18090 (NUS-246)

O

OAK RIDGE NATIONAL LAB., TENN.
A metallographic technique for measuring thin films of zirconium oxide as formed on reactor fuel cladding, 20: 16946 (ORNL-TM-1161, pp 80-4)
Accelerated epoxy mounting using r-f furnace, 20: 16947 (ORNL-TM-1161, pp 98-102)
Atomic and molecular cross sections, 20: 17253 (ORNL-3908, pp 90-9)
Biology and medicine, 20: 16159 (ORNL-3900, pp 150-81)
Choice of a fallout shelter protection factor, 20: 16733 (ORNL-P-1098)
Computer program for predicting coated-particle behavior, 20: 18076 (ORNL-TM-1385)
Conference on metallography, 19th group meeting, Oak Ridge National Lab., 4/65, 20: 16945 (ORNL-TM-1161)
DWBA analysis of $^{90}Zr(d,p)^{91}Zr$ reaction between 3.5 and 5.5 Mev, 20: 17691 (ORNL-TM-1235)
Electrical discharge machining in the metallurgical laboratory, 20: 16951 (ORNL-TM-1161, pp 159-81)
Electron-cyclotron heating, 20: 17888 (ORNL-3908, pp 32-51)
Electron optical study of effect of aging on carbides in Nb–W–Zr alloy, 20: 17023 (ORNL-TM-1161, pp 208-24)
Evaluation and irradiation effects studies on pyrolytic-carbon-coated fuel particles, 20: 17127 (ORNL-3923)
Evaluation of dissolvable epoxy systems for remote metallographic evaluations, 20: 16948 (ORNL-TM-1161, pp 103-11)
Experience with color in metallography, 20: 16949 (ORNL-TM-1161, pp 112-29)
Gamma-ray attenuation coefficients for Ge, 20: 17962 (ORNL-TM-1237)
High-current ion-beam production and injection, 20: 17890 (ORNL-3908, pp 100-7)
High magnification optical microscopy of ceramic materials, 20: 16954 (ORNL-TM-1161, pp 267-71)
Inelastic effects in stripping and other direct reactions, 20: 17692 (ORNL-TM-1414)
Injection and accumulation: single-pass experiments (DCX-1), 20: 17886 (ORNL-3908, pp 1-17)
Injection and accumulation: multiple-pass experiments (DCX-2), 20: 17887 (ORNL-3908, pp 18-31)
Interim postirradiation examination of a europium-bearing control rod from the stationary medium power reactor, 20: 17129 (ORNL-TM-1407)
Isotope development, 20: 16914 (ORNL-3900, pp 182-93)
Lists of available and desired materials (ultrapure inorganic research materials), 20: 16417 (ORNL-RMIC-4)
Magnetics and superconductivity, 20: 17600 (ORNL-3908, pp 114-48)
Metallic inclusions in UO_2, 20: 16953 (ORNL-TM-1161, pp 249-66)
Micro-constituents in Incoloy 800, 20: 17024 (ORNL-TM-1161, pp 236-46)
Microphotometer: application to grain orientation studies and quantitative metallography, 20: 16950 (ORNL-TM-1161, pp 132-45)
Neutron fluctuation measurements at ORNL, 20: 18048 (ORNL-P-1967)
OGRE-G—Monte Carlo code for calculation of dose rate at arbitrary points, 20: 17961 (ORNL-TM-1212)
Phase-shift analysis of elastic scattering: code PEGGY, 20: 17693 (ORNL-TM-1464)
Physical research, 20: 17158 (ORNL-3900, pp 82-149)
Plasma physics, 20: 17889 (ORNL-3908, pp 52-89)
Plasma theory and computation, 20: 17891 (ORNL-3908, pp 108-13)
Preparation of radioactive metallic specimens for replication, 20: 17128 (ORNL-TM-1161, pp 194-207)
Prog. rpt., annual, 1964, 20: 18175 (ORNL-3900)
Prog. rpt. on chemical technology, 11/64, 20: 16556 (ORNL-TM-1090)
Prog. rpt. on thermonuclear research, semiannual, 10/65, 20: 17885 (ORNL-3908)
Project Salt Vault: design and demonstration of equipment, 20: 18165 (ORNL-P-1987)
Reactor development, 20: 18020 (ORNL-3900, pp 2-81)
Shipping cost comparisons for lead-, steel-, and uranium-shielded casks, 20: 16622 (ORNL-3918)
Steam condensate β-γ monitor at fission products lab., 20: 16825 (ORNL-TM-1442)
Thermal conductivity values for solid and liquid promethium, 20: 17025 (ORNL-TM-1424)
Underground highway and parking garage and blast shelter for Manhattan Island, 20: 16623 (ORNL-TM-1381)
Use of image-splitting eyepiece, 20: 16952 (ORNL-TM-1161, pp 182-91)
Vacuum studies, sputtering, adsorption, and diffusion of gases in metals, 20: 17892 (ORNL-3908, pp 149-53)
OESTERREICHISCHE STUDIENGESELLSCHAFT FUER ATOMENERGIE G.M.B.H., SEIBERSDORF.
Radiometric and autoradiographic investigation of production of asbestos cement products, 20: 16920 (SGAE-IB/IA-7/1965)
OHIO STATE UNIV. RESEARCH FOUNDATION, COLUMBUS.
Microtopology of stress-corrosion cracking, 20: 16968 (COO-1319-33)
OREGON STATE UNIV., CORVALLIS.
Prog. rpt. on mechanism of divalent cation uptake by plants, 6/65–5/66, 20: 16174 (RLO-1547-3)

P

PARIS UNIV. (FRANCE).
Bound water of several high specific surface-area oxides, 20: 16413 (CEA-R-2703)
Calculation of pair-interaction function in some normal metals, 20: 17008 (CEA-R-2820)
Diffusion, electrical mobility, and ionic interactions in molten salts, 20: 16414 (CEA-R-2806)
Fluctuations of partial and total radiative widths by neutron capture resonance, 20: 17676 (CEA-R-2810)

PARIS UNIV., ORSAY (FRANCE). LABORATOIRE DE PHYSIQUE THEORIQUE ET HAUTES ENERGIES.
3-Particle nonrelativistic kinematics and phase space, 20: 17351 (N-65-19396)

PENNSYLVANIA STATE UNIV., UNIVERSITY PARK. MATERIALS RESEARCH LAB.
Prog. rpt. on crystal chemistry, 8/15–11/13/65, 20: 17007 (AD-627468)

PHILLIPS PETROLEUM CO. IDAHO FALLS, IDAHO., ATOMIC ENERGY DIV.
In-tank irradiation facilities at test reactor area, 20: 18135 (IDO-17135)
Prog. rpt. on SPERT project, 7–9/65, 20: 18019 (IDO-17146)

PITKIN (LUCIUS) INC., GRAND JUNCTION, COLO. WESTERN URANIUM PROJECT.
Handbook of analytical procedures, 20: 16337 (RMO-3001(Rev.1)(Suppl.))

PITTSBURGH UNIV., PA. DEPT. OF CHEMISTRY.
Prog. rpt. on magnetothermodynamics of para- and antiferromagnets, annual, 3/65–3/66, 20: 17978 (NYO-3402-2)

PRINCETON–PENNSYLVANIA ACCELERATOR, PRINCETON, N. J.
Guideline for use of standard nuclear instrument modules, 20: 16779 (PPAD-584D)
K^+ detector for use with rapid-cycling bubble chamber, 20: 16826 (PPAD-574E)

PRINCETON UNIV., N. J. ELEMENTARY PARTICLES LAB.
Single electron light pulse size distribution from cascaded image intensifier, 20: 16824 (NYO-3406-3)

PRINCETON UNIV., N. J. PLASMA PHYSICS LAB.
Initial transient of a thermonuclear reactor, 20: 17880 (MATT-437)

PRODUCTION GROUP, UNITED KINGDOM ATOMIC ENERGY AUTHORITY, CAPENHURST (ENGLAND).
Radioactive fallout in air and rain: results to middle of 1965, 20: 16660 (AERE-R-4997)

PRODUCTION GROUP, UNITED KINGDOM ATOMIC ENERGY AUTHORITY, SELLAFIELD (ENGLAND).
Effect of sodium alginate on uptake of Sr-85 from G-I tract, 20: 16173 (PG-Report-686)

PUBLIC HEALTH SERVICE, LAS VEGAS, NEV. SOUTHWESTERN RADIOLOGICAL HEALTH LAB.
Potential hazards as result of inhalation of radioiodines: a literature survey, 20: 16734 (TID-22693)

PUBLIC HEALTH SERVICE, WASHINGTON, D. C.
Measurement of airborne radioactivity, 20: 16732 (NP-15898)

PURDUE RESEARCH FOUNDATION, LAFAYETTE, IND.
Steady flow characteristics of single-phase natural circulation loop, 20: 16600 (COO-1177-15)

PURDUE UNIV., LAFAYETTE, IND. DEPT. OF PHYSICS.
Beta-gamma circular polarization correlation of ^{122}Sb, 20: 17677 (COO-1420-112)
Search for higher-order effects in allowed β transitions, 20: 17678 (COO-1420-113)

R

RAND CORP., SANTA MONICA, CALIF.
Underground highway and parking garage and blast shelter for Manhattan Island, 20: 16623 (ORNL-TM-1381)

RCA VICTOR CO., LTD., MONTREAL (QUEBEC). RESEARCH LABS.
Focused microwave systems for plasma diagnostics, 20: 17881 (N-65-19804)

REACTOR GROUP, UNITED KINGDOM ATOMIC ENERGY AUTHORITY, DOUNREAY (SCOTLAND).
Use of Dounreay fast reactor as MTR, 20: 18092 (TRG-Report-1039)

REACTOR GROUP, UNITED KINGDOM ATOMIC ENERGY AUTHORITY, SELLAFIELD (ENGLAND).
Reactor physics calculations with the ARGOSY code, 20: 18051 (TRG-Report-1014)

RENSSELAER POLYTECHNIC INST., TROY, N. Y.
Prog. rpt. on studies of sintering, annual, 1965, 20: 16992 (RPI-2408-4)

ROCHESTER UNIV., N. Y. DEPT. OF PHYSICS AND ASTRONOMY.
Zero-range distorted wave analysis of $^{16}O(^3He,\alpha_0)^{15}O$ reaction, 20: 17696 (UR-875-65)

RURAL COOPERATIVE POWER ASSOCIATION, ELK RIVER, MINN.
Prog. rpt. on Elk River reactor operations safety analysis, 3–5/65, 20: 18090 (NUS-246)

RUTGERS–THE STATE UNIV. OF NEW JERSEY, NEW BRUNSWICK. BUREAU OF ENGINEERING RESEARCH.
Prog. rpt. on gas-solid suspension, 9–12/65, 20: 16606 (TID-22621)

S

SANDIA CORP., ALBUQUERQUE, N. MEX.
High purity de-ionized water cleaning stations, 20: 16590 (SC-TM-66-49)

SANDIA CORP., LIVERMORE, CALIF.
Materials marking system, 20: 18176 (SCL-DR-66-6)

SEA-SPACE SYSTEMS INC., PALOS VERDES ESTATES, CALIF.
Calculation of magnet profile by the method of equivalent currents, 20: 17178 (CONF-650922, pp 96-103)
Magnet-system power supplies, 20: 17202 (CONF-650922, pp 755-68)
Stranded niobium–tin wire solenoids, 20: 17593 (CONF-650922, pp 597-602)

SOUDOMETAL, S. A., BRUSSELS (BELGIUM).
Prog. rpt. on stainless steel cladding of heavy gage steel, 7–9/65, 20: 16990 (EURAEC-1556)
Prog. rpt. on stainless steel cladding of heavy gage steels, 10–12/65, 20: 16991 (EURAEC-1557)

SPACE TECHNOLOGY LABS., INC., CANOGA PARK, CALIF.
Prog. rpt. on low-energy proton experiments, 12/64, 20: 16907 (N-65-17517)

STAATLICHE ZENTRALE FUER STRAHLENSCHUTZ, BERLIN (EAST GERMANY).
Summary of working session on personnel dosimetry, Berlin, 11/64, 20: 16827 (SZS-9(1965))

STANFORD LINEAR ACCELERATOR CENTER, STANFORD UNIV., CALIF.
A precision system for measuring wire trajectories in magnetic fields, 20: 17196 (CONF-650922, pp 497-504)
An achromatic 90° bending magnet system, 20: 17200 (CONF-650922, pp 715-22)
Applying acyclic generators for pulse duty in magnet power supplies, 20: 16772 (CONF-650922, pp 769-75)
Argonne National Laboratory's pion focusing horn, 20: 17198 (CONF-650922, pp 650-6)
Automated logging and processing of NRL cyclotron magnetic field data, 20: 17188 (CONF-650922, pp 415-20)
B-constant magnet pole design, 20: 17184 (CONF-650922, pp 239-47)
Beam transport magnet measurements at DESY, 20: 17192 (CONF-650922, pp 456-66)
Behavior of Hall probes in magnetic gradient fields, 20: 17194 (CONF-650922, pp 483-6)
CERN slim beam transport elements, 20: 17183 (CONF-650922, pp 218-38)
Circular current shim for a cyclotron magnet, 20: 17187 (CONF-650922, pp 377-89)
Closed-loop cooling system for superconducting bubble chamber magnets, 20: 17595 (CONF-650922, pp 611-14)
Conference on magnet technology, Stanford Univ., 9/65, 20: 17156 (CONF-650922)
Contoured poles for d-c accelerator magnets, 20: 17185 (CONF-650922, pp 248-52)
Cryogenic coil for megajoule energy storage, 20: 17597 (CONF-650922, pp 625-9)
Design and construction of magnet and transport system for large liquid helium bubble chamber, 20: 16810 (CONF-650922, pp 356-76)
Design and fabrication of integral coolant passage cryogenic coils for high power density, 20: 17874 (CONF-650922, pp 630-42)
Design, construction, and performance of cryogenically cooled and superconducting electromagnets, 20: 17592 (CONF-650922, pp 574-87)
Design of volume-minimized-split solenoid systems, 20: 17180 (CONF-650992, pp 111-25)
Determination of median planes in cyclotrons with Hall plates, 20: 17189 (CONF-650922, pp 421-7)
Economical magnet design, 20: 16584 (CONF-650922, pp 271-80)
Electromagnets for high-energy physics applications, 20: 17175 (CONF-650992, pp 1-26)
Establishing magnetic field of a solid pole magnet to within ±0.01%, 20: 17206 (CONF-650922, pp 823-34)
Exciting coils for guiding magnet of a 4-Bev electron synchrotron, 20: 17199 (CONF-650922, pp 686-99)
Experiments with superconducting cable, 20: 17591 (CONF-650922, pp 560-7)
Fabrication techniques of coils in the Zero-Gradient Synchrotron complex, 20: 17186 (CONF-650922, pp 356-65)
Field mapping by differential usage of Hall generators, 20: 17193 (CONF-650922, pp 472-5)

Flux pumps as power supplies for superconducting coils, 20: 17596 (CONF-650922, pp 615-24)
High homogeneity-rich field superconducting magnet for nuclear resonance, 20: 17587 (CONF-650922, pp 517-24)
High homogeneous field superconducting magnet for a polarized proton target, 20: 17586 (CONF-650922, pp 509-16)
High power silicon-controlled rectifier thyristors, 20: 16774 (CONF-650922, pp 788-96)
Large spark chamber magnet with tape-wound coils, 20: 16809 (CONF-650922, pp 253-61)
Magnet coil fabrication, 20: 16988 (CONF-650922, pp 305-12)
Magnet technology in high-energy experimental physics, 20: 17176 (CONF-650992, pp 27-55)
Magneto-optical experiments with superconducting magnet, 20: 17588 (CONF-650922, pp 525-9)
Measurements of ion-optical properties of high-resolution spectrometer for electron scattering, 20: 16808 (CONF-650922, pp 154-63)
Megagauss magnets using capacitor discharges, 20: 16587 (CONF-650922, pp 680-3)
New magnet installations at the Kamerlingh Onnes Laboratory, 20: 17598 (CONF-650922, pp 745-52)
NMR magnetometric device with flowing liquids, 20: 16770 (CONF-650922, pp 428-30)
Orthogonal analog model helps to solve magnetic field problems difficult to be treated by analytical methods, 20: 17181 (CONF-650922, pp 126-40)
Potential of interstitial compounds for high-field superconducting magnets, 20: 17589 (CONF-650922, pp 541-9)
Power supply for MURA magnet modeling program, 20: 17203 (CONF-650922, pp 776-8)
Precision current of field-regulated power supplies, 20: 16773 (CONF-650922, pp 779-87)
Precision magnetic field measurements with Hall-effect probes, 20: 17191 (CONF-650922, pp 447-55)
Prestressing method for assembling ZGS ring magnet coils, 20: 17201 (CONF-650922, pp 733-44)
Princeton-Pennsylvania accelerator standard magnet current regulators, 20: 17205 (CONF-650922, pp 817-22)
Quadrupole magnet design, 20: 17182 (CONF-650922, pp 208-17)
Rectifier power supplies for ZGS experimental magnets, 20: 17204 (CONF-650922, pp 808-16)
Search coil measurements of the harmonic content of beam transport magnets, 20: 17195 (CONF-650922, pp 487-96)
Selection of water-cooled conductors for d-c magnets, 20: 16585 (CONF-650922, pp 349-55)
Specifying magnet steels, 20: 17009 (CONF-650922, pp 287-96)
Spectroscopy of quadrupole magnets, 20: 17190 (CONF-650922, pp 431-46)
Terminal characteristics of short samples of superconductors and their effect on coil behavior, 20: 17590 (CONF-650922, pp 550-9)
Testing steels for gradient magnets, 20: 17010 (CONF-650922, pp 297-304)
Three-dimensional potential functions for magnet design, 20: 17177 (CONF-650922, pp. 89-95)
Use of conformal transformation in magnet design and extension of Schwarz-Christoffel transformation, 20: 17179 (CONF-650922, pp 104-110)
Wire orbit measurements with pulley of low friction, 20: 16771 (CONF-650922, pp 467-71)
100 Kilogauss quasi-continuous cryogenic solenoid. I., 20: 16586 (CONF-650922, pp 723-32)
100–300 kg pulse bubble chamber magnet, 20: 16811 (CONF-650922, pp 663-79)
4500-Gauss superconducting magnet for corpuscular ionography experiments, 20: 17594 (CONF-650922, pp 604-10)
90° Superconducting bending magnet for 30-Mev protons, 20: 17197 (CONF-650922, pp 536-40)

STANFORD UNIV., CALIF. INST. FOR PLASMA RESEARCH.
Prog. rpt. on plasma oscillations, 6–8/65, 20: 17893 (SU-IPR-44)
Prog. rpt. on studies of plasma oscillations, 9–11/65, 20: 17894 (SU-IPR-47)

STATE UNIV. OF IOWA, IOWA CITY. DEPT. OF PHYSICS AND ASTRONOMY.
Morphology of outer zone electron distribution, 20: 17538 (N-65-17609)

STATE UNIV. OF NEW YORK, ALBANY.
Prog. rpt. on effects of radiation on genetic structure of heterozygous outbreeding populations of forest trees, annual, 6/65–6/66, 20: 16228 (NYO-3571-2)

STATE UNIV. OF NEW YORK, SYRACUSE. COLL. OF FORESTRY.
Prog. rpt. on effects of radiation on genetic structure of heterozygous outbreeding populations of forest trees, annual, 6/65–6/66, 20: 16228 (NYO-3571-2)

STICHTING VOOR FUNDAMENTEEL ONDERZOEK DER MATERIE, JUTPHAAS (NETHERLANDS). INSTITUUT VOOR PLASMA-FYSICA.
Introduction to general dynamical systems, stability and waves, 20: 17884 (NP-15886)

SYRACUSE UNIV., N. Y. DEPT. OF PHYSICS.
Currents, algebras and dynamical systems, 20: 17435 (NYO-3399-45)
Dynamical mixing of spin and unitary spin, 20: 17434 (NYO-3399-18)
Nature of approximate symmetries of strongly interacting particles, 20: 17433 (NYO-3399-13)

SYRACUSE UNIV. RESEARCH INST., N. Y. DEPT. OF CHEMICAL ENGINEERING AND METALLURGY.
Underground highway and parking garage and blast shelter for Manhattan Island, 20: 16623 (ORNL-TM-1381)

SYSTEMS RESEARCH LABS., INC., DAYTON, OHIO.
Determination of ion excitation energies and densities in low-pressure discharge, 20: 17508 (ARL-65-246)

T

TECHNICAL OPERATIONS RESEARCH, BURLINGTON, MASS.
Development of improved land-surface fallout model, 20: 16735 (TO-B-65-99)

TECHNISCHE HOCHSCHULE, AACHEN (WEST GERMANY). INSTITUT FUER ELEKTRISCHE ANLAGEN UND ENERGIEWIRTSCHAFT.
Maximum credible accident in storage of highly radioactive fission products in salt formations, 20: 16722 (BMwF-FBK-65-03)

TENNESSEE UNIV., KNOXVILLE.
Inelastic effects in stripping and other direct reactions, 20: 17692 (ORNL-TM-1414)

TEXAS AGRICULTURAL AND MECHANICAL UNIV., COLLEGE STATION.
Absorption of injected horse gamma globulin in rabbits following whole-body γ irradiation, 20: 16214 (AD-620438)

THAYER SCHOOL OF ENGINEERING, DARTMOUTH COLL., HANOVER, N. H.
Analysis of liquid film in annular flow, 20: 16604 (NYO-3114-13)

THERMO ELECTRON ENGINEERING CORP., WALTHAM, MASS.
Converter performance test of Re emitter in contact with carbide fuel, 20: 17327 (N-65-19264)

TRACERLAB/RESEARCH, WALTHAM, MASS.
Narrow-band x-ray detector for identification of chemical elements using radioisotope x-ray sources, 20: 16823 (NYO-3160-1)

TRAVELERS RESEARCH CENTER, INC., HARTFORD, CONN.
Prog. rpt. on influence of local winds on fallout, final, 5–12/65, 20: 16661 (ECOM-00392-F)

TRW SPACE TECHNOLOGY LABS., THOMPSON RAMO WOOLDRIDGE INC., REDONDO BEACH, CALIF.
Effects of low-energy protons and high-energy electrons on silicon, 20: 17125 (NASA-CR-404)

TRW SYSTEMS, REDONDO BEACH, CALIF. APPLIED THERMODYNAMICS DEPT.
Prog. rpt. on kinetic studies of heterogeneous water reactors, 6/30/65, 20: 18050 (STL-372-22)

U

UNION CARBIDE CORP., OAK RIDGE, TENN. Y-12 PLANT.
Polyvinyl plastisol quality study, 20: 18179 (Y-1508)
Powder metallurgy in fabrication of very large parts, 20: 16993 (Y-DA-1043)
Y-12 clean room facilities, 20: 16744 (Y-EA-49)

UNION CARBIDE CORP., PARMA, OHIO. CARBON PRODUCTS DIV.
Prog. rpt. on effects of neutron damage on single-crystal graphite, semiannual, 7–12/65, 20: 17027 (TID-22712)
Prog. rpt. on effects of neutron damage on properties of pyrolytic and single-crystal graphite, annual, 4/64–6/65, 20: 17028 (TID-22733)

UNION CARBIDE CORP., TUXEDO, N. Y. NUCLEAR DIV.
Prog. rpt. on research in activation analysis, 8/63–10/64, 20: 16336 (NYO-10175)

UNITED NUCLEAR CORP., ELMSFORD, N. Y.
Prog. rpt. on heat exchangers for sodium-cooled reactors, 10–12/65, 20: 18093 (UNC-5142)

UNITED STATES–EURATOM JOINT RESEARCH AND DEVELOPMENT PROGRAM.
Analysis of liquid film in annular flow, 20: 16604 (NYO-3114-13)
Prog. rpt. on determination of embrittlement in steel, 10–12/65, 20: 17117 (EURAEC-1558)
Prog. rpt. on in-pile corrosion of nuclear materials, 3–8/65, 20: 17118 (EURAEC-2564)
Prog. rpt. on relationship of N content of stainless steels to stress corrosion, 10–12/65, 20: 16969 (EURAEC-1579)
Prog. rpt. on stainless steel cladding of heavy gage steel, 7–9/65, 20: 16990 (EURAEC-1556)
Prog. rpt. on stainless steel cladding of heavy gage steels, 10–12/65, 20: 16991 (EURAEC-1557)

Prog. rpt. on transition boiling heat transfer program, 10–12/65, 20: 16602 (GEAP-5081)
Prog. rpt. on two-phase flow investigation, 10–12/65, 20: 16601 (GEAP-5067)

V

VETERANS ADMINISTRATION HOSPITAL, OMAHA, NEBR.
Effects of radiation on serum enzymes and trace elements in large animals, 20: 16222 (AFWL-TR-65-112)
VIRGINIA POLYTECHNIC INST., BLACKSBURG. DEPT. OF METALS AND CERAMIC ENGINEERING.
Prog. rpt. on relationship of N content of stainless steels to stress corrosion, 10–12/65, 20: 16969 (EURAEC-1579)
VIRGINIA UNIV., CHARLOTTESVILLE. RADIOBIOLOGY AND BIOPHYSICS LAB.
Prog. rpt. on effects of radiation on radiosensitive and radioresistant mammalian cells, final, 20: 16230 (TID-22644)

W

WASHINGTON STATE UNIV., PULLMAN. RESEARCH DIV.
Radioisotope techniques in stream pollution problems in pulp and paper industry, 20: 16921 (TID-22627)
WESTINGHOUSE ELECTRIC CORP., PITTSBURGH, PA. ASTRONUCLEAR LAB.
Curve plot for "SCISRS", 20: 17699 (WANL-TME-1317)
New cross section library for n + ^{235}U reactions, 20: 17697 (WANL-TME-1028)
XO and EXT—IBM-7094 programs, 20: 17698 (WANL-TME-1132)
WESTINGHOUSE ELECTRIC CORP., PITTSBURGH, PA. ATOMIC POWER DIV.
A metallographic technique for measuring thin films of zirconium oxide as formed on reactor fuel cladding, 20: 16946 (ORNL-TM-1161, pp 80-4)
Mechanical, thermal, and hydraulic design of Saxton partial plutonium core, 20: 18095 (WCAP-3385-52)
Micro-constituents in Incoloy 800, 20: 17024 (ORNL-TM-1161, pp 236-46)
Prog. rpt. on CVTR, 7–9/65, 20: 18087 (CVNA-250)
WHERRETT LAB. OF NUCLEAR CHEMISTRY, UNIV. OF PITTSBURGH, PA.
Prog. rpt. on recoil studies of nuclear reactions, annual, 1/65–1/66, 20: 16508 (NYO-2771-13)

Z

ZENTRALINSTITUT FUER KERNPHYSIK, ROSSENDORF BEI DRESDEN (EAST GERMANY).
Decay of ^{79}Kr, 20: 17700 (ZfK-PhA-17)
ZENTRALSTELLE FUER ATOMKERNENERGIE-DOKUMENTATION, GMELIN-INSTITUT FUER ANORGANISCHE CHEMIE UND GRENZGEBIETE, FRANKFURT AM MAIN (WEST GERMANY).
Bibliography on accelerators, 11/65, 20: 17170 (AED-C-18-05)
Bibliography on disposal of radioactive waste material. I., 20: 18153 (AED-C-01-12)
Bibliography on disposal of radioactive waste material. II., 20: 18154 (AED-C-01-13)
Bibliography on direct conversion of nuclear energy into electric energy, 20: 17325 (AED-C-15-09)
Bibliography on direct conversion of nuclear energy into electric energy, 20: 17326 (AED-C-15-10)
Bibliography on high-energy physics, No. 5, 8/65, 20: 17153 (AED-C-23-05)
Bibliography on high-energy physics, No. 6, 8/65, 20: 17154 (AED-C-23-06)
Bibliography on high-energy physics, 8/65, 20: 17155 (AED-C-23-07)
Bibliography on radiation effects on living tissues and organisms, 20: 16219 (AED-C-04-23)
Bibliography on radiation effects on living tissues and organisms, 20: 16220 (AED-C-04-24)
Bibliography on radiation effects on living tissues and organisms, 20: 16221 (AED-C-04-25)

PERSONAL AUTHOR INDEX

Each entry after an author's name is a shortened version of the title of the report or article, followed by the *NSA* volume and abstract number. Report numbers are given in parentheses.

The phrase "Progress report" is abbreviated as "Prog. rpt.," permitting a more rapid and complete alphabetical arrangement of the titles without changing the location of the progress report titles in relation to the other titles.

Because of problems involving the mechanical preparation of this index, all accent marks are omitted. The following changes in spelling have been introduced to reduce some of the confusion which might result from omitting the accents:

ä	becomes	ae
ö		oe
ø		oe
ü		ue (except in transliterated Chinese names)

A

AALTONEN, J., Alpha-gamma and alpha-conversion electron coincidence study of ^{219}Rn, ^{215}Po, and ^{211}Bi, 20: 17703

ABARBANEL, Henry D. I., Calculation of nucleon magnetic moments by dispersion-theory methods, 20: 17390

ABDEL-AZIZ, A., Determination of certain trace impurities in U concentrates by activation analysis, 20: 16399

ABDEL-RASSOUL, A. A., Determination of certain trace impurities in U concentrates by activation analysis, 20: 16399

ABDEL-WAHAB, M. F., Preparation of ^{131}I-tyrosines and ^{131}I-thyroxine, 20: 16496

ABELES, Carl, Nondestructive determination of grade of Be by radiography, 20: 16962

ABRAHAM, P., Estimation of radon and thoron in atmospheric air, 20: 16679

ABRAHAMS, S. C., Symposium on accuracy in x-ray intensity measurement, Suffern, N. Y., 1965, 20: 18017

ABRIKOSOV, A. A., Present state of superconductivity problems, 20: 17628

ACKARET, R. L., In-tank irradiation facilities at test reactor area, 20: 18135 (IDO-17135)

ACKER, H. L., Muonic atoms and charge distribution of deformed nuclei, 20: 17756

ADACHI, Takayoshi, Catalytic tritium exchange reactions with tritiated active methylene compound, 20: 16492

ADAM, G., Effect of ionizing radiation on iron metabolism, 20: 16187

ADAMS, N., Film dosimetry practice with AERE/RPS film holder, 20: 16720 (AERE-R-4669)

ADDISON, L. A., Response characteristics of high-temperature electron-capture detector, 20: 16804

ADIN, A., Electron-transfer reactions of europium(II) in aqueous perchloric acid solutions, 20: 16462

ADLER, Howard I., Repair of radiation-induced damage to cell division mechanism of E. coli, 20: 16200

ADLER, Stephen L., Sum rules giving tests of local current commutation relations in high-energy neutrino reactions, 20: 17387

AEDELROTH, K. E., Hyperfine structure of 16-hour state in ^{119}Te, 20: 17705

AFANAS'EV, A. M., Change of resonance nuclear parameters during scattering on regular systems, 20: 18015

AGARWAL, Y. K., Measurements of the g factors of 2^+ states in even nuclei utilizing hyperfine fields in iron lattice. I., 20: 17747

AGARWALA, S. C., Effect of uv radiation on the oxidation of certain Krebs cycle substrates, 20: 16198

AGULLO-LOPEZ, F., Propagation of cleavage cracks in unirradiated and x-rayed NaCl single crystals, 20: 16513

AHMED, Syed Mansoor, Measurement of gross air activity (lower atmosphere) at Lahore, 20: 16683

AHRENS, L. H., Applied geochronology, 20: 16715

AHRONS, R. W., Bridge cell—superconductive memory cell, 20: 16797

AIDEMIRSKI, P., Brownian movement study by means of Moessbauer effect, 20: 17165

AINSWORTH, E. J., Recovery from radiation injury in dogs as evaluated by the split-dose technique, 20: 16216 (AD-628791)

AITA, Ryoji, Motion of balls, mill charge, and their pulverizing effect in the ball mill, 20: 16957 (LA-tr-66-11)

AITA, Ryoji, Pulverizing of natural graphite particle by hammer mill, 20: 16958 (LA-tr-66-12)

AITA, Ryoji, Shape of particle of natural graphite pulverized by cutter mill, 20: 16956 (LA-tr-66-6)

AITA, Ryoji, Studies on the pulverizing of crystalline graphite, 20: 16955 (LA-tr-66-5)

AJZENBERG-SELOVE, F., Energy levels of ^{31}S, 20: 17780

AKHIEZER, I. O., The fluctuations and scattering of particles in a turbulent plasma, 20: 17941

AKOPYAN, V. O., Interdiffusion between Ti and Mo, 20: 17111

ALBERT, Philippe, Radioactivation analysis of Ti in Al using reaction ^{48}Ti(p,n)^{48}V, 20: 16366

ALBERT, Philippe, Radioactivation analysis of Fe in Al using reaction ^{56}Fe(p,n)^{56}Co, 20: 16367

ALBERTONI, S., Spectrum of neutron transport equation in finite bodies, 20: 17657

ALBRETHSEN, A. E., Votalization of fission products from high-level ceramic wastes, 20: 18156 (BNWL-SA-453)

ALBRITTON, D. L., Ionic drift velocities and ion-molecule reactions in drift-tube mass spectrometer, 20: 17298

ALBURGER, D. E., Properties of the 4.77- and 5.16-Mev states of ^{10}B, 20: 17761

ALCANTARA, Raul, Possible formation of dithymine peroxide in irradiated DNA, 20: 16203

ALDERHOUT, J. J. H., Minimum atmospheric dilution of long-term and short-term emissions from the Eurochemic chimney, 20: 18162 (NP-15754)

ALDERMAN, Donald W., Nuclear spin relaxation in molybdenum metal, 20: 17998

ALDRED, A. T., Magnetization of iron–beryllium alloys, 20: 17985

ALEITE, W., Control of Obrigheim nuclear power plant, 20: 18112

ALEKSANDROV, N. N., Effect of meteorological conditions on effectiveness of radioactive pollutant collection, 20: 16656

ALESHIN, K. P., Moessbauer effect on ^{161}Dy impurity nuclei in metallic Gd, 20: 17988

ALEVRA, A., Angular distributions from ^{12}C(α,n)^{15}O reaction at 14 Mev, 20: 17803

ALEXANDRU, Gr., Transformation of M1-1305 type spectrometer, 20: 16798

ALEXANIAN, Moorad, New series expansion in statistical mechanics, 20: 17527

ALEXEFF, Igor, Plasma physics, 20: 17889 (ORNL-3908, pp 52-89)

ALFILLE, Lucien, Guide tubes for nuclear reactors, 20: 18039

ALFINTSEVA, R. A., Investigation of Cr–Fe–Mo and Cr–Fe–W alloys, 20: 17093

ALFORD, W. Parker, Zero-range distorted wave analysis of ^{16}O(^{3}He,α_0)^{15}O reaction, 20: 17696 (UR-875-65)

ALIX, Denise, Effect of fractionated x-ray doses on hemogram and protein formula of the mouse, 20: 16224 (CEA-R-2848)

ALLAS, R. G., Automated logging and processing of NRL cyclotron magnetic field data, 20: 17188 (CONF-650922, pp 415-20)

ALLAS, R. G., Prog. rpt. on NRL cyclotron, 9/65, 20: 17169 (AD-628928)

ALLEMAND, R., New possibilities offered by boron and uranium detectors,

20: 16896
ALLER, Lawrence H., Abundance of elements in solar atmosphere, 20: 17229
ALLES, W., SU_3 • SU_3 and nonleptonic hyperon decays, 20: 17448
ALLISON, S. K., Atomic and ionic partial stopping powers of He, gas for a He beam, 20: 17305
ALMAGRO, J., Polarographic behavior of hafnium(IV) in aqueous-alcoholic mixtures, 20: 16445
ALTER, H., Age of fission neutrons to In resonance energy in Fe–H_2O mixtures. II., 20: 17660
ALVAREZ RIVAS, J. L., Propagation of cleavage cracks in unirradiated and x-rayed NaCl single crystals, 20: 16513
ALVINERIE, Jacques, Tritium activity of basin pouring from Mont Cenis, 20: 16668
ALYAMOVSKII, S. I., Kinetics of reduction of low-oxide niobium by carbon, 20: 16483
ALYEA, E. D. Jr., π^+ p interactions at 450 Mev, 20: 17384
AMANKULOVA, D. S., Identification of single- and double-charge D particles by means of the δ-electron method, 20: 17358
AMARANTOS, S., Prog. rpt. on evaporation of radioactive wastes by solar energy, final, 12/65, 20: 18164 (NP-15874)
AMBROZHII, M. N., Thermal decomposition of Er and Yb hydroxides, 20: 16441
AMELINCKX, S., Ordering of interstitial impurities in niobium, 20: 18003
AMER, N. M., Dark recovery and glycerol protection for diploid Saccharomyces cerevisiae, 20: 16231 (UCRL-16377)
AMES, Lynford Lenhart, Dissociation energies of gaseous rare-earth monoxides, 20: 16485
AMIEL, S., Delayed neutrons and photoneutrons from fission products, 20: 17830
AMIEL, Sondie, Quantitative radioactivity determination of ^{18}O, 20: 16412
AMRAM, Y., Data processing in nuclear physics, 20: 17708
AMY, J. A., Annealing of uranium quenched from 100 to 4.2°K, 20: 17029 (ANL-Trans-273)
ANDARY, J., Time varying solar cycle protons program manual, 20: 17539 (N-65-18257)
ANDERS, Edward, Canyon Diablo meteorite, 20: 17238
ANDERSON, A. L., Whole-body counter facility, 20: 16737 (UCRL-14534, pp 13-18)
ANDERSON, A. R., Effect of temperature on γ radiolysis of water vapor, 20: 16536
ANDERSON, A. W., Radiation survival of food pathogens in complex media, 20: 16237
ANDERSON, H. L., Fine structure and isotope shift in muonic lead, 20: 17268
ANDERSON, J. R., Computer program for Fermi surface studies, 20: 17973 (IS-1106)
ANDREEV, A. B., Reactions of La and Nd oxides with oxides of Group II elements, 20: 16482
ANDREEVA, I. V., Effect of uv irradiation on temperate phage-bacteria complex, 20: 16270
ANDREEVA, Yu. A., Automatic physical measurements with magnetic β spectrometers, 20: 16854
ANDRES, K., Superconductivity of beta uranium, 20: 17095
ANDRITSOPOULOS, G., Simultaneous measurements of flight times and energies of fission fragments, 20: 17864
ANDRONIKASHVILI, E. L., Attenuation of second sound in rotating He on transition through phase transformation temperature, 20: 17641
ANDRONIKASHVILI, E. L., Relaxation of Onsager-Feynman vortexes in heating of rotating He II above phase transformation temperature, 20: 17642
ANDRONOV, E. A., Uranium sorption by platinized carbon, 20: 16581
ANGELI, I., Measurement of total cross sections of Cs and Rb for 14-Mev neutrons, 20: 17702
ANISOVICH, V. V., Prediction of masses in mesonic multiplets in the simple Quark model, 20: 17443
ANSELL, G. S., Kirkendall-effect densification in sintered W–Mo powder compact, 20: 16994
APALIN, V. F., Neutrons and kinetic energy of fragments in fission of heavy nuclei, 20: 17867
APPELT, H., Construction problems in design of hot cells, 20: 16595
ARAFUNE, J., Current-generated algebra and mass levels of the hadrons, 20: 17471
ARBMAN, G., An energy-weighted M1 sum rule, 20: 17690 (NP-15899)
ARGUE, G. R., Prog. rpt. on radiation effects on Ag and Zn battery electrodes, 7–10/65. II., 20: 17115 (AI-65-264)
ARGUE, G. R., Prog. rpt. on radiation effects on Ni–Cd electrodes. III., 6–9/13/64, 20: 17124 (N-65-17608)
ARINO, H., Prog. rpt. on research in activation analysis, 8/63–10/64, 20: 16336 (NYO-10175)
ARIZAN, Dan, Paramagnetic centers produced in irradiated polycrystalline $Mo_7O_{24}(NH_4)_6 \cdot 4H_2O$, 20: 16529
ARMBRUSTER, P., Average number and energy of γ rays emitted in ^{235}U fission, 20: 17828
ARMBRUSTER, P., Dependence of fission-fragment primary charge on nuclear structure, 20: 17845
ARMBRUSTER, P., Prompt and delayed γ rays from fission, 20: 17827
ARMBRUSTER, R., Multiple-duration monostable multivibrator, 20: 16792
ARMSTRONG, D. A., Cobalt-60 γ radiolysis of hydrogen halides at 77°K, 20: 16519
ARMSTRONG, T., Morphology of outer zone electron distribution, 20: 17538 (N-65-17609)
ARMSTRONG, W. A., Radiolysis of alkaline aqueous solutions containing hydrogen and oxygen, 20: 16520
ARONSON, S., Electrical properties of thorium carbides, 20: 17068
ARP, V., Cryogenic coil for megajoule energy storage, 20: 17597 (CONF-650922, pp 625-9)
ARRINGTON, Cleon Curtis, Chemical species containing ^{32}P and ^{35}S, 20: 16540
ASBURY, J. J., Powder metallurgy in fabrication of very large parts, 20: 16993 (Y-DA-1043)
ASHBROOK, A. W., Uranium and copper extraction by liquid ion exchange, 20: 16572
ASHBROOK, Richard Louis, Modification of eutectic alloys for high-temperature service, 20: 17108
ASHIKAWA, J. K., Dark recovery and glycerol protection for diploid Saccharomyces cerevisiae, 20: 16231 (UCRL-16377)
ASINOVSKII, E. I., Experimental determination of argon plasma heat-conductance factor, 20: 17937
ASLUND, Nils, Band spectrum of ThO, 20: 17254
ASNER, A., CERN alim beam transport elements, 20: 17183 (CONF-650922, pp 218-38)
ASNER, A., Orthogonal analog model helps to solve magnetic field problems difficult to be treated by analytical methods, 20: 17181 (CONF-650922, pp 126-40)
ATKINSON, D., Levinson's theorem for S-matrix theory with inelasticity, 20: 17452
ATTREP, Moses Jr., Fallout from nuclear explosion of October 16, 1964, 20: 16663 (TID-21470)
ATTREP, Moses Jr., Radiochemical measurement of promethium isotopes in nature, 20: 16685
AULT, J. D., Yttrium oxide–titanium dioxide system, 20: 17032
AUSKERN, A. B., Electrical properties of thorium carbides, 20: 17068
AUSTERMAN, Stanley B., Cation diffusion in single-crystal and polycrystalline BeO, 20: 17049
AUXIER, J. A., Free-field radiation-dose distributions from Hiroshima and Nagasaki bombings, 20: 16760
AZIMOV, S. A., Elastic scattering of 5.5-Bev π mesons on protons, 20: 17360

B

BABA, C. V. K., Measurements of the g factors of 2^+ states in even nuclei utilizing hyperfine fields in iron lattice. I., 20: 17747
BABAEV, A. I., Observation of atomic muonium in crystalline quartz, 20: 17361
BABAKOV, A. A., Effect of silicon on mechanical properties and intercrystalline corrosion tendencies of Cr–Ni–Mo alloy, 20: 16983
BABLER, G. M., High-current ion-beam production and injection, 20: 17890 (ORNL-3908, pp 100-7)
BABLIDZE, R. A., Attenuation of second sound in rotating He on transition through phase transformation temperature, 20: 17641
BACCONNET, Eugene, Mobility of Rb^+ and Cs^+ ions in gases at high pressures, 20: 16415 (CEA-R-2861)
BACHMAN, A. H., Pion production in $p\bar{p}$ annihilations at 3.3 and 3.7 Bev/c, 20: 17385
BACMANN, Jean-Jacques, Fritting of uranium dioxide, 20: 17037
BACRY, H., The de Sitter group $L_{4,1}$ and bound states of hydrogen atom, 20: 17263
BAGHDIKIAN, M., Characterization of ^9B excited states populated by ^9Be_A decay, 20: 17807
BAGLIN, J. E. E., $^{12}C(\gamma,n)^{11}C$ cross section to 65 Mev, 20: 17763
BAGLIN, J. E. E., $^{16}O(\gamma,n)^{15}O$ cross section from threshold to 65 Mev, 20: 17762
BAHCALL, John N., Phase-space integrals for β decay and nuclear matrix elements, 20: 17732
BAIBORODOV, Yu. T., Unstable states of a plasma in a trap with combined field, 20: 17925
BAIER, V. N., Electromagnetic particle pair production, 20: 17499
BAIER, V. N., Quantum depolarization of electrons in magnetic field, 20: 17689 (NP-15783)
BAIERL, H., Nanosecond pulse device for a 2-Mev Van de Graaff electron accelerator, 20: 17217
BAILEY, J. M., Atomic interactions of muonium, 20: 17297
BAKKEN, Jon Arne, Small-time solution of snowplough equations for

plasma accelerator, 20: 17903
BALABAN, A. T., Isotope exchange of active methyl hydrogens. III., 20: 16501
BALACHANDRAN, A. P., Dynamical mixing of spin and unitary spin, 20: 17434 (NYO-3399-18)
BALATS, M. Ya., Observation of atomic muonium in crystalline quartz, 20: 17361
BALDIN, A. M., Electromagnetic interactions in the quark model, 20: 17348 (JINR-P-2556)
BALDINGER, E., Preparation of Li-drifted Ge counter diodes, 20: 16890
BALON, G., Inorganic ion exchanger for separation of Cs from high-level radioactive wastes, 20: 16570
BANJI, Mehtab S., Carotenoid pigments of a radiation-resistant Micrococcus species, 20: 16161
BANAS, J., Chromatographic separation of $^{131}I^-$, $^{131}IO_3^-$, and $^{131}IO_4^-$, 20: 16567
BANE, R. W., Spectrophotometric determination of Mn after oxidation with Na perxenate, 20: 16351
BANERJEE, B. M., Resolving times of binary scalers—analytical study, 20: 16802
BARABAS, A., Isotope exchange of active methyl hydrogens. III., 20: 16501
BARANGER, M., Oscillator brackets for Hartree-Fock calculations, 20: 17744
BARDES, R., Prog. rpt. on graphite interface studies, 5/63–9/65, 20: 18127 (GA-6753(Pt.I))
BARDIN, T. T., Magnetic dipole and electric quadrupole hyperfine effects in ^{209}Bi muonic x rays, 20: 17793
BAREISS, Erwin H., Spectral theory for the stationary transport operator in slab geometry, 20: 17658
BARENDREGT, T. J., Eurochemic plant and role in startup of European fuel cycles, 20: 16558
BARENDSEN, G. W., Dose-rate and survival curves, 20: 16750
BARKOW, A. G., Lithium-8 fragments from 28-Bev proton interactions in nuclear emulsion, 20: 17753
BARNARD, A. C. L., Nuclear reaction polarimeter using position-sensitive particle detectors, 20: 16870
BARNETT, C. F., Atomic and molecular cross sections, 20: 17253 (ORNL-3908, pp 90-9)
BAR-NIR, I. M., Renormalization of the strangeness-changing axial-current coupling constant, 20: 17458
BAROCH, C. J., Irradiation performance of alternate cladding materials, 20: 17120 (GEAP-4916)
BARON, V. V., Solid solutions of Ge, Sn, Al, and Be in V_3Si and their superconductivity, 20: 17043
BARRALL, R. C., Health physics for maintenance operation on a homogeneous research reactor, 20: 16757
BARRERA PINERO, R., Pyrolysis of polyphenyls. I., 20: 16491
BARRETT, C. S., Thermal expansion of alpha uranium, 20: 17064
BARRETT, J. H., Role of correlated defects in radiation-enhanced diffusion, 20: 17131
BARRETT, M. J., Techniques applicable to shielding of nuclear particles from space, 20: 17965
BARRETT, R. C., Magnetic dipole and electric quadrupole hyperfine effects in ^{209}Bi muonic x rays, 20: 17793
BARTLETT, D., Transverse polarization of the muon in decay $K^+_{\frac{1}{2}} \rightarrow \mu^+ + \pi^- + \nu$, 20: 17424
BARTON, Donald, Reversing hydrogen isotope effect on rate of gas phase decomposition of oxalic acid, 20: 16455
BARTON, J. P., Radiographic examination through steel using cold neutrons, 20: 16616
BARTOSEK, V., Flat flux in slab reactor with natural uranium, 20: 18058
BARTRAM, R. H., Wave functions for F′ centers in alkali halides, 20: 17977 (NYO-2047-36, App.2)
BARTRAM, Ralph H., Prog. rpt. on investigation of radiation effects in metal oxides and azides, annual, 2/65–1/66, 20: 17975 (NYO-2047-36)
BARYAKHTAR, V. G., Effect of impurities on superconducting transition temperature, 20: 17637
BARYAKHTAR, V. G., Effect of pressure on superconducting transition temperature, 20: 17639
BASILE, L. J., Infrared spectra of rare earth metal chloride complexes of 2,2′-bipyridyl and 1,10-phenanthroline, 20: 16437
BASMANOV, P. I., Basis for using fibrous filter materials, (Petryanov filters), 20: 16653
BASS, F. G., Low-frequency properties of semiconductor plasma in stationary electric field, 20: 18013
BASSETTI, M., Beam optics computation for particle transport systems, 20: 17211 (LNF-65/45)
BASSI, A., Metallographic techniques for optical and electronic observation of Zr–2.5 Nb alloy, 20: 16959
BASSLER, E. A., Mechanical, thermal and hydraulic design of Saxton partial plutonium core, 20: 18095 (WCAP-3385-52)
BATES, D. R., Classical calculations on electron capture, 20: 17275
BATES, Roger G., Dissociation of acetic acid-d_3 in aqueous solution and related isotope effects, 20: 16458
BATYEV, E. G., Coexistence of singlet and triplet pairs in an anisotropic superconductor, 20: 17645
BAUDACH, H., Effect of radiation on distribution of ^{32}P-labeled Yoshida sarcoma cells, 20: 16188
BAUMEL, P., Pion production in $p\bar{p}$ annihilations at 3.3 and 3.7 Bev/c, 20: 17385
BAYHURST, B. P., Symmetry of neutron-induced ^{239}Pu fission in resonance region, 20: 17858
BE, C. A., Metallographic techniques for optical and electronic observation of Zr–2.5 Nb alloy, 20: 16959
BEARD, E., Converting portable survey meter's ion chamber into continuous air monitor, 20: 16832 (UCRL-14534, pp 32-40)
BEAUCAGE, D. R., Multiple spectrometer control by computer, 20: 16869
BEAUDET, C. A., Inorganic ion exchanger for separation of Cs from high-level radioactive wastes, 20: 16570
BECIRSPAHIC, Sulejman, Improvement of heat transfer of fuel element with polyzonal spiral finning, 20: 18078
BECK, Harold L., Environmental γ radiation from deposited fission products, 1960–1964, 20: 16168
BECK, J. N., Fallout from nuclear explosion of October 16, 1964, 20: 16663 (TID-21470)
BECK, Juergen, Detectors for reactor instrumentation, 20: 18023
BECK, R., Development of a laser light source for the Mach-Zehnder interferometer, 20: 17875 (IPP-1/35)
BECKER, G., Image characteristics of short magnetic deflection systems for atomic beams with regard to velocity distribution. II., 20: 17225
BEERNTSEN, D. J., Critical currents in superconducting single-crystal NbSe, 20: 17609
BEIL, H., Measurement of capture cross section of Na between 10 and 135 kev, 20: 17718
BEKKER, J. H., Immunity in experimental syphilis. IV., 20: 16199
BELEW, W. L., Controlled-potential polarography and coulometry as microanalytical techniques, 20: 16390
BELEW, W. L., Determination of trace quantities of U, 20: 16389
BELEZOS, N. K., Local estrogen and uv irradiation in treatment of alopecia, 20: 16248
BELL, George I., Neutron capture cross sections of some rare earth nuclei, 20: 17653 (LA-3463)
BELL, J. T., Absorption spectrum of the uranyl ion in perchlorate media. I., 20: 16450
BELL, P. R., Injection and accumulation: multiple-pass experiments (DCX-2), 20: 17887 (ORNL-3908, pp 18-31)
BELLE, Yu. S., Radiometric properties of large liquid scintillation counter, 20: 16865
BELLENI-MORANTE, A., Reactor kinetics equation as direct consequence of Boltzmann equation, 20: 18067
BELLMAN, Richard, Existence and uniqueness theorems in invariant imbedding. II., 20: 16935
BELLOCQ, Anne-Marie, Vibration spectra of imidazole, imidazole (D)-1, imidazole (D_3)-2,4,5, and imidazole (D_4). I., 20: 16499
BELLOCQ, Anne-Marie, Vibration spectra of imidazole, imidazole (D)-1, imidazole (D_3)-2,4,5, and imidazole (D_4). II., 20: 16500
BELMONT, Jean-Loup, Production of intense source of microsecond proton pulses, 20: 17172 (CEA-R-2802)
BELOUS, V. N., Corrosion resistance of structural materials in boron-containing solutions, 20: 16976
BELOV, K. P., Magnetostriction of rare earth metals in paramagnetic, antiferromagnetic and ferromagnetic regions, 20: 18012
BELSKY, Theodore, Chemical evolution and organic geochemistry, 20: 16633 (UCRL-16605)
BENAKSAS, D., Deuteron electromagnetic form factors, 20: 17349 (LAL-1155)
BENEDICT, G., Comparison of observed delayed-neutron abundances with calculated fission yields of neutron precursors, 20: 17831
BENESOVSKY, F., Ternary phases with $MgZn_2$ type, 20: 17075
BENISZ, J., Possibility of introduction of maximum quantity of boron into nuclear emulsions, 20: 16891
BENJAMIN, R. W., Gamma rays produced in $^{56}Fe(n,n'\gamma)^{56}Fe$ reaction, 20: 17736
BENOIST, P., Heterogeneity calculation for fast reactors by a perturbation method, 20: 18063
BENUSKA, K. L., Reusability of buildings after a warfire, 20: 16621 (AD-625867)
BENZ, Mark G., Stranded niobium–tin wire solenoids, 20: 17593 (CONF-650922, pp 597-603)
BENZI, V., Monte Carlo analysis of some enriched ^{235}U fast critical assemblies, 20: 18057
BERGER, K. C., Polonium-210 analyses of vegetables, cured and uncured tobacco, and associated soils, 20: 16189
BERGGREN, T., Quasi-free proton-proton scattering in light nuclei at 460 Mev, 20: 17741

BERGLES, A. E., Investigation of boiling water flow regimes at high pressure, 20: 16605 (NYO-3304-8)
BERGMANN, W. H., 100–300 kg pulse bubble chamber magnet, 20: 16811 (CONF-650922, pp 663-79)
BERGNER, K. G., Rapid determination of important radionuclides in foodstuffs and water. II., 20: 16369
BERNHARD, M., Prog. rpt. on radioactive contamination of the sea, annual, 1964, 20: 16725 (EUR-2543.e)
BERKES, Branko, Behavior of Hall-probes in magnetic gradient fields, 20: 17194 (CONF-650922, pp 483-6)
BERMAN, B. L., Photoneutron cross sections for ^{12}C and ^{27}Al, 20: 17773
BERMAN, S. S., Direct determination of small quantities of rare earth and yttrium oxides in thoria by emission spectroscopy, 20: 16393
BERNARDINI, E. J., Use of electronic flash units in proximity with explosives, 20: 16739 (UCRL-14534, pp 44-9)
BERNSTEIN, Richard B., Long-range interatomic forces from predissociation data and resonances in atomic scattering, 20: 17266
BERNSTEIN, Richard B., Velocity analysis of reactive scattering in crossed molecular beams, 20: 17296
BERTINOV, A. I., Axi-symmetric linear MGD flow with a Hall effect in two-component magnetic field, 20: 17521
BERLYAND, M. E., Effect of vertical distribution of temperature and wind velocity on the atmospheric diffusion of radioactive pollutants, 20: 16651
BES, D. R., Exact diagonalization of quadrupole and pairing forces in nuclear d-s shell, 20: 17801
BESKROVNYI, I. M., Automatic physical measurements with magnetic β spectrometers, 20: 16854
BESSONOV, A. F., X-ray study of oxidation of UO_2, 20: 16474
BEUKERS, R., Effect of proflavine on uv-induced dimerization of thymine in DNA, 20: 16280
BEVERIDGE, J. H., Development problems of nuclear rocket engines, 20: 18128
BEWILOGUA, L., Heat transfer in boiling hydrogen, neon, nitrogen, and argon, 20: 16610
BEYNON, T. D., Calculation of cross section for $^{238}U(n,\gamma)^{239}U$ at 10 kev to 3 Mev, 20: 17720
BEYSTER, J. R., Prog. rpt. on graphite interface studies, 5/63–9/65, 20: 18127 (GA-6753(Pt.1))
BEZIN, G. I., Experimental radiation sickness induced with ^{210}Po, 20: 16268
BEZUGLYI, P. A., Nonlinear effects in ultrasonic absorption in superconducting indium, 20: 17635
BHATNAGAR, K. G., Large plastic scintillators of parabolic shape, 20: 16849
BHATTACHARYA, Tapan K., Radiation effects on fracture surface energy of KCl, 20: 17137
BHATTACHERJEE, S. K., Measurements of the g factors of 2^+ states in even nuclei utilizing hyperfine fields in iron lattice. I., 20: 17747
BHAWALKAR, D. V., Large plastic scintillators of parabolic shape, 20: 16849
BHIDAY, M. R., Large plastic scintillators of parabolic shape, 20: 16849
BHIDE, G. K., Effect of Tl concentration on performance of NaI(Tl) scintillation crystals, 20: 16850
BHUTANI, O. P., General study of plane steady flows in nonequilibrium magnetogasdynamics, 20: 17515
BIALECKE, E. P., Rapid electron-density oscillations on axis of theta pinch, 20: 17918
BICAK, J., Rainich geometrization of vector meson field in Kibble theory, 20: 17441
BICHSEL, Hans, Wire orbit measurements with pulley of low friction, 20: 16771 (CONF-650922, pp 467-71)
BIEBER, Erhard, Conversion electron spectrum of ^{104}Rh after neutron capture, 20: 17810
BIEFER, G. J., Effects of U and Mo alloying additions on corrosion resistance of AISI type 430 stainless steel, 20: 16975 (NP-15900)
BIERNACKA, Irmina, Studies on viruses of asiatic influenza. III., 20: 16239
BIERTER, W., Group theoretical classification of transitions, 20: 17488
BIGGERS, R. E., Absorption spectrum of the uranyl ion in perchlorate media. I., 20: 16450
BIJWAARD, G., Prog. rpt. on two-phase flow investigation, 10–12/65, 20: 16601 (GEAP-5067)
BILDSTEIN, H., Reprocessing of graphite-carbide fuel for high-temperature reactors, 20: 16575
BILGER, H. R., Optimum energy resolution of semiconductor radiation detectors, 20: 16871
BINDELL, J., Interference fringes formed by x rays scattered from thin films, 20: 17163
BINDER, I., Preparation and properties of superconducting Nb–Sn sandwiches, 20: 17649
BIRKEBAK, Richard C., Prediction of mode transition in an arc with a transpiration-cooled anode, 20: 17514
BIRKHOFER, A., Unstationary temperature distribution in cylindrical and annular, 20: 16613
BIRSS, I. R., Use of Dounreay fast reactor as MTR, 20: 18092 (TRG-Report-1039)
BISCAYE, Pierre E., Prog. rpt. on radiochemical analyses of filter samples collected under Project Stardust, 1963. Appendix, 20: 16727 (HASL-168)
BISHOP, T. P., Use of Dounreay fast reactor as MTR, 20: 18092 (TRG-Report-1039)
BISSELL, R. C., Guideline for use of standard nuclear instrument modules, 20: 16779 (PPAD-584D)
BITTER, Francis, Megagauss magnets using capacitor discharges, 20: 16587 (CONF-650922, pp 680-3)
BITTNER, H., Problem of the carbohydrides, 20: 17074
BJORKEN, J. D., Inequality for electron and muon scattering from nucleons, 20: 17399
BLAGA, Liviu, Distribution of deuterium in fractions obtained in pretreatment of crude oil, 20: 16475
BLAGA, Lucia, Distribution of deuterium in fractions obtained in pretreatment of crude oil, 20: 16475
BLANC, Joseph, Deuterium isotope effect on performance of europium chelate lasers, 20: 16781
BLANCHARD, R. C., Time varying solar cycle protons program manual, 20: 17539 (N-65-18257)
BLANK, Howard A., 400-Ton copper vacuum tube, 20: 16999
BLANKS, B. L., Experiments with foil-film combinations and collimators for neutron radiography, 20: 16619
BLAU, L. M., Zero-range distorted wave analysis of $^{16}O(^3He,\alpha_0)^{15}O$ reaction, 20: 17696 (UR-875-65)
BLAZHIEVSKII, L. F., Calculation of free energy on basis of representation of interaction in collective variables, 20: 17530
BLENDEN, D. C., Incorporation of disaster preparedness in curriculum of school of veterinary medicine, 20: 16761
BLIZARD, Everitt P., Choice of a fallout shelter protection factor, 20: 16733 (ORNL-P-1098)
BLOCH, J., Variation of the parameters of weakly irradiated UC, 20: 17140
BLOCH, S. C., Heterodyne generation by electromagnetic fields in gaseous plasma, 20: 17905
BLOCK, S., Converting portable survey meter's ion chamber into continuous air monitor, 20: 16832 (UCRL-14534, pp 32-40)
BLOCK, S., Source of intermediate-energy neutrons for dosimeter calibration, 20: 16830 (UCRL-14534, pp 8-12)
BLOK, J., Temperature scale for Nd ethylsulfate below 1°K, 20: 17614
BLOK, Johan, Systematic variation of quadrupole crystal-field shielding in rare-earth ethyl sulfates, 20: 17996
BLOKHIN, V. I., Photometric determination of Np by means of xylenol orange, 20: 16408
BLOKHINTSEV, D. I., Backward scattering of high-energy particles, 20: 17373
BLOMEKE, J. O., Project Salt Vault, 20: 18169
BLONS, J., Measurement and analysis of fission cross section of ^{239}Pu from 0 to 5 kev, 20: 17851
BLUDMAN, S. A., Distinction between composite and elementary particles in a model field theory, 20: 17472
BLUET, J. C., Measurement of capture cross section of Na between 10 and 135 kev, 20: 17718
BLUMENSTOCK, Joe W., Prog. rpt. on ionizing radiation, injury, prevention, and treatment, annual, 10/65, 20: 16303 (AD-626384)
BOBOVNIKOVA, Ts. I., Strontium-90 in fresh-water reservoirs of the Soviet Union in 1961-1962, 20: 16705
BOCHNACKI, Zbigniew, Transverse spin polarization of odd-mass deformed nuclei, 20: 17682 (INP-428/PL)
BOCKMANN, Rolf, Possibility of radiological hydrogen determination in solids, especially in coals, 20: 16356
BOCOLA, W., Separation of oxygen isotopes by gas chromatography, 20: 16930
BODENSTEDT, E., Lifetime of the $^{31}/_2$ three-particle state of ^{177}Hf, 20: 17811
BODERGAT, R., Comparison of effects of mutagenic substances by studying mutagenesis of plants, 20: 16225 (EUR-2715.f)
BODNER, Stephen Elliott, Quasi-linear theory of electrostatic instabilities, 20: 17957
BOEER, K. W., Prog. rpt. on radiation damage in CdS, 7–12/64, 20: 17123 (N-65-17505)
BOEGLY, W. J. Jr., Project Salt Vault: design and demonstration of equipment, 20: 18165 (ORNL-P-1987)
BOEGLY, W. J. Jr., Project Salt Vault, 20: 18169
BOEHLER, Torstein, Organic-cooled irradiation loop in the HFR at Petten, 20: 18137 (KR-82)
BOEHM, E., Digital recording system of air shower experiment at Kiel, 20: 16873
BOEKELHEIDE, Irving, Graphing self-absorption curves with ordinary γ absorption data, 20: 17966

BOERSCH, H., Superconducting hollow cylinder as magnetic lens, 20: 17631
BOETTCHER, A., Second Foratom Congress. Fuel elements, 20: 16566
BOEUF, A., Flux distribution in D_2O-moderated lattice, 20: 18055
BOGARD, D. D., Noble gases from Peace River, Lalande, and Achilles meteorites, 20: 16672
BOGARD, D. D., Xenon anomalies in Pasamonte meteorite, 20: 17239
BOGDANOV, V. S., Jump in volume and melting curve of Cs at pressures up to 17,000 kg/cm², 20: 17071
BOGEN, Donald C., Prog. rpt. on radiochemical analyses of filter samples collected under Project Stardust, 1963. Appendix, 20: 16727 (HASL-168)
BOGEN, Donald C., Prog. rpt. on radiochemical analyses of filter samples collected under Project Stardust, 1964, 20: 16728 (HASL-169)
BOGOLYUBOV, P. N., Magnetic moment of Dirac particle in the potential well, 20: 17431 (JINR-P-2569)
BOGOLYUBOVA, I. V., Interdiffusion between Ti and Mo, 20: 17111
BOJARSKI, Zbigniew, Neutron-diffraction investigation of iron–tungsten carbides, 20: 17015 (INR-665/II/PS)
BOKHARI, M. Sibtain, Deuteron polarization from $^{9}Be(p,d)^{8}Be$ reaction at 3 to 5 Mev, 20: 17760
BOKOV, O. G., Electromagnetic interaction of the X meson in higher symmetries, 20: 17342 (JINR-P-2520)
BOLDEMAN, J. W., Liquid scintillator experiment for measuring $\bar{\nu}$ for ^{241}Pu, 20: 17826
BOLDT, Elihu, Do solar flare proton events measure geometry of a diffusion process? 20: 17228 (N-65-18275)
BOLLOK, L., Experiences with measuring systems OZH-1 and OZH-2, 20: 18024
BOLOGNA, G., Highly polarized coherent bremsstrahlung from a diamond target in Bev region, 20: 17679 (DESY-65/15)
BOL'SHAKOVA, O. V., Microstructure of the initial phase of a magnetic storm according to stability of micropulsations, 20: 17549
BONCHEV, L., Positron annihilation in CdS monocrystals, 20: 17983
BONCHEV, Ts., Brownian movement study by means of Moessbauer effect, 20: 17165
BOND, C. D., Automated logging and processing of NRL cyclotron magnetic field data, 20: 17188 (CONF-650922, pp 415-20)
BOND, C. D., Prog. rpt. on NRL cyclotron, 9/65, 20: 17169 (AD-628928)
BONDELID, R. O., Prog. rpt. on NRL cyclotron, 9/65, 20: 17169 (AD-628928)
BONDY, Charles, Radiochemical Laboratory of L'Atome Industriel, 20: 16365
BONI, A. L., Rapid ion exchange analysis of radiocesium in milk, urine, sea water, and environmental samples, 20: 16342
BONNEVIE-SVENDSEN, M., Analysis of chemical state of Pu and fission products in process feed solutions, 20: 16333 (KR-81)
BOOS, E. G., Criterion for selecting nucleon-nucleon events in nuclear emulsion, 20: 17357
BOOZENNY, A., Design and fabrication of integral coolant passage cryogenic coils for high power density, 20: 17874 (CONF-650922, pp 630-42)
BORISOV, M., Positron annihilation in CdS monocrystals, 20: 17983
BORISOV, N. S., Method of obtaining super-low temperature based on a dissolution of ^{3}He in ^{4}He, 20: 17599 (JINR-P-2480)
BORN, W., Radiosensitivity of calcifying Malherbe's epitheliona, 20: 16308
BORNAZ, M., Moessbauer spectrometer, 20: 16872
BOROWITZ, J. L., Synthesis and isotopic analysis of $CH_3{}^{18}OH$ and $CH_3{}^{17}OH$, 20: 16547
BORST, Lyle B., Dispersion relation in liquid helium, 20: 16461
BOS, W. G., Rare earth hydrides, 20: 16453
BOSHOLM, Joergen, Separation chromatography of the rare earths by use of di(2-ethylhexyl) phosphoric acid. III., 20: 16385
BOSSARD, P., Orthogonal analog model helps to solve magnetic field problems difficult to be treated by analytical methods, 20: 17181 (CONF-650922, pp 126-40)
BOSTANJOGLO, O., Superconducting hollow cylinder as magnetic lens, 20: 17631
BOTOS, P. Jr., Single electron light pulse size distribution from cascaded image intensifier, 20: 16824 (NYO-3406-3)
BOTVIN, V. A., Inelastic interactions of antiprotons with neutrons at 3 Bev, 20: 17359
BOUDREAUX, Rodney Ayes, Boundary layer thermodynamic and hydrodynamic characteristics of a flowing liquid hydrogen tank, 20: 17536
BOUNIN, Paul, Application of Fermat principle to magnetic spectrometers, 20: 16821 (LAL-1151)
BOWLER, M. G., Energy spectrum of primary cosmic rays, 20: 17315
BOWMAN, Harry R., Application of high-resolution semiconductor detectors in x-ray emission spectrography, 20: 16887
BOWYER, Charles Stuart, X-ray astronomy: observational results, theoretical aspects, and experimental procedures, 20: 17248
BOX, Harold C., Paramagnetic absorption of irradiated glycine, 20: 16525
BOYKO, E. S., Micro-constituents in Incoloy 800, 20: 17024 (ORNL-TM-1161, pp 236-46)
BOZOKI, G., Multiple scattering constant in emulsion at great cell lengths, 20: 16833
BRAAMS, C. M., Thermonuclear investigations. III., 20: 17928
BRADFORD, E., Moessbauer absorption in presence of electron spin relaxation, 20: 18009
BRADFORD, J. N., Praseodymium-141 photoneutron cross section to 65 Mev, 20: 17764
BRADFORD, J. N., $^{12}C(\gamma,n)^{11}C$ cross section to 65 Mev, 20: 17763
BRADFORD, J. N., $^{16}O(\gamma,n)^{15}O$ cross section from threshold to 65 Mev, 20: 17762
BRADLEY, E. F., Coated Nb alloys can take high turbine heat, 20: 16963
BRADSHAW, R. L., Project Salt Vault: design and demonstration of equipment, 20: 18165 (ORNL-P-1987)
BRADSHAW, R. L., Project Salt Vault, 20: 18169
BRADT, R. C., Kirkendall-effect densification in sintered W–Mo powder compact, 20: 16994
BRAGINSKII, V. B., One method of searching for quarks, 20: 17365
BRALL, U., Photoproduction of pion and nucleon resonances up to 5.5 Bev, 20: 17368
BRAMBLETT, R. L., Photoneutron cross sections for ^{12}C and ^{27}Al, 20: 17773
BRAMMAR, I. S., Electron metallography of dilute alloys of uranium with iron and aluminum, 20: 17058
BRANDES, S., Maximum credible accident storage of highly radioactive fission products in salt formations, 20: 16722 (BMwF-FBK-65-03)
BRANDON, George W. Jr., Heat-shield ablation measurements using radioisotope techniques, 20: 16778 (NASA-TN-D-3329)
BRANDT, John C., Interplanetary gas. XI., 20: 17236
BRANDT, N. B., Effect of uniform compression and plastic deformation of superconducting properties of Ti, 20: 17634
BRANDT, R., Interaction of high-energy protons with U, 20: 17837
BRANDUS, L., Diffusion theory of low-voltage arc plasma, 20: 17907
BRANITSKII, G. A., Effects of preliminary γ irradiation and heating on activity of the $Ag/Ag_2C_2O_4$ catalyst, 20: 16523
BRANSDEN, B. H., Electron capture by fast protons in helium, 20: 17274
BRAUN, Heribert, Influence of whole-body x irradiation on enzymatic activity of lactate dehydrogenase isoenzymes, 20: 16289
BRAUNER, A., Health physics for maintenance operation on a homogeneous research reactor, 20: 16757
BRAY, L. A., Purification of rare earths from Hanford wastes by solvent extraction, 20: 16329 (BNWL-187)
BREAUX, O. P., Photoelectric ion emission from cesiated surfaces, 20: 17267
BRECHNA, H., Conference on magnet technology, Stanford Univ., 9/65, 20: 17156 (CONF-650922)
BRECHNA, H., Electromagnets for high-energy physics applications, 20: 17175 (CONF-650922, pp 1–26)
BREDIN, D. J., Properties of the 4.77- and 5.16-Mev states of ^{10}B, 20: 17761
BREHM, J. J., l-Dependence, singularities, and the double-spectral function, 20: 17367
BRENNER, Abner, Prog. rpt. on W deposition, 11/64–2/65, 20: 17020 (N-65-18466)
BREWER, Leo, Stability of metallic structures, 20: 16418 (UCRL-16250)
BREZINSCAK, Marijan, Development of electromagnets for nuclear research, 20: 17222
BRIGHT, C. D., Optimizing the design of superconducting solenoids, 20: 16592
BRILL, Dieter R., Rotating masses and their effect on inertial frames, 20: 17575
BRIMHALL, J. L., Effects of prestrain and subsequent neutron irradiation on Mo, 20: 17132
BRINKERHOFF, Joris M., Narrow-band x-ray detector for identification of chemical elements using radioisotope x-ray sources, 20: 16823 (NYO-3160-1)
BROCK, William W., Microphotometer: application to grain orientation studies and quantitative metallography, 20: 16950 (ORNL-TM-1161, pp 132-45)
BROCKMEIER, Richard Tabor, Isotope shift of the $K_{\alpha 1}$ x ray in uranium, 20: 17285
BROER, L. J. F., Introduction to general dynamical systems, stability and waves, 20: 17884 (NP-15886)
BROGLIA, R., Exact diagonalization of quadrupole and pairing forces in nuclear d-s shell, 20: 17801
BROMLEY, J., Desorption studies on graphite surfaces irradiated in CO_2, CH_4, and $CO_2/CO/CH_4$ mixtures, 20: 17114 (AERE-R-5163)
BRONCA, G., Calculation of magnet profile by the method of equivalent currents, 20: 17178 (CONF-65022, pp 96-103)
BROOKS, E. J., Tungsten–rhenium alloy thermocouples and use in UO_2-fueled reactor, 20: 16942 (ANL-6981)
BROOKS, W. L., Radioactive fallout in air and rain: results to middle of

1965, 20: 16660 (AERE-R-4997)
BROWMAN, A., Scattering of 150- and 300-Mev positrons and electrons from Bi, 20: 17785
BROWN, D. M., Matrix isolation of unstable halogen radical ions, 20: 16534
BROWN, Louis, Reaction $^{3}He(d,p)^{4}He$ induced with polarized deuterons from 310 to 2935 kev, 20: 17749
BROWN, Louis, Triplet-singlet transitions in D(d,p)T reaction, 20: 17750
BROWNE, C. P., Isobaric-spin selection rule in the $^{10}B(d,\alpha)^{8}Be$ reaction at 7.5 Mev, 20: 17759
BROWNE, Philip L., REZONE—proposal for accomplishing rezoning in two dimensional Lagrangian hydrodynamics problems, 20: 18173 (LA-3455)
BRUCE, C. E. R., Lightning, novae, and quasars, 20: 17243
BRUNER, F., Separation of oxygen isotopes by gas chromatography, 20: 16930
BRUNFELTER, B., Unscrambling of proton-recoil spectra, 20: 16875
BRUNK, W., Argonne National Laboratory's pion focusing horn, 20: 17198 (CONF-650922, pp 650-6)
BRUNNQUELL, H., Scintillator-film combination for fast-neutron dosimetry, 20: 16861
BRUSCHI, L., Second-sound attenuation associated with hot ions in liquid He II, 20: 17615
BRUSH, E. G., Sodium mass transfer. XVI., 20: 16970 (GEAP-4832)
BRUTOVSKY, M., Chromatographic separation of $^{131}I^-$, $^{131}IO_3^-$, and $^{131}IO_4^-$, 20: 16567
BRYANT, Paul J., Cold-cathode magnetron gage characteristics, 20: 16788
BRYZGALOV, V. I., Stationary current in axially symmetric conducting body with strong Hall effect, 20: 17164
BUCCELLA, F., Some remarks on $[SU_6(T) \otimes SU_2(X) \otimes V(Y)]_W$, 20: 17455
BUCCI, Pompeo, Experimental proposal for new method for measurement of fast neutron fluxes, 20: 16851
BUCHANAN, P. S., Gamma rays produced in $^{56}Fe(a,n'\gamma)^{56}Fe$ reaction, 20: 17736
BUCHEL'NIKOVA, N. S., Investigation of drift instability in potassium plasma, 20: 17883 (NP-15784)
BUCHSBAUM, S. J., Longitudinal plasma oscillations near electron cyclotron harmonics, 20: 17934
BUCKMAN, R. William Jr., Refractory alloy tubing for space power systems, 20: 16998
BUCY, Paul C., Value of radioactive brain scans in diagnosis of brain tumors as compared with other methods, 20: 16304
BUCZKOWSKI, Z., Preparation of labeled compounds by tritioboration procedures. I., 20: 16549
BUDBERG, P. B., Interatomic binding in Ti–Nb–Cr system, 20: 17112
BUDZINSKI, Edwin E., Paramagnetic absorption of irradiated glycine, 20: 16525
BUECHNER, W. W., Stripping analysis of $^{46}Ti(d,p)^{47}Ti$ reactions, 20: 17776
BUISHVILI, L. L., Quantum-statistical theory of dynamic polarization of nuclei, 20: 17819
BUKOWIECKI, B., Optimalization of FET spectrometer stages working with semiconductor radiation detector, 20: 16806 (CLOR-44/D)
BUKOWIECKI, B., Radiation-dose-sensitive pocket alarm monitor, 20: 16805 (CLOR-43/D)
BULBULIAN, S., Technetium-99m generator using Fe_2O_3 as sorbent for ^{99}Mo, 20: 16552
BULHAK, Zofia, Hydrophobization of cellulose by radiation-induced grafting of styrene on its surface, 20: 16507 (INR-671/XVII/C)
BULLIS, R. H., Measurement of low-energy cesium ion-cesium atom cross sections by beam techniques, 20: 17299
BULLIS, Robert H., Cesium-diode thermionic converter for laboratory experiments, 20: 17329
BUONANNI, R. M., Beam optics computation for particle transport systems, 20: 17211 (LNF-65/45)
BURBIDGE, G. R., Nature of quasi-stellar sources, 20: 17242
BURDETT, Jane L., Organophosphorus–uranyl complexes studied by NMR spectroscopy, 20: 16422
BURGER, L. L., Organophosphorus–uranyl complexes studied by NMR spectroscopy, 20: 16422
BURLESON, G. R., Polarization of Σ^0 particles in reaction $\pi^- + p \rightarrow K^0 + \Sigma^0$ at 1.5 and 1.8 Bev/c, 20: 17382
BURNETT, D. S., Nucleosynthesis in early history of solar system, 20: 17234
BURSILL, L. A., Natural radiation damage in zircon ($ZrSiO_4$), 20: 17147
BURTSEV, I. I., Washout by precipitation of artificial radioactive aerosols from the atmosphere, 20: 16647
BUSCHERT, R. C., Deformation potential of irradiation induced traps in p-type Ge, 20: 17142
BUSCHERT, R. C., Length changes in electron-irradiated high-purity germanium, 20: 17136
BUSCHERT, R. C., Length changes in electron-irradiated n- and p-type Ge, 20: 17145
BUSH, W. E., Handbook of analytical procedures, 20: 16337 (RMO-3001 (Rev.1)(Suppl.))
BUT, D. A., Axi-symmetric linear MGD flow with a Hall effect in two-component magnetic field, 20: 17521
BUTERA, R. A., Prog. rpt. on magnetothermodynamics of para- and antiferromagnets, annual, 3/65–3/66, 20: 17978 (NYO-3402-2)
BUTLER, G. W., Mass of ^{8}He from the four-neutron transfer reaction $^{26}Mg(a,^{8}He)^{22}Mg$, 20: 17794
BUTLER, T. A., Aluminosilicate ion exchanger for recovery and transport of ^{137}Cs from fission-product wastes, 20: 16578
BUTTERFIELD, James L., Prog. rpt. on ionizing radiation, injury, prevention, and treatment, annual, 10/65, 20: 16303 (AD-626384)
BUTTLER, N., Lifetime of the $^{31}/_{2}$ three-particle state of ^{177}Hf, 20: 17811
BYCKLING, Eero, Effective potential in the degenerate Bose liquid, 20: 17439
BYKHOVSKII, A. V., Observation of hot radioactive particles in the atmosphere during 1962-1964, 20: 16677
BYRNE, J., Production of polarized electron beams by spin exchange collisions, 20: 17273
BYZOVA, N. L., Distribution of pollutants settling into lower layers of atmosphere, 20: 16652

C

CADILHAC, M., Heterogeneity calculation for fast reactors by a perturbation method, 20: 18063
CAILLET, C., Procedure for rapid start-up, 20: 18021
CAIRNS, E. J., Purification and preparation of cesium compounds, 20: 16476
CALDWELL, J. T., Photoneutron cross sections for ^{12}C and ^{27}Al, 20: 17773
CALKINS, John, Alternative multi-target equation useful for fitting survival curves of x-irradiated protozoa, 20: 16273
CALLAGHAN, Edmund E., Magnetics and superconductivity, 20: 17603
CALLAHAN, C. M., Ion exchange in fused salts. II., 20: 16340 (USNRDL-TR-970)
CALLAN, Curtis G. Jr., Calculation of nucleon magnetic moments by dispersion-theory methods, 20: 17390
CAMBRAY, R. S., Radioactive fallout in air and rain: results to middle of 1965, 20: 16660 (AERE-R-4997)
CAMONA, G., Metallographic techniques for optical and electronic observation of Zr–2.5 Nb alloy, 20: 16959
CAO, M. G., Calculation of Racah, Clebsch-Gordan, and Z coefficients, 20: 17559 (EUR-2639.f)
CARACH, Jozef, Contamination of biosphere by ^{137}Cs from weapon test fallout, 20: 16682
CARDOSI, G., Preliminary neutronic project of PRO-II core (UO_2–stainless steel), 20: 18091 (RT/FI(65)45)
CARETTI, G., Determination of dose in intracavitary contact therapy with ^{60}Co beads and in interstitial therapy, 20: 16765
CARPENTER, Donald G., Effect of nuclear-reactor operation in space, 20: 18131
CARPENTER, L., Analysis of Be metal and its compounds by optical emission spectrography, 20: 16352
CARPENTER, S. G., Prog. rpt. on tungsten resonance integrals and Doppler coefficients, 6–12/65, 20: 18045 (AI-66-16)
CARROLL, Harold W., Humoral mediation of radiation-induced motivation in parabiont rats, 20: 16284
CARSWELL, A. I., Focused microwave systems for plasma diagnostics, 20: 17881 (N-65-19804)
CARTER, J. R., Effects of low-energy protons and high-energy electrons on silicon, 20: 17125 (NASA-CR-404)
CARTER, Melvin W., Off-site surveillance for Salmon Event of Project Dribble, 20: 16743 (VUF-1021)
CARTONI, G. P., Separation of oxygen isotopes by gas chromatography, 20: 16930
CASEY, Harold Wilton, Influence of chronic acceleration on effects of whole-body irradiation in rats, 20: 16213 (AD-620403)
CASPARI, M. E., Gamma-gamma angular-correlation study of ^{169}Tm in lutetium iron garnet, 20: 17994
CASSINELLI, Joseph P., Interplanetary gas. XI., 20: 17236
CASTORINA, Thomas C., Radiation-enhanced surface activity of gamma HMX, 20: 16504 (AD-627846)
CATE, J. L., Energy absorption coefficients of dosimetric LiF, 20: 16829 (UCRL-14534, pp 1-7)
CAVALLERI, G., Isotropic monogap chamber pulsed with damped oscillation, 20: 16886
CAVANAUGH, P. J., Combined surgical and radiation management of carcinoma of the laryngopharynx, 20: 16313
CEFOLA, Michael, Prog. rpt. on kinetics and structural studies of chelates, annual, 6/65–6/66, 20: 16416 (NYO-906-68)
CERNY, J., Mass of ^{8}He from the four-neutron transfer reaction $^{26}Mg(a,^{8}He)^{22}Mg$, 20: 17794
CERVELLATI, R., Design and performance of neutron thermopiles, 20: 16899

CESARANO, C., Determination of manganese and arsenic content in steel by neutron activation analysis, 20: 16338 (RT/CHI-(65)36)
CEVOLANI, M., Energy and angular distributions in $^{20}Ne(n,\alpha)^{17}O$ reaction at 14 Mev, 20: 17743
CHACHRA, S. P., Magnetic anisotropy and nature of crystalline electric field of octahydrated neodymium sulfate, 20: 16435
CHACKALACKAL, Scaria M., Infrared spectra of vapors above sulfuric and deuteriosulfuric acids, 20: 16442
CHACKETT, K. F., Yields of potassium isotopes in high-energy bombardments of V, Fe, Co, Ni, Cu, and Zn, 20: 17717
CHADWICK, R. O'Neal, Rhabdomyosarcoma: case report of long-term palliation by irradiation, 20: 16312
CHAKKALAKAL, D. A., Lithium-8 fragments from 28-Bev proton interactions in nuclear emulsion, 20: 17753
CHAKRAVARTI, S. N., Transistorized instruments for reactor control and flux measurement, 20: 18027
CHALLE, J., Eurochemic instrumentation development and studies, 20: 16559
CHAMPION, K. P., Determination of Sr in samples of biological and geological origin, 20: 16345
CHAN, Y. M., Dipole spectrum and properties of helium, 20: 17272
CHANG, Tieo-hsu, Surface catalysis of orthohydrogen-parahydrogen conversion on carbon-supported Gd and Ho sulfates, 20: 16454
CHAPIN, Douglas S., Surface catalysis of orthohydrogen-parahydrogen conversion on carbon-supported Gd and Ho sulfates, 20: 16454
CHAPMAN, G. T., Gamma-ray attenuation coefficients for Ge, 20: 17962 (ORNL-TM-1237)
CHARALAMBOUS, S., Radiation measurements around an insufficiently shielded target, 20: 17212 (UCRL-Trans-1305)
CHARYKOV, A. K., Properties of organic thorium salts, 20: 16497
CHASE, A. B., Data for $LaTaO_4$ and $PrTaO_4$, 20: 16438
CHASE, A. B., Growth and preferential doping of zircon and thorite, 20: 16960
CHASE, L. F. Jr., Properties of the 4.77- and 5.16-Mev states of ^{10}B, 20: 17761
CHASE, L. H., Steam condensate β-γ monitor at fission products lab, 20: 16825 (ORNL-TM-1442)
CHASSARD, J. L., Metoclopramide in treatment of roentgen disease, 20: 16163
CHATTERJEE, R., Separation and determination of Ca, Sr, and Ba, 20: 16388
CHATTERS, Roy M., Radioisotope techniques in stream pollution problems in pulp and paper industry, 20: 16921 (TID-22627)
CHAUDHRY, M. A., Review on wholesomeness of irradiated foods with special reference to wheat, 20: 16918 (AECL-PAK/RB-7)
CHAUVET, G., Reactimeters, 20: 18032
CHEISHVILI, O. D., Flow of a superfluid liquid in porous media, 20: 17644
CHEKA, J. S., Free-field radiation-dose distributions from Hiroshima and Nagasaki bombings, 20: 16760
CHEKHOVSKOI, V. Ya., Thermodynamic properties of Nb at temperature range from 0°K to melting point, 2740°K, 20: 17100
CHEN, H. C., Macroscopic characterization of two-fluid anisotropic warm plasma, 20: 17912
CHENEY, E. S., Stable carbon isotopic composition of biogenic carbonates, 20: 16675
CHENEY, E. S., Stable isotopic geology of the Gas Hills, Wyoming, Uranium District, 20: 16670
CHENG, D. K., Macroscopic characterization of two-fluid anisotropic warm plasma, 20: 17912
CHEPELEV, V. V., Scintillation excitation mechanism in NaI(Tl), 20: 17991
CHEPURNYKH, G. K., Symmetry in nonlinear theory of the spinor field, 20: 17492
CHERMENSKAYA, N. F., Effects of silicon on mechanical properties and intercrystalline corrosion tendencies of Cr–Ni–Mo alloy, 20: 16983
CHERNIKOVA, D. M., Dispersion of sound in superfluid helium, 20: 17611
CHERNIKOVA, D. M., Relaxation phenomena in superfluid helium, 20: 17640
CHERNYSHEVA, P. G., Seasonal changes in radon and thorium concentration in surface boundary layer of atmosphere, 20: 16695
CHESHKOV, A. A., Elastic e-d scattering and CP-invariance breakdown, 20: 17341 (JINR-P-2504)
CHESKOV, A. A., Invariant parametrization of the products of local operators, 20: 17498
CHESLOW, M., Development of radiation-resistant solar cell, 20: 16910 (N-65-18448)
CHESNOKOV, S. V., On pairing with an orbital moment $l \neq 0$, 20: 17646
CHESTER, Arthur N., Reggeization, massless particles and vanishing renormalization constants, 20: 17476
CHHABRA, A. S., Radium-226 in food and man in Bombay and Kerala, India, 20: 16747
CHIANURA, G., Determination of dose in intracavitary contact therapy with ^{60}Co beads and in interstitial therapy, 20: 16765
CHIDA, Katsuhisa, Prog. rpt. on INS isotope separator, 11/5/65, 20: 16928 (INSJ-92)
CHIEVITZ, Eva, Complications and causes of death in polycythemia vera, 20: 16233
CHIFU, Alexandru, Distribution of deuterium in fractions obtained in pretreatment of crude oil, 20: 16475
CHIOTTI, P., Thermodynamic properties of uranium oxycarbides, 20: 16449
CHIOU, C., Superconducting composite Sn and Au films, 20: 17601
CHOMICKI, Oskar, Standardization of measurements of iodine uptake of thyroid gland by ^{131}I, 20: 16315
CHOUDHURY, S. Rai, Effect of dipion resonances on π-N scattering amplitude, 20: 17388
CHOUDHURY, S. S., Resolving times of binary scalers—analytical study 20: 16802
CHRIST, Hans A., Reaction $^3He(d,p)^4He$ induced with polarized deuterons from 310 to 2935 kev, 20: 17749
CHRIST, Hans A., Triplet-singlet transitions in D(d,p)T reaction, 20: 17750
CHRIST, N., Possible tests of C_{ST} and T_{ST} invariances, 20: 17392
CHRISTENSEN, W. R., Intercomparison of pathological fractures in beagles injected with ^{226}Ra, ^{228}Ra, ^{239}Pu or ^{90}Sr, 20: 16253
CHRISTIAN, R., Multiple pion production by 1.89-Bev/c π^-, 20: 17386
CHRISTIAN, R. S., Contoured poles for d-c accelerator magnets, 20: 17185 (CONF-650922, pp 248-52)
CHROMY, V., Reactions of metallochromic indicators of micelles. III., 20: 16394
CHRYSOCHOIEDES, N. G., Individual reactor cell temperature coefficient measurements, 20: 18145
CHU, J., Effects of x rays on growth, maturation, and fertility of rats irradiated at seventh day after birth. I., 20: 16287
CHU, J., Effects of x rays on growth, maturation, and fertility of rats irradiated at seventh day after birth. II., 20: 16288
CHU, N., Radiochemical determination of cadmium isotopes in radioactive debris, 20: 16397
CHUBB, J. N., Hydrogen condensation on to liquid helium-cooled surfaces, 20: 16631
CHUNG, Koo-Seon, Improved method for determination of Sc by neutron-activation analysis, 20: 16383
CHUNG, Suh Urk, Analysis of the B enhancement, 20: 17402
CHURCH, E. L., Double decay processes in ^{114m}In, 20: 17783
CICOGNA, G., Allowed link-up between relativity and internal symmetry, 20: 17454
CIGNA, R., Corrosion of Zr and Zy-2 at low temperatures, 20: 16979
CINELLI, G., Extension of the finite Hankel transform and applications, 20: 16934
CIOBOTARU, Tomaro, Distribution of deuterium in fractions obtained in pretreatment of crude oil, 20: 16475
CIRELLI, R., Analyticity properties of the scattering amplitude for a velocity-dependent potential, 20: 17449
CIRIC, Ivan S., Value of radioactive brain scans in diagnosis of brain tumors as compared with other methods, 20: 16304
CIZERON, Georges, Fritting of uranium dioxide, 20: 17037
CLAES, P., Chemical dosimetry in irradiation at high dose rates. I., 20: 16517
CLAES, P., Chemical dosimetry in irradiation at high dose rates. II., 20: 16518
CLAIBORNE, Lewis T., Deviations from BCS behavior in temperature dependence of ultrasonic absorption in superconducting tin, 20: 17605
CLAIBORNE, Lewis T., Ultrasonic observation of magnetization and flux jumping in a superconducting Nb–Zr alloy, 20: 17606
CLARK, H. K., Effect of distribution of fissile material on critical mass, 20: 18062
CLARKE, William Henry, Recombination line intensities in an attenuated hydrogen plasma, 20: 17952
CLAYTON, Robert N., Measurement of $^{18}O/^{16}O$ ratios of total oxygen of carbonates, 20: 16676
CLEGG, T. B., Nuclear reaction polarimeter using position-sensitive particle detectors, 20: 16870
CLELAND, W. E., Atomic interactions of muonium, 20: 17297
CLINE, D., Zero-range distorted wave analysis of $^{16}O(^3He,\alpha_0)^{15}O$ reaction, 20: 17696 (UR-875-65)
CLINE, David, Method to test for time-reversal invariance violation in K decays, 20: 17404
CLOSS, H., Second Foratom congress. Uranium reserves, 20: 16716
COBB, J., Spectroscopy of quadrupole magnets, 20: 17190 (CONF-650922, pp 431-46)
COBB, J. K., Establishing magnetic field of a solid pole magnet to within ±0.01%, 20: 17296 (CONF-650922, pp 823-34)
COCHE, A., Low energy α-p pulse-shape discrimination with Si surface-barrier detectors, 20: 16900
COCKING, E. C., Liquid scintillation counting of ^{14}C and ^3H samples

using glass-fiber or filter-paper discs, 20: 16177
COCUCCI, S., Biosynthesis of gibberellic acid-^{14}C and 3,4-glucose-^{14}C, 20: 16193 (EUR-2539.i)
COEKELBERGS, Roger, Description of calorimetric measurement of the intensity of low-energy x radiation, 20: 16856
COHAN, Norah V., General theorem for multiple-photon processes, 20: 17401
COHEN, Jeffrey M., Rotating masses and their effect on inertial frames, 20: 17575
COHEN, K. J., Photoproduction cross sections for π^+ and K^+ mesons at 3.4 to 4.0 Bev and comparison with SU(3), 20: 17400
COHEN, R. C., Magnetic dipole and electric quadrupole hyperfine effects in ^{209}Bi muonic x rays, 20: 17793
COLE, R., Spectroscopy of quadrupole magnets, 20: 17190 (CONF-650922, pp 431-46)
COLE, W. F., Device for reducing the radiation hazard in x-ray diffractometry, 20: 16782
COLEGRAVE, E. H. M., Reaction of active nitrogen with ethylene, 20: 16510 (NP-tr-1364)
COLEMAN, L. F., Treatment and disposal of glass melter condensates containing sulfuric acid, 20: 18159 (BNWL-SA-514)
COLEMAN, Paul J. Jr., Interaction of the solar wind with the planets, 20: 17232
COLER, M. A., Non-destructive electrical method of studying the density distribution of a randomly packed bed, 20: 18018 (CONF-651101-73)
COLES, Willard D., Design, construction, and performance of cryogenically cooled and superconducting electromagnets, 20: 17592 (CONF-650922, pp 574-87)
COLLIER, R. S., Energy gap of superconducting tin films in a magnetic field, 20: 17619
COLLIGAN, G. A., Liquid metal-refractory reaction studies, 20: 16984
COLLINS, D. A., Control of fission-product release from advanced gas-cooled reactors, 20: 18110
COLVIN, D. W., Boron pile $\bar{\nu}$ measurements, 20: 17823
COMES, R., Observations of primary defects in crystals of LiF irradiated with thermal neutrons at 77°K, 20: 18007
COMSA, George, Ion collection in the Bayard-Alpert gage, 20: 16787
CONDE, H., Fission-neutron spectra of ^{235}U, ^{239}Pu, and ^{252}Cf, 20: 17825
CONNOR, Jean H., Prog. rpt. on W deposition, 11/64–2/65, 20: 17020 (N-65-18466)
CONSOLI, Terenzio, Acceleration of electrically charged particles of an ionized gas, 20: 17960
CONSTANTINESCU, Maria, Paramagnetic centers produced in irradiated polycrystalline $Mo_7O_{24}(NH_4)_6 \cdot 4H_2O$, 20: 16529
CONSTANTINESCU, Olimpia, Paramagnetic centers produced in irradiated polycrystalline $Mo_7O_{24}(NH_4)_6 \cdot 4H_2O$, 20: 16529
COOK, B. C., Praseodymium-141 photoneutron cross section to 65 Mev, 20: 17764
COOK, B. C., $^{12}C(\gamma,n)^{11}C$ cross section to 65 Mev, 20: 17763
COOK, B. C., $^{16}O(\gamma,n)^{15}O$ cross section from threshold to 65 Mev, 20: 17762
COOK, J. R., Ultraviolet bleaching of synchronized Euglena, 20: 16204
COOKE, Kenneth L., Existence and uniqueness theorems in invariant imbedding. II., 20: 16935
COOLEY, C. R., Waste solidification engineering prototypes technical program, 20: 18158 (BNWL-SA-467)
COONEY, R. W., Applying acyclic generators for pulse duty in magnet power supplies, 20: 16772 (CONF-650922, pp 769-75)
COOPER, A. G. S., Special problems in employment of pregnant women in radiation work, 20: 16762
COOPER, G. P., Effects of various gases within nasal cavities of rats on response of olfactory bulb neurons to x irradiation, 20: 16215 (AD-628443)
COOPER, J. A., Evaluation of Rb and Fe bias in flame photometric K determination for K–Ar dating, 20: 16713
COOPER, Leon N., Approximation methods in many-body perturbation theory, 20: 17570
COPPO, N., Decimal scanner for the modular chain, 20: 16777 (EUR-2702.e)
CORENZWIT, E., Superconductivity of beta uranium, 20: 17095
CORGE, C. R., Data processing in some nuclear physics problems, 20: 17709
CORNELL, T., Prompt-neutron emission from ^{235}U fission fragments, 20: 17824
CORNELL, T., Simultaneous measurements of flight times and energies of fission fragments, 20: 17864
CORWIN, Richard R., Determination of ion excitation energies and densities in low-pressure discharge, 20: 17508 (ARL-65-246)
COSPER, John H., Development of a sensitive liquid dosimeter for integral dose measurement, 20: 16845
COSPER, S. W., Mass of ^6He from the four-neutron transfer reaction $^{26}Mg(\alpha,^6He)^{22}Mg$, 20: 17794
COULTER, Philip Wylie, Effects of inelastic channels on NN, $\pi\pi$, and πN elastic scattering cross sections, 20: 17419
COURT BROWN, W. M., Mortality from cancer and other causes after radiotherapy for ankylosing spondylitis, 20: 16242
COURTNEY, F. E., On-site meteorological tests at Parr, South Carolina, 20: 18084 (CVNA-96)
COURVOISIER, Pierre, Catalysis by alkaline amides of isotopic exchange between hydrogen and liquid ammonia, 20: 16444
COWAN, G., Symmetry of neutron-induced ^{239}Pu fission in resonance region, 20: 17858
COX, D. E., Long-period modulation of stacking order in Au_3Mn, 20: 17066
COX, G. F., Absolute differential cross section in proton-carbon elastic scattering at 145 Mev, 20: 17739
COX, R. J., Reducing effects of electrical interference on nucleonic instruments, 20: 18030
CRAMER, W. A., Measurement of radioactivity in effluents of a gas chromatograph, 20: 16371
CRAPPER, G. D., Steady MGD flow past a source, 20: 17525
CRAWFORD, F. W., Prog. rpt. on plasma oscillations, 6–8/65, 20: 17893 (SU-IPR-44)
CRAWFORD, F. W., Prog. rpt. on studies of plasma oscillations, 9–11/65, 20: 17894 (SU-IPR-47)
CREMERS, C. J., Measurement of thermal radiation from an argon plasmajet, 20: 17898
CREMERS, Clifford J., Prediction of mode transition in an arc with a transpiration-cooled anode, 20: 17514
CRESPI, Henry L., Deuterated organisms: cultivation and uses, 20: 16165
CREVELING, H. F., Steady flow characteristics of single-phase natural circulation loop, 20: 16600 (COO-1177-15)
CREW, R. J., Distribution of volcanic fallout in and about a one-story residence, 20: 16659 (AD-629527)
CROCKER, J. G., Prog. rpt. on SPERT project, 7–9/65, 20: 18019 (IDO-17146)
CROCKET, James H., Radioactivation determination of palladium in basaltic and ultrabasic rocks, 20: 16370
CROOKER, T. W., Analysis of Ti–7Al–2Nb–1Ta and Ti–6Al–4V fractures, 20: 16967 (AD-628277)
CROSS, Ronald Allan, Delayed and persistent expression of induced mutations in Chlamydomonas reinhardi, 20: 16294
CROSSLEY, D., Rapid dissolution of PuO_2 by a Na peroxide sinter and determination of PuO_2 content, 20: 16350
CROUSE, R. S., Accelerated epoxy mounting using r-f furnace, 20: 16947 (ORNL-TM-1161, pp 98-102)
CROUSE, R. S., Experience with color in metallography, 20: 16949 (ORNL-TM-1161, pp 112-29)
CRUCQ, Andre, Description of calorimetric measurement of the intensity of low-energy x radiation, 20: 16856
CSANYI, Piroska, Use of liquid scintillators for measurement of isotopes emitting soft β radiation. III., 20: 16862
CSANYI, Piroska, Use of liquid scintillators for measurement of isotope emitting soft β radiation. IV., 20: 16863
CSONKA, Paul L., General nondynamical formalism for reactions with particles of arbitrary spin, 20: 17479
CSONKA, Paul L., Nondynamical structure of $^3He(d,p)^4He$ reaction, 20: 17770
CSUPKA, Stefan, Contamination of biosphere by ^{137}Cs from weapon test fallout, 20: 16682
CUEVAS, J., Atomic and ionic partial stopping powers of He gas for a He beam, 20: 17305
CULVER, J. S., Injection and accumulation: multiple-pass experiments (DCX-2), 20: 17887 (ORNL-3908, pp 18-31)
CUNNINGHAM, S. P., Bands of D_2 and T_2 originating from lowest excited Σ_g states, 20: 16451
CUPINI, E., Monte Carlo analysis of some enriched ^{235}U fast critical assemblies, 20: 18057
CUROTT, David Richard Francis, Pendulum gravimeter for precision detection of scalar gravitational radiation, 20: 17583
CURRY, B. P., Ionization and recombination in alkali-seeded collision-dominated plasmas, 20: 17872 (AD-627988)
CUTLER, J. A., Non-destructive electrical method of studying the density distribution of a randomly packed bed, 20: 18018 (CONF-651101-73)
CUTLER, William Herbert, Thermal cesium plasma, 20: 17955

D

DAHL, Orin I., Analysis of the B enhancement, 20: 17402
DAHL, R. E., Correlation of radiation damage in boronated graphite, 20: 17116 (BNWL-199)
DAHMEN, H. D., Bound on coupling constant from unitarity and analyticity, 20: 17477
DAIBOG, E. I., Application of unitary symmetry to multiple meson production, 20: 17345 (JINR-P-2531)
DAINTON, F. S., Matrix isolation of unstable halogen radical ions,

20: 16534
DALGARNO, A., Dipole spectrum and properties of helium, 20: 17272
D'AMATO, Constance J., Effects of low levels of ionizing radiation on rat developing cerebral cortex, 20: 16275
DAMGARD, Joergen, Fermi decays of deformed odd nuclei, 20: 17742
DAMJANOVICH, S., Effect of sulfhydryl inhibitors on radiation sensitivity of Ehrlich ascites tumor cells, 20: 16299
DANCEWICZ, Antoni M., Biochemical lesions induced in subcellular structures by ionizing radiation. II., 20: 16277
DANG, Gio Do., Number-conserving approximation for theory of pairing interaction in nuclei, 20: 17765
DANIELI, B., Synthesis of ^{14}C-lanosterol and ^{14}C-desmosterol, 20: 16548
DARONIAN, P., π^+ p interactions at 1.6 Bev, 20: 17374
DAS, T., Two-pion decay modes of K^+ and K^0_2 mesons in SU_3, 20: 17379
DAS, T. P., Electron-nuclear interaction in antimony metal, 20: 18000
DASHEN, R. F., Self-consistent determination of coupling shifts in broken SU(3), 20: 17467
DASHEN, R. F., Weak and electromagnetic interactions of the hadrons in bootstrap theory, 20: 17466
DATZ, Sheldon, Angular distribution of elastically scattered Cs^+ ions from Ar, Kr, and N_2, 20: 17300
DATZ, Sheldon, Measurement of "knock-on" cross section in elastic scattering in H–He systems, 20: 17293
DATZ, Sheldon, Molecular-beam studies of the alkali–halogen reactions, 20: 17295
DAUDIN, A., π^+ p interactions at 1.6 Bev, 20: 17374
DAVID, J. H., Functions L, M, N of the nonlinear spinor theory of elementary particles, 20: 17440
DAVIDSON, Eric, Surface catalysis of orthohydrogen-parahydrogen conversion on carbon-supported Gd and Ho sulfates, 20: 16454
DAVIES, A. J., Space-charge controlled ionization growth in hydrogen, 20: 17518
DAVIES, B., Matrix elements for three-nucleon system. II., 20: 17746
DAVIES, J. W., Liquid scintillation counting of ^{14}C and ^{3}H samples using glass-fiber or filter-paper discs, 20: 16177
DAVIES, K. T. R., Oscillator brackets for Hartree-Fock calculations, 20: 17744
DAVIS, R. C., High-current ion-beam production and injection, 20: 17890 (ORNL-3908, pp 100-7)
DAVIS, R. C., Injection and accumulation: multiple-pass experiments (DCX-2), 20: 17887 (ORNL-3908, pp 18-31)
DAVIS, R. E., Efficiency of Whatman-type ACG/B filter papers for methyl iodide retention in air, 20: 16719 (AEEW-M-568)
DAVIS, W. Jr., Softening and decontaminating waste water by caustic-carbonate precipitants in slowly stirred sludge-blanket column, 20: 18168
DAVYDOV, E. N., Determination of annual ^{90}Sr fallout in polar regions by recording ^{90}Sr content in seasonal layers of snow and ice, 20: 16703
DAVYDOV, E. N., Fluctuations in seasonal concentration of fission products in atmosphere surface layers over Moscow, 20: 16650
DAVYDOV, E. N., Seasonal and geographical changes in ^{210}Pb content of the atmosphere, 20: 16640
DAWSON, J., Computation of x-ray diagnostic exposure tables, 20: 16751
DAYAL, B., Evaluation of specific heats of titanium, zirconium, and hafnium, 20: 17084
DAYAL, B., Lattice dynamics and specific heats of some transition metals on Krebs's model, 20: 17081
DEAN, J. A., Determination of trace quantities of U, 20: 16389
DEAT, M., Procedure for rapid start-up, 20: 18021
DEB, A. R., Airborne radioactivity at Delhi, 20: 16680
DE BORTOLI, M., Some data and comments on ^{22}Na in food chains, 20: 16678
DE BRUIJN, J. H., Immunity in experimental syphilis. IV., 20: 16199
DE CALAN, C., Radiative corrections to inelastic electron scattering with detection in coincidence. II., 20: 17370
DECOOL, F., Safety systems and measurement of neutron flux, 20: 18119
DECOT, Jean, Description of calorimetric measurement of the intensity of low-energy x radiation, 20: 16856
DECUYPER, J. C., Low-voltage ionization chamber, 20: 16902
DEDERICK, Preston K., Electron emission of Pt group metals in Cs vapor, 20: 17333
DE DREUILLE, M., Radium-226 content of milk in France. II., 20: 16753
DE FOUQUET, Jacques, Relation between rational curves of compression and deformation mechanisms of polycrystalline Be, 20: 17040
DEGENKOLB, J. K., Reusability of buildings after a warfire, 20: 16621 (AD-625867)
DEGOLS, Luc, Description of calorimetric measurement of the intensity of low-energy x radiation, 20: 16856
DEGOT, Bernadette, Tritium activity of basin pouring from Mont Cenis, 20: 16668
DE HEER, F. J., Electron capture into excited states by He ions incident on He, 20: 17304
DEHNEN, H., Energy transport by Ozsvath-Schucking solution of gravitational field equations, 20: 17579
DEHNEN, H., Gravitational electric exchange, 20: 17580
DEHOUST, O., Nanosecond pulse device for a 2-Mev Van de Graaff electron accelerator, 20: 17217
DEISS, M., Description of two reactivity measuring apparatuses, 20: 18037
DEKEYSER, R., Convergent expression for partition function of a partially ionized hydrogen plasma, 20: 17935
DE KLERK, D., New magnet installations at the Kamerlingh Onnes Laboratory, 20: 17598 (CONF-650922, pp 745-52)
DE KLUIVER, H., Thermonuclear investigations. III., 20: 17928
DE LANY, Vincent Miles, Dynamical equations for scattering of particles with spin and analytic continuation in angular momentum, 20: 17420
DELARUE, M. R., Dosimetry of ionizing radiations by means of lumidosimeters, 20: 16837
DELCROIX, V., Fast period meter with integrated circuits, 20: 18029
DELCROIX, V., New possibilities offered by boron and uranium detectors, 20: 16896
DELEPLANQUE, Michel, Study of double nitrate of La and Mg between 4000 and 1250 cm^{-1}, 20: 16429
DEL MARMOL, P., Research for delayed-neutron precursors in antimony and arsenic fission products, 20: 17833
DELMAS, Robert, Catalysis by alkaline amides of isotopic exchange between hydrogen and liquid ammonia, 20: 16444
DELMAS, Roger, Fritting of uranium dioxide, 20: 17037
DE LOTTO, I., Method to correct amplitude distortions due to pile-up effects, 20: 16795
DELVAILLE, J. P., Search for discrete sources of cosmic γ rays above 1 Bev, 20: 17320
DE MATTEIS, A., Monte Carlo analysis of some enriched ^{235}U fast critical assemblies, 20: 18057
DEMBINSKI, Wojciech, Determination of powder density particularly of uranium compounds, 20: 16425
DE MEVERGNIES, M. Neve, Research for delayed-neutron precursors in antimony and arsenic fission products, 20: 17833
DEMIDOV, A. M., Spectrum of γ rays emitted during capture of thermal neutrons in tellurium, 20: 17681 (IAE-966)
DEMIDOV, B. A., Search for Raman scattering of electromagnetic waves in microwave band with aid of turbulent plasma, 20: 17923
DE MIER, W. V., Transient thermal behavior in fixation of radioactive materials, 20: 18155 (BNWL-157)
DEM'YANOVICH, V. K., Effect of vertical distribution of temperature and wind velocity on the atmospheric diffusion of radioactive pollutants, 20: 16651
DENFELD, Richard E., Effect of nuclear-reactor operation in space, 20: 18131
DEO, B., Neutron exchange in reaction $p + p \rightarrow d + \pi^+$, 20: 17394
DEPIREUX, J., Artificial radioactive carbonization, 20: 16514
DEPOITIER, J., Increase in the diameter of composite tubes used in atomic power applications, 20: 17088
DEPTULA, Andrzej, Determination of powder density, particularly of uranium compounds, 20: 16425
DEREM, A., Functions L, M, N of the nonlinear spinor theory of elementary particles, 20: 17440
DERMENDZHIEV, E., Interaction of neutrons with ^{235}U nuclei at 2 ev to 30 kev, 20: 17856
DEROW, H., Prog. rpt. on SNAP-8 materials, semiannual, 1–6/65, 20: 16972 (NASA-CR-54719)
DERUYTTER, A. J., Variation of the binary-ternary fission ratio for ^{235}U, 20: 17540
DE SAUSSURE, G., Measurement and analysis of fission cross section of ^{239}Pu from 0 to 5 kev, 20: 17851
DESHPANDE, N. G., Distinction between composite and elementary particles in a model field theory, 20: 17472
DESPORTES, H., High homogeneous field superconducting magnet for a polarized proton target, 20: 17586 (CONF-650922, pp 509-16)
DESPOTOVIC, R., Heterogeneous exchange of precipitates. X., 20: 16432
DETRAZ, C., Mass of ^{8}He from the four-neutron transfer reaction ^{26}Mg(α,^{6}He)^{22}Mg, 20: 17794
DEVANEY, R. A., Time varying solar cycle protons program manual, 20: 17539 (N-65-18257)
DEVANI, M., Influence of phosphate ester structure and the character of metal ions of fourth subgroup on dephosphorylation, 20: 16420
DE VOE, James R., Prog. rpt. on radiochemical analysis, 7/64–6/65, 20: 16335 (NBS-TN-276)
DEVONS, S., Magnetic dipole and electric quadrupole hyperfine effects in ^{209}Bi muonic x rays, 20: 17793
DE VROEY, M., Fission cross-section of ^{240}Pu for 0.03- to 2.0-Mev neutrons, 20: 17855
DEWEY, M. A. P., Electron metallography of dilute alloys of uranium with iron and aluminum, 20: 17058
DE WITTE, R., Eurochemic pulse columns for countercurrent liquid-liquid extraction, 20: 16561

DEY, Arun K., Separation and determination of Ca, Sr, and Ba, 20: 16388
DICKEL, G., Calculation of squared-off cascades for isotope separation by diffusion, 20: 16929
DICKENS, J. K., Dependence of proton optical-model parameters upon experimental uncertainties, 20: 17768
DIEHL, J., Thermally activated processes in deformation of neutron-irradiated Cu single crystals. II., 20: 17980 (ANL-Trans-274)
DIEKE, G. H., Bands of D_2 and T_2 originating from lowest excited Σ_g states, 20: 16451
DIENST, W., Irradiation possibilities and safety considerations concerning irradiations at reactor FR-2, 20: 18146
DIETER, Lowell H., Spectrophotometric determination of Ce with sulfanilic acid, 20: 16398
DI GIACOMO, C., Experimental reactor safety circuits involving numerical data processing, 20: 18038
DISCHINGER, R. H., Prog. rpt. on heat exchangers for sodium-cooled reactors, 10–12/65, 20: 18093 (UNC-5142)
DISCHLER, B., ESR of sulfur and selenium radicals in alkali halides, 20: 18005
DITCHEK, T., Medical x-ray survey packet, 20: 16843
DJORDJEVIC, O., Effect of native isologous DNA on incorporation of thymidine-^{3}H into uv-irradiated L-strain cells, 20: 16279
DJURIC, Branko, Isothermal transformation kinetics of a U–1.85 wt.% Nb alloy, 20: 17036
DMITRENKO, I. M., High-frequency Josephson current, 20: 17636
DMITRIEV, I. S., Autoionization of nitrogen and oxygen ions after passage through a solid, 20: 17262
DMITRIEVA, G. P., Investigation of Cr–Fe–Mo and Cr–Fe–W alloys, 20: 17093
DMITRIEVA, G. P., Phase equilibrium diagram of Hf–Ta system in solid state, 20: 17092
DMITRIEVA, G. V., Appearance on the earth's surface of areas of increased concentrations of stratospheric radioactive products, 20: 16698
DMITRIEVA, G. V., Radioactivity of atmosphere over oceans and relationship to meteorological factors, 20: 16699
DMITRIEVA, G. V., Synoptic-climatic sketch maps of global stratospheric radioactive fallout, 20: 16697
DOBKOWSKI, Zbigniew, Stable isotope dilution analysis. II., 20: 16362
DOBROLYUBSKAYA, T. S., Determination of uranium(VI) in carbonate solutions, 20: 16354
DODE, Maurice, High-temperature x-ray study in controlled atmosphere of system uranium–oxygen, 20: 16471
DOEDERLEIN, J. M., DATAPREP-II—reactor lattice homogenization and BIGG-II data preparation computer code, 20: 18047 (KR-78)
DOERING, H., Effect of electron-bombardment heating on tensile properties of tungsten, 20: 17073
DOLEZEL, M., Long-term follow-up in detection and treatment of cervical cancer, 20: 16326
DOLGOV, A. D., Predictions of unitary symmetry for hadron photoproduction reactions, 20: 17412
DOLL, Richard, Mortality from cancer and other causes after radiotherapy for ankylosing spondylitis, 20: 16242
DOMANGE, Louis, Divalent rare earth sulfide–trivalent rare earth sulfide systems, 20: 16431
DOMMERGUES, P., Comparison of effects of mutagenic substances by studying mutagenesis of plants, 20: 16225 (EUR-2715.f)
DONADIEU, L. J., 4500-Gauss superconducting magnet for corpuscular ionography experiments, 20: 17594 (CONF-650922, pp 604-10)
DONHOWE, J. M., Determination of nuclear reaction widths from reaction
DONOHUE, Paul C., Modification of structures of ternary oxides by cation yield curves, 20: 17778
substitution. I., 20: 16436
DONOVAN, P. F., Properties of the 4.77- and 5.16-Mev states of ^{10}B, 20: 17761
DOOHER, John Patrick, Effect of vector mesons on lepton production by scattering of muon neutrinos and protons, 20: 17504
DORMAN, I. V., Modulation of protons and α particles of small rigidities and cosmic-ray spectrum in the galaxy, 20: 17312
DORMAN, L. I., Effects of small flares in hard component of cosmic rays of magnetically quiet and disturbed days, 20: 17313
DORMAN, L. I., Modulation of protons and α particles of small rigidities and cosmic-ray spectrum in the galaxy, 20: 17312
DOTHAN, Y., Self-consistent determination of coupling shifts in broken SU(3), 20: 17467
DOTTI, D., Method to correct amplitude distortions due to pile-up effects, 20: 16795
DOUDNEY, C. O., Formation of RNA during recovery of DNA synthetic system of bacteria damaged by uv light, 20: 16202
DOUGAL, Arwin A., International developments in controlled thermonuclear fusion, 20: 17914
DOWDY, Edward Joseph, Nuclear resonance fluorescence using recoil-broadened γ rays from radiative capture of thermal neutrons, 20: 17842
DOWKER, J. S., Minimal coupling of massless charged particles, 20: 17484
DOWNING, R. G., Effects of low-energy protons and high-energy electrons on silicon, 20: 17125 (NASA-CR-404)
DOWNING, R. G., Prog. rpt. on low-energy proton experiments, 12/64, 20: 16907 (N-65-17517)
DRABKIN, G. M., Critical scattering of polarized neutrons in nickel, 20: 17986
DRACKA, Oldrich, Prog. rpt. on hydrodynamics of disposal of low-level liquid radioactive wastes in soil, final, 1965, 20: 18163 (NP-15859)
DRAGULESCU, C., Uranyl pyrophosphate complexes, 20: 16472
DRASIL, V., Effect of sulfhydryl inhibitors on radiation sensitivity of Ehrlich ascites tumor cells, 20: 16299
DRAWBAUGH, D. W., New cross section library for n + ^{235}U reactions, 20: 17697 (WANL-TME-1028)
DRESIA, H., Measurement of humidity of large-lump coke with neutrons, 20: 16922
DRICKEY, D., Deuteron electromagnetic form factors, 20: 17349 (LAL-1155)
DROEGE, T. F., Guideline for use of standard nuclear instrument modules, 20: 16779 (PPAD-584D)
DRUIN, V. A., Radioactive properties of nuclei of heaviest elements, 20: 17688 (JINR-P-2539)
DRUMMOND, J. L., Potentiometric determination of Pu by argentic oxidation, ferrous reduction, and dichromate titration, 20: 16405
DUBINI, M., Preparation of ^{32}P-labeled compounds from carrier-free ^{32}P, 20: 16551
DUBOVIK, V. M., Elastic e-d scattering and CP-invariance breakdown, 20: 17341 (JINR-P-2504)
DUBOVIKOV, M. S., Use of polarized proton target to determine isobar parity, 20: 17362
DUCHENE, J. P., Radiation detectors for reactor control, 20: 16903
DUFAY, Philippe, Preparation of α and β anomers of desoxy-2′ adenosine, labeled with ^{14}C, 20: 16545
DUFTSCHMID, K. E., Radiometric and autoradiographic investigation of production of asbestos cement products, 20: 16920 (SGAE-IB/IA-7/1965)
DUMITRESCU, R., Angular distributions from ^{12}C(α,n)^{15}O reaction at 14 Mev, 20: 17803
DUNAITSEV, A. F., Measurement of π^+ meson lifetime, 20: 17346 (JINR-P-2534)
DUNLAP, J. L., Injection and accumulation: single-pass experiments (DCX-1), 20: 17886 (ORNL-3908, pp 1-17)
DUNLOP, J. I., ESR studies of uv-irradiated keratin and related proteins, 20: 16205
DUNN, A. L., Determination of Ca, Cu, Mn, and Mg in serum by neutron activation analysis, 20: 16347
DUNWOODY, N. T., Magnetohydrodynamic natural convection in a cylinder, 20: 17516
DUPAY, F., Carbon dioxide–coolant gas of G.2 and G.3 reactors, 20: 18120
DURAND, Georges Louis, Dating of the Beillard peat bog by the ^{14}C method, 20: 16712
DURGAPRASAD, N., Multiply charged nuclei of primary cosmic radiation. III., 20: 17321
DURING, G., Fission-neutron spectra of ^{235}U, ^{239}Pu, and ^{252}Cf, 20: 17825
DUSHIN, L. A., Bremsstrahlung in infrared region from plasma of electrodeless induction discharge, 20: 17931
DUTIYABODHI, Pisawat, Radiation survival of food pathogens in complex media, 20: 16237
DUTRANNOIS, J., Radiation measurements around an insufficiently shielded target, 20: 17212 (UCRL-Trans-1305)
DVORAK, James R., High magnification optical microscopy of ceramic materials, 20: 16954 (ORNL-TM-1161, pp 267-71)
DVORINA, L. A., Physico-chemical properties of rare-earth silicides, 20: 17047
DVORNIKOVA, L. M., Thermal decomposition of Er and Yb hydroxides, 20: 16441
DWYER, Orrington E., Heat transfer to liquid metals flowing turbulently in eccentric annuli. I., 20: 16612
D'YACHENKO, P. P., Multi-parameter investigations of fast fission fragments, 20: 17868
DYBCZYNSKI, Rajmund, Determination of rare earths by neutron activation method using ion-exchange chromatography. Analysis of spectrally pure erbium oxide, 20: 16363
DYBROVINA, S. M., Fission distribution in neutron-induced fission of ^{230}Th, ^{238}Pu, and ^{241}Am, 20: 17848
DYER, John K., Radiation survival for food pathogens in complex media, 20: 16237
DYMNIKOV, A. D., On the paper "third order abberations of an electric strong-focusing doublet", 20: 17219
D'YUK, F. Zh., Effectiveness of magnetic spectrometer for recording $K^0 \to \pi^+ + \pi^-$ decay, 20: 16814 (ITEF-386)
DYUMIN, N. E., Experimental observation of fourth sound in ^{3}He–^{4}He solutions, 20: 17159

E

EBERHAGEN, A., Electromagnetic radiation from plasmas of high temperature and density, 20: 17944

ECCLESHALL, D., Coulomb excitation of low-energy states in Ce, Nd, and Sm isotopes, 20: 17734

ECCLESHALL, D., Fission following (d,p) and (t,p) reactions in uranium isotopes, 20: 17844

ECKARDT, A., Recent state of betatron development and application, 20: 17216

ECKHARDT, W., Comparison of observed delayed-neutron abundances with calculated fission yields of neutron precursors, 20: 17831

ECKSTEIN, H., Synchronized budding yeast cells. I., 20: 16240

EDELMAN, V. S., Landau damping and resonance damping of magnetoplasma waves in bismuth, 20: 18011

EDER, G., Density of energy states in light nuclei, 20: 17745

EDGECUMBE, J., Thin film densities, 20: 17070

EDMONDSON, L. F., Removal of radiostrontium from milk with tricalcium phosphate and resulting changes in milk composition, 20: 16382

EDVINSSON, Gunnar, Band spectrum of ThO, 20: 17254

EDWARDS, R. S., Injection and accumulation: single-pass experiments (DCX-1), 20: 17886 (ORNL-3908, pp 1-17)

EDWARDS, W. T., Determination of oxygen in sodium, 20: 16349

EFIMOV, Yu. V., Solid solutions of Ge, Sn, Al, and Be in V_3Si and their superconductivity, 20: 17043

EGAMI, Nobuo, Effect of temperature on survival period of Oryzias latipes following irradiation, 20: 16236

EGAMI, Nobuo, Effects of x irradiation on females of the teleost, Oryzias latipes, 20: 16263

EGGENSBERGER, H., Nuclear resonance magnetometer with frequency modulation, 20: 16791

EGOROV, E. V., Ionizing radiation effects on ion exchange materials, 20: 16583

EGOROV, V. N., Excitation and characteristics of Th spectrum in electrodeless discharge tubes, 20: 16464

EHRENBERG, W., Electron-bombardment-induced conductivity in fused silica, 20: 17133

EHRLICH, R. D., M1 and E2 hyperfine structure in muonic K and L x rays of bismuth, 20: 17792

EICH, W. J., Consistency in analysis of high-buckling critical experiments, 20: 18065

EICHHOLZ, G. G., Neutron detection by corrugated-plate spark counters, 20: 16894

EINSPRUCH, Norman G., Deviations from BCS behavior in temperature dependence of ultrasonic absorption in superconducting tin, 20: 17605

EINSPRUCH, Norman G., Ultrasonic observation of magnetization and flux jumping in a superconducting Nb–Zr alloy, 20: 17606

EISBERG, Robert, Survey of nuclear reactions induced by 57-Mev protons. II., 20: 17725

EISELE, J. A., Prog. rpt. on NRL cyclotron, 9/65, 20: 17169 (AD-628928)

EIWECK, Ladislaus, Device for shutdown of nuclear reactors with an electromagnetic collision momentum generator, 20: 18044

EKIMENKO, T. M., Preparation of thin layers of zirconium carbide by electrophoresis, 20: 17004

EKSTROM, A., Radiolysis of binary mixtures. I., 20: 16530

ELARDE, Paul F., Testing steels for gradient magnets, 20: 17010 (CONF-650922, pp 207-304)

ELDREDGE, Arnold L., Retort furnace anneals and brazes 266,000 components, 20: 17000

EL-ELA, M. Abu, Slow neutron spectrum of neutron beam from UA-RR-1 reactor, 20: 18147

ELINGS, V. B., Photoproduction cross sections for π^+ and K^+ mesons at 3.4 to 4.0 Bev and comparison with SU(3), 20: 17400

ELLERT, G. V., Excitation transfer from crystal lattice to rare earth ions, 20: 18010

ELLIS, David, Coupled-channel Schroedinger-equation model for high-energy peripheral collisions, 20: 17397

ELSTON, J., Crystal structure of oxides and their neutron irradiation behavior at 80°C, 20: 17148

ELYUTIN, V. P., Interaction between Nb and alumina, 20: 16978

EMELYANOV, I. Ya., Logical-element system for reactor control, 20: 18031

EMMETT, M. B., OGRE-G—Monte Carlo code for calculation γ dose rate at arbitrary points, 20: 17961 (ORNL-TM-1212)

EMPSON, F. M., Project Salt Vault: design and demonstration of equipment, 20: 18165 (ORNL-P-1987)

EMPSON, F. M., Project Salt Vault, 20: 18169

ENDO, Michio, Catalytic tritium exchange reactions with tritiated active methylene compound, 20: 16492

ENGEL, Ronald E., Potential hazards as result of inhalation of radioiodines: a literature survey, 20: 16734 (TID-22693)

ENGLE, G. B., Irradiation behavior of graphite joints and graphite-coated particles in carbonized pitch matrix, 20: 17119 (GAMD-6789)

ENYO, Michio, Relation between forward and backward rates of hydrogen electrode reaction in isotopically mixed system, 20: 16459

ERBAN, Jiri, Possibility of absolute measurements of radioisotope activity using scintillation γ spectrometry, 20: 16858

ERDMANN, K., Inhibition of absorption of glucose in small intestine of rats by x radiation, 20: 16274

ERHARDT, W. H., Polonium-210 analyses of vegetables, cured and uncured tobacco, and associated soils, 20: 16189

ERICKSON, Lyndon E., EPR absorption by Nd(III) ions in $LaCl_3$ and lanthanum ethyl sulfate, 20: 17997

ERK, Vernon, Radioactive material in teeth of children in northern New Jersey area, 20: 16763

ERMOLAEV, N. P., Photometric determination of Np by means of xylenol orange, 20: 16408

EROKHIN, R. A., Use of γ spectrometry for determination of Pu in the living organism, 20: 16864

ERRAMUSPE, H. J., Scattering chamber for use with solid-state detectors, 20: 16883

ERSKINE, J. R., Isobaric-spin selection rule in the $^{10}B(d,\alpha)^8Be$ reaction at 7.5 Mev, 20: 17759

ERWIN, A. R., Multiple pion production by 1.89-Bev/c π^-, 20: 17386

ESCHNAUER, H., Fuel cores for plate fuel elements, 20: 16995

ESEL'SON, B. N., Experimental observation of fourth sound in ^3He–^4He solutions, 20: 17159

ETOH, Hisami, Effect of temperature on survival period of Oryzias latipes following irradiation, 20: 16236

ETTINGER, H. J., Iodine sampling with silver nitrate-impregnated filter paper, 20: 16756

EU, Byung Chan, Applications of R-matrix theory to reactive and elastic molecular scattering, 20: 17259

EVANGELISTI, R., Electrical resistivity measurement of Na, 20: 17026 (RT/ING-(65)17)

EVANS, C. J., Space-charge controlled ionization growth in hydrogen, 20: 17518

EVANS, E. A., Stability of a radioactive drug—tetrasodium 2-methyl-1,4-naphthaquinol diphosphate labeled with tritium, 20: 16535

EVANS, E. Anthony, Control of self-irradiation decomposition of tritium-labeled compounds at high specific activity, 20: 16533

EVANS III, E. C., Wounding response and polar transport of ^{45}Ca in isolated root segments of Zea mays, 20: 16170 (AD-628805)

EVANS, Robley D., Lithium-drifted Ge detectors: applications to neutron-activation analysis, 20: 16888

F

FAATZ, H., FHT 800 A: measurement device for Moessbauer effect experiments, 20: 16866

FADIN, V. S., Electromagnetic particle pair production, 20: 17499

FAIER, Harry, Meson decays and the Σ hypothesis, 20: 17422

FAIRCHILD II, Edward J., Changes in thyroid ^{131}I activity in ozone-tolerant and ozone-susceptible rats, 20: 16190

FALK, W. R., Positron annihilation in noble gases, 20: 17423

FALKO, I. I., Effect of impurities on superconducting transition temperature, 20: 17637

FANALE, Fraser Partington, Helium in magnetite, 20: 16714

FANCHENKO, S. D., Search for Raman scattering of electromagnetic waves in microwave band with aid of turbulent plasma, 20: 17923

FARAGO, P. S., Production of polarized electron beams by spin exchange collisions, 20: 17273

FARGE, Y., Optical observation of interstitial Li in irradiated LiF, 20: 17143

FARRIS, Gerald C., Strontium-90 in antlers and selected bones of Colorado mule deer, 20: 16724 (COO-1156-12)

FARWELL, B. E., Prog. rpt. on SNAP-8 materials, semiannual, 1–6/65, 20: 16972 (NASA-CR-54719)

FAST, R. W., Contoured poles for d-c accelerator magnets, 20: 17185 (CONF-650922, pp 248-52)

FAUST, H., Chemical treatment of nitrogen compounds for isotope analysis of nitrogen by emission spectrometry, 20: 16376

FECHTER, H. R., Multiple pion production by 1.89-Bev/c π^-, 20: 17386

FECHTIG, H., Tritium diffusion measurements on four stone meteorites, 20: 17247

FEDOROV, T. F., Phase equilibrium in ternary Zr–Co–C and Nb–Fe–C systems, 20: 17086

FEDOROV, Yu. F., EPR in irradiated quartz single crystals containing aluminum impurity, 20: 16539

FEDOROVSKII, L. L., Experimental radiation sickness induced with ^{210}Po, 20: 16268

FEDOTOV, V. P., Experimental radiation sickness induced with ^{210}Po, 20: 16268

FEDRIGHINI, A. C., Evaluation of the first BR3 core, 20: 18108

FEELY, Herbert W., Prog. rpt. on radiochemical analyses of filter samples collected under Project Stardust, 1963. Appendix, 20: 16727 (HASL-168)

FEELY, Herbert W., Prog. rpt. on radiochemical analyses of filter samples collected under Project Stardust, 1964, 20: 16728 (HASL-169)
FEINBERG, E. L., High-energy successive interactions, 20: 17418
FELDER, R. M., Energy distribution of energetic atoms in an irradiated medium. II., 20: 17257
FELDMAN, J. M., Quantitative measurements of optical emission from dense theta-pinch discharges, 20: 17523
FERBEL, T., Pion production in $p\bar{p}$ annihilations at 3.3 and 3.7 Bev/c, 20: 17385
FERGUSON, A. T. G., Fission cross-section of ^{240}Pu for 0.03- to 2.0-Mev neutrons, 20: 17855
FERRARO, J. R., Infrared spectra of rare earth metal chloride complexes of 2,2'-bipyridyl and 1,10-phenanthroline, 20: 16437
FERRIS, Leslie M., High-temperature immiscibility of uranium mono- and dicarbides, 20: 17057
FERRY, James A., Determination of nuclear reaction widths from reaction yield curves, 20: 17778
FIEDLER, J., Comparison of observed delayed-neutron abundances with calculated fission yields of neutron precursors, 20: 17831
FIL, V. D., Nonlinear effects in ultrasonic absorption in superconducting indium, 20: 17635
FILIPIAK, B., Determination of mixture of thermal-neutron and γexposures by film badges, 20: 16807 (CLOR-IBJ-42/D)
FILIPPOV, A. G., Logical-element system for reactor control, 20: 18031
FILIPPOV, N. I., Moessbauer effect on ^{161}Dy impurity nuclei in metallic Gd, 20: 17988
FILLOLEAU, Etienne, Device for movement of control rod in a nuclear reactor, 20: 18042
FILOTI, G., Moessbauer spectrometer, 20: 16872
FINK, H. J., Inherent low-frequency losses of the superconducting surface sheath, 20: 17620
FIORE, Nicholas F., Test of viscous dislocation damping theory, 20: 17138
FIRESTONE, A., Pion production in $p\bar{p}$ annihilations at 3.3 and 3.7 Bev/c, 20: 17385
FIRSOV, V. G., Observation of atomic muonium in crystalline quartz, 20: 17361
FISCHER, B., Image characteristics of short magnetic deflection systems for atomic beams with regard to velocity distribution. II., 20: 17225
FISCHER, D. C., Mechanical, thermal and hydraulic design of Saxton partial plutonium core, 20: 18095 (WCAP-3385-52)
FISCHER, J., Discrete degenerate representations of non-compact unitary groups, 20: 17426 (IC-66/16)
FISCHER, P., New determination of the neutron scattering amplitude of zinc, 20: 17667
FISHER, D. J., Controlled-potential polarography and coulometry as microanalytical techniques, 20: 16390
FISHER, D. J., Determination of trace quantities of U, 20: 16389
FISHER, E. M. R., Radioactive fallout in air and rain: results to middle of 1965, 20: 16660 (AERE-R-4997)
FISHER, E. S., Temperature dependence of elastic moduli in alpha-U single crystals. IV., 20: 17063
FISHER, William D., Repair of radiation-induced damage to cell division mechanism of E. coli, 20: 16200
FISHER, P. C., High-sensitivity detectors for few-kev x rays, 20: 16901
FLAGELLA, P. N., Creep-rupture properties of Re and Re alloys, 20: 17011 (CONF-651025-14)
FLAHAUT, J., Manganese carbides, 20: 17030 (LA-tr-66-1)
FLAHAUT, Jean, Divalent rare earth sulfide—trivalent rare earth sulfide systems, 20: 16431
FLAMM, D., Coupling constants in broken $\bar{U}(12)$ symmetry, 20: 17481
FLAMMERSFELD, A., Isomer of ^{197}Au, 20: 17812
FLANNAGAN, Charles A., Approximating by synthesis a many, short-time increment depletion calculation, 20: 18052 (WAPD-T-1836)
FLEGONTOV, V. M., Measurements of β activity of fission products, 20: 16707
FLEISCHER, R. L., Ternary fission of heavy compound nuclei in thorite track detectors, 20: 17788
FLEROV, G. N., Isomeric yield ratio for the 14-ms fissioning isomer from deuteron irradiation of, 20: 17857
FLEROV, G. N., Radioactive properties of nuclei of heaviest elements, 20: 17688 (JINR-P-2539)
FLEURY, Alain, Simultaneous separations of Ra, Pu, U, Am, and Cm from irradiated Th, 20: 16359
FLIPOT, A. J., Increase in the diameter of composite tubes used in atomic power applications, 20: 17088
FLORA, John W., Nuclear reactor with aqueous fuel solution and a catalytic recombiner, 20: 18075
FLOUX, Francis, Study of plasma created by focusing of laser beam in air, 20: 17908
FLOYD, Frank W., Solar wind deuterium detector and charge spectrum analyzer, 20: 17307 (CONF-651001-34)
FLUEGGE, S., New approach to potential scattering. II., 20: 17491
FOCARDI, S., Production mechanism of $\overline{K}^*(891)$ in K⁻-p interaction at 3 Bev, 20: 17380
FORKER, M., Lifetime of the $^{31}/_2$ three-particle state of ^{177}Hf, 20: 17811
FORSBERG, S., Radiochemical separation of carrier-free Zr from yttrium oxide, 20: 16353
FORSEN, Harold Kay, Two-stage magnetic mirror compression experiment using a rotating plasma source, 20: 17953
FORSLING, W., Radiochemical separation of carrier-free Zr from yttrium oxide, 20: 16353
FORSYTH, Richard, Narrow-band x-ray detector for identification of chemical elements using radioisotope x-ray sources, 20: 16823 (NYO-3160-1)
FORTI, G., Evaluation of the first BR3 core, 20: 18108
FOSDICK, Lloyd D., Path-integral calculation of two-particle Slater sum for ^4He, 20: 17613
FOSTER, K. W., Radioisotopes for heat sources. II., 20: 16927 (MLM-1297)
FOWLER, J. F., Nomograms for radiobiologically equivalent fractionated x-ray doses, 20: 16749
FOWLER, P. H., Energy spectrum of primary cosmic rays, 20: 17315
FOWLER, William A., Nucleosynthesis in early history of solar system, 20: 17234
FRANCE, E. D., Determination of oxygen in sodium, 20: 16349
FRANCIS, C. W., Polonium-210 analyses of vegetables, cured and uncured tobacco, and associated soils, 20: 16189
FRANCIS, J. E. Jr., Excitation heating of ions to high temperature, 20: 17900
FRANKE, H., Radiosensitivity of human spinal cord, 20: 16251
FRANKE, Th., Calculation of radiation dose resulting from natural and artificial radioactive isotopes in the ground by γ spectrometry, 20: 16687
FRANKEVICH, D. P., New compounds of rare earths with Mn and Fe, and their crystal structures, 20: 17096
FRANK-KAMENETSKII, D. A., Drift waves of non-potential nature in a stationary magnetoacoustic plasma, 20: 17949
FRAPART, P., Chromatographic separations of iodide, iodate, tellurite, and tellurate ions on ion-exchange cellulose papers and control of $Na^{131}I$ gelatin capsules, 20: 16372
FRASER, H. J., Variable-width pulse generator using avalanche transistors and charge-storage diodes, 20: 16793
FRASER, J. S., Energy release in low-energy fission, 20: 17862
FRAUTSCHI, S. C., Self-consistent determination of coupling shifts in SU(3), 20: 17467
FRAUTSCHI, S. C., Weak and electromagnetic interactions of the hadrons in bootstrap theory, 20: 17466
FRAYSSE, G., Fission cross-section measurement of ^{235}U and ^{239}Pu for low-energy neutrons, 20: 17854
FREIDBERG, J. P., Unified theory of nonlinear oscillations of a cold plasma, 20: 17919
FRENKEL, A., Intermediate fields withoug particles, 20: 17437
FRENNET, Alfred, Description of calorimetric measurement of the intensity of low-energy x radiation, 20: 16856
FREREJACQUE, D., Deuteron electromagnetic form factors, 20: 17349 (LAL-1155)
FREUND, Harold G., Paramagnetic absorption of irradiated glycine, 20: 16525
FREY, A., Peptization of solid thorium oxide, 20: 16419 (UCRL-Trans-1301(L))
FRIDDLE, R. J., Phase diagram of Pu at pressures up to 75 kbar, 20: 17061
FRIEDBERG, C., Transverse polarization of the muon in decay $K_2^0 \to \mu^+ + \pi^- + \nu$, 20: 17424
FRIEDBERG, Richard Michael, Radiative decay of intermediate boson, 20: 17421
FRIEDLAENDER, E. M., Distribution of transverse moments in high-energy meson production, 20: 17371
FRIEDLING, G., Apparatus for measuring fast doubling times of the CABRI reactor, 20: 18150
FRIEDLING, G., Automatic control system of PEGGY reactor, 20: 18151
FRIEDMAN, Herbert, X-ray astronomy, 20: 17244
FRIEDMAN, Jerome H., Production and decay properties of $K_2^0(892)$, 20: 17403
FRIEDMAN, N. F., Parameter study of large fast reactor meltdown accidents, 20: 18123
FRIEND, James P., Prog. rpt. on radiochemical analyses of filter samples collected under Project Stardust, 1963. Appendix, 20: 16727 (HASL-168)
FRIMMER, M., Use of dimethyl sulfoxide as solvent in measuring scintillation mixtures, 20: 16355
FRISCHAT, G. H., Residual activity method for determination of self-diffusion coefficients in solids, 20: 16478
FRISH, I., Symmetry groups in classical and quantum mechanics, 20: 17429 (JINR-P-2529)
FRISHMAN, Y., Wave functions and production amplitudes for any spin, 20: 17462
FRISOLI, A., Medical x-ray survey packet, 20: 16843
FROMAGEOT, P., Preparation and purification of actinomycin-D-^3H,

20: 16550
FRONSDAL, C., Strong vertex according to SL(6,C), 20: 17427 (IC-66/20)
FROSCH, Robert Peter, Spectra of molecules trapped in rare gases and theory of electron relaxation in solid phase, 20: 18016
FRY, Arthur, Prog. rpt. on tracer and isotope effect studies in organic chemistry, annual, 1965, 20: 16542 (TID-22646)
FRY, D. N., Neutron fluctuation measurements at ORNL, 20: 18048 (ORNL-P-1967)
FRYBERGER, D., M1 and E2 hyperfine structure in muonic K and L x rays of bismuth, 20: 17792
FUCHS, G., Radiative corrections to inelastic electron scattering with detection in coincidence, II., 20: 17370
FUCHS, G., Role of radiation in pathogenesis of bronchial carcinoma, 20: 16264
FUJII, M., Ultrasonic attenuation and magnetic properties of superconducting Nb in mixed state, 20: 17608
FUJII, Taro, Chlorophyll mutations in Einkorn wheat induced by radiation, 20: 16285
FUKUSHIMA, Naoshi, Seasonal change of auroral zone in corrected geomagnetic latitudes, 20: 17556
FUKUZAWA, Fumio, Medium dependence of charge changing collisions for 9.7-Mev carbon ions, 20: 17724
FULLER, E. L. Jr., Heats of immersion in the Th oxide–water system. II., 20: 16456
FULTON, Margaret J., Electron capture by helium ions in neutral helium, 20: 17276
FULTZ, S. C., Photoneutron cross sections for ^{12}C and ^{27}Al, 20: 17773
FURET, J., Control and safety assembly for reactors of very high flux, 20: 18152
FURET, J., Description of two reactivity measuring apparatuses, 20: 18037
FURET, J., Evolution of safety systems for control of CEA reactors, 20: 18026
FURET, J., Procedure for rapid start-up, 20: 18021
FURET, J., Reactor control instrumentation design in France, 20: 18035
FURNICA, Gh., Modification of stability of complex metal–protein compounds in proteins subjected to action of γ rays, 20: 16211
FURNICA, Gheorghe, Modification of electrical conductivity of irradiated biopolymers, 20: 16194
FURSA, A. D., Capture of π^- mesons in H and D, 20: 17278
FURUHASHI, Akira, Radiation-induced graft copolymerization of butadiene to polyethylene and polypropylene, 20: 16527
FURUKAWA, T., Low-drift solid-state d-c amplifier, 20: 16803
FURUKAWA, T., Solid-state neutron flux monitoring instruments for nuclear reactor, 20: 18034

G

GABBIANI, G., Mechanism of experimental soft-tissue calcification, 20: 16162
GAGLIONE, P., Some data and comments on ^{22}Na in food chains, 20: 16678
GAILLOUD, M., Pion production in $p\bar{p}$ annihilations at 3.3 and 3.7 Bev/c, 20: 17385
GAL, Dezso, Kinetics and mechanism of isotopic exchange reactions on surface of solid catalysts. I., 20: 16460
GALIBA, Ilona, Kinetics and mechanism of isotopic exchange reactions on surface of solid catalysts. I., 20: 16460
GALLIA, A. S. Jr., BF_3 counters for use in field instrumentation, 20: 16895
GALLIGANI, I., Numerical solution of diffusion equations with the Kantorovich method, 20: 17656
GALLMANN, A., Properties of the 4.77- and 5.16-Mev states of ^{10}B, 20: 17761
GALSKOV, A., Labeling of corticotropin with ^{125}I, 20: 16494
GANAPATHY, R., Fallout from nuclear explosion of October 16, 1964, 20: 16663 (TID-21470)
GANGLBERGER, E., Problem of the carbohydrides, 20: 17074
GANGLBERGER, E., Ternary phases with $MgZn_2$ type, 20: 17075
GARBALYAUSKAS, Ch. A., Radioactive fallout in Vilnius in 1962, 20: 16700
GARCIA, R., Ultrasonic-induced cavitation studies in mercury and water, 20: 16974 (NP-15889)
GARD, E., Isotope exchange of active methyl hydrogens. III., 20: 16501
GARELICK, D. A., Photoproduction cross sections for π^+ and K^+ mesons at 3.4 to 4.0 Bev and comparison with SU(3), 20: 17400
GARIOD, R., Low-voltage ionization chamber, 20: 16902
GARIOD, R., Reactimeters, 20: 18032
GARNETT, J. L., Radiolysis of binary mixtures. I., 20: 16530
GARRISON, J. G., Effects of U and Mo alloying additions on corrosion resistance of AISI type 430 stainless steel, 20: 16975 (NP-15900)
GASC, Claude, Relation between rational curves of compression and deformation mechanisms of polycrystalline Be, 20: 17040
GASKILL, J. R., Vacuum-operated, foam-entrainment milk evaporator, 20: 16741 (UCRL-14534, pp 54-6)
GATLAND, I. R., Line-profile effects in stimulated scattering, 20: 17464
GATOS, H. C., Superconductivity in transition metal carbides, 20: 17607
GATOS, H. C., Superconductivity in close-packed intermediate phases of V–Ir, Nb–Ir, Nb–Rh, Ta–Rh, Nb–Pt, Ta–Pt, and other related systems, 20: 17624
GATTI, E., Isotropic monogap chamber pulsed with damped oscillation, 20: 16886
GATTO, R., Models for nonleptonic decays based on Chiral $U_3 \otimes U_3$ algebra, 20: 17456
GAVRILOV, K. A., Solvent extraction of Cf, Fm, and Md, 20: 16404
GAY, William I., Radiation hygiene, 20: 16296
GAYER, K. H., Rare earth hydrides, 20: 16453
GAZIEV, Ya. I., Dispersion of aerosols in global radioactive pollution of the atmosphere, 20: 16642
GAZIEV, Ya. I., Dispersion of radioactive aerosols in the stratosphere, 20: 16643
GAZIEV, Ya. I., Fluctuations in dispersed composition of radioactive aerosols in surface boundary layer of the atmosphere, 20: 16644
GEBALLE, R., Electron capture into excited states by He ions incident on He, 20: 17304
GEBALLE, T. H., Superconductivity of beta uranium, 20: 17095
GEDEONOV, L. I., Accumulation of ^{90}Sr and ^{137}Cs in soils of Leningrad region, 20: 16702
GEDEONOV, L. I., Chemical composition of atmospheric precipitation and fallout in vicinity of Leningrad, 20: 16704
GEDEONOV, L. I., Fallout of ^{90}Sr and ^{137}Cs isotopes in vicinity of Leningrad in 1961-1963, 20: 16701
GEDEONOV, L. I., Measurements of β activity of fission products, 20: 16707
GEILIKMAN, B. T., Jump in specific heat on going from superconducting to normal state, 20: 17612
GEILIKMAN, B. T., Shell effects in nuclear fission, 20: 17846
GEIS, Jack W., Research and development of electric propulsion, 20: 16628
GELBERG, A., Moessbauer spectrometer, 20: 16872
GELBERG, D., Optical properties of the neutron crystal spectrometers, 20: 16874
GEL'D, P. V., Kinetics of reduction of low-oxide niobium by carbon, 20: 16483
GEL'D, P. V., Self-diffusion of Nb in single crystal and molten specimens, 20: 17090
GELINAS, R. J., Reactor noise analysis by photon observation, 20: 18064
GELLER, Leonard, Outlook for uranium. Survey of U. S. U market, 20: 16718
GENESTE, P., Secondary deuterium isotope effect in addition reactions on carbonyl compounds, 20: 16555
GENIKHOVICH, E. L., Effect of vertical distribution of temperature and wind velocity on the atmospheric diffusion of radioactive pollutants, 20: 16651
GENTNER, W., Tritium diffusion measurements on four stone meteorites, 20: 17247
GENTRY, Robert V., Abnormally long α-particle tracks in biotite, 20: 16667
GEORGES, N. J., Mechanical, thermal and hydraulic design of Saxton partial plutonium core, 20: 18095 (WCAP-3385-52)
GERARDO, J. B., Rapid electron-density oscillations on axis of theta pinch, 20: 17918
GERASIMOV, V. V., Corrosion resistance of structural materials in boron-containing solutions, 20: 16976
GERBER, Abraham, Outlook for uranium. Survey of U. S. U market, 20: 16718
GERHARDT, P., Heinz body formation and chronic radiation burden, 20: 16250
GERHOLM, T. R., Double decay processes in ^{114m}In, 20: 17783
GERMAN, V. O., Investigation of performance of direct-current plasmatron, 20: 17938
GERWIN, R. A., Field-aligned flow of a conducting fluid past a source of magnetism, 20: 17509 (D-1-82-0469)
GESKE, G., Recent state of betatron development and application, 20: 17216
GETOFF, Nikola, Carboxylation of formic acid in aqueous solutions under influence of uv light, 20: 16538
GEVERS, R., Ordering of interstitial impurities in niobium, 20: 18003
GEWISS, Claude, Guide tubes for nuclear reactors, 20: 18039
GEY, Albert, Determination of number of neutrons emitted simultaneously by a source, 20: 16905
GHATIKAR, M. N., Zeeman-field-dependent quadrupolar interaction in rare-earth trichlorides, 20: 18008
GHIDINI, B., $\pi^+ p$ interactions at 1.6 Bev, 20: 17374
GIAEVER, I., Flux pinning and flux-flow resistivity in magnetically coupled superconducting films, 20: 17623
GIBSON, G., New cross section library for n + ^{235}U reactions, 20: 17697 (WANL-TME-1028)
GIBSON, G., XO and EXT—IBM-7094 programs temperature target, 20: 17698 (WANL-TME-1132)
GIBSON, W. M., Thermal-neutron-induced fission of ^{235}U, ^{233}U, and ^{239}Pu,

20: 17863
GILAT, G., Normal vibrations in aluminum and derived thermodynamic properties, 20: 18001
GILBODY, H. B., Charge transfer in proton-atomic H collisions above 50 kev, 20: 17302
GILET, Roland, Extrapolation number from survival curves of various populations of x-irradiated Chlorella pyrenoidosa, 20: 16246
GILLIAM, O. R., Paramagnetic resonance of F_2 ions trapped in electron-irradiated KF_2, 20: 17976 (NYO-2047-36, App.1)
GILLIAM, Otis R., Prog. rpt. on investigation of radiation effects in metal oxides and azides, annual, 2/65–1/66, 20: 17975 (NYO-2047-36)
GILLOT, J., Comparison of effects of mutagenic substances by studying mutagenesis of plants, 20: 16225 (EUR-2715.f)
GILMORE, J. S., Symmetry of neutron-induced ^{239}Pu fission in resonance region, 20: 17858
GILSON, Albert J., Development of a sensitive liquid dosimeter for integral dose measurement, 20: 16845
GILTINAN, D., Distorted-wave theory of the one-meson-exchange reaction, 20: 17474
GIMBLE, Francis S., Radioactive material in teeth of children in northern New Jersey area, 20: 16763
GINTER, Marshall L., Spectrum and structure of the He_2 molecule. III., 20: 16452
GINZBURG, N. I., Effect of uniform compression and plastic deformation of superconducting properties of Ti, 20: 17634
GIORCELLI, M., Numerical solution of diffusion equations with the Kantorovich method, 20: 17656
GISLON, R., Design and performance of neutron thermopiles, 20: 16899
GIUDICI, G., Third annual meteorological report of Center for Nuclear Studies at Casaccia, 1964, 20: 16635 (RT/PROT(65)-40)
GLADISHEVSKII, E. I., Continuous transition between structural types α-$ThSi_2$ and α-$GdSi_2$ in homogeneity region of $LaSi_2$, 20: 17042
GLADISHEVSKII, E. I., Solid solutions of Ge, Sn, Al, and Be in V_3Si and their superconductivity, 20: 17043
GLADKII, Ya., Spark chambers for studying elastic scattering of π^+ mesons by protons at 180°, 20: 16815 (JINR-P-2506)
GLASS, C. D., CVTR initial core loading, 20: 18085 (CVNA-173)
GLASS, H. Bentley, Prog. rpt. on effects of radiation and other mutagenic agents on inducing mutation in Drosophila, final, 5/53–12/65, 20: 16229 (NYO-1472-1)
GLASSGOLD, A. E., Spin-exchange scattering in uniform magnetic fields, 20: 17291
GLAUBERMAN, A. E., Effect of excitons on scattering of neutrons by crystals, 20: 18006
GLENDENIN, L. E., Primary nuclear charge from characteristic K x-ray emission in spontaneous fission of ^{252}Cf, 20: 17859
GODDEN, William R., Effects of radiation on serum enzymes and trace elements in large animals, 20: 16222 (AFWL-TR-65-112)
GODSHALL, John L., Refractory alloy tubing for space power systems, 20: 16998
GOEBEL, K., Radiation measurements around an insufficiently shielded target, 20: 17212 (UCRL-Trans-1305)
GOLD, Harold, Description and operation of spacecraft SERT I ion thrustor flight test, 20: 16625 (N-65-19272)
GOLDBERG, Hyman, nn Scattering length, 20: 17350 (N-65-19395)
GOLDBERG, M., K^--p interaction at 2.24 Bev/c, 20: 17383
GOLDBLITH, Samuel A., Discrepancies in application of triangle test to evaluation of irradiated whole-egg magma, 20: 16923
GOLDMAN, I. I., Law of conservation for free fields, 20: 17500
GOLDSCHMIDT, Z. B., Low odd levels of erbium I., 20: 17261
GOLDSTEIN, R., Performance measurements on pulsed ablating thruster, 20: 16626
GOLUBEV, V. A., Theoretical and experimental studies of water vapor plasma radiation, 20: 17936
GOLUBEVA, L. S., Deformed Zr–Ti–O–Fe alloy for high-pressure chambers, 20: 17003
GOMBOSI, E., Multiple scattering constant in emulsion at great cell lengths, 20: 16833
GONGWER, Nancy Ruth, Kerr magneto-optic effect as applied to rare-earth metals, 20: 17974 (IS-T-63)
GONZALES, B. A., Portable vacuum cleaner for recovering spilled mercury, 20: 16738 (UCRL-14534, pp 41-3)
GOODE, R. J., Analysis of Ti–7Al–2Nb–1Ta and Ti–6Al–4V fractures, 20: 16967 (AD-628277)
GOODIER, I. W., Half life of ^{32}P, 20: 17712
GOOGIN, J. M., Powder metallurgy in fabrication of very large parts, 20: 16993 (Y-DA-1043)
GOPAL, N. S., Chromatographic separations of iodide, iodate, tellurite, and tellurate ions on ion-exchange cellulose papers and control of $Na^{131}I$ gelatin capsules, 20: 16372
GOPALAN, K., Radioactive disequilibrium in minerals by α spectroscopy, 20: 16717
GOPALAN, K., Simple and flexible differential and integral pulse-height selector, 20: 16786
GORBATKOV, S. A., Axi-symmetric linear MGD flow with a Hall effect in two-component magnetic field, 20: 17521
GORBUNKOV, V. M., Illumination of a bubble chamber by means of a ruby laser, 20: 16841
GORBUNOV, L. M., Plasma instability in strong high-frequency field, 20: 17948
GORDON, H. S., Conference on magnet technology, Stanford Univ., 9/65, 20: 17156 (CONF-650922)
GORETZKI, H., Problem of the carbohydrides, 20: 17074
GORLOVOI, G. D., Tritium emitters, 20: 16916
GORODETZKY, S., Multiple-duration monostable multivibrator, 20: 16792
GOROSHKO, B. B., Effect of meteorological conditions on effectiveness of radioactive pollutant collection, 20: 16656
GOSSELIN, Charles M., Cold-cathode magnetron gage characteristics, 20: 16788
GOTT, Yu. V., Unstable states of a plasma in a trap with combined field, 20: 17925
GOUJON, Jean, New swimming pool reactor Osiris will go critical at Saclay in 1966, 20: 18148
GOULDING, F. S., Mass of ^6He from the four-neutron transfer reaction $^{26}Mg(\alpha,^6He)^{22}Mg$, 20: 17794
GOULIANOS, K., Transverse polarization of the muon in decay $K^\pm_{\mu 3} \rightarrow \mu^+ + \pi^- + \nu$, 20: 17424
GOYAL, I. C., Diffusion parameters of graphite, 20: 17661
GRABARI, V., Moessbauer spectrometer, 20: 16872
GRABOWSKI, Z. W., Beta-gamma circular polarization correlation of ^{122}Sb, 20: 17677 (COO-1420-112)
GRABOWSKI, Z. W., Search for higher-order effects in allowed β transitions, 20: 17678 (COO-1420-113)
GRAEFFE, G., Alpha-gamma and alpha-conversion electron coincidence study of ^{219}Rn, ^{215}Po, and ^{211}Bi, 20: 17703
GRAFF, G., Angular distribution of γ rays from fission of ^{235}U, 20: 17829
GRAFTIEAUX, J., Fission-product detectors for detection of burst fuel element cans, 20: 18036
GRAHAM, Stuart L., Changes in thyroid ^{131}I activity in ozone-tolerant and ozone-susceptible rats, 20: 16190
GRANOVSKII, Yu. I., Two axial octets, 20: 17442
GRANT, R. A., Potentiometric determination of Pu by argentic oxidation, ferrous reduction, and dichromate titration, 20: 16405
GRASS, G., Study of liquid metal boiling under forced convection, 20: 16608 (ANL-Trans-257)
GRAY, R. J., Conference on metallography, 19th group meeting, Oak Ridge National Lab., 4/65, 20: 16945 (ORNL-TM-1161)
GRAY, R. J., Experience with color in metallography, 20: 16949 (ORNL-TM-1161, pp 112-29)
GRAY, Robert J., High-temperature immiscibility of uranium mono- and dicarbides, 20: 17057
GRECHUKHIN, D. P., Tables of cross sections of photoionization of the hydrogen atom, 20: 17251 (IAE-873)
GRECHUSHKINA, M. P., Fractionation of radioactive products of nuclear explosion, 20: 16696
GREENSLADE, D. J., ESR studies of irradiated silver halides, 20: 17981
GREISEN, K. I., Search for discrete sources of cosmic γ rays above 1 Bev, 20: 17320
GRIBOV, B. S., Critical thermal fluxes in forced motion of MIPB–benzol, 20: 16614
GRIEM, H. R., Determination of atomic-resonance line-oscillator strengths, 20: 17932
GRIEPENTROG, E., Analysis of electrical networks using the ZRA 1 type computer, 20: 16790
GRIEPENTROG, E., Numerical treatment of kinetic reactor equations, 20: 18061
GRIFFEL, Jack, Forced convection boiling burnout for water in uniformly heated tubular test sections, 20: 16603 (NYO-187-7)
GRIFFIN, D. A., Atomic and molecular cross sections, 20: 17253 (ORNL-3908, pp 90-9)
GRIFFIN, H. C., Primary nuclear charge from characteristic K x-ray emission in spontaneous fission of ^{252}Cf, 20: 17859
GRIFFIN, J. E., Praseodymium-141 photoneutron cross section to 65 Mev, 20: 17764
GRIFFIN, J. E., $^{12}C(\gamma,n)^{11}C$ cross section to 65 Mev, 20: 17763
GRIFFIN, J. E., $^{16}O(\gamma,n)^{15}O$ cross section from threshold to 65 Mev, 20: 17762
GRIGOR'EVA, G. Ya., Criterion for selecting nucleon-nucleon events in nuclear emulsion, 20: 17357
GRIM, Alfred C., Discrepancies in application of triangle test to evaluation of irradiated whole-egg magma, 20: 16923
GRISHIN, V. G., Possible experiments aimed at testing isotopic structure of electromagnetic interaction, 20: 17428 (JINR-P-2498)
GRITCHENKO, Z. G., Accumulation of ^{90}Sr and ^{137}Cs in soils of Leningrad region, 20: 16702
GRITCHENKO, Z. G., Measurements of β activity of fission products,

20: 16707
GRITSYUK, Yu. N., Neutrons and kinetic energy of fragments in fission of heavy nuclei, 20: 17867
GRIVET, P., High homogeneity-rich field superconducting magnet for nuclear resonance, 20: 17587 (CONF-650922, pp 517-24)
GRODZNS, L., Nuclear transition probability, B(E2), for $0^+_{g.s.} \rightarrow 2^+_{first}$ transitions, 20: 17730
GROHMANN, K., Superconducting hollow cylinder as magnetic lens, 20: 17631
GROMOV, K. Ya., Decay of ^{159}Ho, 20: 17685 (JINR-P-2497)
GROMOVA, A. I., Corrosion resistance of structural materials in boron-containing solutions, 20: 16976
GROSHEV, L. V., Spectrum of γ rays emitted during capture of thermal neutrons in tellurium, 20: 17681 (IAE-966)
GROSSE, N., Preparation and purification of actinomycin-D-^{3}H, 20: 16550
GROSSER, Arthur E., Velocity analysis of reactive scattering in crossed molecular beams, 20: 17296
GROSSE-RUYKEN, Heinz, Separation chromatography of the rare earths by use of di(2-ethylhexyl) phosphoric acid. III., 20: 16385
GROSSETETE, B., Scattering of 150- and 300-Mev positrons and electrons from Bi, 20: 17785
GROZDOV, S. P., Experimental radiation sickness induced with ^{210}Po, 20: 16268
GRUEMM, H., Dynamics of nuclear fuel cycles, 20: 18116
GRUEMM, H., Simplified method for calculation of fuel cost fraction, 20: 18101
GRUETTER, Fritz, Magnet-system power supplies, 20: 17202 (CONF-650922, pp 755-68)
GRUGER, Alain, Infrared spectrometric study of phenylmethanes, 20: 16498
GRUZIN, P. L., Interaction of radiation-induced point defects with dislocations, 20: 17135
GRYCZ, Bronislav, Plasma of combustion products of $C_2H_2 + O_2$. II., 20: 17519
GSCHNEIDNER, K. A. Jr., Solid solubility of gold-rich rare-earth and lanthanide-rich magnesium alloys, 20: 17016
GUDDEN, F., Energy loss of 53-Mev electrons in graphite, 20: 17970
GUDEHUS, H., Cost regression in nuclear power plants, 20: 18102
GUDZHABIDZE, G. V., Relaxation of Onsager-Feynman vortexes in heating of rotating He II above phase transformation temperature, 20: 17642
GUDZHABIDZE, G. V., Relaxation processes related to temperature changes in rotating He II, 20: 17643
GUERLET, Jean-Paul, Behavior of Cu during CO_2 oxidation of Zr–Cu alloys, 20: 16977
GUGENBERGER, P., Conference on nuclear physics, Paris, 7/64. II., 20: 17871
GUILLET, Bernard, Dating of the Beillard peat bog by the ^{14}C method, 20: 16712
GUILLOTEAU, Rene, Machine for extraction of nuclear cartridges, 20: 16598
GUINIER, A., Observations of primary defects in crystals of LiF irradiated with thermal neutrons at 77°K, 20: 18007
GUINIER, A., Optical observation of interstitial Li in irradiated LiF, 20: 17143
GUIRAGOSSIAN, Zaven G. T., Analysis of the B enhancement, 20: 17402
GUPTA, R. P., Evaluation of specific heats of titanium, zirconium, and hafnium, 20: 17084
GUPTA, Sachchidanande, S-wave baryon-baryon scattering in broken SU(3), 20: 17468
GUSEVA, L. N., Phase transformation in Cr–Ta and Cr–Nb alloys, 20: 17046
GUS'KOV, Y. N., Spark chambers for studying elastic scattering of π^+ mesons by protons at 180°, 20: 16815 (JINR-P-2506)
GUTAN, V. B., Electron-bombardment-induced conductivity in fused silica, 20: 17133
GUTBROD, F., Pair production and heavy electron, 20: 17338 (DESY-65/10)
GUTFREUND, H., Direct capture mechanism for intermediate-energy nucleons, 20: 17737
GVUZDZ, E., Solvent extraction of Cf, Fm, and Md, 20: 16404
GWIAZDOWSKA, Barbara, Standardization of measurements of iodine uptake of thyroid gland by ^{131}I, 20: 16315
GWIAZDOWSKI, Bohdan, Standardization of measurements of iodine uptake of thyroid gland by ^{131}I, 20: 16315

H

HAAS, P. A., Prog. rpt. on chemical technology, 11/64, 20: 16556 (ORNL-TM-1090)
HAAS, T. W., Use of molybdenum in getter ion pumps, 20: 16789
HABEL, R., Isotropic monogap chamber pulsed with damped oscillation, 20: 16886
HABERMAN, Jerome, Radiation-enhanced surface activity of gamma HMX, 20: 16504 (AD-627846)
HACKFORTH, H. L., Energy spectrum of primary cosmic rays, 20: 17315
HADHAZI, Ca., Effect of ionizing radiation on iron metabolism, 20: 16187
HAEBLER, D. V., Automatization of nuclear-ship reactor plant, 20: 18130
HAEFNER, Klaus, Inactivation criteria for single cells, 20: 16255
HAELG, W., Double-axis neutron diffractometer and general criteria for optimization of its resolution for powder investigations, 20: 16799
HAELG, W., New determination of the neutron scattering amplitude of zinc, 20: 17667
HAFFEMAYER, Marcel, Device for movement of control rod in a nuclear reactor, 20: 18042
HAGEDOORN, H. L., 90° Superconducting bending magnet for 30-Mev protons, 20: 17197 (CONF-650922, pp 536-40)
HAGEE, G. Richard, Weak α and electron-capture decay in ^{208}Po and ^{209}Po, 20: 17841
HAGELSTEEN, John., Static electricity in anesthetic flowmeters eliminated by radioactive pistol, 20: 16783
HAGUE, J. F., Measurement of wide-angle bremsstrahlung at 28 Mev, 20: 17798
HAHN, George Max, Radiation sensitivity of cultured mammalian cells, 20: 16298
HAINS, F. D., Acceleration of NGD flow through the sonic velocity, 20: 17513
HALACSY, Andrew A., Use of conformal transformation in magnet design and extension of Schwarz-Christoffel transformation, 20: 17179 (CONF-650922, pp 104-110)
HALL, R. R., High-current ion-beam production and injection, 20: 17890 (ORNL-3908, pp 100-7)
HALL, Richard B., Acceleration of electrically charged particles of an ionized gas, 20: 17960
HALLER, Harry F., Underground highway and parking garage and blast shelter for Manhattan Island, 20: 16623 (ORNL-TM-1381)
HALNAN, Keith E., Non-surgical methods in diagnosis and management, 20: 16307
HALPERN, Jack, Homogeneous catalysis of D_2–H_2O exchange by Ru(III) chloride, 20: 16423
HALPERN, Jack, Reactivity of hydrogen atoms toward some cobalt(III) complexes in aqueous solutions, 20: 16526
HALZL, Jozsef, Effect of utilization factor on economy of heat-generating atomic power stations, 20: 18124
HAMADA, Kunihiko, Studies on renal clearance. II., 20: 16234
HAMEKA, H. F., General theorem for multiple-photon processes, 20: 17401
HAMELIN, J., Calculation of magnet profile by the method of equivalent currents, 20: 17178 (CONF-65022, pp 96-103)
HAMILTON, E. I., Applied geochronology, 20: 16715
HAMILTON, E. I., Distribution of uranium in some natural minerals, 20: 16684
HAMILTON, J., Elementary introduction to elementary particle physics, 20: 17432 (NP-15902)
HAMILTON, J. H., Internal conversion, 20: 17795
HAMMAN, Donald J., Effects of radiation on electronic components, 20: 16911
HAMMITT, F. G., Ultrasonic-induced cavitation studies in mercury and water, 20: 16974 (NP-15889)
HAMMOND, Martin Lewis, Metal diffusion in pyrolytic graphite, 20: 17107
HAMMOND, R. H., Nuclear spin relaxation in gallium metal, 20: 17995
HAMOUDA, I., Slow neutron spectrum of neutron beam from UA-RR-1 reactor, 20: 18147
HANAUER, S. H., Neutron fluctuation measurements at ORNL, 20: 18048 (ORNL-P-1967)
HANNA, G. L., Strength of irradiated BeO fueled with UO_2–ThO_2, 20: 17113 (AAEC-E-140)
HANNER, D. W., High-temperature testing of graphite helical-screw expanders and compressors, 20: 16591 (UCRL-14660)
HANRAHAN, D. J., Role of inductance in superconducting energy storage systems, 20: 17625
HANSEN, Luisa F., Ground-state (p,n) reactions in mirror nuclei and quasielastic model of (p,n) reactions, 20: 17775
HANUS, H., Possibility of introduction of maximum quantity of boron into nuclear emulsions, 20: 16891
HARARI, H., Particle masses and SU(6) symmetry breaking, 20: 17480
HARCHOL, M., Preparation of self-supporting targets of brittle metals, 20: 17218
HARDAWAY, John E., Prog. rpt. on radiochemical analyses of filter samples collected under Project Stardust, 1964, 20: 16728 (HASL-169)
HARDAWAY, John E., Prog. rpt. on radiochemical analyses of filter samples collected under Project Stardust, 1963. Appendix, 20: 16727 (HASL-168)
HARDIGREE, Alice A., Repair of radiation-induced damage to cell division mechanism of E. coli, 20: 16200
HARDING, John T., Density of niobium, 20: 17053
HARDT, Werner, Accelerator magnet of German electron synchrotron (DESY), 20: 17213 (UCRL-Trans-1312)
HARDY, Edward P. Jr., Prog. rpt. on fallout program, 9–12/65, 20: 16662

(HASL-165)
HARGROVE, C. K., Fine structure and isotope shift in muonic lead, 20: 17268
HAROLDSEN, G. O., Water chemistry of hermetically sealed boiling water reactors, 20: 18089 (NAA-SR-Memo-10178)
HARPOOTLIAN, Harry, Dispenser for addition of internal standard in liquid scintillation counting, 20: 16834
HARRIS, B., Temperature and strain-rate dependence of flow stress of solution-hardened Nb alloy, 20: 17082
HARRIS, C. A., Establishing magnetic field of a solid pole magnet to within ±0.01%, 20: 17206 (CONF-650922, pp 823-34)
HARRISON, D., Reducing effects of electrical interference on nucleonic instruments, 20: 18030
HARTLEY, P. E., Method for digital computer processing of data from radioisotope sediment tracing studies, 20: 16632 (AAEC/TM-303)
HARUN-AR-RASHID, A. M., Pion-nucleon coupling constant from spin-flip dispersion relation, 20: 17336 (AECD/TP-5)
HARVEY, L. M., Applying acyclic generators for pulse duty in magnet power supplies, 20: 16772 (CONF-650922, pp 769-75)
HARVEY, R. R., Photoneutron cross sections for ^{12}C and ^{27}Al, 20: 17773
HASEGAWA, Akinori, ESR of sodium polyphosphate glass irradiated with γ rays, 20: 16516
HASEGAWA, Akira, Longitudinal plasma oscillations near electron cyclotron harmonics, 20: 17934
HASSITT, A., Average atmosphere for particles trapped in the earth's magnetic field, 20: 17540 (N-65-18914)
HASTE, G. R., Injection and accumulation: single-pass experiments (DCX-1), 20: 17886 (ORNL-3908, pp 1-17)
HATZIKAKIDIS, A., Prog. rpt. on evaporation of radioactive wastes by solar energy, final, 12/65, 20: 18164 (NP-15874)
HAUG, H., Curium(III) phosphates, 20: 16470
HAUGHNEY, Louis C., Sputtering of single-crystal copper, 20: 17256
HAVELL, Richard F., High-temperature electrical properties of insulators, 20: 17022 (N-65-18933)
HAVEN, G. T., Determination of Ca, Cu, Mn, and Mg in serum by neutron activation analysis, 20: 16347
HAVEN, M. C., Determination of Ca, Cu, Mn, and Mg in serum by neutron activation analysis, 20: 16347
HAWERSAAT, William H., Description and operation of spacecraft SERT I ion thrustor flight test, 20: 16625 (N-65-19272)
HAWTHORNE, J. R., Radiation damage surveillance of power reactor pressure vessels, 20: 17126 (NRL-6349)
HAYAKAWA, Satio, Lunar x rays excited by energetic terrestrial electrons, 20: 17246
HAYES, F. N., Quench monitoring and efficiency calibration through external standardization, 20: 16820 (LA-DC-7222)
HAYWOOD, F. F., Free-field radiation-dose distributions from Hiroshima and Nagasaki bombings, 20: 16760
HAZEN, K. A., Analysis of Be metal and its compounds by optical emission spectrography, 20: 16352
HAZEN, Richard W., Neoplasms following irradiation of the head, 20: 16245
HAZUE, Masaaki, Catalytic tritium exchange reactions with tritiated active methylene compound, 20: 16492
HEARD, M. J., Film dosimetry practice with AERE/RPS film holder, 20: 16720 (AERE-R-4669)
HECHT, P., Utilization of multiclone dust for decontaminating sewage waters containing ^{137}Cs and $^{90}Sr/^{90}Y$, 20: 18170
HEDIN, Bengt, Three-dimensional potential functions for magnet design, 20: 17177 (CONF-650922, pp 89-95)
HEDIN, R. A., Power supply system for ZGS ring magnet, 20: 17227
HEGER, A., Effect of penetrating radiation on properties of polyamide fibers. I., 20: 16522
HEIL, H., Ionization cross section of cesium at threshold, 20: 17287
HELLMAN, W. S., Goldstone behavior in some model theories, 20: 17473
HELLSTRAND, Eric, Fission integrals of ^{235}U and ^{239}Pu with cadmium and boron filters, 20: 17751
HELMER, R. G., Decay of ^{149}Nd, 20: 17787
HEMMI, Seizaburo, Influence of γ radiation on germination of Rauwolfia serpentina. II., 20: 16249
HEMPELMANN, Louis H., Neoplasms following irradiation of the head, 20: 16245
HENKE, G., Determination of radioactivity in drinking and rain water, 20: 16407
HENMI, Masatake, B-constant magnet pole design, 20: 17184 (CONF-650922, pp 239-47)
HENMI, Masatake, Field mapping by differential usage of Hall generators, 20: 17193 (CONF-650922, pp 472-5)
HENNEN, N. M., Shielding calculations for β radiation sources of high activity, 20: 17968
HENRY, Roger P., Lorentz force maximization in continuous-flow Hall current plasma accelerators, 20: 17897
HENSON, Robert Maurice, Plasma interaction with a cylindrical magnetic field, 20: 17956
HERBERT, W. C., Underground highway and parking garage and blast shelter for Manhattan Island, 20: 16623 (ORNL-TM-1381)
HEREWARD, H. G., What are the equations for the phase oscillations in a synchrotron? 20: 17174 (CERN-66-6)
HERGET, Camillo, Carbonyl compounds of technetium, 20: 16480
HERMANN, G., Comparison of observed delayed-neutron abundances with calculated fission yields of neutron precursors, 20: 17831
HERMANSDORFER, H., Measurement of high electron densities on linear Z pinch using new microwave reflection probe, 20: 17876 (IPP-1/37)
HERRMANN, Adele B., Accelerator magnet of German electron synchrotron (DESY), 20: 17213 (UCRL-Trans-1312)
HERRMANN, D., Summary of working session on personnel dosimetry, Berlin, 11/64, 20: 16827 (SZS-9(1965))
HERRMANN, G. F., Echo processes in a plasma, 20: 17933
HERZENBERG, A., Quasi-stationary-state approach to resonances in scattering of electrons, 20: 17289
HERZMANN, H., Labeling of proteins with radioactive iodine, especially ^{133}I, 20: 16257
HESP, R., Effect of sodium alginate on uptake of Sr-85 from G-I tract, 20: 16173 (PG-Report-686)
HESSE, E., Nanosecond pulse device for a 2-Mev Van de Graaff electron accelerator, 20: 17217
HEUFNER, Joerg, Muonic atoms in the neighborhood of lead, 20: 17281
HEYM, A., Axial high-frequency discharge, 20: 17879 (LRP-19/65)
HEYMANN, Dieter, Canyon Diablo meteorite, 20: 17238
HEYMANN, Dieter, Rare gas evidence for two paired meteorite falls, 20: 16673
HEYMANN, F., Unstationary temperature distribution in cylindrical and annular, 20: 16613
HICKS, Samuel P., Effects of low levels of ionizing radiation on rat developing cerebral cortex, 20: 16275
HIEBER, Walter, Carbonyl compounds of technetium, 20: 16480
HIEMANN, D., Density-independent moisture gage using neutron radiation, 20: 16924
HIGASHIMURA, Takenobu, Thermoluminescence dosimetry of γ rays from atomic bombs in Hiroshima and Nagasaki, 20: 16759
HIGGINS, L. J., Handbook of analytical procedures, 20: 16337 (RMO-3001(Rev.1)(Suppl.))
HILDITCH, R. J., Strength of irradiated BeO fueled with UO_2–ThO_2, 20: 17113 (AAEC-E-140)
HILLER, D. M., Thoron monitor, 20: 16842
HILZ, H., Synchronized budding yeast cells. I., 20: 16240
HINCKS, E. P., Fine structure and isotope shift in muonic lead, 20: 17268
HINTENBERGER, H., Argonne National Laboratory's pion focusing horn, 20: 17198 (CONF-650922, pp 650-6)
HINZPETER, M., Relation between the total β activity and individual radionuclide content in fission-product mixtures, 20: 16766
HIRSCH, R. L., Rapid electron-density oscillations on axis of theta pinch, 20: 17918
HITCHCOCK, H. C., Design of volume-minimized-split solenoid systems, 20: 17180 (CONF-650922, pp 111-25)
HITE, Mark, Changes in thyroid ^{131}I activity in ozone-tolerant and ozone-susceptible rats, 20: 16190
HITLIN, D., Magnetic dipole and electric quadrupole hyperfine effects in ^{209}Bi muonic x rays, 20: 17793
HITZIG, K., Current feed and instrumentation of electrically heated 2.8-Mw superheating loop, 20: 16609
HO, J. C., Superconductivity of beta uranium, 20: 17095
HODGKINSON, J. G., Measurement of fission cross sections for neutrons of energies in range 40 to 500 kev, 20: 17852
HOEFT, Lothar O., Microwave heating: critical exposure variables for man and experimental animals, 20: 16235
HOEKS, Bas, Transverse waves in accelerated parallel-flow electron beams with constant magnetic field, 20: 17505
HOENIG, Arnost, Computation of thickness of lead shielding against γ radiation, 20: 17963 (ORNL-tr-1059)
HOENIG, Arnost, Computation of thickness of water shields against γ radiation, 20: 17964 (ORNL-tr-1061)
HOEVERMANN, Georg, Pleochroic halos in biotite, hornblende and cordierite, and relations to the α rays of radioactive elements, 20: 16666 (ORNL-tr-923)
HOFFMAN, George A., Underground highway and parking garage and blast shelter for Manhattan Island, 20: 16623 (ORNL-TM-1381)
HOFFMAN, Roy C., Penetration seals for N-reactor plant, 20: 18125 (RL-SA-25)
HOFFMANN, J. P., Irradiation performance of alternate cladding materials, 20: 17120 (GEAP-4916)
HOFMAN, A., Some properties of U–1 wt.% Mo alloy after thermal treatment, 20: 17014 (INR-645/XIV/PS)
HOFMANN, A., High-order double focusing in magnetic field, 20: 16868
HOGERTON, John F., Outlook for uranium. Survey of U. S. U market,

20: 16718
HOLLANDER, J. M., Internal conversion, 20: 17795
HOLLIDAY, R. J., Hyperfine magnetic fields at nuclei of indium in iron and nickel, 20: 17992
HOLM, K., Beam transport magnet measurements at DESY, 20: 17192 (CONF-650922, pp 456-66)
HOLMES, H. F., Heats of immersion in the Th oxide–water system. II., 20: 16456
HOLT, P. D., Film dosimetry practice with AERE/RPS film holder, 20: 16720 (AERE-R-4669)
HOLTZ, Frederick C., High-temperature electrical properties of insulators, 20: 17022 (N-65-18933)
HOLZWARTH, Gottfried, Polarization effects in electron-electron and positron-electron scattering, 20: 17489
HOMMA, S., Photoproduction cross sections for π^+ and K^+ mesons at 3.4 to 4.0 Bev and comparison with SU(3), 20: 17400
HONJYO, Takaharu, Solvent extraction of europium ions, 20: 16565
HONSTEAD, J. F., Disposal of radioactive wastes into fresh water, 20: 18157 (BNWL-SA-466)
HONZAWA, Tadao, Anomalous bremsstrahlung and anomalous cyclotron emission from partially ionized gases, 20: 17921
HOOD, C. Gregory, Interactions and relativity, 20: 17574
HOPPER, Arthur F., Depletion of intestinal epithelium of the mouse following exposure to lethal whole-body radiation, 20: 16223 (BNL-8952)
HOREN, D. J., Levels of ^{85}Sr populated in decay of ^{85}Y and ^{85m}Y, 20: 17670 (AD-629576)
HORNUNG, Goenter, Influence of whole-body x irradiation on enzymatic activity of lactate dehydrogenase isoenzymes, 20: 16289
HORTON, M. D., Applying acyclic generators for pulse duty in magnet power supplies, 20: 16772 (CONF-650922, pp 769-75)
HORTON, R. W., Prog. rpt. on chemical technology, 11/64, 20: 16556 (ORNL-TM-1090)
HOUSTON, John M., Electron emission of Pt-group metals in Cs vapor, 20: 17333
HOUTMAN, J. P. W., Measurement of radioactivity in effluents of a gas chromatograph, 20: 16371
HOUZE, Gerald Lucien Jr., Segregation processes and the omega transformation in Zr–Nb alloys, 20: 17105
HOWARD, R. C., Converter performance test of Re emitter in contact with carbide fuel, 20: 17327 (N-65-19264)
HOYLE, F., Nature of quasi-stellar sources, 20: 17242
HOYLE, F., Nucleosynthesis in early history of solar system, 20: 17234
HRASTNIK, B., g-Factor of 87-kev excited state in ^{155}Gd, 20: 17683 (INP-430/PL)
HRYNKIEWICZ, A. Z., g-Factor of 87-kev excited state in ^{155}Gd, 20: 17683 (INP-430/PL)
HSIUNG, Y. C., Effects of x rays on growth, maturation, and fertility of rats irradiated at seventh day after birth. I., 20: 16287
HSIUNG, Y. C., Effects of x rays on growth, maturation, and fertility of rats irradiated at seventh day after birth. II., 20: 16288
HUANG, Robert Y.-M., Structure and properties of cellulose graft copolymers. I., 20: 16528
HUBBARD, E. L., Ternary fission of heavy compound nuclei in thorite track detectors, 20: 17788
HUDDLE, R. A. U., Development of coated-particle fuel for high-temperature reactors, 20: 18098
HUDGENS, C. R., Handling α-active specimens in the electron microprobe x-ray analyzer, 20: 16554
HUDSON, W. R., Combined surgical and radiation management of carcinoma of the laryngopharynx, 20: 16313
HUEGEL, Helmut, Electric arc in a supersonic plasma jet, 20: 17904
HUEGEL, Helmut, Phenomena on arc cathodes in flowing gases at low pressures, 20: 17517
HUESTON, F. H., Uranium monocarbide—new nuclear fuel concept for Canada, 20: 16966
HUGHES, A., Radioactive fallout in air and rain: results to middle of 1965, 20: 16660 (AERE-R-4997)
HUGHES, V. W., Atomic interactions of muonium, 20: 17297
HUIZENGA, J. R., Fission-fragment angular, energy, and mass division correlations for the $^{234}U(d,pf)$ reaction, 20: 17865
HULETT, S. H., Environmental radiation levels and concentrations [at Portsmouth, Ohio gaseous diffusion plant], 20: 16726 (GAT-506)
HULL, G. W. Jr., Superconductivity of beta uranium, 20: 17095
HULLIGER, F., C23-type modification of $ThAs_2$, 20: 17077
HUMMEL, John P., Cross sections for $^{27}Al(\gamma,\pi^+)^{27}Mg$ reaction, 20: 17779
HUMMEL, R. H., Pulse-shape discrimination in organic scintillators, 20: 16839
HUNT, Edward L., Humoral mediation of radiation-induced motivation in parabiont rats, 20: 16284
HUNT, W., Ultraviolet bleaching of synchronized Euglena, 20: 16204
HUNYADI, I., Measurement of total cross sections of Cs and Rb for 14-Mev neutrons, 20: 17702
HUSAK, Vaclav, Possibility of absolute measurements of radioisotope activity using scintillation γ spectrometry, 20: 16858
HUSSAIN, Masud, 1001 reactions of the Ar and Kr ion doublets, 20: 17255
HUTCHINSON, D., Transverse polarization of the muon in decay $K_2^+ \rightarrow \mu^+ + \pi^- + \nu$, 20: 17424
HUTCHINSON, D. R., Praseodymium-141 photoneutron cross section to 65 Mev, 20: 17764
HUYCKE, Edward J., Prog. rpt. on ionizing radiation, injury, prevention, and treatment, annual, 10/65, 20: 16303 (AD-626384)
HUYNH VINH DINH, Fluctuations of partial and total radiative widths by neutron capture resonance, 20: 17676 (CEA-R-2810)
HYDE, Earl K., Application of high-resolution semiconductor detectors in x-ray emission spectrography, 20: 16887
HYGH, E. H., Electron-nuclear interaction in antimony metal, 20: 18000

I

ICHIKAWA, Yonota, Thermoluminescence dosimetry of γ rays from atomic bombs in Hiroshima and Nagasaki, 20: 16759
IGI, K., High-energy behavior of real part of scattering amplitudes and consequences from SU_3, 20: 17378
IGNATOV, D. V., Rate of oxidation of metallic Sc, 20: 16985
IIZUMI, Masashi, Calculation of effective cutoff energies taking into account scattering and higher resonances of filters, 20: 17663
IKEBUCHI, Hidekaru, Contamination of ^{90}Sr in stock rainwater in lighthouses, 20: 16671
IKEDA, Masamichi, Reaction of active nitrogen with ethylene, 20: 16510 (NP-tr-1364)
IKEDA, Minoo, Generalization of the spherical complex function, 20: 16941
IKUSHIMA, A., Ultrasonic attenuation and magnetic properties of superconducting Nb in mixed state, 20: 17608
IL'INSKAYA, T. I., Chemical composition of atmospheric precipitation and fallout in vicinity of Leningrad, 20: 16704
ILLASZEWICZ, A., New type of radiometric titrator: Redox and chelatometric microtitrations, 20: 16386
IMAEDA, K., Primary-energy estimate for jets based on momentum and angular distributions of secondaries, 20: 17316
IMANISHI, Nobutsugu, Medium dependence of charge changing collisions for 9.7-Mev carbon ions, 20: 17724
INDREAS, Gr., Acceleration of negative hydrogen ions in the U-120 cyclotron, 20: 17224
INDREAS, Gr., NMR magnetometric device with flowing liquids, 20: 16770 (CONF-650922, pp 428-30)
INDURKAR, V. S., New design of ratio circuit for fission-fragment study, 20: 17870
INGLE, N. A., Automatic data logging system for meteorological studies in reactor environment, 20: 16710
INOKUTI, M., Generalized oscillator strength and relation to inelastic scattering of charged particles, 20: 17306
INOPIN, E. V., Inelastic diffraction scattering treated by the complex angular momentum method, 20: 17817
INOPIN, E. V., Theory of diffraction scattering of particles by complex nuclei, 20: 17816
IOFFE, M. S., Unstable states of a plasma in a trap with combined field, 20: 17925
IOFFE, V. A., EPR in irradiated quartz single crystals containing aluminum impurity, 20: 16539
ISACCHINI, F., Electrical resistivity measurement of Na, 20: 17026 (RT/ING-(65)17)
ISACSSON, P., Quasi-free proton-proton scattering in light nuclei at 460 Mev, 20: 17741
ISELIN, Ch., Orthogonal analog model helps to solve magnetic field problems difficult to be treated by analytical methods, 20: 17181 (CONF-650922, pp 126-40)
ISHIHAMA, H., Tritium measurement with liquid scintillation counter, 20: 16373
ISHIHARA, Takeaki, Medical survey of Japanese exposed to fallout radiation in 1954, 20: 16226 (NP-15891)
ISHIZAKI, Yoshihide, Survey of nuclear reactions induced by 57-Mev protons. II., 20: 17725
ISLAM, Md. Mozharul, Pion-nucleon coupling constant from spin-flip dispersion relation, 20: 17336 (AECD/TP-5)
ISMATOV, E., Polarization of products of ^6Li breakup in electromagnetic field of the nucleus, 20: 17806
ISRAEL, Werner, New interpretation of the extended Schwarzschild manifold, 20: 17576
ISRAEL, Werner, Radial motion in Schwarzschild field and gravitational collapse, 20: 17569
ISSA, I. M., Analysis of uranium in phosphate ores, 20: 16381
ITOH, Koichi, Stereospecific addition of hydrogen to fumaric acid in irradiated single crystals of succinic acid, 20: 16537
IVANCHEV, N., Positron annihilation in CdS monocrystals, 20: 17983
IVANOV, E., Isomeric yield ratio for the 14-ms fissioning isomer from

deuteron irradiation of, 20: 17857
IVANOV, K. G., Did the IMP 1 observe the magnetic wake of the moon or earth? 20: 17235
IVANOV, P. P., Singularities of MGD generator performance at large Hall numbers, 20: 17332
IVANOV, V. I., Effects of small flares in hard component of cosmic rays of magnetically quiet and disturbed days, 20: 17313
IVANOV, V. I., X-ray and infrared study of perrhenate tetrahydrates of rare earths and yttrium, 20: 16473
IWASAKI, Y., Current-generated algebra and mass levels of the hadrons, 20: 17471
IYER, R. S., Neutron-induced fission of ^{227}Ac, ^{231}Pr, and ^{237}Np: mass distribution, 20: 17861
IZRAEL, Yu. A., Adsorption method of determining radon concentration in the air from an airplane, 20: 16708
IZRAEL, Yu. A., Fractionation of radioactive products of nuclear explosion, 20: 16696

J

JABIOL, M. A., π^+ p interactions at 1.6 Bev, 20: 17374
JACKSON, A. G., Use of molybdenum in getter ion pumps, 20: 16789
JACKSON, D. F., Interpretation of structure of ^{7}Li from proton scattering, 20: 17800
JACQUELIN, R., Rapsodie reactor—control rod mechanisms, 20: 18096 (ORNL-tr-987)
JACQUESSON, Jacques, Determination of number of neutrons emitted simultaneously by a source, 20: 16905
JAEGERHUBER, P., Rapid determination of important radionuclides in foodstuffs and water. II., 20: 16369
JAIDANE, S., Calculation of magnet profile by the method of equivalent currents, 20: 17178 (CONF-650922, pp 96-103)
JAIN, H. C., Neutron-induced fission of ^{227}Ac, ^{231}Pr, and ^{237}Np: mass distribution, 20: 17861
JAIN, S. C., Integrated photodisintegration cross section of He with velocity-dependent nuclear potential, 20: 17774
JAMES, Brian R., Homogeneous catalysis of D_2–H_2O exchange by Ru(III) chloride, 20: 16423
JAMES, D., Medical x-ray survey packet, 20: 16843
JAMES, M. F., CWF and TABLE—two FORTRAN programs for calculation of Coulomb penetration and shift factors, 20: 17671 (AEEW-M-611)
JANIN, Joseph, Thermoluminescence of calcium oxide activated by IVa Group elements, 20: 17982
JANOSSY, L., Two subgroups of Lorentz group and their physical significance, 20: 17564
JANSEN, G. Jr., Transient thermal behavior in fixation of radioactive materials, 20: 18155 (BNWL-157)
JARED, Richard C., Application of high-resolution semiconductor detectors in x-ray emission spectrography, 20: 16887
JAROSCHEK, K., Second Foratom congress. Present types of nuclear power plants, 20: 18104
JARRETT, H. F., Underground highway and parking garage and blast shelter for Manhatten Island, 20: 16623 (ORNL-TM-1381)
JARVIS, O. N., Absolute differential cross section in proton-carbon elastic scattering at 145 Mev, 20: 17739
JARVIS, O. N., Analysis of 140-Mev nucleon scattering data for beryllium and carbon, 20: 17740
JARVIS, O. N., Measurements of proton-nucleus triple scattering parameters near 140 Mev, 20: 17738
JASKE, R. T., Evaluation of use of selective discharges from Lake Roosevelt to cool Columbia River, 20: 18172 (BNWL-208)
JATHAR, N. B., Automatic data logging system for meteorological studies in reactor environment, 20: 16710
JEAN-LOUIS, Francois, Plastic deformation of polycrystalline uranium, by straining at various rates, between 20 and 850°C, 20: 17039
JEDLICKA, M., On the sensitivity of photocathodes to x rays, 20: 17984
JEE, W. S. S., Intercomparison of pathological fractures in beagles injected with ^{226}Ra, ^{228}Ra, ^{239}Pu or ^{90}Sr, 20: 16253
JEEVANANDAM, Maloyappa, Isotope effects among oxides of nitrogen in gaseous and liquid phases, 20: 16486
JELLEY, J. V., High-energy γ absorption in space by a 3.5°K microwave field, 20: 17319
JENIK, L., Multiple scattering constant in emulsion at great cell lengths, 20: 16833
JENKINS, P. M., Excitation heating of ions to high temperature, 20: 17900
JENNINGS, R. E., Measurement of wide-angle bremsstrahlung at 28 Mev, 20: 17798
JENSEN, D. A., M1 and E2 hyperfine structure in muonic K and L x rays of bismuth, 20: 17792
JENSEN, M. L., Stable isotopic geology of the Gas Hills, Wyoming, Uranium District, 20: 16670
JENSEN, M. L., Stable carbon isotopic composition of biogenic carbonates, 20: 16675
JIN, Y. S., Forward peak at high energies, 20: 17459
JOE, E. G., Uranium and copper extraction by liquid ion exchange, 20: 16572
JOERGENSEN, C. Barker, Hormonal dependency of molting in amphibians, 20: 16252
JOHANSEN, H. A., Potential of interstitial compounds for high-field superconducting magnets, 20: 17589 (CONF-650922, pp 541-9)
JOHNSON, O. W., Isotopic mass dependence of Li diffusion in rutile, 20: 17052
JOHNSON, R. G., Praseodymium-141 photoneutron cross section to 65 Mev, 20: 17764
JOHNSON, R. H., Enhancement of ductility in alpha-uranium, 20: 17076
JOHNSON, Virginia Ann, Bibliography on electrets. II., 20: 17971 (AD-299256)
JONES, B. L., Normal-Fermi-liquid theory for electrons in solids, 20: 17993
JONES, C. Edward, Numerical solution of non-Fredholm (singular) integral equations by matrix inversion, 20: 16936
JONES, C. K., Potential of interstitial compounds for high-field superconducting magnets, 20: 17589 (CONF-650922, pp 541-9)
JONES, Frank C., Inverse Compton scattering of cosmic-ray electrons, 20: 17309 (N-65-19716)
JONES, G., Positron annihilation in noble gases, 20: 17423
JONES, H. C., Controlled-potential polarography and coulometry as microanalytical techniques, 20: 16390
JONES, I. G., Rapid dissolution of PuO_2 by a Na peroxide sinter and determination of PuO_2 content, 20: 16350
JONES, Ieuan R., Beryllium pressure bar having a submicrosecond risetime, 20: 17018 (LRP-20/66)
JONES, M. B., Radiological environmental survey manual, 20: 18083 (CVNA-63)
JONES, Norman D., Effects of radiation on serum enzymes and trace elements in large animals, 20: 16222 (AFWL-TR-65-112)
JONES, T. D., Free-field radiation-dose distributions from Hiroshima and Nagasaki bombings, 20: 16760
JONES, W. D., Plasma physics, 20: 17889 (ORNL-3908, pp 52-89)
JORDAN, Harry F., Path-integral calculation of two-particle Slater sum for ^{4}He, 20: 17613
JOSEPH, A. D., Coated Nb alloys can take high turbine heat, 20: 16963
JOSEPH, R. R., Solid solubility of gold-rich rare-earth and lanthanide-rich magnesium alloys, 20: 17016 (IS-1175)
JOSHI, C. W., Automatic data logging system for meteorological studies in reactor environment, 20: 16710
JOSHI, V., Plasmas under the influence of stationary crossed electric and magnetic fields, 20: 17943
JOSIEN, Marie-Louise, Vibration spectra of imidazole, imidazole (D)-1, imidazole (D_3)-2,4,5, and imidazole (D_4). I., 20: 16499
JOUSSEAUME, C., Measurement and analysis of fission cross section of ^{239}Pu from 0 to 5 kev, 20: 17851
JOUSSET, J. C., Annealing of uranium quenched from 100 to 4.2°K, 20: 17029 (ANL-Trans-273)
JOVER, P., Control and safety assembly for reactors of very high flux, 20: 18152
JUDY, R. W. Jr., Analysis of Ti–7Al–2Nb–1Ta and Ti–6Al–4V fractures, 20: 16967 (AD-628277)
JUDY, Ray W., Dispenser for addition of internal standard in liquid scintillation counting, 20: 16834
JULEAN, I., Uranyl pyrophosphate complexes, 20: 16472
JUNG, L., Distribution system for multichannel pulse-height analyzer, 20: 16817 (JUL-270-RB)
JURA, G., Magnetic and structural properties of europium metal and EuO at high pressure, 20: 17999

K

KACHI, S., Prog. rpt. on crystal chemistry, 8/13–11/13/65, 20: 17007 (AD-627468)
KADONAGA, Masao, Radiation-induced graft copolymerization of butadiene to polyethylene and polypropylene, 20: 16527
KAGAN, Yu., Change of resonance nuclear parameters during scattering on regular systems, 20: 18015
KAHANE, Andre, Study of double nitrate of La and Mg between 4000 and 1250 cm^{-1}, 20: 16429
KAHN, J. S., Electron transmission microscopy of polycrystalline BeO, 20: 17054
KAIDALOV, A. B., Possible radiative decays of heavy mesons involving violation of charge parity, 20: 17501
KAINZ, Gerald, Determination of ^{14}C, tritium, or ^{35}S after combustion of an organic sample at a system of nozzles, 20: 16387
KAJAMAA, J., Small neutron diffractometer, 20: 16882
KALAB, D., Uv-induced photodimerization of thymine and 5-hydroxymethyluracil in frozen water solutions, 20: 16197
KALASHNIKOV, N. P., Quantum effects in multiple scattering, 20: 17497
KALASHNIKOV, V. P., Transfer theory in non-equilibrium systems of

particles in a strong magnetic field, 20: 17487
KALINNIKOV, V. G., New isotopes ^{157}Eu, ^{157}Ho, and ^{156}Er, 20: 17808
KALINOVICH, D. F., Mobility of atoms in a Mo–W alloy, 20: 17101
KALMON, B., Environmental radiation levels and concentrations [at Portsmouth, Ohio gaseous diffusion plant], 20: 16726 (GAT-506)
KALMUS, P. I. P., Polarization of Σ^0 particles in reaction $\pi^- + p \rightarrow K^0 + \Sigma^0$ at 1.5 and 1.8 Bev/c, 20: 17382
KAMETANI, Katsuaki, Contamination by ^{90}Sr and ^{137}Cs of dry milk products in 1962, 20: 16755
KAMLAH, A., Measurement of g_J factor of $^5D_4$ ground state of ^{56}Fe, 20: 17280
KAMMERER, O. F., Effect of electron-spin paramagnetism on critical field of thin Al films, 20: 17622
KAMPER, R. A., Energy gap of superconducting tin films in a magnetic field, 20: 17619
KANAYA, K., Comment on "aberrations of focused beams of charged particles caused by space charge," 20: 16784
KANAZIR, D., Effect of native isologous DNA on incorporation of thymidine-^{3}H into uv-irradiated L-strain cells, 20: 16279
KANDA, Keiji, Orthogonal expansion method for deducing thermal neutron spectra from activation rates, 20: 16857
KANDROR, V. I., Hypophysis and adrenals in presence of radiation injuries, 20: 16232 (JPRS-34120)
KANEKO, Kumetaro, Prog. rpt. on INS isotope separator, 11/5/65, 20: 16928 (INSJ-92)
KANGOS, James D., Prog. rpt. on influence of local winds on fallout, final, 20: 16661 (ECOM-00392-F)
KANNO, M., Thermodynamic properties of uranium oxycarbides, 20: 16449
KANNO, Masayoshi, Oxidation behavior of Nb and Nb–V alloys, 20: 16982
KANNO, Masayoshi, Processing of uranium oxide fuel by oxidation-reduction cycle, 20: 16576
KAPLAN, Morton, Effects of angular momentum in decay of samarium compound nuclei, 20: 17784
KAPLIT, M., Electron emission from metals in vapors of Cs and F, 20: 17334
KAPOOR, N. K., Effect of uv radiation on the oxidation of certain Krebs cycle substrates, 20: 16198
KAPUR, Shobhay Laxmi, Ultrasonic velocity in aqueous solution of thorium nitrate, 20: 16477
KARASAWA, Takeshi, B-constant magnet pole design, 20: 17184 (CONF-650922, pp 239-47)
KARASAWA, Takeshi, Circular current shim for a cyclotron magnet, 20: 17187 (CONF-650922, pp 377-89)
KARASAWA, Takeshi, Field mapping by differential usage of Hall generators, 20: 17193 (CONF-650922, pp 472-5)
KARNAUKHOV, V. A., Proton emitters among Te isotopes, 20: 17687 (JINR-P-2514)
KAROL, I. L., Accumulation of ^{90}Sr and ^{137}Cs in soils of Leningrad region, 20: 16702
KAROL, I. L., Adsorption method of determining radon concentration in the air from an airplane, 20: 16708
KAROL, I. L., Appearance on the earth's surface of areas of increased concentrations of stratospheric radioactive products, 20: 16698
KAROL, I. L., Basis for using fibrous filter materials, (Petryanov filters), 20: 16653
KAROL, I. L., Chemical composition of atmospheric precipitation and fallout in vicinity of Leningrad, 20: 16704
KAROL, I. L., Determination of annual ^{90}Sr fallout in polar regions by recording ^{90}Sr content in seasonal layers of snow and ice, 20: 16703
KAROL, I. L., Dispersion of aerosols in global radioactive pollution of the atmosphere, 20: 16642
KAROL, I. L., Dispersion of radioactive aerosols in the stratosphere, 20: 16643
KAROL, I. L., Distribution of pollutants settling into lower layers of atmosphere, 20: 16652
KAROL, I. L., Effect of vertical-exchange intensity on the distribution of natural radioactive matter in the free atmosphere, 20: 16637
KAROL, I. L., Effect of advection on radioactivity distribution in the atmosphere, 20: 16638
KAROL, I. L., Effect of meteorological conditions on effectiveness of radioactive pollutant collection, 20: 16656
KAROL, I. L., Emission of radon from surface of some types of soils in European USSR and Kazakhstan, 20: 16691
KAROL, I. L., Estimate of the rate of formation of certain radioactive isotopes in the atmosphere, 20: 16689
KAROL, I. L., Fallout of ^{90}Sr and ^{137}Cs isotopes in vicinity of Leningrad in 1961-1963, 20: 16701
KAROL, I. L., Fluctuations in dispersed composition of radioactive aerosols in surface boundary layer of the atmosphere, 20: 16644
KAROL, I. L., Fluctuations in seasonal concentration of fission products in atmosphere surface layers over Moscow, 20: 16650
KAROL, I. L., Fractionation of radioactive products of nuclear explosion, 20: 16696
KAROL, I. L., Global distribution in the atmosphere and fallout of the radioactive products of nuclear explosions, 20: 16649
KAROL, I. L., Making the coefficients of aerosol collection by horizontal sheets more precise, 20: 16657
KAROL, I. L., Measurements of β activity of fission products, 20: 16707
KAROL, I. L., Methods of measurement of ultra-small α activities, 20: 16411
KAROL, I. L., Method for selecting cloud water samples using cyclone precipitators, 20: 16658
KAROL, I. L., Nature of accumulation of atmospheric aerosols on ocean surfaces, 20: 16706
KAROL, I. L., Observations of hot particles in surface boundary layer of atmosphere in Moscow region, 1961-63, 20: 16645
KAROL, I. L., Optimum conditions for measurements on radioactive preparations, 20: 16410
KAROL, I. L., Parameters of vertical exchange and average rate of aerosol removal by clouds, 20: 16639
KAROL, I. L., Planetary distribution of ^{210}Pb in free atmosphere, 20: 16641
KAROL, I. L., Problems in investigation of natural radioactivity of the atmosphere, 20: 16688
KAROL, I. L., Properties of fibrous filters in rarefied air, 20: 16654
KAROL, I. L., Radiation-sedimentation method for aerosol studies, 20: 16655
KAROL, I. L., Radioactive isotopes in atmosphere and their use in meteorology, 20: 16636
KAROL, I. L., Radioactivity of atmosphere over oceans and relationship to meteorological factors, 20: 16699
KAROL, I. L., Radioactive fallout in Vilnius in 1962, 20: 16700
KAROL, I. L., Radon as indicator of atmospheric stability, 20: 16694
KAROL, I. L., Radon concentration and vertical turbulent mixing in surface boundary layer of atmosphere, 20: 16692
KAROL, I. L., Seasonal and geographical changes in ^{210}Pb content of the atmosphere, 20: 16640
KAROL, I. L., Seasonal changes in radon and thorium concentration in surface boundary layer of atmosphere, 20: 16695
KAROL, I. L., Spectra of dimensions and mobility of natural radioactive aerosols in the atmosphere, 20: 16690
KAROL, I. L., Strontium-90 in fresh-water reservoirs of the Soviet Union in 1961-1962, 20: 16705
KAROL, I. L., Synoptic-climatic sketch maps of global stratospheric radioactive fallout, 20: 16697
KAROL, I. L., Variation in radon-concentration field in atmosphere in presence of sectors with nonhomogeneous exhalation values, 20: 16693
KAROL, I. L., Washout by precipitation of artificial radioactive aerosols from the atmosphere, 20: 16647
KAROL, I. L., Washout of fission products from the atmosphere, 20: 16648
KARPUSHKINA, E. I., Tables of cross sections of photoionization of the hydrogen atom, 20: 17251 (IAE-873)
KASATKINA, V. I., Appearance on the earth's surface of areas of increased concentrations of stratospheric radioactive products, 20: 16698
KASHTANOV, A. I., Dispersion fuel elements for nuclear reactors, 20: 18079
KASIDA, Y., Tritium measurement with liquid scintillation counter, 20: 16373
KASMAN, Yu. A., Critical scattering of polarized neutrons in nickel, 20: 17986
KASTRUP, H. A., Position operators, gauge transformations, and the conformal group, 20: 17577
KATHREN, R. L., Estimation of area enclosed by a fallout isoconcentration line, 20: 16664 (UCRL-14534, pp 19-22)
KATKIEWICZ, W., Optimalization of FET spectrometer stages working with semiconductor radiation detector, 20: 16806 (CLOR-44/D)
KATO, Kiyoo, Excitation of plasma oscillation by parametric resonance, 20: 17920
KATZ, Joseph J., Deuterated organisms: cultivation and uses, 20: 16165
KATZ, Lewis, Modification of structures of ternary oxides by cation substitution. I., 20: 16436
KAUFMANN, Richard L., Evidence for rapid motion of outer boundary of the magnetosphere, 20: 17541 (N-65-19719)
KAVANAGH, R. W., ^{3}He + p elastic scattering below 1 Mev, 20: 17771
KAWAHARA, F. K., Distribution of volcanic fallout in and about a one-story residence, 20: 16659 (AD-629527)
KAWAI, T., High-energy behavior of real part of scattering amplitudes and consequences from SU_3, 20: 17378
KAWAKATSU, H., Comment on "aberrations of focused beams of charged particles caused by space charge," 20: 16784
KAWATANI, Toyohiko, Influence of γ radiation on germination of Rauwolfia serpentina. II., 20: 16249
KAYE, S., Development of radiation-resistant solar cell, 20: 16910 (N-65-18448)
KAZACHKOVSKY, O. D., Fast power reactors, 20: 18097
KAZANSKAYA, A. P., Helium particles emitted during 17.5-Bev π-meson

collisions with photoemulsion nuclei, 20: 17716
KAZANSKAYA, A. P., Identification of single- and double-charge D particles by means of the δ-electron method, 20: 17358
KEBLER, R. W., Preparation and properties of superconducting Nb–Sn sandwiches, 20: 17649
KEEREETAVEEP, J., Energy spectrum of primary cosmic rays, 20: 17315
KEIL, R. A., Calculation of radiation dose resulting from natural and artificial radioactive isotopes in the ground by γ spectrometry, 20: 16687
KELER, E. K., Reactions of La and Nd oxides with oxides of Group II elements, 20: 16482
KELLER, C., Composition of transuranium elements, 20: 16543
KELLER, G. E., Ionic drift velocities and ion-molecule reactions in drift-tube mass spectrometer, 20: 17298
KELLEY, G. G., High-current ion-beam production and injection, 20: 17890 (ORNL-3908, pp 100-7)
KELLEY, M. A., Multiple spectrometer control by computer, 20: 16869
KELLEY, M. T., Controlled-potential polarography and coulometry as microanalytical techniques, 20: 16390
KELLEY, M. T., Determination of trace quantities of U, 20: 16389
KELLY, G. M., Nuclear spin relaxation in gallium metal, 20: 17995
KELLY, W. H., Levels of ^{85}Sr populated in decay of ^{85}Y and ^{85m}Y, 20: 17670 (AD-629576)
KEMOKLIDZE, M. P., Dynamics of a superfluid Fermi gas, 20: 17647
KEMPTER, C. P., Isothermal compressibility of UC, 20: 17062
KEMPTER, Charles P., Manganese carbides, 20: 17030 (LA-tr-66-1)
KERTZ, W., Ring current variations during the IGY, 20: 17544
KERWIN, Lorkin, 1001 reactions of the Ar and Kr ion doublets, 20: 17255
KERWIN, Robert Eugene, Osmotic and activity coefficients of some alkali halides in D_2O at 25°C, 20: 16488
KHAIKIN, M. S., Landau damping and resonance damping of magnetoplasma waves in bismuth, 20: 18011
KHAIRALLAH, A., Heterogeneity calculation for fast reactors by a perturbation method, 20: 18063
KHALATNIKOV, I. M., Dispersion of sound in superfluid helium, 20: 17611
KHALATNIKOV, I. M., Relaxation phenomena in superfluid helium, 20: 17640
KHAN, J. M., Microgram surface density measurements by observation of proton-produced x rays, 20: 17051
KHAN, R. M., Scattering of electromagnetic waves by plasma, 20: 17915
KHAN, T. P., Scattering of electromagnetic waves by plasma, 20: 17915
KHAN, Umar Hayat, Measurement of gross air activity (lower atmosphere) at Lahore, 20: 16683
KHANKINA, S. I., Low-frequency properties of semiconductor plasma in stationary electric field, 20: 18013
KHEIFETS, M. I., Electromagnetic radiation emitted during passage of a fast charged particle through a semiconductor, 20: 17494
KHELASHVILI, A. A., Scattering of a complex particle on the force center, 20: 17430 (JINR-P-2565)
KHERRMAN, E., New isotopes ^{157}Eu, ^{157}Ho, and ^{156}Er, 20: 17808
KHODYREVA, M. A., Penetration of ^{239}Pu through the skin, 20: 16183
KHOVRIN, S. K., Theoretical and experimental studies of water vapor plasma radiation, 20: 17936
KHOZE, V. A., Electromagnetic particle pair production, 20: 17499
KHRAPKO, R. I., Uniqueness of central-symmetric gravitational field in vacuum, 20: 17582
KIDO, Yasumasa, Contamination of ^{90}Sr in stock rainwater in lighthouses, 20: 16671
KIEFER, Hans, Instrument for simultaneous and separate measurement of α and β activity of radiating nuclei, 20: 16906
KIESEWETTER, W., Summary of working session on personnel dosimetry, Berlin, 11/64, 20: 16827 (SZS-9(1965))
KIKINDAI, Tivadar, Kinetics of ion exchange on zirconium phosphate, 20: 16568
KIKKAWA, K., Current-generated algebra and mass levels of the hadrons, 20: 17471
KIKUCHI, Ken, Survey of nuclear reactions induced by 57-Mev protons. II., 20: 17725
KILLENS, Richard, Changes in thyroid ^{131}I activity in ozone-tolerant and ozone-susceptible rats, 20: 16190
KIM, Young S., Polarization of Σ⁰ particles in reaction $\pi^- + p \rightarrow K^0 + \Sigma^0$ at 1.5 and 1.8 Bev/c, 20: 17382
KIMELDORF, D. J., Effects of various gases within nasal cavities of rats on response of olfactory bulb neurons to x irradiation, 20: 16215 (AD-628443)
KIMELDORF, Donald J., Humoral mediation of radiation-induced motivation in parabiont rats, 20: 16284
KINELL, Per-Olof, ESR absorption of hexane/silica gel systems γ irradiated at low temperatures, 20: 16511
KING, H. T., Radiological environmental survey manual, 20: 18083 (CVNA-63)
KING, R. W., Boson masses, 20: 17393
KIRICHENKO, L. V., Radioactive isotopes in atmosphere and their use in meteorology, 20: 16636
KIRICHENKO, L. V., Variation in radon-concentration field in atmosphere in presence of sectors with nonhomogeneous exhalation values, 20: 16693
KIRILLIN, A. V., Experimental determination of argon plasma heat-conductance factor, 20: 17937
KIRILLIN, V. A., Thermodynamic properties of Nb at temperature range from 0°K to melting point, 2740°K, 20: 17100
KIRILLOVA, L. F., Real part of pp elastic scattering amplitude at 2, 4, 6, 8 and 10 Bev, 20: 17417
KIRILLOVA, L. F., Real part of pn scattering amplitude at 2 to 10 Bev, 20: 17363
KIRILYUK, A. L., Influence of VVR-M active zone configuration on neutron spectra from horizontal channel, 20: 18140
KIRYUTIN, A. A., Critical thermal fluxes in forced motion of MIPB–benzol, 20: 16614
KIRZ, James, Analysis of the B enhancement, 20: 17402
KISLYI, P. S., Preparation of zirconium diboride, 20: 17085
KISS, A. E., Measurement of quantum efficiency of scintillation counters for x rays, 20: 16836
KISTNER, G., Appearance of activation products from neutron explosions in food (^{54}Mn), 20: 16167
KISTNER, O. C., Decay of ^{108m}Ag, 20: 17786
KITZ, A., Density of energy states in light nuclei, 20: 17745
KIYAMA, Satoru, Excitation of plasma oscillation by parametric resonance, 20: 17920
KLAR, H., New approach to potential scattering. I., 20: 17490
KLAR, H., New approach to potential scattering. II., 20: 17491
KLECZKOWSKI, A., Proper use of short-wavelength reversal of uv light inactivation of nucleic acids, 20: 16207
KLEIN, Abraham, Number-conserving approximation for theory of pairing interaction in nuclei, 20: 17765
KLEIN, F. S., Synthesis and isotopic analysis of $CH_3{}^{18}OH$ and $CH_3{}^{17}OH$, 20: 16547
KLEINBAUER, Karel, Possibility of absolute measurements of radioisotope activity using scintillation γ spectrometry, 20: 16858
KLENER, Vladislav, Loss of an emitter in defectoscopic field work, 20: 16764
KLIMA, R., High-frequency heating of low-pressure plasma, 20: 17909
KLIMAN, G. B., Terminal properties of Alfven waveguides, 20: 17522
KLIMOVA, E. N., Disturbance of conditioned reflex activity in chronic action of ^{90}Sr, 20: 16266
KLODT, Donald T., Prog. rpt. on phase equilibria of Ta-rich region of Ta–W–Hf and Ta–W–Zr systems, final, 9/64–11/65, 20: 17012 (DRI-1092-226)
KLOKHOLM, E., Superconducting composite Sn and Au films, 20: 17601
KLOOSTERZIEL, H., Kinetic protium–deuterium isotope effect in intramolecular 1-5 shift of hydrogen, 20: 16503
KLOTZ, Paul, Synergistic effect of tri-n-octylamine on solvent extraction of Am by TTA, 20: 16571
KLUG, H., Phagocytosis of radiation-injured lymphocytes in thymus of rats, 20: 16293
KLUSMANN, Arno, Possibility of radiological hydrogen determination in solids, especially in coals, 20: 16356
KLYUCHAREV, A. P., Deuteron and α-particle pickup in interaction between ^{10}B and ^{16}O, 20: 17815
KNAPP, H. A., Magnitude and distribution of weapon effects for design of shelters for protection against fallout, 20: 16620 (AD-624370)
KNAUER, W., Diocotron instability in plasmas and gas discharges, 20: 17916
KNEZEVIC, Z. V., Determination of D_2O content in water by infrared spectrometry, 20: 16377
KNIGHT, B., Effect of temperature on γ radiolysis of water vapor, 20: 16536
KNOBELOCH, G. W., Symmetry of neutron-induced ^{239}Pu fission in resonance region, 20: 17858
KNOENER, R., Heat transfer in boiling hydrogen, neon, nitrogen, and argon, 20: 16610
KNOTIK, K., Reprocessing of graphite-carbide fuel for high-temperature reactors, 20: 16575
KNOWLES, D. J., Steam condensate β-γ monitor at fission products lab, 20: 16825 (ORNL-TM-1442)
KNOX, J. M., Effect of uv exposure on succinic dehydrogenase activity, 20: 16196
KOBAYASHI, Masao, Breeding of medicinal plants exposed to γ irradiation. I., 20: 16290
KOBAYASHI, Setsuo, Fuel rod scanner for reactor power density distribution measurement, 20: 18025
KOBAYASHI, Toshio, Radiation osteitis and colitis from radiotherapy, 20: 16322
KOBAYASHI, Yoshii, Electrodeposition of Ru from Ru(III) and Ru(IV) solution and a fission-product solution, 20: 16563
KOBZEV, V. A., Effects of cascade process on yield of energetic He isotopes, 20: 17713
KOCH, R. O., Measurement of radioactivity in effluents of a gas

chromatograph, 20: 16371
KOCH, S., Sensitivity and accuracy of measurements in quantitative analyses by means of β backscattering, 20: 16378
KOCHENOV, A. S., Comparison of theoretical and experimental parameters for homogeneous uranium–water critical assembly, 20: 18053
KOCHERGIN, S. M., Effective decontaminating solutions to remove ^{60}Co from Duralumin and steel-3 by ultrasonic cleaning, 20: 16767
KOCHERZHINSKII, Yu. A., Phase diagrams of systems $NbCr_2$–$TiCr_2$ and $NbCr_2$–Ti, 20: 17091
KOCHOWSKI, C., $\pi^+ p$ interactions at 1.6 Bev, 20: 17374
KOCKUM, J., Unscrambling of proton-recoil spectra, 20: 16875
KODAIRA, Kiyoshi, Cesium-137 in Japanese soil and rice, 20: 16169
KOHLBERG, I., Development of improved land-surface fallout model, 20: 16735 (TO-B-65-99)
KOHLSCHUETTER, V., Peptization of solid thorium oxide, 20: 16419 (UCRL-Trans-1301(L))
KOHN, Sidney I., Radioactive material in teeth of children in northern New Jersey area, 20: 16763
KOICKI, A., Gamma-gamma angular-correlation study of ^{169}Tm in lutetium iron garnet, 20: 17994
KOICKI, S., Gamma-gamma angular-correlation study of ^{169}Tm in lutetium iron garnet, 20: 17994
KOIKE, Masahiro, Electrical detection system for broad-range magnetic analyzer, 20: 16859
KOK, L. P., Phenomenology of nuclear forces. I., 20: 17727
KOK, L. P., Phenomenology of nuclear forces. II., 20: 17728
KOLLTVEIT, Kristofer, Stripping reactions A(d,n)(A + 1), 20: 17704
KOLM, Henry H., Closed-loop cooling system for superconducting bubble chamber magnets, 20: 17595 (CONF-650922, pp 611-14)
KOLOMEYETS, E. V., Effects of small flares in hard component of cosmic rays of magnetically quiet and disturbed days, 20: 17313
KOLONTSOVA, E. V., Structural changes in neutron irradiated α-quartz, 20: 17149
KOMPANEETS, A. S., Quantum electrodynamics with two fermions, 20: 17581
KONONENKO, Y. I., Bremsstrahlung in infrared region from plasma of electrodeless induction discharge, 20: 17931
KONOVALOV, E. A., Tangential channels and construction of thermal column in VVR-M reactor, 20: 18139
KONRADI, Andrei, Evidence for rapid motion of outer boundary of magnetosphere, 20: 17541 (N-65-19719)
KON'SHIN, V. A., Fission cross sections of ^{181}Ta, Re, Pt, ^{197}Au, Pb, Bi, Th, ^{235}U and ^{239}U for protons at 150 to 660 Mev, 20: 17838
KONTOS, J., Pattern generator, 20: 16881
KOPPEL, J. U., Slow neutron spectra in molecular hydrogen at low temperatures, 20: 17664
KOPVILLEM, U. Kh., Inertial echo and coherent gravitational waves, 20: 17567
KORABLEV, L. V., Quasilinear theory of current instability in a plasma, 20: 17950
KORNILOV, I. I., Diffusion of nickel into solid solutions of intermetallic compounds of Ni_3Nb and Ni_3Ta, 20: 17089
KOROBEINIKOVA, V. G., Investigation of Cr–Fe–Mo and Cr–Fe–W alloys, 20: 17093
KOROBKIN, V. V., Illumination of a bubble chamber by means of a ruby laser, 20: 16841
KOROES, Endre, Solvent effect in isotope exchange reactions. III., 20: 16502
KOROLKOV, V. S., Fine structure of spectra of Eu coordination compounds of MX_3 type. I., 20: 16467
KOROSIN, J., Determination of Cd in U compounds by atomic absorption spectrophotometry, 20: 16368
KOSHURNIKOVA, N. A., Use of γ spectrometry for determination of Pu in the living organism, 20: 16864
KOSKI, W. S., Reaction of hydrogen atoms with some conjugated ring systems at 77°K, 20: 16524
KOSTIC, Lj., Effect of native isologous DNA on incorporation of thymidine-^3H into uv-irradiated L-strain cells, 20: 16279
KOSTIKOV, Yu. I., Radiometric properties of large liquid scintillation counter, 20: 16865
KOSTIN, M. D., Energy distribution of energetic atoms in an irradiated medium. II., 20: 17257
KOTLENSKY, W. V., Analysis of high-temperature creep in pyrolytic carbon, 20: 17017 (JPL-TR-32-889)
KOTTOWSKI, H., Study of liquid metal boiling under forced convection, 20: 16608 (ANL-Trans-257)
KOVACIC, D. L., Infrared spectra of rare earth metal chloride complexes of 2,2'-bipyridyl and 1,10-phenanthroline, 20: 16437
KOVALENKO, G. S., Photometric determination of Np by means of xylenol orange, 20: 16408
KOVALENKO, V. G., Effect of meteorological conditions on effectiveness of radioactive pollutant collection, 20: 16656
KOVALEVA, E. S., Crystalline structure of $Cs_2[UO_2Br_4]$, 20: 16484
KOVANIC, P., Static programming of data handling, 20: 18121
KOVBASYUK, V. I., Singularities of MGD generator performance at large Hall numbers, 20: 17332
KOVENSKII, I. I., Mobility of atoms in a Mo–W alloy, 20: 17101
KOVRIZHNYKH, L. M., Interaction between electron beams and a non-isothermal plasma and the nonlinear stabilization of beam instability, 20: 17951
KOWALEW, A., Salt-boiling fast reactor "SAWA", 20: 18088 (INR-699/C)
KOYAMA, Kenichi, Inductively coupled a-c MHD electrical power generator, 20: 17330
KOYANAKA, Yoshio, Separation of fission products by flotation method, 20: 16392
KOZLOV, A. N., Possibility of super-thermal conductivity in semiconductors, 20: 18014
KRAAK, W., Reprocessing studies at Kjeller, 20: 16569
KRAMER, G., Application of spectral representations to nonrelativistic and relativistic Bethe-Salpeter equation, 20: 17425 (DESY-66/1)
KRAMER, G., Influence of absorption on peripheral photoproduction of vector mesons, 20: 17414
KRAMER, H. H., Prog. rpt. on research in activation analysis, 8/63–10/64, 20: 16336 (NYO-10175)
KRAMER, P., 90°Superconducting bending magnet for 30-Mev protons, 20: 17197 (CONF-650922, pp 536-40)
KRAMER, W. C., Tungsten–rhenium alloy thermocouples and use in UO_2-fueled reactor, 20: 16942 (ANL-6981)
KRANER, Hobart W., Lithium-drifted Ge detectors, applications to neutron-activation analysis, 20: 16888
KRASNOPEVTSEV, Yu. V., Radioactive isotopes in atmosphere and their use in meteorology, 20: 16636
KRASNOPEVTSEV, Yu. V., Radioactivity of atmosphere over oceans and relationship to meteorological factors, 20: 16699
KRASOVITSKII, V. B., Nonlinear theory of beam instability under conditions of the anomalous Doppler effect, 20: 17533
KRAUS, W., Summary of working session on personnel dosimetry, Berlin, 11/64, 20: 16827 (SZS-9(1965))
KRAUSE, H., Decontamination of radioactive wastes of Karlsruhe nuclear research center from 1963 to 1965, 20: 18171
KRAUSE, M. O., Atomic and molecular cross sections, 20: 17253 (ORNL-3908, pp 90-9)
KRAUSE, Siegfried, Electric arc in a supersonic plasma jet, 20: 17904
KRAUT, A., How are physical equations treated?, 20: 17160
KRESIN, V. Z., Jump in specific heat on going from superconducting to normal state, 20: 17612
KRESNIN, A. A., Theory of diffraction scattering of particles by complex nuclei, 20: 17816
KRIEGE, Owen H., Analysis of rare earth sulfides, selenides, and tellurides, 20: 16395
KRIEN, K., Lifetime of the $^{25}/_2$ three-particle state of ^{177}Hf, 20: 17811
KRIMIGIS, S. M., Observation of ~500-kev protons in interplanetary space with Mariner IV, 20: 17318
KRINBERG, I. A., Effects of ionization reactions on plasma thermal conductivity, 20: 17940
KRINSKY, Norman I., Carotenoid pigments of a radiation-resistant Micrococcus species, 20: 16161
KRIPYAKEVICH, P. I., New compounds of rare earths with Mn and Fe, and their crystal structures, 20: 17096
KRISHNA MURTI, G. S. R., Airborne radioactivity at Delhi, 20: 16680
KRIVIT, William, Hyperbaric oxygen, whole-body x irradiation, and cyclophosphamide combination therapy in mouse leukemia, 20: 16262
KRONLUND, Kenneth H., Effect of nuclear-reactor operation in space, 20: 18131
KROT, N. N., Photometric determination of Np by means of xylenol orange, 20: 16408
KROUSE, H. R., Isotopic mass dependence of Li diffusion in rutile, 20: 17052
KRUEGER, H., New approach to potential scattering. I., 20: 17490
KRUEGER, H., New approach to potential scattering. II., 20: 17491
KRUSE, F. W. Jr., Precision current of field-regulated power supplies, 20: 16773 (CONF-650922, pp 779-87)
KRUTIKOV, I. E., Neutrons and kinetic energy of fragments in fission of heavy nuclei, 20: 17867
KSHIRSAGAR, S. G., Discrimination between Sr and Ca in bone and transfer from blood to bone, 20: 16178
KUDINOV, N. N., Naval nuclear power installations, 20: 18132
KUDO, Ken-ichi, Catalytic tritium exchange reactions with tritiated active methylene compound, 20: 16492
KUDRYAVTSEVA, A. V., New isotopes ^{157}Eu, ^{157}Ho, and ^{156}Er, 20: 17808
KUHLMANN, W. R., Arrangement for position and energy determination with semiconductor detectors, 20: 16878
KUHLMANN, W. R., Position-sensitive counter, 20: 16880
KUHLMANN, W. R., Pulse-division circuit, 20: 16879
KULAGIN, S. G., States with population inversion in a self-compressed

discharge, 20: 17924
KULESSA, R., g-Factor of 87-kev excited state in ^{155}Gd, 20: 17683 (INP-430/PL)
KULIKOV, O. F., Method of investigating betatron oscillation resonances, 20: 17221
KULIKOVA, A. O., Continuous transition between structural types α–$ThSi_2$ and α–$GdSi_2$ in homogeneity region of $LaSi_2$, 20: 17042
KULLANDER, S., Quasi-free proton-proton scattering in light nuclei at 460 Mev, 20: 17741
KULUNDZIC, Predrag, Improvement of heat transfer of fuel element with polyzonal spiral finning, 20: 18078
KUMAGAI, Hiroo, B-constant magnet pole design, 20: 17184 (CONF-650922, pp 239-47)
KUMAR, Aditya, Effect of dipion resonances on π-N scattering amplitude, 20: 17388
KUMATORI, Toshiyuki, Medical survey of Japanese exposed to fallout radiation in 1954, 20: 16226 (NP-15891)
KUNDU, S. K., Vector-scalar fields and renormalization, 20: 17465
KURBATOV, I. M., Optimum control of a nuclear reactor by thermal processes, 20: 18054
KURDIANI, N. I., Electrical properties of InSb irradiated by neutrons at 77°K and by electrons at 300°K, 20: 17150
KURGANSKAYA, V. M., Radioactive isotopes in atmosphere and their use in meteorology, 20: 16636
KURILKO, V. I., Nonlinear theory of beam instability under conditions of the anomalous Doppler effect, 20: 17533
KURITA, Susumu, Magneto-optical experiments with superconducting magnet, 20: 17588 (CONF-650922, pp 525-9)
KURODA, P. K., Fallout from nuclear explosion of October 16, 1964, 20: 16663 (TID-21470)
KUSTOM, R. L., Large spark chamber magnet with tape-wound coils, 20: 16809 (CONF-650922, pp 253-61)
KUT'IN, V. M., Search for $\pi^0 \to 3\gamma$ decay, 20: 17340 (JINR-P-2322)
KUVIK, Vilius, New principle of activation-analysis separations. X., 20: 16396
KUZENKOVA, M. A., Preparation of zirconium diboride, 20: 17085
KUZHEVSKII, B. M., Dependence of chemical composition of cosmic rays on nature of their motion in the galaxy, 20: 17324
KUZIN, I. A., Uranium sorption by platinized carbon, 20: 16581
KUZMA, Yu. B., Phase equilibrium in ternary Zr–Co–C and Nb–Fe–C systems, 20: 17086
KUZ'MINOV, B. D., Angular anisotropy and mass asymmetry of ^{232}Th fission fragments, 20: 17869
KUZ'MINOV, B. D., Multi-parameter investigations of fast fission fragments, 20: 17868
KUZNETSOV, G. I., A remark on the many-dimensional Coulomb problem, 20: 17252 (JINR–P–2522)
KUZNETSOV, V. G., Crystalline structure of $Cs_2[UO_2Br_4]$, 20: 16484
KUZNETSOVA, V. V., Fine structure of spectra of Eu coordination compounds of MX_3 type. I., 20: 16467
KYRS, M., Stability constants of complexes from non-equilibrium distribution of metal between aqueous phase and ion exchanger, 20: 16481

L

LA, S. Y., Wave functions for F′ centers in alkali halides, 20: 17977 (NYO-2047-36, App.2)
LACOMBE, Paul, Plastic deformation of polycrystalline uranium, by straining at various rates, between 20 and 850°C, 20: 17039
LACOUR, J., Fast period meter with integrated circuits, 20: 18029
LADANYI, Laszlo, Solvent effect in isotope exchange reactions. III., 20: 16502
LAGERWALL, Torbjoern, Diffusion and capture of Ar in neutron-irradiated CaF_2, 20: 17804
LAGERWALL, Torbjoern, Neutron cross sections for some threshold reactions, 20: 17809
LAGOMARSINO, Raymond J., Prog. rpt. on radiochemical analyses of filter samples collected under Project Stardust, 1964, 20: 16728 (HASL-169)
LAGOMARSINO, Raymond J., Prog. rpt. on radiochemical analyses of filter samples collected under Project Stardust, 1963. Appendix, 20: 16727 (HASL-168)
LAI, C. S., $p\bar{p}$ Annihilation into two mesons, 20: 17377
LAJTAI, A., Angular distribution of γ rays from fission of ^{235}U, 20: 17829
LAKIN, R. W., Personnel alarm dosimeter LE 14507-1, 20: 16831 (UCRL-14534, pp 28-31)
LAL, Krishan, Diffusion of cerium and lanthanum in magnesium, 20: 17038
LAM, C. S., Operator and generalized gauge transformations in quantum electrodynamics, 20: 17446
LAMATY, G., Secondary deuterium isotope effect in addition reactions on carbonyl compounds, 20: 16555
LAMB, E., Aluminosilicate ion exchanger for recovery and transport of ^{137}Cs from fission-product wastes, 20: 16578
LAMB, Lawrence E., Aerospace medicine, 20: 16745
LAMB, William H. Jr., Search coil measurements of the harmonic content of beam transport magnets, 20: 17195 (CONF-650922, pp 487-96)
LAMBERT, M., Observations of primary defects in crystals of LiF irradiated with thermal neutrons at 77°K, 20: 18007
LAMBERT, M., Optical observation of interstitial Li in irradiated LiF, 20: 17143
LAMORRE, Yves, Preparation of α and β anomers of deoxy-2′ adenosine, labeled with ^{14}C, 20: 16545
LAMPORT, James E., Cosmic-ray telescope for Mariner-Mars mission, 20: 16822 (N-65-19927)
LANCUCKI, C. J., Device for reducing the radiation hazard in x-ray diffractometry, 20: 16782
LANDGREBE, A. R., Removal of radiostrontium from milk with tricalcium phosphate and resulting changes in milk composition, 20: 16382
LANDIS, D. A., Mass of ^8He from the four-neutron transfer reaction $^{26}Mg(\alpha,^8He)^{22}Mg$, 20: 17794
LANE, Nancy J., Effects of arginine deprivation, uv, and x radiation on cultured KB cells, 20: 16258
LANE, R. C., Measurement of critical mass of enriched U in reflectors of wood, concrete, polyethylene, and water, 20: 16721 (AWRE-NR-1/66)
LANG, David V., Fine structure in energy spectra of electrons from gases bombarded by positive ions, 20: 17292
LANGE, E. A., Analysis of Ti–7Al–2Nb–1Ta and Ti–6Al–4V fractures, 20: 16967 (AD-628277)
LANGE, Gerald, High-energy fission of ^{238}U, 20: 17790
LANGHAM, W. H., Neutron activation of sulfur in hair, application in a nuclear accident dosimetry study, 20: 16758
LANGMANN, H.-J., Preparation and study of thick depleted surface-barrier detectors, 20: 16818 (KFK-328)
LANTELME, Frederic, Diffusion, electrical mobility, and ionic interactions in molten salts, 20: 16414 (CEA-R-2806)
LA PATRA, J. W., Radiation measurement utilizing communication theory, 20: 16893
LAPIDUS, Gabriel, Reversing hydrogen isotope effect on rate of gas phase decomposition of oxalic acid, 20: 16455
LAPINS, K., Compact mutants of Lambert cherry produced by ionizing radiation, 20: 16244
LAPOSTOLLE, Pierre, Particle accelerators, 20: 17226
LARI, R. J., A precision system for measuring wire trajectories in magnetic fields, 20: 17196 (CONF-650922, pp 497-504)
LARI, Robert J., Search coil measurements of the harmonic content of beam transport magnets, 20: 17195 (CONF-650922, pp 487-96)
LAROCCI, E., Isotropic monogap chamber pulsed with damped oscillation, 20: 16886
LARSEN, Lis Olesen, Hormonal dependency of molting in amphibians, 20: 16252
LARSEN, Ole Steen, Static electricity in anesthetic flowmeters eliminated by radioactive pistol, 20: 16783
LARSEN, W. L., Phase studies of high-Nb-content Nb–Zr–O alloys, 20: 16980
LASKORIN, B. N., Extraction of uranium(VI) with D2EHP and MLPA from H_3PO_4 solutions, 20: 16579
LASKORIN, B. N., Uranium and Th extraction from H_3PO_4 solutions by acid and neutral alkylphosphorus compounds, 20: 16580
LASSETTRE, E. N., Test of low-energy limit of the Born approximation, 20: 17258
LATYSHEV, G. D., Automatic physical measurements with magnetic β spectrometers, 20: 16854
LATYSHEVA, V. I., Phase diagrams of systems $NbCr_2$–$TiCr_2$ and $NbCr_2$–Ti, 20: 17091
LATZKOVITS, Laszlo, Kinetics and mechanism of isotopic exchange reactions on surface of solid catalysts. I., 20: 16460
LAUNOIS, M., Modulated gain detectors and digital data storage unit to record pulsed reactor excursions, 20: 18028
LAURENCE, James C., Design, construction, and performance of cryogenically cooled and superconducting electromagnets, 20: 17592 (CONF-650922, pp 574-87)
LAUTERJUNG, K. H., Arrangement for position and energy determination with semiconductor detectors, 20: 16878
LAUTERJUNG, K. H., Position-sensitive counter, 20: 16880
LAVERICK, C., Experiments with superconducting cable, 20: 17591 (CONF-650922, pp 560-7)
LAVIOLETTE, P., Action of ^{60}Co γ rays on mortality and fertility of the rice weevil, 20: 16243
LAWROSKI, Stephen, Reactor Fuel Processing, Vol. 8, No. 4, 20: 16582
LAZARENKO, L. O., Polarization coefficients in photoproduction reactions of pseudoscalar particles on a nucleon, 20: 17407
LAZAREVA, T. P., Helium particles emitted during 17.5-Bev π-meson collisions with photoemulsion nuclei, 20: 17716
LAZAREVA, T. P., Production of high-energy fragments by 7.5-Bev π mesons, 20: 17715
LAZZARINI, E., Distribution of some fission products between core and

recombiner of L54M reactor. V., 20: 18142
LEA, R. M., Pion production in $p\bar{p}$ annihilations at 3.3 and 3.7 Bev/c, 20: 17385
LEACH, J. S. Llewelyn, Corrosion of Zr and Zy-2 at low temperatures, 20: 16979
LEBAS, Jeanne Marie, Infrared spectrometric study of phenylmethanes, 20: 16498
LEBEDEV, B. I., Experimental radiation sickness induced with ^{210}Po, 20: 16268
LEBEDEV, N. A., New isotopes ^{157}Eu, ^{157}Ho, and ^{156}Er, 20: 17808
LEBEDEV, V. I., Neutrons and kinetic energy of fragments in fission of heavy nuclei, 20: 17867
LE BLANC, M. A. R., Pattern of current flow in nonideal type-II superconductors in longitudinal magnetic fields. I., 20: 17617
LECIEJEWICZ, Janusz, Neutron-diffraction investigation of iron–tungsten carbides, 20: 17015 (INR-665/II/PS)
LE COUVIOUR, M., Comparison of effects of mutagenic substances by studying mutagenesis of plants, 20: 16225 (EUR-2715.f)
LEE, Chul, Improved method for determination of Sc by neutron-activation analysis, 20: 16383
LEE, T. D., Possible tests of C_{st} and T_{st} invariances, 20: 17392
LEE, Y. C., Hard-core potential and boundary-condition model for nuclear matter, 20: 17772
LEHMANN, A., Use of beta radiations (^{90}Sr–^{90}Y) in dermatology, 20: 16325
LEHMANN, Frank-Guenter, Influence of whole-body x irradiation on enzymatic activity of lactate dehydrogenase isoenzymes, 20: 16289
LEHR, Pierre, Behavior of Cu during CO_2 oxidation of Zr–Cu alloys, 20: 16977
LEIGHTON, Stuart A., Preparation of radioactive metallic specimens for replication, 20: 17128 (ORNL-TM-1161, pp 194-207)
LEITER, Edgar, Measurement devices for nuclear reactors, 20: 18022
LEITNER, J., K^--p interaction at 2.24 Bev/c, 20: 17383
LEJEUNE, S., Influence of self-absorption on absolute measurement of Moessbauer fraction, 20: 17990
LEMONNE, J., Production of hyperfragments from the interactions of of 3.0- and 5.0-Bev/c K^- mesons with emulsion nuclei, 20: 17752
LENEL, F. V., Kirkendall-effect densification in sintered W–Mo powder compact, 20: 16994
LENEL, Fritz V., Prog. rpt. on studies of sintering, annual, 1965, 20: 16992 (RPI-2409-4)
LEO, Micah W. M., Prog. rpt. on radiochemical analyses of filter samples collected under Project Stardust, 1964, 20: 16728 (HASL-169)
LEONCHUK, M. P., Optimum control of a nuclear reactor by thermal processes, 20: 18054
LEONE, J. A., Reaction of hydrogen atoms with some conjugated ring systems at 77°K, 20: 16524
LEONG, G. F., Recovery from radiation injury in dogs as evaluated by the split-dose technique, 20: 16216 (AD-628791)
LEONTOVICH, A. M., Illumination of a bubble chamber by means of a ruby laser, 20: 16841
LERCHE, I., Synchrotron radiation from a primary cosmic ray, 20: 17314
LE RIGOLEUR, C., Measurement of capture cross section of Na between 10 and 135 kev, 20: 17718
LEROY, J. L., Measurement of capture cross section of Na between 10 and 135 kev, 20: 17718
LEROY, Jean-Marie, Uranium semipentoxide, 20: 16430
LESNIAK, Ch., Slip casting of powdered carbides, 20: 16997
LETARDI, T., Isotropic monogap chamber pulsed with damped oscillation, 20: 16886
LEV, I. E., Photometric determination of Ce in simple and stainless steel, 20: 16380
LEVAY, Bela, Use of liquid scintillators for measurement of isotopes emitting soft β radiation. III., 20: 16862
LEVAY, Bela, Use of liquid scintillators for measurement of isotope emitting soft β radiation. IV., 20: 16863
LEVEQUE, A., Information processing for high-energy corpuscular physics experiments, 20: 16838
LEVEQUE, Paul, Tritium activity of basin pouring from Mont Cenis, 20: 16668
LEVIN, Sheldon G., Output of self-rectified dental x-ray machines, 20: 16844
LEVINE, Melvin M., Monte Carlo methods in resonance absorption, 20: 18046 (BNL-9644)
LEVITIN, R. Z., Magnetostriction of rare earth metals in paramagnetic, antiferromagnetic and ferromagnetic regions, 20: 18012
LEVITMAN, M. Kh., Influence of ^{35}S on growth of bones, 20: 16267
LEVY, Viviane, Diffusion of cerium and lanthanum in magnesium, 20: 17038
LEVY-LEBLOND, Jean-Marc, 3-Particle nonrelativistic kinematics and phase space, 20: 17351 (N-65-19396)
LEVY-NAHAS, Monique, 3-Particle nonrelativistic kinematics and phase space, 20: 17351 (N-65-19396)
LEWIN, C., π^+ p interactions at 1.6 Bev, 20: 17374
LEWIN, G., Reemission of ionically pumped H_2 and He from a stainless steel surface, 20: 17922
LEWINS, J., Reactor optimization, 20: 18074
LEWINS, J., Variational principle for ratios in critical systems, 20: 18059
LEWIS, R. A., Photoproduction cross sections for π^+ and K^+ mesons at 3.4 to 4.0 Bev and comparison with SU(3), 20: 17400
LEWIS, R. E., Aluminosilicate ion exchanger for recovery and transport of ^{137}Cs from fission-product wastes, 20: 16578
LEWIS, R. E., Device for reducing the radiation hazard in x-ray diffractometry, 20: 16782
LEWIS, R. W., Analysis of Be metal and its compounds by optical emission spectrography, 20: 16352
LEWIS, S. M., Hematological complications of polycythemia vera and treatment with radioactive phosphorus, 20: 16241
LIBERMAN, Irving, Doping of crystals by ion bombardment, 20: 17151
LIBURG, M. Yu., Method of obtaining super-low temperature based on a dissolution of ^3He in ^4He, 20: 17599 (JINR-P-2480)
LICHTENBERG, D. B., Coupled-channel Schroedinger-equation model for high-energy peripheral collisions, 20: 17397
LICHTMAN, S., K^--p interaction at 2.24 Bev/c, 20: 17383
LIEBENBERG, D. H., Cryogenic evaluation laboratory test of cryogenic low-pressure coupling, 20: 16588 (LA-3454)
LIEBENBERG, Donald H., Quantitative analysis of ^3H by gas chromatography, 20: 16348
LIEMOHN, H. B., Partial electron velocity spectra from cyclotron absorption of Whistler power, 20: 17558
LIESER, K. H., Cation exchange and adsorption of radionuclides on glass surfaces, 20: 16469
LIGHTBODY, J. W., Measurements of ion-optical properties of high-resolution spectrometer for electron scattering, 20: 16808 (CONF-650922, pp 154-63)
LIKHACHEV, M. F., Designs of gaseous threshold and differential Cherenkov counters, 20: 16816 (JINR-P-2528)
LIKHACHEV, V. M., States with population inversion in a self-compressed discharge, 20: 17924
LINCKE, R., Determination of atomic-resonance line-oscillator strengths, 20: 17932
LINDEKEN, C. L., Effect of variation of airborne radon daughter concentration on whole-body counter background, 20: 16665 (UCRL-14534, pp 23-7)
LINDEKEN, C. L., Removal of C dust from high-speed printer, 20: 16740 (UCRL-14534, pp 50-3)
LINDEMAN, H., Counting characteristics of G-M counters at higher intensities, 20: 16884
LINDGREN, I., Hyperfine structure of 16-hour state in ^{119}Te, 20: 17705
LIPKIN, H. J., Spin independence, W spin, parity, and SU(6) symmetry, 20: 17475
LIPSCHUTZ, Michael E., Canyon Diablo meteorite, 20: 17238
LIPTAI, R. G., Phase diagram of Pu at pressures up to 75 kbar, 20: 17061
LISAGOR, W. Barry, Oxidation-resistant coatings on Nb–10Ti–5Zr alloy sheet at 2000, 2400, and 2700°F, 20: 16973 (NASA-TN-D-3275)
LISTER, D., Elastic scattering of neutrons from carbon and oxygen at 3.0 to 4.7 Mev, 20: 17767
LITOMISKY, Miroslav, Equipment for measuring superconducting properties of superconductors for strong magnetic fields, 20: 17602
LITTING, B. G., Role of non-destructive testing in manufacture of welded and clad pressure vessels, 20: 16617
LITTLE, J. C., Y-12 clean room facilities, 20: 16744 (Y-EA-49)
LITVIN, D. F., Deformed Zr–Ti–O–Fe alloy for high-pressure chambers, 20: 17003
LIVINGOOD, John, Neoplasms following irradiation of the head, 20: 16245
LIVINGSTON, Peter M., Methods of quadrature for Euler transform integrals, 20: 16937
LLOYD, Elizabeth, Discrimination between Sr and Ca in bone and transfer from blood to bone, 20: 16178
LLOYD, Lowell T., Thermal expansion of alpha uranium, 20: 17064
LOBASHOV, V. M., Possibility of investigating weak N-N interactions, 20: 17413
LOBASHOV, V. M., Search for parity nonconservation in nuclear γ transitions, 20: 17444
LOBODZINSKA, Maria, Studies on viruses of asiatic influenza. III., 20: 16239
LODDE, G. M., Changes in ^{137}Cs retention and routes of elimination as effected by external factors, 20: 16180
LODDING, A., Inter-diffusion of Li isotopes in liquid lithium metal, 20: 17104
LOESCH, P. J. Jr., Effect of mutated background genotype on mutant expression in Arachis hypogaea, 20: 16247
LOEVINGER, R., Design and operation of extrapolation chamber with removable electrodes, 20: 16852
LOEWENTHAL, John, Irradiation injury to the colon, 20: 16309
LOGAN, W. L., An improved method of Rossi oscillator-oscilloscope

coupling, 20: 16776 (EGG-1183-1156)
LOHMANN, Wolfgang, Advances in radioisotope instrumentation, 20: 16855
LOMBARD, David B., Potential application of nuclear explosives for recovery of oil from shale, 20: 16589 (UCRL-12224-T)
LOMMATZSCH, P., Possibilities of β therapy of tumors of the eye, 20: 16305
LONDON, G. W., K⁻-p interaction at 2.24 Bev/c, 20: 17383
LONER, Charles John, Reactions of hydrocarbons with deuterium on chromium oxide gel, 20: 16487
LONG, David M., Transient radiation response of insulated gate field-effect transistors, 20: 16913
LONG, E. L. Jr., Evaluation and irradiation effects studies on pyrolytic-carbon-coated fuel particles, 20: 17127 (ORNL-3923)
LONGLEY, William W. Jr., Cold-cathode magnetron gage characteristics, 20: 16788
LONTAI, Laszlo M., 100-Kilogauss quasi-continuous cryogenic solenoid. I., 20: 16586 (CONF-650922, pp 723-32)
LOPATO, L. M., Interaction of rare earth oxides with strontium oxide, 20: 17044
LOPEZ-MENCHERO, E., Final purification of plutonium and conditioning of products, 20: 16560
LOPEZ-MENCHERO, Emilio, High-energy fission of ^{238}U, 20: 17790
LORIUS, C., Use of isotopes in glaciological study of the polar caps, 20: 16686
LOTTSFELDT, Fredrik I., Hyperbaric oxygen, whole-body x irradiation, and cyclophosphamide combination therapy in mouse leukemia, 20: 16262
LOUCKS, T. L., Relativistic electronic structure in crystals. II., 20: 18002
LOUNASMAA, O. V., Specific heat of Eu and Yb metals between 3 and 25°K, 20: 17080
LOVAS, Istvan, Microscopic description of collective vibrations of nuclei, 20: 17711
LOWENTHAL, G. C., Standardization of radioactivity, 20: 16746
LOYA, B. R., Reusability of buildings after a warfire, 20: 16621 (AD-625867)
LU, Ching-chiang, Real part of pn scattering amplitude at 2 to 10 Bev, 20: 17363
LU, Pou-Chang, Rayleigh's problem in magnetogasdynamics with Hall effect, 20: 17512
LUCAS, J., Growth of pre-breakdown current in helium, 20: 17520
LUCCHINI, G., Biosynthesis of gibberellic acid-^{14}C and 3,4-glucose-^{14}C, 20: 16193 (EUR-2539.i)
LUCKEY, P. D., Photoproduction cross sections for π^+ and K⁺ mesons at 3.4 to 4.0 Bev and comparison with SU(3), 20: 17400
LUDWIG, G. H., Measurement of low-energy primary cosmic-ray protons on IMP-1, 20: 17308 (N-65-18274)
LUDWIG, H. B., Final purification of plutonium and conditioning of products, 20: 16560
LUENOW, W., Diffraction of electromagnetic waves on plasma cylinders, 20: 17877 (IPP-6/44)
LUIPPOLD, H. E., Mitotic delay and apparent synergism of far-red radiation and x rays in chromosome aberrations, 20: 16278
LUITEN, A. L., 90° Superconducting bending magnet for 30-Mev protons, 20: 17197 (CONF-650922, pp 536-40)
LUKAS, I. R., Angular distributions from ^{12}C(α,n)^{15}O reaction at 14 Mev, 20: 17803
LUKASHEVICH, I. I., Moessbauer effect on ^{161}Dy impurity nuclei in metallic Gd, 20: 17988
LUMLEY, E. J., Estimation of cerium in chromium-base alloys, 20: 16334 (N-65-18292)
LUND, Anders, ESR absorption of hexane/silica gel systems γ irradiated at low temperatures, 20: 16511
LUTGEN, P., Chemical dosimetry in irradiation at high dose rates. I., 20: 16517
LUTGEN, P., Chemical dosimetry in irradiation at high dose rates. II., 20: 16518
LUTHARDT, G., Comparison of observed delayed-neutron abundances with calculated fission yields of neutron precursors, 20: 17831
LUTZ, G., Highly polarized coherent bremsstrahlung from a diamond target in Bev region, 20: 17679 (DESY-65/15)
LUX, Franz, Carbonyl compounds of technetium, 20: 16480
LUYANAS, V. Yu., Estimate of the rate of formation of certain radioactive isotopes in the atmosphere, 20: 16689
LYASHCHENKO, N. Yu., Comparison of theoretical and experimental parameters for homogeneous uranium–water critical assembly, 20: 18053
LYMAN, J. T., Dark recovery and glycerol protection for diploid Saccharomyces cerevisiae, 20: 16231 (UCRL-16377)
LYONS, A. R., Cancer of the breast: results of treatment in northern Ireland, 1955–1959, 20: 16324
LYSOV, B. S., Interaction between Nb and alumina, 20: 16978
LYTKIN, V. B., Fast power reactors, 20: 18097
LYUBIMOV, A. L., Spark chambers for studying elastic scattering of π^+ mesons by protons at 180°, 20: 16815 (JINR-P-2506)
LYUBIMOV, V. D., Kinetics of reduction of low-oxide niobium by carbon, 20: 16483
LYUBIMOV, V. D., Self-diffusion of Nb in single crystal and molten specimens, 20: 17090
LYUBOSHITS, V. L., Possible experiments aimed at testing isotopic structure of electromagnetic interaction, 20: 17428 (JINR-P-2498)
LYUBOSHITS, V. L., Radiation anisotropy of the hydrogen atom in an electric field, 20: 17282

M

MAAYOUF, R., Slow neutron spectrum of neutron beam from UA-RR-1 reactor, 20: 18147
MACAGNO, E., Magnetic dipole and electric quadrupole hyperfine effects in ^{209}Bi muonic x rays, 20: 17793
MACKRIE, Vladimir, Prog. rpt. on hydrodynamics of disposal of low-level liquid radioactive wastes in soil, final, 1965, 20: 18163 (NP-15859)
MAEDA, Ken-ichi, Magnetospheric current along the geomagnetic lines of force, 20: 17553
MAGDA, M. T., Angular distributions from ^{12}C(α,n)^{15}O reaction at 14 Mev, 20: 17803
MAGDON, E., Effect of radiation on distribution of ^{32}P-labeled Yoshida sarcoma cells, 20: 16188
MAHAFFEY, Michael Kent, Velocity transfer function analysis of forced convection heat transfer, 20: 16607 (TID-22663)
MAHALANABIS, J., Interpretation of structure of ^{7}Li from proton scattering, 20: 17800
MAHANTAPPA, K. T., Two-pion decay modes of K± and K$^0_1$ mesons in SU$_3$, 20: 17379
MAHENC, Jean, Effect of composition of gaseous phase on isotopic separation of ^{15}N, 20: 16443
MAHESH, P. S., Lattice dynamics and specific heats of some transition metals on Krebs's model, 20: 17081
MAIANI, L., Vector-meson dominance and U$_{6,6}$, 20: 17457
MAIER, B. P., Energy levels of ^{170}Tm, 20: 17782
MAIER-LEIBNITZ, H., Average number and energy of γ rays emitted in ^{235}U fission, 20: 17828
MAIER-LEIBNITZ, H., Prompt and delayed γ rays from fission, 20: 17827
MAJUMDAR, B., Transistorized instruments for reactor control and flux measurement, 20: 18027
MAKARENKO, G. N., Nature of chemical bond in rare earth dicarbides, 20: 17048
MAKAROV, A. A., Two-meson annihilation of baryons in broken SL(6,C) symmetry, 20: 17347 (JINR-P-2547)
MAKAROV, S. P., New isotopes ^{157}Eu, ^{157}Ho, and ^{156}Er, 20: 17808
MAKAROV, V. I., Effect of impurities on superconducting transition temperature, 20: 17637
MAKAROV, V. I., Effect of pressure on superconducting transition temperature, 20: 17639
MAKHON'KO, K. P., Observations of hot particles in surface boundary layer of atmosphere in Moscow region, 1961-63, 20: 16645
MAKHON'KO, K. P., Washout of fission products from the atmosphere, 20: 16648
MAKIOS, W., Microwave interferometer measurements of electron density distribution behind shock fronts and discharge plasmas, 20: 17510 (IPP-3/25)
MAKOWSKA, E., Residual nuclei observed in interactions of 25-Bev/c protons with heavy emulsion nuclei, 20: 17748
MAKSIMOV, L. A., Possibility of super-thermal conductivity in semiconductors, 20: 18014
MAKSYUTENKO, B. P., Delayed neutrons of the fission threshold of ^{232}Th, 20: 17680 (FEI-26)
MAKSYUTENKO, B. P., Variation of relative yields of delayed neutrons, 20: 17832
MALAKHOV, S. G., Fluctuations in seasonal concentration of fission products in atmosphere surface layers over Moscow, 20: 16650
MALAKHOV, S. G., Global distribution in the atmosphere and fallout of the radioactive products of nuclear explosions, 20: 16649
MALAKHOV, S. G., Observations of hot particles in surface boundary layer of atmosphere in Moscow region, 1961-63, 20: 16645
MALAKHOV, S. G., Radioactive isotope in atmosphere and their use in meteorology, 20: 16636
MALAKHOV, S. G., Radon concentration and vertical turbulent mixing in surface boundary layer of atmosphere, 20: 16692
MALAKHOV, S. G., Seasonal changes in radon and thorium concentration in surface boundary layer of atmosphere, 20: 16695
MALAKHOV, S. G., Seasonal and geographical changes in ^{210}Pb content of the atmosphere, 20: 16640
MALAKHOV, S. G., Washout of fission products from the atmosphere, 20: 16648
MALCIC, Stjepan, Monoclinic α'_L phase in U–Nb system, 20: 17035
MALEEV, S. V., Scattering of polarized neutrons in magnets near phase-transition point, 20: 17987

MALHOTRA, P. K., Energy spectrum of primary cosmic rays, 20: 17315
MALINOWSKI, W., Apparatus for internal friction and Young's moduli measurements in kilocycle range, 20: 17013 (INR-632/XIV/PS)
MALKO, A. I., Determination of deuteron polarization parameters from experiments on double scattering by nuclei, 20: 17805
MALLARD, J. R., Small-gamma camera, 20: 16853
MALMBERG, J. H., Prog. rpt. on fundamental modes of collisionless plasma, 3/10–6/10/64, 20: 17882 (N-65-19862)
MALVICINI, A., Some data and comments on ^{22}Na in food chains, 20: 16678
MALYKHIN, V. M., Optimum conditions for measurements on radioactive preparations, 20: 16410
MALYSHEV, V. I., Determination of nitrogen and oxygen in UF_6, 20: 16409
MAMALADZE, Yu. G., Flow of a superfluid liquid in porous media, 20: 17644
MANDZHUKOV, I., Brownian movement study by means of Moessbauer effect, 20: 17165
MANEE, Roger, Supporting post for solid moderator pile of a nuclear reactor, 20: 18040
MANERO RODRIGUEZ, J., Pyrolysis of polyphenyls. I., 20: 16491
MANI, R. S., Preparation of brom sulfalein labeled with ^{82}Br and ^{197}Hg, 20: 16495
MANUEL, O. K., Noble gases from Peace River, Lalande, and Achilles meteorites, 20: 16672
MAPLETON, R. A., Classical calculations on electron capture, 20: 17275
MAQUEDA, E., Exact diagonalization of quadrupole and pairing forces in nuclear d-s shell, 20: 17801
MARAVIGLIA, B., Second-sound attenuation associated with hot ions in liquid He II, 20: 17615
MARAZZI, Carlos A., Secondary emission effects in ion beams, 20: 16624 (N-65-17749)
MARCANTONIO, Arthur, Specifying magnet steels, 20: 17009 (CONF-650922, pp 287-96)
MARCOTTE, V. C., Phase studies of high-Nb-content Nb–Zr–O alloys, 20: 16980
MARCUS, F. R., Role of waste management at Eurochemic, 20: 18167
MARGHITU, Silvia, Ion sources with a magnetic field, 20: 17223
MARINKOVIC, Slobodan, Methods for determination of reactor-grade graphite characteristics, 20: 17079
MARINOV, M., Positron annihilation in CdS monocrystals, 20: 17983
MARIOTTI, D., Method to correct amplitude distortions due to pile-up effects, 20: 16795
MARKERT, Clement L., Prog. rpt. on pathways of metabolism in embryonic development, 6/58–6/65, 20: 16172 (NYO-2194-1)
MARKLEY, F., Argonne National Laboratory's pion focusing horn, 20: 17198 (CONF-650922, pp 650-6)
MARKLEY, F., Fabrication techniques of coils in the Zero-Gradient Synchrotron complex, 20: 17186 (CONF-650922, pp 356-65)
MARKOV, M., Search for specific interactions between μ mesons and ν neutrinos at ultrahigh energies, 20: 17366
MARKUZON, E. V., States with population inversion in a self-compressed discharge, 20: 17924
MARMER, E. N., Tungsten heater stability in vacuum at temperatures up to 3273°K, 20: 16596
MARSH, D. J., Electron metallography of dilute alloys of uranium with iron and aluminum, 20: 17058
MARSH, R. C., High-purity de-ionized water cleaning stations, 20: 16590 (SC-TM-66-49)
MARSHALL, H., Muonic atoms and charge distribution of deformed nuclei, 20: 17756
MARSHALL, W., Moessbauer absorption in presence of electron spin relaxation, 20: 18009
MARSTON, Peter G., 100-Kilogauss quasi-continuous cryogenic solenoid. I., 20: 16586 (CONF-650922, pp 723-32)
MARTALOGU, N., Angular distributions from $^{12}C(\alpha,n)^{15}O$ reaction at 14 Mev, 20: 17803
MARTALOGUE, N., Isomeric yield ratio for the 14-ms fissioning isomer from deuteron irradiation of, 20: 17857
MARTH, W., Irradiation possibilities and safety considerations concerning irradiations at reactor FR 2, 20: 18146
MARTIN, D. W., Ionic drift velocities and ion-molecule reactions in drift-tube mass spectrometer, 20: 17298
MARTIN, D. W., Ionization and charge-transfer cross sections for fast neutral He atoms (0.15 to 1.0 Mev), 20: 17301
MARTIN, G., Reemission of ionically pumped H_2 and He from a stainless steel surface, 20: 17922
MARTIN, G. P., An improved method of Rossi oscillator-oscilloscope coupling, 20: 16776 (EGG-1183-1156)
MARTIN, H., New gonad protector, 20: 16321
MARTIN, H. J. Jr., π^+p Interactions at 450 Mev, 20: 17384
MARTIN, I. D., Evaluation of Rb and Fe bias in flame photometric K determination for K–Ar dating, 20: 16713
MARTINI, V., Analysis of chemical state of Pu and fission products in process feed solutions, 20: 16333 (KR-81)
MARUNA, Frank A. Jr., Description and operation of spacecraft SERT I ion thruster flight test, 20: 16625 (N-65-19272)
MARUYAMA, Masatomo, Reactor fuel reprocessing plant safety in foreign countries, 20: 16577
MAS, Roland, Device for recovering radioactive waste, 20: 18160 (CEA-R-2894)
MASHKOVA, G. B., Distribution of pollutants settling into lower layers of atmosphere, 20: 16652
MASLIN, E. E., Prompt-neutron emission from ^{238}U fission fragments, 20: 17824
MASON, D. W., Apparatus for detection and energy analysis of fast neutral atoms, 20: 17873 (CLM-R-49)
MASON, E. A., Effect of reactor irradiation on Santowax WR, 20: 17122 (MIT-334-34)
MASON, Warren P., Determination of the superconducting energy gaps of metals, 20: 17618
MASSENGILL, L. A., Injection and accumulation: single-pass experiments (DCX-1), 20: 17886 (ORNL-3908, pp 1-17)
MASTEL, B., Effect of prestrain and subsequent neutron irradiation on Mo, 20: 17132
MASTRUP, F. N., Performance measurements on pulsed ablating thruster, 20: 16626
MASUDA, Akimasa, Difference in lanthanide abundance pattern between the crust and the chondrite, 20: 17233
MATHE, I. G., Experiences with measuring systems OZH-1 and OZH-2, 20: 18024
MATHE, I. Gyoergy, Low-capacity atomic power stations, 20: 18107
MATHEWS, J., Neutron exchange in reaction $p + p \rightarrow d + \pi^+$, 20: 17394
MATHEWS, P. M., Invariant scalar product and observables in a relativistic theory of particles of arbitrary spin, 20: 17572
MATHEWS, P. M., Relativistic Schroedinger equations for particles of arbitrary spin, 20: 17571
MATHIAS, B. T., Superconductivity of beta uranium, 20: 17095
MATHIS, Agostino, Simulation of nuclear plants, 20: 18106
MATHUR, V. S., Algebra of currents and K_{e3}, 20: 17405
MATHUR, V. S., Algebra of currents and low-energy $K\pi$ interaction, 20: 17470
MATILE, G., Preparation of Li-drifted Ge counter diodes, 20: 16890
MATSUDA, Kazuhisa, Electrical detection system for broad-range magnetic analyzer, 20: 16859
MATSUDA, Kazuhisa, Survey of nuclear reactions induced by 57-Mev protons. II., 20: 17725
MATSUDA, S., Current-generated algebra and mass levels of the hadrons, 20: 17471
MATSUDA, Shuuji, Cesium-137 in Japanese soil and rice, 20: 16169
MATSUDA, Yasuo, Breeding of medicinal plants exposed to γ irradiation. I., 20: 16290
MATSUI, Masakuzu, Solvent extraction of europium ions, 20: 16565
MATSUI, Yoshito, Difference in lanthanide abundance pattern between the crust and the chondrite, 20: 17233
MATSUOKA, Kenichi, Fuel rod scanner for reactor power density distribution measurement, 20: 18025
MATSUURA, Noboru, Diabetes mellitus in relation to atomic bomb exposure, 20: 16254
MATTHES, Franz, Reaction of oxalatohydrates of rare earth metals with hydrogen chloride. I., 20: 16446
MATTHES, Franz, Reaction of oxalatohydrates of rare earth metals with hydrogen chloride. II., 20: 16447
MATTHES, Franz, Reaction of oxalatohydrates of rare earth metals with hydrogen chloride. III., 20: 16448
MATTHES, W., Measurement of transfer function with statistical methods, 20: 18066
MATULYAVICHENE, V. I., Spectra of dimensions and mobility of natural radioactive aerosols in the atmosphere, 20: 16690
MATUSEVICH, E. S., Fission cross sections of ^{181}Ta, Re, Pt, ^{197}Au, Pb, Bi, Th, ^{235}U and ^{239}U for protons at 150 to 660 Mev, 20: 17838
MATVEEV, V. A., Some effects in the Quark Model, 20: 17343 (JINR-P-2524)
MATYUSHIN, A. T., Spark chambers for studying elastic scattering of π^+ mesons by protons at 180°, 20: 16815 (JINR-P-2506)
MAULARD, Jean, Device for movement of control rod in a nuclear reactor, 20: 18042
MAUSBERG, W., Bibliography on accelerators, 11/65, 20: 17170 (AED-C-18-05)
MAUSHART, Rupprecht, Instrument for simultaneous and separate measurement of α and β activity of radiating nuclei, 20: 16906
MAWARDI, O. K., Langmuir probes for low-density plasma diagnostics, 20: 17899
MAXIE, E. C., Ethylene formation in pea epicotyl tissues following irradiation with γ rays from ^{60}Co, 20: 16281
MAY, James, Irradiation injury to the colon, 20: 16309
MAY, Serge, Determination of silicon by neutron radioactivation and

application to nuclear graphites and alumina, 20: 16360
MAYDAN, D., Search for level structure near 2.86 Mev in ^{10}B, 20: 17797
MAYES, V. M., Energy spectrum of primary cosmic rays, 20: 17315
MAZZOLDI, P., Second-sound attenuation associated with hot ions in liquid He II, 20: 17615
MC ALLISTER, D. R., Economical magnet design, 20: 16584 (CONF-650922, pp 271-80)
MC CABE, E. A., Mechanical, thermal and hydraulic design of Saxton partial plutonium core, 20: 18095 (WCAP-3385-52)
MC CARTHY, G. J., Prog. rpt. on crystal chemistry, 8/13–11/13/65, 20: 17007 (AD-627468)
MC CLAIN, W. C., Project Salt Vault: design and demonstration of equipment, 20: 18165 (ORNL-P-1987)
MC CLURE, J. W., Normal-Fermi-liquid theory for electrons in solids, 20: 17993
MC COLLUM, W. A., Prog. rpt. on radiation effects on Ag and Zn battery electrodes, 7–10/65. II., 20: 17115 (AI-65-264)
MC COLLUM, W. A., Prog. rpt. on radiation effects on Ni–Cd electrodes. III., 6–9/13/64, 20: 17124 (N-65-17608)
MC CORLEY, G. C., Effects of various gases within nasal cavities of rats on response of olfactory bulb neurons to x irradiation, 20: 16215 (AD-628443)
MC DANIEL, E. W., Ionic drift velocities and ion-molecule reactions in drift-tube mass spectrometer, 20: 17298
MC DONALD, F. B., Measurement of low-energy primary cosmic-ray protons on IMP-1, 20: 17308 (N-65-18274)
MC DONALD, L. W., Dark recovery and glycerol protection for diploid Saccharomyces cerevisiae, 20: 16231 (UCRL-16377)
MC DONALD, R. E., Properties of the 4.77- and 5.16-Mev states of ^{10}B, 20: 17761
MC ELROY, D. L., Thermal conductivity values for solid and liquid promethium, 20: 17025 (ORNL-TM-1424)
MC ELROY, J. L., High-temperature testing of graphite helical-screw expanders and compressors, 20: 16591 (UCRL-14660)
MC ELROY, W. N., Health physics for maintenance operation on a homogeneous research reactor, 20: 16757
MC GUIRE, Stephen A., Dose-monitoring instrument for neutrons from thermal to 100 Mev, 20: 16819 (LA-3435)
MC INTOSH, A. E., Control of fission-product release from advanced gas-cooled reactors, 20: 18110
MC ISAAC, L. D., Decay of ^{149}Nd, 20: 17787
MCKAMEY, A., Fabrication techniques of coils in the Zero-Gradient Synchrotron complex, 20: 17186 (CONF-650922, pp 356-65)
MC KAY, M. H., Function arising from second-order approximations to the effective resonance integral, 20: 17650 (AAEC/E-144)
MC KEE, D. W., Catalytic exchange of methane with deuterium on palladium–gold alloys, 20: 16457
MC KEE, R. J., Fine structure and isotope shift in muonic lead, 20: 17268
MC KENZIE, D. E., Prog. rpt. on radiation effects on Ni–Cd electrodes. III., 6–9/13/64, 20: 17124 (N-65-17608)
MC LAREN, A. C., Natural radiation damage in zircon ($ZrSiO_4$), 20: 17147
MC LAUGHLIN, W. L., Microscopic visualization of dose distributions, 20: 16521
MC MASTERS, O. D., Solid solubility of gold-rich rare-earth and lanthanide-rich magnesium alloys, 20: 17016 (IS-1176)
MC MILLAN, W. L., Electron interference in a normal metal induced by superconducting contacts, 20: 17621
MC NALLY, J. Read Jr., Excitation heating of ions to high temperature, 20: 17900
MC PEAK, D. W., Changes in ^{137}Cs retention and routes of elimination as effected by external factors, 20: 16180
MC WHAN, D. B., Magnetic and structural properties of europium metal and EuO at high pressure, 20: 17999
MEAD, C. Alden, Observable consequences of fundamental-length hypotheses, 20: 17573
MEADS, P. F. Jr., IBM-7094 beam quadrupole abberation program, 20: 17220
MEDICUS, G., Photoelectric ion emission from cesiated surfaces, 20: 17267
MEDICUS, H. A., Scandium-44 isomeric yield ratios, 20: 17777
MEERS, J. T., Prog. rpt. on effects of neutron damage on single-crystal graphite, semiannual, 7–12/65, 20: 17027 (TID-22712)
MEERS, J. T., Prog. rpt. on effects of neutron damage on properties of pyrolytic and single-crystal graphite, annual, 4/64–6/65, 20: 17028 (TID-22733)
MEETZ, K., Application of spectral representations to nonrelativistic and relativistic Bethe-Salpeter equation, 20: 17425 (DESY-66/1)
MEGAHED, Y. M., Preparation of ^{131}I-tyrosines and ^{131}I-thyroxine, 20: 16496
MEHROTRA, R. C., Organic compounds of lanthanide elements. V., 20: 16434
MEHTA, G. K., Long-range α particles in fission of ^{235}U and ^{239}Pu, 20: 17839
MEHTA, M. L., Correlation functions for eigenvalues of real quaternian matrices, 20: 16938
MEIER, G., Isotope analysis of nitrogen by emission spectroscopy with photoelectric recording, 20: 16375
MEIFFREN, J., Carbon dioxide–coolant gas of G.2 and G.3 reactors, 20: 18120
MEIFFREN, J., Safety systems and measurement of neutron flux, 20: 18119
MEINERS, Dieter, Discharge of the θ pinch at high initial densities, 20: 17945
MELKONIAN, E., Long-range α particles in fission of ^{235}U and ^{239}Pu, 20: 17839
MELLENTIN, K., Bibliography on high-energy physics, No. 5, 8/65, 20: 17153 (AED-C-23-05)
MELLENTIN, K., Bibliography on high-energy physics, No. 6, 8/65, 20: 17154 (AED-C-23-06)
MELLENTIN, K., Bibliography on high-energy physics, 8/65, 20: 17155 (AED-C-23-07)
MELNICK, M. M., New cross section library for n + ^{235}U reactions, 20: 17697 (WANL-TME-1028)
MELNICK, M. M., XO and EXT—IBM-7094 programs temperature target, 20: 17698 (WANL-TME-1132)
MELNICK, Marion M., Curve plot for "SCISRS", 20: 17699 (WANL-TME-1317)
MENENDEZ, Manuel G., Angular distribution of elastically scattered Cs^+ ions from Ar, Kr, and N_2, 20: 17300
MENKES, Civel K., Glass dosimeter washing technique for improved reproducibility, 20: 16847
MERCER, B. W., Treatment and disposal of glass melter condensates containing sulfuric acid, 20: 18159 (BNWL-SA-514)
MERLIN, H. B., World and Canadian energy today and tomorrow. I., 20: 18082 (AECL-2390)
MESHITSUKA, Gisuke, Reaction of active nitrogen with ethylene, 20: 16510 (NP-tr-1364)
MESHKOV, S., Spin independence, W spin, parity, and SU(6) symmetry, 20: 17475
MEYER, H., Equalizing system for small differential nonlinearity with a one-nanosecond digital time coder, 20: 16794
MEYER, O., Preparation and study of thick depleted surface-barrier detectors, 20: 16818 (KFK-328)
MEYER, P., Lifetime of the $^{25}/_{2}$ three-particle state of ^{177}Hf, 20: 17811
MEYER, R. A., Parameter study of large fast reactor meltdown accidents, 20: 18123
MEYERAND, Russell G. Jr., Cesium-diode thermionic converter for laboratory experiments, 20: 17329
MEYEROTT, A. J., High-sensitivity detectors for few-kev x rays, 20: 16901
MEZZETTI, F., Low-frequency internal friction of Al–Al_2O_3 dispersed-phase alloys (SAP), 20: 17065
MIA, M. M., Effect of γ irradiation on seeds of Corchorus capsularis and C. olitorius, 20: 16217 (AECD-AG-7)
MIA, M. M., Interspecific hybridization in jute, 20: 16218 (AECD-AG-12)
MIAH, Md. Hanifuddin, Pion-nucleon coupling constant from spin-flip dispersion relation, 20: 17336 (AECD/TP-5)
MICHAUDON, A., Measurement and analysis of fission cross section of ^{239}Pu from 0 to 5 kev, 20: 17851
MICHON, G., Organization of a control of radioactive pollution of milk, 20: 16754
MICHON, G., Radium-226 content of milk in France. I., 20: 16752
MICHON, G., Radium-226 content of milk in France. II., 20: 16753
MIDDLETON, Roy, Study of ^{19}O by $^{17}O(tp)^{19}O$ and $^{18}O(d,p)^{19}O$ reactions, 20: 17758
MIELCARSKI, M., Salt-boiling fast reactor "SAWA", 20: 18088 (INR-699/C)
MIGDAL, A. B., Nuclear magnetic moments, 20: 17733
MIHAJLOVIC, Aleksandar, Monoclinic α'_3 phase in U–Nb system, 20: 17035
MIHRAN, Theodore G., Nonlinear limiting of double-stream instability, 20: 17917
MIHUL, Eleonora, Symmetries in elementary particle physics, 20: 17486
MIKAELYAN, L. A., Neutrons and kinetic energy of fragments in fission of heavy nuclei, 20: 17857
MIKAELYAN, L. A., The neutrino, 20: 17406
MIKELSON, A., Modulation of forces acting on conducting bodies in travelling magnetic field of a cylindrical inductor, 20: 17162
MIKHAILOV, Yu. N., Crystalline structure of $Cs_2[UO_2Br_4]$, 20: 16484
MIKHEEV, N. B., Application of co-crystallization and adsorption in the solution of current problems of radiochemistry, 20: 16557
MIKI, Isao, Processing of uranium oxide fuel by oxidation-reduction cycle, 20: 16576
MIKOLEIT, W., Automatic control of a four-stage evaporator for treating contaminated waters, 20: 16594
MIKUMO, Takeshi, Survey of nuclear reactions induced by 57-Mev protons. II., 20: 17725
MILFORD, S. N., Double-inelastic collisions of excited H atoms with excited H atoms, 20: 17290

MILICIC, Miodrag, Developing production methods for reactor-grade graphite, 20: 17002
MILIN, V. B., Radon concentration and vertical turbulent mixing in surface boundary layer of atmosphere, 20: 16692
MILLER, Donald H., Analysis of the B enhancement, 20: 17402
MILLER, H. W., Economical magnet design, 20: 16584 (CONF-650922, pp 271-80)
MILLER, J. K., Absorption and gastric secretion of ^{131}I and ^{36}Cl in dairy calves, 20: 16186
MILLER, James N., Immunity in experimental syphilis. IV., 20: 16199
MILLER, Laurence Frederick, Effects of radiation quality on radiolysis of water, 20: 16509
MILLER, T. G., Liquid-helium, time-of-flight coincidence neutron polarimeter, 20: 16876
MILLER, T. M., Ionic drift velocities and ion-molecule reactions in drift-tube mass spectrometer, 20: 17298
MILLIKIN, A. D., Power supply system for ZGS ring magnet, 20: 17227
MILLIOT, B., Study of liquid metal boiling under forced convection, 20: 16608 (ANL-Trans-257)
MILLS, Robert G., Initial transient of a thermonuclear reactor, 20: 17880 (MATT-437)
MILNER, A., Prog. rpt. on fabrication of W alloy tubing, 10/23/65–1/1/66, 20: 16989 (COO-1518-2)
MILNER, G. W. C., Rapid dissolution of PuO_2 by a Na peroxide sinter and determination of PuO_2 content, 20: 16350
MILTENYI, L., Effect of ionizing radiation on iron metabolism, 20: 16187
MINARDI, E., Thermonuclear investigations. III., 20: 17928
MINARDI, E., Thermonuclear investigations. IV., 20: 17929
MINCZEWSKI, Jerzy, Determination of rare earths by neutron activation method using ion-exchange chromatography. Analysis of spectrally pure erbium oxide, 20: 16363
MINGUZZI-RANZI, A., Production mechanism of $\bar{K}^*o(891)$ in K⁻-p interaction at 3 Bev, 20: 17380
MINKOV, L., Tolerance of x-ray moving-beam irradiation, 20: 16317
MINTURN, Robert E., Molecular-beam studies of the alkali–halogen reactions, 20: 17295
MISHEV, I. T., Possibility of obtaining a standard source of thermal neutrons, 20: 17654 (RT/PROT-(65)31)
MISRA, S. N., Organic compounds of lanthanide elements. V., 20: 16434
MISRA, T. N., Organic compounds of lanthanide elements. V., 20: 16434
MITCHARD, F. S., Vacuum/gas leak testing of boiler elements for nuclear power stations, 20: 16618
MITCHELL, John C., Proton dosimetry measurements performed in support of primate irradiations, 20: 16283
MITIN, B. S., Interaction between Nb and alumina, 20: 16978
MITSUI, Hidehiko, Measurement of distribution of fission fragments recoiling into aluminum, 20: 17721
MITTLEMAN, M. H., Electron capture by helium ions in neutral helium, 20: 17276
MIURA, Masaji, ESR of sodium polyphosphate glass irradiated with γ rays, 20: 16516
MIURA, Motoi, Diabetes mellitus in relation to atomic bomb exposure, 20: 16254
MIYAGAWA, Ichiro, Stereospecific addition of hydrogen to fumaric acid in irradiated single crystals of succinic acid, 20: 16537
MIYAHARA, Syokei, Magnetic susceptibilities of V, Zr, and Nb, 20: 17069
MIYANO, Kazumasa, Nonexistence of reported 0.58-Mev γ ray in decay of ^{42}K, 20: 17723
MIYAZAWA, Yoshitoshi, B-constant magnet pole design, 20: 17184 (CONF-650922, pp 239-47)
MIYAZAWA, Yoshitoshi, Circular current shim for a cyclotron magnet, 20: 17187 (CONF-650922, pp 377-89)
MIYOSHI, Kazuo, Medical survey of Japanese exposed to fallout radiation in 1954, 20: 16226 (NP-15891)
MOAURO, A., Determination of manganese and arsenic content in steel by neutron activation analysis, 20: 16338 (RT/CHI-(65)36)
MOBLEY, R. M., Atomic interactions of muonium, 20: 17297
MOEBIUS, P., Derivation of weak current in framework of unitary symmetry, 20: 17415
MOEBIUS, Rolf, Reaction of oxalatohydrates of rare earth metals with hydrogen chloride. I., 20: 16446
MOEBIUS, Rolf, Reaction of oxalatohydrates of rare earth metals with hydrogen chloride. III., 20: 16448
MOEBIUS, Rolf, Reaction of oxalatohydrates of rare earth metals with hydrogen chloride. II., 20: 16447
MOHOS, B., ESR studies on trapped free radicals in irradiated aqueous H_2O_2 solutions, 20: 16512
MOISEENKO, S. K., Effective decontaminating solutions to remove ^{60}Co from Duralumin and steel-3 by ultrasonic cleaning, 20: 16767
MOISEIWITSCH, B. L., Tamm variational principle and its generalization to the scattering amplitude, 20: 17271
MOLDOVAN, C., Diffusion theory of low-voltage arc plasma, 20: 17907
MOLINSKI, V. J., Prog. rpt. on research in activation analysis, 8/63–10/64, 20: 16336 (NYO-10175)
MONARI, L., Production mechanism of $\bar{K}^*o(891)$ in K⁻-p interaction at 3 Bev, 20: 17380
MONCASSOLI, A. M., Evaluation of the first BR3 core, 20: 18108
MONGELLI, S., π^+ p interactions at 1.6 Bev, 20: 17374
MONGON, A., Eurochemic instrumentation development and studies, 20: 16559
MONTAGNINI, B., Spectrum of neutron transport equation in finite bodies, 20: 17657
MONTALDI, E., Analyticity properties of the scattering amplitude for a velocity-dependent potential, 20: 17449
MONTAN, D. N., Effect of variation of airborne radon daughter concentration on whole-body counter background, 20: 16665 (UCRL-14534, pp 23-7)
MOONEY, Paul J., Electronic design of spectrometer for monitoring solar x radiation in space, 20: 16904
MOORE, David P., Prog. rpt. on mechanism of divalent cation uptake by plants, 6/65–5/66, 20: 16174 (RLO-1547-3)
MOORE, George E., Measurement of "knock-on" cross section in elastic scattering in H–He systems, 20: 17293
MOORE, P. W., Polarographic determination of H_2O_2 in irradiated H_2O, 20: 16327 (AAEC/TM-301)
MOORE, W. H., Source of high-energy particles from an internal target in the AGS, 20: 17171 (BNL-10030)
MORAVCSIK, Michael J., General nondynamical formalism for reactions with particles of arbitrary spin, 20: 17479
MORAVCSIK, Michael J., Non-dynamical structure of particle reactions, 20: 17436 (UCRL-14321-T)
MORAVCSIK, Michael J., Nondynamical structure of $^3He(d,p)^4He$ reaction, 20: 17770
MOREY, R. E., Analysis of Ti–7Al–2Nb–1Ta and Ti–6Al–4V fractures, 20: 16967 (AD-628277)
MORGAN, C. G., Space-charge controlled ionization growth in hydrogen, 20: 17518
MORGAN, D., Levinson's theorem for S-matrix theory with inelasticity, 20: 17452
MORGAN, D. T., Effect of reactor irradiation on Santowax WR, 20: 17122 (MIT-334-34)
MORGAN, I. L., Gamma rays produced in $^{56}Fe(n,n'\gamma)^{56}Fe$ reaction, 20: 17736
MORGAN, J. G., Evaluation and irradiation effects studies on pyrolytic-carbon-coated fuel particles, 20: 17127 (ORNL-3923)
MORGAN, O. B., High-current ion-beam production and injection, 20: 17890 (ORNL-3908, pp 100-7)
MORK, K. J., Differential cross section for pair production by photons on electrons, 20: 17354
MOROZ, B. B., Experimental radiation sickness induced with ^{210}Po, 20: 16268
MOROZ, E. M., Method of investigation betatron oscillation resonances, 20: 17221
MOROZOV, A. I., A similarity parameter in theory of plasma flows, 20: 17910
MOROZOV, A. I., Plasma flow between electrodes with weak longitudinal conductivity, 20: 17939
MOROZOV, A. I., Stationary current in axially symmetric conducting body with strong Hall effect, 20: 17164
MOROZOV, M. G., Investigation of performance of direct-current plasmatron, 20: 17938
MOROZOVA, P. V., Helium particles emitted during 17.5-Bev π-meson collisions with photoemulsion nuclei, 20: 17716
MOROZUMI, Henry M., Diurnal variation of auroral zone geophysical disturbances, 20: 17554
MORPURGO, G., Is a non-relativistic approximation possible for internal dynamics of elementary particles?, 20: 17482
MORRIS, R. A., Experiments with foil-film combinations and collimators for neutron radiography, 20: 16619
MORRIS, T. W., Pion production in $p\bar{p}$ annihilations at 3.3 and 3.7 Bev/c, 20: 17385
MOSER, Pierre, Magnetic hysteresis study of iron contaminated by nickel traces and irradiated with neutrons, 20: 17134
MOSKVIN, Yu. V., Theoretical and experimental studies of water vapor plasma radiation, 20: 17936
MOSTERT, P., 50-Mw boiling water reactor of Dodewaard, 20: 18103
MOTEFF, John, Effect of neutron radiation on creep properties of W, 20: 17152
MOTOJIMA, Kenji, Spectrophotometric determination of Mn in Be, 20: 16361
MOTONAGA, Shoshichi, B-constant magnet pole design, 20: 17184 (CONF-650922, pp 239-47)
MOTONAGA, Shoshichi, Circular current shim for a cyclotron magnet, 20: 17187 (CONF-650922, pp 377-89)
MOTONAGA, Shoshchi, Field mapping by differential usage of Hall generators, 20: 17193 (CONF-650922, pp 472-5)
MOULTON, William G., Magnetic and electrical properties of selected materials, 20: 17019 (N-65-17873)

MUCSI, O., Effect of ionizing radiation on iron metabolism, 20: 16187
MUELLER, A., Calculation of lattice parameters of the WWER core, 20: 18143
MUELLER, G., Isotope analysis of nitrogen by emission spectroscopy with photoelectric recording, 20: 16375
MUELLER, G., The animal in radiation experiments, 20: 16164
MUELLER, K., New type of radiometric titrator: Redox and chelatometric microtitrations, 20: 16386
MUELLER, Karl-Heinz, Particular solutions of energy-dependent Boltzmann equation, 20: 18068
MUENZEL, Helmut, High-energy fission of ^{238}U, 20: 17790
MUKAIBO, Takeshi, Oxidation behavior of Nb and Nb–V alloys, 20: 16982
MUKAIBO, Takeshi, Processing of uranium oxide fuel by oxidation-reduction cycle, 20: 16576
MUKHTASIMOV, F. N., Decay of ^{159}Ho, 20: 17685 (JINR-P-2497)
MULADY, James R., Precision magnetic field measurements with Hall-effect probes, 20: 17191 (CONF-650922, pp 447-55)
MULAS, Pablo M., Energy degradation of fission fragments in light materials, 20: 17821
MULLER, O., Prog. rpt. on crystal chemistry, 8/13–11/13/65, 20: 17007 (AD-627468)
MULLER-BUSCHBAUM, H. K., Fluorescence of rare earths. III., 20: 16466
MURAKAMI, Yukito, Influence of metal ions and metal chelates on hydrolysis of α-D-glucose 1-phosphate, 20: 16421
MURATA, Hiroo, Magnetospheric current along the geomagnetic lines of force, 20: 17553
MUROHASHI, Toyoho, Effect of uv irradiation on acid fastness and gram positivity of mycobacteria, 20: 16195
MURRAY, G., Scattering of high-energy electrons by ^{7}Li, 20: 17799
MURRAY, J. S., Cross section and polarization of Balmer α radiation produced in collisions of protons with N_2, 20: 17269
MUSA, G., Diffusion theory of low-voltage arc plasma, 20: 17907
MUSER, A., Multiple-duration monostable multivibrator, 20: 16792
MUSIALOWICZ, T., Determination of mixture of thermal-neutron and γ exposures by film badges, 20: 16807 (CLOR-IBJ-42/D)
MUSTELIER, J. P., Variation of the parameters of weakly irradiated UC, 20: 17140
MUTA, Nobuyoshi, Subcutaneous nodules following ^{60}Co teleradiation, 20: 16323
MUZIOL, G., New isotopes ^{157}Eu, ^{157}Ho, and ^{156}Er, 20: 17808
MYASISHCHEVA, G. G., Observation of atomic muonium in crystalline quartz, 20: 17361
MYKYTIUK, A., Direct determination of small quantities of rare earth and yttrium oxides in thoria by emission spectroscopy, 20: 16393
MYZNIKOV, K. P., Slow ejection of the proton beam from the synchrophasotron, 20: 17208 (JINR-P-2537)

N

NABOICHENKO, K. V., Critical thermal fluxes in forced motion of MIPB–benzol, 20: 16614
NAGASAWA, Kakuma, Contamination of ^{90}Sr in stock rainwater in light-houses, 20: 16671
NAGASAWA, Kakuma, Contamination by ^{90}Sr and ^{137}Cs of dry milk products in 1962, 20: 16755
NAGASHIMA, Nobuo, Study on Al–Zr alloys. I., 20: 17072
NAGAYA, Yutaka, Fallout radionuclides in deep waters around Japan, 20: 16681
NAGIBAROV, V. R., Inertial echo and coherent gravitational waves, 20: 17567
NAGIBAROV, V. R., Quadrupole and nuclear spin interaction via the optical phonon virtual field, 20: 17818
NAGLE, A. K., Instrumentation for control and safety of zero energy reactor Zerlina, 20: 18149
NAGY, E., Multiple scattering constant in emulsion at great cell lengths, 20: 16833
NAGY, L., Angular distribution of γ rays from fission of ^{235}U, 20: 17829
NAKAJIMA, Yutaka, Survey of nuclear reactions induced by 57-Mev protons. II., 20: 17725
NAKAMURA, K., Current-generated algebra and mass levels of the hadrons, 20: 17471
NAKANISHI, Noriyoshi, B-constant magnet pole design, 20: 17184 (CONF-650922, pp 239-47)
NAKANISHI, Noriyoshi, Circular current shim for a cyclotron magnet, 20: 17187 (CONF-650922, pp 377-89)
NAKANISHI, Yuh H., Effects of x irradiation on females of the teleost, Oryzias latipes, 20: 16263
NAKASHIMA, Noritsugu, Protective effects of two drugs against radiation injury, 20: 16302
NAMBOODIRI, M. N., Neutron-induced fission of ^{227}Ac, ^{231}Pr, and ^{237}Np: mass distribution, 20: 17861
NARATH, Albert, Nuclear spin relaxation in molybdenum metal, 20: 17998
NARAYANA, K. L., Low-lying even-parity levels of ^{18}F, 20: 17710
NARDON, P., Action of ^{60}Co γ rays on mortality and fertility of the rice weevil, 20: 16243
NASIRUDDIN, Review on wholesomeness of irradiated foods with special reference to wheat, 20: 16918 (AECL-PAK/RB-7)
NATARAJAN, R., Airborne radioactivity at Delhi, 20: 16680
NATER, K. A., Plutonium-containing fuel, 20: 16996
NAUMKIN, O. P., Rate of oxidation of metallic Sc, 20: 16985
NAZARENKO, V. A., Search for parity nonconservation in nuclear γ transitions, 20: 17444
NAZAROV, L. E., Dispersion of radioactive aerosols in the atmosphere, 20: 16643
NAZAROV, L. E., Fluctuations in dispersed composition of radioactive aerosols in surface boundary layer of the atmosphere, 20: 16644
NEAL, L. G., Prog. rpt. on kinetic studies of heterogeneous water reactors, 6/30/65, 20: 18050 (STL-372-22)
NEDYALKOVA, N., Brownian movement study by means of Moessbauer effect, 20: 17165
NEELEY, A. C., Powder metallurgy in fabrication of very large parts, 20: 16993 (Y-DA-1043)
NEGANOV, B. S., Method of obtaining super-low temperature based on a dissolution of ^{3}He in ^{4}He, 20: 17599 (JINR-P-2480)
NEHRT, Lee C., International marketing of nuclear power plants, 20: 18117
NEHRU, A. Y., Corrosion of Zr and Zy-2 at low temperatures, 20: 16979
NEIDIGH, R. V., Plasma physics, 20: 17889 (ORNL-3908, pp 52-89)
NEILL, J. M., Prog. rpt. on graphite interface studies, 5/63–9/65, 20: 18127 (GA-6753(Pt.1))
NEKHOROSHEVA, M. P., Determination of annual ^{90}Sr fallout in polar regions by recording ^{90}Sr content in seasonal layers of snow and ice, 20: 16703
NEKHOROSHEVA, M. P., Fluctuations in seasonal concentration of fission products in atmosphere surface layers over Moscow, 20: 16650
NEKHOROSHEVA, M. P., Washout of fission products from the atmosphere, 20: 16648
NELSON, Carl Walter, Acoustical relaxation processes in Zr–Nb alloys, 20: 17106
NELSON, Neal S., Radiation hygiene, 20: 16296
NEMETHY, L., Rare earth metals in stainless steel making, 20: 17078
NENOV, N., Determination of arsenic in ores and rocks with high Mn by neutron activation analysis, 20: 16364
NENTWICH, H., 100-MHz prescaler in biquinary tunnel diode transistor mode, 20: 16775 (DESY-65/17)
NENTWICH, O., Decontamination of radioactive wastes of Karlsruhe nuclear research center from 1963 to 1965, 20: 18171
NESS, S., Photomultiplier base system with high-voltage divider network remote from the photomultiplier, 20: 16796
NESTERENKO, V., Slow neutron spectrum of neutron beam from UA-RR-1 reactor, 20: 18147
NEUBAUER, H., Preparation and superconductivity of Nb_3Sn diffusion layers with addition of Zr or Ti, 20: 17632
NEUDACHIN, V. G., Nucleon clusters in light nuclei, 20: 17707
NEUMANN, L., Temperature dependence of magnetization in mixed state of superconducting alloys, 20: 17633
NEUMEISTER, K., Osteoradionecroses in area of the hand, 20: 16210
NEVE DE MEVERGNIES, M., Variation of the binary-ternary fission ratio for ^{235}U, 20: 17840
NEVEU-RENE, Monique, Analysis of the B enhancement, 20: 17402
NEW, T. C., High power silicon-controlled rectifier thyristors, 20: 16774 (CONF-650922, pp 788-96)
NEWMAN, Leonard, Synergistic effect of tri-n-octylamine on solvent extraction of Am by TTA, 20: 16571
NGUEN VAN, Hieu, Electromagnetic interaction of the X meson in higher symmetries, 20: 17342 (JINR-P-2520)
NGUYEN LUONG THAN, Solution of the diffusion equation, 20: 17652 (CEA-R-2867)
NICHOLLS, C. H., ESR studies of uv-irradiated keratin and related proteins, 20: 16205
NICKLOW, R. M., Normal vibrations in aluminum and derived thermodynamic properties, 20: 18001
NIELSEN, Betty, Canyon Diablo meteorite, 20: 17238
NIELSEN, C. E., Injection and accumulation: single-pass experiments (DCX-1), 20: 17886 (ORNL-3908, pp 1-17)
NIEMANN, L., Thermally activated processes in deformation of neutron-irradiated Cu single crystals. II., 20: 17980 (ANL-Trans-274)
NIFENECKER, H., Analysis of fission cross section of ^{233}U for neutrons between 1.7 and 30 ev, 20: 17853
NIKISHOV, A. I., Ionization of systems bound by short-range forces under action of an EM wave, 20: 17284
NIKITIN, V. A., Real part of pp elastic scattering amplitude at 2, 4, 6, 8 and 10 Bev, 20: 17417
NIKOLAEV, V., Modulation of forces acting on conducting bodies in travelling magnetic field of a cyliadrical inductor, 20: 17162
NIKOLAEV, V. S., Autoionization of nitrogen and oxygen ions after passage

through a solid, 20: 17262
NIKOLSKII, I. K., Bremsstrahlung in infrared region from plasma of electrodeless induction discharge, 20: 17931
NIR, Aharon, Quantitative radioactivity determination of ^{18}O, 20: 16412
NISHIHARA, Hiroshi, Burnup characteristics of large Pu–U fast reactors, 20: 18060
NISHIKAWA, Seiichi, Study on Al–Zr alloys. I., 20: 17072
NISHINA, Yoichiro, Magneto-optical experiments with superconducting magnet, 20: 17588 (CONF-650922, pp 525-9)
NISSIM-SABAT, C., Magnetic dipole and electric quadrupole hyperfine effects in ^{209}Bi muonic x rays, 20: 17793
NISSIM-SABAT, C., M1 and E2 hyperfine structure in muonic K and L x rays of bismuth, 20: 17792
NISTOR, C., Moessbauer spectrometer, 20: 16872
NOGGLE, T. S., Reduction in radiation damage due to channeling of 51-Mev iodine ions in gold, 20: 17146
NONAKA, Ituro, Survey of nuclear reactions induced by 57-Mev protons. II., 20: 17725
NORDEMANN, D., Radioactivity induced by cosmic rays in the Bogou meteorite, 20: 16674
NORMENT, H. G., Development of improved land-surface fallout model, 20: 16735 (TO-B-65-99)
NORTH, J. C., Deformation potential of irradiation induced traps in p-type Ge, 20: 17142
NORTH, J. C., Length changes in electron-irradiated high-purity germanium, 20: 17136
NORTH, J. C., Length changes in electron-irradiated n- and p-type Ge, 20: 17145
NORTON, D. S., CWF and TABLE—two FORTRAN programs for calculation of Coulomb penetration and shift factors, 20: 17671 (AEEW-M-611)
NOSKOV, A. S., Determination of nitrogen and oxygen in UF_6, 20: 16409
NOSSAL, Ralph, Validity of convolution approximation for the Van Hove G(r,t) function, 20: 17665
NOVAK, Alexandre, Vibration spectra of imidazole, imidazole (D)-1, imidazole (D_3)-2,4,5, and imidazole (D_4). I., 20: 16499
NOVAK, Alexandre, Vibration spectra of imidazole, imidazole (D)-1, imidazole (D_3)-2,4,5, and imidazole (D_4). II., 20: 16500
NOVIKOFF, Alex B., Effects of arginine deprivation, uv, and x radiation on cultured KB cells, 20: 16258
NOVIKOV, L. N., Optical orientation of ^{201}Hg atoms using the 1850 A line, 20: 17755
NOVIKOV, P. D., Ionizing radiation effects on ion exchange materials, 20: 16583
NOVIKOVA, A. P., Distribution of U in dogs at long periods after inhalation of U_3O_8, 20: 16184
NOWALK, T. P., High power silicon-controlled rectifier thyristors, 20: 16774 (CONF-650922, pp 788-96)
NOWOTNY, H., Problem of the carbohydrides, 20: 17074
NOWOTNY, H., Ternary phases with $MgZn_2$ type, 20: 17075
NURMIA, M., Alpha-gamma and alpha-conversion electron coincidence study of ^{219}Rn, ^{215}Po, and ^{211}Bi, 20: 17703
NYSTROM, R. E., Ultrasonic-induced cavitation studies in mercury and water, 20: 16974 (NP-15889)
NYSTROM, R. F., Preparation of labeled compounds by tritioboration procedures. I., 20: 16549

O

OAKLEY, A. E., Standardization of radioactivity, 20: 16746
OBUKHOV, Yu. V., Observation of atomic muonium in crystalline quartz, 20: 17361
OEGELMAN, H. B., Search for discrete sources of cosmic γ rays above 1 Bev, 20: 17320
OEHME, Reinhard, Current algebras and approximate symmetries, 20: 17463
OEL, H. J., Residual activity method for determination of self-diffusion coefficients in solids, 20: 16478
OEN, O. S., Reduction in radiation damage due to channeling of 51-Mev iodine ions in gold, 20: 17146
OGATA, Yoshiyu, Principal substance inducing leukocytosis after x irradiation, 20: 16265
OGAWA, S. Y., Irradiation performance of alternate cladding materials, 20: 17120 (GEAP-4916)
OGAWA, S. Y., Performance of fuel rods containing boron burnable poison, 20: 17121 (GEAP-4918)
OGAZA, S., g-Factor of 87-kev excited state in ^{158}Gd, 20: 17683 (INP-430/PL)
OGAZA, Stanislaw, Transverse spin polarization in odd-mass deformed nuclei, 20: 17682 (INP-428/PL)
OGGERO, Mario, Experimental research on electric propulsion. VII., 20: 16629
OGIEVETSKII, V. I., Possible experiments aimed at testing isotopic structure of electromagnetic interaction, 20: 17428 (JINR-P-2498)
OGORODNIKOV, B. I., Basis for using fibrous filter materials, (Petryanov filters), 20: 16653
OGORODNIKOV, B. I., Properties of fibrous filters in rarefied air, 20: 16654
OGURA, R., Effect of uv exposure on succinic dehydrogenase activity, 20: 16196
OHLSEN, H., Summary of working session on personnel dosimetry, Berlin, 11/64, 20: 16827 (SZS-9(1965))
OHSHIMA, Tomoyo, Effects of x irradiation on females of the teleost, Oryzias latipes, 20: 16263
OHTA, Masao, Burnup characteristics of large Pu–U fast reactors, 20: 18060
OHTSUKI, Sozi, Propagation of normal region in superconducting magnet, 20: 17610
OI, Noboru, Xe diffusion in UO_2 single crystals, 20: 17103
OKOROKOV, A. I., Critical scattering of polarized neutrons in nickel, 20: 17986
OKSMAN, Juhani, Slant sporadic E reflections, 20: 17542
OKUBO, S., Algebra of currents and low-energy theorem, 20: 17375
OKUBO, S., Algebra of currents and $K_{\ell 3}$, 20: 17405
OKUDA, H., Cosmic rays in upper atmosphere, 20: 17322
OKUN, L. B., Quarks: astrophysical and physicochemical aspects, 20: 17411
OKUNO, Hisataru, Electrodeposition of Ru from Ru(III) and Ru(IV) solution and a fission-product solution, 20: 16563
OLIPHANT, Thomas A. Jr., Spherical harmonic reduction of Fokker-Planck equation, 20: 17878 (LA-3437)
OLLIVIER, Jean-Yves, Kinetics of ion exchange on zirconium phosphate, 20: 16568
OLSEN, J. M., Proton-proton singlet S-state interaction, 20: 17353
OLSEN, Tore, Deviations from BCS behavior in temperature dependence of ultrasonic absorption in superconducting tin, 20: 17605
OLSMATS, M., Hyperfine structure of 16-hour state in ^{119}Te, 20: 17705
OMORI, Tokushi, Chemical effects associated with the β-decay process. II., 20: 16544
OMUKA, Iku, Report by Director, Bureau of Public Health [on health of populations exposed to atomic bombs], 20: 16271
ONIKUL, R. I., Effect of vertical distribution of temperature and wind velocity on the atmospheric diffusion of radioactive pollutants, 20: 16651
ONISHCHUK, V. A., Effect of atomic hyperfine interaction on nuclear γ transitions, 20: 17686 (JINR-P-2512)
ONISHCHUK, V. A., Radiation anisotropy of the hydrogen atom in an electric field, 20: 17282
OPHIR, D., Multiple spectrometer control by computer, 20: 16869
ORBAN, Miklos, Solvent effect in isotope exchange reactions. III., 20: 16502
ORLANDINI, K. A., Preparation of carrier-free ^{207}Bi for β spectrometry, 20: 16546
ORLOV, Yu. F., Quantum depolarization of electrons in magnetic field, 20: 17689 (NP-15783)
ORNSTEIN, L. Th. M., Thermonuclear investigations. III., 20: 17928
ORTH, P. H. R., Positron annihilation in noble gases, 20: 17423
OSBORN, R. K., Reactor noise analysis by photon observation, 20: 18064
OSBORNE, L. S., Photoproduction cross sections for π^+ and K^+ mesons at 3.4 to 4.0 Bev and comparison with SU(3), 20: 17400
OSIPOV, Yu. S., Distribution of pollutants settling into lower layers of atmosphere, 20: 16652
OSMER, Judith A., Growth and preferential doping of zircon and thorite, 20: 16960
OTA, Masaxiro, Geomagnetic diurnal variation in north polar region with corrected geomagnetic latitude, 20: 17555
OTROTSENKO, G. A., Fission distribution in neutron-induced fission of ^{230}Th, ^{238}Pu, and ^{241}Am, 20: 17848
OTT, A., Inter-diffusion of Li isotopes in liquid lithium metal, 20: 17104
OTTER, J. M., Prog. rpt. on tungsten resonance integrals and Doppler coefficients, 6–12/65, 20: 18045 (AI-66-16)
OTTO, Fred B., Paramagnetic resonance of F_2 ions trapped in electron-irradiated KF_2, 20: 17976 (NYO-2047-36, App.I)
OTTO, R., Utilization of multiclone dust for decontaminating sewage waters containing ^{137}Cs and $^{90}Sr/^{90}Y$, 20: 18170
OWEN, L. W., Phase-shift analysis of elastic scattering: code PEGGY, 20: 17693 (ORNL-TM-1464)
OWENS, C. M., Metallographic technique for measuring thin films of zirconium oxide as formed on reactor fuel cladding, 20: 16946 (ORNL-TM-1161, pp 80-4)
OWENS, C. M., Micro-constituents in Incoloy 800, 20: 17024 (ORNL-TM-1161, pp 236-46)
OYA, Hiroshi, Effect of resonances on admittance of an r-f plasma probe surrounded by an ion sheath, 20: 17552

P

PAABO, Maya, Dissociation of acetic acid-d_3 in aqueous solution and

related isotope effects, 20: 16458
PAAS, Herman J. Jr., Radiological appraisal of Monticello Project, San Juan County, Monticello, Utah, 20: 16729 (IDO-12049)
PADALKO, O. V., Structure of sintered Mo–ZrO_2 materials, 20: 17109
PAGANINI, L., Metallographic techniques for optical and electronic observation of Zr–2.5 Nb alloy, 20: 16959
PAGNON, P., Metoclopramide in treatment of roentgen disease, 20: 16163
PAL, B. K., $K^- + p \rightarrow \eta + \Lambda$ scattering near threshold, 20: 17376
PALENZONA, A., MX_3 intermetallic phase of rare earths with Hg, In, Tl, Pb, 20: 17060
PALMER, B. D., Fallout from nuclear explosion of October 16, 1964, 20: 16663 (TID-21470)
PALMER, D. W., Determination of nuclear reaction widths from reaction yield curves, 20: 17778
PALMER, Rita B. J., Stopping power of hydrogen and hydrocarbon vapors for α particles at 1 to 8 Mev, 20: 17277
PALMER, S. M., Polarography of solochrome violet rs-metal complexes at high pH. I., 20: 16406
PALMS, J. M., Ionization produced by energetic Ge atoms within a Ge lattice, 20: 17265
PAN, V. M., Effect of degree of purity of refractory metals on their melting points, 20: 17094
PANCHAPAKESAN, N., Low-energy interaction of Ξ^- with proton and deuteron, 20: 17389
PANDE, Lalit Kumar, S-wave baryon-baryon scattering in broken SU(3), 20: 17468
PANDHARIPANDE, V. R., Low-lying excited states in ^{115}In and ^{117}In, 20: 17766
PANDIT, L. K., Algebra of currents and K_{e3}, 20: 17405
PANDIT, L. K., Algebra of currents and low-energy $K\pi$ interaction, 20: 17470
PANFILOVA, G. A., Effect of meteorological conditions on effectiveness of radioactive pollutant collection, 20: 16656
PANKOV, V. G., Tangential channels and construction of thermal column in VVR-M reactor, 20: 18139
PANONTIN, J. A., High-energy fission of ^{238}U, 20: 17790
PANSARE, M. G., Instrumentation for control and safety of zero energy reactor Zerlina, 20: 18149
PANT, L. M., Diffuse x-ray scattering from neutron-irradiated graphite, 20: 17130
PANZERI, D., Preliminary neutronic project of PRO-II core (UO_2–stainless steel), 20: 18091 (RT/FI(65)45)
PAPADAKIS, A. C., Charge collection in certain types of semiconductor radiation detectors, 20: 16885
PAPASTAMATIOU, H. J., Vector-meson dominance and $U_{6,6}$, 20: 17457
PARFENOV, Yu. D., Distribution of U in dogs at long periods after inhalation of U_3O_8, 20: 16184
PARILLE, D., Liquid metal-refractory reaction studies, 20: 16984
PARISI, B., Biosynthesis of gibberellic acid-^{14}C and 3,4-glucose-^{14}C, 20: 16193 (EUR-2539.i)
PARKER, F. L., Project Salt Vault: design and demonstration of equipment, 20: 18165 (ORNL-P-1987)
PARKER, F. L., Project Salt Vault, 20: 18169
PARKER, P. D., Properties of the 4.77- and 5.16-Mev states of ^{10}B, 20: 17761
PARKER, P. D., ^{3}He + p elastic scattering below 1 Mev, 20: 17771
PARKINSON, Michael, Meson production in $\bar{p}N$ annihilation, 20: 17396
PARKS, J. E., Portable scaler, 20: 16846
PARR, W. H., Changes in ^{137}Cs retention and routes of elimination as effected by external factors, 20: 16180
PARRA, C., Radiosensitivity of calcifying Malherbe's epithelioma, 20: 16308
PASCARU, Ioncov, Paramagnetic centers produced in irradiated polycrystalline $Mo_7O_{24}(NH_4)_6 \cdot 4H_2O$, 20: 16529
PASCHALL, R. K., Age of fission neutrons to In resonance energy in Fe–H_2O mixtures. I., 20: 17659
PASCHALL, R. K., Prog. rpt. on tungsten resonance integrals and Doppler coefficients, 6–12/65, 20: 18045 (AI-66-16)
PASSARI, L., Low-frequency internal friction of Al–Al_2O_3 dispersed-phase alloys (SAP), 20: 17065
PASSE, Jean, Measurement of periodic variation of neutron flux density in a nuclear reactor, 20: 18043
PASTUKHOVA, Z. V., Radioactive molybdenum isotopes, 20: 16917
PASZTOR, Laszlo C., Comparison of neutron-activation analysis and hot-extraction analysis of oxygen content of steel, 20: 16400
PATAKI, Laszlo, Solvent effect in isotope exchange reactions. III., 20: 16502
PATANKAR, A. V., ESR of color centers in γ-irradiated planar lead halides, 20: 16531
PATH, M. C., Hematological complications of polycythemia vera and treatment with radioactive phosphorus, 20: 16241
PATHAK, M. A., Effect of single dose of uv radiation on epidermal melanocytes, 20: 16261
PATLA, N., Measurement of quantum efficiency of scintillation counters for x rays, 20: 16836
PATRICK, Richard M., Performance characteristics of a magnetic annular arc, 20: 16627
PATRO, A. P., Backscattering of electrons from phosphors, 20: 16867
PATWARDHAN, P. K., New design of ratio circuit for fission-fragment study, 20: 17870
PATZELT, P., Comparison of observed delayed-neutron abundances with calculated fission yields of neutron precursors, 20: 17831
PAURI, M., Canonical realizations of Lie symmetry groups, 20: 16939
PAVLICHENKO, O. S., Bremsstrahlung in infrared region from plasma of electrodeless induction discharge, 20: 17931
PAVLINCHUK, V. A., Pairing effects in fission of even-even compound nuclei near the threshold, 20: 17847
PAYNE, J. R., Design and fabrication of integral coolant passage cryogenic coils for high power density, 20: 17874 (CONF-650922, pp 630-42)
PEACOCK, D. E., Temperature and strain-rate dependence of flow stress of solution-hardened Nb alloy, 20: 17082
PEARSON, Dorothy, Treatment of tumors in children by radiotherapy, 20: 16306
PEASLEE, D. C., Boson masses, 20: 17393
PEEBLES, P. J. E., Primeval helium abundance and primeval fireball, 20: 17245
PEED, W. F., Plasma physics, 20: 17889 (ORNL-3908, pp 52-89)
PEEK, James M., Proton-hydrogen atom system at large distances, 20: 17264
PEEK, James M., Proton-hydrogen atom system at large distances, 20: 17303
PEGUSHEVSKII, V. I., Fission cross sections of ^{181}Ta, Re, Pt, ^{197}Au, Pb, Bi, Th, ^{235}U and ^{239}U for protons at 150 to 660 Mev, 20: 17838
PEHL, R. H., Mass of ^{8}He from the four-neutron transfer reaction ^{26}Mg(α,^{8}He)^{22}Mg, 20: 17794
PENNER, S., Measurements of ion-optical properties of high-resolution spectrometer for electron scattering, 20: 16808 (CONF-650922, pp 154-63)
PENNY, S. K., Inelastic effects in stripping and other direct reactions, 20: 17692 (ORNL-TM-1414)
PENSELIN, S., Measurement of g_J factor of $^5D_4$ ground state of ^{56}Fe, 20: 17280
PERCHARD, Claudine, Vibration spectra of imidazole, imidazole (D)-1, imidazole (D_3)-2,4,5, and imidazole (D_4). I., 20: 16499
PERCHARD, Claudine, Vibration spectra of imidazole, imidazole (D)-1, imidazole (D_3)-2,4,5, and imidazole (D_4). II., 20: 16500
PERDIJON, J., Rapid and nondestructive determination of oxygen in steels by radioactivation, 20: 16357
PERELOMOV, A. M., Lorentz group as a dynamic symmetry group of the hydrogen atom, 20: 17283
PEREZ GARCIA, M., Analysis of polyphenyls by gas chromatography. I., 20: 16341
PERFILOV, N. A., Nuclear fission at high and medium energy of excitation, 20: 17836
PERKINS, O. J. E., Measurement of critical mass of enriched U in reflectors of wood, concrete, polyethylene, and water, 20: 16721 (AWRE-NR-1/66)
PERKINS, W. H., Advances in radioisotope instrumentation, 20: 16855
PERKO, Lawrence Marion, Asymptotic matching in the restricted three-body problem, 20: 17584
PERLA, Harold F., Underground highway and parking garage and blast shelter for Manhattan Island, 20: 16623 (ORNL-TM-1381)
PERRET, R., Observations of primary defects in crystals of LiF irradiated with thermal neutrons at 77°K, 20: 18007
PERRIN, G., Analysis of fission cross section of ^{233}U for neutrons between 1.7 and 30 ev, 20: 17853
PERUCCA, G. P., Preparation of ^{32}P-labeled compounds from carrier-free ^{32}P, 20: 16551
PERVYKH, V. G., X-ray and infrared study of perrhenate tetrahydrates of rare earths and yttrium, 20: 16473
PESKIN, Richard L., Prog. rpt. on gas-solid suspension, 9–12/65, 20: 16606 (TID-22621)
PESSALL, N., Potential of interstitial compounds for high-field superconducting magnets, 20: 17589 (CONF-650922, pp 541-9)
PETERMANN, P., Intercomparison of pathological fractures in beagles injected with ^{226}Ra, ^{228}Ra, ^{239}Pu or ^{90}Sr, 20: 16253
PETERS, C. W., BF_3 counters for use in field instrumentation, 20: 16895
PETERS, Theo, Electric arc in a supersonic plasma jet, 20: 17904
PETERSEN, D. F., Neutron activation of sulfur in hair: application in a nuclear accident dosimetry study, 20: 16758
PETERSON, F. L., Power supply for MURA magnet modeling program, 20: 17203 (CONF-650922, pp 776-8)
PETERSON, Richard L., Radioisotope techniques in stream pollution problems in pulp and paper industry, 20: 16921 (TID-22627)
PETILLAT, Georges, Machine for extraction of nuclear cartridges, 20: 16598
PETRALIA, S., Energy and angular distributions in ^{20}Ne(n,α)^{17}O reaction

at 14 Mev, 20: 17743
PETRASOVA, Marie, Contamination of biosphere by ^{137}Cs from weapon test fallout, 20: 16682
PETROCK, K. F., Effect of variation of airborne radon daughter concentration on whole-body counter background, 20: 16665 (UCRL-14534, pp 23-7)
PETROV, K. I., X-ray and infrared study of perrhenate tetrahydrates of rare earths and yttrium, 20: 16473
PETROV, L. A., Proton emitters among Te isotopes, 20: 17687 (JINR-P-2514)
PETROV, M. M., Dispersion theory of magnetic dipole photo-splitting of the deuteron, 20: 17408
PETROV, Yu. V., Resonance radiation from liquid helium, 20: 17638
PETRUKHIN, V. I., Search for $\pi^0 \to 3\gamma$ decay, 20: 17340 (JINR-P-2322)
PETRYANOV, I. V., Properties of fibrous filters in rarefied air, 20: 16654
PETUCHOV, V. A., Method of investigating betatron oscillation resonances, 20: 17221
PFANNEBECKER, George William, Analytical investigation of MHD boundary layers with Hall effects, 20: 17534
PFEIFFER, K., Device for calculation of γ shielding problems, 20: 17969
PFENDER, E., Measurement of thermal radiation from an argon plasmajet, 20: 17898
PHILLIPS, G., Rapid dissolution of PuO_2 by a Na peroxide sinter and determination of PuO_2 content, 20: 16350
PHILLIPS, G. M., Computation of x-ray diagnostic exposure tables, 20: 16751
PHILLIPS, N. E., Superconductivity of beta uranium, 20: 17095
PHILLIPS, R. J. N., Tests for T invariance in N-N scattering, 20: 17337 (AERE-R-5138)
PHILLIPS, T. L., Radiation effects on renal enlargement in the mouse, 20: 16282
PHILLIPS, T. L., Suppression of DNA synthesis in weanling rat kidneys by short-term fasting, 20: 16158 (AD-628360)
PHIPPS, C., Liquid metal-refractory reaction studies, 20: 16984
PIALOUX, André, High-temperature x-ray study in controlled atmosphere of system uranium–oxygen, 20: 16471
PICCIARELLI, V., $\pi^+ p$ interactions at 1.6 Bev, 20: 17374
PICCOT, Denis, Determination of silicon by neutron radioactivation and application to nuclear graphites and alumina, 20: 16360
PICHAT, Louis, Preparation of α and β anomers of desoxy-2′ adenosine, labeled with ^{14}C, 20: 16545
PICK, Robert, Calculation of pair-interaction function in some normal metals, 20: 17008 (CEA-R-2820)
PICON, M., Manganese carbides, 20: 17030 (LA-tr-66-1)
PIEPER, A. G., Automated logging and processing of NRL cyclotron magnetic field data, 20: 17188 (CONF-650922, pp 415-20)
PIEPER, A. G., Prog. rpt. on NRL cyclotron, 9/65, 20: 17169 (AD-628928)
PIERCE, G. V., Controlled-potential polarography and coulometry as microanalytical techniques, 20: 16390
PIEROTTI, Theodore, Effect of fractionated x-ray doses on hemogram and protein formula of the mouse, 20: 16224 (CEA-R-2848)
PIERQUIN, B., Symptomatic medication associated with radiotherapy, 20: 16319
PIET, G. J., Measurement of radioactivity in effluents of a gas chromatograph, 20: 16371
PIETERMAAT, F., Plasma and its technical applications, 20: 16593
PIFER, James W., Neoplasms following irradiation of the head, 20: 16245
PIKEL'NEV, S. B., Quarks: astrophysical and physicochemical aspects, 20: 17411
PIKHTELEV, R. N., Measurement of π^+ meson lifetime, 20: 17346 (JINR-P-2534)
PINDER, D. N., Slow-wave propagation in a nonuniform plasma, 20: 17913
PINON, Y., Fast period meter with integrated circuits, 20: 18029
PIPER, J., Preparation and properties of superconducting Nb–Sn sandwiches, 20: 17649
PIRET, J., Inorganic ion exchanger for separation of Cs from high-level radioactive wastes, 20: 16570
PISUT, J., Effect of inelastic processes on the P_{11} phase shift in πN scattering, 20: 17355
PITAEVSKII, L. P., Dynamics of a superfluid Fermi gas, 20: 17647
PIXLEY, R. E., Properties of the 4.77- and 5.16-Mev states of ^{10}B, 20: 17761
PLACAK, O. R., Off-site surveillance for Salmon Event of Project Dribble, 20: 16743 (VUF-1021)
PLACIDI, M., Beam optics computation for particle transport systems, 20: 17211 (LNF-65/45)
PLATT, A. M., Waste solidification engineering prototypes technical program, 20: 18158 (BNWL-SA-467)
PLATZMAN, R. L., Generalized oscillator strength and relation to inelastic scattering of charged particles, 20: 17306
PLETNEV, V. D., Dynamics of a geomagnetic trap and origin of the earth's radiation belts, 20: 17547
PLEVE, A. A., Isomeric yield ratio for the 14-ms fissioning isomer from deuteron irradiation of, 20: 17857
PLINGEN, K.-G., Lifetime of the $^{11}/_2$ three-particle state of ^{177}Hf, 20: 17811
PLOSTINARU, D., Angular distributions from $^{12}C(\alpha,n)^{15}O$ reaction at 14 Mev, 20: 17803
PLYUSHCHEV, V. E., Cerium perrhenate and its crystal hydrates, 20: 16440
PLYUSHCHEV, V. E., X-ray and infrared study of perrhenate tetrahydrates of rare earths and yttrium, 20: 16473
POBELL, F., Isomeric shift of the 23.8-kev γ line of ^{119}Sn in various alloy phases, 20: 18004
PODERGIN, V. A., Aluminothermic production of aluminum–cerium alloys, 20: 16964
PODGORETSKII, M. I., Possible experiments aimed at testing isotopic structure of electromagnetic interaction, 20: 17428 (JINR-P-2498)
PODGORETSKII, M. I., Radiation anisotropy of the hydrogen atom in an electric field, 20: 17282
PODOBNIK, B., Determination of Cd in U compounds by atomic absorption spectrophotometry, 20: 16368
POENARU, D., Angular distributions from $^{12}C(\alpha,n)^{15}O$ reaction at 14 Mev, 20: 17803
POENARU, D., Isomeric yield ratio for the 14-ms fissioning isomer from deuteron irradiation of, 20: 17857
POENARU, D., Semiconductor radiation detectors. III-a., 20: 16889
POGUDIN, A. P., Making the coefficients of aerosol collection by horizontal sheets more precise, 20: 16657
POIRIER, C. P., $\pi^+ p$ interactions at 450 Mev, 20: 17384
POKORNY, J., Contributions to chemistry of rare earths. XVII., 20: 16426
POKORNY, J., Contributions to chemistry of rare earths. XVIII., 20: 16427
POLAK, L. S., Kinetics and thermodynamics of chemical reactions in low-temperature plasma, 20: 17959
POLIEVKTOV-NIKOLADZE, N. M., Non-Einsteinian gravitation, 20: 17568
POLIKANOV, S. M., Isomeric yield ratio for the 14-ms fissioning isomer from deuteron irradiation of, 20: 17857
POLLACK, Gerald L., Effect of normal-fluid motion on third sound in liquid-helium films, 20: 17616
POLLACK, I., Argonne National Laboratory's pion focusing horn, 20: 17198 (CONF-650922, pp 650-6)
POLLACK, I., Selection of water-cooled conductors for d-c magnets, 20: 16585 (CONF-650922, pp 349-55)
POLLARD, I. E., Hydrogen condensation on to liquid helium-cooled surfaces, 20: 16631
POLLARD, J. P., Function arising from second-order approximations to the effective resonance integral, 20: 17650 (AAEC/E-144)
POMILLA, Frank R., Double-inelastic collisions of excited H atoms with excited H atoms, 20: 17290
PONOMAREV, B. K., Magnetostriction of rare earth metals in paramagnetic, antiferromagnetic and ferromagnetic regions, 20: 18012
PONOMAR'KOV, Y. I., Experimental radiation sickness induced with ^{210}Po, 20: 16258
PONYATOVSKII, E. G., Deformed Zr–Ti–O–Fe alloy for high-pressure chambers, 20: 17003
POP, Iulia, Paramagnetism of polycrystalline metallic Gd, Ho, and Er, 20: 17098
POPESCU, I., Diffusion theory of low-voltage arc plasma, 20: 17907
POPESKU, Ion M., Optical orientation of ^{201}Hg atoms using the 1850 A line, 20: 17755
POPOV, B. M., Autoionization of nitrogen and oxygen ions after passage through a solid, 20: 17262
POPOV, Ch., Determination of arsenic in ores and rocks with high Mn by neutron activation analysis, 20: 16364
POPOV, N. I., Nature of accumulation of atmospheric aerosols on ocean surfaces, 20: 16706
POPOV, V. S., Lorentz group as a dynamic symmetry group of the hydrogen atom, 20: 17283
POPOVA, N. M., Phase equilibrium in ternary Zr–Co–C and Nb–Fe–C systems, 20: 17086
POPOVICI, M., Optical properties of the neutron crystal spectrometers, 20: 16874
POPPEI, H., Inhibition of absorption of glucose in small intestine of rats by x radiation, 20: 16274
PORTER, E. H., Radium implant dosimetry with small digital computer, 20: 16748
PORTMANN, J., X-inflammation irradiation, 20: 16314
POSTMA, H., Injection and accumulation: single-pass experiments (DCX-1), 20: 17886 (ORNL-3908, pp 1-17)
POTANINA, L. V., Effects of preliminary γ irradiation and heating on activity of the $Ag/Ag_2C_2O_4$ catalyst, 20: 16523
POTTER, D. L., Microgram surface density measurements by observation of proton-produced x rays, 20: 17051
POTTS, Kevin T., Prog. rpt. on derivatives of five-membered heterocycles as radiation-protective agents, final, 12/65, 20: 16490 (TID-22681)
POTURAJ-GUTNIAK, S., Salt-boiling fast reactor "SAWA", 20: 18088

(INR-669/C)
POWELL, Brian W., Analysis of track chamber photographs using flying spot digitizers, 20: 16840
POWER, Geoffrey, Plane gasdynamic flows with orthogonal magnetic and velocity field distributions, 20: 17532
POWERS, Edward Joseph Jr., Anomalous diffusion across a magnetic field in an r-f discharge, 20: 17954
POWERS, R. J., M1 and E2 hyperfine structure in muonic K and L x rays of bismuth, 20: 17792
PRADOS, J. W., Computer program for predicting coated-particle behavior, 20: 18076 (ORNL-TM-1385)
PRAEG, W. F., Control of ZGS magnet current, 20: 17215
PRAKASH, Satya, Ultrasonic velocity in aqueous solution of thorium nitrate, 20: 16477
PRANAL, Y., Measurement and analysis of fission cross section of ^{239}Pu from 0 to 5 kev, 20: 17851
PRASAD, K. G., Low-lying excited states in ^{115}In and ^{117}In, 20: 17766
PRASILOVA, Jarmila, Substoichiometric determination of manganese by neutron-activation analysis, 20: 16403
PREMACHANDRA, B. N., Thyroidal ^{131}I determination in the small laboratory animal, 20: 16179
PREPAROTA, G., Vector-meson dominance and $U_{6,6}$, 20: 17457
PRESSLEY, Robert J., Deuterium isotope effect on performance of europium chelate lasers, 20: 16781
PRESTWOOD, R. S., Symmetry of neutron-induced ^{239}Pu fission in resonance region, 20: 17858
PRETSCH, J., German policy of reactor development, 20: 18111
PREVO, C. T., Energy absorption coefficients of dosimetric LiF, 20: 16829 (UCRL-14534, pp 1-7)
PREVO, C. T., Source of intermediate-energy neutrons for dosimeter calibration, 20: 16830 (UCRL-14534, pp 8-12)
PRICE, A. T., Quiet-day magnetic variations during the IGY, 20: 17545
PRICE, P. B., Ternary fission of heavy compound nuclei in thorite track detectors, 20: 17788
PRIME, M., K⁻-p interaction at 2.24 Bev/c, 20: 17383
PRITCHARD, Daphne H., Half life of ^{32}P, 20: 17712
PRIVOROTSKII, I. A., On pairing with an orbital moment $l \neq 0$, 20: 17646
PROKOSHKIN, Yu. D., Measurement of π^+ meson lifetime, 20: 17346 (JINR-P-2534)
PROKOSHKIN, Yu. D., Search for $\pi^0 \to 3\gamma$ decay, 20: 17340 (JINR-P-2322)
PROSDOCIMI, A., Fission cross-section measurement of ^{238}U and ^{239}Pu for low-energy neutrons, 20: 17854
PROSPERI, G. M., Analyticity properties of the scattering amplitude for a velocity-dependent potential, 20: 17449
PROSPERI, G. M., Canonical realizations of Lie symmetry groups, 20: 16939
PROSPERO, J. M., Determination of mixing and circulation in the ocean with radioactive tracers, 20: 16828 (TID-22763)
PROTASOV, V. S., The crystal structure of ternary phases in the Sc–Cu–Al system, 20: 17097
PROZOROVA, E. I., Elastic scattering of 5.5-Bev π mesons on protons, 20: 17360
PRUDEN, Brenda Lamont, ESR studies of irradiated nucleic acids and constituents of nucleic acids, 20: 16541
PRYOR, William Harold, Absorption of injected horse gamma globulin in rabbits following whole-body γ irradiation, 20: 16214 (AD-620438)
PSZONICKI, Leon, Precise titrimetric determination of uranium in high-purity uranium compounds, 20: 16401
PUCKETT, L. J., Ionization and charge-transfer cross sections for fast neutral He atoms (0.15 to 1.0 Mev), 20: 17301
PUDLOWSKA, B., g-Factor of 87-kev excited state in ^{155}Gd, 20: 17683 (INP-430/PL)
PUDOVKIN, I. B., Method for selecting cloud water samples using cyclone precipitations, 20: 16658
PUJANTE, A., Polarographic behavior of hafnium(IV) in aqueous-alcoholic mixtures, 20: 16445
PUSTOVOIT, L. T., Nature of chemical bond in rare earth dicarbides, 20: 17048

Q

QUEYROUX, F., Systems formed by lime with the oxides of type C rare-earth elements, 20: 17087
QUINN, E. P., Vibration of SEFOR fuel rods in parallel flow, 20: 18134 (GEAP-4966)

R

RABANI, Joseph, Reactivity of hydrogen atoms toward some cobalt(III) complexes in aqueous solutions, 20: 16526
RABICHEV, V. A., Logical-element system for reactor control, 20: 18031
RABINKOVA, E. V., Excretion of thymidine with urine in ^{90}Sr-affected rats, 20: 16201
RABINOFF, Carter V., Graphing self-absorption curves with ordinary γ absorption data, 20: 17966
RABINOVICH, M. S., States with population inversion in a self-compressed discharge, 20: 17924
RACAH, G., Low odd levels of erbium I., 20: 17261
RACZKA, R., Discrete degenerate representations of non-compact unitary groups, 20: 17426 (IC-66/16)
RADELOFF, J., Lifetime of the $^{23}/_{2}$ three-particle state of ^{177}Hf, 20: 17811
RADU, Minodora, Modification of electrical conductivity of irradiated biopolymers, 20: 16194
RAE, E. R., Cross sections for low-energy neutron-induced fission, 20: 17850
RAEUBER, A., ESR of sulfur and selenium radicals in alkali halides, 20: 18005
RAFIQUE, M. M., Bibliography on Pu, 20: 16328 (AECL-Pak/Lib-10)
RAGHAVAN, R. S., Beta-gamma circular polarization correlation of ^{122}Sb, 20: 17677 (COO-1420-112)
RAGHAVAN, R. S., Nuclear-resonance fluorescence in ^{159}Tb, 20: 17789
RAGHAVAN, R. S., Search for higher-order effects in allowed β transitions, 20: 17678 (COO-1420-113)
RAGUPATHY, S., Multichannel analysis system for low levels of fission products in reactor coolants, 20: 16898
RAHMAN, Saidur, Effect of γ irradiation on seeds of Corchorus capsularis and C. olitorius, 20: 16217 (AECD-AG-7)
RAINWATER, J., Magnetic dipole and electric quadrupole hyperfine effects in ^{209}Bi muonic x rays, 20: 17793
RAIS, J., Stability constants of complexes from non-equilibrium distribution of metal between aqueous phase and ion exchanger, 20: 16481
RAIZER, Yu. P., Breakdown and heating of gas by a laser beam, 20: 17531
RAJKISHORE, M. Rajagopalan, Neutron-induced fission of ^{227}Ac, ^{231}Pr, and ^{237}Np: mass distribution, 20: 17861
RAKAVY, G., Direct capture mechanism for intermediate-energy nucleons, 20: 17737
RAMACHANDRAN, R., Quasi-free proton-proton scattering in light nuclei at 460 Mev, 20: 17741
RAMAMURTY, G. V. N., Effect of Tl concentration on performance of NaI(Tl) scintillation crystals, 20: 16850
RAMAN, A., Tantalum–aluminum system, 20: 17034
RAMANIAH, M. V., High-energy fission of ^{238}U, 20: 17790
RAMANIAH, M. V., Neutron-induced fission of ^{227}Ac, ^{231}Pr, and ^{237}Np: mass distribution, 20: 17861
RAMASESHAN, S., Use of anomalous scattering of neutrons in solution of crystal structures containing large molecules, 20: 17041
RAMM, C. A., Magnet technology in high-energy experimental physics, 20: 17176 (CONF-650922, pp 27-55)
RAMSBOTTOM, B., Effect of sodium alginate on uptake of Sr-85 from G-I tract, 20: 16173 (PG-Report-686)
RAND, R. E., Measurement of wide-angle bremsstrahlung at 28 Mev, 20: 17798
RANDALL, D. D., An achromatic 90° bending magnet system, 20: 17200 (CONF-650922, pp 715-22)
RANDLES, J., Feedback due to elastic waves and Doppler coefficient during excursions of pulsed fast reactor, 20: 18056
RANKOWITZ, S., Multiple spectrometer control by computer, 20: 16869
RAO, C. L., Neutron-induced fission of ^{227}Ac, ^{231}Pr, and ^{237}Np: mass distribution, 20: 17861
RAO, E. V. R., Ionization chambers for reactor control, 20: 16897
RAO, M. N., Fallout from nuclear explosion of October 16, 1964, 20: 16663 (TID-21470)
RAPAPORT, J., Stripping analysis of ^{46}Ti(d,p)^{47}Ti reactions, 20: 17776
RAPHAEL, R., Decay of nuclear giant resonance states following electroexcitation, 20: 17757
RASHID, M. A., Particle masses and SU(6) symmetry breaking, 20: 17480
RASMUSSEN, J. O., Internal conversion, 20: 17795
RASTOGI, R. C., Prog. rpt. on fixation of low- and medium-level radioactive waste in stable solid media, 2–10/65, 20: 18166 (TID-22531)
RASZL, Karoly, Reactor for university instruction, 20: 18141
RATNER, L. G., A precision system for measuring wire trajectories in magnetic fields, 20: 17196 (CONF-650922, pp 497-504)
RAU, R. R., K⁻-p interaction at 2.24 Bev/c, 20: 17383
RAUSCH, Doyle William, Initial oxidation of tungsten and tantalum, 20: 16987
RAVERA, Oscar, Measurement of ^{54}Mn in Unio pictorum of Lake Maggiore, 20: 16185
RAVIN, V. K., Effect of uv irradiation on temperate phage-bacteria complex, 20: 16270
RAVINDRAN, N., Neutron-induced fission of ^{227}Ac, ^{231}Pr, and ^{237}Np: mass distribution, 20: 17861
RAVIV, A., Synthesis and isotopic analysis of $CH_3{}^{18}OH$ and $CH_3{}^{17}OH$, 20: 16547
RAVOIRE, Jean, Catalysis by alkaline amides of isotopic exchange between hydrogen and liquid ammonia, 20: 16444

RAY, J. A., Atomic and molecular cross sections, 20: 17253 (ORNL-3908, pp 90-9)
READ, A. H., Computer techniques used to study charged particle trajectories in magnetic field, 20: 17906
REAGAN, P. E., Evaluation and irradiation effects studies on pyrolytic-carbon-coated fuel particles, 20: 17127 (ORNL-3923)
RECHT, H. L., Prog. rpt. on radiation effects on Ag and Zn battery electrodes, 7–10/65. II., 20: 17115 (AI-65-264)
RECHT, H. L., Prog. rpt. on radiation effects on Ni–Cd electrodes. III., 6–9/13/64, 20: 17124 (N-65-17608)
REHFELD, C. E., Intercomparison of pathological fractures in beagles injected with ^{226}Ra, ^{228}Ra, ^{239}Pu or ^{90}Sr, 20: 16253
REID, C. N., Dislocation widths in anisotropic bcc crystals, 20: 17033
REID, W. B., Pulse-shape discrimination in organic scintillators, 20: 16839
REILLY, Pamela C., Evaluation of existing criteria for judging quality of science exhibits, 20: 18178 (TID-22703)
REIMANN, G., Photoproduction of pion and nucleon resonances up to 5.5 Bev, 20: 17368
REIMANN, R., Nuclear resonance magnetometer with frequency modulation, 20: 16791
REINER, A. S., Bound on coupling constant from unitarity and analyticity, 20: 17477
REINES, Frederick, Neutrinos from atmosphere and beyond, 20: 17323
REINHARDT, R. G., Injection and accumulation: single-pass experiments (DCX-1), 20: 17886 (ORNL-3908, pp 1-17)
RENNER, J., Structure of tantalum suboxides, 20: 17059
RENZLER, G., Current detectors for the linac with impulse transformers, 20: 17210 (LNF-65/37)
RETVARI, Laszlo, Thermodynamic characteristics of an organic cooling agent, 20: 16493
REVOLINSKY, E., Critical currents in superconducting single-crystal NbSe, 20: 17609
REYNOLDS, G. F., Polarography of solochrome violet rs-metal complexes at high pH. I., 20: 16406
REYNOLDS, Geo. T., Single electron light pulse size distribution from cascaded image intensifier, 20: 16824 (NYO-3406-3)
RHYNE, M. K., Computer program for Fermi surface studies, 20: 17973 (IS-1106)
RIBRAG, M., Mass spectra of fission fragments after prompt neutron emission, 20: 17866
RICHARD, C., Focused microwave systems for plasma diagnostics, 20: 17881 (N-65-19804)
RICHARDSON, A. S., In-tank irradiation facilities at test reactor area, 20: 18135 (IDO-17135)
RICHT, A. E., Interim postirradiation examination of a europium-bearing control rod from the stationary medium power reactor, 20: 17129 (ORNL-TM-1407)
RICKER, C. W., Neutron fluctuation measurements at ORNL, 20: 18048 (ORNL-P-1967)
RIDER, P. E., Solid solubility of gold-rich rare-earth and lanthanide-rich magnesium alloys, 20: 17016 (IS-1175)
RIEDEL, J., Princeton-Pennsylvania accelerator standard magnet current regulators, 20: 17205 (CONF-650922, pp 817-22)
RIEDEL, Jozef Tadeusz, Investigation of boron isotopes, 20: 16915
RIEPE, G., Distribution system for multichannel pulse-height analyzer, 20: 16817 (JUL-270-RB)
RIESE, Gretchen R., Manganese carbides, 20: 17030 (LA-tr-66-1)
RIESSBECK, K.-H., Determining radiation responses of organism in tumor therapy, 20: 16209
RIETJENS, L. H. Th., Thermonuclear investigations. I., 20: 17926
RIETJENS, L. H. Th., Thermonuclear investigations. III., 20: 17928
RIGGSBY, William S., Effects of radiation on serum enzymes and trace elements in large animals, 20: 16222 (AFWL-TR-65-112)
RIJK, J., Rectifier power supplies for ZGS experimental magnets, 20: 17204 (CONF-650922, pp 808-16)
RINDI, A., Radiation measurements around an insufficiently shielded target, 20: 17212 (UCRL-Trans-1305)
RINK, R. E., Terminal properties of Alfven waveguides, 20: 17522
RISCH, Rudolf, Energy losses in feeding of superconducting coils with magnetic flux pumps, 20: 17630
RISPOLI, B., Design and performance of neutron thermopiles, 20: 16899
RITCEY, G. M., Uranium and copper extraction by liquid ion exchange, 20: 16572
RITCHIE, E. E., Evaluation of dissolvable epoxy systems for remote metallographic evaluations, 20: 16948 (ORNL-TM-1161, pp 103-11)
RITTENHOUSE, John B., Space materials handbook, 20: 16944 (NASA-SP-3025)
RITUS, V. I., Ionization of systems bound by short-range forces under action of an EM wave, 20: 17284
RIVERA, Joseph, Prog. rpt. on fallout program, 9–12/65, 20: 16662 (HASL-165)
RIVIERE, Andre, Sedimentological significance of natural radioactivity of beaches of Gulf of Lion, 20: 16669
ROBASCHIK, D., Plus-parity mesons and the 189-plet of SU(6), 20: 17339 (JINR-E-2557)
ROBERTS, A., Polarization of Σ^0 particles in reaction $\pi^- + p \rightarrow K^0 + \Sigma^0$ at 1.5 and 1.8 Bev/c, 20: 17382
ROBERTS, E., Argonne National Laboratory's pion focusing horn, 20: 17198 (CONF-650922, pp 650-6)
ROBERTS, F. P., Purification of rare earths from Hanford wastes by solvent extraction, 20: 16329 (BNWL-187)
ROBERTS, J. B. G., Impact of plasma on a dipole magnetic field, 20: 17551
ROBERTS, M. J., Moment relations for Schroedinger two-body cross sections, 20: 17483
ROBINSON, Alan Hedley, Transport calculation of the disadvantage factor, 20: 17668
ROBINSON, E., High-temperature testing of graphite helical-screw expanders and compressors, 20: 16591 (UCRL-14660)
ROBINSON, K. W., Possible use of the CEA directly as a colliding beam facility, 20: 17173 (CEAL-1029)
ROBINSON, P. S., Production of radioactive sources by electrospraying, 20: 16553
ROBINSON, R. A., Dissociation of acetic acid-d_3 in aqueous solution and related isotope effects, 20: 16458
ROBINSON, W. C., Thermodynamic properties of uranium oxycarbides, 20: 16449
ROBOTTI, Aurelio C., Experimental research on electric propulsion. VII., 20: 16629
RODGERS, A. L., Prompt-neutron emission from ^{235}U fission fragments, 20: 17824
RODGERS, A. L., Simultaneous measurements of flight times and energies of fission fragments, 20: 17864
ROESCH, D. L., Handling α-active specimens in the electron microprobe x-ray analyzer, 20: 16554
ROGANOV, V. S., Observation of atomic muonium in crystalline quartz, 20: 17361
ROGUIN, A., Fission-product detectors for detection of burst fuel element cans, 20: 18036
ROGUIN, A., Radiation detectors for reactor control, 20: 16903
ROKHLENKO, A. V., Bound states of a nonlocal separable potential, 20: 17495
ROKHLIN, L. L., Magnesium alloys containing neodymium, 20: 17110
ROLL, P. G., Cosmic background radiation at 3.2 cm—support for cosmic black-body radiation, 20: 17317
ROMA, Carlo, Direct conversion into electrical energy of γ radiation, 20: 17331
ROMAN, Harriet R., Use of image-splitting eyepiece, 20: 16952 (ORNL-TM-1161, pp 182-91)
ROMAN, P., Goldstone behavior in some model theories, 20: 17473
ROMAN, R., Fabrication techniques of coils in the Zero-Gradient Synchrotron complex, 20: 17186 (CONF-650922, pp 356-65)
ROMANOWSKI, T. A., Polarization of Σ^0 particles in reaction $\pi^- + p \rightarrow K^0 + \Sigma^0$ at 1.5 and 1.8 Bev/c, 20: 17382
ROMETSCH, R., Eurochemic plant and role in startup of European fuel cycles, 20: 16558
RONA, P., Synthesis and isotopic analysis of $CH_3{}^{18}OH$ and $CH_3{}^{17}OH$, 20: 16547
ROONEY, D. M., Metallic inclusions in UO_2, 20: 16953 (ORNL-TM-1161, pp 249-66)
ROOSE, U. J., Digital recording system of air shower experiment at Kiel, 20: 16873
ROOT, Richard M., Microfield approximations in plasmas, 20: 17896
ROPERS, Jean, Guide tubes for nuclear reactors, 20: 18039
ROSA, R. J., Scaling laws and envelope of allowable operating conditions for MHD generator using inert gases, 20: 17328
ROSATELLI, Carlo, Milan University's cyclotron, 20: 17214
ROSE, B., Measurements of proton-nucleus triple scattering parameters near 140 Mev, 20: 17738
ROSEN, Carol Zwick, Specular reflection of phonons in superfluid He below 0.33°K, 20: 17648
ROSEN, S. P., Theory of parity-violating nonleptonic decay, 20: 17398
ROSENBERG, Theodore Jay, Spatial and temporal characteristics of auroral zone electron precipitation, 20: 17557
ROSENKILDE, Per, Hormonal dependency of molting in amphibians, 20: 16252
ROSESCU, Th., Integral nucleus method in nuclear reactor physics, 20: 18069
ROSNER, Carl H., Stranded niobium–tin wire solenoids, 20: 17593 (CONF-650922, pp 597-603)
ROSNER, Jonathan Lincoln, Exchange of massive particles in Bethe-Salpeter equation, 20: 17502
ROSS, Daniel L., Deuterium isotope effect on performance of europium chelate lasers, 20: 16781
ROSS, John, Applications of R-matrix theory to reactive and elastic molecular scattering, 20: 17259

ROSS, Ronald R., Production and decay properties of $K_3^*(892)$, 20: 17403
ROSSET, Robert, Properties of the aminodiacetate resin Dowex A-1. II., 20: 16358
ROSYANOV, S. P., Accumulation of ^{90}Sr and ^{137}Cs in soils of Leniagrad region, 20: 16702
ROTHBERG, J. E., Atomic interactions of muonium, 20: 17297
ROTHE, W., Summary of working session on personnel dosimetry, Berlin, 11/64, 20: 16827 (SZS-9(1965))
ROTHE, William E., Prog. rpt. on ionizing radiation, injury, prevention, and treatment, annual, 10/65, 20: 16303 (AD-626384)
ROUGE, Pierre, Supporting post for solid moderator pile of a nuclear reactor, 20: 18040
ROUQUEROL, Jean, Bound water of several high specific surface-area oxides, 20: 16413 (CEA-R-2703)
ROUSSEL, F., Cladding temperatures used in automatic control for a power reactor, 20: 18105
ROUX, D. P., Neutron fluctuation measurements at ORNL, 20: 18048 (ORNL-P-1967)
ROWCLIFFE, A. F., Helium bubbles in irradiated 20 Cr–25 Ni–Ti stainless steel, 20: 17141
ROWE, M. W., Noble gases from Peace River, Lalande, and Achilles meteorites, 20: 16672
ROWE, M. W., Xenon anomalies in Pasamonte meteorite, 20: 17239
ROWELL, J. M., Electron interference in a normal metal induced by superconducting contacts, 20: 17621
ROWENHORST, D. D., Prog. rpt. on fabrication of W alloy tubing, 10/23/65–1/1/66, 20: 16989 (COO-1518-2)
ROY, Rustum, Prog. rpt. on crystal chemistry, 8/13–11/13/65, 20: 17007 (AD-627468)
ROYDEN, H. N., Prog. rpt. on tungsten resonance integrals and Doppler coefficients, 6–12/65, 20: 18045 (AI-66-16)
ROYET, J., 4500-Gauss superconducting magnet for corpuscular ionography experiments, 20: 17594 (CONF-650922, pp 604-10)
RUD, B. M., Nature of chemical bond in rare earth dicarbides, 20: 17048
RUDAKOV, L. I., Quasilinear theory of current instability in a plasma, 20: 17950
RUDAVSKII, E. Ya., Experimental observation of fourth sound in ^3He–^4He solutions, 20: 17159
RUDD, M. Eugene, Fine structure in energy spectra of electrons from gases bombarded by positive ions, 20: 17292
RUDENKO, N. P., Radioactive molybdenum isotopes, 20: 16917
RUDENKO, N. S., Isotropic spark chamber, 20: 16860
RUDIN, Hermann, Reaction $^3He(d,p)^4He$ induced with polarized deuterons from 310 to 2935 kev, 20: 17749
RUDNITSKII, Yu. P., Excitation transfer from crystal lattice to rare earth ions, 20: 18010
RUDO, F. S., Non-destructive electrical method of studying the density distribution of a randomly packed bed, 20: 18018 (CONF-651101-73)
RUEFENACHT, J., Experimental studies on the degradation phenomena in small superconducting coils of Nb-25 Zr, 20: 17629
RUEGG, H., C and T invariance and number of SU_3 amplitudes, 20: 17453
RUGGIERO, Umberto, Improvements and limitations in vapor cycle of Magnox reactors, 20: 18109
RULIS, Raymond J., Description and operation of spacecraft SERT I ion thrustor flight test, 20: 16625 (N-65-19272)
RUMFELDT, R. C., Cobalt-60 γ radiolysis of hydrogen halides at 77°K, 20: 16519
RUNGE, K., Magnetic dipole and electric quadrupole hyperfine effects in ^{209}Bi muonic x rays, 20: 17793
RUNKOV, O. V., Excitation and characteristics of Th spectrum in electrodeless discharge tubes, 20: 16464
RUSANOV, V. D., Drift waves of non-potential nature in a stationary magnetoacoustic plasma, 20: 17949
RUSCHER, J., Multiple-duration monostable multivibrator, 20: 16792
RUSHBROOKE, J. G., Decays of baryon resonances of any spin, 20: 17395
RUSSELL, D. S., Direct determination of small quantities of rare earth and yttrium oxides in thoria by emission spectroscopy, 20: 16393
RUSSO, G., Synthesis of ^{14}C-lanosterol and ^{14}C-desmosterol, 20: 16548
RUST, John H., Radiation hygiene, 20: 16296
RUTKEVICH, N. Ye., Deuteron and α-particle pickup in interaction between ^{10}B and ^{16}O, 20: 17815
RUVINSKII, M. A., Effect of excitons on scattering of neutrons by crystals, 20: 18006
RUZICKA, Jaromir, New principle of activation-analysis separations. X., 20: 16396
RUZICKA, Jaromir, Substoichiometric determination of manganese by neutron-activation analysis, 20: 16403
RUZICKA, Jiri, Equipment for measuring superconducting properties of superconductors for strong magnetic fields, 20: 17602
RYABOV, Yu. V., Interaction of neutrons with ^{235}U nuclei at 2 ev to 30 kev, 20: 17856
RYAZANOV, M. I., Quantum effects in multiple scattering, 20: 17497
RYDING, G., Charge transfer in proton-atomic H collisions above 50 kev, 20: 17302
RYE, Robert Orph, Carbon, hydrogen, and oxygen isotopic composition of hydrothermal fluids responsible for lead–zinc deposits, 20: 16634
RYON, A. D., Prog. rpt. on chemical technology, 11/64, 20: 16556 (ORNL-TM-1090)
RYVAL'CHENKO, M. K., Structure of sintered Mo–ZrO_2 materials, 20: 17109
RZEKIECKI, Roger, Sorption of ^{90}Sr on an aluminum oxide, 20: 16330 (CEA-R-2851)

S

SABU, D. D., Fallout from nuclear explosion of October 16, 1964, 20: 16663 (TID-21470)
SACTON, J., Production of hyperfragments from the interactions of 3.0- and 5.0-Bev/c K^- mesons with emulsion nuclei, 20: 17752
SADAGAPAN, V., Superconductivity in transition metal carbides, 20: 17607
SADAGOPAN, V., Superconductivity in close-packed intermediate phases of V–Ir, Nb–Ir, Nb–Rh, Ta–Rh, Nb–Pt, Ta–Pt, and other related systems, 20: 17624
SADEH, D., Synthesis and isotopic analysis of $CH_3{}^{18}OH$ and $CH_3{}^{17}OH$, 20: 16547
SADLER, A. M., Removal of radiostrontium from milk with tricalcium phosphate and resulting changes in milk composition, 20: 16382
SADOFSKY, J., Electrical properties of thorium carbides, 20: 17068
SAENKO, L. F., Search for parity nonconservation in nuclear γ transitions, 20: 17444
SAFARIK, I., ESR studies on trapped free radicals in irradiated aqueous H_2O_2 solutions, 20: 16512
SAFFORD, G. J., Thermal-neutron-induced fission of ^{235}U, ^{233}U, and ^{239}Pu, 20: 17863
SAFKO, John Lorne, Peratization of scalar particle-graviton interaction, 20: 17503
SAGAR, P., Effect of uv radiation on the oxidation of certain Krebs cycle substrates, 20: 16198
SAGE, Harold H., Duct ligation and small-dose x radiation, 20: 16316
SAHINI, M., Multiple scattering constant in emulsion at great cell lengths, 20: 16833
ST. LORANT, S. J., Residual nuclei observed in interactions of 25-Bev/c protons with heavy emulsion nuclei, 20: 17748
SAJI, Yoshio, Survey of nuclear reactions induced by 57-Mev protons. II., 20: 17725
SAKAI, Mitsuo, Prog. rpt. on INS isotope separator, 11/5/65, 20: 16928 (INSJ-92)
SAKISAKA, Masaketsu, Medium dependence of charge changing collisions for 9.7-Mev carbon ions, 20: 17724
SAKKA, Masatoshi, X-ray-induced shortening of life span of adult Sarcophaga peregrina, 20: 16291
SAKWA, W., Slip casting of powdered carbides, 20: 16997
SALAMA, M., Slow neutron spectrum of neutron beam from UA-RR-1 reactor, 20: 18147
SALMON, Royes, Shipping cost comparisons for lead-, steel-, and uranium-shielded casks, 20: 16622 (ORNL-3918)
SALOMON, Mark, Isotope effects in mixtures of liquid H_2O and T_2O, 20: 16424
SALTER, L., Radiochemical determination of cadmium isotopes in radioactive debris, 20: 16397
SALZANO, F. J., Electrical properties of thorium carbides, 20: 17068
SALZMAN, F., Electric dipole moments of Fermi particles, 20: 17372
SALZMAN, G., Electric dipole moments of Fermi particles, 20: 17372
SAMIOS, N. P., K^--p interaction at 2.24 Bev/c, 20: 17383
SAMOILOV, A. G., Dispersion fuel elements for nuclear reactors, 20: 18079
SAMOILOV, B. N., Moessbauer effect on ^{161}Dy impurity nuclei in metallic Gd, 20: 17988
SAMSAHL, K., Selective sorption of trace elements in neutron-irradiated biological material, 20: 16171 (AE-215)
SAMSONOV, G. V., Aluminothermic production of aluminum–cerium alloys, 20: 16964
SAMSONOV, G. V., Formation of Tb(IV) compounds, 20: 16433
SAMUEL, D., Synthesis and isotopic analysis of $CH_3{}^{18}OH$ and $CH_3{}^{17}OH$, 20: 16547
SAMUELS, D. E. J., Design factors influencing the containment of internal explosion in fast reactors, 20: 18122
SANADA, J., Deformed ion source at positive potential in f-m cyclotron, 20: 17207 (INSJ-93)
SANCHO, J., Polarographic behavior of hafnium(IV) in aqueous-alcoholic mixtures, 20: 16445
SANDERS, Harold, K^+ detector for use with rapid-cycling bubble chamber, 20: 16826 (PPAD-574E)
SANDWEISS, J., Pion production in $p\bar{p}$ annihilations at 3.3 and 3.7 Bev/c, 20: 17385
SANGAL, Satendra P., Chromogenic reaction of the uranium–aluminon

chelate in solution, 20: 16428
SANGERMANO, L. D., Purification and preparation of cesium compounds, 20: 16476
SANGIUST, V., Distribution of some fission products between core and recombiner of L54M reactor. V., 20: 18142
SANKARANARAYANAN, A., Covariant multipole polarization operators and density matrices for any spin, 20: 17451
SANNER, L., Hyperfine structure of 16-hour state in ^{119}Te, 20: 17705
SARGENT, W. L. W., Nature of quasi-stellar sources, 20: 17242
SARMA, P. L., Spectrophotometric determination of Ce with sulfanilic acid, 20: 16398
SARVER, J. F., Preparation and luminescent properties of Ti-activated zirconia, 20: 17056
SASIELA, R., Unified theory of nonlinear oscillations of a cold plasma, 20: 17919
SATO, H., Long-period modulation of stacking order in Au_3Mn, 20: 17066
SATO, Shin, Nitrous oxide as electron scavenger in radiolysis of hydrocarbons, 20: 16515
SATO, Taichi, Uranium(VI) extraction from hydrochloric acid solutions by tri-n-octylamine, 20: 16391
SATTLER, A. R., Ionization produced by energetic Ge atoms within a Ge lattice, 20: 17265
SATYANARAYANA, L., Ionization chambers for reactor control, 20: 16897
SAULITE, U., Modulation of forces acting on conducting bodies in travelling magnetic field of a cylindrical inductor, 20: 17162
SAUR, E., Preparation and superconductivity of Nb_3Sn diffusion layers with addition of Zr or Ti, 20: 17632
SAURO, J. P., Interference fringes formed by x rays scattered from thin films, 20: 17163
SAUZADE, M., High homogeneity-rich field superconducting magnet for nuclear resonance, 20: 17587 (CONF-650922, pp 517-24)
SAVAGE, Howard F., Problem associated with elastic waves produced by heating of targets with pulsed-ion beam, 20: 17139
SAVARY, A., Review of economic scope for various uses of nuclear energy in certain overseas countries, 20: 16919 (EUR-2619.f)
SAVENKO, I. A., Measurements of protons with energy of 0.4- to 8-Mev on Cosmos 41 satellite, 20: 17548
SAVENKO, I. A., Measuring low-energy protons on the Kosmos-41 satellite, 20: 17310 (AD-623948)
SAVIN, I. A., Designs of gaseous threshold and differential Cherenkov counters, 20: 16816 (JINR-P-2528)
SAVIN, I. A., Spark chambers for studying elastic scattering of π^+ mesons by protons at 180°, 20: 16815 (JINR-P-2506)
SAVITSKAYA, Yu. S., Preparation of thin layers of zirconium carbide by electrophoresis, 20: 17004
SAVITSKII, E. M., Solid solutions of Ge, Sn, Al, and Be in V_3Si and their superconductivity, 20: 17043
SAWAGUCHI, Tetsuo, Study on Al–Zr alloys. I., 20: 17072
SAXENA, R. P., Effect of dipion resonances on π-N scattering amplitude, 20: 17388
SAYRES, A., Elastic scattering of neutrons from carbon and oxygen at 3.0 to 4.7 Mev, 20: 17767
SCADRON, Michael D., General nondynamical formalism for reactions with particles of arbitrary spin, 20: 17479
SCADRON, Michael D., Nondynamical structure of ^{3}He(d,p)^{4}He reaction, 20: 17770
SCANDRETT, J. H., π^+p interactions at 450 Mev, 20: 17384
SCHAEFER, Hermann J., Radiation exposure from heavy nuclei in solar particle beams in space systems of low shielding, 20: 16300
SCHAENZLER, L., Lifetime of the $^{23}/_{4}$ three-particle state of ^{177}Hf, 20: 17811
SCHAFFER, W. F. Jr., Project Salt Vault: design and demonstration of equipment, 20: 18165 (ORNL-P-1987)
SCHAFFER, W. F. Jr., Project Salt Vault, 20: 18169
SCHARBERT, T., Half life of second excited state in ^{133}Cs, 20: 17701
SCHEEL, Lester D., Changes in thyroid ^{131}I activity in ozone-tolerant and ozone-susceptible rats, 20: 16190
SCHERB, Frank, Solar wind deuterium detector and charge spectrum analyzer, 20: 17307 (CONF-651001-34)
SCHILDKNECHT, D., Pair production and heavy electron, 20: 17338 (DESY-65/10)
SCHILL, W. J., Injection and accumulation: single-pass experiments (DCX-1), 20: 17886 (ORNL-3908, pp 1-17)
SCHILLER, Diethard H., Electron-ion bremsstrahlung of non-relativistic plasmas, 20: 17947
SCHILLING, K., Influence of absorption on peripheral photoproduction of vector mesons, 20: 17414
SCHIMMER, B., Arrangement for position and energy determination with semiconductor detectors, 20: 16878
SCHIMMER, B., Position-sensitive counter, 20: 16880
SCHIMMER, B., Pulse-division circuit, 20: 16879
SCHLEIFE, F., Sensitivity and accuracy of measurements in quantitative analyses by means of β backscattering, 20: 16378
SCHLESSINGER, J. E., Radium implant dosimetry with small digital computer, 20: 16748
SCHLIER, C., Velocity dependence of total scattering cross section of K on rare gases, 20: 17294
SCHMID, A., Effect of pyridoxine on renal excretion of Sr, Ca, and phosphate, 20: 16176
SCHMIDT, Albrecht, Apparatus for production of nuclear reactions on a parallel electrode, 20: 17669
SCHMIDT, C. T., Whole-body counter facility, 20: 16737 (UCRL-14534, pp 13-18)
SCHMIDT, Gerhard, Nuclear reactor fuel element cluster, 20: 18080
SCHMIDT, Paul H., Purification of lithium metal by high-vacuum fractional distillation, 20: 16961
SCHMIDT-OTT, W.-D., Isomer of ^{197}Au, 20: 17812
SCHMITT, C. R., Polyvinyl plastisol quality study, 20: 18179 (Y-1508)
SCHMITT, H. W., Average number and energy of γ rays emitted in ^{235}U fission, 20: 17828
SCHMITZ, N., Strongly decaying elementary particles, 20: 17445
SCHNEIDER, E. E., ESR of color centers in γ-irradiated planar lead halides, 20: 16531
SCHNEIDER, H., Scintillator-film combination for fast-neutron dosimetry, 20: 16861
SCHNEIDER, J., ESR of sulfur and selenium radicals in alkali halides, 20: 18005
SCHNEIDERMAN, Arthur M., Performance characteristics of a magnetic annular arc, 20: 16627
SCHOFIELD, J. M. S., Apparatus for detection and energy analysis of fast neutral atoms, 20: 17873 (CLM-R-49)
SCHÖNFELD, E., Softening and decontaminating waste water by caustic-carbonate precipitants in slowly stirred sludge-blanket column, 20: 18168
SCHOOL, H.-G., Preparation and superconductivity of Nb_3Sn diffusion layers with addition of Zr or Ti, 20: 17632
SCHOROCHOFF, G., Production of hyperfragments from the interactions of 3.0- and 5.0-Bev/c K⁻ mesons with emulsion nuclei, 20: 17752
SCHRAM, B. L., Cross section formulae for ionization and excitation of atoms by high-energy electrons, 20: 17270
SCHREIBER, Franz, Electromagnetic jack for control rods in marine nuclear reactors with a center latch system, 20: 18041
SCHRENK, G. L., Electron emission from metals in vapors of Cs and F, 20: 17334
SCHROEDER, Gerald L., Lithium-drifted Ge detectors: applications to neutron-activation analysis, 20: 16888
SCHUELLER, W., Safety precautions to prevent criticality accidents, 20: 16562
SCHUESSLER, H. D., Comparison of observed delayed-neutron abundances with calculated fission yields of neutron precursors, 20: 17831
SCHULTZ, C. W., Thermoelectric power in Nb–Zr alloys, 20: 17067
SCHULZ, H. D., Highly polarized coherent bremsstrahlung from a diamond target in Bev region, 20: 17679 (DESY-65/15)
SCHURICHT, V., Density-independent moisture gage using neutron radiation, 20: 16924
SCHWAMB, F. E., Multiple pion production by 1.89-Bev/c π^-, 20: 17386
SCHWARTZ, L. J., Assessing mutagenic action of uv radiation on Emericellopsis glabra, 20: 16238
SCHWARTZ, Laurent-Marcel, Thermoluminescence of calcium oxide activated by IVa Group elements, 20: 17982
SCHWARTZ, Samuel, Hyperbaric oxygen, whole-body x irradiation, and cyclophosphamide combination therapy in mouse leukemia, 20: 16262
SCHWARZWAELDER, Reiner, Boiler superheating elements for superheat reactor of the AEG, 20: 18077
SCHWEIKERT, Emile, Radioactivation analysis of Ti in Al using reaction ^{48}Ti(p,n)^{48*}V, 20: 16366
SCHWEIKERT, Emile, Radioactivation analysis of Fe in Al using reaction ^{56}Fe(p,n)^{56*}Co, 20: 16367
SCHWENKE, T. W., Development of improved land-surface fallout model, 20: 16735 (TO-B-65-99)
SCHWETJE, W., Density of energy states in light nuclei, 20: 17745
SCINTEI, N., NMR magnetometric device with flowing liquids, 20: 16770 (CONF-650922, pp 428-30)
SCOTT, B. W., Ionization cross section of cesium at threshold, 20: 17287
SEABORN, G. B., Improved portable fast neutron detector, 20: 16848
SEARS, Mildred Bradley, High-temperature immiscibility of uranium mono- and dicarbides, 20: 17057
SECEROV, Mileta, Developing production methods for reactor-grade graphite, 20: 17002
SECOY, C. H., Heats of immersion in the Th oxide–water system. II., 20: 16456
SEDOV, L. I., Energy-momentum tensor and macroscopic internal interactions in gravitational field and in material media, 20: 17566
SEHGAL, J. D., Prog. rpt. on fixation of low- and medium-level radioactive waste in stable solid media, 2–10/65, 20: 18166 (TID-22531)
SEIDEL, G. P., Thermally activated processes in deformation of neutron-

irradiated Cu single crystals. II., 20: 17980 (ANL-Trans-274)
SEIFERT, A. M., Scattering chamber for use with solid-state detectors, 20: 16883
SEKIGUCHI, Tadashi, Inductively coupled a-c MHD electrical power generator, 20: 17330
SEKINE, Tatsuyo, Liquid-liquid partition systems. III., 20: 16564
SELIN, Lars-Erik, Band spectrum of ThO, 20: 17254
SELLEY, G., Experiences with measuring systems OZH-1 and OZH-2, 20: 18024
SELLEY, Gabor, Low-capacity atomic power stations, 20: 18107
SELLSCHOP, J. P. F., Neutrinos from atmosphere and beyond, 20: 17323
SEN, P., Backscattering of electrons from phosphors, 20: 16867
SENG, Wang Tung, Solvent extraction of Cf, Fm, and Md, 20: 16404
SERBIN, I. A., Experimental observation of fourth sound in $^{3}He-^{4}He$ solutions, 20: 17159
SEREBRYAKOVA, T. I., Nature of chemical bond in transition metal compounds with boron, 20: 16439
SEREDA, G. A., Strontium-90 in fresh-water reservoirs of the Soviet Union in 1961-1962, 20: 16705
SEREDAG, A., Radioactive isotopes in atmosphere and their use in meteorology, 20: 16636
SERGACHEV, A. I., Angular anisotropy and mass asymmetry of ^{232}Th fission fragments, 20: 17869
SERPAN, C. Z. Jr., Radiation damage surveillance of power reactor pressure vessels, 20: 17126 (NRL-6349)
SERRA, Alberto, Study of double nitrate of La and Mg between 4000 and 1250 cm^{-1}, 20: 16429
SERRA, P., Production mechanism of $\bar{K}^{*0}(891)$ in K⁻-p interaction at 3 Bev, 20: 17380
SETLOW, Jane K., Proper use of short-wavelength reversal and pyrimidine dimers in biological inactivation, 20: 16206
SETLOW, R. B., Proper use of short-wavelength reversal and pyrimidine dimers in biological inactivation, 20: 16206
SETO, Yoshio, Fallout radionuclides in deep waters around Japan, 20: 16681
SEVIN, W., Use of beta radiations ($^{90}Sr-^{90}Y$) in dermatology, 20: 16325
SEYFARTH, H., Beta activity of fission products from thermal-neutron fission of ^{233}U, ^{235}U and ^{239}Pu, 20: 17835
SHADIEV, N., Spectrum of γ rays emitted during capture of thermal neutrons in tellurium, 20: 17681 (IAE-966)
SHAH, J., Ethylene formation in pea epicotyl tissues following irradiation with γ rays from ^{60}Co, 20: 16281
SHAH, T. P., Primary-energy estimate for jets based on momentum and angular distributions of secondaries, 20: 17316
SHAHINIAN, P., Effect of electron-bombardment heating on tensile properties of tungsten, 20: 17073
SHAIKH, A. Q., Interspecific hybridization in jute, 20: 16218 (AECD-AG-12)
SHAKHOVA, K. I., Interatomic binding in Ti–Nb–Cr system, 20: 17112
SHAKIN, Carl, Foundations for Hartree-Fock calculations with singular potentials, 20: 17791
SHALABY, Laila A., Analysis of uranium in phosphate ores, 20: 16381
SHALAGINA, E. V., Effects of cascade process on yield of energetic He isotopes, 20: 17713
SHALIMOV, V. P., Dynamics of a geomagnetic trap and origin of the earth's radiation belts, 20: 17547
SHAL'MAN, M. P., Technological and thermotechnical control of nuclear power stations, 20: 18118
SHAMOV, V. P., Radiometric properties of large liquid scintillation counter, 20: 16865
SHAPIRO, E. L., Radiometric properties of large liquid scintillation counter, 20: 16865
SHAPIRO, P., Prog. rpt. on NRL cyclotron, 9/65, 20: 17169 (AD-628928)
SHAPOVALOVA, E. T., Corrosion resistance of structural materials in boron-containing solutions, 20: 16976
SHAPPERT, L. B., Shipping cost comparisons for lead-, steel-, and uranium-shielded casks, 20: 16622 (ORNL-3918)
SHARAPOV, K. V., Inelastic interactions of antiprotons with neutrons at 3 Bev, 20: 17359
SHARE, Irwin, Wave propagation in plasma, 20: 17911
SHARMA, Arun Kumar, Effect of moisture on radiosensitivity in root tips of Vicia sativa, 20: 16276
SHARMA, H. D., Neutron-induced fission of ^{227}Ac, ^{231}Pr, and ^{237}Np: mass distribution, 20: 17861
SHARMA, R. P., Low-lying excited states in ^{115}In and ^{117}In, 20: 17766
SHARMA, S. K., Measurement of pressure in high and ultrahigh vacuum regions using ionization gages. I., 20: 16630
SHARMA, Tuleshwar, Measurement of $^{18}O/^{16}O$ ratios of total oxygen of carbonates, 20: 16676
SHARP, D. H., Self-consistent determination of coupling shifts in broken SU(3), 20: 17467
SHARP, David H., Calculation of nucleon magnetic moments by dispersion-theory methods, 20: 17390
SHAVRIN, P. I., Measurements of protons with energy of 0.4- to 8-Mev on Cosmos 41 satellite, 20: 17548
SHCHEGOLEVA, R. P., Deformed Zr–Ti–O–Fe alloy for high-pressure chambers, 20: 17003
SHCHETININ, N. N., Adsorption method of determining radon concentration in the air from an airplane, 20: 16708
SHEBEKO, A. V., Inelastic diffraction scattering treated by the complex angular momentum method, 20: 17817
SHEFCIK, J. J., In-tank solidification of radiochemical wastes, 20: 18161 (ISO-SA-1)
SHEINDLIN, A. E., Thermodynamic properties of Nb at temperature range from 0°K to melting point, 2740°K, 20: 17100
SHEKHTER, V. M., Broken unitary symmetry and possible Ω^- (1875) resonance, 20: 17364
SHELINE, R. K., Energy levels of ^{170}Tm, 20: 17782
SHELUPSKY, David Irwin, Translations of discrete Bose-Einstein operators, 20: 17506
SHERIDAN, J. R., Cross section and polarization of Balmer α radiation produced in collisions of protons with N_2, 20: 17269
SHERMAN, Michael, Thermal stability of completely confined fluids including MHD effects, 20: 17535
SHERWOOD, B. A., M1 and E2 hyperfine structure in muonic K and L x rays of bismuth, 20: 17792
SHETTEL, Harris H., Evaluation of existing criteria for judging quality of science exhibits, 20: 18178 (TID-22703)
SHEVCHENKO, O. A., Nonlinear effects in ultrasonic absorption in superconducting indium, 20: 17635
SHEVCHENKO, V., Nature of the giant resonance in photonuclear reactions, 20: 17706
SHEVCHENKO, V. V., Logical-element system for reactor control, 20: 18031
SHIGEMATSU, Tsunesabu, Solvent extraction of europium ions, 20: 16565
SHIGIN, V. A., Fission distribution in neutron-induced fission of ^{230}Th, ^{238}Pu, and ^{241}Am, 20: 17848
SHIH, Chang-ho, Magnetodynamic instability of plasma beam, 20: 17942
SHIM, Sun Shik, Factors affecting bone blood flow based on bone clearance of radiostrontium (^{85}Sr), 20: 16192
SHIMADA, Syoichiro, NELKER: code for scattering kernel calculation for bound hydrogen, 20: 17684 (JAERI-1085)
SHIMAMOTO, Susumu, Propagation of normal region in superconducting magnet, 20: 17610
SHIMIZU, Kiyoshi, Survey on atomic bomb casualties, 20: 16272
SHINOZAKI, Yoshiharu, Reaction of active nitrogen with ethylene, 20: 16510 (NP-tr-1364)
SHINSAKA, Kyoji, Nitrous oxide as electron scavenger in radiolysis of hydrocarbons, 20: 16515
SHINYAEV, A. Ya., Interdiffusion between Ti and Mo, 20: 17111
SHINYAYEV, A. Ya., Diffusion of nickel into solid solutions of intermetallic compounds of Ni_3Nb and Ni_3Ta, 20: 17089
SHIOKAWA, Takanobu, Chemical effects associated with the β-decay process. II., 20: 16544
SHIOZAKI, Masaru, Fallout radionuclides in deep waters around Japan, 20: 16681
SHIPLEY, K. L., Spectroscopic measurements of a supersonic plasmajet, 20: 17902
SHIRANE, G., Long-period modulation of stacking order in Au_3Mn, 20: 17066
SHIRINOV, Kh., Utilization of atomic energy in the national economy, 20: 18182
SHIRLEY, D. A., Hyperfine magnetic fields at nuclei of indium in iron and nickel, 20: 17992
SHIRLEY, D. A., Systematic variation of quadrupole crystal-field shielding in rare-earth ethyl sulfates, 20: 17996
SHIRLEY, D. A., Temperature scale for Nd ethylsulfate below 1°K, 20: 17614
SHIRN, G. A., Heat-treatment of anodic oxide films on Ta. IV., 20: 17055
SHKAROFSKY, I. P., Laboratory simulation of disturbances produced by bodies moving through plasma and solar wind-magnetosphere interaction, 20: 17546
SHOENHALS, R. J., Steady flow characteristics of single-phase natural circulation loop, 20: 16600 (COO-1177-15)
SHOPAUSKAS, K. K., Effect of vertical-exchange intensity on the distribution of natural radioactive matter in the free atmosphere, 20: 16637
SHOPAUSKAS, K. K., Effect of advection on radioactivity distribution in the atmosphere, 20: 16638
SHOPAUSKAS, K. K., Radioactivity, sizes, and compositions of α-radiating aerosols, 20: 16646
SHORIN, K. N., Method of investigating betatron oscillation resonances, 20: 17221
SHUBIN, A. P., Plasma flow between electrodes with weak longitudinal conductivity, 20: 17939
SHUKLA, P. G., Energy spectrum of primary cosmic rays, 20: 17315
SHULTS, W. D., Controlled-potential polarography and coulometry as

microanalytical techniques, 20: 16390
SHUMILOV, S. N., Deuteron and α-particle pickup in interaction between ^{10}B and ^{16}O, 20: 17815
SHURIN, A. K., Phase equilibrium diagram of Hf–Ta system in solid state, 20: 17092
SHUTTLEWORTH, E., Nomograms for radiobiologically equivalent fractionated x-ray doses, 20: 16749
SHVACHUNOV, I. N., Dynamics of a geomagnetic trap and origin of the earth's radiation belts, 20: 17547
SHVEDOV, N. P., Radioactive fallout in Vilnius in 1962, 20: 16700
SHVEIKIN, G. P., Kinetics of reduction of low-oxide niobium by carbon, 20: 16483
SHVEYKIN, G. P., Self-diffusion of Nb in single crystal and molten specimens, 20: 17090
SIDEI, Tunehiko, Thermoluminescence dosimetry of γ rays from atomic bombs in Hiroshima and Nagasaki, 20: 16759
SIEMINSKA, J., Residual nuclei observed in interactions of 25-Bev/c protons with heavy emulsion nuclei, 20: 17748
SIFFERT, P., Low energy α-p pulse-shape discrimination with Si surface-barrier detectors, 20: 16900
SIGNARBIEUX, C., Mass spectra of fission fragments after prompt neutron emission, 20: 17866
SILIN, V. P., Plasma instability in strong high-frequency field, 20: 17948
SILJANDER, W. A., Large spark chamber magnet with tape-wound coils, 20: 16809 (CONF-650922, pp 253-61)
SILJANDER, W. A., Prestressing method for assembling ZGS ring magnet coils, 20: 17201 (CONF-650922, pp 733-44)
SILL, Claude W., Determination of radioisotopes of Ce, Ba, La, and Np after separation by $BaSO_4$, 20: 16343
SILVERMAN, S. M., Test of low-energy limit of the Born approximation, 20: 17258
SIMNAD, Massoud T., Fuel element for nuclear reactors, 20: 18081
SIMONIUS, M., Group theoretical classification of transitions, 20: 17488
SIMONOFF, Gabriel, Simultaneous separations of Rs, Pu, U, Am, and Cm from irradiated Th, 20: 16359
SIMONOV, Yu. A., Three-body problem. Complete system of angular functions, 20: 17560 (ITEF-384)
SIMONOV, Yu. N., Measurement of π^+ meson lifetime, 20: 17346 (JINR-P-2534)
SIMONS, E. L., Purification and preparation of cesium compounds, 20: 16476
SIMONS, Lennart, Alpha-particle excitations in atomic nuclei, 20: 17802
SIMPSON, J. J., Coulomb excitation of low-energy states in Ce, Nd, and Sm isotopes, 20: 17734
SINESI, S. J., Effect of single dose of uv radiation on epidermal melanocytes, 20: 16261
SIN FAI LAM, L. T., Electron capture by fast protons in helium, 20: 17274
SINGLETARY, John B., Space materials handbook, 20: 16944 (NASA-SP-3025)
SINGRU, R. M., Low-lying excited states in ^{115}In and ^{117}In, 20: 17766
SINHA, Shyama P., Investigation on rare earth terpyridyl system. IV., 20: 16479
SIRUGUE-COLLIN, M., Approximate calculation of asymptotic operators, 20: 17450
SISIGINA, T. I., Emission of radon from surface of some types of soils in European USSR and Kazakhstan, 20: 16691
SISIGINA, T. I., Radon concentration and vertical turbulent mixing in surface boundary layer of atmosphere, 20: 16692
SISIGINA, T. I., Radon as indicator of atmospheric stability, 20: 16694
SISTEMICH, K., Position-sensitive counter, 20: 16880
SIWICKI, Henryk, Standardization of measurements of iodine uptake of thyroid gland by ^{131}I, 20: 16315
SKALKO, Richard G., Effect of ^{60}Co radiation on development and DNA synthesis in the 11-day rat embryo, 20: 16260
SKATKIN, V. M., Statistical characteristics of functional ratemeters, 20: 16835
SKAVLEM, S., Proton-proton singlet S-state interaction, 20: 17353
SKIDMORE, M. R., Excitation heating of ions to high temperature, 20: 17900
SKINNER II, Loren C., Temperature variation of Ginzburg-Landau parameter in Nb single crystals, 20: 17585 (AD-627910)
SKIPPEN, George B., Radioactivation determination of palladium in basaltic and ultrabasic rocks, 20: 16370
SKLYAREVSKII, V. V., Moessbauer effect on ^{161}Dy impurity nuclei in metallic Gd, 20: 17988
SKOLOZDRA, R. V., Phase equilibrium in ternary Zr–Co–C and Nb–Fe–C systems, 20: 17086
SKORCHEV, B., Brownian movement study by means of Moessbauer effect, 20: 17165
SKREPPEN, Helge, Organic-cooled irradiation loop in the HFR at Petten, 20: 18137 (KR-82)
SKURATOVICH, A. A., Biological effects of fast electrons under continuous and pulsed irradiation of rat skins, 20: 16269
SKURIDIN, G. A., Dynamics of a geomagnetic trap and origin of the earth's radiation belts, 20: 17547
SKURSKA, Zofia, Studies on viruses of asiatic influenza. III., 20: 16239
SLATER, J. V., Dark recovery and glycerol protection for diploid Saccharomyces cerevisiae, 20: 16231 (UCRL-16377)
SLATTERY, G. F., Electron metallography of dilute alloys of uranium with iron and aluminum, 20: 17058
SLIEKER, C. J. G., Thermal diffusion in isotopic hydrogen and H–He mixtures. II., 20: 16468
SLIVNIK, Jože, Plutonium hexafluoride synthesis, 20: 16463
SMEND, F., Isomer of ^{197}Au, 20: 17812
SMETANA, Andrew F., Radiation-enhanced surface activity of gamma HMX, 20: 16504 (AD-627846)
SMILEY, D. C., Health physics for maintenance operation on a homogeneous research reactor, 20: 16757
SMILJANIC, Daniel, Development of electromagnets for nuclear research, 20: 17222
SMIRNOV, V. F., Extraction of uranium(VI) with D2EHP and MLPA from H_3PO_4 solutions, 20: 16579
SMIRNOV, V. F., Uranium and Th extraction from H_3PO_4 solutions by acid and neutral alkylphosphorus compounds, 20: 16580
SMIRNOV, Yu. F., Nucleon clusters in light nuclei, 20: 17707
SMITH, Charles G., Determination of median planes in cyclotrons with Hall plates, 20: 17189 (CONF-650922, pp 421-7)
SMITH, P. D., Linear thermal expansion of beryllia, 20: 17006 (AAEC/TM-300)
SMITH, T. J., Microtopology of stress-corrosion cracking, 20: 16968 (COO-1319-33)
SMITH, William R., DWBA analysis of $^{90}Zr(d,p)^{91}Zr$ reaction between 3.5 and 5.5 Mev, 20: 17691 (ORNL-TM-1235)
SMITH-SAVILLE, R. J., Photomultiplier base system with high-voltage divider network remote from the photomultiplier, 20: 16796
SMOLIN, M. D., Mobility of atoms in a Mo–W alloy, 20: 17101
SMORODINSKII, Ya. A., Symmetry groups in classical and quantum mechanics, 20: 17429 (JINR-P-2529)
SMOTRITSKII, L. M., Search for parity nonconservation in nuclear γ transitions, 20: 17444
SMYTH, D. M., Heat treatment of anodic oxide films on Ta. IV., 20: 17055
SNOUSE, T. W., Sputtering of single-crystal copper, 20: 17256
SNYDER, A. L., BF_3 counters for use in field instrumentation, 20: 16895
SODD, Vincent Joseph, Semiconductor detector studies of recoils from 15-Mev deuterons on ^{12}C, 20: 17820
SODHA, M. S., Second-order diffusion of electrons in ionized gases, 20: 17529
SOERENSSEN, A., Theoretical total cross sections for high-energy nuclear-field pair production in light elements, 20: 17754
SOKIRYANSKII, L. F., Interdiffusion between Ti and Mo, 20: 17111
SOLOV'EV, L. S., A similarity parameter in theory of plasma flows, 20: 17910
SOLOV'EV, V. V., Predictions of unitary symmetry for hadron photoproduction reactions, 20: 17412
SOLTAN, M., Residual nuclei observed in interactions of 25-Bev/c protons with heavy emulsion nuclei, 20: 17748
SONDHAUS, C. A., Dark recovery and glycerol protection for diploid Saccharomyces cerevisiae, 20: 16231 (UCRL-16377)
SOOD, P. C., Reformulation for the meson-atomic model of the nucleon, 20: 17356
SORANTIN, H., Technetium-99m generator using Fe_2O_3 as sorbent for ^{99}Mo, 20: 16552
SOUERS, P. C., Magnetic and structural properties of europium metal and EuO at high pressure, 20: 17999
SOWERBY, M. G., Boron pile ρ measurements, 20: 17823
SOWERBY, M. G., $^{10}B(n,\alpha)$ branching ratio, 20: 17719
SOWMAN, H. G., Prog. rpt. on fabrication of W alloy tubing, 10/23/65–1/1/66, 20: 16989 (COO-1518-2)
SPAMER, E., Nuclear levels of ^{10}B and ^{11}B by inelastic electron scattering, 20: 17813
SPECHT, H. J., Beta activity of fission products from thermal-neutron fission of ^{233}U, ^{235}U and ^{239}Pu, 20: 17835
SPECHT, H. J., Prompt and delayed γ rays from fission, 20: 17827
SPECTOR, Nissan, Analysis of spectrum of neutral erbium (Er I)., 20: 17260
SPEECKE, A., Research for delayed-neutron precursors in antimony and arsenic fission products, 20: 17833
SPERDUTO, A., Stripping analysis of $^{46}Ti(d,p)^{47}Ti$ reactions, 20: 17776
SPICER, G. S., Radioactive fallout in air and rain: results to middle of 1965, 20: 16660 (AERE-R-4997)
SPIERING, G. A., Critical currents in superconducting single-crystal NbSe, 20: 17609
SPINELLI, John, Effect of hypoxanthine on flavor of fresh and stored low-dose-irradiated petrale sole fillets, 20: 16925
SPINRAD, R. J., Multiple spectrometer control by computer, 20: 16869
SPIRIN, V. D., Methods of measurement of ultra-small α activities,

20: 16411
SPITSYN, V. I., Application of co-crystallization and adsorption in the solution of current problems of radiochemistry, 20: 16557
SPITZY, H., New type of radiometric titrator: Redox and chelatometric microtitrations, 20: 16386
SPRAWLS, Perry Jr., Development of a sensitive liquid dosimeter for integral dose measurement, 20: 16845
SPRING, E., Coincidence method for studies of internal pair formation from annihilation radiation, 20: 17731
SREDNIAVA, B., Electromagnetic interaction of the X meson in higher symmetries, 20: 17342 (JINR-P-2520)
SRIKANTIAH, G., Control of reactivity in high-conversion-ratio, plutonium-fueled thermal power reactors, 20: 18115
SRIVASTAVA, B. K., Integrated photodisintegration cross section of He with velocity-dependent nuclear potential, 20: 17774
SRIVASTAVA, H. K., Second-order diffusion of electrons in ionized gases, 20: 17529
SRIVASTAVA, P. K., Correlation functions for eigenvalues of real quaternian matrices, 20: 16938
SRIVASTAVA, Som Prakash, Ultrasonic velocity in aqueous solution of thorium nitrate, 20: 16477
STACEY, G. M., Tamm variational principle and its generalization to the scattering amplitude, 20: 17271
STACH, E., Artificial radioactive carbonization, 20: 16514
STAEHLE, R. W., Microtopology of stress-corrosion cracking, 20: 16968 (COO-1319-33)
STAHLHOFEN, W., Bibliography on radiation effects on living tissues and organisms, 20: 16219 (AED-C-04-23)
STAHLHOFEN, W., Bibliography on radiation effects on living tissues and organisms, 20: 16220 (AED-C-04-24)
STAHLHOFEN, W., Bibliography on radiation effects on living tissues and organisms, 20: 16221 (AED-C-04-25)
STAIRS, Gerald R., Prog. rpt. on effects of radiation on genetic structure of heterozygous outbreeding populations of forest trees, annual, 6/65–6/66, 20: 16228 (NYO-3571-2)
STAMM'LER, R. J. J., DATAPREP-II—reactor lattice homogenization and BIGG-II data preparation computer code, 20: 18047 (KR-78)
STANCHI, L., Decimal scanner for the modular chain, 20: 16777 (EUR-2702.e)
STANFORD, Fred E., Infrared spectra of vapors above sulfuric and deuteriosulfuric acids, 20: 16442
STANICEK, J., Long-term follow-up in detection and treatment of cervical cancer, 20: 16326
STANISLAW, Pszona, Measurement of ratio of slow to fast components of scintillation in stilbene in a wide range of dE/dx, 20: 16813 (INR-653/IA/D)
STAPLETON, George E., Repair of radiation-induced damage to cell division mechanism of E. coli, 20: 16200
STARFELT, N., Fission cross-section of ^{240}Pu for 0.03- to 2.0-Mev neutrons, 20: 17855
STARY, J., Solvent extraction of Cf, Fm, and Md, 20: 16404
STARY, Jiri, Separation of transplutonium elements, 20: 16402
STAUB, F. W., Prog. rpt. on two-phase flow investigation, 10–12/65, 20: 16601 (GEAP-5067)
STAUBERT, R., Digital recording system of air shower experiment at Kiel, 20: 16873
STAUFFER, J. F., Assessing mutagenic action of uv radiation on Ericericellopsis glabra, 20: 16238
STAVINSKII, V. S., Designs of gaseous threshold and differential Cherenkov counters, 20: 16816 (JINR-P-2528)
STECHER, M., Recent state of betatron development and application, 20: 17216
STECURA, Stephen, Phase transformations of La_2O_3, Nd_2O_3, Sm_2O_3, Eu_2O_3, and Gd_2O_3, 20: 16489
STEEB, S., Structure of tantalum suboxides, 20: 17059
STEELE, E. L., Helium-3 charged particles in activation analysis, 20: 16331 (GA-6568)
STEELE, E. L., Variable-energy neutron activation analysis, 20: 16332 (GA-6691)
STEELE, L. E., Radiation damage surveillance of power reactor pressure vessels, 20: 17126 (NRL-6349)
STEFANOV, G., Determination of arsenic in ores and rocks with high Mn by neutron activation analysis, 20: 16364
STEFFEN, K. G., Beam transport magnet measurements at DESY, 20: 17192 (CONF-650922, pp 456-66)
STEFFEN, R. M., Beta-gamma circular polarization correlation of ^{122}Sb, 20: 17677 (COO-1420-112)
STEFFEN, R. M., Search for higher-order effects in allowed β transitions, 20: 17678 (COO-1420-113)
STEIN, Bland A., Oxidation-resistant coatings on Nb–10Ti–5Zr alloy sheet at 2000, 2400, and 2700°F, 20: 16973 (NASA-TN-D-3275)
STEIN, Otto L., Prog. rpt. on use of tritiated thymidine as internal source of radiation in study of lateral root initiation, annual, 1965–66, 20: 16227 (NYO-3561-2)
STEINBERG, Meyer, Chemonuclear and radiation chemical process research and development, 20: 16506 (BNL-10020)
STEINEMANN, A., Experimental studies on the degradation phenomena in small superconducting coils of Nb-25 Zr, 20: 17629
STEINERT, C., Fuel utilization in a joint economy of converters and breeders, 20: 18100
STEKERT, J. J., Cherenkov interaction in a uniformly loaded waveguide, 20: 17485
STEKLY, Z. J. J., Terminal characteristics of short samples of superconductors and their effect on coil behavior, 20: 17590 (CONF-650922, pp 550-9)
STELLA, P., Numerical resolution of magnetic field diffusion problem, 20: 17157 (EUR-2620.i)
STELSON, P. H., Nuclear transition probability, B(E2), for $0^+_{g.s.} \rightarrow 2^+_{first}$ transitions, 20: 17730
STELTS, Marion L., Ground-state (p,n) reactions in mirror nuclei and quasielastic model of (p,n) reactions, 20: 17775
STEPANENKO, V. A., Tritium emitters, 20: 16916
STEPANOV, A. V., Chemical composition of atmospheric precipitation and fallout in vicinity of Leningrad, 20: 16704
STEPANOV, E. P., Moessbauer effect on ^{161}Dy impurity nuclei in metallic Gd, 20: 17988
STEPANOV, S. A., Singularities of MGD generator performance at large Hall numbers, 20: 17332
STEPHENS, D. R., Compression of lithium hydride, 20: 17979 (UCRL-12386)
STEPHENS, R. E., Anomalous contraction of invertebrate striated muscle, 20: 16259
STEPHENS, S. A., Energy spectrum of primary cosmic rays, 20: 17315
STEPHENSON, S. E., Neutron fluctuation measurements at ORNL, 20: 18048 (ORNL-P-1967)
STERKIN, Carol K., Interactions of spacecraft and other moving bodies with natural plasmas, 20: 17537 (JPLAI/LS-541)
STERMAN, L. S., Effects of thermal decomposition of organic coolants on heat exchange in large-volume boiling, 20: 16615
STERNBERG, J., Radiocontamination of the environment and effects on the mother and fetus. I., 20: 16301
STERNHEIMER, R. M., Linear mass relations for elementary particles and resonant states, 20: 17391
STERNHEIMER, R. M., Wave functions for quadrupole antishielding factors, 20: 17250 (BNL-8850)
STEVENS, G., Specialized use of optical instruments in construction of nuclear power stations, 20: 18114
STEVENS, R. K., Response characteristics of high-temperature electron-capture detector, 20: 16804
STEWART, K. B., BNW master library. I., 20: 17673 (BNWL-CC-325 (Vol.1))
STEWART, K. B., BNW master library. II., 20: 17674 (BNWL-CC-325 (Vol.2))
STEWART, K. B., BNW master library. III., 20: 17675 (BNWL-CC-325 (Vol.3))
STIER, P. M., Prog. rpt. on research in activation analysis, 8/63–10/64, 20: 16336 (NYO-10175)
STIEVE, F. E., Estimation of radiation dose in diagnostic radiology, 20: 16318
STIRLING, W. L., Plasma physics, 20: 17889 (ORNL-3908, pp 52-89)
STOELAN, Birger, Approximation methods in many-body perturbation theory, 20: 17570
STOLL, E., Double-axis neutron diffractometer and general criteria for optimization of its resolution for powder investigations, 20: 16799
STOLL, E., New determination of the neutron scattering amplitude of zinc, 20: 17667
STONE, D. J., Quiet-day magnetic variations during the IGY, 20: 17545
STONE, N. J., Hyperfine magnetic fields at nuclei of indium in iron and nickel, 20: 17992
STONE, N. J., Temperature scale for Nd ethylsulfate below 1°K, 20: 17614
STOREY, E., Experimental epiphyseal cartilage growth anomalies, 20: 16181
STORRER, F., Heterogeneity calculation for fast reactors by a perturbation method, 20: 18063
STRACHAN, C., Scattering of high-energy electrons by ^{7}Li, 20: 17799
STRATTON, R. F., High-current ion-beam production and injection, 20: 17890 (ORNL-3908, pp 100-7)
STREKALOVSKII, V. N., X-ray study of oxidation of UO_2, 20: 16474
STRELOW, F. W. E., Determination of rare earths and Sc in South African carbonatites, 20: 16346
STRELOW, F. W. E., Separation of Sc from Y, La, and rare-earth metals, 20: 16574
STRIGACHEV, A., Brownian movement study by means of Moessbauer effect, 20: 17165
STRONG, Grant H., Penetration seals for N-reactor plant, 20: 18125 (RL-

SA-25)
STRONGIN, Myron, Effect of electron-spin paramagnetism on critical field of thin Al films, 20: 17622
STRUMINSKII, B. V., Some effects in the quark model, 20: 17343 (JINR-P-2524)
STRUNCK, H. J., Velocity dependence of total scattering cross section of K on rare gases, 20: 17294
STRUTINSKII, V. M., Angular anisotropy of fission and the liquid drop model, 20: 17849
STRUTINSKII, V. M., Pairing effects in fission of even-even compound nuclei near the threshold, 20: 17847
STUEBER, W., Subtractor circuit with integrated logic elements, 20: 16940
STUKANOV, A. F., Tungsten heater stability in vacuum at temperatures up to 3273°K, 20: 16596
STUPAK, A., Slow neutron spectrum of neutron beam from UA-RR-1 reactor, 20: 18147
STUPAR, J., Determination of Cd in U compounds by atomic absorption spectrophotometry, 20: 16368
STURNIOLO, D., Radiochemical determination of cadmium isotopes in radioactive debris, 20: 16397
STYCZEN, J., g-Factor of 87-kev excited state in ^{155}Gd, 20: 17683 (INP-430/PL)
STYKO, B. I., Radioactive fallout in Vilnius in 1962, 20: 16700
STYRO, B. I., Problems in investigation of natural radioactivity of the atmosphere, 20: 16688
STYRO, B. I., Radioactivity, sizes, and composition of α-radiating aerosols, 20: 16646
STYRO, B. I., Spectra of dimensions and mobility of natural radioactive aerosols in the atmosphere, 20: 16690
SUCHORZEWSKA, J., Residual nuclei observed in interactions of 25-Bev/c protons with heavy emulsion nuclei, 20: 17748
SUDARSHAN, E. C. G., Currents, algebras and dynamical systems, 20: 17435 (NYO-3399-45)
SUDARSHAN, E. C. G., Nature of approximate symmetries of strongly interacting particles, 20: 17433 (NYO-3399-13)
SUDARSHAN, E. C. G., Sum rule for two-pion decay amplitudes of K mesons, 20: 17369
SUDDATH, J. C., Prog. rpt. on chemical technology, 11/64, 20: 16556 (ORNL-TM-1090)
SUEVEGES, M., Theory of congruence in gravitational fields. I., 20: 17562
SUEVEGES, M., Theory of congruence in gravitational fields. II., 20: 17563
SUGARMAN, Nathan, High-energy fission of ^{238}U, 20: 17790
SUGIURA, Masahisa, Hourly values of equatorial Dst for the IGY, 20: 17543
SUKHANOV, A. D., Equation of motion for a half S matrix and some consequences, 20: 17493
SULC, Vlastimil, Operation of experimental sodium loop with natural convection, 20: 16611
SUNDBERG, O., Quasi-free proton-proton scattering in light nuclei at 460 Mev, 20: 17741
SUNDBOM, L., Irradiation planning in radiotherapy, 20: 16320
SUNTZOV, A. S., Properties of fibrous filters in rarefied air, 20: 16654
SUNYAR, A. W., Decay of ^{108m}Ag, 20: 17786
SUO, M., Investigation of boiling water flow regimes at high pressure, 20: 16605 (NYO-3304-8)
SURDIN, M., X-ray emission from very dense stars, 20: 17240
SUTOVSKII, V. M., States with population inversion in a self-compressed discharge, 20: 17924
SUTTON, J., Electron tunneling evidence for fluxon entry into thin type II superconducting films, 20: 17627
SUTTON, William Wallace, Effects of ionizing radiations on peritrichs, 20: 16295
SUZUKI, Arata, Survey of nuclear reactions induced by 57-Mev protons. II., 20: 17725
SUZUKI, Harohiko, Magnetic susceptibilities of V, Zr, and Nb, 20: 17069
SUZUKI, T., Ultrasonic attenuation and magnetic properties of superconducting Nb in mixed state, 20: 17608
SVEC, Jan, Prog. rpt. on hydrodynamics of disposal of low-level liquid radioactive wastes in soil, final, 1965, 20: 18163 (NP-15859)
SVECHNIKOV, V. N., Phase diagrams of systems $NbCr_2$–$TiCr_2$ and $NbCr_2$–Ti, 20: 17091
SVECHNIKOV, V. N., Phase equilibrium diagram of Hf–Ta system in solid state, 20: 17092
SVESTKA, Zdenek, Spectral analysis of solar flares, 20: 17230
SVIDERSKAYA, Z. A., Magnesium alloys containing neodymium, 20: 17110
SVIRIDOV, V. A., Real part of pp elastic scattering amplitude at 2, 4, 6, 8 and 10 Bev, 20: 17417
SVIRIDOV, V. V., Effects of preliminary γ irradiation and heating on activity of the $Ag/Ag_2C_2O_4$ catalyst, 20: 16523
SVISTUNOVA, T. V., Effects of silicon on mechanical properties and intercrystalline corrosion tendencies of Cr–Ni–Mo alloy, 20: 16983
SVOBODA, C. J., Treatment and disposal of glass melter condensates containing sulfuric acid, 20: 18159 (BNWL-SA-514)
SVOBODA, V., Reactions of metallochromic indicators of micelles. III., 20: 16394
SWARTZ, John M., Analysis of effect of fast-neutron bombardment on current-voltage characteristic of conductivity-modulated p-i-n diode, 20: 16912
SWEET, George Henry, Serological and physicochemical studies on radiation-aggregated human gamma-globulin, 20: 16212
SWIATECKI, W. J., Review of fission theory, 20: 17843
SWINT, J. B., Nuclear reaction polarimeter using position-sensitive particle detectors, 20: 16870
SYKES, A. G., Electron-transfer reactions of europium(II) in aqueous perchloric acid solutions, 20: 16462
SYKES, E. C., Enhancement of ductility in alpha-uranium, 20: 17076
SYROVATSKII, S. I., Dependence of chemical composition of cosmic rays on nature of their motion in the galaxy, 20: 17324
SZABO, G., Effect of single dose of uv radiation on epidermal melanocytes, 20: 16261
SZUR, L., Hematological complications of polycythemia vera and treatment with radioactive phosphorus, 20: 16241

T

TABUSHI, Masayoki, Solvent extraction of europium ions, 20: 16565
TAFT, H. D., Pion production in pp annihilations at 3.3 and 3.7 Bev/c, 20: 17385
TAKAGI, J., Evaporation behavior of non-gaseous fission products from UO_2, 20: 17102
TAKAHASHI, Kenji, Creep rupture strength of Incoloy (32Ni–20Cr steel), 20: 17031 (ORNL-tr-962)
TAKAYAMA, Kazuo, Anomalous bremsstrahlung and anomalous cyclotron emission from partially ionized gases, 20: 17921
TAKIBAEV, Zh. S., Effects of cascade process on yield of energetic He isotopes, 20: 17713
TAKIBAEV, Zh. S., Helium particles emitted during 17.5-Bev π-meson collisions with photoemulsion nuclei, 20: 17716
TAKIBAEV, Zh. S., Inelastic interactions of antiprotons with neutrons at 3 Bev, 20: 17359
TAKIBAEV, Zh. S., Production of high-energy fragments by 7.5-Bev π mesons, 20: 17715
TALBOOM, F. P., Coated Nb alloys can take high turbine heat, 20: 16963
TALBURT, Dwight Edmond, Effects of rare earths and yttrium on growth and metabolism of Aspergillus niger, 20: 16191
TALUKDAR, Chitra, Effect of moisture on radiosensitivity in root tips of Vicia sativa, 20: 16276
TAMURA, Nori, Spectrophotometric determination of Mn in Be, 20: 16361
TANAKA, Kunihide, Magneto-optical experiments with superconducting magnet, 20: 17588 (CONF-650922, pp 525-9)
TANAKA, Michio, Influence of metal ions and metal chelates on hydrolysis of α-D-glucose 1-phosphate, 20: 16421
TANAKA, Shigetoshi, Anomalous bremsstrahlung and anomalous cyclotron emission from partially ionized gases, 20: 17921
TANG, K. T., Potential scattering, 20: 17438
TANSKANEN, Pekka J., Variation of cosmic-ray meson intensity at sea level in connection with atmospheric disturbances, 20: 17311
TARONI, A., Numerical resolution of magnetic field diffusion problem, 20: 17157 (EUR-2620.i)
TARR, C. O., Creep-rupture properties of Re and Re alloys, 20: 17011 (CONF-651025-14)
TARTAKOVSKII, V. K., Polarization of products of ^{6}Li breakup in electromagnetic field of the nucleus, 20: 17806
TASSAN, S., Flux distribution in D_2O-moderated lattice, 20: 18055
TASSO, H., Resonant ohmic damping of linearized magnetoacoustic waves, 20: 17946
TATARCZUK, J. R., Scandium-44 isomeric yield ratios, 20: 17777
TATTEGRAIN, A., Fast period meter with integrated circuits, 20: 18029
TAUBE, M., Salt-boiling fast reactor "SAWA", 20: 18088 (INR-669/C)
TAUSHKANOV, V. P., Uranium sorption by platinized carbon, 20: 16581
TAUSSIG, Robert T., Normal ionizing shock waves, 20: 17511 (NP-15894)
TAUTH, Th., Acceleration of negative hydrogen ions in the U-120 cyclotron, 20: 17224
TAVKHELEDZE, A. N., Some effects in the quark model, 20: 17343 (JINR-P-2524)
TAYLOR, A. E., Measurements of proton-nucleus triple scattering parameters near 140 Mev, 20: 17738
TAYLOR, Edward A., Quadrupole magnet design, 20: 17182 (CONF-650922, pp 208-17)
TAYLOR, G. N., Intercomparison of pathological fractures in beagles injected with ^{226}Ra, ^{228}Ra, ^{239}Pu or ^{90}Sr, 20: 16253
TAYLOR, G. O., Ionization and charge-transfer cross sections for fast neutral He atoms (0.15 to 1.0 Mev), 20: 17301
TAYLOR, J. C., Determination of Sr in samples of biological and geological origin, 20: 16345
TAYLOR, R., Control of fission-product release from advanced gas-cooled

reactors, 20: 18110
TAYLOR, R. D., Portable vacuum cleaner for recovering spilled mercury, 20: 16738 (UCRL-14534, pp 41-3)
TAYLOR, R. D., Removal of C dust from high-speed printer, 20: 16740 (UCRL-14534, pp 50-3)
TELEGDI, V. L., Argonne National Laboratory's pion focusing horn, 20: 17198 (CONF-650922, pp 650-6)
TELEGDI, V. L., M1 and E2 hyperfine structure in muonic K and L x rays of bismuth, 20: 17792
TELEGINA, I. V., Structural changes in neutron irradiated α-quartz, 20: 17149
TEL'TSOV, M. V., Measurements of protons with energy of 0.4- to 8-Mev on Cosmos 41 satellite, 20: 17548
TEMPLETON, W. M., Neutron detection by corrugated-plate spark counters, 20: 16894
TEODORESCU, I. E., Ion sources with a magnetic field, 20: 17223
TEPEL, J. W., Computer program for analysis of time-of-flight spectra, 20: 16877
TER-AKOP'YAN, G. M., Proton emitters among Te isotopes, 20: 17687 (JINR-P-2514)
TERAO, Terumi, Nitrous oxide as electron scavenger in radiolysis of hydrocarbons, 20: 16515
TER BORG, A. P., Kinetic protium–deuterium isotope effect in intramolecular 1-5 shift of hydrogen, 20: 16503
TERNOVSKII, I. A., Use of γ spectrometry for determination of Pu in the living organism, 20: 16864
TERRANI, M., Distribution of some fission products between core and recombiner of L54M reactor. V., 20: 18142
TESLYUK, M. Yu., The crystal structure of ternary phases in the Sc–Cu–Al system, 20: 17097
TEVIKIAN, R. V., Law of conservation for free fields, 20: 17500
TEWORDT, L., Temperature dependence of magnetization in mixed state of superconducting alloys, 20: 17633
THEIDE, Torben, Complications and causes of death in polycythemia vera, 20: 16233
THEISSEN, H., Energy loss of 53-Mev electrons in graphite, 20: 17970
THEODORE, Mary Louise, Analysis of rare earth sulfides, selenides, and tellurides, 20: 16395
THEUS, R. B., Automated logging and processing of NRL cyclotron magnetic field data, 20: 17188 (CONF-650922, pp 415-20)
THEUS, R. B., Prog. rpt. on NRL cyclotron, 9/65, 20: 17169 (AD-628928)
THODOROV, D., Tolerance of x-ray moving-beam irradiation, 20: 16317
THOMAS, E. J., Optimizing the design of superconducting solenoids, 20: 16592
THOMAS, K. T., Prog. rpt. on fixation of low- and medium-level radioactive waste in stable solid media, 2–10/65, 20: 18166 (TID-22531)
THOMAS, Richard C., Dispenser for addition of internal standard in liquid scintillation counting, 20: 16834
THOMAS, T. D., Thermal-neutron-induced fission of ^{235}U, ^{233}U, and ^{239}Pu, 20: 17863
THOMPSON, Stanley G., Application of high-resolution semiconductor detectors in x-ray emission spectrography, 20: 16887
THORNGATE, J. H., Free-field radiation-dose distributions from Hiroshima and Nagasaki bombings, 20: 16760
THORNGATE, J. H., Portable scaler, 20: 16846
THURSTON, Merlin O., Analysis of effect of fast-neutron bombardment on current-voltage characteristic of conductivity-modulated p-i-n diode, 20: 16912
TIEN, Vovan, Divalent rare earth sulfide–trivalent rare earth sulfide systems, 20: 16431
TIKHAYA, M. G., Distribution of U in dogs at long periods after inhalation of U_3O_8, 20: 16184
TIKTOPOULOS, George, Numerical solution of non-Fredholm (singular) integral equations by matrix inversion, 20: 16936
TILBURY, R. S., Prog. rpt. on research in activation analysis, 8/63–10/64, 20: 16336 (NYO-10175)
TILGER, C. A., π+p interactions at 450 Mev, 20: 17384
TIMM, U., Highly polarized coherent bremsstrahlung from a diamond target in Bev region, 20: 17679 (DESY-65/15)
TIMMERMAN, Lucien, Description of calorimetric measurement of the intensity of low-energy x radiation, 20: 16856
TIMMINS, T. H., Effect of reactor irradiation on Santowax WR, 20: 17122 (MIT-334-34)
TIMMONS, Darrel Holt, Noise analysis applied to a liquid-solid fluidized bed, 20: 18071 (TID-22665)
TISHCHENKO, B. I., Inelastic diffraction scattering treated by the complex angular momentum method, 20: 17817
TISHCHENKO, O. P., Adsorption method of determining radon concentration in the air from an airplane, 20: 16708
TITUS, Albert C., Weighing irradiated fuel specimens in water, 20: 16780 (TID-22689)
TLEUBERGENOVA, G. A., Helium particles emitted during 17.5-Bev π-meson collisions with photoemulsion nuclei, 20: 17716
TLEUBERGENOVA, G. A., Production of high-energy fragments by 7.5-Bev π mesons, 20: 17715
TOAFF, S., Low odd levels of erbium I., 20: 17261
TOBAILEM, J., Radioactivity induced by cosmic rays in the Bogou meteorite, 20: 15674
TOBIAS, C. A., Dark recovery and glycerol protection for diploid Saccharomyces cerevisiae, 20: 16231 (UCRL-16377)
TOBOCMAN, W., Distorted-wave theory of the one-meson-exchange reaction, 20: 17474
TODD, P. W., Dark recovery and glycerol protection for diploid Saccharomyces cerevisiae, 20: 16231 (UCRL-16377)
TOELGYESSY, J., Determination of arsenic in ores and rocks with high Mn by neutron activation analysis, 20: 16364
TOLMAN, E. L., Compton detector development report, 20: 16812 (EGG-1183-1174)
TOMBRELLO, T. A., Phase-shift analysis of T(n,n)T, 20: 17769
TOMIYASU, Fujio, Creep rupture strength of Incoloy (32Ni–20Cr steel), 20: 17031 (ORNL-tr-962)
TOMLINSON, L., Short-lived antimony and arsenic isotopes formed in fission, 20: 17834
TOMOV, T., Determination of arsenic in ores and rocks with high Mn by neutron activation analysis, 20: 16364
TONDINELLI, L., Comparative examination of methods for disadvantage factor calculations, 20: 18049 (RT/FI(65)-42)
TORGERSON, Ronald, Field-theoretic formulation of the optical model at high energies, 20: 17469
TORMA, Miklos, Effect of utilization factor on economy of heat-generating atomic power stations, 20: 18124
TORO, T., Heisenberg nonlinear spinor field equation in presence of gravitation for a nonlocal spin connection, 20: 17565
TORRES, P., Atomic and ionic partial stopping powers of He gas for a He beam, 20: 17305
TOTH, J. L., Automated logging and processing of NRL cyclotron magnetic field data, 20: 17188 (CONF-650922, pp 415-20)
TOTH, J. L., Prog. rpt. on NRL cyclotron, 9/65, 20: 17169 (AD-628928)
TOTH, R. S., Long-period modulation of stacking order in Au_3Mn, 20: 17066
TOUHILL, C. J., Treatment and disposal of glass melter condensates containing sulfuric acid, 20: 18159 (BNWL-SA-514)
TOURIN, Richard H., Spectroscopy of plasmajets and electric arcs, 20: 17901
TOURKY, A. Riad, Analysis of uranium in phosphate ores, 20: 16381
TOURNIER, E., Reactimeters, 20: 18032
TOUVIN, H., Comparison of effects of mutagenic substances by studying mutagenesis of plants, 20: 16225 (EUR-2715.f)
TOVEY, S. N. Energy spectrum of primary cosmic rays, 20: 17315
TOYOOKA, Edward T., Neoplasms following irradiation of the head, 20: 16245
TOZONI, O. V., Mathematical models for computing electric and magnetic fields, 20: 17161
TRAINOR, L. E. H., Reformulation for the meson-atomic model of the nucleon, 20: 17356
TRAPMANN, H., Influence of phosphate ester structure and the character of metal ions of fourth subgroup on dephosphorylation, 20: 16420
TREGUIER, R., Metoclopramide in treatment of roentgen disease, 20: 16163
TRESVYATSKII, S. G., Interaction of rare earth oxides with strontium oxide, 20: 17044
TRIDOT, Gabriel, Uranium semipentoxide, 20: 16430
TRIKHA, S. K., Diffusion parameters of graphite, 20: 17661
TRINKLER, E., Effect of γ radiation on magnetic diffusion in nickel–zinc ferrites, 20: 16532
TRINKO, J. R., Neutron fluctuation measurements at ORNL, 20: 18048 (ORNL-P-1967)
TRIPP, T. B., Heat treatment of anodic oxide films on Ta. IV., 20: 17055
TROETSCH, E., Calculation of squared-off cascades for isotope separation by diffusion, 20: 16929
TROFIMOV, A. S., Optimum control of a nuclear reactor by thermal processes, 20: 18054
TROST, A., Industrial moisture measurement with neutrons, 20: 16926
TROXELL, G. E., Reusability of buildings after a warfire, 20: 16621 (AD-625867)
TRUBEY, D. K., OGRE-G—Monte Carlo code for calculation γ dose rate at arbitrary points, 20: 17961 (ORNL-TM-1212)
TRUELLE, Marcel A., Loss of an emitter in defectoscopic field work, 20: 16764
TRUEMPER, J., Digital recording system of air shower experiment at Kiel, 20: 16873
TRUTIA, E., Angular distributions from $^{13}C(\alpha,n)^{15}O$ reaction at 14 Mev, 20: 17803
TSAI, B., High homogeneous field superconducting magnet for a polarized proton target, 20: 17586 (CONF-650922, pp 509-16)
TSAKADZE, Dzh. S., Attenuation of second sound in rotating He on

transition through phase transformation temperature, 20: 17641
TSAKADZE, Dzh. S., Relaxation of Onsager-Feynman vortexes in heating of rotating He II above phase transformation temperature, 20: 17642
TSAKADZE, Dzh. S., Relaxation processes related to temperature changes in rotating He II, 20: 17643
TSAPKIN, V. V., Excitation transfer from crystal lattice to rare earth ions, 20: 18010
TSCHIRF, E., Device for calculation of γ shielding problems, 20: 17969
TSCHOPP, Peter A., Design and construction of magnet and transport system for large liquid helium bubble chamber, 20: 16810 (CONF-650922, pp 366-76)
TSCHOPP, Peter A., Exciting coils for guiding magnet of A 4-Bev electron synchrotron, 20: 17199 (CONF-650922, pp 686-99)
TSERKOVNITSKAYA, I. A., Properties of organic thorium salts, 20: 16497
TSKHAKAYA, D. D., Compton scattering in a magnetic field, 20: 17409
TSUCHIHASHI, Keiichiro, Calculation of effective cutoff energies taking into account scattering and higher resonances of filters, 20: 17663
TU, Pham Qui, Photoproduction of vector mesons at high energies, 20: 17410
TUCCIARONE, A., Relativistic treatment of the three-body problem, 20: 17417
TUCHWEBER, B., Mechanism of experimental soft-tissue calcification, 20: 16162
TUGOV, I. I., p-Separation of variables in the Schroedinger equation, 20: 17561 (JINR-P-2532)
TUNKELO, E., Small neutron diffractometer, 20: 16882
TURNER, D. N., Linear thermal expansion of beryllia, 20: 17006 (AAEC/TM-300)
TURNER, J. M., Analysis of liquid film in annular flow, 20: 16604 (NYO-3114-13)
TURNER, J. P., Impact of plasma on a dipole magnetic field, 20: 17551
TURNER, T. A., The renogram: radioactive isotopes and renal disease, 20: 16311
TURGVTSEVA, A. M., Determination of nitrogen and oxygen in UF_6, 20: 16409
TUTTER, M., Diffraction of electromagnetic waves on plasma cylinders, 20: 17877 (IPP-6/44)
TVERBAKH, O. P., DATAPREP-II—reactor lattice homogenization and BIGG-II data preparation computer code, 20: 18047 (KR-78)
TYREN, H., Quasi-free proton-proton scattering in light nuclei at 460 Mev, 20: 17741
TYROR, J. G., Reactor physics calculations with the ARGOSY code, 20: 18051 (TRG-Report-1014)

U

UBERSCHLAG, J., Control and safety assembly for reactors of very high flux, 20: 18152
UCHIKAWA, Isamu, X-ray-induced mutants of European common wheat, 20: 16286
UEBERALL, H., Decay of nuclear giant resonance states following electroexcitation, 20: 17757
UEDA, Toshio, Medical survey of Japanese exposed to fallout radiation in 1954, 20: 16226 (NP-15891)
UEMURA, Yoshiaki, Medium dependence of charge changing collisions for 9.7-Mev carbon ions, 20: 17724
UGLIRZH, M., Symmetry groups in classical and quantum mechanics, 20: 17429 (JINR-P-2529)
UHLMANN, A., Plus-parity mesons and the 189-plet of SU(6), 20: 17339 (JINR-E-2557)
UMANSKAYA, S. L., Logical-element system for reactor control, 20: 18031
UNGER, K., Calibration of neutron-γ probes used in moisture and density measurement of solids, 20: 16374
UNIK, J. P., Fission-fragment angular, energy, and mass division correlations for the ^{234}U(d,pf) reaction, 20: 17865
UNIK, J. P., Primary nuclear charge from characteristic K x-ray emission in spontaneous fission of ^{252}Cf, 20: 17859
UPTON, A. C., Choice of a fallout shelter protection factor, 20: 16733 (ORNL-P-1098)
URBAN, W., ESR spectrometer with continuously variable frequency and high sensitivity, 20: 16800
USHAKOV, V. V., Direct interactions in reactions with finite nuclei in highly excited states, 20: 17714
USPENSKAYA, M. S., Excretion of thymidine with urine in ^{90}Sr-affected rats, 20: 16201
UST'YANTSEV, V. M., X-ray study of oxidation of UO_2, 20: 16474

V

VAENNGARD, Tore, ESR absorption of hexane/silica gel systems γ irradiated at low temperatures, 20: 16511
VAETH, J. M., Radiation effects on renal enlargement in the mouse, 20: 16282
VALLI, K., Alpha-gamma and alpha-conversion electron coincidence study of ^{219}Rn, ^{215}Po, and ^{211}Bi, 20: 17703
VAN ALLEN, J. A., Observation of ~500-kev protons in interplanetary space with Mariner IV, 20: 17318
VAN CAMPEN, Darrell R., Effects of Zn, Cd, Ag, and Hg on absorption and distribution of ^{64}Cu in rats, 20: 16182
VANDENBOSCH, R., Fission-fragment angular, energy, and mass division correlations for the ^{234}U(d,pf) reaction, 20: 17865
VAN DER VALK, Fred, Measurement of "knock-on" cross section in elastic scattering in H–He systems, 20: 17293
VAN ELST, H. C., Prog. rpt. on determination of embrittlement in steel, 10–12/65, 20: 17117 (EURAEC-1558)
VAN GEEL, J., Final purification of plutonium and conditioning of products, 20: 16560
VAN LANDUYT, J., Ordering of interstitial impurities in niobium, 20: 18003
VAN NORTON, R., Multiple spectrometer control by computer, 20: 16869
VAN TORNE, L. I., Specific electrical conductivities of Ta–Mo alloy single crystals, 20: 17083
VAN WAGENINGEN, R., Phenomenology of nuclear forces. I., 20: 17727
VAN WAGENINGEN, R., Phenomenology of nuclear forces. II., 20: 17728
VARFOLOMEEV, M. B., Cerium perrhenate and its cyrstal hydrates, 20: 16440
VARFOLOMEEV, M. B., X-ray and infrared study of perrhenate tetrahydrates of rare earths and yttrium, 20: 16473
VASARU, Gh., Enrichment of the molecular species $^{14}N^{15}N$ by thermal diffusion. I., 20: 16931
VASILESCU, A., Isotope exchange of active methyl hydrogens. III., 20: 16501
VASILEV, A. N., Whiteman type functional for two-particle scattering, 20: 17496
VASIL'EV, G. Ya., Tangential channels and construction of thermal column in VVR-M reactor, 20: 18139
VASILIEVSKAYA, V. V., Experimental radiation sickness induced with ^{210}Po, 20: 16268
VASILIU, S., Methods used for measurement of thermal conductivity and specific heat on small samples, 20: 17099
VASS, D. G., Search for level structure near 2.86 Mev in ^{10}B, 20: 17797
VAUGHAN, B. E., Wounding response and polar transport of ^{45}Ca in isolated root segments of Zea mays, 20: 16170 (AD-628805)
VAUGHAN, Janet, Discrimination between Sr and Ca in bone and transfer from blood to bone, 20: 16178
VDOVIN, V. L., Drift waves of non-potential nature in a stationary magnetoacoustic plasma, 20: 17949
VEBRA, E. Yu., Radioactivity, sizes, and composition of α-radiating aerosols, 20: 16646
VEDENOV, A. A., Theory of turbulent plasma, 20: 17958
VEGORS, S. H., Multiple pion production by 1.89-Bev/c π^-, 20: 17386
VEHAUC, Aleksander, Improvement of heat transfer of fuel element with polyzonal spiral finning, 20: 18078
VELDRE, V. Yu., Effective cross sections of electron collisions with atoms, 20: 17286
VENKATASUBRAMANIAN, V. S., Radioactive disequilibrium in minerals by α spectroscopy, 20: 16717
VENKATESWARLU, U., Instrumentation for control and safety of zero energy reactor Zerlina, 20: 18149
VENKATESWARLU, U., Transistorized instruments for reactor control and flux measurement, 20: 18027
VERBINSKI, Victor V., Deuteron polarization from $^{9}Be(p,d)^{8}Be$ reaction at 3 to 5 Mev, 20: 17760
VERGLAS, A., Production mechanism of $\bar{K}^*0(891)$ in K–p interaction at 3 Bev, 20: 17380
VERINK, Ellis Daniel Jr., Oxidation mechanism of uranium in moist, flowing nitrogen and in nitrogen–oxygen mixtures, 20: 16986
VERMEULEN, L. W., Recovery of thorium from uranium solutions, 20: 16573
VERNHET, Solange, Sedimentological significance of natural radioactivity of beaches of Gulf of Lion, 20: 16669
VERNON, M. J., Evaluation of Rb and Fe bias in flame photometric K determination for K–Ar dating, 20: 16713
VERNOV, S. N., Measurements of protons with energy of 0.4- to 8-Mev on Cosmos 41 satellite, 20: 17548
VERNOV, S. N., Measuring low-energy protons on the Kosmos-41 satellite, 20: 17310 (AD-623948)
VERON, Harry, Propagation of glow discharge into annular gap between discharge tube wall and cathode, 20: 17524
VERSCHUUR, K. A., Calculation methods of neutron shielding of reactors, 20: 17967
VERTEBNYI, V. P., Influence of VVR-M active zone configuration on neutron spectra from horizontal channel, 20: 18140
VERTOGRADOV, L. S., Proton emitters among Te isotopes, 20: 17687 (JINR-P-2514)
VERVIER, J., Effective N-N interactions in nuclei with 29 and 30 neutrons,

20: 17735
VERZILOV, E. E., Radiation-sedimentation method for aerosol studies, 20: 16655
VETTE, James I ., Space radiation environment, 20: 17249
VEYRIE, Pierre, Study of plasma created by focusing of laser beam in air, 20: 17908
VIDO, Ludovico, Measurement of ^{54}Mn in Unio pictorum of Lake Maggiore, 20: 16185
VIERK, I., Bibliography on high-energy physics, No. 5, 8/65, 20: 17153 (AED-C-23-05)
VIERK, I., Bibliography on high-energy physics, No. 6, 8/65, 20: 17154 (AED-C-23-06)
VIERK, I., Bibliography on high-energy physics, 8/65, 20: 17155 (AED-C-23-07)
VIGIER, Pierre, Magnetic hysteresis study of iron contaminated by nickel traces and irradiated with neutrons, 20: 17134
VIGLIN, A. S., Electrodynamics of homogeneous anisotropic and dispersive medium, 20: 17166
VIGNEAUX, Michel, Tritium activity of basin pouring from Mont Cenis, 20: 16668
VIJAYALAKSHMI, B., Energy spectrum of primary cosmic rays, 20: 17315
VILCEANU, Nicolete, Uranyl pyrophosphate complexes, 20: 16472
VILCOV, I., Angular distributions from $^{12}C(\alpha,n)^{15}O$ reaction at 14 Mev, 20: 17803
VILCOV, N., Angular distributions from $^{12}C(\alpha,n)^{15}O$ reaction at 14 Mev, 20: 17803
VILCOV, N., Isomeric yield for the 14-ms fissioning isomer from deuteron irradiation of, 20: 17857
VILCOV, N., Semiconductor radiation detectors. III-a., 20: 16889
VILEMAS, Yu., Effects of thermal decomposition of organic coolants on heat exchange in large-volume boiling, 20: 16615
VILENSKII, V. D., Parameters of vertical exchange and average rate of aerosol removal by clouds, 20: 16639
VILENSKII, V. D., Radioactivity of atmosphere over oceans and relationship to meteorological factors, 20: 16699
VILENSKII, V. D., Seasonal and geographical changes in ^{210}Pb content of the atmosphere, 20: 16640
VINOGRADOVA, L. I., Autoionization of nitrogen and oxygen ions after passage through a solid, 20: 17262
VINOGRADOVA, V. K., Accumulation of ^{90}Sr and ^{137}Cs in soils of Leningrad region, 20: 16702
VISENTIN, R., Isotropic monogap chamber pulsed with damped oscillation, 20: 16886
VISWANATHAN, L., Instrumentation for control and safety of zero energy reactor Zerlina, 20: 18149
VLASOV, M. F., Influence of VVR-M active zone configuration on neutron spectra from horizontal channel, 20: 18140
VODOPYANOV, L. K., Electron-bombardment-induced conductivity in fused silica, 20: 17133
VODOPYANOV, L. K., Electrical properties of InSb irradiated by neutrons at 77°K and by electrons at 300°K, 20: 17150
VOGEL, H., Argonne National Laboratory's pion focusing horn, 20: 17198 (CONF-650922, pp 650-6)
VOHRA, K. G., Multichannel analysis system for low levels of fission products in reactor coolants, 20: 16898
VOJINOVIC, Mirko, Effect of driving pulse duration on threshold level of trigger circuits, 20: 16785
VOLKOV, V. I., Tables of cross sections of photoionization of the hydrogen atom, 20: 17251 (IAE-873)
VOLKOV, V. S., Dispersion fuel elements for nuclear reactors, 20: 18079
VOLODKO, L. V., Luminescence spectra and structure of hydrated uranyl nitrates, 20: 16465
VON BUSCH, F., Velocity dependence of total scattering cross section of K on rare gases, 20: 17294
VON GUNTEN, H. R., Fission yields of isotopes in fission of ^{232}Th by reactor neutrons, 20: 17860
VON SALLMANN, Ludwig, Effects of x rays, myerlan, and TEM on lens epithelium, 20: 16256
VON ZUR MUEHLER, M., Ship reactor development in Japan, 20: 18129
VOOK, F. L., Ionization produced by energetic Ge atoms within a Ge lattice, 20: 17265
VOROB'EV, G. A., Isotropic spark chamber, 20: 16860
VORONOV, B. L., π-N Interaction in axiomatic approach, 20: 17416
VOROTNIKOV, P. E., Fission distribution in neutron-induced fission of ^{230}Th, ^{238}Pu, and ^{241}Am, 20: 17848
VOSS, G. A., Possible use of the CEA directly as a colliding beam facility, 20: 17173 (CEAL-1029)
VOSS, Milo D., Survey of environmental radioactivity, 20: 18136 (IS-1320)
VOSSEN, J. L., Plasma-anodized La titanate films, 20: 17045
VOVENKO, A. S., Spark chambers for studying elastic scattering of π^+ mesons by protons at 180°, 20: 16815 (JINR-P-2506)
VRIENS, L., Cross section formulae for ionization and excitation of atoms by high-energy electrons, 20: 17270

W

WACHBERGER, Eugen, Determination of ^{14}C, tritium, or ^{35}S after combustion of an organic sample at a system of nozzles, 20: 16387
WACHTEL, L. W., Suppression of DNA synthesis in weanling rat kidneys by short-term fasting, 20: 16158 (AD-628360)
WADA, Sueo, Diabetes mellitus in relation to atomic bomb exposure, 20: 16254
WADE, J. T., Evaluation of dissolvable epoxy systems for remote metallographic evaluations, 20: 16948 (ORNL-TM-1161, pp 103-11)
WADLEIGH, Willa, Electron transmission microscopy of polycrystalline BeO, 20: 17054
WAGEMANN, K., Future fuel needs of nuclear power plants, 20: 18099
WAGHMARE, Yeshwant R., Foundations for Hartree-Fock calculations with singular potentials, 20: 17791
WAGNER, H., Influence of serum of irradiated rats on Jensen sarcoma in vitro. III., 20: 16208
WAGNER, H.-F., Lifetime of the $^{31}/_2$ three-particle state of ^{177}Hf, 20: 17811
WAGNER, J. W., Cation diffusion in single-crystal and polycrystalline BeO, 20: 17049
WAHBA, S. S., Determination of certain trace impurities in U concentrates by activation analysis, 20: 16399
WAHL, W. H., Prog. rpt. on research in activation analysis, 8/63--10/64, 20: 16336 (NYO-10175)
WAHLGREN, M. A., Preparation of carrier-free ^{207}Bi for β spectrometry, 20: 16546
WAHLMAN, L., Radiochemical separation of carrier-free Zr from yttrium oxide, 20: 16353
WAINFAN, N., Interference fringes formed by x rays scattered from thin films, 20: 17163
WAINFAN, Nathan, Propagation of glow discharge into annular gap between discharge tube wall and cathode, 20: 17524
WAKAYAMA, N., Low-drift solid-state d-c amplifier, 20: 16803
WAKAYAMA, N., Solid-state neutron flux monitoring instruments for nuclear reactor, 20: 18034
WALKER, B. J., New type of superconducting magnet for traveling-wave masers, 20: 17626
WALKER, Dennis, Plane gasdynamic flows with orthogonal magnetic and velocity field distributions, 20: 17532
WALKER, J. A. J., Determination of oxygen in sodium, 20: 16349
WALKER, R. M., Ternary fission of heavy compound nuclei in thorite track detectors, 20: 17788
WALKER, W. D., Multiple pion production by 1.89-Bev/c π^-, 20: 17386
WALL, G. J., Measurement of fission cross sections for neutrons of energies in range 40 to 500 kev, 20: 17852
WALLACE, Walter Paul, Fuel element for nuclear reactors, 20: 18081
WALLERSTEIN, George, Analysis of abundances of rare earths in the sun, 20: 17237
WALLIS, G. B., Analysis of liquid film in annular flow, 20: 16604 (NYO-3114-13)
WALSTAM, R., Irradiation planning in radiotherapy, 20: 16320
WALTER, H. E., Removal of radiostrontium from milk with tricalcium phosphate and resulting changes in milk composition, 20: 16382
WALTERS, William B., Cross sections for $^{27}Al(\gamma,\pi^+)^{27}Mg$ reaction, 20: 17779
WANG, Shih Yi, Possible formation of dithymine peroxide in irradiated DNA, 20: 16203
WANG, Shih-Hi, Interaction of neutrons with ^{235}U nuclei at 2 ev to 30 kev, 20: 17856
WANG, Yung-ch'ang, Interaction of neutrons with ^{235}U nuclei at 2 ev to 30 kev, 20: 17856
WAPSTRA, A. H., Two-proton and two-neutron binding-energy systematics and α-decay energies, 20: 17729
WARAKSA, Irene, Nondestructive determination of grade of Be by radiography, 20: 16962
WARD, Roland, Modification of structures of ternary oxides by cation substitution. I., 20: 16436
WARING, R. C., Praseodymium-141 photoneutron cross section to 65 Mev, 20: 17764
WATANABE, Hitoshi, Ductility of metallic uranium containing carbide inclusions at rolling, 20: 17001
WATANABE, Shinsuke, Excitation of plasma oscillation by parametric resonance, 20: 17920
WATSON, C. D., Prog. rpt. on chemical technology, 11/64, 20: 16556 (ORNL-TM-1090)
WATSON, C. E., Energy levels of ^{170}Tm, 20: 17782
WATSON, J. H. P., Magnetization of synthetic filamentary superconductors. I., 20: 17604
WEENINK, M. P. H., Thermonuclear investigations. II., 20: 17927
WEGENER, H., Applications of Moessbauer effect, 20: 17989

WEIBEL, E. S., Axial high-frequency discharge, 20: 17879 (LRP-19/65)
WEIGEL, F., Curium(III) phosphates, 20: 16470
WEILL, J., Procedure for rapid start-up, 20: 18021
WEILL, J., Reactor control instrumentation design in France, 20: 18035
WEINBERG, I., Thermoelectric power in Nb–Zr alloys, 20: 17067
WEINER, Richard M., Check of C, P, and T conservation at large momentum transfer as test of conventional quantum electrodynamics, 20: 17578
WEIRAUCH, W., Isomer of ^{197}Au, 20: 17812
WEISBERGER, William I., Unsubtracted dispersion relations and renormalization of weak axial-vector coupling constants, 20: 17478
WEISS, H., Power measurements and automatic reactor control by Cherenkov or γ radiation, 20: 18033
WEISS, Z., DATAPREP-II—reactor lattice homogenization and BIGG-II data preparation computer code, 20: 18047 (KR-78)
WELCH, A. J. E., Yttrium oxide–titanium dioxide system, 20: 17032
WELLS, E. R., Injection and accumulation: single-pass experiments (DCX-1), 20: 17886 (ORNL-3908, pp 1-17)
WELLS, W. M., High-temperature testing of graphite helical-screw expanders and compressors, 20: 16591 (UCRL-14660)
WENDT, G., Determination of nuclear reaction widths from reaction yield curves, 20: 17778
WENT, J. J., Homogeneous suspension reactor project, 20: 18072
WENTZ, L. B., Prog. rpt. on kinetic studies of heterogeneous water reactors, 6/30/65, 20: 18050 (STL-372-22)
WENZEL, P., Thermal breeding by utilizing thorium–uranium fuel cycle, 20: 18073
WERNER, E., Inclusion of core excitations in quasi-particle theory of nuclear structure, 20: 17814
WESLEY, E. J., Radiation measurement utilizing communication theory, 20: 16893
WESOLOWSKI, Jerome J., Ground-state (p,n) reactions in mirror nuclei and quasielastic model of (p,n) reactions, 20: 17775
WESTERMAN, R., Charging Zircaloy-2 with hydrogen beyond the solubility limit, 20: 16981
WHATLEY, M. E., Prog. rpt. on chemical technology, 11/64, 20: 16556 (ORNL-TM-1090)
WHICKER, F. W., Factors influencing accumulation of fallout ^{137}Cs in mule deer, 20: 16723 (COO-1156-11)
WHITE, P. H., Measurement of fission cross sections for neutrons of energies in range 40 to 500 kev, 20: 17852
WHITE, R., Strong vertex according to SL(6,C), 20: 17427 (IC-66/20)
WHITE, W. B., Prog. rpt. on crystal chemistry, 8/13–11/13/65, 20: 17007 (AD-627468)
WHITEHEAD, A. Bruce, Yield and energy spectrum of secondary electrons generated by fission fragments, 20: 17168
WHITEHOUSE, J. E., Electron irradiation of p-type Ge at 4.2°K, 20: 17144
WHITMER, R. F., Echo processes in a plasma, 20: 17933
WHITMORE, G. F., Radiobiology at the cellular level, 20: 16292
WHITMORE, R. E., Plasma-anodized La titanate films, 20: 17045
WHITTAKER, J. M., Cosmological model, 20: 17241
WHITTEM, R. N., Determination of Sr in samples of biological and geological origin, 20: 16345
WIELGOZ, Karoline, High-energy fission of ^{238}U, 20: 17790
WIGNER, Eugene P., Choice of a fallout shelter protection factor, 20: 16733 (ORNL-P-1098)
WIKNER, E. G., Nuclear spin relaxation in gallium metal, 20: 17995
WILIP, Elmar K., Thermally activated processes in deformation of neutron-irradiated Cu single crystals. II., 20: 17980 (ANL-Trans-274)
WILKINSON, D. H., Properties of the 4.77- and 5.16-Mev states of ^{10}B, 20: 17761
WILKINSON, David T., Cosmic background radiation at 3.2 cm—support for cosmic black-body radiation, 20: 17317
WILKS, R. J., Small-gamma camera, 20: 16853
WILLCOX, B. A. M., Computation of x-ray diagnostic exposure tables, 20: 16751
WILLIAMS, David C., Decay of ^{194}Ir and ^{194}Os, 20: 17781
WILLIAMS, H. T. Jr., Consistency in analysis of high-buckling critical experiments, 20: 18065
WILLIAMS, J. M. E., Efficiency of Whatman-type ACG/B filter papers for methyl iodide retention in air, 20: 16719 (AEEW-M-568)
WILLIAMS, M. M. R., Neutron flux perturbations due to infinite plane absorbers. II., 20: 17655
WILLIAMS, R. K., Thermal conductivity values for solid and liquid promethium, 20: 17025 (ORNL-TM-1424)
WILLIAMS, W. T., Space-charge controlled ionization growth in hydrogen, 20: 17518
WILLIAMSON, H. E., Irradiation performance of alternate cladding materials, 20: 17120 (GEAP-4916)
WILLIAMSON, H. E., Performance of fuel rods containing boron burnable poison, 20: 17121 (GEAP-4918)
WILLIS, Conrad P., Determination of radioisotopes of Ce, Ba, La, and Np after separation by $BaSO_4$, 20: 16343
WILLIS, W. J., Pion production in p$\bar{p}$ annihilations at 3.3 and 3.7 Bev/c, 20: 17385
WILLMARTH, T. E., Electron optical study of effect of aging on carbides in Nb–W–Zr alloy, 20: 17023 (ORNL-TM-1161, pp 208-24)
WILLS, John G., Coupled-channel Schroedinger-equation model for high-energy peripheral collisions, 20: 17397
WILMORE, D., Computer program for calculation of compound nuclear cross sections by Hauser-Feshbach theory, 20: 17672 (AERE-R-5053)
WILSON, J. C., Electrical discharge machining in the metallurgical laboratory, 20: 16951 (ORNL-TM-1161, pp 159-81)
WILSON, R. Gale, Hemispherical spectral emittance of ablation chars, carbon, and zirconia to 3700°K, 20: 17021 (N-65-18607)
WING, J., Preparation of carrier-free ^{207}Bi for β spectrometry, 20: 16546
WINKLER, Keith G., Output of self-rectified dental x-ray machines, 20: 16844
WINOGRAD, H., Power supply system for ZGS ring magnet, 20: 17227
WINSTON, R., Argonne National Laboratory's pion focusing horn, 20: 17198 (CONF-650922, pp 650-6)
WINTER, D. F., Field-aligned flow of a conducting fluid past a source of magnetism, 20: 17509 (D-1-82-0469)
WINTER, Georg, Decay of ^{79}Kr, 20: 17700 (ZfK-PhA-17)
WINTER, J. A., Effect of temperature on γ radiolysis of water vapor, 20: 16536
WINTERNITZ, P., Symmetry groups in classical and quantum mechanics, 20: 17429 (JINR-P-2529)
WINTERNITZ, P., Two-meson annihilation of baryons in broken SL(6,C) symmetry, 20: 17347 (JINR-P-2547)
WIPF, S. L., Flux pumps as power supplies for superconducting coils, 20: 17596 (CONF-650922, pp 615-24)
WISHART, R. C., Materials marking system, 20: 18176 (SCL-DR-66-6)
WITTEBORN, Fred Carl, Free-fall experiments with negative ions and electrons, 20: 17167
WITZMANN, H., Fluorescence of rare earths. III., 20: 16466
WIZA, J. L., Energy levels of ^{31}S, 20: 17780
WIZA, Joseph L., Study of ^{19}O by ^{17}O(tp)^{19}O and ^{18}O(d,p)^{19}O reactions, 20: 17758
WOHLLEBEN, D. F., Superconductivity of beta uranium, 20: 17095
WOJTASZEK, Joseph Henry, Electromagnetic mass differences of baryons, mesons, and $\frac{1}{2}^+$ resonances, 20: 17507
WOLF, A., Fuel cores for plate fuel elements, 20: 16995
WOLF, G., Heat transfer in boiling hydrogen, neon, nitrogen, and argon, 20: 16610
WOLFE, B., Parameter study of large fast reactor meltdown accidents, 20: 18123
WOLFF, Sheldon, Mitotic delay and apparent synergism of far-red radiation and x rays in chromosome aberrations, 20: 16278
WOLFF, U. E., Metallic inclusions in UO_2, 20: 16953 (ORNL-TM-1161, pp 249-66)
WOLKE, Robert L., Prog. rpt. on recoil studies of nuclear reactions, annual, 1/65–1/66, 20: 16508 (NYO-2771-13)
WOLTEN, G. M., Data for $LaTaO_4$ and $PrTaO_4$, 20: 16438
WOLTER, W., Dynamic behavior of a research reactor, 20: 18144
WOLTERBEEK MULLER, L., Electron capture into excited states by He ions incident on He, 20: 17304
WONG, K. W., Hard-core potential and boundary-condition model for nuclear matter, 20: 17772
WOOD, D. E., Comparison of neutron-activation analysis and hot-extraction analysis of oxygen content of steel, 20: 16400
WOOD, G. T., Gamma-gamma angular-correlation study of ^{169}Tm in lutetium iron garnet, 20: 17994
WOOD, J., Existence of higher time decay constants in pulsed neutron experiments, 20: 17662
WORLEY, R. D., Microgram surface density measurements by observation of proton-produced x rays, 20: 17051
WORTMAN, D. E., New series expansion in statistical mechanics, 20: 17527
WRIGHT, Donald, Ground-state energy of charged Bose gas, 20: 17526
WRIGHT, R. W., Prog. rpt. on kinetic studies of heterogeneous water reactors, 6/30/65, 20: 18050 (STL-372-22)
WRIGHT, Thomas Rea, System UO_2–ZrO_2, 20: 17005
WU, C. S., Magnetic dipole and electric quadrupole hyperfine effects in ^{209}Bi muonic x rays, 20: 17793
WU, Tai Tsun, Born approximation and large-momentum-transfer processes in potential scattering, 20: 17460
WU, Tai Tsun, High-energy large-momentum-transfer processes and analyticity in coordinate space, 20: 17461
WYSOPOLSKI, J., Determination of mixture of thermal-neutron and γ exposures by film badges, 20: 16807 (CLOR-IBJ-42/D)
WYTTENBACH, A., Fission yields of isotopes in fission of ^{232}Th by reactor neutrons, 20: 17860

Y

YAGODOVSKII, I. V., Radioactive isotopes in atmosphere and their use in

meteorology, 20: 16636
YAKOVENKO, V. M., Low-frequency properties of semiconductor plasma in stationary electric field, 20: 18013
YAKOVLEVA, G. V., Radioactive fallout in Vilnius in 1962, 20: 16700
YAKUBOV, I. T., Energy emitted by argon plasma in spectral lines, 20: 17930
YAMAGATA, Noboru, Cesium-137 in Japanese soil and rice, 20: 16169
YAMAGUCHI, Hisashi, Survey of nuclear reactions induced by 57-Mev protons. II., 20: 17725
YAMAKIDO, Michio, Diabetes mellitus in relation to atomic bomb exposure, 20: 16254
YAMAMOTO, Albert S., Prog. rpt. on phase equilibria of Ta-rich region of Ta–W–Hf and Ta–W–Zr systems, final, 9/64–11/65, 20: 17012 (DRI-1092-226)
YAMAMOTO, S. S., K⁻-p interaction at 2.24 Bev/c, 20: 17383
YAMAMOTO, Y., Cosmic rays in upper atmosphere, 20: 17322
YAMANISHI, Kiyoshi, Breeding of medicinal plants exposed to γ irradiation. I., 20: 16290
YAMASHITA, Yoshihiko, Diabetes mellitus in relation to atomic bomb exposure, 20: 16254
YAMATERA, Hideo, Electrodeposition of Ru from Ru(III) and Ru(IV) solution and a fission-product solution, 20: 16563
YAMAUCHI, Yuzuru, Protective effects of two drugs against radiation injury, 20: 16302
YAMAWAKI, Michio, Oxidation behavior of Nb and Nb–V alloys, 20: 16982
YAMAZAKI, H., Comment on "aberrations of focused beams of charged particles caused by space charge," 20: 16784
YAMAZAKI, M., Tritium measurement with liquid scintillation counter, 20: 16373
YAMAZAKI, Tomohisa, Breeding of medicinal plants exposed to γ irradiation. I., 20: 16290
YANG, John Y., Radioassay of tritium- and ^{14}C-labeled polymer, 20: 16384
YANKWICH, Peter E., Reversing hydrogen isotope effect on rate of gas phase decomposition of oxalic acid, 20: 16455
YANSON, I. K., High-frequency Josephson current, 20: 17636
YAREMENKO, Z. A., Interaction of rare earth oxides with strontium oxide, 20: 17044
YAROV, A. S., Method of investigating betatron oscillation resonances, 20: 17221
YASHIN, D. A., Tangential channels and construction of thermal column in VVR-M reactor, 20: 18139
YASUNO, Takehiko, Measurement of resonance fission integral of ^{233}U, 20: 17722
YATES, M. J. L., Coulomb excitation of low-energy states in Ce, Nd, and Sm isotopes, 20: 17734
YATES, M. J. L., Fission following (d,p) and (t,p) reactions in uranium isotopes, 20: 17844
YAUGER, W. L., Response characteristics of high-temperature electron-capture detector, 20: 16804
YAVOR, S. Ya., On the paper "third order abberations of an electric strong-focusing doublet", 20: 17219
YDO, H. J., Euratom's role in creation of a nuclear industry, 20: 18180
YOCK, P. C. M., One-particle exchange model for inelastic p-p scattering, 20: 17381
YOKOYAMA, Takamitsu, Relation between forward and backward rates of hydrogen electrode reaction in isotopically mixed system, 20: 16459
YOSELI, Morihiro, Excitation of plasma oscillation by parametric resonance, 20: 17920
YOSHIDA, Konosuke, Effect of uv irradiation on acid fastness and gram positivity of mycobacteria, 20: 16195
YOSHIDA, Kunio, Motion of balls, mill charge, and their pulverizing effect in the ball mill, 20: 16957 (LA-tr-66-11)
YOSHIDA, Kunio, Pulverizing of natural graphite particle by hammer mill, 20: 16958 (LA-tr-66-12)
YOSHIDA, Kunio, Shape of particle of natural graphite pulverized by cutter mill, 20: 16956 (LA-tr-66-6)
YOSHIDA, Kunio, Studies on the pulverizing of crystalline graphite, 20: 16955 (LA-tr-66-5)
YOUNG, J. A., Prog. rpt. on graphite interface studies, 5/63–9/65, 20: 18127 (GA-6753(Pt.1))
YOUNG, James A., Slow neutron spectra in molecular hydrogen at low temperatures, 20: 17664
YOUNG, R. A., Injection and accumulation: single-pass experiments (DCX-1), 20: 17886 (ORNL-3908, pp 1-17)
YOUNG, S. J., Cross section and polarization of Balmer α radiation produced with N_2, 20: 17269
YOUNT, D., Scattering of 150- and 300-Mev positrons and electrons from Bi, 20: 17785
YU, Wen-Shih, Heat transfer to liquid metals flowing turbulently in eccentric annuli. I., 20: 16612
YUDIN, N., Nature of the giant resonance in photonuclear reactions, 20: 17706
YUGETA, REI, Nitrous oxide as electron scavenger in radiolysis of hydrocarbons, 20: 16515
YUILLE, W. D., Control of fission-product release from advanced gas-cooled reactors, 20: 18110
YULDASHEV, A. A., Elastic scattering of 5.5-Bev π mesons on protons, 20: 17360
YULE, Herbert P., Data convolution and peak location, peak area, and peak energy measurements in scintillation spectrometry, 20: 16344
YUL'MET'EV, R. M., Quasiclassical approximation in theory of slow neutron scattering, 20: 17666
YUNG, J. M., Cladding temperatures used in automatic control for a power reactor, 20: 18105
YUPKO, V. L., Nature of chemical bond in rare earth dicarbides, 20: 17048
YURKA, G. E., Large spark chamber magnet with tape-wound coils, 20: 16809 (CONF-650922, pp 253-61)
YUROVA, L. N., Certain problems in physics and technology nuclear reactors, 20: 18070
YUSHMANOV, E. E., Unstable states of a plasma in a trap with combined field, 20: 17925

Z

ZABIDAROV, E. I., Critical scattering of polarized neutrons in nickel, 20: 17986
ZABLOCKI, H. S., Non-destructive electrical method of studying the density distribution of a randomly packed bed, 20: 18018 (CONF-651101-73)
ZADUBAN, M., Chromatographic separation of $^{131}I^-$, $^{131}IO_3^-$, and $^{131}IO_4^-$, 20: 16567
ZAKHARKO, Ye. M., Scintillation excitation mechanism in NaI(Tl), 20: 17991
ZAKHAROV, V. I., Possible radiative decays of heavy mesons involving violation of charge parity, 20: 17501
ZAKRZEWSKI, Janusz, Discovery of heavy hypernuclei, 20: 17796
ZAPLATYNSKY, I., Zeta phase in system Ta–C, 20: 17050
ZARAEV, O. M., Observation of hot radioactive particles in the atmosphere during 1962-1964, 20: 16677
ZEL'DOVICH, Ya. B., Quarks: astrophysical and physicochemical aspects, 20: 17411
ZELDOVICH, Ya. B., Survey of modern cosmology, 20: 17231
ZEMAN, Adolf, New principle of activation-analysis separations. X., 20: 16396
ZEMAN, Adolf, Substoichiometric determination of manganese by neutron-activation analysis, 20: 16403
ZEN, J., Multiple-duration monostable multivibrator, 20: 16792
ZENKER, W., Calculation of lattice parameters of the WWER core, 20: 18143
ZETTERSTROEM, H.-O., Unscrambling of proton-recoil spectra, 20: 16875
ZEZULA, R., Flat flux in slab reactor with natural uranium, 20: 18058
ZHABOTINSKII, M. E., Excitation transfer from crystal lattice to rare earth ions, 20: 18010
ZHAROV, Yu. D., Interaction of radiation-induced point defects with dislocations, 20: 17135
ZHELEV, Zh. T., New isotopes ^{157}Eu, ^{157}Ho, and ^{156}Er, 20: 17808
ZHILKINA, M. I., Chemical composition of atmospheric precipitation and fallout in vicinity of Leningrad, 20: 16704
ZHILKINA, M. I., Fallout of ^{90}Sr and ^{137}Cs isotopes in vicinity of Leningrad in 1961-1963, 20: 16701
ZHIRKIN, Y. N., Deformed Zr–Ti–O–Fe alloy for high-pressure chambers, 20: 17003
ZHIVULINA, L. I., Preparation of thin layers of zirconium carbide by electrophoresis, 20: 17004
ZHUKOV, V. V., Tungsten heater stability in vacuum at temperatures up to 3273°K, 20: 16596
ZHUKOVA, I. A., Thermodynamic properties of Nb at temperature range from 0°K to melting point, 2740°K, 20: 17100
ZIELINSKI, Waclaw, Hydrophobization of cellulose by radiation-induced grafting of styrene on its surface, 20: 16507 (INR-671/XVII/C)
ZIL'BERSHTEIN, Kh. I., EPR in irradiated quartz single crystals containing aluminum impurity, 20: 16539
ZIMANYI, Jozsef, Circular polarization of γ radiation following the stripping reaction, 20: 17726
ZIMBRICK, J. D., Health physics for maintenance operation on a homogeneous research reactor, 20: 16757
ZIMMERMAN, Ben, Magnet coil fabrication, 20: 16988 (CONF-650922, pp 305-12)
ZIMMERMAN, D. R., Low work function collector: strontium tungstate, 20: 17335
ZIMMERMANN, W., Highly polarized coherent bremsstrahlung from a diamond target in Bev region, 20: 17679 (DESY-65/15)
ZINOV'EV, G. M., Inelastic π^+-p interaction at high energies and statistical model, 20: 17344 (JINR-P-2530)
ZIPF, K., Effect of pyridoxine on renal excretion of Sr, Ca, and phosphate, 20: 16176
ZMBOV, K. F., Isotopic analysis of sulfur by solid source mass spectrom-

etry, 20: 16379
ZOLIN, L. S., Real part of pn scattering amplitude at 2 to 10 Bev, 20: 17363
ZORINA, K. I., Radon concentration and vertical turbulent mixing in surface boundary layer of atmosphere, 20: 16692
ZUBER, N., Prog. rpt. on two-phase flow investigation, 10–12/65, 20: 16601 (GEAP-5067)
ZUEND, H., Safety precautions to prevent criticality accidents, 20: 16562
ZUGENMAIER, P., Theory of molecular beam production with help of cylindrical tubes, 20: 17279
ZWICKER, Earl F., Radiation effects on fracture surface energy of KCl, 20: 17137

SUBJECT INDEX

Main entries in this index are generally specific materials, things, and processes. These are followed by modifiers that describe the properties of, and processes applied to, the main entries.

The number preceding the colon is the *NSA* volume number, and the number following is the abstract number. The designation (R) following the abstract number indicates that the abstract is of a progress report; (P) indicates a patent; and (T) indicates a translation. Abstracts for reports other than progress reports carry no letter designation. References to report numbers, where appropriate, are included after the abstract number of the citation. Published literature (journal article or book) is identifiable by the absence of a report number.

The user should bear in mind that the ideas presented in the original literature, rather than key words, have been indexed. The indexers have tried to select what seemed the most probable and logical place to look for typical information. Since it is not possible to anticipate where a user would look for information, numerous cross references are included in cumulative indexes to assist him in his search.

Experience in using an index of this type will be the best guide in obtaining the desired information, and a consideration of synonymous or closely related terms will prove valuable.

Information must be so indexed as to be of the greatest use to the greatest number of users. This requires that a topic be indexed to headings that most specifically describe it and not ordinarily to the headings that describe its ultimate use, nor to the general class headings that include the specific headings. For example, information on the treatment of thyroid disease with I-131 would be indexed under Thyroid Gland and under Iodine Isotopes I-131, but not necessarily under Radiotherapy. A study of the effects of x radiation on hair would be indexed under both X Radiation and Hair. However, the information would not be indexed under the experimental animal, e.g., Rats, unless the report discusses the effects on rat hair as compared with the effect on the hair of other animals.

The broad, general class headings are used only for general information or for comprehensive reports or articles.

Subject Heading Styles

Generally, the direct form of subject entry is used rather than inverted headings, e.g., Amino Acids rather than Acids, Amino; Helium Isotopes He-4 rather than Helium—isotopes He-4 or Helium—He-4 isotopes. Note, however, that in some cases parenthetic modifying terms or inverted headings of the form Neutrons, Fast are used in preference to a direct entry that would result in the scattering of information. Organic compounds are usually entered in the index in the inverted form so that substituted compounds can be listed near the parent compound; e.g., Benzene, Bromo- rather than Bromobenzene. In general, the style of nomenclature used is that of Chemical Abstracts, except that some items listed in that publication as subheadings are elevated to form part of the main heading; e.g., Butyric Acid, Methyl Ester rather than Butyric Acid—methyl ester.

Alphabetization

Main headings are alphabetized word-by-word. A parenthetic qualifier following a main heading is disregarded in alphabetizing unless there are two or more headings identical except for the parenthetic qualifier, in which case the qualifier determines the order. Headings involving Greek letters are arranged as if the names of the letters were spelled out.

Examples:

M-Capture
see Electron Capture
Magnesium
Magnesium Alloys
Manganese Fluorides
Manganese(II) Fluorides
Mesons
Mesons (π)
Mesons (ρ)
3-Pentanol, 2,4-Dimethyl-
2-Pentanol, 2-Methyl-
2-Pentanol, 4-Methyl-

Nomenclature of Inorganic Compounds

Inorganic compounds are indexed in the direct form, listing cations in the order of increasing valence in the case of polycationic salts of varying valence and in alphabetic order for polycationic salts in which all cations have the same valence; e.g., Sodium Aluminum Silicates and Potassium Sodium Sulfates.

Multicomponent Alloys and Other Systems

Multicomponent alloys, except well-known trade names, are indexed under a main heading in the form "element alloy" for each element in the alloy. The modifier begins with element symbols for each component arranged alphabetically as if the English name for the element were spelled out.

Example: Copper-Gold Alloy is indexed
Copper Alloys
Cu-Au...
Gold Alloys
Cu-Au...

Well-known alloys such as Zircaloy-2 are indexed directly to the trade name; cross references referring from each component of the alloy to the entry for the trade name appear in cumulative indexes.

Multicomponent systems of non-metallic elements are indexed in a manner similar to alloys except the main heading used contains the word "Systems" in place of "Alloys."

Example: Silicon–Tungsten Systems are indexed
Silicon Systems
Si-W...
Tungsten Systems
Si-W...

Multicompound systems and mixtures of compounds are indexed under the main heading for each component com-

pound; the modifiers begin with an alphabetical listing of compound formulas.

Example: Lead Titanate–Lead Zirconate is indexed
Lead Titanates
$PbTiO_3$-$PbZrO_3$...
Lead Zirconates
$PbTiO_3$-$PbZrO_3$...

A mixed system of compounds and elements is indexed using a combined form of the above conventions, e.g., a dispersion of copper and alumina would be indexed

Aluminum Oxides
Al_2O_3-Cu...
Copper Systems
Al_2O_3-Cu..

Physical States and Configurations of Materials

Specification of the physical state, if other than normal, or geometric configuration of the material is included in the modifying phrase, i.e., liquid metals would be indexed to the metal with "liquid" in the modifier, and carbon crucibles would be indexed to Carbon with "crucibles" appropriately placed in the modifier and also to Crucibles if appropriate.

Modifying Phrases

The modifiers appearing under a main heading are written specifically to describe the relation of the item being indexed to that main heading. The modifier, therefore, will generally contain more useful information about that relation than will a title or a phrase written to be used under every main heading assigned to the item. Effort is exerted to begin the modifier with the word judged to be of greatest use to the greatest number of users; this, however, does not obviate the need to consider all modifiers under the main heading(s) of interest.

Modifiers are usually intended to form a meaningful phrase when combined with the main heading. Some are intended to be read following the main heading, e.g., the entry Hydrogen—sorption by charcoal is read "hydrogen sorption by charcoal"; however, as a result of placing the important word first, many modifiers must be arranged for smooth reading, e.g., Formaldehyde—yields in radiolysis of ethyl ether, effects of deuterium on is read "effects of deuterium on formaldehyde yields in radiolysis of ethyl ether" and Uranium—crystal structure of, effect of cooling rate on allotropic transformations in is read "effect of cooling rate on allotropic transformations in crystal structure of uranium." Prepositions are sometimes omitted if no ambiguity results.

Special characters are added to modifiers in the field of physics; if the modifier does not establish the experimental or theoretical character of a reference, a symbol (E), (T), or (E/T) is placed immediately after the modifying phrase and before the journal reference number. The value of this identification has been established by the American Institute of Physics.

A

ABSTRACTS
on electrets, 20: 17971 (AD-299256)
on electronic and atomic collisions, 20: 17288
on radioactive waste disposal, 20: 18153 (AED-C-01-12)
on radioactive waste disposal, 20: 18154 (AED-C-01-13)
ACCELERATORS
beam quantum depolarization in, storage rings of high-energy electron, (T), 20: 17689 (NP-15783)
beam transport system design for, computer program for, 20: 17211 (LNF-65/45)
bibliography, 20: 17170 (AED-C-18-05)
book: *Particle Accelerators*, 20: 17226
control of, computer systems for, 20: 17209(R) (LA-3479)
design and research programs using, at Saclay, 20: 18181
development, 20: 17209(R) (LA-3479)
magnet development for, 20: 17222
operation at Risö, 20: 18174(R) (NP-15771)
power supplies for, development of, 20: 17209(R) (LA-3479)
waveguides for, development and testing of, 20: 17209(R) (LA-3479)
ACCIDENTS
criticality, at Eurochemic irradiated fuel reprocessing plant, methods of preventing, 20: 16562
planning for maximum credible, in waste storage in salt caverns, (T), 20: 16722 (BMwF-FBK-65-03)
radiation dose to personnel from IIT reactor, 20: 16757
radiation dosimetry in criticality, using hair activation, 20: 16758
ACETIC ACID
corrosive effects of, on iron-base alloys, mechanisms of stress-, 20: 16968 (COO-1319-33)
dissociation of, in aqueous solutions at 0 to 50°C, effects of deuterium on, 20: 16458
effects on uranium sorption by platinized carbon, 20: 16581
ACETIC ACID, CHLORO-
scandium salts of, preparation and properties of, 20: 16427
ACETIC ACID, DICHLORO-
scandium salts of, preparation and properties of, 20: 16427
ACETIC ACID, (ETHYLENEDIAMINE)TETRA- COMPLEXES
with cerium, chemical properties of praseodymium-144 produced by beta decay of cerium-144 in, 20: 16544
with iron, effects on hydrolysis of α-D-glucose 1-phosphate, 20: 16421
with thorium, effects on hydrolysis of α-D-glucose 1-phosphate, 20: 16421
ACETIC ACID, IODO-
radiosensitivity effects on tumor cells in culture, 20: 16299
ACETIC ACID, TRICHLORO-
scandium salts of, preparation and properties of, 20: 16427
ACETONE
effects on radioinduced rayon to styrene graft polymerization, 20: 16528
formation by disproportionation of aliphatic ketones in perchloric acid, 20: 16542(R) (TID-22646)
reduction by borohydride ions, secondary deuterium isotope effects in, 20: 16555
ACETONE, THENOYLTRIFLUORO-
complexes with cerium, lanthanum, neodymium, praseodymium, and samarium, magnetic susceptibilities of, 20: 16416(R) (NYO-906-68)
complexes with praseodymium, preparation, properties, and structure of, 20: 16416 (NYO-906-68)
complexes with praseodymium, Szilard-Chalmers reaction in, 20: 16416(R) (NYO-906-68)
solvent properties for americium, synergistic effects of tri-*n*-octylamine on, 20: 16571
ACETONITRILE
yields in reactions between ethylene and active nitrogen, 20: 16510(T) (NP-tr-1364)
ACETOPHENONE
reactions with phosphoric acid, products formed by disproportionation in, 20: 16542(R) (TID-22646)
reduction by borohydride ions, secondary deuterium isotope effects in, 20: 16555
2,2,2-triphenyl-, formation by rearrangement of benzopinacol in perchloric acid, 20: 16542(R) (TID-22646)
ACETYLENE
formation in reactions between rare earth dicarbides and water, 20: 17048
production from hydrocarbons in plasma jet, 20: 17959
production from methane in plasma jets, 20: 17959
spectra of x-irradiated deuterated and normal, trapped in solid rare gases, 20: 18016
acetylene–O, transport coefficients for combustion products of, (T), 20: 17519
ACRIDINES
effects on mutations in yeast, 20: 16159(R) (ORNL-3900, pp 150-81)
effects on phage-bacteria complex in *Escherichia coli*, 20: 16270(T)
ACRIFLAVINE
effect on synthesis of RNA during recovery of DNA synthetic system in uv-damaged *E. coli*, 20: 16202
ACTINIDE OXIDES
preparation and properties, 20: 17158(R) (ORNL-3900, pp 82-149)
ACTINIUM ISOTOPES Ac-227
neutron fission of, fragment mass distributions from, (E), 20: 17861
production by neutron irradiation of radium-226, calculations for, 20: 16927 (MLM-1297)
properties as heat source, 20: 16927 (MLM-1297)
ACTINOMYCIN
preparation and purification of tritium-labeled, 20: 16550
ACTIVATION ANALYSIS
bibliography on, 20: 16336(R) (NYO-10175)
equipment and methods for, 20: 16365
equipment and methods for, 20: 16335(R) (NBS-TN-276)
equipment and procedure for, of steel for oxygen, 20: 16357
equipment for, calibration of, 20: 16374
indicators for, properties of metastable nuclear isomers for use as sensitive, 20: 16336(R) (NYO-10175)
methods and techniques of neutron, 20: 17822
neutron, methods using lithium-drifted germanium detectors, 20: 16888
neutron, variable-energy, 20: 16332 (GA-6691)
radiochemical separations in, 20: 16336(R) (NYO-10175)
sensitivities of helium-3 reactions for, 20: 16331 (GA-6568)
ACTIVATION DETECTORS
design of lithium-6-iodide scintillation, for neutrons, 20: 16819 (LA-3435)
performance for thermal neutron spectra determination, orthogonal expansion method for, (E/T), 20: 16857
ADENINE
effects on viability of stored erythrocytes, 20: 16303(R) (AD-626384)
ADENOSINE, DEOXY-
preparation of carbon-14-labeled alpha and beta anomers of, method for, 20: 16545
ADENOSINEPHOSPHORIC ACIDS
hydrolysis of, effects of hafnium, thorium, titanium, and zirconium catalysts on, 20: 16420
ADHESIVES
performance and selection of, for use in space vehicles, 20: 16944 (NASA-SP-3025)
ADRENAL GLANDS
radiation effects on, following tumor therapy, 20: 16209
radiation effects on dog, α, 20: 16268
radiosensitivity effects on mice and rats, review on, 20: 16232(T) (JPRS-34120)
ADRENALINE
effects on bone blood flow, 20: 16192
ADRENOCORTICOTROPIC HORMONE
labeling with iodine-125, 20: 16494
ADVANCED TEST REACTOR
materials irradiation testing in, handbook for, 20: 18135 (IDO-17135)
AEROSOLS
accumulation of radioactive, on land and ocean surfaces, 20: 16706
composition of radioactive, in surface boundary layer of atmosphere, 20: 16644
conference on atmospheric, 20: 16636
deposition rate of radioactive, on pasture grass, 20: 16160 (UCRL-14739(Pt.2))
diffusion in atmosphere, vertical turbulent, 20: 16639
diffusion of radioactive, in atmosphere, 20: 16651
dispersion of radioactive, in atmosphere, 20: 16642
dispersion of radioactive, in stratosphere, 20: 16643
distribution in lower layers of atmosphere, 20: 16652
particle dimensions and mobility of radioactive, in atmosphere, 20: 16690
properties of, in surface boundary layer of atmosphere over Moscow, 20: 16645
properties of, in atmosphere over Vilnius, Russia, 20: 16646
removal from atmosphere by clouds and precipitation, 20: 16639
removal from atmosphere by clouds and precipitation, 20: 16641
removal from atmosphere by precipitation, 20: 16647
sample collection using horizontal sheets, 20: 16657
sampling of radioactive, effects of meteorological conditions on effectiveness of, 20: 16656
sampling of, using fibrous filters, 20: 16654
sedimentation techniques for study of radioactive, 20: 16655
use in studies of radioactivity of atmosphere, 20: 16688
AFRICA
nuclear energy in, economics of, 20: 16919 (EUR-2619.f)
AGE ESTIMATION
argon–potassium and cosmic ray exposure methods of, for meteorites,

20: 16672
argon–potassium method of, 20: 17804
carbon-14 method of, for Beillard peat bog, 20: 16712
development of, for rocks, 20: 16711(R) (MIT-1381-13)
methods of, book, 20: 16715
potassium–argon method of, effects of iron and rubidium on flame photometric determination of potassium in, 20: 16713
use of potassium–argon method for, 20: 16711(R) (MIT-1381-13)
use of rubidium–strontium and strontium-87/-86 for, of granite, quartzite, and slate in Massachusetts, 20: 16711(R) (MIT-1381-13)
use of strontium-87/-86 ratio method for Archean Seas, 20: 16711(R) (MIT-1381-13)

AGRICULTURE
plant mutations in, use of γ-ray- and chemically induced, 20: 16225 (EUR-2715.f)

AIR
electromagnetic field interactions in plasma of, heterodyne generation from, (E/T), 20: 17905
mass exchange in Northern Hemisphere, 20: 16640
radiosensitivity effects on olfactory bulb neurons in rats, 20: 16215 (AD-628443)
radon content in atmospheric, method for determining, 20: 16708
reactions with scandium at 300 to 900°C, 20: 16985
sampling of, using fibrous filters, 20: 16654

ALANINE
radiation effects on oxidation of, in *Vibrio cholerae*, 20: 16198

ALARM SYSTEMS
design of radiation dosimetric, 20: 16831(R) (UCRL-14534, pp 28-31)
development of beta-gamma monitor for steam condensate, 20: 16825 (ORNL-TM-1442)

ALCOHOLS
effects on solvent extraction of europium using benzoyltrifluoroacetone, 20: 16565

ALGAE
analysis for carbon and phosphorus, methods for, 20: 16175(R) (RT/BIO(65)-1)
cultivation and use of deuterium-labeled, 20: 16165
mutations induced in, delayed and persistent expression of, 20: 16294

ALGINIC ACID
sodium salts, effects on strontium-85 uptake from human gastrointestinal tract, 20: 16173 (PG-Report-686)

ALKALI METAL HALIDES
color centers in, wave functions for F, (T), 20: 17977(R) (NYO-2047-36, App.2)
light emission and absorption by crystalline, 20: 17158(R) (ORNL-3900, pp 82-149)
selenium ion ESR in single-crystal, 20: 18005
sulfur ion ESR in single-crystal, 20: 18005

ALKALI METAL IONS
effects on acetylcholinesterase activity in vagal heart preparations from frogs, 20: 16160 (UCRL-14739(Pt.2))
effects on biological systems, 20: 16160 (UCRL-14739(Pt.2))

ALKALI METALS
analysis for carbon, hydrogen, and oxygen, procedures for, 20: 17158(R) (ORNL-3900, pp 82-149)
reactions of atoms of, with halogens, (E/T), 20: 17295
reactions with halogens, stripping effects in, 20: 17158(R) (ORNL-3900, pp 82-149)
separation from scandium by ion exchange chromatography, 20: 16574

ALKALINE EARTH OXIDES
color centers in, g-values for F, (T), 20: 17975(R) (NYO-2047-36)

ALKALINE EARTH SELENIDES
color centers in, g-values for F, (T), 20: 17975(R) (NYO-2047-36)

ALKALINE EARTH SULFIDES
color centers in, g-values for F, (T), 20: 17975(R) (NYO-2047-36)

ALKANES
determination of isoprenoid, in geological samples, 20: 16633 (UCRL-16605)

ALKENES
production from hydrocarbons in plasma jet, 20: 17959

ALLENES
yields in reactions between ethylene and active nitrogen, 20: 16510(T) (NP-tr-1364)

ALLOYS
electric charge distribution in, measurement of, (E/T), 20: 17158(R) (ORNL-3900, pp 82-149)
magnetization in mixed state of superconducting, temperature dependence of, (T), 20: 17633

ALPHA BEAMS
effects on microstructure of zircons, 20: 17147

ALPHA PARTICLES
activity in rain water and water supplies, method for determining, 20: 16407
activity of, methods for measuring low-level, 20: 16411
detection and measurement of, design of extrapolation chamber for, 20: 16852
detection and measurement simultaneously with beta particles, instrument for, 20: 16906(P)
detection using silicon surface-barrier detectors, pulse-shape discrimination system for, 20: 16900
doses of solar-flare, in low-shielding space systems, 20: 16300
effects on carbonization of coal, 20: 16514
effects on dog skeleton, 20: 16253
effects on dogs, 20: 16268
effects on yeasts, effects of dark recovery and glycerol on, 20: 16231 (UCRL-16377)
emission from excited states in light nuclei, cluster model for, (T), 20: 17802
production in proton reactions with emulsion nuclei at 9 Bev, cascade effects on, (E), 20: 17713
ranges in hydrogen and hydrocarbon vapors at 1 to 8 Mev, (E/T), 20: 17277
reactions (α,α') with titanium-48, cross sections for, (T), 20: 17692 (ORNL-TM-1414)
reactions (α,γ) with lithium-6, boron-10 4.77- and 5.16-Mev levels from, (E), 20: 17761
reactions (α,He-3) with magnesium-26 at 80.0 Mev, helium-3 mass from, (E), 20: 17794
reactions (α,n) with beryllium-9, spectra from, (E), 20: 18020(R) (ORNL-3900, pp 2-81)
reactions (α,n) with nuclei, neutron production for activation analysis in, 20: 16332 (GA-6691)
reactions (α,n) with carbon-12 at 14 Mev, angular distributions from, (E), 20: 17803
reactions in biotite, mechanism for abnormally long tracks from, 20: 16667
reactions with argon, energy levels from, 20: 16159(R) (ORNL-3900, pp 150-81)
reactions with arsenic-75 at 7 Mev, gamma spectra from, (E), 20: 17158(R) (ORNL-3900, pp 82-149)
yields from plutonium-239 and uranium-235 resonance neutron fission, (E), 20: 17839

ALPHA SOURCES
content in atmosphere and surface waters at Portsmouth Gaseous Diffusion Plant, 1965, 20: 16726 (GAT-506)
detection and measurement on hands and shoes, engineering drawings of counter for, 20: 16769
determination in air, dust, rock, and water samples, radiochemical methods for, 20: 16337 (RMO-3001(Rev.1)(Suppl.))
determination of natural decay series, from tracks in biotite, 20: 16667
preparation and handling of, for electron-microprobe x-ray analyzer, 20: 16554
production of, electrospraying method for, 20: 16553
radiation emission by, relation of pleochroic halos to, 20: 16666(T) (ORNL-tr-923)

ALUMINUM
analysis for iron by proton activation analysis, 20: 16367
analysis for oxygen, activation, 20: 16331 (GA-6568)
analysis for trace amounts of gallium, activation, 20: 16396
analysis of zone-purified, for titanium by proton activation methods, 20: 16366
carbon ion reactions at 9.7 Mev, charge-exchange cross sections and ionization from, (E), 20: 17724
cavitation damage in water, 20: 16974 (NP-15889)
corrosion by boron-containing solutions, 20: 16976
crystal lattice vibrations in, frequency distribution for Debye-Waller coefficient and specific heat from normal, (T), 20: 18001
density of thin films of, proton-produced x rays for determining surface, 20: 17051
density of thin films of, 20: 17070
determination in semiconducting silicon by neutron activation, 20: 17822
determination in steel, computer use for activation, 20: 16335(R) (NBS-TN-276)
determination of trace amounts of, in beryllium by spectrography, 20: 16352
effects on high-temperature properties of eutectic alloys, 20: 17108
effects on radioinduced EPR spectra in quartz, 20: 16539(T)
effects on uranium separation from phosphate rocks, 20: 16381
fission fragment ranges in, distribution of, (E), 20: 17721
ion beam reactions with, elastic waves from heating in pulsed argon, 20: 17139
ion pairing interactions in, (T), 20: 17008 (CEA-R-2820)
polarography of, in solochrome violet RS, 20: 16406
reactions of liquid, with water jets, pressure-wave generation by, 20: 18050(R) (STL-372-22)

recoil-ion ranges in, from proton reactions with uranium at 0.55 and 18.2 Bev, (E), 20: 17837
separation from scandium by ion exchange chromatography, 20: 16574
separation from uranium and thorium by solvent extraction using alkyl phosphates, 20: 16580
solubility in vanadium silicide, 20: 17043
superconducting critical fields of films of, (E/T), 20: 17622
thermal capacity and Debye-Waller coefficient for, phonon-dispersion curve analysis for frequency distribution for, (T), 20: 18001

ALUMINUM ALLOYS
corrosion by aqueous sodium chloride, factors affecting, 20: 17158(R) (ORNL-3900, pp 82-149)
decontamination of Duralumin, ultrasonic, 20: 16767
development for fuel cladding, 20: 17158(R) (ORNL-3900, pp 82-149)
development of dispersion-strengthened, 20: 18174(R) (NP-15771)
radiation effects on, neutron, 20: 18020(R) (ORNL-3900, pp 2-81)
Al–Ce, production of, aluminothermic, 20: 16964
Al–Co, effects of additives on high-temperature properties of eutectic, 20: 17108
Al–Co–V, phase studies on intermetallic compounds in, 20: 17075
Al–Co–W, phase studies on intermetallic compounds in, 20: 17075
Al–Cu–Sc, crystal structure of ternary phases in, 20: 17097(T)
Al–Fe–Ta, phase studies on intermetallic compounds in, 20: 17075
Al–Fe–U, metallography of, correlation of particle distribution and swelling characteristics of, 20: 17058
Al–Hf–Mo, phase studies on intermetallic compounds in, 20: 17075
Al–Nb–Ta–Ti, corrosion cracking in titanium-base, stress-, 20: 16967 (AD-628277)
Al–Ta, phase studies at 900 to 1300°C, 20: 17034
Al–Ti–V, corrosion cracking in titanium-base, stress-, 20: 16967 (AD-628277)
Al–U, fabrication of fuel plates of, specifications for, 20: 16995
Al–U, metallography of, correlation of particle distribution and swelling characteristics of, 20: 17058
Al–U, thermal expansion of clad fuels of, calculation of force due to, 20: 17088
Al–V–Zr, phase studies on intermetallic compounds in, 20: 17075
Al–Zr, crystallization of, effects of zirconium additions on, 20: 17072

ALUMINUM IONS
sorption by aminodiacetate resin Dowex A-1, 20: 16358
wave functions for, including effect of nuclear quadrupole moment, 20: 17250 (BNL-8850)

ALUMINUM ISOTOPES Al-26
beta decay of, phase-space integrals for, (T), 20: 17732
content in Bogou iron meteorite, 20: 16674

ALUMINUM ISOTOPES Al-27
bremsstrahlung reactions (γ,π^+) at 100 to 300 Mev, cross sections for, (E), 20: 17779
electron reactions with, absolute differential cross section for bremstrahlung production in, (E/T), 20: 17798
energy levels in, properties of, (E), 20: 17651(R) (AD-612192)
energy levels in, polarization of resonance radiation from 2.21 Mev, (E), 20: 17651(R) (AD-612192)
gamma reactions (γ,n) at 13 to 37 Mev, levels from, (E), 20: 17773
helium-3 reactions (He-3,2p) at 12 Mev, Q value for, 20: 16331 (GA-6568)
neutron reactions (n,p) with, sensitivity of, for activation analysis, 20: 16332 (GA-6691)
neutron reactions (n,2n2p), threshold cross section and energy for, 20: 16335(R) (NBS-TN-276)
proton reactions (p,n) at 6.0 to 7.5 Mev, absolute cross sections and angular distributions for, (E/T), 20: 17775
proton reactions (p,γ), widths from yield curves for, (E), 20: 17778
proton reactions (p,d) at 57 Mev, energy spectra from, (E), 20: 17725
proton reactions (p,2p) at 140 Mev, energy spectra and angular correlation distributions from, (E), 20: 17741

ALUMINUM ISOTOPES Al-28
half life, 20: 16331 (GA-6568)

ALUMINUM OXIDES
analysis for silicon, interferences in activation, 20: 16360
carbon ion reactions at 9.7 Mev, charge-exchange cross sections and ionization from, (E), 20: 17724
color centers in, g-values for F, (T), 20: 17975(R) (NYO-2047-36)
compatibility with refractory metals and alloys, 20: 17022 (N-65-18933)
dehydration at 150 to 1100°C, bound water in, 20: 16413 (CEA-R-2703)
determination in Moldavites by spectrophotometry and x-ray fluorescence, 20: 16711(R) (MIT-1381-13)
electric conductivity at 1100 to 1600°C, 20: 17022 (N-65-18933)
fabrication of large insulators of, by powder metallurgy techniques, 20: 16993 (Y-DA-1043)
radiation effects on structure of, neutron, 20: 17148
radioinduced defects in, ESR of, (E/T), 20: 17975(R) (NYO-2047-36)
reactions with lanthanum or neodymium oxides or oxides of Group II elements, 20: 16482
reactions with molten AMS 5350 steel and Inconel 713C, 20: 16984
reactions with niobium, 20: 16978
sample preparation for high-magnification optical microscopy of, 20: 16954 (ORNL-TM-1161, pp 267-71)
sorptive properties for strontium-90 in waste solutions, mechanism of, 20: 16330 (CEA-R-2851)
Al_2O_3–Ag, preparation of wires of, with oxide homogeneously dispersed, 20: 16992(R) (RPI-2408-4)
Al_2O_3–SiO_2, effects of dehydration on bound water in, 20: 16413 (CEA-R-2703)

ALUMINUM STEEL
magnetic properties of flat-rolled, variation with processing techniques, 20: 17009 (CONF-650922, pp 287-96)

ALUMINUM SYSTEMS
Al–Si–V, superconductivity of solid solutions in, 20: 17043

AMERICIUM
dissociation in hydrochloric acid–bis(2-ethylhexyl) phosphate–toluene system, constants for, 20: 16404
production, 20: 16543
separation from aqueous sodium thiocyanate solutions by solvent extraction using tributyl phosphate, 20: 16564
separation from aqueous solutions by solvent extraction using thenoyltrifluoroacetone, synergistic effects of trioctylamine on, 20: 16571
separation from irradiated thorium, method for, 20: 16359
separation from irradiated fuel elements by ion exchange and solvent extraction, 20: 16582

AMERICIUM ISOTOPES Am-241
determination in living tissues, using gamma spectrometry, 20: 16864
neutron fission at 0.1 to 1.2 and 4 and 5 Mev, fragment angular distributions from, (E/T), 20: 17848
production of alpha sources of, electrospraying method for, 20: 16553

AMERICIUM ISOTOPES Am-242
fission of isomeric, spontaneous, (E), 20: 17857
production in plutonium (d,2n) reactions at 7 to 12 Mev, isomeric yield ratios in, (E), 20: 17857

AMES RESEARCH REACTOR
environs monitoring, 20: 18136 (IS-1320)

AMIDE POLYMERS
radiation effects on properties of fibers of, gamma, 20: 16522

AMINES
effects on solvent extraction of europium using benzoyltrifluoroacetone, 20: 16565
solvent properties of tertiary, for americium and curium, 20: 16582

AMINO ACIDS
radiolysis of tritium-labeled, effects of low temperature and scavengers on self-, 20: 16533

AMMETERS
design for measuring superconducting critical currents, 20: 17602

AMMONIA
deuterium exchange between liquid and hydrogen, catalytic effects of alkaline amides on, 20: 16444

AMMONIUM BORATES
corrosive effects on structural materials, 20: 16976

AMMONIUM CHLORIDES
effects on uranium sorption by platinized carbon, 20: 16581

AMMONIUM MOLYBDATES
radiation effects on, EPR studies of gamma, 20: 16529

AMPLIFIERS
design and performance of pre-, for semiconductor detectors, 20: 16806 (CLOR-44/D)
design of charge-sensitive pulse, 20: 16159(R) (ORNL-3900, pp 150-81)
design of solid-state, for reactor control systems, 20: 18027
design of solid-state d-c, 20: 16803
signal-to-noise ratio for pulse, for semiconductor detectors, 20: 16871

ANALYSIS
beta backscattering techniques for, 20: 16378

ANEMIA
effects on iron absorption, tracer study, 20: 16303(R) (AD-626384)

ANEMOMETERS
development for measuring statistical properties of fluid velocity in suspension, 20: 16606(R) (TID-22621)

ANESTHESIA
flowmeters for, design of γ-active static eliminator for, 20: 16783

ANIMAL CELLS
effects of space flight on mammalian, 20: 16231 (UCRL-16377)
enzyme synthesis in embryonic, during differentiation, 20: 16172(R) (NYO-2194-1)
freezing of, effects of water loss on, 20: 16159(R) (ORNL-3900, pp 150-81)
radiation effects on mammalian, cytogenetic, 20: 16159(R) (ORNL-3900, pp 150-81)
radiation effects on depression, replication, and synthesis of DNA in,

20: 16230(R) (TID-22644)
radiation effects on cultured carcinoma, uv and x, 20: 16258
radiation effects on thymidine uptake in cultures of, uv, 20: 16279
radiosensitivity of, effects of divisional cycle on, 20: 16292
radiosensitivity of, 20: 16296
radiosensitivity of cultured mammalian, effects of serum and temperature on, 20: 16298
radiosensitivity of cultured tumor, effects of monoiodoacetic acid and p-chloromercuribenzoate on, 20: 16299
trace metals in, electron microscopy for determining, 20: 16160 (UCRL-14739(Pt.2))
ANIMAL REPRODUCTION
mating patterns on Drosophila, effects on life spans, 20: 16229(R) (NYO-1472-1)
radiation effects on rat, x, 20: 16287
radiation effects on rat, x, 20: 16288
ANIMALS
cellular specificity in verterbrate, epigenetic control of, 20: 16159(R) (ORNL-3900, pp 150-81)
effects of microwaves on, thermal, 20: 16235
iodine-131 metabolism by, review on, 20: 16734 (TID-22693)
proton irradiation at 32 to 400 Mev, depth-dose distribution of, 20: 16283
radiation effects on, bibliography on, 20: 16220 (AED-C-04-24)
radiation effects on, biological, 20: 16296
use in radiobiological experiments, errors from, 20: 16164
ANION EXCHANGE MATERIALS
radiation effects on resin, 20: 16583
ANIONS
gravitational force on free, measurement of, 20: 17167
ANNEALING
effects on creep-rupture properties of irradiated tungsten, 20: 17152
ANOXIA
radiation effects on dog, α, 20: 16268
ANTARCTICA
deuterium abundance in levels of polar cap of, variation of, 20: 16686
ANTHRACENE
scintillation response functions for monoenergetic electrons, 20: 16867
ANTIFERROMAGNETIC MATERIALS
magnetothermodynamics of, instrument for determining, 20: 17978(R) (NYO-3402-2)
properties of, tables for, 20: 17972 (IAE-942)
ANTIGENS
immune reactions to, effects of age on mouse, 20: 16159(R) (ORNL-3900, pp 150-81)
radiation effects on serological reactivity of Treponema, γ, 20: 16199
ANTIMONY
content in marine organisms, 20: 16725(R) (EUR-2543.e)
determination in asbestos using ion exchange, activation, 20: 16336(R) (NYO-10175)
electron reactions with nuclear fields in, field gradient and Knight shift for, (T), 20: 18000
separation from fission products, method for, 20: 17834
ANTIMONY ALLOYS
Sb–Cs, photosensitivity of, 20: 17984
Sb–Cs–K–Na, photosensitivity of, 20: 17984
Sb–Cs–K–Na–Te, photosensitivity of, 20: 17984
Sb–In, radiation effects on electric properties of, electron and neutron, 20: 17150(T)
Sb–Sn, tin-119 isomeric shift in, 20: 18004
ANTIMONY ISOTOPES
neutron emission from fission fragments of, delayed, (E), 20: 17833
separation of, performance of separator for, 20: 16928(R) (INSJ-92)
ANTIMONY ISOTOPES Sb-122
beta decay of, beta-gamma circular polarization correlations in, (E), 20: 17677 (COO-1420-112)
sensitivity for activation analysis using beta-gamma-gamma sum-coincidence gamma spectrometer, 20: 16335(R) (NBS-TN-276)
ANTIMONY ISOTOPES Sb-124
beta transitions in, higher-order effects in allowed, (E), 20: 17678 (COO-1420-113)
content in stratospheric and tropospheric samples in Project Star Dust, 1963, 20: 16727(R) (HASL-168)
content in stratospheric and tropospheric samples in Project Star Dust, 1964, 20: 16728(R) (HASL-169)
incorporation in heavy water-moderated beryllium neutron sources, 20: 16830(R) (UCRL-14534, pp 8-12)
ANTIMONY ISOTOPES Sb-125
content in atmospheric dust and rain water, 1964–65, 20: 16660 (AERE-R-4997)
content in rain water, Fayetteville, Arkansas, Oct. 1964, 20: 16663 (TID-21470)
content in stratospheric and tropospheric samples in Project Star Dust, 1963, 20: 16727(R) (HASL-168)
content in stratospheric and tropospheric samples in Project Star Dust, 1964, 20: 16728(R) (HASL-169)
ground water contamination by, in Shoal Event, hazards from, 20: 16742 (VUF-1014)
ANTIMONY ISOTOPES Sb-128
gamma spectra, (E), 20: 17834
ANTIMONY ISOTOPES Sb-129
gamma spectra, (E), 20: 17834
ANTIMONY ISOTOPES Sb-130
gamma spectra, (E), 20: 17834
ANTIMONY ISOTOPES Sb-135
neutron emission from fission products of, delayed, (E), 20: 17834
ANTIPROTONS
interactions with protons, SL(6,C) symmetry for two-meson annihilation, 20: 17347 (JINR-P-2547)
interactions with neutrons in emulsion at 3 Bev/c, inelastic, (E), 20: 17359
interactions with protons at rest, coupling constants in SU(3) for two-body meson production in annihilation, (T), 20: 17377
interactions with protons at high energies, real amplitudes for, (T), 20: 17378
interactions with protons at 3.3 and 3.7 Bev/c, meson (π) production in annihilation, (E), 20: 17385
interactions with nucleons, meson production in annihilation, (T), 20: 17396
ANTIPYRINE, 4-IODO-
iodine-131 exchange with iodine, effects of solvents on, 20: 16502
ARGININE
content in culture media, effects on KB cells of, 20: 16258
ARGON
alpha reactions with, energy levels from, 20: 16159(R) (ORNL-3900, pp 150-81)
argon ion reactions with atomic, ionization probability effects on 1001 cross sections for, (E), 20: 17255
cesium ion elastic scattering at 2.3 to 11.6 ev, (E/T), 20: 17300
content in magnetites, determination and origin of, 20: 16714
content in silts, age estimation from, 20: 16711(R) (MIT-1381-13)
determination in silicon single crystals, activation, 20: 16335(R) (NBS-TN-276)
electric arcs in plasma jets of, structure of, (E), 20: 17904
electron scattering by atomic, cross sections for, (T), 20: 17286
heat transfer in boiling, 20: 16610
ionic mobility of cesium and rubidium in, at high pressures, (E/T), 20: 16415 (CEA-R-2861)
magnetohydrodynamic flow of seeded, Rayleigh problem in, (T), 20: 17512
positron annihilation in, in electric fields, (T), 20: 17423
production of plasmas of, spectroscopic studies of, 20: 17902
radio wave emission from plasma of, negative-absorption effects on anomalous bremsstrahlung and cyclotron, (E), 20: 17921
radiosensitivity effects on olfactory bulb neurons in rats, 20: 16215 (AD-628443)
reactions with helium atoms, charge transfer and ionization in, (E), 20: 17301
spectra of molecules trapped in solid, 20: 18016
spectra of plasma of, emission, 20: 17930(T)
thermal conductivity of plasma of, (E), 20: 17937
thermal radiation from plasma jets of, measurement of, (E), 20: 17898
ARGON IONS
reactions on aluminum targets, elastic waves from heating in, 20: 17139
reactions with argon atoms, ionization probability effects on 1001 cross sections for, (E), 20: 17255
reactions with thorium at 400 Mev, compound nucleus binary and ternary fission cross sections for, (E), 20: 17788
sputtering on copper single crystals at 0.1 to 200 kev, yields from, (E), 20: 17256
ARGON ISOTOPES
abundance in Achilles, LaLande, and Peace River chondrites, 20: 16672
ARGON ISOTOPES Ar-40
proton reactions (p,2p) at 140 Mev, energy spectra and angular correlation distributions from, (E), 20: 17741
ARGON ISOTOPES Ar-41
diffusion and capture in neutron-irradiated calcium fluoride, properties of, (E), 20: 17804
production by neutron reactions (n,p) with potassium-41 and (n,α) with calcium-44, cross sections for, (E/T), 20: 17809
ARGON SYSTEMS
Ar–methane, distribution in nonequilibrium plasma of, 20: 17959
ARGONNE SYNCHROTRON
magnet coils for, fabrication of, 20: 17186 (CONF-650922, pp 356-65)
magnet coils for, prestressing of ring, (E/T), 20: 17201 (CONF-650922, pp 733-44)
magnet current control system for, 20: 17215
magnet power supplies for, design of, 20: 17204 (CONF-650922,

pp 808-16)
power supply for ring magnet of, design of, 20: 17227
ARKANSAS
fallout monitoring in rain water in Fayetteville, Oct. 1964, 20: 16663 (TID-21470)
radionuclide content of rain in, in Oct. 1964, 20: 16685
ARMY REACTORS (SM-1)
radiation and thermal damage in pressure vessel in, 20: 17126 (NRL-6349)
radiation effects on europium oxide–stainless steel control rod in, reactor, 20: 17129 (ORNL-TM-1407)
ARSENIC
determination by radiometric titration, 20: 16386
determination in ores and rocks in presence of manganese, activation, 20: 16364
determination in stainless steel, activation, 20: 16338 (RT/CHI-(65)36)
separation from fission products, method for, 20: 17834
ARSENIC ISOTOPES
neutron emission from fission fragments of, delayed, (E), 20: 17833
ARSENIC ISOTOPES As-75
alpha reactions at 7 Mev, gamma spectra from, (E), 20: 17158(R) (ORNL-3900, pp 82-149)
neutron reactions (n,p) with, sensitivity of, for activation analysis, 20: 16332 (GA-6691)
ARSENIC ISOTOPES As-85
neutron emission from fission products of, delayed, (E), 20: 17834
ARSENIC ISOTOPES As-87
neutron emission from fission products of, delayed, (E), 20: 17834
ASBESTOS
analysis of, method for activation, 20: 16336(R) (NYO-10175)
distribution and structure in products with cement, use of neutron-induced sodium-24 for determining, 20: 16920 (SGAE-IB/IA-7/1965)
ASPARTIC ACID
radiation effects on oxidation of, in *Vibrio cholerae*, 20: 16198
radiosensitivity effects on mice and rabbits, 20: 16302
ASTRONAUTS
radiation hazards for, 20: 16745
ASTRONOMY
development of x-ray, 20: 17244
ASTROPHYSICS
nucleosynthesis in early history of solar system, 20: 17234
ATMOSPHERE
aerosol diffusion in and removal from, 20: 16639
analysis for alpha and beta sources, radiochemical methods for, 20: 16337 (RMO-3001(Rev.1)(Suppl.))
analysis for radon and thoron, alpha and beta activity measurements for, 20: 16679
cesium-137 content in Cache la Poudre, Colorado, 20: 16723 (COO-1156-11)
cesium-137 content in, in Yugoslavia from weapons testing in 1962 and 1963, 20: 16682
contamination by dispersion of radioactive aerosols, global, 20: 16642
cosmic nucleon attenuation by, (T), 20: 17651(R) (AD-612192)
diffusion of fission products in, 20: 16651
distribution of pollutants in low layers of, 20: 16652
electron precipitation in auroral zone of, spatial and temporal characteristics of, 20: 17557
fallout in, deposition and distribution of, 20: 16649
fallout monitoring in global, 1965, 20: 16662(R) (HASL-165)
fallout monitoring, 1964–65, 20: 16660 (AERE-R-4997)
fallout monitoring of, 1962 to 1964, 20: 16677
fallout monitoring in lower, Lahore, Pakistan, 20: 16683
fallout perturbations by local sea breezes, 20: 16661(R) (ECOM-00392-F)
fallout transport in, 20: 16698
fallout transport in, incorporation of, in fallout prediction model, 20: 16735 (TO-B-65-99)
fission product release to, from volatilization of ceramic wastes, 20: 18156 (BNWL-SA-453)
fission products in, dosimetry of gamma emission from, 20: 16168
fission-product content over Heis Island and Moscow, seasonal variations in, 20: 16650
iodine-131 content in, review on radiation hazards to man from, 20: 16734 (TID-22693)
lead-210 content in atmosphere, seasonal and geographical variations in, 20: 16640
lead-210 content in, planetary, 20: 16641
light diffusion in, spectral theory for stationary transport operator for, 20: 17658
meteorological measurements in, at Casaccia, Italy, 1964, 20: 16635 (RT/PROT(65)-40)
monitoring for radioactivity, methods for, 20: 16732 (NP-15898)
monitoring ground, for beta activity in Germany, 1961 to 1963, 20: 16766
monitoring of, engineering drawings of instrument for plutonium alpha, 20: 16768
particle dimensions and mobility of radioactive aerosols in, 20: 16690
properties of particles in surface boundary layer of, over Moscow, 20: 16645
properties of particles in, over Vilnius, Russia, 20: 16646
radiation monitoring for Salmon Event, 20: 16743 (VUF-1021)
radioactive aerosols in surface boundary layer of, composition of, 20: 16644
radioactivity distribution in, effect of advection on, 20: 16638
radioactivity in Japan, 1964, 20: 16730 (NP-15882)
radioactivity in Monticello Project Area, Utah, 20: 16729 (IDO-12049)
radioactivity in, distribution of, 20: 16637
radioactivity in, in Japan, 1964, 20: 16731 (NP-15883)
radioactivity monitoring of, at Portsmouth Gaseous Diffusion Plant, 1965, 20: 16726 (GAT-506)
radioactivity of, use of aerosols in studies of, 20: 16688
radioactivity over oceans, dependence of, on, 20: 16699
radon content in surface boundary layer of, effect of vertical turbulent mixing on, 20: 16692
radon content in surface boundary layer of, seasonal variations in, 20: 16695
radon content in, distribution of, 20: 16693
radon content in, method for determining, (E), 20: 16708
removal of radioactive aerosols from, by precipitation, 20: 16647
retention of methyl iodide in, efficiency of Whatman Type ACG/B filter paper for, 20: 16719 (AEEW-M-568)
thorium content in surface boundary layer of, seasonal variations in, 20: 16695
tracer studies of, using lead-210, 20: 16641
turbulence in, tracer studies of, using radon, 20: 16694
ATOMIC BEAMS
focusing of, image characteristics of magnetic systems for, (T), 20: 17225
ATOMIC CLOUDS
growth and rise of, dynamics of, 20: 16735 (TO-B-65-99)
particulate matter in long-term, washout of, 20: 16160 (UCRL-14739 (Pt.2))
ATOMIC ENERGY
bibliography of bibliographies on, Dec. 1965 and Jan. 1966, 20: 18177 (TID-3733)
book: *Utilization of Atomic Energy in National Economy (Power Plant, Petroleum Industry and Technology)*, in Azerbaidzhan, 20: 18182
organization, legislation, and training in, in the Netherlands, 20: 18183
research programs on, at Saclay, 20: 18181
sources and uses of, world, 20: 18082 (AECL-2390)
use in African countries in agriculture and hydrology, economics of, 20: 16919 (EUR-2619.f)
ATOMIC ENERGY, LEGAL ASPECTS
book: *International Marketing of Nuclear Power Plants*, 20: 18117
ATOMIC EXPLOSIONS
effects on diabetes incidence in residents of Hiroshima, 20: 16254
effects on health of population of Hiroshima and Nagasaki, 20: 16271
fallout from, deposition and distribution of, 20: 16649
fallout from, deposition and distribution of, 20: 16697
fallout from, monitoring 1962 to 1964, 20: 16677
fission products from, fractionation of, 20: 16696
fission products from, beta activity of, 20: 16707
radiation dose distribution from, free field, 20: 16760
radiation effects of, on Hiroshima population, 20: 16272
radiation from Japanese, doses from, in dwelling, 20: 16159(R) (ORNL-3900, pp 150-81)
radiation shielding from, 20: 18020(R) (ORNL-3900, pp 2-81)
radioactivity induced by Hiroshima and Nagasaki, thermoluminescent dosimetry of, 20: 16759
sample-marking system for positive identification following, 20: 18176 (SCL-DR-66-6)
use of underground, for recovery of oil from shale, 20: 16589 (UCRL-12224-T)
ATOMIC WEAPONS
effects of, distribution and magnitude of, for shelter design, 20: 16620 (AD-624370)
ATOMS
charged-particle inelastic scattering by, (T), 20: 17306
electron reactions at high energies, cross sections for excitation and ionization in, (T), 20: 17270
electron scattering by, resonances in, (T), 20: 17289
electron scattering by, in uniform magnetic fields, (T), 20: 17291
emission from plasma, system for analyzing neutral, 20: 17873 (CLM-R-49)
hyperfine interactions in, effects on nuclear gamma transitions, (T), 20: 17686 (JINR-P-2512)
ion reactions with, classical calculations on electron capture in,

20: 17275
reactions of single species of energetic and thermal, energy distributions from, (T), 20: 17257
reactions with atoms, (T), 20: 17266
reactions with atoms and molecules, conference on, 20: 17288
reactions with muonium, 20: 17297
AURINTRICARBOXYLIC ACID, AMMONIUM SALTS
complexes with uranium, formation and stability of, 20: 16428
AURORAL STORMS
electron precipitation in, spatial and temporal characteristics of, 20: 17557
intensity variations at South Pole, diurnal, 20: 17554
properties of, seasonal latitude changes of, 20: 17556
sounding data for slant sporadic E reflections over Finland, 20: 17542
AUSTRALIA
radioisotope standards establishment in, 20: 16746
AUTORADIOGRAPHY
use in determining plutonium-239 sorption through rabbit skin, 20: 16183
AVIATION PERSONNEL
body mass, effects of airborne training on lean, 20: 16303(R) (AD-626384)
6-AZAURACIL
effect on synthesis of RNA during recovery of DNA synthetic system in uv-damaged *E. coli*, 20: 16202
AZO DYES
analysis for tritium by scintillation counting, use of oxygen-flask combustion method in, 20: 16373
AZULENE, 4,6,8-TRIMETHYL-
preparation of deuterated, from 2,4,6-tri-d_3-methylpyrylium perchlorate, 20: 16501

B

BACTERIA
carotenoid pigment from radioresistant Micrococcus, characterization of, 20: 16161
cultivation and use of deuterium-labeled, 20: 16165
growth and metabolism of, effects of rare earths and yttrium on, 20: 16191
radiation effects on division, growth, and recovery in, 20: 16159(R) (ORNL-3900, pp 150-81)
radiation effects on staining characteristics of mycobacteria, uv, 20: 16195
radiation effects on oxidation of Krebs cycle substrates in *Vibrio cholerae*, 20: 16198
radiation effects on serological activity of antigens from Treponema, γ, 20: 16199
radiation effects on survival curves of, in complex media, 20: 16237
radiosensitivity of DNA in *Bacillus subtilis*, effects of proflavine on uv, 20: 16280
transfer of DNA during mating of, mechanism of, 20: 16159(R) (ORNL-3900, pp 150-81)
BACTERIOPHAGES
desoxyribonucleic acid breakage and reunion in, during infections, 20: 16159(R) (ORNL-3900, pp 150-81)
radiation effects on infection of *Escherichia coli* by, uv, 20: 16270(T)
BALANCES
development for weighing irradiated fuel elements in water, 20: 16780 (TID-22689)
BALL MILLS
design of, effects of, on pulverizing efficiency of graphite, 20: 16957(T) (LA-tr-66-11)
BARIUM
abundance in sun, (E), 20: 17237
determination in presence of calcium and strontium by ring oven techniques, 20: 16388
separation from other fission products by precipitation with barium sulfate, 20: 16343
sorption by chabazite in lithium, potassium, and sodium nitrates, 20: 16340 (USNRDL-TR-970)
BARIUM CHLORIDES
ion exchange and sorption on glass surfaces, 20: 16469
BARIUM IONS
sorption by aminodiacetate resin Dowex A-1, 20: 16358
BARIUM ISOTOPES
separation of, performance of separator for, 20: 16928(R) (INSJ-92)
BARIUM ISOTOPES Ba-130
neutron reactions (n,γ), activation cross section for, (E), 20: 16336(R) (NYO-10175)
BARIUM ISOTOPES Ba-131
half life of isomeric, from neutron reactions (n,γ), (E), 20: 16336(R) (NYO-10175)
half life of, from neutron reactions (n,γ), (E), 20: 16336(R) (NYO-10175)
BARIUM ISOTOPES Ba-133
determination by precipitation with barium sulfate and gamma spectroscopy, 20: 16343
production in deuteron reactions (d,2n) with cesium-133, cross sections for, 20: 16508(R) (NYO-2771-13)
BARIUM ISOTOPES Ba-134
deuteron reactions (d,n), cross sections for lanthanum-135 production in, 20: 16508(R) (NYO-2771-13)
BARIUM ISOTOPES Ba-135
deuteron reactions (d,2n), cross sections for lanthanum-135 production in, 20: 16508(R) (NYO-2771-13)
BARIUM ISOTOPES Ba-136
carbon-12 reactions (C-12,6n), angular momentum effects on excitation functions for, (E), 20: 17784
BARIUM ISOTOPES Ba-137
carbon-12 reactions (C-12,7n) with barium-137, angular momentum effects on excitation functions for, (E), 20: 17784
half life of isomeric, from neutron reactions (n,n′), (E), 20: 16336(R) (NYO-10175)
neutron reactions (n,n′), activation cross section for, (E), 20: 16336(R) (NYO-10175)
BARIUM ISOTOPES Ba-138
carbon-12 reactions (C-12,8n), angular momentum effects on excitation functions for, (E), 20: 17784
deuteron reactions (d,γ), cross sections for lanthanum-140 production by, 20: 16508(R) (NYO-2771-13)
neutron reactions (n,γ), activation cross section for, (E), 20: 16336(R) (NYO-10175)
neutron reactions (n,α) with, cross sections for, (E/T), 20: 17809
BARIUM ISOTOPES Ba-139
half life of, from neutron reactions (n,γ), (E), 20: 16336(R) (NYO-10175)
BARIUM ISOTOPES Ba-140
content in atmospheric dust and rain water, 1964–65, 20: 16660 (AERE-R-4997)
content in milk and plants before and after Salmon Event, 20: 16743 (VUF-1021)
content in milk, measures for controlling, 20: 16754
content in rain water, Fayetteville, Arkansas, Oct. 1964, 20: 16663 (TID-21470)
content in rainwater and snow in Germany, 1961 to 1963, 20: 16766
content in stratospheric and tropospheric samples in Project Star Dust, 1963, 20: 16727(R) (HASL-168)
determination in milk, gamma spectrometric, 20: 16369
ranges of fission products of, in aluminum, (E), 20: 17721
yields from thorium-232 fission, (E), 20: 17860
yields in plutonium-239 fission in resonance region, (E), 20: 17858
BARIUM ISOTOPES Ba-141
yields from thorium-232 fission, (E), 20: 17860
BARIUM NITRATES
ion exchange and sorption on glass surfaces, 20: 16469
BARIUM OXIDES
reactions with aluminum oxides and lanthanum or neodymium oxides at 1400 to 1500°C, 20: 16482
BaO–IrO_2–SrO, crystal structure, 20: 16436
BaO–RuO_2–SrO, crystal structure, 20: 16436
BARIUM TITANATES
response to 300-kev hydrogen beams, 20: 17253(R) (ORNL-3908, pp 90-9)
BARLEY
manganese sorption by roots of, effects of divalent cations on, 20: 16174(R) (RLO-1547-3)
radiation effects on seeds of, protective effects of inorganic salts against, 20: 16297(R) (EUR-2548.f)
BARYONS
annihilation with antibaryons, CT invariance for SU(3) amplitudes in octet, (T), 20: 17453
interactions of, CT invariance for SU(3) amplitudes in octet, (T), 20: 17453
interactions with mesons, symmetry group for coupling in, (T), 20: 17455
interactions with mesons in broken SU(3) symmetry, self-consistent determination of coupling in, 20: 17467
interactions with baryons in broken SU(3), sum rules for S-state amplitudes for, 20: 17468
mass of, quark model for, 20: 17343 (JINR-P-2524)
masses of, electromagnetic, (T), 20: 17507
meson couplings to currents of, vector-meson dominance and U(6,6) symmetry for, 20: 17457
production in high-energy cascade showers, transverse momentum distribution for, (T), 20: 17371
BARYONS, RESONANCE
decay of, isotopic structure of electromagnetic, (T), 20: 17428 (JINR-P-2498)
decay widths of, (T), 20: 17395

lifetime of Ω⁻(1875), (T), 20: 17364(T)
mass relations for, linear, 20: 17391
masses of ¾⁺, electromagnetic, (T), 20: 17507
parity of, method for determining, (T), 20: 17362(T)
photoproduction of N*(1238), on protons at 0.3 and 5.5 Bev, (E), 20: 17368
production in meson (K⁻) interactions with protons at 2.24 Bev/c, (E), 20: 17383
production of Δ⁰ and Δ⁺, in photon-proton interactions, (T), 20: 17348 (JINR-P-2556)
production of mass-2098-Mev/c Λ-N, by helium–hyperon reactions, (E/T), 20: 17158(R) (ORNL-3900, pp 82-149)
production of N*₊, in proton-proton inelastic interactions, (T), 20: 17381
production of N*₃₃⁺ in meson (π⁺)-proton interactions at 1.6 Bev/c, cross sections for, (E), 20: 17374

BEHAVIOR
effects of Drosophila reproductive, on life span, 20: 16229(R) (NYO-1472-1)
radiation effects on dog, after chronic enteral administration of strontium-90, β, 20: 16266
radiation effects on conditioned, in parabiont rats, x, 20: 16284

BELGIAN REACTOR-2
experimental facilities and operation, 20: 18133(R) (EUR-2625.e)

BELGIAN REACTOR-3
criticality, 20: 18108
development of, review of, 20: 18104

BENZENE
formation by disproportionation of acetophenone, butyrophenones, and propiophenone in phosphoric acid, 20: 16542(R) (TID-22646)
radiolysis of, nitrous oxide as electron scavenger in, 20: 16515
reactions with deuterium, catalyzed by chromium oxide gel, 20: 16487
spectra of deuterated and normal, trapped in solid rare gases, 20: 18016
tritium exchange with tritiated ethyl malonate, effects of catalysts on, 20: 16492
benzene–nitrobenzene, effects on isotopic exchange between elementary iodine and 1-phenyl-2,3-dimethyl-4-iodopyrazolone, 20: 16502
benzene–cyclohexane–cyclohexene, radiolysis of, nitrous oxide as electron scavenger in, 20: 16515
benzene–methanol, radiolysis of, fuel-radical scavenging in, 20: 16530
benzene–isopropylbiphenyl, thermal fluxes in boiling, in forced flow in channels, 20: 16614

BENZENE, NITRO-
benzene–nitrobenzene, effects on isotopic exchange between elementary iodine and 1-phenyl-2,3-dimethyl-4-iodopyrazolone, 20: 16502
chloroform–nitrobenzene, effects on isotopic exchange between elementary iodine and 1-phenyl-2,3-dimethyl-4-iodopyrazolone, 20: 16502

m-BENZENEDISULFONIC ACID, 4,5-DIHYDROXY-, SODIUM SALT
complexes with thorium, effects on hydrolysis of α-D-glucose 1-phosphate, 20: 16421

BENZENESULFONIC ACID, 4-HYDROXY-3-[(2-HYDROXY-1-NAPHTHYL)AZO]-
complexes with metals, polarography of, 20: 16406

BENZOIC ACID
formation by Friedel-Crafts reactions on aromatic-aliphatic ketones, 20: 16542(R) (TID-22646)
oxygen-18 exchange reactions between *p*-substituted, and water, 20: 16542(R) (TID-22646)

BENZOIC ACID, *p*-CHLORO-, MERCURY SALT
radiosensitivity effects on tumor cells in culture, 20: 16299

BENZOPHENONES
oxygen-18 exchange reactions between *p*-substituted, and water, 20: 16542(R) (TID-22646)

BENZYL ALCOHOLS
effects on self-irradiation decomposition of tritium-labeled organic compounds, 20: 16533

BERKELIUM
production, 20: 16543

BERYLLIUM
analysis for manganese, spectrophotometric, 20: 16361
analysis for trace impurities by optical emission spectrography, 20: 16352
deformation of polycrystalline, mechanisms of, 20: 17040
diffusion in single-crystal and polycrystalline beryllia, 20: 17049
gamma reactions (γ,n) in moderators of, (E/T), 20: 17830
grade of, nondestructive radiographic determination of, 20: 16962
helium-3 reactions (He-3,n) with, neutrons yields for activation analysis in, 20: 16332 (GA-6691)
incorporation in heavy water-moderated antimony-124 neutron sources, 20: 16830(R) (UCRL-14534, pp 8-12)
neutron decay constants in, pulsed, (T), 20: 17662
neutron spectra in, thermal, (E/T), 20: 18127(R) (GA-6753(Pt.1))
neutron total cross section, 20: 18127(R) (GA-6753(Pt.1))
nucleon elastic scattering at 140 Mev, parametrization analysis for, (T), 20: 17740
pressure response in bars of, 20: 17018 (LRP-20/66)
production by high-energy solar particles, 20: 17234
properties as reactor fuel material, 20: 18182
proton reactions (p,d) at 3 to 5 Mev, deuteron polarization in, (E), 20: 17760
proton reactions at 30.5 Bev, secondaries from, (E/T), 20: 17171 (BNL-10030)
proton reactions at 19.2 Bev/c, radiation levels from, 20: 17212(T) (UCRL-Trans-1305)
proton scattering at 140 Mev, parameters for triple, (E/T), 20: 17738
separation from scandium by ion exchange chromatography, 20: 16574
solubility in vanadium silicide, 20: 17043

BERYLLIUM ALLOYS
Be–Fe, magnetic moments of bcc, atomic, 20: 17985

BERYLLIUM COMPOUNDS
analysis for trace impurities by optical emission spectrography, 20: 16352

BERYLLIUM FLUORIDES
BeF_2–LiF, viscosity at 710 to 1720°F, 20: 17158(R) (ORNL-3900, pp 82-149)

BERYLLIUM IONS
sorption by aminodiacetate resin Dowex A-1, 20: 16358

BERYLLIUM ISOTOPES Be-7
beta decay of, energy and lifetime values and nuclear matrix elements for, (T), 20: 17732
content in stratospheric and tropospheric samples in Project Star Dust, 1963, 20: 16727(K) (HASL-168)
content in stratospheric and tropospheric samples in Project Star Dust, 1964, 20: 16728(R) (HASL-169)
half life, 20: 16331 (GA-6568)

BERYLLIUM ISOTOPES Be-8
energy levels from boron-10 (d,α) reactions, isotopic spin rule violation in, (E), 20: 17759
energy levels from boron-9 decay, spins of, (T), 20: 17807

BERYLLIUM ISOTOPES Be-9
alpha reactions (α,n) with, spectra from, (E), 20: 18020(R) (ORNL-3900, pp 2-81)
alpha reactions (α,n) with, neutron production for activation analysis in, 20: 16332 (GA-6691)
deuteron reactions (d,n) with, neutron production for activation analysis in, 20: 16332 (GA-6691)
deuteron reactions (d,n) at 600 kev, boron-10 level structure from, (E), 20: 17797
gamma reactions (γ,n) with, neutron production for activation analysis in, 20: 16332 (GA-6691)
helium-3 reactions (He-3,n) at 12 Mev, Q value for, 20: 16331 (GA-6568)
proton reactions (p,2p) at 140 Mev, energy spectra and angular correlation distributions from, (E), 20: 17741

BERYLLIUM OXIDES
compatibility with refractory metals and alloys, 20: 17022 (N-65-18933)
dehydration at 150 to 1100°C, bound water in, 20: 16413 (CEA-R-2703)
diffusion of beryllium in single-crystal and polycrystalline, 20: 17049
electric conductivity at 1100 to 1600°C, 20: 17022 (N-65-18933)
mechanical properties and structure of polycrystalline, 20: 17054
radiation effects on structure of, neutron, 20: 17148
reactions with aluminum oxides and lanthanum or neodymium oxides at 1400 to 1500°C, 20: 16482
thermal expansion at 20 to 1000°C, linear, 20: 17006 (AAEC/TM-300)

BERYLLIUM OXIDES (IMPREGNATED)
radiation effects on mechanical properties of thoria–urania, reactor, 20: 17113 (AAEC-E-140)

BERYLLIUM SYSTEMS
Be–Si–V, superconductivity of solid solutions in, 20: 17043

BESSEL FUNCTIONS
solution of, with asymmetric endpoint conditions, 20: 16934

BETA DECAY
coupling constants in, dispersion relations and renormalization of weak axial-vector, 20: 17478
phase-space integrals for nuclear matrix elements for, (T), 20: 17732

BETA PARTICLES
activity in ground air in Germany, 1961 to 1963, 20: 16766
activity in rain water and water supplies, method for determining, 20: 16407
activity of fission products, 20: 16707
detection and measurement in biological materials, sample preparation for, 20: 16177
detection and measurement of, design of extrapolation chamber for,

20: 16852
detection and measurement simultaneously with alpha particles, instrument for, 20: 16906(P)
dosimetry in thyroid gland, method for, 20: 16160 (UCRL-14739(Pt.2))
effects of, combined with cytostatic drugs on polycythemia, complications from, 20: 16233
effects on aqueous hydrogen peroxide solutions at 77°K, ESR studies of, 20: 16512
effects on behavior in dogs after chronic enteral administration, 20: 16266
effects on blood picture following polycythemia therapy, 20: 16241
effects on dog skeleton, 20: 16253
effects on root growth of corn and pea seedlings, 20: 16227(R) (NYO-3561-2)
effects on skeletal growth in rats, 20: 16267
effects on thymidine excretion by rats, 20: 16201
monitoring in steam condensate, 20: 16825 (ORNL-TM-1442)
scattering of, use in quantitative analysis, 20: 16378

BETA SOURCES
activity in stratospheric and tropospheric samples in Project Star Dust, 1964, 20: 16728(R) (HASL-169)
activity in stratospheric and tropospheric samples in Project Star Dust, 1963, 20: 16727(R) (HASL-168)
content in atmosphere and surface waters at Portsmouth Gaseous Diffusion Plant, 1965, 20: 16726 (GAT-506)
content in atmosphere and rain water in Japan, 1964, 20: 16730 (NP-15882)
determination in air, dust, rock, and water samples, radiochemical methods for, 20: 16337 (RMO-3001(Rev.1)(Suppl.))
fabrication, 20: 16914(R) (ORNL-3900, pp 182-93)
shielding calculations for strontium-90–yttrium-90, 20: 17968
use for therapy of skin tumors, 20: 16325
use for treatment of eye tumors, 20: 16305

BETA SPECTROMETERS
magnetic field for, high-order double-focusing, 20: 16868
spectra corrections for scintillation, backscattering and resolution, 20: 16867
use of magnetic, for automatic measurements, 20: 16854

BETATRONS
development and uses, 20: 17216

BIBLIOGRAPHIES
of biblicgraphies on atomic energy literature, Dec. 1965 and Jan. 1966, 20: 18177 (TID-3733)
on accelerators, 20: 17170 (AED-C-18-05)
on activation analysis, 20: 16336(R) (NYO-10175)
on chemical composition and origin of tektites in Moldavia, 20: 16711(R) (MIT-1381-13)
on chemical evolution and organic geochemistry, 20: 16633 (UCRL-16605)
on coolant purification systems for sealed boiling-water power reactors, 20: 18089 (NAA-SR-Memo-10178)
on criteria for judging quality of science exhibits, 20: 18178 (TID-22793)
on direct conversion of nuclear into electric energy, 20: 17325 (AED-C-15-09)
on direct conversion of nuclear into electric energy, 20: 17326 (AED-C-15-10)
on electrets, 20: 17971 (AD-299256)
on factors affecting cesium-137 content in mule deer, 20: 16723 (COO-1156-11)
on fallout, 20: 16662(R) (HASL-165)
on geologic dating of sediments using potassium–argon method, 20: 16711(R) (MIT-1381-13)
on giant resonance in photonuclear reactions, 20: 17706
on hazards from inhalation of radioiodines, 20: 16734 (TID-22693)
on high-energy physics, 20: 17153 (AED-C-23-05)
on high-energy physics, 20: 17154 (AED-C-23-06)
on high-energy physics, 20: 17155 (AED-C-23-07)
on living organisms and tissues, 20: 16219 (AED-C-04-23)
on neutrinos, 20: 17352 (NEIC-RR-21)
on nucleon clustering in light nuclei, 20: 17707
on pleochroic halos in biotite, cordierite, and hornblende, and relation to α rays in radioactive elements, 20: 16666(T) (ORNL-tr-923)
on plutonium technology, 20: 16328 (AECL-Pak/Lib-10)
on radiation effects on living organisms and materials, 20: 16220 (AED-C-04-24)
on radiation effects on living organisms and tissues, 20: 16221 (AED-C-04-25)
on radiation effects on ion exchange materials, 20: 16583
on radiation environment in space, 20: 17249
on radioactive waste disposal, 20: 18153 (AED-C-01-12)
on radioactive waste disposal, 20: 18154 (AED-C-01-13)
on separation of transplutonium elements, 20: 16402
on strontium-90 in antlers and bones of Colorado mule deer, 20: 16724 (COO-1156-12)

BIG ROCK POINT POWER REACTOR
radiation and thermal damage in pressure vessel in, 20: 17126 (NRL-6349)

BIOLOGICAL MATERIALS
analysis for β activity, sample preparation for, 20: 16177
radiation effects on, molecular, 20: 16160 (UCRL-14739(Pt.2))
radionuclide and elemental content and distribution in, 20: 16160 (UCRL-14739(Pt.2))
trace elements in neutron activated, anion exchange method for selective sorption of, 20: 16171 (AE-215)

BIOLOGICAL MODELS
of radiation effects and recovery of cells in culture, 20: 16292

BIOLOGICAL STRESS
radiosensitivity effects of acceleration-induced, in rats, 20: 16213 (AD-620403)

BIOLOGICAL SYSTEMS
effects of alkali metal ions on, 20: 16160 (UCRL-14739(Pt.2))
hydrogen pathways in, deuterioörganic compounds for studying, 20: 16165
radiation effects on, enzymatic assessment of, 20: 16160 (UCRL-14739(Pt.2))
radiation effects on, bibliography on, 20: 16220 (AED-C-04-24)

BIOMETRY
use in survival studies on irradiated Chlorella, 20: 16246

BIOTITES
alpha tracks in, mechanism for abnormally long, 20: 16667
pleochroic halos in, dimensions and relation to α rays in radioactive elements, 20: 16666(T) (ORNL-tr-923)

BIPHENYL
analysis of, by gas chromatography, thermal conductivity, and flame ionization, 20: 16341
tritium exchange with tritiated ethyl malonate, effects of catalysts on, 20: 16492
biphenyl–phenyl ether, thermodynamic properties of eutectic mixture of, for use as reactor coolant, 20: 16493

BIPHENYL, ISOPROPYL-
benzene–isopropylbiphenyl, thermal fluxes in boiling, in forced flow in channels, 20: 16614

BIPYRIDINES
complexes with rare earths, infrared spectra of, 20: 16437

BIREFRINGENCE
measurement in biotite, hornblende, and cordierite, 20: 16666(T) (ORNL-tr-923)

BISMUTH
content in marine organisms, 20: 16725(R) (EUR-2543.e)
determination of trace amounts of, in beryllium by spectrography, 20: 16352
electron and positron scattering at 150 and 300 Mev, cross sections and electron-positron ratios from, (E), 20: 17785
energy levels of μ-mesic atoms of, resonances in, (T), 20: 17281
hydromagnetic waves in single crystal of, Landau and resonance damping of, (E), 20: 18011
hyperfine structure of μ-mesic atoms of, E2 and M1, (E), 20: 17792
proton fission at 150 to 660 Mev, cross sections for, (E), 20: 17838

BISMUTH ALLOYS
Bi–Sn, tin-119 isomeric shift in, 20: 18004

BISMUTH ISOTOPES Bi-207
production of carrier-free, 20: 16546

BISMUTH ISOTOPES Bi-209
hyperfine structure of, E2 and M1, (E), 20: 17793
nucleon capture at 10 to 40 Mev, cross sections and mechanism for direct, (T), 20: 17737
proton reactions (p,d) at 57 Mev, energy spectra from, (E), 20: 17725

BISMUTH ISOTOPES Bi-211
alpha decay of, thallium-207 levels from, (E), 20: 17703
energy levels from polonium-215 decay, (E), 20: 17703

BLAST EFFECTS
protection from, design data for shelters for, 20: 16620 (AD-624370)
resistance to nuclear weapons, calculation of, 20: 16621 (AD-625867)

BLOOD
analysis for iron by neutron activation, 20: 17822
flow in bones, determination and factors affecting, 20: 16192
plutonium-239 content in rabbit, after sorption through intact skin, 20: 16183
radiation effects on transplanted Yoshida sarcoma cells in rat, tracer study, 20: 16188
radioinduced behavior stimulus in parabiont rat, transference of x, 20: 16284
strontium-85 content in human, effects of sodium alginate on, 20: 16173 (PG-Report-686)

BLOOD CELLS

radiation effects on, pre-space-flight testing of, 20: 16159(R) (ORNL-3900, pp 150-81)
radiation effects on mouse, fractionated-dose x, 20: 16224 (CEA-R-2848)
radiosensitivity of, 20: 16322

BLOOD FORMATION
radiation effects on dog, α, 20: 16268

BLOOD PLASMA
calcium-45 uptake by rabbit, 20: 16178
chlorine-36 content in calf, after ingestion, 20: 16186
iodine-131 content in calf, after ingestion, 20: 16186
strontium-90 uptake by rabbit, 20: 16178

BLOOD SERUM
analysis for magnesium, activation, 20: 16336(R) (NYO-10175)
radiation effects on growth inhibition in rat, effects of cysteine on, 20: 16208
radiation effects on copper and zinc content and enzyme activity in, 20: 16222 (AFWL-TR-65-112)

BODY FLUIDS
analysis for elements, quantitative, 20: 16160 (UCRL-14739(Pt.2))

BODY VOLUME
effects of training on body mass of aviation personnel, 20: 16303(R) (AD-626384)

BOILERS
development of sodium-heated superheating, 20: 16599(R) (BAW-1280-34)
performance in sodium-cooled reactors, computer analysis of, 20: 18093(R) (UNC-5142)
testing of, vacuum-gas leak, 20: 16618

BOILING
burnout in uniformly heated tubes, forced convection, (E), 20: 16603 (NYO-187-7)
detection of nucleate, by neutron power spectral density measurements in reactors, 20: 18048 (ORNL-P-1967)
heat transfer by monoisopropylbiphenyl-benzol, in forced flow in channels, 20: 16614
heat transfer in forced flow three-rod sections, film and transition, (E/T), 20: 16602(R) (GEAP-5081)
heat transfer in large-volume, effects of thermal decomposition of organic coolants on, 20: 16615
heat transfer in two-phase steady-state flows, 20: 16601(R) (GEAP-5067)
heat transfer of transition, from finned reactor fuel rods, (E), 20: 16602(R) (GEAP-5081)
in annular two-phase flow, analysis of liquid film from, (T), 20: 16604 (NYO-3114-13)

BOILING REACTORS
coolant purification systems for hermetically sealed power, 20: 18089 (NAA-SR-Memo-10178)
fuel elements for AEG, development of, 20: 18077
kinetics of heterogeneous, 20: 18050(R) (STL-372-22)

BONDS, CHEMICAL
effects on x-ray spectra, 20: 16160 (UCRL-14739(Pt.2))

BONE FRACTURES
effects on bone blood flow in femur, 20: 16192
radioinduced in dogs by plutonium-239, radium-226, -228, and strontium-90, 20: 16253

BONE MARROW
radiation effects on, following polycythemia therapy, β, 20: 16241
radiosensitivity of, 20: 16322

BONES
blood flow in, determination and factors affecting, 20: 16192
calcium-45 uptake by rabbit, 20: 16178
citrate synthesis in, measurement of enzyme for, 20: 16160 (UCRL-14739(Pt.2))
radiation effects on transplanted Yoshida sarcoma cells in rat, tracer study, 20: 16188
radiodiagnostic procedure for, gallium-68, 20: 16310
radioinduced necrosis in hand, following eczema therapy, 20: 16210
radiosensitivity of, 20: 16322
strontium-90 content in Colorado mule deer, 20: 16724 (COO-1156-12)
strontium-90 content in, of U. S. children, 1965, 20: 16662(R) (HASL-165)
strontium-90 uptake by rabbit, 20: 16178

BORAX
use in nuclear emulsions for neutron detection, 20: 16891

BORIC ACID
corrosive effects on structural materials, 20: 16976

BORIDES
chemical bonding and electric conductivity of transition metal, 20: 16439

BOROHYDRIDE IONS
reduction of ketones by, secondary deuterium isotope effects in, 20: 16555

BORON
determination of trace amounts of, in beryllium by spectrography, 20: 16352
effects on high-temperature properties of eutectic alloys, 20: 17108
helium-3 reactions (He-3,n) with, neutrons yields for activation analysis in, 20: 16332 (GA-6691)
natural deposits of, isotopic composition in, 20: 16915
photon reactions with Coulomb field of, pair production total cross sections for high-energy, (T), 20: 17754
production by high-energy solar particles, 20: 17234

BORON IONS
charge states of recoil, target thickness problem in studies on equilibrium, 20: 16508(R) (NYO-2771-13)

BORON ISOTOPES B-8
beta decay of, energy and lifetime values and nuclear matrix elements for, (T), 20: 17732

BORON ISOTOPES B-9
decay of, angular correlations from, (T), 20: 17807
energy levels from $_{4}Be^{9}$ decay, parity and spin of, (T), 20: 17807

BORON ISOTOPES B-10
abundance in nature, 20: 16915
alpha reactions (α,n) with, neutron production for activation analysis in, 20: 16332 (GA-6691)
deuteron reactions (d,α) at 7.5 Mev, isotopic spin rule violation in beryllium-8 levels from, (E), 20: 17759
deuteron reactions (d,pγ) at 420 kev, gamma polarization from, (E/T), 20: 17726
electron inelastic scattering at 32 to 57 Mev, multipolarity and width of levels from, (E), 20: 17813
energy level structure from deuteron reactions (d,n) with beryllium-9 at 600 kev, (E), 20: 17797
energy levels from boron-11 (He-3,α) and lithium-6 (α,γ) reactions, (E), 20: 17761
helium-3 reactions (He-3,d), Q value for, 20: 16331 (GA-6568)
neutron reactions (n,α) at 23 ev to 0.5 Mev, excited-to-ground state branching ratio for, (E), 20: 17719
proton reactions (p,2p) at 140 Mev, energy spectra and angular correlation distributions from, (E), 20: 17741
proton scattering at 140 Mev, parameters for triple, (E/T), 20: 17738
reactions (B-10,3α) with oxygen-16 at 100 Mev, excitation function and nitrogen-14 angular distributions from, (E), 20: 17815
reactions (B-10,7n) with lanthanum-139, angular momentum effects on excitation functions for, (E), 20: 17784
spectra of recoil, from deuteron reactions with carbon-12, (E), 20: 17820

BORON ISOTOPES B-11
abundance in nature, 20: 16915
electron inelastic scattering at 32 to 57 Mev, multipolarity and width of levels from, (E), 20: 17813
helium-3 reactions (He-3,n) and (He-3,t) at 12 Mev, Q values for, 20: 16331 (GA-6568)
helium-3 reactions (He-3,α) at 3.5 Mev, boron-10 4.77- and 5.16-Mev levels from, (E), 20: 17761
proton reactions (p,2p) at 140 Mev, energy spectra and angular correlation distributions from, (E), 20: 17741
reactions (B-11,8n) with lanthanum-139, angular momentum effects on excitation functions for, (E), 20: 17784

BORON ISOTOPES B-12
beta decay of, phase-space integrals for, (T), 20: 17732

BORON NITRIDES
compatibility with refractory metals and alloys, 20: 17022 (N-65-18933)
electric conductivity at 1100 to 1600°C, 20: 17022 (N-65-18933)

BORON OXIDES
reactions with rare earth oxides at high temperatures, 20: 16489

BORON SYSTEMS
B–stainless steels, mechanical properties of irradiated fuel cladding of, 20: 17121 (GEAP-4918)
B–stainless steel, radiation effects on corrosion resistance of modified austenitic, neutron, 20: 17118(R) (EURAEC-1564)

BOSONS
decay of intermediate W, radiative, (T), 20: 17421
energy levels of gases of charged, ground-state, (T), 20: 17526
interactions in liquids of, effective potential for, (T), 20: 17439
interactions of intermediate vector, renormalization theory of weak, 20: 17437
interactions with spinless fermions, approximate calculation of asymptotic operators for, 20: 17450
mass scale for, (T), 20: 17393
reactions with fermions, invariant amplitudes for structure of, (T), 20: 17770
scattering by nuclei, complex angular momentum method for inelastic diffraction, (T), 20: 17817

BOUNDARY LAYER
hydrodynamic and thermodynamic characteristics of, in liquid hydrogen tanks, 20: 17536
magnetohydrodynamic, influence of Hall effects on, 20: 17534

BRAIN
radiation effects on transplanted Yoshida sarcoma cells in rat, tracer study, 20: 16188
radiation effects on developing rat, x, 20: 16275
BRAIN TUMORS
localization using mercury-197 or mercury-203 neohydrin, 20: 16304
BRASS
analysis for tellurium, activation, 20: 16335(R) (NBS-TN-276)
BREASTS
radiotherapy of cancers of, after surgery, 20: 16324
BREEDER REACTORS
development in Germany, policy for, 20: 18111
development of thorium–uranium, review of, 20: 18073
fuel economics of, uranium–plutonium cycle, 20: 18100
research programs on advanced, 20: 18020(R) (ORNL-3900, pp 2-81)
BREMSSTRAHLUNG
emission by electron-ion interactions in nonrelativistic plasmas, 20: 17947
emission by successive interactions of electrons, (T), 20: 17418
emission from rare gas plasma, negative absorption effects on, (E), 20: 17921
emission in infrared region from hydrogen discharge plasma, (E), 20: 17931(T)
interactions with protons at 0.3 and 5.5 Bev, meson (π) and nucleon resonance production from, (E), 20: 17368
production in electron reactions with aluminum-27, absolute differential cross section for, (E/T), 20: 17798
production of polarized coherent, in electron reactions with diamonds, (E), 20: 17679 (DESY-65/15)
reactions (γ,n) with oxygen-16 to 65 Mev, cross section structure from, (E), 20: 17762
reactions (γ,n) with carbon-12 to 65 Mev, giant resonance structure in cross sections for, (E), 20: 17763
reactions (γ,n) with praseodymium-141 to 65 Mev, cross section for, (E), 20: 17764
reactions (γ,n) with scandium-45 at 24, 36, and 48 Mev, scandium-44 isomeric yield ratio from, (E), 20: 17777
reactions (γ,np) with titanium-46 at 24, 36, and 48 Mev, scandium-44 isomeric yield ratio from, (E), 20: 17777
reactions (γ,π^+) with aluminum-27 at 100 to 300 Mev, cross sections for, (E), 20: 17779
reactions with helium-4, velocity-dependent potential for disintegration, (T), 20: 17774
BRITISH REACTORS
development of, review of, 20: 18104
BROMINE
proton reactions in emulsions at 25 Bev/c, lithium-8 fragment recoil from, (E), 20: 17748
reactions of molecules of, with potassium atoms, 20: 17296
BROMINE ISOTOPES
recoil from proton reactions with uranium at 0.55 and 18.2 Bev, ranges in aluminum, (E), 20: 17837
BROMINE ISOTOPES Br-79
neutron reactions (n,n′) with, sensitivity of, for activation analysis, 20: 16332 (GA-6691)
BROMINE ISOTOPES Br-82
incorporation in bromosulfalein, 20: 16495
sensitivity for activation analysis using beta-gamma-gamma sum-coincidence gamma spectrometer, 20: 16335(R) (NBS-TN-276)
BROMOSULFALEIN SODIUM
labeling with bromine-82 and mercury-197, 20: 16495
BROOKHAVEN ALTERNATING-GRADIENT SYNCHROTRON
particle production in, high-energy, (E/T), 20: 17171 (BNL-10030)
BUBBLE CHAMBERS
magnet power supplies for, use of acyclic generators as, 20: 16772 (CONF-650922, pp 769-75)
magnets for large, design of, 20: 16810 (CONF-650922, pp 366-76)
magnets for, cooling system for superconducting, 20: 17595 (CONF-650922, pp 611-14)
magnets for, design of pulsed, 20: 16811 (CONF-650922, pp 663-79)
particle tracks in, flying spot digitizers for analysis of, 20: 16840
particle tracks in, pulse-pattern generator for analysis of, 20: 16881
photograph scanning and measuring system for, 20: 16838
track illumination and photography using ruby lasers, 20: 16841
BUILDING MATERIALS
gamma emission by tile, thermoluminescent dosimetry of, 20: 16759
BUTADIENE
radioinduced graft polymerization with polyethylene and polypropylene, gamma, 20: 16527
1,3-BUTANEDIONE, 1-PHENYL- COMPLEXES
with europium, fine structure spectra of, 20: 16467(T)
with praseodymium, Szilard-Chalmers reaction in, 20: 16416(R) (NYO-906-68)
1,3-BUTANEDIONE, 4,4,4-TRIFLUORO-1-PHENYL-
complexes with europium, performance of lasers of, deuterium isotope effects on, 20: 16781
solvent properties for europium, 20: 16565
2-BUTANONE
formation by disproportionation of aliphatic ketones in perchloric acid, 20: 16542(R) (TID-22646)
reactions with perchloric acid, disproportionation in rearrangement, 20: 16542(R) (TID-22646)
BUTYL PHOSPHATES
solvent properties for plutonium, 20: 16560
solvent properties for americium and europium, 20: 16564
BUTYROPHENONES
reactions with phosphoric acid, products formed by disproportionation in, 20: 16542(R) (TID-22646)

C

CABLES
performance of magnet coils using superconducting, 20: 17591 (CONF-650922, pp 560-7)
CADARACHE REACTORS
control system of PEGASE, automatic system for correction of amplifier gains in, 20: 18152
CADARACHE REACTORS (RAPSODIE)
control rods for, testing of gripper for, 20: 18096(T) (ORNL-tr-987)
CADMIUM
analysis of ideal solutions of, differential controlled-potential coulometric, 20: 16335(R) (NBS-TN-276)
content in marine organisms, 20: 16725(R) (EUR-2543.e)
determination in uranium compounds by atomic absorption spectrophotometry, 20: 16368
effects on gastrointestinal absorption of copper-64 in rats, 20: 16182
performance of foils of, in neutron radiography, 20: 16619
performance of neutron filters of, effective cutoff energies for, (T), 20: 17663
radiation effects on battery electrodes of, gamma, 20: 17124(R) (N-65-17608)
separation from scandium by ion exchange chromatography, 20: 16574
CADMIUM ALLOYS
Cd–Sn, tin-119 isomeric shift in, 20: 18004
CADMIUM IONS
sorption by aminodiacetate resin Dowex A-1, 20: 16358
CADMIUM ISOTOPES
separation of, performance of separator for, 20: 16928(R) (INSJ-92)
CADMIUM ISOTOPES Cd-109
content in stratospheric and tropospheric samples in Project Star Dust, 1963, 20: 16727(R) (HASL-168)
content in stratospheric and tropospheric samples in Project Star Dust, 1964, 20: 16728(R) (HASL-169)
determination in fission products and fallout, radiochemical, 20: 16397
distribution of atmospheric, from Operation Dominic, 20: 16662(R) (HASL-165)
distribution of atmospheric, from SNAP-9A high-altitude burn-up, predictions for, 20: 16662(R) (HASL-165)
CADMIUM ISOTOPES Cd-113
beta emission by, detection of, 20: 16508(R) (NYO-2771-13)
content in stratospheric and tropospheric samples in Project Star Dust, 1963, 20: 16727(R) (HASL-168)
content in stratospheric and tropospheric samples in Project Star Dust, 1964, 20: 16728(R) (HASL-169)
determination of isomer of, in fallout and fission products, radiochemical, 20: 16397
ground water contamination by, in Shoal Event, hazards from, 20: 16742 (VUF-1014)
CADMIUM ISOTOPES Cd-114
deuteron reactions (d,p) at 15 Mev, isomeric yield ratios for, 20: 16508(R) (NYO-2771-13)
CADMIUM ISOTOPES Cd-115
beta decay of, indium-115 low-lying levels from, (E), 20: 17766
determination of isomer of, in fallout and fission products, radiochemical, 20: 16397
production of isomeric, in deuteron reactions (d,p) at 15 Mev, 20: 16508(R) (NYO-2771-13)
yields in plutonium-239 fission in resonance region, (E), 20: 17858
CADMIUM ISOTOPES Cd-117
beta decay of, indium-117 low-lying levels from, (E), 20: 17766
CADMIUM OXIDES
reactions with aluminum oxides and lanthanum or neodymium oxides at 1400 to 1500°C, 20: 16482
CADMIUM SULFIDES
electric properties of, effects of heat treatments in sulfur vapor at 300 to 750°C on, 20: 17123(R) (N-65-17505)

preparation of single-crystal, 20: 17123(R) (N-65-17505)
radiation effects on photoconductivity of, x-, 20: 17123(R) (N-65-17505)
CALCIFICATION
mechanisms of soft-tissue, 20: 16162
CALCITES
carbon-13 content of, in epigenetic pyrite deposits, Gas Hills Area, Wyoming, 20: 16675
deuterium content of fluid inclusions in, from Mexico, 20: 16634
isotopic composition of Mexican, carbon and oxygen, 20: 16634
CALCIUM
analysis for magnesium, polarographic, 20: 16406
content in Great Lakes and Hudson Bay, geochemistry of, 20: 16711(R) (MIT-1381-13)
content in rabbit skeleton, 20: 16178
determination in presence of barium and strontium by ring oven techniques, 20: 16388
determination in serum, activation, 20: 16347
determination of trace amounts of, in beryllium by spectrography, 20: 16352
effects of, with ferric and ferrous iron on manganese sorption by barley roots, 20: 16174(R) (RLO-1547-3)
effects of, with strontium on manganese sorption by barley roots, 20: 16174(R) (RLO-1547-3)
effects of, with strontium on manganese sorption by barley roots, 20: 16174(R) (RLO-1547-3)
effects on high-temperature properties of eutectic alloys, 20: 17108
effects on uranium separation from phosphate rocks, 20: 16381
excretion in rats, effects of pyridoxine on, 20: 16176
neutron reactions in, short-lived activities from, (E), 20: 16336(R) (NYO-10175)
polarography of, in solochrome violet RS, 20: 16406
sorption by chabazite in lithium, potassium, and sodium nitrates, 20: 16340 (USNRDL-TR-970)
CALCIUM CARBONATES
analysis for manganese, substoichiometric activation, 20: 16403
CALCIUM FLUORIDES
diffusion and capture of argon in neutron-irradiated, properties of, (E), 20: 17804
radiation damage in crystals of, neutron, 20: 17804
sintering of, studies on, 20: 16992(R) (RPI-2408-4)
CALCIUM IONS
sorption by aminodiacetate resin Dowex A-1, 20: 16358
CALCIUM ISOTOPES Ca-40
energy level density of, oscillator model for determining, 20: 17745
energy levels in, excitation of alpha-cluster, (T), 20: 17802
helium-3 reactions (He-3,α) with, optical-model analysis of, (T), 20: 17696 (UR-875-65)
CALCIUM ISOTOPES Ca-41
energy level density of, oscillator model for determining, 20: 17745
CALCIUM ISOTOPES Ca-42
energy level density of, oscillator model for determining, 20: 17745
energy level transitions from potassium-42 decay, 0.58-Mev, (E), 20: 17723
helium-3 reactions (He-3,p) at 12 Mev, Q value for, 20: 16331 (GA-6568)
CALCIUM ISOTOPES Ca-43
energy level density of, oscillator model for determining, 20: 17745
CALCIUM ISOTOPES Ca-44
energy level density of, oscillator model for determining, 20: 17745
neutron reactions (n,α), cross sections for, (E), 20: 17804
neutron reactions (n,α) with, cross sections for, (E/T), 20: 17809
CALCIUM ISOTOPES Ca-45
energy level density of, oscillator model for determining, 20: 17745
transport in paired corn root segments, method for determining wounding response in, 20: 16170 (AD-628805)
uptake by rabbit bones and plasma, 20: 16178
CALCIUM ISOTOPES Ca-46
energy level density of, oscillator model for determining, 20: 17745
CALCIUM ISOTOPES Ca-47
energy level density of, oscillator model for determining, 20: 17745
CALCIUM ISOTOPES Ca-48
energy level density of, oscillator model for determining, 20: 17745
CALCIUM ISOTOPES Ca-49
nucleon interactions in, properties from effective, (T), 20: 17735
CALCIUM MOLYBDATES
radioinduced defects in, ESR of, (E/T), 20: 17975(R) (NYO-2047-36)
CALCIUM OXIDES
determination in Moldavites by mass spectrometry and x-ray fluorescence, 20: 16711(R) (MIT-1381-13)
radioinduced thermoluminescence of hafnium-, thorium-, titanium-, and zirconium-activated, 20: 17982
reactions with aluminum oxides and lanthanum or neodymium oxides at 1400 to 1500°C, 20: 16482
$CaO-Dy_2O_3$, phase studies, 20: 17087
$CaO-SiO_2-Na_2O$, diffusion of sodium-22 in solid, residual activity method for self-, 20: 16478
$CaO-Yb_2O_3$, phase studies, 20: 17087
CALCIUM PHOSPHATES
analytical properties for separation of strontium isotopes from milk, 20: 16382
CALCIUM SULFIDES
positron annihilation in monocrystalline, resistivity from angular distributions of, (E), 20: 17983
CALDER HALL REACTORS
cooling cycle limitations in Magnox, 20: 18109
design of Dungeness A, 20: 18113
CALIFORNIUM
dissociation in hydrochloric acid–bis(2-ethylhexyl) phosphate–toluene system, constants for, 20: 16404
production, 20: 16543
separation from fermium and mendelevium by extraction chromatography using bis(2-ethylhexyl) orthophosphate, 20: 16404
CALIFORNIUM ISOTOPES Cf-252
fission fragment primary charge from, nuclear structure effects on, (T), 20: 17845
fission fragment primary charge from, (E), 20: 17859
fission fragments from, energy degradation in light materials, (E), 20: 17821
fission neutron spectra from, spontaneous, (E), 20: 17825
fission of, neutron yields from spontaneous, (E), 20: 17823
CALORIMETERS
design for measuring x-ray intensity, 20: 16856
CALUTRONS
operation for isotope separation at ORNL, 1964 summary of, 20: 16914(R) (ORNL-3900, pp 182-93)
CAMBRIDGE SYNCHROTRON
use for colliding beam experiments, 20: 17173 (CEAL-1039)
CANADA
geologic dating of volcanic rocks in Lower Cambrian in Atlantic Provinces of, 20: 16711(R) (MIT-1381-13)
CARBAMIC ACID, DIETHYLDITHIO–
solvent properties for manganese-56, 20: 16336(R) (NYO-10175)
CARBON
creep properties of pyrolytic, effects of structure on, 20: 17017 (JPL-TR-32-889)
determination by isotopic dilution, 20: 16362
determination in algae, method for, 20: 16175(R) (RT/BIO(65)-1)
determination in steel and welded joints, activation, 20: 16331 (GA-6568)
effects on ductility and rolling properties of uranium, 20: 17001
effects on high-temperature properties of eutectic alloys, 20: 17108
emissivity and reflectivity at 2100 to 3700°K, 20: 17021 (N-65-18607)
fission gas diffusion through coatings of pyrolytic, effects of coating structure on, 20: 17127 (ORNL-3923)
nucleon elastic scattering at 140 Mev, parametrization analysis for, (T), 20: 17740
proton elastic scattering at 145 Mev, absolute differential cross sections for, (E), 20: 17739
proton scattering at 140 Mev, parameters for triple, (E/T), 20: 17738
radioinduced failures of coatings of pyrolytic, on reactor fuel pellets, 20: 18076 (ORNL-TM-1385)
reactions with niobium oxides at 1400 to 1600°C, 20: 16483
sorptive properties for iodine, 20: 18110
CARBON (ACTIVATED)
sorptive properties for uranium, effects of platinum on, 20: 16581
CARBON BLACK
removal from high-speed printers using cyclone scrubbers, 20: 16740(R) (UCRL-14534, pp 50-3)
CARBON COMPOUNDS
analysis for carbon-14, scintillation counter for, 20: 16862
CARBON DIOXIDES
radiation effects on desorption of graphite surfaces in, 20: 17114 (AERE-R-5163)
reactions with copper–zirconium alloy at 800°C, 20: 16977
Co_2–CO–methane, radiation effects on desorption of graphite surfaces in, 20: 17114 (AERE-R-5163)
CARBON IONS
charge states of recoil, target thickness problem in studies on equilibrium, 20: 16508(R) (NYO-2771-13)
reactions with thin foils at 9.7 Mev, charge-exchange cross sections and ionization from, (E), 20: 17724
CARBON ISOTOPES
abundance ratios in sandstone-type uranium deposits, Gas Hills District, Wyoming, 20: 16670
content in calcite in Mexico, 20: 16634
separation of, performance of separator for, 20: 16928(R) (INSJ-92)
CARBON ISOTOPES C-10

beta decay of, energy and lifetime values and nuclear matrix elements for, (T), 20: 17732

CARBON ISOTOPES C-11
energy levels from carbon-12 (He-3,α) reactions, (E), 20: 17780
half life, 20: 16331 (GA-6568)

CARBON ISOTOPES C-12
alpha reactions (α,n) at 14 Mev, angular distributions from, (E), 20: 17803
bremsstrahlung reactions (γ,n) to 65 Mev, giant resonance structure in cross section for, (E), 20: 17763
decay in oxygen-16 (B-10,3α) reactions, (E), 20: 17815
deuteron reactions (d,n) with, neutron production for activation analysis in, 20: 16332 (GA-6691)
deuteron reactions (d,d′) and (d,p) at 15 Mev, recoils from, (E), 20: 17820
deuteron reactions (d,pγ) at 13.5 Mev, gamma polarization from, (E/T), 20: 17726
electron inelastic scattering by angular distributions for giant resonance decay from, (T), 20: 17757
gamma reactions (γ,n) at 18 to 37 Mev, levels from, (E), 20: 17773
helium-3 reactions (He-3,α) and (He-3,d) at 12 Mev, Q values for, 20: 16331 (GA-6568)
helium-3 reactions (He-3,α) at 12.1 Mev, carbon-11 levels from, (E), 20: 17780
neutron elastic scattering at 3.0 to 4.7 Mev, differential cross sections for, (E), 20: 17767
proton double elastic scattering at 6.14 Mev, polarization angular distributions from, (E), 20: 16870
proton reactions (p,d) at 57 Mev, energy spectra from, (E), 20: 17725
proton reactions (p,2p) at 140 Mev, energy spectra and angular correlations distributions from, (E), 20: 17741
reactions (C-12,6n) with barium-136, angular momentum effects on excitation functions for, (E), 20: 17784
reactions (C-12,7n) with barium-137, angular momentum effects on excitation functions for, (E), 20: 17784
reactions (C-12,8n) with barium-138, angular momentum effects on excitation functions for, (E), 20: 17784
spectra of recoil, from deuteron reactions with carbon-12, (E), 20: 17820

CARBON ISOTOPES C-13
alpha reactions (α,n) with, neutron production for activation analysis in, 20: 16332 (GA-6691)
content in calcite in epigenetic pyrite deposits, Gas Hills Area, Wyo., 20: 16675
energy levels from neutron scattering by carbon-12, (E), 20: 17767
production by high-energy solar particles, 20: 17234
spectra of recoil, from deuteron reactions with carbon-12, (E), 20: 17820

CARBON ISOTOPES C-14
determination in compounds, scintillation detector for, 20: 16862
determination in organic sample by combustion and scintillation, counting, 20: 16387
determination in organic compounds by gas chromatography and scintillation counting, 20: 16371
determination in polystyrene by combustion and liquid scintillation counting, 20: 16384
incorporation in alpha and beta anomers of deoxy-2′-adenosine, method for, 20: 16545
incorporation in desmosterol and lanosterol, 20: 16548
production process improvement, 20: 16914(R) (ORNL-3900, pp 182-93)

CARBON MONOXIDES
radiation synthesis of, developments in, 20: 16506 (BNL-10020)
reactions with cupric oxide in fixed beds, kinetics of, 20: 16556(R) (ORNL-TM-1090)
reactions with niobium oxides, 20: 16483
separation from helium by oxidation and sorption by molecular sieves, 20: 16556(R) (ORNL-TM-1090)
CO_2–CO–methane, radiation effects on desorption of graphite surfaces in, 20: 17114 (AERE-R-5163)

CARBON STEEL
bonding to stainless steel, testing of, 20: 16617
corrosion by boron-containing solutions, 20: 16976

CARBON SYSTEMS
C–Co–Zr, phase studies, 20: 17086
C–Fe–Nb, phase studies, 20: 17086
C–Fe–W, crystal structure of Fe_3W_3C and Fe_6W_6C in, 20: 17015 (INR-665/II/PS)
C–Hf–Mo, superconducting transition temperature of $Mo_{0.95}Hf_{0.05}C_{0.75}$, 20: 17607
C–Mo–Si, superconducting transition temperature of $Mo_{4.8}Si_3C_{0.6}$, 20: 17607
C–Nb–W–Zr, microstructure of D-43, effects of aging on, 20: 17023 (ORNL-TM-1161, pp 208-24)
C–Nb–W–Zr, properties as hollow turbine vanes, 20: 16963
C–Ta, phase studies on zeta-phase in, 20: 17050

CARBON TETRACHLORIDE
effects on radioinduced rayon to styrene graft polymerization, 20: 16528

CARBONATES
oxygen-16/oxygen-18 ratios in, 20: 16676

CARBONATITES
analysis of South African, for rare earths, 20: 16346

CARBOXYLASES
effects of metal ions on potato, 20: 16160 (UCRL-14739(Pt.2))
hydrolysis of, effects of hafnium, thorium, titanium, and zirconium catalysts on, 20: 16420

CARCINOGENS
protection against, using AET, 20: 16159 (ORNL-3900, pp 150-81)

CARCINOMAS
radiation effects on cell cultures from oral, uv and x, 20: 16258
radioinduced lung, etiology of, 20: 16264
radiotherapy of bronchial, esophageal, and lung, moving-beam x, 20: 16317
radiotherapy of laryngeal, γ, 20: 16313
radiotherapy of scalp, 20: 16308

CAROLINAS-VIRGINIA TUBE REACTOR
criticality, 20: 18086 (CVNA-174)
loading operations, 20: 18085 (CVNA-173)
operation and performance analyses of, 20: 18087(R) (CVNA-250)
radiological environment data for, 20: 18083 (CVNA-63)
site meteorological tests for, 20: 18084 (CVNA-96)

CAROTENOIDS
characterization of, isolated from radioresistant Micrococcus, 20: 16161

CARTILAGE
growth in rats, effects of dietary strontium on, 20: 16181

CASCADE SHOWERS
baryon and meson (π) transverse-momentum distribution in high-energy, (T), 20: 17371
detection of EAS, digital recording system for, 20: 16873
energy estimate for, secondary angular distribution and momentum for primary, (T), 20: 17316

CASCADES
calculations of squared-off, for isotope separation by diffusion, 20: 16929

CATALASES
radiation effects on activity of, in rat liver and spleen, 20: 16277

CATHODES
electric arc structure in flowing gases at low pressures, (E), 20: 17517
performance of molybdenum, in getter ion pumps, 20: 16789

CATION EXCHANGE MATERIALS
radiation effects on resin, 20: 16583
sorptive properties of Decalso, for cesium, 20: 16578
sorptive properties of chabazite, for alkali and alkaline earth metals in nitrate solutions, 20: 16340 (USNRDL-TR-970)

CATIONS
effects of polyvalent, on manganese sorption by barley roots, 20: 16174(R) (RLO-1547-3)
uptake of divalent, effects of metabolism on, 20: 16174(R) (RLO-1547-3)

CATTLE
chlorine-36 metabolism in, after ingestion, 20: 16186
iodine-131 content in thyroid gland of, Japan, 1964, 20: 16730 (NP-15882)
iodine-131 metabolism in, after ingestion, 20: 16186
radionuclide transfer in dairy, system for measuring, 20: 16160 (UCRL-14739(Pt.2))

CAVES
design, 20: 16595
design of, at Saclay, 20: 18181
uses at Risö, 20: 18174(R) (NP-15771)

CAVITATION
damage tests on materials by mercury and water, (E), 20: 16974 (NP-15889)

CAVITY RESONATORS
design for plasma acceleration, 20: 17960(P)

CELLULOSE
radioinduced grafting on styrene, properties of product in, 20: 16507 (INR-671/XVII/C)
radioinduced polymerization of rayon with styrene, 20: 16528

CEMENTS
distribution and structure of asbestos in products of, use of neutron-induced sodium-24 for determining, 20: 16920 (SGAE-IB/IA-7/1965)

CERAMIC MATERIALS
dislocation motion in, size distribution of obstacles to, 20: 17980(T) (ANL-Trans-274)
performance and selection of, for use in space vehicles, 20: 16944 (NASA-SP-3025)
properties as reactor fuel material, 20: 18182
sample preparation for high-magnification optical microscopy of, 20: 16954 (ORNL-TM-1161, pp 267-71)

CERIUM

abundance in sun, (E), 20: 17237
determination in chromium-base alloys, method for, 20: 16334 (N-65-18292)
determination in presence of rare earths using sulfanilic acid, spectrophotometric, 20: 16398
diffusion from ceramic wastes, effects of volatilization on, 20: 18156 (BNWL-SA-453)
diffusion in magnesium, 20: 17038
effects on high-temperature properties of eutectic alloys, 20: 17108
effects on soft-tissue calcification in rats, 20: 16162
evaporation from irradiated uranium dioxide at 750 to 1600°C, 20: 17102
separation from Hanford wastes by solvent extraction, 20: 16329 (BNWL-187)
separation from other fission products by precipitation with barium sulfate, 20: 16343
separation from rare earths, solvent extraction method for, 20: 16329 (BNWL-187)
solubility in gold, solid, 20: 17016 (IS-1175)
solvent properties for magnesium, solid, 20: 17016 (IS-1175)

CERIUM ALLOYS
Al–Ce, production of, aluminothermic, 20: 16964
Ce–Mg, spectrophotometric analysis for cerium using sulfanilic acid, 20: 16398

CERIUM CARBIDES
properties of, chemical and physical, 20: 17048
reactions with water, formation of gaseous products in, 20: 17048

CERIUM COMPLEXES
with EDTA, chemical properties of praseodymium-144 produced by beta decay of cerium-144 in, 20: 16544
with thenoyltrifluoroacetone, magnetic susceptibilities of, 20: 16416(R) (NYO-906-68)

CERIUM HYDRIDES
properties and structure, 20: 16453

CERIUM IONS
sorption by aminodiacetate resin Dowex A-1, 20: 16358

CERIUM ISOTOPES Ce-137
content in food chain, ratio to fallout of, 20: 16678
gamma angular distributions from isomeric, aligned in neodymium ethyl sulfate, (E), 20: 17614
nuclear magnetic moment of isomeric, (E), 20: 17614

CERIUM ISOTOPES Ce-140
oxygen-16 scattering at 31 to 45 Mev, B(E2) values for transitions from, (E), 20: 17734

CERIUM ISOTOPES Ce-141
content in fallout and precipitation near Leningrad, 20: 16704
content in rain water, Fayetteville, Arkansas, Oct. 1964, 20: 16663 (TID-21470)
content in stratospheric and tropospheric samples in Project Star Dust, 1963, 20: 16727(R) (HASL-168)
content in surface layer of atmosphere over Heis Island and Moscow, 20: 16650
determination by precipitation with barium sulfate and gamma spectroscopy, 20: 16343
fallout monitoring at Vilnius, Soviet Union, in 1962, 20: 16700
yields from thorium-232 fission, (E), 20: 17860

CERIUM ISOTOPES Ce-142
nucleon capture at 10 to 40 Mev, cross sections and mechanism for direct, (T), 20: 17737
oxygen-16 scattering at 31 to 45 Mev, B(E2) values for transitions from, (E), 20: 17734

CERIUM ISOTOPES Ce-143
sensitivity for activation analysis using beta-gamma-gamma sum-coincidence gamma spectrometer, 20: 16335(R) (NBS-TN-276)

CERIUM ISOTOPES Ce-144
beta decay in EDTA complexes, chemical properties of praseodymium-144 recoils from, 20: 16544
content in atmospheric dust and rain water, 1964–65, 20: 16660 (AERE-R-4997)
content in atmosphere in Japan, 1964, 20: 16731 (NP-15883)
content in fallout and precipitation near Leningrad, 20: 16704
content in plants before and after Salmon Event, 20: 16743 (VUF-1021)
content in stratospheric and tropospheric samples in Project Star Dust, 1963, 20: 16727(R) (HASL-168)
content in stratospheric and tropospheric samples in Project Star Dust, 1964, 20: 16728(R) (HASL-169)
content in surface layer of atmosphere over Heis Island and Moscow, 20: 16650
determination by precipitation with barium sulfate and gamma spectroscopy, 20: 16343
dispersion of aerosols of, in stratosphere, 20: 16643
distribution in deep sea water near Japan, vertical, 20: 16681
fallout monitoring at Vilnius, Soviet Union, in 1962, 20: 16700
ground water contamination by, in Shoal Event, hazards from, 20: 16742 (VUF-1014)
yields from thorium-232 fission, (E), 20: 17860

CERIUM OXALATES
reactions of hydrated, with hydrochloric acid, 20: 16447

CERIUM OXIDES
determination in thorium oxide by emission spectroscopy, 20: 16393
CeO_2–La_2O_3–Sm, fluorescence properties of, 20: 16466(T)
CeO_2–Sm_2O_3, fluorescence properties of, 20: 16466(T)
CeO_2–Sm–ThO_2, samarium fluorescence in, 20: 16466(T)

CERIUM PERRHENATES
preparation and properties of anhydrous and hydrated, 20: 16440

CERIUM SILICIDES
properties of, physicochemical, 20: 17047

CERIUM SULFIDES
Ce_2S_3–EuS, compound formation in, 20: 16431
Ce_2S_3–SmS, compound formation in, 20: 16431
Ce_2S_3–YbS, compound formation in, 20: 16431

CERIUM TANTALATES
$CeTaO_4$–$KTaO_3$, crystal structure, 20: 16438

CERMETS
casting of cobalt–tungsten carbide, process for slip, 20: 16997

CESIUM
cesium ion reactions with atoms of, at low energies, (E), 20: 17299
electron scattering by atomic, cross sections for, (T), 20: 17286
ionization by electrons, cross sections for, 20: 17287
loss from waste sludge-containing glass during firing, 20: 18166(R) (TID-22531)
melting at high pressures, 20: 17071(T)
neutron total cross sections at 14 Mev, (E), 20: 17702
production and properties of plasma of, (E), 20: 17955
separation from high-level waste solutions by ion exchange, 20: 16570
separation from sewage water by sorption on multiclone dust from gasification of coke, 20: 18170
sorption by chabazite in lithium, potassium, and sodium nitrates, 20: 16340 (USNRDL-TR-970)
uptake by erythrocyte membranes, 20: 16160 (UCRL-14739(Pt.2))

CESIUM ALLOYS
Sb–Cs, photosensitivity of, 20: 17984
Sb–Cs–K–Na, photosensitivity of, 20: 17984
Sb–Cs–K–Na–Te, photosensitivity of, 20: 17984

CESIUM CARBONATES
preparation and purification, 20: 16476

CESIUM CHLORIDES
activity and osmotic coefficients in heavy water at 25°C, 20: 16488

CESIUM HYDROXIDES
preparation and purification, 20: 16476

CESIUM IODIDES
density of thin films of, 20: 17070
scintillation response functions for monoenergetic electrons, 20: 16867

CESIUM IONS
mobility in argon, helium, and nitrogen at high pressures, (E/T), 20: 16415 (CEA-R-2861)
reactions with cesium atoms at low energies, cross section for, (E), 20: 17299
scattering by argon, krypton, and nitrogen at 2.3 to 11.6 ev, elastic, (E/T), 20: 17300
wave functions for, including effect of nuclear quadrupole moment, 20: 17250 (BNL-8850)

CESIUM ISOTOPES Cs-133
deuteron reactions (d,2n), cross sections for barium-133 production in, 20: 16508(R) (NYO-2771-13)
energy levels of, half life of second excited, (E), 20: 17701
nitrogen-14 reactions (N-14,5n), angular momentum effects on excitation functions for, (E), 20: 17784
nuclear radius, (E), 20: 17702

CESIUM ISOTOPES Cs-134
beta transitions in, higher-order effects in allowed, (E), 20: 17678 (COO-1420-113)
sensitivity for activation analysis using beta-gamma-gamma sum-coincidence gamma spectrometer, 20: 16335(R) (NBS-TN-276)

CESIUM ISOTOPES Cs-137
accumulation in soils near Leningrad, 20: 16702
content in atmospheric dust and rain water, 1964–65, 20: 16660 (AERE-R-4997)
content in atmosphere in Yugoslavia from weapons testing in 1962 and 1963, 20: 16682
content in atmosphere, human urine, milk, rain water, and water supplies in Japan, 1964, 20: 16731 (NP-15883)
content in body and urine of Japanese, 20: 16226 (NP-15891)
content in Colorado mule deer, effects of foliage contamination and food habits on, 20: 16723 (COO-1156-11)
content in diet in U. S., 1965, 20: 16662(R) (HASL-165)
content in fallout and precipitation near Leningrad, 20: 16704

content in human placentas, 20: 16301
content in Japanese rice and soil, 20: 16169
content in man, 1965, 20: 16303(R) (AD-626384)
content in milk and plants before and after Salmon Event, 20: 16743 (VUF-1021)
content in powdered milk in Japan, 1962 and 1963, 20: 16755
content in rain water, Fayetteville, Arkansas, Oct. 1964, 20: 16663 (TID-21470)
content in stratospheric and tropospheric samples in Project Star Dust, 1963, 20: 16727(R) (HASL-168)
content in stratospheric and tropospheric samples in Project Star Dust, 1964, 20: 16728(R) (HASL-169)
content in surface layer of atmosphere over Heis Island and Moscow, 20: 16650
determination in milk, sea water, urine, and environmental samples by ion exchange and gamma spectroscopy, 20: 16342
determination in milk, solid foods, and water, methods for, 20: 16339
diffusion from ceramic wastes, effects of volatilization on, 20: 18156 (BNWL-SA-453)
dispersion of aerosols of, in stratosphere, 20: 16643
distribution in deep sea water near Japan, vertical, 20: 16681
fallout monitoring near Leningrad in 1961–1963, 20: 16701
ground water contamination by, in Shoal Event, hazards from, 20: 16742 (VUF-1014)
radiation effects combined with cold on rat retention of, x, 20: 16180
separation from aqueous solutions by flotation, 20: 16392
separation from fission products, ion exchanger for, 20: 16578
yields from thorium-232 fission, (E), 20: 17860

CESIUM OXALATES
preparation and purification, 20: 16476

CESIUM SYSTEMS
Cs–F, electron emission from metals in vapors of, thermionic, (T), 20: 17334

CESIUM URANYL BROMIDES
crystal structure of, from x-ray-diffraction studies, 20: 16484

CESIUM URANYL CHLORIDES
crystal lattice energy transfer to rare earth ions in, effective-excitation, (E), 20: 18010

CHALKS
analysis for manganese, substoichiometric activation, 20: 16403

CHARCOAL
reactions with niobium oxides at 1400 to 1600°C, 20: 16483

CHARGED PARTICLE BEAMS
aberrations in focused, space-charge effects on coefficients for, (T), 20: 16784
interactions with turbulent plasma, (T), 20: 17958
transport system for, computer program for designing, 20: 17211 (LNF-65/45)

CHARGED PARTICLES
charge and energy flows in nonequilibrium system of, in strong magnetic field, (T), 20: 17487
detection and measurement using magnetic analyzers, 20: 16859
emission in neutron-induced reactions, Coulomb penetration and shift factors for, 20: 17671 (AEEW-M-611)
interactions in turbulent plasma, (T), 20: 17958
interactions in turbulent plasma, (T), 20: 17941
interactions of massless, minimal electromagnetic, 20: 17484
interactions with photons, pair production in, (T), 20: 17499
interactions with photons in magnetic field, Compton effect in, (T), 20: 17409
motion in geomagnetic fields, (T), 20: 17540 (N-65-18914)
motion in magnetic field, computer for determining, 20: 17906
motion in magnetic spectrometers, Fermat principle for, (T), 20: 16821 (LAL-1151)
orbits in magnetic fields, measurement using current-carrying wire, 20: 16771 (CONF-650922, pp 467-71)
production in meson (π) and proton reactions in emulsions, identification by delta electrons, (E), 20: 17358
production of high-energy, in meson (π) reactions with emulsion nuclei at 7.5 Bev, 20: 17715
scattering by atoms and molecules, inelastic, (T), 20: 17306
scattering by complex nuclei, analysis of diffraction, (T), 20: 17816
scattering of, quantum effects in multiple, (T), 20: 17497
shielding of space vehicles against, calculations for, 20: 17965
trajectories in magnetic fields, measurement using current-carrying wire, (E/T), 20: 17196 (CONF-650922, pp 497-504)
transmission through semiconductors, electromagnetic radiation emission from, (T), 20: 17494

CHEMICAL ANALYSIS
developments in nuclear and radio-, summary for ORNL, 20: 16914(R) (ORNL-3900, pp 182-93)
equipment and procedures for determining carbon, hydrogen, and oxygen in alkali metals, 20: 17158(R) (ORNL-3900, pp 82-149)
radiation effects on results of, gamma, 20: 17158(R) (ORNL-3900, pp 82-149)

CHEMICAL ENGINEERING
process for removal of carbon monoxide and hydrogen from helium coolants, 20: 16556(R) (ORNL-TM-1090)

CHEMICALS AND REAGENTS
radioinduced synthesis of, developments in, 20: 16506 (BNL-10020)

CHEMISTRY
radiation synthesis in, developments in, 20: 16506 (BNL-10020)

CHEMOTHERAPY
nausea in, properties of metoclopramide for preventing, 20: 16163

CHERENKOV DETECTORS
design and performance of gaseous, 20: 16816 (JINR-P-2528)

CHERENKOV RADIATION
emission by electron stream in uniformly loaded waveguides, (T), 20: 17485
emission from charged particles passing through semiconductors, properties of, (T), 20: 17494
use in reactor power control and measurement, 20: 18033

CHICKENS
embryos of, metabolic pathways in developing, 20: 16172(R) (NYO-2194-1)

CHLORAMPHENICOL
effect on synthesis of RNA during recovery of DNA synthetic system in uv-damaged *E. coli*, 20: 16202

CHLORELLA
radiation effects on survival in, mathematical analysis of, 20: 16246

CHLORINE
determination in polystyrene, activation, 20: 16335(R) (NBS-TN-276)
effects of impurity of, on electric conductivity of irradiated fused silica, 20: 17133
neutron reactions in, short-lived activities from, (E), 20: 16336(R) (NYO-10175)
photon reactions with Coulomb field of, pair production total cross sections for high-energy, (T), 20: 17754

CHLORINE IONS
wave functions for, including effect of nuclear quadrupole moment, 20: 17250 (BNL-8850)

CHLORINE ISOTOPES Cl-34
beta decay of, phase-space integrals for, (T), 20: 17732
half life, 20: 16331 (GA-6568)

CHLORINE ISOTOPES Cl-35
helium-3 reactions (He-3,α) at 12 Mev, Q value for, 20: 16331 (GA-6568)

CHLORINE ISOTOPES Cl-36
metabolism in calves after ingestion, 20: 16186
neutron reactions, production of phosphorus-33 in, 20: 16914(R) (ORNL-3900, pp 182-93)

CHLORINE ISOTOPES Cl-37
helium-3 reactions (He-3,2p) at 12 Mev, Q value for, 20: 16331 (GA-6568)
proton reactions (p,n) with, neutron production for activation analysis in, 20: 16332 (GA-6691)

CHLORINE ISOTOPES Cl-38
half life, 20: 16331 (GA-6568)

CHLOROFORM
chloroform–nitrobenzene, effects on isotopic exchange between elementary iodine and 1-phenyl-2,3-dimethyl-4-iodopyrazolone, 20: 16502

CHOLINESTERASES
activity in vagal heart preparations from frogs, effects of alkali metal ions on, 20: 16160 (UCRL-14739(Pt.2))

CHROMATOGRAPHY
gas, catalytic detectors for use with, 20: 17158(R) (ORNL-3900, pp 82-149)

CHROMIUM
complexes with protein, radiation chemistry of, γ, 20: 16211
determination in asbestos using ion exchange, activation, 20: 16336(R) (NYO-10175)
determination in presence of manganese, activation, 20: 16332 (GA-6691)
determination in uranium concentrates, oxides, and metal, activation, 20: 16399
determination of trace amounts of, in beryllium by spectrography, 20: 16352
dislocation parameters for, 20: 17033
melting point of, effects of gas impurities on, 20: 17094

CHROMIUM ALLOYS
analysis for cerium, method for, 20: 16334 (N-65-18292)
Cr–Co, effects of additives on high-temperature properties of eutectic, 20: 17108
Cr–Co–Nb, phase studies on intermetallic compounds in, 20: 17075
Cr–Fe–Mo, phase studies, 20: 17093
Cr–Fe–Ni, corrosion cracking in, mechanisms of stress-, 20: 16968 (COO-1319-33)
Cr–Fe–W, phase studies, 20: 17093

Cr–Ga–Nb, phase studies on intermetallic compounds in, 20: 17075
Cr–Ge–Nb, phase studies on intermetallic compounds in, 20: 17075
Cr–Nb, phase transformations in, 20: 17046
Cr–Nb–Ti, phase studies, 20: 17091
Cr–Nb–Ti, tensile properties of, effects of composition on, 20: 17112
Cr–Ni–Nb, phase studies on intermetallic compounds in, 20: 17075
Cr–Ta, phase transformations in, 20: 17046
Cr–U, superconductivity of beta-phase, 20: 17095

CHROMIUM BORIDES
chemical bonding and electric conductivity of, 20: 16439

CHROMIUM IONS
sorption by aminodiacetate resin Dowex A-1, 20: 16358

CHROMIUM ISOTOPES Cr-48
gamma spectra, 20: 16508(R) (NYO-2771-13)

CHROMIUM ISOTOPES Cr-49
half life, 20: 16331 (GA-6568)

CHROMIUM ISOTOPES Cr-50
helium-3 reactions (He-3,α) and (He-3,d) at 12 Mev, Q values for, 20: 16331 (GA-6568)

CHROMIUM ISOTOPES Cr-52
neutron reactions (n,p) with, sensitivity of, for activation analysis, 20: 16332 (GA-6691)

CHROMIUM ISOTOPES Cr-53
nucleon interactions in, properties from effective, (T), 20: 17735

CHROMIUM ISOTOPES Cr-54
nucleon interactions in, properties from effective, (T), 20: 17735

CHROMIUM OXIDES
catalytic properties in deuterium–hydrocarbon reactions, 20: 16487

CHROMIUM STEEL
Cr–Mo, corrosion of Croloy 2¼ steel by sodium and sodium hydroxides, 20: 16599(R) (BAW-1280-34)
Cr–Mo, corrosion by mercury, corrosion loop testing of, 20: 16972(R) (NASA-CR-54719)
Cr–Mo, properties of, effects of potassium–sodium environment on, 20: 16972(R) (NASA-CR-54719)

CHROMIUM SYSTEMS
Cr–Fe–Ni–P, corrosion cracking in, mechanisms of stress-, 20: 16968 (COO-1319-33)
Cr–Fe–Ni–Si, corrosion cracking in, mechanisms of stress-, 20: 16968 (COO-1319-33)

CHROMOSOMES
differentiation in developing embryos, 20: 16172(R) (NYO-2194-1)
meiotic division in, distributive pairing theory of, 20: 16159(R) (ORNL-3900, pp 150-81)
model for, 20: 16160 (UCRL-14739(Pt.2))
radiation effects on sister chromated exchanges in, 20: 16159(R) (ORNL-3900, pp 150-81)
radiation effects on number and structure of, computer system for analyzing, 20: 16160 (UCRL-14739(Pt.2))
radiation effects on, low-dose, 20: 16160 (UCRL-14739(Pt.2))
radioinduced aberrations in human, effects of dose on, 20: 16230(R) (TID-22644)
radioinduced aberrations of, effects of infrared radiation on x, 20: 16278

CIRCUITS
analysis of electric, computer program for, 20: 16790
design for studying mass distributions of fission fragments, 20: 17870
design of subtractor, with integrated logic elements, 20: 16940
radiation effects on microelectronic, gamma and neutron, 20: 16908 (N-65-17526)
threshold level of trigger, effects of driving pulse duration on, 20: 16785

CITRATES
synthesis in bone tissues, measurement of enzyme for, 20: 16160 (UCRL-14739(Pt.2))

CIVILIAN DEFENSE
fallout shelter protection factor for, calculation of, 20: 16733 (ORNL-P-1098)
role of veterinarians in, 20: 16761
shelters for urban populations, design of tunnel-grid, 20: 16159(R) (ORNL-3900, pp 150-81)
use of underground highway and parking garage for Manhattan Island, engineering study on, 20: 16623 (ORNL-TM-1381)

CLEAN ROOMS
contamination control in, de-ionized water-laminar air flow system for, 20: 16590 (SC-TM-66-49)
description of, at Y-12, 20: 16744 (Y-EA-49)
design for centrifugal separation of viruses, engineering drawings of, 20: 16166

CLEANING
equipment for recovery of spilled mercury, 20: 16738(R) (UCRL-14534, pp 41-3)
method for glass dosimeter, 20: 16847
methods for, description of, 20: 16744 (Y-EA-49)
systems for, high-purity de-ionized water, 20: 16590 (SC-TM-66-49)

CLINCH RIVER
radioactive waste disposal in, safety hazards from, 20: 18020(R) (ORNL-3900, pp 2-81)

CLOUDS
water sample selection from, using cyclone precipitators, 20: 16658

COAL
analysis for hydrogen by beta absorption, 20: 16356
radioinduced carbonization, 20: 16514

COATINGS
properties of pyrolytic carbon, 20: 18020(R) (ORNL-3900, pp 2-81)

COBALT
determination in asbestos using ion exchange, activation, 20: 16336(R) (NYO-10175)
determination in nickel oxide solutions, tracer technique for, 20: 16335(R) (NBS-TN-276)
determination in uranium concentrates, oxides, and metal, activation, 20: 16399
determination of trace amounts of, in beryllium by spectrography, 20: 16352
determination of, radiometric and substoichiometric methods for trace, 20: 16335(R) (NBS-TN-276)
electron and positron scattering at 150 Mev, cross sections for, (E), 20: 17785
preparation of self-supporting radiation targets of, 20: 17218
proton reactions at 590 Mev and 18.3 Bev, potassium isotope yields in, (E), 20: 17717
separation from scandium by ion exchange chromatography, 20: 16574

COBALT ALLOYS
Al–Co, effects of additives on high-temperature properties of eutectic, 20: 17108
Al–Co–V, phase studies on intermetallic compounds in, 20: 17075
Al–Co–W, phase studies on intermetallic compounds in, 20: 17075
Co–Mo, effects of additives on high-temperature properties of eutectic, 20: 17108
Co–W, effects of additives on high-temperature properties of eutectic, 20: 17108
Cr–Co, effects of additives on high-temperature properties of eutectic, 20: 17108
Cr–Co–Nb, phase studies on intermetallic compounds in, 20: 17075

COBALT COMPLEXES
radiation effects on reduction of, by hydrogen in ethanol solutions, 20: 16526

COBALT IONS
effects on hydrolysis of α-D-glucose 1-phosphate, 20: 16421
sorption by aminodiacetate resin Dowex A-1, 20: 16358

COBALT ISOTOPES Co-54
beta decay of, phase-space integrals for, (T), 20: 17732

COBALT ISOTOPES Co-56
beta transitions in, higher-order effects in allowed, (E), 20: 17678 (COO-1420-113)
nucleon interactions in, properties from effective, (T), 20: 17735

COBALT ISOTOPES Co-57
content in stratospheric and tropospheric samples in Project Star Dust, 1964, 20: 16728(R) (HASL-169)
nucleon interactions in, properties from effective, (T), 20: 17735

COBALT ISOTOPES Co-58
half life, 20: 16335(R) (NBS-TN-276)

COBALT ISOTOPES Co-59
proton reactions (p,2p) at 140 Mev, energy spectra and angular correlation distributions from, (E), 20: 17741

COBALT ISOTOPES Co-60
content in Bogou iron meteorite, 20: 16674
content in stratospheric and tropospheric samples in Project Star Dust, 1964, 20: 16728(R) (HASL-169)
determination in irradiated materials by extraction and precipitation, gamma spectrometric, 20: 16336(R) (NYO-10175)
gamma dosimetry for, in contact and interstitial therapy, 20: 16765
gamma emission from, liquid photographic emulsions for dosimetry of, 20: 16845
performance in rocket engines, 20: 16914(R) (ORNL-3900, pp 182-93)
removal from Duralumin and steel-3 by ultrasonic cleaning in acid media, 20: 16767
sensitivity for activation analysis using beta-gamma-gamma sum-coincidence gamma spectrometer, 20: 16335(R) (NBS-TN-276)

COBALT ISOTOPES Co-61
nucleon capture at 10 to 40 Mev, cross sections and mechanism for direct, (T), 20: 17737

COBALT NITRATES
effects of iodine-131 exchange between silver iodide and iodide ions, 20: 16432

COBALT OXIDES
electronic properties of single-crystal, effects of ion-bombardment on,

20: 17151
COBALT SYSTEMS
C–Co–Zr, phase studies, 20: 17086
Co–TiC–WC, casting of cermets of, slip, 20: 16997
Co–WC, casting of cermets of, slip, 20: 16997
COILS
design for measurement of harmonic content of beam transport magnets, 20: 17195 (CONF-650922, pp 487-96)
COINCIDENCE COUNTERS
design for Mariner C, 20: 16822 (N-65-19927)
design of cubical meson telescope for sea level observations, 20: 17311
COKE
analysis for water using neutron probes, 20: 16926
moisture content of, neutron absorption measurements of, 20: 16922
reactions with niobium oxides at 1400 to 1600°C, 20: 16483
COLLOIDS
radiation effects on sedimentation of sewage, gamma, 20: 16505 (BNL-949)
COLORADO
cesium-137 content in atmosphere, deer, plants, and soils of Cache la Poudre, 20: 16723 (COO-1156-11)
COLUMBIA RIVER
cooling program for, evaluation of use of selective discharges from Lake Roosevelt in, 20: 18172 (BNWL-208)
COMMUNICATION THEORY
use in radiation detection and measurement, 20: 16893
COMPLEXES
stability constants of, determination of, by metal distribution between aqueous phase and ion exchanger, 20: 16481
COMPTON EFFECT
cross sections for, in photon reactions with lithium fluoride, 20: 16829(R) (UCRL-14534, pp 1-7)
use in direct energy conversion, 20: 17331
COMPUTER PROGRAMS
ARGOSY, use in analysis of reactor kinetics, 20: 18051 (TRG-Report-1014)
CPS, for neutron cross section curve plotting, FORTRAN II, 20: 17699 (WANL-TME-1317)
CWF, for Coulomb penetration, EGTRAN and FORTRAN for IBM 7090 and KDF9, 20: 17671 (AEEW-M-611)
DATAPREP-II, for reactor lattice homogenization, FORTRAN-63 for CDC 3600, 20: 18047 (KR-78)
development of, for analysis of whole-body counting data, 20: 16737(R) (UCRL-14534, pp 13-18)
developments on, at Risö, 20: 18174(R) (NP-15771)
EXT, for Maxwellian Doppler broadened Breit-Wigner resonances, IBM 7094, 20: 17698 (WANL-TME-1132)
for analysis of charged-particle motion in geomagnetic fields, 20: 17540 (N-65-18914)
for analyzing electrical circuits using ZRA-1 computer, 20: 16790
for automatic neutron time-of-flight spectra analysis using least square methods, in FORTRAN IV, 20: 16877
for calculating transient temperatures for fixation of radioactive material in hollow and solid cylinders and slabs, 20: 18155 (BNWL-157)
for calculation of proton density variation in radiation belts with solar cycle, FORTRAN II for IBM 7094, 20: 17539 (N-65-18257)
for calculation of neutron disadvantage factor, 20: 17668
for compound nuclear cross sections, S2 for IBM 7030, 20: 17672 (AERE-R-5053)
for data convolution techniques for determining peak area, peak energy, and peak location in scintillation spectra, 20: 16344
for effects of local sea breezes on fallout transport, 20: 16661(R) (ECOM-00392-F)
for Fermi surfaces of crystals, FORTRAN, 20: 17973 (IS-1106)
for flow calculations in liquid hydrogen tanks, 20: 17536
for processing data from radioisotope sediment tracing studies, FORTRAN IV for IBM 7040, 20: 16632 (AAEC/TM-303)
for reactor evaluations, 20: 18020(R) (ORNL-3900, pp 2-81)
for third-order aberrations of magnet systems, in FAP and FORTRAN, 20: 17220
HUNTER, for optical-model analysis of nuclear reactions, (T), 20: 17696 (UR-875-65)
ISOCRUNCH, for isotope yields, 20: 16914(R) (ORNL-3900, pp 182-93)
ISOTOPES, for isotope yields, 20: 16914(R) (ORNL-3900, pp 182-93)
MYRA, for fuel shipping costs, 20: 18020(R) (ORNL-3900, pp 2-81)
NELKER, for scattering kernel calculation for hydrogen, FORTRAN II for IBM 7090, 20: 17684 (JAERI-1085)
NORA, for fuel processing costs, 20: 18020(R) (ORNL-3900, pp 2-81)
OGRE-G, for gamma dose rates in arbitrary geometries, 20: 17961 (ORNL-TM-1212)
OR TEP, for crystal structures, 20: 17158(R) (ORNL-3900, pp 82-149)
PEGGY, for phase-shift analysis of elastic scattering, FORTRAN for CDC-1604, 20: 17693 (ORNL-TM-1464)
REZONE, for two-dimensional Lagrangian hydrodynamics problems, 20: 18173 (LA-3455)
STRETCH, for radioinduced failures of pyrolytic-carbon coatings on reactor fuel pellets, 20: 18076 (ORNL-TM-1385)
SYTRAN, for charged particle beam transport system design, for IBM 7040, 20: 17211 (LNF-65/45)
TABLE, for Coulomb shift factors, EGTRAN and FORTRAN for IBM 7090 and KDF9, 20: 17671 (AEEW-M-611)
TASCO, for waste disposal costs, 20: 18020(R) (ORNL-3900, pp 2-81)
TNT02, for flux depletion in reactors, 20: 18052 (WAPD-T-1836)
TURBO, for flux depletion in reactors, 20: 18052 (WAPD-T-1836)
use of matrix inversion for unfolding proton recoil spectra, for IBM-7090, 20: 16875
use with flying spot digitizers for track chamber photograph analysis, 20: 16840
XO, for resonance cross sections for zero temperature target, IBM 7094, 20: 17698 (WANL-TME-1132)
COMPUTERS
circuit design for IBM 7094, subtractor, 20: 16940
description of digital, for data processing, 20: 16335(R) (NBS-TN-276)
design for operation and control of system of neutron and x-ray spectrometers, 20: 16869
programming of digital data handling, static, 20: 18121
use at ORNL in mathematics research, 20: 17158(R) (ORNL-3900, pp 82-149)
use for accelerator control, 20: 17209(R) (LA-3479)
use in activation analysis, 20: 16335(R) (NBS-TN-276)
use in calculating gamma attenuation by lithium fluoride crystals, 20: 16829(R) (UCRL-14534, pp 1-7)
use in determining radiation effects on chromosome number and structure, 20: 16160 (UCRL-14739(Pt.2))
use in determining patient exposure during radiography, 20: 16751
use in mass difference calculations for baryons, mesons, and ¾*, resonances, IBM 7074, 20: 17507
use in processing of nuclear data, 20: 17709
use of analog, for charged-particle motion in magnetic field, 20: 17906
use of digital, for nuclear data processing, 20: 17708
use of digital, in radium implant dosimetry, 20: 16748
CONCRETES
analysis for water using neutron probes, 20: 16926
CONFERENCES
see also introduction to Report Number Index
Nuclear Physics, International Congress of, Paris, July, 1964, 20: 17871
CONSTANTS AND CONVERSION FACTORS
calculations of Clebsch-Gordan and Z coefficients, 20: 17559 (EUR-2639.f)
CONTAMINATION
control in clean rooms, methods for, 20: 16744 (Y-EA-49)
CONVECTION
magnetohydrodynamic, in vertical cylinders, (T), 20: 17516
CONVERSION ELECTRONS
emission from nuclei, review of data on, 20: 17795
COPPER
analysis for selenium by neutron activation, 20: 17822
analysis for silver by radioisotope dilution, 20: 16335(R) (NBS-TN-276)
analysis for vanadium, activation, 20: 16332 (GA-6691)
brazing of disks and cylinders of, for linear accelerator waveguide, 20: 16999
cavitation damage in water, 20: 16974 (NP-15889)
content in marine organisms, 20: 16725(R) (EUR-2543.e)
defects in crystalline, x-ray determination of, 20: 17158(R) (ORNL-3900, pp 82-149)
determination by radiometric titration, 20: 16386
determination in asbestos using ion exchange, activation, 20: 16336(R) (NYO-10175)
determination in lung tissue, activation, 20: 16335(R) (NBS-TN-276)
determination in serum, activation, 20: 16347
determination of trace amounts of, in beryllium by spectrography, 20: 16352
deuteron sputtering at 30 kev, yields from, 20: 17892(R) (ORNL-3908, pp 149-53)
dislocation motion in, size distribution of obstacles to, 20: 17980(T) (ANL-Trans-274)
effects on iodine diffusion from L54M fuels, 20: 18142
proton reactions at 590 Mev and 18.3 Bev, potassium isotope yields in, (E), 20: 17717
proton scattering at 140 Mev, parameters for triple, (E/T), 20: 17738
radiation effects on internal friction of, electron-beam, 20: 17135
radiation effects on content in blood serum of mammals, 20: 16222 (AFWL-TR-65-112)
separation from scandium by ion exchange chromatography, 20: 16574
separation from sulfuric acid leach slurries by liquid ion exchange, 20: 16572

sputtering by argon ions at 0.1 to 200 kev, yields from, (E), 20: 17256
x ray scattering by thin films of, interference fringes from, (E/T), 20: 17163
COPPER ALLOYS
Al–Cu–Sc, crystal structure of ternary phases in, 20: 17097(T)
Cu–Ge, radiation effects on viscous dislocation damping in dilute, gamma, 20: 17138
Cu–Zn, cavitation damage in water, 20: 16974 (NP-15889)
Cu–Zr, oxidation by carbon dioxide at 800°C, 20: 16977
COPPER IONS
effects on hydrolysis of α-D-glucose 1-phosphate, 20: 16421
sorption by aminodiacetate resin Dowex A-1, 20: 16358
COPPER ISOTOPES Cu-63
neutron reactions (n,γ), threshold cross section and energy for, 20: 16335(R) (NBS-TN-276)
COPPER ISOTOPES Cu-64
half life, 20: 16335(R) (NBS-TN-276)
sorption in rats, effects of cadmium, mercury, silver, and zinc on gastrointestinal, 20: 16182
COPPER ISOTOPES Cu-65
deuteron reactions (d,2n), cross sections for zinc-65 production in, 20: 16508(R) (NYO-2771-13)
proton reactions (p,n) with, neutron production for activation analysis in, 20: 16332 (GA-6691)
COPPER OXIDES
reactions in fixed beds with carbon monoxide and hydrogen, kinetics of, 20: 16556(R) (ORNL-TM-1090)
CORDIERITES
pleochroic halos in, dimensions and relation to α rays in radioactive elements, 20: 16666(T) (ORNL-tr-923)
CORROSION LOOPS
operation of mercury forced-convection, 20: 16972(R) (NASA-CR-54719)
operation of potassium–sodium, 20: 16972(R) (NASA-CR-54719)
COSMIC ALPHA PARTICLES
flux modulation at low rigidities, (T), 20: 17312(T)
COSMIC ELECTRONS
detection and measurement of primary, background estimates for, 20: 17322
energy losses by synchrotron radiation and inverse Compton scattering, (T), 20: 17309 (N-65-19716)
COSMIC MESONS
detection and measurement at sea level, cubical telescope for, 20: 17311
intensity variations from atmospheric disturbances, evaluation of, 20: 17311
COSMIC MESONS (μ)
interactions with cosmic neutrinos, (T), 20: 17366(T)
COSMIC NEUTRINOS
interactions with cosmic mesons (μ), (T), 20: 17366(T)
COSMIC NEUTRONS
research on high-energy, review of, 20: 17323
COSMIC NUCLEONS
attenuation in atmosphere, altitude effects on, (E), 20: 17651(R) (AD-612192)
propagation through atmosphere, (T), 20: 17651(R) (AD-612192)
COSMIC PARTICLES
energy spectrum of nuclei in primary, (E), 20: 17315
synchrotron radiation from charged, (T), 20: 17314
COSMIC PHOTONS
detection and measurement of primary, background estimates for, 20: 17322
interactions with electrons, (T), 20: 17309 (N-65-19716)
COSMIC PROTONS
distribution of solar, diffusion effects in, (T), 20: 17228 (N-65-18275)
energy and intensity spectrum of low-energy primary, (E), 20: 17308 (N-65-18274)
flux modulation at low rigidities, (T), 20: 17312(T)
intensity variations of low-energy, 20: 17310(T) (AD-623948)
synchrotron radiation from primary, (T), 20: 17314
COSMIC RADIATION
absorption of high-energy gamma, by thermal microwave field, (T), 20: 17319
abundances of nuclei with $Z \geq 4$ in primary, (E), 20: 17321
detection and measurement at sea level, cubical telescope for, 20: 17311
detection and measurement of microwave black-body, (E), 20: 17317
detection and measurement of high-energy gamma, (E), 20: 17320
detection and measurement at high altitudes, secondary-component effects on, 20: 17322
detection and measurement of, Mariner C instrumentation for, 20: 16822 (N-65-19927)
detection and measurement of x, using gas proportional counters, 20: 16901
energy of primary, from secondary angular distribution and momentum, (T), 20: 17316
energy spectrum of nuclei in primary, (E), 20: 17315
intensity gradient and variation in interplanetary space, (T), 20: 17312(T)
intensity measurements on, in equatorial, mid-latitude, and plateau regions, (E), 20: 17651(R) (AD-612192)
intensity of, effects of solar flares on, (E), 20: 17313(T)
motion in galaxy, models for, (T), 20: 17324
properties of, 20: 16745
quark production in, (T), 20: 17411
reactions in atmosphere, production of radioisotopes by, 20: 16689
research on, (E/T), 20: 17651(R) (AD-612192)
sources of x, 20: 17248
spectra in galaxy, (T), 20: 17312(T)
transport of, spectral theory for stationary operator for, 20: 17658
COSMIC SHOWERS
energy estimate for, secondary angular distribution and momentum for primary, (T), 20: 17316
COSMOLOGY
evolution of universe, review of, 20: 17231
evolution of universe, (T), 20: 17243
evolution of universe, (T), 20: 17245
model of universe, (T), 20: 17241
radiation emission and propagation from quasi-stellar radio sources, (T), 20: 17242
universe in, origin of Lorentz group for, 20: 17563
COULOMETRY
electrodes for controlled-potential, 20: 16390
tracer use in, 20: 16335(R) (NBS-TN-276)
CRITICAL ASSEMBLIES
critical experiments for, consistency in analysis of high-buckling, (T), 20: 18065
criticality of enriched uranium, configuration effects on, 20: 18020(R) (ORNL-3900, pp 2-81)
criticality of homogeneous uranium–water systems, (E/T), 20: 18053
criticality of uranium-235–enriched fast, Monte Carlo analysis of, 20: 18057
design and research programs using, at Saclay, 20: 18181
neutron disadvantage factor calculations in hydrogeneous-moderator, (T), 20: 18049 (RT/FI(65)-42)
neutron reaction probabilities in, variational principle for ratios of, (T), 20: 18059
CRITICALITY STUDIES
of aqueous solutions and fuel elements, 20: 18020(R) (ORNL-3900, pp 2-81)
of reflected enriched-uranium assemblies, 20: 16721 (AWRE-NR-1/66)
CROSS SECTIONS
calculation of compound nuclear, computer program for, 20: 17672 (AERE-R-5053)
CRUSTACEA
radioinduced muscle inactivation in, combined with polarization microscopy for contraction studies, uv, 20: 16259
CRYOGENICS
testing of couplings for hydrogen transfer lines, 20: 16588 (LA-3454)
use in electronic equipment, power-loss reduction from, 20: 17603
CRYSTALLOGRAPHY
crystal Fermi surfaces, computer analysis of, 20: 17973 (IS-1106)
CRYSTALS
ion reactions with ordered lattices of, channeling effects in, (E), 20: 17158(R) (ORNL-3900, pp 82-149)
lists of available and desired ultrapure inorganic, for research, 20: 16417 (ORNL-RMIC-4)
neutron magnetic scattering by nonlocalized Mott and Dyknan-Pekar excitons in, (T), 20: 18006
neutron scattering by, phase determination from, 20: 17041
properties of, computer analysis of Fermi surfaces, 20: 17973 (IS-1106)
radiation scattering on, change of nuclear resonance parameters by, 20: 18015
x-ray diffraction analysis of, intensity measurements in, 20: 18017
CULTURE MEDIA
arginine content in, effects on KB cells of, 20: 16258
effects of serum content and temperature of, on growth of mammalian cells, 20: 16298
CURIUM
dissociation in hydrochloric acid–bis(2-ethylhexyl) phosphate–toluene system, constants for, 20: 16404
production, 20: 16543
separation from irradiated thorium, method for, 20: 16359
separation from irradiated fuel elements by ion exchange and solvent extraction, 20: 16582
CURIUM PHOSPHATES
crystal structure, 20: 16470

CURRENT REGULATORS
design for magnets at Princeton Synchrotron, 20: 17205 (CONF-650922, pp 817-22)
CYCLOHEXANE
effects on hydrogen yields from gamma radiolysis of water vapor, 20: 16536
properties as chemical dosimeter, 20: 16518
radiolysis of, nitrous oxide as electron scavenger in, 20: 16515
tritium exchange with tritiated ethyl malonate, effects of catalysts on, 20: 16492
benzene–cyclohexane–cyclohexene, radiolysis of, nitrous oxide as electron scavenger in, 20: 16515
cyclohexane–cyclohexene, properties as chemical dosimeter, 20: 16518
CYCLOHEXANONES
reduction by borohydride ions, secondary deuterium isotope effects in, 20: 16555
CYCLOHEXENE
preparation of tritium-labeled, by tritioboration of 1-(*N*-piperidino)-cyclohexene, 20: 16549
radiolysis of, nitrous oxide as electron scavenger in, 20: 16515
reactions with deuterium, catalyzed by chromium oxide gel, 20: 16487
benzene–cyclohexane–cyclohexene, radiolysis of, nitrous oxide as electron scavenger in, 20: 16515
cyclohexane–cyclohexene, properties as chemical dosimeter, 20: 16518
CYCLOOCTA-1,3,6-TRIENE
isomerization of, deuterium effects on thermal, 20: 16503
CYCLONE SEPARATORS
design for removal of carbon black from high-speed printers, 20: 16740(R) (UCRL-14534, pp 50-3)
CYCLOPENTANONE
reduction by borohydride ions, secondary deuterium isotope effects in, 20: 16555
CYCLOTRON RADIATION
emission by cosmic electrons, (T), 20: 17309 (N-65-19716)
emission by cosmic charged particles, (T), 20: 17314
emission from quasi-stellar radio sources, (T), 20: 17242
emission from rare gas plasma, negative absorption effects on, (E), 20: 17921
emission from thermonuclear reactors, (T), 20: 17929
CYCLOTRONS
design of separated-orbit, 20: 17158(R) (ORNL-3900, pp 82-149)
design of 45-Mev proton, at Milan University, 20: 17214
ion sources for, development of deformed, 20: 17207 (INSJ-93)
ion sources for, negative hydrogen, 20: 17224
magnetic field distribution in, correction of radial, 20: 17187 (CONF-650922, pp 377-89)
magnetic field measurements in, automatic data logging and processing system for, 20: 17188 (CONF-650922, pp 415-20)
magnetic fields in, measurement using Hall effect, 20: 17191 (CONF-650922, pp 447-55)
magnetic median plane in, determination using Hall effect, 20: 17189 (CONF-650922, pp 421-7)
CYLINDERS
fabrication of Nb_3Sn, using concentric diffusion layers, 20: 17649
fissile-material critical mass in water-reflected, distribution effects on, (T), 20: 18062
fixation of radioactive materials in hollow and solid, calculations of transient temperatures for, 20: 18155 (BNWL-157)
magnetohydrodynamic natural convection in vertical, (T), 20: 17516
temperatures in finite hollow, from asymmetrical internal heat source, 20: 16934
CYSTEIC ACID
radiation chemistry of, neutron, 20: 16540
CYSTEINE
radiation chemistry of, neutron, 20: 16540
radiosensitivity effects on growth inhibition by rat serum, x, 20: 16208
CYSTINE
radiation chemistry of, neutron, 20: 16540
CYTIDINE
radiation effects on, ESR studies of gamma, 20: 16541
CYTOLOGY
radiation effects on cells in culture, 20: 16292
radiation effects on phagocytosis of lymphocytes in rat thymus, 20: 16293

D

DATA RECORDING SYSTEMS
design for EAS detection equipment, 20: 16873
design for experiments, engineering drawings for, 20: 16597
design for measurement of cycloiron magnetic fields, 20: 17188 (CONF-650922, pp 415-20)
design of automatic, for meteorological studies at reactor sites, 20: 16710
development and uses at Risö, 20: 18174(R) (NP-15771)
electronic equipment in, description of, 20: 16335(R) (NBS-TN-276)
for production of temperature-vs-thermocouple-emf tables, 20: 17158(R) (ORNL-3900, pp 82-149)
DATA TABULATIONS
antiferromagnetic materials, properties of, 20: 17972 (IAE-942)
boson reactions with fermions, structure of observables for, 20: 17770
electron and positron scattering by bismuth and cobalt, cross sections and electron-positron ratios for, 20: 17785
electron pair-production cross sections for light elements, 20: 17754
erbium energy levels, 20: 17261
geomagnetic equatorial Dst hourly values for IGY, 20: 17543
geomagnetic quiet-day variations during IGY, 20: 17545
geomagnetic ring current variations during IGY, 20: 17544
hydrogen photoionization cross sections, (T), 20: 17251 (IAE-873)
neutron elastic scattering by carbon-12 and oxygen-16, coefficients for, 20: 17767
neutron filter effective cutoff energies, (T), 20: 17663
neutron slowing down in iron-water mixtures, Legendre scattering coefficients for fission, 20: 17660
nuclear deformation parameters and E2 transition probabilities, 20: 17730
on mass transport in deep-bed copper oxide tests with carbon monoxide and hydrogen, 20: 16556(R) (ORNL-TM-1090)
samarium compound nuclei decay cross sections and excitation functions, 20: 17784
thorium oxide band-spectrum term values, 20: 17254
thulium-170 energy levels, 20: 17782
DECAY SERIES
alpha tracks in biotite from natural, parent determination in, 20: 16667
DECONTAMINATING SOLUTIONS
efficiency of, for ultrasonic cleaning of cobalt-60 from Duralumin and steel-3, 20: 16767
DECONTAMINATION
systems for, high-purity de-ionized water, 20: 16590 (SC-TM-66-49)
DEER
cesium-137 content in Colorado mule, effects of foliage contamination and food habits on, 20: 16723 (COO-1156-11)
strontium-90 content in antlers and bones of Colorado mule, 20: 16724 (COO-1156-12)
DEHYDROGENASES
genetic control of lactate, 20: 16172(R) (NYO-2194-1)
DENMARK
activities in International Atomic Energy Agency and regional cooperation in Europe, 20: 18174(R) (NP-15771)
DENSITOMETERS
development of radiometric, 20: 18182
DENSITY
determination in randomly packed pebble beds, 20: 18018 (CONF-651101-73)
measurement in liquids, automated equipment for, engineering drawings of, 20: 16801
DEUTERIOÖRGANIC COMPOUNDS
use for following hydrogen in biological systems, 20: 16165
DEUTERIUM
abundance in primeval universe, (T), 20: 17245
abundance of primeval, (T), 20: 17245
abundance variations in polar caps, 20: 16686
content in hydrothermal fluids responsible for lead–zinc deposits in Mexico, 20: 16634
content in solar wind, system for determining, 20: 17307 (CONF-651001-34)
deuteron reactions (d,n) with, neutron production for activation analysis in, 20: 16332 (GA-6691)
deuteron reactions (d,n) at 1.5 and 1.9 Mev, polarization from, (E), 20: 16876
deuteron reactions (d,p) at 400, 850, and 1280 kev, triplet-singlet transitions from polarization effects on, (E), 20: 17750
effects on dissociation of acetic acid in aqueous solutions at 0 to 50°C, 20: 16458
effects on electron relaxation rates in solids, theory of, 20: 18016
effects on gas-phase decomposition of oxalic acid, 20: 16455
effects on infrared and Raman spectra of imidazole, 20: 16500
effects on infrared and Raman spectra of imidazole, 20: 16499
effects on ketone reduction by borohydride ions, secondary, 20: 16555
effects on morphology of organisms, 20: 16165
effects on thermal isomerization of cycloocta-1,3,6-triene, 20: 16503
exchange between hydrogen and liquid ammonia, catalytic effects of alkaline amides on, 20: 16444
exchange with hydrogen in methane, catalytic effects of gold–palladium alloy on, 20: 16457
fission-fragment energy degradation in, (E), 20: 17821
gamma reactions (γ,n) in moderators of, (E/T), 20: 17830
incorporation in diphenyl methane, 20: 16498
incorporation in methyl groups of organic compounds, 20: 16501

isotope effects on europium chelate lasers, 20: 16781
isotopic exchange with water, catalytic effects of ruthenium chloride on, 20: 16423
meson (π^-) capture by, probabilities for fine-structure-level, (T), 20: 17278
production by high-energy solar particles, 20: 17234
reactions with benzene, cyclohexene, and toluene, catalyzed by chromium oxide gel, 20: 16487
scattering of molecules of, by helium atoms, (E), 20: 17293
separation from hydrogen in crude-oil fractionation, 20: 16475
spectra of, bands from lowest excited states in vibrational, 20: 16451

DEUTERIUM IONS
detection and measurement in solar wind, system for, 20: 17307 (CONF-651001-34)

DEUTERIUM SYSTEMS
D–H, thermal diffusion in, 20: 16468

DEUTERON BEAMS
polarization parameters for, (T), 20: 17805

DEUTERONS
form factors of, electromagnetic, (E), 20: 17349 (LAL-1155)
interactions with electrons, CP-invariance breakdown in, (T), 20: 17341 (JINR-P-2504)
interactions with electrons, form factors from, (E), 20: 17349 (LAL-1155)
interactions with protons at 1 to 10 Bev, elastic, (E), 20: 17363(T)
interactions with electrons, radiative corrections for disintegration in, (T), 20: 17370
interactions with hyperons (Ξ^-) at low energies, hyperon (Λ) production in, (T), 20: 17389
interactions with photons, dispersion theory for magnetic-dipole splitting in, 20: 17408
production in neutron interactions with protons, 20: 17413
reactions (d,α) with boron-10 at 7.5 Mev, isotopic spin rule violation in beryllium-8 levels from, (E), 20: 17759
reactions (d,d′) and (d,p) with carbon-12 at 15 Mev, recoils from, (E), 20: 17820
reactions (d,γ), (d,n), (d,2n), and (d,p) with nuclei, production cross sections for, 20: 16508(R) (NYO-2771-13)
reactions (d,γ) and (d,2n) with nuclei, compound-nucleus-statistical mechanisms in, 20: 16508(R) (NYO-2771-13)
reactions (d,n) with nuclei, amplitudes for, (T), 20: 17704
reactions (d,n) with nuclei for neutron production for activation analysis, 20: 16332 (GA-6691)
reactions (d,n) with molybdenum-92 and zirconium-94 at 15 Mev, calculated isomeric yield ratios for, 20: 16508(R) (NYO-2771-13)
reactions (d,n) with deuterium at 1.5 and 1.9 Mev, polarization from, (E), 20: 16876
reactions (d,n) with beryllium-9 at 600 kev, boron-10 level structure from, (E), 20: 17797
reactions (d,n) with tritium at 100 kev, tensor and vector polarization effects on, (E), 20: 17749
reactions (d,pf) with uranium isotopes at 13 Mev, fragment-proton coincidences in, (E), 20: 17844
reactions (d,pf) with uranium-234, fragment angular, energy, and mass distributions from, (E), 20: 17865
reactions (d,pγ) with boron-10 and carbon-11 at 420 kev and 13.5 Mev, gamma polarization in, (E/T), 20: 17726
reactions (d,p) at 15 Mev, isomeric yield ratios for, 20: 16508(R) (NYO-2771-13)
reactions (d,p) with zirconium-90 at 3.5 to 5.5 Mev, angular distributions from, (T), 20: 17691 (ORNL-TM-1235)
reactions (d,p) with magnesium-24 and tungsten-182 near 10 Mev, angular distributions from, (T), 20: 17692 (ORNL-TM-1414)
reactions (d,p) with thulium-169 at 12 Mev, thulium-170 levels from, (E), 20: 17782
reactions (d,p) with helium-3 at 310 to 2935 kev, tensor and vector polarization effects on, (E), 20: 17749
reactions (d,p) with deuterium at 400, 850, and 1280 kev, triplet-singlet transitions from polarization effects on, (E), 20: 17750
reactions (d,p) with oxygen-18 at 12 Mev, oxygen-19 levels from, (E), 20: 17758
reactions (d,p) with helium-3, asymmetry and polarization relation in structure of, (T), 20: 17770
reactions (d,p) with titanium-46 at 7.0 Mev, titanium-47 energy levels from, (E), 20: 17776
reactions (d,2n) with plutonium-242 at 7 to 12 Mev, isomeric yield ratios from, (E), 20: 17857
scattering by nuclei, polarization parameters from double elastic, (T), 20: 17805
sputtering on metals at 30 kev, yields from, 20: 17892(R) (ORNL-3908, pp 149-53)

DIABETES
incidence in residents of Hiroshima exposed to radiation from atomic bomb, 20: 16254

DIAMONDS
electron reactions at 4.8 Bev, coherent bremsstrahlung from, (E), 20: 17679 (DESY-65/15)

DIET
cesium-137 content in U. S., 1965, 20: 16662(R) (HASL-165)
effects on DNA synthesis in weanling rat kidneys, 20: 16158 (AD-628360)
strontium-90 content in U. S., 1960 to 1965, 20: 16662(R) (HASL-165)

DIFFERENTIAL EQUATIONS
numerical solution of non-Fredholm, matrix-inversion, 20: 16936

DIFFERENTIAL THERMAL ANALYSIS
method for studying bound water in alumina, beryllia, and silica during dehydration, 20: 16413 (CEA-R-2703)

DIFFUSION
method for measuring inter-, in metals by gamma radiation attenuation, 20: 17111

DIODES
radiation effects on HPA-1002 and IN1616, gamma and neutron, 20: 16908 (N-65-17526)
radiation effects on IN540 and IN649, gamma and neutron, 20: 16909 (N-65-18250)
radiation effects on type SIN752A Zener, gamma and neutron, 20: 16909 (N-65-18250)

DIOXANE
dioxane–H_2O, effects on equilibrium in keto-enol tautomerism of 2,4-pentanedione, 20: 16416(R) (NYO-906-68)
dioxane–H_2O, effects on isotopic exchange between elementary iodine and 1-phenyl-2,3-dimethyl-4-iodopyrazolone, 20: 16502

DIRECT ENERGY CONVERSION DEVICES
bibliography, 20: 17325 (AED-C-15-09)
bibliography, 20: 17326 (AED-C-15-10)
design of dual-electrode system for gamma conversion by way of Compton electrons, 20: 17331

DISEASES
radiotherapy of skin, effects on bones, 20: 16210

DITHIZONE
properties of cobalt-60-labeled, for determining VYNS target film thickness, 20: 16508(R) (NYO-2771-13)

DODECYLAMINE
solvent properties for neptunium, 20: 16582

DODEWAARD POWER REACTOR
description, 20: 18103

DOGS
bone blood flow in, determination and factors affecting, 20: 16192
radiation effects on copper and zinc content and enzyme activity in blood serum of, 20: 16222 (AFWL-TR-65-112)
radiation effects on behavior in, after chronic enteral administration of, strontium-90, β, 20: 16266
radiation injuries in, use of split-dose technique for evaluating recovery from, 20: 16216 (AD-628791)
radiation sickness in, characteristics of polonium-210-induced, 20: 16268
radioinduced bone fractures in, plutonium-239, radium-226, -228, and strontium-90, 20: 16253
radioisotope excretion in urine of, pathway for, 20: 16160 (UCRL-14739 (Pt.2))
uranium oxide content in lungs of, after inhalation, 20: 16184

DOMINIC OPERATION
cadmium-109 distribution in atmosphere from Starfish Burst, 20: 16662(R) (HASL-165)

DOSIMETERS
calibration of, neutron sources for, 20: 16830(R) (UCRL-14534, pp 8-12)
design and performance of photoluminescent, 20: 16837
design of alarm, for personnel, 20: 16831(R) (UCRL-14534, pp 28-31)
development and performance of lithium fluoride, 20: 16829(R) (UCRL-14534, pp 1-7)
development for personnel monitoring, review on, 20: 16827 (SZS-9(1965))
development of solid-state, for medical uses, 20: 16855
evaluation of chemical, for irradiations at high dose rates, 20: 16517
evaluation of chemical, for irradiations at high dose rates, 20: 16518
performance of alanine and glass rod, in measurement of protons, 20: 16283
performance of liquid-emulsion, for γ and x radiations, 20: 16845
performance of scintillator-film combination, for fast neutrons, 20: 16861
reproducibility of glass, washing technique for improved, 20: 16847

DOUNREAY FAST REACTOR
use for materials testing, 20: 18092 (TRG-Report-1039)

DROSOPHILA
radioinduced mutations in, effects of sex on, 20: 16229(R) (NYO-1472-1)
suppressor genes in, action of, 20: 16229(R) (NYO-1472-1)

DRUGS
effectiveness of metoclopramide as emetic in chemo- and radiotherapy,

20: 16163
effects of, combined with beta or x radiation on polycythemia, complications from, 20: 16233
DUSTS
analysis for alpha and beta sources, radiochemical methods for, 20: 16337 (RMO-3001(Rev.1)(Suppl.))
analysis for uranium, methods for, 20: 16337 (RMO-3001(Rev.1)(Suppl.))
radon-220 measurement in, monitor for, 20: 16842
removal of carbon, from high-speed printers using cyclone scrubbers, 20: 16740(R) (UCRL-14534, pp 50-3)
sorptive properties of multiclone, from gasification of coke, for cesium, strontium, and yttrium, 20: 18170
DYES
uses for radiation dosimetry, 20: 16521
DYSPROSIUM
analysis for yttrium using bis(2-ethylhexyl) phosphate, chromatographic, 20: 16385
determination by neutron activation and ion-exchange chromatography, 20: 16363
magnetic structure of, determination using Kerr effect, 20: 17974 (IS-T-63)
magnetostriction in antiferromagnetic, ferromagnetic, and paramagnetic regions, (E), 20: 18012
performance of foils of, in neutron radiography, 20: 16619
solubility in gold, solid, 20: 17016 (IS-1175)
solvent properties for magnesium, solid, 20: 17016 (IS-1175)
DYSPROSIUM ALLOYS
Dy–Fe, crystal structure of Dy_6Fe_{23} in, 20: 17096(T)
Dy–Hg, crystal structure of $DyHg_3$, 20: 17060
Dy–Mn, crystal structure of Dy_6Mn_{23} in, 20: 17096(T)
Dy–Tl, crystal structure of $DyTl_3$, 20: 17060
DYSPROSIUM COMPLEXES
with phenanthroline, infrared spectra of, 20: 16436
with 2,2′-bipyridyl, infrared spectra of, 20: 16437
DYSPROSIUM HYDRIDES
properties and structure, 20: 16453
DYSPROSIUM IONS
nuclear quadrupolar interactions in lanthanum trichloride, Zeeman-field dependent, 20: 18008
DYSPROSIUM ISOTOPES Dy-159
energy levels from holmium-159 decay, parity and spin of, (E), 20: 17685 (JINR-P-2497)
DYSPROSIUM ISOTOPES Dy-161
Mössbauer effect in gadolinium, (E), 20: 17988(T)
DYSPROSIUM ISOTOPES Dy-164
neutron capture by, conversion-electron spectrum from thermal, 20: 17822
DYSPROSIUM OXIDES
determination in thorium oxide by emission spectroscopy, 20: 16393
CaO–Dy_2O_3, phase studies, 20: 17087
Dy_2O_3–ReO_2, phase studies at 1130 and 1300°C, 20: 17007(R) (AD-627468)
DYSPROSIUM SULFIDES
Dy_2S_3–EuS, compound formation in, 20: 16431
Dy_2S_3–SmS, compound formation in, 20: 16431
Dy_2S_3–YbS, compound formation in, 20: 16431

E

EARTH
magnetism of interior of, conference on, 20: 17550
magnetohydrodynamic wake of, observation using IMP-1, 20: 17235(T)
rare earths abundance pattern in crust of, comparison with chondrites, 20: 17233
rubidium–strontium ratio in, differentiation of mantle by studying, 20: 16711(R) (MIT-1381-13)
ECOLOGY
research programs on freshwater and terrestrial, 20: 16159(R) (ORNL-3900, pp 150-81)
EGGS
biochemical activity of yolk and sac membrane in chicken, 20: 16172(R) (NYO-2194-1)
radiation effects on protein synthesis in sea urchin, 20: 16160 (UCRL-14739(Pt.2))
radiation processing of, evaluation of effects on flavor, 20: 16923
EINSTEINIUM
production, 20: 16543
ELECTRETS
bibliography on, 20: 17971 (AD-299256)
ELECTRIC ARC FURNACES
design for melting and casting heat-resisting alloys, 20: 16965
ELECTRIC ARCS
energy transfer in and from, spectroscopic studies of, 20: 17901
flute stabilization in deuterium-fed, (E/T), 20: 17158(R) (ORNL-3900, pp 82-149)
ion heating in, excitation, (E), 20: 17900
operation mode transitions in, with transpiration cooled anode, (E), 20: 17514
performance of hydrogen–nitrogen arc jets for propulsion, 20: 16629
structure in flowing gases at low pressures, (E), 20: 17517
structure of traverse, in supersonic plasma jet, (E), 20: 17904
ELECTRIC CONDENSERS
radiation effects on, review of, 20: 16911
ELECTRIC CONDUCTORS
electric current flow in weakly deformed axially symmetric, with strong Hall effect, (T), 20: 17164
forces on, in traveling magnetic field of cylindrical inductor, (T), 20: 17162
ELECTRIC DISCHARGE
ion excitation energies and densities in, (E), 20: 17508 (ARL-65-246)
light emission from theta-pinch, in dense gases, (E), 20: 17523
plasma diffusion across magnetic fields in r-f, anomalous, (E), 20: 17954
plasma production by, microwave measurements of electron density in, (E), 20: 17510 (IPP-3/25)
plasma production by h-f, properties of, (E/T), 20: 17879 (LRP-19/65)
ELECTRIC FIELDS
book: *Mathematical Models for Computing Electric and Magnetic Fields*, 20: 17161
distributions in plasma, (T), 20: 17896
effects of crossed magnetic and, on plasma, (E), 20: 17943
hydrogen atom radiative transitions in external, anisotropy of, (T), 20: 17282
plasma instability in strong h-f, collisionless, (T), 20: 17948
ELECTRIC GENERATORS
use of acyclic, as power supplies for pulsed magnets, 20: 16772 (CONF-650922, pp 769-75)
ELECTRIC INSULATORS
radiation effects on, review of, 20: 16911
ELECTRIC PROBES
development for studying density distribution of randomly packed bed, 20: 18018 (CONF-651101-73)
ion collection in Bayard-Alpert gage, factor for, (T), 20: 16787
ion sheath effects on admittance of r-f, in plasma, (T), 20: 17552
performance of Langmuir, for plasma diagnostics, 20: 17899
properties of Langmuir, (T), 20: 17889(R) (ORNL-3908, pp 52-89)
ELECTRICITY
production by conversion of nuclear energy, bibliography on, 20: 17325 (AED-C-15-09)
production by conversion of nuclear energy, bibliography on, 20: 17326 (AED-C-15-10)
production of, role of nuclear energy in future, 20: 18082 (AECL-2390)
ELECTRODES
development of carbon, for amperometry, potentiometry, and voltammetry, 20: 17158(R) (ORNL-3900, pp 82-149)
use of rhenium, in nuclear-thermionic cells, 20: 17327 (N-65-19264)
ELECTRODYNAMICS
formalism for homogeneous anisotropic and dispersive medium, 20: 17166
ELECTROLYTES
radiation effects on oxidation-reduction potential of, neutron, 20: 17118(R) (EURAEC-1564)
ELECTROMAGNETIC FIELDS
book: *Mathematical Models for Computing Electric and Magnetic Fields*, 20: 17161
charged particle motion in permanent, Fermat principle for, (T), 20: 16821 (LAL-1151)
induction from arbitrary sources, equations for strength of, 20: 17166
interaction potential energy in relativity theory, 20: 17574
interactions in air plasma, heterodyne generation from, (E/T), 20: 17905
interactions with gravitational fields, 20: 17580
ELECTROMAGNETIC LENSES
aberration properties of magnet systems for, computer program for third-order, 20: 17220
aberrations in, space-charge effects on coefficents for, 20: 16784
charged-particle trajectories in, analog computer techniques for determining, 20: 17906
design for beam transport systems of CERN proton synchrotron, 20: 17183 (CONF-650922, pp 218-38)
design for focusing of meson (π) beams, 20: 17198 (CONF-650922, pp 650-6)
focusing image characteristics for atomic beams, approximations for, (T), 20: 17225
magnetic fields in quadrupole, method for measuring, 20: 17190 (CONF-650922, pp 431-46)
performance of superconducting hollow cylinders for electron optics, 20: 17631
ELECTROMAGNETIC WAVES

diffraction by plasma, (T), 20: 17877 (IPP-6/44)
emission from charged particles passing through semiconductors, properties of, (T), 20: 17494
emission from electron beams, instability with anomalous Doppler effect in, (T), 20: 17533
emission from high-temperature and -density plasmas, 20: 17944
interactions with turbulent plasma, (T), 20: 17958
propagation in nonuniform plasma, (T), 20: 17913
propagation in plasma, 20: 17537 (JPLAI/LS-641)
propagation in plasma, review on theory and uses for, 20: 17911
propagation in semiconductor plasma in stationary electric fields, (T), 20: 18013
reactions with neutral and charged bound systems, ionization by, (T), 20: 17284
reflection and refraction in homogeneous plasma, in magnetic fields, (T), 20: 17915
scattering by plasma, Raman, (E/T), 20: 17923(T)

ELECTRON BEAMS

effects on electric properties of indium–antimony alloys, 20: 17150(T)
effects on electronic energy levels in p-type germanium, 20: 17142
effects on internal friction of copper, 20: 17135
effects on optical absorption spectra of lithium fluoride, 20: 17143
effects on rat skin, continuous- and pulsed-exposure, 20: 16269
effects on structure of solar cells, 20: 16910 (N-65-18448)
effects on tensile properties of tungsten by heating with low-energy, 20: 17073
electromagnetic wave excitation by, instability with anomalous Doppler effect in one-dimensional, (T), 20: 17533
focusing by superconducting hollow cylinders, 20: 17631
interactions with nonisothermal plasma, 20: 17951
interactions with plasma, heating mechanisms in, (E/T), 20: 17158(R) (ORNL-3900, pp 82-149)
interactions with plasma, properties of, (E), 20: 17889(R) (ORNL-3908, pp 52-89)
interactions with plasma, diagnostics from, (E/T), 20: 17893(R) (SU-IPR-44)
interactions with plasma, diagnostics from, (E/T), 20: 17894(R) (SU-IPR-47)
magnet system for 90° bending of 100-Mev, design of, 20: 17200 (CONF-650922, pp 715-22)
noise fluctuations in, effects of beam length and magnetic field on, (T), 20: 17505
polarization in storage ring magnetic fields, quantum effects on, (T), 20: 17689 (NP-15783)
production of polarized, by spin exchange collisions, 20: 17273

ELECTRON CAPTURE CROSS SECTIONS

capture cross sections determination using swarm-beam methods, 20: 16159(R) (ORNL-3900, pp 150-81)

ELECTRON MICROSCOPES

performance of Phillips EM 200, 20: 17158(R) (ORNL-3900, pp 82-149)

ELECTRON MICROSCOPY

method for determining trace metals in cells and cellular components, 20: 16160 (UCRL-14739(Pt.2))
techniques for, status, 20: 16160 (UCRL-14739(Pt.2))

ELECTRON PAIRS

production cross sections for, in photon-electron interactions, 20: 17354
production in Coulomb field of light elements, total cross sections for high-energy, (T), 20: 17754
production of, heavy electron analysis for, (T), 20: 17338 (DESY-65/10)

ELECTRON SCATTERING CROSS SECTIONS

measurement of, magnetic spectrometer for, 20: 16808 (CONF-650922, pp 154-63)

ELECTRON TUBES

performance in semiconductor detector preamplifiers, 20: 16871
performance of cold-cathode magnetron gages, pressure response curves for, 20: 16788
radiation effects on, review of, 20: 16911

ELECTRONIC EQUIPMENT

coupling of oscillators to oscilloscopes, method of, 20: 16776 (EGG-1183-1156)
description of, for handling data from pulse height analyzers, 20: 16335(R) (NBS-TN-276)
design of data-processing, for multichannel pulse-height analyzers, 20: 16817 (JUL-270-RB)
electric interference in reactor instrumentation, 20: 18030
performance and selection of, for use in space vehicles, 20: 16944 (NASA-SP-3025)
power loss reduction for, use of low temperatures for, 20: 17603

ELECTRONS

acceleration of plasma, method and device for, 20: 17960(P)
bremsstrahlung emission in successive interactions of, (T), 20: 17418
density in axis of theta pinch plasma, rapid oscillations in, (E), 20: 17918
density in discharge and shock produced plasmas, microwave measurements of, (E), 20: 17510 (IPP-3/25)
density in z-pinch plasma, microwave reflection probe for measuring, 20: 17876 (IPP-1/37)
detection and measurement of secondary, method for, 20: 17168
diffusion in infinite plane low-voltage arc plasma, coefficient for, (T), 20: 17907
diffusion in ionized gases, second-order, (T), 20: 17529
distribution in lower regions of outer radiation belt, (E), 20: 17538 (N-65-17609)
dosimetry of, using cyanides of triphenylmethane dyes, 20: 16521
effects on defects in silicon solar cells, 20: 17125 (NASA-CR-404)
effects on dimensional stability of high-purity single-crystal germanium, (E), 20: 17136
effects on DNA synthesis in mammalian cells, 20: 16230(R) (TID-22644)
effects on electric conductivity of fused silica, 20: 17133
effects on electric conductivity and dimensional stability of *n*- and *p*-type, germanium, 20: 17145
effects on electronic components in space, review of, 20: 16911
effects on *p*-type germanium, electric conductivity and Hall effect from, 20: 17144
effects on potassium acid fluoride, EPR spectra of, 20: 17976(R) (NYO-2047-36, App.1)
electric dipole moments of, in intermediate vector boson theory, 20: 17372
emission by metals in cesium vapor, thermionic, (E), 20: 17333
emission from metals in cesium-fluorine vapors, thermionic, (T), 20: 17334
emission from surfaces of strontium tungstate in vacuum, thermionic, (E), 20: 17335
emission of, from metals, photon-induced, 20: 17984
energy spectra from hydrogen ion reactions with gases, (E), 20: 17292
gravitational force on free, measurement of, 20: 17167
intensity in outer radiation belt, 20: 17310(T) (AD-623948)
interactions in solids, normal-Fermi-liquid theory for, 20: 17993
interactions in uniformly loaded waveguides, Cherenkov radiation from, (T), 20: 17485
interactions of, gauge transformations for, (T), 20: 17446
interactions with photons, line-profile effects in stimulated beam, (T), 20: 17464
interactions with gravitons and photons, Reggeization in field theory for, 20: 17476
interactions with electrons and positrons, polarization effects in, (T), 20: 17489
interactions with ion-acoustic oscillations in plasma, quasilinear theory for, 20: 17950
interactions with deuterons, CP-invariance breakdown in, (T), 20: 17341 (JINR-P-2504)
interactions with deuterons, form factors from, (E), 20: 17349 (LAL-1155)
interactions with photons, cross sections for pair production in, (T), 20: 17354
interactions with particles, radiative corrections for, (T), 20: 17370
interactions with deuterons, radiative corrections for disintegration in, (T), 20: 17370
interactions with nucleons, inelastic, (T), 20: 17399
magnetic moment of Dirac particles in potential wells, (T), 20: 17431 (JINR-P-2569)
motion in plasma, cyclotron echoes from, (T), 20: 17933
precipitation in auroral zone, spatial and temporal characteristics of, 20: 17557
production of secondary, in fission-fragment reactions with metal foils, 20: 17168
reactions with aluminum-27, absolute differential cross section for bremsstrahlung production in, (E/T), 20: 17798
reactions with atoms at high energies, cross sections for excitation and ionization in, (T), 20: 17270
reactions with atoms and molecules, conference on, 20: 17288
reactions with cesium, ionization cross sections for, (E), 20: 17287
reactions with diamonds at 4.8 Bev, coherent bremsstrahlung from, (E), 20: 17679 (DESY-65/15)
reactions with helium, Born approximation of cross sections for, 20: 17258
reactions with polyatomic molecules, 20: 16159(R) (ORNL-3900, pp 150-81)
relaxation in solids, theory of, 20: 18016
scattering by anthracene, cesium iodides, and plastics, response functions for monoenergetic, (E), 20: 16867
scattering by atoms, cross sections for, (T), 20: 17286
scattering by atoms and molecules, resonances in, (T), 20: 17289
scattering by atoms in uniform magnetic fields, (T), 20: 17291
scattering by bismuth at 150 and 300 Mev, cross sections for, (E), 20: 17785
scattering by carbon-12 and oxygen-16, angular distributions for giant

resonance decay from inelastic, (T), 20: 17757
scattering by cobalt at 150 Mev, cross sections for, (E), 20: 17785
scattering by hydrogen atoms, variational principle for elastic, (T), 20: 17271
scattering by lithium-7 at high energies, kinematics of, (T), 20: 17799
scattering by nuclei, excitation of analog states by inelastic, (E), 20: 17651(R) (AD-612192)
scattering by nuclei, electron and nucleon angular distributions for giant resonance decay from inelastic, (T), 20: 17757
scattering on boron-10 and -11 at 32 to 57 Mev, multipolarity and width levels from inelastic, (E), 20: 17813
scavenging in hydrocarbon radiolysis using nitrous oxide, 20: 16515
thermodynamic properties of gas of, representation of interactions in collective variables for calculating, 20: 17530
track density of delta, from proton and meson (π) reactions in emulsions, (E), 20: 17358
transfer mechanisms in tetravalent terbium compounds, 20: 16433
transmission in graphite at 53 Mev, energy loss and half width from, 20: 17970
transmission in solids at 3 ev, mean free path of, 20: 16159(R) (ORNL-3900, pp 150-81)
velocity distribution in magnetosphere, determination from whistler attenuation, (T), 20: 17558

ELECTROPHORESIS
use for separation of transplutonium elements, review on, 20: 16402

ELECTROSTATIC LENSES
aberrations in, space-charge effects on coefficients for, 20: 16784
aberrations of strong-focusing doublet, third-order, (T), 20: 17219

ELEMENT ONE HUNDRED AND THREE
production, 20: 16543

ELEMENTARY PARTICLES
annihilation and properties of quarks, (T), 20: 17411
coupling constant in strangeness-changing beta decay, renormalization of axial-vector, (T), 20: 17458
decay of strongly interacting, tests of C and T invariances in leptonic, 20: 17392
decay of, renormalization of weak axial-vector coupling constants for leptonic, 20: 17478
decay of, strong, (T), 20: 17445
detection of quarks, method for, (T), 20: 17365(T)
field theory for composite and, Zachariasen model, 20: 17472
field theory for massless, Reggeization and vanishing renormalization constants in, 20: 17476
interactions at high energies, large momentum-transfer processes in strong, (T), 20: 17461
interactions in broken $\bar{U}(12)$ symmetry, coupling constants for, 20: 17481
interactions in nonrelativistic three-body systems of, (T), 20: 17351 (N-65-19396)
interactions in quantum field theory, eigenvalue problem of Bethe-Salpeter equation for, (T), 20: 17425 (DESY-66/1)
interactions of arbitrary-spin, covariant-multipole-polarization operators and density matrices for, (T), 20: 17451
interactions of arbitrary-spin, nondynamical formalism for composite, 20: 17479
interactions of hadrons, bootstrap theory for weak and electromagnetic, 20: 17466
interactions of massless charged, minimal electromagnetic, 20: 17484
interactions of massive, in Bethe-Salpeter equation, 20: 17502
interactions of scalar, peratization of graviton-exchanging, (T), 20: 17503
interactions of, approximate calculation of asymptotic operators for, 20: 17450
interactions of, bibliography on, 20: 17154 (AED-C-23-06)
interactions of, bibliography on, 20: 17155 (AED-C-23-07)
interactions of, bibliography on, 20: 17153 (AED-C-23-05)
interactions of, distorted-wave theory of one-meson-exchange, 20: 17474
interactions of, isotopic structure of electromagnetic, (T), 20: 17428 (JINR-P-2498)
interactions of, relativistic treatment of three-body, (T), 20: 17447
interactions of, S-matrix with inelasticity for, 20: 17452
interactions of, SU(6) symmetry and spin independence in strong, 20: 17475
interactions of, structure for, (T), 20: 17436 (UCRL-14321-T)
interactions with electrons, radiative corrections for, (T), 20: 17370
kinetics of, nonrelativistic approximation for internal, (T), 20: 17482
mass formulas and strong interactions in SU(6) symmetry, 20: 17480
mass relations for, linear, 20: 17391
mass splittings of U(3) multiplets of strongly interacting, 20: 17471
operators for, invariant parametrization of products of local, (T), 20: 17498
polarization of scalar, in electromagnetic fields, (T), 20: 17498
production amplitudes and wave functions for, (T), 20: 17462
production of quarks, in cosmic rays and quasars, (T), 20: 17411
scattering by complex nuclei, analysis of diffraction, (T), 20: 17816
scattering by nuclei, phase-shift analysis for 0- and ½-spin elastic, (T), 20: 17693 (ORNL-TM-1464)
symmetries for, properties of, 20: 17435 (NYO-3399-45)
symmetries for, strong vertex from SL(6,C), 20: 17427 (IC-66/20)
symmetries of strongly interacting, approximate, (T), 20: 17433 (NYO-3399-13)
symmetries of, from dynamical mixing of spin and unitary spin, (T), 20: 17434 (NYO-3399-18)
symmetry and current algebras for, spurion scheme of U(6,6), 20: 17463
symmetry for classification of transitions in, 20: 17488
symmetry for, allowed link-up between relativity and internal, (T), 20: 17454
symmetry for, derivation of weak current in unitary, 20: 17415
symmetry for, SU(2), 20: 17429 (JINR-P-2529)
symmetry group for, discrete degenerate representations of U(p,q), 20: 17426 (IC-66/16)
symmetry groups for, 20: 17486
theory for, 20: 17432 (NP-15902)
theory of, L,M,N functions in nonlinear spinor, 20: 17440
transitions of systems of interacting, multi-photon, (T), 20: 17401
transport of, invariant imbedding for, (T), 20: 16935
wave equation for arbitary-spin, relativistic covariant Schroedinger, 20: 17572
wave equations for nonzero-mass, relativistic Schroedinger, 20: 17571

ELEMENTS
abundance of, nucleosynthesis theory for, 20: 17234
abundances in solar atmosphere, 20: 17229
abundances in solar wind, (T), 20: 17236
content and distribution in biological pool, 20: 16160 (UCRL-14739 (Pt.2))
determination in biological fluids and tissues, 20: 16160 (UCRL-14739 (Pt.2))
sorption of trace, anion exchange method of selective, 20: 16171 (AE-215)

ELK RIVER POWER REACTOR
operations safety analysis for March, 1965, 20: 18090(R) (NUS-246)

EMBRYONIC TISSUES
enzyme synthesis in, during cell differentiation, 20: 16172(R) (NYO-2194-1)
protein synthesis in, during cell differentiation, 20: 16172(R) (NYO-2194-1)
role of egg yolk in glucose and glycogen metabolism by chick embryos, 20: 16172(R) (NYO-2194-1)

EMBRYOS
metabolic pathways in developing, tracer studies, 20: 16172(R) (NYO-2194-1)
metabolic pathways of developing chick, 20: 16172(R) (NYO-2194-1)
radiation effects on DNA synthesis in rat, γ, 20: 16260

EMESIS
prevention during chemo- and radiotherapy using metoclopramide, 20: 16163

ENDOXAN
effects of, combined with x radiation and hyperbaric oxygen on leukemic mice, 20: 16262

ENERGY
storage of, superconducting system for, 20: 17625
storage of, use of superconductor magnetic fields for, 20: 17603

ENGINEERING
evaluation of underground highway and parking garage for fallout shelter for Manhattan Island, 20: 16623 (ORNL-TM-1381)

ENGINEERING TEST REACTOR
materials irradiation testing in, handbook for, 20: 18135 (IDO-17135)

ENTROPY
determination of, for melting of binary systems, 20: 16711(R) (MIT-1381-13)

ENZYMES
determination in tissue homogenates after electrophoretic separation, 20: 16172(R) (NYO-2194-1)
effects of metal ions on polymerase, 20: 16160 (UCRL-14739(Pt.2))
effects on uv-irradiated deoxyribonucleic acid, 20: 16159(R) (ORNL-3900, pp 150-81)
genetic control of, 20: 16172(R) (NYO-2194-1)
measurement of citrate-cleavage, in bone tissues, 20: 16160 (UCRL-14739(Pt.2))
radiation effects on activity of, in blood of mammals, 20: 16222 (AFWL-TR-65-112)
radiation effects on activity of, in rat tissue homogenates, x, 20: 16289
role of manganese in, by which RNA is synthesized, 20: 16160 (UCRL-14739(Pt.2))
synthesis during cell differentiation, 20: 16172(R) (NYO-2194-1)

EPITHELIUM
radiosensitivity of intestinal, 20: 16322

EQUATION OF STATE
approximations for, virial coefficients of molecular models for, 20: 17527
ERBIUM
determination by neutron activation and ion-exchange chromatography, 20: 16363
determination in carbonatites by ion exchange chromatography and oxalate precipitation, 20: 16346
determination in simple and stainless steels, photometric, 20: 16380
energy levels, (E), 20: 17260
energy levels of, low odd, (E/T), 20: 17261
magnetic properties of polycrystalline, 20: 17098
magnetostriction in paramagnetic region, (E), 20: 18012
solubility in gold, solid, 20: 17016 (IS-1175)
ERBIUM ALLOYS
Er–Fe, crystal structure of Er_6Fe_{23} in, 20: 17096(T)
Er–Hg, crystal structure of $ErHg_3$, 20: 17060
Er–Mn, crystal structure of Er_6Mn_{23} in, 20: 17096(T)
Er–Tl, crystal structure of $ErTl_3$, 20: 17060
ERBIUM COMPLEXES
with phenanthroline, infrared spectra of, 20: 16436
with 2,2′-bipyridyl, infrared spectra of, 20: 16437
ERBIUM HYDRIDES
properties and structure, 20: 16453
ERBIUM HYDROXIDES
decomposition of, products of thermal, 20: 16441
ERBIUM ISOTOPES Er-156
half life, (E), 20: 17808
ERBIUM ISOTOPES Er-157
half life, (E), 20: 17808
ERBIUM ISOTOPES Er-166
neutron reactions (n,γ), activation cross section for, (E), 20: 16336(R) (NYO-10175)
ERBIUM ISOTOPES Er-167
half life of isomeric, from neutron reactions (n,γ), (E), 20: 16336(R) (NYO-10175)
half life of isomeric, from neutron reactions (n,n′), (E), 20: 16336(R) (NYO-10175)
half life of isomeric, from neutron reactions (n,2n), (E), 20: 16336(R) (NYO-10175)
neutron reactions (n,n′), activation cross section for, (E), 20: 16336(R) (NYO-10175)
ERBIUM ISOTOPES Er-168
neutron reactions (n,2n), activation cross section for, (E), 20: 16336(R) (NYO-10175)
ERBIUM OXIDES
analysis for impurities by neutron activation and ion-exchange chromatography, 20: 16363
determination in thorium oxide by emission spectroscopy, 20: 16393
determination of hydrated, from erbium hydroxide thermal decomposition, 20: 16441
Er_2O_3–SrO, properties of compounds formed by interactions in, 20: 17044
ERYTHROCYTES
lipid function in membranes of sheep, 20: 16160 (UCRL-14739(Pt.))
radiation effects on, morphological, 20: 16250
viability of stored, effects of adenine on, 20: 16303(R) (AD-626384)
ESCHERICHIA COLI
radiation effects on gibberellic acid synthesis in, tracer study, 20: 16193 (EUR-2539.i)
radiation effects on mitotic mechanism in, repair of x, 20: 16200
radiation effects on survival curves of, in complex media, 20: 16237
radiation effects on phage infection of, uv, 20: 16270(T)
ribonucleic acid separation from, 20: 17158(R) (ORNL-3900, pp 82-149)
synthesis of RNA during recovery of DNA synthetic system of uv-damaged, 20: 16202
ESOPHAGUS
radiotherapy of carcinomas in, moving-beam x, 20: 16317
ESTERS
effects on solvent extraction of europium using benzoyltrifluoroacetone, 20: 16565
ESTROGENS
radiosensitivity effects on skin, uv, 20: 16248
ETHANE
formation in reactions between rare earth dicarbides and water, 20: 17048
ETHANOL
effects on self-irradiation decomposition of tritium-labeled organic compounds, 20: 16533
ethanol–H_2O, effects on isotopic exchange between elementary iodine and 1-phenyl-2,3-dimethyl-4-iodopyrazolone, 20: 16502
ethanol–naphthalene, radiation effects on hydrogen atom reactions in, 20: 16524
methanol–naphthalene, radiation effects on hydrogen atom reactions in, 20: 16524
ETHYL RADICALS
yield from gamma radiolysis of hexane–silica gel systems, 20: 16511
ETHYL SULFATES
effects on plants, review of mutagenic, 20: 16225 (EUR-2715.f)
ETHYLENE
formation in reactions between rare earth dicarbides and water, 20: 17048
radioinduced in plant tissues, γ, 20: 16281
reactions with active nitrogen, products of, 20: 16510(T) (NP-tr-1364)
ETHYLENE, CHLORO- POLYMERS
plastisols of, defects in molds of, effects of moisture on, 20: 18179 (Y-1508)
ETHYLENE GLYCOL
tetraphenyl-, rearrangement to benzopinacolone by reactions with perchloric acid, 20: 16542(R) (TID-22646)
yields from gamma radiolysis of benzene–methanol mixture, 20: 16530
ETHYLENE POLYMERS
radiation effects on, neutron, 20: 17822
radioinduced graft polymerization with butadiene, gamma, 20: 16527
radioinduced preparation of, 20: 16505 (BNL-949)
EUGLENA
radiation effects reproduction of, uv, 20: 16204
EUROPEAN ATOMIC ENERGY COMMUNITY
nuclear industry development in, 20: 18180
EUROPIUM
abundance in sun, (E), 20: 17237
compressibility and Néel temperature, (E), 20: 17999
separation by solvent extraction using benzoyltrifluoroacetone, effects of nitrogen- and oxygen-containing solvents on, 20: 16565
separation from aqueous sodium thiocyanate solutions by solvent extraction using tributyl phosphate, 20: 16564
thermal capacity at 3 to 25°K, 20: 17080
EUROPIUM ALLOYS
Eu–Hg, magnetic properties of $EuHg_3$, 20: 17060
Eu–Pb, crystal structure and magnetic properties of $EuPb_3$, 20: 17060
Eu–Tl, crystal structure and magnetic properties of $EuTl_3$, 20: 17060
EUROPIUM COMPLEXES
with phenanthroline, infrared spectra of, 20: 16436
with 1-phenyl-1,3-butanedione, fine structure spectra of, 20: 16467(T)
with 2,2′-bipyridyl, infrared, spectra of, 20: 16437
with 4,4,4-trifluoro-1-phenyl-1,3-butanedione, performance of lasers of, deuterium isotope effects on, 20: 16781
EUROPIUM COMPOUNDS
spectra of MX_3-type, fine structure, 20: 16467(T)
EUROPIUM HYDRIDES
properties and structure, 20: 16453
EUROPIUM IONS
reactions of divalent, in aqueous perchloric acid solutions, electron transfer in, 20: 16462
EUROPIUM ISOTOPES
content in Arkansas rain water in Oct. 1964, 20: 16685
EUROPIUM ISOTOPES Eu-154
orientation in neodymium ethyl sulfate, quadrupole crystal-field shielding from, (E), 20: 17996
EUROPIUM ISOTOPES Eu-155
content in rain water, Fayetteville, Arkansas, Oct. 1964, 20: 16663 (TID-21470)
ground water contamination by, in Shoal Event, hazards from, 20: 16742 (VUF-1014)
EUROPIUM ISOTOPES Eu-156
beta decay of, transition rates for, (T), 20: 17742
content in rain water, Fayetteville, Arkansas, Oct. 1964, 20: 16663 (TID-21470)
EUROPIUM OXIDES
compressibility and Curie temperature of, (E), 20: 17999
crystallographic modifications and phase transformations of, 20: 16489
preparation of, methods for, 20: 17007(R) (AD-627468)
reactions with boron oxides at high temperatures, 20: 16489
Eu_2O_3–stainless steel, radiation effects on control rods of, reactor, 20: 17129 (ORNL-TM-1407)
EUROPIUM SULFIDES
Ce_2S_3–EuS, compound formation in, 20: 16431
Dy_2S_3–EuS, compound formation in, 20: 16431
EuS–Gd_2S, compound formation in, 20: 16431
EuS–La_2S_3, compound formation in, 20: 16431
EuS–Nd_2S_3, compound formation in, 20: 16431
EuS–Pr_2S_3, compound formation in, 20: 16431
EuS–Sm_2S_3, compound formation in, 20: 16431
EuS–Tb_2S_3, compound formation in, 20: 16431
EVAPORATORS
control of four-stage, for treatment of contaminated water, 20: 16594
design of solar, for waste solutions, 20: 18164(R) (NP-15874)
development of vacuum, for milk, 20: 16741(R) (UCRL-14534, pp 54-6)
EVOLUTION
chemical, in geological samples, 20: 16633 (UCRL-16605)

EXERCISE
effects on bone blood flow, 20: 16192
EXPERIMENTAL BREEDER REACTOR-II
fuel cycle facility for, 20: 16582
EXPERIMENTAL GAS COOLED REACTOR
development, 20: 18020(R) (ORNL-3900, pp 2-81)
EXPLOSIONS
sample-marking system for positive identification following, 20: 18176 (SCL-DR-66-6)
EXPLOSIVES
photography of, evaluation of flash equipment for, 20: 16739(R) (UCRL-14534, pp 44-9)
EYES
radiation effects on mitosis in lens epithelium of rat, x, 20: 16256
radiotherapy of tumors of, using β applicators, 20: 16305

F

FALLOUT
activity level of, near New Delhi, 20: 16680
analysis for cadmium isotopes, radiochemical, 20: 16397
bibliography on, 20: 16662(R) (HASL-165)
cesium-137 content in, uptake by food chain, 20: 16678
composition near Leningrad, 20: 16704
content in rain in Arkansas in Oct. 1964, 20: 16685
content in rainfall, measurement of, 20: 16168
deposition from atmosphere, 20: 16649
deposition of atmospheric, estimation of areal isoconcentration line for, 20: 16664(R) (UCRL-14534, pp 19-22)
deposition of, data on, 20: 16697
deposition of, effects of precipitation on, 20: 16647
deposition of, effects of precipitation on, 20: 16648
deposition on pasture grass, rate of, 20: 16160 (UCRL-14739(Pt.2))
effects on biological systems, enzymatic assessment of, 20: 16160 (UCRL-14739(Pt.2))
effects on Japanese, medical survey of 10-year, 20: 16226 (NP-15891)
effects on lungs, pathological, 20: 16264
mass and particle size distribution of, volcanic simulation, 20: 16659 (AD-629527)
measurement at Risö, 20: 18174(R) (NP-15771)
monitoring at global locations, 1964 and 1965, 20: 16662(R) (HASL-165)
monitoring at Vilnius, Soviet Union, 1962, 20: 16700
monitoring atmospheric, 1962 to 1964, 20: 16677
monitoring for beta activity in ground air in Germany, 1961 to 1963, 20: 16766
monitoring in atmospheric dust and rain water, 1964–65, 20: 16660 (AERE-R-4997)
monitoring in Japan, 1962 and 63, 20: 16671
monitoring in Japan, 1964, 20: 16730 (NP-15882)
monitoring in Japan, 1964, 20: 16731 (NP-15883)
monitoring in lower atmosphere, Lahore, Pakistan, 20: 16683
monitoring in rain water at Fayetteville, Arkansas, Oct. 1964, 20: 16663 (TID-21470)
monitoring in stratosphere and troposphere in Project Star Dust, 1963, 20: 16727(R) (HASL-168)
monitoring in stratosphere and troposphere during 1963 in Project Star Dust, 1964, 20: 16728(R) (HASL-169)
monitoring near Leningrad in 1961–1963, 20: 16701
monitoring of strontium-90, in polar regions of Soviet Union, 20: 16703
prediction model for, effects of cloud rise and particle transport in, 20: 16735 (TO-B-65-99)
protection from, design data for shelters for, 20: 16620 (AD-624370)
sample collection using horizontal sheets, 20: 16657
sampling of, effects of meteorological conditions on effectiveness of, 20: 16656
sodium-22 content in, uptake by food chain, 20: 16678
transport in atmosphere, 20: 16698
wind effects on, analysis of local sea-breeze, 20: 16661(R) (ECOM-00392-F)
FAST REACTORS
core explosions in, containment of, 20: 18122
core meltdown accidents in, energy release in, 20: 18123
design of molten-salt power-breeder, 20: 18088 (INR-669/C)
development for power production, 20: 18097
development in Germany, policy for, 20: 18111
fuel burnup in large plutonium–uranium, effects on breeding ratio, multiplication factor, and sodium-void reactivity, 20: 18060
neutron flux and multiplication factor in, heterogeneity effects on, (T), 20: 18063
reactivity feedback of pulsed, during excursions, (T), 20: 18056
FECES
chlorine-36 content in calf, after ingestion, 20: 16186
iodine-131 content in calf, after ingestion, 20: 16186
strontium-85 content in human, effects of sodium alginate on, 20: 16173 (PG-Report-686)
FERMIONS
boson reactions with, invariant amplitudes for structure of, (T), 20: 17770
hydrodynamic equations for superfluid gas of, 20: 17647
interactions with scalar bosons, approximate calculation of asymptotic operators for, 20: 17450
production of pairs of, in photon interactions with charged particles, (T), 20: 17499
quantum electrodynamics of, (T), 20: 17581
transport properties of normal systems of, dissipative effects in finite-temperature, (T), 20: 17528
FERMIUM
dissociation in hydrochloric acid–bis(2-ethylhexyl) phosphate–toluene system, constants for, 20: 16404
production, 20: 16543
separation from californium and mendelevium by extraction chromatography using bis(2-ethylhexyl) orthophosphate, 20: 16404
FERROMAGNETIC MATERIALS
neutron scattering near phase-transition point, polarized, (T), 20: 17987(T)
FETUSES
cesium-137 contamination of, effects of diet and environmental contamination on, 20: 16301
radiation effects on brain of rat, pathological x, 20: 16275
FFAG SYNCHROTRONS
magnet poles for, fabrication of contoured, 20: 17185 (CONF-650922, pp 248-52)
magnets for, power supply for MURA modeling program on, 20: 17203 (CONF-650922, pp 776-8)
FIELD THEORY
Bethe-Salpeter equation for massive particles, 20: 17502
conservation laws for free fields in, 20: 17500
elementary particle interactions in quantum, eigenvalue problem of Bethe-Salpeter equation for, (T), 20: 17425 (DESY-66/1)
elementary particles and bound states in Zachariasen model, 20: 17472
formulation of optical model at high energies, 20: 17469
geometrization of vector meson, Rainich, 20: 17441
model for vector-scalar fields in, renormalization theory for, 20: 17465
models in, Goldstone behavior in, 20: 17473
S-matrix in, equation of motion for half, 20: 17493
S-matrix theory for intermediate fields without particles, 20: 17437
spinor field equation in presence of gravitation for nonlocal spin connection, 20: 17565
spinor fields in, symmetry in nonlinear theory of, 20: 17492
FILMS
density of thin, 20: 17070
magnetic flux motion in magnetically coupled superconducting, (E/T), 20: 17623
preparation of thin oxide, 20: 17158(R) (ORNL-3900, pp 82-149)
thickness of VYNS target, for determining equilibrium charge states of boron and carbon recoil ions, 20: 16508(R) (NYO-2771-13)
x ray scattering by thin copper, interference fringes from, (E/T), 20: 17163
FILTER MATERIALS
properties of fibrous, 20: 16653
FILTER PAPERS
efficiency of Whatman Type ACG/B, for methyl iodide retention in air, 20: 16719 (AEEW-M-568)
radioiodine sampling with silver nitrate-impregnated, efficiency of, 20: 16756
FILTERS
performance of neutron, effective cutoff energies for, (T), 20: 17663
properties of fibrous, 20: 16653
properties of fibrous, for sampling aerosols, 20: 16654
FILTRATION
research programs on reverse–osmatic, 20: 17158(R) (ORNL-3900 (pp 82-149)
FINLAND
ionospheric sounding for 1958 to 1960 over Sodankylae, 20: 17542
FINNED TUBES
heat transfer from, 20: 18078
FISH
analysis for zinc in marine, polarographic, 20: 16175(R) (RT/BIO(65)-1)
embryos of, metabolic pathways in developing, 20: 16172(R) (NYO-2194-1)
phosphorus-32 uptake by, from radioactive wastes in fresh water, 20: 18157 (BNWL-SA-466)
radiation effects on development of female *Oryzias latipes*, effects of steroids on, 20: 16263
radiation effects on flavor of, effects of hypoxanthine on, 20: 16925
radiation processing of, effects on wholesomeness, 20: 16925

radiosensitivity of *Oryzias latipes*, effects of water temperature on, 20: 16236
FISSION
chemistry and physics of, conference on, 20: 17694 (STI/PUB/101 (Vol.1))
chemistry and physics of, conference on, 20: 17695 (STI/PUB/101 (Vol.2))
energy release in thermal, (T), 20: 17862
gamma emission from, delayed and prompt, (E/T), 20: 17827
mechanisms of, determination from energy and mass of fission fragments, (E/T), 20: 17158(R) (ORNL-3900, pp 82-149)
neutron energy spectra and yields from, delayed, (E/T), 20: 17830
nuclear moment of inertia at saddle point in drop model for, (T), 20: 17849
nucleon pairing effects on even-even compound nuclei, near threshold, (T), 20: 17847
research at high and medium energies, review of, (E/T), 20: 17836
theory of, review of, 20: 17843
theory of, shell effects in, 20: 17846
FISSION CHAMBERS
design for neutron detection and measurement in reactors, 20: 16903
use in neutron flux measurements in reactors, 20: 16896
FISSION FRAGMENTS
angular anisotropy and mass asymmetry of thorium-232 fast neutron, (E), 20: 17869
angular distributions from americium-241, plutonium-238, and thorium-230, (E/T), 20: 17848
beta activity of uranium-233 and -235 and plutonium-239, (E), 20: 17835
charge distributions of, nuclear structure dependence of, (T), 20: 17845
charge distributions from californium-252, (E), 20: 17859
distributions from plutonium-239 and uranium-233 and -235, energy and mass, (E), 20: 17863
distributions from uranium-234 (d,pf) reactions, angular, energy, and mass, (E), 20: 17865
energy degradation in light materials, (E), 20: 17821
energy distributions of, method for measuring, 20: 17864
energy distributions of uranium-235, 20: 17867
energy of uranium-235, mass dependence of, (E/T), 20: 17868
gamma emission from, energy and intensity of, (E/T), 20: 17830
mass distributions from actinium-227, neptunium-237, and protactinium-231, (E), 20: 17861
mass distributions of, after prompt neutron emission, (E/T), 20: 17866
mass distributions of, circuit for studying, 20: 17870
neutron emission from uranium-235, prompt, (E), 20: 17824
neutron emission from, delayed, (E/T), 20: 17830
neutron emission from antimony and arsenic isotopes, delayed, (E), 20: 17833
reactions with metal foils, secondary electron production in, 20: 17168
separation of antimony and arsenic from, method for, 20: 17834
yields from plutonium-239 and uranium-235 resonance neutron fission, (E), 20: 17839
yields from thorium-232, (E), 20: 17860
yields of delayed neutron precursors, (E/T), 20: 17831
FISSION PRODUCTS
accumulation of cesium-137 and strontium-90, in soils near Leningrad, 20: 16702
accumulation of, on land and ocean surfaces, 20: 16706
analysis for cadmium isotopes, radiochemical, 20: 16397
behavior in fuel-meltdown, 20: 18020(R) (ORNL-3900, pp 2-81)
beta activity of, from atomic explosions, 20: 16707
content in surface layer of atmosphere over Heis Island and Moscow, 20: 16650
deposition of, from atmosphere, effects of precipitation on, 20: 16648
detection in reactor coolants, systems for, 20: 18036
determination in reactor coolants using gamma spectrometry, equipment for, 20: 16898
determination in rain water and water supplies, method for, 20: 16407
diffusion from ceramic wastes, effects of volatilization on, 20: 18156 (BNWL-SA-453)
diffusion from pyrolytic-carbon-coated fuel particles, effects of coating structure on gaseous, 20: 17127 (ORNL-3923)
diffusion from uranium fuels, 20: 18020(R) (ORNL-3900, pp 2-81)
diffusion in atmosphere, 20: 16651
distribution in atmosphere, global, 20: 16649
fractionation of, from nuclear explosions, 20: 16696
gamma emissions from, dosimetry of, 20: 16168
hazards from, prediction of, 20: 16160 (UCRL-14739(Pt.2))
monitoring in stratosphere and troposphere in Project Star Dust, 1963, 20: 16727(R) (HASL-168)
monitoring in stratosphere and troposphere during 1963 in Project Star Dust, 1964, 20: 16728(R) (HASL-169)
production from proton reactions with uranium-238 at 400 Mev, recoil properties from, (E), 20: 17790
release from AGR, control of, 20: 18110
separation from sulfuric acid in waste condensates, methods for, 20: 18159 (BNWL-SA-514)
separation of cesium-137 from, ion exchanger for, 20: 16578
separation of ruthenium from solutions of, by electrodeposition, 20: 16563
steam condensate from, system for monitoring, 20: 16825 (ORNL-TM-1442)
uptake and placental transfer of, effects of environmental contamination on, 20: 16301
FISSIONABLE MATERIAL
availability for future needs, 20: 18099
diffusion of rare gases in, activation entropy for, (T), 20: 17804
FLAVINES
radiosensitivity effects in bacterial DNA, 20: 16280
FLOWMETERS
static eliminator for, design of γ-active, 20: 16783
FLUID FLOW
boiling heat transfer in annular two-phase, analysis of liquid film in, (T), 20: 16604 (NYO-3114-13)
density profiles for suspensions in, (E/T), 20: 16606(R) (TID-22621)
heat transfer in steady-state two-phase, 20: 16601(R) (GEAP-5067)
heat transfer in two-phase, in water, 20: 16605 (NYO-3304-8)
hydrodynamics of waste disposal in soil by injection, 20: 18163(R) (NP-15859)
magnetohydrodynamic, around magnet source, (T), 20: 17509 (D-1-82-0469)
magnetohydrodynamic, with orthogonal magnetic and velocity field distributions, (T), 20: 17532
structure of, effects of suspensions on statistical, (T), 20: 16606(R) (TID-22621)
FLUID FLOW (LAMINAR)
magnetohydrodynamic, in natural convection in vertical cylinders, (T), 20: 17516
properties of single-phase natural circulation, (T), 20: 16600 (COO-1177-15)
FLUID FLOW (TURBULENT)
properties of single-phase natural circulation, (T), 20: 16600 (COO-1177-15)
FLUID FUEL REACTORS
development of single-zone circulating suspension, 20: 18072
neutron losses in, delayed, 20: 18048 (ORNL-P-1967)
FLUIDIZATION
kinetics of liquid-solid fluidized beds, determination using noise analysis, 20: 18071 (TID-22665)
FLUIDS
thermal stability of completely confined, calculation of, 20: 17535
FLUORIDE VOLATILITY PROCESSES
development, 20: 16582
FLUORIDES
effects of distribution of ferric thiocyanate in 2-methyl-1-propanol--water, 20: 16335(R) (NBS-TN-276)
FLUORINE
determination in presence of oxygen, activation, 20: 16332 (GA-6691)
determination in zinc electrorefining solutions, feasibility of activation, 20: 16339(R) (TID-22662)
photon reactions with Coulomb field of, pair production total cross sections for high-energy, (T), 20: 17754
reactions with plutonium tetrafluoride to prepare plutonium hexafluoride, 20: 16463
FLUORINE COMPOUNDS
radioinduced preparation of, 20: 16505 (BNL-949)
FLUORINE ISOTOPES F-18
energy levels of, two-nucleon interaction energy matrices for low-lying, (T), 20: 17710
half life, 20: 16331 (GA-6568)
FLUORINE ISOTOPES F-19
helium-3 reactions (He-3,α) at 12 Mev, Q value for, 20: 16331 (GA-6568)
neutron reactions (n,p) with, sensitivity of, for activation analysis, 20: 16332 (GA-6691)
FLUORINE SYSTEMS
Cs–F, electron emission from metals in vapors of, thermionic, (T), 20: 17334
F–O, analysis for fluorine, activation, 20: 16332 (GA-6691)
FLUOROCARBONS
radioinduced preparation of, 20: 16505 (BNL-949)
FOOD
analysis for radioisotopes, methods for, 20: 16369
manganese-54 content in barley, rye, tea leaves, and wheat, 20: 16167
radiosterilization of, status, 20: 16918 (AECL-PAK/RB-7)
radium-226 content in, Bombay and Kerala, India, 20: 16747
sodium-22 uptake from fallout, 20: 16678

FORMIC ACID
effects on self-irradiation decomposition of tritium-labeled organic compounds, 20: 16533
radiation effects on carboxylation of, kinetics of uv, 20: 16538
FRANCE
radioactivity variations on beaches of Gulf of Lion, 20: 16669
radium-226 content in milk in, 20: 16752
radium-226 content in milk in, 20: 16753
tritium content in Mont Cenis Lake, 1964 and 1965, 20: 16668
FREE RADICALS
electron spin resonance spectra of, in aqueous hydrogen peroxide at 77°K, 20: 16512
paramagnetic resonance in liquids, (E/T), 20: 17158(R) (ORNL-3900, pp 82-149)
radioinduced in crystals of deuterated glycine, controlled-temperature ESR spectral studies on, 20: 16525
radioinduced in keratin, uv, 20: 16205
repairing long-lived, kinetics of, 20: 16159(R) (ORNL-3900, pp 150-81)
yields from gamma radiolysis of hexane–silica gel systems, 20: 16511
FRENCH REACTORS
development of, review of, 20: 18104
FRIEDEL-CRAFTS REACTIONS
effects on decomposition and rearrangement in aromatic-aliphatic ketones, 20: 16542(R) (TID-22646)
FROGS
embryos of, metabolic pathways in developing, 20: 16172(R) (NYO-2194-1)
molting of, effects of thyroid hormones on, 20: 16252
radiation thyroidectomy in, effects on molting, 20: 16252
FRUITS
radioinduced mutants of sweet cherry, 20: 16244
FUMARATES
radiation effects on oxidation of, in *Vibrio cholerae*, 20: 16198
FUMARIC ACID
radioinduced addition of hydrogen to, in single crystals of succinic acid, (E), 20: 16537
FUNGI
cultivation and use of deuterium-labeled, 20: 16165
growth and metabolism of *A. niger*, effects of rare earths and yttrium on, 20: 16191
radioinduced mutations in Emericellopsis, methods for assaying uv, 20: 16238
FURAN, DIHYDRO-
formation by disproportionation of aliphatic ketones in perchloric acid, 20: 16542(R) (TID-22646)
FURAN, 3,5-DIMETHYL-2-ACETYL-
preparation of deuterated, from 2,4,6-tri-d_3-methylpyrylium perchlorate, 20: 16501
FURNACES
description of retort, for brazing and annealing copper waveguides, 20: 17000
FUSED SALTS
crystal structure of metal-fluoride, 20: 17158(R) (ORNL-3900, pp 82-149)
design of all-metal, for equilibrium potential measurement, 20: 17158(R) (ORNL-3900, pp 82-149)
spectra of metal–fluoride, absorption, 20: 17158(R) (ORNL-3900, pp 82-149)

G

GADOLINIUM
abundance in sun, (E), 20: 17237
determination in carbonatites by ion exchange chromatography and oxalate precipitation, 20: 16346
dysprosium-161 Mössbauer effect in, (E), 20: 17988(T)
electronic properties of single-crystal, effects of ion-bombardment on, 20: 17151
magnetic properties, (E), 20: 17988(T)
magnetic properties of polycrystalline, 20: 17098
magnetic structure of, determination using Kerr effect, 20: 17974 (IS-T-63)
performance of foils of, in neutron radiography, 20: 16619
performance of neutron filters of, effective cutoff energies for, (T), 20: 17663
solubility in gold, solid, 20: 17016 (IS-1175)
solvent properties for magnesium, solid, 20: 17016 (IS-1175)
GADOLINIUM ALLOYS
Gd–Hg, crystal structure of $GdHg_3$, 20: 17050
Gd–Mn, crystal structure of Gd_6Mn_{23} in, 20: 17096(T)
GADOLINIUM CARBIDES
properties of, chemical and physical, 20: 17048
reactions with water, formation of gaseous products in, 20: 17048
GADOLINIUM COMPLEXES
with phenanthroline, infrared spectra of, 20: 16436
with 2,2′-bipyridyl, infrared spectra of, 20: 16437
GADOLINIUM HYDRIDES
properties and structure, 20: 16453
GADOLINIUM ISOTOPES Gd-153
ground water contamination by, in Shoal Event, hazards from, 20: 16742 (VUF-1014)
GADOLINIUM ISOTOPES Gd-155
energy levels of, g-factors for 87-kev, (E), 20: 17683 (INP-430/PL)
GADOLINIUM ISOTOPES Gd-156
energy levels from europium-156 decay, (T), 20: 17742
GADOLINIUM ISOTOPES Gd-159
beta decay of, terbium-159 levels from, (E), 20: 17789
orientation in neodymium ethyl sulfate, quadrupole crystal-field shielding from, (E), 20: 17996
GADOLINIUM OXIDES
crystallographic modifications and phase transformations of, 20: 16489
determination in thorium oxide by emission spectroscopy, 20: 16393
reactions with boron oxides at high temperatures, 20: 16489
GADOLINIUM SULFATES
effects on orthohydrogen–parahydrogen conversion at 77°K, catalytic, 20: 16454
GADOLINIUM SULFIDES
EuS–Gd_2S, compound formation in, 20: 16431
Gd_2S_3–SmS, compound formation in, 20: 16431
Gd_2S_3–YbS, compound formation in, 20: 16431
GAGES
design of radiometric, for moisture determination, 20: 16924
ion collection in Bayard-Alpert, factor for, (T), 20: 16787
use of radiometric, for measuring moisture in coke, concretes, and sand, 20: 16926
GALAXIES
cosmic particle motion in, models for, (T), 20: 17324
radiation emission by, (T), 20: 17243
GALLIUM
determination of trace amounts of, activation, 20: 16396
nuclear spin relaxation in metallic, at 1.1 to 307°K, (E), 20: 17995
GALLIUM ALLOYS
Cr–Ga–Nb, phase studies on intermetallic compounds in, 20: 17075
GALLIUM ISOTOPES Ga-68
use in bone scanning, 20: 16310
GALLIUM ISOTOPES Ga-69
nuclear quadrupole resonance in gallium metal, at 1.1 to 300°K, 20: 17995
GALLIUM ISOTOPES Ga-71
nuclear quadrupole resonance in gallium metal, at 1.1 to 300°K, 20: 17995
GALLIUM ISOTOPES Ga-72
sensitivity for activation analysis using beta-gamma-gamma sum-coincidence gamma spectrometer, 20: 16335(R) (NBS-TN-276)
GALLIUM SELENIDES
magneto-optical properties of, measurement using superconducting magnet, (E), 20: 17588 (CONF-650922, pp 525-9)
GAMMA CAMERAS
development of scintillation, for radiodiagnosis, 20: 16855
image transfer system modifications, digital print-out of counts, and setting-up procedures for, 20: 16853
GAMMA RADIATION
absorption curves for, method of graphing self-, 20: 17966
absorption of high-energy cosmic, by thermal microwave field, (T), 20: 17319
activity in rain water and water supplies, method for determining, 20: 16407
attenuation by lithium fluoride crystals, 20: 16829(R) (UCRL-14534, pp 1-7)
attenuation in germanium, coefficients for, (T), 20: 17962 (ORNL-TM-1237)
detection and measurement of high-energy cosmic, (E), 20: 17320
detection and measurement in reactors, instruments for, 20: 16903
detection of, fabrication and performance of lithium-drifted germanium diodes for, 20: 16890
detection of, spherical dielectric Compton detector for, 20: 16812 (EGG-1183-1174)
dose buildup factors for lead, 20: 17963(T) (ORNL-tr-1059)
dose buildup factors for water, 20: 17964(T) (ORNL-tr-1061)
dosimetry in arbitrary geometries, computer program for, 20: 17961 (ORNL-TM-1212)
dosimetry in soils, methods for, 20: 16687
dosimetry in thermal neutron background using film badges, 20: 16807 (CLOR/IBJ-42/D)
dosimetry of, from roof tiles using thermoluminescence, 20: 16759
dosimetry of, liquid photographic emulsions for, 20: 16845
dosimetry of, oxygen enhancement ratio for, 20: 16750

dosimetry of, using hair activation, 20: 16758
dosimetry of, using cyanides of triphenylmethane dyes, 20: 16521
dosimetry using digital computers, 20: 16748
effects of fallout, Japanese medical survey of 10-year, 20: 16226 (NP-15891)
effects on activity of silver–silver oxalate catalyst, 20: 16523
effects on alkaline aqueous solution containing hydrogen and oxygen, 20: 16520
effects on benzene–methanol mixture, 20: 16530
effects on cadmium and nickel battery electrodes, 20: 17124(R) (N-65-17608)
effects on chemical analyses, 20: 17158(R) (ORNL-3900, pp 82-149)
effects on chromium-protein complexes, 20: 16211
effects on chromosome aberrations in man, 20: 16230(R) (TID-22644)
effects on copper and zinc content and enzyme activity in blood of mammals, 20: 16222 (AFWL-TR-65-112)
effects on corrosion resistance of type 304L stainless steel, 20: 17118(R) (EURAEC-1564)
effects on corrosion of vermiculite glass containing cesium, (E/T), 20: 18166(R) (TID-22531)
effects on cytidine, DNA, and thymidine, ESR resonance studies of, 20: 16541
effects on diffusion in solids, effects of correlated defects on, 20: 17131
effects on diodes and transistors, 20: 16909 (N-65-18250)
effects on diodes, transistors, and microelectronic circuits, 20: 16908 (N-65-17526)
effects on DNA synthesis in rat embryos, 20: 16260
effects on dog skeleton, 20: 16253
effects on electric conductivity of DNA and γ-globulin solutions, 20: 16194
effects on electronic components in space, review of, 20: 16911
effects on ESR spectra of sodium polyphosphate glasses, 20: 16516
effects on fertility and mortality of rice weevils, 20: 16243
effects on germination of *Rauwolfia serpentina* seed, 20: 16249
effects on graft polymerization of butadiene to polyethylene and polypropylene, 20: 16527
effects on graft polymerization of rayon with styrene, 20: 16528
effects on hexaammonium molybdate, EPR studies of, 20: 16529
effects on hexane, silica gel, and their systems, ESR studies of, 20: 16511
effects on human gamma globulin, chemical, physical, and serological, 20: 16212
effects on immune reactions in rabbits, 20: 16214 (AD-620438)
effects on iron metabolism in rats, tracer study, 20: 16187
effects on jute seeds, 20: 16217 (AECD-AG-7)
effects on jute, hybridization, 20: 16218 (AECD-AG-12)
effects on laryngeal carcinomas, 20: 16313
effects on magnetic diffusion in nickel zinc ferrites, 20: 16532
effects on pea tissues, ethylene formation in, 20: 16281
effects on peritrichs, 20: 16295
effects on physical properties of Santowax WR at 425 to 800°F, 20: 17122 (MIT-334-34)
effects on planar lead chloride and iodide at liquid nitrogen temperatures, 20: 16531
effects on plants, review of mutagenic, 20: 16225 (EUR-2715.f)
effects on potassium chloride fracture surface energy, 20: 17137
effects on praseodymium complexes with β-diketones, 20: 16416(R) (NYO-906-68)
effects on pre-meiotic male flower buds of *Pinus nigra*, dose effects on, 20: 16228(R) (NYO-3571-2)
effects on properties of polyamide fibers, 20: 16522
effects on pyrolytic carbon coatings of reactor-fuel pellets, 20: 18076 (ORNL-TM-1385)
effects on reduction by hydrogen of cobalt complexes in ethanol solutions, 20: 16526
effects on sedimentation of sewage colloids, 20: 16505 (BNL-949)
effects on seeds of medicinal plants, genetic, 20: 16290
effects on serological reactivity of Treponema antigens, 20: 16199
effects on silver bromide and silver chloride, ESR from, (E), 20: 17981
effects on silver battery electrodes, 20: 17115(R) (AI-65-264)
effects on skin, therapeutic-dose, 20: 16323
effects on sodium bromide, chloride, and iodide in sulfuric acid glasses at 77°K, 20: 16534
effects on solid polycrystalline hydrobromic and hydrochloric acids at 77°K, 20: 16519
effects on surface activity of γ-octahydro-1,3,5,7-tetranitro-1,3,5,7-tetrazocine, 20: 16504 (AD-627846)
effects on survival curves of bacteria in complex media, 20: 16237
effects on thermoluminescence of calcium oxides, 20: 17982
effects on viscous dislocation damping in dilute copper–germanium alloys, 20: 17138
effects on water vapor at 100 to 350°C, 20: 16536
effects on water, reaction rates and yields from, (T), 20: 16509
(TID-22666)
effects on wheat seed, genetic, 20: 16285
emission following stripping reactions (d,p), polarization in, (E/T), 20: 17726
emission from fuel rods, scanner for measuring, 20: 18025
emission from nuclear explosions, dosimetry of, 20: 16760
emission in neutron capture by nitrogen-14, (E), 20: 17842
emission in nuclear fission, delayed and prompt, (E), 20: 17827
energy conversion into electrical energy by way of Compton electrons, 20: 17331
energy spectra and yields from uranium-235 thermal fission, (E), 20: 17828
interactions with protons, SU(3) predictions for, 20: 17412
monitoring in Plowshare tests, radiological telemetering system for, 20: 16160 (UCRL-14739(Pt.2))
monitoring in steam condensate, 20: 16825 (ORNL-TM-1442)
production by 160-Mev proton bombardment of water, spectra from, (E), 20: 17158(R) (ORNL-3900, pp 82-149)
production in neutron interactions with protons, 20: 17413
reactions (γ,n) with nuclei, neutron production for activation analysis in, 20: 16332 (GA-6691)
reactions (γ,n) with carbon-12 at 18 to 37 Mev, energy levels from, (E), 20: 17773
reactions (γ,n) with aluminum-27 at 13 to 37 Mev, energy levels from, (E), 20: 17773
reactions with lead, 7.3-Mev level excitation in, (E), 20: 17842
use for therapy of scalp carcinoma, 20: 16308
use in reactor power control and measurement, 20: 18033

GAMMA SHIELDING
calculation of, design of device for, 20: 17969
thickness of lead, 20: 17963(T) (ORNL-tr-1059)
thickness of water, 20: 17964(T) (ORNL-tr-1061)

GAMMA SOURCES
activity of, devices for measuring, 20: 16505 (BNL-949)
content in atmosphere and surface waters at Portsmouth Gaseous Diffusion Plant, 1965, 20: 16726 (GAT-506)
development of portable, 20: 18182
fabrication of sealed cesium-137, method for, 20: 16335(R) (NBS-TN-276)
loss in defectoscopic field work, exposure hazard from, 20: 16764
use of tin-119m-labeled palladium–tin alloy for use as, 20: 16335(R) (NBS-TN-276)

GAMMA SPECTRA
analysis of, use of computer program and scintillation detector in, 20: 16344

GAMMA SPECTROMETERS
design of beta-gamma-gamma coincidence sum, for activation analysis, 20: 16335(R) (NBS-TN-276)
design of coincidence-counting, for oceanography studies, 20: 16828 (TID-22763)
design of drift-free, 20: 16335(R) (NBS-TN-276)
design of Mössbauer, 20: 16872
development and performance of lithium-drifted germanium, 20: 16159(R) (ORNL-3900, pp 150-81)
performance of scintillation, for absolute activity measurements, 20: 16858
pulse height analyzers for, design of auxiliary electronics for, 20: 16817 (JUL-270-RB)
use in determining americium-241 and plutonium-239 in living tissues, 20: 16864

GAMMA SPECTROSCOPY
detectors for, lithium-drifted germanium, 20: 16160 (UCRL-14739(Pt.2))
detectors for, performance of lithium–drifted germanium, (E), 20: 17158(R) (ORNL-3900, pp 82-149)
milk condensation equipment for, 20: 16741(R) (UCRL-14534, pp 54-6)

GARIGLIANO POWER REACTOR
development of, review of, 20: 18104

GAS COOLED REACTORS
control of, effects of cladding and coolant temperature on, 20: 18105
cooling cycle limitations in Magnox, 20: 18109
fission-product release from advanced, control of, (E), 20: 18110
fuel cost optimization for, 20: 18020(R) (ORNL-3900, pp 2-81)
fuel element failure in, detection systems for, 20: 18036

GAS FLOW
magnetohydrodynamic, Rayleigh problem in, (T), 20: 17512
magnetohydrodynamic, ultrasonic, (T), 20: 17513
magnetohydrodynamic, plane steady, (T), 20: 17515
magnetohydrodynamic, Hall effect in axial-symmetric, (T), 20: 17521
magnetohydrodynamic, around bodies, (T), 20: 17525
magnetohydrodynamic, with orthogonal magnetic and velocity field distributions, (T), 20: 17532

GAS HILLS AREA (WYO.)
carbon-13 content of calcite in epigenetic pyrite of, 20: 16675

carbon, oxygen, and sulfur isotope ratios in uranium deposits in, 20: 16670
GASEOUS DIFFUSION PLANTS
environs monitoring at Portsmouth, 1965, 20: 16726 (GAT-506)
GASEOUS DIFFUSION PROCESS
cascades in, calculations of squared-off, 20: 16929
model of, 20: 17158(R) (ORNL-3900, pp 82-149)
GASES
effects on small particles, thermal-force, (T), 20: 16606(R) (TID-22621)
electric arc structure in flowing, at low pressures, (E), 20: 17517
electric discharges in, microwave measurements of electron density in, (E), 20: 17510 (IPP-3/25)
electric discharges in, properties of h-f, (E/T), 20: 17879 (LRP-19/65)
electron diffusion in ionized, second-order, (T), 20: 17529
energy levels of charged Bose, ground-state, (T), 20: 17526
energy partitions in mixed, model of, 20: 16159(R) (ORNL-3900, pp 150-81)
hydrodynamic equations for superfluid Fermi, 20: 17647
hydrogen ion reactions with, electron spectra from, (E), 20: 17292
laser beam reactions with, breakdown and heating in focused, 20: 17531
light emission from theta-pinch discharges in dense, (E), 20: 17523
shock propagation in, properties of ionizing, (T), 20: 17511 (NP-15894)
shock wave propagation in, microwave measurement of electron density in, (E), 20: 17510 (IPP-3/25)
spectra of, over deuterated and normal sulfuric acid, 20: 16442
stability of discharge, wave-interaction model for diocotron effect in, 20: 17916
thermodynamics of electron, 20: 17530
virial coefficients for, equations of state from, 20: 17527
gas–solid, efficiency as working fluid in Brayton cycle, (T), 20: 16606(R) (TID-22621)
GASTROINTESTINAL TRACT
copper-64 uptake by rat, 20: 16182
strontium-85 uptake from human, effects of sodium alginate on, 20: 16173 (PG-Report-686)
GEIGER-MUELLER TUBES
counting characteristics of, at high intensities, 20: 16884
use in personnel alarm dosimeters, 20: 16831(R) (UCRL-14534, pp 28-31)
GENES
metabolism by developing embryo, control of, 20: 16172(R) (NYO-2194-1)
suppressor activity of, mechanism in Drosophila for, 20: 16229(R) (NYO-1472-1)
GENETICS
effects on experimental error in radiobiology, 20: 16164
radiation effects on jute, γ, 20: 16218 (AECD-AG-12)
GEOCHEMISTRY
chemical evolution and organic, 20: 16633 (UCRL-16605)
of argon, calcium, lead, potassium, rubidium, strontium, thorium, and uranium, comparative, 20: 16715
rubidium–strontium ratio in geological materials, differentiation of Earth's mantle by studying, 20: 16711(R) (MIT-1381-13)
rubidium-87 decay in geological materials, 20: 16711(R) (MIT-1381-13)
GEOLOGY
book: *Applied Geochronology*, 20: 16715
GEOMAGNETIC FIELDS
charged-particle motion in, (T), 20: 17540 (N-65-18914)
conference, 20: 17550
disturbances in, hourly values of equatorial Dst for, (E), 20: 17543
disturbances in, latitudinal and seasonal dependences of, 20: 17556
electrons in solar-geomagnetic cavity, bombardment of lunar surface by, 20: 17246
intensity variations during IGY, ring current, 20: 17544
intensity variations during IGY, quiet-day, (E), 20: 17545
intensity variations during auroral storms over South Pole, 20: 17554
intensity variations in north polar region, diurnal, 20: 17555
interactions with solar corpuscular stream, (T), 20: 17547(T)
interactions with solar plasma, (E), 20: 17551
ion currents in, from ionospheric dynamo theory, 20: 17553
mapping in north polar region with corrected latitude, 20: 17555
pulsations in initial phase of magnetic storms, stable, (T), 20: 17549(T)
solar wind interactions with, (T), 20: 17232
GEOMAGNETIC STORMS
geomagnetic field pulsations in initial phase of, stable, 20: 17549(T)
intensity of, hourly values of equatorial Dst for, (E), 20: 17543
GERMAN REACTORS
development of, policy for, 20: 18111
development of, review of, 20: 18104
fuel elements for AEG, development of, 20: 18077
GERMANIUM
fabrication of diodes of, for gamma detection, 20: 16890
gamma attenuation coefficients for, (T), 20: 17962 (ORNL-TM-1237)
ionization spectra of recoil atomic, energy dependence in germanium for, (E), 20: 17265
neutron reactions at 0.4 to 18.6 Mev, germanium recoil atom ionization spectrum from, (E), 20: 17265
performance of lithium-drifted, for gamma spectroscopy, 20: 16160 (UCRL-14739(Pt.2))
radiation effects on electronic energy levels in p-type, electron-beam, 20: 17142
radiation effects on p-type, electric conductivity and Hall Effect from electron, 20: 17144
radiation effects on electric conductivity and dimensional stability of n- and p-type, electron, (E), 20: 17145
radioinduced dimensional instability in high-purity single-crystal, electron, (E), 20: 17136
use of lithium-drifted detectors of, in neutron activation analysis, 20: 16888
GERMANIUM ALLOYS
Cr–Ge–Nb, phase studies on intermetallic compounds in, 20: 17075
Cu–Ge, radiation effects on viscous dislocation damping in dilute, gamma, 20: 17138
Ge–Ta–V, phase studies on intermetallic compounds in, 20: 17075
GERMANIUM ISOTOPES Ge-77
sensitivity for activation analysis using beta-gamma-gamma sum-coincidence gamma spectrometer, 20: 16335(R) (NBS-TN-276)
GERMANIUM SYSTEMS
Ge–Si–V, superconductivity of solid solutions in, 20: 17043
GERMANY
cesium-137 content in residents of, 1965, 20: 16303(R) (AD-626384)
monitoring ground air in, 1961 to 1963, 20: 16766
stable isotope production and uses in, 20: 16933
GIBBERELLIC ACID
radiation effects on synthesis of, in *E. coli*, 20: 16193 (EUR-2539.i)
GLACIERS
age estimation of polar caps by radioisotope abundances in, 20: 16686
GLASS
cesium loss from waste sludge-containing, during firing, 20: 18166(R) (TID-22531)
cleaning dosimeters of, method for, 20: 16847
composition of waste sludge-containing, chemical analysis of, 20: 18166(R) (TID-22531)
ion exchange and sorption of radionuclides on, effects of solution concentration on, 20: 16469
leaching of radioactive waste-containing, aqueous, 20: 18166(R) (TID-22531)
magnetic flux jumping in superconducting indium-impregnated, field sweep-rate and temperature dependence of, (E), 20: 17604
phosphorescence of containers of, in liquid scintillation counters, 20: 16863
radiation effects on corrosion of, containing cesium and strontium, (E/T), 20: 18166(R) (TID-22531)
waste fixation in, simulation studies of, 20: 18166(R) (TID-22531)
waste incinerator ash fixation in, 20: 18166(R) (TID-22531)
GLOBULIN
isolation by zonal centrifugation, 20: 16159(R) (ORNL-3900, pp 150-81)
radiation effects on electric conductivity in gamma, 20: 16194
radiation effects on human gamma, 20: 16212
radiation effects on absorption of foreign, by rabbits, γ, 20: 16214 (AD-620438)
radiation effects on mouse, fractionated-dose x, 20: 16224 (CEA-R-2848)
GLOW DISCHARGES
propagation in hydrogen, structure between tube wall and cathode, (E) 20: 17524
GLUCOSE
metabolism by developing embryos, 20: 16172(R) (NYO-2194-1)
radiation effects on oxidation of, in *Vibrio cholerae*, 20: 16198
radiation effects on rat intestinal metabolism of, x, 20: 16274
synthesis of 3,4-carbon-14-labeled, from carbon-14-labeled pyruvates, 20: 16193 (EUR-2539.i)
GLUCOSE PHOSPHATES
hydrolysis of, effects of metal ions and metal chelates on, 20: 16421
GLUTAMIC ACID
radiation effects on oxidation of, in *Vibrio cholerae*, 20: 16198
GLUTARIC ACID, 2-OXO-
radiation effects on oxidation of, in *Vibrio cholerae*, 20: 16198
GLYCEROL
radiosensitivity effects on yeasts, α and x, 20: 16231 (UCRL-16377)
GLYCINE
radiation effects on crystals of deuterated, controlled-temperature ESR spectral studies on, 20: 16525
GLYCOGEN
metabolism by developing embryos, 20: 16172(R) (NYO-2194-1)
GOLD
analysis for oxygen, activation, 20: 16331 (GA-6568)

carbon ion reactions at 9.7 Mev, charge-exchange cross sections and ionization from, (E), 20: 17724
density of thin films of, 20: 17070
determination of, design of narrow-band detector for, 20: 16823 (NYO-3160-1)
iodine-127 reactions at 51 Mev, effect of channeling on radiation damage from, (E), 20: 17146
metabolism in rats, 20: 16160 (UCRL-14739(Pt.2))
performance of foils of, in neutron radiography, 20: 16619
solvent properties for rare earth metals, 20: 17016 (IS-1175)

GOLD ALLOYS
Au–Mn, crystal structure of Au_3Mn, 20: 17066
Au–Pd, effects on isotopic exchange between methane and deuterium at 90 to 200°C, catalytic, 20: 16457
Au–Sn, superconductivity properties of thin composite films of, 20: 17601
Au–Yb, phase studies, 20: 17016 (IS-1175)

GOLD ISOTOPES Au-197
half life of isomeric, from neutron reactions (n,n′), (E), 20: 16336(R) (NYO-10175)
isomeric transitions in, conversion coefficients and multipolarity of, (E), 20: 17812
neutron reactions (n,n′), activation cross section for, (E), 20: 16336(R) (NYO-10175)
neutron reactions (n,γ), threshold cross section and energy for, 20: 16335(R) (NBS-TN-276)
production of isomeric, (E), 20: 17812
proton fission at 150 to 660 Mev, cross sections for, (E), 20: 17838
proton reactions (p,d) at 57 Mev, energy spectra from, (E), 20: 17725

GOLD ISOTOPES Au-198
metabolism in rats, 20: 16160 (UCRL-14739(Pt.2))

GONADS
shielding of male, during diagnostic radiography, 20: 16321

GRANITES
age of Massachusetts, rubidium–strontium and strontium-87/-86 estimation of, 20: 16711(R) (MIT-1381-13)

GRAPHITE
analysis for silicon, interferences in activation, 20: 16360
crushing in ball mills, 20: 16957(T) (LA-tr-66-11)
deformation properties of pyrolytic and single-crystal, 20: 17028(R) (TID-22733)
diffusion of metals in pyrolytic, at 1450 to 1950°C, 20: 17107
elastic constants of pyrolytic, methods for measurement of, 20: 17028(R) (TID-22733)
electron transmission at 53 Mev, energy loss and half width from, 20: 17970
emissivity and reflectivity at 2100 to 3700°K, 20: 17021 (N-65-18607)
mechanical properties of pyrolytic and single-crystal, apparatus and methods development for measuring, 20: 17027(R) (TID-22712)
neutron decay constants in, pulsed, (T), 20: 17662
neutron diffusion parameters of, pulsed and static, (E/T), 20: 17661
neutron spectra in, thermal, (E/T), 20: 18127(R) (GA-6753(Pt.1))
particle shape of, pulverized by hammer mills, 20: 16958(T) (LA-tr-66-12)
particle shape of, pulverized by cutter mills, 20: 16956(T) (LA-tr-66-6)
particle size distribution and shape of pulverized, effects of pulverizing method and time on, 20: 16955(T) (LA-tr-66-5)
production of reactor-grade, 20: 17002
production of single-crystal, 20: 17028(R) (TID-22733)
properties as reactor fuel material, 20: 18182
properties of, review of methods for determining, 20: 17079
radiation effects on joints in, fast-neutron, 20: 17119 (GAMD-6789)
radiation effects on particles coated with, in carbonized pitch matrix, fast-neutron, 20: 17119 (GAMD-6789)
radiation effects in boronated, fast- and thermal-neutron, 20: 17116 (BNWL-199)
radiation effects on desorption on surface of, in carbon dioxide, carbon monoxide, and methane, 20: 17114 (AERE-R-5163)
radiation effects on crystal structure of, x-ray studies of neutron, 20: 17130
reactions with manganese, composition and structure of carbides formed by, 20: 17030(T) (LA-tr-66-1)
reactions with niobium oxides at 1400 to 1600°C, 20: 16483
spectra of hot-pressed, optical, 20: 16159(R) (ORNL-3900, pp 150-81)
structure of, methods for characterization of, 20: 17028(R) (TID-22733)
testing helical-screw expanders and compressors of, 20: 16591 (UCRL-14660)

GRAPHITE (IMPREGNATED)
development of spherically shaped, 20: 18020(R) (ORNL-3900, pp 2-81)
processing irradiated for fuel recovery, 20: 18020(R) (ORNL-3900, pp 2-81)

GRAPHITE MODERATED REACTORS
control of gas-cooled, effects of cladding and coolant temperature on, 20: 18105

GRASS
radioactive particle deposition on pasture, rate of, 20: 16160 (UCRL-14739(Pt.2))

GRAVITATION
effects on free electrons and negative ions, measurement of, 20: 17167
electron interactions with gravitons, Reggeization in field theory for, 20: 17476
energy transport by, Einstein field equations for, 20: 17579
energy-momentum tensors for continuous media in general relativity for, 20: 17566
field equations for, Lagrangian density of non-Einsteinian, 20: 17568(T)
fields in vacuum, uniqueness of central-symmetric, (T), 20: 17582
graviton exchange in scalar-particle interactions, peratization of, (T), 20: 17503
interaction potential energy in relativity theory, 20: 17574
interactions with electromagnetic fields, 20: 17580
measurement of, fundamental-length hypothesis for minimum uncertainty in, 20: 17573
measurement of, pendulum gravimeter for, (E), 20: 17583
particle motion in Schwarzschild field, 20: 17569
production and detection of waves of, technique for, 20: 17567(T)
spinor field equation in presence of, Heisenberg nonlinear, 20: 17565
theory of congruence in fields of, geodesics and red shift from, 20: 17562
theory of congruence in fields of, 20: 17563

GREAT BRITAIN
fallout monitoring in atmosphere and rain water in, 1964–65, 20: 16660 (AERE-R-4997)

GREENLAND
geological investigations in, 20: 18174(R) (NP-15771)

GROUND WATERS
flow velocities and radioactive decay in Shoal Event, hazards from, 20: 16742 (VUF-1014)
isotopic composition of Mexican, responsible for lead–zinc deposits, 20: 16634

GROWTH
effects of rare earths and yttrium on, of bacteria, fungi, molds, and yeasts, 20: 16191
effects of serum and temperature on cultured mammalian-cell, 20: 16298

GUANIDINE
nitroso-, mutations induced in algae by, patterns of expression of, 20: 16294

GUINEA PIGS
radiation effects on skin pigments in, uv, 20: 16261

H

HAFNIUM
determination in zirconium, activation, 20: 16335(R) (NBS-TN-276)
determination of polarographic, 20: 16445
effects on hydrolysis of adenosine-2-phosphate and carboxylase, catalytic, 20: 16420
polarographic behavior in aqueous-alcohol solutions, 20: 16445
specific heat, (T), 20: 17084

HAFNIUM ALLOY COUPLES
Hf–Ta/Ta–W, fabrication by roll cladding and hot spinning, rocket nozzle, 20: 16943(R) (IITRI-B237-45)

HAFNIUM ALLOYS
Al–Hf–Mo, phase studies on intermetallic compounds in, 20: 17075
Hf–Ta, diffusion into tantalum–10 tungsten alloy, effects of niobium and tantalum barriers on, 20: 16943(R) (IITRI-B237-45)
Hf–Ta, phase studies, 20: 17092
Hf–Ta–W, fabrication of tubing of T-111, 20: 16998
Hf–Ta–W, phase studies at 1100 and 1600°C, 20: 17012(R) (DRI-1092-226)

HAFNIUM ISOTOPES Hf-177
energy levels of, half life of $^{25}/_2$ rotational, (E), 20: 17811

HAFNIUM ISOTOPES Hf-181
beta decay of, gamma polarization in, (E), 20: 17444(T)

HAFNIUM NITRIDES
HfN–NbC–NbN, superconducting properties, 20: 17589 (CONF-650922, pp 541-9)

HAFNIUM OXIDES
mechanical and thermal properties of plasma-sprayed, 20: 16943(R) (IITRI-B237-45)
HfO_2–Ta, development of composites of, by controlled oxidation of alloy, 20: 16943(R) (IITRI-B237-45)
HfO_2–W, mechanical and thermal properties of plasma-sprayed composite layers of, 20: 16943(R) (IITRI-B237-45)
HfO_2–Y_2O_3, mechanical and thermal properties of plasma-sprayed, 20: 16943(R) (IITRI-B237-45)

HAFNIUM SYSTEMS
C–Hf–Mo, superconducting transition temperature of $Mo_{0.98}Hf_{0.08}C_{0.75}$,

20: 17607
HAIR
analysis for sulfur, radiation exposure determination from, 20: 16758
radiation effects on growth of, effects of estrogen on uv, in cases of total baldness, 20: 16248
radiation effects on growth of animal, protective effects of sulfur compounds against, 20: 16297(R) (EUR-2548.f)
HALL EFFECT
effects on magnetohydrodynamic boundary layers, 20: 17534
measurement for superconducting magnets, 20: 17600(R) (ORNL-3908, pp 114-48)
use in determination of magnetic median plane in cyclotrons, 20: 17189 (CONF-650922, pp 421-7)
use in measurement of magnetic fields, 20: 17191 (CONF-650922, pp 447-55)
use in measurement of magnetic fields, method of, 20: 17193 (CONF-650922, pp 472-5)
use in measurement of gradient magnetic fields, 20: 17194 (CONF-650922, pp 483-6)
HALOGEN COMPOUNDS
with pyridine, preparation of, 20: 16416(R) (NYO-906-68)
HALOGENS
effects on infrared and Raman spectra of imidazole, 20: 16499
reactions with alkali metals, stripping effects in, 20: 17158(R) (ORNL-3900, pp 82-149)
reactions with alkali metal atoms, (E/T), 20: 17295
HAMBURG ELECTRON SYNCHROTRON
magnetic fields in beam transport systems of, semiautomatic system for, 20: 17192 (CONF-650922, pp 456-66)
magnets for, design of, 20: 17213(T) (UCRL-Trans-1312)
HAMSTERS
radiosensitivity of cultured cells of, effects of serum and temperature on, 20: 16298
HANDBOOKS AND MANUALS
for capsule irradiation experiments at NRTS, 20: 18135 (IDO-17135)
for standard nuclear instrument modules, 20: 16779 (PPAD-584D)
on analytical procedures, 20: 16337 (RMO-3001(Rev.1)(Suppl.))
HANDS
radiation effects on bones of, following eczema therapy, 20: 16210
HANFORD PRODUCTION REACTORS (N)
ventilation system of, penetration seals for, 20: 18125 (RL-SA-25)
HARDTACK OPERATION
rhodium-102 distribution from, atmospheric, 20: 16662(R) (HASL-165)
HASTELLOY C
corrosion of weldments of, effects of silicon content on intergranular, 20: 16983
HEAD
radiotherapy of carcinoma of scalp, 20: 16308
radiotherapy of, tumorigenic effects of, 20: 16245
HEALTH PHYSICS
activities at ORNL, 1964, 20: 16159(R) (ORNL-3900, pp 150-81)
gamma source loss in field work, exposure hazard from, 20: 16764
program for reactor maintenance, 20: 16757
programs at Risö, 20: 18174(R) (NP-15771)
HEART
acetylcholinesterase activity in vagal preparations of frog, effects of alkali metal ions on, 20: 16160 (UCRL-14739(Pt.2))
radiation effects on transplanted Yoshida sarcoma cells in rat, tracer study, 20: 16188
HEAT
performance of tungsten, in vacuum at 2273 to 3233°K, 20: 16596
HEAT EXCHANGERS
development of, review of, 20: 18182
performance in sodium-cooled reactors, computer analysis of, 20: 18093(R) (UNC-5142)
HEAT OF FUSION
determination from binary system phase diagram, 20: 16711(R) (MIT-1381-13)
HEAT-RESISTING ALLOYS
melting and casting of, design of furnace for, 20: 16965
properties of cobalt- and nickel-base eutectic, effects of additives on, 20: 17108
testing in high-velocity potassium vapor, 20: 18020(R) (ORNL-3900, pp 2-81)
HEAT TRANSFER
ablation measuring device for reentering bodies, 20: 16778 (NASA-TN-D-3329)
analysis in two-phase steady-state flows, 20: 16601(R) (GEAP-5067)
analysis in two-phase water flows, 20: 16605 (NYO-3304-8)
boiling burnout in uniformly heated tubes, forced convection, (E), 20: 16603 (NYO-187-7)
boiling transition in finned fuel rods, geometrical effects on, (E), 20: 16602(R) (GEAP-5081)
by fuel elements with polyzonal spiral finning, 20: 18078
coefficients for, in gas–solid systems, (E), 20: 16606(R) (TID-22621)
in boiling two-phase annular flow, analysis of liquid film from, (T), 20: 16604 (NYO-3114-13)
in forced flow three-rod test sections, film and transition boiling, (E/T), 20: 16602(R) (GEAP-5081)
in helium, organic coolants, and water, research on, 20: 18174(R) (NP-15771)
in liquid metal turbulent flow, annulus eccentricity effects on, 20: 16612
in reactor cooling systems, by forced convection, 20: 16607 (TID-22663)
in suspensions, effects of thermal plate-out on, (T), 20: 16606(R) (TID-22621)
research programs on reactor, 20: 18020(R) (ORNL-3900, pp 2-81)
HEAT TRANSFER SYSTEMS
design and instrumentation of electric superheated, 20: 16609
design for shipping radioactive materials, 20: 18165 (ORNL-P-1987)
operation of sodium natural convection, properties of, 20: 16611
HEAVY WATER REACTORS
control elements for plutonium-fueled, thermal, power breeder, 20: 18115
control systems for, design using numerical data processing, 20: 18038
description of National Bureau of Standards, 20: 16335(R) (NBS-TN-276)
fuel distribution for flat flux in natural uranium slab, (T), 20: 18058
neutron flux distribution in organic-cooled, hyperfine structure of thermal, 20: 18055
HELIUM
abundance in primeval universe, (T), 20: 17245
abundance of primeval, (T), 20: 17245
content in magnetites, determination and origin of, 20: 16714
dispersion relation in liquid, 20: 16461
electric discharges in, pre-breakdown current in, (T), 20: 17520
electron capture by monovalent helium ions in, (E), 20: 17304
electron reactions with, Born approximation of cross sections for, 20: 17258
flow of superfluid liquid II, in porous media, 20: 17644
helium ion energy losses in, (E), 20: 17305
helium ion reactions in, electron capture in, (T), 20: 17276
hydrogen condensation on surfaces cooled by liquid, 20: 16631
hyperon (Σ^-) reactions with, resonance baryon production in, (E/T), 20: 17158(R) (ORNL-3900, pp 82-149)
ion motion in liquid II, second-sound attenuation associated with hot, (E), 20: 17615
ionic mobility of cesium and rubidium in, at high pressures, (E/T), 20: 16415 (CEA-R-2861)
liquid motion in films of liquid II, third-sound effects of normal, (T), 20: 17616
molecule scattering by atomic, deuterium and hydrogen, 20: 17293
phonon specular reflection in superfluid, (E), 20: 17648
photon reactions with Coulomb field of, pair production total cross sections for high-energy, (T), 20: 17754
pinch discharge in high-density, θ, 20: 17945
production in meson (π) reactions with emulsion nuclei at 17.5 Bev, cross sections for, (E), 20: 17716
properties and dipole spectrum of, (T), 20: 17272
proton reactions at 0.03 to 10 Mev, cross sections for electron capture in, (T), 20: 17274
radio wave emission from plasma of, negative-absorption effects on anomalous bremsstrahlung and cyclotron, (E), 20: 17921
radioinduced formation of bubbles of, in stainless steel, 20: 17141
reactions of atoms of, with argon, helium, hydrogen, and nitrogen, (E), 20: 17301
reactions with helium atoms, charge transfer and ionization in, (E), 20: 17301
relaxation in superfluid, (T), 20: 17640
relaxation processes in rotating liquid II, effect of temperature changes on, (E), 20: 17643
separation of reactor-coolant, from carbon monoxide and hydrogen, model of, 20: 16556(R) (ORNL-TM-1090)
sound dispersion in liquid II, (T), 20: 17611(T)
sound wave propagation in superfluid, equations for, (T), 20: 17640
spectra and structure of diatomic molecule of, 20: 16452
spectra of plasma of, recombination lines in, (T), 20: 17952
use of liquid, in neutron time-of-flight polarimeters, 20: 16876
vortex formation in rotating, during phase transition, (E), 20: 17641
vortex lines in rotating liquid II, relaxation of Onsager-Feynman, (E), 20: 17642
HELIUM IONS
electron capture by monovalent, in helium, (E), 20: 17304
energy losses in helium, (E), 20: 17305
reactions in helium, electron capture by, (T), 20: 17276
reactions with stellarator stainless steel wall, re-emission rates for, (E), 20: 17922
HELIUM ISOTOPES
abundance in Achilles, LaLande, and Peace River chondrites, 20: 16672

HELIUM ISOTOPES He-3
- binding energies in compound nucleus systems, 20: 16331 (GA-6568)
- content in primary cosmic radiation, 20: 17324
- determination using gas chromatography, 20: 16348
- deuteron reactions (d,p) at 310 to 2935 kev, tensor and vector polarization effects on, (E), 20: 17749
- deuteron reactions (d,p), with, asymmetry and polarization relation in structure of, (T), 20: 17770
- proton elastic scattering at 0.125 to 1 Mev, helium-4 levels from, (E), 20: 17771
- reactions (He-3,α) with calcium-40 and oxygen-16, optical-model analysis of, (T), 20: 17696 (UR-875-65)
- reactions (He-3,α) with boron-11 at 3.5 Mev, boron-10 4.77- and 5.16-Mev levels from, (E), 20: 17761
- reactions (He-3,α) with carbon-12, oxygen-16, and sulphur-32 at 12.1 Mev, energy levels from, (E), 20: 17780
- reactions (He-3,d) with nickel-62 at 22 Mev, angular distributions from, (T), 20: 17692 (ORNL-TM-1414)
- reactions (He-3,n) with beryllium, boron, and lithium for neutron production for activation analysis, 20: 16332 (GA-6691)
- reactions with nuclei, sensitivities for activation analysis, 20: 16331 (GA-6568)
- reactions with nuclei at 12 Mev, Q values for, 20: 16331 (GA-6568)
- scattering by oxygen-16, optical-model analysis of, (T), 20: 17696 (UR-875-65)
- spectra of liquid, resonance lines in, (T), 20: 17638
- use in activation analysis, sensitivities for, 20: 16331 (GA-6568)
- ^{3}He–^{4}He, fourth sound in liquid, 20: 17159(T)
- He-3–He-4, use for obtaining very low temperatures, 20: 17599 (JINR-P-2480)

HELIUM ISOTOPES He-4
- content in primary cosmic radiation, 20: 17324
- energy levels from proton scattering by helium-3, (E), 20: 17771
- particle Slater sum at 2 to 273°K, path-integral calculation of two-body, 20: 17613
- photodisintegration cross section for, velocity-dependent potential for, (T), 20: 17774
- proton reactions (p,2p) at 140 Mev, energy spectra and angular correlation distributions from, (E), 20: 17741
- reactions (He-4,4n) with neodymium-142, angular momentum effects on excitation functions for, (E), 20: 17784
- spectra of liquid, resonance lines in, (T), 20: 17638
- ^{3}He–^{4}He, fourth sound in liquid, 20: 17159(T)
- He-3–He-4, use for obtaining very low temperatures, 20: 17599 (JINR-P-2480)

HELIUM ISOTOPES He-6
- beta decay of, energy and lifetime values and nuclear matrix elements for, (T), 20: 17732

HELIUM ISOTOPES He-8
- mass, (E), 20: 17794

HELIUM SYSTEMS
- He–H, atomic-resonance line-oscillator strengths in T-tube plasma of, (E), 20: 17932
- He–H, thermal diffusion in, 20: 16468

HEMOGLOBIN
- compound with hydrocyanic acid, iron-57 Mössbauer absorption spectra of, 20: 18009

HEPTANE
- tritium exchange with tritiated ethyl malonate, effects of catalysts on, 20: 16492

HETEROCYCLIC COMPOUNDS
- effects on solvent extraction of europium using benzoyltrifluoroacetone, 20: 16565

HETEROGENEOUS REACTORS
- kinetics of water cooled, 20: 18050(R) (STL-372-22)
- neutron and multiplication factor in, heterogeneity effects on, (T), 20: 18063
- neutron spectra in, computer program for, 20: 18047 (KR-78)

HEXANE
- radiolysis of, at 77°K, ESR studies of, 20: 16511
- hexane–SiO_2, radiolysis of, at 77°K, ESR studies of, 20: 16511

HIGH ENERGY INJECTION DEVICES
- development, 20: 17890(R) (ORNL-3908, pp 100-7)
- development of DCX–1 and DCX–2, 20: 17158(R) (ORNL-3900, pp 82-149)
- plasma heating in, properties of electron cyclotron, (E/T), 20: 17888(R) (ORNL-3908, pp 32-51)
- plasma properties in DCX-2, determination of, (E/T), 20: 17887(R) (ORNL-3908, pp 18-31)
- plasma stability in, (T), 20: 17891(R) (ORNL-3908, pp 108-13)
- plasma stabilization in DCX-1, (E/T), 20: 17886(R) (ORNL-3908, pp 1-17)

HIGH TEMPERATURE GAS COOLED REACTOR EXPERIMENT
- fuel element development for, coated-particle, 20: 18098

HIROSHIMA
- atomic explosions at, free-field radiation dose from, 20: 16760
- diabetes incidence in residents of, exposed to radiation from atomic bomb, 20: 16254
- gamma emissions from roof tiles in, thermoluminescent dosimetry of, 20: 16759
- health of population exposed to atomic bomb at, 20: 16271
- radiation exposure of residents of, survey, 20: 16272

HOLMIUM
- determination by neutron activation and ion-exchange chromatography, 20: 16363
- magnetic properties of polycrystalline, 20: 17098
- magnetostriction in antiferromagnetic, ferromagnetic, and paramagnetic regions, (E), 20: 18012
- preparation of self-supporting radiation targets of, 20: 17218

HOLMIUM ALLOYS
- Ho–Fe, crystal structure of Ho_6Fe_{23} and Ho_2Fe_{17} in, 20: 17096(T)
- Ho–Hg, crystal structure of $HoHg_3$, 20: 17060
- Ho–Mn, crystal structure of Ho_6Mn_{23} in, 20: 17096(T)
- Ho–Tl, crystal structure of $HoTl_3$, 20: 17060

HOLMIUM COMPLEXES
- with phenanthroline, infrared spectra of, 20: 16436
- with 2,2′-bipyridyl, infrared spectra of, 20: 16437

HOLMIUM HYDRIDES
- properties and structure, 20: 16453

HOLMIUM ISOTOPES Ho-157
- half life, (E), 20: 17808

HOLMIUM ISOTOPES Ho-159
- decay of, conversion electron spectra from, (E), 20: 17685 (JINR-P-2497)

HOLMIUM ISOTOPES Ho-165
- neutron capture by, conversion-electron spectrum from thermal, 20: 17822

HOLMIUM OXIDES
- determination in thorium oxide by emission spectroscopy, 20: 16393
- Ho_2O_3–SrO, properties of compounds formed by interactions in, 20: 17044

HOLMIUM SULFATES
- effects on orthohydrogen–parahydrogen conversion at 77°K, catalytic, 20: 16454

HOLMIUM SULFIDES
- Ho_2S_3–YbS, compound formation in, 20: 16431

HOMOGENEOUS REACTORS
- design using aqueous fuel solution and catalytic recombiner, 20: 18075(P)
- development of single-zone circulating suspension, 20: 18072
- maintenance of IIT, health physics program for, 20: 16757

HORMONES
- radiation effects on urinary content of dehydroepiandrosterone, use in determining radiation response, 20: 16209

HORNBLENDE
- pleochroic halos in, dimensions and relation to α rays in radioactive elements, 20: 16666(T) (ORNL-tr-923)

HYDRIODIC ACID
- effects on peptization of solid thorium oxide, mechanism of, 20: 16419(T) (UCRL-Trans-1301(L))

HYDROBROMIC ACID
- effects on peptization of solid thorium oxide, mechanism of, 20: 16419(T) (UCRL-Trans-1301(L))
- radiolysis of solid polycrystalline, hydrogen yields in γ, 20: 16519

HYDROCARBONS
- alpha-particle ranges in vapors of, at 1 to 8 Mev, (E/T), 20: 17277
- determination in fuel burnup test assemblies, methods for, 20: 17155(R) (ORNL-3900, pp 82-149)

HYDROCHLORIC ACID
- effects on peptization of solid thorium oxide, mechanism of, 20: 16419(T) (UCRL-Trans-1301(L))
- effects on uranium sorption by platinized carbon, 20: 16581
- radiolysis of solid polycrystalline, hydrogen yields in γ, 20: 16519
- reactions with rare earth oxalates, thermal decomposition of products from, 20: 16446
- reactions with rare earth oxalate hydrates, 20: 16447
- reactions with rare earth oxalate hydrates, 20: 16448
- separation of uranium from, by solvent extraction using trioctylamine, 20: 16391
- bis(2-ethylhexyl) phosphate–HCl–toluene, extraction constants for americium, californium, curium, and fermium in, 20: 16404
- bis(2-ethylhexyl) phosphate–HCl–toluene, solvent properties for californium, fermium, and mendelevium, 20: 16404

HYDRODYNAMICS
- numerical analysis in, rezoning code for Lagrangian, 20: 18173 (LA-3455)

HYDROFLUORIC ACID
- reactions with plutonium dioxide to prepare plutonium tetrafluoride, 20: 16463

HYDROGEN
alpha-particle ranges in, at 1 to 8 Mev, (E/T), 20: 17277
bremsstrahlung emission in infrared region from discharge plasma of, (E), 20: 17931(T)
condensation on liquid-helium-cooled surfaces, sticking coefficients of, 20: 16631
determination by isotopic dilution, 20: 16362
determination in solids by beta absorption, 20: 16356
deuterium exchange with liquid ammonia, catalytic effects of alkaline amides on, 20: 16444
effects on yields of hydrogen peroxide from radiolysis of water, 20: 16520
electric discharge in, space-charge controlled ionization growth in, (E), 20: 17518
electron elastic scattering by atomic, variational principle for, 20: 17271
electron scattering by atomic, cross sections for, (T), 20: 17286
energy level transitions in external electric field, anisotropy of radiative, (T), 20: 17282
energy levels of nonrelativistic atomic, de Sitter group $L_{4,1}$ for, (T), 20: 17263
energy levels of, Fock problem on, (T), 20: 17252 (JINR-P-2522)
fission-fragment energy degradation in, (E), 20: 17821
flow in tanks, boundary layer characteristics of liquid, 20: 17536
formation in reactions between rare earth dicarbides and water, 20: 17048
glow discharge propagation in, structure between tube wall and cathode, (E), 20: 17524
heat transfer in boiling, 20: 16610
ion velocity distribution in, in electric fields, (E), 20: 17298
laser-beam heating of gaseous, for thermonuclear reactions, 20: 17531
meson (π^-) capture by, probabilities for fine-structure-level, (T), 20: 17278
neutron scattering by molecular, cross sections and spectra for slow, (T), 20: 17664
neutron scattering by, computer program for thermal, 20: 17684 (JAERI-1085)
ortho–para conversion of, at 77°K, catalytic effects of gadolinium and holmium sulfates on, 20: 16454
partition function for partially ionized plasma of, (T), 20: 17935
photoionization cross sections for n = 1 to n = 15 states, tables of, (T), 20: 17251 (IAE-873)
photon reactions with Coulomb field of, pair production total cross sections for high-energy, (T), 20: 17754
proton reactions with atoms of, charge transfer in, (E), 20: 17302
proton reactions with atoms of, charge transfer in, (T), 20: 17303
proton reactions with atomic, resonant charge transfer in, (T), 20: 17264
radiation effects on reactions of atomic, in ethanol or methanol mixtures with naphthalene, 20: 16524
radiation effects on reduction of cobalt complexes by, in ethanol solutions, 20: 16526
radiation synthesis of, developments in, 20: 16506 (BNL-10020)
radioinduced addition to fumaric acid in single crystals of succinic acid, 20: 16537
reactions of excited atoms of, double-inelastic, (T), 20: 17290
reactions of, in isotopically mixed systems, forward and backward unidirectional rates of, electrode, 20: 16459
reactions with cupric oxide in fixed beds, kinetics of, 20: 16556(R) (ORNL-TM-1090)
reactions with helium atoms, charge transfer and ionization in, (E), 20: 17301
scattering of molecules of, by helium atoms, (E), 20: 17293
separation from helium by oxidation and sorption by molecular sieves, 20: 16556(R) (ORNL-TM-1090)
solubility in Zircaloy-2, effects of thermal cycling on, 20: 16981
spectra of plasma of, recombination lines in, (T), 20: 17952
symmetry group for atomic, Lorentz, 20: 17283
wave excitation in stationary magneto-acoustic plasma of, drift, (E), 20: 17949
yield from gamma radiolysis of solid polycrystalline hydrobromic and hydrochloric acids at 77°K, 20: 16519
yields from gamma radiolysis of benzene–methanol mixture, 20: 16530
yields from gamma radiolysis of water vapor, effects of cyclohexane scavenger on, 20: 16536
HYDROGEN ION CONCENTRATION
effects on plant uptake of divalent cations, 20: 16174(R) (RLO-1547-3)
effects on uranyl ion sorption by barley roots, 20: 16174(R) (RLO-1547-3)
HYDROGEN IONS
acceleration of negative, in U-120 cyclotrons, 20: 17224
decay of magnetically trapped fast, effects of hot electron plasma on, (E/T), 20: 17158(R) (ORNL-3900, pp 82-149)
dissociation of molecular, into neutral atoms, 20: 17253(R) (ORNL-3908, pp 90-9)
effects on reactions of sodium pyrophosphates with uranyl nitrates, 20: 16472
energy levels of diatomic molecular, eigenvalues of, (T), 20: 17264
energy levels of excited molecular, 20: 17253(R) (ORNL-3908, pp 90-9)
reactions of molecular, with gases, electron spectra from, (E), 20: 17292
reactions with stellarator stainless steel wall, re-emission rates for, (E), 20: 17922
velocity distribution in hydrogen in electric fields, (E), 20: 17298
HYDROGEN ISOTOPES H-4
energy levels from neutron inelastic scattering by tritium, (T), 20: 17769
HYDROGEN PEROXIDES
determination in irradiated water, polarographic, 20: 16327 (AAEC/TM-301)
radiolysis of, ESR spectra of trapped free radicals from, 20: 16512
yield from gamma radiolysis of alkaline solutions containing hydrogen and oxygen, 20: 16520
HYDROGEN SYSTEMS
D–H, thermal diffusion in, 20: 16468
He–H, atomic-resonance line-oscillator strengths in T-tube plasma of, (E), 20: 17932
He–H, thermal diffusion in, 20: 16468
HYDROLOGY
ground water flow velocities and radioactive decay in Shoal Event, hazards from, 20: 16742 (VUF-1014)
tracer studies on silts, computer program for processing data from, 20: 16632 (AAEC/TM-303)
HYDROMAGNETIC WAVES
propagation in bismuth single crystals, Landau and resonance damping of, (E), 20: 18011
properties in cylindrical Alfvén waveguides, terminal, (T), 20: 17522
HYPERFRAGMENTS
decay of $_{\Lambda}Be^{9}$, boron-9 production from, (T), 20: 17807
production and decay in nuclear emulsions, identification of, 20: 17796
production in meson (K⁻) reactions with emulsion nuclei at 3.0 and 5.0 Bev/c, (E), 20: 17752
HYPERONS
decay of, symmetry group for weak nonleptonic, (T), 20: 17455
decays of, models based on chiral U(3) ⊗ U(3) algebra for nonleptonic, 20: 17456
decays of, SU(3) ⊗ SU(3) for nonleptonic, (T), 20: 17448
interactions with nucleons in broken SU(3), sum rules for S-state amplitudes for, 20: 17468
symmetry for, electromagnetic form factors from, (T), 20: 17455
HYPERONS (Λ)
coupling constant in strangeness-changing beta decay, renormalization of axial-vector, (T), 20: 17458
interactions with hyperons (Λ), effect of Ξ-N channel on, (T), 20: 17389
production in hyperon (Ξ⁻) interactions with deuterons and protons at low energies, 20: 17389
production in meson (K⁻)-proton interactions, cross section and scattering length for, (T), 20: 17376
HYPERONS (Λ^0)
production in photon-proton interactions, quark model for, (T), 20: 17348 (JINR-P-2556)
HYPERONS (Σ^-)
reactions with helium, resonance baryon production by, (E/T), 20: 17158(T) (ORNL-3900, pp 82-149)
HYPERONS (Σ^0)
coupling constant in strangeness-changing beta decay, renormalization of axial-vector, (T), 20: 17458
polarization in meson (π^-) interactions with protons at 1.5 and 1.8 Bev/c, (E), 20: 17382
production in photon-proton interactions, quark model for, (T), 20: 17348 (JINR-P-2556)
HYPERONS (Σ^+)
decay of, parity-violating nonleptonic, (T), 20: 17398
HYPERONS (Ξ^-)
interactions with deuterons and protons at low energies, hyperon (Λ) production in, (T), 20: 17389
HYPOXANTHINE
effects on flavor of irradiated fish, 20: 16925

I

ICE
neutron diffusion parameters for, 20: 18020(R) (ORNL-3900, pp 2-81)
IMAGE BRIGHTNESS INTENSIFIERS
light pulse size distribution from noise and single photoelectrons, 20: 16824 (NYO-3406-3)
IMIDAZOLE

spectra of, effects of deuterium and halogens on infrared and Raman, 20: 16499
spectra of, effects of deuterium on infrared and Raman, 20: 16500

IMMUNE REACTIONS
radiation effects on, of Treponema antigens, γ, 20: 16199
radiation effects on, in rabbits, γ, 20: 16214 (AD-620438)

IN-PILE LOOPS
design and operation of organic-cooled, in Netherlands High Flux Reactor, 20: 18137 (KR-82)
neutron flux spectrum for, in NRL Research Reactor, 20: 16335(R) (NBS-TN-276)
performance of OZH-1 and OZH-2, 20: 18024

INCOLOY
creep properties at high temperatures of Japanese-manufactured, 20: 17031(T) (ORNL-tr-962)
microstructure of type 800, study of precipitates in, 20: 17024 (ORNL-TM-1161, pp 236-46)
radiation effects on fuel cladding of type 800, reactor, 20: 17120 (GEAP-4916)

INCONEL
reactions of molten type 713C, with alumina, fused silica, zircon, and zirconia, 20: 16984

INDIA
radium-226 content in food and man at Bombay and Kerala, 20: 16747

INDIUM
magnetic fields in iron and nickel, hyperfine, (E), 20: 17992
magnetic flux jumping in glass impregnated with superconducting, field sweep-rate and temperature dependence of, (E), 20: 17604
magnetostriction in antiferromagnetic and ferromagnetic regions, (E), 20: 18012
performance of foils of, in neutron radiography, 20: 16619
ultrasonic absorption in superconducting, nonlinear effects in, (E), 20: 17635

INDIUM ALLOYS
In–Fe, indium hyperfine magnetic field in, (E), 20: 17992
In–Ni, indium hyperfine magnetic field in, (E), 20: 17992
In–Pb, electron tunneling in superconducting thin films of, as evidence of fluxon entry, (E/T), 20: 17627
In–Sm, crystal structure of $SmIn_3$, 20: 17060
In–Sn, tin-119 isomeric shift in, 20: 18004
In–Yb, crystal structure of $YbIn_3$, 20: 17060
Sb–In, radiation effects on electric properties of, electron and neutron, 20: 17150(T)

INDIUM IONS
sorption by aminodiacetate resin Dowex A-1, 20: 16358

INDIUM ISOTOPES In-114
decay of isomeric, upper limits for double internal conversion in, (E), 20: 17783

INDIUM ISOTOPES In-115
energy levels from cadmium-115 decay, parity and spin of low-lying, (E), 20: 17766
neutron capture by, indium-116 isomers from, 20: 17822

INDIUM ISOTOPES In-116
energy levels of, indium-115 (n,γ) reactions for isomeric, 20: 17822

INDIUM ISOTOPES In-117
energy levels from cadmium-117 decay, half-life, parity, and spin of low-lying, (E), 20: 17766

INFECTIONS
radiation effects on phage-bacteria complex in *Escherichia coli*, uv, 20: 16270(T)

INFLAMMATION
radiotherapy of, 20: 16314

INFLUENZA VIRUS
radiation effects on properties of Asiatic, uv, 20: 16239

INFORMATION CENTERS
functions of NSIC, 20: 18020(R) (ORNL-3900, pp 2-81)
organization for atomic and molecular collision processes, 20: 17158(R) (ORNL-3900, pp 82-149)

INFRARED RADIATION
effects on seeds, genetic, 20: 16278

INSECTS
radiation control of *Sitophilus sasakii*, γ, 20: 16243
radiation effects on life span and reproduction of *Sarcophaga peregrina*, x, 20: 16291

INSTRUMENTATION
design for measuring reactivity, 20: 18032
design of control and safety, for zero-power reactors, 20: 18149
development at ORNL, 20: 17158(R) (ORNL-3900, pp 82-149)
development for Eurochemic fuel reprocessing plant, 20: 16559
electric interference in reactor, 20: 18030

INSTRUMENTS
design of decimal scanner, 20: 16777 (EUR-2702.e)
design of high-temperature electron capture detector, 20: 16804
manual for standard nuclear instrument modules, 20: 16779 (PPAD-584D)
use of optical, in construction of nuclear power plants, 20: 18114

INTERFEROMETERS
development of Mach-Zehnder laser, for plasma diagnostics, 20: 17875 (IPP-1/35)
use for measuring Doppler velocity, 20: 16335(R) (NBS-TN-276)

INTERNAL CONVERSION
coefficients of, coincidence method for determination of, 20: 17731

INTESTINE
chlorine-36 content in calf, after ingestion, 20: 16186
iodine-131 content in calf, after ingestion, 20: 16186
radiation effects on epithelium of mouse, lethal whole-body x, 20: 16223 (BNL-8952)
radiation effects on depression, replication, and synthesis of DNA in cells in, 20: 16230(R) (TID-22644)
radiation effects on transplanted Yoshida sarcoma cells in rat, tracer study, 20: 16188
radiation effects on glucose absorption by rat, x, 20: 16274
radioinduced tumors of, after therapy, 20: 16309

IODATES
separation from iodides, tellurates, and tellurites by paper chromatography, 20: 16372
separation of iodine-131-labeled, from labeled iodides and periodates, chromatographic, 20: 16567

IODIDES
separation from iodates, tellurates, and tellurites by paper chromatography, 20: 16372
separation of iodine-131-labeled, from labeled iodates and periodates, chromatographic, 20: 16567
transport system for, location of, 20: 16160 (UCRL-14739(Pt.2))

IODINE
diffusion from L54M fuels, effects of copper on, 20: 18142
iodine-131 exchange with 1-phenyl-2,3-dimethyl-4-iodopyrazolone, effects of solvents on, 20: 16502
sorption by carbon, 20: 18110

IODINE IONS
iodine-131 exchange with silver iodide, effects of cobalt and uranyl nitrates on, 20: 16432
wave functions for, including effect of nuclear quadrupole moment, 20: 17250 (BNL-8850)

IODINE ISOTOPES
recoil from proton reactions with uranium at 0.55 and 18.2 Bev, ranges in aluminum, (E), 20: 17837

IODINE ISOTOPES I-125
incorporation in corticotropin, 20: 16494

IODINE ISOTOPES I-126
production by deuteron reactions (d,n) and (d,2n) with tellurium-125 and -126, cross sections for, 20: 16508(R) (NYO-2771-13)

IODINE ISOTOPES I-127
reactions with gold at 51 Mev, effect of channeling on radiation damage from, (E), 20: 17146

IODINE ISOTOPES I-128
production in deuteron reactions (d,2n) with tellurium-128, cross sections for, 20: 16508(R) (NYO-2771-13)

IODINE ISOTOPES I-130
production in deuteron reactions (d,2n) with tellurium-130, cross sections for, 20: 16508(R) (NYO-2771-13)

IODINE ISOTOPES I-131
beta emission from, dosimetry in thyroid of, 20: 16160 (UCRL-14739 (Pt.2))
content in atmospheric dust and rain water, 1964–65, 20: 16660 (AERE-R-4997)
content in atmosphere, human urine, milk, rain water, and thyroid glands in Japan, 1964, 20: 16730 (NP-15882)
content in milk and plants before and after Salmon Event, 20: 16743 (VUF-1021)
content in milk, measures for controlling, 20: 16754
content in rain water, Fayetteville, Arkansas, Oct. 1964, 20: 16663 (TID-21470)
content in thyroid carcinoma patients after therapy, 20: 16303(R) (AD-626384)
determination in milk, solid foods, and water, methods for, 20: 16369
exchange between elementary iodine and 1-phenyl-2,3-dimethyl-4-iodopyrazolone, effects of solvents on, 20: 16502
exchange between potassium iodide and silver iodide, kinetics of, 20: 16460
exchange between silver iodide and iodide ions, effects of cobalt and uranyl nitrates on, 20: 16432
half life on plants, formula for determining effective, 20: 16160 (UCRL-14739(Pt.2))
incorporation in L-thyroxine and tyrosines, 20: 16496
metabolism by animals, review on, 20: 16734 (TID-22693)

metabolism in calves after ingestion, 20: 16186
metabolism in dairy cattle, system for measuring, 20: 16160 (UCRL-14739(Pt.2))
metabolism in rats, measurement methods for analyzing, 20: 16179
monitoring in reactor wastes, efficiency of silver nitrate-impregnated filter paper for, 20: 16756
production in deuteron reactions (d,n) and (d,p) with tellurium-130, cross sections for, 20: 16508(R) (NYO-2771-13)
production process improvement, 20: 16914(R) (ORNL-3900, pp 182-93)
radiation hazards to man from inhalation of, review on, 20: 16734 (TID-22693)
separation of iodate, iodide, and periodate labeled with, chromatographic, 20: 16567
uptake by rats, effects of ozone on, 20: 16190
uptake by thyroid, measurement standardization for, 20: 16315
use for tests of kidney function, 20: 16311
use for therapy of thyroid cancers, 20: 16307
yields from thorium-232 fission, (E), 20: 17860

IODINE ISOTOPES I-132
incorporation in protein, equipment for, 20: 16257

ION BEAMS
effects of positive, on electronic properties of semiconducting crystals, 20: 17151
focusing in magnetic spectrometers, 20: 16808 (CONF-650922, pp 154-63)

ION EXCHANGE
method for selective sorption of trace elements in neutron activated biological materials, 20: 16171 (AE-215)
use for separation of transplutonium elements, review on, 20: 16402
use in determining stability constants of complexes in aqueous phase, 20: 16481

ION EXCHANGE MATERIALS
book: *Ionizing Radiation Effects on Ion Exchange Materials*, 20: 16583
properties of zirconium phosphate, 20: 16568
sorptive properties of aminodiacetate resin Dowex A-1 for di- and trivalent cations, 20: 16358

ION EXCHANGERS
design for trace element separation from biological materials, 20: 16171 (AE-215)

ION PUMPS
performance of getter, using molybdenum cathodes, 20: 16789

ION SOURCES
construction and operating characteristics for linear accelerators, 20: 17223
design and uses of h-f plasmatrons, 20: 17959
design of duoplasmatron, for production of proton pulses, 20: 17172 (CEA-R-2802)
development for variable energy cyclotrons, 20: 17207 (INSJ-93)
development of, for radioisotope separator, 20: 16928(R) (INSJ-92)

IONIZATION
properties of, in electric-discharge plasma, (E), 20: 17508 (ARL-65-246)

IONIZATION CHAMBERS
design and performance of, for thoron monitoring, 20: 16842
design for gamma detection and measurement in reactors, 20: 16903
design for neutron flux measurements in reactors, 20: 16897
design for survey meters, engineering drawings on, 20: 16892
design of extrapolation, for measurements with alpha, beta, and x-ray sources, 20: 16852
properties of low-voltage, in recombination mode, 20: 16902
use for in-pile neutron flux monitoring, 20: 18043(P)

IONOSPHERE
density variations in E region over Finland, 1958 to 1960, 20: 17542
disturbances in, vlf phenomena in, 20: 17554
interactions with moving bodies, 20: 17537 (JPLAI/LS-641)
ion currents in, from ionospheric dynamo theory, 20: 17553
ion sheath effects on r-f probe admittance in, (T), 20: 17552

IONS
acceleration of plasma, method and device for, 20: 17960(P)
effects of competitive, on plant uptake of divalent cations, 20: 16174(R) (RLO-1547-3)
effects of metal, on protein synthesis systems, 20: 16160 (UCRL-14739(Pt.2))
electromagnetic-wave reactions with molecular, (T), 20: 17284
emission from cesiated surfaces at room temperature, photoelectric, (E/T), 20: 17267
explosion of multicharged molecular, mechanisms of, (E/T), 20: 17158(R) (ORNL-3900, pp 82-149)
heating to high temperature, inelastic collision processes for excitation, 20: 17900
oscillations in plasma, quasilinear theory for electron interactions with, 20: 17950
oscillations in plasma, determination of ion acoustic wave velocity from, (E/T), 20: 17158(R) (ORNL-3900, pp 82-149)
reactions of metal, with ligands, 20: 16160 (UCRL-14739(Pt.2))
reactions of metal, chelate formation in, 20: 16160 (UCRL-14739(Pt.2))
reactions with atoms, classical calculations on electron capture in, 20: 17275
slowing down in crystalline solids, computer analysis of, 20: 17158(R) (ORNL-3900, pp 82-149)
trajectory of fast heavy, in ordered crystal lattices, (E), 20: 17158(R) (ORNL-3900, pp 82-149)

IRIDIUM
deposition on refractory metal rocket engine components, 20: 16943(R) (IITRI-B237-45)
diffusion in tungsten to 4000°F, inter-, 20: 16943(R) (IITRI-B237-45)
electron emission in cesium vapor, thermionic, (E), 20: 17333

IRIDIUM ALLOYS
Ir–Nb, superconductivity in close-packed intermediate phases of, 20: 17624
Ir–V, superconductivity in close-packed intermediate phases of, 20: 17624

IRIDIUM ISOTOPES Ir-191
half life of isomeric, from neutron reactions (n,n′), (E), 20: 16336(R) (NYO-10175)
neutron reactions (n,γ), activation cross section for, (E), 20: 16336(R) (NYO-10175)
neutron reactions (n,n′), activation cross section for, (E), 20: 16336(R) (NYO-10175)

IRIDIUM ISOTOPES Ir-192
beta decay of, platinum-192 2⁺-level g factors from, (E), 20: 17747
half life of isomeric, from neutron reactions (n,γ), (E), 20: 16336(R) (NYO-10175)
half life of, from neutron reactions (n,γ), (E), 20: 16336(R) (NYO-10175)
preparation for radiographic sources, 20: 16914(R) (ORNL-3900, pp 182-93)

IRIDIUM ISOTOPES Ir-193
neutron reactions (n,γ), activation cross section for, (E), 20: 16336(R) (NYO-10175)

IRIDIUM ISOTOPES Ir-194
beta decay of, platinum-194 energy levels from, (E), 20: 17781
beta decay of, platinum-194 2⁺level g factors from, (E), 20: 17747
energy levels from osmium-194 decay, (E/T), 20: 17781
half life of, from neutron reactions (n,γ), (E), 20: 16336(R) (NYO-10175)

IRIDIUM OXIDES
BaO–IrO_2–SrO, crystal structure, 20: 16436

IRON
analysis for tellurium, activation, 20: 16335(R) (NBS-TN-276)
crystal lattice dynamics of α, Krebb's model for, 20: 17081
determination by radiometric titration, 20: 16386
determination in asbestos using ion exchange, activation, 20: 16336(R) (NYO-10175)
determination in aluminum by proton activation analysis, 20: 16367
determination in blood by neutron activation, 20: 17822
determination in nickel oxide samples by radioisotope dilution, 20: 16335(R) (NBS-TN-276)
determination in presence of cobalt, activation, 20: 16332 (GA-6691)
determination in uranium concentrates, oxides, and metal, activation, 20: 16399
determination of trace amounts of, using controlled-potential coulometry, 20: 16390
determination of trace amounts of, in beryllium by spectrography, 20: 16352
dislocation parameters for, 20: 17033
effects on light-induced chlorosis in tomato leaves, 20: 16174(R) (RLO-1547-3)
effects on potassium determination by flame photometry, 20: 16713
effects on uranium separation from phosphate rocks, 20: 16381
neutron reactions in, short-lived activities from, (E), 20: 16336(R) (NYO-10175)
neutron reactions (n,n′γ) at 0.95 to 4.0 Mev, angular distributions and level parities and spins from, (E), 20: 17736
proton reactions at 590 Mev and 18.3 Bev, potassium isotope yields in, (E), 20: 17717
radiation effects on atomic arrangement in, 20: 18020(R) (ORNL-3900, pp 2-81)
radiation effects on metabolism of, by rats, 20: 16187
radiation effects on magnetic hysteresis of, combined nickel impurity and fast-neutron, 20: 17134
separation from scandium by ion exchange chromatography, 20: 16574
separation from uranium and thorium by solvent extraction using alkyl phosphates, 20: 16580
sorption in anemic patients, tracer study, 20: 16303(R) (AD-626384)
thermal capacity of α, Krebb's model for lattice contributions to, 20: 17081

IRON ALLOYS
Al–Fe–Ta, phase studies on intermetallic compounds in, 20: 17075
Al–Fe–U, metallography of, correlation of particle distribution and swelling characteristics of, 20: 17058
Be–Fe, magnetic moments of bcc, atomic, 20: 17985
Cr–Fe–Mo, phase studies, 20: 17093
Cr–Fe–Ni, corrosion cracking in, mechanisms of stress-, 20: 16968 (COO-1319-33)
Cr–Fe–W, phase studies, 20: 17093
Dy–Fe, crystal structure of Dy_6Fe_{23} in, 20: 17096(T)
Er–Fe, crystal structure of Er_6Fe_{23} in, 20: 17096(T)
Fe–Lu, crystal structure of Lu_6Fe_{23} in, 20: 17096(T)
Fe–Pr, crystal structure of Pr_2Fe_{17} in, 20: 17096(T)
Fe–Tb, crystal structure of Tb_6Fe_{23} and Tb_2Fe_{17} in, 20: 17096(T)
Fe–Tm, crystal structure of Tm_6Fe_{23} in, 20: 17096(T)
Fe–U, metallography of, correlation of particle distribution and swelling characteristics of, 20: 17058
Fe–Y, crystal structure of Y_6Fe_{23} in, 20: 17096(T)
Ho–Fe, crystal structure of Ho_6Fe_{23} and Ho_2Fe_{17} in, 20: 17096(T)
In–Fe, indium hyperfine magnetic field in, (E), 20: 17992
IRON(III) CHLORIDES
corrosive effects of, on iron-base alloys, mechanisms of stress-, 20: 16968 (COO-1319-33)
IRON COMPLEXES
with ethylenediaminetetraacetate, effects on hydrolysis of α-D-glucose 1-phosphate, 20: 16421
with kojate, effects on hydrolysis of α-D-glucose 1-phosphate, 20: 16421
IRON(II) COMPOUNDS
effects of, with calcium or magnesium on manganese sorption by barley roots, 20: 16174(R) (RLO-1547-3)
IRON(III) COMPOUNDS
effects of, with calcium or magnesium on manganese sorption by barley roots, 20: 16174(R) (RLO-1547-3)
IRON IONS
effects on hydrolysis of α-D-glucose 1-phosphate, 20: 16421
sorption by aminodiacetate resin Dowex A-1, 20: 16358
IRON ISOTOPES
separation of, performance of separator for, 20: 16928(R) (INSJ-92)
IRON ISOTOPES Fe-55
content in stratospheric and tropospheric samples in Project Star Dust, 1963, 20: 16727(R) (HASL-168)
content in stratospheric and tropospheric samples in Project Star Dust, 1964, 20: 16728(R) (HASL-169)
ground water contamination by, in Shoal Event, hazards from, 20: 16742 (VUF-1014)
nucleon interactions in, properties from effective, (T), 20: 17735
IRON ISOTOPES Fe-56
electron energy levels of, gyromagnetic ratio for ground state, (E), 20: 17280
neutron reactions (n,p) with, sensitivity of, for activation analysis, 20: 16332 (GA-6691)
neutron reactions (n,nγ) at 0.95 to 4.0 Mev, angular distributions and level parities and spins from, (E), 20: 17736
nucleon interactions in, properties from effective, (T), 20: 17735
IRON ISOTOPES Fe-57
Mössbauer effect in stainless steel, self-absorption effects on, (E), 20: 17990
Mössbauer spectra in prescence of ESR, (T), 20: 18009
IRON ISOTOPES Fe-59
content in stratospheric and tropospheric samples in Project Star Dust, 1963, 20: 16727(R) (HASL-168)
determination in irradiated materials by extraction and precipitation, gamma spectrometric, 20: 16336(R) (NYO-10175)
IRON NITRATES
ion exchange and sorption on glass surfaces, 20: 16469
IRON OXIDES
determination in Moldavites by mass spectrometry and x-ray fluorescence, 20: 16711(R) (MIT-1381-13)
IRON(III) OXIDES
sorptive properties for molybdenum and technetium, 20: 16552
IRON(II) SULFATES
properties as chemical dosimeter, 20: 16517
IRON SYSTEMS
C–Fe–Nb, phase studies, 20: 17086
C–Fe–W, crystal structure of Fe_3W_3C and Fe_6W_6C in, 20: 17015 (INR-665/II/PS)
Cr–Fe–Ni–P, corrosion cracking in, mechanisms of stress-, 20: 16968 (COO-1319-33)
Cr–Fe–Ni–Si, corrosion cracking in, mechanisms of stress-, 20: 16968 (COO-1319-33)
Fe–H_2O, neutron age to indium resonance energy in, fission, (E), 20: 17659
Fe–H_2O, neutron slowing down density distributions in, Monte Carlo code for, 20: 17660
Fe–O–Ti–Zr, fabrication and properties of sintered, deformable, 20: 17003
IRON THIOCYANATES
solvent distribution in 2-methyl-1-propanol–water, effects of fluoride on, 20: 16335(R) (NBS-TN-276)
IRRADIATION FACILITIES
development for reactor fuels and materials, 20: 18174(R) (NP-15771)
ISOTOPE EFFECTS
of deuterium on thermal isomerization of cycloocta-1,3,6-triene, 20: 16503
on activity and osmotic coefficients of alkali halides in water, 20: 16488
on dissociation of acetic acid in aqueous solutions at 0 to 50°C, 20: 16458
on energy of K_α x rays from uranium, 20: 17285
on infrared and Raman spectra of imidazole, 20: 16499
on infrared and Raman spectra of imidazole, 20: 16500
on ionization and proton transfer in water, 20: 16424
on kinetics of hydrogen electrode system, 20: 16459
on rate of gas-phase decomposition of oxalic acid, reversing-hydrogen, 20: 16455
ISOTOPE SEPARATION METHODS
development of, Pierrelatte plant for, 20: 16932
diffusion, calculation of squared-off cascades for, 20: 16929
ISOTOPIC EQUILIBRATION
method for trace element determinations, 20: 16335(R) (NBS-TN-276)
uses in analysis, 20: 16362
ISOTOPIC EXCHANGE
between deuterium and water, catalytic effects of ruthenium chloride on, 20: 16423
between deuterium and methane, catalytic effects of gold–palladium alloy on, 20: 16457
between hydrogen and liquid ammonia, catalytic effects of alkaline amides on, 20: 16444
between iodine and 1-phenyl-2,3-dimethyl-4-iodopyrazolone, effects of solvents on, 20: 16502
in hydrogen electrode reaction, kinetics of, 20: 16459
of iodine-131 and silver-110, in silver iodide–silver nitrate and potassium iodide–silver iodide systems, kinetics of, 20: 16460
of tritium between ethyl malonate and hydrocarbons, effects of catalysts on, 20: 16492
ITALY
manganese-54 content in mollusks in Lake Maggiore, 20: 16185
meteorological measurements at Casaccia, 1964, 20: 16635 (RT/PROT(65)-40)

J

JAPAN
fallout monitoring, 1962-3, 20: 16755
fallout monitoring, 1962 and 63, 20: 16671
radiation effects on fishermen in, 10-year fallout, 20: 16226 (NP-15891)
radioactivity monitoring in, 1964, 20: 16730 (NP-15882)
radioactivity monitoring in, 1964, 20: 16731 (NP-15883)

K

KANSAS
waste disposal in salt mines of Lyons, 20: 18169
KERATINS
radioinduced free radicals in, uv, 20: 16205
KETONES
effects on solvent extraction of europium using benzoyltrifluoroacetone, 20: 16565
Friedel-Crafts reactions with aromatic-aliphatic, decomposition and rearrangement in, 20: 16542(R) (TID-22646)
reactions with perchloric acid, mechanism of rearrangement, 20: 16542(R) (TID-22646)
reactions with perchloric acid, disproportionation in rearrangement, 20: 16542(R) (TID-22646)
reduction of *cis*-2-decalone, diethyl ketone, and noncamphor by borohydride ions, secondary deuterium isotope effects in, 20: 16555
KIDNEYS
desoxyribonucleic acid synthesis in weanling rat, effects of fasting on, 20: 16158 (AD-628360)
function tests using iodine-131-hippuran, 20: 16311
preparation of artificial, using radioinduced PVA membrane in, 20: 16505 (BNL-949)
radiation effects on rabbit, x, 20: 16234
radiation effects on weight of, in nephrectomized mice, x, 20: 16282
KRYPTON
cesium ion elastic scattering at 2.3 to 11.6 ev, (E/T), 20: 17300

krypton ion reactions with atomic, ionization probability effects on 1001 cross sections for, (E), 20: 17255
radio wave emission from plasma of, negative-absorption effects on anomalous bremsstrahlung and cyclotron, (E), 20: 17921
spectra of molecules trapped in solid, 20: 18016
KRYPTON IONS
reactions with krypton atoms, ionization probability effects on 1001 cross sections for, (E), 20: 17255
KRYPTON ISOTOPES Kr-79
decay of, L/K capture ratio for, (E), 20: 17700 (ZfK-PhA-17)
gamma spectra, (E), 20: 17700 (ZfK-PhA-17)
KRYPTON ISOTOPES Kr-85
concentration by thermal diffusion, 20: 16914(R) (ORNL-3900, pp 182-93)

L

LABORATORIES
operation of HIRDL, at Brookhaven, 20: 16505 (BNL-949)
LABORATORY EQUIPMENT
design and operation of, for activation analysis, 20: 16365
LANTHANUM
abundance in sun, (E), 20: 17237
crystal structure of solid solutions of, in lanthanum disilicide, 20: 17042
determination using Xylenol Orange, spectrophotometric, 20: 16394
diffusion in magnesium, 20: 17038
effects on high-temperature properties of eutectic alloys, 20: 17108
effects on manganese sorption by barley roots, 20: 16174(R) (RLO-1547-3)
effects on soft-tissue calcification in rats, 20: 16162
evaporation from irradiated uranium dioxide at 750 to 1600°C, 20: 17102
separation from other fission products by precipitation with barium sulfate, 20: 16343
solubility in gold, solid, 20: 17016 (IS-1175)
solvent properties for magnesium, solid, 20: 17016 (IS-1175)
LANTHANUM CARBIDES
properties of, chemical and physical, 20: 17048
reactions with water, formation of gaseous products in, 20: 17048
LANTHANUM CHLORIDES
dysprosium ion quadrupolar interactions in, Zeeman-field-dependent, (E/T), 20: 18008
neodymium ion EPR absorption in single crystals of, in zero fields, (E), 20: 17997
LANTHANUM COMPLEXES
with phenanthroline, infrared spectra of, 20: 16436
with solochrome violet RS, polarography of, 20: 16406
with thenoyltrifluoroacetone, magnetic susceptibilities of, 20: 16416(R) (NYO-906-68)
with 2,2'-bipyridyl, infrared spectra of, 20: 16437
LANTHANUM ETHYL SULFATES
neodymium ion EPR absorption in, in zero fields, (E), 20: 17997
LANTHANUM HYDRIDES
properties and structure, 20: 16453
LANTHANUM HYPOPHOSPHITES
preparation and properties of, 20: 16426
LANTHANUM IONS
sorption by aminodiacetate resin Dowex A-1, 20: 16358
LANTHANUM ISOTOPES La-135
production in deuteron reactions (d,n) and (d,2n) with barium-134 and -135, cross sections for, 20: 16508(R) (NYO-2771-13)
LANTHANUM ISOTOPES La-139
boron-10 reactions (B-10,7n), angular momentum effects on excitation functions for, (E), 20: 17784
boron-11 reactions (B-11,8n), angular momentum effects on excitation functions for, (E), 20: 17784
LANTHANUM ISOTOPES La-140
determination by precipitation with barium sulfate and gamma spectroscopy, 20: 16343
determination in milk, gamma spectrometric, 20: 16369
orientation in neodymium ethyl sulfate, quadrupole crystal-field shielding from, (E), 20: 17996
production in deuteron reactions (d,γ) with barium-138, cross sections for, 20: 16508(R) (NYO-2771-13)
ranges of fission products of, in aluminum, (E), 20: 17721
sensitivity for activation analysis using beta-gamma-gamma sum-coincidence gamma spectrometer, 20: 16335(R) (NBS-TN-276)
use as tracer in paper industry, 20: 16921 (TID-22627)
LANTHANUM OXALATES
reactions of hydrated, with hydrochloric acid, 20: 16447
LANTHANUM OXIDES
crystallograpaic modifications and phase transformations of, 20: 16489
determination in thorium oxide by emission spectroscopy, 20: 16393
reactions with aluminum oxide and oxides of Group II elements at 1400 to 1500°C, 20: 16482
reactions with boron oxides at high temperatures, 20: 16489
CeO_2–La_2O_3–Sm, fluorescence properties of, 20: 16466(T)
LANTHANUM SILICIDES
crystal structure of lanthanum solid solutions in, 20: 17042
properties of, physicochemical, 20: 17047
LANTHANUM SULFIDES
EuS–La_2S_3, compound formation in, 20: 16431
La_2S_3–SmS, compound formation in, 20: 16431
La_2S_3–YbS, compound formation in, 20: 16431
LANTHANUM TANTALATES
crystal structure, 20: 16438
LANTHANUM TITANATES
preparation and dielectric properties of plasma-anodized films of, 20: 17045
LARYNX
radiotherapy of carcinomas of, γ, 20: 16313
radiotherapy of carcinomas in, moving-beam x, 20: 16317
LATINA POWER REACTOR
development of, review of, 20: 18104
LEAD
content in marine organisms, 20: 16725(R) (EUR-2543.e)
corrosion by boron-containing solutions, 20: 16976
crystal properties of, computer analysis of Fermi surfaces, 20: 17973 (IS-1106)
determination by radiometric titration, 20: 16386
determination of trace amounts of, in beryllium by spectrography, 20: 16352
effects on soft-tissue calcification in rats, 20: 16162
energy levels of μ-mesic atoms of, resonances in, (T), 20: 17281
gamma shielding by, thickness calculations for, 20: 17963(T) (ORNL-tr-1059)
hyperfine structure of μ-mesic, (E), 20: 17268
proton fission at 150 to 660 Mev, cross sections for, (E), 20: 17838
proton scattering at 140 Mev, parameters for triple, (E/T), 20: 17738
superconducting energy gap of, effects of electron-damped dislocations on determination of, 20: 17618
LEAD ALLOYS
Eu–Pb, crystal structure and magnetic properties of $EuPb_3$, 20: 17060
In–Pb, electron tunneling in superconducting thin films of, as evidence of fluxon entry, (E/T), 20: 17627
Pb–Sn, tin-119 isomeric shift in, 20: 18004
Pb–Yb, crystal structure of $YbPb_3$, 20: 17060
LEAD CHLORIDES
radioinduced color centers in planar, ESR of γ, 20: 16531
LEAD IODIDES
radioinduced color centers in planar, ESR of γ, 20: 16531
LEAD IONS
sorption by aminodiacetate resin Dowex A-1, 20: 16358
LEAD ISOTOPES Pb-205
energy levels from polonium-209 decay, parity and spin of, (E), 20: 17841
LEAD ISOTOPES Pb-206
hyperfine structure of μ-mesic, (E), 20: 17268
LEAD ISOTOPES Pb-207
content in stratospheric and tropospheric samples in Project Star Dust, 1963, 20: 16727(R) (HASL-168)
LEAD ISOTOPES Pb-208
energy level excitation by 7.3-Mev gamma rays, (E), 20: 17842
energy-level transitions in, internal-pair formation of 2615-kev, (E), 20: 17731
hyperfine structure of μ-mesic, (E), 20: 17268
neutron scattering cross sections at 1 to 4.2 Mev, (E), 20: 18020(R) (ORNL-3900, pp 2-81)
nucleon capture at 10 to 40 Mev, cross sections and mechanism for direct, (T), 20: 17737
LEAD ISOTOPES Pb-209
nucleon capture at 10 to 40 Mev, cross sections and mechanism for direct, (T), 20: 17737
LEAD ISOTOPES Pb-210
content in atmosphere, seasonal and geographical variations in, (E), 20: 16640
content in stratospheric and tropospheric samples in Project Star Dust, 1964, 20: 16728(R) (HASL-169)
distribution in atmosphere over oceans, dependence of, on meteorological factors, 20: 16699
distribution in free atmosphere, planetary, (E), 20: 16641
tracer use in studies of atmosphere, 20: 16641
LEAD NITRATES
ion exchange and sorption on glass surfaces, 20: 16469
LEAVES
light-induced chlorosis in tomato, effects of iron on expression of, 20: 16174(R) (RLO-1547-3)
LEPTONS

interactions with neutrinos at high energies, local-current commutation relations for, 20: 17387
interactions with nucleons for tests of C and T invariances, 20: 17392
production by neutrino (ν_μ)-proton interactions, effects of vector mesons on, (T), 20: 17504

LEUKEMIA
radiation effects on mouse, combined with cyclophosphamide and hyperbaric oxygen, 20: 16262
radioinduced by therapeutic doses of x radiation, 20: 16242
radioinduced, effects of viruses on transmission of, 20: 16159(R) (ORNL-3900, pp 150-81)
radioinduced, following polycythemia therapy, β, 20: 16241
radiotherapy of, effectiveness in children, 20: 16306

LEUKOCYTES
radiation effects on production of rabbit, x, 20: 16265

LEVEL INDICATORS
development of radiometric, 20: 18182

LIFE SPANS
effects of mating pattern on Drosophila, 20: 16229(R) (NYO-1472-1)

LIGHT
absorption and emission by alkali halide crystals, (E/T), 20: 17158(R) (ORNL-3900, pp 82-149)
diffusion in atmosphere, spectral theory for stationary transport operator for, 20: 17658
effects on chlorosis in tomato leaves, effects of iron on, 20: 16174(R) (RLO-1547-3)
effects on silver bromide and silver chloride, ESR from, (E), 20: 17981
emission from theta-pinch discharges in dense gases, (E), 20: 17523
resonance scattering on mercury-201, orientation of magnetic moment by, 20: 17755(T)

LIGHTNING
theory, 20: 17243

LINEAR ACCELERATORS
beam detectors for pulsed electron, design of magnetic, 20: 17210 (LNF-65/37)
beam dynamics in Alvarez, (T), 20: 17209(R) (LA-3479)
fabrication of copper waveguide for, by brazing, 20: 16999
ion sources for, optimum design of, 20: 17223
operation characteristics of, for activation analyses, 20: 16335(R) (NBS-TN-276)
use for activation analyses, 20: 16335(R) (NBS-TN-276)

LIPIDS
function of, in sheep erythrocyte membranes, 20: 16160 (UCRL-14739 (Pt.2))

LIQUID FLOW
boundary layer characteristics of hydrogen, in tanks, 20: 17536
heat transfer in steady-state two-phase, 20: 16601(R) (GEAP-5067)
heat transfer to metal, annulus eccentricity effects on, 20: 16612

LIQUID METAL COOLED REACTORS
cooling system testing for space-oriented medium-power, 20: 18020(R) (ORNL-3900, pp 2-81)
core explosions in fast, containment of, 20: 18122
core meltdown accidents in fast, energy release in, 20: 18123
fuel burnup in large plutonium–uranium, effects on breeding ratio, multiplication factor, and sodium-void reactivity, 20: 18060
heat exchangers for sodium, computer analysis of, 20: 18093(R) (UNC-5142)

LIQUIDS
hydrodynamic equations for ideal, 20: 17647
radiation effects on coalescence in mixed, 20: 17158(R) (ORNL-3900, pp 82-149)

LITHIUM
diffusion in titanium dioxide, isotopic mass dependence of, 20: 17052
diffusion of lithium-6 and lithium-7 in liquid, at 195 to 450°C, 20: 17104
electron scattering by atomic, cross sections for, (T), 20: 17286
helium-3 reactions (He-3,n) with, neutrons yields for activation analysis in, 20: 16332 (GA-6691)
ion pairing interactions in, (T), 20: 17008 (CEA-R-2820)
production by high-energy solar particles, 20: 17234
purification by high-vacuum fractional distillation, 20: 16961

LITHIUM BERYLLIUM FLUORIDES
crystal structure, 20: 17158(R) (ORNL-3900, pp 82-149)

LITHIUM CHLORIDES
activity and osmotic coefficients in heavy water at 25°C, 20: 16488
determination by titration, semiquantitative, 20: 17158(R) (ORNL-3900, pp 82-149)

LITHIUM DEUTERIDES
compression at 25°C, 20: 17979 (UCRL-12386)

LITHIUM FLUORIDES
gamma absorption coefficient at 0.01 to 10 Mev, effects of impurities on, 20: 16829(R) (UCRL-14534, pp 1-7)
photon reactions at 0.01 to 10 Mev, calculated cross sections for, 20: 16829(R) (UCRL-14534, pp 1-7)
radiation effects on crystal structure of, point defects from thermal neutron, 20: 18007
radiation effects on optical absorption spectra of, electron-beam and thermal-neutron, 20: 17143
BeF_2–LiF, viscosity at 710 to 1720°F, 20: 17158(R) (ORNL-3900, pp 82-149)

LITHIUM HYDRIDES
compression at 25°C, 20: 17979 (UCRL-12386)
fabrication of reactor shields of, by powder metallurgy techniques, 20: 16993 (Y-DA-1043)

LITHIUM ISOTOPES Li-6
alpha reactions (α,γ), boron-10 4.77- and 5.16-Mev levels from, (E), 20: 17761
diffusion in liquid lithium metal at 195 to 450°C, 20: 17104
helium-3 reactions (He-3,d), Q value for, 20: 16331 (GA-6568)
nuclear breakup of, polarization of products from, 20: 17806
proton reactions (p,2p) at 140 Mev, energy spectra and angular correlation distributions from, (E), 20: 17741
reactions (Li-6,5n), angular momentum effects on excitation functions for, (E), 20: 17784

LITHIUM ISOTOPES Li-7
diffusion in liquid lithium metal at 195 to 450°C, 20: 17104
electron scattering at high energies, kinematics of, (T), 20: 17799
helium-3 reactions (He-3,t) at 12 Mev, Q value for, 20: 16331 (GA-6568)
production in boron-10 (n,α) reactions at 23 ev to 0.5 Mev, excited-to-ground state branching ratio for, (E), 20: 17719
proton reactions (p,n) with, neutron production for activation analysis in, 20: 16332 (GA-6691)
proton reactions (p,2p) at 140 Mev, energy spectra and angular correlation distributions from, (E), 20: 17741
proton scattering at 150 to 185 Mev, level structure from, (T), 20: 17800
reactions (Li-7,6n) with praseodymium-141, angular momentum effects on excitation functions for, (E), 20: 17784

LITHIUM ISOTOPES Li-8
beta decay of, energy and lifetime values and nuclear matrix elements for, (T), 20: 17732
production from proton reactions with bromine and silver in emulsions at 25 Bev/c, recoil from, (E), 20: 17748
production from proton reactions with emulsion nuclei at 28 Bev, evaporation theory for, (E/T), 20: 17753

LITHIUM ISOTOPES Li-9
beta decay of, energy and lifetime values and nuclear matrix elements for, (T), 20: 17732

LITHIUM NITRATES
diffusion and electric mobility of ions in, tracer study on, 20: 16414 (CEA-R-2806)
ion exchange distribution of alkali and alkaline earth metals between chabazite and fused, 20: 16340 (USNRDL-TR-970)
$LiNO_3$–KNO_3, diffusion and electric mobility of ions in, 20: 16414 (CEA-R-2806)
$LiNO_3$–$NaNO_3$, diffusion and electric mobility of ions in, 20: 16414 (CEA-R-2806)

LIVER
radiation effects on depression, replication, and synthesis of DNA in cells in, 20: 16230(R) (TID-22644)
radiation effects on iron metabolism in rat, tracer study of y, 20: 16187
radiation effects on transplanted Yoshida sarcoma cells in rat, tracer study, 20: 16188
radiation effects on catalase activity in rat, 20: 16277

LOOPS
development of high-temperature potassium, 20: 18020(R) (ORNL-3900, pp 2-81)
fluid flow in closed, properties of natural convection, (E/T), 20: 16600 (COO-1177-15)

LUBRICANTS
performance and selection of, for use in space vehicles, 20: 16944 (NASA-SP-3025)

LUMINESCENT DETECTORS
development for ionizing radiation dosimetry, 20: 16837

LUNGS
analysis for copper and zinc, activation, 20: 16335(R) (NBS-TN-276)
radiation effects on transplanted Yoshida sarcoma cells in rat, tracer study, 20: 16188
radioinduced carcinomas of, etiology of, 20: 16264
radiotherapy of carcinomas in, moving-beam x, 20: 16317
uranium oxide content in dog, after inhalation, 20: 16184

LUTETIUM
determination by neutron activation and ion-exchange chromatography, 20: 16363
solubility in gold, solid, 20: 17016 (IS-1175)
solvent properties for magnesium, solid, 20: 17016 (IS-1175)

LUTETIUM ALLOYS
Fe–Lu, crystal structure of Lu_6Fe_{23} in, 20: 17096(T)

Lu–Hg, crystal structure of $LuHg_3$, 20: 17060
Lu–Mn, crystal structure of Lu_6Mn_{23} in, 20: 17096(T)
Lu–Tl, crystal structure of $LuTl_3$, 20: 17060
LUTETIUM COMPLEXES
with phenanthroline, infrared spectra of, 20: 16436
with 2,2'-bipyridyl, infrared spectra of, 20: 16437
LUTETIUM FERRATES(III)
thulium ion hyperfine magnetic fields in, (E), 20: 17994
LUTETIUM HYDRIDES
properties and structure, 20: 16453
LUTETIUM ISOTOPES Lu-170
beta decay of, transition rates for, (T), 20: 17742
LUTETIUM ISOTOPES Lu-176
neutron capture by, lutetium-177 levels from, 20: 17822
LUTETIUM ISOTOPES Lu-177
energy levels from lutetium-176 (n,γ) reactions, 20: 17822
orientation in neodymium ethyl sulfate, quadrupole crystal-field shielding from, (E), 20: 17996
LUTETIUM OXIDES
Lu_2O_3–SrO, properties of compounds formed by interactions in, 20: 17044
LYMPH SYSTEM
uranium oxide content in dog, after inhalation, 20: 16184
LYSOSOMES
radiation effects on KB cell, uv and x, 20: 16258

M

MACHINING
design of equipment for electrical-discharge, of metallographic specimens, 20: 16951 (ORNL-TM-1161, pp 159-81)
equipment for spent fuel element, 20: 16598(P)
MAGNESIUM
conference on geomagnetism, 20: 17550
determination by radiometric titration, 20: 16386
determination in blood serum and ores, activation, 20: 16336(R) (NYO-10175)
determination in calcium, polarographic, 20: 16406
determination in serum, activation, 20: 16347
determination of trace amounts of, in beryllium by spectrography, 20: 16352
diffusion of cerium and lanthanum in, 20: 17038
effects of, with calcium on manganese sorption by barley roots, 20: 16174(R) (RLO-1547-3)
effects of, with ferric and ferrous iron on manganese sorption by barley roots, 20: 16174(R) (RLO-1547-3)
effects on high-temperature properties of eutectic alloys, 20: 17108
photon reactions with Coulomb field of, pair production total cross sections for high-energy, (T), 20: 17754
separation from scandium by ion exchange chromatography, 20: 16574
solubility in lanthanide metals, solid, 20: 17016 (IS-1175)
MAGNESIUM ALLOYS
Ce–Mg, spectrophotometric analysis for cerium using sulfanilic acid, 20: 16398
Lu–Mn, crystal structure of Lu_6Mn_{23} in, 20: 17096(T)
Mg–Ag, photosensitivity of, 20: 17984
Mg–Nd, properties and structure of, 20: 17110
Mn–Tm, crystal structure of Tm_6Mn_{23} in, 20: 17096(T)
MAGNESIUM CHLORIDES
corrosive effects of, on iron-base alloys, mechanisms of stress-, 20: 16968 (COO-1319-33)
MAGNESIUM COMPLEXES
with solochrome violet RS, polarography of, 20: 16406
MAGNESIUM IONS
sorption by aminodiacetate resin Dowex A-1, 20: 16358
MAGNESIUM ISOTOPES
separation of, performance of separator for, 20: 16928(R) (INSJ-92)
MAGNESIUM ISOTOPES Mg-24
deuteron reactions (d,p) at 10.1 Mev, angular distributions for, (T), 20: 17692 (ORNL-TM-1414)
neutron reactions (n,p) with, sensitivity of, for activation analysis, 20: 16332 (GA-6691)
neutron reactions (n,p), threshold cross section and energy for, 20: 16335(R) (NBS-TN-276)
MAGNESIUM ISOTOPES Mg-26
alpha reactions (α,He-8) at 80.0 Mev, helium-8 mass from, (E), 20: 17794
helium-3 reactions (He-3,p) at 12 Mev, Q value for, 20: 16331 (GA-6568)
MAGNESIUM ISOTOPES Mg-27
gamma spectra of neutron-irradiated, 20: 16336(R) (NYO-10175)
separation from manganese-56 by solvent extraction using diethyl-dithiocarbamic acid, 20: 16336(R) (NYO-10175)
MAGNESIUM LANTHANUM NITRATES
spectra of hydrated, at 20 to 290°K, infrared, 20: 16429
MAGNESIUM OXIDES
compatibility with refractory metals and alloys, 20: 17022 (N-65-18933)
determination in Moldavites by mass spectrometry and x-ray fluorescence, 20: 16711(R) (MIT-1381-13)
electric conductivity at 1100 to 1600°C, 20: 17022 (N-65-18933)
radiation effects on structure of, neutron, 20: 17148
reactions with aluminum oxides and lanthanum or neodymium oxides at 1400 to 1500°C, 20: 16482
MAGNET COILS
design and fabrication for 4-Bev electron synchrotron, 20: 17199 (CONF-650922, pp 686-99)
design and fabrication of cryogenic, with integral coolant passages, 20: 17874 (CONF-650922, pp 630-42)
design for use in high-energy physics, (T), 20: 17175 (CONF-650922, pp 1-26)
design for water-cooled d-c magnets, 20: 16585 (CONF-650922, pp 349-55)
design of cryogenic, for energy storage, 20: 17597 (CONF-650922, pp 625-9)
design of high-field superconducting, 20: 17598 (CONF-650922, pp 745-52)
design of superconducting Helmholtz, 20: 17586 (CONF-650922, pp 509-16)
development of cryogenically cooled and superconducting, 20: 17592 (CONF-650922, pp 574-87)
energy losses from superconducting, (E), 20: 17630
fabrication, 20: 16988 (CONF-650922, pp 305-12)
fabrication for Argonne Synchrotron, 20: 17186 (CONF-650922, pp 356-65)
fabrication of ZGS ring, prestressing techniques in, 20: 17201 (CONF-650922, pp 733-44)
field properties of large-volume, (E), 20: 17600(R) (ORNL-3908, pp 114-48)
Hall effect measurements on superconduction niobium–zirconium, 20: 17600(R) (ORNL-3908, pp 114-48)
performance of superconducting, 20: 17590 (CONF-650922, pp 550-9)
performance of, with superconducting cables, 20: 17591 (CONF-650922, pp 560-7)
power supplies for superconducting, use of flux pumps as, (E/T), 20: 17596 (CONF-650922, pp 615-24)
MAGNETIC FIELDS
book: *Mathematical Models for Computing Electric and Magnetic Fields*, 20: 17161
charged-particle charge and energy flows in strong, nonequilibrium system of, (T), 20: 17487
charged-particle motion in, computer for determining, 20: 17906
charged-particle orbits in, measurement using current-carrying wire, 20: 16771 (CONF-650922, pp 467-71)
charged-particle trajectories in, measurement using current-carrying wire, (E/T), 20: 17196 (CONF-650922, pp 497-504)
design of high-order double focusing, for beta spectrometers, 20: 16868
distribution in cyclotrons, correction of radial, 20: 17187 (CONF-650922, pp 377-89)
effects of crossed electric and, on plasma, (E), 20: 17943
effects of traveling, on conducting bodies, (T), 20: 17162
effects on noise fluctuations in electron beams, (T), 20: 17505
electromagnetic wave reflection and refraction by plasma in, plane, (T), 20: 17915
electron beam quantum depolarization in, storage ring high-energy, (T), 20: 17689 (NP-15783)
flux compression by cylindrical liners, (T), 20: 17157 (EUR-2620.i)
interactions of dipole, with plasma, (E), 20: 17551
measurement in beam transport systems, semiautomatic system for, 20: 17192 (CONF-650922, pp 456-66)
measurement in cyclotrons, automatic data logging and processing system for, 20: 17188 (CONF-650922, pp 415-20)
measurement in cyclotrons, using Hall effect, 20: 17189 (CONF-650922, pp 421-7)
measurement of gradient, using Hall effect, 20: 17194 (CONF-650922, pp 483-6)
measurement of harmonic content in beam transport systems, search coils for, 20: 17195 (CONF-650922, pp 487-96)
measurement of quadrupole, method for, 20: 17190 (CONF-650922, pp 431-46)
measurement of, NMR device for, 20: 16770 (CONF-650922, pp 428-30)
measurement using Hall effect, 20: 17191 (CONF-650922, pp 447-55)
measurement using Hall effect, method of, 20: 17193 (CONF-650922, pp 472-5)
model for studying, analog, 20: 17181 (CONF-650922, pp 126-40)
plasma containment and heating by, (T), 20: 17927
plasma containment and heating by, (E), 20: 17928
plasma diffusion across, in r-f discharges, (E), 20: 17954
plasma interactions with cylindrical, (T), 20: 17956
potential functions for, three-dimensional, 20: 17177 (CONF-650922,

pp 89-95)
MAGNETIC MATERIALS
radiation effects on, review of, 20: 16911
MAGNETIC MIRROR MACHINES
charged-particle trajectories in, analog computer techniques for determining, 20: 17906
magnet coil design for, cryogenic, 20: 17874 (CONF-650922, pp 630-42)
plasma heating in, properties of electron cyclotron, (E/T), 20: 17888(R) (ORNL-3908, pp 32-51)
plasma production and properties in two-stage, 20: 17953
MAGNETITES
age estimation from helium content of, 20: 16714
argon and helium content of, origin of, 20: 16714
solubility in water at high temperatures, 20: 17158(R) (ORNL-3900, pp 82-149)
MAGNETOHYDRODYNAMIC CELLS
bibliography, 20: 17326 (AED-C-15-10)
design and performance of inductively coupled a-c, 20: 17330
performance at large Hall numbers, (T), 20: 17332
performance using inert gases, 20: 17328
power output of Hall effect, (T), 20: 17521
MAGNETOHYDRODYNAMICS
boundary layer behavior in, influence of Hall effects on, 20: 17534
damping of linearized magnetoacoustic waves, resonant ohmic, 20: 17946
fluid flow around magnets, field-aligned, (T), 20: 17509 (D-1-82-0469)
gas flow around bodies, (T), 20: 17525
gas flow in nonequilibrium, plane steady, (T), 20: 17515
gas flow in, Hall effect in axial-symmetric, (T), 20: 17521
gas flow in, ultrasonic, (T), 20: 17513
gas flow with Hall effect in, Rayleigh problem in, (T), 20: 17512
gas flow with orthogonal magnetic and velocity field distributions, (T), 20: 17532
plasma flow in magnetic fields, similarity analysis of, (T), 20: 17910
thermal stability of completely confined fluids in, (T), 20: 17535
MAGNETOMETERS
design of NMR, 20: 16791
design of NMR, using flowing liquid samples, 20: 16770 (CONF-650922, pp 428-30)
MAGNETOSPHERE
boundary of, motion of outer, (E), 20: 17541 (N-65-19719)
boundary with solar wind, 20: 17249
electron velocity distribution in, determination from whistler attenuation, (T), 20: 17558
interaction with solar wind, field perturbation from simulated, (E), 20: 17546
interactions with moving bodies, 20: 17537 (JPLAI/LS-641)
ion currents in, from ionospheric dynamo theory, 20: 17553
solar wind interactions with, (T), 20: 17232
MAGNETS
aberration properties of systems of octopole and quadrupole, computer program for third-order, 20: 17220
calibration in beam transport system of Stanford Linear Accelerator, 20: 17206 (CONF-650922, pp 823-34)
cooling system for superconducting, for bubble chambers, 20: 17595 (CONF-650922, pp 611-14)
cost factors, 20: 16584 (CONF-650922, pp 271-80)
current regulators for Princeton Synchrotron, design of, 20: 17205 (CONF-650922, pp 817-22)
current shim for cyclotron, 20: 17187 (CONF-650922, pp 377-89)
design for beam transport systems of CERN proton synchrotron, 20: 17183 (CONF-650922, pp 218-38)
design for Hamburg Electron Synchrotron, 20: 17213(T) (UCRL-Trans-1312)
design for large bubble chambers, 20: 16810 (CONF-650922, pp 366-76)
design for spark chambers, using tape-wound coils, 20: 16809 (CONF-650922, pp 253-61)
design for use in high-energy physics, (T), 20: 17175 (CONF-650922, pp 1-26)
design for 90°bending of 100-Mev electron beams, 20: 17200 (CONF-650922, pp 715-22)
design of cryogenic, for energy storage, 20: 17597 (CONF-650922, pp 625-9)
design of high-field superconducting, 20: 17598 (CONF-650922, pp 745-52)
design of megagauss, using capacitor discharges, 20: 16587 (CONF-650922, pp 680-3)
design of pulsed, for bubble chambers, 20: 16811 (CONF-650922, pp 663-79)
design of superconducting, for traveling-wave masers, 20: 17626
design of superconducting, for 90° deflection of 30-Mev protons, 20: 17197 (CONF-650922, pp 536-40)
design of superconducting, for polarized proton targets, 20: 17586 (CONF-650922, pp 509-16)
design of superconducting, for magneto-optical studies, 20: 17588 (CONF-650922, pp 525-9)
design of superconducting, 20: 17594 (CONF-650922, pp 604-10)
design of water-cooled d-c, 20: 16585 (CONF-650922, pp 349-55)
design of, three-dimensional potential functions for, 20: 17177 (CONF-650922, pp 89-95)
design of, use of conformal transformation in, 20: 17179 (CONF-650922, pp 104-110)
design with uniform induction, 20: 17184 (CONF-650922, pp 239-47)
development for particle accelerators, 20: 17222
development of cryogenically cooled and superconducting, 20: 17592 (CONF-650922, pp 574-87)
fabrication of contoured poles for FFAG accelerator, 20: 17185 (CONF-650922, pp 248-52)
field quality in quadrupole, method of calculating, 20: 17182 (CONF-650922, pp 208-17)
magnetic properties of steels for use in, 20: 17009 (CONF-650922, pp 287-96)
magnetic properties of steels for use in gradient, 20: 17010 (CONF-650922, pp 297-304)
pole profile calculations using method of equivalent currents, 20: 17178 (CONF-650922, pp 96-103)
power supplies for, survey of, 20: 17202 (CONF-650922, pp 755-68)
power supplies for ZGS, design of, (E), 20: 17204 (CONF-650922, pp 808-16)
power supplies for pulsed, use of acyclic generators as, 20: 16772 (CONF-650922, pp 769-75)
power supplies for, status of solid-state, 20: 16773 (CONF-650922, pp 779-87)
power supply for MURA FFAG magnet modeling program, design of, 20: 17203 (CONF-650922, pp 776-8)
power supply for ZGS ring, design of, 20: 17227
technology of, conference on, 20: 17156 (CONF-650922)
technology of, for high-energy physics, 20: 17176 (CONF-650922, pp 27-55)
MAIZE
calcium-45 transport in paired root segments of, method for determining wounding response in, 20: 16170 (AD-628805)
radiation effects on root growth in seedlings of, from tritiated water and tritiated thymidine, 20: 16227(R) (NYO-3561-2)
MALATES
radiation effects on oxidation of, in *Vibrio cholerae*, 20: 16198
MALONIC ACID, DIETHYL ESTER
tritium exchange with hydrocarbons, effects of catalysts on, 20: 16492
MAMMALS
radioinduced mutations in, neutron, 20: 16159(R) (ORNL-3900, pp 150-81)
MAN
cesium-137 content in urine of, Japan, 1964, 20: 16731 (NP-15883)
cesium-137 content of, whole-body, 20: 16303(R) (AD-626384)
effects of microwaves on, thermal, 20: 16235
effects of space flight on, 20: 16231 (UCRL-16377)
fallout hazards to, prediction of, 20: 16160 (UCRL-14739(Pt.2))
iodine-131 content in thyroid gland and urine of, Japan, 1964, 20: 16730 (NP-15882)
radiation effects on Japanese, medical survey of 10-year fallout, 20: 16226 (NP-15891)
radiation effects on morphology of erythrocytes in, x, 20: 16250
radiation effects on skin pigments in, uv, 20: 16261
radiation hazards to, from inhalation of radioiodines, 20: 16734 (TID-22693)
radiation hazards to, program for control of, 20: 16160 (UCRL-14739 (Pt.2))
radiation hazards to, in atmosphere, 20: 16732 (NP-15898)
radiation hazards to fetal, from placental transfer of fission products, 20: 16301
radioinduced chromosome aberrations in, effects of dose on, 20: 16230(R) (TID-22644)
radiosensitivity of spinal cord of, x, 20: 16251
radiosensitivity of tissues of, 20: 16322
radiotherapy of malignant diseases in children, effectiveness of, 20: 16306
radium-226 content in, Bombay and Kerala, India, 20: 16747
strontium-85 uptake from gastrointestinal tract of, effects of sodium alginate on, 20: 16173 (PG-Report-686)
strontium-90 content in bones of children in U. S., 1965, 20: 16662(R) (HASL-165)
strontium-90 content in primary teeth of children in New Jersey, 20: 16763
strontium-90 content of, whole-body, 20: 16303(R) (AD-626384)
MANGANESE
determination in asbestos using ion exchange, activation, 20: 16336(R) (NYO-10175)
determination in beryllium, spectrophotometric, 20: 16361

determination in calcium carbonate, chalk, and potassium hydroxide, substoichiometric activation, 20: 16403
determination in stainless steel, activation, 20: 16338 (RT/CHI-(65)36)
determination in serum, activation, 20: 16347
determination of trace amounts of, in beryllium by spectrography, 20: 16352
determination using sodium perxenate, spectrophotometric, 20: 16351
effects on activation determination of arsenic in ores and rocks, 20: 16364
preparation of self-supporting radiation targets of, 20: 17218
reactions with graphite, composition and structure of carbides formed in, 20: 17030(T) (LA-tr-66-1)
role in enzyme systems by which RNA is synthesized, 20: 16160 (UCRL-14739(Pt.2))
separation from Hanford wastes by solvent extraction, 20: 16329 (BNWL-187)
separation from rare earths, solvent extraction method for, 20: 16329 (BNWL-187)
separation from scandium by ion exchange chromatography, 20: 16574
sorption by barley roots, effects of polyvalent cations on, 20: 16174(R) (RLO-1547-3)

MANGANESE ALLOYS
Au–Mn, crystal structure of Au_3Mn, 20: 17066
Dy–Mn, crystal structure of Dy_6Mn_{23} in, 20: 17096(T)
Er–Mn, crystal structure of Er_6Mn_{23} in, 20: 17096(T)
Gd–Mn, crystal structure of Gd_6Mn_{23} in, 20: 17096(T)
Ho–Mn, crystal structure of Ho_6Mn_{23} in, 20: 17096(T)
Mn–Sm, crystal structure of Sm_6Mn_{23} in, 20: 17096(T)
Mn–Tb, crystal structure of Tb_6Mn_{23} in, 20: 17096(T)
Mn–Y, crystal structure of Y_6Mn_{23} in, 20: 17096(T)

MANGANESE BROMIDES
preparation of high purity crystalline, 20: 17978(R) (NYO-3402-2)

MANGANESE CARBIDES
preparation, composition, and structure of, 20: 17030(T) (LA-tr-66-1)

MANGANESE COMPLEXES
with solochrome violet RS, polarography of, 20: 16406

MANGANESE IONS
effects on hydrolysis of α-D-glucose 1-phosphate, 20: 16421
sorption by aminodiacetate resin Dowex A-1, 20: 16358

MANGANESE ISOTOPES Mn-51
half life, 20: 16331 (GA-6568)

MANGANESE ISOTOPES Mn-54
content in atmospheric dust and rain water, 1964–65, 20: 16660 (AERE-R-4997)
content in barley, rye, tea leaves, and wheat, 20: 16167
content in Bogou iron meteorite, 20: 16674
content in mollusks in Lake Maggiore, Italy, 20: 16185
content in plants before and after Salmon Event, 20: 16743 (VUF-1021)
content in stratospheric and tropospheric samples in Project Star Dust, 1963, 20: 16727(R) (HASL-168)
content in stratospheric and tropospheric samples in Project Star Dust, 1964, 20: 16728(R) (HASL-169)
metabolism in aquatic organisms, 20: 16160 (UCRL-14739(Pt.2))
nucleon interactions in, properties from effective, (T), 20: 17735

MANGANESE ISOTOPES Mn-55
helium-3 reactions (He-3,2p) at 12 Mev, Q value for, 20: 16331 (GA-6568)
nucleon interactions in, properties from effective, (T), 20: 17735

MANGANESE ISOTOPES Mn-56
half life, 20: 16331 (GA-6568)
separation from magnesium-27 by solvent extraction using diethyl-dithiocarbamic acid, 20: 16336(R) (NYO-10175)

MANGANESE OXIDES
electronic properties of single-crystal, effects of ion-bombardment on, 20: 17151

MARCOULE REACTORS (G-2)
coolant activity, analysis, and leaks, 20: 18120
power control and measurement systems for, 20: 18119

MARCOULE REACTORS (G-3)
coolant activity, analysis, and leaks, 20: 18120
power control and measurement systems for, 20: 18119

MARITIME REACTORS
control rod latch system for, 20: 18041(P)
design of forced-circulation, pressurized-water, 20: 18126 (EUR-2629.i(Vol.1))
development of PWR, for oceanographic research ship, 20: 18129
startup sequence for, automation of, 20: 18130

MASERS
superconducting magnets for traveling-wave, 20: 17626

MASERS (OPTICAL)
beam absorption by plasma, effects from, 20: 17531
beam focusing in air, plasma production by, (E), 20: 17908
beam reactions with gases, breakdown and heating in focused, 20: 17531
beam scattering from, line-profile effects in stimulated, (T), 20: 17464
development for Mach-Zehnder interferometers, for plasma diagnostics, 20: 17875 (IPP-1/35)
effects of giant pulsed, on solid targets, 20: 17531
laser emission by pinch plasma, (E), 20: 17924(T)
performance of europium chelate, deuterium isotope effects on, 20: 16781
radiation effects on, 20: 16505 (BNL-949)
use in bubble chamber illumination and photography, 20: 16841
uses of gas, for plasma diagnostics, (E), 20: 17508 (ARL-65-246)

MASS SPECTROGRAPHY
use in isotopic analysis of sulfur, 20: 16379

MASS SPECTROMETERS
design changes for M1-1305, 20: 16798
design of drift-tube, 20: 17298
operation of double-magnetic-deflection, 20: 17158(R) (ORNL-3900, pp 82-149)

MASSACHUSETTS
geologic dating of granites, quartzites, and slates in, use of rubidium–strontium and strontium-87/-86 methods for, 20: 16711(R) (MIT-1381-13)

MATERIALS TESTING
nondestructive methods development at ORNL, 20: 18020(R) (ORNL-3900, pp 2-81)
nondestructive methods of, for pressure vessels, 20: 16617

MATERIALS TESTING REACTOR
materials irradiation testing in, handbook for, 20: 18135 (IDO-17135)

MATHEMATICS
book: *Mathematical Models for Computing Electric and Magnetic Fields*, 20: 17161
difference algorithm in, convergence of, 20: 16935
equations for fallout isoconcentration line determination, 20: 16664(R) (UCRL-14534, pp 19-22)
generalization of complex spherical function to four dimensions, 20: 16941
integral equations in, numerical solution of singular, 20: 16936
integral transforms in, method for quadrature for Euler, 20: 16937
Lie groups in, canonical realizations of, 20: 16939
matrices in, correlation functions for eigenvalues of real quaternian, 20: 16938
methods in equation development, 20: 17160
research programs at ORNL on, 20: 16159(R) (ORNL-3900, pp 150-81)
restricted three-body problem, asymptotic matching in, 20: 17584

MEATS
radiation effects on survival curves of bacteria in crab, γ, 20: 16237

MECHANICS
Lie groups in, canonical realizations of, 20: 16939
parameters in statistical, power-series expansion for, 20: 17527
symmetry in classical, SU(2), 20: 17429 (JINR-P-2529)

MEDICAL PERSONNEL
employment of pregnant women in radiation work, 20: 16762

MEDICINE
survey of 10-year radiation effects from fallout on Japanese, 20: 16226 (NP-15891)
use in treating injuries resulting from radiotherapy, 20: 16319
veterinary, curriculum of, 20: 16761

MEIOSIS
radiation effects on jute, γ, 20: 16217 (AECD-AG-7)

MELAMINE, TRIETHYLENE-
effects on mitosis in rat lens epithelium, 20: 16256

MEMBRANES
biochemical activity of yolk sac, during cell differentiation in chick embryos, 20: 16172(R) (NYO-2194-1)
lipid content of sheep erythrocyte, function of, 20: 16160 (UCRL-14739(Pt.2))
radioinduced PVA, for use in artificial kidney, 20: 16505 (BNL-949)

MEMORY DEVICES
development of superconductive bridge cells, 20: 16797

MENDELEVIUM
production, 20: 16543
separation from californium and fermium by extraction chromatography using bis(2-ethylhexyl) orthophosphate, 20: 16404

MERCHANT VESSELS
book: *Naval Nuclear Power Installations*, 20: 18132
design of nuclear-powered tanker using forced-circulation pressurized-water reactor, 20: 18126 (EUR-2629.i(Vol.1))
reactor startup sequence for, automation of, 20: 18130
visit of N.S. *Savannah*, at Copenhagen, 20: 18174(R) (NP-15771)

MERCURY
cavitation damage to materials in, (E), 20: 16974 (NP-15889)
effects on gastrointestinal absorption of copper-64 in rats, 20: 16182
heat transfer properties of, effects of rubidium additions on, 20: 16972(R) (NASA-CR-54719)
recovery of spilled, equipment for, 20: 16738(R) (UCRL-14534, pp 41-3)

separation from scandium by ion exchange chromatography, 20: 16574

MERCURY ALLOYS
Dy–Hg, crystal structure of $DyHg_3$, 20: 17060
Er–Hg, crystal structure of $ErHg_3$, 20: 17060
Eu–Hg, magnetic properties of $EuHg_3$, 20: 17060
Gd–Hg, crystal structure of $GdHg_3$, 20: 17060
Hg–Tb, crystal structure of $TbHg_3$, 20: 17060
Hg–Tm, crystal structure of $TmHg_3$, 20: 17060
Hg–Yb, crystal structure of $YbHg_3$, 20: 17060
Ho–Hg, crystal structure of $HoHg_3$, 20: 17060
Lu–Hg, crystal structure of $LuHg_3$, 20: 17060

MERCURY IONS
sorption by aminodiacetate resin Dowex A-1, 20: 16358

MERCURY ISOTOPES Hg-196
deuteron reactions (d,p) at 15 Mev, isomeric yield ratios for, 20: 16508(R) (NYO-2771-13)
neutron reactions (n,γ), activation cross section for, (E), 20: 16336(R) (NYO-10175)

MERCURY ISOTOPES Hg-197
half life of isomeric, from neutron reactions (n,γ), (E), 20: 16336(R) (NYO-10175)
half life of, from neutron reactions (n,γ), (E), 20: 16336(R) (NYO-10175)
incorporation in bromosulfalein, 20: 16495
production of isomeric, in deuteron reactions (d,p) at 15 Mev, 20: 16508(R) (NYO-2771-13)
use for diagnosis of brain tumors, 20: 16304

MERCURY ISOTOPES Hg-201
photon resonance scattering on, optical orientation of magnetic moment in, 20: 17755(T)

MERCURY ISOTOPES Hg-203
use for diagnosis of brain tumors, 20: 16304

MESIC ATOMS
energy levels of deformed (μ), resonances in, (T), 20: 17281
hyperfine structure of μ-mesic lead, (E), 20: 17268
hyperfine structure of μ-mesic bismuth, E2 and M1, (E), 20: 17792
x-ray spectra from (μ⁻), nuclear charge distribution from, (T), 20: 17756

MESITYL OXIDE
formation by disproportionation of 3-methyl-3-penten-2-one in perchloric acid, 20: 16542(R) (TID-22646)

MESON BEAMS
focusing of pi, electromagnetic lenses for, 20: 17198 (CONF-650922, pp 650-6)

MESONS
classification of positive-parity, using 189-plet of SU(6), (T), 20: 17339 (JINR-E-2557)
decay rates of, quark model for, 20: 17343 (JINR-P-2524)
effects of vector, on lepton production by neutrino (ν_μ)-proton interactions, (T), 20: 17504
exchange in elementary-particle interactions, distorted-wave theory for one-, 20: 17474
field theory for vector, Rainich geometrization of, 20: 17441
interactions of vector, renormalization theory for coupling in, 20: 17465
interactions with mesons, CT invariance for SU(3) amplitudes in octet, (T), 20: 17453
interactions with baryons, symmetry group for coupling in, (T), 20: 17455
interactions with baryons in broken SU(3) symmetry, self-consistent determination of coupling in, 20: 17467
mass of, quark model for, 20: 17343 (JINR-P-2524)
masses of pseudoscalar, electromagnetic, (T), 20: 17507
photoproduction of, symmetry group for backward and forward, (T), 20: 17455
photoproduction of vector, on protons and mesons (π^+), cross sections for, 20: 17410
production in antiproton-proton annihilation at rest, coupling constants in SU(3) for two-body, (T), 20: 17377
production in antiproton-nucleon annihilation, (T), 20: 17396
theory for axial and tensor, 20: 17442(T)

MESONS, RESONANCE
classification of positive-parity, using 189-plet of SU(6), (T), 20: 17339 (JINR-E-2557)
decay of A_1 and A_2, charge-parity violation in radiative, (T), 20: 17501
decay of χ(960), U(12) symmetry for radiative, 20: 17342 (JINR-P-2520)
decay of, isotopic structure of electromagnetic, (T), 20: 17428 (JINR-P-2498)
effects of 2π (400) and (730), on meson (π)-nucleon scattering amplitudes, (T), 20: 17388
mass of, quark model for determining, 20: 17443(T)
mass relations for, linear, 20: 17391
production in meson (K⁻) interactions with protons at 2.24 Bev/c, (E), 20: 17383
production of $\bar{K}^*0(891)$ in meson (K⁻)-proton interactions at 3 Bev/c, mechanism for, (E), 20: 17380
properties of $K_\delta^*(892)$, (E), 20: 17403
theory for axial and tensor, 20: 17442(T)

MESONS (B)
decay of, charge-parity violation in radiative, (T), 20: 17501
production of, model for, (E/T), 20: 17402

MESONS (η)
decay of, sigma hypothesis in, 20: 17422
photoproduction on protons at 0.3 and 5.5 Bev, (E), 20: 17368
production in meson (K⁻)-proton interactions, cross section and scattering length for, (T), 20: 17376

MESONS (η')
production in nucleon interactions at high energies, SU(3) for multiple, (T), 20: 17345 (JINR-P-2531)

MESONS (f^0)
decay of, charge-parity violation in radiative, (T), 20: 17501

MESONS (K)
decay of, matrix elements for leptonic, 20: 17415
decay of, sigma hypothesis in, 20: 17422
decay of, time-reversal invariance in, (E/T), 20: 17404
interactions with mesons (π) at low energies, sum rules for, 20: 17470
photoproduction on nucleons, polarization coefficients for, (T), 20: 17407

MESONS (K^-)
decay of, weak interaction theory in SU(3) for 2π, 20: 17379
interactions with protons, cross section and scattering length for hyperon (Λ) and meson (η) production in, (T), 20: 17376
interactions with neutrons and protons at high energies, real amplitudes for, (T), 20: 17378
interactions with protons at 2.24 Bev/c, (E), 20: 17383
interactions with protons at 3 Bev/c, mechanism for $\bar{K}^*0(891)$ yields from, (E), 20: 17380
interactions with protons at 2.10, 2.45, and 2.64 Bev/c, $K_\delta^*(892)$ resonances in, (E), 20: 17403
reactions with emulsion nuclei at 3.0 and 5.0 Bev/c, hyperfragment production from, (E), 20: 17752

MESONS (K^0)
decay of K_1^0, weak interaction theory for 2π, 20: 17379
decay of K_2^0, meson (μ^+) polarization in, (E), 20: 17424
decay of, magnetic spectrometer performance for recording 2π, 20: 16814 (ITEF-386)
decay of, sum rule for amplitudes of 2π, (T), 20: 17369

MESONS (K^+)
decay of, sum rule for amplitudes of 2π, (T), 20: 17369
decay of, time-reversal invariance in $\pi^+\pi^0\gamma$, (E/T), 20: 17404
decay of, weak interaction theory in SU(3) for 2π, 20: 17379
detection system for, scintillation, 20: 16826 (PPAD-574E)
interactions with neutrons and protons at high energies, real amplitudes for, (T), 20: 17378
photoproduction on protons at 3.4 to 4.0 Bev, cross sections for, (E/T), 20: 17400
production in photon-proton interactions, quark model for, (T), 20: 17348 (JINR-P-2556)

MESONS (K_{e3})
decay of, current algebra for, (T), 20: 17405

MESONS (μ)
electric dipole moments of, in intermediate vector boson theory, 20: 17372
interactions with neutrinos (ν_μ) at very high energies, (T), 20: 17366(T)
interactions with nucleons, inelastic, (T), 20: 17399

MESONS (μ^+)
polarization in decay of mesons ($K_{\mu 3}^0$), (E), 20: 17424

MESONS (ω)
coupling to baryon current, vector-meson dominance and U(6,6) symmetry for, 20: 17457
photoproduction on protons at 0.3 and 5.5 Bev, (E), 20: 17368
photoproduction on nucleons, effect of absorption on peripheral, (T), 20: 17414

MESONS (φ)
coupling to baryon current, vector-meson dominance and U(6,6) symmetry for, 20: 17457

MESONS (π)
decay of, matrix elements for leptonic, 20: 17415
interactions with nucleons, high-energy successive field, (T), 20: 17418
interactions with mesons (π) and nucleons, inelastic effects on cross sections for elastic, (T), 20: 17419
interactions with mesons (π) and nucleons, dynamical equations for, 20: 17420
interactions with mesons (K) at low energies, sum rules for, 20: 17470
interactions with nucleons, coupling constants for, (T), 20: 17336 (AECD/TP-5)
interactions with nucleons, inelastic effects on P_{11} phase shift in, (T), 20: 17355
interactions with mesons (π), l-dependence, singularities, and double-spectral function for, (T), 20: 17367

interactions with nucleons at high energies, optical model for backward, (T), 20: 17373
interactions with nucleons, effect of dipion resonances on amplitude for, (T), 20: 17388
interactions with nucleons, minimal singularity in axiomatic approach to charge-symmetry, (T), 20: 17416
interactions with nucleons, coupled-channel Schroedinger equation model for, 20: 17397
photoproduction on protons at 0.3 and 5.5 Bev, (E), 20: 17368
photoproduction on nucleons, current algebra for, (T), 20: 17375
photoproduction on nucleons, polarization coefficients for, (T), 20: 17407
production in antiproton-neutron interactions in emulsions at 3 Bev/c, (E), 20: 17359
production in antiproton-proton annihilation at 3.3 and 3.7 Bev/c, (E), 20: 17385
production in high-energy cascade showers, transverse momentum distribution for, (T), 20: 17371
production in meson (π^-) interactions with protons at 1.89 Bev/c, multiple, (E), 20: 17386
production in nucleon interactions at high energies, SU(3) for multiple, (T), 20: 17345 (JINR-P-2531)
reactions in nuclear emulsions at 7.5 and 17.5 Bev, charged-particle identification from delta electrons in, (E), 20: 17358
reactions with emulsion nuclei at 7.5 Bev, production of high-energy fragments in, (E), 20: 17715
reactions with emulsion nuclei at 17.5 Bev, helium particle emission in, (E), 20: 17716

MESONS (π^-)
capture by hydrogen and deuterium, probabilities for fine-structure-level, (T), 20: 17278
interactions with protons in emulsions at 5.5 Bev/c, cross sections for elastic, (E), 20: 17360
interactions with protons at high energies, real amplitudes for, (T), 20: 17378
interactions with protons at 1.5 and 1.8 Bev/c, polarization of hyperons (Σ^0) from, (E), 20: 17382
interactions with protons at 1.89 Bev/c, multiple meson (π) production in, (E), 20: 17386
interactions with protons at 3.2 and 4.2 Bev/c, meson (B) production in, (E/T), 20: 17402

MESONS (π^0)
decay of, 3γ, (E), 20: 17340 (JINR-P-2322)
production in nucleon interactions at high energies, SU(3) for multiple, (T), 20: 17345 (JINR-P-2531)

MESONS (π^+)
interactions with protons at 1 to 4 Bev, inelastic, (T), 20: 17344 (JINR-P-2530)
interactions with protons at high energies, real amplitudes for, (T), 20: 17378
interactions with protons at 1.6 Bev/c, mesons (ρ^+) and N_{33}^{*++} production from, (E), 20: 17374
interactions with protons at 450 Mev, cross sections for elastic and inelastic, (E), 20: 17384
interactions with photons, cross sections for vector meson production in, 20: 17410
interactions with protons at 180°, spark chamber for recording, 20: 16815 (JINR-P-2506)
lifetime, (E), 20: 17346 (JINR-P-2534)
photoproduction on protons at 3.4 to 4.0 Bev, cross sections for, (E/T), 20: 17400
production in photon-proton interactions, quark model for, (T), 20: 17348 (JINR-P-2556)

MESONS (ρ)
coupling to baryon current, vector-meson dominance and U(6,6) symmetry for, 20: 17457
photoproduction on protons at 0.3 and 5.5 Bev, (E), 20: 17368
photoproduction on nucleons, effect of absorption on peripheral, (T), 20: 17414

MESONS (ρ^+)
production in meson (π^+)-proton interactions at 1.6 Bev/c, cross sections for, (E), 20: 17374

MESONS (σ)
role in decay of mesons (η), (K), and (X^0), (T), 20: 17422

MESONS (X^0)
decay of, sigma hypothesis in, 20: 17422

METABOLISM
effects of rare earths and yttrium on, in bacteria, fungi, molds, and yeasts, 20: 16191
effects on plant uptake of divalent cations, 20: 16174(R) (RLO-1547-3)
pathways of, in embryonic development, tracer studies, 20: 16172(R) (NYO-2194-1)

METALLIC FILMS
density of thin aluminum, proton-produced x rays for determining surface, 20: 17051

METALLIC FOILS
fission-fragment reactions with, secondary electron production in, 20: 17168

METALLOGRAPHY
conference on, ORNL, April 20–22, 1965, 20: 16945 (ORNL-TM-1161)
sample mounting in epoxy resin using a radio-frequency furnace, accelerated, 20: 16947 (ORNL-TM-1161, pp 98-102)
sample mounting resins for irradiated specimens, evaluation of, 20: 16948 (ORNL-TM-1161, pp 103-11)
sample preparation techniques for irradiated specimens in, for electron microscope studies, 20: 17128 (ORNL-TM-1161, pp 194-207)
sample preparation for, using electrical-discharge machining, design and operation of equipment for, 20: 16951 (ORNL-TM-1161, pp 159-81)
sample preparation of urania containing metallic inclusions for, 20: 16953 (ORNL-TM-1161, pp 249-66)
sample preparation for high-magnification examination of ceramic materials, 20: 16954 (ORNL-TM-1161, pp 267-71)
uses of color film in, 20: 16949 (ORNL-TM-1161, pp 112-29)
uses of image-splitting eyepiece in, 20: 16952 (ORNL-TM-1161, pp 182-91)
uses of microphotometers in, 20: 16950 (ORNL-TM-1161, pp 132-45)

METALS
boiling of liquid, under forced convection, 20: 16608(T) (ANL-Trans-257)
coating with zirconium carbide by electrophoresis at 19 to 20 mv, 20: 17004
crystal structure of, effects of fabrication on, 20: 17158(R) (ORNL-3900, pp 82-149)
defects in, study by electron microscopy, 20: 17158(R) (ORNL-3900, pp 82-149)
determination trace amounts in cells, electron microscopic, 20: 16160 (UCRL-14739(Pt.2))
diffusion of tritium in, research on, 20: 17892(R) (ORNL-3908, pp 149-53)
dislocation motion in, size distribution of obstacles to, 20: 17980(T) (ANL-Trans-274)
effects of ions of, on protein synthesis systems, 20: 16160 (UCRL-14739(Pt.2))
electron emission from, in cesium-fluorine vapors, (T), 20: 17334
electron tunneling into normal, from superconducting films, electron interference effects in, (E/T), 20: 17621
heat transfer to turbulently flowing liquid, annulus eccentricity effects on, 20: 16612
internal friction and Young's modulus of, design of apparatus for measurement of, 20: 17013 (INR-632/XIV/PS)
ion emission from cesiated surfaces of, at room temperature, (E/T), 20: 17267
ion pairing interactions in normal, (T), 20: 17008 (CEA-R-2820)
performance and selection of, for use in space vehicles, 20: 16944 (NASA-SP-3025)
preparation of pure, review of progress on, 20: 17158(R) (ORNL-3900, pp 82-149)
radiation enhanced diffusion in, effects of correlated defects in gamma-, 20: 17131
reflectivity of, microphotometer for measuring, 20: 16950 (ORNL-TM-1161, pp 132-45)
specific heat of superconducting, at transition point, (T), 20: 17612(T)

METEORITES
age estimation, 20: 16715
analysis of Canyon Diablo, mass spectrometric and metallographic, 20: 17238
diffusion of tritium in stone, 20: 17247
radioactivity from gamma emitters of Bogou iron, 20: 16674
rare earths abundance in, comparison with earth's crust, 20: 17233
rare gas contents and isotopic abundances in Achilles, LaLande, and Peace River, 20: 16672
rare gas contents in, evidence for paired falls from, 20: 16673
uranium distribution in, 20: 16684
xenon isotope content in Pasamonte, anomalies from, 20: 17239

METEOROLOGY
conference on use of radioisotopes in, 20: 16636
data recording system for meteorological studies at reactor sites, design of automatic, 20: 16710
effects of meteorological conditions on sampling of fallout, 20: 16656
effects of meteorological conditions on radioactivity in atmosphere over oceans, 20: 16699
fallout perturbations by local sea breezes, 20: 16661(R) (ECOM-00392-F)
measurements at Casaccia, Italy, 1964, 20: 16635 (RT/PROT(65)-40)

METHANE
deuterium exchange with hydrogen in, catalytic effects of gold–palladium alloy on, 20: 16457

formation in reactions between rare earth dicarbides and water, 20: 17048
radiation effects on desorption of graphite surfaces in, 20: 17114 (AERE-R-5163)
reactions in plasma jets, 20: 17959
Ar–methane, distribution in nonequilibrium plasma of, 20: 17959
CO_2–CO–methane, radiation effects on desorption of graphite surfaces in, 20: 17114 (AERE-R-5163)
METHANE, CHLORODIPHENYL-
spectra of, infrared and Raman, 20: 16498
METHANE, DIPHENYL-
preparation and spectra of deuterated, 20: 16498
spectra of, infrared and Raman, 20: 16498
METHANE, IODO-
retention in atmosphere, efficiency of Whatman Type ACG/B filter paper for, 20: 16719 (AEEW-M-568)
METHANE, TRIPHENYL-
determination in polyphenyls by chromatography, thermal conductivity, and flame ionization, 20: 16341
METHANE, TRIPHENYL-, DERIVATIVES
uses for radiation dosimetry, 20: 16521
METHANESULFONIC ACID, ETHYL ESTER
effects on algae, patterns of expressions of mutagenic, 20: 16294
METHANESULFONIC ACID, TETRAMETHYLENE ESTER
effects on mitosis in rat lens epithelium, 20: 16256
METHANOL
effects on radioinduced rayon to styrene graft polymerization, 20: 16528
labeling with oxygen-17 and -18, 20: 16547
benzene–methanol, radiolysis of, free-radical scavenging in, 20: 16530
METHYL RADICALS *(Free Radicals)*
yield from gamma radiolysis of hexane–silica gel systems, 20: 16511
METHYL SULFOXIDE
properties of, for use as solvent in measuring scintillation mixtures, 20: 16355
MICE
immune reactions to antigens in, effects of age on, 20: 16159(R) (ORNL-3900, pp 150-81)
radiation effects on intestinal epithelium of, lethal whole-body x, 20: 16223 (BNL-8952)
radiation effects on, protective effects of 1,3,4-oxadiazolium salts and s-triazole derivatives against, 20: 16490(R) (TID-22681)
radiation effects on succinic dehydrogenase activity in, uv, 20: 16196
radiation effects on blood cells, globulins, and proteins in, fractionated-dose x, 20: 16224 (CEA-R-2848)
radiation effects on, role of adrenal and pituitary glands in, 20: 16232(T) (JPRS-34120)
radiation effects on leukemic, combined with cyclophosphamide and hyperbaric oxygen, x, 20: 16262
radiation effects on body and renal weight in nephrectomized, x, 20: 16282
radiation effects on, protective effects of sulfur compounds against, 20: 16297(R) (EUR-2548.f)
radioinduced leukemia transmission in, effects of viruses on, 20: 16159(R) (ORNL-3900, pp 150-81)
radiosensitivity of cultured cells of, effects of serum and temperature on, 20: 16298
radiosensitivity of, effects of aspartic acid and Solcoseryl on, 20: 16302
MICROORGANISMS
content in marine ecosystem, 20: 16175(R) (RT/BIO(65)-1)
MICROSCOPES
performance of image-splitting eyepieces in, in metallographic applications, 20: 16952 (ORNL-TM-1161, pp 182-91)
MICROSCOPY
sample preparation of ceramic materials for high-magnification optical, 20: 16954 (ORNL-TM-1161, pp 267-71)
use of polarization, in muscle contraction studies, 20: 16259
MICROSOMES
chemical dissection of rat liver, method for, 20: 16160 (UCRL-14739 (Pt.2))
function of, electron microscopic analysis of, 20: 16160 (UCRL-14739 (Pt.2))
MICROWAVE EQUIPMENT
development of waveguides, for accelerators, 20: 17209(R) (LA-3479)
electron interactions in uniformly loaded waveguides, Cherenkov radiation from, (T), 20: 17485
properties of Alfvén cylindrical waveguides, terminal, (T), 20: 17522
MICROWAVES
effects on man and experimental animals, thermal, 20: 16235
scattering by plasma, electron density determination by, 20: 17876 (IPP-1/37)
use for plasma electron density measurements, (E), 20: 17510 (IPP-3/25)
use of focused beams of, in plasma diagnostics, (E/T), 20: 17881 (N-65-19804)
MILK
analysis for cesium-137 by ion exchange and gamma spectroscopy, 20: 16342
analysis for radioisotopes, methods for, 20: 16369
cesium-137 content in powdered, in Japan, 1962 and 1963, 20: 16755
evaporation for gamma pulse-height analysis, equipment for, 20: 16741(R) (UCRL-14534, pp 54-6)
iodine-131 content in Japan, 1964, 20: 16730 (NP-15882)
radiation monitoring for Salmon Event, 20: 16743 (VUF-1021)
radioactive contamination of, control measures for, 20: 16754
radioactivity from cesium-137 and strontium-90, in Japan, 1964, 20: 16731 (NP-15883)
radium-226 content in French, 20: 16752
radium-226 content in French, 20: 16753
separation of strontium-85, -89, and -90 from, using calcium phosphate precipitation method, 20: 16382
sodium-22 uptake from fallout, 20: 16678
strontium-90 content in U. S., 1965, 20: 16662(R) (HASL-165)
strontium-90 content in powdered, in Japan, 1962 and 1963, 20: 16755
MINERAL METABOLISM
radiation effects on rat, tracer study of γ, 20: 16187
MINERALS
analysis for niobium and tantalum simultaneously, activation, 20: 16336(R) (NYO-10175)
phase diagrams of binary systems of, entropy of melting of, 20: 16711(R) (MIT-1381-13)
uranium distribution in, 20: 16684
MISSISSIPPI (LAMAR CO.)
environs monitoring for Salmon Event, 20: 16743 (VUF-1021)
MITOCHONDRIA
role in radioisotope accumulation by higher animals, 20: 16160 (UCRL-14739(Pt.2))
MITOSIS
effects of myleran and TEM on, in rat lens epithelium, 20: 16256
effects of stage of, on radiosensitivity of cells, 20: 16292
radiation effects on, in Saccharomyces, 20: 16255
radiation effects on, low-dose, 20: 16160 (UCRL-14739(Pt.2))
radiation effects on *E. coli*, repair of x, 20: 16200
radiation effects on jute, γ, 20: 16217 (AECD-AG-7)
radiation effects on, in rat lens epithelium, 20: 16256
radiation effects on, in *Vicia faba* seeds, effects of infrared radiation on x, 20: 16278
MOLDS
defects in polyvinyl chloride plastisol, effects of moisture on, 20: 18179 (Y-1508)
growth and metabolism of, effects of rare earths and yttrium on, 20: 16191
MOLECULAR BEAMS
production using cylindrical tubes, (T), 20: 17279
MOLECULES
charged-particle inelastic scattering by, (T), 20: 17306
electromagnetic-wave reactions with, ionization by, (T), 20: 17284
electron scattering by, resonances in, (T), 20: 17289
radiation effects on biological, 20: 16160 (UCRL-14739(Pt.2))
radiation effects on, 20: 16160 (UCRL-14739(Pt.2))
reactions of polyatomic, with electrons, 20: 16159(R) (ORNL-3900, pp 150-81)
reactions with muonium, 20: 17297
scattering of, R-matrix theory for elastic and reactive, (T), 20: 17259
MOLLUSKS
manganese-54 content in Lake Maggiore, Italy, 20: 16185
manganese-54 metabolism in fresh-water, 20: 16160 (UCRL-14739(Pt.2))
radioinduced muscle inactivation in, combined with polarization microscopy for contraction studies, uv, 20: 16259
zinc-65 metabolism in fresh-water, 20: 16160 (UCRL-14739(Pt.2))
zinc-65 uptake by, from radioactive wastes in fresh water, 20: 18157 (BNWL-SA-466)
MOLTEN SALT REACTOR EXPERIMENT
components development and testing, 20: 18020(R) (ORNL-3900, pp 2-81)
fuel processing for, 20: 16582
neutron losses in, delayed, 20: 18048 (ORNL-P-1967)
MOLTEN SALT REACTORS
design of power-breeder, 20: 18088 (INR-669/C)
MOLYBDENUM
analysis for oxygen, activation, 20: 16331 (GA-6568)
compatibility with alumina, beryllia, magnesia, and boron nitride, 20: 17022 (N-65-18933)
creep-rupture properties at high temperatures, 20: 17011 (CONF-651025-14)
crystal lattice dynamics of, Krebb's model for, 20: 17081
determination of trace amounts of, in beryllium by spectrography, 20: 16352

deuteron sputtering at 30 kev, yields from, 20: 17892(R) (ORNL-3908, pp 149-53)
diffusion in molybdenum–tungsten alloys at 1500 to 2400°C, tracer studies of, 20: 17101
diffusion in titanium at 905 to 1210°C, inter-, 20: 17111
dislocation parameters for, 20: 17033
effects of alloying additions of, on corrosion resistance of type 430 stainless steel, 20: 16975 (NP-15900)
evaporation from irradiated uranium dioxide at 750 to 1600°C, 20: 17102
melting point of, effects of gas impurities on, 20: 17094
nuclear spin relaxation in metallic, (E), 20: 17998
radioinduced defects in, effects of prestrain on fast-neutron, 20: 17132
separation from technetium by sorption on iron oxide, 20: 16552
thermal capacity of, Krebb's model for lattice contributions to, 20: 17081
use as cathodes for getter ion pumps, 20: 16789

MOLYBDENUM ALLOY COUPLES
Mo/Mo–W, densification of sintered tungsten–molybdenum powder compact, Kirkendall-effect in, 20: 16994

MOLYBDENUM ALLOYS
Al–Hf–Mo, phase studies on intermetallic compounds in, 20: 17075
Co–Mo, effects of additives on high-temperature properties of eutectic, 20: 17108
Cr–Fe–Mo, phase studies, 20: 17093
Mo–Nb–Ta–W, deformation mechanisms in solution-hardened niobium-base, 20: 17082
Mo–Nb–Ta–W, properties as hollow turbine vanes, 20: 16963
Mo–Nb–V–Zr, fabrication of tubing of B-66, 20: 16998
Mo–Re, creep-rupture properties at high temperatures, 20: 17011 (CONF-651025-14)
Mo–Re–W, fabrication of rods of, by extrusion and sintering, 20: 16989(R) (COO-1518-2)
Mo–Ta, electric conductivity of single-crystal, specific, 20: 17083
Mo–Ti, cavitation damage in mercury and water, 20: 16974 (NP-15889)
Mo–Ti–Zr, compatibility of TZM, with alumina, beryllia, magnesia, and boron nitride, 20: 17022 (N-65-18933)
Mo–U, mechanical properties and structure of, effects of heat treatments on, 20: 17014 (INR-645/XIV/PS)
Mo–W, diffusion of molybdenum and tungsten in, at 1500 to 2400°C, tracer studies of, 20: 17101

MOLYBDENUM BORIDES
chemical bonding and electric conductivity of, 20: 16439

MOLYBDENUM CARBIDES
superconducting transition temperature of, 20: 17607
MoC–NbN, superconducting properties, 20: 17589 (CONF-650922, pp 541-9)

MOLYBDENUM COUPLES
Mo/Mo–W, densification of sintered tungsten–molybdenum powder compact, Kirkendall-effect in, 20: 16994

MOLYBDENUM ISOTOPES
book: *Radioactive Molybdenum Isotopes*, in Russian, 20: 16917

MOLYBDENUM ISOTOPES Mo-92
deuteron reactions (d,n) at 15 Mev, isomeric yield ratios for, 20: 16508(R) (NYO-2771-13)
neon-20 and -22 reactions with, delayed proton emitters from, (E), 20: 17687 (JINR-P-2514)

MOLYBDENUM ISOTOPES Mo-93
production, separation, and uses of, 20: 16917

MOLYBDENUM ISOTOPES Mo-94
neon-20 reactions with, delayed proton emitters from, (E), 20: 17687 (JINR-P-2514)

MOLYBDENUM ISOTOPES Mo-95
nuclear moments of, E2 and M1, (E), 20: 17998
nuclear spin relaxation in molybdenum metal, (E), 20: 17998

MOLYBDENUM ISOTOPES Mo-97
nuclear moments of, E2 and M1, (E), 20: 17998
nuclear spin relaxation in molybdenum metal, (E), 20: 17998

MOLYBDENUM ISOTOPES Mo-99
content in rain water, Fayetteville, Arkansas, Oct. 1964, 20: 16663 (TID-21470)
content in stratospheric and tropospheric samples in Project Star Dust, 1963, 20: 16727(R) (HASL-168)
production, separation, and uses of, 20: 16917
sensitivity for activation analysis using beta-gamma-gamma sum-coincidence gamma spectrometer, 20: 16335(R) (NBS-TN-276)
yields from thorium-232 fission, (E), 20: 17860
yields in plutonium-239 fission in resonance region, (E), 20: 17858

MOLYBDENUM STEEL
Cr–Mo, corrosion of Croloy 2¼ steel by sodium and sodium hydroxides, 20: 16599(R) (BAW-1280-34)
Cr–Mo, corrosion by mercury, corrosion loop testing of, 20: 16972(R) (NASA-CR-54719)
Cr–Mo, properties of, effects of potassium–sodium environment on, 20: 16972(R) (NASA-CR-54719)

MOLYBDENUM SYSTEMS
C–Hf–Mo, superconducting transition temperature of $Mo_{0.95}Hf_{0.05}C_{0.75}$, 20: 17607
C–Mo–Si, superconducting transition temperature of $Mo_{4.8}Si_3C_{0.6}$, 20: 17607
Mo–ZrO_2, structure of dispersion-hardened, effects of sintering process on, 20: 17109

MONAZITES
analysis for scandium, activation, 20: 16383

MONOCHROMATORS
design and theory of gamma, 20: 16505 (BNL-949)

MONTANA
geologic datings in Jardine-Crevasse Mountain area in, rubidium–strontium method for, 20: 16711(R) (MIT-1381-13)

MONTE CARLO METHOD
use for analysis of uranium-235–enriched fast critical assemblies, 20: 18057
use in neutron resonance absorption calculations, 20: 18046 (BNL-9644)

MONTICELLO DISTRICT (UTAH)
environs monitoring, 20: 16729 (IDO-12049)

MOON
electron excitation of x rays on surface of, from solar-geomagnetic cavity tail, 20: 17246
magnetohydrodynamic wake of, observation using IMP-1, 20: 17235(T)

MÖSSBAUER EFFECT
detection of, spectrometer for, 20: 16872
effects of twinning on, in tin oxides, 20: 16335(R) (NBS-TN-276)
electron spin relaxation effects on, (T), 20: 18009
measurement device for, design of, 20: 16866
measurement of absolute fraction of self-absorption effects on, (E/T), 20: 17990
measurement using Doppler effect, cosine effect in, 20: 16335(R) (NBS-TN-276)
spectra of, properties of sodium nitroprusside for use as standard in, 20: 16335(R) (NBS-TN-276)
theory, 20: 18015
use in measurement of electric charge distribution in alloys, (E/T), 20: 17158(R) (ORNL-3900, pp 82-149)
uses in metallurgy, 20: 17158(R) (ORNL-3900, pp 82-149)
uses in solid state physics, (E/T), 20: 17158(R) (ORNL-3900, pp 82-149)
uses in studies of chemical and physical properties, 20: 17989

MULTIPLICATION FACTOR
measurement in reactors, system for, 20: 18032

MUONIUM
reactions with atoms and molecules, 20: 17297
spin precession in quartz, in magnetic field, (E), 20: 17361(T)

MUSCLES
radiation effects on transplanted Yoshida sarcoma cells in rat, tracer study, 20: 16188
radioinduced inactivation of, combined with polarization microscopy for contraction studies, uv, 20: 16259

MUTATIONS
induced in algae, delayed and persistent expression of, 20: 16294
of yeast, effects of 5-aminoacridine on, 20: 16159(R) (ORNL-3900, pp 150-81)
radioinduced in *Arachis hypogaea* peanuts, 20: 16247
radioinduced in Drosophila, effects of sex on, 20: 16229(R) (NYO-1472-1)
radioinduced in Emericellopsis, methods for assaying uv, 20: 16238
radioinduced in jute, γ, 20: 16217 (AECD-AG-7)
radioinduced in mammals, neutron, 20: 16159(R) (ORNL-3900, pp 150-81)
radioinduced in medicinal plants, γ, 20: 16290
radioinduced in plants, review of agricultural use of γ, 20: 16225 (EUR-2715.f)
radioinduced in *Prunus avium* cherries, 20: 16244
radioinduced in Vicia, x, 20: 16276
radioinduced in wheat, γ and x, 20: 16285
radioinduced in wheat, x, 20: 16286

N

NAGASAKI
atomic explosions at, free-field radiation dose from, 20: 16760
gamma emissions from roof tiles in, thermoluminescent dosimetry of, 20: 16759
health of population exposed to atomic bomb at, 20: 16271

NAPHTHALENE
spectra of deuterated and normal, trapped in solid rare gases, 20: 18016
ethanol–naphthalene, radiation effects on hydrogen atom reactions in, 20: 16524
methanol–naphthalene, radiation effects on hydrogen atom reactions in, 20: 16524

1,4-NAPHTHALENEDIOL, 2-METHYL- DIPHOSPHATE, SODIUM SALTS
radiolysis of tritium-labeled, self-, 20: 16535
NAPHTHALENES
efficiency of scintillators of, for x-ray detection, 20: 16836
NATIONAL REACTOR TESTING STATION
irradiation experiments at, handbook for in-pile, 20: 18135 (IDO-17135)
NATURAL WATERS
waste disposal in, hazards and movement in, 20: 18157 (BNWL-SA-466)
NAVAL REACTORS
book: *Naval Nuclear Power Installations*, 20: 18132
NEODYMIUM
abundance in sun, (Σ), 20: 17237
solubility in gold, solid, 20: 17016 (IS-1175)
solvent properties for magnesium, solid, 20: 17016 (IS-1175)
NEODYMIUM ALLOYS
Mg–Nd, properties and structure of, 20: 17110
NEODYMIUM CARBIDES
properties of, chemical and physical, 20: 17048
reactions with water, formation of gaseous products in, 20: 17048
NEODYMIUM COMPLEXES
with phenanthroline, infrared, spectra of, 20: 16436
with thenoyltrifluoroacetone, magnetic susceptibilities of, 20: 16416(R) (NYO-906-68)
with 2,2′-bipyridyl, infrared spectra of, 20: 16437
with 2,4-pentanedioae, preparation, 20: 16434
NEODYMIUM ETHYL SULFATES
rare-earth quadrupole crystal-field shielding in, systematic variation of, (E), 20: 17996
temperature scale for, below 1°K, 20: 17614
NEODYMIUM HYDRIDES
properties and structure, 20: 16453
NEODYMIUM ISOTOPES
content in Arkansas rain water in Oct. 1964, 20: 16685
NEODYMIUM ISOTOPES Nd-142
helium-4 reactions (He-4,4n), angular momentum effects on excitation functions for, (E), 20: 17784
oxygen-16 scattering at 31 to 45 Mev, B(E2) values for transitions from, (E), 20: 17734
NEODYMIUM ISOTOPES Nd-143
nuclear magnetic moment, (E), 20: 17997
oxygen-16 scattering at 31 to 45 Mev, B(E2) values for transitions from, (E), 20: 17734
NEODYMIUM ISOTOPES Nd-144
oxygen-16 scattering at 31 to 45 Mev, B(E2) values for transitions from, (E), 20: 17734
NEODYMIUM ISOTOPES Nd-145
nuclear magnetic moment, (E), 20: 17997
oxygen-16 scattering at 31 to 45 Mev, B(E2) values for transitions from, (E), 20: 17734
NEODYMIUM ISOTOPES Nd-146
oxygen-16 scattering at 31 to 45 Mev, B(E2) values for transitions from, (E), 20: 17734
NEODYMIUM ISOTOPES Nd-147
content in rain water, Fayetteville, Arkansas, Oct. 1964, 20: 16663 (TID-21470)
NEODYMIUM ISOTOPES Nd-148
oxygen-16 scattering at 31 to 45 Mev, B(E2) values for transitions from, (E), 20: 17734
NEODYMIUM ISOTOPES Nd-149
beta decay of, promethium-149 levels from, (E), 20: 17787
half life, (E), 20: 17787
NEODYMIUM ISOTOPES Nd-150
oxygen-16 scattering at 31 to 45 Mev, B(E2) values for transitions from, (E), 20: 17734
NEODYMIUM OXALATES
reactions of hydrated, with hydrochloric acid, 20: 16447
NEODYMIUM OXIDES
crystallographic modifications and phase transformations of, 20: 16489
determination in thorium oxide by emission spectroscopy, 20: 16393
reactions with aluminum oxide and oxides of Group II elements at 1400 to 1500°C, 20: 16482
reactions with boron oxides at high temperatures, 20: 16489
Nd_2O_3–ReO_2, phase studies at 1130 and 1300°C, 20: 17007(R) (AD-627468)
NEODYMIUM SILICIDES
properties of, physicochemical, 20: 17047
NEODYMIUM SULFATES
crystal structure, cation electric field, and magnetic anisotropy in octahydrated, 20: 16435
NEODYMIUM SULFIDES
EuS–Nd_2S_3, compound formation in, 20: 16431
Nd_2S_3–SmS, compound formation in, 20: 16431
Nd_2S_3–YbS, compound formation in, 20: 16431
NEODYMIUM TANTALATES
$NdTaO_4$–$KTaO_3$, crystal structure, 20: 16438
NEON
composition of atmospheric, isotopic, 20: 17158(R) (ORNL-3900, pp 82-149)
electron scattering by atomic, cross sections for, (T), 20: 17286
heat transfer in boiling, 20: 16610
ion excitation energies and densities in plasma of, (E), 20: 17508 (ARL-65-246)
photon reactions with Coulomb field of, pair production total cross sections for high-energy, (T), 20: 17754
radio wave emission from plasma of, negative-absorption effects on anomalous bremsstrahlung and cyclotron, (E), 20: 17921
NEON ISOTOPES
abundance in Achilles, LaLande, and Peace River chondrites, 20: 16672
NEON ISOTOPES Ne-20
neutron reactions (n,α) at 14.2 Mev, angular and energy distributions from, (E), 20: 17743
reactions with molybdenum-92 and -94, delayed proton emitters from, (E), 20: 17687 (JINR-P-2514)
NEPTUNIUM
determination using xylenol orange, photometric, 20: 16408
production, 20: 16543
separation from irradiated fuels, 20: 16582
separation from other fission products by precipitation with barium sulfate, 20: 16343
NEPTUNIUM ISOTOPES Np-234
beta decay of, transition rates for, (T), 20: 17742
NEPTUNIUM ISOTOPES Np-237
neutron fission cross sections at 40 to 500 kev, (E), 20: 17852
neutron fission of, fragment mass distributions from, (E), 20: 17861
production of alpha sources of, electrospraying method for, 20: 16553
NEPTUNIUM ISOTOPES Np-239
determination by precipitation with barium sulfate and gamma spectroscopy, 20: 16343
NERVE CELLS
radiation effects on rat olfactory bulb, effects of gases in nasal cavities on x, 20: 16215 (AD-628443)
NERVES
effects of section of sciatic, on bone blood flow, 20: 16192
NERVOUS SYSTEM
radiation effects on dog, α, 20: 16268
NETHERLANDS
nuclear energy organization, legislation, and training in, 20: 18183
NEUROSPORA
ad-3B mutants in, reversibility and type of nitrous acid-induced, 20: 16159(R) (ORNL-3900, pp 150-81)
radioinduced mutation rates in ad-3 regions of, x, 20: 16159(R) (ORNL-3900, pp 150-81)
NEUTRINOS
bibliography, 20: 17352 (NEIC-RR-21)
interactions with leptons at high energies, local-current commutation relations for, 20: 17387
properties of, review of, 20: 17406
NEUTRINOS (ν_μ)
interactions with protons, effects of vector mesons on lepton production by, (T), 20: 17504
interactions with mesons (μ) at very high energies, (T), 20: 17366(T)
NEUTRON ACTIVATION CROSS SECTIONS
tables of, for metastable isomers, 20: 16336(R) (NYO-10175)
NEUTRON BEAMS
spectra in UA-RR-1 thermal column, 20: 18147
NEUTRON CAPTURE CROSS SECTIONS
calculation for rare-earth nuclei from 1 to 10 kev, 20: 17653 (LA-3463)
NEUTRON CROSS SECTIONS
calculation of, computer programs for, 20: 17698 (WANL-TME-1132)
data plotting of, computer program for, 20: 17699 (WANL-TME-1317)
library for nuclei $1 \leq A \leq 91$, 20: 17673 (BNWL-CC-325(Vol.1))
library for nuclei $90 \leq A \leq 161$, 20: 17674 (BNWL-CC-325(Vol.2))
library for nuclei $159 \leq A \leq 239$, 20: 17675 (BNWL-CC-325(Vol.3))
tabulations for uranium-235 from 1.86 ev to 10 Mev, 20: 17697 (WANL-TME-1028)
NEUTRON-DIFFRACTION ANALYSIS
use in determining magnetic properties of solid, 20: 17158(R) (ORNL-3900, pp 82-149)
NEUTRON DIFFRACTOMETERS
design and performance of small automatic, 20: 16882
operation and performance of double-axis, for powder investigations, 20: 16799
NEUTRON FISSION CROSS SECTIONS
measurement and interpretation of low-energy, (T), 20: 17850
NEUTRON PHOTOGRAPHY

collimators and foil-film combinations for, 20: 16619
NEUTRON SOURCES
design of parallel-electrode, 20: 17669(P)
design of standard thermal, 20: 17654 (RT/PROT-(65)31)
development of antimony–beryllium, with heavy water moderator, 20: 16830(R) (UCRL-14534, pp 8-12)
fabrication, 20: 16914(R) (ORNL-3900, pp 182-93)
spectra analysis for beryllium-polonium and plutonium-240, computer program for, 20: 16875
yields from photo-, for activation analysis, 20: 16332 (GA-6691)
NEUTRON SPECTRA
analysis of time-of-flight, computer program for, 20: 16877
measurement in NRL Research Reactor, 20: 16335(R) (NBS-TN-276)
NEUTRON SPECTROMETERS
luminosity and resolution of crystal, (T), 20: 16874
operation and control of system of, computer for, 20: 16869
operation at ORR, 20: 17158(R) (ORNL-3900, pp 82-149)
spectra unfolding in proton-recoil, computer program for, 20: 16875
NEUTRONS
absorption by tungsten, resonance integrals for, (E/T), 20: 18045(R) (AI-66-16)
absorption of underground explosion, activation of terrestrial environment in, 20: 16160 (UCRL-14739(Pt.2))
absorption of, Monte Carlo methods for calculation of resonance, 20: 18046 (BNL-9644)
angular distributions from alpha reactions (α,n) with carbon-12 at 14 Mev, (E), 20: 17803
binding energy of pairs of, in nuclei, variation with neutron numbers, 20: 17729
capture by nuclei, resonance widths in, (E), 20: 17676 (CEA-R-2810)
capture by rare earth nuclei at 1 to 10 kev, cross sections for, (T), 20: 17653 (LA-3463)
capture by rhodium-103, conversion electron spectrum from, (E), 20: 17810
capture by sodium at 10 to 135 kev, cross sections for, (E), 20: 17718
decay of, phase-space integrals for, (T), 20: 17732
detection and measurement at 0.025 ev to 100 Mev, detector for, 20: 16819 (LA-3435)
detection and measurement using corrugated-plate spark chambers, 20: 16894
detection and measurement using boron trifluoride proportional detectors, 20: 16895
detection and measurement in reactors, instruments for, 20: 16903
diffraction by zinc, scattering length for, (E), 20: 17667
diffusion equations for, technique for solving, (T), 20: 17652 (CEA-R-2867)
diffusion equations for, numerical solution by Kantorovich method, (T), 20: 17656
diffusion in graphite, parameters for pulsed and static, (E/T), 20: 17661
effects on aluminum alloys, 20: 18020(R) (ORNL-3900, pp 2-81)
effects on calcium fluoride crystals, damage from, 20: 17804
effects on corrosion resistance of boron-modified austenitic stainless steels, 20: 17118(R) (EURAEC-1564)
effects on crystal structure of graphite, x-ray studies of, 20: 17130
effects on cysteic acid, cysteine, and cystine, chemical, 20: 16540
effects on diodes and transistors, 20: 16909 (N-65-18250)
effects on diodes, transistors, and microelectronic circuits, 20: 16908 (N-65-17526)
effects on electric properties of indium–antimony alloys, 20: 17150(T)
effects on electronic components in space, review of, 20: 16911
effects on induced activity in polyethylene, 20: 17822
effects on lattice parameters of uranium monocarbide, annealing of, 20: 17140
effects on metal oxides, effects of crystal structure on, 20: 17148
effects on mutations in mammals, 20: 16159(R) (ORNL-3900, pp 150-81)
effects on oxidation-reduction potential of electrolytes, 20: 17118(R) (EURAEC-1564)
effects on praseodymium complexes with β-diketones, 20: 16416(R) (NYO-906-68)
effects on pyrolytic carbon coatings of reactor fuel pellets, 20: 18076 (ORNL-TM-1385)
effects on structure of alpha-quartz, 20: 17149(T)
effects on water at 14.6 Mev, reaction rates and yields from, (T), 20: 16509 (TID-22666)
embrittlement of Soudotenax and T-1 pressure vessel steels by, 20: 17117 (EURAEC-1558)
emission in fission and (α,n) reactions, counter design for simultaneous measurement of, 20: 16905(P)
exchange in proton interactions with protons in Bev range, (T), 20: 17394
flux and multiplication in fast reactors, heterogeneity effects on, (T), 20: 18063
flux decay constants in beryllium and graphite, pulsed, (T), 20: 17662
flux in reactors, detectors for monitoring, 20: 18023
flux in reactors, few-time-step depletion calculations of, 20: 18052 (WAPD-T-1836)
flux in slab reactor with natural uranium, production of flat, (T), 20: 18058
flux measurement in reactors, method and device for, 20: 18043(P)
flux measurements in reactors, using fission chambers and proportional detectors, 20: 16896
flux measurements in reactors, ionization chambers for, 20: 16897
flux measurements in reactors using thermopiles, 20: 16899
flux measurements in NRL Research Reactor, 20: 16335(R) (NBS-TN-276)
flux monitoring in reactors, solid-state instrumentation for, 20: 18034
flux monitoring in reactors, instrumentation for, 20: 18035
flux perturbations of, effects of infinite plane absorbers on exponential, (T), 20: 17655
form factors of, electromagnetic, (E), 20: 17349 (LAL-1155)
half life measurement, 20: 18174(R) (NP-15771)
interactions with nucleons, scattering lengths for, (T), 20: 17350 (N-65-19395)
interactions with antiprotons in emulsions at 3 Bev/c, inelastic, (E), 20: 17359
interactions with protons at 2 to 10 Bev, amplitude for, (E), 20: 17363(T)
interactions with mesons (K^-) and (K^+) at high energies, real amplitudes for, (T), 20: 17378
interactions with protons, deuteron and gamma production in, 20: 17413
magnetic moment of, dispersion-theoretical calculation of, 20: 17390
multiplication in aluminum- and Zircaloy-clad uranium dioxide, effective, (T), 20: 18065
photoproduction on beryllium and deuterium by fission gamma rays, (E/T), 20: 17830
polarimeter for, time-of-flight, 20: 16876
polarization from deuteron reactions (d,n) with deuterium at 1.5 and 1.9 Mev, (E), 20: 16876
reactions (n,α) with boron-10 at 23 ev to 0.5 Mev, excited-to-ground state branching ratio for, (E), 20: 17719
reactions (n,α) with calcium-44, cross sections for, (E), 20: 17804
reactions (n,α) with barium-138 and calcium-44, cross sections for, (E/T), 20: 17809
reactions (n,α) with neon-20 at 14.2 Mev, angular and energy distributions from, (E), 20: 17743
reactions (n,α) at 3.0 and 4.7 Mev, total cross sections for, (E), 20: 17767
reactions (n,γ) with uranium-238 at 0.01 to 3 Mev, cross sections for, (T), 20: 17720
reactions (n,γ) with copper-64 and gold-197, threshold cross sections and energies for, 20: 16335(R) (NBS-TN-276)
reactions (n,n') and (n,p) with excited nuclei, cross sections for direct, (T), 20: 17714
reactions (n,n'γ) with iron-56 at 0.95 to 4.0 Mev, angular distributions and level parities and spins from, (E), 20: 17736
reactions (n,p) with magnesium-24 and nickel-58, threshold cross sections and energies for, 20: 16335(R) (NBS-TN-276)
reactions (n,p) with potassium-41, cross sections for, (E/T), 20: 17809
reactions (n,2n2p) with aluminum-27, threshold cross section and energy for, 20: 16335(R) (NBS-TN-276)
reactions (n,2n) with scandium-45 at 14 Mev, scandium-44 isomeric yield ratio from, (E), 20: 17777
reactions in critical systems, variational principle for ratios of, (T), 20: 18059
reactions with actinium-227, neptunium-237, and protactinium-231, fission fragment mass distributions from, (E), 20: 17861
reactions with americium-241, plutonium-238, and thorium-230 at 0.1 to 1.2 Mev, fission fragment angular distributions from, (E/T), 20: 17848
reactions with americium-241 at 4 and 5 Mev, fission fragment angular distributions from, (E/T), 20: 17848
reactions with cesium and niobium at 14 Mev, total cross sections for, (E), 20: 17702
reactions with germanium at 0.4 to 18.6 Mev, germanium recoil atom ionization spectrum from, (E), 20: 17265
reactions with neptunium, plutonium, and uranium isotopes at 40 to 500 kev, fission cross sections for, (E), 20: 17852
reactions with nuclei, computer programs for charged particle cross sections from, 20: 17671 (AEEW-M-611)
reactions with nuclei, sensitivities of, for activation analysis, 20: 16332 (GA-6691)
reactions with plutonium-239 and uranium-235, fission neutron spectra from, (E), 20: 17825
reactions with plutonium-239 and uranium-235, alpha particle and fission fragment energies and yields from fission, (E), 20: 17839
reactions with plutonium-239 at 0.16 ev to 5 kev, fission cross sections for, (E/T), 20: 17851

reactions with plutonium-239 and uranium-235 at 0.0322 to 0.275 ev, fission cross sections for, (E), 20: 17854
reactions with plutonium-240 at 0.03 to 2.0 Mev, fission cross sections for, (E), 20: 17855
reactions with plutonium-239 at 200 to 600 ev, symmetry of fission, (E), 20: 17858
reactions with plutonium-239 and uranium-233 and -235, fission fragment distributions from, (E), 20: 17863
reactions with thorium-232 and uranium-238 at 14 Mev, delayed neutron precursors from, (E/T), 20: 17831
reactions with thorium-232, fission fragment yields from, (E), 20: 17860
reactions with uranium-235 and -238, twenty-group cross sections for, 20: 18057
reactions with uranium-235 at 1.86 ev to 10 Mev, cross sections for, 20: 17697 (WANL-TME-1028)
reactions with uranium-235, nucleon pairing effects on threshold fission, (T), 20: 17847
reactions with uranium-235 at 2 ev to 30 kev, fission, radiative capture, and total cross sections for, (E), 20: 17856
reactions with uranium-235, fission fragment kinetic energy from, (E/T), 20: 17867
reactions with uranium-233 at 1.7 to 30 ev, least-squares analysis of fission cross sections for, (T), 20: 17853
reactions with uranium-233, resonance fission integral for, (E), 20: 17722
resonance integrals for, second order approximations for effective, 20: 17650 (AAEC/E-144)
scattering by carbon-12 and oxygen-16 at 3.0 to 4.7 Mev, carbon-13 and oxygen-17 level parameters from elastic, (E), 20: 17767
scattering by crystals, phase determination from, 20: 17041
scattering by excitons in crystals, cross sections for, (T), 20: 18006
scattering by ferromagnetic materials near phase-transition point, polarized, (T), 20: 17987(T)
scattering by nickel phase transitions in small-angle polarized, (E/T), 20: 17986(T)
scattering by tritium at 1.0 to 6.0 Mev, phase-shift analysis for elastic, (T), 20: 17769
transport in lattices, disadvantage factor calculations for, (T), 20: 18049 (RT/FI(65)-42)
transport in reactors, solutions of energy-dependent Boltzman equation for, 20: 18068
transport in reactors, (T), 20: 18070
transport in slab geometry, spectral theory for stationary operator for, 20: 17658
transport in two-region slab lattice, calculation of disadvantage factor for, 20: 17668
transport of, kernel method in equation for, 20: 18069
use in moisture gages, 20: 16924

NEUTRONS, COLD
scattering by molecular hydrogen, cross sections and spectra for, (T), 20: 17664
use in steel radiography, 20: 16616

NEUTRONS, DELAYED
emission from antimony and arsenic fission products, (E), 20: 17833
emission in thorium-232 fission at 1.6 to 2.6 Mev, (E), 20: 17680 (FEI-26)
energy spectra and yields of, (E/T), 20: 17830
yields from fission fragments, (E/T), 20: 17831
yields from uranium-238 fast fission, (E), 20: 17832

NEUTRONS, EPITHERMAL
effects on neutron filter cutoff energies, (T), 20: 17663
reactions with plutonium-239 and uranium-235, fission resonance integral for, (E), 20: 17751

NEUTRONS, FAST
detection of, design and performance of portable monitor for, 20: 16848
dosimetry of, scintillator-film combination for, 20: 16861
dosimetry of, using hair activation, 20: 16758
effects on boronated graphite, 20: 17116 (BNWL-199)
effects on creep-rupture properties of tungsten, 20: 17152
effects on electric properties of conductivity-modulated silicon p-i-n diodes, 20: 16912
effects on graphite joints and graphite-coated particles in carbonized pitch matrix, 20: 17119 (GAMD-6789)
effects on magnetic hysteresis of iron, combined nickel impurity and, 20: 17134
effects on physical properties of Santowax WR at 425 to 800°F, 20: 17122 (MIT-334-34)
effects on semiconductors, radiosensitivity levels for, 20: 16911
effects on structure of molybdenum, effects of prestrain on, 20: 17132
emission from nuclear explosions, dosimetry of, 20: 16760
flux of, quartz and silicon dioxide films for measuring, 20: 16851
penetration and scattering of, shielding materials effects on, 20: 18020(R) (ORNL-3900, pp 2-81)
reactions with plutonium-241, prompt neutron yields from fission, (E), 20: 17826
reactions with thorium-232 at 1.6 to 2.6 Mev, delayed neutrons from fission, (E), 20: 17680 (FEI-26)
reactions with thorium-232, fission fragment angular anisotropy and mass asymmetry from, (E), 20: 17869
reactions with uranium-235 at 100 kev to 2.6 Mev, fission neutron yields from, (E), 20: 17823
reactions with uranium-238 at 1.5 to 15 Mev, delayed neutron yields from fission, (E), 20: 17832
reactions with uranium-235, mass dependence of fission fragment energies from, (E/T), 20: 17868

NEUTRONS, FISSION
age to indium resonance energy in iron-water mixtures, (E), 20: 17659
effects on copper and zinc content and enzyme activity in blood of mammals, 20: 16222 (AFWL-TR-65-112)
effects on ductility of stainless steel, 20: 17141
slowing-down density distribution in iron-water mixtures at indium resonance energy, Monte Carlo code for, 20: 17660
yields from californium, plutonium, and uranium isotopes, (E), 20: 17823

NEUTRONS, PROMPT
emission from uranium-235 fission fragments, (E), 20: 17824
emission of, time-of-flight method for measuring, 20: 17864

NEUTRONS, THERMAL
capture by dysprosium-164, conversion-electron spectrum from, 20: 17822
capture by holmium-165, conversion-electron spectrum from, 20: 17822
capture by indium-115, indium-116 isomers from, 20: 17822
capture by lutetium-176, lutetium-177 levels from, 20: 17822
capture by tellurium, gamma spectra from, (E), 20: 17681 (IAE-966)
detection and measurement using borax-impregnated K-2 emulsion plates, 20: 16891
dosimetry in gamma background using film badges, 20: 16807 (CLOR/IBJ-42/D)
effects on boronated graphite, 20: 17116 (BNWL-199)
effects on ductility of stainless steel, 20: 17141
effects on lithium fluoride crystals, point defects from, 20: 18007
effects on optical absorption spectra of lithium fluoride, 20: 17143
effects on sweet cherry trees, genetic, 20: 16244
flux distribution in heavy water moderated, organic-cooled reactors, hyperfine structure of, 20: 18055
reactions (n,γ) with thulium-169, thulium-170 levels from, (E), 20: 17782
reactions with plutonium and uranium isotopes, fission neutron yields from, 20: 17823
reactions with plutonium-241, prompt neutron yields from fission, (E), 20: 17826
reactions with plutonium-239 and uranium-235, fission resonance integral for, (E), 20: 17751
reactions with uranium-235, prompt neutron yields from fission, (E), 20: 17824
reactions with uranium-235, gamma energies and yields from fission, (E), 20: 17828
reactions with uranium-235, gamma angular distributions from fission, (E), 20: 17829
reactions with uranium-235 at 0.005 to 0.2 ev, ratio of binary-to-ternary fission in, (E), 20: 17840
reactions with uranium-235, fission fragment mass distributions after prompt neutron emission, (E/T), 20: 17866
reactions with uranium-235, mass dependence of fission fragment energies from, (E/T), 20: 17868
scattering by hydrogen, computer program for, 20: 17684 (JAERI-1085)
scattering by molecular hydrogen, cross sections and spectra for, (T), 20: 17664
scattering of, convolution approximation of Van Hove function for, 20: 17665
scattering of, quasiclassical approximation in theory of, 20: 17666
spectra in beryllium and graphite, (E/T), 20: 18127(R) (GA-6753(Pt.1))
spectra of, deduction from activation rates of foils, (E/T), 20: 16857
transport equation in finite bodies, spectrum of, (T), 20: 17657

NEW ENGLAND REGION
geologic dating of Ammonoosuc volcanics and Monson gneiss in, rubidium–strontium method for, 20: 16711(R) (MIT-1381-13)

NEW JERSEY
strontium-90 content of primary teeth of children in, 20: 16763

NICKEL
cavitation damage in water, 20: 16974 (NP-15889)
determination by radiometric titration, 20: 16386
determination in asbestos using ion exchange, activation, 20: 16336(R) (NYO-10175)
determination of trace amounts of, in beryllium by spectrography, 20: 16352
effects on magnetic hysteresis of iron, combined fast-neutron radiation and, 20: 17134
effects on tritium exchange between tritiated ethyl malonate and hydrocarbons, catalytic, 20: 16492

neutron scattering by, phase transitions in small-angle polarized, (E/T), 20: 17986(T)
proton reactions at 590 Mev and 18.3 Bev, potassium isotopes yields in, in, (E), 20: 17717
radiation effects on battery electrodes of, gamma, 20: 17124(R) (N-65-17608)
separation from scandium by ion exchange chromatography, 20: 16574

NICKEL ALLOYS
Cr–Fe–Ni, corrosion cracking in, mechanisms of stress-, 20: 16968 (COO-1319-33)
Cr–Ni–Nb, phase studies on intermetallic compounds in, 20: 17075
In–Ni, indium hyperfine magnetic field in, (E), 20: 17992
Ni–Nb–Ta, diffusion of nickel in, effects of annealing temperature and composition on, 20: 17089
Ni–Ta, effects of additives on high-temperature properties of eutectic, 20: 17108
Ni–W, effects of additives on high-temperature properties of eutectic, 20: 17108
Ni–Zr, effects of additives on high-temperature properties of eutectic, 20: 17108

NICKEL IONS
effects on hydrolysis of α-D-glucose 1-phosphate, 20: 16421
reactions with 2,4-pentanedione in 2-propanol–water, thermodynamics of, 20: 16416(R) (NYO-906-68)
sorption by aminodiacetate resin Dowex A-1, 20: 16358

NICKEL ISOTOPES Ni-57
nucleon interactions in, properties from effective, (T), 20: 17735

NICKEL ISOTOPES Ni-58
neutron reactions (n,p) threshold cross section and energy for, 20: 16335(R) (NBS-TN-276)
nucleon interactions in, properties from effective, (T), 20: 17735
proton reactions (p,d) at 57 Mev, energy spectra from, (E), 20: 17725

NICKEL ISOTOPES Ni-60
nucleon capture at 10 to 40 Mev, cross sections and mechanism for direct, (T), 20: 17737

NICKEL ISOTOPES Ni-62
helium-3 reactions (He-3,d) at 22 Mev, angular distributions from, (T), 20: 17692 (ORNL-TM-1414)

NICKEL OXIDES
analysis for cobalt, tracer technique for, 20: 16335(R) (NBS-TN-276)
analysis for iron by radioisotope dilution, 20: 16335(R) (NBS-TN-276)

NICKEL SYSTEMS
Cr–Fe–Ni–P, corrosion cracking in, mechanisms of stress-, 20: 16968 (COO-1319-33)
Cr–Fe–Ni–Si, corrosion cracking in, mechanisms of stress-, 20: 16968 (COO-1319-33)

NICKEL ZINC FERRITES
radiation effects on magnetic diffusion in, gamma, 20: 16532

NIOBIUM
density, 20: 17053
determination in process feed solutions by extraction chromatography, 20: 16333 (KR-81)
determination simultaneously with tantalum in minerals and ores, activation, 20: 16336(R) (NYO-10175)
diffusion barriers between hafnium–20 tantalum cladding on tantalum–10 tungsten, performance of, 20: 16943(R) (IITRI-B237-45)
diffusion in, effects of annealing temperature and porosity on self-, 20: 17090
diffusion of tin in, containing zirconium or titanium, 20: 17632
dislocation parameters for, 20: 17033
impurities in, ordering of interstitial, 20: 18003
magnetic susceptibilities of, temperature dependence of, 20: 17069
melting point of, effects of gas impurities on, 20: 17094
oxidation of, temperature dependence of, 20: 16982
properties of superconducting mixed-state, magnetic and ultrasonic attenuation, 20: 17608
reactions with alumina, 20: 16978
reactions with niobium oxides, 20: 16483
superconductivity of, temperature dependence of Ginzburg-Landau parameter for, 20: 17585 (AD-627910)
thermodynamic properties at 0 to 2740°K, 20: 17100

NIOBIUM ALLOYS
Al–Nb–Ta–Ti, corrosion cracking in titanium-base, stress-, 20: 16967 (AD-628277)
Cr–Co–Nb, phase studies on intermetallic compounds in, 20: 17075
Cr–Ga–Nb, phase studies on intermetallic compounds in, 20: 17075
Cr–Ge–Nb, phase studies on intermetallic compounds in, 20: 17075
Cr–Nb, phase transformations in, 20: 17046
Cr–Nb–Ti, phase studies, 20: 17091
Cr–Nb–Ti, tensile properties of, effects of composition on, 20: 17112
Cr–Ni–Nb, phase studies on intermetallic compounds in, 20: 17075
Ir–Nb, superconductivity in close-packed intermediate phases of, 20: 17624
Mo–Nb–Ta–W, deformation mechanisms in solution-hardened niobium-base, 20: 17082
Mo–Nb–Ta–W, properties as hollow turbine vanes, 20: 16963
Mo–Nb–V–Zr, fabrication of tubing of B-66, 20: 16998
Nb–Pt, superconductivity in close-packed intermediate phases of, 20: 17624
Nb–Rh, superconductivity in close-packed intermediate phases of, 20: 17624
Nb–Sn, fabrication of superconducting solenoids from stranded wires of, 20: 17593 (CONF-650922, pp 597-603)
Nb–Sn, preparation of superconducting Nb_3Sn using diffusion layers, 20: 17649
Nb–Sn, superconductivity of diffusion layers of Nb_3Sn, (E), 20: 17632
Nb–Ta, current flow patterns in superconducting, in longitudinal fields, (E/T), 20: 17617
Nb–Ta–W–Zr, properties as hollow turbine vanes, 20: 16963
Nb–Ti–Zr, oxidation-resistant coatings on D-36, performance of commercial, 20: 16973 (NASA-TN-D-3275)
Nb–U, phase studies, 20: 17035
Nb–U, phase transformation kinetics in, 20: 17036
Nb–V, oxidation of, temperature dependence of, 20: 16982
Nb–W–Zr, properties as hollow turbine vanes, 20: 16963
Nb–Zr, cavitation damage in mercury and water, 20: 16974 (NP-15889)
Nb–Zr, degradation phenomena in small superconducting coils of, (E), 20: 17629
Nb–Zr, electric properties of normal region in superconducting magnet of, 20: 17610
Nb–Zr, Hall effect measurements on superconducting magnets of, 20: 17600(R) (ORNL-3908, pp 114-48)
Nb–Zr, internal friction and relaxation processes in, 20: 17106
Nb–Zr, magnetic susceptibility, 20: 17106
Nb–Zr, metallographic techniques for preparation of, for microscopy, 20: 16959
Nb–Zr, omega transformation and segregation processes in, 20: 17105
Nb–Zr, properties for containment of potassium at high temperatures, 20: 18020(R) (ORNL-3900, pp 2-81)
Nb–Zr, solvent properties for oxygen at 1000 to 1200°C, 20: 16980
Nb–Zr, thermoelectric power at 9.2 to 330°K, effects of zirconium content on, 20: 17067
Nb–Zr, ultrasonic attenuation in nonideal superconducting, flux jumping and magnetization effects on, (E), 20: 17606
Ni–Nb–Ta, diffusion of nickel in, effects of annealing temperature and composition on, 20: 17089

NIOBIUM BORIDES
chemical bonding and electric conductivity of, 20: 16439

NIOBIUM CARBIDES
HfN–NbC–NbN, superconducting properties, 20: 17589 (CONF-650922, pp 541-9)
NbC–NbN, superconducting properties, 20: 17589 (CONF-650922, pp 541-9)
NbC–NbN–VN, superconducting properties, 20: 17589 (CONF-650922, pp 541-9)
NbC–NbN–ZrN, superconducting properties, 20: 17589 (CONF-650922, pp 541-9)

NIOBIUM ISOTOPES Nb-95
content in plants before and after Salmon Event, 20: 16743 (VUF-1021)
diffusion in pyrolytic graphite, 20: 17107
fallout monitoring at Vilnius, Soviet Union, in 1962, 20: 16700
production of isomeric, in deuteron reactions (d,n) at 15 Mev, 20: 16508(R) (NYO-2771-13)
ranges of fission products of, in aluminum, (E), 20: 17721

NIOBIUM NITRIDES
HfN–NbC–NbN, superconducting properties, 20: 17589 (CONF-650922, pp 541-9)
MoC–NbN, superconducting properties, 20: 17589 (CONF-650922, pp 541-9)
NbC–NbN, superconducting properties, 20: 17589 (CONF-650922, pp 541-9)
NbC–NbN–VN, superconducting properties, 20: 17589 (CONF-650922, pp 541-9)
NbC–NbN–ZrN, superconducting properties, 20: 17589 (CONF-650922, pp 541-9)
NbN–TaC, superconducting properties, 20: 17589 (CONF-650922, pp 541-9)
NbN–TiC, superconducting properties, 20: 17589 (CONF-650922, pp 541-9)
NbN–TiN, superconducting properties, 20: 17589 (CONF-650922, pp 541-9)
NbN–VC, superconducting properties, 20: 17589 (CONF-650922, pp 541-9)
NbN–VN, superconducting properties, 20: 17589 (CONF-650922, pp 541-9)

NIOBIUM OXIDES

reactions with niobium, 20: 16483
reduction by carbon at 1400 to 1600°C, effects of potash and soda on, 20: 16483
reduction by carbon monoxide, 20: 16483
reduction by hydrogen at 1000°C, 20: 16483
NbO_2–VO_2, crystal structure of double oxide $NbVO_4$, 20: 16982

NIOBIUM SELENIDES
superconducting critical currents in single-crystal, effects of stoichiometry on peak, (E), 20: 17609

NIOBIUM SYSTEMS
C–Fe–Nb, phase studies, 20: 17086
C–Nb–W–Zr, microstructure of D-43, effects of aging on, 20: 17023 (ORNL-TM-1161, pp 208-24)
C–Nb–W–Zr, properties as hollow turbine vanes, 20: 16963
Nb–O–Zr, phase studies, 20: 16980

NITRATE COMPLEXES
rare earth terpyridyl, preparation and infrared spectra of, 20: 16479

NITRATES
analysis for plutonium by argentic oxidation, ferrous reduction, and dichromate titration, 20: 16405

NITRIC ACID
corrosive effects of, on iron-base alloys, mechanisms of stress-, 20: 16968 (COO-1319-33)
effects on peptization of solid thorium oxide, mechanism of, 20: 16419(T) (UCRL-Trans-1301(L))
properties for use in ultrasonic cleaning of cobalt-60 from Duralumin and steel-3, 20: 16767

NITROGEN
cesium ion elastic scattering at 2.3 to 11.6 ev, (E/T), 20: 17300
determination by isotopic dilution, 20: 16362
determination in uranium hexafluoride, spectrographic, 20: 16409
effects on stress-corrosion of austenitic stainless steels, 20: 16969(R) (EURAEC-1579)
fission-fragment energy degradation in, (E), 20: 17821
heat transfer in boiling, 20: 16610
ion velocity distribution in, in electric fields, (E), 20: 17298
ionic mobility of cesium and rubidium in, at high pressures, (E/T), 22: 16415 (CEA-R-2861)
isotopic analysis of, by emission spectroscopy with photoelectric recording, 20: 16375
isotopic analysis of, by emission spectroscopy, 20: 16376
photon reactions with Coulomb field of, pair production total cross sections for high-energy, (T), 20: 17754
production of plasmas of, spectroscopic studies of, 20: 17902
proton reactions at 2 to 35 kev, Balmer-alpha radiation in, (E), 20: 17269
radiation fixation of, developments in, 20: 16506 (BNL-10020)
radiosensitivity effects on olfactory bulk neurons in rats, 20: 16215 (AD-628443)
reactions of active, with ethylene, 20: 16510(T) (NP-tr-1364)
reactions with helium atoms, charge transfer and ionization in, (E), 20: 17301

NITROGEN COMPOUNDS
isotopic analysis of nitrogen from, procedures for, 20: 16376

NITROGEN IONS
ionization after passage through solids, auto-, (E), 20: 17262(T)
velocity distribution in nitrogen in electric fields, (E), 20: 17298

NITROGEN ISOTOPES
concentration of nitrogen-14/-15 molecules by thermal diffusion, 20: 16931
distribution between gaseous nitrogen oxides and liquid organic solutions, 20: 16486

NITROGEN ISOTOPES N-12
beta decay of, phase-space integrals for, (T), 20: 17732

NITROGEN ISOTOPES N-13
half life, 20: 16331 (GA-6568)
spectra of recoil, from deuteron reactions with carbon-12, (E), 20: 17820

NITROGEN ISOTOPES N-14
helium-3 reactions (He-3,α) at 12 Mev, Q value for, 20: 16331 (GA-6568)
production in oxygen-16 (B-10,3α) reactions, angular distributions from, (E), 20: 17815)
proton reactions (p,2p) at 140 Mev, energy spectra and angular correlation distributions from, (E), 20: 17741
reactions (N-14,5n) with cesium-133, angular momentum effects on excitation functions for, (E), 20: 17784

NITROGEN ISOTOPES N-15
separation from other nitrogen isotopes by chemical exchange between nitric solutions and nitrous vapors, 20: 16443

NITROGEN OXIDES
analysis of mixtures of, spectrophotometric method for, 20: 16486
effects on radioinduced surface activity of γ-octahydro-1,3,5,7-tetranitro-1,3,5,7-tetrazocine, 20: 16504 (AD-627846)
nitrogen isotope distribution between gaseous and liquid phases of, 20: 16486
production in plasma jets, 20: 17959
properties as electron scavenger in radiolysis of hydrocarbons, 20: 16515
spectra of x-ray excited, trapped in solid rare gases, 20: 18016

NITROGEN SYSTEMS
N–H_2O, oxidative effects on uranium, mechanism of, 20: 16986
N–O–H_2O, oxidative effects on uranium, mechanism of, 20: 16986

NITROUS ACID
effects on algae, patterns of expression of mutagenic, 20: 16294

NOBELIUM
production, 20: 16543

NOISE
fluctuations in electron-beam, effects of beam length and magnetic field on, 20: 17505

NORWAY
fuel element reprocessing pilot plant research, Kjeller, 20: 16569

NOSE
radiosensitivity effects of gases in, on olfactory bulb neurons in rats, 20: 16215 (AD-628443)

NOZZLES
cladding bores of, welding techniques for, 20: 16617

NRL ISOCHRONOUS CYCLOTRON
development, 20: 17169(R) (AD-628928)

NRL RESEARCH REACTOR
neutron flux spectrum for pneumatic tube system in, 20: 16335(R) (NBS-TN-276)

NUCLEAR EMULSIONS
meson (K$^-$) reactions at 3.0 and 5.0 Bev/c, hyperfragment production from, (E), 20: 17752
meson (π) reactions at 7.5 Bev, production of high-energy fragments in, (E), 20: 17715
meson (π) reactions at 17.5 Bev, helium particle emission in, (E), 20: 17716
nucleon interactions with nucleons in, particle-track distributions from, (E), 20: 17357
particle multiple scattering constant in, effect of cell length on, 20: 16833
performance of boron-impregnated type K-2, for neutron detection, 20: 16891
proton reactions at 28 Bev, lithium-8 production from, (E/T), 20: 17753
proton reactions at 9 Bev with, cascade effects on alpha yields in, (E), 20: 17713
proton reactions with bromine and silver at 25 Bev/c in, lithium-8 recoil from, (E), 20: 17748

NUCLEAR HEATING PLANTS
economics of small dual-purpose, 20: 18124

NUCLEAR MAGNETIC MOMENTS
calculation of, 20: 17733

NUCLEAR MAGNETIC RESONANCE
use in protein studies, deuterated organisms for, 20: 16165

NUCLEAR MODELS
description for collective vibrations of nuclei, 20: 17711
energy levels in core-excitation, quasi-particle, 20: 17814
potential in boundary-condition, hard-core, (T), 20: 17772

NUCLEAR MODELS (DROP)
nuclear moment of inertia at fission saddle point in, (T), 20: 17849

NUCLEAR MODELS (OPTICAL)
proton scattering parameters in, experimental uncertainty of, (T), 20: 17768

NUCLEAR PHYSICS
bibliography on high-energy, 20: 17153 (AED-C-23-05)
bibliography on high-energy, 20: 17154 (AED-C-23-06)
bibliography on high-energy, 20: 17155 (AED-C-23-07)
conference, 20: 17871
data processing in, use of digital computers for, 20: 17708
data processing in, 20: 17709
research on, (E/T), 20: 17651(R) (AD-612192)

NUCLEAR POWER PLANTS
book: *International Marketing of Nuclear Power Plants*, 20: 18117
book: *Technological and Thermotechnical Control of Nuclear Power Stations*, 20: 18118
construction costs, 20: 18102
construction of, use of optical instruments in, 20: 18114
control of, use of static programming of digital data handling in, 20: 18121
development of, in European Atomic Energy Community, 20: 18180
economics of low-capacity, 20: 18107
magnetohydrodynamic generator for, 20: 17328
simulation of, concepts and methods of, 20: 18106
site selection for, 20: 16709

NUCLEAR REACTIONS

amplitudes for (d,n) stripping, (T), 20: 17704
cross sections for compound nucleus, computer program for calculating, 20: 17672 (AERE-R-5053)
gamma circular polarization in stripping, (E/T), 20: 17726
neutron production in, for activation analysis, 20: 16332 (GA-6691)
theory for one-meson-exchange, distorted-wave, 20: 17474
theory for pickup and stripping, quasi-particle, 20: 17814
theory for, inelastic effects in, (T), 20: 17692 (ORNL-TM-1414)

NUCLEAR STRUCTURE
nuclear forces in, phenomenological treatment of, 20: 17727
nuclear forces in, phenomenological treatment of, 20: 17728
nucleon quadrupole and pairing forces in, (T), 20: 17801
potentials for Hartree-Fock calculations of, singular, (T), 20: 17791
theory of, core excitations in quasi-particle, 20: 17814

NUCLEAR THEORY
forces in, oscillator brackets for Hartree-Fock calculations for two-body, 20: 17744
nuclear forces in, phenomenological treatment of, 20: 17727
nucleon quadrupole and pairing forces in, (T), 20: 17801

NUCLEI
abundances of $Z \geq 4$, in primary cosmic radiation, (E), 20: 17321
alpha decay energies of, variation with neutron number, 20: 17729
beta transitions in, higher-order effects in allowed, (E), 20: 17678 (COO-1420-113)
binding energies of, methods of calculating, (E/T), 20: 17158(R) (ORNL-3900, pp 82-149)
boson inelastic diffraction scattering by, complex angular momentum method for spin-zero, (T), 20: 17817
charge distribution of deformed, from x-ray spectra from μ-mesic atoms of, (T), 20: 17756
conversion electrons from, review of data on, 20: 17795
deformation parameters for even-even, 20: 17730
deuteron double elastic scattering by, polarization parameters from, (T), 20: 17805
deuteron reactions (d,n) with, amplitudes for, (T), 20: 17704
deuteron reactions (d,n) with, neutron production for activation analysis in, 20: 16332 (GA-6691)
effects of heavy solar-flare, on low-shielding space systems, 20: 16300
electron inelastic scattering by, electron and nucleon angular distributions for giant resonance decay from, (T), 20: 17757
elementary particle elastic scattering by, phase-shift analysis for 0- and ½-spin, (T), 20: 17693 (ORNL-TM-1464)
energy level transitions in, P violation in, (E/T), 20: 17444(T)
energy level transitions in, effects of atomic hyperfine interactions on, (T), 20: 17686 (JINR-P-2512)
energy level transitions in, energy-weighted sum rule for M1, (T), 20: 17690 (NP-15899)
energy level transitions in, multi-photon, (T), 20: 17401
energy level transition probabilities for even-even, E2, 20: 17730
energy levels in, excitation of alpha-cluster, (T), 20: 17802
energy levels of odd, transverse spin polarization effects on, (T), 20: 17682 (INP-428/PL)
energy levels of three-nucleon, matrix elements of three velocity-dependent operators for arbitrary, 20: 17746
energy levels of, lifetimes of, (E), 20: 17676 (CEA-R-2810)
energy levels of, model for collective vibrations of, 20: 17711
forces in, oscillator brackets for Hartree-Fock calculations for two-body, 20: 17744
gamma emission by, measurement using lithium-drifted germanium detectors, (E), 20: 17158(R) (ORNL-3900, pp 82-149)
neutron capture by, resonance widths in, (E), 20: 17676 (CEA-R-2810)
neutron reactions with, computer programs for charged particle cross sections from, 20: 17671 (AEEW-M-611)
neutron reactions (n,n') and (n,p) with excited, cross sections for direct, (T), 20: 17714
neutron resonance integrals for, second order approximations for effective, 20: 17650 (AAEC/E-144)
nucleon binding energies in, systematics of, 20: 17729
nucleon clustering in light, review on, 20: 17707
nucleon interactions in, hard-core potential in boundary-condition model for, (T), 20: 17772
nucleon pairing interactions in, approximation for, (T), 20: 17765
nucleon quadrupole and pairing forces in d-s shell of, (T), 20: 17801
particle scattering by complex, analysis of diffraction, (T), 20: 17816
photon reactions with, giant resonance in, (E/T), 20: 17706
polarization of, quantum-statistical theory of dynamic, 20: 17819
proton reactions with, pickup effects in, (E/T), 20: 17158(R) (ORNL-3900, pp 82-149)
proton scattering by, optical model parameters for, (T), 20: 17768
spin and quadrupole interaction in, via optical phonon virtual field, (T), 20: 17818
structure of, determination from isobaric analog states, (E/T), 20: 17158(T) (ORNL-3900, pp 82-149)

NUCLEIC ACIDS
radiation effects on metabolism of, 20: 16160 (UCRL-14739(Pt.2))
radiation effects on primer function of, 20: 16160 (UCRL-14739(Pt.2))
radiation effects on properties of virus, uv, 20: 16206
radiation effects on properties of virus, uv, 20: 16207
reactions with radionuclides, injuries from, 20: 16160 (UCRL-14739 (Pt.2))

NUCLEONS
capture by nuclei at 10 to 40 Mev, cross sections and mechanism for direct, (T), 20: 17737
clustering in light nuclei, review on, 20: 17707
electric dipole moments of, in intermediate vector boson theory, 20: 17372
energy levels of three-body system of, matrix elements of three velocity-dependent operators for arbitrary, 20: 17746
interactions at high energies, SU(3) for multiple meson production in, (T), 20: 17345 (JINR-P-2531)
interactions in nuclei, phenomenological treatment of, 20: 17728
interactions with meson field, high-energy successive, (T), 20: 17418
interactions with mesons (π) and nucleons, inelastic effects on cross sections for elastic, (T), 20: 17419
interactions with mesons (π) and nucleons, dynamical equations for, 20: 17420
interactions with nucleons, velocity-dependent potential from amplitude of low-energy, (T), 20: 17449
interactions with hyperons in broken SU(3), sum rules for S-state amplitudes for, 20: 17468
interactions with mesons (π), coupling constants for, (T), 20: 17336 (AECD/TP-5)
interactions with nucleons, T-invariance tests in, (T), 20: 17337 (AERE-R-5138)
interactions with neutrons, scattering lengths for, (T), 20: 17350 (N-65-19395)
interactions with mesons (π), inelastic effects on P_{11} phase shift in, (T), 20: 17355
interactions with nucleons in nuclear emulsions, particle-track distributions from, (E), 20: 17357
interactions with mesons (π) at high energies, optical model for backward, (T), 20: 17373
interactions with photons, current algebra for meson (π) production from, (T), 20: 17375
interactions with mesons (π), effect of dipion resonances on amplitude for, (T), 20: 17388
interactions with antiprotons, meson production in annihilation, (T), 20: 17396
interactions with mesons (π), coupled-channel Schroedinger equation model for, 20: 17397
interactions with electrons and mesons (μ), inelastic, (T), 20: 17399
interactions with photons, polarization coefficients for mesons (K) and (π) production from, (T), 20: 17407
interactions with photons, cross sections for vector meson production in, (T), 20: 17414
interactions with mesons (π), minimal singularity in axiomatic approach to charge-symmetry, (T), 20: 17416
interactions with charged leptons, tests of C and T invariances in, 20: 17392
interactions with nucleons in nuclei, hard-core potential in boundary-condition model for, (T), 20: 17772
interactions with nucleons in nuclei with N = 29 and 30, properties from effective, (T), 20: 17735
magnetic moment of, dispersion-theoretical calculation of, 20: 17390
model for, reformulation for meson-atomic, 20: 17356
pairing effects on fission of even-even compound nuclei near threshold, (T), 20: 17847
pairing interactions in nuclei, approximation for, (T), 20: 17765
scattering by beryllium and carbon at 140 Mev, parametrization analysis for elastic, (T), 20: 17740
symmetry for, electromagnetic form factors from, (T), 20: 17455

NUCLEOSIDES
radiolysis of tritium-labeled, effects of low temperature and scavengers on self-, 20: 16533

NUCLEOTIDES
radiation effects on, in intestine and liver cells, 20: 16230(R) (TID-22644)

O

OAK RIDGE NATIONAL LAB., TENN.
activities for education, information, and training during 1964, 20: 18175(R) (ORNL-3900)

OBRIGHEIM POWER REACTOR (*Germany*)
control system of, design of, 20: 18112

OCEANOGRAPHY

potassium-40 background in sea water, sensitivity of gamma spectrometer and scintillation detectors for, 20: 16828 (TID-22763)
OILS
analysis for isoprenoid alkanes, methods for, 20: 16633 (UCRL-16605)
deposition on tissue specimens, tracer study of, 20: 16159(R) (ORNL-3900, pp 150-81)
ONTARIO
geologic dating of rocks in, developments in, 20: 16711(R) (MIT-1381-13)
OOGENESIS
radiation effects on Drosophila, mutagenic, 20: 16229(R) (NYO-1472-1)
OPTICAL SYSTEMS
use in construction of nuclear power plants, 20: 18114
ORES
analysis for arsenic, effects of manganese on activation, 20: 16364
analysis for magnesium, activation, 20: 16336(R) (NYO-10175)
analysis for niobium and tantalum simultaneously, activation, 20: 16336(R) (NYO-10175)
analysis of silicate, methods for, 20: 16337 (RMO-3001(Rev.1)(Suppl.))
ORGANIC ACIDS
reactions with thorium, properties of salts from, 20: 16497
ORGANIC COMPOUNDS
analysis for carbon-14, sulfur-35, and tritium by combustion and scintillation counting, 20: 16387
analysis for radioisotopes, use of chromatography and flame ionization detector in, 20: 16371
heat transfer in, for reactor coolants, 20: 18070
performance and selection of, for use in space vehicles, 20: 16944 (NASA-SP-3025)
radiolysis of tritium-labeled, effects of low temperature and scavengers on self, 20: 16533
thermal decomposition of, in large-volume boiling, 20: 16615
ORGANIC COOLED REACTORS
neutron flux distribution in heavy water moderated, hyperfine structure of, 20: 18055
ORGANISMS
radiation effects on living, bibliography on, 20: 16219 (AED-C-04-23)
radiation effects on living, bibliography on, 20: 16221 (AED-C-04-25)
radioisotope uptake, distribution, and excretion by marine, factors affecting, 20: 16725(R) (EUR-2543.e)
ORNL FAST BURST REACTOR
operation, 1964, 20: 16159(R) (ORNL-3900, pp 150-81)
ORNL HIGH FLUX ISOTOPE REACTOR
design and development, 20: 18020(R) (ORNL-3900, pp 2-81)
reactivity measurements in core for, subcritical, 20: 18048 (ORNL-P-1967)
ORNL RELATIVISTIC ISOCHRONOUS CYCLOTRON
design and operation of, 20: 17158(R) (ORNL-3900, pp 82-149)
ORNL RESEARCH REACTOR
boiling in, neutron power spectral density measurements for detection of, 20: 18048 (ORNL-P-1967)
OSCILLATORS
coupling to oscilloscopes, method of, 20: 16776 (EGG-1183-1156)
OSCILLOGRAPHS
coupling of oscillators to oscilloscopes, method of, 20: 16776 (EGG-1183-1156)
OSMIUM
electron emission in cesium vapor, thermionic, (E), 20: 17333
OSMIUM ISOTOPES Os-189
neutron reactions (n,γ), activation cross section for, (E), 20: 16336(R) (NYO-10175)
OSMIUM ISOTOPES Os-190
half life of isomeric, from neutron reactions (n,γ), (E), 20: 16336(R) (NYO-10175)
half life of isomeric, from neutron reactions (n,n′), (E), 20: 16336(R) (NYO-10175)
neutron reactions (n,n′), activation cross section for, (E), 20: 16336(R) (NYO-10175)
OSMIUM ISOTOPES Os-194
beta decay of, iridium-194 levels from, (E/T), 20: 17781
OXADIAZOLES
salts of, protective effects against radiation injuries in mice, 20: 16490(R) (TID-22681)
OXALIC ACID
decomposition of, effects of deuterium on gas-phase, 20: 16455
properties as chemical dosimeter, 20: 16517
yields in uv carboxylation of formic acid, effects of acidity on, 20: 16538
OXYGEN
determination by isotopic dilution, 20: 16362
determination in metals and welded joints, activation, 20: 16331 (GA-6568)
determination in steel, comparison of hot-extraction and activation, 20: 16400
determination in sodium by distillation and titration, 20: 16349
determination in steel, activation, 20: 16357
determination in thin metallic foils, activation, 20: 16331 (GA-6568)
determination in uranium hexafluoride, spectrographic, 20: 16409
effects of hyperbaric, combined with x radiation and cyclophosphamide on leukemic mice, 20: 16262
effects on radiation chemistry of cysteic acid, cysteine, and cystine, 20: 16540
effects on yields of hydrogen peroxide from radiolysis of water, 20: 16520
photon reactions with Coulomb field of, pair production total cross sections for high-energy, (T), 20: 17754
radiosensitivity effects on olfactory bulb neurons in rats, 20: 16215 (AD-628443)
radiosensitivity effects of, effects of dose on γ and x, 20: 16750
solubility in niobium–zirconium alloys at 1000 to 1200°C, 20: 16980
OXYGEN IONS
ionization after passage through solids, auto-, (E), 20: 17262(T)
OXYGEN ISOTOPES
abundance ratios in sandstone-type uranium deposits, Gas Hills District, Wyoming, 20: 16670
content in calcite in Mexico, 20: 16634
content in hydrothermal fluids responsible for lead–zinc deposits in Mexico, 20: 16634
distribution between gaseous and liquid phases of nitrogen oxide systems, 20: 16486
OXYGEN ISOTOPES O-14
beta decay of, phase-space integrals for, (T), 20: 17732
OXYGEN ISOTOPES O-15
energy levels from oxygen-16 (He-3,α) reactions, (E), 20: 17780
OXYGEN ISOTOPES O-16
boron-10 reactions (B-10,3α) at 100 Mev, excitation function and nitrogen-14 angular distributions from, (E), 20: 17815
bremsstrahlung reactions (γ,n) to 65 Mev, cross section structure from, (E), 20: 17762
content ratio to oxygen-18 in carbonates, 20: 16676
electron inelastic scattering by, angular distributions for giant resonance decay from, (T), 20: 17757
energy level density of, oscillator model for determining, 20: 17745
helium-3 reactions (He-3,α) with, optical-model analysis of, (T), 20: 17696 (UR-875-65)
helium-3 reactions (He-3,n) and (He-3,p) at 12 Mev, Q values for, 20: 16331 (GA-6568)
helium-3 reactions (He-3,α) at 12.1 Mev, oxygen-15 levels from, (E), 20: 17780
helium-3 scattering by, optical-model analysis of, (T), 20: 17696 (UR-875-65)
neutron elastic scattering at 3.0 to 4.7 Mev, differential cross sections for, (E), 20: 17767
neutron reactions (n,α) at 3.0 to 4.7 Mev, total cross section for, (E), 20: 17767
proton reactions (p,2p) at 140 Mev, energy spectra and angular correlation distributions from, (E), 20: 17741
scattering by even and odd nuclei at 31 to 45 Mev, B(E2) values for transitions from, (E), 20: 17734
separation from oxygen-18 by gas chromatography, 20: 16930
spallation by high-energy solar particles, 20: 17234
OXYGEN ISOTOPES O-17
energy levels from neutron scattering by oxygen-16, (E), 20: 17767
incorporation in methanol, 20: 16547
triton reactions (t,p) at 12 Mev, oxygen-19 levels from, (E), 20: 17758
OXYGEN ISOTOPES O-18
content ratio to oxygen-16 in carbonates, 20: 16676
determination by activation methods, 20: 16412(P)
deuteron reactions (d,p) at 12 Mev, oxygen-19 levels from, (E), 20: 17758
exchange between *p*-substituted benzoate anions and water, mechanism of, 20: 16542(R) (TID-22646)
exchange between *p*-substituted benzophenones and water, reaction medium for, 20: 16542(R) (TID-22646)
incorporation in methanol, 20: 16547
separation from oxygen-16 by gas chromatography, 20: 16930
tracer use in studies on benzopinacol rearrangement to benzopinacolone, 20: 16542(R) (TID-22646)
OXYGEN ISOTOPES O-19
energy levels from oxygen-17 (t,p) and oxygen-18 (d,p) reactions, parity and spin of, (E), 20: 17758
OXYGEN SYSTEMS
acetylene–O, transport coefficients for combustion products of, (T), 20: 17519
Fe–O–Ti–Zr, fabrication and properties of sintered, deformable, 20: 17003
F–O, analysis for fluorine, activation, 20: 16332 (GA-6691)
Nb–O–Zr, phase studies, 20: 16980

N–O–H_2O, oxidative effects on uranium, mechanism of, 20: 16986
O–H_2O, oxidative effects on uranium, mechanism of, 20: 16986
O–V, phase studies, 20: 17007(R) (AD-627468)
OZONE
effects on iodine-131 uptake by rats, 20: 16190
radiation synthesis of, developments in, 20: 16506 (BNL-10020)

P

PAIR PRODUCTION
cross sections for photo-, 20: 16829(R) (UCRL-14534, pp 1-7)
PAKISTAN
fallout monitoring in lower atmosphere at Lahore, 20: 16683
radiosterilization of food in, feasibility, 20: 16918 (AECL-PAK/RB-7)
PALLADIUM
determination in rocks, activation, 20: 16370
effects on tritium exchange between tritiated ethyl malonate and hydrocarbons, catalytic, 20: 16492
electron emission in cesium vapor, thermionic, (E), 20: 17333
PALLADIUM ALLOYS
Au–Pd, effects on isotopic exchange between methane and deuterium at 90 to 200°C, catalytic, 20: 16457
Pd–Sn, preparation and properties of, for use as Mössbauer source, 20: 16335(R) (NBS-TN-276)
Pt–Ta, superconductivity in close-packed intermediate phases of, 20: 17624
PALLADIUM ISOTOPES Pd-106
neutron reactions (n,γ), activation cross section for, (E), 20: 16336(R) (NYO-10175)
PALLADIUM ISOTOPES Pd-107
half life of isomeric, from neutron reactions (n,γ), (E), 20: 16336(R) (NYO-10175)
PALLADIUM ISOTOPES Pd-108
energy levels from isomeric silver-108 decay, (E), 20: 17786
neutron reactions (n,γ), activation cross section for, (E), 20: 16336(R) (NYO-10175)
PALLADIUM ISOTOPES Pd-109
half life of isomeric, from neutron reactions (n,γ), (E), 20: 16336(R) (NYO-10175)
sensitivity for activation analysis using beta-gamma-gamma sum-coincidence gamma spectrometer, 20: 16335(R) (NBS-TN-276)
PALLADIUM ISOTOPES Pd-110
deuteron reactions (d,p) at 15 Mev, isomeric yield ratios for, 20: 16508(R) (NYO-2771-13)
PALLADIUM ISOTOPES Pd-111
production of isomeric, in deuteron reactions (d,p) at 15 Mev, 20: 16508(R) (NYO-2771-13)
PALLADIUM ISOTOPES Pd-112
yields from thorium-232 fission, (E), 20: 17860
PAPER
production of, tracer techniques for stream pollution problems in, 20: 16921 (TID-22627)
PARAMAGNETIC MATERIALS
magnetothermodynamics of, instrument for determining, 20: 17978(R) (NYO-3402-2)
PARAMECIUM
radiation effects on, equation of survival from, 20: 16273
PARTICLE STATISTICS
canonical commutation relations in, effects of operator translations on, 20: 17506
PARTICLE TRACKS
analysis of bubble- and spark-chamber, flying spot digitizers for, 20: 16840
PARTICLE TRAJECTORIES
determination in magnetic fields using analog computer, 20: 17906
PARTICLES
dispersion of radioactive, in atmosphere, 20: 16642
dispersion of radioactive, in stratosphere, 20: 16643
distribution in lower layers of atmosphere, 20: 16652
motion in Schwarzschild field, 20: 17569
motion in three-body systems, mathematical treatment of, 20: 17584
properties of alpha-emitting, in atmosphere over Vilnius, Russia, 20: 16646
properties of radioactive, in surface boundary layer of atmosphere over Moscow, 20: 16645
PEAS
radiation effects on root growth in seedlings of, from tritiated water and tritiated thymidine, 20: 16227(R) (NYO-3561-2)
radiation effects on flour from, role of water content in, 20: 16297(R) (EUR-2548.f)
radioinduced ethylene in, γ, 20: 16281
PEAT
age estimation of Beillard bog, carbon-14 method for, 20: 16712
PEBBLE BED REACTORS
core density distribution in randomly packed, nondestructive electrical method for determining, 20: 18018 (CONF-651101-73)
2,4-PENTANEDIONE
reactions with nickel(II) in 2-propanol–water, thermodynamics of, 20: 16416(R) (NYO-906-68)
tautomerism of, solvent effects of dioxane–water on equilibrium in keto-enol, 20: 16416(R) (NYO-906-68)
2,4-PENTANEDIONE COMPLEXES
with neodymium and praseodymium, preparation, 20: 16434
with praseodymium, Szilard-Chalmers reaction in, 20: 16416(R) (NYO-906-68)
2-PENTANONE
formation by disproportionation of aliphatic ketones in perchloric acid, 20: 16542(R) (TID-22646)
formation by rearrangement reactions of 3-pentanone with perchloric acid, mechanism of, 20: 16542(R) (TID-22646)
3-PENTANONE
formation by disproportionation of aliphatic ketones in perchloric acid, 20: 16542(R) (TID-22646)
reactions with perchloric acid, mechanism of 2-pentanone formation by rearrangement, 20: 16542(R) (TID-22646)
2-PENTANONE, 4-METHYL-
reactions with perchloric acid, disproportionation in, 20: 16542(R) (TID-22646)
PERCHLORIC ACID
effects on rearrangement of benzopinacol to benzopinacolone, oxygen-18 tracer studies on, 20: 16542(R) (TID-22646)
europium ion reactions in aqueous solutions of, electron transfer in, 20: 16462
reactions with aliphatic ketones, mechanism of rearrangement, 20: 16542(R) (TID-22646)
reactions with aliphatic ketones, disproportionation in rearrangement, 20: 16542(R) (TID-22646)
PERIODATES
separation of iodine-131-labeled, from labeled iodides and iodates, chromatographic, 20: 16567
PERSONNEL
education and training at Risö, 20: 18174(R) (NP-15771)
radiation dose to reactor, from leaks, 20: 16757
radiation dosimetry for, equipment and methods for, 20: 16827 (SZS-9(1965))
radiation monitoring of hands and shoes of, engineering drawings of instrument for alpha, 20: 16769
radiation monitoring of, using photographic film detectors, 20: 16720 (AERE-R-4669)
PERTURBATION THEORY
approximation methods in many-body, 20: 17570
PETROLEUM
fractionation of crude, deuterium distribution in, 20: 16475
recovery from shale, use of nuclear explosions for, 20: 16589 (UCRL-12224-T)
PHANTOMS
use of plastic neck, for iodine-131 measurement standardization, 20: 16315
PHENANTHROLINE COMPLEXES
with rare earths, infrared spectra of, 20: 16437
PHENYL ETHER
biphenyl–phenyl ether, thermodynamic properties of eutectic mixture of, for use as reactor coolant, 20: 16493
PHONONS
reflection in superfluid helium, specular, (E), 20: 17648
PHOSPHATE GLASS
leaching of radioactive waste-containing, aqueous, 20: 18166(R) (TID-22531)
processing and disposal of condensates of, containing sulfuric acid, 20: 18159 (BNWL-SA-514)
radiation effects on ESR spectra of, γ, 20: 16516
PHOSPHATE ROCKS
separation of uranium from, ion exchange methods for, 20: 16381
PHOSPHATES
excretion in rats, effects of pyridoxine on, 20: 16176
PHOSPHINE SULFIDE, TRIOCTYL-
bis(2-ethylhexyl) phosphate–trioctylphosphine oxide, solvent properties for thorium and uranium, 20: 16580
PHOSPHONIC ACID, METHYL-, DIPENTYL ESTER
bis(2-ethylhexyl) phosphate–dipentyl methylphosphonate, solvent properties for thorium and uranium, 20: 16580
PHOSPHONIC ACIDS
dimethyl ester, labeling with phosphorus-32 from carrier-free source, 20: 16551
PHOSPHOR BRONZE
analysis for phosphorus, activation, 20: 16332 (GA-6691)

PHOSPHORIC ACID
reactions with acetophenone, butyrophenones, and propiophenone, products formed by disproportionation in, 20: 16542(R) (TID-22646)
PHOSPHORIC ACID, BIS(2-ETHYLHEXYL) ESTER
analytical use in chromatographic separation of yttrium from dysprosium and terbium, 20: 16385
solvent properties for cerium in rare earth solutions, 20: 16329 (BNWL-187)
solvent properties for uranium, 20: 16579
solvent properties for thorium and uranium, 20: 16580
bis(2-ethylhexyl) phosphate–HCl–toluene, extraction constants for americium, californium, curium, and fermium in, 20: 16404
bis(2-ethylhexyl) phosphate–trioctylphosphine oxide, solvent properties for thorium and uranium, 20: 16580
bis(2-ethylhexyl) phosphate–dipentyl methylphosphonate, solvent properties for thorium and uranium, 20: 16580
bis(2-ethylhexyl) phosphate–HCl–toluene, solvent properties for californium, fermium, and mendelevium, 20: 16404
PHOSPHORIC ACID, DIETHYLOCTYL ESTER
solvent properties for uranium, 20: 16579
PHOSPHORODITHIOIC ACID
dimethyl ester, labeling with phosphorus-32 from carrier-free source, 20: 16551
PHOSPHORS
preparation and performance of large parabolic, 20: 16849
scintillation pulse-shape discrimination in organic, circuit for determining, 20: 16839
scintillation quenching correction by external standardization of sources, 20: 16820 (LA-DC-7222)
scintillation response of organic, time-dependent, 20: 16813 (INR-653/1A/D)
use of NE102, with photographic film for fast neutron dosimetry, 20: 16861
PHOSPHORUS
determination in algae, method for, 20: 16175(R) (RT/BIO(65)-1)
determination in phosphor bronze, activation, 20: 16332 (GA-6691)
photon reactions with Coulomb field of, pair production total cross sections for high-energy, (T), 20: 17754
PHOSPHORUS CHLORIDES
labeling with phosphorus-32 from carrier-free source, 20: 16551
PHOSPHORUS COMPOUNDS
organic, solvent properties for thorium in uranium leach solutions, 20: 16573
organo-, NMR studies of coupling in uranyl complexes with, 20: 16422
PHOSPHORUS ISOTOPES P-30
half life, 20: 16331 (GA-6568)
PHOSPHORUS ISOTOPES P-31
energy levels in, properties of, (E), 20: 17651(R) (AD-612192)
helium-3 reactions (He-3,α) at 12 Mev, Q value for, 20: 16331 (GA-6568)
proton reactions (p,α) at 6.0 to 7.5 Mev, absolute cross sections and angular distributions for, (E/T), 20: 17775
proton reactions (p,2p) at 140 Mev, energy spectra and angular correlation distributions from, (E), 20: 17741
PHOSPHORUS ISOTOPES P-32
chemical species containing, following neutron irradiation of cysteic acid, cysteine, and cystine, 20: 16540
content in stratospheric and tropospheric samples in Project Star Dust, 1963, 20: 16727(R) (HASL-168)
content in stratospheric and tropospheric samples in Project Star Dust, 1964, 20: 16728(R) (HASL-169)
effects of, combined with cytostatic drugs on polycythemia, complications from, 20: 16233
effects on blood picture following polycythemia therapy, 20: 16241
half life, (E), 20: 17712
incorporation of carrier-free, in inorganic and organic compounds, 20: 16551
preparation for radiation sources, 20: 16914(R) (ORNL-3900, pp 182-93)
radiation effects on distribution of Yoshida sarcoma cell-incorporated, in rats, 20: 16188
uptake by aquatic foodstuffs from radioactive wastes in fresh water, 20: 18157 (BNWL-SA-466)
PHOSPHORUS ISOTOPES P-33
content in stratospheric and tropospheric samples in Project Star Dust, 1964, 20: 16728(R) (HASL-169)
content in stratospheric and tropospheric samples in Project Star Dust, 1963, 20: 16727(R) (HASL-168)
production, 20: 16914(R) (ORNL-3900, pp 182-93)
PHOSPHORUS OXIDES
effects on uranium separation from phosphate rocks, 20: 16381
PHOSPHORUS SULFIDES
labeling with phosphorus-32 from carrier-free source, 20: 16551
PHOSPHORUS SYSTEMS
Cr–Fe–Ni–P, corrosion cracking in, mechanisms of stress-, 20: 16968 (COO-1319-33)
PHOSPHORYL CHLORIDES
labeling with phosphorus-32 from carrier-free source, 20: 16551
PHOTOCHEMISTRY
reaction mechanisms for DNA, 20: 16203
PHOTOELECTRIC CELLS
radiation effects on junctions, proton, 20: 16907(R) (N-65-17517)
PHOTOELECTRIC EFFECT
cross sections for, in photon reactions with lithium fluoride, 20: 16829(R) (UCRL-14534, pp 1-7)
electron yields from photocathodes, 20: 17984
ion emission from cesiated surfaces at room temperature, (E/T), 20: 17267
PHOTOGRAPHIC EMULSIONS
performance of liquid, for γ- and x-ray dosimetry, 20: 16845
PHOTOGRAPHIC FILM
performance with activation foils in neutron radiography, 20: 16619
use with scintillators for fast neutron dosimetry, 20: 16861
PHOTOGRAPHIC FILM DETECTORS
design and performance of, for medical use, 20: 16843
performance for personnel monitoring, 20: 16720 (AERE-R-4669)
use for determining properties of dental x-ray equipment, 20: 16844
use in gamma and thermal-neutron dosimetry, 20: 16807 (CLOR/IBJ-42/D)
PHOTOGRAPHY
equipment for, of high explosives, evaluation of flash, 20: 16739(R) (UCRL-14534, pp 44-9)
PHOTOMULTIPLIER TUBES
base system for, with high-voltage divider remote from photomultiplier, 20: 16796
cathodes for, sensitivity of, 20: 17984
PHOTONS
detection of, use in reactor noise analysis, 20: 18064
emission from electron-irradiated slabs, spectra of, 20: 16159(R) (ORNL-3900, pp 150-81)
interactions with particles, isotopic structure of, (T), 20: 17428 (JINR-P-2498)
interactions with electrons and photons, line-profile effects in stimulated beam, (T), 20: 17464
interactions with charged particles, pair production in, (T), 20: 17499
interactions with protons, quark model for hyperon production in, (T), 20: 17348 (JINR-P-2556)
interactions with electrons, cross sections for pair production in, (T), 20: 17354
interactions with nucleons, current algebra for meson (π) production from, (T), 20: 17375
interactions with protons at 3.4 to 4.0 Bev, meson (K^+) and (π^+) production in, (E/T), 20: 17400
interactions with nucleons, polarization coefficients for mesons (K) and (π) production from, (T), 20: 17407
interactions with deuterons, dispersion theory for magnetic-dipole splitting in, 20: 17408
interactions with charged particles in magnetic field, Compton effect in, (T), 20: 17409
interactions with mesons (π^+) and protons, cross sections for vector meson production in, 20: 17410
interactions with nucleons, cross sections for vector meson production in, (T), 20: 17414
reactions with hydrogen atoms, tables of ionization cross sections from, (T), 20: 17251 (IAE-873)
reactions with metals, electron yields from, 20: 17984
reactions with nuclei, giant resonance in, (E/T), 20: 17706
transport in slab geometry, spectral theory for stationary operator for, 20: 17658
PHOTOSYNTHESIS
energy conversion steps in, 20: 16159(R) (ORNL-3900, pp 150-81)
instrumentation for, 20: 16159(R) (ORNL-3900, pp 150-81)
PHYSICS
equation development in, 20: 17160
PIEZOELECTRIC CRYSTALS
radiation effects on, review of, 20: 16911
PIGMENTS
radiation effects on skin, in guinea pigs and man, uv, 20: 16261
PINCH EFFECT
electron density in theta, rapid oscillations in, (E), 20: 17918
laser emission by plasma in, (T), 20: 17924(T)
light emission from theta, in dense gases, (E), 20: 17523
plasma kinetics in theta, (T), 20: 17878 (LA-3437)
PIPE JOINTS
testing of low-pressure, for hydrogen transfer lines, 20: 16588 (LA-3454)
PITCHBLENDES
processing for promethium isotope separation, 20: 16685

PITUITARY GLAND
radiation effects on, following tumor therapy, 20: 16209
radiation exposure of thyroid and, carcinogenic effects of x, 20: 16245
radiosensitivity effects on mice and rats, review on, 20: 16232(T) (JPRS-34120)
PLACENTA
fission product transfer by, radiation hazards to fetus from, 20: 16301
PLANETS
earth-to-Mars trajectories, three-body analysis of, 20: 17584
solar wind interactions with, (T), 20: 17232
PLANKTON
distribution in marine ecosystem, 20: 16175(R) (RT/BIO(65)-1)
radioactive contamination in, equation for predicting, 20: 16175(R) (RT/BIO(65)-1)
radioisotope uptake, distribution, and excretion by, factors affecting, 20: 16725(R) (EUR-2543.e)
PLANT CELLS
trace metals in, electron microscopy for determining, 20: 16160 (UCRL-14739(Pt.2))
PLANT PATHOLOGY
research at Risö on, 20: 18174(R) (NP-15771)
PLANTS
cesium-137 content in, effects on cesium-137 burdens in Colorado mule deer, 20: 16723 (COO-1156-11)
cultivation and use of deuterium-labeled, 20: 16165
growth without cell division, abnormal and normal, 20: 16159(R) (ORNL-3900, pp 150-81)
manganese-54 content in barley, rye, tea leaves, and wheat, 20: 16167
mineral uptake by, factors affecting, 20: 18174(R) (NP-15771)
polonium-210 uptake from soils by, effects on plant content of, 20: 16189
radiation effects on jute, γ, 20: 16217 (AECD-AG-7)
radiation effects on, bibliography on, 20: 16220 (AED-C-04-24)
radiation monitoring for Salmon Event, 20: 16743 (VUF-1021)
radioactivity in Monticello Project Area, Utah, 20: 16729 (IDO-12049)
radioinduced ethylene formation in, γ, 20: 16281
radioinduced hybridization in jute, γ, 20: 16218 (AECD-AG-12)
radioinduced mutations in, review of agricultural use of γ, 20: 16225 (EUR-2715.f)
radioinduced mutations in peanut, x, 20: 16247
radioinduced mutations in, research at Risö on, 20: 18174(R) (NP-15771)
radioinduced mutations in medicinal, γ, 20: 16290
radioisotope contamination of, formula for determining effective half life of, 20: 16160 (UCRL-14739(Pt.2))
sodium-22 uptake from fallout, 20: 16678
PLASMA
acceleration of, method and device for, 20: 17960(P)
accelerators for, snowplow equations for, 20: 17903
atom emission from magnetically confined, system for analysis of, 20: 17873 (CLM-R-49)
book: *Kinetics and Thermodynamics of Chemical Reactions in Low-Temperature Plasma*, 20: 17959
book: *The Theory of Turbulent Plasma*, 20: 17958
bremsstrahlung emission from nonrelativistic, electron-ion, 20: 17947
bremsstrahlung emission in infrared region from hydrogen discharge, (E), 20: 17931(T)
charged-particle interactions in turbulent, (T), 20: 17941
containment and heating by magnetic fields, (T), 20: 17927
containment and heating by magnetic fields, (E), 20: 17928
current instability in, quasilinear theory of, 20: 17950
cyclotron echo processes in, (T), 20: 17933
diagnostics of low-density, use of Langmuir probes for, 20: 17899
diagnostics of, Mach-Zehnder laser interferometer for, 20: 17875 (IPP-1/35)
diagnostics using focused microwave beams, (E/T), 20: 17881 (N-65-19804)
diagnostics using electromagnetic wave reflection and refraction, (T), 20: 17915
diffusion across magnetic fields in r-f discharges, anomalous, (E), 20: 17954
diffusion in infinite plane low-voltage arc, electron coefficient of, (T), 20: 17907
electric field distributions in, (T), 20: 17896
electromagnetic field interactions in air, heterodyne generation from, (E/T), 20: 17905
electromagnetic properties of anisotropic hot two-component, (T), 20: 17912
electromagnetic radiation from high-temperature and -density, 20: 17944
electromagnetic wave propagation in, 20: 17537 (JPLAI/LS-641)
electromagnetic wave diffraction by, (T), 20: 17877 (IPP-6/44)
electromagnetic wave propagation in, review on theory and uses for, 20: 17911
electromagnetic wave propagation in nonuniform, (T), 20: 17913
electromagnetic wave reflection and refraction in homogeneous, in magnetic fields, (T), 20: 17915
electromagnetic wave scattering by, Raman, (E/T), 20: 17923(T)
electron beam interactions with nonisothermal, 20: 17951
electron beam interactions with, properties of, (E), 20: 17889(R) (ORNL-3908, pp 52-89)
electron beam interactions with, diagnostics from, (E/T), 20: 17893(R) (SU-IPR-44)
electron beam interactions with, diagnostics from, (E/T), 20: 17894(R) (SU-IPR-47)
electron density in discharge and shock produced, microwave interferometry of, (E), 20: 17510 (IPP-3/25)
electron density in z-pinch, microwave reflection probe for measuring, 20: 17876 (IPP-1/37)
electron density in axis of theta pinch, rapid oscillations in, (E), 20: 17918
energy emission by argon, 20: 17930(T)
flow between electrodes with weak longitudinal conductivity, Hall effect in, (E/T), 20: 17939
flow in magnetic fields, similarity analysis of two-fluid, (T), 20: 17910
heating in injection devices, electron cyclotron, (E/T), 20: 17888(R) (ORNL-3908, pp 32-51)
heating of low-pressure, high-frequency, 20: 17909
interactions with dipole magnetic fields, (E), 20: 17551
interactions with cylindrical magnetic fields, (T), 20: 17956
interactions with electron beams, heating mechanisms in, (E/T), 20: 17158(R) (ORNL-3900, pp 82-149)
ion excitation energies and densities in, (E), 20: 17508 (ARL-65-246)
ion heating in discharge, inelastic collision processes for excitation, (E), 20: 17900
ion sheath effects on r-f probe admittance in, (T), 20: 17552
ion wave propagation in, instabilities from, (E/T), 20: 17893(R) (SU-IPR-44)
ion wave propagation in, instabilities from, (E/T), 20: 17894(R) (SU-IPR-47)
ionization and recombination in alkali-seeded collision-dominated, model for, (T), 20: 17872 (AD-627988)
kinetics of, spherical-harmonic reduction of Fokker-Planck equation for, (T), 20: 17878 (LA-3437)
laser beam absorption by, effects from focused, 20: 17531
laser emission by pinch, (E), 20: 17924(T)
magnetohydrodynamic perturbations in, resonant ohmic damping of, 20: 17946
oscillation amplitudes in d-c arc, 20: 17938
oscillation modes of collisionless, research progress on, 20: 17882(R) (N-65-19862)
oscillations in, parametric resonance excitation of, (E), 20: 17920
oscillations near electron cyclotron harmonics, longitudinal, (T), 20: 17934
oscillations of cold, unified theory of nonlinear, 20: 17919
partition function of partially ionized hydrogen, (T), 20: 17935
pinch discharge in helium, at high densities, 20: 17945
production and properties in two-stage magnetic mirror compression, 20: 17953
production and properties of thermal cesium, (E), 20: 17955
production by laser beam focusing in air, properties of, (E), 20: 17908
properties of h-f discharge, (E/T), 20: 17879 (LRP-19/65)
properties of, effect of stationary crossed electric and magnetic fields on, (E), 20: 17943
radio wave emission from rare gas, negative absorption effects on anomalous bremsstrahlung and cyclotron, (E), 20: 17921
research programs at Risö on, 20: 18174(R) (NP-15771)
satellite motion through tenuous, scaling conditions for sheaths from simulated, (E), 20: 17546
spectra of helium and hydrogen, recombination lines in, (T), 20: 17952
spectra of T-tube, atomic-resonance line-oscillator strengths in, (E), 20: 17932
stability in magnetic traps, (E), 20: 17925(T)
stability of beam, magnetohydrodynamic, (T), 20: 17942
stability of collisionless, in strong h-f field, (T), 20: 17948
stability of fusion, (T), 20: 17891(R) (ORNL-3908, pp 108-13)
stability of potassium, drift, (E/T), 20: 17883 (NP-15784)
stability of thermonuclear, initial, (T), 20: 17880 (MATT-437)
stability of, quasi-linear theory of electrostatic, 20: 17957
stability of, wave-interaction model for diocotron effect in, 20: 17916
stability theory for, review of, 20: 17884 (NP-15886)
temperature determination in argon and nitrogen, by spectroscopy, 20: 17902
thermal conductivity of argon, (E), 20: 17937
thermal conductivity of, effect of ionization reactions on, (T), 20: 17940
transport coefficients for acetylene–oxygen combustive, (T), 20: 17519
wave excitation in stationary magneto-acoustic hydrogen, drift, (E), 20: 17949

wave propagation in positive column, properties of, (T), 20: 17893(R) (SU-IPR-44)
wave propagation in positive column, properties of, (E/T), 20: 17894(R) (SU-IPR-47)
wave propagation theory for, review of, 20: 17884 (NP-15886)
PLASMA JETS
chemical reactions in, kinetics and thermodynamics of, 20: 17959
current sheet in, snowplow equations for, 20: 17903
development of thruster for, experiments for, 20: 17904
electric arcs in supersonic, (E), 20: 17904
energy transfer in and from, spectroscopic studies of, 20: 17901
Lorentz force maximization in Hall current, (T), 20: 17897
performance of d-c, 20: 17938
performance of Hall current, 20: 16627
performance of hydrogen–nitrogen arc jets for propulsion, 20: 16629
performance of pulsed ablating thruster, 20: 16626
radiation emission from water-vapor, (E/T), 20: 17936
stability of, nonlinear limiting of double-stream, (T), 20: 17917
thermal radiation from argon, measurement of, (E), 20: 17898
uses in metallurgy, 20: 16593
PLASTICS
efficiency of Naton II scintillators for x-ray detection, 20: 16836
scintillation response functions for monoenergetic electrons, 20: 16867
plastics–wood, radiation processing of materials of, 20: 16505 (BNL-949)
PLATINUM
analysis for oxygen, activation, 20: 16331 (GA-6568)
effects on sorption of uranium by activated carbon, 20: 16581
effects on tritium exchange between tritiated ethyl malonate and hydrocarbons, catalytic, 20: 16492
electron emission in cesium vapor, thermionic, (E), 20: 17333
photosensitivity of, 20: 17984
proton fission at 150 to 660 Mev, cross sections for, (E), 20: 17838
PLATINUM ALLOYS
Nb–Pt, superconductivity in close-packed intermediate phases of, 20: 17624
Pt–U, superconductivity of beta-phase, 20: 17095
PLATINUM ISOTOPES Pt-192
energy levels from iridium-192 decay, g factors for 2+, (E), 20: 17747
PLATINUM ISOTOPES Pt-194
energy levels from iridium-194 decay, (E), 20: 17781
energy levels from iridium-194 decay, g factors for 2+, (E), 20: 17747
PLATINUM ISOTOPES Pt-196
deuteron reactions (d,p) at 15 Mev, isomeric yield ratios for, 20: 16508(R) (NYO-2771-13)
neutron reactions (n,γ), activation cross section for, (E), 20: 16336(R) (NYO-10175)
PLATINUM ISOTOPES Pt-197
half life of isomeric, from neutron reactions (n,γ), (E), 20: 16336(R) (NYO-10175)
production of isomeric, in deuteron reactions (d,p) at 15 Mev, 20: 16508(R) (NYO-2771-13)
PLATINUM ISOTOPES Pt-198
neutron reactions (n,γ), activation cross section for, (E), 20: 16336(R) (NYO-10175)
PLATINUM ISOTOPES Pt-199
half life of isomeric, from neutron reactions (n,γ), (E), 20: 16336(R) (NYO-10175)
half life of, from neutron reactions (n,γ), (E), 20: 16336(R) (NYO-10175)
PLATINUM OXIDES
effects on tritium exchange between tritiated ethyl malonate and hydrocarbons, catalytic, 20: 16492
PLUTONIUM
cost factors and requirements for, 20: 16716
determination in nitrate solutions by argentic oxidation, ferrous reduction, and dichromate titration, 20: 16405
determination in plutonium dioxide by differential spectrophotometry, 20: 16350
determination of trace amounts of, using controlled-potential coulometry, 20: 16390
fabrication of fuel elements of, 20: 16996
fabrication, production, and separation of, bibliography on, 20: 16328 (AECL-Pak/Lib-10)
monitoring in air, engineering drawings of instrument for, 20: 16768
phase transformations in, effects of pressure to 75 kbar on, 20: 17061
production, 20: 16543
properties as reactor fuel material, 20: 18182
separation from irradiated fuels, Eurochemic facility for, 20: 16558
separation from irradiated fuels by solvent extraction using TBP and tridodecylamine, 20: 16560
separation from irradiated fuels by ion exchange, 20: 16582
separation from irradiated thorium, method for, 20: 16359
PLUTONIUM ALLOYS
fabrication of fuel elements of, 20: 16996
PLUTONIUM CARBIDES
production, 20: 16582
PuC–UC, burnup in fast reactors, effects on breeding ratio, multiplication factor, and sodium-void reactivity, 20: 18060
PLUTONIUM COMPOUNDS
fabrication of fuel elements of, 20: 16996
PLUTONIUM(IV) FLUORIDES
reactions with fluorine to prepare plutonium hexafluoride, 20: 16463
PLUTONIUM(VI) FLUORIDES
preparation of high-purity, 20: 16463
PLUTONIUM IONS
determination of chemical state of, in process feed solutions by extraction chromatography, 20: 16333 (KR-81)
PLUTONIUM ISOTOPES Pu-238
content in stratospheric and tropospheric samples in Project Star Dust, 1964, 20: 16728(R) (HASL-169)
distribution of atmospheric, from SNAP-9A high-altitude burn-up, predictions for, 20: 16662(R) (HASL-165)
neutron fission at 0.1 to 1.2 Mev, fragment angular distributions from, (E/T), 20: 17848
PLUTONIUM ISOTOPES Pu-239
content in stratospheric and tropospheric samples in Project Star Dust, 1963, 20: 16727(R) (HASL-168)
content in stratospheric and tropospheric samples in Project Star Dust, 1964, 20: 16728(R) (HASL-169)
critical mass in water-reflected cylinder, distribution effects on, (T), 20: 18062
determination in living tissues, using gamma spectrometry, 20: 16864
effects on dog skeleton, 20: 16253
neutron fission cross sections at 40 to 500 kev, (E), 20: 17852
neutron fission cross sections at 0.0322 to 0.75 ev, (E), 20: 17854
neutron fission cross sections at 0.16 ev to 5 kev, (E/T), 20: 17851
neutron fission in resonance region, symmetry of, (E), 20: 17858
neutron fission of, neutron spectra from, (E), 20: 17825
neutron fission of, beta activity of products from thermal, (E), 20: 17835
neutron fission of, alpha particle and fragment energies and yields from resonance, (E), 20: 17839
neutron fission of, fragment energy and mass distributions from thermal, (E), 20: 17863
neutron fission of, neutron yields from thermal, (E), 20: 17823
neutron resonance fission integral for, epithermal and thermal, (E), 20: 17751
sorption of nitrated, through intact rabbit skin, 20: 16183
PLUTONIUM ISOTOPES Pu-240
fission of, neutron yields from spontaneous, (E), 20: 17823
neutron fission cross sections at 0.03 to 2.0 Mev, (E), 20: 17855
PLUTONIUM ISOTOPES Pu-241
neutron fission cross sections at 40 to 500 kev, (E), 20: 17852
neutron fission of, prompt neutron yields from fast and thermal, (E), 20: 17826
neutron fission of, neutron yields from thermal, (E), 20: 17823
PLUTONIUM ISOTOPES Pu-242
deuteron reactions (d,2n) at 7 to 12 Mev, isomeric yield ratios from, (E), 20: 17857
PLUTONIUM NITRATES
analysis for plutonium by argentic oxidation, ferrous reduction, and dichromate titration, 20: 16405
sorption of plutonium-239, by intact rabbit skin, 20: 16183
PLUTONIUM(IV) OXIDES
analysis for plutonium, spectrophotometric, 20: 16350
dissolution by sintering with sodium peroxide, rapid, 20: 16350
reactions with hydrofluoric acid to prepare plutonium tetrafluoride, 20: 16463
PuO_2–UO_2, burnup in fast reactors, effects on breeding ratio, multiplication factor, and sodium-void reactivity, 20: 18060
PuO_2–UO_2, development as fuel rods, 20: 18095 (WCAP-3385-52)
POCKET CHAMBERS
design of personnel monitor with audible alarm, 20: 16805 (CLOR-43/D)
POLARISCOPES
design and performance of nuclear reaction, using position-sensitive particle detectors, 20: 16870
design and performance of liquid helium, time-of-flight, neutron, 20: 16876
POLAROGRAPHS
design of voltammeter-incorporating d-c, 20: 17158(R) (ORNL-3900, pp 82-149)
POLAROGRAPHY
electrodes for controlled-potential, 20: 16390
POLLEN
radiation effects on *Liriodendron tulipifera*, used in diallel mating scheme, 20: 16228(R) (NYO-3571-2)
radiosensitivity of conifer, 20: 16228(R) (NYO-3571-2)

use of irradiated *Picea glauca*, in poly-cross breeding, 20: 16228(R) (NYO-3571-2)
POLONIUM
radiation emission by, relation of pleochroic halos to alpha, 20: 16666(T) (ORNL-tr-923)
POLONIUM ISOTOPES Po-208
decay scheme, (E), 20: 17841
POLONIUM ISOTOPES Po-209
decay scheme, (E), 20: 17841
POLONIUM ISOTOPES Po-210
content in soils, tobacco, and vegetables, 20: 16189
content in stratospheric and tropospheric samples in Project Star Dust, 1963, 20: 16727(R) (HASL-168)
content in stratospheric and tropospheric samples in Project Star Dust, 1964, 20: 16728(R) (HASL-169)
content in tobacco smoke, 20: 16264
effects on dogs, 20: 16268
POLONIUM ISOTOPES Po-214
particle dimensions and mobility of aerosols containing, in atmosphere, 20: 16690
POLONIUM ISOTOPES Po-215
alpha decay of, bismuth-211 levels from, (E), 20: 17703
energy levels from radon-219 decay, (E), 20: 17703
POLYCYTHEMIA
radiation effects on, complications from cytostatic drugs combined with β or x, 20: 16233
radiotherapy of, hematological complications from phosphorus-32, 20: 16241
POLYMERS
radiation effects on, 20: 16505 (BNL-949)
radioinduced preparation of, 20: 16505 (BNL-949)
POLYPHENYL SYSTEMS
radiation effects on physical properties of Santowax WR at 425 to 800°F, fast-neutron and gamma, 20: 17122 (MIT-334-34)
POLYPHENYLS
analysis of, by gas chromatography, thermal conductivity, and flame ionization, 20: 16341
POPULATIONS
protection against atomic weapons, shelter design for, 20: 16620 (AD-624370)
radiation control of rice weevil, 20: 16243
radiation effects on health of Hiroshima and Nagasaki, 20: 16271
radiation effects on *Sarcophaga peregrina*, x, 20: 16291
radiation exposure to, in vicinity of Monticello Project, Utah, 20: 16729 (IDO-12049)
radiation exposure of Hiroshima, 20: 16272
POSITRON BEAMS
polarization in storage ring magnetic fields, quantum effects on, (T), 20: 17689 (NP-15783)
POSITRONS
annihilation in cadmium sulfide monocrystals, resistivity from angular distributions of, (E), 20: 17983
annihilation in rare gases, in electric fields, (T), 20: 17423
interactions with electrons, polarization effects in, (T), 20: 17489
scattering by bismuth at 150 and 300 Mev, cross sections for, (E), 20: 17785
scattering by cobalt at 150 Mev, cross sections for, (E), 20: 17785
POTASH
effects on reduction of niobium oxide using carbon, 20: 16483
POTASSIUM
boiling of liquid metals under forced convection, 20: 16608(T) (ANL-Trans-257)
containment at 1200°C, materials for, 20: 18020(R) (ORNL-3900, pp 2-81)
content in silts, age estimation from, 20: 16711(R) (MIT-1381-13)
determination by flame photometry, effects of iron and rubidium on, 20: 16713
determination in Moldavites by flame photometry and x-ray fluorescence, 20: 16711(R) (MIT-1381-13)
electron scattering by atomic, cross sections for, (T), 20: 17286
ion pairing interactions in, (T), 20: 17008 (CEA-R-2820)
reactions of atoms of, with bromine and hydrogen bromides, 20: 17296
scattering of atoms of, by rare gases, (E), 20: 17294
sorption by barley roots, effects of uranium(IV) oxides on, 20: 16174(R) (RLO-1547-3)
sorption by chabazite in lithium, potassium, and sodium nitrates, 20: 16340 (USNRDL-TR-970)
stability of plasma of, drift, (E/T), 20: 17883 (NP-15784)
POTASSIUM ACID FLUORIDES
radioinduced defects in, EPR spectra of electron, 20: 17976(R) (NYO-2047-36, App.1)
POTASSIUM ALLOYS
K–Na, effects on properties of chromium–molybdenum steels, 20: 16972(R) (NASA-CR-54719)
Sb–Cs–K–Na, photosensitivity of, 20: 17984
Sb–Cs–K–Na–Te, photosensitivity of, 20: 17984
POTASSIUM AMIDE
effects on isotopic exchange between hydrogen and liquid ammonia, 20: 16444
POTASSIUM BROMIDES
color centers in, wave functions for F, (T), 20: 17977(R) (NYO-2047-36, App.2)
production in reactions of potassium atoms with bromine and hydrogen bromides, (E), 20: 17296
POTASSIUM CARBONATES
ion exchange and sorption on glass surfaces, 20: 16469
POTASSIUM CHLORIDES
density of thin films of, 20: 17070
photosensitivity of, 20: 17984
radiation effects on fracture surface energy of, gamma, 20: 17137
radiation effects on external surface energy of, x, 20: 17137
transfer from heavy water to water, free energy and entropy of, 20: 16488
POTASSIUM CHROMATES
$K_2Cr_2O_7$–H_2SO_4, properties for use in ultrasonic cleaning of cobalt-60 from Duralumin and steel-3, 20: 16767
POTASSIUM FLUORIDES
radioinduced defects in, ESR of, (E/T), 20: 17975(R) (NYO-2047-36)
POTASSIUM HYDROXIDES
analysis for manganese, substoichiometric activation, 20: 16403
corrosive effects on zirconium and Zircaloy-2 at 50 to 90°C, effects of electrode potential on, 20: 16979
POTASSIUM IODIDES
iodine-131 exchange between, and silver iodide, kinetics of, 20: 16460
POTASSIUM ISOTOPES K-38
half life, 20: 16331 (GA-6568)
production in proton reactions with cobalt, copper, iron, nickel, vanadium, and zinc at 590 Mev and 18.3 Bev, (E), 20: 17717
POTASSIUM ISOTOPES K-39
helium-3 reactions (He-3,α) at 12 Mev, Q value for, 20: 16331 (GA-6568)
POTASSIUM ISOTOPES K-40
background activity in sea water from, sensitivity of gamma spectrometer and scintillation detectors for, 20: 16828 (TID-22763)
content in Bogou iron meteorite, 20: 16674
content in plants before and after Salmon Event, 20: 16743 (VUF-1021)
determination in milk, gamma spectrometric, 20: 16369
POTASSIUM ISOTOPES K-41
neutron reactions (n,p) with, cross sections for, (E/T), 20: 17809
POTASSIUM ISOTOPES K-42
beta decay of, 0.58-Mev gamma transition in, (E), 20: 17723
production in proton reactions with cobalt, copper, iron, nickel, vanadium, and zinc at 590 Mev and 18.3 Bev, (E), 20: 17717
sensitivity for activation analysis using beta-gamma-gamma sum-coincidence gamma spectrometer, 20: 16335(R) (NBS-TN-276)
POTASSIUM ISOTOPES K-43
production in proton reactions with cobalt, copper, iron, nickel, vanadium, and zinc at 590 Mev and 18.3 Bev, (E), 20: 17717
POTASSIUM ISOTOPES K-44
production in proton reactions with cobalt, copper, iron, nickel, vanadium, and zinc at 590 Mev and 18.3 Bev, (E), 20: 17717
POTASSIUM ISOTOPES K-45
production in proton reactions with cobalt, copper, iron, nickel, vanadium, and zinc at 590 Mev and 18.3 Bev, (E), 20: 17717
POTASSIUM NITRATES
diffusion and electric mobility of ions in, tracer study on, 20: 16414 (CEA-R-2806)
ion exchange distribution of alkali and alkaline earth metals between chabazite and fused, 20: 16340 (USNRDL-TR-970)
KNO_3–$NaNO_3$, diffusion and electric mobility of ions in, 20: 16414 (CEA-R-2806)
$LiNO_3$–KNO_3, diffusion and electric mobility of ions in, 20: 16414 (CEA-R-2806)
POTASSIUM OXIDES
determination in Moldavites by mass spectrometry and x-ray fluorescence, 20: 16711(R) (MIT-1381-13)
POTASSIUM PERMANGANATES
$KMnO_4$–H_2SO_4, properties for use in ultrasonic cleaning of cobalt-60 from Duralumin and steel-3, 20: 16767
POTASSIUM SULFATES
corrosive effects on zirconium and Zircaloy-2 at 50 to 90°C, effects of electrode potential on, 20: 16979
POTASSIUM TANTALATES
$CeTaO_4$–$KTaO_3$, crystal structure, 20: 16438
$KTaO_3$–$PrTaO_4$, crystal structure, 20: 16438
$NdTaO_4$–$KTaO_3$, crystal structure, 20: 16438
POTATOES

carboxylase systems in, effects of metal ions on, 20: 16160 (UCRL-14739(Pt.2))
POWDER METALLURGY
methods for fabrication of very large parts of ceramic or metal powders, 20: 16993 (Y-DA-1043)
POWDERS
analysis for hydrogen by beta absorption, 20: 16356
analysis of metallic, by beta backscattering techniques, 20: 16378
density of, method for measuring, 20: 16425
POWER BREEDER REACTORS
control elements for plutonium-fueled, heavy-water-moderated, thermal, 20: 18115
design of molten-salt fast, 20: 18088 (INR-669/C)
POWER BURST FACILITY
reactivity feedback during short-period transients in, method for calculation of Doppler, 20: 18019(R) (IDO-17146)
POWER REACTORS
boiler leak testing for, 20: 16618
book: *Technological and Thermotechnical Control of Nuclear Power Stations*, 20: 18118
construction of, use of optical instruments in, 20: 18114
coolant purification systems for hermetically sealed boiling-water, 20: 18089 (NAA-SR-Memo-10178)
design, 20: 18174(R) (NP-15771)
design and feasibility for desalting uses, 20: 18020(R) (ORNL-3900, pp 2-81)
development in Germany, policy for, 20: 18111
development of fast, 20: 18097
economics of small dual-purpose, 20: 18124
fuel costs of, method for calculating, 20: 18101
fuel cycle calculations, 20: 18116
fuel development for high-temperature, coated-particle, 20: 18098
fuels for, future needs for, 20: 18099
heat exchangers for sodium-cooled, computer analysis of, 20: 18093(R) (UNC-5142)
operation of, survey for countries in western Europe, 20: 18104
reactivity calculations for PRO-II, 20: 18091 (RT/F1(65)45)
POWER SUPPLIES
design for high-field superconducting magnets, 20: 17598 (CONF-650922, pp 745-52)
design for magnets, survey of, 20: 17202 (CONF-650922, pp 755-68)
design for MURA FFAG magnet modeling program, 20: 17203 (CONF-650922, pp 776-8)
design for ring magnet of Argonne Synchrotron, 20: 17227
design for ZGS magnets, 20: 17204 (CONF-650922, pp 808-16)
development of r-f, for accelerators, 20: 17209(R) (LA-3479)
development status of solid-state, for magnets, 20: 16773 (CONF-650922, pp 779-87)
use of flux pumps with superconducting magnet coils, 20: 17596 (CONF-650922, pp 615-24)
PRASEODYMIUM
abundance in sun, (E), 20: 17237
preparation of self-supporting radiation targets of, 20: 17218
preparation of spherical polycrystalline, 20: 17978(R) (NYO-3402-2)
solvent properties for magnesium, solid, 20: 17016 (IS-1175)
PRASEODYMIUM ALLOYS
Fe–Pr, crystal structure of Pr_2Fe_{17} in, 20: 17096(T)
POTASSIUM CHLORIDES
color centers in, wave functions for F, (T), 20: 17977(R) (NYO-2047-36, App.2)
PRASEODYMIUM CARBIDES
properties of, chemical and physical, 20: 17048
reactions with water, formation of gaseous products in, 20: 17048
PRASEODYMIUM CHLORIDES
electric and magnetic properties, 20: 17019 (N-65-17873)
PRASEODYMIUM COMPLEXES
with β-diketones, Szilard-Chalmers reactions in, 20: 16416(R) (NYO-906-68)
with thenoyltrifluoroacetone, preparation, properties, and structure of, 20: 16416(R) (NYO-906-68)
with 2,4-pentanedione, preparation, 20: 16434
PRASEODYMIUM HYDRIDES
properties and structure, 20: 16453
PRASEODYMIUM IONS
wave functions for, including effect of nuclear quadrupole moment, 20: 17250 (BNL-8850)
PRASEODYMIUM ISOTOPES Pr-140
decay of, yield curves for, (E), 20: 17764
PRASEODYMIUM ISOTOPES Pr-141
bremsstrahlung reactions (γ,n) to 65 Mev, cross section for, (E), 20: 17764
lithium-6 reactions (Li-6,5n), angular momentum effects on excitation functions for, (E), 20: 17784
lithium-7 reactions (Li-7,6n), angular momentum effects on excitation functions for, (E), 20: 17784
PRASEODYMIUM ISOTOPES Pr-143
nucleon capture at 10 to 40 Mev, cross sections and mechanism for direct, (T), 20: 17737
PRASEODYMIUM ISOTOPES Pr-144
fallout monitoring at Vilnius, Soviet Union, in 1962, 20: 16700
reactions of recoil, in cerium-144 EDTA complexes, 20: 16544
PRASEODYMIUM OXALATES
reactions of hydrated, with hydrochloric acid, 20: 16447
PRASEODYMIUM OXIDES
determination in thorium oxide by emission spectroscopy, 20: 16393
PRASEODYMIUM SILICIDES
properties of, physicochemical, 20: 17047
PRASEODYMIUM SULFIDES
EuS–Pr_2S_3, compound formation in, 20: 16431
Pr_2S_3–SnS, compound formation in, 20: 16431
Pr_2S_3–YbS, compound formation in, 20: 16431
PRASEODYMIUM TANTALATES
crystal structure, 20: 16438
$KTaO_3$–$PrTaO_4$, crystal structure, 20: 16438
PRECIPITATION, ATMOSPHERIC
composition near Leningrad, 20: 16704
effect on accumulation of cesium-137 and strontium-90 in soils near Leningrad, 20: 16702
effects on deposition of fallout, 20: 16648
effects on fallout level, near New Delhi, 20: 16680
effects on particulate matter in atomic clouds, 20: 16160 (UCRL-14739 (Pt.2))
effects on radioactive aerosols in atmosphere, 20: 16647
fallout monitoring in global, 1965, 20: 16662(R) (HASL-165)
radioactivity of, from barium-140 and zirconium-95 content in Germany, 1961 to 1963, 20: 16766
PRECIPITATORS
use of cyclone, in selection of cloud water samples, 20: 16658
PREGNANCY
effects on employment in radiation work, 20: 16762
PRESSURE
measurement in vacuum systems, using hot-cathode ionization gages, 20: 16630
PRESSURE GAGES
performance of cold-cathode magnetron, 20: 16788
properties of beryllium for pressure bar gages, 20: 17018 (LRP-20/66)
PRESSURE VESSELS
radiation and thermal damage in, surveillance program for, 20: 17126 (NRL-6349)
testing of stainless steel-clad, nondestructive, 20: 16617
PRESSURIZED WATER REACTORS
design of forced-circulation, for use in nuclear-powered tanker, 20: 18126 (EUR-2629.i(Vol.1))
development and engineering of, 20: 18094(R) (WAPD-MRP-115)
development of Austrian, Spanish, and Swiss, 20: 18104
startup sequence for, automation of, 20: 18130
PRINCETON SYNCHROTRON
magnet current regulators for, design of, 20: 17205 (CONF-650922, pp 817-22)
PROMETHIUM
atomic volume of liquid, 20: 17025 (ORNL-TM-1424)
diffusion in liquid, coefficient for self-, 20: 17025 (ORNL-TM-1424)
effects on uranium separation from phosphate rocks, 20: 16381
electric conductivity, 20: 17025 (ORNL-TM-1424)
thermal conductivity of liquid and solid, 20: 17025 (ORNL-TM-1424)
PROMETHIUM ISOTOPES
separation from pitchblende and rain by ion exchange, 20: 16685
PROMETHIUM ISOTOPES Pm-146
neutron cross section for burnup in promethium-147, 20: 16914(R) (ORNL-3900, pp 182-93)
PROMETHIUM ISOTOPES Pm-147
burnup of promethium-146 in, cross section for, 20: 16914(R) (ORNL-3900, pp 182-93)
content in rain water, Fayetteville, Arkansas, Oct. 1964, 20: 16663 (TID-21470)
content in stratospheric and tropospheric samples in Project Star Dust, 1963, 20: 16727(R) (HASL-168)
content in stratospheric and tropospheric samples in Project Star Dust, 1964, 20: 16728(R) (HASL-169)
ground water contamination by, in Shoal Event, hazards from, 20: 16742 (VUF-1014)
preparation for radistion sources, 20: 16914(R) (ORNL-3900, pp 182-93)
yield from uranium-238 fission, 20: 16685
PROMETHIUM ISOTOPES Pm-149
content in rain water, Fayetteville, Arkansas, Oct. 1964, 20: 16663 (TID-21470)

energy levels from promethium-149 decay, (E), 20: 17787
yield from uranium-238 fission, 20: 16685
1,3-PROPANEDIONE, 1,3-DIPHENYL-
complexes with praseodymium, Szilard-Chalmers reaction in, 20: 16416(R) (NYO-906-68)
2-PROPANOL
2-propanol–H_2O, thermodynamics of reactions between nickel(II) and 2,4-pentanedione in, 20: 16416(R) (NYO-906-68)
1-PROPANOL, 2-METHYL-
2-methyl-1-propanol–water, effects of fluoride on distribution of ferric thiocyanate in, 20: 16335(R) (NBS-TN-276)
PROPENE POLYMERS
radioinduced graft polymerization with butadiene, gamma, 20: 16527
PROPIONITRILES
yields in reactions between ethylene and active nitrogen, 20: 16510(T) (NP-tr-1364)
PROPIOPHENONES
reactions with phosphoric acid, products formed by disproportionation in, 20: 16542(R) (TID-22646)
PROPORTIONAL DETECTORS
design for neutron detection and measurement in reactors, 20: 16903
energy resolution of position-sensitive, 20: 16880
use in detection and measurement of cosmic x radiation, 20: 16901
use in neutron flux measurements in reactors, 20: 16896
use of boron trifluoride, in neutron detection and measurement, 20: 16895
use with magnetic analyzers, for charged particles, 20: 16859
PROPULSION
electric systems for space, mission performance of, 20: 16628
electric, perfomance of pulsed ablating thruster for, 20: 16626
electric, performance of hydrogen–nitrogen arc jets for, 20: 16629
ion engines for space, effects of secondary electron emission in, 20: 16624 (N-65-17749)
ion engines for space, flight testing of, 20: 16625 (N-65-19272)
plasma jet, thrust efficiencies of Hall current, 20: 16627
PROPYNE
yields in reactions between ethylene and active nitrogen, 20: 16510(T) (NP-tr-1364)
PROTACTINIUM
chemistry of, 20: 17158(R) (ORNL-3900, pp 82-149).
PROTACTINIUM ISOTOPES Pa-231
neutron fission of, fragment mass distributions from, (E), 20: 17861
PROTACTINIUM ISOTOPES Pa-234
decay energy levels of, 20: 18174(R) (NP-15771)
PROTEINS
complexes with chromium, radiation chemistry of, γ, 20: 16211
labeling with iodine-132, equipment for, 20: 16257
metabolism by developing embryos, 20: 16172(R) (NYO-2194-1)
radiation effects on synthesis of, in sea urchin eggs, 20: 16160 (UCRL-14739(Pt.2))
radiation effects on ESR spectra of, uv, 20: 16205
radiation effects on mouse, fractionated-dose x, 20: 16224 (CEA-R-2848)
structure models for, 20: 17158(R) (ORNL-3900, pp 82-149)
synthesis of, effects of metal ions on, 20: 16160 (UCRL-14739(Pt.2))
synthesis of, enzymic mechanisms in, 20: 16159(R) (ORNL-3900, pp 150-81)
synthesis of, genetic control, 20: 16172(R) (NYO-2194-1)
PROTON BEAMS
deflection of 30-Mev, superconducting magnet for right-angle, 20: 17197 (CONF-650922, pp 536-40)
effects on structure of solar cells, 20: 16910 (N-65-18448)
production of, pulsed duoplasmatron ion source for, 20: 17172 (CEA-R-2802)
PROTONS
angular distributions from zirconium-90 (d,p) reactions at 3.5 to 5.5 Mev, (T), 20: 17691 (ORNL-TM-1235)
binding energy of pairs of, in nuclei, variation with atomic number, 20: 17729
density variation in radiation belts with solar cycle, computer program for calculation of, 20: 17539 (N-65-18257)
detection using silicon surface-barrier detectors, pulse-shape discrimination system for, 20: 16900
doses of solar-flare, in low-shielding space systems, 20: 16300
dosimetry measurement using alanine and glass rods, 20: 16283
effects on defects in silicon solar cells, 20: 17125 (NASA-CR-404)
effects on direct energy conversion devices, 20: 16907(R) (N-65-17517)
effects on electronic components in space, review of, 20: 16911
intensity in radiation belts at $3.5 \leq L \leq 10$, (E), 20: 17548(T)
intensity of low-energy solar, in space, (E), 20: 17318
interactions with protons with large momentum transfer, cross section for elastic, (T), 20: 17461
interactions with protons above 8 Bev/c, optical model for forward amplitude of, 20: 17469
interactions with neutrinos (ν_μ), effects of vector meson on lepton production by, (T), 20: 17504
interactions with mesons (π^+) at 1 to 4 Bev, inelastic, (T), 20: 17344 (JINR-P-2530)
interactions with antiprotons, SL(6,C) symmetry for two-meson annihilation, 20: 17347 (JINR-P-2547)
interactions with photons, quark model for hyperon production in, (T), 20: 17348 (JINR-P-2556)
interactions with protons in singlet S-state, (T), 20: 17353
interactions with nucleons at 19.8 Bev/c in nuclear emulsions, particle-track distributions from, (E), 20: 17357
interactions with mesons (π^-) in emulsions at 5.5 Bev/c, cross sections for elastic, (E), 20: 17360
interactions with neutrons at 2 to 10 Bev, amplitude for, (E), 20: 17363(T)
interactions with deuterons at 1 to 10 Bev, elastic, (E), 20: 17363(T)
interactions with bremsstrahlung at 0.3 and 5.5 Bev, meson (π) and nucleon resonance production from, (E), 20: 17368
interactions with mesons (K-), cross sections and scattering length for hyperon (Λ) and meson (η) production in, (T), 20: 17376
interactions with antiprotons at rest, coupling constants in SU(3) for two-body meson production in annihilation, (T), 20: 17377
interactions with protons at high energies, real amplitudes for, (T), 20: 17378
interactions with mesons (K-) and (K+) at high energies, real amplitudes for, (T), 20: 17378
interactions with mesons (π^-) and (π^+) at high energies, real amplitudes for, (T), 20: 17378
interactions with antiprotons at high energies, real amplitudes for, (T), 20: 17378
interactions with protons, one-particle exchange model for inelastic, (T), 20: 17381
interactions with mesons (π^+) at 1.6 Bev/c, mesons (ρ^+) and N^{*++}_{33} production from, (E), 20: 17374
interactions with mesons (π^-) at 1.5 and 1.8 Bev/c, polarization of hyperons (Σ^0) from, (E), 20: 17382
interactions with mesons (K-) at 2.24 Bev/c, (E), 20: 17383
interactions with mesons (π^+) at 450 Mev, cross sections for elastic and inelastic, (E), 20: 17384
interactions with antiprotons at 3.3 and 3.7 Bev/c, meson (π) production in annihilation, (E), 20: 17385
interactions with mesons (π^-) at 1.89 Bev/c, multiple meson (π) production in, (E), 20: 17386
interactions with hyperons (Ξ^-) at low energies, hyperon (Λ) production in, (T), 20: 17389
interactions with protons in Bev range, neutron exchange in, (T), 20: 17394
interactions with photons at 3.4 to 4.0 Bev, meson (K+) and (π^+) production in, (E/T), 20: 17400
interactions with mesons (π^-) at 3.2 and 4.2 Bev/c, meson (B) production in, (E/T), 20: 17402
interactions with photons, cross sections for vector meson production in, 20: 17410
interactions with protons, SU(3) predictions for, 20: 17412
interactions with neutrons, deuteron and gamma production in, 20: 17413
interactions with protons at 2 to 10 Bev, real part of amplitude for elastic, (E/T), 20: 17417
interactions with mesons (K-) at 3 Bev/c, mechanism for $\bar{K}^{*0}(891)$ yields from, (E), 20: 17380
interactions with mesons (K-) at 2.10, 2.45, and 2.64 Bev/c, $K^0_S(892)$ resonances in, (E), 20: 17403
interactions with mesons (π^+) at 180°, spark chamber for recording, 20: 16815 (JINR-P-2506)
magnetic moment of, dispersion-theoretical calculation of, 20: 17390
penetration in primates at 32 to 400 Mev, depth-dose distribution of, 20: 16283
reactions (p,d) with beryllium-9 at 3 to 5 Mev, deuteron polarization in, (E), 20: 17760
reactions (p,γ), with aluminum-27 widths from yield curves for, (E), 20: 17778
reactions (p,n) with nuclei, threshold energies for, 20: 16332 (GA-6691)
reactions (p,n) with aluminum-27, phosphorus-31, and silicon-27 at 6.0 to 7.5 Mev, absolute cross sections and angular distributions for, (E/T), 20: 17775
reactions (p,p') with zinc-64, cross sections for, (T), 20: 17692 (ORNL-TM-1414)
reactions (p,2p) with nuclei at 140 Mev, energy spectra and angular correlation distributions from, (E), 20: 17741
reactions in helium at 0.03 to 10 Mev, cross sections for electron capture in, (T), 20: 17274
reactions in nuclear emulsions at 19.5 Bev, charged-particle identification from delta electrons in, (E), 20: 17358
reactions with beryllium at 30.5 Bev, secondaries from, (E/T),

20: 17171 (BNL-10030)
reactions with beryllium at 19.2 Bev/c, radiation levels from, 20: 17212(T) (UCRL-Trans-1305)
reactions with bromine and silver in emulsions at 25 Bev/c, lithium-8 fragment recoil from, (E), 20: 17748
reactions with cobalt, copper, iron, nickel, vanadium, and zinc at 590 Mev and 18.3 Bev, potassium isotope yields in, (E), 20: 17717
reactions with emulsion nuclei at 28 Bev, lithium-8 production from, (E/T), 20: 17753
reactions with emulsion nuclei at 9 Bev, cascade effects on alpha yields in, (E), 20: 17713
reactions with gases, electron spectra from, (E), 20: 17292
reactions with heavy nuclei at 150 to 660 Mev, fission cross sections for, (E), 20: 17838
reactions with hydrogen atoms, charge transfer in, (E), 20: 17302
reactions with hydrogen atoms, charge transfer in, 20: 17303
reactions with hydrogen atoms, resonant charge transfer in, (T), 20: 17264
reactions with nitrogen at 2 to 35 kev, Balmer-alpha radiation in, (E), 20: 17269
reactions with nuclei, pickup effects in, (E/T), 20: 17158(R) (ORNL-3900, pp 82-149)
reactions with thin aluminum films, determination of surface density from x-ray production from, 20: 17051
reactions with uranium at 0.55 and 18.2 Bev, bromine and iodine isotope recoils from, (E), 20: 17837
reactions with uranium-238 at 450 Mev, recoil ion properties from fission, (E), 20: 17790
recoil spectra analysis for, computer program for, 20: 16875
scattering by carbon-12 at 6.14 Mev, polarization angular distributions from double elastic, (E), 20: 16870
scattering by carbon at 145 Mev, absolute differential cross sections for elastic, (E), 20: 17739
scattering by helium-3 at 0.125 to 1 Mev, helium-4 levels from, (E), 20: 17771
scattering by lithium-7 at 150 to 185 Mev, level structure from, (T), 20: 17800
scattering by nuclei, optical model parameters for, (T), 20: 17768
scattering by nuclei at 140 Mev, parameters for triple, (E/T), 20: 17738
shielding of space vehicles against, calculations for, 20: 17965

PROTOZOA
radiation effects on *Vorticella microstoma* and *Teletrochidium henneguyi*, 20: 16295

PSEUDOUREA, 2-(2-AMINOETHYL)-2-THIO-
protective effects against carcinogens in mice, 20: 16159(R) (ORNL-3900, pp 150-81)

PULSE ANALYZERS
amplitude distortions in, correction for pile-up-effect, 20: 16795
data processing equipment for multichannel, 20: 16817 (JUL-270-RB)
design and calibration of, for oxygen determination in steel, 20: 16400
design and operation of differential- and integral-selector, 20: 16786
design and performance for organic scintillator pulse-shape discrimination, 20: 16839
design of decimal scanner for, 20: 16777 (EUR-2702.e)
design of multichannel, 20: 16898
operation of 20,000-channel, for nuclear data processing, (E/T), 20: 17158(R) (ORNL-3900, pp 82-149)

PULSE COLUMNS
design and efficiency of, for countercurrent liquid-liquid extraction at Eurochemic, 20: 16561
flow capacity prediction for, 20: 17158(R) (ORNL-3900, pp 82-149)

PULSE GENERATORS (ELECTRONICS)
design and performance of nanosecond, for 2-Mev Van de Graaff, 20: 17217
design and performance of multiple-duration monostable multivibrator, 20: 16792
design and performance of variable-width, using avalanche transistors and charge-storage diodes, 20: 16793
design of pattern generator, for bubble and spark chamber data analysis, 20: 16881

PULSE MODIFIERS
performance of division circuit, for particle detectors, 20: 16879

PUREX PROCESS
analysis for chemical states of fission products and plutonium in solutions of, by extraction chromatography, 20: 16333 (KR-81)
equipment and flowsheet for, in Eurochemic plant, 20: 16558
equipment and methods for, Kjeller, Norway, 20: 16569
fission product release from ceramic wastes from, effects of volatilization on, 20: 18156 (BNWL-SA-453)

PYRIDINE COMPLEXES
with polyhalogens, preparation of, 20: 16416(R) (NYO-906-68)

PYRIDINE, 2,4,6-TRIMETHYL-
preparation of deuterated, from 2,4,6-tri-d_3-methylpyrylium perchlorate, 20: 16501

PYRIDOXINE
effects on strontium excretion in rats, 20: 16176

PYRITES
carbon-13 content of calcites in deposits of epigenetic, Gas Hills Area, Wyoming, 20: 16675

PYROMETERS
design of optical, for plasma jets, 20: 17959

4-PYRONE, 5-HYDROXY-2-(HYDROXYMETHYL)-
complexes with iron, effects on hydrolysis of α-D-glucose 1-phosphate, 20: 16421

PYROPHOSPHATES
complexes with uranium, preparation of, effects of hydrogen ions on, 20: 16472

PYRUVATES
radiation effects on oxidation of, in *Vibrio cholerae*, 20: 16198
synthesis of carbon-14-labeled, glucose from carbon-14-labeled, 20: 16193 (EUR-2539.i)

Q

QUANTUM ELECTRODYNAMICS
electromagnetic interactions in, C, P, and T conservation in large-momentum-transfer, 20: 17578
formation of optical model at high energies, 20: 17469
gauge transformations in, operation and generalized, 20: 17446
theory with two fermions in, 20: 17581

QUANTUM MECHANICS
canonical commutation relations in, effects of operator translations on, 20: 17506
magnetic moment of Dirac particles in potential wells, (T), 20: 17431 (JINR-P-2569)
operators in, calculations of Clebsch-Gordan, Racah, and Z, 20: 17559 (EUR-2639.f)
position operators in, Lie algebra of conformal group for, 20: 17577
symmetry in, SU(2), 20: 17429 (JINR-P-2529)
three-body problem in, angular functions for, 20: 17560 (ITEF-384)
wave equations for nonzero-mass particles in, relativistic Schroedinger, 20: 17571
wave equations for arbitrary-spin particles in, relativistic covariant Schroedinger, 20: 17572
wave equations in, separation of variables in Schroedinger, 20: 17561 (JINR-P-2532)

QUARTZ
age of Massachusetts, rubidium–strontium and strontium-87/-86 estimation of, 20: 16711(R) (MIT-1381-13)
deuterium content of fluid inclusions in, from Mexico, 20: 16634
muonium spin precession in, in magnetic field, (E), 20: 17361(T)
performance of thin films of, for fast neutron flux measurements, 20: 16851
radiation effects on structure of, neutron, 20: 17148
radioinduced EPR spectra in, effects of aluminum impurity on, 20: 16539(T)
radioinduced structural changes in alpha-, neutron, 20: 17149(T)

R

RABBITS
bone blood flow in, determination and factors affecting, 20: 16192
calcium-45 metabolism in blood and bones, 20: 16178
plutonium-239 sorption through skin of, 20: 16183
radiation effects on absorption of injected horse gamma globulin by, γ, 20: 16214 (AD-620438)
radiation effects on kidneys of, x, 20: 16234
radiation effects on formation of leukocyte-regulating factor in, x, 20: 16265
radiosensitivity of, effects of aspartic acid and Solcoseryl on, 20: 16302
strontium-90 metabolism in blood and bones of, 20: 16178

RACAH COEFFICIENTS
calculations of, using IBM 7090, 20: 17559 (EUR-2639.f)

RADIATION
detection and measurement of, use of communication theory in, 20: 16893
dose from internally deposited radioactive materials, estimation of, 20: 16159(R) (ORNL-3900, pp 150-81)
dosimetry of fallout, volcanic simulation of, 20: 16659 (AD-629527)
dosimetry of, review of methods for, 20: 18182
dosimetry using photoluminescent detectors, 20: 16837
effects of atomic-explosion, on population of Hiroshima, 20: 16272
effects of space, cyclotron simulation of, 20: 16914(R) (ORNL-3900, pp 182-93)
effects on adrenals and pituitary following tumor therapy, measurement of, 20: 16209
effects on animals, biological, 20: 16296

effects on biological molecules, 20: 16160 (UCRL-14739(Pt.2))
effects on bones following eczema therapy, 20: 16210
effects on catalase activity in rat liver and spleen, 20: 16277
effects on chromosomes and mitosis, quantitative, 20: 16160 (UCRL-14739(Pt.2))
effects on clonal material of *Populus tremuloides*, 20: 16228(R) (NYO-3571-2)
effects on crosslinking in PVA for use as membrane in artificial kidney, 20: 16505 (BNL-949)
effects on desorption on graphite surfaces in carbon dioxide, carbon monoxide, and methane, 20: 17114 (AERE-R-5163)
effects on diabetes incidence in residents of Hiroshima, 20: 16254
effects on Drosophila females and males, mutagenic, 20: 16229(R) (NYO-1472-1)
effects on food wholesomeness, 20: 16918 (AECL-PAK/RB-7)
effects on ion exchange materials, 20: 16583
effects on *Liriodendron tulipifera* pollen used in diallel mating scheme, 20: 16228(R) (NYO-3571-2)
effects on living organisms and tissues, bibliography on, 20: 16219 (AED-C-04-23)
effects on living organisms and tissues, bibliography on, 20: 16221 (AED-C-04-25)
effects on mice and rats, role of adrenal and pituitary glands in, 20: 16232(T) (JPRS-34120)
effects on nucleic acid metabolism, 20: 16160 (UCRL-14739(Pt.2))
effects on optical maser materials, 20: 16505 (BNL-949)
effects on pollen of *Picea glauca*, use in poly-cross breeding studies, 20: 16228(R) (NYO-3571-2)
effects on protein synthesis in sea urchin eggs, 20: 16160 (UCRL-14739(Pt.2))
effects on styrene grafting on cellulose, properties of product in, 20: 16507 (INR-671/XVII/C)
scattering by crystal lattices, change of nuclear resonance parameters by, 20: 18015
transport in stellar atmospheres, spectral theory for stationary operator for, 20: 17658
use in synthesis of inorganic and organic compounds, 20: 16505 (BNL-949)
use in synthesis of chemicals, developments in, 20: 16506 (BNL-10020)

RADIATION CHEMISTRY
electron scavenging in hydrocarbon, using nitrous oxide, 20: 16515
mechanisms in, of cysteic acid, cysteine, and cystine, 20: 16540
research programs on, at Risö, 20: 18174(R) (NP-15771)

RADIATION DETECTION INSTRUMENTS
description of reactor neutron, 20: 18023
design and use for cosmic x-radiation measurements, 20: 17248
design for simultaneous and separate measurement of alpha and beta activity, 20: 16906(P)
design of spherical dielectric Compton detector for gamma radiation, 20: 16812 (EGG-1183-1174)
design of, for gamma activity, 20: 16505 (BNL-949)

RADIATION DETECTION INSTRUMENTS (ION CURRENT TYPE)
development for continuous air monitoring, 20: 16832(R) (UCRL-14534, pp 32-40)
ionization chambers for, engineering drawings on, 20: 16892
operation and performance of neutron multiplicity detector for cosmic ray studies, (E), 20: 17651(R) (AD-612192)

RADIATION DETECTION INSTRUMENTS (PULSE TYPE)
circuitry for, pulse division, 20: 16879
design for alpha monitoring of hands and shoes, engineering drawings for, 20: 16769
design for continuous plutonium alpha monitoring in air, engineering drawings for, 20: 16768
design for simultaneous determination of neutrons from fission and (α,n) reactions, 20: 16905(P)
design of fuel rod scanner, for power-density distribution measurement, 20: 18025
design of narrow-band, for x-ray fluorescence analysis, 20: 16823 (NYO-3160-1)
development for beta-gamma monitoring of steam condensate, 20: 16825 (ORNL-TM-1442)
performance of scintillation, for absolute gamma activity measurements, 20: 16858

RADIATION DETECTORS
design and performance of portable fast-neutron, 20: 16848
development and performance of lithium-drifted germanium, 20: 16159(R) (ORNL-3900, pp 150-81)
development at Risö, 20: 18174(R) (NP-15771)
for determination of americium-241 and plutonium-239 in lungs, 20: 16737(R) (UCRL-14534, pp 13-18)
performance of quartz and silicon dioxide films for fast neutron flux measurements, 20: 16851

RADIATION EXPOSURE CHAMBERS
design of scattering chamber for use with solid-state detectors, 20: 16883

RADIATION INJURIES
diagnosis of, after radiotherapy, 20: 16309
medication for, during radiotherapy, 20: 16319
pathology of rat, effects of biological stress following acceleration on, 20: 16213 (AD-620403)
pathology of, in developing rat brain, 20: 16275
pathology of, induced by radiotherapy, 20: 16322
protection against, effects of 1,3,4-oxidiazolium salts and *s*-triazole derivatives in mice, 20: 16490(R) (TID-22681)
recovery from, use of split-dose technique for evaluation of, 20: 16216 (AD-628791)

RADIATION MONITORING
equipment and methods for personnel, 20: 16827 (SZS-9(1965))
equipment design and performance for thoron, 20: 16842
equipment design for alpha, of hands and shoes, 20: 16769
equipment emergency crews, pocket chamber, 20: 16805 (CLOR-43/D)
equipment for alpha, 20: 16768
equipment for continuous air, conversion of survey meters for, 20: 16832(R) (UCRL-14534, pp 32-40)
equipment for whole-body, effects of radon and thoron daughters on, 20: 16665(R) (UCRL-14534, pp 23-7)
equipment for whole-body, development and performance of, 20: 16737(R) (UCRL-14534, pp 13-18)
film badges for medical, design and performance of, 20: 16843
of airborne decay products from radon and thoron, 20: 16665(R) (UCRL-14534, pp 23-7)
program for off-site, during Salmon Event, 20: 16743 (VUF-1021)
system for, of radioactive steam condensate, 20: 16825 (ORNL-TM-1442)

RADIATION PROTECTION
against nuclear explosions, research on, 20: 18020(R) (ORNL-3900, pp 2-81)
methods for patient, during radiographic examination, 20: 16318
methods for, review, 20: 16296
research in, using large scintillation counters, 20: 16865

RADIATION SICKNESS
polonium-210-induced, characteristics in dogs, 20: 16268

RADIATION SOURCES
fabrication of sealed, method for, 20: 16335(R) (NBS-TN-276)

RADIATION TARGET CANS
irradiation in NRTS reactors, handbook for, 20: 18135 (IDO-17135)
response of cylinders of type-304 and type-304L stainless steel to explosive loads, 20: 18019(R) (IDO-17146)

RADIATION TARGETS
fabrication and uses of tritium-containing, 20: 16916
laser beam effects on solid, giant pulsed, 20: 17531
magnet for polarized proton, design of superconducting, 20: 17586 (CONF-650922, pp 509-16)
preparation of self-supporting brittle metal, 20: 17218
preparation of, summary for ORNL, 1964, 20: 16914(R) (ORNL-3900, pp 182-93)
thickness of VYNS-film, use of cobalt-60-labeled dithizone for determining, 20: 16508(R) (NYO-2771-13)

RADIO WAVES
emission from rare gas plasma, negative absorption effects on anomalous bremsstrahlung and cyclotron, (E), 20: 17921

RADIOACTIVE CONTAMINATION
control of, role of veterinarians in, 20: 16761
equation for predicting, in plankton, 20: 16175(R) (RT/BIO(65)-1)
marine, studies on, 20: 16175(R) (RT/BIO(65)-1)

RADIOACTIVE MATERIALS
activity of, optimum conditions for measurement of, 20: 16410
alpha activity of, methods for measuring low-level, 20: 16411
alpha emission by, relation of pleochroic halos in biotite, cordierite, and hornblende, to, 20: 16666(T) (ORNL-tr-923)
fixation in hollow and solid cylinders and slabs, calculations of transient temperatures for, 20: 18155 (BNWL-157)
handling, storage, and transfer of, equipment for, 20: 18165 (ORNL-P-1987)
preparation and handling of alpha, for electron microprobe x-ray analyzer, 20: 16554

RADIOACTIVE MINERALS
sources and transport of alluvial deposits of, on Gulf of Lion, France, 20: 16669

RADIOACTIVE STATIC ELIMINATORS
design of cesium-137, for anesthetic flowmeters, 20: 16783

RADIOACTIVITY
accumulation of, on land and ocean surfaces, 20: 16706
content in biosphere, program for estimating, 20: 16160 (UCRL-14739 (Pt.2))
distribution in atmosphere, 20: 16637
distribution in atmosphere, effect of advection on, 20: 16638

dosimetry of natural, in soils, 20: 16687
measurement in effluents of gas chromatograph, flame ionization detector for, 20: 16371
measurement of, optimum conditions for, 20: 16410
monitoring atmospheric, methods for, 20: 16732 (NP-15898)
monitoring environmental, for Salmon Event, 20: 16743 (VUF-1021)
monitoring in atmosphere, plants, and water in Monticello Project Area, Utah, 20: 16729 (IDO-12049)
of atmosphere over oceans, dependence of, on meteorological factors, 20: 16699
release to atmosphere from Eurochemic chimney, estimates of minimum dilution for, 20: 18162 (NP-15754)

RADIOAPPLICATORS
development for irradiation of eye tumors, 20: 16305
dosimetry using digital computers, 20: 16748
use of strontium-90–yttrium-90, for therapy of skin tumors, 20: 16325

RADIOBIOLOGY
experimental error in, from use of animals, 20: 16164
research in, using large scintillation counters, 20: 16865
x-ray dosimetry in, nomogram for fractionated, 20: 16749

RADIOCHEMICAL PROCESSING PLANTS
operating capacity of, 20: 16566

RADIOCHEMISTRY
separation processes in, review of, 20: 16557

RADIODIAGNOSIS
equipment development for, 20: 16855
iodine-131-hippuran for kidney function tests, 20: 16311
mercury-197- mercury-203-neohydrin for brain tumor, 20: 16304
use of gallium-68 in bone scanning, 20: 16310

RADIOFREQUENCY SPECTROMETERS
design and performance of ESR, with variable frequency, 20: 16800
magnets for NMR, design of superconducting, 20: 17587 (CONF-650922, pp 517-24)

RADIOGRAPHY
dosimetry in medical, tables for, 20: 16751
dosimetry in medical, 20: 16843
personnel in, hazards to female, 20: 16762
radiation protection of patients during, 20: 16318
shielding male gonads during diagnostic, 20: 16321
uses for nondestructive determination of grade of beryllium, 20: 16962

RADIOISOTOPES
activity standardization for, in Australia, 20: 16746
alpha activity of, methods for measuring low-level, 20: 16411
book: *Utilization of Atomic Energy in National Economy (Power Plant, Petroleum Industry and Technology)*, in Azerbaidzhan, 20: 18182
conference on use in meteorology, 20: 16636
content and distribution in biological pool, 20: 16160 (UCRL-14739 (Pt.2))
content in biosphere, program for estimating, 20: 16160 (UCRL-14739 (Pt.2))
content in higher animals, role of mitochondrial transport system in, 20: 16160 (UCRL-14739(Pt.2))
counting and identification of, 20: 18174(R) (NP-15771)
determination in labeled compounds by scintillation counting, dimethyl sulfoxide as solvent for, 20: 16355
determination in mixtures by gamma spectroscopy, 20: 17158(R) (ORNL-3900, pp 82-149)
distribution in soils, model for, 20: 16168
effects on enzyme systems, 20: 16160 (UCRL-14739(Pt.2))
emissions from, effects on macromolecules, 20: 16160 (UCRL-14739 (Pt.2))
excretion by dogs, pathway for urinary, 20: 16160 (UCRL-14739(Pt.2))
half lives on plants, formula for determining effective, 20: 16160 (UCRL-14739(Pt.2))
ion exchange and sorption of, on glass surfaces, effects of solution concentration on, 20: 16469
metabolism in dairy cattle, system for measuring, 20: 16160 (UCRL-14739(Pt.2))
production, 20: 18174(R) (NP-15771)
production by cyclotron irradiation, targets for, 20: 16914(R) (ORNL-3900, pp 182-93)
production of short-lived, generators for, 20: 16914(R) (ORNL-3900, pp 182-93)
production of, in atmosphere by cosmic-ray reactions, 20: 16689
properties and separation of reactor-produced, 20: 16914(R) (ORNL-3900, pp 182-93)
reactions with nucleic acids, injuries from, 20: 16160 (UCRL-14739 (Pt.2))
separation by sorption and cocrystallization, 20: 16557
tracer studies on silts, computer program for processing data from, 20: 16632 (AAEC/TM-303)
uptake, distribution, and excretion by marine organisms, factors affecting, 20: 16725(R) (EUR-2543.e)
use in controlled-potential coulometry, 20: 16335(R) (NBS-TN-276)
uses in glaciological studies of polar cap, 20: 16686

RADIOLOGICAL DEFENSE
role of veterinarians in, 20: 16761

RADIOLOGICAL TELEMETERING SYSTEMS
development for gamma monitoring in Plowshare tests, 20: 16160 (UCRL-14739(Pt.2))

RADIOMETRIC ANALYSIS
chelatometric and redox microtitrations in, 20: 16386
electron capture detector for, design and response of high-temperature, 20: 16804
measurements in, optimum conditions for, 20: 16410
method for trace determination of cobalt, 20: 16335(R) (NBS-TN-276)
methods for, 20: 16337 (RMO-3001(Rev.1)(Suppl.))
sample preparation for, of carbon-14- and tritium-labeled biological materials, 20: 16177

RADIOMIMETIC SUBSTANCES
effects on yeast, metabolic, 20: 16240

RADIOPROTECTIVE COMPOUNDS
preparation and evaluation of 1,3,4-oxadiazolium salts and *s*-triazole derivatives as, in mice, 20: 16490(R) (TID-22681)
radiosensitivity effects in animals, evaluation of, 20: 16296

RADIOSENSITIVITY
effects of aspartic acid and Solcoseryl on, in mice and rabbits, 20: 16302
effects of biological stress induced by acceleration on, of rats, 20: 16213 (AD-620403)
effects of cell division stage on *Euglena gracilis*, uv, 20: 16204
effects of chemical protective compounds on, in animals, 20: 16296
effects of moisture on *Rauwolfia serpentina* seed, 20: 16249
effects of moisture on *Vicia sativa*, x, 20: 16276

RADIOSTERILIZATION
effects on flavor, evaluation of, 20: 16923
status of food, 20: 16918 (AECL-PAK/RB-7)

RADIOTHERAPY
beam focussing methods for, 20: 16320
dosimetry in contact and interstitial γ, 20: 16765
effects on rhabdomyosarcoma, 20: 16312
effects on tumor incidence, 20: 16309
evaluation of, for treatment of malignant diseases in children, 20: 16306
evaluation of, for treatment of breast cancer after surgery, 20: 16324
injuries from, prevention and treatment, 20: 16319
nausea in, properties of metoclopramide for preventing, 20: 16163
pathological effects of, delayed, 20: 16322
results of cervical-cancer, 40-year survey, 20: 16326
tolerance to moving-beam, 20: 16317

RADIUM
content in man, whole-body, 20: 16303(R) (AD-626384)
dosimetry using digital computers, 20: 16748
effects of deposited, in lungs, carcinogenic, 20: 16264
radiation emission by, relation of pleochroic halos to, 20: 16666(T) (ORNL-tr-923)
separation from irradiated thorium, method for, 20: 16359

RADIUM ISOTOPES Ra-226
content in food and man in India, 20: 16747
content in milk in France, 20: 16752
content in milk in France, 20: 16753
effects on dog skeleton, 20: 16253
neutron reactions with, calculations for actinium-227 production by, 20: 16927 (MLM-1297)
separation from wastes by sorption, 20: 17158(R) (ORNL-3900, pp 82-149)

RADIUM ISOTOPES Ra-228
effects on dog skeleton, 20: 16253

RADON
content in atmosphere, seasonal and geographical variations in, 20: 16640
content in atmosphere, distribution of, 20: 16693
content in atmosphere, method for determining, 20: 16708
content in surface boundary layer of atmosphere, effect of vertical turbulent mixing on, 20: 16692
content in surface boundary layer of atmosphere, seasonal variations in, 20: 16695
determination in atmosphere, alpha and beta activity measurements for, 20: 16679
distribution in atmosphere over oceans, dependence of, on meteorological factors, 20: 16699
emission from soils in European USSR and Kazakhstan, 20: 16691
particle dimensions and mobility of aerosols containing, in atmosphere, 20: 16690
tracer use in studies of atmospheric turbulence, 20: 16694

RADON ISOTOPES Rn-219
alpha decay of, polonium-215 levels from, (E), 20: 17703

RADON ISOTOPES Rn-220

decay products from, measurement of atmospheric, 20: 16665(R) (UCRL-14534, pp 23-7)
detection in dusts, monitor for, 20: 16842
determination in atmosphere, alpha and beta activity measurements for, 20: 16679

RADON ISOTOPES Rn-222
decay products from, measurement of atmospheric, 20: 16665(R) (UCRL-14534, pp 23-7)

RAIN WATER
effects on fallout level, near New Delhi, 20: 16680
fallout content in, measurement of, 20: 16168
fallout monitoring in Fayetteville, Arkansas, Oct. 1964, 20: 16663 (TID-21470)
fallout monitoring, 1964–65, 20: 16660 (AERE-R-4997)
radioactivity from cesium-137 and strontium-90 in, in Japan, 1964, 20: 16731 (NP-15883)
radioactivity in Japan, 1964, 20: 16730 (NP-15882)
radioactivity in, method for determining alpha, beta, and gamma, 20: 16407
radioactivity of, from barium-140 and zirconium-95 content in Germany, 1961 to 1963, 20: 16766
radioactivity of, in Japan, 1962 and 63, 20: 16671
radionuclide content of, in Arkansas, 20: 16685
sample selection from, using cyclone precipitators, 20: 16658

RAMJET ENGINES
use in supersonic plasma jet experiments, 20: 17904

RARE EARTH BORIDES
chemical bonding and electric conductivity of, 20: 16439

RARE EARTH CHLORIDES
rare earth ion quadrupolar interactions in, Zeeman-field-dependent, (E/T), 20: 18008

RARE EARTH COMPLEXES
oxalatochloride, thermal decomposition of, 20: 16446
terpyridyl nitrate, preparation and infrared spectra of, 20: 16479

RARE EARTH ETHYL SULFATES
crystal-field shielding in, systematic variation of quadrupole, (E), 20: 17996

RARE EARTH HYDRIDES
properties and structure, 20: 16453

RARE EARTH IONS
energy transfer from cesium uranyl tetrachloride lattices to, effective-excitation, (E), 20: 18010
nuclear quadrupolar interactions in rare-earth trichlorides, Zeeman-field-dependent, (E/T), 20: 18008

RARE EARTH ISOTOPES
neutron capture cross sections at 1 to 10 kev, (T), 20: 17653 (LA-3463)

RARE EARTH OXALATES
reactions of hydrates of, with hydrochloric acid, thermal decomposition of products from, 20: 16446
reactions of hydrated, with hydrochloric acid, 20: 16447
thermal decomposition of hydrates of, in hydrochloric acid, 20: 16448

RARE EARTH OXIDES
determination in thorium oxide by emission spectroscopy, 20: 16393
dissociation energies of gaseous monoxides, relation of, to atomic number, 20: 16485

RARE EARTH PERRHENATES
crystal structure and infrared spectra of tetrahydrates of, 20: 16473(T)

RARE EARTH SELENIDES
analysis of, evaluation of methods for, 20: 16395

RARE EARTH SULFIDES
analysis of, evaluation of methods for, 20: 16395
compound formations in systems of divalent and trivalent, 20: 16431

RARE EARTH TELLURIDES
analysis of, evaluation of methods for, 20: 16395

RARE EARTHS
abundance patterns in chondrites and earth's crust, 20: 17233
analysis for cerium in presence of, spectrophotometric, 20: 16398
determination by neutron activation and ion-exchange chromatography, 20: 16363
determination in carbonatites by ion exchange chromatography and oxalate precipitation, 20: 16346
determination in selenides, sulfides, and tellurides by titration using EDTA and Xylenol Orange, 20: 16395
effects of alloying additions of, on properties of types 310 and 316 stainless steels, 20: 17078
effects on growth and metabolism of bacteria, fungi, molds, and yeasts, 20: 16191
oxidation of, effects of electron orbit structure on kinetics of, 20: 16985
separation from Hanford wastes by solvent extraction, 20: 16329 (BNWL-187)
separation from uranium and thorium by solvent extraction using alkyl phosphates, 20: 16580
separation of cerium and manganese from, solvent extraction methods for, 20: 16329 (BNWL-187)
separation of scandium from, by ion exchange chromatography, 20: 16574

RARE GASES
content and isotopic abundances in Achilles, LaLande, and Peace River chondrites, 20: 16672
content in meteorite of paired falls, mass spectrometric studies of, 20: 16673
diffusion in fissionable materials, activation entropy for, (T), 20: 17804
positron annihilation in, in electric fields, (T), 20: 17423
potassium atom scattering by, (E), 20: 17294
purification system for, design of, 20: 16971(R) (N-65-18444)

RATE METERS
voltage of functional, statistical variations of output, 20: 16835

RATS
calcification of soft tissues in, 20: 16162
cartilage growth in, effects of dietary strontium on, 20: 16181
copper-64 sorption by, gastrointestinal, 20: 16182
desoxyribonucleic acid synthesis in kidneys of weanling, effects of fasting on, 20: 16158 (AD-628360)
gold-198 metabolism in, 20: 16160 (UCRL-14739(Pt.2))
iodine-131 content of thyroid gland of, measurement using scintillation detectors, 20: 16179
iodine-131 uptake by, effects of ozone on, 20: 16190
radiation effects on DNA and nucleotides in intestine and liver cells in, electron and x, 20: 16230(R) (TID-22644)
radiation effects combined with cold on cesium-137 retention in, x, 20: 16180
radiation effects on iron metabolism in, tracer study of γ, 20: 16187
radiation effects on distribution of phosphorus-32-labeled Yoshida sarcoma cells in, 20: 16188
radiation effects on thymidine excretion by, β, 20: 16201
radiation effects on growth inhibitors in serum of, x, 20: 16208
radiation effects on olfactory bulb neurons in, effects of gases in nasal cavities on x, 20: 16215 (AD-628443)
radiation effects on, role of adrenal and pituitary glands in, 20: 16232(T) (JPRS-34120)
radiation effects on mitosis in lens epithelium of, x, 20: 16256
radiation effects on DNA synthesis in embryos of, γ, 20: 16260
radiation effects on skeletal growth in, β, 20: 16267
radiation effects on skin of, continuous and pulsed electron, 20: 16269
radiation effects on glucose absorption in intestine of, x, 20: 16274
radiation effects on developing brain in, x, 20: 16275
radiation effects on catalase activity of liver and spleen in, 20: 16277
radiation effects on conditioned behavior in parabiont, x, 20: 16284
radiation effects on fertility, growth, and maturation of young female, x, 20: 16287
radiation effects on fertility, growth, and maturation of young male, x, 20: 16288
radiation effects on enzyme activity in tissue homogenates from, x, 20: 16289
radiation effects on physiology of reticulum cells in thymus of, x, 20: 16293
radiation effects on, protective effects of sulfur compounds against, 20: 16297(R) (EUR-2548.f)
radiosensitivity of, effects of biological stress induced by acceleration on, 20: 16213 (AD-620403)
strontium excretion in, effects of pyridoxine on, 20: 16176
tungsten-181 metabolism in, 20: 16160 (UCRL-14739(Pt.2))
tungsten-187 metabolism in, 20: 16160 (UCRL-14739(Pt.2))

REACTION MECHANISMS
kinetics and thermodynamics of reactions in low-temperature plasma, 20: 17959

REACTOR COMPONENTS
design of period meter for CABRI research reactor, 20: 18150
instrumentation for neutron flux monitoring, status in France, 20: 18035
instrumentation for measurement of reactivity, design of, 20: 18037
radiography of, equipment for neutron, 20: 16619

REACTOR CONTROL RODS
development for EGCR, 20: 18020(R) (ORNL-3900, pp 2-81)
drive mechanism for, 20: 18042(P)
locking device for, 20: 18041(P)
testing of gripper for Rapsodie, 20: 18096(T) (ORNL-tr-987)

REACTOR CONTROL SYSTEMS
amplifier gains in PEGASE, automatic system for correction of, 20: 18152
book: *Technological and Thermotechnical Control of Nuclear Power Stations*, 20: 18118
design for heavy water reactors using numerical data processing, 20: 18038
design of automatic, for French research reactor PEGGY, 20: 18151
design of shutdown, 20: 18044(P)
design using logic elements, 20: 18031
development, 20: 18020(R) (ORNL-3900, pp 2-81)

instrumentation for, design of solid-state, 20: 18027
instrumentation for, electric interference in, 20: 18030
instrumentation for neutron flux monitoring, solid-state, 20: 18034
instrumentation for neutron flux monitoring, 20: 18035
instrumentation for zero-power reactors, 20: 18149
operation of automatic, effects of fuel-cladding and gas-coolant temperatures on, 20: 18105
safety aspects of CEA, 20: 18026
testing of ERR, 20: 18090(R) (NUS-246)

REACTOR COOLANTS
analysis for fission products using gamma spectrometry, equipment for, 20: 16898
boiling of liquid metals under forced convection, 20: 16608(T) (ANL-Trans-257)
fission-product detection in, systems for, 20: 18036
purification systems for hermetically sealed boiling-water power plants, 20: 18089 (NAA-SR-Memo-10178)
separation of helium, from carbon monoxide and hydrogen, 20: 16556(R) (ORNL-TM-1090)
thermal decomposition of organic, in large-volume boiling, 20: 16615
thermodynamic properties of organic, 20: 16493

REACTOR COOLING SYSTEMS
book: *Technological and Thermotechnical Control of Nuclear Power Stations*, 20: 18118
development and testing boiling potassium, 20: 18020(R) (ORNL-3900, pp 2-81)
heat transfer in, by forced convection, 20: 16607 (TID-22663)
purification systems for hermetically sealed boiling-water power plants, 20: 18089 (NAA-SR-Memo-10178)

REACTOR ENGINEERING
developments on, at Risö, 20: 18174(R) (NP-15771)

REACTOR EXPERIMENTAL FACILITIES
uses at NRTS, handbook for, 20: 18135 (IDO-17135)

REACTOR FUEL ALLOYS
dimensional stability of, effects of particle distributions on, 20: 17058

REACTOR FUEL ELEMENTS
design, 20: 18081(P)
design of rod-cluster, 20: 18080(P)
development for EGCR, 20: 18020(R) (ORNL-3900, pp 2-81)
fabrication of, capacity of facilities for, 20: 16566
failure of, detection systems for, 20: 18036
fuel tube deformation in ERR, 20: 18090(R) (NUS-246)
heat transfer from polyzonal spiral-finned, 20: 18078
machining spent, equipment design for, 20: 16598(P)
processing of beryllium oxide-based, 20: 16582
processing of irradiated, at Eurochemic, waste management in, 20: 18167
processing of irradiated, Eurochemic plant for, 20: 16558
processing of irradiated, instrumentation problems at Eurochemic plant for, 20: 16559
processing of irradiated, at Eurochemic, safety precautions to prevent criticality accidents in, 20: 16562
processing of irradiated, facility for, Kjeller, Norway, 20: 16569
processing of irradiated, review of safety precautions in, 20: 16577
processing of irradiated, technical progress review on, 20: 16582
processing of irradiated highly enriched and uranium dioxide, by fluoride volatility methods, 20: 16582
processing of, German program for, 20: 18111
weighing in water, equipment for error elimination in, 20: 16780 (TID-22689)

REACTOR FUEL ELEMENTS (CERAMIC)
design of plutonia–urania, for Saxton core II, 20: 18095 (WCAP-3385-52)
mechanical properties of boron-containing, 20: 17121 (GEAP-4918)
performance of boron-containing, 20: 17121 (GEAP-4918)

REACTOR FUEL ELEMENTS (DISPERSION)
book: *Dispersion Fuel Elements for Nuclear Reactors*, 20: 18079
processing of irradiated, 20: 16575

REACTOR FUEL ELEMENTS (THERMOELECTRIC)
preparation of strontium titanate, 20: 16914(R) (ORNL-3900, pp 182-93)

REACTOR FUEL PLATES
fabrication of aluminum–uranium, specifications for, 20: 16995

REACTOR FUEL RODS
cladding temperature variations of, effect of heat capacity on, (E/T), 20: 16602(R) (GEAP-5081)
gamma activity of, scanner for measuring, 20: 18025
heat transfer from finned, geometrical effects on, (E), 20: 16602(R) (GEAP-5081)
heat transfer in annular and cylindrical, time-dependent temperature distribution for, (T), 20: 16613
heat transfer in forced flow three rod sections, film and transition boiling, (E/T), 20: 16602(R) (GEAP-5081)

REACTOR FUEL SPHERES
density distribution of randomly packed, nondestructive electrical method for determining, 20: 18018 (CONF-651101-73)
radioinduced failures of pyrolytic-carbon coatings on fuel pellets, 20: 18076 (ORNL-TM-1385)

REACTOR FUEL TUBES
deformation in ERR fuel elements, 20: 18090(R) (NUS-246)
development of urania-filled SAP, 20: 18174(R) (NP-15771)

REACTOR FUELS
cycle analysis factors, 20: 16566
development and testing of coated-particle, 20: 18098
distribution in reactors, method for optimizing, 20: 18074
economics in breeder reactors, 20: 18100
economics of power reactor, 20: 18101
energy density in, following reactor power excursions, 20: 18019(R) (IDO-17146)
fabrication and properties of oxide-pellet, 20: 17005
fabrication of plutonium-containing, 20: 16996
processing irradiated, for recovery of fertile and fissile materials, 20: 18020(R) (ORNL-3900, pp 2-81)
processing of irradiated uranium dioxide pellet, by oxidation-reduction cycles, 20: 16576
radioinduced failures of pyrolytic-carbon coatings on fuel pellets, 20: 18076 (ORNL-TM-1385)
shipping casks for spent, economics of lead, steel, and uranium-shielded, 20: 16622 (ORNL-3918)

REACTOR FUELS (FUSED SALTS)
development and processing of MSRE, 20: 18020(R) (ORNL-3900, pp 2-81)

REACTOR MATERIALS
radiation effects on, 20: 18174(R) (NP-15771)

REACTOR MATRICES
neutron disadvantage factor of two-region slab, calculation of, 20: 17668

REACTOR MODERATORS
support structure for solid, design of, 20: 18040(P)

REACTOR SAFETY
core meltdown accidents in fast reactors, energy release in, 20: 18123
maintenance program for, 20: 16757
systems for, coincidence magnet for, 20: 18020(R) (ORNL-3900, pp 2-81)

REACTOR SAFETY EXPERIMENTS
core explosions in meltdown accidents, containment of, 20: 18122
reactivity feedback during short-period transients in Spert I, Doppler, 20: 18019(R) (IDO-17146)
reactivity measurements on Capsule Driver core in Spert IV, 20: 18019(R) (IDO-17146)

REACTOR SHIELDING
calculational methods for, historical review of, 20: 17967
development for SNAP, 20: 18020(R) (ORNL-3900, pp 2-81)

REACTOR THERMAL COLUMNS
design for VVR-M, 20: 18139

REACTOR TUBES
design of insulated, 20: 18039(P)

REACTORS
book: *Certain Problems in Physics and Technology of Nuclear Reactors*, 20: 18070
control of CEA, safety aspects of, 20: 18026
control of, use of thermal processes for optimum, (T), 20: 18054
control of, use of static programming of digital data handling in, 20: 18121
criticality accidents at, analysis of hair activation for dosimetry in, 20: 16758
development of, review of, 20: 18182
energy density distribution in, following power excursions, 20: 18019(R) (IDO-17146)
fuel materials distribution in, method for optimizing, 20: 18074
instrumentation for, development of, 20: 18022
kinetics of, analysis using ARGOSY program, 20: 18051 (TRG-Report-1014)
kinetics of, differential-difference equation of retarded type for, 20: 18067
kinetics of, numerical methods for solving equations for, 20: 18061
neutron diffusion equations for, Kantorovich method for solving, (T), 20: 17656
neutron flux in, few-time-step depletion calculations of, 20: 18052 (WAPD-T-1836)
neutron flux measurement in, method and device for, 20: 18043(P)
neutron flux measurements in, using fission chambers and proportional detectors, 20: 16896
neutron flux measurements in, ionization chambers for, 20: 16897
neutron flux measurements in, using thermopiles, 20: 16899
neutron flux monitoring in, detectors for, 20: 18023
neutron flux monitoring instrumentation for, solid-state, 20: 18034
neutron flux monitoring instrumentation for, status in France, 20: 18035
neutron physics calculations for, kernel method in, 20: 18069
neutron power spectral density measurements in, 20: 18048 (ORNL-P-1967)

neutron resonance absorption in, calculation using Monte Carlo method, 20: 18046 (BNL-9644)
neutron transport in, solutions of energy-dependent Boltzman equation for, 20: 18068
noise analysis for, photon detection for, 20: 18064
operation in space environment, electrostatic energy from, (T), 20: 18131
power control and measurement using Cherenkov radiation and gamma radiation, 20: 18033
power excursions in, system for recording, 20: 18028
power-density distribution in, fuel rod scanner for measuring, 20: 18025
reactivity of, instrumentation for measurement of, 20: 18037
reactivity of, system for measuring, 20: 18032
reactivity transfer function of, statistical methods for measuring, 20: 18066
shutdown device for, 20: 18044(P)
startup procedure for, automatic, 20: 18021

RECOIL IONS
angular and energy distributions from proton fission of uranium-238 at 400 Mev, (E), 20: 17790
spectra from carbon-12 (d,d′) and (d,p) reactions, semiconductor studies of, (E), 20: 17820

REFRACTORY COATINGS
development for halogen and hydrocarbon environment, 20: 16943(R) (IITRI-B237-45)
performance of commercial oxidation-resistant, on niobium–titanium–zirconium alloys, 20: 16973 (NASA-TN-D-3275)

REFRACTORY MATERIALS
oxidation of metallic, mechanisms of, 20: 17158(R) (ORNL-3900, pp 82-149)

RELATIVITY THEORY
electromagnetic and gravitational interactions in, potential energy of, 20: 17574
energy-momentum tensors for continuous media in gravitational field in general, 20: 17566
gravitational wave production and detection for proving, 20: 17567(T)
inertial frames in, effect of rotating masses on, 20: 17575
Lorentz group in, subgroups of, 20: 17564
Schwarzschild manifold in, analytic extensions at, 20: 17576

REMOTE-CONTROL EQUIPMENT
design for hot cells, 20: 16595
design for machining spent fuel elements, 20: 16598(P)
design for specific gravity, engineering drawings of, 20: 16801

RESEARCH REACTORS
control system for French PEGGY, design of automatic, 20: 18151
control systems for heavy-water-cooled-and-moderated, design using numerical data processing, 20: 18038
core configuration of VVR-M, optimization of, 20: 18140
description of heavy water-moderated, enriched-fuel, tank-type, at National Bureau of Standards, 20: 16335(R) (NBS-TN-276)
design of homogeneous suspension-fueled KSTR, 20: 18072
design of 10 kw, 20: 18141
development and instrumentation of DR-3, for physics and safety experiments, 20: 18174(R) (NP-15771)
experimental facilities of Triga Mark II, neutron diffractometer, 20: 16882
experimental facilities of Netherlands High Flux, design and operation of organic-cooled in-pile loop, 20: 18137 (KR-82)
experimental facilities for VVR-M, beam holes and thermal column, 20: 18139
experimental facilities in FR-2, characteristics of in-pile, 20: 18146
experimental facilities of UA-RR-1, beam spectra from thermal column, 20: 18147
fuel materials and reactor materials irradiation in DR-3, 20: 18174(R) (NP-15771)
fuels for L54M, copper ion effects on iodine escape from, 20: 18142
instrumentation of zero-power, control and safety, 20: 18149
maintenance of IIT, health physics program for, 20: 16757
neutron lattice parameters of WWER, 20: 18143
operation of DR-2 and DR-3, 20: 18174(R) (NP-15771)
period meter for CABRI, design of, 20: 18029
period meter for CABRI, design of, 20: 18150
power density of WWRM, 20: 18144
reactivity measurements in NORA, (E), 20: 18138(R) (TID-22697)

RESINS
carbon ion reactions with formvar at 9.7 Mev, charge-exchange cross sections and ionization from, (E), 20: 17724
performance as metallographic sample mounting of irradiated specimens, 20: 16948 (ORNL-TM-1161, pp 103-11)
radiation effects on ion-exchange, 20: 16583
sample mounting in epoxy, using a radio-frequency furnace, accelerated metallographic, 20: 16947 (ORNL-TM-1161, pp 98-102)
sorptive properties of aminodiacetate resin Dowex A-1 for di- and trivalent cations, 20: 16358

RESISTANCE FURNACES
design of silicon carbide, for fusing glass, 20: 18166(R) (TID-22531)

RESISTORS
radiation effects on, review of, 20: 16911

RETICULO-ENDOTHELIAL SYSTEM
radiation effects on physiology of rat, x, 20: 16293

RHENIUM
creep-rupture properties at high temperatures, 20: 17011 (CONF-651025-14)
diffusion in pyrolytic graphite, 20: 17107
diffusion in tungsten to 4000°F, inter-, 20: 16943(R) (IITRI-B237-45)
proton fission at 150 to 660 Mev, cross sections for, (E), 20: 17838

RHENIUM ALLOY COUPLES
Re–W/Re–W, performance to 2760°C, 20: 16942 (ANL-6981)
W/Re–W, performance to 2760°C, 20: 16942 (ANL-6981)

RHENIUM ALLOYS
Mo–Re, creep-rupture properties at high temperatures, 20: 17011 (CONF-651025-14)
Mo–Re–W, fabrication of rods of, by extrusion and sintering, 20: 16989(R) (COO-1518-2)
Re–W, creep-rupture properties at high temperatures, 20: 17011 (CONF-651025-14)
Re–W, fabrication of tubing of, by extrusion and sintering, 20: 16989(R) (COO-1518-2)
Re–W, microstructure of vapor-deposited, 20: 18020(R) (ORNL-3900, pp 2-81)

RHENIUM CARBIDES
properties of metastable, 20: 17107

RHENIUM ISOTOPES Re-184
production in deuteron reactions (d,n) and (d,2n), with tungsten-183 and -184, cross sections for, 20: 16508(R) (NYO-2771-13)

RHENIUM OXIDES
Dy_2O_3–ReO_2, phase studies at 1130 and 1300°C, 20: 17007(R) (AD-627468)
Nd_2O_3–ReO_2, phase studies at 1130 and 1300°C, 20: 17007(R) (AD-627468)
ReO_2–Yb_2O_3, phase studies at 1130 and 1300°C, 20: 17007(R) (AD-627468)

RHODIUM
electron emission in cesium vapor, thermionic, (E), 20: 17333
performance of foils of, in neutron radiography, 20: 16619

RHODIUM ALLOYS
Nb–Rh, superconductivity in close-packed intermediate phases of, 20: 17624
Rh–Ta, superconductivity in close-packed intermediate phases of, 20: 17624

RHODIUM ISOTOPES Rh-102
content in stratospheric and tropospheric samples in Project Star Dust, 1963, 20: 16727(R) (HASL-168)
distribution of atmospheric, from operation Hardtack, 20: 16662(R) (HASL-165)

RHODIUM ISOTOPES Rh-103
neutron capture by, conversion electron spectrum from, (E), 20: 17810

RIBONUCLEIC ACID
separation from *Escherichia coli*, 20: 17158(R) (ORNL-3900, pp 82-149)
synthesis in recovery of DNA synthetic system of uv-damaged *E. coli*, 20: 16202
synthesis of, role of manganese in enzyme systems for, 20: 16160 (UCRL-14739(Pt.2))

RIBONUCLEIC ACID, DESOXY-
breakage and reunion in bacteriophage infections, mechanisms of, 20: 16159(R) (ORNL-3900, pp 150-81)
photochemistry of, 20: 16203
radiation effects on, effects of enzymes on uv, 20: 16159(R) (ORNL-3900, pp 150-81)
radiation effects on depression, replication, and synthesis of, in mammalian cells, 20: 16230(R) (TID-22644)
radiation effects on electric conductivity of, 20: 16194
radiation effects on rat, β, 20: 16201
radiation effects on synthesis in rat embryos, y, 20: 16260
radiation effects on, ESR studies of gamma, 20: 16541
radiation effects on bacterial, uv, 20: 16280
synthesis in recovery of uv-damaged *E. coli*, 20: 16202
synthesis in weanling rat kidneys, effects of fasting on, 20: 16158 (AD-628360)
transfer in bacterial mating, 20: 16159(R) (ORNL-3900, pp 150-81)

RICE
cesium-137 content in Japanese, 20: 16169

ROCKET MOTOR NOZZLES
development, 20: 16943(R) (IITRI-B237-45)

ROCKET REACTORS
operation in space environment, electrostatic energy from, 20: 18131

ROCKET REACTORS (KIWI)

development problems, 20: 18128
ROCKS
age estimation, 20: 16715
age of Massachusetts, rubidium–strontium and strontium-87/-86 estimation of, 20: 16711(R) (MIT-1381-13)
age of New England Ammonoosuc volcanic and Monson metamorphic, estimation of, 20: 16711(R) (MIT-1381-13)
age of volcanic, at Kirkland Lake, Ontario, 20: 16711(R) (MIT-1381-13)
age of volcanic, in Lower Cambrian in Canada, 20: 16711(R) (MIT-1381-13)
age of, developments in estimation of, 20: 16711(R) (MIT-1381-13)
analysis for alpha and beta sources, radiochemical methods for, 20: 16337 (RMO-3001(Rev.1)(Suppl.))
analysis for arsenic, effects of manganese on activation, 20: 16364
analysis for isoprenoid alkanes, methods for, 20: 16633 (UCRL-16605)
analysis for palladium, activation, 20: 16370
analysis for rubidium/strontium ratio by x-ray spectrography, 20: 16711(R) (MIT-1381-13)
analysis for uranium, methods for, 20: 16337 (RMO-3001(Rev.1)(Suppl.))
rubidium-87 decay in, 20: 16711(R) (MIT-1381-13)
ROOTS
calcium-45 transport in paired corn, method for determining wounding response in, 20: 16170 (AD-628805)
manganese sorption by barley, effects of divalent cations on, 20: 16174(R) (RLO-1547-3)
radiation effects on corn and pea seedlings, from tritiated water and tritiated thymidine, 20: 16227(R) (NYO-3561-2)
radiation effects on *Vicia sativa*, x, 20: 16276
ROTARY PUMPS
development for radioactive steam condensate pumping from underground tanks, 20: 16825 (ORNL-TM-1442)
ROTORS
testing graphite helical-screw, 20: 16591 (UCRL-14660)
RUBIDIUM
content in Ammonoosuc volcanics and Monson gneiss in New England, age estimations from, 20: 16711(R) (MIT-1381-13)
content in granites, quartzites, and slate in Massachusetts, age estimation from, 20: 16711(R) (MIT-1381-13)
content in Jardine-Crevasse Mountain area, Montana, age estimation from, 20: 16711(R) (MIT-1381-13)
content in tektites in Moldavia, age estimation from, 20: 16711(R) (MIT-1381-13)
content ratio to strontium in geological materials, differentiation of Earth's mantle by studying, 20: 16711(R) (MIT-1381-13)
determination in Moldavites by mass spectrometry and x-ray fluorescence, 20: 16711(R) (MIT-1381-13)
determination in rocks by x-ray spectrography, 20: 16711(R) (MIT-1381-13)
effects on heat transfer properties of mercury, 20: 16972(R) (NASA-CR-54719)
effects on potassium determination by flame photometry, 20: 16713
electron scattering by atomic, cross sections for, (T), 20: 17286
neutron total cross sections at 14 Mev, (E), 20: 17702
nuclear radius of, mean, (E), 20: 17702
sorption by chabazite in lithium, potassium, and sodium nitrates, 20: 16340 (USNRDL-TR-970)
RUBIDIUM IONS
mobility in argon, helium, and nitrogen at high pressures, (E/T), 20: 16415 (CEA-R-2861)
RUBIDIUM ISOTOPES Rb-87
decay in geological materials, 20: 16711(R) (MIT-1381-13)
RUBIDIUM OXIDES
content in Keewatin and Timiskaming volcanic rocks at Kirkland Lake, Ontario, age estimations from, 20: 16711(R) (MIT-1381-13)
content in volcanic rocks in Lower Cambrian in Canada, age estimation from, 20: 16711(R) (MIT-1381-13)
RUMANIA
geologic dating of tektites in Moldavia, using rubidium–strontium method, 20: 16711(R) (MIT-1381-13)
Moldavites in, composition and origin of, 20: 16711(R) (MIT-1381-13)
RUTHENIUM
determination in process feed solutions by extraction chromatography, 20: 16333 (KR-81)
diffusion from ceramic wastes, effects of volatilization on, 20: 18156 (BNWL-SA-453)
electron emission in cesium vapor, thermionic, (E), 20: 17333
evaporation from irradiated uranium dioxide at 750 to 1600°C, 20: 17102
separation from fission product solutions by electrodeposition, 20: 16563
RUTHENIUM CHLORIDES
effects on isotopic exchange between deuterium and water, 20: 16423
RUTHENIUM ISOTOPES Ru-103
content in plants before and after Salmon Event, 20: 16743 (VUF-1021)
content in rain water, Fayetteville, Arkansas, Oct. 1964, 20: 16663 (TID-21470)
sensitivity for activation analysis using beta-gamma-gamma sum-coincidence gamma spectrometer, 20: 16335(R) (NBS-TN-276)
yields from thorium-232 fission, (E), 20: 17860
RUTHENIUM ISOTOPES Ru-106
content in atmospheric dust and rain water, 1964–65, 20: 16660 (AERE-R-4997)
content in plants before and after Salmon Event, 20: 16743 (VUF-1021)
content in rain water, Fayetteville, Arkansas, Oct. 1964, 20: 16663 (TID-21470)
ground water contamination by, in Shoal Event, hazards from, 20: 16742 (VUF-1014)
use for radiotherapy, 20: 16305
yields from thorium-232 fission, (E), 20: 17860
RUTHENIUM OXIDES
BaO–RuO_2–SrO, crystal structure, 20: 16436

S

SACLAY REACTORS
design of OSIRIS, 20: 18181
SACLAY REACTORS (EL-2)
operation experience, 20: 18181
SACLAY REACTORS (EL-3)
design and research program using, 20: 18181
SACLAY REACTORS (OSIRIS)
description, 20: 18148
SAFETY
evaluation of flash units for photographing explosives, 20: 16739(R) (UCRL-14534, pp 44-9)
in fabrication and use of radioisotopic sources, 20: 16914(R) (ORNL-3900, pp 182-93)
requirements for, in reprocessing irradiated fuels, review of, 20: 16577
research programs on nuclear, at ORNL, 20: 18020(R) (ORNL-3900, pp 2-81)
SAFETY HAZARDS
evaluation of, in reactor fuel reprocessing, 20: 16582
gamma source loss in field work, exposure hazard from, 20: 16764
SALIVARY GLANDS
radiotherapy of Mikulicz's disease of, x, 20: 16316
SALT DEPOSITS
fission product storage in, dimensioning for maximum credible accident in, (T), 20: 16722 (BMwF-FBK-65-03)
waste disposal in, demonstration of high-level, 20: 18169
waste storage in, equipment for, 20: 18165 (ORNL-P-1987)
SALTS
radiosensitivity effects of inorganic, on barley seeds, 20: 16297(R) (EUR-2548.f)
SAMARIUM
abundance in sun, (E), 20: 17237
determination in carbonatites by ion exchange chromatography and oxalate precipitation, 20: 16346
performance of neutron filters of, effective cutoff energies for, (T), 20: 17663
solubility in gold, solid, 20: 17016 (IS-1175)
SAMARIUM ALLOYS
In–Sm, crystal structure of $SmIn_3$, 20: 17060
Mn–Sm, crystal structure of Sm_6Mn_{23} in, 20: 17096(T)
SAMARIUM COMPLEXES
with phenanthroline, infrared spectra of, 20: 16436
with thenoyltrifluoroacetone, magnetic susceptibilities of, 20: 16416(R) (NYO-906-68)
with 2,2'-bipyridyl, infrared spectra of, 20: 16437
SAMARIUM HYDRIDES
properties and structure, 20: 16453
SAMARIUM ISOTOPES
content in Arkansas rain water in Oct. 1964, 20: 16685
decay of compound nucleus of, excitation functions from, (E), 20: 17784
SAMARIUM ISOTOPES Sm-142
production in heavy ion reactions with nuclei, angular momentum effects on excitation functions for, (E), 20: 17784
SAMARIUM ISOTOPES Sm-144
oxygen-16 scattering at 31 to 45 Mev, B(E2) values for transitions from, (E), 20: 17734
SAMARIUM ISOTOPES Sm-148
oxygen-16 scattering at 31 to 45 Mev, B(E2) values for transitions from, (E), 20: 17734
SAMARIUM ISOTOPES Sm-150
decay scheme, 20: 18174(R) (NP-15771)
oxygen-16 scattering at 31 to 45 Mev, B(E2) values for transitions from, (E), 20: 17734
SAMARIUM ISOTOPES Sm-151
content in rain water, Fayetteville, Arkansas, Oct. 1964, 20: 16663

(TID-21470)
ground water contamination by, in Shoal Event, hazards from, 20: 16742 (VUF-1014)
SAMARIUM ISOTOPES Sm-153
content in rain water, Fayetteville, Arkansas, Oct. 1964, 20: 16663 (TID-21470)
SAMARIUM OXIDES
crystallographic modifications and phase transformations of, 20: 16489
preparation of, methods for, 20: 17007(R) (AD-627468)
reactions with boron oxides at high temperatures, 20: 16489
CeO_2–Sm_2O_3, fluorescence properties of, 20: 16466(T)
SAMARIUM SULFIDES
Ce_2S_3–SmS, compound formatioa in, 20: 16431
Dy_2S_3–SmS, compound formation in, 20: 16431
EuS–Sm_2S_3, compound formation in, 20: 16431
Gd_2S_3–SmS, compound formation in, 20: 16431
La_2S_3–SmS, compound formation in, 20: 16431
Nd_2S_3–SmS, compound formation in, 20: 16431
Pr_2S_3–SmS, compound formation in, 20: 16431
SmS–Tb_2S_3, compound formation in, 20: 16431
Sm_2S_3–YbS, compound formation in, 20: 16431
SAMARIUM SYSTEMS
CeO_2–La_2O_3–Sm, fluorescence properties of, 20: 16466(T)
CeO_2–Sm–ThO_2, samarium fluorescence in, 20: 16466(T)
SAMPLING
equipment and methods for, in marine ecosystems, 20: 16175(R) (RT/BIO(65)-1)
marking system for materials exposed to nuclear blast environment, 20: 18176 (SCL-DR-66-6)
SANDS
analysis for water using neutron probes, 20: 16926
SAP (SINTERED ALUMINUM PRODUCTS)
fabrication and testing for reactor cooling channels, 20: 18174(R) (NP-15771)
internal friction of, low-frequency, 20: 17065
SARCOMAS
radiation effects on distribution of cells of phosphorus-32-labeled Yoshida, in rat tissues, 20: 16188
radiotherapy of, x, 20: 16312
SATELLITES
motion in tenuous plasma, scaling conditions for sheaths from simulated, (E), 20: 17546
SAXTON POWER REACTOR
core II design, 20: 18095 (WCAP-3385-52)
SCALERS
design and performance of portable, 20: 16846
design of 100-Mc, in biquinary tunnel diode mode, 20: 16775 (DESY-65/17)
resolving time of binary, 20: 16802
SCANDIUM
abundance in sun, (E), 20: 17237
determination by neutron activation methods, 20: 16383
determination in asbestos using ion exchange, activation, 20: 16336(R) (NYO-10175)
determination in carbonatites by ion exchange chromatography and oxalate precipitation, 20: 16346
oxidation by air at 300 to 900°C, 20: 16985
preparation of self-supporting radiation targets of, 20: 17218
separation from other metals by ion exchange chromatography, 20: 16574
SCANDIUM ALLOYS
Al–Cu–Sc, crystal structure of ternary phases in, 20: 17097(T)
SCANDIUM COMPLEXES
with phenanthroline, infrared spectra of, 20: 16436
with 2,2′-bipyridyl, infrared spectra of, 20: 16437
SCANDIUM COMPOUNDS
organic, preparation and properties of scandium chloroacetates, 20: 16427
SCANDIUM HYPOPHOSPHITES
preparation and properties of, 20: 16426
SCANDIUM ISOTOPES Sc-44
half life, 20: 16331 (GA-6568)
yield ratios for isomeric, from (γ,n), (γ,np), and (n,2n) reactions, (E), 20: 17777
SCANDIUM ISOTOPES Sc-45
bremsstrahlung reactions (γ,n) at 24, 36, and 48 Mev, scandium-44 isomeric yield ratio from, (E), 20: 17777
neutron reactions (n,2n) at 14 Mev, scandium-44 isomeric yield ratio from, (E), 20: 17777
proton reactions (p,n) with, neutron production for activation analysis in, 20: 16332 (GA-6691)
SCANDIUM ISOTOPES Sc-46
determination in irradiated materials by extraction and precipitation, gamma spectrometric, 20: 16336(R) (NYO-10175)
sensitivity for activation analysis using beta-gamma-gamma sum-coincidence gamma spectrometer, 20: 16335(R) (NBS-TN-276)
SCANDIUM ISOTOPES Sc-50
nucleon interactions in, properties from effective, (T), 20: 17735
SCANDIUM OXIDES
determination in thorium oxide by emission spectroscopy, 20: 16393
SCANDIUM SILICIDES
properties of, physicochemical, 20: 17047
SCATTERING
amplitude for high-energy elastic, forward peak in, 20: 17459
amplitudes for potential, 20: 17438
amplitudes for potential, S-matrix for low- and high-energy, 20: 17491
cross sections for two-body, moment relations for Schroedinger, 20: 17483
potential, Born approximation and large-momentum transfer in, 20: 17460
potential, S-matrix theory for, 20: 17490
potential, three-body, 20: 17430 (JINR-P-2565)
potentials in, bound states of nonlocal separable, 20: 17495
S-matrix for, equation of motion for half, 20: 17493
S-matrix theory for coupling constant bounds, unitarity and analyticity in, 20: 17477
S-matrix with inelasticity in, Levinson's theorem for, 20: 17452
theory of high-energy, analyticity and large-momentum-transfer processes in, 20: 17461
theory of two-particle, Whiteman-type functional for, 20: 17496
SCIENCE
evaluation of existing criteria for judging quality of exhibits on, 20: 18178 (TID-22793)
SCINTILLATION DETECTORS
design for meson (K^+) detection, 20: 16826 (PPAD-574E)
design modification of liquid, for carbon-14 determination, 20: 16862
design of lithium-6-iodide activation, for neutrons, 20: 16819 (LA-3435)
development for radiodiagnosis, review of, 20: 16855
efficiency for x ray detection, 20: 16836
efficiency of, using larger parabolic phosphors, 20: 16849
performance of liquid, phosphorescence effects of glass containers on, 20: 16863
performance of sodium iodide, for absolute gamma activity measurements, 20: 16858
performance of thallium-activated sodium iodide, for measuring radionuclide transfer in cows, 20: 16160 (UCRL-14739(Pt.2))
pulse-shape discrimination in organic, circuits for, 20: 16839
radiometric properties of, 20: 16865
sensitivity of, for oceanography studies, 20: 16828 (TID-22763)
spectra from, computer program for analysis of, 20: 16344
standards for, dispersion for addition of internal, 20: 16834
use for counting β activity in biological materials, 20: 16177
use for measuring iodine-131 in rat thyroid gland, 20: 16179
use for whole-body measurements of strontium-90 in man, 20: 16303(R) (AD-626384)
use with magnetic analyzers, for charged particles, 20: 16859
use with photographic film for fast neutron dosimetry, 20: 16861
SCRUBBERS
design and development of wet cyclone, for collection of carbon black, 20: 16740(R) (UCRL-14534, pp 50-3)
SEA URCHINS
radiation effects on protein synthesis in eggs of, 20: 16160 (UCRL-14739(Pt.2))
SEA WATER
analysis for cesium-137 by ion exchange and gamma spectroscopy, 20: 16342
analysis for trace amounts of uranium by controlled-potential polarography, 20: 16389
bacteria in, studies on, 20: 16175(R) (RT/BIO(65)-1)
desalination of, chemical research on, 20: 17158(R) (ORNL-3900, pp 82-149)
desalination of, development of nuclear systems for, 20: 18020(R) (ORNL-3900, pp 2-81)
fallout radionuclide distribution in deep offshore, of Japan, 20: 16681
plankton distribution in ecosystem of, 20: 16175(R) (RT/BIO(65)-1)
potassium-40 background activity in, sensitivity of gamma spectrometer and scintillation detectors for, 20: 16828 (TID-22763)
strontium isotopic composition in, age estimation from, 20: 16711(R) (MIT-1381-13)
SEALING MATERIALS
performance and selection of, for use in space vehicles, 20: 16944 (NASA-SP-3025)
SEDIMENTATION
use in studies of radioactive aerosols, 20: 16655
SEED
radiation effects on germination of *Rauwolfia serpentina*, γ, 20: 16249
radiation effects on barley, protective effects of inorganic salts against, 20: 16297(R) (EUR-2548.f)

radioinduced mutations in jute, γ, 20: 16217 (AECD-AG-7)
radiosensitivity of *Vicia sativa*, effects of moisture on, 20: 16276
radiosensitivity of *Vicia faba*, effects of infrared radiation on x, 20: 16278
radiosensitivity of wheat, γ and x, 20: 16285
radiosensitivity of wheat, x, 20: 16286
radiosensitivity of medicinal plant, γ, 20: 16290

SEEDLINGS
radiation effects on corn and pea, from tritiated water and tritiated thymidine, 20: 16227(R) (NYO-3561-2)

SELENIUM
determination in copper by neutron activation, 20: 17822
determination in rare earth selenides, 20: 16395

SELENIUM IONS
electron spin resonance of molecular, in alkali halide single crystals, (E/T), 20: 18005

SELENIUM ISOTOPES Se-80
deuteron reactions (d,p) at 15 Mev, isomeric yield ratios for, 20: 16508(R) (NYO-2771-13)

SELENIUM ISOTOPES Se-81
production of isomeric, in deuteron reactions (d,p) at 15 Mev, 20: 16508(R) (NYO-2771-13)

SEMICONDUCTOR DETECTORS
amplifiers for, design and performance of pre-, 20: 16806 (CLOR-44/D)
charge collection in, properties of, (T), 20: 16885
design and uses of, review on, 20: 16869
design of system of, for energy and position determination, 20: 16878
development of lithium-drifted germanium, for high resolution spectroscopy, 20: 16160 (UCRL-14739(Pt.2))
energy resolution of, preamplifiers, bipolar and FET transistors, and tubes for optimum, 20: 16871
fabrication and performance of lithium-drifted germanium, for gamma radiation, 20: 16890
fabrication by neutron transmutation methods, 20: 16505 (BNL-949)
performance for beta spectra, backscattering and resolution corrections for, 20: 16867
performance for prompt neutrons and fission fragments, 20: 17864
performance in x-ray emission spectrography, 20: 16887
performance of silicon, for hydrogen and nitrogen ion detection, 20: 17253(R) (ORNL-3908, pp 90-9)
performance of silicon surface-barrier, in studies of recoil nuclei, 20: 17820
preparation and performance of depleted surface-barrier, 20: 16818 (KFK-328)
pulse-shape discrimination between alpha particles and protons, system for, 20: 16900
response to electrons below 30 kev, 20: 17168
scattering chamber for use with, 20: 16883
use of lithium-drifted germanium, in neutron activation analysis, 20: 16888

SEMICONDUCTORS
charged-particle passage through, electromagnetic radiation emission from, (T), 20: 17494
electromagnetic-wave propagation in plasma of, in stationary electric fields, (T), 20: 18013
electronic properties of single-crystal, effects of ion-bombardment on, 20: 17151
radiation effects on, 20: 17158(R) (ORNL-3900, pp 82-149)
radiation effects on junctions of, proton, 20: 16907(R) (N-65-17517)
radiation effects on, review of, 20: 16911
radiosensitivity levels for types of, fast-neutron, 20: 16911
thermal conductivity in, existence of super-, (T), 20: 18014

SENA POWER REACTOR
development of, review of, 20: 18104

SEPARATION PROCESSES
development of, for use in radiochemistry, review of, 20: 16557
instrumentation for, for fuel element reprocessing, 20: 16559
methods for transplutonium elements, review on, 20: 16402

SEPARATORS
performance of radioisotope, at Institute for Nuclear Study, Japan, 20: 16928(R) (INSJ-92)

SERUMS
analysis for calcium, copper, magnesium, and manganese, activation, 20: 16347
content in culture, effects of, on radiosensitivity of mammalian cells, 20: 16298

SHALES
analysis for isoprenoid alkanes, methods for, 20: 16633 (UCRL-16605)
oil recovery from, use of nuclear explosions for, 20: 16589 (UCRL-12224-T)

SHEEP
lipid function in membranes of, 20: 16160 (UCRL-14739(Pt.2))
radiation effects on copper and zinc content and enzyme activity in blood serum of, 20: 16222 (AFWL-TR-65-112)

SHELTERS
design of tunnel-grid, for urban populations, 20: 16159(R) (ORNL-3900, pp 150-81)
design of, distribution and magnitude of weapon effects for, 20: 16620 (AD-624370)
protection factor for fallout, calculation of, 20: 16733 (ORNL-P-1098)
use of underground highway and parking garage for Manhattan Island fallout, engineering study on, 20: 16623 (ORNL-TM-1381)

SHIELDED CONTAINERS
development for radioactive materials, 20: 18020(R) (ORNL-3900, pp 2-81)
economics of lead, steel, and uranium, comparison of, 20: 16622 (ORNL-3918)

SHIELDING
calculations for space vehicles, 20: 17965
design for protection of male gonads during diagnostic radiography, 20: 16321
development for whole-body counter facility, 20: 16737(R) (UCRL-14534, pp 13-18)
method of filtration, x-ray equipment, 20: 16844
performance of accelerator and space vehicle, methods of calculating, (E/T), 20: 17158(R) (ORNL-3900, pp 82-149)

SHIPPING
casks for spent fuel, economics of lead, steel, and uranium-shielded, 20: 16622 (ORNL-3918)
container and equipment for radioactive materials, design of, 20: 18165 (ORNL-P-1987)

SHIPPINGPORT PRESSURIZED WATER REACTOR
core materials for, metallurgy of, 20: 18094(R) (WAPD-MRP-115)
design of, mechanical and thermal, 20: 18094(R) (WAPD-MRP-115)
development and engineering of, 20: 18094(R) (WAPD-MRP-115)
reactivity calculations for core 2 assemblies, 20: 18094(R) (WAPD-MRP-115)

SHIPS
nuclear-powered, development of oceanographic research, 20: 18129

SHOCK WAVES
generation by water impacts on liquid aluminum in vacuum, 20: 18050(R) (STL-372-22)
plasma production by, microwave measurements of electron density in, (E), 20: 17510 (IPP-3/25)
propagation in gases, properties of ionizing, (T), 20: 17511 (NP-15894)

SILICATE ROCKS
analysis of, methods for, 20: 16337 (RMO-3001(Rev.1)(Suppl.))

SILICON
analysis for aluminum by neutron activation, 20: 17822
analysis for argon, activation, 20: 16335(R) (NBS-TN-276)
analysis for trace amounts of gallium, activation, 20: 16396
determination in alumina and graphite, interferences in activation, 20: 16360
determination of trace amounts of, in beryllium by spectrography, 20: 16352
electronic properties of single-crystal, effects of ion-bombardment on, 20: 17151
performance of semiconductors of, for hydrogen and nitrogen ion detection, 20: 17253(R) (ORNL-3908, pp 90-9)
photon reactions with Coulomb field of, pair production total cross sections for high-energy, (T), 20: 17754
production in h-f electrodeless plasmatron, 20: 17959
radiation effects on electric properties of conductivity-modulated p-i-n diodes of, 20: 16912
radiation effects on defects in solar cells of, effects of impurities on electron and proton, 20: 17125 (NASA-CR-404)

SILICON ISOTOPES Si-27
proton reactions (p,n) at 6.0 to 7.5 Mev, absolute cross sections and angular distributions for, (E/T), 20: 17775

SILICON ISOTOPES Si-28
energy level lifetimes, (E), 20: 17651(R) (AD-612192)
helium-3 reactions (He-3,p) at 12 Mev, Q value for, 20: 16331 (GA-6568)
neutron reactions (n,p) with, sensitivity of, for activation analysis, 20: 16332 (GA-6691)
proton reactions (p,2p) at 140 Mev, energy spectra and angular correlation distributions from, (E), 20: 17741

SILICON ISOTOPES Si-29
helium-3 reactions (He-3,d), Q value for, 20: 16331 (GA-6568)

SILICON ISOTOPES Si-30
deuteron reactions (d,γ), cross sections for phosphorus-32 production by, 20: 16508(R) (NYO-2771-13)

SILICON OXIDES
determination in Moldavites by spectrophotometry and x-ray fluorescence, 20: 16711(R) (MIT-1381-13)
performance of thin films of, for fast neutron flux measurements, 20: 16851
production in h-f electrodeless plasmatron, 20: 17959

radiation effects on structure of, neutron, 20: 17148
radioinduced electric conductivity in fused, effects of crystalline form and impurity on electron, 20: 17133
radiolysis of colloids of, at 77°K, ESR studies of, 20: 16511
reactions with molten AMS 5350 steel and Inconel 713C, 20: 16984
Al_2O_3–SiO_2, effects of dehydration on bound water in, 20: 16413 (CEA-R-2703)
CaO–SiO_2–Na_2O, diffusion of sodium-22 in solid, residual activity method for self-, 20: 16478
hexane–SiO_2, radiolysis of, at 77°K, ESR studies of, 20: 16511

SILICON STEEL
magnetic properties of flat-rolled, variation with processing techniques, 20: 17009 (CONF-650922, pp 287-96)

SILICON SYSTEMS
Al–Si–V, superconductivity of solid solutions in, 20: 17043
Be–Si–V, superconductivity of solid solutions in, 20: 17043
C–Mo–Si, superconducting transition temperature of $Mo_{4.8}Si_3C_{0.6}$, 20: 17607
Cr–Fe–Ni–Si, corrosion cracking in, mechanisms of stress-, 20: 16968 (COO-1319-33)
Ge–Si–V, superconductivity of solid solutions in, 20: 17043
Si–Sn–V, superconductivity of solid solutions in, 20: 17043
Si–Ta–V, phase studies on intermetallic compounds in, 20: 17075

SILTS
analysis for isoprenoid alkanes, methods for, 20: 16633 (UCRL-16605)
geologic dating of, using potassium–argon method, 20: 16711(R) (MIT-1381-13)
tracer studies on, computer program for processing data from, 20: 16632 (AAEC/TM-303)

SILVER
carbon ion reactions at 9.7 Mev, charge-exchange cross sections and ionization from, (E), 20: 17724
determination in copper samples by radioisotope dilution, 20: 16335(R) (NBS-TN-276)
determination of trace amounts of, in beryllium by spectrography, 20: 16352
effects on gastrointestinal absorption of copper-64 in rats, 20: 16182
electron spin resonance in colloidal solutions and films of, (E), 20: 17981
proton reactions (p,d) at 57 Mev, energy spectra from, (E), 20: 17725
proton reactions in emulsions at 25 Bev/c, lithium-8 fragment recoil from, (E), 20: 17748
radiation effects on battery electrodes of, gamma-, 20: 17115(R) (AI-65-264)
sintering of, studies on, 20: 16992(R) (RPI-2408-4)

SILVER ALLOYS
Mg–Ag, photosensitivity of, 20: 17984

SILVER BROMIDES
radioinduced ESR in, gamma, light, and uv, (E), 20: 17981

SILVER CHLORIDES
radioinduced ESR in, gamma, light, and uv, (E), 20: 17981

SILVER IODIDES
iodine-131 exchange with iodine ions, effects of cobalt and uranyl nitrates on, 20: 16432
iodine-131 exchange between, and potassium iodide, kinetics of, 20: 16460
silver-110 exchange between, and silver nitrate, kinetics of, 20: 16460

SILVER IONS
photoluminescence of neutralized, use in dosimeters, 20: 16837

SILVER ISOTOPES Ag-108
decay of isomeric, (E), 20: 17786
energy levels from isomer decay, (E), 20: 17786

SILVER ISOTOPES Ag-110
content in stratospheric and tropospheric samples in Project Star Dust, 1963, 20: 16727(R) (HASL-168)
content in stratospheric and tropospheric samples in Project Star Dust, 1964, 20: 16728(R) (HASL-169)
exchange between silver iodide and silver nitrate, kinetics of, 20: 16460
sensitivity for activation analysis using beta-gamma-gamma sum-coincidence gamma spectrometer, 20: 16335(R) (NBS-TN-276)

SILVER ISOTOPES Ag-111
content in rain water, Fayetteville, Arkansas, Oct. 1964, 20: 16663 (TID-21470)
yields from thorium-232 fission, (E), 20: 17860

SILVER NITRATES
incorporation in filter papers for radioiodine sampling, 20: 16756
ion exchange and sorption on glass surfaces, 20: 16469
silver-110 exchange between, and silver iodide, kinetics of, 20: 16460

SILVER OXALATES
Ag–silver oxalate, gamma radiation effects on catalytic acitivity of, 20: 16523

SILVER SYSTEMS
Ag–silver oxalate, gamma radiation effects on catalytic activity of, 20: 16523
Al_2O_3–Ag, preparation of wires of, with oxide homogeneously dispersed, 20: 16992(R) (RPI-2408-4)

SINGLE CRYSTALS
preparation of urania, 20: 17158(R) (ORNL-3900, pp 82-149)

SINTERING
studies on, 20: 16992(R) (RPI-2408-4)

SKELETON
calcium-strontium discrimination in rabbit, 20: 16178
radiation dose to dog, after chronic enteral administration of strontium-90, β, 20: 16266
radiation effects on growth of rat, β, 20: 16267

SKIN
plutonium-239 sorption through rabbit, 20: 16183
radiation effects on transplanted Yoshida sarcoma cells in rat, tracer study, 20: 16188
radiation effects on pigments in human and guinea pig, uv, 20: 16261
radiation effects on rat, continuous and pulsed electron, 20: 16269
radiosensitivity of, γ, 20: 16323
radiotherapy of tumors of, β, 20: 16325

SMOKES
polonium-210 content in tobacco, 20: 16264

SNOW
radioactivity of, from barium-140 and zirconium-95 content in Germany, 1961 to 1963, 20: 16766

SODIUM
analysis for oxygen by distillation and titration, 20: 16349
corrosive effects on type 316 stainless steel at 1100 and 1200°C, mechanisms of, 20: 16970 (GEAP-4832)
corrosive effects on Croloy 2¼ steel, 20: 16599(R) (BAW-1280-34)
determination in asbestos using ion exchange, activation, 20: 16336(R) (NYO-10175)
electric conductivity at 100 to 1000°C, 20: 17026 (RT/ING-(65)17)
electron scattering by atomic, cross sections for, (T), 20: 17286
ion pairing interactions in, (T), 20: 17008 (CEA-R-2820)
neutron capture at 10 to 135 kev, cross sections for, (E), 20: 17718
photon reactions with Coulomb field of, pair production total cross sections for high-energy, (T), 20: 17754
sorption by barley roots, effects of uranium(IV) oxides on, 20: 16174(R) (RLO-1547-3)
sorption by chabazite in lithium, potassium, and sodium nitrates, 20: 16340 (USNRDL-TR-970)

SODIUM ACID CARBONATES
effects on reduction of niobium oxide using carbon, 20: 16483

SODIUM ALLOYS
K–Na, effects on properties of chromium–molybdenum steels, 20: 16972(R) (NASA-CR-54719)
Sb–Cs–K–Na, photosensitivity of, 20: 17984
Sb–Cs–K–Na–Te, photosensitivity of, 20: 17984

SODIUM ALUMINUM SILICATES
sorptive properties of Decalso, for cesium, 20: 16578

SODIUM BROMIDES
activity and osmotic coefficients in heavy water at 25°C, 20: 16488
NaBr–H_2SO_4, radioinduced absorption spectra in, at 77°K, 20: 16534

SODIUM CARBONATES
analysis for uranium(VI) by u-v absorption, 20: 16354

SODIUM CHLORIDES
activity and osmotic coefficients in heavy water at 25°C, 20: 16488
color centers in, wave functions for F, (T), 20: 17977(R) (NYO-2047-36, App.2)
radiation effects on cleavage crack propagation in single-crystal, 20: 16513
transfer from heavy water to water, free energy and entropy of, 20: 16488
NaCl–H_2SO_4, radioinduced absorption spectra in, at 77°K, 20: 16534

SODIUM FLUORIDES
radioinduced defects in, ESR of, (E/T), 20: 17975(R) (NYO-2047-36)

SODIUM FORMATES
effects on self-irradiation decomposition of tritium-labeled organic compounds, 20: 16533

SODIUM HYDRIDES
Na–NaH–NaOH, corrosive effects on Croloy 2¼ steel, 20: 16599(R) (BAW-1280-34)

SODIUM HYDROXIDES
corrosive effects on Croloy 2¼ steel, 20: 16599(R) (BAW-1280-34)
effects on uranium sorption by platinized carbon, 20: 16581
Na–NaH–NaOH, corrosive effects on Croloy 2¼ steel, 20: 16599(R) (BAW-1280-34)
Na–NaOH, corrosive effects on Croloy 2¼ steel, 20: 16599(R) (BAW-1280-34)

SODIUM IODIDES
activity and osmotic coefficients in heavy water at 25°C, 20: 16488
analysis of iodine-131-labeled, by paper chromatography, 20: 16372

efficiency of thallium-doped scintillators of, for x-ray detection, 20: 16836
purification of iodine-131-labeled, by paper chromatography, 20: 16372
radioinduced luminescence of thallium-activated, excitation mechanism in x, 20: 17991(T)
scintillation performance of thallium-doped, activator concentration effects on, 20: 16850
NaI–H_2SO_4, radioinduced absorption spectra in, at 77°K, 20: 16534
SODIUM ISOTOPES Na-22
beta decay of, energy of positron group from, (E), 20: 16867
beta transitions in, higher-order effects in allowed, (E), 20: 17678 (COO-1420-113)
content in Bogou iron meteorite, 20: 16674
content in food chain, ratio to fallout of, 20: 16678
content in stratospheric and tropospheric samples in Project Star Dust, 1963, 20: 16727(R) (HASL-168)
content in stratospheric and tropospheric samples in Project Star Dust, 1964, 20: 16728(R) (HASL-169)
diffusion in sodium oxide–calcium oxide–silicon oxide systems, residual activity method for self-, 20: 16478
half life, 20: 16331 (GA-6568)
SODIUM ISOTOPES Na-23
helium-3 reactions (He-3,α) at 12 Mev, Q value for, 20: 16331 (GA-6568)
neutron reactions (n,p) with, sensitivity of, for activation analysis, 20: 16332 (GA-6691)
SODIUM ISOTOPES Na-24
radioinduced in asbestos cement products by neutrons, tracer use of, 20: 16920 (SGAE-IB/IA-7/1965)
sensitivity for activation analysis using beta-gamma-gamma sum-coincidence gamma spectrometer, 20: 16335(R) (NBS-TN-276)
SODIUM NEODYMIUM FLUORIDES
crystal structure, 20: 17158(R) (ORNL-3900, pp 82-149)
SODIUM NITRATES
diffusion and electric mobility of ions in, tracer study on, 20: 16414 (CEA-R-2806)
ion exchange distribution of alkali and alkaline earth metals between chabazite and fused, 20: 16340 (USNRDL-TR-970)
KNO_3–$NaNO_3$, diffusion and electric mobility of ions in, 20: 16414 (CEA-R-2806)
$LiNO_3$–$NaNO_3$, diffusion and electric mobility of ions in, 20: 16414 (CEA-R-2806)
SODIUM NITROPRUSSIDE
properties for use as standard for Mössbauer spectroscopy, 20: 16335(R) (NBS-TN-276)
SODIUM OXIDES
determination in Moldavites by mass spectrometry and x-ray fluorescence, 20: 16711(R) (MIT-1381-13)
CaO–SiO_2–Na_2O, diffusion of sodium-22 in solid, residual activity method for self-, 20: 16478
SODIUM PEROXIDE
sintering with plutonium dioxide, 20: 16350
SODIUM PERXENATES
uses in spectrophotometric determination of manganese, 20: 16351
SODIUM PYROPHOSPHATES
reactions with uranyl nitrate, 20: 16472
SODIUM SULFATES
effects of sulfur-35-labeled, on skeletal growth in rats, 20: 16267
SODIUM SYSTEMS
Na–NaH–NaOH, corrosive effects on Croloy 2¼ steel, 20: 16599(R) (BAW-1280-34)
Na–NaOH, corrosive effects on Croloy 2¼ steel, 20: 16599(R) (BAW-1280-34)
SODIUM TETRABORATES
corrosive effects on structural materials, 20: 16976
SOILS
cesium-137 content in, of Cache la Poudre, Colorado, 20: 16723 (COO-1156-11)
cesium-137 content in, in Japan, 20: 16169
cesium-137 in, uptake by plants, 20: 16678
density and moisture of, calibration of neutron-gamma probe for, 20: 16374
gamma dosimetry in, methods for, 20: 16687
polonium-210 content in, 20: 16189
properties of, effects of, on plant uptake of radioisotopes, 20: 18174(R) (NP-15771)
radioactive particle deposition on pasture, rate of, 20: 16160 (UCRL-14739(Pt.2))
radioisotope distribution in, model for, 20: 16168
radium-226 content in, Bombay and Kerala, India, 20: 16747
radon emission from, in European USSR and Kazakhstan, 20: 16691
sodium-22 in, uptake by plants, 20: 16678
waste disposal in injection in, hydrodynamics of, 20: 18163(R) (NP-15859)
SOLAR BATTERIES
development of radiation-resistant, 20: 16910 (N-65-18448)
radiation damage in, electron and proton, 20: 16910 (N-65-18448)
radiation effects on defects in silicon, effects of impurities on electron and proton, 20: 17125 (NASA-CR-404)
radiation effects on junctions, proton, 20: 16907(R) (N-65-17517)
SOLAR FLARES
effects on intensity of cosmic radiation, (E), 20: 17313(T)
properties of, spectral analysis for determining, 20: 17230
proton distribution from, diffusion effects in, (T), 20: 17228 (N-65-18275)
spectral analysis of, 20: 17230
SOLAR RADIATION
boundary of solar wind with magnetosphere, 20: 17249
charge distribution of corpuscular, system for determining, 20: 17307 (CONF-651001-34)
detection and measurement of x, instruments for, 20: 16904
deuterium abundance in, system for determining, 20: 17307 (CONF-651001-34)
doses in low-shielding space systems, 20: 16300
element abundances in solar wind, (T), 20: 17236
intensity of low-energy protons in space, (E), 20: 17318
interaction of solar wind with magnetosphere, magnetic field perturbation from simulated, (E), 20: 17546
interactions of solar corpuscular stream with geomagnetic fields, (T), 20: 17547(T)
interactions of solar plasma with geomagnetic fields, (E), 20: 17551
interactions of solar wind with planets, (T), 20: 17232
model for solar wind, exospheric, (T), 20: 17236
properties of, 20: 16745
reactions of, nuclear synthesis in, 20: 17234
use in waste evaporation, 20: 18164(R) (NP-15874)
SOLCOSERYL
radiosensitivity effects on mice and rabbits, 20: 16302
SOLDERS
design of superconducting, optimization of, 20: 16592
SOLENOIDS
beam focusing by superconducting, (T), 20: 17197 (CONF-650922, pp 536-40)
design and fabrication of cryogenic, with integral coolant passages, 20: 17874 (CONF-650922, pp 630-42)
design of high-field d-c, 20: 17158(R) (ORNL-3900, pp 82-149)
design of superconducting, for NMR spectrometers, 20: 17587 (CONF-650922, pp 517-24)
design of superconducting, for magneto-optical studies, 20: 17588 (CONF-650922, pp 525-9)
design of symmetrically separated pairs of, with minimum volume, 20: 17180 (CONF-650922, pp 111-25)
electric properties of normal region in superconducting niobium–zirconium, 20: 17610
fabrication of superconducting, from stranded niobium–tin wire, 20: 17593 (CONF-650922, pp 597-603)
stress analysis of cryogenic high-field, 20: 16586 (CONF-650922, pp 723-32)
SOLID STATE REACTIONS
research programs at Risö on, 20: 18174(R) (NP-15771)
SOLIDS
analysis for hydrogen by beta absorption, 20: 16356
density profiles in turbulent flow, (E/T), 20: 16606(R) (TID-22621)
effects on statistical structure of turbulence in fluid flow, (T), 20: 16606(R) (TID-22621)
electron relaxation in, theory of, 20: 18016
electron transmission in, mean free path of, at 3 ev, 20: 16159(R) (ORNL-3900, pp 150-81)
electrons in, normal-Fermi-liquid theory for, 20: 17993
magnetic properties of, determination by neutron diffraction, 20: 17158(R) (ORNL-3900, pp 82-149)
radiation effects on, with surface-sorbed gases, 20: 17158(R) (ORNL-3900, pp 82-149)
radiation enhanced diffusion in, effects of correlated defects in gamma-, 20: 17131
gas–solid, efficiency as working fluid in Brayton cycle, (T), 20: 16606(R) (TID-22621)
SOLUTIONS
analysis for sulfur in aqueous, activation, 20: 16331 (GA-6568)
separation of cesium-137 from aqueous, by flotation, 20: 16392
specific gravity of, automated equipment for measuring, engineering drawings of, 20: 16801
SOLVENT EXTRACTION PROCESSES
equipment design for, 20: 16582
mechanisms of, research on, 20: 17158(R) (ORNL-3900, pp 82-149)
pulse columns for countercurrent, at Eurochemic, 20: 16561
use for separation of transplutonium elements, review on, 20: 16402

SOLVENTS
effects of organic, on nitrogen isotope distribution between oxides in gaseous and liquid phases, 20: 16486
SOUND
absorption by liquid helium II, (T), 20: 17611(T)
propagation in superfluid helium, equations for, (T), 20: 17640
SOUTHWEST EXPERIMENTAL FAST OXIDE REACTOR
fuel rod vibrations in, effects of coolant flow on, (E), 20: 18134 (GEAP-4966)
SOVIET UNION
fallout monitoring at Vilnius in 1962, 20: 16700
fallout monitoring near Leningrad, 1961–1963, 20: 16701
fallout monitoring of strontium-90 in polar regions of, 20: 16703
stable isotope production and uses in, 20: 16933
strontium-90 content in surface waters in, 1961–1962, 20: 16705
SPACE
cosmic-ray intensity gradient and variation in interplanetary, (T), 20: 17312(T)
radiation environment in, review on, 20: 17249
radiation environment in, review of effects on electronic components, 20: 16911
reactor operation in, electrostatic energy from, (T), 20: 18131
SPACE FLIGHT
effects on man, 20: 16231 (UCRL-16377)
radiation hazards during, 20: 16745
SPACE VEHICLES
heat-shield ablation, instrumentation for measurement of, 20: 16778 (NASA-TN-D-3329)
instrumentation of Mariner C, for detection and measurement of cosmic radiation, 20: 16822 (N-65-19927)
interactions with ionized media, 20: 17537 (JPLAI/LS-641)
ion engines for, effects of secondary electron emission in, 20: 16624 (N-65-17749)
ion engines for, flight testing of, 20: 16625 (N-65-19272)
materials used in, performance and selection of, 20: 16944 (NASA-SP-3025)
propulsion systems for, mission performance of electric, 20: 16628
radiation doses from solar-flare heavy nuclei, 20: 16300
shielding calculations for, 20: 17965
SPARK CHAMBERS
design of isotropic, 20: 16860(T)
development of isotropic monogap, pulsed with damped oscillations, 20: 16886
magnets for, design using tape-wound coils, 20: 16809 (CONF-650922, pp 253-61)
particle tracks in, flying spot digitizers for analysis of, 20: 16840
particle tracks in, pulse-pattern generator for analysis of, 20: 16881
performance for recording meson (π^+)-proton interactions at 180°, 20: 16815 (JINR-P-2506)
performance of corrugated-plate, in neutron detection and measurement, 20: 16894
SPECTROMETERS
charged particle trajectories in magnetic, Fermat principle for, (T), 20: 16821 (LAL-1151)
design of double-focusing magnetic, for electron scattering studies, 20: 16808 (CONF-650922, pp 154-63)
performance of magnetic, for meson (K^0) decays, 20: 16814 (ITEF-386)
uses in physics research, 20: 18174(R) (NP-15771)
SPECTROSCOPY
methods for plasma-jet, 20: 17901
proton magnetic resonance, use of deuterated organisms in, 20: 16165
SPERMATOGENESIS
radiation effects on Drosophila, mutagenic, 20: 16229(R) (NYO-1472-1)
SPHALERITES
deuterium content of fluid inclusions in, from Mexico, 20: 16634
SPINAL CORD
radiosensitivity of, in man, 20: 16251
SPLEEN
radiation effects on iron metabolism in rat, tracer study of γ, 20: 16187
radiation effects on transplanted Yoshida sarcoma cells in rat, tracer study, 20: 16188
radiation effects on catalase activity in rat, 20: 16277
SPONTANEOUS FISSION
energy release in, (T), 20: 17862
SPORES
photoproducts induced in bacterial, by uv, 20: 16159(R) (ORNL-3900, pp 150-81)
STABLE ISOTOPES
book: *Stable Isotopes. Catalog for Stable Isotopes, Compounds, and Products with Enriched Stable Isotopes*, 20: 16933
STACK DISPOSAL
dilution of long- and short-term emissions in Eurochemic, estimates of minimum, 20: 18162 (NP-15754)
STAINING
radiation effects on response of mycobacteria to, 20: 16195
STAINLESS STEEL
analysis for arsenic and manganese, activation, 20: 16338 (RT/CHI-(65)36)
analysis for cerium, photometric, 20: 16380
analysis for oxygen, activation, 20: 16331 (GA-6568)
bonding to carbon steel pressure vessels, testing of, 20: 16617
corrosion by boron-containing solutions, 20: 16976
corrosion of type 304, effects on nitrogen content on stress-, 20: 16969(R) (EURAEC-1579)
corrosion of type 316, by sodium at 1100 and 1200°C, mechanisms of, 20: 16970 (GEAP-4832)
corrosion of 300-series, in in-pile high-purity boiling water, 20: 18089 (NAA-SR-Memo-10178)
corrosion resistance of type 430, effects of molybdenum or uranium alloying additions on, 20: 16975 (NP-15900)
deposition on heavy gage steels by welding, development of methods for, 20: 16991(R) (EURAEC-1557)
deposition on low alloy steel by welding, development of methods for, 20: 16990(R) (EURAEC-1556)
ion reactions with stellarator walls of, re-emission rates for helium and hydrogen, (E), 20: 17922
iron-57 Mössbauer effect in, self-absorption effects on, (E), 20: 17990
properties of types 310 and 316, effects of rare earth alloying additions on, 20: 17078
radiation effects on corrosion resistance of type 304L, gamma, 20: 17118(R) (EURAEC-1564)
radiation effects on fuel cladding of type 304, reactor, 20: 17120 (GEAP-4916)
radiation effects on ductility of, role of helium bubbles in, 20: 17141
reduction of oxide films on type 304, effects of surface treatment on coulometric, 20: 17118(R) (EURAEC-1564)
response of cylinders of 304 and 304L, to explosive loads, 20: 18019(R) (IDO-17146)
sputtering by deuterons at 30 kev, yields from, 20: 17892(R) (ORNL-3908, pp 149-53)
B–stainless steels, mechanical properties of irradiated fuel cladding of, 20: 17121 (GEAP-4918)
B–stainless steel, radiation effects on corrosion resistance of modified austenitic, neutron, 20: 17118(R) (EURAEC-1564)
Eu_2O_3–stainless steel, radiation effects on control rods of, reactor, 20: 17129 (ORNL-TM-1407)
STANDARDS
development for radioisotopes in Australia, 20: 16746
specifications for iodine-131, for thyroidal uptake measurements, 20: 16315
use of internal, in liquid scintillation counting, dispenser for, 20: 16834
STANFORD LINEAR ACCELERATOR
beam transport magnets for, calibration of, 20: 17206 (CONF-650922, pp 823-34)
STARS
quark production in quasars, (T), 20: 17411
radiation emission and propagation from quasi-stellar radio sources, (T), 20: 17242
theory of novas and quasi-, 20: 17243
x-ray emission from neutron, (T), 20: 17240
x-ray emission from, review and analysis of, 20: 17248
STATISTICS
parameters in, power-series expansion for, 20: 17527
radiation transport in, spectral theory for stationary operator for, 20: 17658
STEAM
monitoring of, from fission products, 20: 16825 (ORNL-TM-1442)
STEEL
analysis for aluminum, computer use for activation, 20: 16335(R) (NBS-TN-276)
analysis for carbon, activation, 20: 16331 (GA-6568)
analysis for cerium, photometric, 20: 16380
analysis for oxygen, comparison of hot-extraction and activation, 20: 16400
analysis for oxygen, activation, 20: 16357
coating with stainless steel by welding, development of methods for, 20: 16990(R) (EURAEC-1556)
coating with stainless steel by welding, development of methods for, 20: 16991(R) (EURAEC-1557)
decontamination of, ultrasonic, 20: 16767
magnetic properties of flat-rolled, variation with composition and processing techniques, 20: 17009
magnetic properties for use in gradient magnets, determination of, 20: 17010 (CONF-650922, pp 297-304)
radiation effects on atomic arrangement in, 20: 18046(R) (ORNL-3900,

pp 2-81)
radiation embrittlement of Soudotenax and T-1, neutron, 20: 17117 (EURAEC-1558)
radiography using cold neutrons, 20: 16616
reactions of molten AMS 5350, with alumina, fused silica, zircon, and zirconia, 20: 16984
STELLARATORS (A-2)
ion reactions with stainless steel wall of, re-emission rates for helium and hydrogen, (E), 20: 17922
STEROIDS
effects on development of female fish, 20: 16263
STEROIDS, 17-KETO-
radiation effects on, following tumor therapy, 20: 16209
use in determining radiation response, 20: 16209
STEROLS
labeling of desmosterol and lanosterol with carbon-14, 20: 16548
STILBENE
scintillation pulse-shape discrimination in, circuit for determining, 20: 16839
scintillation response of, time-dependent, 20: 16813 (INR-653/1A/D)
STRATOSPHERE
dispersion of radioactive aerosols in, 20: 16643
fallout content and transport in, 20: 16698
fallout in, deposition and distribution of, 20: 16697
fallout monitoring in Star Dust Project, 1963, 20: 16727(R) (HASL-168)
fallout monitoring in Project Star Dust, 1964, 20: 16728(R) (HASL-169)
STRESS ANALYSIS
of cryogenic high-field solenoids, 20: 16586 (CONF-650922, pp 723-32)
STRONTIUM
abundance in sun, (E), 20: 17237
content in Ammonoosuc volcanics and Monson gneiss in New England, age estimations from, 20: 16711(R) (MIT-1381-13)
content in granites, quartzites, and slate in Massachusetts, age estimation from, 20: 16711(R) (MIT-1381-13)
content in Great Lakes and Hudson Bay, geochemistry of, 20: 16711(R) (MIT-1381-13)
content in Jardine-Crevasse Mountain area, Montana, age estimation from, 20: 16711(R) (MIT-1381-13)
content in rabbit skeleton, 20: 16178
content in tektites in Moldavia, age estimation from, 20: 16711(R) (MIT-1381-13)
content ratio to rubidium in geological materials, differentiation of Earth's mantle by studying, 20: 16711(R) (MIT-1381-13)
determination in biological and geological samples by x-ray fluorescence methods, 20: 16345
determination in Moldavites by mass spectrometry and x-ray fluorescence, 20: 16711(R) (MIT-1381-13)
determination in presence of barium and calcium by ring oven techniques, 20: 16388
determination in rocks by x-ray spectrography, 20: 16711(R) (MIT-1381-13)
diffusion from ceramic wastes, effects of volatilization on, 20: 18156 (BNWL-SA-453)
effects of, with calcium on manganese sorption by barley roots, 20: 16174(R) (RLO-1547-3)
effects on cartilage growth in rats, 20: 16181
excretion in rats, effects of pyridoxine on, 20: 16176
separation from sewage water by sorption on multiclone dust from gasification of coke, 20: 18170
STRONTIUM COMPLEXES
stability constants of, determination of, by metal distribution between aqueous phase and ion exchanger, 20: 16481
STRONTIUM IONS
sorption by aminodiacetate resin Dowex A-1, 20: 16358
STRONTIUM ISOTOPES
separation of, performance of separator for, 20: 16928(R) (INSJ-92)
STRONTIUM ISOTOPES Sr-85
energy levels from yttrium-85 decay, parity and spin of, (E), 20: 17670 (AD-629576)
separation from milk using calcium phosphate precipitation method, 20: 16382
uptake from human gastrointestinal tract, effects of sodium alginate on, 20: 16173 (PG-Report-686)
use in measurement of bone blood flow, 20: 16192
STRONTIUM ISOTOPES Sr-86
content in Archean Seas, age estimation from, 20: 16711(R) (MIT-1381-13)
content in granites, quartzites, and slate in Massachusetts, age estimation from, 20: 16711(R) (MIT-1381-13)
content in Great Lakes and Hudson Bay, geochemistry of, 20: 16711(R) (MIT-1381-13)
STRONTIUM ISOTOPES Sr-87
content in Archean Seas, age estimation from, 20: 16711(R) (MIT-1381-13)
content in granites, quartzites, and slate in Massachusetts, age estimation from, 20: 16711(R) (MIT-1381-13)
content in Great Lakes and Hudson Bay, geochemistry of, 20: 16711(R) (MIT-1381-13)
production in geological materials by rubidium-87 decay, 20: 16711(R) (MIT-1381-13)
STRONTIUM ISOTOPES Sr-89
content in fallout at 156 world land sites, 1957 to 1965, 20: 16662(R) (HASL-165)
content in fallout and precipitation near Leningrad, 20: 16704
content in milk and plants before and after Salmon Event, 20: 16743 (VUF-1021)
content in rain water, Fayetteville, Arkansas, Oct. 1964, 20: 16663 (TID-21470)
content in stratospheric and tropospheric samples in Project Star Dust, 1964, 20: 16728(R) (HASL-169)
content in stratospheric and tropospheric samples in Project Star Dust, 1963, 20: 16727(R) (HASL-168)
determination in milk, solid foods, and water, methods for, 20: 16369
separation from milk using calcium phosphate precipitation method, 20: 16382
STRONTIUM ISOTOPES Sr-90
accumulation in soils near Leningrad, 20: 16702
content in antlers and bones of Colorado mule deer, 20: 16724 (COO-1156-12)
content in atmospheric dust and rain water, 1964–65, 20: 16660 (AERE-R-4997)
content in atmosphere, milk, rain water, water supplies, and wheat in Japan, 1964, 20: 16731 (NP-15883)
content in body and urine of Japanese, 20: 16226 (NP-15891)
content in bones of children in U. S., 1965, 20: 16662(R) (HASL-165)
content in diet in U. S., 1960 to 1965, 20: 16662(R) (HASL-165)
content in fallout at 156 world land sites, 1957 to 1965, 20: 16662(R) (HASL-165)
content in fallout and precipitation near Leningrad, 20: 16704
content in man, whole-body, 20: 16303(R) (AD-626384)
content in milk and plants before and after Salmon Event, 20: 16743 (VUF-1021)
content in powdered milk in Japan, 1962 and 1963, 20: 16755
content in primary teeth of children, 20: 16763
content in rain water, Fayetteville, Arkansas, Oct. 1964, 20: 16663 (TID-21470)
content in rain water in Japan, 1962 and 63, 20: 16671
content in stratospheric and tropospheric samples in Project Star Dust, 1964, 20: 16728(R) (HASL-169)
content in stratospheric and tropospheric samples in Project Star Dust, 1963, 20: 16727(R) (HASL-168)
content in surface layer of atmosphere over Heis Island and Moscow, 20: 16650
content in surface waters in Soviet Union, 1961–1962, 20: 16705
determination in milk, solid foods, and water, methods for, 20: 16369
dispersion of aerosols of, in stratosphere, 20: 16643
distribution in atmosphere over oceans, dependence of, on meteorological factors, 20: 16699
distribution in deep sea water near Japan, vertical, 20: 16681
effects on behavior in dogs after chronic enteral administration, 20: 16266
effects on dog skeleton, 20: 16253
effects on thymidine excretion by rats, 20: 16201
fallout monitoring near Leningrad in 1961–1963, 20: 16701
fallout monitoring in polar regions of Soviet Union, 20: 16703
ground water contamination by, in Shoal Event, hazards from, 20: 16742 (VUF-1014)
incorporation in titanate pellets for thermoelectric generators, 20: 16914(R) (ORNL-3900, pp 182-93)
separation from milk using calcium phosphate precipitation method, 20: 16382
sorption from waste solutions by aluminum oxide, mechanism of, 20: 16330 (CEA-R-2851)
uptake by rabbit bones and plasma, 20: 16178
use for radiotherapy, 20: 16305
use for therapy of skin tumors, 20: 16325
yields from thorium-232 fission, (E), 20: 17860
STRONTIUM NITRATES
ion exchange and sorption on glass surfaces, 20: 16469
STRONTIUM OXIDES
content in Keewatin and Timiskaming volcanic rocks at Kirkland Lake, Ontario, age estimations from, 20: 16711(R) (MIT-1381-13)
content in volcanic rocks in Lower Cambrian in Canada, age estimation from, 20: 16711(R) (MIT-1381-13)
reactions with aluminum oxides and lanthanum or neodymium oxides at

1400 to 1500°C, 20: 16482
BaO–IrO_2–SrO, crystal structure, 20: 16436
BaO–RuO_2–SrO, crystal structure, 20: 16436
Er_2O_3–SrO, properties of compounds formed by interactions in, 20: 17044
Ho_2O_3–SrO, properties of compounds formed by interactions in, 20: 17044
La_2O_3–SrO, properties of compounds formed by interactions in, 20: 17044
SrO–Tm_2O_3, properties of compounds formed by interactions in, 20: 17044
SrO–Yb_2O_3, properties of compounds formed by interactions in, 20: 17044
SrO–Y_2O_3, properties of compounds formed by interactions in, 20: 17044

STRONTIUM TITANATES
preparation of strontium-90-bearing pellets of, 20: 16914(R) (ORNL-3900, pp 182-93)

STRONTIUM TUNGSTATES
thermionic emission from surfaces of, in vacuum, (E), 20: 17335

STRUCTURES
nuclear blast effects on, calculation of fire resistance to, 20: 16621 (AD-625867)

STYRENE
radioinduced grafting on cellulose fibers, properties of product in, 20: 16507 (INR-671/XVII/C)
radioinduced polymerization with rayon, 20: 16528

STYRENE POLYMERS
analysis for carbon-14 and tritium by combustion and liquid scintillation counting, 20: 16384
analysis for chlorine, activation, 20: 16335(R) (NBS-TN-276)

SUCCINATES
radiation effects on oxidation of, in *Vibrio cholerae*, 20: 16198

SUCCINIC ACID
radioinduced addition of hydrogen to fumaric acid in single crystals of, 20: 16537

SUCCINIC DEHYDROGENASE
radiation effects on activity of, in mouse tissue homogenates and skin, uv, 20: 16196

SULFANILIC ACID
analytical use for spectrophotometric determination of cerium, 20: 16398

SULFONATES
effects on plants, review of mutagenic, 20: 16225 (EUR-2715.f)

SULFUR
determination by isotopic dilution, 20: 16362
determination in aqueous solutions, activation, 20: 16331 (GA-6568)
determination in hair of accident victims, radiation dosimetry from, 20: 16758
determination in rare earth sulfides, 20: 16395
isotopic analysis of, mass spectrometric, 20: 16379
photon reactions with Coulomb field of, pair production total cross sections for high-energy, (T), 20: 17754

SULFUR COMPOUNDS
radiosensitivity effects in animals and plants, 20: 16297(R) (EUR-2548.f)

SULFUR IONS
electron spin resonance of molecular, in alkali halide single crystals, (E/T), 20: 18005

SULFUR ISOTOPES
abundance ratios in sandstone-type uranium deposits, Gas Hills District, Wyoming, 20: 16670
separation of, performance of separator for, 20: 16928(R) (INSJ-92)

SULFUR ISOTOPES S-31
energy levels from sulfur-32 (He-3,α) reactions, (E), 20: 17780

SULFUR ISOTOPES S-32
energy levels in, excitation of alpha-cluster, (T), 20: 17802
helium-3 reactions (He-3,p) at 12 Mev, Q value for, 20: 16331 (GA-6568)
helium-3 reactions (He-3,α) at 12.1 Mev, sulphur-31 levels from, (E), 20: 17780
proton reactions (p,2p) at 140 Mev, energy spectra and angular correlation distributions from, (E), 20: 17741

SULFUR ISOTOPES S-33
neutron reactions, production of phosphorus-33 in, 20: 16914(R) (ORNL-3900, pp 182-93)

SULFUR ISOTOPES S-35
chemical species containing, following neutron irradiation of cysteic acid, cysteine, and cystine, 20: 16540
determination in organic sample by combustion and scintillation counting, 20: 16387
determination in organic compounds by gas chromatography and scintillation counting, 20: 16371
effects of sodium sulfate-incorporated, on skeletal growth in rats, 20: 16267

SULFURIC ACID
effects on peptization of solid thorium oxide, mechanism of, 20: 16419(T) (UCRL-Trans-1301(L))
processing and disposal of glass melter condensates containing, methods for, 20: 18159 (BNWL-SA-514)
radiation effects on glasses of, with sodium bromide, chloride, and iodide, 20: 16534
separation from fission products in waste condensates, methods for, 20: 18159 (BNWL-SA-514)
solvent properties for thorium in uranium leach solutions, 20: 16573
spectra of vapors over deuterated and normal, infrared, 20: 16442
$K_2Cr_2O_7$–H_2SO_4, properties for use in ultrasonic cleaning of cobalt-60 from Duralumin and steel-3, 20: 16767
$KMnO_4$–H_2SO_4, properties for use in ultrasonic cleaning of cobalt-60 from Duralumin and steel-3, 20: 16767
NaBr–H_2SO_4, radioinduced absorption spectra in, at 77°K, 20: 16534
NaCl–H_2SO_4, radioinduced absorption spectra in, at 77°K, 20: 16534
NaI–H_2SO_4, radioinduced absorption spectra in, at 77°K, 20: 16534

SUN
atmosphere of, abundance of elements in, 20: 17229
element abundance analysis of, (E), 20: 17237
rare earth abundance analysis of, (E), 20: 17237
x-ray emission from, review and analysis of, 20: 17248

SUPERCONDUCTIVITY
research on, review of, 20: 17628

SUPERCONDUCTORS
coupling constant range for coexistence of singlet and triplet pairs in anisotropic, 20: 17645
critical currents in, equipment for measuring, 20: 17602
critical currents in niobium diselenide single crystals, effects of stoichiometry on peak, (E), 20: 17609
critical fields of niobium-, temperature dependence of Ginsberg-Landau parameter for, 20: 17585 (AD-627910)
critical fields of aluminum film, (E/T), 20: 17622
critical magnetic field strength of pure, pressure effects on, (T), 20: 17639
current flow patterns in nonideal type II, in longitudinal fields, (E/T), 20: 17617
design modification for energy-storage-system, 20: 17625
design of magnets of, for traveling-wave masers, 20: 17626
electric properties of normal region of niobium–zirconium magnets, 20: 17610
electron tunneling from films of, into normal metals, electron interference effects in, (E/T), 20: 17621
electron tunneling evidence for fluxon entry into thin type II, (E/T), 20: 17627
electron tunneling in tin-junction, structure of high-frequency Josephson, (E), 20: 17636
energy gap of tin, (E), 20: 17619
energy gaps of, effects of electron-damped dislocations on determination of, (T), 20: 17618
energy losses from magnet coils of, (E), 20: 17630
fabrication of Nb_3Sn cylinder and ribbon, using diffusion layers, 20: 17649
Hall effect measurements on niobium–zirconium magnets, 20: 17600(R) (ORNL-3908, pp 114-48)
magnetic flux jumping in high-field indium-impregnated porous glass, field sweep-rate and temperature dependence of, (E), 20: 17604
magnetic flux motion in magnetically coupled films of, (E/T), 20: 17623
magnetization in mixed state of alloys of, temperature dependence of, (T), 20: 17633
performance of hollow cylindrical, as magnetic lens, 20: 17631
power degradation phenomena in coils of niobium–zirconium, (E), 20: 17629
power losses of surface sheath of, I-f, (T), 20: 17620
properties of titanium iodide, compression and deformation effects on, (E), 20: 17634
specific heat at transition point, (T), 20: 17612(T)
transition temperature of pure, pressure effects on, (T), 20: 17639
transition temperature of, diamagnetic impurity effects on, (T), 20: 17637
ultrasonic absorption in tin single-crystal, temperature dependence of, (E), 20: 17605
ultrasonic absorption in indium, nonlinear effects in, (E), 20: 17635
ultrasonic attenuation in nonideal niobium–zirconium, flux jumping and magnetization effects on, (E), 20: 17606
use for strong magnetic field production and memory devices, review of, 20: 17628
use in bridge cell for memory devices, 20: 16797
use in electronic equipment, power-loss reduction from, 20: 17603

SUPERFLUIDITY
theory of, two-particle excitation spectrum in Landau, 20: 17646

SUPERHEATERS
development of sodium-heated steam, 20: 16599(R) (BAW-1280-34)

SUPERHEATERS (NUCLEAR)
fuel elements for AEG, development of, 20: 18077

SURFACE WATERS
geochemistry of Great Lakes and Hudson Bay, 20: 16711(R) (MIT-1381-13)
radioactivity in Monticello Project Area, Utah, 20: 16729 (IDO-12049)

radioactivity monitoring of, at Portsmouth Gaseous Diffusion Plant, 1965, 20: 16726 (GAT-506)
strontium-90 content in Soviet Union, 1961–1962, 20: 16705
tritium content variations in levels of Mont Cenis Lake, France, 1964 and 1965, 20: 16668
SURGERY
use for breast cancers, evaluation of effects of radiotherapy after, 20: 16324
use for carcinomas of larynx, 20: 16313
use for therapy of thyroid cancers, 20: 16307
SUSPENSIONS
density profiles in turbulent flow, (E/T), 20: 16606(R) (TID-22621)
effects on statistical structure of turbulence in fluid flow, (T), 20: 16606(R) (TID-22621)
efficiency as working fluid in Brayton cycle, (T), 20: 16606(R) (TID-22621)
heat transfer by, effects of thermal plate-out on, (T), 20: 16606(R) (TID-22621)
heat transfer coefficients in gas–solid, (E), 20: 16606(R) (TID-22621)
thermal force effects in dense, (T), 20: 16606(R) (TID-22621)
thermal force effects in dense, (T), 20: 16606(R) (TID-22621)
SWIMMING POOL REACTORS
reactivity temperature coefficients of, method for measuring, (E/T), 20: 18145
SWINE
radiation effects on copper and zinc content and enzyme activity in blood serum of, 20: 16222 (AFWL-TR-65-112)
SWITCHES
status of silicon-controlled rectifier thyristor, 20: 16774 (CONF-650922, pp 788-96)
use of superconducting, energy losses in, (E), 20: 17630
SYNCHROCYCLOTRONS
magnetic median plane in, determination using Hall effect, 20: 17189 (CONF-650922, pp 421-7)
SYNCHROTRONS
beam ejection from proton synchrophasotrons, slow, 20: 17208 (JINR-P-2537)
beam transport magnets of CERN proton, 20: 17183 (CONF-650922, pp 218-38)
betatron oscillation resonances in, 20: 17221
magnet coils for 4-Bev electron, design and fabrication of, 20: 17199 (CONF-650922, pp 686-99)
magnet power supplies for proton, 20: 17202 (CONF-650922, pp 755-68)
phase oscillations in, (T), 20: 17174 (CERN-66-6)
radiation levels near CERN proton, 20: 17212(T) (UCRL-Trans-1305)
SYNERGISTIC ACTION
of calcium and magnesium on manganese sorption by barley roots, 20: 16174(R) (RLO-1547-3)
of calcium and strontium on manganese sorption by barley roots, 20: 16174(R) (RLO-1547-3)
of ferrous iron and calcium or magnesium on manganese sorption by barley roots, 20: 16174(R) (RLO-1547-3)
SYSTEMS FOR NUCLEAR AUXILIARY POWER
development of, review of, 20: 18182
materials for, corrosion testing of, 20: 18020(R) (ORNL-3900, pp 2-81)
SYSTEMS FOR NUCLEAR AUXILIARY POWER (SNAP-9)
cadmium-109 distribution in atmosphere from high-altitude burn-up of, predictions for, 20: 16662(R) (HASL-165)
plutonium-238 distribution in atmosphere from high-altitude burn-up of, predictions for, 20: 16662(R) (HASL-165)
SZILARD-CHALMERS REACTIONS
effects on praseodymium complexes with β-diketones, 20: 16416(R) (NYO-906-68)

T

TANKS
flow in liquid-hydrogen, boundary layer characteristics in, 20: 17536
TANTALUM
analysis for oxygen, activation, 20: 16331 (GA-6568)
compatibility with alumina, beryllia, magnesia, and boron nitride, 20: 17022 (N-65-18933)
determination in asbestos using ion exchange, activation, 20: 16336(R) (NYO-10175)
determination simultaneously with niobium in minerals and ores, activation, 20: 16336(R) (NYO-10175)
diffusion barriers between hafnium–20 tantalum cladding on tantalum–10 tungsten, performance of, 20: 16943(R) (IITRI-B237-45)
diffusion in tungsten to 4000°F, inter-, 20: 16943(R) (IITRI-B237-45)
dislocation parameters for, 20: 17033
oxidation of substrates of, at 30 to 1500°C, mechanism of initial, 20: 16987
TANTALUM ALLOY COUPLES
Hf–Ta/Ta–W, fabrication by roll cladding and hot spinning, rocket nozzle, 20: 16943(R) (IITRI-B237-45)
TANTALUM ALLOYS
Al–Fe–Ta, phase studies on intermetallic compounds in, 20: 17075
Al–Nb–Ta–Ti, corrosion cracking in titanium-base, stress-, 20: 16967 (AD-628277)
Al–Ta, phase studies at 900 to 1300°C, 20: 17034
Cr–Ta, phase transformations in, 20: 17046
Ge–Ta–V, phase studies on intermetallic compounds in, 20: 17075
Hf–Ta, diffusion into tantalum–10 tungsten alloy, effects of niobium and tantalum barriers on, 20: 16943(R) (IITRI-B237-45)
Hf–Ta, phase studies, 20: 17092
Hf–Ta–W, fabrication of tubing of T-111, 20: 16998
Hf–Ta–W, phase studies at 1100 and 1600°C, 20: 17012(R) (DRI-1092-226)
Mo–Nb–Ta–W, deformation mechanisms in solution-hardened niobium-base, 20: 17082
Mo–Nb–Ta–W, properties as hollow turbine vanes, 20: 16963
Mo–Ta, electric conductivity of single-crystal, specific, 20: 17083
Nb–Ta, current flow patterns in superconducting, in longitudinal fields, (E/T), 20: 17617
Nb–Ta–W–Zr, properties as hollow turbine vanes, 20: 16963
Ni–Nb–Ta, diffusion of nickel in, effects of annealing temperature and composition on, 20: 17089
Ni–Ta, effects of additives on high-temperature properties of eutectic, 20: 17108
Pt–Ta, superconductivity in close-packed intermediate phases of, 20: 17624
Rh–Ta, superconductivity in close-packed intermediate phases of, 20: 17624
Ta–Sn, tin-119 isomeric shift in, 20: 18004
Ta–W, compatibility with alumina, beryllia, magnesia, and boron nitride, 20: 17022 (N-65-18933)
Ta–W, diffusion into hafnium–20 tantalum cladding, effects of niobium and tantalum barriers on, 20: 16943(R) (IITRI-B237-45)
Ta–W–Zr, phase studies at 1100 and 1600°C, 20: 17012(R) (DRI-1092-226)
TANTALUM BORIDES
chemical bonding and electric conductivity of, 20: 16439
TANTALUM CARBIDES
NbN–TaC, superconducting properties, 20: 17589 (CONF-650922, pp 541-9)
TANTALUM ISOTOPES Ta-181
energy level transitions in, gamma polarization in, (E), 20: 17444(T)
neutron reactions (n,γ), activation cross section for, (E), 20: 16336(R) (NYO-10175)
proton fission at 150 to 660 Mev, cross sections for, (E), 20: 17838
TANTALUM ISOTOPES Ta-182
half life of isomeric, from neutron reactions (n,γ), (E), 20: 16336(R) (NYO-10175)
half life of, from neutron reactions (n,γ), (E), 20: 16336(R) (NYO-10175)
neutron reactions (n,γ), activation cross section for, (E), 20: 16336(R) (NYO-10175)
TANTALUM OXIDES
dielectric properties of films of, on anodized tantalum, effects of anodization electrolyte on, 20: 17055
structure of single-crystal films of, on electropolished tantalum, 20: 17059
TANTALUM SYSTEMS
C–Ta, phase studies on zeta-phase in, 20: 17050
HfO_2–Ta, development of composites of, by controlled oxidation of alloy, 20: 16943(R) (IITRI-B237-45)
Si–Ta–V, phase studies on intermetallic compounds in, 20: 17075
TECHNETIUM
separation from molybdenum by sorption on iron oxide, 20: 16552
TECHNETIUM CARBONYLS
preparation and properties of, 20: 16480
TECHNETIUM COMPLEXES
carbonyl, preparation and properties, 20: 16480
TECHNETIUM ISOTOPES Tc-93
production of isomeric, in deuteron reactions (d,n) at 15 Mev, 20: 16508(R) (NYO-2771-13)
TECHNETIUM ISOTOPES Tc-99
preparation by deposition on metal foils, method for, 20: 16914(R) (ORNL-3900, pp 182-93)
production of radiochemically pure isomer, 20: 16552
TECHNICAL REPORTS
lists of available and desired ultrapure inorganic materials for research, 20: 16417 (ORNL-RMIC-4)
TECHNOLOGY
evaluation of existing criteria for judging quality of science exhibits, 20: 18178 (TID-22793)
TEETH

strontium-90 content of children's primary, 20: 16763
TEKTITES
age of Moldavian, rubidium–strontium estimation of, 20: 16711(R) (MIT-1381-13)
composition and origin of, in Moldavia, 20: 16711(R) (MIT-1381-13)
TELLURATE IONS
separation from iodates, iodides, and tellurites by paper chromatography, 20: 16372
TELLURITE IONS
separation from iodates, iodides, and tellurates by paper chromatography, 20: 16372
TELLURIUM
determination in brass and cast iron, activation, 20: 16335(R) (NBS-TN-276)
determination in rare earth tellurides, 20: 16395
evaporation from irradiated uranium dioxide at 750 to 1600°C, 20: 17102
TELLURIUM ISOTOPES
neutron capture by, gamma spectra from thermal, (E), 20: 17681 (IAE-966)
TELLURIUM ISOTOPES Te-106
production in molybdenum-92 (Ne-20, 6n) reactions, cross sections for, (E), 20: 17687 (JINR-P-2514)
TELLURIUM ISOTOPES Te-108
production in molybdenum-92 (Ne-20, 4n) reactions, cross sections for, (E), 20: 17687 (JINR-P-2514)
TELLURIUM ISOTOPES Te-109
production of delayed proton emitters of, (E), 20: 17687 (JINR-P-2514)
TELLURIUM ISOTOPES Te-111
production of delayed proton emitters of, (E), 20: 17687 (JINR-P-2514)
TELLURIUM ISOTOPES Te-119
hyperfine structure of isomeric, (E), 20: 17705
nuclear magnetic moment, (E), 20: 17705
TELLURIUM ISOTOPES Te-121
energy levels, (E), 20: 17681 (IAE-966)
TELLURIUM ISOTOPES Te-122
energy level transitions from antimony-122 decay, (E), 20: 17677 (COO-1420-112)
TELLURIUM ISOTOPES Te-123
energy levels, (E), 20: 17681 (IAE-966)
TELLURIUM ISOTOPES Te-124
energy levels, (E), 20: 17681 (IAE-966)
TELLURIUM ISOTOPES Te-125
deuteron reactions (d,n), cross sections for iodine-126 production in, 20: 16508(R) (NYO-2771-13)
energy levels, (E), 20: 17681 (IAE-966)
TELLURIUM ISOTOPES Te-126
deuteron reactions (d,2n), cross sections for iodine-126 production in, 20: 16508(R) (NYO-2771-13)
energy levels, (E), 20: 17681 (IAE-966)
TELLURIUM ISOTOPES Te-127
energy levels, (E), 20: 17681 (IAE-966)
sensitivity for activation analysis using beta-gamma-gamma sum-coincidence gamma spectrometer, 20: 16335(R) (NBS-TN-276)
TELLURIUM ISOTOPES Te-128
deuteron reactions (d,2n), cross sections for iodine-128 production in, 20: 16508(R) (NYO-2771-13)
TELLURIUM ISOTOPES Te-129
content in rain water, Fayetteville, Arkansas, Oct. 1964, 20: 16663 (TID-21470)
energy levels, (E), 20: 17681 (IAE-966)
TELLURIUM ISOTOPES Te-130
deuteron reactions (d,p) at 15 Mev, isomeric yield ratios for, 20: 16508(R) (NYO-2771-13)
deuteron reactions (d,2n), cross sections for iodine-130 production in, 20: 16508(R) (NYO-2771-13)
deuteron reactions (d,n) and (d,p), cross sections for iodine-131 production in, 20: 16508(R) (NYO-2771-13)
TELLURIUM ISOTOPES Te-131
energy levels, (E), 20: 17681 (IAE-966)
production of isomeric, in deuteron reactions (d,p) at 15 Mev, 20: 16508(R) (NYO-2771-13)
TELLURIUM SYSTEMS
Sb–Cs–K–Ne–Te, photosensitivity of, 20: 17984
TEMPERATURE
calculation of transient, for fixation of radioactive material in hollow and solid cylinders and slabs, 20: 18155 (BNWL-157)
effects of low, combined with x radiation on cesium-137 retention in rats, 20: 16180
effects on electron relaxation rates in solids, theory of, 20: 18016
effects on initial oxidation of tantalum and tungsten substrates, 20: 16987
effects on nitrogen isotope distribution between oxides in gaseous and liquid phases, 20: 16486
measurement of high, methods for, 20: 17158(R) (ORNL-3900, pp 82-149)
radiosensitivity effects on goldfish, 20: 16236
radiosensitivity effects on peritrichs, 20: 16295
radiosensitivity effects on cultured mammalian cells, 20: 16298
TERBIUM
analysis for yttrium using bis(2-ethylhexyl) phosphate, chromatographic, 20: 16385
magnetic structure of, determination using Kerr effect, 20: 17974 (IS-T-63)
magnetostriction in antiferromagnetic, ferromagnetic, and paramagnetic regions, (E), 20: 18012
solubility in gold, solid, 20: 17016 (IS-1175)
TERBIUM ALLOYS
Fe–Tb, crystal structure of Tb_6Fe_{23} and Tb_2Fe_{17} in, 20: 17096(T)
Hg–Tb, crystal structure of $TbHg_3$, 20: 17060
Mn–Tb, crystal structure of Tb_6Mn_{23} in, 20: 17096(T)
Tb–Tl, crystal structure of $TbTl_3$, 20: 17060
TERBIUM COMPOUNDS
formation of tetravalent, role of electron transfers in, 20: 16433
TERBIUM FLUORIDES
formation of tetravalent, role of electron transfer in, 20: 16433
TERBIUM HYDRIDES
properties and structure, 20: 16453
TERBIUM ISOTOPES Tb-159
energy levels from gadolinium-159 decay, mean lives and quadrupole moments for, (E), 20: 17789
TERBIUM ISOTOPES Tb-160
beta transitions in, higher-order effects in allowed, (E), 20: 17678 (COO-1420-113)
TERBIUM NITRIDES
formation of tetravalent, role of electron transfer in, 20: 16433
TERBIUM OXIDES
determination in thorium oxide by emission spectroscopy, 20: 16393
formation of tetravalent, role of electron transfer in, 20: 16433
TERBIUM SULFIDES
EuS–Tb_2S_3, compound formation in, 20: 16431
SmS–Tb_2S_3, compound formation in, 20: 16431
Tb_2S_3–YbS, compound formation in, 20: 16431
TEREPHTHALIC ACID, ETHYLENE POLYMER ESTERS
fission-fragment energy degradation in Mylar, (E), 20: 17821
TERPHENYL
analysis of, by gas chromatography, thermal conductivity, and flame ionization, 20: 16341
pyrolysis of, kinetics of, 20: 16491
testing for reactor coolants, 20: 18174(R) (NP-15771)
TERPYRIDINE
complexes with rare earth nitrates, preparation and infrared spectra of, 20: 16479
1,3,5,7-TETRAZOCINE, OCTAHYDRO-1,3,5,7-TETRANITRO-
radiation effects on surface activity of polymorphic, gamma, 20: 16504 (AD-627846)
THALLIUM
energy levels of μ-mesic atoms of, resonances in, (T), 20: 17281
THALLIUM ALLOYS
Dy–Tl, crystal structure of $DyTl_3$, 20: 17060
Er–Tl, crystal structure of $ErTl_3$, 20: 17060
Eu–Tl, crystal structure and magnetic properties of $EuTl_3$, 20: 17060
Ho–Tl, crystal structure of $HoTl_3$, 20: 17060
Lu–Tl, crystal structure of $LuTl_3$, 20: 17060
Tb–Tl, crystal structure of $TbTl_3$, 20: 17060
Tl–Tm, crystal structure of $TmTl_3$, 20: 17060
THALLIUM ISOTOPES Tl-204
content in stratospheric and tropospheric samples in Project Star Dust, 1963, 20: 16727(R) (HASL-168)
THALLIUM ISOTOPES Tl-207
energy levels from bismuth-211 decay, (E), 20: 17703
THERMAL CONDUCTIVITY
measurement methods, 20: 17158(R) (ORNL-3900, pp 82-149)
THERMAL RADIATION
emission from argon plasma jet, measurement of, (E), 20: 17898
THERMAL RADIATION SHIELDING
ablation of, radioisotope technique for measuring, 20: 16778 (NASA-TN-D-3329)
performance and selection of, for use in space vehicles, 20: 16944 (NASA-SP-3025)
THERMAL REACTORS
control elements for plutonium-fueled, heavy-water-moderated, power breeder, 20: 18115
development of thorium–uranium, review of, 20: 18073
neutron spectra in, computer program for, 20: 18047 (KR-78)
THERMIONIC CELLS
performance of nuclear-, using rhenium emitters on uranium carbide, 20: 17327 (N-65-19264)
use of cesium-diode, for laboratory experiments, 20: 17329

THERMOCOUPLES
welding metal-sheathed, 20: 18174(R) (NP-15771)
THERMODYNAMICS
parameters in, power-series expansion for, 20: 17527
THERMOLUMINESCENT DETECTORS
use in dosimetry of roof tile gamma emissions, 20: 16759
THERMONUCLEAR EXPLOSIONS
fallout from, monitoring 1962 to 1964, 20: 16677
peaceful use of, bioenvironmental feasibility, 20: 16160 (UCRL-14739 (Pt.2))
THERMONUCLEAR REACTIONS
research, 20: 17895(T) (AEC-tr-6669)
research, 20: 17885(R) (ORNL-3908)
research on controlled, review of, 20: 17914
THERMONUCLEAR REACTORS
development of, review of, 20: 17914
development status, 20: 17926
energy balance in, (T), 20: 17929
plasma containment and heating in, (T), 20: 17927
plasma containment and heating in, (E), 20: 17928
plasma stability in, initial, (T), 20: 17880 (MATT-437)
plasma stability in magnetic traps, (E), 20: 17925(T)
THERMOPILES
use in neutron flux measurements in reactors, 20: 16899
THICKNESS GAGES
development of radiometric, 20: 18182
THIOCYANIC ACID
effects on uranium sorption by platinized carbon, 20: 16581
THIOPHOSPHORYL CHLORIDE
labeling with phosphorus-32 from carrier-free source, 20: 16551
THORITES
growth and doping of single-crystal, 20: 16960
THORIUM
argon ion reactions at 400 Mev, compound nucleus binary and ternary fission cross sections for, (E), 20: 17788
content in surface boundary layer of atmosphere, seasonal variations in, 20: 16695
effects on hydrolysis of adenosine-2-phosphate and carboxylase, catalytic, 20: 16420
properties as reactor fuel material, 20: 18182
proton fission at 150 to 660 Mev, cross sections for, (E), 20: 17838
separation from aluminum, iron, and rare earths by solvent extraction using alkyl phosphates, 20: 16580
separation from granites, economics of, 20: 17158(R) (ORNL-3900, pp 82-149)
separation from phosphoric acid solutions by solvent extraction using alkyl phosphates, 20: 16580
separation from uranium ore leach solution by solvent extraction using organic phosphorus compound and sulfuric acid, 20: 16573
separation of lower actinides and radium from irradiated, method for simultaneous, 20: 16359
spectra of, in electrodeless discharge tubes, 20: 16464(T)
THORIUM ARSENIDES
crystal structure, (E), 20: 17077
THORIUM CARBIDES
electric properties of hot-pressed, effects of annealing and composition on, 20: 17068
ThC_2–UC_2, fission gas diffusion from pyrolytic-carbon-coated particles of, effects of coating structure on, 20: 17127 (ORNL-3923)
THORIUM COMPLEXES
with ethylenediaminetetraacetate, effects on hydrolysis of α-D-glucose 1-phosphate, 20: 16421
with iron, effects on hydrolysis of α-D-glucose 1-phosphate, 20: 16421
THORIUM IONS
effects on hydrolysis of α-D-glucose 1-phosphate, 20: 16421
THORIUM ISOTOPES Th-230
neutron fission at 0.1 to 1.2 Mev, fragment angular distributions from, (E/T), 20: 17848
THORIUM ISOTOPES Th-232
neutron fission at 1.6 to 2.6 Mev, delayed neutrons from, (E), 20: 17680 (FEI-26)
neutron fission at 14 Mev, delayed neutron precursors from, (E/T), 20: 17831
neutron fission of, fragment yields from, (E), 20: 17860
neutron fission of, fragment angular anisotropy and mass asymmetry from fast, (E), 20: 17869
production of alpha sources of, electrospraying method for, 20: 16553
THORIUM NITRATES
ion exchange and sorption on glass surfaces, 20: 16469
ultrasonic velocity and adiabatic compressibilities of aqueous solutions of, 20: 16477
THORIUM ORES
processing of, research on, 20: 18174(R) (NP-15771)
THORIUM OXIDES
heat of adsorption of water on, 20: 16456
peptization of solid, mechanism of, 20: 16419(T) (UCRL-Trans-1301(L))
spectra of, band, (E), 20: 17254
CeO_2–Sm–ThO_2, samarium fluorescence in, 20: 16466(T)
THORIUM(IV) OXIDES
analysis for rare earth oxides by emission spectroscopy, 20: 16393
content in man, whole-body, 20: 16303(R) (AD-626384)
surface chemistry of, 20: 17158(R) (ORNL-3900, pp 82-149)
ThO_2–UO_2, effects of dispersions of, on mechanical properties of beryllia, 20: 17113 (AAEC-E-140)
ThO_2–UO_2, fission gas diffusion from pyrolytic-carbon-coated particles of, effects of coating structure on, 20: 17127 (ORNL-3923)
ThO_2–UO_2, preparation of microspheres of, 20: 18020(R) (ORNL-3900, pp 2-81)
THORIUM PHOSPHIDES
crystal structure, (E), 20: 17077
THORIUM SALTS
composition and properties of organic, 20: 16497
THRESHOLD DETECTORS
use for neutron flux measurements in NRL Research Reactor, 20: 16335(R) (NBS-TN-276)
THULIUM
solubility in gold, solid, 20: 17016 (IS-1175)
THULIUM ALLOYS
Fe–Tm, crystal structure of Tm_6Fe_{23} in, 20: 17096(T)
Hg–Tm, crystal structure of $TmHg_3$, 20: 17060
Mn–Tm, crystal structure of Tm_6Mn_{23} in, 20: 17096(T)
Tl–Tm, crystal structure of $TmTl_3$, 20: 17060
THULIUM COMPLEXES
with phenanthroline, infrared spectra of, 20: 16437
with 2,2′-bipyridyl, infrared spectra of, 20: 16437
THULIUM HYDRIDES
properties and structure, 20: 16453
THULIUM IONS
magnetic hyperfine field in lutetium iron garnet, 20: 17994
wave functions for, including effect of nuclear quadrupole moment, 20: 17250 (BNL-8850)
THULIUM ISOTOPES Tm-169
deuteron reactions (d,p) at 12 Mev, thulium-170 levels from, (E), 20: 17782
energy levels of, transverse spin polarization effects on, (T), 20: 17682 (INP-428/PL)
energy levels of, g factors for, (E), 20: 17994
neutron reactions (n,γ), thulium-170 levels from thermal, (E), 20: 17782
THULIUM ISOTOPES Tm-170
energy levels from thulium-169 (d,p) and (n,γ) reactions, (E), 20: 17782
THULIUM OXIDES
determination in thorium oxide by emission spectroscopy, 20: 16393
SrO–Tm_2O_3, properties of compounds formed by interactions in, 20: 17044
THYMIDINE
effects of tritium-labeled, on root growth of corn and pea seedlings, 20: 16227(R) (NYO-3561-2)
radiation effects on rat urinary excretion of, β, 20: 16201
radiation effects on, ESR studies of gamma, 20: 16541
radiation effects on uptake by L cells in culture, uv, 20: 16279
radiolysis of tritium-labeled, effects of low temperature and scavengers on self-, 20: 16533
use of tritiated, as measure of DNA synthesis in irradiated rats, 20: 16230(R) (TID-22644)
THYMINE
radioinduced dimerization of, in frozen aqueous solution, 20: 16197
THYMUS GLAND
radiation effects on physiology of reticulum cells in rat, x, 20: 16293
THYROID GLAND
iodide transport in, site for, 20: 16160 (UCRL-14739(Pt.2))
iodine-131 content of rat, methods for measuring, 20: 16179
iodine-131 content in cattle and human, Japan, 1964, 20: 16730 (NP-15882)
iodine-131 dosimetry in, method for, 20: 16160 (UCRL-14739(Pt.2))
iodine-131 uptake by rat, effects of ozone on, 20: 16190
iodine-131 uptake by, measurement standardization for, 20: 16315
radiation exposure of pituitary and, carcinogenic effects of x, 20: 16245
radioinduced malignancies of, after combined pituitary and thyroid exposure, 20: 16245
radiotherapy of cancers of, 20: 16307
THYROID HORMONES
effects on molting in amphibians, 20: 16252
effects on molting in amphibians, 20: 16252
THYROXINE
labeling with iodine-131, 20: 16496
TIMING CIRCUITS
design and performance of equalizing system for small differential non-

linearity in nanosecond, 20: 16794
TIN
determination of trace amounts of, in beryllium by spectrography, 20: 16352
diffusion in niobium containing zirconium or titanium, 20: 17632
electron tunneling in superconducting junctions of, structure of high-frequency Josephson, (E), 20: 17636
magnetic flux motion in magnetically coupled films of superconducting, (E/T), 20: 17623
proton reactions (p,d) at 57 Mev, energy spectra from, (E), 20: 17725
superconducting energy gap, (E), 20: 17619
ultrasonic absorption in single-crystals of superconducting, temperature dependence of, (E), 20: 17605
TIN ALLOYS
Au–Sn, superconductivity properties of thin composite films of, 20: 17601
Bi–Sn, tin-119 isomeric shift in, 20: 18004
Cd–Sn, tin-119 isomeric shift in, 20: 18004
In–Sn, tin-119 isomeric shift in, 20: 18004
Nb–Sn, fabrication of superconducting solenoids from stranded wires of, 20: 17593 (CONF-650922, pp 597-603)
Nb–Sn, preparation of superconducting Nb_3Sn using diffusion layers, 20: 17649
Nb–Sn, superconductivity of diffusion layers of Nb_3Sn, (E), 20: 17632
Pb–Sn, tin-119 isomeric shift in, 20: 18004
Pd–Sn, preparation and properties of, for use as Mössbauer source, 20: 16335(R) (NBS-TN-276)
Sb–Sn, tin-119 isomeric shift in, 20: 18004
Ta–Sn, tin-119 isomeric shift in, 20: 18004
TIN ISOTOPES
separation of, performance of separator for, 20: 16928(R) (INSJ-92)
TIN ISOTOPES Sn-117
neutron capture gamma spectra from, (E), 20: 17158(R) (ORNL-3900, pp 82-149)
TIN ISOTOPES Sn-119
gamma line isomeric shift in tin alloys, 23.8 kev, 20: 18004
Mössbauer effect in tin-oxide suspensions, study of Brownian movement from, (E), 20: 17165
TIN ISOTOPES Sn-122
neutron reactions (n,γ), activation cross section for, (E), 20: 16336(R) (NYO-10175)
TIN ISOTOPES Sn-123
half life of, from neutron reactions (n,γ), (E), 20: 16336(R) (NYO-10175)
TIN ISOTOPES Sn-124
neutron reactions (n,γ), activation cross section for, (E), 20: 16336(R) (NYO-10175)
TIN ISOTOPES Sn-125
half life of isomeric, from neutron reactions (n,γ), (E), 20: 16336(R) (NYO-10175)
TIN OXIDES
Mössbauer line broadening in, twinning effects in, 20: 16335(R) (NBS-TN-276)
tin-119 Mössbauer effect in suspensions of, study of Brownian movement from, (E), 20: 17165
TIN SYSTEMS
Si–Sn–V, superconductivity of solid solutions in, 20: 17043
TISSUE CULTURES
radiation effects on KB, uv and x, 20: 16258
radiation effects on thymidine uptake by cells in, uv, 20: 16279
radiosensitivity of cells in, 20: 16292
TISSUE HOMOGENATES
radiation effects on enzyme activity in rat, x, 20: 16289
TISSUES
analysis for copper and zinc in lung, activation, 20: 16335(R) (NBS-TN-276)
analysis for elements, quantitative, 20: 16160 (UCRL-14739(Pt.7))
analysis for enzyme composition, 20: 16172(R) (NYO-2194-1)
analysis of living, for americium-241 and plutonium-239, 20: 16864
calcification of soft, mechanisms for, 20: 16162
radiation effects on living, bibliography on, 20: 16219 (AED-C-04-23)
radiation effects on, bibliography on, 20: 16220 (AED-C-04-24)
radiation effects on living, bibliography on, 20: 16221 (AED-C-04-25)
radiation effects on dog, α, 20: 16268
radioinduced ethylene in plant, γ, 20: 16281
TITANIUM
analysis for oxygen, activation, 20: 16331 (GA-6568)
corrosion by boron-containing solutions, 20: 16976
corrosion by saline water, factors affecting, 20: 17158(R) (ORNL-3900, pp 82-149)
determination in zone-purified aluminum by proton activation methods, 20: 16366
determination of trace amounts of, in beryllium by spectrography, 20: 16352
diffusion in molybdenum at 905 to 1210°C, inter-, 20: 17111
effects on high-temperature properties of eutectic alloys, 20: 17108
effects on hydrolysis of adenosine-2-phosphate and carboxylase, catalytic, 20: 16420
specific heat, (T), 20: 17084
superconducting properties of, plastic deformation and uniform compression effects on, (E), 20: 17634
TITANIUM ALLOYS
Al–Nb–Ta–Ti, corrosion cracking in titanium-base, stress-, 20: 16967 (AD-628277)
Al–Ti–V, corrosion cracking in titanium-base, stress-, 20: 16967 (AD-628277)
Cr–Nb–Ti, phase studies, 20: 17091
Cr–Nb–Ti, tensile properties of, effects of composition on, 20: 17112
Mo–Ti, cavitation damage in mercury and water, 20: 16974 (NP-15889)
Mo–Ti–Zr, compatibility of TZM, with alumina, beryllia, magnesia, and boron nitride, 20: 17022 (N-65-18933)
Nb–Ti–Zr, oxidation-resistant coatings on D-36, performance of commercial, 20: 16973 (NASA-TN-D-5275)
TITANIUM BORIDES
chemical bonding and electric conductivity of, 20: 16439
TITANIUM CARBIDES
Co–TiC–WC, casting of cermets of, slip, 20: 16997
NbN–TiC, superconducting properties, 20: 17589 (CONF-650922, pp 541-9)
TITANIUM IODIDES
superconducting properties of, plastic deformation and uniform compression effects on, (E), 20: 17634
TITANIUM ISOTOPES Ti-44
content in Bogou iron meteorite, 20: 16674
TITANIUM ISOTOPES Ti-46
bremsstrahlung reactions (γ,np) at 24, 36, and 48 Mev, scandium-44 isomeric yield ratio from, (E), 20: 17777
deuteron reactions (d,p) at 7.0 Mev, titanium-47 levels from, (E), 20: 17776
TITANIUM ISOTOPES Ti-47
energy levels from titanium-46 (d,p) reactions, (E), 20: 17776
helium-3 reactions (He-3,n) at 12 Mev, Q value for, 20: 16331 (GA-6568)
TITANIUM ISOTOPES Ti-48
alpha reactions (α,α′) at 43 Mev, angular distributions from, (T), 20: 17692 (ORNL-TM-1414)
TITANIUM ISOTOPES Ti-51
nucleon interactions in, properties from effective, (T), 20: 17735
TITANIUM NITRIDES
NbN–TiN, superconducting properties, 20: 17589 (CONF-650922, pp 541-9)
TITANIUM OXIDES
determination in Moldavites by mass spectrometry and x-ray fluorescence, 20: 16711(R) (MIT-1381-13)
electronic properties of single-crystal, effects of ion-bombardment on, 20: 17151
TiO_2–Y_2O_3, phase studies, 20: 17032
TITANIUM(IV) OXIDES
diffusion of lithium in, isotopic mass dependence of, 20: 17052
TITANIUM PHOSPHATES
properties for use as ion exchange material in radioactive waste processing, 20: 16570
TITANIUM SYSTEMS
Fe–O–Ti–Zr, fabrication and properties of sintered, deformable, 20: 17003
T–Ti, fabrication and uses of targets of, 20: 16916
TOBACCO
polonium-210 content in, 20: 16189
polonium-210 content in smoke from, 20: 16264
TOLUENE
reactions with deuterium, catalyzed by chromium oxide gel, 20: 16487
tritium exchange with tritiated ethyl malonate, effects of catalysts on, 20: 16492
bis(2-ethylhexyl) phosphate–HCl–toluene, extraction constants for americium, californium, curium, and fermium in, 20: 16404
bis(2-ethylhexyl) phosphate–HCl–toluene, solvent properties for californium, fermium, and mandelevium, 20: 16404
TOMATOES
leaf chlorosis induced by continuous light in, effects of iron on expression of, 20: 16174(R) (RLO-1547-3)
TRACER TECHNIQUES
development for paper and pulp industry, 20: 16921 (TID-22627)
development of, review, 20: 18182
for deposition of vacuum pump oil on tissue specimens, 20: 16159(R) (ORNL-3900, pp 150-81)
TRACER TECHNIQUES (AGRICULTURE)
use in African countries, economics of, 20: 16919 (EUR-2619.f)

TRACER TECHNIQUES (BIOLOGY)
for distribution of Yoshida sarcoma cells in rats, phosphorus-32, 20: 16188
for location of iodide pump, iodine-131, 20: 16160 (UCRL-14739(Pt.2))
for thyroidal iodine-131 in small animals, 20: 16179
sample preparation for, in carbon-14- and tritium-labeled materials, 20: 16177
TRACER TECHNIQUES (BOTANY)
for gibberellic acid synthesis by *E. coli*, 20: 16193 (EUR-2539.1)
TRACER TECHNIQUES (CHEMISTRY)
development of, 20: 16335(R) (NBS-TN-276)
TRACER TECHNIQUES (HYDROLOGY)
use in African countries, economics of, 20: 16919 (EUR-2619.f)
TRACER TECHNIQUES (MEDICINE)
use of gallium-68 in bone scanning, 20: 16310
TRACER TECHNIQUES (METEOROLOGY)
use of radon in studies of atmospheric turbulence, 20: 16694
TRANSCURIUM ELEMENTS
production, 20: 16543
TRANSDUCERS
design for measurement of water velocity, 20: 18019(R) (IDO-17146)
radiation effects on, review of, 20: 16911
TRANSISTORS
performance of bipolar and FET, in semiconductor detector circuitry, 20: 16871
radiation effects on S2N1724 and 2N2222, gamma and neutron, 20: 16908 (N-65-17526)
radiation effects on 2N834, gamma and neutron, 20: 16909 (N-65-18250)
radiation effects on MOS field-effect, transient, 20: 16913
TRANSITION METALS
bonding in, theory of atomic, 20: 16418 (UCRL-16250)
compounds with boron, chemical bonding and electric conductivity of, 20: 16439
sublimation of, enthalpy of, 20: 16418 (UCRL-16250)
TRANSPLUTONIC ELEMENTS
separation of, review on methods for, 20: 16402
TRANSURANIC ELEMENTS
fission of, spontaneous, 20: 17688 (JINR-P-2539)
processing plant operation for, 20: 17158(R) (ORNL-3900, pp 82-149)
production, 20: 16543
radioactivity, 20: 17688 (JINR-P-2539)
TREES
radiation effects on pre-meiotic male flower buds of *Pinus nigra*, dose effects on, 20: 16228(R) (NYO-3571-2)
radiation effects on clonal material of *Populus tremuloides*, 20: 16228(R) (NYO-3571-2)
radiation effects on seed of *Rauwolfia serpentina*, γ, 20: 16249
radioinduced mutants of sweet cherry, 20: 16244
TRIAZOLES
effects against radiation injuries in mice, 20: 16490(R) (TID-22681)
TRIDODECYLAMINE
solvent properties for plutonium, 20: 16560
TRINO POWER REACTOR
development of, review of, 20: 18104
TRIOCTYLAMINE
effects on solvent extraction of americium by thenoyltrifluoroacetone, synergistic, 20: 16571
solvent properties for uranium in hydrochloric acid solutions, 20: 16391
TRITIUM
beta decay of, phase-space integrals for, (T), 20: 17732
content variations in levels of Mont Cenis Lake, France, 1964 and 1965, 20: 16668
decay of, in organic compounds, effects of low temperature and scavengers on decomposition from, 20: 16533
decay of, in tetrasodium 2-methyl-1,4-naphthaquinol, self-radiolysis from, 20: 16535
determination in azo dyes by scintillation counting, use of oxygen-flask combustion method in, 20: 16373
determination in organic compounds by gas chromatography and scintillation counting, 20: 16371
determination in organic sample by combustion and scintillation counting, 20: 16387
determination in polystyrene by combustion and liquid scintillation counting, 20: 16384
deuteron reactions (d,n) with, neutron production for activation analysis in, 20: 16332 (GA-6691)
deuteron reactions (d,n) at 100 kev, tensor and vector polarization effects on, (E), 20: 17749
diffusion in metals, research on, 20: 17892(R) (ORNL-3908, pp 149-53)
diffusion in stone meteorites, 20: 17247
effects of water- and thymidine-incorporated, on root growth of corn and pea seedlings, 20: 16227(R) (NYO-3561-2)
effects on proton transfer in water, 20: 16424
exchange between tritiated ethyl malonate and hydrocarbons, effects of catalysts on, 20: 16492
ground water contamination by, in Shoal Event, hazards from, 20: 16742 (VUF-1014)
incorporation in actinomycin-D, 20: 16550
incorporation in cyclohexene by tritioboration of 1-(*N*-piperidino)-cyclohexene, 20: 16549
neutron elastic scattering at 1.0 to 6.0 Mev, phase-shift analysis for, (T), 20: 17769
production in atmosphere, 20: 16689
proton reactions (p,n) with, neutron production for activation analysis in, 20: 16332 (GA-6691)
spectra of, bands from lowest excited states in vibrational, 20: 16451
use in instrumentation, 20: 16916
TRITIUM SYSTEMS
T–Ti, fabrication and uses of targets of, 20: 16916
T–Zr, fabrication and uses of targets of, 20: 16916
TRITONS
reactions (t,pf) with uranium isotopes at 13 Mev, fragment-proton coincidences in, (E), 20: 17844
reactions (t,p) with oxygen-17 at 12 Mev, oxygen-19 levels from, (E), 20: 17758
TROPOSPHERE
fallout monitoring in Star Dust Project, 1963, 20: 16727(R) (HASL-158)
fallout monitoring in Project Star Dust, 1964, 20: 16728(R) (HASL-169)
TUBES
boiling burnout in uniformly heated, forced convection, (E), 20: 16603 (NYO-187-7)
TUMORS
radioinduced after head exposure, x, 20: 16245
radioinduced by therapeutic doses of x radiation, 20: 16242
radioinduced intestinal, after therapy, 20: 16309
radioinduced thyroid, after combined pituitary and thyroid exposure, x, 20: 16245
radiosensitivity of cultured cells of, effects of monoiodoacetic acid and p-chloromercuribenzoate on, 20: 16299
radiotherapy of breast, after surgery, 20: 16324
radiotherapy of cervical, 20: 16326
radiotherapy of eye, using β applicators, 20: 16305
radiotherapy of skin, β, 20: 16325
radiotherapy of thyroid, using iodine-131 or x radiation, 20: 16307
radiotherapy of, beam focussing methods for, 20: 16320
radiotherapy of, effects on 17-ketosteroids, 20: 16209
radiotherapy of, effectiveness in children, 20: 16306
radiotherapy of, formation of subcutaneous nodules after, 20: 16323
radiotherapy of, late pathological effects, 20: 16322
TUNGSTEN
analysis for oxygen, activation, 20: 16331 (GA-6568)
compatibility with alumina, beryllia, magnesia, and boron nitride, 20: 17022 (N-65-18933)
creep-rupture properties at high temperatures, 20: 17011 (CONF-651025-14)
crystal lattice dynamics of, Krebb's model for, 20: 17081
determination in asbestos using ion exchange, activation, 20: 16336(R) (NYO-10175)
deuteron sputtering at 30 kev, yields from, 20: 17892(R) (ORNL-3908, pp 149-53)
diffusion in iridium, rhenium, and tantalum to 4000°F, inter-, 20: 16943(R) (IITRI-B237-45)
diffusion in molybdenum–tungsten alloys at 1500 to 2400°C, tracer studies of, 20: 17101
dislocation parameters for, 20: 17033
electron band structure of, relativistic effects on Fermi, (T), 20: 18002
electron emission in cesium vapor, thermionic, (E), 20: 17333
fabrication of large crucibles of, by powder metallurgy techniques, 20: 16993 (Y-DA-1043)
metabolism in rats, 20: 16160 (UCRL-14739(Pt.2))
neutron Doppler coefficients and resonance integrals for, (E/T), 20: 18045(R) (AI-66-16)
oxidation of substrates of, at 30 to 1500°C, mechanism of initial, 20: 16987
performance as heater electrodes in vacuum at 2273 to 3233°K, 20: 16596
physical properties of vapor-deposited, 20: 17020(R) (N-65-18466)
radiation effects on creep-rupture properties at 900 to 1700°C, fast-neutron, 20: 17152
tensile properties of, effects of electron-bombardment heating on, 20: 17073
thermal capacity of, Krebb's model for lattice contributions to, 20: 17081
TUNGSTEN ALLOY COUPLES
Hf–Ta/Ta–W, fabrication by roll cladding and hot spinning, rocket nozzle, 20: 16943(R) (IITRI-B237-45)
Mo/Mo–W, densification of sintered tungsten–molybdenum powder compact, Kirdendall-effect in, 20: 16994

Re–W/Re–W, performance to 2760°C, 20: 16942 (ANL-6981)
W/Re–W, performance to 2760°C, 20: 16942 (ANL-6981)

TUNGSTEN ALLOYS
Al–Co–W, phase studies on intermetallic compounds in, 20: 17075
Co–W, effects of additives on high-temperature properties of eutectic, 20: 17108
Cr–Fe–W, phase studies, 20: 17093
Hf–Ta–W, fabrication of tubing of T-111, 20: 16998
Hf–Ta–W, phase studies at 1100 and 1600°C, 20: 17012(R) (DRI-1092-226)
Mo–Nb–Ta–W, deformation mechanisms in solution-hardened niobium-base, 20: 17082
Mo–Nb–Ta–W, properties as hollow turbine vanes, 20: 16963
Mo–Re–W, fabrication of rods of, by extrusion and sintering, 20: 16989(R) (COO-1518-2)
Mo–W, diffusion of molybdenum and tungsten in, at 1500 to 2400°C, tracer studies of, 20: 17101
Nb–Ta–W–Zr, properties as hollow turbine vanes, 20: 16963
Nb–W–Zr, properties as hollow turbine vanes, 20: 16963
Ni–W, effects of additives on high-temperature properties of eutectic, 20: 17108
Re–W, creep-rupture properties at high temperatures, 20: 17011 (CONF-651025-14)
Re–W, fabrication of tubing of, by extrusion and sintering, 20: 16989(R) (COO-1518-2)
Re–W, microstructure of vapor-deposited, 20: 18020(R) (ORNL-3900, pp 2-81)
Ta–W, compatibility with alumina, beryllia, magnesia, and boron nitride, 20: 17022 (N-65-18933)
Ta–W, diffusion into hafnium–20 tantalum cladding, effects of niobium and tantalum barriers on, 20: 16943(R) (IITRI-B237-45)
Ta–W–Zr, phase studies at 1100 and 1600°C, 20: 17012(R) (DRI-1092-226)

TUNGSTEN BORIDES
chemical bonding and electric conductivity of, 20: 16439

TUNGSTEN CARBIDES
Co–TiC–WC, casting of cermets of, slip, 20: 16997
Co–WC, casting of cermets of, slip, 20: 16997

TUNGSTEN COUPLES
W/Re–W, performance to 2760°C, 20: 16942 (ANL-6981)

TUNGSTEN ISOTOPES W-181
content in stratospheric and tropospheric samples in Project Star Dust, 1963, 20: 16727(R) (HASL-168)
metabolism in rats, 20: 16160 (UCRL-14739(Pt.2))

TUNGSTEN ISOTOPES W-182
deuteron reactions (d,p) at 11.96 Mev, angular distributions from, (T), 20: 17692 (ORNL-TM-1414)

TUNGSTEN ISOTOPES W-183
deuteron reactions (d,n), cross sections for rhenium-184 production in, 20: 16508(R) (NYO-2771-13)

TUNGSTEN ISOTOPES W-184
deuteron reactions (d,2n), cross sections for rhenium-184 production in, 20: 16508(R) (NYO-2771-13)

TUNGSTEN ISOTOPES W-185
content in stratospheric and tropospheric samples in Project Star Dust, 1963, 20: 16727(R) (HASL-168)

TUNGSTEN ISOTOPES W-186
neutron Doppler coefficients and resonance integrals for, (E/T), 20: 18045(R) (AI-66-16)

TUNGSTEN ISOTOPES W-187
metabolism in rats, 20: 16160 (UCRL-14739(Pt.2))

TUNGSTEN SYSTEMS
C–Fe–W, crystal structure of Fe_3W_3C and Fe_6W_6C in, 20: 17015 (INR-665/II/PS)
C–Nb–W–Zr, microstructure of D-43, effects of aging on, 20: 17023 (ORNL-TM-1161, pp 208-24)
C–Nb–W–Zr, properties as hollow turbine vanes, 20: 16963
HfO_2–W, mechanical and thermal properties of plasma-sprayed composite layers of, 20: 16943(R) (IITRI-B237-45)
W–UO_2, neutron Doppler coefficients and resonance integrals for, (E/T), 20: 18045(R) (AI-66-16)

TURBINES
rotors for, graphite helical-screw, 20: 16591 (UCRL-14660)

TYROSINE, IODO-
labeling with iodine-131, 20: 16496

U

ULTRASONICS
absorption in superconducting tin single crystals, temperature dependence of, (E), 20: 17605
absorption in superconducting indium, nonlinear effects in, (E), 20: 17635
attenuation by superconducting mixed-state niobium, 20: 17608
attenuation in niobium–zirconium nonideal superconductors, flux jumping and magnetization effects on, (E), 20: 17606
use for cavitation studies in mercury and water, 20: 16974 (NP-15889)
uses in decontamination of metal surfaces in acid media, 20: 16767

ULTRAVIOLET RADIATION
effects on algae, patterns of expression of mutagenic, 20: 16294
effects on aqueous hydrogen peroxide solutions at 77°K, ESR studies of, 20: 16512
effects on Asiatic influenza virus, 20: 16239
effects on bacterial DNA, 20: 16280
effects on carboxylation of formic acid, kinetics of, 20: 16538
effects on cultured KB cells, 20: 16258
effects on dimerization of 5-hydroxymethyluracil and thymine in frozen aqueous solutions, 20: 16197
effects on Emericellopsis, methods for assaying uv, 20: 16238
effects on *Euglena gracilis*, biological, 20: 16204
effects on hair growth in cases of total baldness, effects of estrogen on, 20: 16248
effects on keratin, chemical, 20: 16205
effects on mitosis in Saccheromyces, 20: 16255
effects on nucleic acids in viruses, inactivating, 20: 16206
effects on nucleic acids in viruses, inactivating, 20: 16207
effects on oxidation of Krebs cycle substrates in *Vibrio cholerae*, 20: 16198
effects on phage-bacteria complex in *Escherichia coli*, 20: 16270(T)
effects on pigments in skin of guinea pigs and man, 20: 16261
effects on silver bromide and silver chloride, ESR from, (E), 20: 17981
effects on spores, 20: 16159(R) (ORNL-3900, pp 150-81)
effects on staining characteristics of mycobacteria, 20: 16195
effects on succinic dehydrogenase activity in mouse tissue homogenates and skin, 20: 16196
effects on thermoluminescence of calcium oxides, 20: 17982
effects on thymidine metabolism in cultured cells, uv, 20: 16279
polarization methods for, 20: 16159(R) (ORNL-3900, pp 150-81)
use in muscle contraction studies, 20: 16259

UNDERGROUND EXPLOSIONS
products of nuclear, biological implications, 20: 16160 (UCRL-14739 (Pt.2))
use for recovery of oil from shale, economics of, 20: 16589 (UCRL-12224-T)

UNITED STATES
fallout monitoring, 1964 and 1965, 20: 16662(R) (HASL-165)

URACIL, 5-HYDROXYMETHYL-
radioinduced dimerization of, in frozen aqueous solution, 20: 16197

URANIUM
analysis for cadmium by atomic absorption spectrophotometry, 20: 16368
analysis for chromium, cobalt, iron, and zinc, activation, 20: 16399
availability for future needs, 20: 18099
cost factors and requirements for enriched, 20: 16716
criticality studies of reflected assemblies of enriched, 20: 16721 (AWRE-NR-1/66)
determination in dust, rocks, urine, and water samples, methods for, 20: 16337 (RMO-300(Rev.1)(Suppl.))
determination in high-purity uranium compounds, titrimetric, 20: 16401
determination of hexavalent, in carbonate solutions by u-v absorption, 20: 16354
determination of trace quantities of, by controlled-potential polarography, 20: 16389
determination of trace amounts of, using controlled-potential coulometry, 20: 16390
distribution in meteorites and minerals, 20: 16684
ductility of, effects of carbon on, 20: 17001
effects of alloying additions of, on corrosion resistance of type 430 stainless steel, 20: 16975 (NP-15900)
effects of deposited, in lungs, carcinogenic, 20: 16264
elastic properties of monocrystals of alpha-, at 298 to 923°K, 20: 17063
electric conductivity of, effects of quenching from 100 to 4.2°K on, 20: 17029(T) (ANL-Trans-273)
enrichment and private ownership of, legal aspects of, 20: 16566
fabrication by rolling, effects of carbon on, 20: 17001
oxidation in moist nitrogen and nitrogen–oxygen mixtures, mechanism of, 20: 16986
plastic deformation at 20 to 850°C of polycrystalline, effects of grain size and strain rate on, 20: 17039
production by reduction of tetrafluoride or dioxide, 20: 16582
production of, economics and future outlook on, 20: 16718
properties as reactor fuel material, 20: 18182
proton reactions at 0.55 and 18.2 Bev, bromine and iodine isotope recoils from, (E), 20: 17837
radiation effects on ductility in alpha-, under varying temperature, 20: 17076
separation from aluminum, iron, and rare earths by solvent extraction

using alkyl phosphates, 20: 16580
separation from hydrochloric acid solutions by solvent extraction using trioctylamine, 20: 16391
separation from irradiated fuels, Eurochemic facility for, 20: 16558
separation from irradiated thorium, method for, 20: 16359
separation from phosphate rocks, ion exchange methods for, 20: 16381
separation from phosphoric acid solutions by solvent extraction using alkyl phosphates, 20: 16579
separation from phosphoric acid solutions by solvent extraction using alkyl phosphates, 20: 16580
separation from sulfuric acid leach slurries by liquid ion exchange, 20: 16572
sorption by platinized carbon, effects of acids and bases on, 20: 16581
superconductivity of alpha-phase, 20: 17095
thermal expansion of alpha-, at 50 to 923°K, 20: 17064

URANIUM ALLOYS
analysis for manganese using sodium persenate, spectrophotometric, 20: 16351
Al–Fe–U, metallography of, correlation of particle distribution and swelling characteristics of, 20: 17058
Al–U, fabrication of fuel plates of, specifications for, 20: 16995
Al–U, metallography of, correlation of particle distribution and swelling characteristics of, 20: 17058
Al–U, thermal expansion of clad fuels of, calculation of force due to, 20: 17088
Cr–U, superconductivity of beta-phase, 20: 17095
Fe–U, metallography of, correlation of particle distribution and swelling characteristics of, 20: 17058
Mo–U, mechanical properties and structure of, effects of heat treatments on, 20: 17014 (INR-645/XIV/PS)
Nb–U, phase studies, 20: 17035
Nb–U, phase transformation kinetics in, 20: 17036
Pt–U, superconductivity of beta-phase, 20: 17095

URANIUM CARBIDES
compressibility of UC, isothermal, 20: 17062
fission gas diffusion from pyrolytic-carbon-coated particles of, effects of coating structure on, 20: 17127 (ORNL-3923)
immiscibility of UC and UC_2, high-temperature, 20: 17057
preparation of monocarbide, 20: 16966
production, 20: 16582
radiation effects on lattice parameters of, annealing of neutron, 20: 17140
sintering, 20: 16582
PuC–UC, burnup in fast reactors, effects on breeding ratio, multiplication factor, and sodium-void reactivity, 20: 18060
ThC_2–UC_2, fission gas diffusion from pyrolytic-carbon-coated particles of, effects of coating structure on, 20: 17127 (ORNL-3923)
UC–UO, thermodynamic properties, 20: 16449

URANIUM COMPLEXES
pyrophosphate, preparation of, effects of hydrogen ions on, 20: 16472
with ammonium aurintricarboxylate, formation and stability of, 20: 16428

URANIUM COMPOUNDS
analysis for cadmium by atomic absorption spectrophotometry, 20: 16368
density of powders of, method for measuring, 20: 16425
properties as reactor fuel material, 20: 18182

URANIUM CONCENTRATES
analysis for chromium, cobalt, iron, and zinc, activation, 20: 16399
analysis for uranium, titrimetric, 20: 16401
production methods and prices, 20: 16716

URANIUM(III) FLUORIDES
equilibria with uranium tetrafluoride, 20: 17158(R) (ORNL-3900, pp 82-149)

URANIUM(IV) FLUORIDES
equilibria with uranium trifluorides, 20: 17158(R) (ORNL-3900, pp 82-149)

URANIUM(V) FLUORIDES
preparation, 20: 16582

URANIUM(VI) FLUORIDES
analysis for nitrogen and oxygen, spectrographic, 20: 16409

URANIUM ISOTOPES
separation of, design of Pierrelatte plant for, 20: 16932
x rays from, isotope shift in energy of electronic K, 20: 17285

URANIUM ISOTOPES U-233
critical mass in water-reflected cylinder, distribution effects on, (T), 20: 18062
deuteron reactions (d,pf) at 13 Mev, fragment-proton coincidences in, (E), 20: 17844
fuel value studies on, 20: 18020(R) (ORNL-3900, pp 2-81)
neutron fission cross sections at 40 to 500 kev, (E), 20: 17852
neutron fission cross sections at 1.7 to 30 ev, least-squares analysis of, (T), 20: 17853
neutron fission of, neutron yields from thermal, (E), 20: 17823
neutron fission of, beta activity of products from thermal, (E), 20: 17835
neutron fission of, fragment energy and mass distributions from thermal, (E), 20: 17863
neutron resonance fission integral of, (E), 20: 17722
production of alpha sources of, electrospraying method for, 20: 16553
triton reactions (t,pf) at 13 Mev, fragment-proton coincidences in, (E), 20: 17844

URANIUM ISOTOPES U-234
deuteron reactions (d,pf) at 13 Mev, fragment-proton coincidences in, (E), 20: 17844
deuteron reactions (d,pf) with, fragment angular, energy, and mass distributions from, (E), 20: 17865
energy levels from neptunium-234 decay, (T), 20: 17742
neutron fission cross sections at 40 to 500 kev, (E), 20: 17852
triton reactions (t,pf) at 13 Mev, fragment-proton coincidences in, (E), 20: 17844

URANIUM ISOTOPES U-235
critical mass in water-reflected cylinder, distribution effects on, (T), 20: 18062
deuteron reactions (d,pf) at 13 Mev, fragment-proton coincidences in, (E), 20: 17844
fission fragment primary charge from, nuclear structure effects on, (T), 20: 17845
neutron cross sections for, twenty-group, 20: 18057
neutron cross sections at 1.86 ev to 10 Mev, 20: 17697 (WANL-TME-1028)
neutron fission at 3 to 10 Mev, cross sections for, 20: 18020(R) (ORNL-3900, pp 2-81)
neutron fission at 100 kev to 2.6 Mev, neutron yields from, (E), 20: 17823
neutron fission at 0.005 to 0.2 ev, binary-to-ternary ratio for, (E), 20: 17840
neutron fission cross sections at 0.0322 to 0.275 ev, (E), 20: 17854
neutron fission near threshold, nucleon pairing effects on, (T), 20: 17847
neutron fission of, neutron yields from thermal, (E), 20: 17823
neutron fission of, prompt neutron yields from thermal, (E), 20: 17824
neutron fission of, neutron spectra from, (E), 20: 17825
neutron fission of, gamma energies and yields from thermal, (E), 20: 17828
neutron fission of, gamma angular distributions from thermal, (E), 20: 17829
neutron fission of, beta activity of products from thermal, (E), 20: 17835
neutron fission of, alpha particle and fragment energies and yields from resonance, (E), 20: 17839
neutron fission of, fragment energy and mass distributions from thermal, (E), 20: 17863
neutron fission of, fragment mass distributions after prompt neutron emission, (E/T), 20: 17866
neutron fission of, fragment kinetic energy from, (E/T), 20: 17867
neutron fission of, mass dependence of fragment energy in fast and thermal, (E/T), 20: 17868
neutron reactions at 2 ev to 30 kev, fission, radiative capture, and total cross sections for, (E), 20: 17856
neutron resonance fission integral for, epithermal and thermal, (E), 20: 17751
production of alpha sources of, electrospraying method for, 20: 16553
proton fission at 150 to 660 Mev, cross sections for, (E), 20: 17838
triton reactions (t,pf) at 13 Mev, fragment-proton coincidences in, (E), 20: 17844

URANIUM ISOTOPES U-236
deuteron reactions (d,pf) at 13 Mev, fragment-proton coincidences in, (E), 20: 17844
neutron fission cross sections at 40 to 500 kev, (E), 20: 17852
triton reactions (t,pf) at 13 Mev, fragment-proton coincidences in, (E), 20: 17844

URANIUM ISOTOPES U-238
deuteron reactions (d,pf) at 13 Mev, fragment-proton coincidences in, (E), 20: 17844
neutron cross sections for, twenty-group, 20: 18057
neutron fission at 14 Mev, delayed neutron precursors from, (E/T), 20: 17831
neutron fission at 1.5 to 15 Mev, delayed neutron yields from, (E), 20: 17832
neutron reactions (n,γ) at 0.01 to 3 Mev, cross sections for, (T), 20: 17720
production of alpha sources of, electrospraying method for, 20: 16553
proton fission at 150 to 660 Mev, cross sections for, (E), 20: 17838
proton fission at 450 Mev, recoil ion properties from, (E), 20: 17790
triton reactions (t,pf) at 13 Mev, fragment-proton coincidences in, (E), 20: 17844

URANIUM LEACH SOLUTIONS
processing for thorium recovery by solvent extraction using organic phosphorus compound and sulfuric acid, 20: 16573
separation of copper and uranium from, by liquid ion exchange, 20: 16572

URANIUM MINERALS

age estimation of, from radioactive disequilibrium in, 20: 16717
occurrence and requirements in Europe and western countries, 20: 16716
radioactivity of, determination of relative abundances of uranium decay products from, 20: 16717
URANIUM NITRATES
analysis for plutonium by argentic oxidation, ferrous reduction, and dichromate titration, 20: 16405
URANIUM NITRIDES
sintering, 20: 16582
URANIUM ORES
carbon, oxygen, and sulfur isotope ratios in, Gas Hills District, Wyoming, 20: 16670
processing of, research on, 20: 18174(R) (NP-15771)
reserves and resources of, in U. S., 20: 16718
URANIUM OXIDES
analysis for manganese using sodium perxenate, spectrophotometric, 20: 16351
reduction, 20: 16582
UC–UO, thermodynamic properties, 20: 16449
URANIUM OXIDES (STAINLESS STEEL CLAD)
meltdown in reactors, fission product behavior in, 20: 18020(R) (ORNL-3900, pp 2-81)
URANIUM(IV) OXIDES
coating with ceramics or metals, 20: 16582
diffusion of fission products from, 20: 18020(R) (ORNL-3900, pp 2-81)
diffusion of xenon in single crystals and particles of, at 600 to 2400°C, 20: 17103
effects on potassium and sodium sorption by barley roots, 20: 16174(R) (RLO-1547-3)
effects on uranyl ion sorption by barley roots, 20: 16174(R) (RLO-1547-3)
evaporation of non-gaseous fission products from, at 750 to 1600°C, 20: 17102
fritting of, at 700 to 850°C, 20: 17037
growth of single-crystal, 20: 17158(R) (ORNL-3900, pp 82-149)
inclusions in, effects of thermal history on metallic, 20: 16953 (ORNL-TM-1161, pp 249-66)
neutron multiplication factors for aluminum- and Zircaloy-clad, effective, (T), 20: 18065
oxidation in air at 200 to 360°C, phase transitions in, 20: 16474(T)
oxidation to U_3O_8, x-ray diffraction study of, 20: 16471
preparation from uranium hexafluoride, pyrolytic, 20: 18020(R) (ORNL-3900, pp 2-81)
preparation of metallographic samples of, containing metallic inclusions, 20: 16953 (ORNL-TM-1161, pp 249-66)
processing of irradiated, by oxidation-reduction cycles, 20: 16576
production and sintering, 20: 16582
radiation effects on structure of, neutron, 20: 17148
specific heat and thermal conductivity of, methods for measuring, 20: 17099
PuO_2–UO_2, burnup in fast reactors, effects on breeding ratio, multiplication factor, and sodium-void reactivity, 20: 18060
PuO_2–UO_2, development as fuel rods, 20: 18095 (WCAP-3385-52)
ThO_2–UO_2, effects of dispersions of, on mechanical properties of beryllia, 20: 17113 (AAEC-E-140)
ThO_2–UO_2, fission gas diffusion from pyrolytic-carbon-coated particles of, effects of coating structure on, 20: 17127 (ORNL-3923)
ThO_2–UO_2, preparation of microspheres of, 20: 18020(R) (ORNL-3900, pp 2-81)
UO_2–ZrB_2, radiation testing of fuel elements of, 20: 17121 (GEAP-4918)
UO_2–ZrO_2, fabrication and properties, 20: 17005
W–UO_2, neutron Doppler coefficients and resonance integrals for, (E/T), 20: 18045(R) (AI-66-16)
URANIUM(IV-VI) OXIDES
analysis for chromium, cobalt, iron, and zinc, activation, 20: 16399
analysis for uranium, titrimetric, 20: 16401
content in dog lungs after inhalation, 20: 16184
URANIUM(V) OXIDES
preparation and properties, 20: 16430
URANIUM(VI) OXIDES
production, 20: 16582
URANYL IONS
diffusion in cesium uranyl chloride crystals, energy transfer from, (E), 20: 18010
effects on hydrolysis of α-D-glucose 1-phosphate, 20: 16421
separation from phosphoric acid solution by solvent extraction using alkyl phosphates, 20: 16579
sorption by aminodiacetate resin Dowex A-1, 20: 16358
sorption by barley roots, effects of pH and uranium(VI) oxide concentration on, 20: 16174(R) (RLO-1547-3)
spectra of, in perchlorate media, resolution of overlapping band structure in, 20: 16450
URANYL NITRATE COMPLEXES
with organophosphorus compounds, NMR studies of coupling in, 20: 16422
URANYL NITRATES
effects on iodine-131 exchange in silver iodide–iodide ion systems, 20: 16432
ion exchange and sorption on glass surfaces, 20: 16469
reactions with sodium pyrophosphate, 20: 16472
spectra and structure of hydrated, luminescence, 20: 16465(T)
URINE
analysis for cesium-137 by ion exchange and gamma spectroscopy, 20: 16342
analysis for uranium, methods for, 20: 16337 (RMO-3001(Rev.1)(Suppl.))
cesium-137 content in human, in Japan, 1964, 20: 16731 (NP-15883)
chlorine-36 content in calf, after ingestion, 20: 16186
iodine-131 content in human, in Japan, 1964, 20: 16730 (NP-15882)
iodine-131 content in calf, after ingestion, 20: 16186
radiation effects on thymidine excretion in rat, β, 20: 16201
radiation effects on content of dehydroepiandrosterone in, use in determining radiation response, 20: 16209
radiation monitoring in Japan, cesium-137 and strontium-90, 20: 16226 (NP-15891)
radioisotope excretion in dog, pathway of, 20: 16160 (UCRL-14739(Pt.2))
strontium-85 content in human, effects of sodium alginate on, 20: 16173 (PG-Report-686)
UTAH (SAN JUAN CO.)
environs monitoring of Monticello Project in, 20: 16729 (IDO-12049)
UTERUS
radiotherapy of cancers of, 20: 16326

V

VACUUM
gravitational fields in, uniqueness of central-symmetric, (T), 20: 17582
VACUUM SYSTEMS
pressure measurements in, using hot-cathode ionization gages, 20: 16630
VACUUM VESSELS
design of scattering chamber for use with solid-state detectors, 20: 16883
VAN ALLEN RADIATION BELTS
electron and proton intensity in, 20: 17310(T) (AD-623948)
electron distribution in lower regions of outer, (E), 20: 17538 (N-65-17609)
origin, (T), 20: 17547(T)
proton density variation with solar cycle, computer program for calculation of, 20: 17539 (N-65-18257)
proton intensity at $3.5 \leq L \leq 10$, (E), 20: 17548(T)
VAN DE GRAAFF ACCELERATORS
pulse generator for 2-Mev, nanosecond, 20: 17217
VANADIUM
analysis for oxygen, activation, 20: 16331 (GA-6568)
determination in copper, activation, 20: 16332 (GA-6691)
determination of trace amounts of, in beryllium by spectrography, 20: 16352
dislocation parameters for, 20: 17033
magnetic susceptibilities of, temperature dependence of, 20: 17069
melting point of, effects of gas impurities on, 20: 17094
proton reactions at 590 Mev and 18.3 Bev, potassium isotope yields in, (E), 20: 17717
separation from scandium by ion exchange chromatography, 20: 16574
VANADIUM ALLOYS
Al–Co–V, phase studies on intermetallic compounds in, 20: 17075
Al–Ti–V, corrosion cracking in titanium-base, stress-, 20: 16967 (AD-628277)
Al–V–Zr, phase studies on intermetallic compounds in, 20: 17075
Ge–Ta–V, phase studies on intermetallic compounds in, 20: 17075
Ir–V, superconductivity in close-packed intermediate phases of, 20: 17624
Mo–Nb–V–Zr, fabrication of tubing of B-66, 20: 16998
Nb–V, oxidation of, temperature dependence of, 20: 16982
VANADIUM BORIDES
chemical bonding and electric conductivity of, 20: 16439
VANADIUM CARBIDES
NbN–VC, superconducting properties, 20: 17589 (CONF-650922, pp 541-9)
VANADIUM ISOTOPES V-46
beta decay of, phase-space integrals for, (T), 20: 17732
VANADIUM ISOTOPES V-51
helium-3 reactions (He-3,2p) at 12 Mev, Q value for, 20: 16331 (GA-6568)
neutron reactions (n,p) with, sensitivity of, for activation analysis, 20: 16332 (GA-6691)
proton reactions (p,α) with, neutron production for activation analysis in, 20: 16332 (GA-6691)

proton reactions (p,2p) at 140 Mev, energy spectra and angular correlation distributions from, (E), 20: 17741
VANADIUM ISOTOPES V-52
half life, 20: 16331 (GA-6568)
nucleon interactions in, properties from effective, (T), 20: 17735
VANADIUM ISOTOPES V-53
nucleon interactions in, properties from effective, (T), 20: 17735
VANADIUM NITRIDES
NbC–NbN–VN, superconducting properties, 20: 17589 (CONF-650922, pp 541-9)
NbN–VN, superconducting properties, 20: 17589 (CONF-650922, pp 541-9)
VANADIUM OXIDES
NbO_2–VO_2, crystal structure of double oxide $NbVO_4$, 20: 16982
V_2O_3–V_2O_5, phase studies, 20: 17007(R) (AD-627468)
VANADIUM SILICIDES
solvent properties for aluminum and beryllium, 20: 17043
superconductivity of, effects of aluminum, beryllium, germanium, and tin on, 20: 17043
VANADIUM SYSTEMS
Al–Si–V, superconductivity of solid solutions in, 20: 17043
Be–Si–V, superconductivity of solid solutions in, 20: 17043
Ge–Si–V, superconductivity of solid solutions in, 20: 17043
O–V, phase studies, 20: 17007(R) (AD-627468)
Si–Sn–V, superconductivity of solid solutions in, 20: 17043
Si–Te–V, phase studies on intermetallic compounds in, 20: 17075
VANADYL IONS
sorption by aminodiacetate resin Dowex A-1, 20: 16358
VELA PROJECT
environs monitoring for Salmon Event, 20: 16743 (VUF-1021)
ground water flow velocities and radioactive decay in Shoal Event, hazards from, 20: 16742 (VUF-1014)
VERMICULITES
radiation effects on corrosion of cesium-containing, 20: 18166(R) (TID-22531)
VESSELS
design and properties of, for radio-induced chemical reactions, 20: 16505 (BNL-949)
design of stainless steel, for recovering radioactive waste, 20: 18160 (CEA-R-2894)
fixation of radioactive materials in, calculations of transient temperatures for, 20: 18155 (BNWL-157)
VINYL ALCOHOL POLYMERS
radioinduced crosslinking in, for use as membrane in artificial kidneys, 20: 16505 (BNL-949)
VIRUSES
isolation of leukemia, in mice, 20: 16159(R) (ORNL-3900, pp 150-81)
radiation effects on nucleic acids in, uv, 20: 16206
radiation effects on nucleic acids in, uv, 20: 16207
separation from other materials using ultracentrifuges, 20: 16159(R) (ORNL-3900, pp 150-81)
separation of, engineering drawings of containment system for centrifugal, 20: 16166
VITAMIN B_{12}
sorption by patients, tracer study, 20: 16303(R) (AD-626384)
VOLCANOES
deposits from Costa Rica, inside and outside of one-story residences, 20: 16659 (AD-629527)
VOLTAMMETRY
method for x-ray equipment, using photographic film, 20: 16844

W

WASTE DISPOSAL
bibliography on, 20: 18153 (AED-C-01-12)
bibliography on, 20: 18154 (AED-C-01-13)
fixation in glass, simulation studies on, 20: 18166(R) (TID-22531)
fixation in soils by injection, hydrodynamics of, 20: 18163(R) (NP-15859)
fresh water, hazards and movement in, 20: 18157 (BNWL-SA-466)
incorporation in asphalt, feasibility of, 20: 18020(R) (ORNL-3900, pp 2-81)
methods for glass melter condensates containing sulfuric acid, 20: 18159 (BNWL-SA-514)
methods of, review of safety precautions in, 20: 16577
methods of, review of, 20: 16582
salt mine, field demonstration of, 20: 18020(R) (ORNL-3900, pp 2-81)
salt mine, field experiment for demonstration of high-level, 20: 18169
solidification, processes for high-level materials, 20: 18020(R) (ORNL-3900, pp 2-81)
storage in salt caverns, dimensioning for maximum credible accidents in, (T), 20: 16722 (BMwF-FBK-65-03)
storage in salt formations, equipment for, 20: 18165 (ORNL-P-1987)
WASTE PROCESSING
equipment and methods for, at Eurochemic fuel reprocessing plant, 20: 18167
evaporation and fixation in bitumens, Karlsruhe, 1963 to 1965, 20: 18171
fission product release in, effects of volatilization on, 20: 18156 (BNWL-SA-453)
incineration, fixation of ash from, in glass, 20: 18166(R) (TID-22531)
methods for glass melter condensates containing sulfuric acid, 20: 18159 (BNWL-SA-514)
methods of, in reactor fuel reprocessing facilities, 20: 16582
solidification, objectives and plans for engineering prototypes for, 20: 18158 (BNWL-SA-467)
WASTE SOLUTIONS
analysis for trace amounts of uranium by controlled-potential polarography, 20: 16389
decontamination using caustic-carbonate precipitants in sludge-blanket column, 20: 18168
evaporation by solar energy, design of equipment for, 20: 18164(R) (NP-15874)
recovery of, design of equipment for, 20: 18160 (CEA-R-2894)
separation of cesium-137, strontium-90, and yttrium-90 from, using multiclone dust, 20: 18170
separation of cesium from high-level, by ion exchange, 20: 16570
separation of manganese and rare earths from, solvent extraction methods for, 20: 16329 (BNWL-187)
separation of strontium-90 from, by sorption by aluminum oxide, 20: 16330 (CEA-R-2851)
solidification of, performance of in-tank, 20: 18161 (ISO-SA-1)
WATER
analysis for alpha and beta sources, radiochemical methods for, 20: 16337 (RMO-3001(Rev.1)(Suppl.))
analysis for cesium-137 by ion exchange and gamma spectroscopy, 20: 16342
analysis for heavy water by infrared spectroscopy, 20: 16377
analysis for hydrogen peroxides in irradiated, polarographic, 20: 16327 (AAEC/TM-301)
analysis for uranium, methods for, 20: 16337 (RMO-3001(Rev.1)(Suppl.))
analysis of, methods for, 20: 16337 (RMO-3001(Rev.1(Suppl.))
bonding in alumina, beryllia, and silica during dehydration at 150 to 1100°C, 20: 16413 (CEA-R-2703)
cavitation damage to materials in, (E), 20: 16974 (NP-15889)
decomposition by electric-arc heating of vaporous, plasma radiation from, (E/T), 20: 17936
determination in coke by neutron absorption, 20: 16922
determination in coke, concretes, and sand using neutron probes, 20: 16926
determination in samples by neutron absorption, gage for, 20: 16924
deuterium exchange with, catalytic effects of ruthenium chloride on, 20: 16423
evaporator for treatment of contaminated, automatic control of, 20: 16594
fissile-material critical mass in, distribution effects on, (T), 20: 18062
fuel element weighing in, equipment for error elimination in irradiated, 20: 16780 (TID-22689)
gamma shielding by, thickness calculations for, 20: 17964(T) (ORNL-tr-1061)
heat of adsorption on thorium oxide, 20: 16456
heat transfer characteristics in two-phase flow, 20: 16605 (NYO-3304-8)
ionization and proton transfer in, effects of tritium on, 20: 16424
oxygen-18 exchange reactions between *p*-substituted benzoate anions and, mechanism of, 20: 16542(R) (TID-22646)
oxygen-18 exchange reactions between *p*-substituted benzophenones and, 20: 16542(R) (TID-22646)
radiolysis of, effects of hydrogen and oxygen on yields of hydrogen peroxide from, 20: 16520
radiolysis of, reaction rates and yields in, (T), 20: 16509 (TID-22666)
radiosensitivity effects on *Rauwolfia serpentina* seed, γ, 20: 16249
radiosensitivity effects on *Vicia sativa*, x, 20: 16276
radiosensitivity effects on pea flour, 20: 16297(R) (EUR-2548.f)
reactions of jets of, with liquid aluminum, pressure-wave generation by, 20: 18050(R) (STL-372-22)
reactions with rare earth dicarbides, formation of gaseous products in, 20: 17048
solvent properties for magnetite at high temperatures, 20: 17158(R) (ORNL-3900, pp 82-149)
systems for de-ionized, for cleaning stations, 20: 16590 (SC-TM-66-49)
dioxane–H_2O, effects on equilibrium in keto-enol tautomerism of 2,4-pentanedione, 20: 16416(R) (NYO-906-68)
dioxane–H_2O, effects on isotopic exchange between elementary iodine and 1-phenyl-2,3-dimethyl-4-iodopyrazolone, 20: 16502
ethanol–H_2O, effects on isotopic exchange between elementary iodine and 1-phenyl-2,3-dimethyl-4-iodopyrazolone, 20: 16502
Fe–H_2O, neutron age to indium resonance energy in, fission, (E), 20: 17659

Fe–H_2O, neutron slowing down density distributions in, Monte Carlo code for, 20: 17660
N–H_2O, oxidative effects on uranium, mechanism of, 20: 16986
N–O–H_2O, oxidative effects on uranium, mechanism of, 20: 16986
O–H_2O, oxidative effects on uranium, mechanism of, 20: 16986
2-methyl-1-propanol–water, effects of fluoride on distribution of ferric thiocyanate in, 20: 16335(R) (NBS-TN-276)
2-propanol–H_2O, thermodynamics of reactions between nickel(II) and 2,4-pentanedione in, 20: 16416(R) (NYO-906-68)

WATER-d_2
alkali halide activity and osmotic coefficients in, at 25°C, 20: 16473
determination in water by infrared spectroscopy, 20: 16377

WATER-t_2
effects on root growth of corn and pea seedlings, 20: 16227(R) (NYO-3561-2)

WATER COOLED REACTORS
core configuration of VVR-M, optimization of, 20: 18140
experimental facilities for VVR-M, beam holes and thermal column, 20: 18139
kinetics of heterogeneous, 20: 18050(R) (STL-372-22)

WATER MODERATED REACTORS
core configuration of VVR-M, optimization of, 20: 18140
criticality parameters for epithermal, (E/T), 20: 18053
experimental facilities for VVR-M, beam holes and thermal column, 20: 18139

WATER PURIFICATION EQUIPMENT
design for operation on high-purity coolant of hermetically sealed boiling reactors, 20: 18089 (NAA-SR-Memo-10178)

WATER SUPPLIES
analysis for radioisotopes, methods for, 20: 16369
radioactivity from cesium-137 and strontium-90 in, in Japan, 1964, 20: 16731 (NP-15883)
radioactivity in, method for determining alpha, beta, and gamma, 20: 16407
strontium-90 content in U. S., 1965, 20: 16662(R) (HASL-165)

WATER VAPOR
radiolysis of, effects of temperature and cyclohexane scavenger on yields of hydrogen from gamma, 20: 16536

WELDED JOINTS
analysis for carbon and oxygen, activation, 20: 16331 (GA-6568)

WELDING
use of plasma jets for, 20: 16593

WELDS
testing of electric resistance and flash butt, 20: 16618

WELL LOGGING
methods of, gamma-gamma and neutron-gamma, 20: 18182

WHEAT
radioinduced mutations in, γ and x, 20: 16285
radioinduced mutations in, 20: 16286
radiosterilization of, status, 20: 16918 (AECL-PAK/RB-7)
strontium-90 content in, in Japan, 1964, 20: 16731 (NP-15883)

WHISTLERS
power spectra of, electron velocity distributions from, (T), 20: 17558

WIND
effects on fallout level, near New Delhi, 20: 16680
effects on particulate matter in atomic clouds, 20: 16160 (UCRL-14739 (Pt.2))
fallout perturbations by local sea breezes, 20: 16661(R) (ECOM-00392-F)

WIND TUNNELS
development of plasma, experiments for, 20: 17904

WOOD
pulp flow through mills, tracer technique for studying, 20: 16921 (TID-22627)
plastics–wood, radiation processing of materials of, 20: 16505 (BNL-949)

WYOMING
carbon-13 content of calcite in epigenetic pyrite deposits, Gas Hills Area, 20: 16675
carbon, oxygen, and sulfur isotope ratios in uranium deposits in Gas Hills district, 20: 16670

X

X RADIATION
detection and measurement of, design of narrow-band apparatus for, 20: 16823 (NYO-3160-1)
detection and measurement of, design of extrapolation chamber for, 20: 16852
detection and measurement of cosmic, using gas proportional counters, 20: 16901
detection and measurement of solar, instruments for, 20: 16904
detection of, scintillation counter efficiency for, 20: 16836
dosimetry of fractionated, nomogram for, 20: 16749
dosimetry of medical, 20: 16843
dosimetry of radiographic, tables for, 20: 16751
dosimetry of, liquid photographic emulsions for, 20: 16845
dosimetry of, oxygen enhancement ratio for, 20: 16750
dosimetry of, using cyanides of triphenylmethane dyes, 20: 16521
effects after head therapy, tumorigenic, 20: 16245
effects of therapeutic doses of, delayed carcinogenic, 20: 16242
effects of, combined with cold on cesium-137 retention in rats, 20: 16180
effects of, combined with cytostatic drugs on polycythemia, complications from, 20: 16233
effects of, combined with cyclophosphamide and hyperbaric oxygen in leukemic mice, 20: 16262
effects on blood cells, globulins, and proteins in mice, fractionated-dose, 20: 16224 (CEA-R-2848)
effects on body and renal weight in nephrectomized mice, 20: 16282
effects on bronchial, esophageal, and lung carcinomas, moving-beam, 20: 16317
effects on conditioned behavior in parabiont rats, x, 20: 16284
effects on copper and zinc content and enzyme activity in blood of mammals, 20: 16222 (AFWL-TR-65-112)
effects on crystals of deuterated glycine, controlled-temperature ESR spectral studies on, 20: 16525
effects on cultured KB cells, 20: 16258
effects on development of *Oryzias latipes* females, effects of steroids on, 20: 16263
effects on developing rat brain, pathological, 20: 16275
effects on DNA synthesis in mammalian cells, 20: 16230(R) (TID-22644)
effects on enzyme activity in rat tissue homogenates, 20: 16289
effects on EPR spectra of quartz with aluminum impurity, 20: 16539(T)
effects on erythrocyte morphology in man, chronic-exposure, 20: 16250
effects on ethanol or methanol mixtures with naphthalene, spectra of hydrogen atom reactions in, 20: 16524
effects on formation of leukocyte-regulating factor in rabbits, 20: 16265
effects on function and histology of rabbit kidneys, 20: 16234
effects on glucose absorption in rat intestine, 20: 16274
effects on goldfish, effects of water temperature on lethal, 20: 16236
effects on growth inhibition by rat serum, protective effects of cysteine against, 20: 16208
effects on intestinal epithelium in mice, lethal whole-body exposure, 20: 16223 (BNL-8952)
effects on life span and reproduction of *Sarcophaga peregrina*, 20: 16291
effects on luminescence of thallium-activated sodium-iodide crystals, excitation mechanism of, 20: 17991(T)
effects on mice and rats, protective effects of sulfur compounds against, 20: 16297(R) (EUR-2548.f)
effects on mice, protective effects of 1,3,4-oxadiazolium salts and s-triazole derivatives against, 20: 16490(R) (TID-22681)
effects on Mikulicz's disease, therapeutic, 20: 16316
effects on mitosis in Saccharomyces, 20: 16255
effects on mitosis in rat lens epithelium, 20: 16256
effects on mitotic mechanism in *E. coli*, repair of, 20: 16200
effects on MOS field-effect transistors, transient, 20: 16913
effects on mutation rates in ad-3 regions of *Neurospora*, 20: 16159(R) (ORNL-3900, pp 150-81)
effects on olfactory bulb neurons in rats, effects of gases in nasal cavities on, 20: 16215 (AD-628443)
effects on *Paramecium Aurelia*, equation for survival from, 20: 16273
effects on peanuts, genetic, 20: 16247
effects on peritrichs, 20: 16295
effects on photoconductivity of cadmium sulfide, 20: 17123(R) (N-65-17505)
effects on physiology of reticulum cells in rat thymus, 20: 16293
effects on potassium chloride external surface energy, 20: 17137
effects on propagation of cleavage cracks in sodium chloride single crystals, 20: 16513
effects on rats, biological, 20: 16287
effects on rats, biological, 20: 16288
effects on sarcoma, therapeutic, 20: 16312
effects on seeds of Vicia, genetic, 20: 16276
effects on seeds, effects of infrared radiation on genetic, 20: 16278
effects on spinal cord, pathological, 20: 16251
effects on survival in Chlorella, mathematical analysis of, 20: 16246
effects on sweet cherry trees, genetic, 20: 16244
effects on transference mechanism in parabiont rats, 20: 16284
effects on wheat seed, genetic, 20: 16285
effects on wheat seeds, genetic, 20: 16286
effects on yeast, metabolic, 20: 16240
effects on yeasts, effects of dark recovery and glycerol on, 20: 16231 (UCRL-16377)
emission from cosmic sources, observation and theory of, 20: 17248
emission from lunar surface following electron bombardment, 20: 17246

emission from neutron stars, (T), 20: 17240
emission from thin aluminum films, determination of surface density from proton-induced, 20: 17051
intensity measurement of, instrumentation for calorimetric, 20: 16856
intensity of, accuracy in measurement of, 20: 18017
isotope shift of K_α, in uranium, 20: 17285
scattering by neutron-irradiated graphite, 20: 17130
scattering by thin copper films, interference fringes from, (E/T), 20: 17163
use for therapy of thyroid cancers, 20: 16307
use for therapy of scalp carcinoma, 20: 16308
use in astronomy, 20: 17244
use in therapy of inflammations, 20: 16314
X-RAY-ABSORPTION ANALYSIS
equipment and methods for, 20: 17158(R) (ORNL-3900, pp 82-149)
X-RAY-DIFFRACTION ANALYSIS
intensity measurements in, conference on accuracy of, 20: 18017
X-RAY DIFFRACTOMETERS
operation of, safety in, 20: 16782
X-RAY EQUIPMENT
properties of dental, photographic film for determining, 20: 16844
X-RAY FLUORESCENCE ANALYSIS
detector design for, narrow-band, 20: 16823 (NYO-3160-1)
X-RAY MICROSCOPY
alpha source preparation and handling for electron-microprobe analyzer for, 20: 16554
X-RAY SPECTRA
effects of chemical bonding on, 20: 16160 (UCRL-14739(Pt.2))
X-RAY SPECTROMETERS
operation and control of system of, computer for, 20: 16869
X-RAY SPECTROSCOPY
semiconductor detectors for use in, 20: 16887
XENON
diffusion in uranium dioxide single crystals and particles at 600 to 2400°C, 20: 17103
radio wave emission from plasma of, negative-absorption effects on anomalous bremsstrahlung and cyclotron, (E), 20: 17921
spectra of molecules trapped in solid, 20: 18016
XENON ISOTOPES
abundance in Achilles, LaLande, and Peace River chondrites, 20: 16672
content in Pasamonte meteorite, anomalies from, 20: 17239
XENON ISOTOPES Xe-133
production process improvement, 20: 16914(R) (ORNL-3900, pp 182-93)
XENON ISOTOPES Xe-135
production by neutron reactions (n,α) with barium-138, cross sections for, (E/T), 20: 17809
XYLENE
tritium exchange with tritiated ethyl malonate, effects of catalysts on, 20: 16492
2,4-XYLENOL
preparation of deuterated, from 2,4,6-tri-d_3-methylpyrylium perchlorate, 20: 16501
XYLENOL ORANGE
uses for determination of rare earths in selenides, sulfides, and tellurides, 20: 16395
uses for spectrophotometric determination of lanthanum, 20: 16394
uses in photometric determination of neptunium, 20: 16408

Y

YANKEE POWER REACTOR
radiation and thermal damage in pressure vessel in, 20: 17126 (NRL-6349)
YEASTS
growth and metabolism of, effects of rare earths and yttrium on, 20: 16191
metabolism and reproduction in, effects of radiomimetic compounds on, 20: 16240
mutations in growing, effects of 5-aminoacridine on, 20: 16159(R) (ORNL-3900, pp 150-81)
radiation effects on, protective effects of dark recovery and glycerol against α and x, 20: 16231 (UCRL-16377)
radiation effects on metabolism and reproduction of, x, 20: 16240
radiation effects on mitosis in, uv and x, 20: 16255
YTTERBIUM
determination in carbonatites by ion exchange chromatography and oxalate precipitation, 20: 16346
thermal capacity at 3 to 25°K, 20: 17080
YTTERBIUM ALLOYS
Au–Yb, phase studies, 20: 17016 (IS-1175)
Hg–Yb, crystal structure of $YbHg_3$, 20: 17060
In–Yb, crystal structure of $YbIn_3$, 20: 17060
Pb–Yb, crystal structure of $YbPb_3$, 20: 17060
YTTERBIUM HYDRIDES
properties and structure, 20: 16453
YTTERBIUM HYDROXIDES
decomposition of, products of thermal, 20: 16441
YTTERBIUM ISOTOPES Yb-169
gamma angular correlations from, in lutetium iron garnet, (E), 20: 17994
YTTERBIUM ISOTOPES Yb-170
energy levels from lutetium-170 decay, (T), 20: 17742
YTTERBIUM ISOTOPES Yb-171
energy level scheme for, (E), 20: 17158(R) (ORNL-3900, pp 82-149)
YTTERBIUM OXIDES
determination in thorium oxide by emission spectroscopy, 20: 16393
determination of hydrated, from ytterbium hydroxide thermal decomposition, 20: 16441
$CaO–Yb_2O_3$, phase studies, 20: 17087
$ReO_3–Yb_2O_3$, phase studies at 1130 and 1300°C, 20: 17007(R) (AD-627468)
$SrO–Yb_2O_3$, properties of compounds formed by interactions in, 20: 17044
YTTERBIUM SULFIDES
Ce_2S_3–YbS, compound formation in, 20: 16431
Dy_2S_3–YbS, compound formation in, 20: 16431
Gd_2S_3–YbS, compound formation in, 20: 16431
Ho_2S_3–YbS, compound formation in, 20: 16431
La_2S_3–YbS, compound formation in, 20: 16431
Nd_2S_3–YbS, compound formation in, 20: 16431
Pr_2S_3–YbS, compound formation in, 20: 16431
Sm_2S_3–YbS, compound formation in, 20: 16431
Tb_2S_3–YbS, compound formation in, 20: 16431
YbS–Y_2S_3, compound formation in, 20: 16431
YTTRIUM
abundance in sun, (E), 20: 17237
determination in dysprosium and terbium using bis(2-ethylhexyl) phosphate, chromatographic, 20: 16385
effects on growth and metabolism of bacteria, fungi, molds, and yeasts, 20: 16191
effects on high-temperature properties of eutectic alloys, 20: 17108
preparation of self-supporting radiation targets of, 20: 17218
separation from sewage water by sorption on multiclone dust from gasification of coke, 20: 18170
YTTRIUM ALLOYS
Fe–Y, crystal structure of Y_6Fe_{23} in, 20: 17096(T)
Mn–Y, crystal structure of Y_6Mn_{23} in, 20: 17096(T)
YTTRIUM CARBIDES
properties of, chemical and physical, 20: 17048
reactions with water, formation of gaseous products in, 20: 17048
YTTRIUM COMPLEXES
stability constants of, determination of, by metal distribution between aqueous phase and ion exchanger, 20: 16481
with phenanthroline, infrared spectra of, 20: 16436
with solochrome violet RS, polarography of, 20: 16406
with 2,2′-bipyridyl, infrared spectra of, 20: 16437
YTTRIUM HYPOPHOSPHITES
preparation and properties of, 20: 16426
YTTRIUM ISOTOPES Y-85
beta decay of isomeric, half life for, (E), 20: 17670 (AD-629576)
energy levels of, parity and spin of, (E), 20: 17670 (AD-629576)
YTTRIUM ISOTOPES Y-88
content in stratospheric and tropospheric samples in Project Star Dust, 1963, 20: 16727(R) (HASL-168)
content in stratospheric and tropospheric samples in Project Star Dust, 1964, 20: 16728(R) (HASL-169)
YTTRIUM ISOTOPES Y-89
half life of isomeric, from neutron reactions (n,n′), (E), 20: 16336(R) (NYO-10175)
neutron reactions (n,n′), activation cross section for, (E), 20: 16336(R) (NYO-10175)
YTTRIUM ISOTOPES Y-90
use for therapy of skin tumors, 20: 16325
YTTRIUM ISOTOPES Y-91
content in fallout and precipitation near Leningrad, 20: 16704
content in stratospheric and tropospheric samples in Project Star Dust, 1963, 20: 16727(R) (HASL-168)
content in stratospheric and tropospheric samples in Project Star Dust, 1963, 20: 16728(R) (HASL-169)
YTTRIUM OXIDES
determination in thorium oxide by emission spectroscopy, 20: 16393
separation of zirconium-89 from irradiated, by ion exchange, 20: 16353
$HfO_2–Y_2O_3$, mechanical and thermal properties of plasma-sprayed, 20: 16943(R) (IITRI-B237-45)
$SrO–Y_2O_3$, properties of compounds formed by interactions in, 20: 17044
$TiO_2–Y_2O_3$, phase studies, 20: 17032
YTTRIUM SILICIDES
properties of, physicochemical, 20: 17047

YTTRIUM SULFIDES
YbS–Y_2S_3, compound formation in, 20: 16431
YUGOSLAVIA
cesium-137 content in atmosphere in, from weapons testing in 1962 and 1963, 20: 16682

Z

ZINC
analysis for fluorine in electrorefining solutions of, feasibility of activation, 20: 16339(R) (TID-22662)
content in marine organisms, 20: 16725(R) (EUR-2543.e)
determination by radiometric titration, 20: 16386
determination in asbestos using ion exchange, activation, 20: 16336(R) (NYO-10175)
determination in lung tissue, activation, 20: 16335(R) (NBS-TN-276)
determination in marine organisms, polarographic, 20: 16175(R) (RT/BIO(65)-1)
determination in uranium concentrates, oxides, and metal, activation, 20: 16399
effects on gastrointestinal absorption of copper-64 in rats, 20: 16182
effects on manganese sorption by barley roots, 20: 16174(R) (RLO-1547-3)
neutron diffraction by, scattering length for, (E), 20: 17667
proton reactions at 590 Mev and 18.3 Bev, potassium isotope yields in, (E), 20: 17717
radiation effects on content in blood serum of mammals, 20: 16222 (AFWL-TR-65-112)
separation from scandium by ion exchange chromatography, 20: 16574
ZINC ALLOYS
Cu–Zn, cavitation damage in water, 20: 16974 (NP-15889)
ZINC COMPLEXES
with solochrome violet RS, polarography of, 20: 16406
ZINC IONS
effects on hydrolysis of α-D-glucose 1-phosphate, 20: 16421
sorption by aminodiacetate resin Dowex A-1, 20: 16358
ZINC ISOTOPES
separation of, performance of separator for, 20: 16928(R) (INSJ-92)
ZINC ISOTOPES Zn-64
proton reactions (p,p′) with, cross sections for, (T), 20: 17692 (ORNL-TM-1414)
ZINC ISOTOPES Zn-65
determination in irradiated materials by extraction and precipitation, gamma spectrometric, 20: 16336(R) (NYO-10175)
metabolism in aquatic organisms, 20: 16160 (UCRL-14739(Pt.2))
production in deuteron reactions (d,2n) with copper-65, cross sections for, 20: 16508(R) (NYO-2771-13)
uptake by aquatic foodstuffs from radioactive wastes in fresh water, 20: 18157 (BNWL-SA-466)
ZINC ISOTOPES Zn-68
deuteron reactions (d,p) at 15 Mev, isomeric yield ratios for, 20: 16508(R) (NYO-2771-13)
neutron reactions (n,γ), activation cross section for, (E), 20: 16336(R) (NYO-10175)
ZINC ISOTOPES Zn-69
half life of isomeric, from neutron reactions (n,γ), (E), 20: 16336(R) (NYO-10175)
production of isomeric, in deuteron reactions (d,p) at 15 Mev, 20: 16508(R) (NYO-2771-13)
ZINC ISOTOPES Zn-70
neutron reactions (n,γ), activation cross section for, (E), 20: 16336(R) (NYO-10175)
ZINC ISOTOPES Zn-71
half life of isomeric, from neutron reactions (n,γ), (E), 20: 16336(R) (NYO-10175)
half life of, from neutron reactions (n,γ), (E), 20: 16336(R) (NYO-10175)
ZINC OXIDES
reactions with aluminum oxides and lanthanum or neodymium oxides at 1400 to 1500°C, 20: 16482
ZINC SULFATES
activity and osmotic coefficients in heavy water at 25°C, 20: 16488
ZIRCALOY-2
corrosion by potassium hydroxide and potassium sulfate at 50 to 90°C, effects of electrode potential on, 20: 16979
diffusion of hydrogen in, effects of thermal cycling on, 20: 16981
metallography and stress analyses of, 20: 18020(R) (ORNL-3900, pp 2-81)
radiation effects on fuel cladding of, reactor, 20: 17120 (GEAP-4916)
ZIRCONIUM
abundance in sun, (E), 20: 17237
analysis for hafnium, activation, 20: 16335(R) (NBS-TN-276)
analysis for oxygen, activation, 20: 16331 (GA-6568)
corrosion by potassium hydroxide and potassium sulfate at 50 to 90°C, effects of electrode potential on, 20: 16979
determination in process feed solutions by extraction chromatography, 20: 16333 (KR-81)
effects on high-temperature properties of eutectic alloys, 20: 17108
effects on hydrolysis of adenosine-2-phosphate and carboxylase, catalytic, 20: 16420
magnetic susceptibilities of, temperature dependence of, 20: 17069
neutron reactions in, short-lived activities from, (E), 20: 16336(R) (NYO-10175)
properties as reactor fuel material, 20: 18182
radioinduced corrosion of, 20: 17158(R) (ORNL-3900, pp 82-149)
specific heat, (T), 20: 17084
ZIRCONIUM ALLOYS
Al–V–Zr, phase studies on intermetallic compounds in, 20: 17075
Al–Zr, crystallization of, effects of zirconium additions on, 20: 17072
Cu–Zr, oxidation by carbon dioxide at 800°C, 20: 16977
Hf–Ta–W, phase studies at 1100 and 1600°C, 20: 17012(R) (DRI-1092-226)
Mo–Nb–V–Zr, fabrication of tubing of B-66, 20: 16998
Mo–Ti–Zr, compatibility of TZM, with alumina, beryllia, magnesia, and boron nitride, 20: 17022 (N-65-18933)
Nb–Ta–W–Zr, properties as hollow turbine vanes, 20: 16963
Nb–Ti–Zr, oxidation-resistant coatings on D-36, performance of commercial, 20: 16973 (NASA-TN-D-3275)
Nb–W–Zr, properties as hollow turbine vanes, 20: 16963
Nb–Zr, cavitation damage in mercury and water, 20: 16974 (NP-15889)
Nb–Zr, degradation phenomena in small superconducting coils of, (E), 20: 17629
Nb–Zr, electric properties of normal region in superconducting magnet of, 20: 17610
Nb–Zr, Hall effect measurements on superconducting magnets of, 20: 17600(R) (ORNL-3908, pp 114-48)
Nb–Zr, internal friction and relaxation processes in, 20: 17106
Nb–Zr, magnetic susceptibility, 20: 17106
Nb–Zr, metallographic techniques for preparation of, for microscopy, 20: 16959
Nb–Zr, omega transformation and segregation processes in, 20: 17105
Nb–Zr, properties for containment of potassium at high temperatures, 20: 18020(R) (ORNL-3900, pp 2-81)
Nb–Zr, solvent properties for oxygen at 100 to 1200°C, 20: 16980
Nb–Zr, thermoelectric power at 9.2 to 330°K, effects of zirconium content on, 20: 17067
Nb–Zr, ultrasonic attenuation in nonideal superconducting, flux jumping and magnetization effects on, (E), 20: 17606
Ni–Zr, effects of additives on high-temperature properties of eutectic, 20: 17108
ZIRCONIUM BORIDES
chemical bonding and electric conductivity of, 20: 16439
preparation and properties of, 20: 17085
UO_2–ZrB_2, radiation testing of fuel elements of, 20: 17121 (GEAP-4918)
ZIRCONIUM CARBIDE HYDRIDES
crystal structure of, from thermal-neutron powder diffraction studies, 20: 17074
ZIRCONIUM CARBIDES
deposition on metals by electrophoresis at 19 to 20 mv, 20: 17004
ZIRCONIUM COMPLEXES
stability constants of, determination of, by metal distribution between aqueous phase and ion exchanger, 20: 16481
ZIRCONIUM ISOTOPES Zr-89
separation from yttrium oxides using ion exchange, radiochemical method for, 20: 16353
ZIRCONIUM ISOTOPES Zr-90
deuteron reactions (d,p) at 3.5 to 5.5 Mev, angular distributions from, (T), 20: 17691 (ORNL-TM-1235)
nucleon capture at 10 to 40 Mev, cross sections and mechanism for direct, (T), 20: 17737
ZIRCONIUM ISOTOPES Zr-91
nucleon capture at 10 to 40 Mev, cross sections and mechanism for direct, (T), 20: 17737
ZIRCONIUM ISOTOPES Zr-94
deuteron reactions (d,n) at 15 Mev, isomeric yield ratios for, 20: 16508(R) (NYO-2771-13)
ZIRCONIUM ISOTOPES Zr-95
content in atmospheric dust and rain water, 1964–65, 20: 16660 (AERE-R-4997)
content in plants before and after Salmon Event, 20: 16743 (VUF-1021)
content in rain water, Fayetteville, Arkansas, Oct. 1964, 20: 16663 (TID-21470)
content in rainwater and snow in Germany, 1961 to 1963, 20: 16766
content in stratospheric and tropospheric samples in Project Star Dust, 1963, 20: 16727(R) (HASL-168)
content in stratospheric and tropospheric samples in Project Star Dust,

1964, 20: 16728(R) (HASL-169)
content in surface layer of atmosphere over Heis Island and Moscow, 20: 16650
fallout monitoring at Vilnius, Soviet Union, in 1962, 20: 16700
ranges of fission products of, in aluminum, (E), 20: 17721

ZIRCONIUM NITRIDES
NbC–NbN–ZrN, superconducting properties, 20: 17589 (CONF-650922, pp 541-9)

ZIRCONIUM OXIDES
emissivity and reflectivity at 2100 to 3700°K, 20: 17021 (N-65-18607)
luminescent properties of titanium-activated, 20: 17056
preparation of thin films of, 20: 16946 (ORNL-TM-1161, pp 80-4)
preparation of titanium-activated, 20: 17056
radiation effects on structure of, neutron, 20: 17148
reactions with molten AMS 5350 steel and Inconel 713C, 20: 16984
Mo–ZrO_2, structure of dispersion-hardened, effects of sintering process on, 20: 17109
UO_2–ZrO_2, fabrication and properties, 20: 17005

ZIRCONIUM PHOSPHATES
properties for use as ion exchanger, 20: 16568
properties for use as ion exchanger, 20: 16582

ZIRCONIUM SILICATES
reactions with molten AMS 5350 steel and Inconel 713C, 20: 16984

ZIRCONIUM SYSTEMS
C–Co–Zr, phase studies, 20: 17086
C–Nb–W–Zr, microstructure of D-43, effects of aging on, 20: 17023 (ORNL-TM-1161, pp 208-24)
C–Nb–W–Zr, properties as hollow turbine vanes, 20: 16963
Fe–O–Ti–Zr, fabrication and properties of sintered, deformable, 20: 17003
Nb–O–Zr, phase studies, 20: 16980
T–Zr, fabrication and uses of targets of, 20: 16916

ZIRCONS
growth and doping of single-crystal, 20: 16960
radiation damage in, alpha, 20: 17147

REPORT NUMBER INDEX

Reports, conference papers and proceedings, numbered translations, and patents abstracted during the period are included in this index. Each item is listed by report number; this is followed by the abstract number and a brief notation regarding public availability. The index entries show which reports are on file in the depository libraries, which reports have been published in open-literature journals (journal citation given), and which reports can be purchased (source and price). Whenever a report is identified by more than one number, cross references from secondary to primary report numbers are cited.

The report number codes apply to AEC reports unless designated otherwise. Non-AEC reports are identified by parenthetical notes after the report codes; e.g., (non-AEC), (British), (Canadian), (French). The note (Misc.) identifies those codes used for both USAEC and non-AEC reports. Patents are listed under the heading "PATENTS"; the country of origin is included in parentheses.

A comprehensive listing of both AEC and non-AEC report codes is contained in TID-85(5th Rev.), *Report Number Series Used by the Division of Technical Information in Cataloging Reports*. This information is also included in the Cumulative Report Number Index (issued annually).

Public Availability of USAEC Reports

All USAEC reports abstracted in *NSA* are available to the public through one or more of the following sources:

(1) Depository libraries in the United States, in other countries, and in international agencies. A list of these depositories appears on the inside covers of each issue of *NSA*.

(2) Scientific and technical journals or other publications.

(3) Microcard Editions, Inc., in Microcard and micronegative form. Orders and inquiries should be sent to: Accounting and Shipping Department, West Salem, Wisconsin 54669.

(4) Clearinghouse for Federal Scientific and Technical Information, U. S. Department of Commerce, Springfield, Virginia 22151.

(5) Superintendent of Documents, U. S. Government Printing Office, Washington, D. C. 20402.

Public Availability of Non-AEC Reports

U. S. Reports. Many reports of U. S. Government agencies are available to the public from the Clearinghouse for Federal Scientific and Technical Information (CFSTI). This availability is given when known. Such reports should be ordered by AD number or NASA-N number. If availability is not shown, inquiries may be directed to CFSTI. In the case of NP numbers, inquiries should be by title and author.

Non-U. S. Reports. Many reports of atomic energy establishments of other countries are deposited in the libraries listed on the inside covers of each issue of *NSA*.

Additionally, the following have made their reports available as indicated.

AUSTRALIA

Australian Atomic Energy Commission Research Establishment. Available upon request from the Library, Australian Atomic Research Establishment, Private Mail Bag, Sutherland, New South Wales, Australia.

BELGIUM

Centre d'Étude de l'Énergie Nucléaire. Available upon request to individuals and organizations, from the Centre d'Étude de l'Énergie Nucléaire (CEN), 31, Rue Belliard, Bruxelles, Belgium.

CANADA

Atomic Energy of Canada Limited. For sale by the Technical Information Officer, Atomic Energy of Canada Limited, Chalk River, Ontario, Canada. Copies are also deposited in libraries in the United Kingdom.

National Research Council of Canada. Available from the National Research Council of Canada, Ottawa 2, Ontario, Canada.

DENMARK

Atomic Energy Commission Research Establishment, Risø. Available on exchange from the Library, Danish Atomic Energy Commission, Risø, Roskilde, Denmark. Also for sale by Jul. Gjellerup, Booksellers, 87 Sölvgade, København K., Denmark.

Danatom. Available on loan from Research Establishment, Risø, Roskilde, Denmark. Copies are available from Danatom, Aurehøjvej 2, Hellerup, Denmark.

EURATOM

Reports from the Commission of the European Atomic Energy Community are available from: Presses academiques europeennes, 98, chaussee de Charleroi, Brussels 6, Belgium; and Office central de vente des publications des Communautes eurodeennes 2, place de Metz, Luxemburg.

FRANCE

Commissariat à l'Énergie Atomique. Inquiries for reports numbered 1-2199 should be addressed to Commissariat à l'Énergie Atomique, Service Central de Documentation, Centre d'Études Nucléaires de Saclay, Boite Postale No. 2, Gif-sur-Yvette (S. et O.), France. Reports numbered 2200 and above are available from La Documentation Francaise, 16 Rue Lord-Byron, Paris VIII, France.

Service Central de Protection contre les Rayonnements Ionisants. Copies are available from Ministère de la Santé Publique, Service Central de Protection contre les Rayonnements Ionisants, B. P. n° 35–LE VESINET (S. et O.), France.

GERMANY

Deutsches Elektronen-Synchrotron DESY. Copies are available from Deutsches Elektronen-Synchrotron Desy, Dokumentation, 2000 Hamburg-Gr. Flottbek 1, Notkestieg 1, Germany.

Gesellschaft für Kernforschung mbH (KFK). Copies are available from Gesellschaft für Kernforschung mbH, 75 Karlsruhe, Postfach 947, Germany. Copies are also deposited in many national nuclear centers in the world.

Kernforschungsanlage. Copies may be ordered from Zentralbibliothek der Kernforschungsanlage Jülich, Jülich, Bundesrepublik Deutschland.

Hahn-Meitner-Institute für Kernforschung. Available without charge from Hahn-Meitner-Institute für Kernforschung Berlin, Bibliothek, Glienicker Strasse 100, 1 Berlin

39, Germany. Copies are deposited in many national nuclear centers in the world.

Johann-Wolfgang-Goethe Universität, Frankfurt Am Main, Institut für Kernphysik, (IKF). Copies are available from Gmelin Institut, 40-42 Varrentrappstrasse, Frankfurt (Main), West Germany.

ISRAEL

Israel Atomic Energy Commission. Available without charge from Ministry of Defence/Atomic Energy Commission, Soreq Research Establishment, Yavne, Israel. Copies are deposited in libraries in Israel and in other countries.

ITALY

Centro Informazioni Studi Esperienze (CISE). For sale at CISE Press Office, Casella Postale 3986, Milano, Italy. Copies are deposited in libraries in Italy.

Comitato Nazionale per l'Energia Nucleare. Copies are available from Comitato Nazionale per l'Energia Nucleare, Divisione Affari Internazionali e Studi Economici, Ufficio Pubblicazioni, Via Belisario, 15, Roma, Italy.

JAPAN

Japan Atomic Energy Research Institute (JAERI). Available from the Staff Supply Cooperative of Japan Atomic Energy Research Institute (JAERI), 1-1 Tamura-Cho, Shiba, Minato-Ku, Tokyo, Japan. Copies are deposited in depositories in Tokyo, Nagoya, and Osaka.

Nagoya University. Copies are available from Research Information Center, Institute of Plasma Physics, Nagoya University, Nagoya, Japan.

University of Tokyo. Available free of charge from Institute for Nuclear Study, University of Tokyo, Tanashi-Machi, Kitatama-gun, Tokyo, Japan.

NETHERLANDS

Reactor Centrum Nederland. For sale by Reactor Centrum Nederland, 112 Scheveningseweg, 's-Gravenhage, The Netherlands. Copies are deposited in university libraries in Holland and in many national nuclear centers in the world.

NEW ZEALAND

Institute of Nuclear Sciences. Copies are available from Librarian, Institute of Nuclear Sciences, D.S.I.R., Private Bag, Lower Hutt, New Zealand. Copies are deposited in other countries.

NORWAY

Forsvarets Forskningsinstitutt. Copies available from Norwegian Defence Research Establishment, Library, P. O. Box 25, Kjeller, Norway.

Institutt for Atomenergi. "KR" reports are available on an exchange basis from the Library, Institutt for Atomenergi, Box 40, Kjeller, Norway. Other series are not generally available to the public.

Norwegian Reactor School. Copies are available from The Library, Institutt for Atomenergi, P. O. Box 40, Kjeller, Norway.

PAKISTAN

Atomic Energy Center. Copies are available from Atomic Energy Center, P. O. Box 658, Lahore, (West Pakistan).

POLAND

Reports of the Polish nuclear institutes are published by the Nuclear Energy Information Center of the Government Commissioner for Use of Nuclear Energy. Copies are available from Ośrodek Informacji o Energii Jądrowej, Warszawa, PKiN, Poland.

SPAIN

Junta de Energia Nuclear. "JEN" reports are available without charge from Servicio de Documentation, Junta de Energia Nuclear, Ciudad Universitaria, Madrid (3), Spain.

SWEDEN

Aktiebolaget Atomenergi. "AE" reports are for sale from Aktiebolaget Atomenergi, Library Section, Box 43041, Stockholm 43, Sweden. Bibliographies and literature surveys of the VDDIT- series may be obtained from Aktiebolaget Atomenergi, Information Office, Scientific and Technical Information, Box 43041, Stockholm 43, Sweden. Other series are not generally available to the public. Organizations in the atomic energy field may obtain copies from Aktiebolaget Atomenergi. Microcopy of AE reports is available from the International Documentation Centre, Tumba, Sweden.

SWITZERLAND

CERN European Organization for Nuclear Research. Available without charge from CERN European Organization for Nuclear Research, Geneva 23, Switzerland. Copies are deposited in libraries in 13 countries.

Eidgenössisches Institut für Reaktorforschung. "EIR" reports are available from Eidgenössiches Institut für Reaktorforschung, c/o Bibliothek, Würenlingen/Ag, Switzerland.

TURKEY

Turkish Atomic Energy Commission. Copies are available free of charge from T.A.E.C., Çekmece Nuclear Research Center, P. O. Box 1, Airport, İstanbul, Turkey.

UNITED KINGDOM

United Kingdom Atomic Energy Authority. Some reports are for sale in the United States by the British Information Service (BIS), 845 Third Avenue, New York, N. Y. 10022. United Kingdom reports generally may be purchased from Her Majesty's Stationery Office, London. Copies not for sale by Her Majesty's Stationery Office may be purchased in microcopy form from Micro Methods Limited, East Ardsley, Wakefield, Yorks, England. Report copies are deposited in a large number of libraries in England.

Conferences

Published conference proceedings as well as individual unpublished papers from conferences are included in this index. A CONF number is assigned to the conference if published proceedings are received and also if only a single paper is received. The base number used is year-month-sequence. Thus, the number CONF-650101 would indicate that the conference was held in 1965, in January, and that this was the first January 1965 conference so received. This number would be assigned to complete published proceedings, or if individual papers are received, the base number would be extended to include a paper number, i.e., CONF-650101-1. As additional papers are received, they will be assigned consecutive numbers in the series, CONF-650101-1, 2, 3, 4, etc. This numbering system ensures that all papers received from a conference will be associated with that conference in this index.

If published proceedings are received after the receipt of individual papers, the complete proceedings will be abstracted and the abstract number will appear in this index with the base CONF number.

Abbreviations Used in Availability Column

AECL	For sale by Atomic Energy of Canada Ltd., Chalk River, Ontario, Canada.
BIS	For sale by British Information Service, 845 Third Avenue, New York, N. Y. 10022
CFSTI	For sale by the Clearinghouse for Federal Scientific and Technical Information, U. S. Department of Commerce, Spring-

field, Virginia 22151. The symbol "cy" indicates that the format of the item sold may be either a printed document or a photographic reproduction (two-thirds of original size) depending upon the availability of printed stock. The indicated price is for either format. The symbol "mn" is used to indicate that copy is also available in the form of micronegatives (microfiche).

Dep. — AEC reports: Full-size copy is on deposit in the depository libraries both inside and outside the United States. These reports are also for sale by Microcard Editions, Inc., Accounting and Shipping Department, West Salem, Wisconsin 54669.

Non-AEC reports: Full-size copy on deposit in the depository libraries in the United States only.

Dep.(mc) — Same as for Dep., except copy is in Microcard form.

Dep.(mn) — Same as for Dep., except copy is in micronegative (microfiche) form.

DSIR — For sale by the National Lending Library for Science and Technology (D.S.I.R.), Boston Spa, Yorkshire, England.

DTI Extension — Available from the U. S. Atomic Energy Commission, Division of Technical Information Extension, P. O. Box 62, Oak Ridge, Tennessee 37830.

EM — Blueprints and microcopy of AEC engineering drawings are available from Clearinghouse for Federal Scientific and Technical Information, U. S. Department of Commerce, Springfield, Virginia 22151. Current prices of the CAPE- packages may be obtained from this address. TID-4100, available from the Division of Technical Information Extension, P. O. Box 62, Oak Ridge, Tennessee 37831, contains information on all the CAPE- packages for sale.

Gmelin — Available at a nominal charge and under the AED- number shown from Atomic Energy Documentation Center, Gmelin Institute, 40-42 Varrentrappstrasse Frankfurt (Main), West Germany.

GPO — For sale by the Superintendent of Documents, Government Printing Office, Washington, D. C. 20402.

HMSO — Her Majesty's Stationery Office, London.

IAEA — Available from the International Atomic Energy Agency, Vienna, Austria, and from its sales agencies in various countries throughout the world. A list of these agencies is found in each STI/DOC and STI/PUB publication.

JCL — For sale by the Special Libraries Association Translation Center, John Crerar Library, 35 West 33rd Street, Chicago, Illinois 60616.

LC — For sale by the Library of Congress, Photoduplication Service, Washington, D. C. 20540.

NAS — National Academy of Sciences, National Research Council, Washington, D. C. 20418.

NRC — For sale by the National Research Council of Canada, Ottawa, Ontario, Canada.

ORINS — Available on interlibrary loan from the Library, Oak Ridge Associated Universities, Post Office Box 117, Oak Ridge, Tennessee 37830.

OTS — See CFSTI.

UKAEA, London — Available from United Kingdom Atomic Energy Authority, 11 Charles II Street, London, S. W. 1.

UN — United Nations Bookshop, United Nations Headquarters, New York, New York.

USGS — Available free of charge from the U. S. Geological Survey, Washington, D. C. 20242.

[The symbols "ph," "mf," and "fs" are used to designate that copy is available only in photostat, microfilm, or facsimile form. The symbol "mn" is used to designate that copy is available in micronegative (microfiche) form. The symbol "cy" is used to designate full size or photographically enlarged copy (two-thirds of original size).]

Report No.	Abstract No.	Availability
AAEC-E–	**(Australian)**	
140	20-17113	Dep. mn
144	20-17650	Dep. mn
AAEC-TM–	**(Australian)**	
300	20-17006	Dep. mn
301	20-16327	Dep. mn
303	20-16632	Dep. mn
AD–	**(Misc.)**	
299256	20-17971	CFSTI $2.75 cy, $0.75 mn
612192	20-17651	CFSTI $1.00 cy, $0.50 mn
620403	20-16213	CFSTI $3.00 cy, $0.75 mn
620438	20-16214	CFSTI $2.00 cy, $0.50 mn
623948	20-17310	CFSTI $1.00 cy, $0.50 mn
624370	20-16620	CFSTI $4.00 cy, $0.75 mn
625867	20-16621	CFSTI $3.00 cy, $0.75 mn
626384	20-16303	CFSTI $1.00 cy, $0.50 mn
627468	20-17007	CFSTI $2.00 cy, $0.50 mn
627846	20-16504	CFSTI $2.00 cy, $0.50 mn
627910	20-17585	CFSTI $2.00 cy, $0.50 mn
627988	20-17872	CFSTI $2.00 cy, $0.50 mn
628277	20-16967	CFSTI $1.00 cy, $0.50 mn
628360	20-16158	CFSTI $2.00 cy, $0.50 mn
628443	20-16215	CFSTI $1.00 cy, $0.50 mn
628791	20-16216	CFSTI $2.00 cy, $0.50 mn
628805	20-16170	CFSTI $1.00 cy, $0.50 mn
628928	20-17169	CFSTI $3.00 cy, $0.50 mn
629527	20-16659	CFSTI $3.00 cy, $0.75 mn
629576	20-17670	CFSTI $2.00 cy, $0.50 mn
AE–	**(Non-AEC)**	
215	20-16171	Dep. mn
AEC-tr–	**(For complete listing see TID-4025)**	
6669	20-17895	CFSTI $3.00 cy, $0.75 mn. JCL $8.10 fs, $2.69 mf
AECD-AG–	**(Pakistani)**	
7	20-16217	Dep. mn
12	20-16218	Dep. mn
AECD-TP–	**(Pakistani)**	
5	20-17336	Dep. mn
AECL–	**(Canadian)**	
2390	20-18082	Dep. mn. AECL $0.50
AECL-Pak–	**(Pakistani)**	
Lib-10	20-16328	Dep. mn
RB-7	20-16918	Dep. mn
AED-C–	**(Non-AEC)**	
01-12	20-18153	Dep. mn
01-13	20-18154	Dep. mn
04-23	20-16219	Dep. mn
04-24	20-16220	Dep. mn
04-25	20-16221	Dep. mn
15-09	20-17325	Dep. mn
15-10	20-17326	Dep. mn
18-05	20-17170	Dep. mn
23-05	20-17153	Dep. mn
23-06	20-17154	Dep. mn
23-07	20-17155	Dep. mn
AEDC-TR–	**(Non-AEC)**	
65-260	20-17872	See AD-627988
AEEW-M–	**(British)**	
568	20-16719	Dep. BIS $0.50. HMSO 2s. 6d.
611	20-17671	Dep. BIS $0.50. HMSO 2s. 6d.
AERE-R–	**(British)**	
4669	20-16720	Dep. BIS $2.40. HMSO 12s.
4997	20-16660	Dep. BIS $1.40. HMSO 7s.
5004	20-17738	Nucl. Phys., 79: 275-96(1966)
5005	20-17740	Nucl. Phys., 79: 305-20(1966)
5006	20-17739	Nucl. Phys., 79: 297-304(1966)
5053	20-17672	Dep. BIS $0.50. HMSO 2s. 6d.
5138	20-17337	Dep. BIS $0.50. HMSO 2s. 6d.
5163	20-17114	Dep. BIS $1.00. HMSO 5s.
AFWL-TR–	**(Non-AEC)**	
65-112	20-16222	CFSTI $2.00 cy, $0.50 mn
AI–	**(Misc.)**	
64-240	20-17124	See N-65-17608
65-264	20-17115	
66-16	20-18045	
ANL–		
6981	20-16942	Dep. mn. CFSTI $2.00 cy, $0.50 mn
ANL-Trans–		
257	20-16608	Dep. mn. JCL $3.60 fs, $1.16 mf
273	20-17029	Dep. mn. JCL $1.60 fs, $0.80 mf
274	20-17980	Dep. mn. JCL $2.60 fs, $0.83 mf
ARL–	**(Non-AEC)**	
65-246	20-17508	CFSTI $2.00 cy, $0.50 mn
ARL-MET–	**(Australian)**	
21	20-16334	See N-65-18292
AWRE-NR–	**(British)**	
1/66	20-16721	Dep. BIS $1.40. HMSO 7s. 0d.
BAW–	**(Misc.)**	
1280-34	20-16599	Dep. mn. CFSTI $2.00 cy, $0.50 mn
BMwF-FBK–	**(German)**	
65-03	20-16722	Dep. mn
BNL–		
949	20-16505	Dep. mn. CFSTI $3.00 cy, $0.75 mn
8850	20-17250	Dep. mn. CFSTI $1.00 cy, $0.50 mn
8952	20-16223	Dep. mn. CFSTI $1.00 cy, $0.50 mn
9275	20-16869	Nucl. Instrum. Methods, 40: 26-44(1966)
9313	20-16571	Inorg. Chem., 5: 461-6(1966)
9368	20-17066	J. Phys. Chem. Solids, 27: 413-21(1966)
9487	20-17391	Phys. Rev., 143: 1262-8(1966)
9542	20-17383	Phys. Rev., 143: 1034-91(1966)
9547	20-17783	Phys. Rev., 143: 879-94(1966)
9583	20-17761	Phys. Rev., 143: 692-711(1966)
9584	20-17786	Phys. Rev., 143: 918-22(1966)
9623	20-17385	Phys. Rev., 143: 1096-1104(1966)
9630	20-17475	Phys. Rev., 143: 1269-74(1966)
9644	20-18046	Dep. mn. CFSTI $2.00 cy, $0.50 mn
10020	20-16506	Dep. mn. CFSTI $2.00 cy, $0.50 mn
10030	20-17171	Dep. mn. CFSTI $1.00 cy, $0.50 mn
BNWL–		
157	20-18155	Dep. mn. CFSTI $4.00 cy, $0.75 mn
187	20-16329	Dep. mn. CFSTI $2.00 cy, $0.50 mn
199	20-17116	Dep. mn. CFSTI $2.00 cy, $0.50 mn
208	20-18172	Dep. mn. CFSTI $3.00 cy, $0.75 mn
BNWL-CC–		
325(Vol.1)	20-17673	ORAU
325(Vol.2)	20-17674	ORAU
325(Vol.3)	20-17675	ORAU
BNWL-SA–		
300	20-17132	Acta Met., 14: 539-41(1966)
453	20-18156	Dep. mn. CFSTI $1.00 cy, $0.50 mn
466	20-18157	Dep. mn. CFSTI $2.00 cy, $0.50 mn
467	20-18158	Dep. mn. CFSTI $1.00 cy, $0.50 mn
514	20-18159	Dep. mn. CFSTI $1.00 cy, $0.50 mn
CALT–		
68-50	20-17476	Phys. Rev., 143: 1275-92(1966)
68-51	20-17467	Phys. Rev., 143: 1185-90(1966)
68-52	20-17466	Phys. Rev., 143: 1171-84(1966)
CAPE–		
1259	20-16801	
1276	20-16892	
1278	20-16597	
1322	20-16166	
1323	20-16768	
1325	20-16769	
1327	20-16965	
CEA-R–	**(French)**	

Report No.	Abstract No.	Availability
2703	20-16413	Dep. mn
2802	20-17172	Dep. mn
2806	20-16414	Dep. mn
2810	20-17676	Dep. mn
2820	20-17008	Dep. mn
2848	20-16224	Dep. mn
2851	20-16330	Dep. mn
2861	20-16415	Dep. mn
2867	20-17652	Dep. mn
2894	20-18160	Dep. mn
CEAL–		
1029	20-17173	Dep. mn. CFSTI $1.00 cy, $0.50 mn
CERN–	(European Organization for Nuclear Research)	
66-6	20-17174	Dep. mn
CLM-R–	(British)	
49	20-17873	Dep. BIS $0.60. HMSO 3s.
CLOR–	(Polish)	
43/D	20-16805	Dep.
44/D	20-16806	Dep.
CLOR-IBJ–	(Polish)	
42/D	20-16807	Dep.
CONF-502–	(International Congress of Nuclear Physics, Paris, July 1964)	
vol.2	20-17871	Paris, Centre National de la Recherche Scientifique, 1964.
CONF-747–	(4th Symposium on Radioactivity in Scandinavia, Riso, Denmark, Oct. 5–6, 1964)	
9	20-16687	ORINS
CONF-640208–	20-16636	(Scientific Conference on Nuclear Meteorology, Obninsk, U.S.S.R., Feb. 3–6, 1964) Moscow, Atomizdat, 1964.
CONF-641025–	(9th Symposium on Advances in Tracer Methodology, San Francisco, Oct. 22–24, 1964)	
1	20-16820	See LA-DC-7222
CONF-641128–	20-17550	(IAGA Symposium on Magnetism of the Earth's Interior, Pittsburgh, Nov. 16–20, 1964) J. Geomagnet. Geoelec., 17: 165-541(1965)
CONF-641129	20-16827	(2nd Working Session on Personnel Dosimetry, Berlin, Nov. 11–14, 1964) See SZS-9(1965)
CONF-650202–	(American Crystallographic Assn., Suffern, N. Y., Feb. 22–26, 1965)	
Vol.1	20-18017	Pittsburgh, Polycrystal Book Service, 1965. $3.50.
CONF-650301–	(Symposium on the Physics and Chemistry of Fission, Salzburg, Mar. 22–26, 1965)	
Vol.1	20-17694	See STI/PUB/101(Vol.1)
Vol.2	20-17695	See STI/PUB/101(Vol.2)
CONF-650414–	20-16945	(19th Metallographic Group Meeting, Oak Ridge, Tenn., Apr. 20–22, 1965) See ORNL-TM-1161
CONF-650602–	(American Nuclear Society 11th Annual Meeting, Gatlinburg, Tenn., June 20–24, 1965)	
27	20-18062	Nucl. Sci. Eng., 24: 133-41(1966)
CONF-650668–	(2nd International Symposium on Basic Environmental Problems of Man in Space, Paris, June 14–16, 1965)	
1	20-16231	See UCRL-16377
CONF-650804–	(5th Rare Earth Research Conference, Ames, Iowa, Aug. 30–Sept. 1, 1965)	
2	20-17016	See IS-1175
CONF-650806–	(7th International Conference on Phenomena in Ionized Gases, Belgrade, Aug. 22–27, 1965)	
21	20-17510	See IPP-3/25
CONF-650833–	20-17288	(4th International Conference on the Physics of Electronic and Atomic Collisions, Quebec, Canada, Aug. 3–7, 1965) New York, Science Bookcrafters, Inc.
CONF-650922–	20-17156	(1st International Symposium on Magnet Technology, Stanford, Calif., Sept. 8–10, 1965) Dep. mn. CFSTI $8.50 cy, $3.50 mn
CONF-650965–	(1st International Conference on Medical Physics, Harrogate, England, Sept. 1965)	
1	20-16173	See PG-Report-686
CONF-651001–	(IEEE Nuclear Science Symposium, San Francisco, Oct. 1965)	
21	20-16893	ORAU. Gmelin, AED-CONF-65-293-6
22	20-16894	ORAU. Gmelin, AED-CONF-65-293-15
23	20-16895	ORAU. Gmelin, AED-CONF-65-293-11
24	20-17168	ORAU. Gmelin, AED-CONF-65-293-59
26	20-16901	ORAU. Gmelin, AED-CONF-65-293-26
27	20-16900	ORAU. Gmelin, AED-CONF-65-293-27
33	20-16826	See PPAD-574E
34	20-17307	Dep. mn. CFSTI $1.00 cy, $0.50 mn
CONF-651009–	(Conference on Safety, Fuels and Core Design in Large Fast Power Reactors, Argonne, Oct. 11–14, 1965)	
17	20-18122	ORAU. Gmelin, AED-CONF-65-307-18
21	20-18123	ORAU. Gmelin, AED-CONF-65-307-43
CONF-651019–	(15th Canadian Chemical Engineering Conference, Quebec City, Canada, Oct. 25, 1965)	
2	20-16966	ORAU. Gmelin, AED-CONF-65-294-2
CONF-651025–	(Symposium on Physical Metallurgy of Refractory Metals, French Lick, Ind., Oct. 3–5, 1965)	
14	20-17011	Dep. mn. CFSTI $1.00 cy, $0.50 mn
CONF-651031–	(American Society of Metals Meeting, Detroit, Oct. 19, 1965)	
4	20-17649	ORAU. Gmelin, AED-CONF-65-331-2
CONF-651043–	(Weak Interactions Conference, Argonne, Ill., Oct. 25–27, 1965)	
6	20-17424	ORAU. Gmelin, AED-CONF-65-320-6
CONF-651049–	(IEEE Thermionic Conversion Specialist Conference, San Diego, Calif., Oct. 25–27, 1965)	
6	20-17287	ORAU. Gmelin, AED-CONF-65-324-2
7	20-17333	ORAU. Gmelin, AED-CONF-65-324-7
8	20-17334	ORAU. Gmelin, AED-CONF-65-324-5
11	20-17335	ORAU. Gmelin, AED-CONF-65-324-4
CONF-651053–	(Joint IEEE–URSI Meeting, Hanover, N. H., Oct. 4–6, 1965)	
1	20-17558	ORAU. Gmelin, AED-CONF-65-278-2
CONF-651054–	(Assn. of Official Agricultural Chemists, 79th Annual Meeting, Washington, D. C., Oct. 11–14, 1965)	
1	20-16804	ORAU. Gmelin, AED-CONF-65-291-1
CONF-651057–	(IEEE East Coast Conference on Aerospace and Navigational Electronics, Baltimore, Md., Oct. 27–29, 1965)	
1	20-16913	ORAU. Gmelin, AED-CONF-65-313-3
2	20-16904	ORAU. Gmelin, AED-CONF-65-313-2
3	20-17249	ORAU. Gmelin, AED-CONF-65-313-1
CONF-651061–	(21st National Electronics Conference and Exhibition, Chicago, Oct. 25–27, 1965)	
3	20-17227	ORAU. Gmelin, AED-CONF-65-326-3
CONF-651064–	20-16505	(5th Annual Contractors Meeting, Upton, N. Y., Oct. 7–8, 1965) See BNL-949
CONF-651101–	20-3647 20-9102	(American Nuclear Society, Winter Meeting, Washington, D. C., Nov. 15–18, 1965) (Revised 11-8-65)
68	20-18052	See WAPD-T-1836

Report No.	Abstract No.	Availability
73	20-18018	Dep. mn. CFSTI $1.00 cy, $0.50 mn
CONF-651105–	**(Conference on Nuclear Electronics, Bombay, India, Nov. 22–26, 1965)**	
3	20-16896	ORAU
4	20-18030	ORAU
5	20-16902	ORAU
6	20-18037	ORAU
7	20-18038	ORAU
8	20-16903	ORAU
9	20-18031	ORAU
10	20-18021	ORAU
11	20-16899	ORAU
12	20-18032	ORAU
13	20-16802	ORAU
14	20-18150	ORAU
15	20-18151	ORAU
16	20-18026	ORAU
17	20-18035	ORAU
18	20-18034	ORAU
19	20-18036	ORAU
20	20-16710	ORAU
21	20-18152	ORAU
22	20-18121	ORAU
23	20-18029	ORAU
24	20-18028	ORAU
25	20-18120	ORAU
26	20-18119	ORAU
27	20-17870	ORAU
28	20-16898	ORAU
29	20-16897	ORAU
30	20-18149	ORAU
31	20-18027	ORAU
32	20-16803	ORAU
33	20-18033	ORAU
CONF-651134–	**(Eastern Theoretical Conference, Stony Brook, N. Y., Nov. 1965)**	
1	20-17435	See NYO-3399-45
CONF-660110–	**(Canadian Electrical Assn. Eastern Zone Meetings, Halifax, Nova Scotia, Jan. 24–27, 1966)**	
1	20-18082	See AECL-2390
CONF-660203–	**(National Topical Meeting on Reactor Physics in the Resonance and Thermal Regions, San Diego, Calif., Feb. 7–9, 1966)**	
1	20-18046	See BNL-9644
CONF-660206–	**(Symposium on Neutron Noise, Waves, and Pulse Propagation, Gainesville, Feb. 14–16, 1966)**	
2	20-18048	See ORNL-P-1967
CONF-660208–	**(Symposium on Solidification and Long-Term Storage of Highly Radioactive Wastes, Richland, Wash., Feb. 14–18, 1966)**	
4	20-18165	See ORNL-P-1987
5	20-18156	See BNWL-SA-453
6	20-18158	See BNWL-SA-467
7	20-18159	See BNWL-SA-514
8	20-18161	See ISO-SA-1
CONF-660305–	**(American Nuclear Society, Topical Meeting, Augusta, Ga., Mar. 21–23, 1966)**	
18	20-15506	See BNL-10020
CONF-660402–	**(American Society of Tool and Mfg. Engineers, Annual Conference and Tool Show, Detroit, Apr. 18–22, 1966)**	
2	20-16993	See Y-DA-1043
COO–		
264-295	20-17377	Nuovo Cimento (10), 41A: 606-8(1966)
382-54	20-17238	J. Geophys. Res., 71: 619-41(1966)
382-56	20-16673	Geochim. Cosmochim. Acta, 29: 1203-8 (1965)
1142-62	20-16455	J. Phys. Chem., 70: 407-11(1966)
1156-11	20-16723	Dep. mn. CFSTI $6.00 cy, $1.25 mn
1156-12	20-16724	Dep. mn. CFSTI $3.00 cy, $0.75 mn
1177-15	20-16600	Dep. mn. CFSTI $2.00 cy, $0.50 mn
1261-20	20-17382	Phys. Rev., 143: 1028-33(1966)
1319-33	20-16968	Dep. mn. CFSTI $3.00 cy, $0.75 mn
1420-112	20-17677	Dep. mn. CFSTI $1.00 cy, $0.50 mn
1420-113	20-17678	Dep. mn. CFSTI $1.00 cy, $0.50 mn
1518-2	20-16989	Dep. mn. CFSTI $1.00 cy, $0.50 mn
CVNA–	**(Misc.)**	
63	20-18083	Dep. mn. CFSTI $2.00 cy, $0.50 mn
96	20-18084	
173	20-18085	
174	20-18086	Dep. mn. CFSTI $1.00 cy, $0.50 mn
250	20-18087	Dep. mn. CFSTI $3.00 cy, $0.75 mn
D–	**(Misc.)**	
1-82-0469	20-17509	
DCBRL–	**(Canadian)**	
482	20-16520	Can. J. Chem., 44: 737-41(1966)
DESY–	**(German)**	
65/10	20-17338	Dep. mn
65/15	20-17679	Dep. mn
65/17	20-16775	Dep. mn
66/1	20-17425	Dep. mn
DPSPU–		
65-30-7	20-16342	Anal. Chem., 38: 89-92(1966)
DRI–	**(Misc.)**	
1092-226	20-17012	Dep. mn. CFSTI $2.00 cy, $0.50 mn
2296	20-17012	See DRI-1092-226
DUBNA REPORTS	**(Russian)**	
See JINR (Russian)		
ECOM–	**(Non-AEC)**	
00392-F	20-16661	CFSTI
01309-1	20-16735	See TO-B-65-99
EFINS–	**(Misc.)**	
65-53	20-16673	See COO-382-56
65-64	20-17790	Phys. Rev., 143: 952-?(1966)
EGG–		
1183-1156	20-16776	Dep. mn. CFSTI $2.00 cy, $0.50 mn
1183-1174	20-16812	Dep. mn. CFSTI $1.00 cy, $0.50 mn
EOS–	**(Non-AEC)**	
2080-Final	20-16910	See N-65-18448
ER–	**(Misc.)**	
7510	20-16908	See N-65-17526
7620	20-16909	See N-65-18250
ETR–	**(Belgian)**	
173	20-18162	See NP-15754
EUR–	**(European Atomic Energy Community)**	
2239.e	20-16175	See RT/BIO(65)-1
2539.i	20-16193	Dep. mn
2543.e	20-16725	Dep. mn
2548.f	20-16297	Dep. mn
2619.f	20-16919	Dep. mn
2620.i	20-17157	Dep. mn
2625.e	20-18133	Dep. mn
2629.i(Vol.1)	20-18126	Dep. mn
2639.f	20-17559	Dep. mn
2697	20-16990	See EURAEC-1556
2698	20-16991	See EURAEC-1557
2699	20-17117	See EURAEC-1558
2702.e	20-16777	Dep. mn
2715.f	20-16225	Dep. mn
2902	20-17118	See EURAEC-1564
EURAEC–		
1491	20-18095	See WCAP-3385-52
1556	20-16990	Dep. mn. CFSTI $1.00 cy, $0.50 mn
1557	20-16991	Dep. mn. CFSTI $1.00 cy, $0.50 mn
1558	20-17117	Dep. mn. CFSTI $2.00 cy, $0.50 mn
1564	20-17118	Dep. mn. CFSTI $2.00 cy, $0.50 mn
1570	20-16602	See GEAP-5081
1572	20-16604	See NYO-3114-13
1575	20-16601	See GEAP-5067
1579	20-16969	Dep. mn. CFSTI $1.00 cy, $0.50 mn

Report No.	Abstract No.	Availability
FEI–	**(Russian)**	
26	20-17680	Dep. mn
FTD-TT–	**(Non-AEC)**	
65-1642	20-17310	For translation see AD-623948
GA–	**(Misc.)**	
6003	20-17664	Nukleonik, 8: 40-5(1966)
6568	20-16331	Dep. mn. CFSTI $2.00 cy, $0.50 mn
6691	20-16332	Dep. mn. CFSTI $2.00 cy, $0.50 mn
6753(Pt.1)	20-18127	Dep. mn. CFSTI $3.00 cy, $0.75 mn
GACD–	**(Non-AEC)**	
5403	20-17882	See N-65-19862
GAMD–	**(Misc.)**	
6789	20-17119	Dep. mn. CFSTI $1.00 cy, $0.50 mn
GAT–		
506	20-16726	Dep. mn. CFSTI $1.00 cy, $0.50 mn
GE-TM–		
65-9-12	20-17011	See CONF-651025-14
GEAP–	**(Misc.)**	
4832	20-16970	Dep. mn. CFSTI $5.00 cy, $1.00 mn
4916	20-17120	Dep. mn. CFSTI $4.00 cy, $0.75 mn
4918	20-17121	Dep. mn. CFSTI $3.00 cy, $0.50 mn
4966	20-18134	Dep. mn. CFSTI $2.00 cy, $0.50 mn
5067	20-16601	Dep. mn. CFSTI $3.00 cy, $0.75 mn
5081	20-16602	Dep. mn. CFSTI $3.00 cy, $0.75 mn
HASL–		
165	20-16662	Dep. mn. CFSTI $7.00 cy, $1.75 mn
168	20-16727	Dep. mn. CFSTI $6.00 cy, $1.25 mn
169	20-16728	Dep. mn. CFSTI $4.00 cy, $1.00 mn
IAE–	**(Non-AEC)**	
873	20-17251	Dep. mn
942	20-17972	Dep. mn
966	20-17681	Dep. mn
IBJ–	**(Polish)**	
See INR		
IC–	**(Misc.)**	
66/16	20-17426	Dep. mn
66/20	20-17427	Dep. mn
IDO–		
12049	20-16729	Dep. mn. CFSTI $1.00 cy, $0.50 mn
17135	20-18135	Dep. mn. CFSTI $3.00 cy, $0.75 mn
17146	20-18019	Dep. mn. CFSTI $2.00 cy, $0.50 mn
IFJ–	**(Polish)**	
See INP		
IITRI–	**(Misc.)**	
B237-45	20-16943	
B6016-17	20-17022	See N-65-18933
INP–	**(Polish)**	
428/PL	20-17682	Dep. mn
430/PL	20-17683	Dep.
INR–	**(Non-AEC)**	
632/XIV/PS	20-17013	Dep.
645/XIV/PS	20-17014	Dep.
653/IA/D	20-16813	Dep.
665/II/PS	20-17015	Dep.
669/C	20-18088	Dep. mn
671/XVII/C	20-16507	Dep.
INSJ–	**(Japanese)**	
92	20-16928	Dep. mn
93	20-17207	Dep. mn
IPP–	**(Non-AEC)**	
1/35	20-17875	Dep. mn
1/37	20-17876	Dep. mn
3/25	20-17510	Dep. mn
6/44	20-17877	Dep. mn
IS–		
1104	20-16980	J. Less-Common Metals, 10: 229-36(1966)
1106	20-17973	Dep. mn. CFSTI $3.00 cy, $0.75 mn
1133	20-17762	Phys. Rev., 143: 712-23(1966)
1160	20-17764	Phys. Rev., 143: 730-5(1966)
1161	20-17763	Phys. Rev., 143: 724-9(1966)
1175	20-17016	Dep. mn. CFSTI $1.00 cy, $0.50 mn
1232	20-18002	Phys. Rev., 143: 506-12(1966)
1233	20-17451	Nuovo Cimento, (10), 41A: 532-42(1966)
1249	20-16449	J. Less-Common Metals, 10: 273-89(1966)
1320	20-18136	Dep. mn. CFSTI $2.00 cy, $0.50 mn
IS-T–		
63	20-17974	Dep. mn. CFSTI $3.00 cy, $0.50 mn
ISO-SA–		
1	20-18161	Dep. mn. CFSTI $1.00 cy, $0.50 mn
ITEF–	**(Russian)**	
384	20-17560	Dep. mn
386	20-16814	Dep. mn
JAERI–	**(Japanese)**	
1085	20-17684	Dep. mn
JINR–	**(Russian)**	
E-2557	20-17339	Dep. mn
P-2322	20-17340	Dep. mn
P-2480	20-17599	Dep. mn
P-2497	20-17685	Dep. mn
P-2498	20-17428	Dep. mn
P-2504	20-17341	Dep. mn
P-2506	20-16815	Dep. mn
P-2512	20-17686	Dep. mn
P-2514	20-17687	Dep. mn
P-2520	20-17342	Dep. mn
P-2522	20-17252	Dep. mn
P-2524	20-17343	Dep. mn
P-2528	20-16816	Dep. mn
P-2529	20-17429	Dep. mn
P-2530	20-17344	Dep. mn
P-2531	20-17345	Dep. mn
P-2532	20-17561	Dep. mn
P-2534	20-17346	Dep. mn
P-2537	20-17208	Dep. mn
P-2539	20-17688	Dep. mn
P-2547	20-17347	Dep. mn
P-2556	20-17348	Dep. mn
P-2565	20-17430	Dep. mn
P-2569	20-17431	Dep. mn
JPL-TR–	**(Non-AEC)**	
32-889	20-17017	
JPLAI-LS–	**(Non-AEC)**	
541	20-17537	
JPRS–	**(Non-AEC)**	
34120	20-16232	CFSTI $1.00 cy, $0.50 mn
JUL–	**(German)**	
270-RB	20-16817	Dep. mn
K-L–		
6036	20-16848	Health Phys., 12: 433-4(1966)
KFK–	**(German)**	
328	20-16818	Dep. mn
KR–	**(Norwegian)**	
78	20-18047	Dep. mn
81	20-16333	Dep. mn
82	20-18137	Dep. mn
LA–		
3435	20-16819	Dep. mn. CFSTI $2.00 cy, $0.50 mn
3437	20-17878	Dep. mn. CFSTI $2.00 cy, $0.50 mn
3454	20-16588	Dep. mn. CFSTI $1.00 cy, $0.50 mn
3455	20-18173	Dep. mn. CFSTI $2.00 cy, $0.50 mn
3463	20-17653	Dep. mn. CFSTI $1.00 cy, $0.50 mn
3479	20-17209	Dep. mn. CFSTI $3.00 cy, $0.75 mn

Report No.	Abstract No.	Availability
LA-DC–		
7044	20-16348	Anal. Chem., 38: 149-50(1966)
7222	20-16820	Dep. mn. CFSTI $2.00 cy, $0.50 mn
7296	20-17265	Phys. Rev., 143: 588-94(1966)
7485	20-17781	Phys. Rev., 143: 855-6(1966)
7497	20-17782	Phys. Rev., 143: 857-8(1966)
7558	20-17858	pp 347-54 of STI/PUB/101(Vol.1)
7629	20-17062	J. Less-Common Metals, 10: 294-5(1966)
LA-tr–		
66-1	20-17030	Dep. mn. JCL $1.10 fs, $0.80 mf
66-5	20-16955	Dep. mn. JCL $2.60 fs, $0.86 mf
66-6	20-16956	Dep. mn. JCL $1.60 fs, $0.80 mf
66-11	20-16957	Dep. mn. JCL $2.60 fs, $1.10 mf
66-12	20-16958	Dep. mn. JCL $1.10 fs, $0.80 mf
LAL–	**(French)**	
1151	20-16821	Dep. mn
1155	20-17349	Dep. mn
LNF–	**(Italian)**	
65/37	20-17210	Dep. mn
65/45	20-17211	Dep. mn
LRP–	**(Swiss)**	
19/65	20-17879	Dep. mn
20/66	20-17018	Dep. mn
MATT–		
336	20-17922	J. Vac. Sci. Technol., 3: 6-10(1966)
437	20-17880	Dep. mn. CFSTI $2.00 cy, $0.50 mn
MIT–	**(Misc.)**	
334-34	20-17122	Dep. mn. CFSTI $6.00 cy, $1.25 mn
1381-13	20-16711	Dep. mn. CFSTI $4.00 cy, $0.75 mn
2098-195	20-17481	Phys. Rev., 143: 1369-74(1966)
2098-200	20-17477	Phys. Rev., 143: 1295-1302(1966)
2098-203	20-17776	Phys. Rev., 143: 808-17(1966)
2098-209	20-17381	Nuovo Cimento, (10), 41A: 635-7(1966)
2098-220	20-17400	Phys. Rev. Lett., 16: 474-7(1966)
ML–	**(Misc.)**	
65853	20-16828	See TID-22763
ML-TDR–	**(Non-AEC)**	
64-40(Suppl.1)	20-16944	See NASA-SP-3025
MLM–		
1297	20-16927	Dep. mn. CFSTI $1.00 cy, $0.50 mn
N–	**(Misc.)**	
17608	20-17124	CFSTI $2.00 cy, $0.50 mn
65-17505	20-17123	CFSTI $3.00 cy, $0.50 mn
65-17517	20-16907	CFSTI $1.00 cy, $0.50 mn
65-17526	20-16908	CFSTI $3.00 cy, $0.75 mn
65-17609	20-17538	CFSTI $3.00 cy, $0.75 mn
65-17749	20-16624	CFSTI $3.00 cy, $0.50 mn
65-17873	20-17019	CFSTI $1.00 cy, $0.50 mn
65-18250	20-16909	CFSTI $2.00 cy, $0.50 mn
65-18257	20-17539	CFSTI $6.00 cy, $1.25 mn
65-18274	20-17308	CFSTI $1.00 cy, $0.50 mn
65-18275	20-17228	CFSTI $1.00 cy, $0.50 mn
65-18292	20-16334	
65-18444	20-16971	CFSTI $1.00 cy, $0.50 mn
65-18448	20-16910	CFSTI $3.00 cy, $0.75 mn
65-18466	20-17020	
65-18607	20-17021	CFSTI $2.00 cy, $0.50 mn
65-18914	20-17540	CFSTI $1.00 cy, $0.50 mn
65-18933	20-17022	CFSTI $5.00 cy, $1.00 mn
65-19264	20-17327	CFSTI $2.00 cy, $0.50 mn
65-19272	20-16625	CFSTI $1.00 cy, $0.50 mn
65-19395	20-17350	
65-19396	20-17351	
65-19716	20-17309	CFSTI $2.00 cy, $0.50 mn
65-19719	20-17541	CFSTI $1.00 cy, $0.50 mn
65-19804	20-17881	
65-19862	20-17882	CFSTI $1.00 cy, $0.50 mn
65-19927	20-16822	CFSTI $1.00 cy, $0.50 mn
NAA-SR-Memo–		
10178	20-18089	Dep. mn. CFSTI $3.00 cy, $0.50 mn

Report No.	Abstract No.	Availability
NASA-CR–	**(Misc.)**	
404	20-17125	CFSTI $0.90 cy, $0.75 mn
54125	20-17022	See N-65-18933
54328	20-17327	See N-65-19264
54719	20-16972	
54888	20-18045	See AI-66-16
57107	20-16909	See N-65-18250
57119	20-16624	See N-65-17749
57132	20-16910	See N-65-18448
57138	20-16971	See N-65-18444
57165	20-17540	See N-65-18914
57469	20-17882	See N-65-19862
57515	20-16822	See N-65-19927
60840	20-16908	See N-65-17526
60866	20-17123	See N-65-17505
60879	20-16907	See N-65-17517
60902	20-17124	See N-65-17608
60905	20-17538	See N-65-17609
60950	20-17019	See N-65-17873
NASA-SP–	**(Misc.)**	
3025	20-16944	CFSTI $3.00 cy, $1.50 mn
NASA-TM–	**(Misc.)**	
X-1077	20-16625	See N-65-19272
X-55134	20-17539	See N-65-18257
X-55138	20-17309	See N-65-19716
X-55141	20-17541	See N-65-19719
X-55160	20-17308	See N-65-18274
X-55161	20-17228	See N-65-18275
NASA-TN–	**(Misc.)**	
D-2704	20-17021	See N-65-18607
D-3275	20-16973	CFSTI $3.00 cy, $0.75 mn
D-3329	20-16778	CFSTI $0.20 cy, $0.50 mn
NBS-TN–	**(Misc.)**	
276	20-16335	GPO $1.00
NC–	**(Norwegian)**	
73	20-18138	See TID-22697
NEIC-RR–	**(Polish)**	
21	20-17352	Dep.
NP–	**(AEC File No. for Non-AEC Reports)**	
15754	20-18162	Dep. mn. CFSTI $2.00 cy, $0.50 mn
15771	20-18174	Dep. mn
15783	20-17689	Dep. mn
15784	20-17883	Dep. mn
15859	20-18163	Dep. mn
15874	20-18164	Dep. mn
15882	20-16730	Dep. mn
15883	20-16731	Dep. mn
15886	20-17884	Dep. mn
15889	20-16974	
15891	20-16226	Dep. mn
15894	20-17511	
15898	20-16732	GPO
15899	20-17690	Dep. mn
15900	20-16975	Dept. of Mines and Technical Surveys, Ottawa $0.50
15902	20-17432	Dep. mn
NP-tr–	**(AEC File No. for Non-AEC Translations)**	
1364	20-16510	Dep. mn. JCL $1.60 fs, $0.80 mf
NRL–	**(Misc.)**	
6330	20-16967	See AD-628277
6349	20-17126	Dep. mn. CFSTI $1.00 cy, $0.50 mn
6366	20-17169	See AD-628928
NUS–	**(Misc.)**	
246	20-18090	Dep. mn. CFSTI $5.00 cy, $1.00 mn
NYO–		
187-7	20-16603	Dep. mn. CFSTI $5.00 cy, $1.00 mn
906-68	20-16416	Dep. mn. CFSTI $3.00 cy, $0.50 mn
1472-1	20-16229	Dep. mn. CFSTI $2.00 cy, $0.50 mn
2047-36	20-17975	Dep. mn. CFSTI $3.00 cy, $0.75 mn
2047-36, App.1	20-17976	

Report No.	Abstract No.	Availability
2047-36, App.2	20-17977	
2194-1	20-16172	Dep. mn. CFSTI $1.00 cy, $0.50 mn
2262-105	20-17459	Phys. Rev., 143: 975-7(1966)
2771-13	20-16508	Dep. mn. CFSTI $3.00 cy, $0.50 mn
3114-13	20-16604	Dep. mn. CFSTI $4.00 cy, $0.75 mn
3160-1	20-16823	Dep. mn. CFSTI $3.00 cy, $0.50 mn
3304-8	20-16605	Dep. mn. CFSTI $3.00 cy, $0.75 mn
3399-13	20-17433	Dep. mn. CFSTI $1.00 cy, $0.50 mn
3399-18	20-17434	Dep. mn. CFSTI $1.00 cy, $0.50 mn
3399-41	20-17369	Nuovo Cimento (10), 41A: 283-5(1966)
3399-45	20-17435	Dep. mn. CFSTI $1.00 cy, $0.50 mn
3402-2	20-17978	Dep. mn. CFSTI $2.00 cy, $0.50 mn
3406-3	20-16824	Dep. mn. CFSTI $1.00 cy, $0.50 mn
3558-2	20-16525	J. Amer. Chem. Soc., 88: 658-61(1966)
3561-2	20-16227	Dep. mn. CFSTI $1.00 cy, $0.50 mn
3571-2	20-16228	Dep. mn. CFSTI $1.00 cy, $0.50 mn
10175	20-16336	Dep. mn. CFSTI $4.00 cy, $1.00 mn
ORNL–		
3900	20-18175	Dep. mn. CFSTI $6.00 cy, $1.25 mn
3908	20-17885	Dep. mn. CFSTI $5.00 cy, $1.00 mn
3918	20-16622	Dep. mn. CFSTI $2.00 cy, $0.50 mn
3923	20-17127	Dep. mn. CFSTI $2.00 cy, $0.50 mn
ORNL-P–	(Misc.)	
340	20-16278	Photochem. Photobiol., 4: 439-45(1965)
1098	20-16733	Dep. mn. CFSTI $1.00 cy, $0.50 mn
1186	20-16846	Health Phys., 12: 385-93(1966)
1341	20-17131	Acta Met., 14: 64-5(1966)
1376	20-16450	J. Mol. Spectros., 18: 247-75(1965)
1411	20-16578	Nucl. Sci. Eng., 24: 118-22(1966)
1530	20-16456	J. Phys. Chem., 70: 436-44(1966)
1540	20-16389	Microchem. J., 10: 301-14(1966)
1549	20-16390	Microchem. J., 10: 315-33(1966)
1638	20-18001	Phys. Rev., 143: 487-94(1966)
1682	20-17744	Nucl. Phys., 79: 403-16(1966)
1716	20-17900	Appl. Opt., 5: 187-94(1966)
1741	20-16200	J. Bacteriol., 91: 737-42(1966)
1754	20-17057	J. Electrochem. Soc., 113: 269-74(1966)
1795	20-17730	Nucl. Data, 1: 21-102(1965)
1825	20-16760	Health Phys., 12: 425-9(1966)
1967	20-18048	Dep. mn. CFSTI $1.00 cy, $0.50 mn
1987	20-18165	Dep. mn. CFSTI $3.00 cy, $0.50 mn
2000	20-17146	Phys. Rev. Lett., 16: 395-8(1966)
ORNL-RMIC–	(Oak Ridge National Lab.)	
4	20-16417	ORNL Free
ORNL-TM–		
1090	20-16556	Dep. mn. CFSTI $3.00 cy, $0.75 mn
1161	20-16945	Dep. mn. CFSTI $6.00 cy, $1.50 mn
1212	20-17961	Dep. mn. CFSTI $2.00 cy, $0.50 mn
1233	20-17760	See ORNL-P-1759
1235	20-17691	Dep. mn. CFSTI $1.00 cy, $0.50 mn
1237	20-17962	Dep. mn. CFSTI $1.00 cy, $0.50 mn
1267	20-17768	Phys. Rev., 143: 758-65(1966)
1381	20-16623	Dep. mn. CFSTI $6.00 cy, $1.25 mn
1385	20-18076	Dep. mn. CFSTI $2.00 cy, $0.50 mn
1407	20-17129	Dep. mn. CFSTI $1.00 cy, $0.50 mn
1414	20-17692	Dep. mn. CFSTI $4.00 cy, $0.75 mn
1424	20-17025	Dep. mn. CFSTI $2.00 cy, $0.50 mn
1442	20-16825	Dep. mn. CFSTI $1.00 cy, $0.50 mn
1464	20-17693	Dep. mn. CFSTI $1.00 cy, $0.50 mn
1759	20-17760	Phys. Rev., 143: 688-91(1966)
ORNL-tr–		
923	20-16666	Dep. mn. JCL $8.60 fs, $2.93 mf
962	20-17031	Dep. mn. JCL $1.00 fs, $0.50 mf
987	20-18096	Dep. mn. JCL $2.60 fs, $0.89 mf
1059	20-17963	Dep. mn. JCL $1.60 fs, $0.80 mf
1061	20-17964	Dep. mn. JCL $1.60 fs, $0.80 mf
PA-TR–	(Non-AEC)	
3282	20-16504	See AD-627846
PAN–	(Polish)	(This series of reports was terminated in 1965. Subsequent reports are identified by the code INR)
PATENTS	(Canadian)	
723,756	20-16412	
724,066	20-16598	
724,285	20-16905	
724,288	20-18039	
724,289	20-18040	
PATENTS	(German)	
1,203,888	20-18080	
1,205,629	20-16906	
1,205,632	20-18081	
1,205,633	20-18075	
1,206,095	20-17669	
1,206,102	20-18041	
1,206,532	20-17960	
1,206,534	20-18042	
1,206,535	20-18043	
1,206,536	20-18044	
PG-Report–	(British)	
686	20-16173	Dep. BIS $0.50. HMSO 2s. 6d.
PPAD–		
574E	20-16826	Dep. mn. CFSTI $1.00 cy, $0.50 mn
584D	20-16779	Dep. mn. $1.00 cy, $0.50 mn
R–	(Misc.)	
2361	20-17118	See EURAEC-1564
RL-SA–		
25	20-18125	Dep. mn. CFSTI $2.00 cy, $0.50 mn
RLO–		
1547-3	20-16174	Dep. mn. CFSTI $1.00 cy, $0.50 mn
RMO–		
3001(Rev.1) (Suppl.)	20-16337	Dep. mn. CFSTI $3.00 cy, $0.75 mn
RPI–	(Misc.)	
2408-4	20-16992	Dep. mn. CFSTI $2.00 cy, $0.50 mn
RT-BIO–	(Italian)	
(65)1	20-16175	Dep. mn
(65)18	20-16725	See EUR-2543.e
RT-CHI–	(Italian)	
(65)36	20-16338	Dep. mn
RT-FI–	(Italian)	
(65)42	20-18049	Dep. mn
(65)45	20-18091	Dep. mn
RT-ING–	(Italian)	
(65)17	20-17026	Dep. mn
RT-PROT–	(Italian)	
(65)31	20-17654	Dep. mn
(65)40	20-16635	Dep. mn
SC-TM–		
66-49	20-16590	Dep. mn. CFSTI $1.00 cy, $0.50 mn
SCL-DR–		
66-6	20-18176	Dep. mn. CFSTI $1.00 cy, $0.50 mn
SGAE-IB–	(Austrian)	
IA-7/1965	20-16920	Dep. mn
SLAC-PUB–		
143	20-17478	Phys. Rev., 143: 1302-9(1966)
153	20-17480	Phys. Rev., 143: 1354-8(1966)
155	20-17070	J. Vac. Sci. Technol., 3: 28-30(1966)
STI-PUB–	(International Atomic Energy Agency)	
101(Vol.1)	20-17694	IAEA: $13.00; S 273,-; £ 3.18.0; F Fr 52,-; DM 45.50
101(Vol.2)	20-17695	IAEA: $10.00; S 210,-; £ 3.0.0; F Fr 40,-; DM 35,-
STL–	(Misc.)	
372-22	20-18050	Dep. mn. CFSTI $2.00 cy, $0.50 mn
4161-6009-SU-000	20-16907	See N-65-17517

Report No.	Abstract No.	Availability
SU-IPR-		
44	20-17893	Dep. mn. CFSTI $2.00 cy, $0.50 mn
47	20-17894	Dep. mn. CFSTI $2.00 cy, $0.50 mn
SUI-	(Misc.)	
64-40	20-17538	See N-65-17609
SWRHL-		
13r	20-16734	See TID-22693
SZS-	(German)	
9(1965)	20-16827	Dep. mn
TB-	(Non-AEC)	
74	20-16975	See NP-15900
TE-	(Non-AEC)	
64-65	20-17327	See N-65-19264
TH-	(Non-AEC)	
83	20-17351	See N-65-19396
85	20-17350	See N-65-19395
TID-		
3733	20-18177	DTI Extension Free
21470	20-16663	Dep. mn. CFSTI $1.00 cy, $0.50 mn
21534	20-16275	Neurology, 15: 1104-16(1965)
22146	20-16870	Nucl. Instrum. Methods, 40: 45-53(1966)
22364	20-17392	Phys. Rev., 143: 1310-21(1966)
22531	20-18166	Dep. mn. CFSTI $2.00 cy, $0.50 mn
22621	20-16606	Dep. mn. CFSTI $1.00 cy, $0.50 mn
22627	20-16921	Dep. mn. CFSTI $1.00 cy, $0.50 mn
22644	20-16230	Dep. mn. CFSTI $2.00 cy, $0.50 mn
22646	20-16542	Dep. mn. CFSTI $2.00 cy, $0.50 mn
22662	20-16339	Dep. mn. CFSTI $1.00 cy, $0.50 mn
22663	20-16607	Dep. mn. CFSTI $3.00 cy, $0.75 mn
22665	20-18071	Dep. mn. CFSTI $4.00 cy, $1.00 mn
22666	20-16509	Dep. mn. CFSTI $6.00 cy, $1.25 mn
22681	20-16490	Dep. mn. CFSTI $4.00 cy, $0.75 mn
22689	20-16780	Dep. mn. CFSTI $1.00 cy, $0.50 mn
22693	20-16734	Dep. mn. CFSTI $3.00 cy, $0.75 mn
22697	20-18138	Dep. mn. CFSTI $2.00 cy, $0.50 mn
22703	20-18178	Dep. mn. CFSTI $1.00 cy, $0.75 mn
22712	20-17027	Dep. mn. CFSTI $2.00 cy, $0.50 mn
22733	20-17028	Dep. mn. CFSTI $4.00 cy, $0.75 mn
22763	20-16828	Dep. mn. CFSTI $2.00 cy, $0.50 mn
TO-B-	(Non-AEC)	
65-99	20-16735	
TR-	(Misc.)	
1074	20-17971	See AD-299256
TRG-Report-	(British)	
952	20-16349	Analyst, 90: 727-31(1965)
1014	20-18051	Dep. BIS $0.90. HMSO 4s. 6d.
1039	20-18092	Dep. BIS $0.60. HMSO 3s.
TT-	(Canadian)	
66-30562	20-16232	See JPRS-34120
UCRL-		
7331	20-17054	J. Appl. Phys., 37: 931-2(1966)
7703	20-17773	Phys. Rev., 143: 790-6(1966)
12107(Rev.1)	20-17051	J. Appl. Phys., 37: 564-7(1966)
12176	20-17775	Phys. Rev., 143: 800-7(1966)
12224-T	20-16589	Dep. mn. CFSTI $1.00 cy, $0.50 mn
12386	20-17979	Dep. mn. CFSTI $1.00 cy, $0.50 mn
14321-T	20-17436	Dep. mn. CFSTI $4.00 cy, $0.75 mn
14325	20-17527	Phys. Rev., 143: 96-103(1966)
14444	20-17800	Proc. Phys. Soc. (London), 87: 677-9(1966)
14478-T	20-17479	Phys. Rev., 143: 1324-39(1966)
14506-T	20-17770	Phys. Rev., 143: 775-9(1966)
14534	20-16736	Dep. mn. CFSTI $3.00 cy, $0.75 mn
14660	20-16591	Dep. mn. CFSTI $3.00 cy, $0.75 mn
14739(Pt.2)	20-16160	Dep. mn. CFSTI $5.00 cy, $1.00 mn
16250	20-16418	Dep. mn. CFSTI $2.00 cy, $0.50 mn
16318	20-17996	Phys. Rev., 143: 278-83(1966)
16345	20-17614	Phys. Rev., 143: 78-84(1966)
16377	20-16231	Dep. mn. CFSTI $2.00 cy, $0.50 mn
16437	20-17992	Phys. Rev., 143: 130-2(1966)
16485	20-16887	Science, 151: 562-8(1966)
16570	20-17402	Phys. Rev. Lett., 16: 481-5(1966)
16604	20-17403	Phys. Rev. Lett., 16: 485-91(1966)
16605	20-16633	Dep. mn. CFSTI $4.00 cy, $1.00 mn
16705	20-17794	Phys. Rev. Lett., 16: 469-73(1966)
UCRL-Trans-		
1301(L)	20-16419	Dep. mn. JCL $5.60 fs, $1.97 mf
1305	20-17212	Dep. mn. JCL $3.60 fs, $1.22 mf
1312	20-17213	Dep. mn. JCL $2.60 fs, $0.95 mf
UNC-	(Misc.)	
5142	20-18093	Dep. mn. CFSTI $2.00 cy, $0.50 mn
UR-		
875-65	20-17696	Dep. mn. CFSTI $1.00 cy, $0.50 mn
875-97	20-17375	Nuovo Cimento (10), 41A: 586-98(1966)
875-103	20-17470	Phys. Rev., 143: 1216-19(1966)
875-113	20-17405	Phys. Rev. Lett., 16: 371-4(1966)
USMRDL-TR-	(Misc.)	
953	20-16659	See AD-629527
956	20-16158	See AD-628360
958	20-16215	See AD-628443
962	20-17670	See AD-629576
963	20-16170	See AD-628805
964	20-16216	See AD-628791
970	20-16340	Dep. mn. CFSTI $2.00 cy, $0.50 mn
VUF-		
1014	20-16742	Dep. mn. CFSTI $3.00 cy, $0.50 mn
1021	20-16743	Dep. mn. CFSTI $3.00 cy, $0.75 mn
WANL-TME-	(Misc.)	
1028	20-17697	Dep. mn. CFSTI $3.00 cy, $0.75 mn
1132	20-17698	Dep. mn. CFSTI $4.00 cy, $1.00 mn
1317	20-17699	Dep. mn. CFSTI $2.00 cy, $0.50 mn
WAPD-MRP-		
115	20-18094	Dep. mn. CFSTI $4.00 cy, $0.75 mn
WAPD-T-		
1836	20-18052	Dep. mn. CFSTI $1.00 cy, $0.50 mn
WCAP-	(Misc.)	
3385-52	20-18095	Dep. mn. CFSTI $2.00 cy, $0.50 mn
X-	(Misc.)	
311-64-371	20-17228	See N-65-18275
611-64-297	20-17541	See N-65-19719
611-64-363	20-17308	See N-65-18274
641-64-288	20-17309	See N-65-19716
642-64-278	20-17539	See N-65-18257
Y-		
1508	20-18179	Dep. mn. CFSTI $2.00 cy, $0.50 mn
Y-DA-		
1043	20-16993	Dep. mn. CFSTI $1.00 cy, $0.50 mn
Y-EA-		
49	20-16744	Dep. mn. CFSTI $2.00 cy, $0.50 mn
ZFK-PHA-	(German)	
17	20-17700	Dep. mn

DEPOSITORIES OF USAEC REPORTS

In Countries Other than the U.S.

ARGENTINA
Buenos Aires, Comisión Nacional de Energía Atómica
AUSTRALIA
Canberra, Australian National Library
Sutherland, New South Wales, Australian Atomic Energy Commission
AUSTRIA
Vienna, Zentral Bibliothek der Physikalischen Institute der Universität
BELGIUM
Mol-Donk, Centre d'Etude de l'Energie Nucleaire
BOLIVIA
La Paz, Comisión Nacional de Energiá Nuclear
BRAZIL
Rio de Janeiro, Instituto Brasileiro de Bibliografia e Documentacao
São Paulo, Instituto de Energia Atomica, Cidade Universitaria São Paulo
BURMA
Rangoon, Union of Burma Applied Research Institute, Atomic Energy Center Library
CANADA
Hamilton, McMaster University
Ottawa, National Research Council Library
Vancouver, University of British Columbia
CHILE
Santiago, Instituto de Fisica y Matematicas, Universidad de Chile
CHINA
Hsinchu, Taiwan, Free China, National Tsing Hua University
COLOMBIA
Bogota, Instituto De Asuntos Nucleares
COSTA RICA
San Pedro, University of Costa Rica Library
DENMARK
Risö, Danish Atomic Energy Commission
ECUADOR
Quito, Escuela Politécnica Nacional
EL SALVADOR
San Salvador, Universidad de El Salvador, Biblioteca de Energia Nuclear
FINLAND
Helsinki, Teknillisen Korkeakoulun Kirjasto
FRANCE
Gif-sur-Yvette, Centre d'Etudes Nucléaires de Saclay
Paris, Académie des Sciences
GERMANY
Berlin, Hahn-Meitner-Institut für Kernforschung Berlin
Frankfurt/Main, Gmelin-Institut
Munich, Technische Hochschule, Bibliothek
GHANA
Accra, University College of Ghana
GREECE
Athens, Nuclear Research Center "Democritus"
GUATEMALA
Guatemala, Comisión Nacional de Energía Nuclear
INDIA
Bombay, Department of Atomic Energy
IRAN
Tehran, Tehran University Nuclear Centre
IRAQ
Baghdad, Iraqi Atomic Energy Commission
IRELAND
Dublin, University College
ISRAEL
Rehovoth, Israel Atomic Energy Commission
ITALY
Rome, Centro di Studi Nucleari della Casaccia
Rome, Comitato Nazionale per l'Energia Nucleare
JAPAN
Tokyo, National Diet Library
KOREA
Seoul, Office of Atomic Energy
LEBANON
Beirut, Lebanese National Council for Scientific Research
LUXEMBOURG
Luxembourg, Ministry of Transport and Electricity
MALAYSIA
Kuala Lumpur, University of Malaysia
MEXICO
Mexico, D.F., Comisión Nacional de Energía Nuclear
NETHERLANDS
The Hague, Reactor Centrum Nederland
NEW ZEALAND
Lower Hutt, Institute of Nuclear Sciences
NIGERIA
Ibadan, University of Ibadan
NORWAY
Lillestrøm, Institutt för Atomenergi
PAKISTAN
Lahore, West Pakistan, Atomic Energy Centre
PERU
Lima, Junta de Control de Energia Atomica
PHILIPPINE REPUBLIC
Manila, Philippine Atomic Energy Commission
POLAND
Warsaw, Biura Pelnomocnika Rzadu do Spraw Wykorzystania Energii Jadrowej
PORTUGAL
Sacavem, Junta de Energía Nuclear
REPUBLIC OF SOUTH AFRICA
Pretoria, Atomic Energy Board Library
REPUBLIC OF THE CONGO
Leopoldville, Université Lovanium
SPAIN
Madrid, Junta de Energía Nuclear, Biblioteca Documentación y Publicaciones, Ciudad Universitaria
SWEDEN
Nyköping, Aktiebolaget Atomenergi
SWITZERLAND
Zürich, Eidgenössische Technische Hochschule, Bibliothek
THAILAND
Bangkok, Office of the Thai Atomic Energy Commission, Department of Science
TURKEY
Ankara, Turkish Atomic Energy Commission, Atomic Energy Library
UNITED ARAB REPUBLIC
Cairo, Atomic Energy Commission
UNITED KINGDOM
Birmingham, Central Library
Boston Spa, National Lending Library for Science and Technology
Kingston upon Hull, Central Library
Liverpool, Central Library
London, Central Library, Acton
London, National Reference Library
London, Science Museum Library, South Kensington
Manchester, Central Library
Newcastle upon Tyne, Central Library
Nottingham, Central Library
Sheffield, Central Library
URUGUAY
Montevideo, Comision Nacional de Energia Atomica
VENEZUELA
Caracas, Instituto Venezolano de Investigaciones Científicas
VIET-NAM
Saigon, Atomic Energy Office
YUGOSLAVIA
Belgrade, Federal Commission for Nuclear Energy

In International Agencies

AUSTRIA
Vienna, International Atomic Energy Agency
BELGIUM
Brussels, La Bibliotheque EURATOM
FRANCE
Paris, European Nuclear Energy Agency, O.E.C.D.
ITALY
Ispra, EURATOM Research Center
SWITZERLAND
Geneva, United Nations Library

UNITED STATES
GOVERNMENT PRINTING OFFICE
DIVISION OF PUBLIC DOCUMENTS
WASHINGTON, D.C. 20402

OFFICIAL BUSINESS

POSTAGE AND FEES PAID
U.S. GOVERNMENT PRINTING OFFICE

TECHNICAL PROGRESS REVIEWS

The Division of Technical Information, U. S. Atomic Energy Commission, also publishes the Technical Progress Reviews, a series of five quarterly journals on nuclear technology. These journals, compiled by specialists and recognized authorities, summarize, evaluate, and reference the progress of development in five important fields.

Isotopes and Radiation Technology P. S. Baker, A. F. Rupp, and associates, Oak Ridge National Laboratory. Reviews AEC-sponsored projects and related significant worldwide developments in radioisotopes and radiation technology.

Nuclear Safety Wm. B. Cottrell, W. H. Jordan, and associates, Oak Ridge National Laboratory. Covers topics relevant to the analysis and control of hazards associated with nuclear reactors and with operations involving fissionable materials and the products of nuclear fission.

Power Reactor Technology Argonne National Laboratory. Reviews research, development, design practices, and operating experiences associated with power reactors, including aerospace applications.

Reactor Fuel Processing Stephen Lawroski and associates, Argonne National Laboratory. Reviews all aspects of the fuel-processing field, including aqueous and nonaqueous processing and waste disposal.

Reactor Materials R. W. Dayton, E. M. Simons, and associates, Battelle Memorial Institute. Covers the properties, behavior, and fabrication processes of materials used in nuclear reactors and associated equipment.

8033 V

Availability

SUBSCRIPTION RATE: The Technical Progress Reviews may be purchased from the Superintendent of Documents, U. S. Government Printing Office, Washington, D. C. 20402, at $2.50 per year for each subscription or $0.70 per issue.

POSTAGE: Postpaid within the United States, Canada, Mexico, and all Central and South American countries except Argentina, Brazil, British and French Guiana, Surinam, and British Honduras. For these Central and South American countries and all other countries, add $0.75 per year or $0.20 per single issue.

REMITTANCE: Payment should be by check, money order, or document coupons and MUST accompany order. Remittances from foreign countries should be made by international money order or draft on an American bank payable to the Superintendent of Documents or by UNESCO book coupons.